UNITED STATES
DEPARTMENT OF THE INTERIOR
GEOLOGICAL SURVEY

ASSESSMENT OF REGIONAL EARTHQUAKE HAZARDS AND RISK ALONG THE WASATCH FRONT, UTAH

VOLUME I

Editors
Paula L. Gori and Walter W. Hays

Contributions from:

UTAH GEOLOGICAL AND MINERAL SURVEY
UTAH DIVISION OF COMPREHENSIVE EMERGENCY MANAGEMENT
UNIVERSITY OF UTAH
UTAH STATE UNIVERSITY

Open File Report 87-585

This report is preliminary and has not been edited or reviewed for conformity with U.S. Geological Survey publication standards and stratigraphic nomenclature. The views and conclusions contained in this document are those of the authors and should not be interpreted as necessarily representing the official policies, either expressed or implied, of the United States Government. Any use of trade names and trademarks in this publication is for descriptive purposes only and does not constitute endorsement by the U.S. Geological Survey.

Reston, Virginia
1987

FOREWORD

This report represents an ongoing U.S. Geological Survey effort to transfer accurate earth science information about earthquake hazards along the Wasatch front, Utah to researchers, public officials, design professionals, land-use planners, and emergency managers in an effort to mitigate the effects of earthquake hazards. This report is a preview of the future U.S. Geological Survey professional paper on regional earthquake hazards and risk along the Wasatch front.

Currently State and local governments, private institutions, and individuals are implementing earthquake hazards reduction measures in Utah. The success of their efforts will depend, in part, on the availability of accurate earth science information. The timeliness and importance of the multidisciplinary research contained in this report and the need for its utilization has made it imperative to release the information in the form of an open-file report while the process of publishing the professional paper is being completed.

The report is organized into 2 volumes. Volume I contains chapters on the tectonic framework and earthquake potential of the Wasatch front area. Volume II contains chapters on the ground shaking hazards and aspects of loss estimation, as well as, chapters on the use of hazards information for urban and regional planning and development. Many of the chapters are in draft format and, therefore, the figures follow the text.

The information contained in this report is the latest and most accurate information available on earthquake hazards along the Wasatch front and may be used and cited until such time as the Professional Paper on "Regional earthquake hazards and risk along the Wasatch front," is published.

Paula L. Gori
Walter W. Hays
Editors

ASSESSMENT OF REGIONAL EARTHQUAKE HAZARDS AND RISK ALONG THE WASATCH FRONT, UTAH

Table of Contents

VOLUME I

INTRODUCTION TO ASSESSMENT OF REGIONAL EARTHQUAKE HAZARDS AND RISK ALONG THE WASATCH FRONT, UTAH

THE TECTONIC FRAMEWORK AND EARTHQUAKE POTENTIAL OF THE WASATCH FRONT AREA

VOLUME II

THE GROUND-SHAKING HAZARDS AND ASPECTS OF LOSS ESTIMATION IN THE WASATCH FRONT AREA

THE USE OF EARTHQUAKE HAZARDS INFORMATION FOR URBAN AND REGIONAL PLANNING AND DEVELOPMENT IN THE WASATCH FRONT AREA

INTRODUCTION TO ASSESSMENT OF REGIONAL EARTHQUAKE HAZARDS AND RISK ALONG THE WASATCH FRONT, UTAH

By

Paula L. Gori and Walter W. Hays

The Earthquake Threat

> "There are many geologists who are very wise, but even they do not understand the forces which produce mountains. And yet it must be admitted, not only that mountains have been made, but that some mountains are still rising. The mysterious forces appear to act in different ways in differenct places, and it is possible that their nature is not unusually the same. Suffice it to say that in the Great Basin the movements they cause are vertical. It is as though something beneath each mountain was slowly, steadily, and irresistibly rising, carrying, the mountain with it." (Salt Lake Daily Tribune, September 16, 1883, p. 4).

So began an article by Grove Karl Gilbert, a geologist, in 1883 warning the citizens of the Great Basin about the potential for damaging earthquakes in their region. After describing the damage and loss of life in a small town in California that he had just visited after an earthquake, Gilbert cautioned that a similar earthquake could occur in Salt Lake City. "It is useless to ask when this disaster [earthquake] will occur. Our occupation of the country has been too brief for us to learn how fast the Wasatch grows, and indeed, it is only by such disasters that we can learn. By the time experience has taught us this, Salt Lake City will have been shaken down. . . ." (Salt Lake Daily Tribune, September 16, 1883, p.4).

After more than a century of research, geologists and other scientists have increased their understanding of the tectonic processes at work in the Wasatch front and are now beginning to answer the questions about the seismicity and tectonics of the Wasatch front that Gilbert and others posed from the time the area was settled in the mid-ninteenth century. Scientists, engineers, architects, urban planners, and emergency managers are not waiting for the disaster that a major earthquake would cause in the Wasatch front area in order to learn the lessons necessary to understand earthquakes in the region and implement measures to mitigate their effects, They are taking actions now to prepare for and to mitigate the physical effects of such an earthquake.

The majority of Utah's population lives adjacent to the Wasatch fault zone, an active, north-south trending, intraplate zone of normal faulting that extends approximately 370 km (220 mi) along the western front of the Wasatch Range from Gunnison, Utah, to Malad City, Idaho. Earthquakes have been felt since settlement of Utah in the mid-ninteenth century. During historic time approximately 8 earthquakes of magnitude $\geq$ 6 have occurred in Utah. The two largest were: the (M_L) 6.6, Hansel Valley earthquake of 1934 and the magnitude (M_L) 6.5, Richfield earthquake of 1901.

The historic record of seismicity has been broadened by incorporating geologic evidence and monitoring small earthquakes. Although no large earthquakes (magnitudes greater than 7.0) have occurred since Utah was settled, clear geologic and geomorphic evidence (Hamblin, 1976) demonstrate that large earthquakes have occurred repeatedly throughout the late Pleistocene (2 million years before present) and Holocene (10,000 years before present) times on segments within the Wasatch fault zone. For this reason, and the continuing low level of seismicity, scientists believe that some parts of segments of the Wasatch fault zone are overdue for a damaging earthquake (Schwartz and Coppersmith, 1984). Machette and others (this report) have identified 12 segments of the Wasatch fault which have produced earthquakes on the average of a couple hundred years to a couple thousand years.

The largest urban centers of Utah are located along the Wasatch front. They are also the largest growth centers. About 80% of Utah's 2 million population live along the Wasatch front. A large earthquake centered near Salt Lake City has the potential to cause extensive damage to buildings, lifelines, and public facilities. The level of ground shaking would be expected to be in the range of 0.2-0.4 g, or possibly greater, depending on site effects. Surface fault rupture and tectonic deformation, as well as landslides and liquefaction, would be expected to occur in many areas. Deaths and injuries could be high, depending on the time of day of the earthquake and the nature and extent of pre-event mitigation actions.

The October 28, 1983, Borah Peak, Idaho, M_s 7.3, earthquake reminded scientists and policymakers that large earthquakes will recur in the intermountain seismic belt. Scientists believe that the Borah Peak, Idaho earthquake is a model of what can happen on the Wasatch front (Smith, 1984). A magnitude 7.0 - 7.5 earthquake nucleating at a depth of 10-15 km is now being considered as a scenario earthquake for the purpose of response planning in Utah.

Purpose and Scope of This Volume

In 1983 the U.S. Geological Survey named the Wasatch front, Utah as the location of a 5-year program of focused research and implementation. The goals were to 1) accelerate the development of the knowledge base on seismic sources, size, frequency of occurrence, and the physical effects of earthquakes in a 10 county area along the Wasatch front, including Salt Lake, Davis, Juab, Weber, Wasatch, Summit, Morgan, Cache, Utah, Box Elder, along the Wasatch front and 2) to foster application of the knowledge base in the form of mitigation measures. Although research by U.S. Geological Survey (USGS) scientists and others had been going on for many years in the area prior to 1984, the knowledge base has not been developed to the point where it could be applied in mitigation measures by officials of State and local government.

The program in the Wasatch front area was conducted under the auspices of the National Earthquake Hazards Reduction Program (NEHRP). It was a part of the "Regional Earthquake Hazards Assessment" element, one of five elements in the Geological Survey's program in the NEHRP. The element was established to provide concentrated and coordinated attention to geographic regions containing large urban areas at risk from earthquakes by utilizing past research and fostering partnerships with universities, the private sector, local government, and State and Federal agencies. The effort provides a technical basis for devising and implementing mitigation and loss reduction measures. Other study areas in this program element include California; Anchorage, Alaska; Puget Sound - Portland area in Washington and Oregon; Central Mississippi Valley; Charleston, South Carolina; the Northeastern United States; Hawaii; and Puerto Rico - Virgin Islands.

In Utah, all five of the interrelated components listed below form the basis of the comprehensive research and implementation program:

1. Information Systems - Produce quality data along with a comprehensive information system, available to both internal and external users, for use in earthquake hazards evaluations, risk assessment, and implementation of loss reduction measures.

2. Synthesis of Geological and Geophysical Data for Evaluation of Data for Evaluation of Earthquake Hazards - Prepare synthesis reports describing the nature, extent, frequency of occurrence, and physical effects of the earthquake hazards of ground shaking, surface faulting, earthquake-induced ground failure, and tectonic deformation and recommend future research to increase the knowledge base required for the creation and implemention of mitigation and loss-reduction measures.

3. Ground Motion Modelling - Produce deterministic and probabilistic ground-motion models and maps of the ground-shaking hazard with commentaries on their use in building codes and land use regulations.

4. Loss Estimation Models - Devise economical methods for acquiring inventories of structures and lifeline systems in urban areas, create a standard model for loss estimation, produce loss and casualty estimates for urban areas, and prepare commentaries giving guidelines for use by agencies of State and local government.

5. Implementation - Foster the creation and implementation of measures to mitigate the earthquake hazards of ground shaking, surface fault rupture, earthquake-induced ground failure, and tectonic deformation in urban areas, providing high-quality scientific information that can be used by local government decisionmakers as a basis for implementing and enforcing them loss-reduction measures.

This report provides a comprehensive treatment of the knowledge gained in the research and implementation program in the Wasatch front area. The report is divided into 3 sections dealing with individual components of the program that collectively define the nature of the earthquake hazards in the Wasatch front area. They are: 1) The tectonic framework and earthquake potential, 2) the ground-shaking hazards and aspects of loss estimation, 3) the use of earthquake hazards information for urban and regional planning and development. Volume I is devoted to the first topic; Volume II is devoted to the latter 2 topics. The research findings contained in this report are the results of studies conducted by scientists and engineers of the U.S. Geological Survey, the Utah Geological Survey, various universities, and private consulting firms. Funding was provided primarily by the U.S. Geological Survey through the NEHRP, using grants to involve non-Survey scientists and engineers.

Tectonic Framework and Earthquake Potential of the Wasatch Front Area

This section of the report contains chapters devoted to geologic and geophysical studies that had the objective of improving the fundamental understanding of the potential for the occurrence of large damaging earthquakes in the Wasatch front area. In some cases, researchers have drawn on studies of other parts of Utah and the Intermountain Seismic Belt to gain an understanding of the large-magnitude earthquakes which may occur in the Wasatch front.

The geologic and seismological/geophysical studies comprising this section are described in 10 chapters:

1. Quaternary Geology Along the Wasatch Fault Zone: Segmentation, Recent Investigations, and Preliminary Conclusions by Michael N. Machette, Stephen F. Personius, and Allan R. Nelson - Ten to twelve discrete segments of the Wasatch fault zone, eight of which have demonstrable Holocene movement, increase the possible number of separate localities where earthquakes may occur.

2. Persistent and Nonpersistent Segmentation of the Wasatch Fault Zone, Utah -- Statistical Analysis for Evaluation of Seismic Hazard by Russell L. Wheeler and Katherine B. Krystinik - The Wasatch fault zone has been persistently segmented at four salients - Pleasant View, Salt Lake, Traverse Mountains, and Payson throughout much or all of its 10-m.y. history and will likely continue to be segmented there throughout the

next several millenia, which is the time span of interest for hazard evaluation.

3. Subsurface Geology Along the Wasatch Front by Don R. Mabey - Magnetic data suggest segment boundaries of the Wasatch fault zone that are generally consistent with segment boundaries inferred from surface mapping of the fault zone.

4. Observational Seismology and the Evaluation of Earthquake Hazards and Risk in the Wasatch Front area, Utah by Walter J. Arabasz, James C. Pechmann, and Ethan D. Brown - Background seismicity predominates on second-order faults in the Wasatch Front area, but it is the largest contributor to the probabilistic ground-shaking hazard for exposure periods of 50 years or less. The earthquake data imply an average return period of 24±10 years for potentially damaging earthquakes of magnitude 5.5 or greater along the Wasatch Front.

5. Superimposed Late Cenozoic, Mesozoic, and Possible Proterozoic Deformation Along the Wasatch Fault Zone in Central Utah by Mary Lou Zoback - The thrust ramping and late Cenozoic normal faulting may be localized by a major west-dipping normal fault zone formed during the early phases of late Precambrian rifting of the western Cordillera.

6. Neotectonic Framework of the Central Sevier Valley Area, Utah, and its Relationship to Seismicity by R. Ernest Anderson and Theodore P. Barnhard - Normal faults in the Wasatch fault zone such as the Sevier fault probably cut one or more levels of potential structural detachment and penetrate to the base of the seismogenic part of the crust. Such faults are more likely to be the source of infrequent large earthquakes than are faults in the complex structural junctures where late Quarternary deformation is concentrated.

7. Neotectonics of the Hansel Valley-Pocatello Valley Corridor, Northern Utah, and Southern Idaho by James McCalpin, Robert M. Robison, and John D. Garr - The 1934 M_L6.6 earthquake may be a typical interpluvial maximum event; i.e., long recurrence time, small displacement, compared to the

larger, more frequent surface-faulting events which are triggered by pluvial lake water loading.

8. Structure of the Salt Lake Segment, Wasatch Normal Fault Zone: Implications for Rupture Propagation During Large Earthquakes by R. L. Bruhn, P. R. Gibler, W. Houghton, and W. T. Parry - There are two potential sites of rupture initiation for large earthquakes in the central and southern ends of the Salt Lake fault segment of the Wasatch normal fault zone. The central site may have been the most common position for repetitive rupture initiation during the last 17 million years.

9. Quaternary Displacement on the Morgan fault, a Back Valley Fault in the Wasatch Range of Northeastern Utah by J. Timothy Sullivan, and Alan R. Nelson - Paleoearthquakes with magnitudes in the range of 6-1/2 to 7 have occurred on the Morgan fault.

10. Late Quaternary History of the James-Peak Fault Southernmost Cashe Valley North-Central Utah by Alan R. Nelson and J. Timothy Sullivan - The James Peak fault may be a westerly splay of the East Cashe fault rather than a separate valley-bounding fault.

The Ground-Shaking Hazard and Aspects of Loss Estimation in the Wasatch Front Area

This section is concerned with the prediction of the effects of local site conditions on ground shaking in the Wasatch front area and the development of loss (risk) estimation procedures.

Ground-motion and loss estimation studies comprising this section are described in six chapters:

1. Site Amplification in the Salt Lake City-Ogden-Provo, Utah, Corridor and the Implications for Earthquake-Resistant Design by Walter W. Hays -

Evaluation of site amplification effects in Utah indicates that the soil deposits in the Salt Lake City-Ogden-Provo urban corridor should be expected to amplify earthquake ground motions especially when the level of shear strain enduced in the soil column is less than about 0.5 percent.

2. Site Response in the Salt Lake City Urban Area Determined from Historic Earthquakes by Sherry D. Oaks - M M intensity of historic earthquakes indicate that intensity increases across Salt Lake City from the Wasatch fault zone to the Jordan River Valley by 2 to 3 intensity units and from east of the Utah State Capitol building south to 17th street south by 1-1/2 intensity units (increase in ground-shaking from east to west and from north to south).

3. Relative Ground Response in Salt Lake City and Areas of Springville-Spanish Fork, Utah by Kenneth W. King, and Robert A. Williams, and David L. Carver - In order to predict the ground-shaking intensity potential for the Wasatch front urban corridor, a better understanding of how shallow underlying geology affects ground shaking was developed.

4. In Situ Poisson's Ratio Measurements Near Provo, Utah by Richard D. Miller, Don W. Steeples, Kenneth W. King, and Ralph W. Knapp - Classification of sites according to response to earthquake energy enables engineers to accurately determine structural requirements for individual sites in high to moderate earthquake risk zones.

5. Predicting Strong Ground Motion in Utah by Kenneth W. Campbell - Near source attenuation relationships for predicting peak horizontal excelleration and velocity in terms of earthquake magnitude, source-to-site distance, and several sources and site parameters are used to estimate strong ground motion in northcentral Utah.

6. Probabilistic Analysis of Earthquake Ground Shaking Hazard Along the Wasatch Front, Utah by R. R. Youngs, F. H. Swan, M. S. Power, D. P. Schwartz, and R. K. Green - The ground shaking hazard along the Wasatch front urban corridor has been assessed using the geological and

seismological data base that has been developed for the region.

7. Earthquake Hazards to Domestic Water Distribution Systems in Salt Lake County, Utah by Lynn M. Highland - In a 7.5 earthquake occurring along the Wasatch Front, Utah significant damage may occur to Salt Lake County's domestic water system.

The Use of Earthquake Hazards Information for Urban and Regional Planning and Development in the Wasatch Front, Utah

This section of the report contains 6 chapters describing the use of earthquake hazards information to reduce potential loss of life and damage to property a damaging earthquake. The 6 chapters are:

1. Making the Implementation Process of the National Earthquake Hazards Reduction Program Work in Utah by Walter W. Hays - Utah has the necessary elements of a program to implement loss-reduction measures designed to mitigate earthquake hazards.

2. Reducing Earthquake Risk in Utah: Past Trends and Future Opportunities by Genevieve Atwood and Don R. Mabey - Utah's political and social structure produces factors that enhance and impede programs that reduce earthquake risk.

3. Emergency Management in Utah for Earthquakes by James L. Tingey and Ralph F. Findlay - Utah State Division of Comprehensive Emergency Management's major challenge has been to provide leadership for the implementation of preparedness and other mitigation strategies within the cities, counties, and State agencies of Utah.

4. Utah Geological and Mineral Survey Escavation and Inspection Program: A Tool for Earthquake Hazard Recognition in Utah by Harold E. Gill - Results of the Utah Geologic and Mineral Survey excavation inspection program have shown the zone of deformation along the Wasatch fault to be highly variable and in some locations up to several hundred meters wide.

5. Rock Fall Hazard Susceptibility Due to Earthquakes, Central Wastach Front Utah, by William F. Case - Property and life loss along a widespread area of the Wasatch front could result from rock falls triggered by nearby earthquakes.

6. Legal Issues Related to Hazard Mitigation Policies by James E. Slosson - Professionals involved in design, construction, and maintenance of structures and facilities may be held responsible to the high standards of practice established outside of Utah. Also planners and public officials may become targets in future litigation and share the burden of court-imposed penalties.

Summary

The efforts in Utah to assess regional earthquake hazards and risk along the Wasatch front in Utah are dynamic and multidisciplinary. This report reflects the nature of the program in Utah. Not only are the topics varied--geology, seismology, engineering geology, urban planning, law, economies, etc., but the level of complexity and sophistication is varied. Some researchers have the benefit of drawing upon many years of research in their discipline in Utah; whereas other researchers are pioneers in their discipline in Utah.

This report is a preview of the future U.S. Geological Survey professional paper on regional earthquake hazards and risk along the Wasatch front in Utah. The timeliness and importance of the research contained herein has made it imperative to release the information in the form of an open-file report while the process of publishing the professional paper is being completed. Plans are also being made to include the results from ongoing research in Utah in a second professional paper which will be a sequel to the first one. Eventually the tectonic processes and their physical and social effects in the Wasatch front will be truly understood and documented.

Acknowledgements

We gratefully acknowledge the efforts of the technical reviewers of the papers which have been included in this report, as well as, the efforts of Charlotte

Jackson (USGS) and her colleagues in Golden, Colorado, who helped coordinate the review process. We especially acknowledge the work of Carla Kitzmiller, Mary Fischer, and Peggy Randalow who prepared the final version of the report.

Selected References

Hamblin, W. K. (1976), Patterns of displacement along the Wasatch fault: Geology, Vol. 4, p. 619-622.

Hays, W. W. and Gori, P. L. eds. (1984), Proceedings of Conference XXVI, a workshop on "Evaluation of regional and urban earthquake hazards and risk in Utah," U.S. Geological Survey Open-File Report 84-763, 674 p.

Hays, W. W. and Gori, P. L. eds. (1987), Proceedings of Conference XXXVIII, a workshop on "Earthquake Hazards Along the Wasatch Front, Utah," Open-File Report 87-154.

Gilbert, G. K., Salt Lake Daily Tribune, September 16, 1883, p. 4.

Schwartz, D. P. and Coppersmith, K. J. (1984), Fault behavior and characteristic earthquakes: Examples from the Wasatch and San Andreas fault zones, Journal of Geophysical Research, vol. 89, p. 5681-5698.

Smith, R. B., Richins and W. D., (1984), Seismicity and Earthquake Hazards of Utah and the Wasatch Front: Paradigm and Paradox, in U.S. Geological Survey Open-File Report 84-763, p. 73-112.

Stein, R. S. and Bucknam, R. C., eds. Proceedings of Conference XXVIII, a workshop on "The Borah Peak, Idaho, earthquake," U.S. Geological Survey Open-File Report 85-290, 686 p.

QUATERNARY GEOLOGY ALONG THE WASATCH FAULT ZONE: SEGMENTATION, RECENT INVESTIGATIONS, AND PRELIMINARY CONCLUSIONS

By Michael N. Machette, Stephen F. Personius, and Alan R. Nelson
U.S. Geological Survey
Denver, Colorado

ABSTRACT

The Wasatch fault zone forms the structural boundary between the Basin and Range province to the west and the Colorado Plateaus and middle Rocky Mountains provinces to the east. It extends about 320 km from Malad City, Idaho, south to Fayette, Utah. Previous studies of the fault zone suggested that it is composed of six discrete segments, each of which tends to act independently during major earthquakes. Since 1983, we have been mapping the surficial geology along the Wasatch front at a publication scale of 1:50,000. The results of this mapping have led us to modify some of the previous segment boundaries, suggest new boundaries, and subdivide four of the original segments.

We now recognize 10 to 12 segments along the Wasatch fault zone. Repeated Holocene movement has been documented along seven segments (the central two-thirds) of the fault zone and an eighth segment moved in the late Holocene. Thus, the heavily urbanized part of the Wasatch Front--between Ogden and Provo--coincides with the part of the fault zone that shows the highest slip rates, shortest recurrence intervals for faulting events, and most recent fault activity.

The 10-12 segments we propose have lengths along their surface traces that are as short as 11-17 km (for the northernmost and southernmost segments) to as long as 57 km for the centrally located Weber segment: their average trace length is about 30 km. The segments with Holocene movement, which form most of the fault zone, average 35 km in length. Historic earthquakes having Moment magnitudes of 6.9-7.5 in nearby parts of the Basin and Range province and the Intermountain Seismic Belt produced surface ruptures of 26 to 36 km (average 31 km). Thus, by analogy, one might expect major (surface rupturing) earthquakes along the Wasatch fault zone to be of similar size (magnitude). One implication of our new segmentation scheme is that the expected length of surface rupturing during a major earthquake on the WFZ could be less than the length suggested by earlier studies (by as much as a factor of 2-3). Because length of surface rupturing is dependent upon earthquake magnitude, the largest earthquake on a single segment would be somewhat less (perhaps 0.3-0.5 M less) than would have been calculated from previous information.

Recent trenching and detailed mapping of Quaternary geology along the Wasatch Front show that the Wasatch fault zone has been active throughout the Holocene (past 10,000 yr). In addition, the recognition of ten to twelve discrete segments of the Wasatch fault zone, eight of which have demonstrable Holocene movement, increases the possible number of separate localities where earthquakes and their associated surface ruptures may occur along the Wasatch Front. Although recurrence intervals for individual segments are still being analyzed, we now think that major earthquakes have and will continue to strike the central heavily urbanized part of the WFZ on an <u>average</u> of once every 250-280 yr (this value is termed the composite-recurrence-interval of faulting).

This preliminary estimate is significantly shorter than the Schwartz and Coppersmith's preferred composite-recurrence-interval of 444 yr. However, we have evidence that large earthquakes (those that cause significant surface-faulting and major ground-shaking damage) have not occurred as recently as the average would demand, and thus one must consider that some form of contagion process (temporal clustering of earthquakes) may be active along the WFZ.

INTRODUCTION

Recent U.S. Geological Survey (USGS) mapping along the Wasatch Front in Utah, from Honeyville on the north to Fayette on the south, has focused on differentiating middle to upper Quaternary deposits (younger than 500,000 yr) that record long- to short-term rates of slip on the Wasatch fault zone (WFZ). This mapping has allowed us to further divide the six segments of the WFZ proposed by Schwartz and Coppersmith (1984). These subdivisions are based on apparent recency of fault movement, amount of displacement of faulted deposits, geometric patterns of surface ruptures and their relations to geology exposed in the footwall block of the fault zone, and the overall history of fault movement during the Holocene and latest Pleistocene. In addition to our detailed mapping studies, the USGS and the Utah Geological and Mineral Survey (UGMS) are engaged in a cooperative study of specific sites on the fault zone where trenching will reveal the age of the most recent ruptures and permit further characterization of major faulting events. Although this work continues (more than 20 radiocarbon dates and 40 thermoluminescence age estimates are pending), our preliminary results are summarized in this report. The reader should be aware that many of the values for recurrence intervals, timing of fault movement, and slip rates are provisional; these values may change when our dating program is completed.

When Schwartz and Coppersmith (1984) proposed a segmentation scheme for the WFZ, they only had excavated trenches at four productive sites along the fault zone. These sites were located, somewhat fortuitously, near the centers of their Ogden, Salt Lake City, Provo, and Nephi segments (sites 5, 7, 11, and 15 of table 1). A natural exposure at Deep Creek (site 17, table 11) along the Levan segment allowed them to constrain the time of most recent faulting there. Their 1984 report on the Wasatch fault zone has been a cornerstone for further investigations. However, having only one trench site on any proposed fault segment left open the possibility that more detailed more would show that different part of the same segments (especially those longer than 40 km) had had different histories of movement.

As an extension of our geologic mapping, the USGS and UGMS undertook a study of newly recognized segments or previously unstudied parts of the WFZ. In September, 1986, thirteen trenches were excavated at three sites on the WFZ near Brigham City, East Ogden, and American Fork Canyon (sites 1, 4, and 9 of table 1). The history of faulting that is being developed from these and additional trenches will help test the suggestion of Machette and others (1986) that the WFZ has at least 10 discrete segments, each of which tends to act independently of the others during major earthquakes (see following discussion of "Fault Segmentation"). In the past two yr trenches also were dug by various governmental groups and private contractors (Machette, 1987). These trenches are at Dresden Place along the East Bench fault (site 6; Salt Lake City segment, WFZ), Dry Creek (site 8; Salt Lake City segment, WFZ), at Woodland Hills (site 14, on a splay of the Spanish Fork segment, WFZ), along the West Valley fault zone (sites 19 and 20, southwest of Salt Lake City), and along the East Cache fault zone near Logan, Utah.

TABLE 1.--Data for exposures of the Wasatch fault zone, Utah

[Trenching sites and natural exposures are listed by fault segment from north to south on Wasatch fault zone, and along subsidary fault zones associated with the Wasatch fault zone. Symbols are as follows: TL, thermoluminescence; MRE, most recent faulting event; RI, recurrence intervals of faulting; Pd., data pending; N.D., not determined, X, unknown number of samples. Slip rates are calculated over intervals B.P.]

Fault segment	Number and name of site	Principal investigator, affilation	Dates of investi-gation	Number of exposures (no. logged)	Age of faulted deposits	Number of datable samples: Organic carbon	Charcoal	TL	Parameters determined: MRE (ka)	RI (1000 yr)	Slip Rate, mm/yr (interval, 1000 yr)
Brigham City	1. Brigham City	S.F. Personius, USGS-Denver.	Sept. 1986	5 (1)	Mid to late Holocene	5	0	2	Pd.	Pd.	Pd.
	2. Pole Patch	S.F. Personius, USGS-Denver.	Sept. 1985	1 (1)	Latest Pleistocene	2	0	0	Pd.	N.d.	N.D.
Weber	3. Garner Canyon	A.R. Nelson, USGS-Denver.	July 1985	1 (1)	Holocene	3	0	0	<1.2	<<2	N.D.
	4. East Ogden	A.R. Nelson, USGS-Denver.	Sept. 1986	5 (5)	Mid to late Holocene	16	3	30	Pd.	Pd.	1.0-1.5 (15)
	5. Kaysville	Woodward-Clyde, Associates.	Summer 1978	7 (7)	Latest Pleistocene	0	1	0	≈0.5	≈2.0	1.3 (8)
Salt Lake City	6. Dresden Place	John Garr, Delta Engin.	Nov. 1986	2 (2)	Late Pleistocene	0	0	6	N.d.	N.d.	0.5 (15)
	7. Little Cottonwood Canyon	Woodward-Clyde, Associates.	Summer 1979	3 (3)	Latest Pleistocene	0	3	0	<<8	2.4-3	0.8 (19)
	8. Dry Creek	D.P. Schwartz, USGS-Menlo Park; W.R. Lund, UGMS.	Summer 1985	5 (5)	Mid Holocene, late Pleistocene	2	0	0	0.9-1.9	Pd.	Pd.
American Fork	9. American Fork Cyn.	M.N. Machette, USGS-Denver.	Sept. 1986	3 (3)	Do.	3	3	10	0.5-<2	1.3-1.9	1.3-2.4 (4.5) 1.0-1.7 (15)
Provo	10. Rock Creek	M.N. Machette, USGS-Denver.	July 1985	1 (1)	Late Holocene	2	0	0	1.1	N.d.	N.D.

TABLE 1.--Data for exposures of the Wasatch fault zone, Utah--continued

Fault segment	Number and name of site	Principal investigator, affilation	Dates of investi- gation	Number of exposures (no. logged)	Age of faulted deposits	Number of datable samples			Parameters determined		
						Organic carbon	Charcoal sample	TL	MRE (ka)	RI (1000 yr)	Slip Rate mm/yr (interval, 1000 yr)
Spanish Fork	11. Hobble Creek	Woodward-Clyde Associates.	Summer 1978	3 (3)	Mid to late Holocene, latest Pleistocene	0	0	0	>1.0	1.7-2.6	0.85-1.0 (14) 1.8-2.5 (17)
	12. Mapleton	W.E. Lund, UGMS.	Summer 1987	5 (2)	Mid(?) Holocene	X	X	7	0.6-0.7	Pd.	Pd.
	13. Water Canyon	D.A. Ostenaa, USBR-Denver.	Spring 1987	3 (3)	Holocene	7 (snails and artifacts)	18	5	Pd.	Pd.	Pd.
	14. Woodland Hills	M.N. Machette, USGS-Denver.	Nov. 1986	2 (1)	Holocene(?) to late Pleistocene	1	0	6	<1.4	50-75 (mean)	0.01-0.02 (150)
Nephi	15. North Creek	Woodward-Clyde Associates.	Sept. 1980	3 (2)	Mid Holocene	2	2	0	<1.1, .3-.5	1.7-2.7	1.3 (4.6)
	16. Red Canyon	M.E. Jackson, Univ. Colorado.	June 1987	1 (1)	Latest(?) Pleistocene	4	0	12	Pd.	Pd.	Pd.
Levan	17. Deep Creek	Woodward-Clyde Associates.	Summer 1980	1 (0)	Early Holocene	0	2	0	<1.8	5.5-7.3	N.D.
	Deep Creek	M.E. Jackson, Univ. Colorado.	June 1987	1 (1)	Do.	0	0	4	Pd.	Pd.	N.D.
	18. Skinner Peaks	M.E. Jackson, Univ. Colorado.	June 1987	1 (1)	Holocene	5	7	10	Pd.	Pd.	Pd.
West Valley fault zone	19. Granger fault	J.R. Keaton, Dames and Moore-Salt Lake City.	1985-1986	2 (2)	Holocene to late Pleistocene	0	0	4	<13	6.5	0.4-0.5 (13) 0.2-0.4 (60) 0.13 (140)
	20. Taylorsville fault	J.R. Keaton, Dames and Moore Salt Lake City.	1985-1986	2 (2)	Holocene and latest Pleistocene	0	0	0	<12	6	0.1-0.2 (<12)

Starting in the spring of 1987, new trenches were opened by the UGMS just south of Mapleton (site 12; Spanish Fork segment, WFZ), by the U.S. Bureau of Reclamation at Water Canyon (site 13; Spanish Fork segment, WFZ), and by Michael Jackson (University of Colorado) at Red Canyon (site 16; Nephi segment, WFZ) and just north of Skinner Peaks (site 18; Levan segment, WFZ). The recent flurry of trenching operations (36 trenches or new exposures in two yr) has provided at least one major trenching site on each of the eight most heavily populated segments (3 major sites on the Spanish Fork segment). The distal fault segments, which are sparsely populated, show little or no evidence of Holocene movement.

REGIONAL QUATERNARY GEOLOGIC FRAMEWORK

Much of our mapping along the Wasatch Front is based on a new understanding of the late Quaternary history of Lake Bonneville. The results of research from 1975-1985 have yielded a simplified stratigraphic framework (see review articles by Scott and others, 1983; Currey and Oviatt, 1985) compared with that developed in the 1950's and 1960's (see Morrison, 1965, for a discussion of pre-1970 stratigraphic concepts). The new framework is based on strategic age determinations coupled with careful discrimination of transgressive and regressive lacustrine sediments deposited before, during, and after isostatic adjustments in the lake basin.

The Quaternary geology along the Wasatch Front is recorded by a series of alluvial, fluvial, colluvial, and eolian deposits. Deposition of these sediments is driven by climatic cycles, either periods of excessive moisture (glacial or pluvial intervals) or restricted moisture (interglacial or interpluvial intervals); deposition or erosion most often coincides with rapid changes in climate (dynamic thresholds).

Stratigraphic and paleontologic evidence suggests that the climate in the eastern Basin and Range was conducive to forming a large and relatively deep lake (Lake Bonneville) at least three times in the past 150 ka (150,000 yr ago). Airfall volcanic ash beds (dated by K-Ar and tephrochronology) in lacustrine sediments show that ancestral Lake Bonneville was present intermittently in early and middle Pleistocene time. Near Beaver, Utah (about 280 km south of Salt Lake City), basin-fill sediments record a major fresh-water lake during late Pliocene and early Pleistocene time. This lake, known as Lake Beaver (Machette, 1985) is an example of lakes that must have occupied basins throughout the eastern Basin and Range province in Quaternary time.

However, the record of these lakes in the Basin and Range province is rarely exposed because much of the province is still undissected (the Bonneville drainage basin still is closed) and young lacustrine and alluvial sediments related to Lake Bonneville largely have obscured the record of all but the most recent lake cycles. Although relatively sparse along the Wasatch Front, there are some exposures of fluvial and lacustrine deposits that extend back into the middle Pleistocene (750 ka-130 ka). For example, extensive alluvial-fan deposits in the Loafer Mountain area of the southeastern part of Utah Valley have thick red argillic B (clay-rich) horizons and thick stage III-IV calcic (calcium-carbonate-rich) horizons that suggest ages of at least several 100 ka (see Birkeland, 1984, for a review of soils and Quaternary geology). The highest and oldest of the fans contains two volcanic ash beds identified by Izett and others (1970) as the Lava Creek B (0.62 Ma; Izett, 1981) and the Bishop (0.74 Ma; Izett, 1982). In the Salt Lake Valley there is a small remnant of fan alluvium or outwash of middle Pleistocene age exposed south of Bells Canyon that has a uranium-trend age of 250 ± 90 ka (Scott and Shroba, 1985: J.N. Rosholt, written commun., 1984, to W.E. Scott).

Most of the surficial deposits that predate the last deep cycle of Lake Bonneville (BLC: Bonneville lake cycle, 32-10 ka) are related to the older Little Valley lake cycle (LVLC; Scott and others, 1983) and glacial drift of the largely contemporaneous Dry Creek advance, or the intervening deposits of the Cutler Dam lake cycle (CDLC; Oviatt and others, 1987; also known as the Hansel Valley lake cycle of McCalpin and others, this volume). These glacial-pluvial cycles (fig. 1) most likely correlate with marine isotope stages 6 and 4, respectively (Richmond and Fullerton, 1987, fig. 2; Martinson and others, 1987, fig. 18). Till of the Dry Creek advance of Madsen and Currey (1979) is exposed at the mouths of Little Cottonwood, Bells, and Dry Creek canyons. Scott and Shroba (1985) suggest the till may be about 150 ka on the basis of its weathering characteristics. Outwash and alluvial-fan deposits of this same general age are preserved at many places along the Wasatch Front. Scott and others (1983) considered the LVLC to be about 150 ka old (it probably persisted for several tens of thousands of years; i.e., marine isotope-stage 6 lasted from 160 ka to 132 ka) on the basis of stratigraphic, soil-morphologic, and amino-acid ratio evidence (see McCoy, 1987).

McCalpin (1986), Keaton and others (1987), and Oviatt and others (1987) have found evidence of a major intermediate-level lake cycle, which Oviatt named the Cutler Dam lake cycle (CSLC), which predates the BLC and postdates the LVLC. No glacial deposits related to the CDLC have been recognized. The radiocarbon dates (infinite?) and amino-acid analyses of Oviatt and others (1987) suggest an age of >40 ka for the CDLC (but an age significantly younger than the LVLC). McCalpin's (1986) two thermoluminescence age estimates are 76 and 82 ka for his Hansel Valley lake cycle (the intermediate lake cycle in the northwestern part of the Bonneville Basin). Keaton and others (1987, table 2) report amino-acid racemization estimates of 45-80 ka for sediments of the intermediate lake cycle in the Salt Lake Valley, but prefer an age of 58 ka for the end of the cycle. If the lake sediments from these three areas all were deposited during marine isotope stage 4, then a reasonable age for the Culter Cam cycle of Lake Bonneville is 60-75 ka.

Most of the units we have mapped along the WFZ were deposited during either the BLC or the largely contemporaneous glaciation of the Wasatch Range, both of which occurred in latest Pleistocene time, between 35 and 10 ka. The following summary of the geologic history during the latest Pleistocene and Holocene is abstracted largely from Madsen and Currey (1979), Currey and others (1983), Scott and others (1983), and Currey and Oviatt (1985).

Glaciers in three canyons advanced beyond the precipitous front of the Wasatch Range and into the eastern Salt Lake and Utah valleys sometime before 22 ka while Lake Bonneville stood at a low to intermediate level during its rise that eventually reached the highest Bonneville shoreline (fig. 1). Till from these glaciers was deposited as large end moraines that extend about 1 km beyond the Wasatch Front at three localities: Little Cottonwood and Bells Canyon south of Salt Lake City and at Dry Creek in the northern Utah Valley. Meltwater from these and the many other glaciers in the Wasatch Mountains deposited gravelly outwash as large fans along the range front and, farther basinward, as deltas in a transgressing Lake Bonneville. The lake's expansion, which started about 32 ka, was interrupted by pauses and minor fluctuations (such as at the Stansbury shoreline, fig. 1), and culminated about 15 ka at the Bonneville shoreline (post-rebound altitudes of 1573-1584 m or 5160-5200 ft, along most of the Wasatch Front). The outwash and alluvial fans along the mountain front were inundated by the lake and, except for small areas near the canyon mouths that stood above the level of the lake, were covered by a veneer of basinward-fining lake sediment.

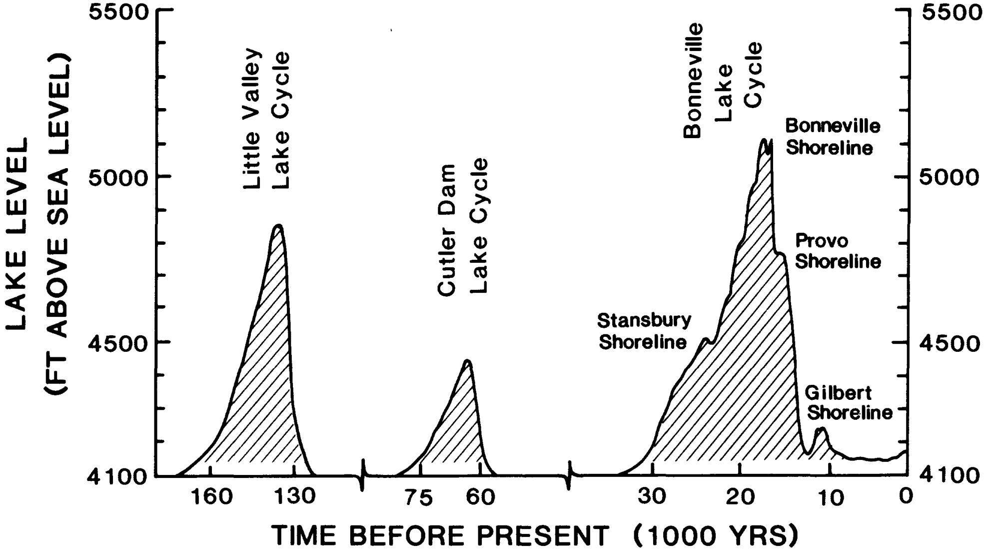

FIGURE 1.--Schematic diagram showing probable levels of Lake Bonneville during the past 150,000 yr. Modified from Currey and Oviatt (1985); extended past 30,000 yr on the basis of recent stratigraphic studies of pre-Bonneville lake cycle deposits by Scott and others (1983), McCalpin and others (this volume), McCoy (1987), and Oviatt and others (1987).

Although most workers agree that the BLC culminated in a major high stand at its natural sill at Red Rock Pass in southern Idaho, Currey and Oviatt (1985) found evidence of a drop and readvance to the overflow level (the Keg Mountain oscillation) sometime between 16 and 15 ka. Others remain skeptical about this oscillation, but Machette's mapping along American Fork Canyon and Scott's reconnaissance of the northern Oquirrh Mountains (W.E. Scott, oral commun., 1987) tends to support an oscillation in the final transgressive phase of the BLC. Gravel pits in the fan-delta complex at the mouth of the American Fork Canyon record two closely series of transgression-regression, separated by what we infer to be the Keg Mountain oscillation.

After Lake Bonneville attained an altitude of 1552 m (5092 feet) it overtopped its natural sill near Red Rock Pass, Idaho, and rapidly downcut about 108 m (355 feet) to the altitude of the major Provo shoreline, where the outlet was stabilized. This fall, which occurred about 15 ka, initiated rapid stream erosion of unconsolidated BLC sediments along former shoreline areas and in mountain canyons. Much of the eroded material was deposited in deltas, bars, and spits at the Provo shoreline. Currey and Oviatt (1985) suggest that Lake Bonneville may have occupied the Provo level for a thousand yr (15 to 14 ka). As the lake retreated below the major Provo shoreline about 14 ka, streams cut terraces into the higher deltas and deposited new deltas graded to successively lower shorelines. This fall was caused by minor downcutting of the outlet at Red Rock Pass, by isostatic uplift of formerly deep areas of Lake Bonneville, and by a progressively more arid climate that marked the end of the Pleistocene epoch.

By 11 ka, the lake had fallen to a level close to that of present Great Salt Lake (1283 m, about 4210 ft), and by about 10.3 ka it had risen briefly to form the Gilbert shoreline (altitude about 1295 m, or 4250 ft) at the end of the BLC. Since 10 ka, Great Salt Lake (a saline remnant of Lake Bonneville) has remained within about 10 m of its present level (Scott and others, 1983; Currey and Oviatt, 1985).

During Holocene time, as climatic conditions became similar to those of the present, rates of alluvial deposition declined, and fan alluvium was restricted to areas close to the mountain front. The mouths of steep canyons continued to be the sites of intermittent debris flows and floods, as they are today. Our unpublished results from radiocarbon dating suggest that a major episode of debris-flow deposition (and fan formation) began after 7000 yr B.P. and ended about 4000-4500 yr B.P. This interval generally correlates with the altithermal (warm) period of Antevs (1948, 1955), which originally was defined from the pollen record in Europe at 4450 to 6950 yr B.P.). Away from the mountain front, reduced flow in streams prevented transport of gravels more than a few km; farther downstream the flood plains became depositional centers for sandy to silty sediment.

SEGMENTATION OF THE WASATCH FAULT ZONE

In Utah the WFZ is the structural boundary between the Basin and Range province (to the west) and the Colorado Plateaus and middle Rocky Mountains provinces (to the east). The WFZ extends about 320 km from Malad City, Idaho, through northern Utah to Fayette.

The first modern study of the Wasatch fault zone was conducted by Cluff and others (1970, 1973, 1974) using low-sun-angle photographs. Their 1:24,000 scale maps have been the most detailed decription of the trace of the WFZ. From 1978-1982 geologists at Woodward-Clyde Consultants made detailed investigations of four trench sites along the WFZ. This work resulted in many important reports, but two major reports focused on paleoseismology of the WFZ. In the first one, Swan and others (1980) speculated on the number of possible segments for the WFZ: they suggested at least 6 on the basis of historic microseismicity on the WFZ and as many as 10 on the basis of geometric variations along the fault zone and on a common rupture length of 30-40 km for normal faults worldwide. In the second one, Schwartz and Coppersmith (1984) proposed that the WFZ in Utah is composed of six major segments (fig. 2); these segments were chosen on the basis of a combination of geomorphic, geophysical, paleoseismicity, and geodetic data. The results of our detailed surficial geologic mapping at 1:50,000 scale (Scott and Shroba, 1985; Personius, 1987; unpublished mapping of Nelson, Personius, and Machette, 1987) have led us to modify some of the previous segment boundaries, suggest new boundaries, and subdivide four of the original segments. Of Schwartz and Coppersmith's (1984) six segments, only the Salt Lake City and Nephi segments of the WFZ remain intact from Schwartz and Coppersmith (1984).

We now recognize as many as 12 segments along the WFZ (fig. 2). Two pairs of adjacent segments (the Malad City-Clarkston Mountain and the American Fork-Provo segments) remain problematic; the subdivision proposed here may change if a detailed fault chronology is ever developed for all these segments. Repeated Holocene movement has been documented along 7 segments (the central two-thirds) of the WFZ, and the Levan segment has evidence of a single movement late in the Holocene. Thus, the heavily urbanized part of the Wasatch Front--between Ogden and Provo--is the section of the WFZ that shows the highest slip rates, shortest recurrence intervals for faulting, and most recent fault activity.

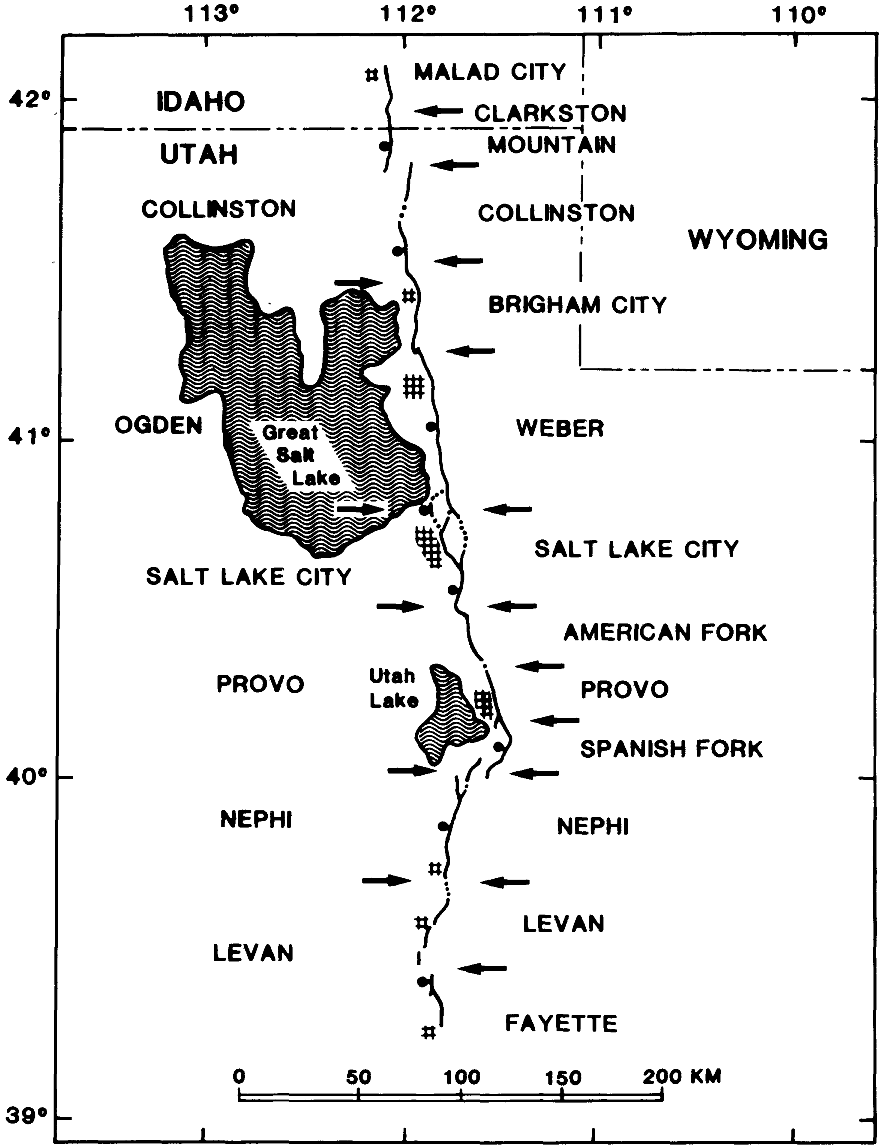

FIGURE 2.--Segmentation of the Wasatch fault zone as proposed by Schwartz and Coppersmith (1984; left column) and by this study (right column). Arrows indicate segment boundaries; major towns shown by hachures.

The 12 segments we propose have lengths along their surface traces that are as short as 11-17 km (for the distal segments) to as long as 57 km for the centrally located Weber segment: their average trace length is about 30 km (table 2). The American Fork (22.5 km) and Provo (18.5 km) segments are suspicious because of their short lengths near the center of the fault zone: if recombined their length would be about 43 km. The segments with Holocene movement, which form most of the fault zone, average 35 km in length.

The lengths of the new proposed segments are generally comparable with the lengths of surface ruptures caused by historic, large-magnitude earthquakes in nearby parts of the Basin and Range province and the Intermountain Seismic Belt. Historic large-magnitude earthquakes in this region include the 1954 Rainbow Mountain-Dixie Valley-Fairview Peak sequence (Slemmons, 1957), the 1959 M 7.5 (moment magnitude) earthquake at Hegben Lake, Montana (Doser, 1985), and the 1983 **M** 7.3 earthquake near Borah Peak, Idaho (Doser and Smith, 1985). The Hegben Lake and Borah Peak earthquakes produced surfaces ruptures of 26 and 34 km length, respectively. The Dixie Valley and Fairview Peak earthquakes of the 1954 sequence occurred on two discrete hypocenters separated by only four minutes in time (Doser, 1986). Doser's body-wave analysis indicates **M** 6.7 for the Dixie Valley earthquake, whereas the preceding Fairview Peak earthquake was between **M** 6.9 and 7.2. These earthquakes produced surface ruptures of 30 and 36 km, respectively (Slemmons, 1957). Therefore, studies of four of the most recent and best studied earthquakes in the Basin and Range province and Intermountain Seismic Belt suggest that rupture lengths of 26-36 km (average 31 km) are associated with historic earthquakes of **M** 6.9-7.5.

TABLE 2.--Lengths of segments and position of boundaries proposed for the Wasatch fault zone, Utah

[Length recorded to closest 0.5 km]

Fault segment	Length of segment (km)		Comments
	Surface trace	Straight line	
Malad City........	17	16.5	No latest Quaternary movement. Length does not include 6-km wide Woodruff spur at south end.
Clarkston Mountain	19	17	No latest Quaternary movement. Extends from spur south to Malad River. 7-km left-step to and 2-km N-S overlap with next segment to south.
Collinston........	30	29.5	No movement younger than 15 ka. North end at Short Divide; fault's position in Bear River area uncertain.
Brigham City......	40	35.5	Repeated Holocene movement. One km left step and 1.5 km N-S overlap at south end; includes most of Pleasant View salient.
Weber.............	57	52	Length to where fault loses evidence of Holocene movement, east of Bountiful and 2 km north of Salt Lake salient (11 km wide).
Salt Lake City....	36.5	31	East Bench and main Wasatch fault south to Corner Canyon, at Traverse Range. Length excludes 7.5 km left step across Traverse Range salient and 4- to 6-km long Warm Springs fault west of Salt Lake salient.
American Fork.....	22.5	21	Extends from Chipman Creek near Alpine south to Provo River. Two-km wide left step into bedrock at south end. No N-S overlap at south end.
Provo.............	18.5	17	Extends from Provo River Canyon to Springville. Includes Springville fault. Overlaps 3 km with Spanish Fork segment.
Spanish Fork......	31.5	24	Major concave-to-west fault. Has 4 km right step and >6 km N-S overlap with Nephi segment.
Nephi.............	42.5	37.5	Extends from Payson to Nephi. Takes major right-step 8.5 km in bedrock between Santaquin Canyon and Juab Valley. 15 km gap in faulting to south.
Levan.............	30	25.5	Has Holocene movement. Length includes 2 major gaps (6 km net) in faulting within segment. Steps 3.5 km left and 5 km south to Fayette segment.
Fayette...........	11	10.5	No Holocene movement. Has a western strand (4 km long) and major range-bounding eastern strand (9 km long). Ends just west of Fayette Cemetery.
TOTAL LENGTH OF SEGMENTS......	356	317	Total length of segments; excludes gaps, overlaps, and salients.
AVERAGE LENGTH OF SEGMENTS	29.5	26.5	Total length divided by 12 segments.
AVERAGE LENGTH OF HOLOCENE SEGMENTS	35	30.5	Total length of Holocene segments divided by 8 segments.
TOTAL LENGTH OF WFZ	369	335	Including gaps and salients, subtracting overlaps.

Note: Schwartz and Coppersmith (1984) proposed six segments. Their Collinston segment is divided here into the Malad City, Clarkston Mountain, and Collinston (restricted sense) segments. Their Odgen segment is divided into the Brigham City and Weber segments (the Brigham City includes about 5 km of the original Collinston segment). Their Provo segment is divided into the American Fork, Provo (restricted sense), and Spanish Fork segments. Their Levan segment is divided into the Levan (restricted sense) and Fayette segments.

One implication of our segmentation scheme is that the expected length of surface rupturing during a major earthquake on the WFZ could be less (by as much as a factor of 2-3). If length of surface rupturing is dependent upon the energy released during an earthquake (i.e. moment magnitude), then the largest earthquake that one could expect along a single segment would be somewhat less (perhaps 0.3-0.5 less on the moment-magnitude scale) for our shorter segments. Implicit in the definition of segments is the concept that a segment defines a distinct part of a fault zone that will rupture during a surface-faulting earthquake (Schwartz and Coppersmith, 1984, p. 5689; Crone and others, 1987). Secondly, the possibility of more segments (10-12 versus 6) increases the number of places that discrete surface rupturing could occur along the WFZ.

Displacement values and slip rates cited in this report refer to only the vertical component of tectonic displacment or slip (NVTD of Schwartz and Coppersmith (1984). This value includes compensation for backtilting, antithetic faults and warping. However, in many cases a lack of good exposures or extensive preservation of the faulted surfaces may allow us to only determine the displacement across a narrow zone or exposure rather than a wider zone that may reflect the far-field effects of tectonism. In such cases, cited values of displacement are crude approximations of the true vertical displacement.

The WFZ has been the focus of extensive trenching efforts (table 1) since the initial investigations of Cluff and others in the 1970's. Including the trench studies currently being conducted, 47 of 53 trenches and 3 natural exposures have been logged and described from 20 sites on 8 segments of the WFZ and an associated fault zone (West Valley). Most of the trenches have provided some control on the time of most recent faulting and set limits on recurrence intervals and slip rates for events at the trench sites. Our additional dating control should refine recurrence intervals and times of most recent faulting, as well as highlight changes in slip rates through time.

To discuss individual fault segments more easily, we divide the WFZ into the northern, central, and southern sections, on the basis of recency of movement and (or) on repetition of faulting in the Holocene. The northern segments show no evidence of Holocene faulting; the central segments show evidence of repeated Holocene faulting; and the southern segments show evidence of one or no faulting events in the Holocene.

NORTHERN WASATCH FAULT ZONE

Segmentation of the northern section of the Wasatch fault zone is difficult to recognize because there is no evidence of faulting in deposits younger than the BLC. Our primary criteria for delineating segments and segment boundaries on the more active part of the Wasatch fault zone are changes in latest Pleistocene and Holocene fault behavior, but because the northern section of the WFZ lacks fault scarps of this age, we have instead used geomorphic and structural relations to identify probable fault segments and boundaries (see Wheeler and Krystinik, 1987a, 1987b, and this volume, for criteria to recognize and methods to analyse fault segmentation). Although we are less confident of these segments compared to those to the south where young surface rupturing is abundant, the structural and geomorphic patterns suggest that the 70-km-long northern section of the WFZ is composed of a 17-km-long Malad City segment, a 19-km-long Clarkston Mountain segment, and a 30-km-long Collinston segment (fig. 2).

Segments along the Malad Range

The northern end of the WFZ, which commonly has been mapped along the west flank of the Malad Range, dies out 4 km northeast of Malad City, Idaho (Cluff and others, 1974). Photo reconnaissance by us and Cluff and others (1974) has shown that lacustrine deposits of the BLC lie undisturbed across most of this section of the fault zone and Cluff and others (1974) recognized some scarps on "older alluvium" (i.e., pre-BLC). On the basis of our photo reconnaissance of this region, we divide the WFZ along the west flank of the Malad Range into two discrete segments: a 17-km-long Malad City segment and a 19-km-long Clarkston Mountain segment.

The boundary we suggest for these two segments is at a 6-km-wide bedrock spur of the the Malad Range, the south edge of which is due east of Woodruff, Idaho. Just south of West Cherry Creek, the front of the Malad Range changes from a steep, linear escarpment that characterizes the Malad City segment, to an irregular zone (the Woodruff spur) that stretches southward to Muddy Creek. From this point south, the range front is marked again by a steep, linear escarpment. The intervening bedrock spur, herein named for the small town of Woodruff, is coincident with a prominent saddle in the gravity data of Peterson (1974) and Zoback (1983); this relation indicates that the net throw across the WFZ decreases at this point. Photo reconnaissance by Cluff and others (1974) suggests that the spur is fractured by numerous faults rather than by a single well defined fault or narrow fault zone. Fractured rock of the spur might disperse and absorb stress as ruptures approach from north or south, thereby decoupling the two adjacent fault segments (King and Nabelek, 1985; Wheeler and Krystinik, this volume) and causing a propagating rupture on either segment to stop at or within the spur.

The Clarkston Mountain segment extends from Muddy Creek south into the Malad River Valley to about 4 km south of the southern end of the Malad Range (Clarkston Mountain). Although the fault does not cut deep-water sediments of the BLC, regressional shorelines at and below the Provo level clearly wrap around a pre-existing escarpment. This escarpment probably is a fault scarp that formed before the regressive phase of the BLC. Surface expression of the Clarkston Mountain segment appears to end near the Malad River, 4 km west of Plymouth, Utah. Although the last movement on the Malad Range segments predates the end of the BLC, steep escarpment along the Malad Range and the presence of older fault scarps along the range front suggest that these two segments have been active in late Pleistocene time.

At the south end of Clarkston Mountain, a prominent down-to-the-south, east-striking normal fault places Tertiary lacustrine sediments (Salt Lake Group) against early Paleozoic sedimentary rocks (Williams, 1958). This fault crosses the Cenozoic structural grain in the region and has been active in late Tertiary and probably Quaternary time. It marks the boundary between the Clarkston Mountain segment and the Collinston segment. The two segments are separated by a 7-km left step and gap in latest Pleistocene faulting. The Collinston segment starts at Short Divide, a low pass just southeast of Clarkston Mountain. The pattern of faulting we recognize in the boundary area differs from that of Cluff and others (1974). They mapped the WFZ as a continuous feature around the southern end of Clarkston Mountain by connecting the fault on the WFZ of the Malad Range (Clarkston Mountain segment) with the WFZ along the Junction Hills (Collinston segment). We believe their presumed connecting fault is a shoreline of Lake Bonneville. The Woodruff spur and the Clarkston Mountain-Collinston segment boundary are shown as major transverse structural features in the gravity maps of Zoback (1983, figs. 3 and 5).

Collinston Segment

The surface trace and history of the Collinston segment is poorly defined because along most of its length there is no evidence for surface faulting in deposits younger than the BLC. The northern end of the segment is probably near Short Divide, where the WFZ intersects the previously discussed, east-striking fault at the south end of Clarkston Mountain. Farther to the south, the Bear River flows southwest from the Cache Valley through a major topographic saddle within the Collinston segment between the south end of Clarkston Mountain and the north end of the Wellsville Mountains. This relatively low topography and a coincident low in the gravity data of Peterson (1974) and Zoback (1983) suggest that the total throw on the WFZ is substantially less on the central part of the Collinston segment than to the south or to the north along the Malad Range. However, the relatively steep escarpment along the Junction Hills (in the topographically low area, but north of the Bear River) and a relatively steep, north-trending gravity gradient suggest that normal faulting extends continuously along the west flank of the Junction Hills, across the Bear River, and south to the west flank of the Wellsville Mountains.

Near the southern boundary of the Collinston segment, Personius (1987) mapped a 2-km-long fault scarp on gravels of the BLC and on early Holocene fan alluvium. This short Holocene scarp is considered part of the Collinston segment, although it probably formed in response to surface faulting originating on the more active, adjacent Brigham City segment. This relationship is similar to the pattern of surface faulting that accompanied the 1983 Borah Peak, Idaho earthquake. Near the northern end of the Lost River fault, the 1983 surface faulting jumped over the segment boundary at the north end of the Thousand Springs segment and ruptured a small part of the

Warm Springs segment (Crone and others, 1987). Sympathetic or subsidiary rupturing is a reasonable explanation for the short Holocene scarp at the southern end of the Collinston segment because no evidence of Holocene faulting is found on the remainder of the segment. Although the most recent faulting on most of the Collinston segment occurred prior to the transgressive phase of the of the BLC (15-10 ka), the steep escarpments along the Wellsville Mountains and the Junction Hills suggest that the segment has probably been active in late Pleistocene time.

The boundary between the Collinston and Brigham City segments is placed at a re-entrant on the west flank of the Wellsville Mountains near the mouth of Jim May Canyon, 2 km northeast of Honeyville, Utah. The boundary is marked by a change in trend of the fault, differences in the amount of displacement of similar-aged pre-BLC deposits, and a general lack of geomorphic evidence for Holocene movement on the Collinston segment (Personius, 1986).

CENTRAL WASATCH FAULT ZONE

The central section of the WFZ is composed of the most active and most recent fault segments. From north to south the seven segments are Brigham City, Weber, Salt Lake City, American Fork, Provo, Spanish Fork, and Nephi (fig. 2). The following discussion highlights evidence from recent investigations along each segment. Determination of additional slip rates along this section of the WFZ awaits radiocarbon dating of samples from recently excavated trenches.

Brigham City Segment

The Brigham City segment is the northernmost segment of the WFZ that exhibits clear evidence of recurrent Holocene faulting along its entire length. The northern part of the segment (from Honeyville to the vicinity of Brigham City) appears to have had lower slip rates than the southern part of the segment. However, near the northern segment boundary our evidence clearly indicates that at least two and probably three faulting events occurred after Lake Bonneville occupied the Provo shoreline (14 ka). Trench studies conducted in September, 1986 near Brigham City revealed evidence that middle Holocene alluvial-fan deposits have been displaced three or possibly four times, although the last event seems to have been in middle to late Holocene time. Just to the south of the trench site, large scarps on the Provo-level delta of Box Elder Creek (and elsewhere along the southern part of the segment) suggest that as many as 8 to 10 surface-faulting events have occurred on the central part of the Brigham City segment since 14 ka. The distribution of fault scarps on different-age Holocene and latest Pleistocene deposits along the segment suggest that the Brigham City segment has remained active in the Holocene. However, only a few small, short and discontinuous scarps near the southern segment boundary are thought to have been formed in latest Holocene time (Personius, 1987). This general lack of young (latest Holocene) activity is in sharp contrast to evidence for three surface faulting events in late Holocene time on the Weber segment to the south (Nelson and others, 1987; see following discussion of the "Weber Segment").

The boundary between the Brigham City and Weber segments is near the northeast corner of the Pleasant View salient, 3 km northeast of North Ogden, Utah (Personius, 1986; Nelson and Personius, 1987). This salient, which was first recognized by Gilbert (1928), seems to be bounded on most (or all) sides by normal faults (Davis, 1985). Here the main trace of the WFZ changes strike and steps left off of the salient, thereby leaving a 2-km-wide gap in Holocene faulting. The Pleasant View salient is a foundered block of Precambrian and lower Paleozoic rock (Davis, 1985) that has been stranded at an intermediate structural level. On the salient, in an area known as the Pole Patch, numerous short normal faults strike at high angles (mainly southwest) to the main trace of the WFZ. At least four of these faults have been active in Holocene time, and they form a network of faults that may disperse the stresses of propagating ruptures in the bedrock salient. Thus, the Pleasant View salient has all the characteristics of a segment boundary.

Weber Segment

The 57-km-long Weber segment of the WFZ extends from Barrett Canyon, 3 km north of North Ogden, to the Salt Lake City salient, a major footwall prong of bedrock that extends westward between Bountiful and northern Salt Lake City. The Weber segment comprises the southern two-thirds of Schwartz and Coppersmith's (1984) 70-km-long Ogden segment, we place the northern boundary of the Weber segment at the Pleasant View salient, well south of their boundary for the Ogden segment. Detailed mapping of late Quaternary deposits along the WFZ by Personius (1987) and Nelson and Personius (1987; unpublished mapping, 1987) suggests that the Pleasant View salient, north of Ogden, Utah, is a nonconservative barrier to fault surface ruptures (see King and Nabelek, 1985, for a discussion of conservative and nonconservative barriers).

Fault slip rates calculated from the amount of surface offset recorded by scarps and from exposures along the main fault on either side of the salient differ significantly. (Surface offset is defined as the amount of displacement of subjacent-correlative alluvial surfaces; Bucknam and Anderson, 1979.) Early and middle Holocene rates are 0.5-1.0 mm/yr on the Brigham City segment and 1.1-1.7 mm/yr on the Weber segment. A comparable difference also has been demonstrated for the late Holocene, where slip rates are <0.3 mm/yr on the Brigham City segment and 0.8-1.2 mm/yr on the Weber segment. These differences in slip rate confirm that the salient is a Holocene (and probably older) boundary between two fault segments (Nelson and Personius, 1987).

The Weber segment of the WFZ is expressed at the surface by almost continuous scarps on Holocene deposits from its northern end to at least as far south as Stone Creek in Bountiful. The majority of these scarps are formed on Holocene alluvial-fan and debris-flow deposits. Nelson's mapping and trenching has shown that debris-flow deposits, almost entirely of late and middle Holocene age, are extensive along the Weber segment. Small landslides are common along the segment, especially where the fault cuts silty deposits of the BLC. Large lateral-spread features appear to be developed in lake deposits near Ogden and Bountiful.

Late Holocene alluvial fans composed of stream and debris-flow sediment are of at least two different ages along the Weber segment, but the degree of soil development and fan surface morphology cannot be used consistently to differentiate two or more ages of fans. A preliminary ^{14}C date from the East Ogden site (discussed below) indicates that even the older Holocene fan remnants exposed along the fault are <5 ka. Fault scarps of differing heights on the late Holocene fans provide the only practical way of distinguishing fans of two ages and this evidence is available at only a few stream drainages. Distinguishing fans by differing scarp height also assumes a spacially and temporally uniform slip rate during the late Holocene.

Scarp heights measured along the fault indicate slip rates of 1.0-1.5 mm/yr over the past 15 ka for the Weber segment. Slip rates appear to decrease as one approaches the boundaries of the segment. This relation was found by topographic profiling forty of the smaller scarps in the field, and making an additional 120 profiles from 1:10,000-scale photographs using the USGS's computer-assisted PG-2 photogrammetric plotter. Analysis of the scarp data shows that most fault-displacement values measured from aerial photographs with the PG-2 plotter are within 10 percent of field measurements made on the same scarps. This measurement error is similar to errors made in estimating displacements from field-measured profiles, especially for scarps >5 m high. In some areas, early vintage photography has been used to measure profiles across scarps that were destroyed as much as 30 yr ago by urbanization.

The exposures at the East Ogden and Garner Canyon sites, near the northern end of the Weber segment, reveal a detailed middle and late Holocene fault history (Nelson and others, 1987). Colluvial wedges found in six exposures at these two sites were deposited following the last three or four events on the fault. The displacements measured in all exposures are similar to values of surface offset calculated from topographic profiles across the scarps. At the Garner Canyon site in north Ogden the last two events, each of 1.4-m displacement, occurred <2 ka and <1.1 ka as determined from ^{14}C mean-residence dates on organic matter concentrated from soil A horizons (fig. 3). At the site in East Ogden, two scarps on middle Holocene fan deposits (^{14}C dated at 4.5 ka) record about 5 m and 7 m of displacement. Where these faults cut two late Holocene fan deposits, the displacements are only 1 m and 2.5 m, respectively, thus indicating recurrent Holocene faulting. The stratigraphy of colluvium exposed in a trench across the 5-m scarp suggests two events of 0.7 m and 2.1 m displacement during the middle Holocene followed by a 2.2-m event in the late Holocene. The 7-m scarp reveals two middle or late Holocene events of about 1.8 m displacment followed by a 2.5-m event during the late Holocene. Trenches across the 5- and 7-m scarps exposed deltaic deposits beneath fan deposits in the hanging-wall block. The deltaic deposits probably formed at the Provo level of the BLC about 14 ka.

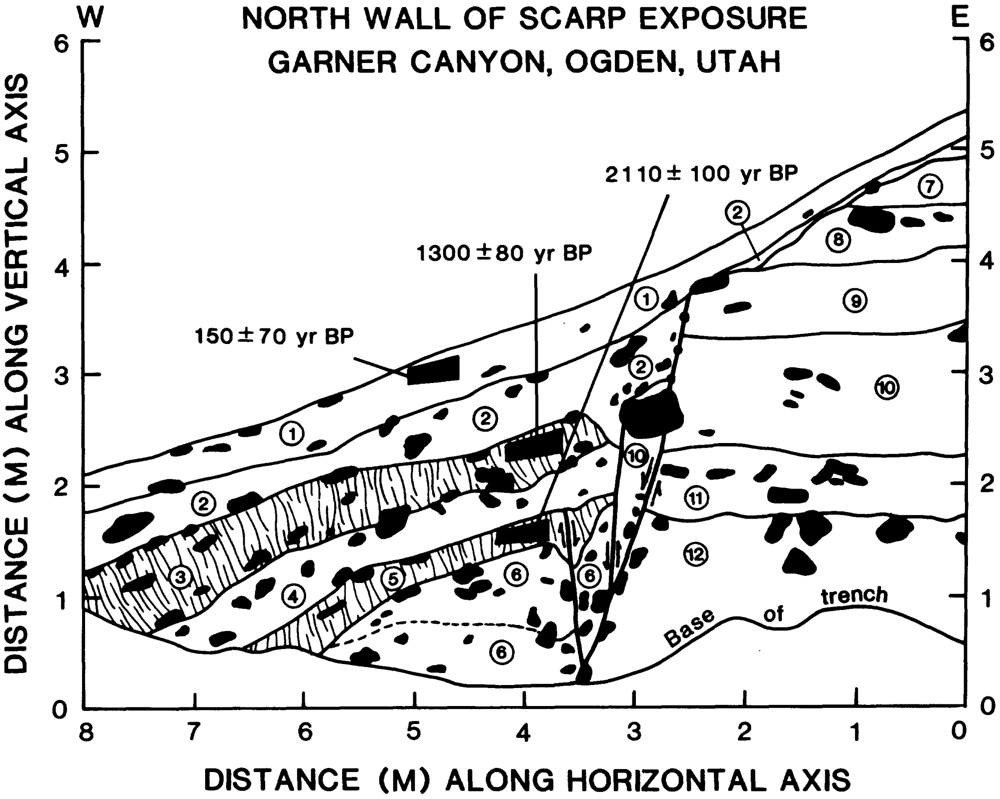

FIGURE 3.--Map of vertical exposure across a fault scarp at Garner Canyon (Weber segment) near Ogden showing fault zone and colluvium produced by faulting events. The scarp (6 m high, 4.4 m displacement) was produced by 3 or probably 4 earthquakes during the middle to late Holocene. Black patches show boulders. Buried A horizons (shown by wavy-line pattern; units 3 and 5) overlie cobbly debris wedges (units 4 and 6) derived from a free face in stream and debris-flow material (units 7-12). The most recent faulting produced a fissure at the base of the free face (easternmost part of unit 2) that was filled with debris. Unit 5 has been displaced by a small antithetic fault. The age of modern A horizons in this area (100-200 yr) subtracted from the ages of the buried A horizons provides approximate maximum ages of 1.1 and 2.0 ka for the last two faulting events at this site on the Weber segment.

The general history of faulting from the two sites near Ogden is similar to that determined for the Kaysville site by Swan and others (1980), 23 km to the south. At Kaysville, Swan and others (1980) have demonstrated at least three surface-faulting events during the past 8 ka (± 2 ka), although the timing of each event is poorly constrained. Discrete colluvial wedges and correlative faulted and back-tilted graben deposits in the trenches were the basis for recognizing three faulting events. The two youngest events occurred within the past 1580 ± 150 ^{14}C yr B.P., and stratigraphic and geomorphic evidence suggests that the most recent event occurred within the past 500 yr, but prior to settlement of the area in 1847. Their best estimate for elapsed time between events is 500-1,000 yr with the longer interval preferred. An early Holocene alluvial fan is displaced 10-11 m, whereas the two most recent events produced similar amounts of displacment; 1.7 and 1.8 m, respectively. The remaining 6.5-7.5 m of displacement may have occurred during the older third event, but more likely it represents the cumulative displacement from two or more events.

Additional ^{14}C dating of soil organic matter and charcoal and thermoluminescence analyses of colluvium (by J.P. McCalpin and S.F. Forman) may provide tighter constraints on the timing of faulting along the Weber segment (table 1). The ages may help resolve unanswered questions such as whether simultaneous movement occurs on parallel faults and whether slip rates have changed significantly during the late Holocene.

Salt Lake City Segment

The Salt Lake segment of the WFZ traverses the most populous part of Utah's Wasatch Front. Detailed mapping along the segment by Scott and Shroba (1985) indicates that most of the recent faulting is concentrated on the Warm Springs fault (western bounding fault of the Salt Lake salient), on the East

Bench fault (intrabasin fault and possible east-bounding fault of the Salt Lake salient), and on the main Wasatch fault that bounds the range front from Olympus Cove south to Corner Canyon on the north flank of the Traverse Mountains.

Scott and Shroba (1985) summarized evidence for Holocene faulting along the Warm Springs fault; little additional knowledge has been gained owing to a lack of new exposures. However, two recent trenches across the East Bench fault near 900 E. and 550 S. (Dresden Place, site 6 of table 1) in Salt Lake City have greatly increased our knowledge of this poorly understood fault. Inspection of these trenches by M.N. Machette and D.R. Currey (Univ. of Utah) and John Garr's mapping of the excavations (written commun., 1987) reveal at least 7 m of deformation in sediments deposited during the BLC (about 26-15 ka at this site). Of the 7 m of deformation, the lower 3 m is expressed as monoclinal warping (plastic deformation) of deep-water sediment. Because plastic deformation requires saturation of the sediment, an early episode of deformation must have occurred before Lake Bonneville fell below the altitude of the site (ca. 4350 ft; 1326 m)--about 12.5 ka as determined from the hydrograph of Lake Bonneville shown in Currey and Oviatt (1985, fig. 2). None of the investigators at this site recognized colluvium within the plastically deformed beds, which suggests that the deformation occurred in a single tectonic event. Plastic deformation was followed by at least 4 m of brittle deformation as indicated by planar fault ruptures that extend to the top of the undisturbed sediment in the trenches. Although the brittle deformation is undated, it seems likely that it corresponds with Holocene movement as indicated by Scott and Shroba's (1985) mapping of the East Bench fault farther to the south.

Previous work by Swan and others (1980) at the mouth of Little Cottonwood Canyon identified several surface-faulting events during the past 19 ka, with at least one event within the past 8 ka. This study indicated a slip rate of 0.76 (+0.6, -0.2) mm/yr, average displacement per event of 2 m, and a recurrence interval of 2400-3000 yr. However, the complex nature of the fault zone complicated the determination of those values and, thus, timing of the most recent event could not be established.

At Dry Creek, about 2 km south of Little Cottonwood Canyon, the UGMS and USGS started a program in 1985 of exploratory trenching, scarp profiling, air photo interpretation, and ^{14}C dating to obtain additional information on elapsed time since the last surface-faulting event, recurrence interval between events, and displacement per event. Trenching and most of the interpretations have been completed, but analysis of recurrence interval and the age of the second most recent faulting event await completion of ^{14}C dating.

The Dry Creek site lies between the steep front of the Wasatch Mountains and the Bonneville shoreline. Here the WFZ is as much as 305 m wide and forms as many as six en echelon, west-facing scarps. Unconsolidated deposits between the mountain front and the shoreline include (from youngest to oldest) Holocene debris-flow deposits, late Pleistocene or early Holocene alluvial-fan and debris-flow deposits, and remnants of middle Pleistocene alluvial-fan deposits (Scott and Shroba, 1985; Lund and Schwartz, 1987). Geomorphic surfaces associated with these deposits are dropped progressively down-to-the-west across the fault zone. The cumulative displacement of these surfaces and deposits becomes greater with increasing age, thus indicating a history of recurrent faulting in the late Quaternary.

A Holocene debris flow along the South Fork of Dry Creek is the youngest deposit (2-4 ka) at the site--its levees have been cut by five of the six faults that form scarps. The sixth fault does not displace the levee, but is buried by it. Schwartz's and Lund's exploratory trenching shows that both single- and multiple-event scarps are present along the faults at this site, with two surface rupture events being the greatest number recognized in any trench. Comparison of the amount of displacement in the levees with those in the trenches shows that for multiple-event scarps, only the most recent event has displaced the levee. The displacement observed in single-event trenches corresponds closely with that on the levees.

Organic matter from buried A horizons exposed in the Dry Creek trenches was concentrated for ^{14}C dating. The organic matter from modern surface soils along the WFZ have radiocarbon dates of as much as several hundred years; thus, dates from buried A horizons should predate the time of burial. This type of radiocarbon determination, which is often referred to as a mean-residence date, could be an important source of error in young soils (less than 1000-2000 yr). A date of 1890 (+50,-60) ^{14}C yr B.P. was obtained for the buried soil on the older of two colluvial wedges; this wedge was subsequently faulted during the most recent event and then buried by a younger colluvial wedge (Lund and Schwartz, 1987). This date places a maximum time limit of about 1700-1800 ^{14}C yr on the most recent event and an absolute minimum limit of about 1900 ^{14}C yr on the prior event. If the older, twice-faulted alluvial fan is middle Holocene (rather than late Pleistocene) like so many others along the WFZ, then the Dry Creek site records two large displacements (ca. 4.5 m) in the past 5 ka and Holocene slip rates are high (>1.8 mm/yr).

Keaton and others (1987) have completed a study of the West Valley fault zone (about 5 km southwest of downtown Salt Lake City). Although this fault zone is 8-10 km west of the East Bench fault of the WFZ, it is included with the Salt Lake City segment because it is a major antithetic fault zone that may be related to the WFZ.

The West Valley fault zone strikes northwest of the Jordan River in the north-central part of Salt Lake County; its closest trace is about 4.8 km southwest of downtown Salt Lake City. Two principal surface traces of the fault zone (the Granger and Taylorsville faults) were identified in the early 1960's on the basis of topographic scarps. Keaton and others (1987) found that the two principal faults each has evidence of Holocene movement. Numerous previously unmapped but suspected fault scarps and lineaments were found as much as 9 km north of the limits of the fault zone as recognized in the 1960's. These features extend the West Valley fault zone to an area about 6.4 km wide and 16 km long.

The Granger fault forms the western of the two traces and has evidence for 4.5 to 12.2 m of normal slip (down-to-the-east) within the past 12 ka; these data yield a minimum slip rate of 0.4-1.0 mm/yr. Sediments of a previous lake cycle (probably the Cutler Dam lake cycle of Oviatt and others, 1987) were found in the trench on the footwall, and in drill holes on the hanging wall. Displacement in the older sediments ranged from 12.2 to 19.8 m and Keaton and others (1987) assumed their age is about 58 ka on the basis of correlation with the end of isotope stage 4. The resulting average slip rates are 0.21-0.34 mm/yr. The markedly different average slip rates (2-3x) between pre- and post-BLC deposits suggested to Keaton and others (1987, p. 25) that the deep water of Lake Bonneville may have suppressed strain release, whereas strain release may have been accelerated after Lake Bonneville started to drain at about 15 ka. Similar evidence of large changes in average slip rate before and after Lake Bonneville's culmination have been noted at a number of points along the WFZ (Machette, 1984; Machette and others, 1986) by comparing the net displacement in different-age late Pleistocene and Holocene deposits (see following section entitled "Discussion of Slip-Rate Data").

The Taylorsville fault, the easternmost of the two traces of the West Valley fault zone, had 1.5 m of monoclinal flexure (down-to-the-east) with minor, but laterally discontinuous faulting in the past 7-5 ka (Keaton and others, 1987). The resulting uplift rate across the flexure is 0.21-0.30 mm/yr. The Taylorsville fault may be the surface expression of an earthquake that was below the threshold magnitude that would create a continuous surface rupture along a discrete fault plane. The detailed analysis of Keaton and others (1987) suggests that earthquakes in the range of Ms 6.9-7.3 would be reasonable for a surface rupture having as much as 1.5 m displacement along the West Valley fault zone. Such faulting would have had an average recurrence interval of 1,000-4,000 yr on the Granger fault and 5,000-7,000 yr on the Taylorsville fault during the past 15,000 yr (recurrence intervals for the preceding period are considerably less).

At the south end of the Salt Lake Valley, the west-trending Traverse Mountains form a major salient that is the boundary between the Salt Lake City segment (on the north) and the American Fork segment (on the south). The Traverse Mountains are one of four such bedrock salients and structural barriers recognized along the WFZ (Wheeler and Krystinick, this volume).

Scott and Shroba (1985) traced the Salt Lake City segment along the Wasatch front as far south as Corner Canyon, where fault scarps turn from a south to southeast strike. Farther south, the WFZ follows Corner Canyon and turns to the east; here it separates rocks of the Little Cottonwood Stock

(Tertiary) from extrusive volcanic rocks (Tertiary) and the underlying Paleozoic Oquirrh Formation (see Davis, 1983a). Machette (unpublished mapping, 1986) has traced the WFZ continuously across the salient from Corner Canyon eastward to the mouth of Chipman Creek (about 3 km northeast of Alpine). Late Quaternary alluvium near the crest of the salient has been offset by the WFZ, indicating that the salient is being actively deformed albeit at an appreciably slower rate than on the segments to the north and south. The major bend in the WFZ corresponds with the westward projection of the Deer Creek fault (see Bruhn and others, 1987). The Deer Creek fault is a transverse structure that allows the WFZ to step 8.5 km to the left from the Salt Lake Valley to the Utah Valley.

American Fork Segment

Schwartz and Coppersmith (1984) suggested that the WFZ from the Traverse Mountains south to Payson Canyon is a single (Provo) segment. As a result of our mapping in the Utah Valley, Machette tentatively has subdivided the original 55-km-long Provo segment into the American Fork, Provo (restricted sense), and Spanish Fork segments. The American Fork segment is shorter than most (about 22.5 km compared to an average of 30 km, table 1) and forms the northeastern border of the Utah Valley. An en echelon 2 km left step in the fault zone at the Provo River is suggested as the southern boundary of the American Fork segment.

In 1986, three 25- to 50-m-long trenches were excavated across a section of the WFZ near American Fork Canyon where the Quaternary geology had been mapped at a scale of 1:10,000 by Machette (unpublished mapping, 1986). The American Fork Canyon site is characterized by a large, well preserved fan-delta complex that was constructed during the transgressive phase of the BLC (about 32 to 15 ka; Currey and Oviatt, 1985, fig. 2). The fan-delta has been deeply incised by streams that became graded to the Provo level of Lake Bonneville between 15 and 14 ka. By 13 ka, recession of Lake Bonneville to an altitude below 4500 feet (1372 m; Currey and Oviatt, 1985, fig. 2) left Utah Lake near its present level, isolated from the progressively more restricted main body of Lake Bonneville. Since Utah Lake is controlled by a natural sill at an altitude of about 4490 feet (1368 m) climatically induced lake expansions (i.e., the Gilbert expansion of Currey and Oviatt, 1985) resulted in overflow rather than a rise in lake level. One practical application of this relation is that none of the shorelines above 4500 feet (1372 m) altitude in the Utah Valley can be much younger than 13 ka. Some of the alluvial-fan complexes mapped as Holocene by Bissel (1963), Hunt (1963), and Miller (1982) have shorelines cut across their distal toes at altitudes of 4520-4560 feet (1378-1390 m); thus, they are related to the Provo level of the BLC, not to Holocene expansions of Utah Lake.

A widespread but thin mantle of calcareous loess was deposited across the landscape as sediments of the BLC were deflated by eolian processes. After the drop to the Provo level, small mountain-front drainages proceeded to build local alluvial fans across lake deposits. These fans consist mainly of coalesced debris-flow deposits of early(?) to middle Holocene age. Their matrix was derived from the loess mantle, which now has been completed eroded from all but the most geomorphically stable landforms (such as the fan-delta complexes graded to the Provo and Bonneville levels). A ^{14}C date from the loess is about 7500 ^{14}C yr B.P., whereas another from near the top of the overlying loess-derived debris flow is about 4,500 ^{14}C yr B.P.

The American Fork segment of the WFZ forms a prominent set of scarps at the foot of the Wasatch Range both north and south of American Fork Canyon. Repeated movement across the fault zone has produced progressively more net displacement in Holocene, latest Pleistocene (BLC) and late to middle Pleistocene deposits. The fan-delta complex at American Fork Canyon is capped by 15-ka transgressive-beach and topset-delta gravels of the BLC. South of the canyon, the gravels are displaced 15-20 m across a wide graben and a single range-bounding fault. North of the canyon, the same gravels are displaced 26 m where there is no graben, but minor backtilting. Using 26 m and 15 m as the maximum and minimum values for net displacement yields average maximum and minimum slip rates of 1.7 and 1.0 mm/yr for the past 15 ka. In contrast, the long-term slip rates recorded by 125- to 250-ka alluvium along this and other segments of the central WFZ has been only 0.1 to 0.2 mm/yr, or almost an order of magnitude less than slip rates recorded since Lake Bonneville fell from its highest level 15,000 yr ago.

The trenches at American Fork Canyon exposed Holocene alluvial fans, which we consider to have been stabilized 4,500 to 5,000 yr ago on the basis of the previously mentioned radiocarbon date. These deposits commonly are dispalced 7-8 m where the fault zone has a simple geometry of parallel normal faults (Machette and Lund, 1987). A preliminary TL age estimate from trench AF-1 (fig. 4) suggests that the most recent faulting event occurred between 400 and 550 yr ago (sample ITL-U23; written commun., S.L. Forman, 1987). (A ^{14}C date from the youngest fault scarp colluvium is 140 ± 120 ^{14}C yr B.P., which we consider to be too young and thus erroneous.) In view of the fault scarp's degraded morphology, Machette and Lund estimated that the youngest event at this site may be as old as 2000 yr. Thus, we are surprised by the young value for the TL estimate.

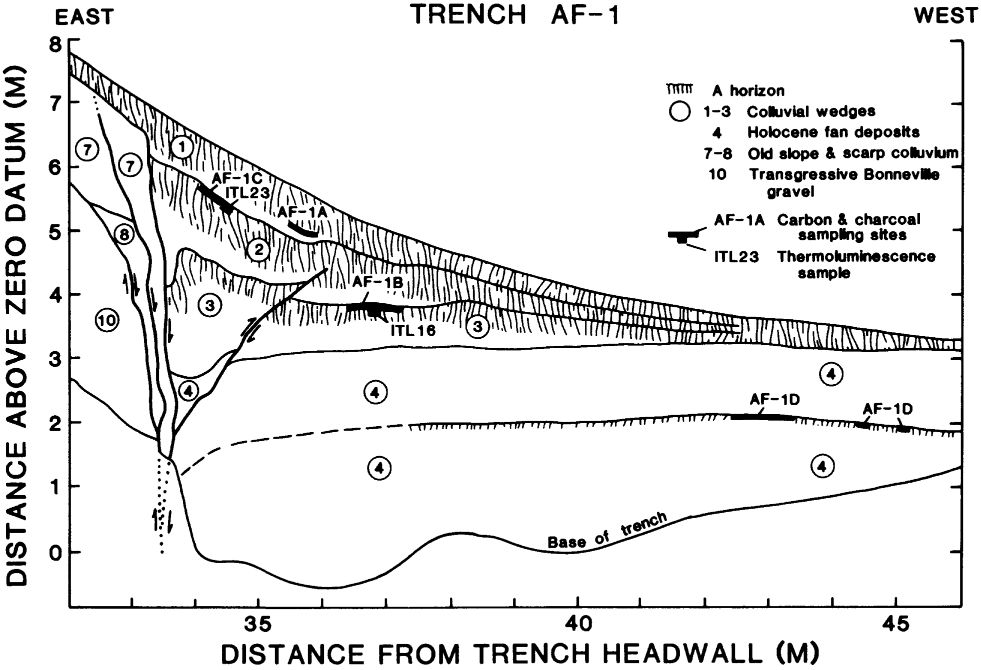

FIGURE 4. Part of the log of trench AF-1, American Fork segment of the WFZ. Diagram shows relation of three colluvial wedges (units 1-3) to units on the upthrown and downdropped fault blocks. Sample numbers refer to dating control shown in table 3.

TABLE 3. Preliminary dating control for faulting events at trench AF-1, American Fork segment of the Wasatch fault zone

[Samples listed in stratigraphic position: young (unit 1) to old (unit 4). Symbols: ^{14}C, radiocarbon date; TLB, thermoluminescence age estimate by the total bleach method; TLR, thermoluminescence age estimate by the regeneration method. TL data from S.L. Forman, written commun., 1987.]

Sample number	Geologic unit, remarks	Type of material; type of age control (and date)
AF-1A	1, near base of upper fault-scarp colluvium.	Charcoal; postdates last event. (^{14}C=140±120 yr B.P.; erroneous)
ITL-23	2, top of middle fault scarp colluvium.	Silty A horizon; time of last event. (TLB=400±50 yr B.P.) (TLR=500±50 and 550±50 yr B.P.)
AF-1C	2, Do.	Organic matter in A horizon; maximum age of last event. (preliminary ^{14}C=920 yr B.P.)
ITL-16	3, top of lower fault scarp colluvium.	Silty A horizon; time of second event. (TLB=3200±300 yr B.P.) (TLR=2400±300 yr B.P.)
AF-1B	3, Do.	Organic matter in A horizon; maximum age of second event. (preliminary ^{14}C=2020 yr B.P.)
AF-1D	4, middle Holocene debris-flow deposit.	Charcoal; predates third event, maximum age of unit 4. (^{14}C=4740±90 yr B.P.)

The TL age estimate from sample ITL-U16 places the second-most-recent fault event at about 2400 to 3200 yr B.P. (S.L. Forman, written commun., 1987), whereas the preliminary radiocarbon date from the buried soil is about 2020 ^{14}C yr B.P. (fig. 4). The third and oldest fault event in trench AF-1 must have occurred after 4740 ± 90 ^{14}C yr B.P. (sample AF-1D), which is the age determined from debris-flow deposits under the third and lowest colluvial wedge. We estimate that the youngest part of the debris flow is about 4500 ^{14}C yr on the basis of the position of the radiocarbon sample and lack of buried soils (the oldest colluvial wedge buried fresh debris-flow material).

Trenching of the fault scarps on Holocene deposits shows that three surface faulting events contributed subequal amounts to the 7-8 m of net displacement recorded since about 4,500 ^{14}C yr B.P. The three Holocene events produced discrete colluvial wedges that were exposed in all the trenches, although only two events are indicated in the third trench (AF-3). Although some of our radiocarbon analyses are still pending, preliminary radiocarbon dates, TL age estimates, and stratigraphic relations constrain the three Holocene fault events between about 500(?) yr and 4500 ^{14}C yr ago. Faulting must have occurred over intervals longer than several hundreds of yr in order to develop the moderately thick A horizons we found on each of the wedges in AF-1 (fig. 4). If one assumes that the most recent surface rupture event was between 500 and <2000 yr B.P. (age estimate from scarp morphology), and that the two prior events (5-6 m displacement) occurred after 4,500 ^{14}C yr B.P. (estimated age of top of unit 4), then there were two events over an interval of 2500 to 4000 ^{14}C yr. The resulting slip rate is 1.3-2.4 mm/yr (5 m/4000 yr to 6 m/2500 yr), which is comparable with the average slip rate of 1.0-1.7 mm/yr during the past 15 ka. These values, although preliminary, confirm that the rate of slip on the WFZ has remained high during the past 15 ka.

Provo Segment

The Provo segment (restricted sense) is the middle of three segments that are subdivided from the original Provo segment of Schwartz and Coppersmith (1984). As redefined, the Provo segment extends from Provo Canyon (where its' most recent splays are in bedrock) south to and including the Springville fault at Springville, Utah, a distance of 18.5 km. South of Little Rock Creek (which is northeast of Provo) the active fault zone is along the western base of the Wasatch Range. North of Little Rock Creek, Davis'(1983b) compilation incorrectly shows large blocks of Paleozoic rock (Oquirrh Formation) thrust upon the uplifted mountain block. Machette's unpubished mapping (1986) indicates that much of the "Oquirrh-like" material is (1) a fanglomeratic facies of the Salt Lake Formation (Tertiary) and elsewhere is (2) composed of large masses of Oquirrh Formation which have slid on Manning Canyon Shale along steep parts of the range. Extensive Quaternary(?) landslide deposits that predate the BLC are also present in this area; these deposits have been derived largely from the Paleozoic Manning Canyon Shale. The Quaternary landslide deposits and Salt Lake Formation, which we believe also have been mapped incorrectly, are bounded by the Provo segment on the east and a buried southward extension of the American Fork segment on the west. The result has been to preserve a coarse-grained facies of the Salt Lake Formation and landslide deposits at intermediate structural levels; usually these deposits are deeply buried in the basins and eroded from the ranges.

Only one exposure of the WFZ has been studied along the Provo segment, and no trenches have been excavated as yet. On the south bank of Rock Creek, at about the midpoint of the Provo segment, Machette and William Mulvey of the UGMS mapped a natural exposure of the fault and determined that there was about 2 m of net displacement (1.5 m of tectonic displacement and 0.5 m of drag) in late to middle(?) Holocene debris flows and alluvium. The resulting scarp has been partly buried by debris-flow and alluvium. Radiocarbon dating of organic matter in fault-scarp colluvium yielded an age of 1110 ± 50 ^{14}C yr B.P. Two corrections need to be considered before using this date. First, the colluvium that was dated may have required several hundred years to accumulate, so this amount of time should be added to the ^{14}C date. Secondly, incorporation of organic matter from the soil on the upthrown fault block may have added a significant amount of 100-300 yr old carbon; this reworked carbon may have made the date too old by several hundred yr. Because these corrections tend to balance one another, we suspect that the reported age may be the approximate time of faulting. Thus, the date indicates that a surface faulting event displaced late(?) Holocene alluvium about 2 m 1100 yr B.P. Larger scarps on middle(?) to early Holocene alluvium about 250 m south and on the same fault strand record 4.5 m of surface offset that probably resulted from two or three faulting events (including the most recent one at about 1100 yr B.P.)

The Provo segment is characterized by multiple parallel to anastomosing strands of the fault zone, and rarely is there a single fault strand on which most of the movement has taken place. The pattern of rupture is complex south of Slate Canyon (east of Provo) where the WFZ strikes across transgressive gravels of the BLC, and regressive gravels at and below the Provo level). These gravels are draped across steeply sloping alluvial-fan deposits that predate the BLC. The history of faulting in this area is difficult to decipher for three reasons: (1) pre-existing fault scarps were modified by the rise and fall of Lake Bonneville, (2) many of these faults were later reactivated, and 3) much of the gravel cover has been disturbed by mining.

The southern end of the Provo segment consists of the Springville fault, which has a 3-km-long fault scarp in Holocene alluvium of Hobble Creek. The fault extends from just east of the State Fish Hatchery (1 km north of Springville) southward to Utah Highway 77, which is a main road leading west from Springville. Scarps along this fault are 0.5 to <2 m high, but they have been extensively modified by man. Bissell (1963) shows another fault scarp about 1 km south of Springville that could be an extension of the Springville fault. However, we agree with Miller's (1982) decision that Bissell's scarp is not a fault, and instead we map it as a part of an extensive, young Provo shoreline that is prominent at 4520 ft (1378 m) altitude in the Utah Valley.

Spanish Fork Segment

As defined by Machette and others (1986), the Spanish Fork segment is restricted to the range- bounding WFZ between Springville and Payson Canyon. It is the southern of three segments that comprise Schwartz and Coppersmith's (1984) original Provo segment. The restricted segment forms a major concave-west bend in the WFZ, the only such prominent bend along the entire fault zone. Southward extension of the Provo segment as the Springville fault and northward extension of the Nephi segment as the Benjamin fault suggests that the two segments may connect in the subsurface west of Spanish Fork, thereby making the Spanish Fork segment the east-bounding fault of the main basin of Utah Valley.

The Spanish Fork segment continues to be the focus of detailed mapping and trenching studies. Swan and others (1980) study of tectonic relations at Hobble Creek, coupled with trenching at Deadmans Hollow (about 2 km to the west) provided the first evidence of repeated Holocene movement on this section of the WFZ. They found evidence for six to seven surface-faulting events that produced 11.5-13.5 m of displacement (NVTD) since formation of the

Provo fan-delta at Hobble Creek about 13.5 ka (we prefer 14 ka on the basis of recent studies). The oldest three to four events are inferred from tectonic strath terraces along Hobble Creek on the upthrown block of the fault. The three youngest events are defined on the basis of colluvial stratigraphy observed in trenches across a faulted alluvial-fan complex at Deadmans Hollow. The number of post-Provo surface-faulting events is probably well constrained, but the absence of organic material prevented determination of individual recurrence intervals. The average interval between events is 1.7-2.6 ka (revised by Schwartz and Coppersmith, 1984). The most recent event was estimated be at least 1,000 yr old on the basis of relatively degraded fault scarps. Individual amounts of displacement for post-Provo events are not well constrained, but the average ranges from 1.6-2.3 m for six to seven events. The net displacement in transgressive sediments of the BLC is difficult to determine because of extensive backtilting and graben formation. Swan and others (1980, table 1) preferred a value of 30 ± 0.5 m, whereas we have estimated about 40-45 m on the basis of a faulting geometry proportional to that seen in the well preserved Provo alluvial surface. If one assumes that the sediments are 17 ± 2 ka, then the resulting average slip rate at Hobble Creek has been between 1.8 mm/yr (Swan and others, 1980) and 2.5 mm/yr (midpoints of our displacement and age values). Because there is 2 to 3 times more net offset recorded in transgressive versus regressive deposits of the BLC, but only a slight difference in age (1-4 ka) we suspect that faulting at this site occurred at a very high rate (perhaps as much as 10 mm/yr) during and after the catastrophic fall of Lake Bonneville 15,000 yr ago (see following discussion of "Causal relation between deep cycles of Lake Bonneville and high slip rates on the Wasatch fault zone").

In order to determine recurrence intervals and the timing of the most recent faulting along this segment, W.R. Lund (UGMS) and D.P. Schwartz (USGS) dug five trenches at two sites south of Mapleton, Utah, in June 1987. Study of these trenches is incomplete (as of August 1987), but their preliminary investigations indicate two surface faulting events; abundant charcoal in several of the trenches should permit dating of the most recent event(s).

Dean Ostenaa of the U.S. Bureau of Reclamation (Denver) is investigating recent movement on the Spanish Fork segment at the Water Canyon site, which is about 6.5 km southwest of Hobble Creek. This investigation is part of a study for the U.S. Bureau of Reclamation's Central Utah Project. Before studying the Water Canyon site, the Bureau excavated two trenches across a 1.5-3 m high fault scarp that is parallel to and above the prominent high shoreline of Lake Bonneville (altitude 5095 feet) at the southeast end of Utah Valley. This fault scarp is herein named the Woodland Hills splay of the Spanish Fork segment (table 1). The larger, western trench was mapped quickly by Machette, Bob Robison (Utah County Geologist), Craig Nelson (Salt Lake County Geologist), Rod Weisser (Bureau of Reclamation-Provo) and James McCalpin (Utah State Univ.-Logan). Their interpretations suggest 3 to 4 major surface faulting events in the past 150 ka (about 3 m net displacement). Radiocarbon dating of a buried, fault-scarp-derived block of A horizon suggests that the most recent faulting event occurred after 1360 ± 60 ^{14}C yr B.P.

The Bureau's study was expanded in 1987 with excavation of three trenches at Water Canyon: two on Holocene terraces at the mouth of the canyon and a third in slope colluvium at a proposed tunnel-portal site several hundred meters to the south. Although final analysis of the trenching investigations awaits ^{14}C dating of charcoal samples, Ostenaa (oral and written communs., 1987) suspects three or possibly four faulting events in the past 6-8 ka.

Between the Mapleton and Water Canyon sites, the trace of the Spanish Fork segment makes a spectacular 100° bend at the mouth of Spanish Fork Canyon. This geometry alone suggests that this bend is a segment boundary. However, Machette's unpublished mapping (1986; 1:10,000 scale) of this area reveals continuous faulting around the bend with a prominent antithetic fault zone crosscutting the bend. The net displacement recorded in deposits of the BLC decreases at the bend in comparison to sites both north and west (perhaps as a result of the geometry and drag). Nevertherless, the continuity of faulting and evidence of repeated Holocene faulting all along the segment suggest that the segment is continuous from just north of Springville to Payson Canyon, where the fault turns southward into massive landslide deposits. We suspect that recent faulting continues several kilometers up Payson Canyon, but we cannot prove it.

Nephi Segment

The Nephi segment, which extends from Payson to Nephi, has two strands: one bounds the west side of the Wasatch Range in northern Juab Valley and the second bounds the west side of the Dry Mountains, east of Santaquin Canyon. Near Mendenhall Creek (about 18.5 km north of Nephi), Holocene ruptures of the western strand turn northeasterly and strike into the bedrock of the range. Although evidence of recent faulting is obscured by vegetation and landslides in the range, we suspect that the WFZ coincides with a major down-to-the-north bedrock fault that strikes NE toward Santaquin Canyon (Davis, 1983b). The Manning Canyon Shale, an incompetent unit that is susceptible to landsliding and intraformational faulting, extends nearly vertically in a northeast direction between this cross fault and the southernmost trace of the eastern strand at Santaquin Canyon. We suspect that the Manning Canyon is a convenient pathway for transferring motion along these two en echelon strands of the Nephi segment. At the northwest end of the Dry Mountains (about 2 km east of Santaquin) the Nephi segment turns northeast again and becomes discontinuous in post-BLC sediments. Young fault scarps (which were originally mapped by Cluff and others, 1973) continue across Payson Canyon, then turn northward and bound a narrow bedrock-cored horst block, which is mantled by beach gravel of the BLC north of Tithing Mountain. At Payson, the Nephi segment looses definition and is largely coincident with fluvial terrace scarps graded to regressive (Provo) levels of Lake Bonneville.

North of Payson, the WFZ may continue another 3.5 km to the Benjamin Cemetery, which is on a low N-S elongated hill underlain by Tertiary Salt Lake Group (Davis, 1983b). This hill is bounded on the west by the Benjamin fault of Hintze (1973), which forms a 1-2 m high fault scarp on BLC silts and clays of the Provo and lower levels. The scarp extends about 2 km south of the hill to within 1.5 km of Payson. Hintze reports that the fault is also expressed as an aligned series of hot springs for almost 4.5 km north of the Benjamin Cemetery (8 km north of Payson; near Lake Shore, Utah). We consider the Benjamin fault as a northward extension of the Nephi segment.

The Nephi segment is one of two segments of Schwartz and Coppersmith (1984) that we have not modified extensively (with the exception of the postulated cross-range fault). The surface trace of the segment is 42.5 km long; if one includes the Benjamin fault and its subsurface projection to the north, the total length is about 50 km. The detailed maps of Cluff and others (1973) show a number of questionable linear features within the city limits of Nephi, but our reconnaissance could not confirm these as faults. The southern limit of continuous faulting on the Nephi segment is at Utah Highway 41, about 2 km north of the Nephi Post Office (city center). We found several fault scarps on alluvial fans (pre-Holocene?) as much as 2 km south of Salt Creek, the major canyon due east of Nephi, but saw no evidence that recent movement has cut the alluvial fan of Salt Creek at Nephi.

Schwartz and others (1983) excavated three trenches at North Creek, their fourth and last major site along the WFZ. At North Creek, the WFZ displaces an alluvial fan that contained charcoal dated at 4580 ± 250 ^{14}C yr B.P. (Bucknam, 1978 and written commun., 1987). A topographic profile across the fan shows the surface has been displaced 7 ± 0.5 m. This displacement is the result of three surface-faulting events, the most recent and second event being represented by scarp-derived colluvium. An older third event is suggested by a tectonic strath terrace cut in the North Creek fan surface on the upthrown block of the fault.

The timing of the most recent event at North Creek is constrained by radiocarbon dates and scarp morphology. Dates of 1110 ± 60 and 1350 ± 70 ^{14}C yr B.P. from charcoal and organic matter in the trenches provide a maximum age for the most recent event. The steep scarp angles (40-42°) along this segment of the fault, the lack of upstream migration of a knickpoint in a channel above the fault scarp, and a generally continuous fault scarp (15 km long) that lacks vegetation all suggested very recent movement (300-500 yr B.P.) to Schwartz and others (1983). They estimated 2.0-2.2 m of displacement per event on the basis of the thickness of scarp-derived colluvial wedges and topographic profiling of surfaces across the fault. Constraint on the minimum time since the second event was provided by a radiocarbon date of 3640 ± 75 ^{14}C yr B.P. from a soil on the second colluvial wedge. The displacement during this event was 2.0-2.5 m. The third event (pre-3640, post-4580 ^{14}C yr B.P.) produced 2.6 m of displacement as indicated by the depth of inset of the strath terrace at the fault. The average of the two recurrence intervals recorded at this site ranges from 1.7-2.7 ka (Schwartz and others, 1983).

However, the individual calculated intervals differ by a factor of at least two (2140-3340 ^{14}C yr versus <940 ^{14}C yr) from the average of two intervals at the site. This example illustrates the problems inherent in using average recurrence intervals for analyses of risk.

In June, 1987, Michael Jackson of the University of Colorado excavated a trench across the southern end of the Nephi segment. His site is just east of Interstate Highway I-15 and about 3.5 km north of Nephi. This trench, which crossed a 5-m-high fault scarp, exposed interbedded distal alluvial-fan sediments (pebbly sand) and thin, locally derived silty debris-flow deposits. Three discrete colluvial wedges were recognized along the main fault, and a fourth (but not necessarily independent) wedge along a subsidiary fault. These relations suggest 3 to 4 major surface faulting events at the site. Radiocarbon dating of soil organic matter and TL analysis of the wedges should provide a second and perhaps longer history of faulting for the Nephi segment.

The southern end of the Nephi segment and the northern end of the Levan segment are separated by a 15 km long gap in recent faulting. These gaps seem typical of distal segments of the WFZ. For example, the boundaries between the Clarkston Mountain and Collinston segments (northern WFZ) and the Levan and Fayette segments (southern WFZ) are marked by discontinuous gaps and steps in faulting. The foothills of the Gunnison Range (the mountains that bound the WFZ between Nephi and Fayette) also step to the left in this gap. However, the foothill (bedrock) and valley (basin fill) contact is fault controlled as evidenced by old degraded fault scarps on middle(?) Pleistocene alluvial fans. Airphoto reconnaissance and detailed mapping of the gap area reveals no evidence of Holocene faulting, and little evidence of faulting of latest Pleistocene (35-10 ka) age.

SOUTHERN WASATCH FAULT ZONE

The southern section of the WFZ comprises segments of the fault zone that do not display Holocene or repeated Holocene movement as contrasted with repeated Holocene movement along the central section of the WFZ. As such, the southern section includes only the 40-km-long Levan segment of Schwartz and Coppersmith (1984). As originally defined, the segment extended from east of Levan south to a point north of Gunnison, Utah. Machette and others (1986) suggested that the Levan segment should be subdivided into the Levan (restricted sense) segment and the Fayette segment, with the boundary between them at the left step from the Juab Valley to Flat Canyon (the south-trending canyon north of Fayette). We make this subdivision on the basis of recency of movement (late Holocene versus no Holocene) and fault geometry (Machette and others, 1986).

Levan Segment

Our mapping and analysis of scarp morphology suggests that the Levan segment has Holocene ruptures from the mouth of Hartleys Canyon (3.8 km northeast of Levan) to as far south as Botham Road, (15 km south of Levan). Just east of Botham Road, the Levan segment steps left about 0.5 km into bedrock. There is clear evidence of Quaternary faulting for another 3 km south on the segment, but we cannot tell if the most recent movement is Holocene or older. The southern end of the Levan segment (including this uncertain part) is about 0.5 km east of where Utah Highway 28 crosses the Juab-San Pete county line. From this point south, the trace of late Quaternary faulting makes a major step about 3.5 km east and 5 km south to the next valley where the WFZ lacks evidence of Holocene movement.

Most of the fault scarps in Holocene deposits along the Levan segment are less that 3 m high and the exposure at Deep Creek suggests that there has only been one faulting event since early Holocene time. However, fault scarps on pre-Holocene alluvium are commonly 5-10 m or larger. Therefore, although we only see evidence for one Holocene event, faulting has occurred repeatedly along the segment in late Quaternary time.

Until recently, no trenches have been excavated on the southern WFZ. However, natural exposures along Deep Creek cross a 2.5-m-high fault scarp of the Levan segment. Schwartz and Coppersmith (1984) and Machette (unpublished mapping, 1984) have studied this exposure and concluded that there is evidence of one faulting event. Machette measured a net displacement (NVTD) of about 1.75 m; this is the product of 2.3 m displacement on the main fault and 0.55 m of offsetting displacement on the graben-bounding antithetic fault. Charcoal in the faulted alluvium at this site has been dated at 7300 ± 1000 ^{14}C yr B.P. (Schwartz and Coppersmith, 1984). At Pigeon Creek, 2 km to the north and due east of Levan, they reported faulted alluvial-fan deposits that contained charcoal dated at 1750 ± 350 ^{14}C yr B.P. (i.e., maximum age of most recent faulting). Extensive flooding in 1984 and construction of flood-control levees has prevented us from restudying the Pigeon Creek site.

Michael Jackson (Univ. of Colorado) excavated a trench across a 3.3 m high fault scarp on Holocene alluvial fan sediments in June, 1987. The site is about 1.5 km northwest of Skinner Peaks and about 200 m east of Utah State Highway 26. Jackson found one colluvial wedge and at least twice as much alluvium on the downdropped block as on the upthrown block. These relations suggest one faulting event after stabilization of the alluvial fan, and perhaps one event during deposition of the fan. Pending ^{14}C dates and TL age estimates may allow Jackson to date a second event on the Levan segment.

Fayette segment

The Fayette segment is the southernmost segment of the 370 km long WFZ. In many ways it is similar to the three segments of the northern WFZ except that the highest level of Lake Bonneville was below the main trace of the fault zone. Evidence of latest Pleistocene or early(?) Holocene faulting is present from just south of Hells Kitchen Canyon south to the Fayette Cemetery. The Fayette segment has two strands: a 4-km-long western strand that strikes south and a 9-km-long eastern strand that also strikes south but is slightly concave to the west. These two strands intersect near the north end of the segment. Scarp morphology data from the two strands suggest that the most recent movement occurred 10-15 ka on the basis of comparison with morphometric data from the Drum Mountains fault scarps (early Holocene; Crone, 1983; Pierce and Colman, 1986) and the highest shoreline of the BLC (15 ka; data of Bucknam and Anderson, 1979). In addition, the fault scarps along this segment typically are eroded at the mouths of canyons, but preserved on terraces that are elevated 2-5 m above stream level. These relations suggest that the Fayette segment is substantially older than and separate from the Levan segment to the north and west.

SUMMARY OF FAULT SEGMENTATION

Our studies show that the WFZ may comprise 10-12 discrete fault segments, each of which is capable of generating large magnitude earthquakes. However, 4 of the 12 segments have not been active in the past 10-15 ka, so we suspect that their slip rates are lower and recurrence intervals are considerably longer than those of the 8 more active segments. Seven of the most active segments show evidence of multiple surface-ruptures during the Holocene. Trenches across these segments generally reveal two or three faulting events in deposits of late to middle Holocene age. Previous studies of segmentation have suggested 6 longer segments, so our results shorten the length of expected surface rupturing and increase the number of segments that could have discrete surface rupturing during major earthquakes along the Wasatch Front.

The average length of all 12 segments of the WFZ is about 30 km (table 2). However, the Holocene segments, which adjoin one another along the central part of the fault zone, average 35 km in length. This value is comparable with the lengths of surface rupturing that have occurred historically in the Basin and Range province and in the Intermountain Seismic Belt. Because the large historic surface ruptures were associated with earthquakes of **M** 6.9-7.5 (Moment magnitude), and because past earthquakes have typically caused about 2 m of surface displacement along the WFZ (Schwartz and Coppersmith, 1984), we see no reason not to expect large-magnitude (**M** 7-7.5) earthquakes along the WFZ in the future.

DISCUSSION OF SLIP-RATE DATA

Slip rates determined from deposits that predate the Bonneville lake cycle (more than 35,000 yr old)

Sediments that predate the Bonneville lake cycle (BLC; more than 35 ka) are rarely exposed on both sides of the WFZ along the northern and central parts of the Wasatch Front. However, south of Santaquin, Utah, the WFZ generally is well above the highest shoreline of the BLC; thereby allowing one to measure the net slip in both post- and pre-BLC alluvial deposits. In addition, several isolated exposures on fault segments to the north of Santaquin provide data on longer-term rates of slip. We have studied these sites in detail to compare slip rates for the time interval before and after the BLC. Figure 5 shows slip rates values calculated at various localities along the WFZ. The fan-shaped array of dashed lines show slip rates (i.e., 0.5-3.0 mm/yr) for different parts of the time scale represented by faulted deposits. In order to plot deposits of Holocene to middle Quaternary age on one diagram, two breaks were made in the time scale, one between 20 ka and 50 ka and a second between 70 ka and about 120 ka. One should note that the slip rate lines do not project through the axis because the scale of the time axis is different for each of the three time intervals. By plotting the slip rate data in this manner, one can compare average slip rates over different time intervals.

For example, at Gardner Creek near Nephi 150-250 ka alluvial-fan deposits that have well developed calcic soils are displaced of about 30 m across the fault zone (see Machette, 1984). Thus, the WFZ has had an average slip rate of 0.12 to 0.20 mm/yr during the past 150-250 ka. At the same site, middle(?) Holocene sediments are displaced 3.9 m, which indicates an average slip rate of 0.8-1.0 mm/yr for the past 4-5 ka. These two average rates (labeled as points A, fig. 5) reflect a 5-fold increase in slip during the latest Quaternary; such changes in slip rate are typical of the central part of the WFZ. Similar large-scale temporal changes in slip rate (fig. 5) have been documented at sites near Santaquin (northern part of Nephi segment), at Dry Creek northeast of Alpine (American Fork segment), at Little and Big Cottonwood Canyons (Salt Lake City segment), at Jim May Canyon (near Honeyville on the Brigham City segment), at on the Granger fault (West Valley fault zone; Keaton and others, 1987).

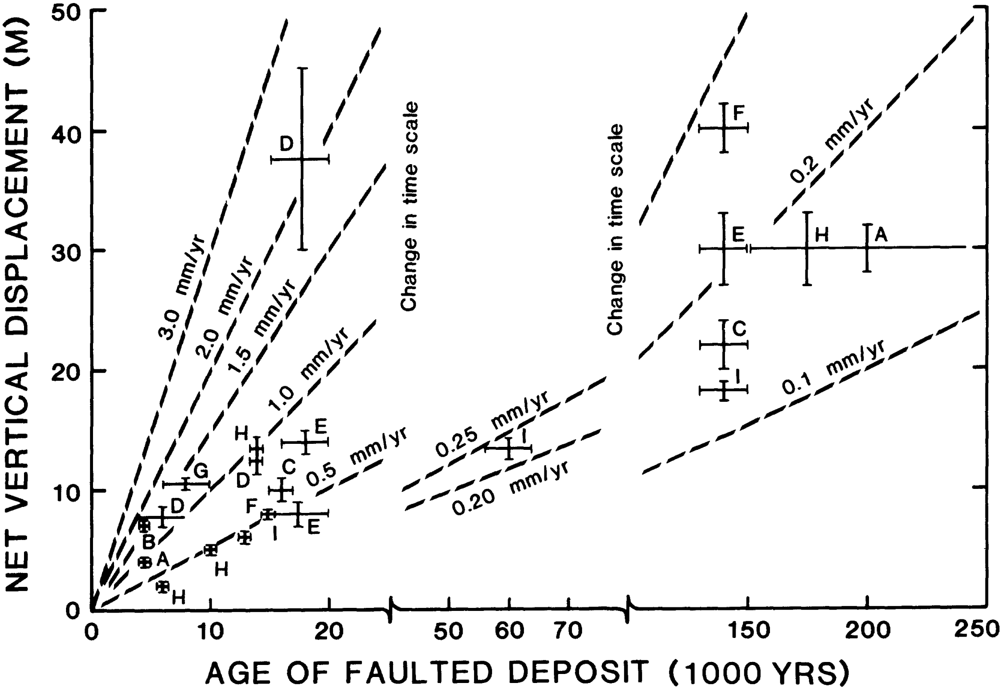

LOCATIONS OF SLIP-RATE DETERMINATIONS

A -- Gardner Creek, Nephi segment, Wasatch fault zone
B -- North Creek, Nephi segment, Wasatch fault zone
C -- Santaquin Valley, Nephi segment, Wasatch fault zone
D -- Hobble Creek, Spanish Fork segment, Wasatch fault zone
E -- Dry Creek, American Fork segment, Wasatch fault zone
F -- Big and Little Cottonwood Creeks, Salt Lake City segment, Wasatch fault zone
G -- Kaysville, Weber segment, Wasatch fault zone
H -- Jim May Canyon, Brigham City segment, Wasatch fault zone
I -- Granger fault, West Valley fault zone (Keaton and others, 1987)

FIGURE 5. Schematic diagram showing some of the slip rates on the Wasatch fault zone determined from deposits of Holocene to pre-Bonneville lake cycle age. Letters indicate locations of slip-rate determinations, some of which are mentioned in the text. Vertical and horizontal bars indicate range in probable amounts of displacement and age of deposits. Dashed lines indicate different rates of slip. Note changes in scale at breaks in horizontal axis (25/40 ka and 80/100 ka).

Slip rates determined from deposits less than 15,000 yr old

Along the northern and central parts of the WFZ, sediments related to the BLC have been deposited against or across pre-existing scarps of the fault zone. Sediments of the BLC (32-10 ka) and Holocene deposits record relatively high rates of slip all along the central part of the WFZ. For example, Swan and others (1980) calculated slip rates for three separate geologic units at the Hobble Creek site (Spanish Fork segment). They range from a maximum of 1.8-2.5 mm/yr in sediments of the highest Bonneville shoreline level (17 ± 2 ka), to 0.85-1.0 mm/yr in the sediments of the Provo level (13.5-14 ka) and 0.65-1.3 mm/yr in middle to early(?) Holocene stream sediments (4.5-9 ka) (these data are labeled as points D on Fig. 5). High-slip rates since culmination of the BLC at about 15 ka have been noted elsewhere along the Wasatch Front (points A, C, F, H on Fig. 5) and on the West Valley fault zone (points I on Fig. 5). The high slip rates during the past 15 ka (at least) are strikingly different from the rates recorded by older deposits. In addition, if you look at the average slip rates recorded between the time of deposition of the older deposit and the culmination of the BLC, the difference in slip rates is even greater. For example, if 200-ka deposits record an average slip rate of 0.2 mm/yr (40 m net slip) and adjacent 15 ka lake sediments record an average slip rate of 1.0 mm/yr (15 m net slip), then the displacement that occurred between deposition of the two units is only 25 m and the maximum time for slip is 185 ka. The resulting slip rate is about 0.14 mm/yr, or about 30 percent less than the long-term (200 ka) average slip rate. Thus, a comparison of intervals of slip rate such as this yields larger changes in slip rate (7x versus 5x). These observations of large and systematic changes in slip rate through time suggest a causal relation between hydrologic cycles of Lake Bonneville and large fluctuations in slip rates on the adjacent WFZ.

CAUSAL RELATIONS BETWEEN DEEP CYCLES OF LAKE BONNEVILLE AND HIGH RATES OF SLIP ON THE WASATCH FAULT ZONE

The pattern, magnitude, and regularity of change in slip rates along the WFZ are of regional extent. The relatively low average slip rates (0.1-0.3 mm/yr) before and possibly during the transgressive phase of the most recent and deepest Quaternary lake cycle in the Bonneville basin (32-15 ka), and high slip rates (typically 0.4-1.8 mm/yr) recorded in sediments less than 15 ka (fig. 5) suggest a regional mechanism is causing large changes in slip on the WFZ. The accelerated rates of slip after the culmination of the BLC suggests that the lake may be a causative or at least related factor.

Several aspects of Lake Bonneville's history may have played a part in increasing slip activity along the WFZ. During the maximum (highest) stand of the lake, most basins of northwestern Utah were flooded to a maximum depth of 300 m (1000 ft). This depth of water imposes the same load as about 130-160 m (425-525 ft) of sedimentary rock. Almost all of this load was on the downthrown block of the WFZ, and much of it accumulated along the Wasatch Front near the fault zone. The lake was deep just a few kilometers west of the central part of the fault zone, where high slip rates have been measured. The hydrologic load and that from accumulating sediments of the BLC increased the confining pressure on the westward-dipping WFZ (and other intrabasin structures such as the West Valley fault zone), although increased pore pressure from the lake may have completely offset any increase in confining pressure. Nevertheless, if one envisions the earth's crust simply as a gently upwarped beam, then during deep lake cycles the beam is shortened (compressed) owing to isostatic depression in the lake basin (as much as 60 m of depression occurred at the high stand of the BLC). The compression would tend to increase horizontal forces across steeply dipping normal faults, and perhaps retard strain release (see Keaton and others, 1987). The catastrophic fall of the lake 15,000 yr ago from the highest Bonneville level to the Provo level (about 100 m lower) was accompanied by rapid isostatic uplift of the basin (see Crittenden, 1963a,b) and deposition of thick wedges of sediment by major streams flowing from the Wasatch Range. The rapid changes that occurred over the Bonneville basin may have triggered rapid slip on the WFZ and some other structures in the area (such as the West Valley fault zone).

Subsequent desication of the lake to near present levels by 10.5 ka was accompanied by additional isostatic rebound; the net rebound in the deep parts of Lake Bonneville was almost 60 m. This crustal rebound (an upward arching; hence, lengthening of the crust) may have allowed the predominant east-west extensional forces that are present in the Basin and Range province to become predominant again.

Thus, there seem to be several possible factors of regional extent related to the most recent and deepest cycle of Lake Bonneville, which together may have led to the recent acceleration of slip rates, and hence paleoseismic activity along the WFZ. Such causal relations are known from other regions of the world. For example, rapid glacio-isostatic rebound after the retreat of late Pleistocene ice caps in Scotland, Finland and Sweden was associated with new and renewed tectonic deformation and (by inference) seismicity (Morner, 1978). Morner (1978, p. 45) concluded that "intense faulting, fracturing, and seismic activity are shown to be linked to the deglaciation phase because of the initiation of changes (our emphasis) in stress and strain when the rate of glacio-isostatic uplift is near its maximum. In addition, changes in water level have been associated with induced seismicity at moderate to large reservoirs throughout the world (see Simpson's 1986 review of induced seismicity).

Recent studies of lake sediments that predate the BLC (e.g., Scott and others, 1983; McCalpin, 1986; McCalpin and others, this volume; McCoy, 1987; Oviatt and others, 1987) suggest that the Bonneville basin may have been occupied by shallow to moderately deep pluvial lakes during most glacial episodes. Oxygen-isotope data from the deep marine record show that major glaciations occur about every 120,000 yr and with by minor glaciations on intervals of 40,000-50,000 yr. If the filling or presence of a deep lake adjacent to the WFZ was a suppressor of strain release (slip) on the WFZ, then older pluvial lakes of somewhat lesser extent (such as the Cutler Dam and Little Valley lake cycles shown in Fig. 5) may also have influenced cyclic movement on the WFZ.

We do not mean to infer that periods of high lake level were times of seismic quiescence on the fault zone, but rather that during these periods the WFZ may have had lower slip rates--rates similar to those determined from late Quaternary faults in the eastern Basin and Range province and backvalleys of the Wasatch Range (rates of 0.1-0.2 mm/yr are most common for active faults). However, the late Cenozoic uplift rate for the central Wasatch Range, as determined by fission-track studies, is about 0.4 to 0.8 mm/yr (Naesar and others, 1983; Parry and Bruhn, 1986, 1987); this value could reflect the average effect of cyclic periods of high slip rates (during low lake levels) and periods of low slip rates (during high lake levels) on the WFZ. If this casual relation is correct, one might view the WFZ as having three "types" of slip rate or tectonic activity: (1) normal rates between deep lake cycles (perhaps approaching the long term average, (2) low rates during the transgressive phase of a lake cycle, and (3) high rates during the regressive phase of a lake cycle. If cyclic patterns such as this exist, it we need to understand where we are in such a pattern along the WFZ.

Although there have been only a few detailed studies of paleoseismicity in the eastern Basin and Range province other than on the WFZ (Nelson and VanArsdale, 1986; Nelson and Sullivan, this volume), regional studies (Bucknam and Algermissen, 1984; Wallace, 1984) show that slip rates on other faults in the province are as much as an order of magnitude less than that documented for the WFZ during the latest Pleistocene and Holocene. These studies include some major range-bounding faults in the transition zone between the Colorado Plateaus and Basin and Range provinces. Many of these faults are considered to be fundamental, deeply penetrating structures capable of generating large-magnitude earthquakes. Because these faults have lower slip rates and generally do not show evidence of short- versus long-term cyclicity in recurrence intervals, we feel that the proximity of the WFZ to former deep lakes in the Bonneville Basin may present a unique set of geologic and hydrologic conditions that could affect assessments of risk from earthquakes along the Wasatch fault zone.

RECURRENCE OF LARGE EARTHQUAKES ON THE WASATCH FAULT ZONE

Schwartz and Coppersmith (1984, table 2) used estimates of 12-13 (minimum) to 18 (probable) faulting events in the past 8000 yr. Using this data, they estimated that a major faulting event should occur once every 615-666 yr on one of their six segments of the WFZ, although their preferred value was 444 yr. This interval is termed the composite recurrence interval of faulting, because it considers the whole (composite) WFZ. The sparse data we have so far (see previous discussions of individual segments) suggest that 18-20 faulting events occurred in the past 5000 yr on the Holocene segments of the WFZ (table 4). These data yield composite recurrence intervals of 250-280 yr. If our calculated level of activity proves to be true, then we would expect to see evidence of 2 or 3 surface faulting events in the past 750-

800 yr. However, our recent studies and Lund and Schwartz's 1987 trenching at Mapleton (site 12, table 1) suggest that some of the most recent faulting events along segments of the WFZ occurred 500-750 yr ago (table 4; sites 9, 12, and perhaps 15). Assuming that a 250-280 yr recurrence interval is valid, there should have been 2 or 3 faulting events since 750 yrs ago, but none have been recorded. This leads us and Schwartz (oral commun., 1987) to suspect that surface faulting along the WFZ may occur in clusters as is presently happening in the Central Nevada Seismic Belt (Wallace and Whitney, 1984). The process of clustering, which is physically manifested as a temporal linking of movement from one fault or fault segment to another, has been termed "contagion" by D.M. Perkins of the USGS (written commun., 1987) after the analogy with contagious behavior.

The implications of a contagion earthquake process are significant for analyses of earthquake risk along the WFZ and other fault zones. For example, assuming a Poisson distribution of earthquakes (the commonly accepted distibution), one would expect a major earthquake somewhere on the central section of the WFZ once every 250-280 yr. This relatively short recurrence interval poses a significant risk for the heavily populated part of the WFZ, where many critical structures and facilities have expected lifespans of 100 yr or more. In the case of contagion earthquakes on the WFZ, if the most recent cluster was about 500-750 yr ago, then one might expect a long period (perhaps 1500-2500 yr) of tectonic quiescence between the last and next episode (cluster) of faulting on the WFZ. In this case, the contagion process represents a significantly lower level of risk (almost an order of magnitude longer time until anticipated surface rupturing) for the central WFZ.

Although our preliminary data presents compelling evidence of non-Poisson distribution of earthquakes on the WFZ, we still have only poor estimates of the variability of earthquake recurrence on individual segments and between clustered episodes of earthquakes. Proving that the contagion-process is valid for the WFZ will require many more ages and more-precise dating control for the past several surface faulting events on most segments of the WFZ.

CONCLUSIONS

> "...the filling of the Bonneville Basin with water added a very considerable weight to the valleys, and therefore to the down-thrown blocks, and made no corresponding addition to the uplifted blocks represented in the mountain ranges....It is therefore theoretically conceivable that during the presence of the lake the process of faulting along the mountain bases was stimulated, and that after the evaporation of the water the process was correspondingly retarded."
>
> (G.K. Gilbert, 1890)

Although we generally concur with Gilbert's suggestion of a causal relation between Lake Bonneville and the Wasatch fault zone, which he made almost 100 yr ago, we suspect that faulting was stimulated by the transgressive rather than regressive phase of Lake Bonneville. There is convincing evidence from the recent trenching and detailed mapping of Quaternary geology along the Wasatch Front that the Wasatch fault zone has continued to be very active in the Holocene (past 10,000 yr). In addition, the recognition of ten to twelve discrete segments of the Wasatch fault zone, eight of which have demonstrable Holocene movement, increases the possible number of separate localities where earthquakes and their associated surface ruptures may occur along the Wasatch Front. Although recurrence intervals for individual segments are still being analyzed, we now think that major earthquakes have and will continue to strike the central heavily urbanized section of the WFZ on an average of once every 250-280 yr. This estimate is significantly shorter than Schwartz and Coppersmith's (1984) preferred composite-recurrence-interval of 444 yr. However, we have no evidence that large earthquakes (those that cause significant surface-faulting) have occurred as recently as the average would demand, thus some form of contagion process (temporal clustering of earthquakes) may be active along the WFZ.

REFERENCES

Antevs, Ernest, 1948, The Great Basin, with emphasis on glacial and post-glacial times, III. Climate changes and pre-white man: University of Utah Bulletin 38, no. 20, p. 168-191.

______1955, Geologic-climatic dating in the west: American Antiquity, v. 20, p. 317-335.

Birkeland, P.W., 1984, Soils and Geomorphology: New York, Oxford University Press, 372 p.

Bissell, H. J., 1963, Lake Bonneville--Geology of southern Utah Valley, Utah: U.S. Geological Survey Professional Paper 257-B, p. 101-130.

Bucknam, R.C., 1978, Northwestern Utah seismic studies, in Summaries of Technical Reports, v. 7: U.S. Geological Survey, p. 64.

Bucknam, R.C., and Algermissen, S.T., 1984, A comparison of geologically determined rates of late Quaternary seismic activity and historic seismicity data in the Great Basin, western United States, in A collection of papers of International Symposium on Continental Seismicity and Earthquake Prediction (Sept. 8-14, 1982, Beijing, China): Seismological Press, Beijing, China. p. 169-176.

Bucknam R.C., and Anderson, R.E., 1979, Estimation of fault-scarp ages from a scarp-height slope-angle relationship: Geology, v. 7, p. 11-14.

Cluff, L.S., Brogan, G.E., and Glass, C.E., 1970, Wasatch fault, northern portion--Earthquake fault investigation and evaluation, prepared for the Utah Geological and Mineral Survey: Woodward-Clyde and Associates, Oakland, California, 27 p., 21 maps, 1:24,000 scale.

______1973, Wasatch fault, southern portion--Earthquake fault investigation and evaluation, prepared for the Utah Geological and Mineral Survey: Woodward-Lundgren and Associates, Oakland, California, 79 p., 23 maps, 1:24,000 scale.

Cluff, L.S., Glass, C.E., and Brogan, G.E., 1974, Investigation and evaluation of the Wasatch fault north of Brigham City and Cache Valley faults, Utah and Idaho--A guide to land-use planning with recommendations for seismic safety, prepared for the U.S. Geological Survey, Contract No. 14-08-001-13665: Woodward-Lungren and Associates, Oakland, California, 147 p., 35 maps, scale 1:24,000.

Crone, A.J., 1983, Amount of displacement and estimated age of a Holocene surface faulting event, eastern Great Basin, Millard County, Utah, _in_, Gurgel, K.D., ed., Geologic Excursions in Neotectonics and Engineering Geology in Utah, Guidebook-Part IV: Utah Geological and Mineral Survey Special Studies 62, p. 49-54.

Crone, A.J., Machette, M.N., Bonilla, M.G., Lienkaemper, J.J., Pierce, K.L., Scott, W.E., and Bucknam, R.C., 1987, Surface faulting accompanying the Borah Peak earthquake and segmentation of the Lost River fault, central Idaho: Bulletin of the Seismological Society of America, v. 77, no. 2, p. 739-770, 3 plates, 1:24,000 scale.

Crittenden, M.D., Jr., 1963a, New data on the isostatic deformation of Lake Bonneville: U.S. Geological Survey Professional Paper 454-E, p. E1-E31.

______1963b, Effective viscosity of the Earth derived from isostatic loading of Pleistocene Lake Bonneville: Journal of Geophysical Research, v. 68, p. 5517-5530.

Currey, D.R., Oviatt, C.G., and Plyler, G.B., 1983, Lake Bonneville stratigraphy, geomorphology, and isostatic deformation in west-central Utah, in Gurgel, K.D., ed., Geologic Excursions in Neotectonics and Engineering Geology in Utah, Guidebook-Part IV: Utah Geological and Mineral Survey Special Studies 62, p. 63-82.

Currey, D.R., and Oviatt, C.G., 1985, Durations, average rates, and probable causes of Lake Bonneville expansion, still-stands, and contractions during the last deep-lake cycle, 32,000 to 10,000 yrs ago, in Kay, P.A., and Diaz, H.F., eds., Problems of and prospects for predicting Great Salt Lake levels--Proceedings of a NOAA Conference held March 26-28, 1985: Center for Public Affairs and Administration, University of Utah, Salt Lake City, Utah, p. 9-24.

Davis, F.D., 1983a, Geologic map of the Central Wasatch Front, Utah: Utah Geological and Mineral Survey Map 54-A, scale 1:100,000.

______1983b, Geologic map of the Southern Wasatch Front, Utah: Utah Geological and Mineral Survey Map 55-A, scale 1:100,000.

______1985, Geologic map of the Northern Wasatch Front, Utah: Utah Geological and Mineral Survey Map 53-A, scale 1:100,000.

Doser, D.I., 1985, Source parameters and faulting processes of the 1959 Hegben Lake, Montana, earthquake sequence: Journal of Geophysical Research, v. 90, no. B6, p. 4537-4555.

______1986, Earthquake processes in the Rainbow Mountain-Fairview Peak-Dixie Valley, Nevada, region 1954-1959: Journal of Geophysical Research, v. 91, no. B12, p. 12572-12586.

Doser, D.I., and Smith, R.B., 1985, Source parameters of the 28 October, 1983, Borah Peak, Idaho, earthquake from body wave analysis: Bulletin of the Seismological Society of America, v. 75, p. 1041-1051.

Gilbert, G.K., 1890, Lake Bonneville: U.S. Geelogical Survey Monograph 1, 438 p.

______1928, Studies of Basin-Range structure: U.S. Geological Survey Professional Paper 153, 89 p.

Hintze, L.F., 1973, Geologic road log of Western Utah and eastern Nevada (part 1): Brigham Young University Geology Studies, v. 20, part 2, p. 10.

Hunt, C.B., Varnes, H.D., and Thomas, H.E., 1953, Lake Bonneville--Geology of northern Utah Valley, Utah: U.S. Geological Survey Professional Paper 257-A, 99 p.

Izett, G.A., Wilcox, R.E., Powers,. H.A., and Desborough, G.A., 1970, The Bishop ash bed, a Pleistocene marker bed in the western United States: Quaternary Research, v. 1, p 121-132.

Izett, G.A., 1981, Volcanic ash beds--recorders of upper Cenozoic silic pyroclastic volcanism in the western United States: Journal of Geophysical Research, v. 86, no. B11, p. 10200-10222.

______1982, The Bishop ash bed and some older compositionally similar ash beds in California, Nevada, and Utah: U.S. Geological Survey Open-File Report 82-582, 44 p., 3 oversize sheets.

Keaton, J.R., Currey, D.R., and Olig, S.J., 1987, Paleoseismicity and earthquake hazards evaluation of the West Valley fault zone, Salt Lake City urban area, Utah: Report to U.S. Geological Survey for Contract No. 14-08-0001-22048, March 6. 1987, 55 p. and 33 p. appendix.

King, Geoffrey, and Nabelek, John, 1985, Role of fault bends in the initiation and termination of earthquake rupture: Science, v. 228, p. 984-987.

Lund, W.R., and Schwartz, D.P., 1987, Fault behavior and earthquake recurrence at the Dry Creek site, Salt Lake segment, Wasatch fault zone, Utah: Geological Society of America Abstracts with Programs, v. 19, no. 5, p. 317.

Machette, M.N., 1984, Preliminary investigations of late Quaternary slip rates along the southern part of the Wasatch fault zone, in Hayes, W.W., and Gori, P.L., eds., Proceedings of Conference XXVI--A workshop on "Evaluation of regional and urban earthquake hazards and risk in Utah": U.S. Geological Survey Open-File Report 84-763, p. 391-406.

______1985, Late Cenozoic geology of the Beaver basin, southwestern Utah: Brigham Young Studies in Geology, v. 32, part 1, p. 19-37.

______1987, Recent studies of the Wasatch fault zone, Utah--A review: Geological Society of America Abstracts with Programs, v. 19, no. 5, p. 317.

Machette, M.N., and Lund, W.R., 1987, Trenching across the American Fork segment of the Wasatch fault zone, Utah: Geological Society of America Abstracts with Programs, v. 19, no. 5, p. 317.

Machette, M.N., Personius, S.F., and Nelson, A.R., 1986, Late Quaternary segmentation and slip-rate history of the Wasatch fault zone, Utah: EOS (Transactions, American Geophysical Union), v. 67, no. 44, p. 1107.

Madsen, D.B., and Currey, D.R., 1979, Late Quaternary glacial and vegetation changes, Little Cottonwood Canyon area, Wasatch Mountains, Utah. Quaternary Research, v. 12, p. 254-270.

Martinson, D.G., Pisias, N.G., Hays, J.D., Imbrie, John, Moore, T.C. Jr., and Shackleton, N.J., 1987, Age dating and the orbital theory of the Ice Ages--Developement of a high-resolution 0 to 300,000-year chronostratigraphy: Quaternary Research, v. 27, p. 1-29.

McCalpin, James, 1986, Thermoluminescence (TL) dating in seismic hazard evaluations--An example from the Bonneville basin, Utah, in Proceedings of the 22nd Symposium on Engineering Geology and Soils Engineering, Boise, Idaho, February 24-26, 1096, p. 156-176.

McCoy, W. D., 1987, Quaternary aminostratigraphy of the Bonneville Basin, Western United States: Geological Society of America Bulletin, v. 98, p. 99-112.

Miller, R.D., 1982, Surficial geologic map along part of the Wasatch Front, Great Salt Lake and Utah Valleys, Utah: U.S. Geological Survey Miscellaneous Field Studies Map MF-1477, scale 1:100,000.

Morner, N.-A., 1978, Faulting, fracturing, and seismicity as functions of glacio-isostasy in Fennoscandia: Geology, v. 6, p. 41-45.

Morrison, R.B., 1965, Quaternary geology of the Great Basin, in Wright, H.E., Jr., and Grey, D.G., eds., Quaternary geology of the United States: Princeton, N.J., Princeton University Press, p. 265-285.

Naeser, C.W., Bryant, Bruce, Crittenden, M.D., Jr., and Sorensen, M.L., 1983, Fission-track ages of apatite in the Wasatch Mountains, Utah--An uplift study, in Miller, D.M., Todd, V.R., and Howard, K.A., eds., Tectonic and stratigraphic studies in the eastern Great Basin: Geological Society of America Memoir 157, p. 29-36.

Nelson, A.R., and Personius, S.F., 1987, A nonconservative barrier to Holocene rupture propagation in the northern Wasatch fault zone, Utah, USA: 1987 International Union for Quaternary Research, 12th International Congress, Ottawa, Canada, July 31-August 9, 1987, Programme with Abstracts, p. 231.

Nelson, A.R., and VanArsdale, R.B., 1986, Recurrent Late Quaternary movement on the Strawberry normal fault, Basin and Range--Colorado Plateau transition zone, Utah: Neotectonics, v. 1, p. 7-37.

Nelson, A.R., Klauk, R.H., Lowe, Michael, and Garr, J.D., 1987, Holocene history of displacement on the Weber segment of the Wasatch fault zone at Ogden, northern Utah: Geological Society of America Abstracts with Programs, v. 19, no. 5, p. 322.

Oviatt, C.G., McCoy, W.E., and Reider, R.G., 1987, Evidence for a shallow early or middle Wisconsin-age lake in the Bonneville basin, Utah: Quaternary Research, v. 27, p. 248-262.

Parry, W.T., and Bruhn, R.L., 1986, Pore fluid and seismogenic characteristics of fault rock at depth on the Wasatch fault, Utah: Journal of Geophysical Research, v. 91, no. B1, p. 730-744.

______1987, Fluid inclusion evidence for minimum 11 km vertical offset on the Wasatch fault, Utah: Geology, v. 15, p. 67-70.

Personius, S.F., 1986, The Brigham City segment--a new segment of the Wasatch fault zone, northern Utah: Geological Society of America Abstracts with Programs, v. 18, no. 5, p. 402.

______1987, Preliminary surficial geologic map of the Brigham City segment and adjacent parts of the Weber and Collinston segments, Wasatch fault zone, Box Elder and Weber Counties, Utah: U.S. Geological Survey Miscellaneous Field Studies Map, scale 1:50,000 (in press).

Personius, S.F., and Gill, H.E., 1987, Holocene displacement on the Brigham City segment of the Wasatch fault zone near Brigham City, Utah: Geological Society of America, Abstracts with Programs, v. 19, no. 5, p. 326.

Peterson, D.L., 1974, Bouguer gravity map of part of the northern Lake Bonneville basin, Utah and Idaho: U.S. Geological Survey Miscellaneous Field Studies Map MF-627, scale 1:250,000.

Pierce, K.L., and Colman, S.M., 1986, Effect of height and orientation (microclimate) on geomorphic degradation rates and processes, late-glacial terrace scarps in central Idaho: Geological Society of America Bulletin, v. 97, p. 869-885.

Richmond, G.M., and Fullerton, D.S., 1987, Introduction to Quaternary glaciation in the United States of America: Quaternary Science Reviews, v. 5, p. 3-10.

Schwartz, D.P., Hanson, K.L., and Swan, F.H., III, 1983, Paleoseismic investigations along the Wasatch fault zone--an update, in Gurgel, K.D., ed., Geologic Excursions in Neotectonics and Engineering Geology in Utah, Guidebook-Part IV: Utah Geological and Mineral Survey Special Studies 62, p. 45-48.

Schwartz, D.P., and Coppersmith, K.J., 1984, Fault behavior and characteristic earthquakes--Examples from the Wasatch and San Andreas fault zones: Journal of Geophysical Research, v. 89, no. B7, p. 5681-5698.

Scott, W.E., and Shroba, R.R., 1985, Surficial geologic map of an area along the Wasatch fault zone in the Salt Lake Valley, Utah: U.S. Geological Survey Open-File Report 85-448, pamphlet and 2 plates, 1:24,000 scale.

Scott, W.E., McCoy, W.D., Shroba, R.R., and Rubin, Meyer, 1983, Reinterpretation of the exposed record of the last two cycles of Lake Bonneville, western United States: Quaternary Research, v. 20, no. 3, p. 261-285.

Simpson, D.W., 1986, Triggered Earthquakes: Annual Review of Earth and Planetary Sciences, 1986, v. 14, p. 21-42.

Slemmons, D.B., 1957, Geological effects of the Dixie Valley-Fairview Peak, Nevada, earthquakes of December 16, 1954: Bulletin of the Seismological Society of America, v. 47, p. 353-375.

Swan, F.H., III, Schwartz, D.P., and Cluff, L.S., 1980, Recurrence of moderate to large magnitude earthquakes produced by surface faulting on the Wasatch fault zone, Utah: Bulletin of the Seismological Society, v. 70, p. 1431-1462.

Wallace, R.E., 1984, Patterns and timing of late Quaternary faulting in the Great Basin Province and relation to some regional tectonic features: Journal of Geophysical Research, v. 89, no. B7, p. 5763-5769.

Wallace, R.E., and Whitney, R.A., 1984, Late Quatenary history of the Stillwater seismic gap, Nevada: Bulletin of the Seismological Society, v. 74, no. 1, p. 301-314.

Wheeler, R.L., and Krystinik, K.B., 1987, Evaluating coinciding anomalies along a fault trace or traverse--Simulations and statistical procedures: U.S. Geological Survey Bulletin 1802, 60 ms p. (in press).

______1987b, Segmentation of the Wasatch fault zone, Utah--Summaries, analyses, and interpretations of geological and geophysical procedures: U.S. Geological Survey Bulletin, 173 ms. p. (in press).

Williams, J.S., 1958, Geologic atlas of Utah, Cache County: Utah Geological and Mineral Survey Bulletin 64, 104 p.

Zoback, M.L., 1983, Structure and Cenozoic tectonism along the Wasatch fault zone, Utah: Geological Society of America Memoir 157, p. 3-27.

PERSISTENT AND NONPERSISTENT SEGMENTATION OF THE WASATCH FAULT ZONE, UTAH--STATISTICAL ANALYSIS FOR EVALUATION OF SEISMIC HAZARD

by

Russell L. Wheeler and Katherine B. Krystinik
U.S. Geological Survey
Denver, Colorado

ABSTRACT

The Wasatch fault zone of central Utah might be divided into segments that tend to rupture independently of each other. If so, ruptures of sufficiently large earthquakes would tend to start and stop at segment boundaries, and would tend not to cross boundaries. The validity of the segmentation hypothesis will affect how seismic hazard is estimated for the Wasatch Front urban corridor, the severity of the estimated hazard, and the degree to which the estimated hazard is concentrated into the state's population centers along the central part of the Wasatch fault zone.

To test the segmentation hypothesis we examined Bouguer gravity data, earthquake epicenters, fault-zone geometry, and aeromagnetic, topographic, and structural data along the fault zone. In each of the six data types we sought the kinds of anomalies (characteristic expressions) that a long-lasting segment boundary should produce. Anomalies in fault-zone geometry are large footwall salients, at which the east (upthrown) wall of the north-striking normal-fault zone projects west into the hanging wall and the fault trace bows westward around the projections. Of 26 anomalies in the six data types, four are salients, from north to south the Pleasant View, Salt Lake, Traverse Mountains, and Payson salients. Salients appear to be the most fundamental anomalies: 17 of the other 22 anomalies coincide with the salients; at each

salient, anomalies in three to five other data types coincide; and no other anomalies coincide elsewhere. Geological processes other than segmentation might have produced any of the anomalies, but only segmentation or chance could produce such coincidings of anomalies in a way that is consistent with the geological evolution of central Utah. With simulation experiments and statistical tests of the results of the simulations we show that the observed degree of anomaly coinciding should not be attributed to chance.

Formation of the salients occupied much or all of the history of the Wasatch fault zone. Fault scarps of late Pleistocene and Holocene age tend to end or change age at the salients, showing that scarps also are segmented there. We conclude that the Wasatch fault zone has been persistently segmented at the four salients throughout much or all of its 10-m.y. history, and will likely continue to be segmented there through at least the next several millenia, which is the time span of interest for hazard evaluation.

From mapping of late Quaternary deposits along the fault zone, other workers detected these four persistent segment boundaries, plus five other boundaries that are little expressed or poorly expressed in our six data types. The five others might be nonpersistent boundaries, alternating between active states in which they control several successive ruptures, and inactive states in which they do not. Although recently active, such boundaries might change state and so are less likely to affect the next few large ruptures than are the persistent boundaries. Fortunately for the estimation of seismic hazard, most of the segment boundaries in the populous central part of the Wasatch fault zone are persistent, so that their past behavior is a reasonable guide to their expected future behavior.

From consideration of the persistent boundaries we conclude that others should exist on other normal-fault zones where exposed or shallowly buried transverse bedrock ridges, some with salients, indicate accumulated slip deficits, and where two or more individual large historic or prehistoric ruptures zones have started or stopped. Testing this model against five historic earthquake sequences in and near the Basin and Range province indicates the existence of two persistent boundaries on the Lost River fault zone of Idaho (which broke in 1983), one persistent boundary between the Dixie Valley and Fairview faults of Nevada (December 1954), and one persistent and one nonpersistent boundaries in the Pleasant View, Nevada, rupture zone (1915). The north end of the Dixie Valley fault is not a segment boundary, persistent or otherwise. Both ends of the Rainbow Mountain, Nevada, rupture zone (July-August 1954), the south end of the Fairview Peak rupture zone, and the north end of the Pleasant Valley rupture zone have too little information available to test the model. The Hebgen Lake, Montana, earthquake (1959) occurred on a fault zone that is too young for the model to apply.

INTRODUCTION

Segmentation

Swan and others (1980) and Schwartz and Coppersmith (1984) hypothesized that the Wasatch fault zone is divided into six segments that are mostly or wholly independent of each other structurally and seismogenically. The proposed segments range in length from at least 30 km to about 70 km (fig. 1). Schwartz and Coppersmith (1984) also hypothesized that seismic energy release on a given segment occurs mostly as earthquakes of a size that is characteristic of the segment. These characteristic earthquakes would rupture the whole segment but would not rupture across segment boundaries into adjacent segments. This report concentrates on the segmentation hypothesis.

FIGURE 1. FOLLOWING TEXT

If the segmentation hypothesis is valid for the Wasatch fault zone, there would be two consequences for hazard evaluation in Utah. First, segmentation would affect the geographic distribution of expected large earthquakes along the Wasatch fault zone. Scarp-forming earthquakes in the last 8,000 years have been concentrated in the four central and most heavily populated of the proposed segments (Schwartz and Coppersmith, 1984, table 2). Compared to the frequencies that would be expected in the central segments if scarp-forming earthquakes were distributed uniformly along the fault zone, the data of Schwartz and Coppersmith (1984) imply that segmentation could nearly double the frequency of scarp-forming earthquakes in the Salt Lake City and Nephi segments, by maintaining the number of large earthquakes in the fault zone as a whole but concentrating them into the middle segments.

Second, segmentation would change probabilistic maps of seismic hazard. Production of such maps requires estimates of three things: the magnitude of the largest expected earthquake, the frequency distribution of earthquakes of various magnitudes, and the geographic area (seismic source zone) over which the estimates of magnitude and frequency apply (Algermissen and others, 1982; Thenhaus, 1983). Segmentation of the Wasatch fault zone would change all three estimates because each segment would become a separate source zone. Each segment would have its own maximum expected magnitude and frequency distribution. Estimates of these things would probably have larger uncertainties than if the whole Wasatch fault zone were treated as a single, unsegmented source zone, because each segment would have to be evaluated using only the comparatively sparse data from within its source zone. The estimated maximum magnitude might decrease because earthquakes large enough to rupture more than one segment (multi-segment earthquakes) might be precluded. Then the estimated frequency of single-segment earthquakes might increase because the strain that would have been released by one multi-segment earthquake would have to be released in several smaller, single-segment earthquakes.

Purpose

Following Schwartz and Coppersmith (1984), our study area is the Wasatch fault zone between lat 39° N. and lat 42° N. (the Utah-Idaho border), a north-south distance of 332 km. For this area we examined several types of geologic and geophysical data that might contain anomalies (characteristic expressions of long-lasting segment boundaries). For each kind of data we expanded or contracted the study area to whatever width was needed to characterize pertinent aspects of the data at the fault zone.

Wheeler (1984) examined the aims of hazard evaluation and analyses of temporal variations in the long historical record of seismicity in a tectonically analogous part of China. He concluded that the geologic records that are most likely to be useful in evaluating segmentation are those that formed during, or can be shown to bear on, the Holocene and late Pleistocene. The importance of Holocene and late Pleistocene records would increase if the degree of independence between segments, and the level of seismic activity on single segments, change over centuries to millenia (Smith and Richins, 1984, p. 79; Machette, 1984; Personius, 1985; Machette and others, in press). In fact, examinations of different parts of the Quaternary geologic record led Maclean (1985), Mayer and Maclean (1986), Personius (1986), Nelson and Personius (1987), and Machette and others (1986, in press) to choose segment boundaries, some of which differ from boundaries recognized in the Holocene record by Schwartz and Coppersmith (1984). These differences might indicate that different segment boundaries have persisted for different lengths of time.

The segmentation hypothesis was based mostly on data from trenches that were dug across scarps of the Wasatch fault zone at only four sites (fig. 1). The trench data are sufficient to suggest the segmentation hypothesis, but one trench site per segment is not enough to evaluate the hypothesis. Schwartz and Coppersmith (1984) observed several apparent spatial associations of the proposed segment boundaries with anomalies in topographic, geophysical, and other data. They suggested that these spatial associations are better than would be expected to occur by chance. Wheeler (1984) noted that an appropriately formulated statistical test could provide a rigorous evaluation of these and other spatial associations, and therefore of the segmentation hypothesis.

Thus, to evaluate the segmentation hypothesis as it applies to the Wasatch fault zone, our purpose is to answer two questions. First, do segments exist along the Wasatch Front, or are they artifacts of subjective perception and a small sample, being indistinguishable from patterns that could arise by chance? Second, if segments exist, have they affected uplift and seismicity along the fault zone both during the Holocene and far enough back in geologic time that the segments can be expected to continue to affect seismicity for the next decades to millenia?

Acknowledgments

Because of the diversity of information that we analyzed and interpreted, we are especially indebted to topical and regional specialists for discussions, corrections, preprints, and sharing of unpublished materials. These generous colleagues include W.J. Arabasz, R.L. Bruhn, A.J. Crone, S.K. Goter, D.R. Mabey, M.N. Machette, Larry Mayer, A.R. Nelson, S.F. Personius, W.E. Scott, D.P. Schwartz, and R.S. Stein. The entire manuscript benefitted from comments by M.N. Machette, A.R. Nelson, K.M. Shedlock, and M.L. Zoback.

METHODS

Anomalies

Wheeler and Krystinik (in press b) examined six kinds of data along the length of the Wasatch fault zone in Utah for the kinds of anomalies that a long-lasting segment boundary might produce. Each data type and its anomalies satisfy seven criteria (Wheeler and Krystinik, in press b) that insure that the anomalies pertain to identification of segment boundaries and to evaluation of seismic hazard, are reliable, and can be analyzed by the statistical and related methods of Wheeler and Krystinik (in press a).

At several places along the fault zone anomalies in two or more data types coincide. (Anomalies in the same data type cannot coincide because they would merge into a single anomaly.) Two anomalies form a coincident pair if either overlaps the center of the other (Wheeler and Krystinik, in press a). Three anomalies can form as many as three coincident pairs. If all three pairs exist, the three anomalies form a triplet. Similarly, m anomalies define an m-tuplet if the anomalies overlap enough to form all of the possible $m(m-1)/2$ coincident pairs (Wheeler and Krystinik, in press a). For example, six anomalies that form 15 coincident pairs form a sextuplet.

Data

The gravity data show transverse anomalies G1-10 (table 1, fig. 2) as groups of east-trending zones of gravity saddles, east-trending gradients, and ends of north-trending gradients and gravity lows. The transverse gravity anomalies match those derived independently by Zoback (1983) and include those of Mabey (in press). All of us interpreted G1-10 to record changes along the normal-fault zone in the depths to the bottoms of adjoining basins in the hanging (west) wall. Wheeler and Krystinik (in press b) argued that basin subsidence probably occurred by seismic slip on the fault zone, so that adjoining hanging-wall basins with different amounts of subsidence would abut parts of the fault zone with different seismic histories. If so, then a transverse gravity anomaly that separates such basins could be a segment boundary. We do not claim that G1-10 must represent segment boundaries. We only observe that long-lasting segment boundaries or their effects should produce transverse anomalies like G1-10, which justifies examination of the gravity data and of G1-10. We make similar observations for the other five data types.

TABLE 1.-- FOLLOWING PAGES

FIGURE 2.-- FOLLOWING TEXT

The total magnetic-intensity data show transverse anomalies M1-3 as east-trending belts of east-trending gradients and of narrow, high-amplitude magnetic highs (Zietz and others, 1976). Mabey and others (1964) attributed M1 to uplifted and exposed Precambrian metamorphic rocks, and M2 and M3 to buried and exposed intrusive and volcanic rocks of Tertiary age, with associated mineral deposits. Wheeler and Krystinik (in press b) suggested that M1 is bounded on the south and perhaps on the north by cross faults along which the metamorphic rocks were uplifted, perhaps on lateral ramps in Cretaceous thrust faults. Wheeler and Krystinik (in press b) also suggested that M2 and M3 might be localized by fracture systems that extend to depths at

TABLE 1.--Locations of transverse anomalies

[Study area is 332 km long, north to south, with north end at Utah-Idaho border. Leaders (---) indicate that the first anomaly in a data type begins south of the Utah-Idaho border. For example, M1 begins 54 km south of the border. Values are from Wheeler and Krystinik (in press b).]

	Distance south of Utah-Idaho border (km)			
Transverse anomaly number	North end of transverse anomaly[1]	South end of transverse anomaly	Transverse anomaly width (km) [2]	Distance to next transverse anomaly to south (km) [3]
Gravity data				
G1	-10	2	2	10
G2	12	17	5	40
G3	57	63	6	5
G4	68	78	10	45
G5	123	135	12	13
G6	148	157	9	9
G7	166	175	9	11
G8	186	192	6	19
G9	211	237	26	42
G10	279	292	13	40
Aeromagnetic data				

---	---	---	---	54
M1	54	130	76	18
M2	148	173	25	54
M3	227	246	19	86

Seismological data

---	---	---	---	59
Se1	59	78	19	42
Se2	120	133	13	8
Se3	141	151	10	62
Se4	213	226	13	106

Fault geometry (salients)

---	---	---	---	70
Sa1	70	76	6	48
Sa2	124	134	10	31
Sa3	165	169	4	48
Sa4	217	230	13	102

Topographic data

---	---	---	---	130
T1	130	140	10	107
T2	247	254	7	78

Structural data

---	---	---	---	112
St1	112	138	26	8
St2	146	167	21	53
St3	220	245	25	87

---

[1] Zoback (1983, fig. 2) showed that transverse anomaly G1 extends 10 km north of Utah-Idaho border. Data north of border lie outside study area and are not used here, so width of G1 is taken as 2 km.

[2] For each data type, sum of these values is length of study area that is occupied by transverse anomalies.

[3] For each data type, last entry is distance from southmost transverse anomaly to south end of study area at lat 39° N. For each data type, sum of values in this column is length of study area not occupied by transverse anomalies.

which magma was generated. Pre-existing faults or other fracture zones that cross the late Tertiary (Naeser and others, 1983) Wasatch fault zone might segment it by separating and decoupling adjoining blocks of one or both fault walls.

Seismological data show anomalies Se1-4 as changes along the fault zone in abundance of epicenters of small earthquakes that occurred near the trace of the fault zone during 1962-1986 (Arabasz and others, 1980; Arabasz, 1984; Smith and Richins, 1984; W.J. Arabasz, oral communs., 1986). The changes could represent differences in present-day rates of seismic slip between adjacent lengths of the fault zone. Such differences could represent different rates of long-term seismic slip, different ratios of seismic to aseismic slip, or different magnitudes and frequencies of the earthquakes by which seismic slip occurs, any of which could arise from independent slip of two fault segments separated by a change in epicentral abundance. Then Se1-4 could be segment boundaries.

The geometry of the fault zone shows anomalies Sa1-4. At each place the footwall projects west into the hanging wall as a large salient, and the mapped trace of the fault zone or one of its strands bends west around the tip of the salient (Hintze, 1980; Davis, 1983a, b, 1985). The trace of the fault zone also forks or steps en echelon at the salients. Respectively, Sa1-4 are the Pleasant View, Salt Lake, Traverse Mountains, and Payson salients (Wheeler and Krystinik, 1987a, b, in press b). If slip vectors change orientation across the salients, then by definition the salients are non-conservative barriers as described by King (1983). King (1983), King and Yielding (1984), and King and Nabelek (1985) suggested a mechanism by which large ruptures would tend to start and stop at non-conservative barriers. Briefly, if two adjacent parts of a fault slip along different vectors, the slip geometry at the junction of the two parts requires the formation of a network of many subsidiary faults surrounding the junction. The network is the process zone of King and Nabelek (1985). The energy of an incoming rupture is absorbed by the process zone and dispersed into small slips on many of its faults. Large ruptures that propagate toward the process zone tend to stop there, so the zone is a barrier. The shattered process zone has low strength but high fracture toughness, so it also acts as an asperity and large ruptures tend to start there and propagate away along the main fault. Accordingly, ruptures tend not to cross the process zone so it becomes a segment boundary. Bruhn and others (in press a,b) concluded from structural measurements and geometric arguments that slip vectors change orientation across the Salt Lake and Traverse Mountains salients. Nelson and Personius (1987) noted that young fault scarps end or change age at the Pleasant View salient, as would be expected of a non-conservative barrier. If the mechanism of King and Nabelek (1985) operates at the salients, they would be segment boundaries.

Transverse topographic anomalies T1-2 are formed where height of the uplifted mountains, their width, or both change abruptly northward or southward. Of all six data types, choice of anomalies in topographic data is the most subjective and the least likely to be give reproducible results. To insure reproducibility Wheeler and Krystinik (in press b) used only those topographic anomalies that were recognized by a majority of 12 independent intepreters. Of 14 suggested topographic anomalies, two were chosen by at least nine interpreters, and no others by more than five. A topographic anomaly could mark a place along the fault zone where a footwall block has been uplifted more than its neighbor across the anomaly. Because much or all uplift has occurred seismically, a topographic anomaly could separate lengths of the fault zone that have different seismic histories and could be a segment boundary.

Structural anomalies St1-St3 were chosen by considering the depths at which large normal faults of the Basin and Range province typically nucleate (about 15 km, at or near the base of the brittle upper crust: Smith and Richins, 1984, p. 97, figs. 9, 11). Large cross-faults that extend to this depth could decouple adjoining lengths of the Wasatch fault zone from each other and could act as segment boundaries. Wheeler and Krystinik (in press b) reviewed the structural evolution of central Utah and found three large, east-striking faults or fault zones (St1-3) that could serve as structural anomalies and could extend to depths of about 15 km. St1 is a buried lateral ramp in thrust sheets that moved eastward into north-central Utah mostly in Cretaceous time (Armstrong and Oriel, 1965; Oriel and Armstrong, 1966; Armstrong, 1968; Royse and others, 1975). The ramp is nowhere exposed but Smith and Bruhn (1984), Schirmer (1985), and Wheeler and Krystinik (in press b) used geometric arguments to conclude that the ramp must dip north. St3, a similar north-dipping lateral ramp at the south end of a more southerly thrust sheet, also formed in Cretaceous time (Crittenden, 1961; Armstrong, 1968; Lawton, 1985; Bryant and Nichols, in press). The top of the ramp is exposed in the south end of the Wasatch Range northeast of Nephi (Hintze, 1980). St2 is the buried fault system that is inferred to bound and underlie the Uinta aulacogen, a long-lasting trough (Forrester, 1937) that extends more than 200 km eastward from the Salt Lake City segment (fig. 1). The aulacogen probably formed as an east-trending continental rift in middle Proterozoic time (Hansen, 1965; Wallace and Crittenden, 1969; Burke and Dewey, 1973). Its existence is inferred from a long stratigraphic record of repeated, superimposed, eastward-elongated uplifts and downwarps from middle Proterozoic and perhaps Archean through Oligocene time (Bryant, 1985; Wheeler and

Krystinik, in press b) and from young, inward-dipping reverse faults that bound the inferred aulacogen along its north and south edges (Bruhn and others, 1983; Gries, 1983; Stone, 1986). However, we found no evidence that the reverse faults penetrate as deeply as 15 km, or that they were active when the aulacogen formed during middle Proterozoic time. Accordingly, Wheeler and Krystinik (in press b) took anomaly St2 to represent the entire system of deep, east-striking, unexposed faults that are inferred to underlie the aulacogen, from the north edge of the aulacogen to the south edge inclusive.

Causes of Coincident Anomalies

Segmentation and other geologic processes might each produce single anomalies of the kinds described above. Coincident anomalies might be produced by segmentation, by some other geologic process that affects more than one data type, or by chance in the form of the spatially random operation of independent geologic processes that each affect only one data type. We will attribute coincident anomalies to segmentation if we can eliminate the two alternative causes. Geologic processes other than segmentation must be eliminated by consideration of the geologic evolution and characteristics of central Utah. Chance must be eliminated statistically before the coincident anomalies can be considered worth interpreting, either as segment boundaries or as manifestations of any other geologic processes.

Geologic Causes of Anomalies other than Segmentation

Transverse anomalies G1-G10 in Bouguer gravity data can be interpreted as separating sediment-filled, hanging-wall basins (Zoback, 1983). Such anomalies would reflect segment boundaries because they would separate parts of the fault zone that have slipped separately and perhaps independently. Overlaying an enlarged version of the Bouguer gravity map of Zoback (1983) on the geologic map of Hintze (1980) indicates that G5-G7 can be tentatively attributed partly to large lateral ramps in thrust sheets. The ramps could act as segment boundaries by decoupling adjacent parts of the Wasatch fault zone so that the parts could slip independently of each other. Other kinds of east-striking cross faults might also cause transverse gravity anomalies, such as east-trending gravity gradients, by juxtaposing rocks of different densities. Deeply penetrating cross faults could also decouple adjacent parts of the Wasatch fault zone and act as segment boundaries. For example, east-striking faults in the Uinta aulacogen or at its edges could cause G6 and G7. Edges of high-density igneous rocks could produce transverse gravity anomalies, but intrusive and extrusive igneous rocks at and near the Wasatch fault zone generally have low densities, some comparable to those of surrounding sedimentary rocks (Zoback, 1983, p. 5, 11). Also, most edges of gravity highs near the fault zone follow the contact between bedrock and basin-filling sediments more faithfully than they follow contacts between igneous rocks and other rocks (Zoback, 1983; Hintze, 1980), and so appear to outline shapes of basins instead of igneous bodies. Facies changes within the sediments that fill some basins could produce lateral density contrasts (Mabey, in press), but these contrasts are likely to be too small to produce the 10-40 mgal of gravity relief that occurs across several of anomalies G1-G10. Thus, segment boundaries of one form or another are the most likely explanation for most of G1-G10.

Mabey and others (1964) attributed transverse anomalies in the aeromagnetic field to exposed Precambrian rocks (M1) and to east-trending belts of igneous rocks (M2, M3). The Precambrian rocks form the main mass of a thrust sheet, whose southern edge is a lateral ramp (Wheeler and Krystinik, in press b). The magma that fed the igneous belts could have risen along east-trending systems of fractures. Both lateral ramps and deeply-penetrating fracture systems could decouple adjacent parts of the Wasatch fault zone, causing its segmentation. Of the various ways to emplace magnetic rock into nonmagnetic surroundings, only thrusting and igneous activity are consistent with the geologic history of north-central Utah. For example, sedimentary processes do not produce magnetic anomalies with the magnetic relief of M1-M3 (200-800 gammas: Zietz and others, 1976), and uplift of magnetic rock in mantled gneiss domes would have been restricted to more westerly parts of the orogen whose eastern parts are preserved along the Wasatch Front. The only reasonable explanations for M1-M3 are consistent with these transverse anomalies being expressions of segment boundaries.

By definition, seismological anomalies Se1-Se4 are segment boundaries for the small earthquakes that were recorded during 1962-1986.

Sa1-Sa4 are salients, where the Wasatch fault splits and rejoins itself to enclose a partly downdropped block (Sa1, Sa2), bends sharply (Sa1, Sa3), or steps en echelon to the east or west (Sa4) (Wheeler and Krystinik, in press b). Our inspection of fault patterns and bedrock lithologies near Sa1-Sa4 (Hintze, 1980) suggests two possible causes for such splits, sharp bends, and steps. In the upper few kilometers of the crust, a massive, unlayered or irregularly layered rock mass might have sufficient fracture toughness that a rupture propagating toward the mass might more easily go partly or entirely around it than straight through it. This might have happened at the south end of the Archean migmatites, schists, and gneisses of the Farmington Canyon Complex (Bryant, 1984) at Sa2, and along the margin of the quartz monzonite of the Little Cottonwood stock (Crittenden, 1965) at Sa3. Alternatively, two ruptures that nucleate independently of each other and propagate toward each other are unlikely to meet perfectly aligned. Their tips would probably propagate past each other for some distance before each rupture curved to join the other. The result could be a sharp bend in the combined fault trace (Sa1, Sa3), a fault trace that appears to split and rejoin itself (Sa1, Sa2), or en echelon steps in the fault trace (Sa4). Whether a salient originates and grows at a tough rock mass, or where two rupture tips barely miss each other, or in both ways, each of the four salients has hundreds to thousands of times the structural relief that it could acquire during one large earthquake. Each salient must have grown over many recurrence intervals of such earthquakes. A salient that grows by similar behavior of many large ruptures is a segment boundary.

Topographic anomalies T1 and T2 could be produced by differences in rates or amounts of uplift across a segment boundary, irregular fault geometry, lithologic variation, variation in geometry of the thrust sheets and related folds that are exposed throughout most of the east wall of the Wasatch fault zone, or variations in erosion rate and stream size. The second through fourth factors might be related to segment boundaries, but need not be. Later we will show that topographic anomalies are poorly associated with inferred segment boundaries. Perhaps the plethora of possible causes of topographic anomalies is the reason for this poor association. T1 is a topographic low (Wheeler and Krystinik, in press b) that coincides with Mesozoic rocks in and near the Parleys Canyon syncline (Crittenden, 1974). The Mesozoic rocks are bounded on north and south by more resistant Precambrian rocks (Hintze, 1980). T2 is also a topographic low (Wheeler and Krystinik, in press b) that coincides with a river that cuts through easily erodable Mesozoic strata

(Hintze, 1980). These strata pass northward under the resistant Paleozoic rocks of a thrust sheet, which form a tall mountain at the north edge of T2 (Hintze, 1980). Thus, both topographic anomalies might arise from lithologic variations that need not be related to segment boundaries.

Anomalies in pre-Cenozoic structure are large lateral ramps that dip moderately northward (St1, St3) and an inferred system of east-striking faults (of unknown geometry) of the Uinta aulacogen (St2) (Wheeler and Krystinik, in press b). St1-St3 are inferred to cut the upper crust. All three could act as segment boundaries by decoupling adjacent parts of the Wasatch fault zone, allowing the parts to operate as independent segments. No other similar structures are known along the fault zone. The best candidate for a similar structure is the north-dipping Willard fault (Crittenden, 1972), which dips too gently to be considered a segment boundary (Wheeler and Krystinik, in press b).

In summary, transverse anomalies in aeromagnetic and seismological data, salients, and pre-Cenozoic structures can be reasonably explained only as expressions of segment boundaries, or of faults and other fractures that could act as segment boundaries. Topographic anomalies can have causes other than segment boundaries, but are the anomalies that are least involved in the inferred segment boundaries of the Wasatch fault zone. There are so many transverse gravity anomalies that one might expect some to have causes other than segment boundaries. Some of the other causes are geologically reasonable, and in fact as we will show later four of the ten transverse gravity anomalies do not coincide with other anomalies (G1, G2, G8, G10: fig. 2). However, the striking grouping of most anomalies into a few anomalous parts of the fault zone (fig. 2) can be reasonably attributed only to the operation of segment boundaries, or to chance.

Simulation and Statistical Procedures

Wheeler and Krystinik (1987a) described or derived several procedures for summarizing and evaluating how anomalies are distributed along the fault zone. They illustrated these procedures by applying them to an artifical data set that resembles a simple version of the real data of figure 2. Among these procedures is modification and use of the Jaccard coefficient J (Cheetham and Hazel, 1969) to identify strongly associated data types, or those which tend to have and lack anomalies at the same places along the fault zone. One nonnegative value of J can be calculated for each pair of data types. Values of J near or larger than 1 identify pairs of data types that are comparatively strongly associated. These data types might be more useful together than separately for interpreting the observed pattern of anomalies. Conversely, values of J near 0 identify pairs of data types that are comparatively unassociated, and which tend to have and lack anomalies without regard to each other. We chose all data types and their anomalies with an eye to identifying segment boundaries, so any data type that tends to be unassociated with the others, and particularly with data types of most interest for identification of segment boundaries, probably can be dropped from further consideration.

Simulations and appropriately designed statistical tests aid in deciding whether anomalies in the observed pattern (fig. 2) coincide more than should be attributed to chance. Each simulation takes the observed number and widths of anomalies in each data type and locates the anomalies randomly along the fault zone. Each simulation produces a simulated anomaly pattern that resembles figure 2 to some degree. For the anomalies of figure 2 we performed 300 simulations. This number was chosen as being large enough to smooth out peculiarities of any small group of simulated patterns, but small enough for the simulations to be computationally feasible.

Each anomaly pattern plots in a three-dimensional graph according to its numbers of triplets, quadruplets, and quintuplets (fig. 3). Only one simulation produced a sextuplet, so this single simulated pattern will be treated individually. Wheeler and Krystinik (in press a) described a simple way to perform the statistical test, by counting the numbers of patterns that plot in serial sections through figure 3 (fig. 4). Each observed or simulated pattern plots on one of a few serial sections. For example, the patterns for the data from the Wasatch fault zone all plot on the first three sections because each pattern has k = 0, 1, or 2 quintuplets. The significance plane S' intersects each section in a dashed line (fig. 4), although only one section and one dashed line contain the point P that corresponds to the observed pattern. N(e) is the number of simulated patterns that plot on or outside (farther from the origin than) the dashed lines, summed over all serial sections. Points C and D (fig. 4) contribute to N(e). N(p) is the total number of simulated patterns in all the sections, so points B-D (fig. 4) all contribute to N(p). The level of significance of the statistical test is N(e)/N(p) (Wheeler and Krystinik, in press a).

FIGURE 3.-- FOLLOWING TEXT

FIGURE 4.-- FOLLOWING TEXT

Locational Uncertainties of Anomaly Edges

The north and south edges of each anomaly have locational uncertainties. Most uncertainties are ±1-5 km (Wheeler and Krystinik, in press b). We investigated effects of uncertainties by analyzing two observed patterns in addition to that of figure 2, which shows the measured and most likely width of each anomaly (table 1). One of the other patterns shows the minimum anomaly widths that are allowed by the locational uncertainties, and was tested against 300 simulations of the locations of these narrowed anomalies. The other pattern shows maximum allowable widths. It was tested against only 100 simulations because the wider anomalies generated more and larger coincidings, and greatly increased computation time made more simulations infeasible. Thus, we did three statistical tests instead of one. We tested for significance with each of these three sets of simulations. The principles of simultaneous inference (Miller, 1981, p. 8) require that each of the three tests use a level of significance of 0.05/3 = 0.0167 instead of the habitual 0.05.

DESCRIPTIVE RESULTS

Observed Pattern of Anomalies

Gravity, aeromagnetic, seismological, and topographic data, salients, and pre-Cenozoic structures together define a total of 26 anomalies along the Wasatch fault zone (fig. 2). Locational uncertainties of anomaly edges define minimum and maximum widths for each anomaly (fig. 5). Most anomalies occupy only a small fraction of the fault's length of 332 km (fig. 6).

FIGURE 5.-- FOLLOWING TEXT

FIGURE 6.-- FOLLOWING TEXT

Anomalous Sections of the Fault Zone

Most of the 26 anomalies fall in four narrow, well demarcated, anomalous sections of the fault zone (fig. 7). Only five anomalies occur singly or elsewhere (fig. 7A). This striking concentration of anomalies into four distinct parts of the fault zone is robust, being weakened little even if each anomaly takes on its extreme widths (figs. 7B, C).

FIGURE 7.-- FOLLOWING TEXT

Triplets, quadruplets, and quintuplets of coincident anomalies are built up from coincident pairs. For example, about at km 70 five anomalies in four data types are involved in eight pairs (fig. 7A). These five anomalies could define as many as ten pairs. Of these ten possible pairs, that between anomalies G3 and G4 is forbidden because two anomalies in the same data type cannot coincide. Anomalies G3 and Sa1 do not overlap and so cannot form a pair. The other eight possible pairs are all present. A triplet is present if and only if all three possible pairs between its three anomalies also are present. At km 70 pair lines define five triplets: G3-M1-Se1, G4-M1-Se1, G4-Se1-Sa1, G4-M1-Sa1, and M1-Se1-Sa1. Similarly, a quadruplet is formed by six pairs among four anomalies. At km 70 the only quadruplet is G4-M1-Se1-Sa1. No quintuplet can link these four anomalies with G3 because the G3-G4 pair is forbidden and the G3-Sa1 pair is not present If anomalies take on their maximum widths, no change occurs in this list of pairs and m-tuplets (fig. 7C). However, using minimum widths breaks the pair G3-Se1, which causes the triplet G3-M1-Se1 to degenerate into its two remaining pairs (fig. 7B).

The six coincident anomalies at km 160 and the five at km 230 can be examined similarly. The six anomalies in six data types at km 130 are linked more complexly (fig. 8). Consideration of figure 8 will reveal the 12 pairs, 11 triplets, five quadruplets, and one quintuplet that are summarized at the right edge of figure 7A. Narrowing anomalies to their minimum widths breaks the pairs G5-M1, G5-T1, M1-Se2, and M1-Sa2 and causes some m-tuplets to degenerate (fig. 7B). Widening anomalies to their maximum widths produces all possible pairs except M1-T1, with the consequent addition of some m-tuplets (fig. 7C).

FIGURE 8.-- FOLLOWING TEXT

Some of these pairs and m-tuplets duplicate each other. A quintuplet comprises five quadruplets, which duplicate it. Similarly, a quadruplet comprises four triplets, and a triplet, three pairs. After duplicates have been deleted, for measured widths, the observed pattern contains one quintuplet, one quadruplet, eight triplets, and one pair (table 2). For minimum widths, the observed pattern contains two quadruplets, two triplets, and seven pairs. For maximum widths, it contains two quintuplets, six quadruplets, one triplet, and one pair (Se3-Sa2).

TABLE 2.-- FOLLOWING PAGES

Anomalies G1, G2, G8, G10, and T2 are singlets (figs. 2, 7A): none coincides with any other anomaly. As widths decrease to their minimums anomalies overlap less, coincident anomalies become scarcer, and these five singlets are joined by G7 and Se3 (figs. 5A, 7B). As widths increase to their maximums the reverse occurs, but the original five singlets do not join any pairs or m-tuplets (figs. 5B, 7C).

Associated Data Types

The 15 possible pairings of the six data types give 15 values of the Jaccard coefficient J (fig. 9). Increased anomaly widths will tend to increase the number of coincident anomalies and the degree of association between any two data types. Decreased anomaly widths will tend to produce the opposite effect. Both effects can be seen by comparing median values of J and histogram shapes in figure 9.

FIGURE 9.-- FOLLOWING TEXT

TABLE 2.--Coincidings of anomalies, with duplicating pairs and m-tuplets deleted

[Pairs and m-tuplets (triplets, quadruplets, and quintuplets) are among those shown in fig. 7. Entries are lists of anomaly names from figs. 2, 5. Leaders (---) mean that none of the indicated kinds of pairs or m-tuplets is present, except as duplicates of parts of larger m-tuplets that might be listed farther to the left for the same location.]

Location[1]	Quintuplets	Quadruplets	Triplets	Pairs
Measured Widths				
70	---	G4-M1-Se1-Sa1	G3-M1-Se1	---
130	G5-M1-Se2-Sa2-St1	---	G5-T1-St1	---
160	---	---	G6-M2-St2 G7-M2-Sa3 M2-Sa3-St2	Se3-St2
230	---	---	G9-Se4-Sa4 G9-M3-St3 G9-Sa4-St3	---
Minimum Widths				
70	---	G4-M1-Se1-Sa1	---	G3-M1
130	---	G5-Se2-Sa2-St1	---	M1-St1 T1-St1
160	---	---	---	G6-M2

				M2-Sa3 M2-St2
230	---	---	G9-Sa4-St3 G9-Se4-Sa4	M3-St3

Maximum Widths

70	---	G4-M1-Se1-Sa1	G3-M1-Se1	---
130	G5-Se2-Sa2-T1-St1 G5-M1-Se2-Sa2-St1	---	---	---
140	---	---	---	Se3-Sa2[2]
160	---	G7-M2-Sa3-St2 G6-M2-Sa3-St2 G6-M2-Se3-St2	---	---
230	---	G9-Se4-Sa4-St3 G9-M3-Sa4-St3	---	---

---

[1] Location means approximate distance south of Utah-Idaho border, in km.

[2] This pair links two anomalous parts of the fault zone by spanning a non-anomalous part, and is indicated by square brackets at the right edge of figure 7C.

The most highly associated data types overall are aeromagnetic data (M) and pre-Cenozoic structure (St). This high association also holds for maximum and minimum anomaly widths. Each structural anomaly coincides with one and only one aeromagnetic transverse anomaly, and vice versa, regardless of whether anomalies take on their measured, minimum, or maximum widths (fig. 7). The data type that is most highly associated with seismological data (Se) is footwall salients (Sa). This association is also robust under the effect of width but is only moderately strong (J = .60, fig. 9A). Each seismological anomaly coincides with one and only one salient, and vice versa, except Se3 and Sa3, which do not coincide with each other (fig. 7A). No change occurs for minimum widths (fig. 7B), but for maximum widths Se2 and Se3 both coincide with Sa2 (fig. 7C).

Each type of data can combine with five others to produce five J values (fig. 9). The median of these five J values indicates how well the data type is associated with the other five types of data overall. Aeromagnetic data are the most strongly associated with other data types overall (median J = .75, .33, and .86 in figures 9A, B, and C, respectively). Most of the aeromagnetic transverse anomalies are connected by pair lines to several other anomalies (fig. 7). In contrast, topographic anomaly T1 is sparsely connected and T2 is not connected to other anomalies. Topographic data are the least strongly associated overall (median J = .00, .00, and .20 in figures 9A, B, and C, respectively).

Diagnostic and Characteristic Data Types

Does any one data type identify anomalous parts of the fault zone particularly well? This question can be answered with techniques that are associated with cluster analysis. The four anomalous parts of the fault zone divide the zone into nine parts (fig. 7), which group naturally into two clusters. The anomalous cluster contains four parts, those around km 70, 130, 160, and 230. The non-anomalous cluster contains five parts, the three intervening parts of the fault zone and the two ends, where anomalies are scarce and coincident anomalies are absent.

The entries in a presence-absence matrix (table 3) allow calculation of two measures called constancy (C) and fidelity (F) (Hazel, 1970). Each is expressed as an integer between 0 and 10. Constancy expresses the degree to which the anomalies of a data type characterize a cluster. Structural anomalies characterize the anomalous cluster moderately well (C = 8, table 3), because one or more of these anomalies are present in most of the fault-zone parts that are in the anomalous cluster. Fidelity expresses the degree to which the anomalies of a data type are diagnostic of a cluster. Structural anomalies are perfectly diagnostic of the anomalous cluster (F = 10, table 3) but undiagnostic of the non-anomalous cluster (F = 0). The occurrence of a structural anomaly in a part of the fault zone indicates that the part belongs in the anomalous cluster.

TABLE 3.-- FOLLOWING PAGES

Most data types have lower C and F values for the non-anomalous cluster than for the anomalous cluster (table 3). This difference is reassuring because the data types were chosen and the anomalies were defined to be likely to reflect the presence of segment boundaries, which should correspond to anomalous parts of the fault zone, instead of segment interiors, which should correspond to non-anomalous parts.

TABLE 3.--Constancy and fidelity for anomalous and non-anomalous parts of the Wasatch fault zone (measured anomaly widths)

Cluster: A is the cluster of four anomalous parts of the fault zone, which are about 70, 130, 160, and 230 km south of the Utah-Idaho border (fig. 7A). N is the cluster of five intervening and surrounding non-anomalous parts of the fault zone, including north and south ends.

Part: part of the fault zone. In each cluster, parts are numbered consecutively from north to south. Leaders (---) mean that this column is not applicable.

Data type: G means gravity data, M means aeromagnetic data, Se means seismological data (epicenters), Sa means salients in fault-zone geometry, T means topographic data, and St means pre-Cenozoic structures.

Cluster	Part	Data type					
		G	M	Se	Sa	T	St
Presence-absence matrix[1]							
N	1	1	0	0	0	0	0
A	1	1	1	1	1	0	0
N	2	0	1	0	0	0	0
A	2	1	1	1	1	1	1
N	3	0	0	0	0	0	0
A	3	1	1	1	1	0	1
N	4	1	0	0	0	0	0
A	4	1	1	1	1	0	1
N	5	1	0	0	0	1	0

Constancy							
A	---	10	10	10	10	2	8
N	---	6	2	0	0	2	0
Fidelity							
A	---	6	8	10	10	5	10
N	---	4	2	0	0	5	0

---

[1] Entry of 1 means that the indicated data type has one or more anomalies in the indicated part of the fault zone. Entry of 0 means that no such anomaly is present in the indicated part. Values of entries were determined by inspection of figure 7A.

We seek data types that are both diagnostic and characteristic of anomalous parts of the fault zone, and which will plot at the upper right corner of a graph of C plotted against F (fig. 10). For measured anomaly widths, salients (Sa) and seismological anomalies (Se) are perfectly characteristic and perfectly diagnostic of anomalous parts of the Wasatch fault zone (fig. 10A). When uncertainty in anomaly widths is considered (figs. 10B, C) seismological anomalies become slightly worse indicators of anomalous parts of the fault zone, but salients remain perfect one-to-one indicators. Aeromagnetic transverse anomalies (M) are perfectly characteristic (C = 10) but only moderately diagnostic (F = 8), and this result is not affected by the uncertainties in anomaly widths. Every anomalous part of the fault zone contains an aeromagnetic transverse anomaly, but such an anomaly can also occur in a non-anomalous part of the fault. F = 8 because the unusually wide anomaly M1 spans two anomalous and the intervening non-anomalous parts of the fault zone (fig. 7).

FIGURE 10.--FOLLOWING TEXT

Recall that the two most highly associated data types are aeromagnetic (M) and pre-Cenozoic structural (St) data. Anomalies in these two data types correspond in parts A2, A3, and A4 of the fault zone, but not in part A1 (fig. 7A, table 3), producing C = 8 and F = 10 for coincident structural and aeromagnetic transverse anomalies in the anomalous cluster. These values do not change with uncertainty in anomaly widths. Thus, the coinciding of structural and aeromagnetic transverse anomalies is perfectly diagnostic but only moderately characteristic of anomalous parts of the fault zone. Coincident transverse anomalies in aeromagnetic and structural data identify parts of the fault zone as anomalous, but one anomalous part of the fault zone (A1) lacks such a coincident pair.

Summary of Descriptive Results

With one exception, the 26 anomalies are of similar widths, with a median that is three percent of the length of the Wasatch fault zone in Utah. Most anomalies coincide with each other in four narrow, anomalous parts of the fault zone.

For the fault zone as a whole aeromagnetic transverse anomalies are the most highly associated with anomalies of other kinds, especially those in structural data. Topographic anomalies are the least well associated with other kinds. The data type that is most highly associated with seismological anomalies is salients, although only moderately so.

For anomalous parts of the fault zone, salients are perfectly diagnostic and perfectly characteristic, seismological anomalies are the second best such one-to-one indicator, aeromagnetic transverse anomalies are perfectly characteristic but only moderately diagnostic, and coincident structural and aeromagnetic transverse anomalies are perfectly diagnostic but only moderately characteristic.

RESULTS FROM SIMULATION AND STATISTICAL TESTING

Is the observed concentration of anomalies into four parts of the fault zone worth interpreting, or should it be dismissed as a likely result of a random scattering of anomalies in unrelated variables along the Wasatch fault zone? The most direct way to answer this question is to compare the observed anomaly pattern with simulated patterns that have each been produced by such a random scattering of anomalies, as Wheeler and Krystinik (in press a) illustrated with an artifical data set.

One-Dimensional Comparisons of Observed and Simulated Patterns

For measured widths few of the simulations produced as many triplets or quintuplets as are observed, and the observed pattern has more quadruplets than do most simulated patterns (fig. 11A). For minimum widths the observed pattern has unusually many quadruplets but not unusually many triplets, and there are no quintuplets in any simulated or observed pattern (fig. 11B). For maximum widths the observed pattern has unusually many quadruplets and quintuplets but unusually few triplets (fig. 11C). Also, one simulation for maximum widths produced the only sextuplet encountered in any anomaly pattern. Thus, these one-dimensional comparisons suggest that anomalies in the observed pattern coincide more than do those in the simulated patterns, but the difference is not striking enough to distinguish clearly the observed degree of coinciding from the effects of chance.

FIGURE 11.-- FOLLOWING TEXT

Three-Dimensional Comparisons of Observed and Simulated Patterns

Histograms of m-tuplet frequencies (fig. 11) are easy to understand, but they lose information by separating a pattern's number of triplets from its numbers of quadruplets and other m-tuplets, and similarly for other combinations of m-tuplets. We retain this information by representing each pattern's triplets, quadruplets, quintuplets, and sextuplets together (fig. 12).

FIGURE 12.-- FOLLOWING TEXT

For measured widths (fig. 12A) 294 of the 300 simulated patterns lack quintuplets and plot in the plane of the page. Five simulated patterns and the observed pattern have one quintuplet each and plot one unit above the page, and a sixth simulated pattern plots two units above the page. Viewed this way, the observed pattern plots near the outside of the group of all points that represent simulated patterns. Accordingly, when all m-tuplets are examined together the anomalies of the observed pattern are seen to coincide strongly when compared to anomalies of the simulated patterns.

For minimum and maximum anomaly widths the picture is similar but less clear cut. For minimum widths no pattern has m-tuplets larger than quadruplets, so all plot in the plane of the page (fig. 12B). The asterisk lies on the edge of the cloud of plotted points from the simulations. At least two simulated patterns have anomalies that coincide at least as strongly as is observed. For maximum widths the observed pattern plots to the right and above the page from the envelope that encloses the plotted locations of all simulated patterns (fig. 12C). The sextuplet is much rarer than are quintuplets, so probably this simulated pattern should be considered to have anomalies that are at least as strongly coincident as are those of the observed pattern.

Therefore, examining all sizes of m-tuplets together shows that the observed pattern has anomalies that coincide more strongly than do those of nearly all simulated patterns. This difference holds whether anomalies take on their measured, minimum, or maximum widths.

Quantitative Comparisons of Observed and Simulated Patterns

For the statistical test of figures 3 and 4, a concise statement of the null hypothesis of Wheeler and Krystinik (in press a) is that the observed pattern was drawn from a population in which anomalies do not tend to coincide more strongly than do anomalies of the simulated patterns. Analogously, the alternative hypothesis is that anomalies in the population do tend to coincide more strongly than do those in the simulations. Each serial section contains a dashed line, the position and slope of which are calculated from the total counts of m-tuplets in all simulations taken together (table 4), and from the value of k that identifies the serial section (fig. 4; figure 10 of Wheeler and Krystinik, in press a, shows equations for the calculations). Any simulated pattern that plots on or outside the dashed line in the appropriate serial section is taken to have anomalies that are at least as strongly coincident as are those of the observed pattern. We performed three tests, one for each of measured, minimum, and maximum anomaly widths, so as described previously we will reject the null hypothesis if N(e)/N(p) is less than 0.0167 for all three tests. N(p) is 300, 300, and 100, respectively, for the three tests. Comparisons of figures 12 and 13 allow counting of N(e). Scale differences preclude combining figures 12 and 13 without sacrificing needed detail, but the observed pattern is represented in both figures by an asterisk to facilitate comparison.

TABLE 4.-- FOLLOWING PAGE

FIGURE 13.-- FOLLOWING TEXT

For measured widths note that the upper right cell of figure 12A has five quadruplets and ten triplets, and would plot at $q = 5$, $t = 10$ in figure 13A. Comparison of the two figures is aided by observing that no simulated patterns can plot above or to the right of this cell in either figure. For $k = 0$ (no quintuplets) all simulated patterns plot to the left of the appropriate dashed line, and so cannot contribute to N(e). The same is true for the five simulated patterns with $k = 1$, all of which have $q = 0$. However, the one simulated pattern that has $k = 2$ plots at (0,1) (fig. 12A), which falls to the right of the appropriate dashed line (fig. 13A). N(e) comprises the following contributions: 0 from $k = 0$, 0 from $k = 1$, and 1 from $k = 2$. The level of significance is 1/300 = 0.0033. This value is smaller than the pre-chosen level of significance 0.0167, so for measured widths we reject the null hypothesis that the observed pattern has anomalies located by random scattering.

TABLE 4.--Total counts of m-tuplets produced by all simulations together

Widths	Triplets	Quadruplets	Quintuplets	Sextuplets
Measured	817	109	7	0
Minimum	517	51	0	0
Maximum	483	155	14	1

For minimum widths the dashed line of figure 13B passes through the center of the cell (2,2) in figure 12B. Because the dashed line slopes steeply down to the right only two simulated patterns plot in cells whose centers lie to the right of the dashed line (fig. 12B). N(e) = 2 so the level of significance is 2/300 = 0.0067. This value is less than 0.0167, so for minimum widths we also reject the null hypothesis.

For maximum widths the upper right cell of figure 12C would plot at q = 10, t = 15 in figure 13C. The point (10,15) lies to the left of the dashed lines for k = 0 and k = 1 (fig. 13C), so for these two serial sections no simulated patterns can plot to the right of the corresponding dashed lines or contribute to N(e). For k = 2 two simulations plot at (0,3) and (1,3) (fig. 12C). Both points lie to the left of the dashed line for k = 2 (fig. 13C). So far no serial section has contributed to N(e). However, we consider that the simulated pattern with the sextuplet (fig. 12C) has more strongly coincident anomalies than does the observed pattern. Then N(e) = 1 so the level of significance is 1/100 = 0.01. This value is less than 0.0167, so for maximum widths we again reject the null hypothesis.

The result of the statistical testing is that, regardless of uncertainties in anomaly widths, the observed pattern contains anomalies that coincide significantly more strongly than would be expected if the anomalies had been scattered randomly along the Wasatch fault zone.

Interpreting a Single Anomalous Part of the Fault Zone

The degree of coinciding among anomalies in the observed pattern is statistically significant because there are unusually many places where unusually many anomalies coincide. All four anomalous parts of the fault zone, and all of their component anomalies, are required to support this conclusion of significance. No one anomalous part of the fault zone can be singled out as significant in itself. For example, random processes occasionally produced a single quintuplet and commonly produced a single quadruplet (fig. 11A). Thus, our analyses allow interpretation of the observed pattern as a whole, but not of any one part of it in isolation. Interpretation of a single anomalous part of the fault zone could be based on a geological description of the history and present state of that part of the fault zone, to demonstrate that the individual anomalies that coincide there are genetically linked instead of randomly coincident. Such description and demonstration lie beyond the scope of this report.

DISCUSSION

Segmented Ruptures

We have shown that the Wasatch fault zone has been segmented persistently through much of the late Cenozoic. We still need to show that ruptures from large earthquakes on the fault zone are segmented at the same places. The Wasatch Range and San Pitch Mountains and the valleys that border them on the west (fig. 1) form a crustal block that is segmented gravitationally, magnetically, seismologically, and structurally. The Wasatch fault zone that traverses this block is itself segmented geometrically by salients. These expressions of segmentation coincide at salients, and only there. We concluded that the coinciding takes place not by chance, but because salients have the same cause as the other expressions of segmentation. We consider the salients to be segment boundaries.

The salients have map widths and structural reliefs that are measured in kilometers (Davis, 1983a, b, 1985; Zoback, 1983, fig. 6). Such structural relief presumably accumulated by seismic rupture. The structural relief of a salient is many hundreds to thousands of times larger than the few meters of relief that would be produced by one rupture. For example, from values given by Zoback (1983) and Schwartz and Coppersmith (1984) the salients have structural reliefs of about 2.6-4.0 km, which was produced about two m at a time by ruptures recurring at intervals of about 2000-8000 years. Such structural relief would have taken about 2.6-16 million years to accumulate, or much or all of the history of the Wasatch fault zone (the past 10 million years or more: Naeser and others, 1983). Thus, the Wasatch fault zone and the rocks adjacent to it are segmented and this segmentation has persisted through much or all of the fault's evolution.

However, none of the six data types of this report record properties of individual large seismic ruptures or groups of large ruptures. The moderate association of the four segment boundaries with seismological anomalies (figs. 7, 9) indicates that the salients affect the seismicity of the fault zone, at least for the small earthquakes that define the seismological anomalies. However, the segmentation hypothesis of Schwartz and Coppersmith (1984) states that large ruptures will tend to start, stop, or do both at segment boundaries, and that no ruptures are likely to cross boundaries into adjacent segments. Results so far are consistent with the possibility that large ruptures might start at salients and propagate in both directions along the fault zone, so that ruptures would span salients and extend simultaneously into both adjacent segments. The nature of the association between the segmented fault zone and the behavior of large seismic ruptures cannot be inferred from information presented so far.

The logical jump from a geometrically segmented fault zone to segmented ruptures requires information about the ruptures. Such information comes from recent USGS mapping of the late Quaternary history of the Wasatch fault zone (Machette and others, 1986, in press; Nelson and Personius, 1987; Personius, 1985, 1986; Scott and Shroba, 1985). From field mapping, analyses of profiles of fault scarps, maps of trenches dug across scarps, and related chronological and stratigraphic information these workers concluded that Holocene and latest Pleistocene surface-rupturing events on the fault zone have been segmented. They infer the existence of ten segments separated by nine boundaries.

Four of these segment boundaries in Holocene to latest Pleistocene surface ruptures occur at the Pleasant View, Salt Lake, Traverse Mountains, and Payson salients. At these four places where the fault zone is geometrically segmented, the surface ruptures that represent the last few large increments of the fault's growth that were caused by seismic activity are also segmented. If one assumes that earlier (Pleistocene) surface ruptures behaved like the younger ruptures, then the older ruptures were also segmented at the four salients. We make that assumption, and conclude that the four salients of the Wasatch fault zone were persistent boundaries for individual large seismic ruptures through most or all of the evolution of the fault zone.

Persistent and Nonpersistent Segment Boundaries

Three studies have inferred segment boundaries from examinations of younger geologic records than we used (fig. 14). Schwartz and Coppersmith (1984) divided the Wasatch fault zone into six segments. Most of their information came from the Holocene record that was exposed in and near trenches at four sites along the fault zone (fig. 1). Maclean (1985) studied morphology and morphometry of 98 drainage basins that evolved throughout the Quaternary in the footwall of the fault zone. For this time span, Maclean (1985) and Mayer and Maclean (1986) divided the fault zone into nine segments. M.N. Machette and coworkers (unpublished data) have mapped and examined the late Quaternary history of the fault zone. Their studies cover nearly all the length of the fault zone in Utah, and record numerous aspects of the single- and multiple-event scarps that form the most striking expression of the late Quaternary seismic history of the fault zone. They divided the fault zone into ten segments. The nine late Quaternary segment boundaries of Machette and others (1986) represent the most complete and uniform description of segmentation of the last few large seismic ruptures on the various parts of the fault zone.

FIGURE 14.-- FOLLOWING TEXT

Each of these three studies of a young geologic record recognized the four persistent segment boundaries, except that Schwartz and Coppersmith (1984) did not identify the Pleasant View boundary (fig. 14). Each of these three studies also interpreted 2-5 additional segment boundaries. However, agreement on these other boundaries was much poorer than on the four persistent boundaries. Other boundaries were inferred at seven or eight places, but only two or three of these boundaries were chosen by two of the three studies, and none was chosen by all three (fig. 14).

Our preferred interpretation of these discrepancies is that most represent real changes through time instead of error by one or more studies including ours. A segment boundary that is recognized in one young geologic record but not in another, and not in the pre-Quaternary record, might be nonpersistent. A nonpersistent boundary is one that nucleates or stops several successive seismic ruptures, but which does not do so before or after the time spanned by these several ruptures. The location, time of turning on, and duration of a nonpersistent boundary might be controlled by older structures, but this control might be so subtle or complex that it cannot be distinguished from the operation of random processes. Then the location, appearance, and disappearance of a nonpersistent boundary could be observed but not predicted.

A useful guide to considering these hypothetical nonpersistent boundaries is the idea of nonconservative barriers (King, 1983; King and Yielding, 1984; King and Nabelek, 1985). Faults contain geometric irregularities such as bends, forks, and bumps. Where an irregularity is extreme enough that the orientation of the slip vector cannot be conserved across it, the irregularity is a nonconservative barrier. Geometric consequences of this change in slip vector orientation cause ruptures to tend to start and stop at nonconservative barriers. Bruhn and others (in press a,b) analyzed the Salt Lake and Traverse Mountains salients and interpreted them as nonconservative barriers. Nelson and Personius (1987) interpreted the Pleasant View boundary similarly. Geometric irregularities such as salients are large enough and extreme enough that they likely will endure considerable slip, and likely will persist through much or all of the history of a fault zone like the Wasatch. Narrower forks, gentler bends, and smaller bumps might force the slip vector to change orientation across them for a few successive ruptures, but then might be smoothed out by abrasion of the bumps and insides of the bends and by abandonment of one branch of each fork. Such lesser geometric irregularities could be formed where lithology, strength, and other rock properties vary along the fault zone. The interactions of these lesser variations with the rupture processes are likely to be complex enough that nonpersistent boundaries could appear to be scattered randomly along the fault zone, and to form and disappear randomly through the history of the fault zone. The idea of nonconservative barriers suggests reasonable explanations for the appearance and disappearance of a nonpersistent boundary, for its expected duration over several successive ruptures, and for any inability to predict its location, time of appearance, or duration.

If nonpersistent boundaries exist, as they appear to, they would pose a problem for hazard evaluation. The past behavior of a persistent boundary is a guide to its likely behavior in the coming decades to millenia, which is the time span of interest to hazard evaluation. A nonpersistent boundary might be the starting or ending point of a rupture, might limit the maximum length of a rupture and therefore the maximum size of the earthquake, or might do neither, without much regard for the recent behavior of the boundary. Fortunately most of the recent boundaries appear to be persistent (three of four) in the populous central part of the Wasatch Front between Brigham City and Provo (fig. 14). Most of the suggested boundaries that might be nonpersistent are farther north or south, where fewer people and engineered structures are at risk.

Bedrock Ridges

Each salient coincides with one or two transverse gravity anomalies (fig. 7A). Although each transverse gravity anomaly is built up from several components (gradients and their ends, ends of elongate highs and lows, and the like), each also has the general form of a gravity saddle: a local interruption in the long gravity low that trends northward along the west side of the Wasatch fault zone (Zoback, 1983). Four of the five saddles with the greatest gravity relief are those that coincide most closely with the salients, transverse anomalies G4, G5, G7, and G9 (fig. 7A). Zoback (1983), Mabey (in press), and we interpret each gravity saddle as the expression of a bedrock ridge, partly or wholly buried by the low-density Cenozoic fillings of the valley basins that underlie the north-trending gravity low. The bedrock ridges trend across the north-trending basins, so the gravity saddles mark places where the basins are less deep than under the adjacent valleys to north and south. Because the basins formed by slip on the Wasatch fault zone, the gravity saddles also mark places where structural relief and the accumulated slip that created the relief are less than to north and south.

The Traverse Mountains segment boundary is the clearest example of a bedrock ridge and its gravity expression (fig. 15). The ridge, partly exposed as the eastern Traverse Mountains, is at least partly bounded by faults that have slipped during the Quaternary, as has the Wasatch fault zone. The isogals show that the bedrock ridge extends across the valley, although the western part of the ridge is buried. Structural relief on the Wasatch fault zone is much less at the ridge than in Salt Lake or Utah Valleys. The relief between the salient and the bottoms of both valleys is partitioned among a network of extensional faults, including the normal fault that separates the salient from the Traverse Mountains (fig. 15), normal faults that are mapped within the eastern Traverse Mountains (Davis, 1983b), normal faults that are mapped as separating the Traverse Mountains from Utah Valley (fig. 15) and are inferred to do the same at Salt Lake Valley (Mattick, 1970; Houghton, 1986, p. 52), and perhaps still other normal and normal-oblique faults that underlie the east-trending gravity gradients at the north end of Utah Valley and the south end of Salt Lake Valley (for example, Okaya and Thompson (1985) described three buried normal faults that step down into the deepest part of a graben and that underlie a gravity gradient in Dixie Valley, Nevada).

FIGURE 15.-- FOLLOWING TEXT

Two processes can explain the observed association of salients with bedrock ridges and small structural relief across the Wasatch fault zone. The first process arises from the requirement that slip for any earthquake must decrease to zero at the edges of the rupture zone. King (1986) postulated that slip measured along the ground rupture of a single earthquake will be largest in the middle and will taper toward the ends of the ground rupture, so that the ends have a slip deficit compared to the middle portion. Measurements on historical ground ruptures of large, normal-faulting earthquakes in and near the Basin and Range province show much local variation along the ruptures, but in general support King's postulate (Byerly, 1956; Tocher, 1956; Slemmons, 1957; Slemmons and others, 1959; Myers and Hamilton, 1964, plate 2; Crone and Machette, 1984; Wallace, 1984, fig. 28). Large ruptures on normal faults will tend to have ends (start, stop, or do both) at persistent segment boundaries, so over time these boundaries will accumulate large slip deficits compared to segment interiors. The slip deficits will be expressed as structural reliefs across the fault zone that are smaller at the boundaries than in segment interiors.

The second process is implicit in the model of a nonconservative barrier (King and Nabelek, 1985). Imagine a simple, planar, normal-fault zone that strikes north, dips west, and slips an arbitrary eight units (fig. 16). For simplicity we ignore slip-tapering toward rupture ends. Tapering of slip only accentuates the result that is described below. Suppose that two strands within the fault zone rupture toward each other, not necessarily simultaneously, with slightly divergent slip vectors. Convergent slip vectors would produce a more complex but otherwise similar result. The divergence causes extension in the hanging wall at the north end of the south rupture; arguments analogous to those that follow apply to the south end of the north rupture. The southward extension in the hanging wall can be accomodated if the north end of the main fault strand forks, say at 45° to the northwest (location A, figure 16). Suppose that the two forks share equally the slip on the single fault strand, so that each branch of the fork slips four units. Geometric requirements of brittle slip force each branch to fork again, and so on down to sizes at which the rock mass no longer acts like distinct rigid blocks (King, 1983). After three forkings, the north end of the hanging wall is broken into blocks that step downward to the south and west (fig. 16), forming a fault network that is the process zone of the nonconservative barrier (King and Nabelek, 1985). Structural relief of the blocks in the hanging wall decreases northward and eastward across the fault network. If a similar thing happens at the south end of the north rupture, the result is a ridge that plunges westward across the barrier, from B to C in figure 16. Slip taper will decrease the westward plunge of the ridge. If the barrier is a persistent segment boundary, then over the course of many ruptures the ridge will increase its structural relief compared to adjacent parts of the footwall.

FIGURE 16.-- FOLLOWING TEXT

Suppose that sediment accumulates on the downdropped blocks, as it has in Salt Lake and Utah Valleys (fig. 15). If the fault pattern of figure 16 were buried to level -0.5, halfway between the top of block D and the top of the footwall block, the result would be a buried bedrock ridge. The low-density sediments would be thinner over the ridge than in the valleys to north and south, creating a gravity saddle. If sediment cover reached only to level -1.5, the eastern, fault-bounded end of the ridge would be exposed as a salient like the Pleasant View and Salt Lake salients, or like the eastern Traverse Mountains. If cover were still thinner, reaching to levels between -5.5 and -7.5, an exposed bedrock ridge would separate the two valleys, as is the case west of the Payson salient (Hintze, 1980).

Consideration of figure 16 suggests a way to estimate the relative persistence of some segment boundaries, averaged over the whole history of the fault zone. If the boundary is perfectly persistent the fault must end there. If the boundary is so persistent that few ruptures cross it, block D of figure 16 will have no throughgoing fault of large throw on its eastern side, and might be part of the footwall block. A bedrock ridge will be exposed across most or all of the valley. This is the case at the Traverse Mountains salient (fig. 15), which is cored by the massive Little Cottonwood stock of Oligocene age (Crittenden and others, 1973). If more ruptures cross the boundary, they will tend to drop block D down a bit more compared to the footwall, but the bedrock ridge might still be exposed. Both are the case at the Payson salient (Davis, 1983b; Machette and others, in press). As successively larger proportions of the ruptures cross the boundary, first the bedrock ridge will be buried (as at the Salt Lake salient; Davis, 1983a), then the salient itself will be buried or nearly buried (as at the Pleasant View salient; Crittenden and Sorenson, 1985), and finally the gravity saddle will flatten and nearly disappear at boundaries that persist for only a few successive ruptures.

Thus, on the Wasatch fault zone the most obvious expression of a persistent segment boundary is an exposed salient, but the key to estimating relative persistence of several boundaries is the relative sizes of the structural reliefs between footwall, salient, bedrock ridge, and adjacent valley bottoms. For segment boundaries of intermediate persistence, or boundaries that have been persistent only for the most recent portion of a fault's history, bedrock ridges might be more diagnostic than are salients. Where Bouguer gravity data are abundant, as along the Wasatch Front, relative structural relief can be estimated easily, but along other fault zones with sparse or no gravity coverage relative structural relief must be estimated indirectly.

Applications to Large Historic Earthquakes

The conclusion that bedrock ridges and salients, where coincident with the ends of large individual ruptures, identify persistent segment boundaries on the Wasatch fault zone can be generalized to other normal-fault zones in and near the Basin and Range province. We test the generalization by examining the ends of ground ruptures from single large historic earthquakes.

Borah Peak, Idaho, October 28, 1983

Crone and others (1987) summarized evidence that the two ends of the mainshock rupture zone occurred at persistent boundaries of the Thousand Springs segment of the Lost River fault zone (fig. 17). At the southeastern boundary, here named the Elkhorn Creek segment boundary, the fault zone cuts the older Borah Peak horst. Geologic mapping and a gravity saddle indicate that the horst extends as a bedrock ridge southwest to the mainshock epicenter (Skipp and Harding, 1985). Crone and others (1987) suggested that the horst and its faults extend to the depth of the mainshock hypocenter (about 15 km: Doser, 1985a; Dewey, 1987) because some of the faults have up to three km of throw and because a similar horst about 25 km to the south is cored by an Eocene pluton. Surface faulting in 1983 followed Holocene scarps along the Thousand Springs segment (Crone and Machette, 1984). A gap of 4 km separates that faulting and those scarps from evidence of recurrent late Quaternary surface faulting along the entire length of the Mackay segment, indicating that at least two pre-1983 ruptures also had ends at the Elkhorn Creek boundary. About 5-10 mgal of gravity relief across the gravity saddle from northwest to southeast (Skipp and Harding, 1985) indicate that many ruptures have had slip deficits, and presumably ends, at the boundary during the evolution of the Lost River fault zone.

FIGURE 17.-- FOLLOWING TEXT

At the northwestern boundary of the main rupture zone, here named the Willow Creek Hills segment boundary, a bedrock ridge is exposed most of the way across the valley. Zones of small, discontinuous surface offsets and cracks fork to extend northwest into the bedrock ridge and north along the Warm Spring segment. However, the main rupture was confined to the Thousand Springs segment, as determined from geological (Crone and Machette, 1984), geodetic (Barrientos and others, 1987), and seismological (Doser and Smith, 1985) evidence. The 1983 rupture of the Thousand Springs segment repeated an early Holocene (Hanks and Schwartz, 1987) rupture of the same segment, with striking fidelity (Salyards, 1985; Vincent, 1985; and especially Schwartz and Crone, 1985). The Warm Springs segment ruptured at about the same time in the early Holocene or more recently, but neither Holocene rupture broke the Willow Creek Hills boundary (Crone and others, 1987). The exposed bedrock ridge indicates that many previous ruptures behaved similarly. Structural relief across the Lost River fault zone there is about half that in the interior of the Thousand Springs segment (Crone and others, 1987).

Thus, both boundaries of the main 1983 rupture have been persistent, and both form bedrock ridges as along the Wasatch fault zone. There is no fault-bounded salient at the Willow Creek Hills boundary. At the Elkhorn Creek boundary, the sharp bend in the Lost River fault zone is much less sharp than the bends in the Wasatch fault zone at the Salt Lake, Traverse Mountains (fig.

15), and Payson salients, but resembles in shape the bend at the Pleasant View salient (Crittenden and Sorensen, 1985). The corner of the footwall block at Elkhorn Creek is broken by several small faults (Susong and Bruhn, 1986), and in this respect has a structural character between the unfaulted Traverse Mountains salient (fig. 15) and the moderately faulted Payson salient (Hintze, 1980). The Pleasant View and Salt Lake salients are separated from the main footwall block by normal faults of much larger throw. We choose not to call the bend at Elkhorn Creek a salient because that would stretch the term beyond the limit of usefulness.

Both boundaries have been interpreted as barriers to the propagation of the rupture zone (Boatwright, 1985; Crone and others, 1985). We further interpret both as nonconservative barriers. Slip-vector orientations are too sparse to determine whether orientations change across either boundary (A.J. Crone, oral commun., 1987), as Bruhn and others (in press a, b) have done for the boundaries of the Salt Lake segment. However, at the Elkhorn Creek boundary many ruptures have had ends at about the same place, including at least the last three ruptures. The northeast-striking normal faults of the Borah Peak horst form a network with the northwest-striking Lost River fault zone. Within the bend in the range front the Lost River fault zone expands into a skein of northwest-striking fault strands that cut diagonally across the bend, and some of the strands were reactivated in 1983 (Susong and Bruhn, 1986). The 1983 rupture started at the horst and propagated unilaterally northwestward. Crone and others (1987, p. 763) speculated that the faults of the horst "...could create irregularities or obstructions on the Lost River fault plane that might inhibit propagating ruptures...." All of these characteristics are properties that would be expected of a nonconservative barrier (King and Nabelek, 1985).

At the Willow Creek Hills boundary at least the last three ruptures and many previous ones have had ends. Early aftershocks in 1983 clustered in the boundary and the northern part of the Thousand Springs segment (Richins and others, 1987). After November, 1983, aftershocks migrated through the boundary into the Warm Springs segment (Zollweg and Richins, 1985). Aftershocks at and near the boundary tended to have large magnitudes, high stress drops, and focal mechanisms with diversely oriented nodal planes (Boatwright, 1985; Richins and others, 1987), as though strain were being accomodated by breaking bit by bit through a network of interlocked faults. Crone and others (1987, p. 764) speculated about intersecting faults there similarly as they did for the Elkhorn Creek boundary. Geodetic modeling (fig. 14 of Barrientos and others, 1987) indicates that rupture in the boundary extended to lesser depths and involved less slip than did rupture on the Thousand Springs segment, as though the boundary at depth had larger fracture toughness than did the segment interior. All of these characteristics are also expected properties of a nonconservative barrier. Thus, although we lack slip-orientation data across the Willow Creek Hills and Elkhorn Creek segment boundaries, the 1983-1984 earthquake sequence revealed enough characteristics of the two boundaries that we conclude they are nonconservative barriers.

Hebgen Lake, Montana, August 17, 1959

The main shock consisted of two subevents (Ryall, 1962), the first at about 10 km depth, followed five seconds later by a much larger subevent at about 15 km depth (Doser, 1985b). Epicenters are poorly constrained but most teleseismic epicenters for the main shock, its subevents, and large aftershocks, and epicenters of small aftershocks determined from a portable network, cluster around the southeastern half of the trace of the Red Canyon fault, near the southeastern end of ground ruptures (fig. 18; Stewart and others, 1964; Trimble and Smith, 1975; Doser, 1985b). Geodetic modeling indicated that rupture occurred on two planes that dip southwest from the traces of the Hebgen and Red Canyon faults, with the rupture down dip from the Hebgen fault extending to greater depth but having about the same length and slip as that down dip from the Red Canyon fault (Barrientos and others, 1987). However, the first subevent was so much smaller than the second that both planes must have slipped during the second subevent (Barrientos and others, 1987). Therefore, it is not known which plane or which outcropping fault slipped first to produce the first subevent and presumably trigger the second.

FIGURE 18.-- FOLLOWING TEXT

The results described above have two interpretations in terms of segment boundaries and barriers. The first is that the fault-bounded Red Canyon fault block (fig. 18) is a salient and a persistent boundary between the Hebgen and Red Canyon segments of the southwest-dipping Hebgen-Red Canyon fault zone. In this interpretation the Hebgen Lake earthquake, the largest normal-faulting shock so far recorded in or near the Basin and Range province, was one of the few earthquakes that rupture past the salient to give it a structural relief intermediate between those of the hanging wall and the footwall. If the salient is a nonconservative barrier, its expected high fracture toughness could require an unusually large earthquake to drive a rupture all the way through the process zone. Alternatively, if previous earthquakes had strained the barrier until it was ready to fail, the comparatively small first subevent could have triggered that failure in the form of the much larger second subevent, with its unusually large slip and stress drop (Barrientos and others, 1987).

We prefer the second interpretation, that the Hebgen-Red Canyon fault zone is young, and that its still-evolving geometry has not yet stabilized enough to justify interpretation in terms of persistent segment boundaries and long-lasting barriers. The youth of the fault zone has several bases. First, Barrientos and others (1987) summarized evidence that the fault zone is part of a fault system about 0.6-2.0 m.y. old, only about 12-50 percent the estimated age of the Lost River fault zone. Second, Witkind and others (1962) and Myers and Hamilton (1964, p. 85-87) observed that younger ground ruptures, including those of 1959, tend to extend into unbroken rock beyond the ends of older faulting. Barrientos and others (1987) suggested that the high stress drops inferred for the mainshock subevents could reflect fresh breaks of largely intact rock. Third, geologic mapping of Witkind and others (1964, plate 5) shows that there is little cumulative slip across the ends of the comparatively short traces of the Hebgen and Red Canyon faults, and that there is no deep, sediment-filled valley on the downthrown block, indicating few slip events and presumably a short history compared to the Lost River or Wasatch fault zones. Fourth, in 1959 the largest ground-level slip on the Red Canyon fault was 9-15 ft (2.7-4.6 m) after correcting for local slumping (Myers and Hamilton, 1964, plate 2). Near the same place the fault has its largest cumulative slip of about 1000 ft (303 m) (Witkind and others, 1964, plate 5). If slip in 1959 was typical of large events on the Red Canyon fault, such events have occurred no more than 67-111 times. Lesser slips in smaller earthquakes would decrease this number. If the fault is 0.6-2.0 m.y. old, the recurrence interval for slips like that of 1959 is at least 5,400-

29,800 yr, which is consistent with evidence for several late Quaternary scarp-forming events on the Hebgen-Red Canyon fault zone (Myers and Hamilton, 1964). Fifth, from structural, geomorphic, and geodetic evidence Myers and Hamilton (1964, p. 91-96) concluded that through Quaternary time a new system of east-striking normal faults has been propagating eastward into the region near and south of Hebgen Lake, cutting across and reactivating parts of older, northwest-striking faults. Although the Hebgen and Red Canyon faults strike northwest, overall subsidence in 1959 formed an east-trending basin (Myers and Hamilton, 1964, plate 2).

That the geometry of the fault zone is still evolving would be suspected from its youth alone. Additional support comes from the observation that the traces of the Hebgen and Red Canyon faults lie near and in the down-dip direction from the traces of older thrust faults (fig. 18). From this Myers and Hamilton (1964) concluded that the normal faults probably reactivated the thrust faults in the shallow subsurface. However, they also note that the thrust complex is probably only a few km thick, so that the shapes of the normal faults in map view are unlikely to resemble their shapes at hypocentral depths. In particular, the curve of the Red Canyon fault around the Red Canyon fault block is probably a near-surface feature, as is the block itself. The two southwest-dipping rupture planes that were inferred from geodetic data converge downward. We speculate that eventually the Hebgen fault will connect with the eastern half of the Red Canyon fault, abandoning the Red Canyon fault block to the footwall of the fault zone. At depth, this evolution might have occurred already. If the Red Canyon fault block is shallow and ephemeral, interpretations of the Hebgen-Red Canyon fault zone in terms of persistent segment boundaries and long-lasting barriers are premature by at least several hundred thousand years.

Rainbow Mountain, Nevada, July 6 and August 24, 1954

The Rainbow Mountain fault zone produced discontinuous, normal-slip, surface ruptures with less than 1 m of surface offset twice within seven weeks (Tocher, 1956). The July mainshock (fig. 19A, epicenter A) comprised two subevents about eight seconds apart, the first and larger occurring at 10 km depth in right-normal slip, and the second at 7 km in mostly normal slip (Doser, 1986). The August mainshock (epicenter C) involved three subevents starting over 22 seconds, all at about 12 km depth, of decreasing sizes, and involving right-normal slip (Doser, 1986). From epicenters, focal mechanisms, and locations of ground ruptures Doser (1986) inferred that the fault zone broke in two overlapping sections, the southern portion in July and the northern portion in August, with each rupture zone propagating northward. Large aftershocks (Doser, 1986) and small earthquakes in 1969-1970 (Ryall and Malone, 1971) clustered near epicenters A and C of fig. 19A. The southern part of the surface breaks passed along the straight east side of Rainbow Mountain (Slemmons, 1956; Stewart and Carlson, 1978), but otherwise the rupture "...did not in its entirety follow any previously recognized fault..." (Tocher, 1956, p. 10). Sparse gravity data between exposed Cenozoic andesites and basalts of Rainbow Mountain and the southern Stillwater Range indicate a thin cover of sediments there, but are too few to support inferences of the shape of the buried bedrock surface (fig. 19B; Erwin and Berg, 1977).

FIGURE 19.-- FOLLOWING TEXT

The Rainbow Mountain earthquakes illustrate an important point about inferring segmentation of a fault zone. Despite the geologic, gravity, and seismological investigations of the earthquake sequence and its surroundings, there are too few data to determine whether any previous earthquakes had ends where the 1954 rupture zones started and stopped. The idea of segmentation requires that at least a few ruptures have had ends at about the same place. We cannot demonstrate coincident ends of successive ruptures on the Rainbow Mountain fault, so we cannot show that the 1954 breaks were not randomly distributed along an unsegmented fault zone. As shown by the discussions of other historic earthquakes in this report, the most useful evidence for such a demonstration comes from field investigations of scarps and other records of Holocene and late Pleistocene earthquakes, and from geophysical delineation of changes in structural relief along a fault zone.

Fairview Peak-Dixie Valley, Nevada, December 16, 1954

Four months after the Rainbow Mountain earthquake sequence another sequence on the opposite side of the Stillwater Range produced information from which segmentation can be inferred. Bilateral rupture near the middle of the graben-bounding Fairview fault began at 15 km depth, involved as many as three subevents starting over 16 seconds, and also broke the opposite bounding fault of the graben (West Gate fault) and a third fault (Gold King fault) that is on strike north of the Fairview fault but dips oppositely to it (fig. 19A; Doser, 1986). Slip was right-normal at the hypocenter and at the surface on the Fairview and southern West Gate faults, but the Gold King and northern West Gate faults showed only normal slip at the surface (Larson, 1957; Slemmons, 1957; Slemmons and others, 1959; Doser, 1986). However, the following summer geodetic measurements detected about 2 m of right slip that had occurred since the summer of 1954 across the southern Gold King and northern West Gate faults (Whitten, 1957), so either coseismic or postseismic right-normal movement characterized all three faults. Small earthquakes in 1966 and 1969-1970 mostly clustered between the mainshock hypocenter of 1954 and the southern part of the trace of the Fairview fault, with right-normal slip (Stauder and Ryall, 1967; Westphal and Lange, 1967; Ryall and Malone, 1971).

Four minutes after the Fairview Peak earthquake, a smaller shock broke the Dixie Valley fault (fig. 19A), beginning at 12-15 km depth in two subevents starting six seconds apart, perhaps propagating bilaterally (Okaya and Thompson, 1985; Doser, 1986). Slip was normal at the hypocenter (Doser, 1986) but at the surface it was right-normal northeast of a sharp bend in the fault trace (at the letters DVF in figure 19A) and left-normal south of the bend (Slemmons, 1957; Slemmons and others, 1969). Small earthquakes in 1969-1970 were few but most clustered between the mainshock epicenter and the trace of the Dixie Valley fault (Ryall and Malone, 1971).

The following evidence indicates that the narrow passage between Dixie and Fairview Valleys is a persistent segment boundary of the fault zones on both sides of the valleys. We name it the Pirouette Mountain boundary. On the east side of the valley, in 1954 the Fairview-West Gate-Gold King rupture ended there. Although surface faulting broke the boundary along the Gold King fault, slip there was small and discontinuous and occurred with opposite dip to that on the Fairview fault (Slemmons, 1957), analogously to surface faulting in 1983 in the Willow Creek Hills boundary on the Lost River fault (fig. 17). The Gold King fault also produced at least 3 miles (5 km) of surface faulting in the Fall of 1903 (Slemmons and others, 1959). The 1903 rupture was confined to the Pirouette Mountain boundary, indicating that the boundary differs mechanically or in its strain history from parts of the same fault zone to north and south. Slemmons (1956, fig. 2) depicted the fault zone on the east sides of Dixie and Fairview Valleys as having had late Quaternary slip. In both valleys the fault zone separates Quaternary sediments from pre-Quaternary bedrock of the Clan Alpine and adjoining ranges (Stewart and Carlson, 1978). Accordingly, in both valleys the fault zone has probably accumulated at least a few tens of meters of structural relief. However, in the Pirouette Mountain boundary the fault zone crosses exposed bedrock as the Gold King fault, with little or no accumulated structural relief (Slemmons and others, 1959). Therefore, at least one and probably several pre-1903 faulting events either stopped at the Pirouette Mountain boundary or decreased their slip markedly for 5-10 km across the boundary. The latter is unlikely, because maps and longitudinal profiles of slip data measured along surface ruptures of large historic earthquakes in and near the Basin and Range province indicate that slip from single earthquakes varies markedly over distance of 1-2 km, and can shift from one fault strand to another where their tips overlap, but that stretches of small slip that are 5-10 km wide usually exist only at the ends of ruptures (Slemmons, 1957; Myers and Hamilton, 1964, plate 2; Crone and Machette, 1984; Wallace, 1984, fig. 28). We conclude that the Pirouette Mountain boundary has been a late Quaternary segment boundary.

Geophysical evidence indicates that the boundary has been persistent. Gravity modeling across Dixie Valley and seismic-reflection profiles, all near the north end of the 1954 ground ruptures, indicate up to 2 km of Quaternary sediments, thickest in the west half of the valley (Okaya and Thompson, 1985). Seismic refraction studies in Dixie Valley indicate depths to pre-Tertiary bedrock as great as 3.2 km in a central graben about 25 km north of

Pirouette Mountain, shallowing southward to 1.1 km in the passage between Dixie and Fairview Valleys (Meister, 1967). Sparse Bouguer gravity data show a poorly defined gravity saddle at the boundary (fig. 19B), with about 20 mgal of gravity relief compared to the centers of Dixie and Fairview Valleys (Erwin and Berg, 1977). A local gravity high, perhaps attributable to exposed Cenozoic and Mesozoic andesites, rhyolites, and tuffs, masks any gravity relief that might exist between the boundary and the narrow valley between the Fairview and West Gate faults (fig. 19B; Erwin and Berg, 1977). Thus, Pirouette Mountain is the exposed eastern end of a largely buried bedrock ridge that separates Dixie and Fairview Valleys. The Pirouette Mountain boundary lacks a fault-bounded salient or a projecting spur like the persistent boundaries of the Wasatch fault zone, and more closely resembles the Willow Creek Hills boundary of the Lost River fault zone, where the bedrock ridge is exposed, and the Elkhorn Creek boundary, where the ridge is buried (fig. 17). Because pre-Tertiary bedrock is shallower at the bedrock ridge than under Dixie and Fairview Valleys, ruptures along the east sides of both valleys have tended to lose slip and probably stop there persistently throughout the evolution of the valleys. The same might be true for the graben and valley between the Fairview and West Gate faults, and was true in 1954.

On the west sides of Dixie and Fairview Valleys, the 1954 Dixie Valley rupture ended at the Pirouette Mountain boundary. The gravity saddle indicates that many other ruptures also did so throughout the evolution of both valleys. Accordingly, the bedrock ridge at Pirouette Mountain has persistently segmented the fault zones on both sides of the valleys.

The manner in which the 1954 ruptures jumped from the east-dipping Fairview fault across the Pirouette Mountain boundary to the east-dipping

Dixie Valley fault suggests an analogy to the north end of the 1983 Borah Peak rupture of the Lost River fault zone (fig. 17). At the Willow Creek Hills boundary the rupture broke discontinuously and with little slip northwestward through the boundary, forming or reactivating faults that dip oppositely to the main rupture along the Thousand Springs segment. Previously we interpreted results of rupture mapping, aftershock studies, and geodetic modeling to suggest that at the Willow Creek Hills boundary the 1983 rupture and its aftershocks broke, bit by bit, through a network of interlocked faults that form the process zone of a nonconservative barrier, after the model of King and Nabelek (1985). For the Dixie Valley and Fairview Peak earthquakes, Snay and others (1985), modeled geodetic data and suggested that slip in 1954 also occurred on a buried fault that strikes north-northwest, dips steeply east-northeast, and underlies southern Dixie Valley, the Pirouette Mountain boundary, and northern Fairview Valley. Perhaps the 1954 and 1983 ruptures represent different expressions of the same phenomenon, in which most large ruptures on the Fairview Valley and Thousand Springs segments stop at the Pirouette Mountain and Willow Creek Hills boundaries, but some break through to rupture the Dixie Valley and Warm Spring segments.

The north end of the 1954 surface rupture of the Dixie Valley fault is not a segment boundary. The end overlaps by 15-20 km the south ends of Holocene and late Pleistocene scarps (Wallace and Whitney, 1984) and there is no gravity saddle there (fig. 19B). Perhaps rupture ends in the central part of the Dixie Valley fault are distributed more or less randomly along the fault, with southern ends bounded by the Pirouette Mountain boundary and with ruptures extending northward various distances according to the amount of strain that has accumulated on this and adjacent parts of the Dixie Valley fault. This example shows the need to demonstrate that two or more rupture ends coincide before inferring the presence of a segment boundary, whether persistent or not.

Pleasant Valley, Nevada, October 2, 1915

Because of its early date little is known of this earthquake seismologically, but geological and gravity evidence and the more recent earthquakes that we have discussed previously allow some interpretation. The mainshock, two large foreshocks, or both produced five main scarps (fig. 20A; Wallace, 1984). Of these, Wallace (1984) suggested that the small Stillwater scarp might have formed by lateral spreading of a ridge instead of tectonic rupture. We will not consider this scarp further.

FIGURE 20.-- FOLLOWING TEXT

Because of its length and large displacements the Pearce scarp dominates the 1915 surface ruptures, providing 70 percent of the total estimated seismic moment (Wallace, 1984). Glass and Slemmons (1969) concluded from examination of low-sun-angle aerial photographs that nearly all the 1915 scarps, including the Pearce scarp, followed still older scarps, although these older scarps could be of diverse ages. From diverse geological observations Wallace (1984) concluded that the Pearce scarp had broken in at least one late Quaternary earthquake with displacement similar to that of 1915, probably between a few thousand and 12,000 years ago. An earthquake with such displacement would probably have broken most or all of the 30 km length of the Pearce scarp, as happened in 1915. From a trench dug across the northern tip of the Pearce scarp Bonilla and others (1984) interpreted several Holocene and late

Pleistocene displacements, each probably less than one meter, and suggested that two of them occurred in the 5,000 years before 1915. Therefore, probably the Pearce scarp has broken at least twice including 1915 and perhaps more often in the Holocene and latest Pleistocene.

To the south, the compilation of Wallace and Whitney (1984) shows no Holocene or late Pleistocene scarps on the Sou Hills scarp or in the Sou Hills, although Wallace (1984, plate 1) showed a few small pre-1915 scarps on the Sou Hills scarp and along strike to the north (fig. 20A). Individual scarps from 1915 are lower, shorter in map view, and less continuous along the Sou Hills scarp than along the Pearce scarp. At its south end the Pearce scarp splays to form numerous very short, low, east- and west-facing scarps, covering an area about five kilometers long and two kilometers wide, and dating from 1915 and earlier (Wallace, 1984, plate 1). The area resembles the shallowly buried Pleasant View salient of the Wasatch fault zone both in size and in the diffuse style of its faulting. Fonseca (1985) described the Sou Hills similarly, contrasting its late Cenozoic faulting style to that of the Tobin and Stillwater Ranges. At locality C of figure 20B a gravity saddle and the exposed bedrock ridge of the Sou Hills separate Pleasant Valley, where Erwin (1974) inferred from gravity data 2,000-2,500 ft (0.6-0.8 km) of Cenozoic alluvial filling, from northern Dixie Valley, where Speed (1976) estimated from gravity modeling 6,000 ft (1.8 km) of Cenozoic filling but Erwin (1974) inferred only about 2,000 ft (0.6 km). These observations and inferences support a suggestion that the 1915 and one or more earlier ruptures had slip deficits at the Sou Hills and stopped there, analogously to the model of figure 16.

By analogy to other fault zones discussed previously, the ending of the 1915 rupture at the Sou Hills, the gravity saddle, and the diffuse style of the 1915 and older faulting indicate that the Sou Hills is a persistent segment boundary, and perhaps a nonconservative barrier also. Fonseca (1985) drew an analogy to the Borah Peak earthquake, during which low, discontinuous surface ruptures broke into the Willow Creek Hills segment boundary and a few kilometers farther north into the Warm Spring segment (fig. 17). Similarly to the Willow Creek Hills, the Sou Hills are fault-bounded, juxtaposing Tertiary rocks of the bedrock ridge to the Triassic rocks of the adjacent Stillwater Range and the Triassic and Permian rocks of the southern Tobin Range (Muller and others, 1951). The Sou Hills have structural relief intermediate between that of the bounding ranges and the relief of Pleasant and Dixie Valleys. We follow Fonseca's (1985) usage in defining the Sou Hills segment boundary, which includes the Sou Hills scarp of Wallace (1984).

North of the Pearce scarp, at the gap that separates it from the Tobin scarp, a gravity saddle indicates a buried bedrock ridge (locality B of fig. 20B). Erwin (1974) inferred from gravity data that Grass Valley contains about 4,000 ft (1.2 km) of Cenozoic filling at the north edge of the area shown in figure 20. Throw across the Tobin scarp is at least 2,500 ft (0.8 km), comparable to Erwin's (1974) inference of 2,000 ft (0.6 km) of Cenozoic filling in northern Pleasant Valley. Throw on the Tobin scarp decreases to zero immediately south of the scarps south end (Muller and others, 1951). This evidence of accumulated slip deficits at the gap could support a speculation of a persistent segment boundary there.

However, we found no evidence that individual ruptures have had ends there. In 1915 the Tobin scarp broke an older scarp as continuously and with as large displacements as did the Pearce scarp (Wallace, 1984). The compilation of Wallace and Whitney (1984) shows late Pleistocene scarps on both sides of the gap. The compilation shows Holocene scarps along the Pearce scarp but not along the Tobin scarp. However, these Holocene scarps are so few that the difference might be erosional instead of tectonic. Also, gravity relief in both Grass and Pleasant Valleys is about 25 mgal between the valley centers and the ranges to the east, and about 40 mgal to the west, whereas relief across the saddle between the valleys is only 10-20 mgal (Erwin, 1974). If structural relief increases with gravity relief, then the structural relief across the Tobin and Pearce scarps is little less at the saddle than north or south of it. There is little accumulated slip deficit at the gap between the Tobin and Pearce scarps. Finally, Wallace (1984) observed that a piedmont surface that spans the gap slopes north and northwest, and appears to be oversteepened. He suggested that structural relief might be expressed in the gap as warping. An old scarp strikes northeast partway across the gap (fig. 20A), and could be evidence of occasional surface rupture across the gap. Thus, with insufficient geologic evidence to determine whether prehistoric ruptures crossed the gap, the buried bedrock ridge might have been produced by warping and occasional throughgoing ruptures instead of by repeated rupture ends at a segment boundary. If there is a boundary there, it did not persist through 1915.

At the north end of the 1915 ground ruptures scarps were few, low, and discontinuous compared to those on the Tobin and Pearce scarps. This was the case in 1915, probably during the Holocene, and during the late Pleistocene (Wallace, 1984; Wallace and Whitney, 1984). The China Mountain scarp is the only one from 1915 to form within a mountain block instead of along a range front. Wallace (1984) and Wallace and Whitney (1984) showed no scarps of any late Quaternary age in the gap between the China Mountain and Tobin scarps, and Wallace (1984) wondered why the 1915 break jumped across the gap to the China Mountain scarp instead of following the older scarps northwestward along the east side of Grass Valley. Which of the two paths was followed by most pre-1915 ruptures is unknown. A wide, gentle gravity saddle centers at locality A of figure 20B, but is poorly defined by a few stations in its northwestern quarter (Erwin, 1974). The existence of the saddle is determined mostly by lows in Pumpernickel Valley north of the area shown in figure 20 and in Grass Valley. The area of the China Mountain scarp, including the gap between it and the Tobin scarp, might be a segment boundary, perhaps persistent, but without more gravity and geologic evidence we cannot settle the issue. Prehistoric ruptures might have tended to end at the gap north of the Tobin scarp, might have continued preferentially northwest along the edge of Grass Valley, or might have begun to abandon Grass Valley in favor of the China Mountain scarp in response to an hypothesized clockwise rotation of the direction of regional extension (Wallace, 1984). Evidence supporting such an hypothesized rotation can be seen in map relations in the Augusta Mountains (fig. 20A). North-striking normal faults within the mountains are truncated by a north-northeast - striking normal fault at the range front (Muller and others, 1951). This range front fault forms the contact between bedrock and Quaternary alluvium, and so has been active during the Quaternary. Similar relations are less clearly evident in the southern Tobin Range.

In conclusion, the Sou Hills are a persistent segment boundary, similar to the Willow Creek Hills boundary on the Lost River fault zone. The gap between the Tobin and Pearce scarps is either not a segment boundary or one of low persistence, similar to the several gravity saddles on the Wasatch fault zone that lack salients, exposed bedrock ridges, or other evidence of recurrent slip deficits. The area of the China Mountain scarp cannot be evaluated with available evidence.

Summary

A segment boundary exists where two or more large historic or prehistoric ruptures have coincident starting or stopping ends. Analysis of the Wasatch fault zone produced a model in which gravity saddles or other evidence of buried bedrock ridges and footwall salients that separate hanging-wall valleys indicate accumulated slip deficits, which are interpreted as evidence of many coincident starting or stopping ends, that is, as persistent segment boundaries.

The Borah Peak rupture of 1983 started at the Elkhorn Creek boundary and ended at the Willow Creek Hills boundary, both persistent and both probably nonconservative barriers.

The Hebgen Lake earthquake of 1959 occurred on a young fault zone whose geometry is still evolving and which should not yet be interpreted in terms of persistent segment boundaries and long-lasting barriers.

The Rainbow Mountain earthquakes of 1954 occurred on a fault zone with too few gravity or geologic data to test the Wasatch model, indicating the need for descriptions of more than one rupture zone before segmentation can be inferred.

The Fairview Peak-Dixie Valley rupture zones of 1954 were separated by the persistent Pirouette Mountain segment boundary, which tends to control large ruptures on both the east and west sides of Fairview and Dixie Valleys, and perhaps in the graben between the Fairview and West Gate faults. The Pirouette Mountain boundary might be a nonconservative barrier. The north end of the Dixie Valley rupture zone is not a segment boundary, persistent or otherwise, which demonstrates that segments need not rupture completely even in large earthquakes. There are too few data to allow evaluation of the south end of the Fairview Peak rupture zone.

The 1915 Pleasant Valley earthquake had its south end at the persistent Sou Hills boundary, which might be a nonconservative barrier. The gap between the Pearce and Tobin scarps is a nonpersistent boundary, which did not end the 1915 rupture zone. The north end of the 1915 rupture lacks enough data for interpretation.

CONCLUSIONS

1. The Wasatch fault zone and most or all of the large seismic ruptures that occur on it are segmented. Large ruptures tend to start, stop, or do both at boundaries between segments, tend to be confined within single segments, and tend not to rupture across boundaries into adjacent segments.
2. Persistent segment boundaries occur at the Pleasant View, Salt Lake, Traverse Mountains, and Payson salients. These boundaries have controlled the seismic evolution of the Wasatch fault zone for much or all of its history, and likely will continue to do so into the near future. Most boundaries in the populous central parts of the Wasatch Front are persistent.
3. Other proposed segment boundaries elsewhere along the fault zone might be nonpersistent, with locations and times of activity that might change unpredictably with time. If boundaries that have affected Holocene and older Quaternary ruptures are not persistent, then these boundaries might not affect the next several ruptures that might occur on the Wasatch fault zone. However, the next ruptures might also be affected by nonpersistent boundaries that have not affected the young geologic record. Present boundaries that might be nonpersistent lie mostly in the comparatively sparsely populated areas north of Brigham City and south of Provo.
4. From 1962 to 1986 epicenters of small earthquakes that occurred near the trace of the Wasatch fault zone changed abundance across the four persistent segment boundaries. In contrast, Arabasz and Julander (1986) suggested that small earthquakes elsewhere along the Wasatch

Front can be controlled in complex ways by little-known structures of buried thrust sheets, and therefore are unlikely to be clearly associated with exposed structure. The association of seismicity near the fault zone with the salients is encouraging for efforts to understand earthquake generation along the Wasatch Front.

5. Analysis of the Wasatch fault zone produced a model that predicts persistent segment boundaries where exposed or shallowly buried transverse bedrock ridges, some with salients, indicate accumulated slip deficits, and where two or more individual large rupture zones have started or stopped.
6. Testing this model against five historic earthquake sequences in and near the Basin and Range province indicates the existence of two persistent segment boundaries on the Lost River fault zone of Idaho, one persistent boundary between the Dixie Valley and Fairview faults of Nevada, and one persistent and one nonpersistent boundaries in the Pleasant View, Nevada, rupture zone. The north end of the Dixie Valley fault is not a segment boundary, persistent or otherwise. Both ends of the Rainbow Mountain, Nevada, rupture zone, the south end of the Fairview Peak rupture zone, and the north end of the Pleasant Valley rupture zone have too little information to test the model there. The Hebgen Lake, Montana, earthquake occurred on a fault zone that is too young for the model to apply.

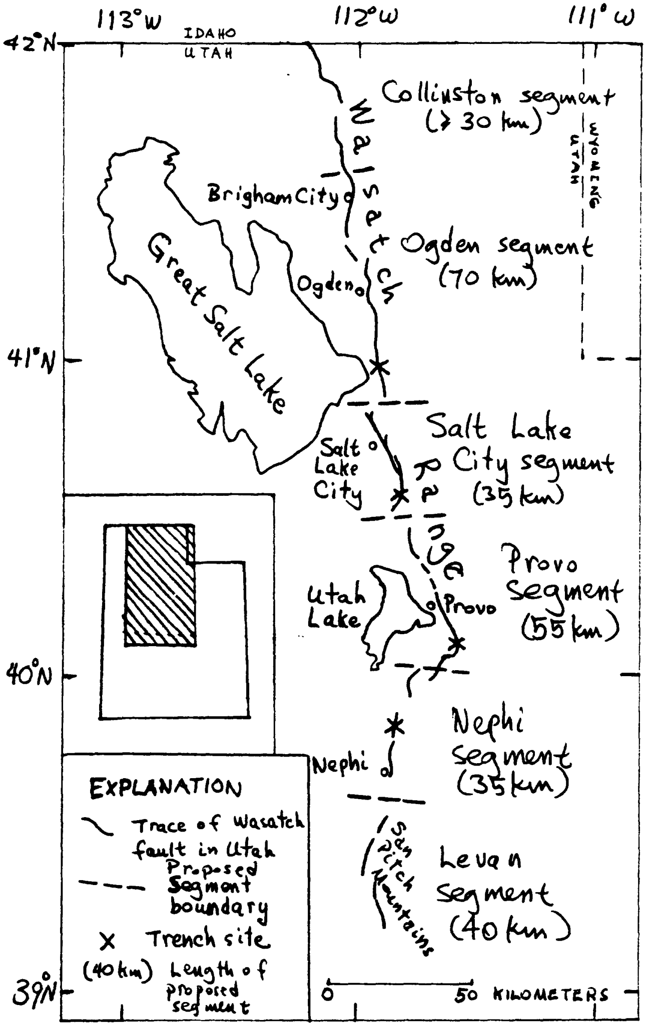

FIGURE 1.--Index map of the Wasatch fault zone in northern central Utah, showing selected towns and cities along the Wasatch Front. The Wasatch Front is usually taken to include the populated valleys that lie along and immediately west of the trace of the Wasatch fault zone (Mabey, in press), and which include most of the population of Utah. Segment boundaries, trench sites, and fault-zone trace are those of Schwartz and Coppersmith (1984), from whose figure 1 this map is modified. Work in progress by several workers has added trench sites and natural fault exposures and has changed some segment boundaries and mapped fault traces. Inset shows location of map area within Utah.

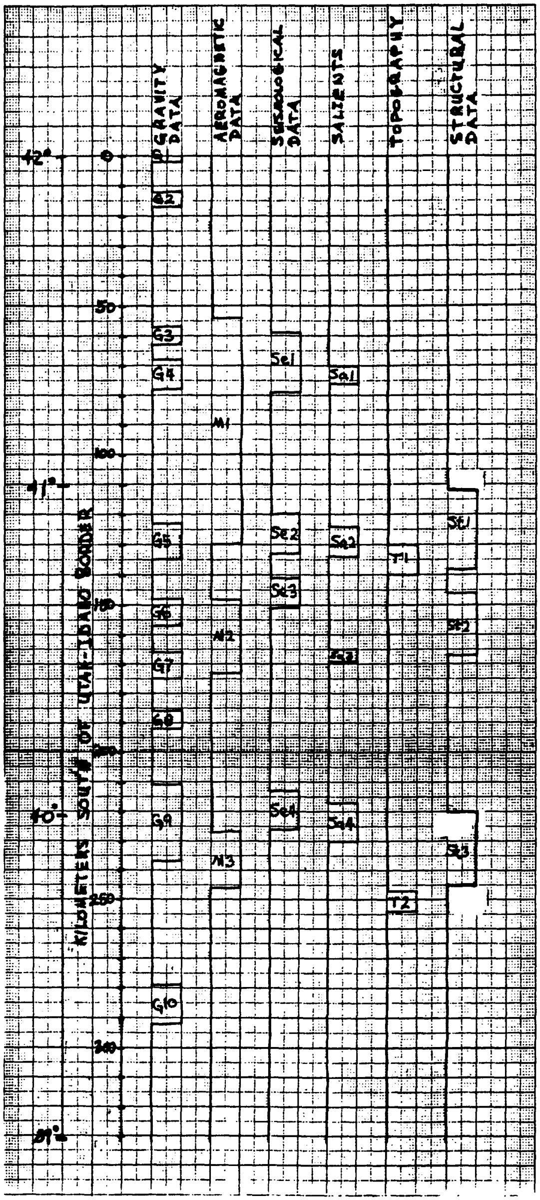

FIGURE 2.-- Observed distribution of anomalies along the Wasatch fault zone. Length of anomaly pattern is 332 km, from Utah-Idaho border at latitude 42° N. to south edge of study area at latitude 39° N. Each of the six data types is represented by a vertical line that steps to the right at one end of an anomaly and back to the left at the other end. Anomaly locations and letter-numeral names are from Wheeler and Krystinik (in press b).

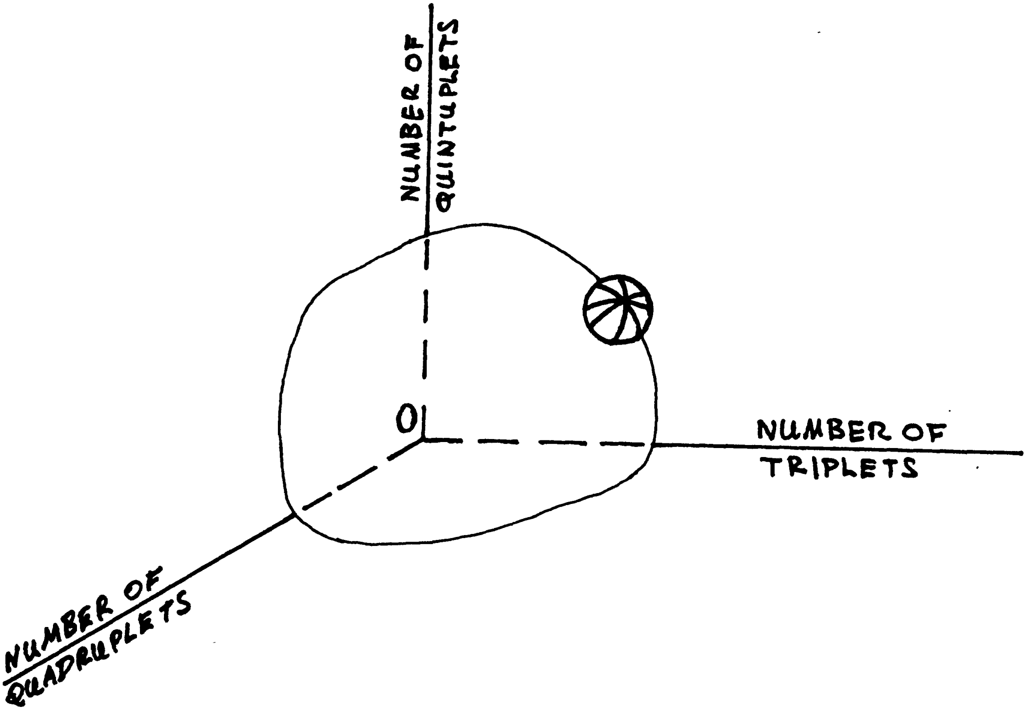

FIGURE 3.--Three-dimensional geometry of comparison of observed anomaly pattern to simulated patterns. Each pattern plots in this graph according to its numbers of triplets, quadruplets, and quintuplets of coincident anomalies, which are identified according to the rules given in the text. Axes are mutually perpendicular, so quadruplets' axis rises out of the page. Thin line outlines cloud of points, one from each simulated pattern. Dashed parts of axes and origin 0 lie behind cloud. Center of small ball with asterisk represents the single observed pattern. Statistical test determines whether this ball is significantly distinct from the cloud of points.

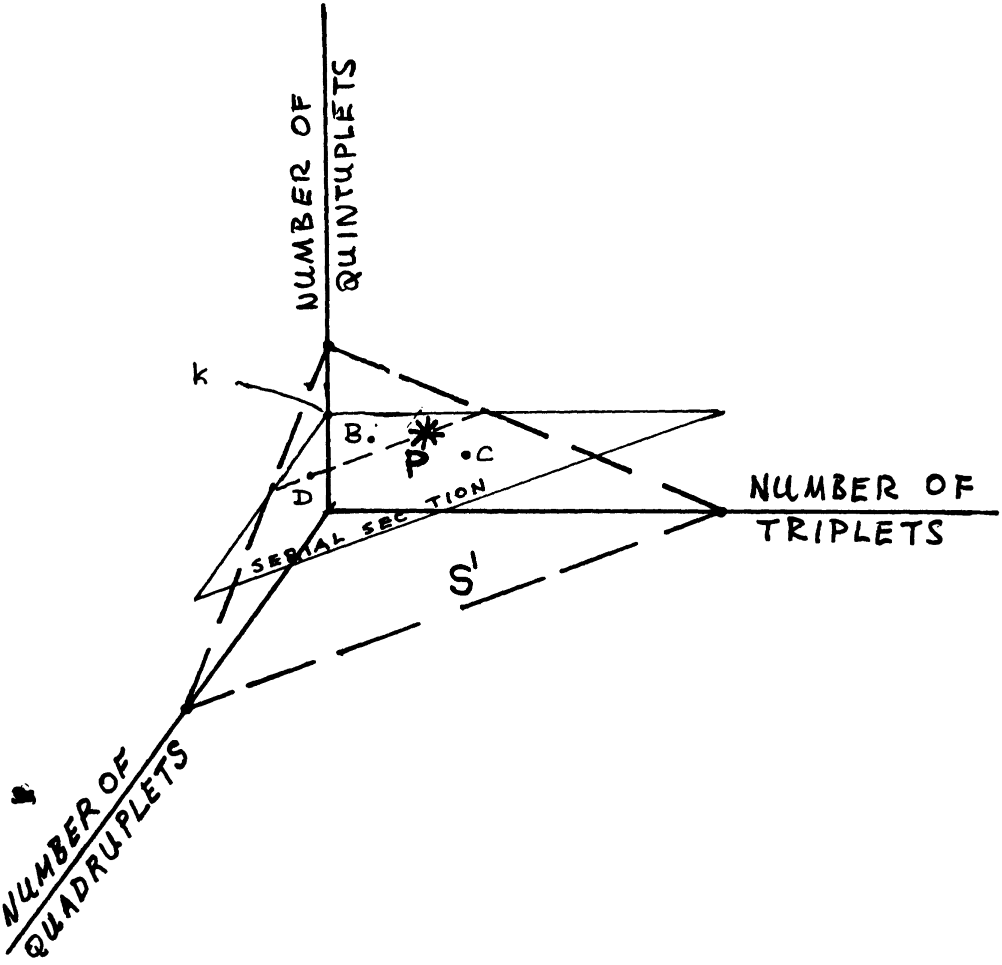

FIGURE 4.--Axes of figure 3, showing a serial section (light lines). Serial section lies parallel to triplets' and quadruplets' axes and intercepts quintuplets' axis perpendicularly at k, so all observed or simulated patterns of anomalies that contain k quintuplets plot in this serial section, for example as points B-D. S' is called the significance plane and intercepts all three axes obliquely. There is one serial section for each value of k, k = 0, 1, 2, ... The section shown here is the one on which the observed pattern plots (point P, shown as an asterisk). S' intersects the serial section in the thin dashed line. S' is constructed so the dashed line passes through P. Modified from Wheeler and Krystinik (in press a).

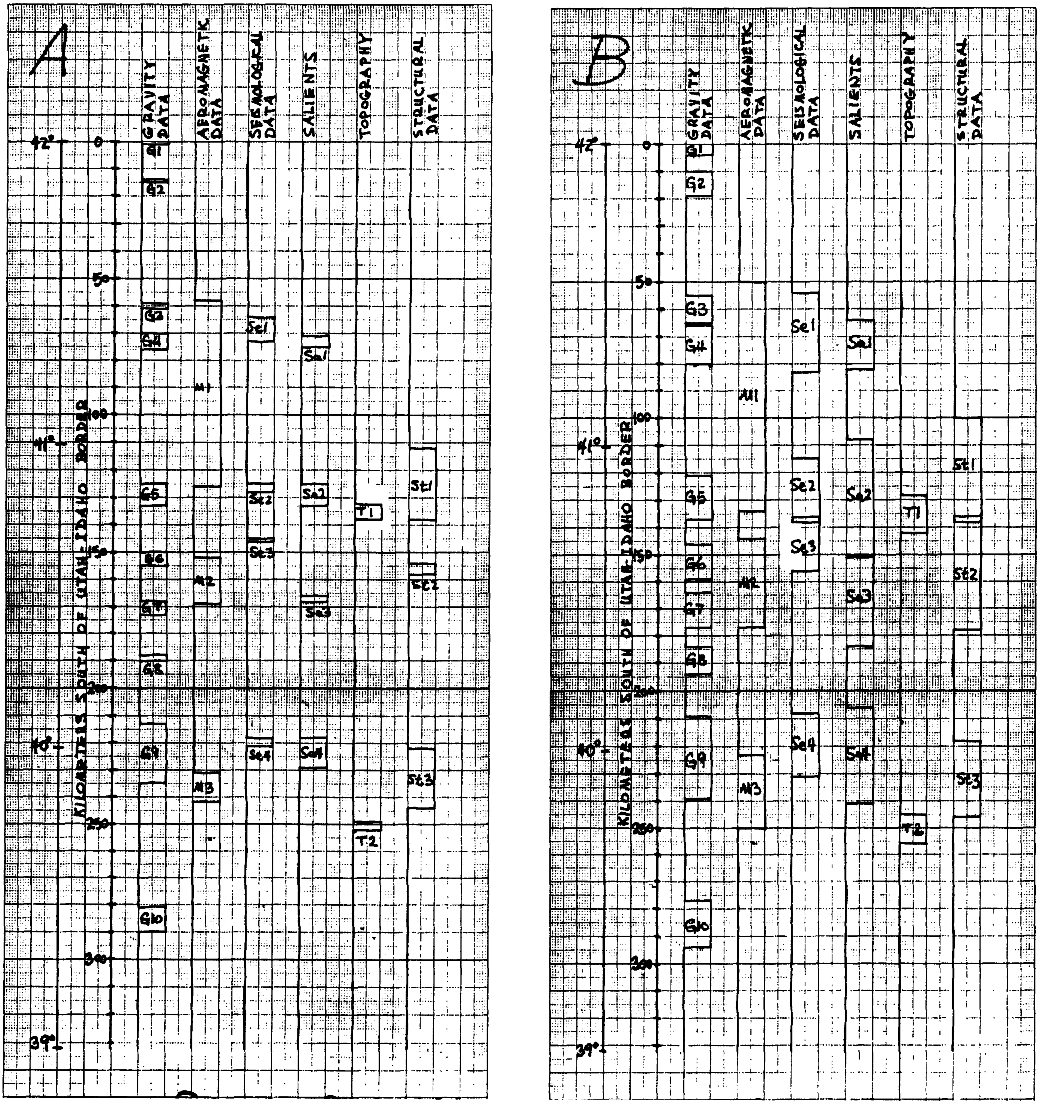

FIGURE 5.--Observed anomaly pattern of figure 2 redrawn to give each anomaly the minimum (A) and maximum (B) widths allowed by locational uncertainties of its edges. Uncertainties are from Wheeler and Krystinik (in press b). In (A) this procedure would give anomaly Se3 a width of zero km. Its minimum width is arbitrarily set at one km. In (B) Se2 and Se3 overlap by two km, as do St1 and St2.

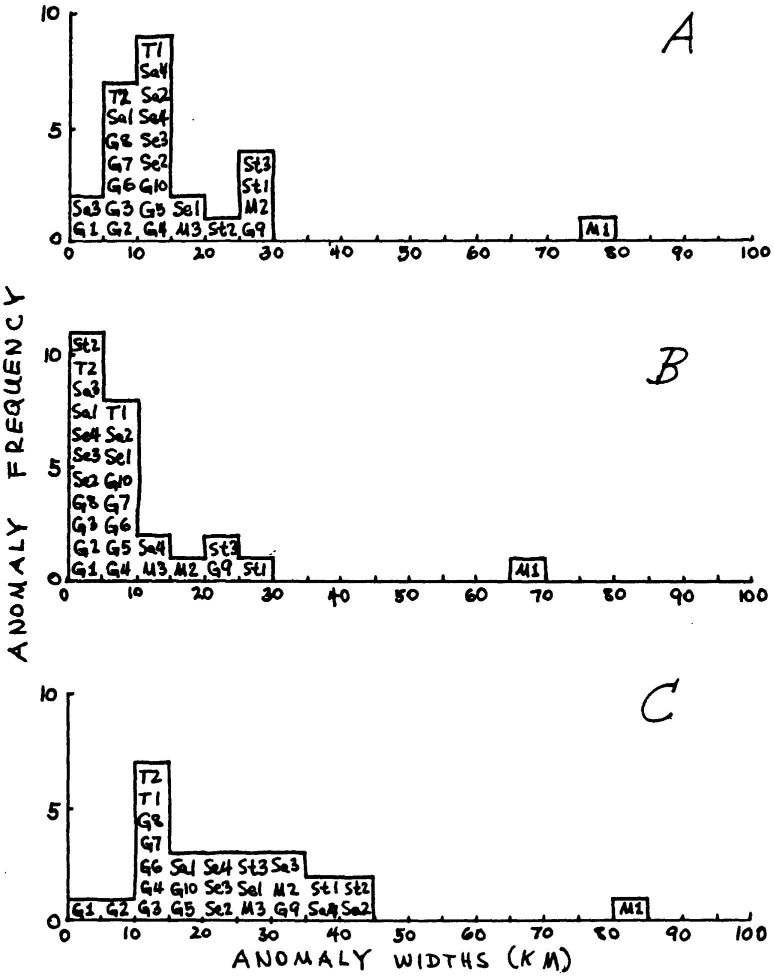

FIGURE 6.--Histograms of anomaly widths. Each anomaly is identified by its letter-numeral name. Widths are from Wheeler and Krystinik (in press b). A, Measured anomaly widths (fig. 2). Median of 26 widths is 11 km, about three percent of the 332 km length of the fault zone in the study area. Widest anomaly after M1 spans eight percent of fault-zone length. B, Minimum widths that are allowed by locational uncertainties of anomaly edges (fig. 5A). Median is 6 km. Widest anomaly after M1 spans eight percent of fault-zone length. C, Maximum allowable widths (fig. 5B), with median of 19 km. Widest anomaly after M1 spans 13 percent of fault-zone length.

FIGURE 7.--Pairs and m-tuplets of coincident anomalies in observed anomaly pattern along the Wasatch fault zone. Figures 2, 5 name each anomaly. Small dots identify anomalies that are involved in pairs and m-tuplets. Solid pair-lines that connect the small dots link anomalies that are paired according to the rule that either anomaly contains the center of the other. An m-tuplet is present wherever all m(m-1)/2 of the possible pairs of the m anomalies are also present (Wheeler and Krystinik, in press a). In parentheses to the right of each group of paired anomalies are the numbers of pairs, triplets, quadruplets, and quintuplets in the group, in that order. There are no sextuplets or larger m-tuplets. Below the plus sign are the totals of pairs and m-tuplets for the whole anomaly pattern. A, Each anomaly is given its measured width (fig. 2). B, Each anomaly is given the minimum width that is allowed by the locational uncertainties of its edges (fig. 5A). C, Each anomaly is given its maximum allowable width (fig. 5B). Numbers in square brackets at right summarize the single pair between anomalies Se3 and Sa2.

Measured Widths

A

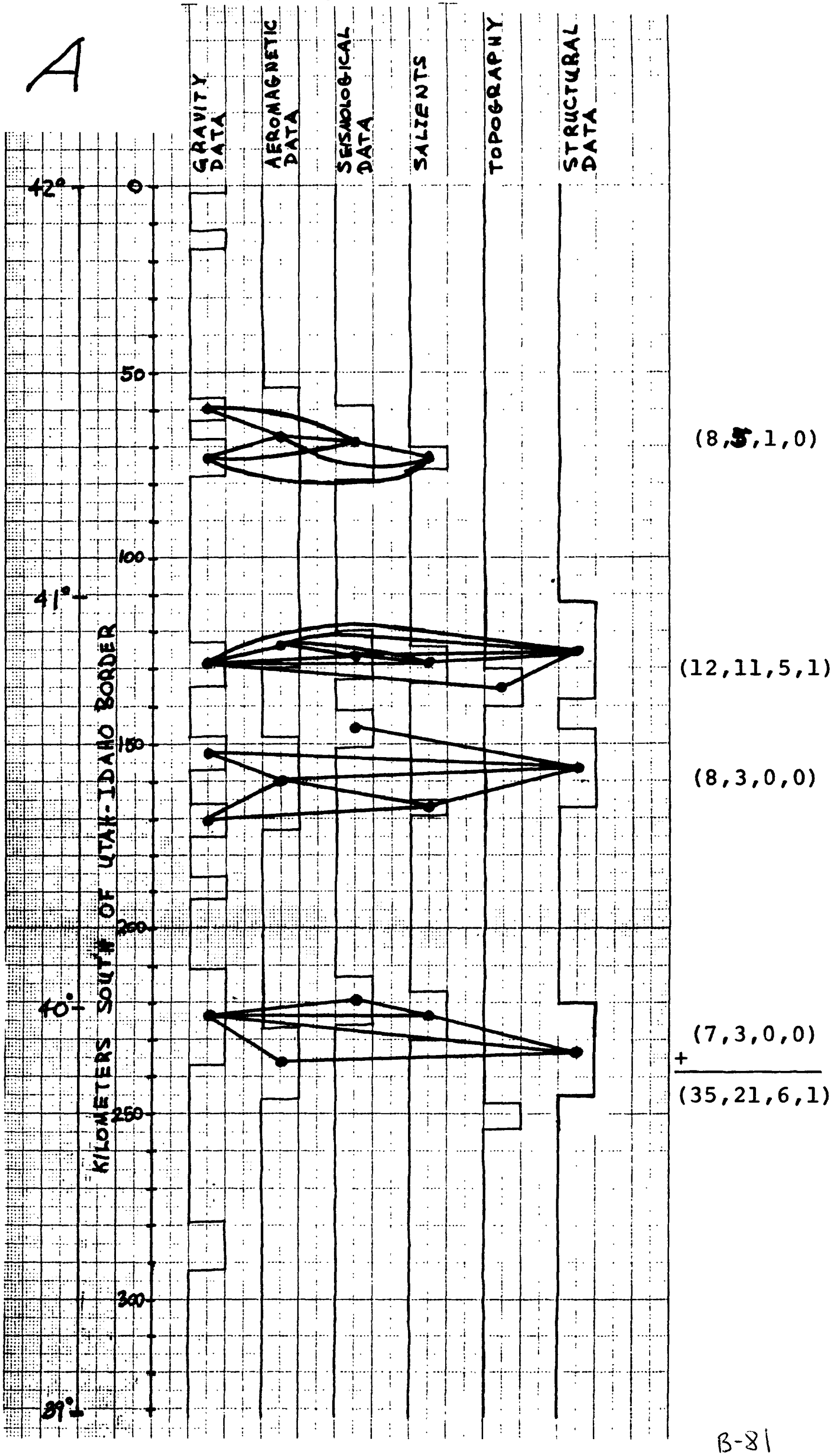

B

Minimum Widths

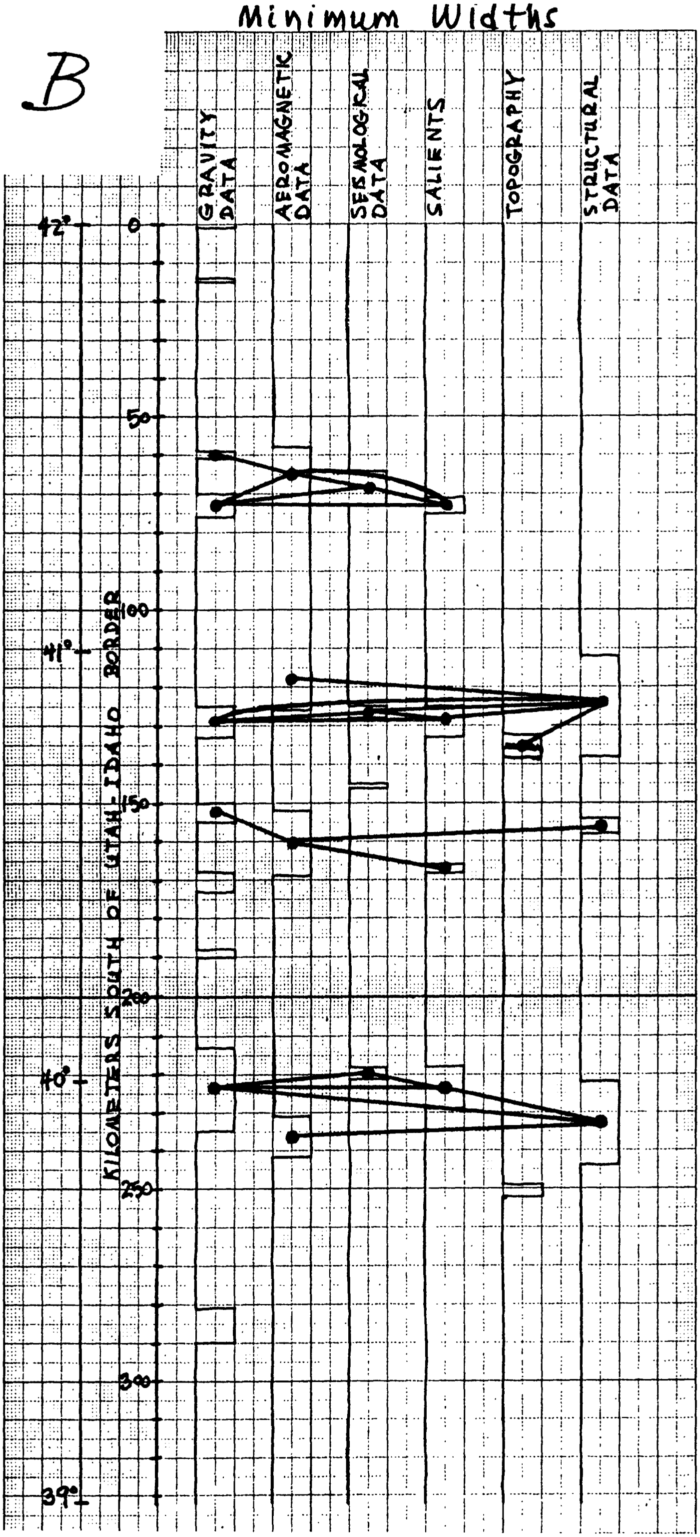

(7,4,1,0)

(8,4,1,0)

(3,0,0,0)

(6,2,0,0)
+
(24,10,2,0)

C

Maximum Widths

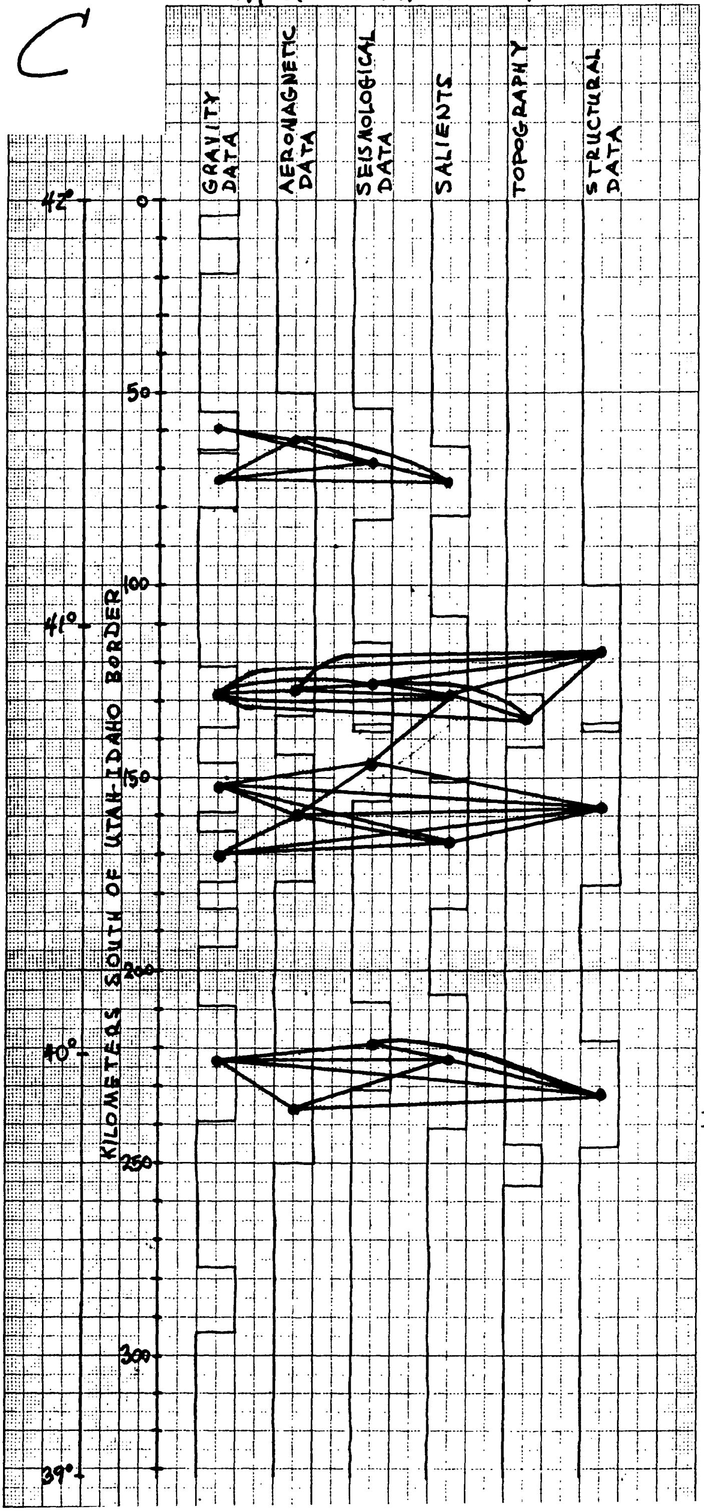

(8,5,1,0)

(14,16,9,2)

[1,0,0,0]

(12,10,3,0)

(9,7,2,0)
\+

(44,38,15,2)

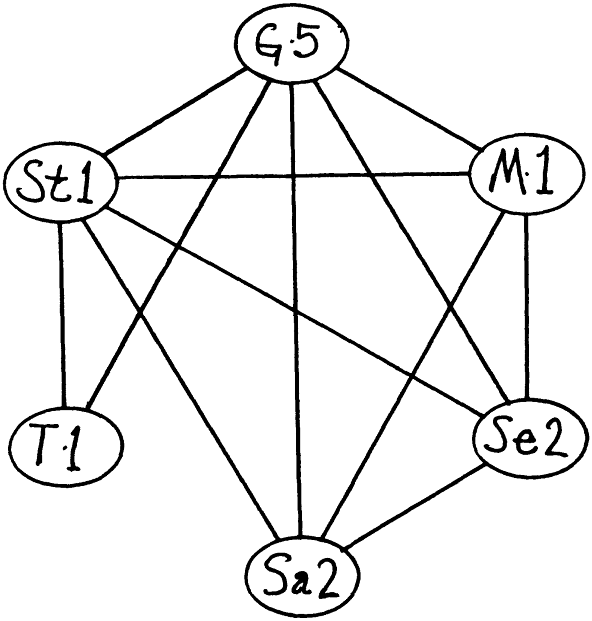

FIGURE 8.--Diagram representing coincidings between anomalies at km 130. Six ellipses represent anomalies that coincide there (figs. 2, 7A). Lines joining ellipses represent the pair lines that identify coincident pairs (fig. 7A). A triplet appears here as three pair lines that form a triangle, as for G5-M1-Se2 or M1-Sa2-St1. The triplet Sa2-T1-St1 is absent because the pair Sa2-T1 is absent (fig. 7A). A quadruplet appears as four ellipses linked by six pair lines that form a closed quadrilateral and its two internal diagonals, as G5-Se2-Sa2-St1. A quintuplet appears as five ellipses, each connected to the others by four pair lines, as G5-M1-Se2-Sa2-St1.

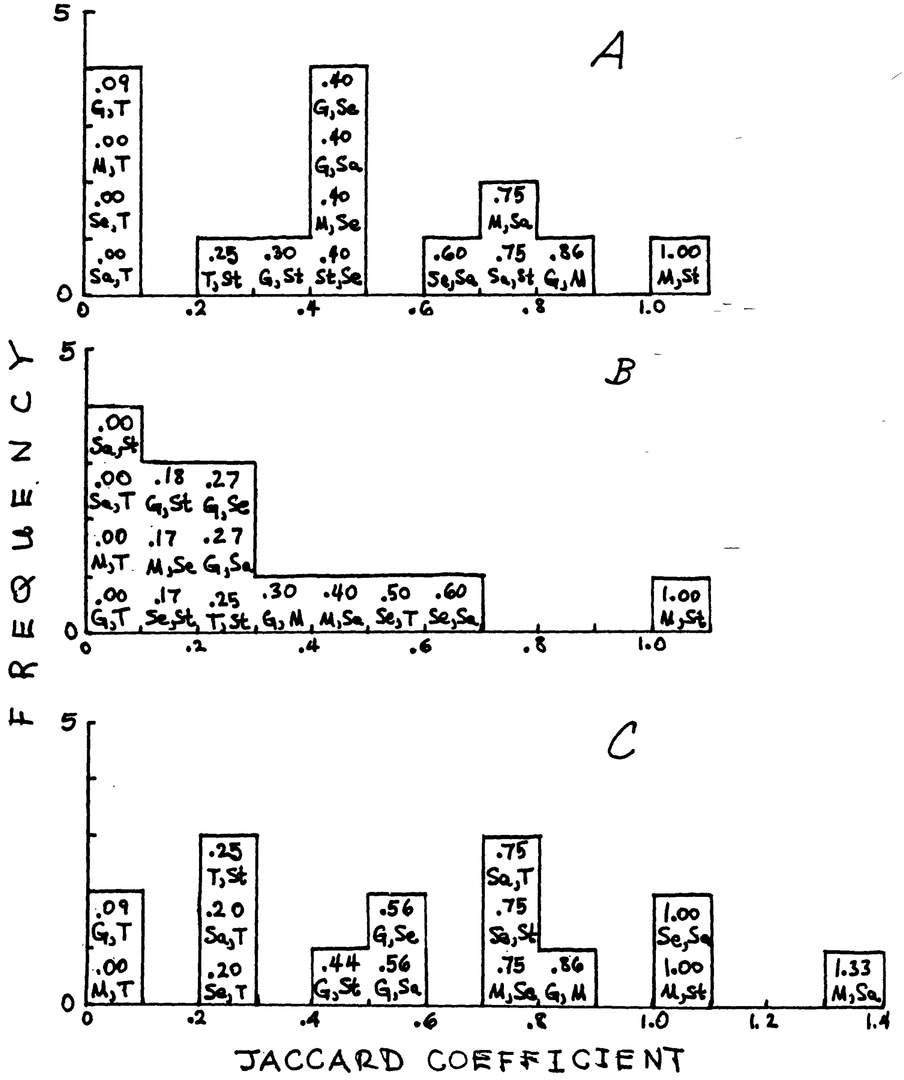

FIGURE 9.--Histograms of values of Jaccard coefficient J for the 15 possible pairs of six data types. For each entry, value of J is written above the letter identifiers of the two data types whose degree of association is summarized by J. G denotes Bouguer gravity data, M denotes aeromagnetic data, Se denotes seismological data, Sa denotes salients, T denotes topographic data, and St denotes pre-Cenozoic structures. For example, in part A structural and aeromagnetic data are highly associated (J = 1.00). A, Measured widths of anomalies (figs. 2, 7A). Median value of J is .40. B, Minimum widths that are allowed by locational uncertainties of anomaly edges (figs. 5A, 7B). Median decreases to .22. C, Maximum allowable widths (figs. 5B, 7C). Median increases to .56.

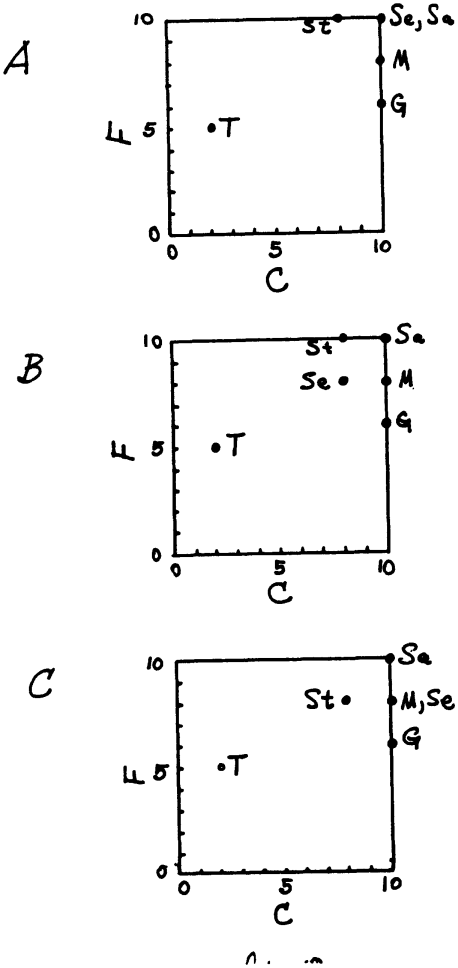

FIGURE 10.--Constancy and fidelity of the six data types in the four anomalous parts of the Wasatch fault zone. High values of constancy C identify data types in which the presence of an anomaly characterizes the cluster of four anomalous parts of the fault zone. High values of fidelity F identify data types in which the presence of an anomaly is diagnostic of the cluster of anomalous parts of the fault zone. G denotes gravity data, M denotes aeromagnetic data, Se denotes seismological data, Sa denotes salients, T denotes topographical data, and St denotes pre-Cenozoic structures. A, Measured widths of anomalies (figs. 2, 7A). Plotted values are from bottom two parts of table 3. B, Minimum widths that are allowed by locational uncertainties of anomaly edges (figs. 5A, 7B). Plotted values are from tables like table 3, and derived from figure 7B. C, Maximum allowable widths (figs. 5B, 7C). Plotted values derived analogously as for B.

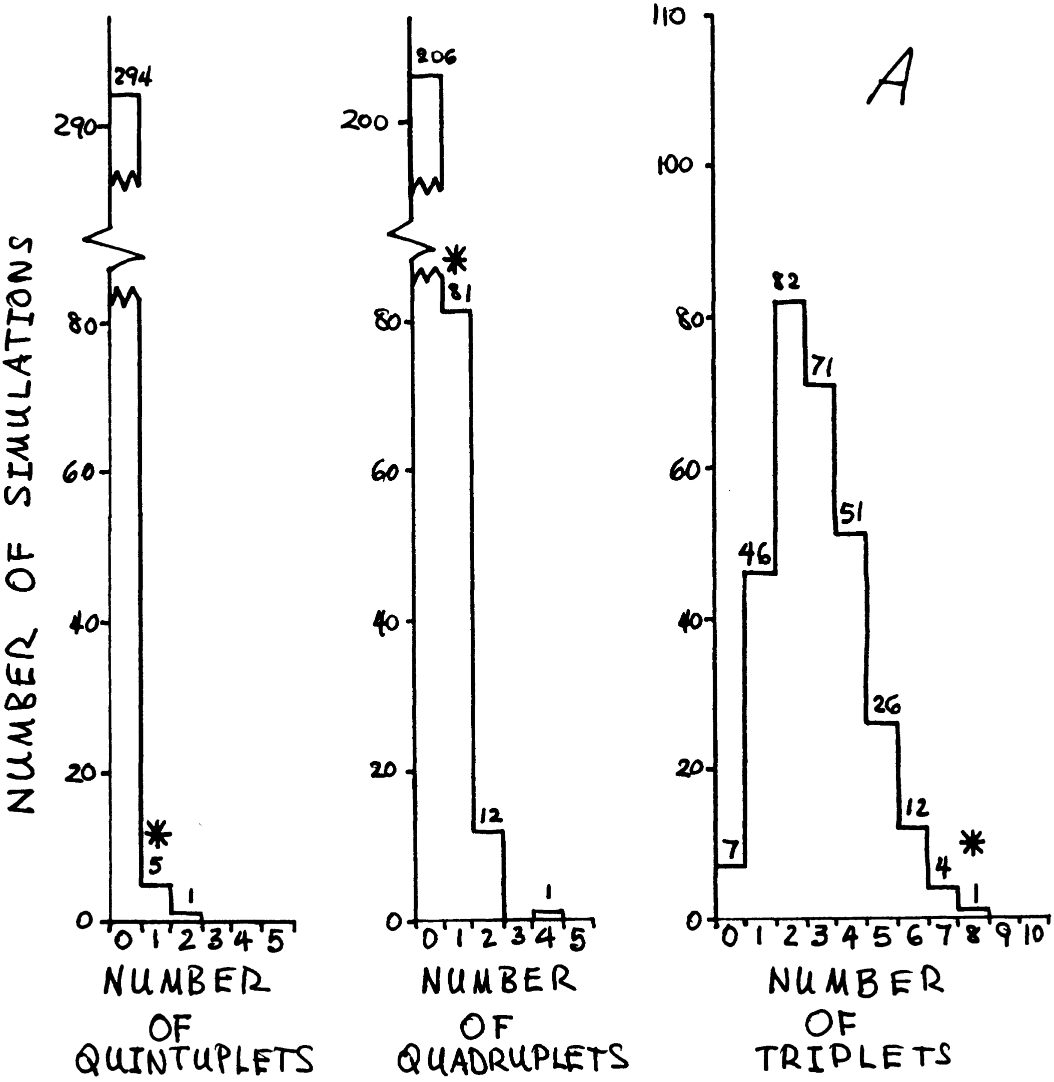

FIGURE 11.--Histograms comparing numbers of m-tuplets in observed and simulated patterns. Histograms summarize simulated patterns. Numeral atop each bar shows its height. Asterisks show numbers of m-tuplets in observed pattern of figure 7. All patterns have had duplicate m-tuplets removed, as for table 2. Pairs are ignored. A, Measured anomaly widths. 300 simulations. No patterns have any sextuplets or larger m-tuplets. B, Minimum widths that are allowed by locational uncertainties of anomaly edges. 300 simulations. No patterns have any quintuplets or larger m-tuplets. C, Maximum allowable widths. 100 simulations. No patterns have any m-tuplets larger than sextuplets.

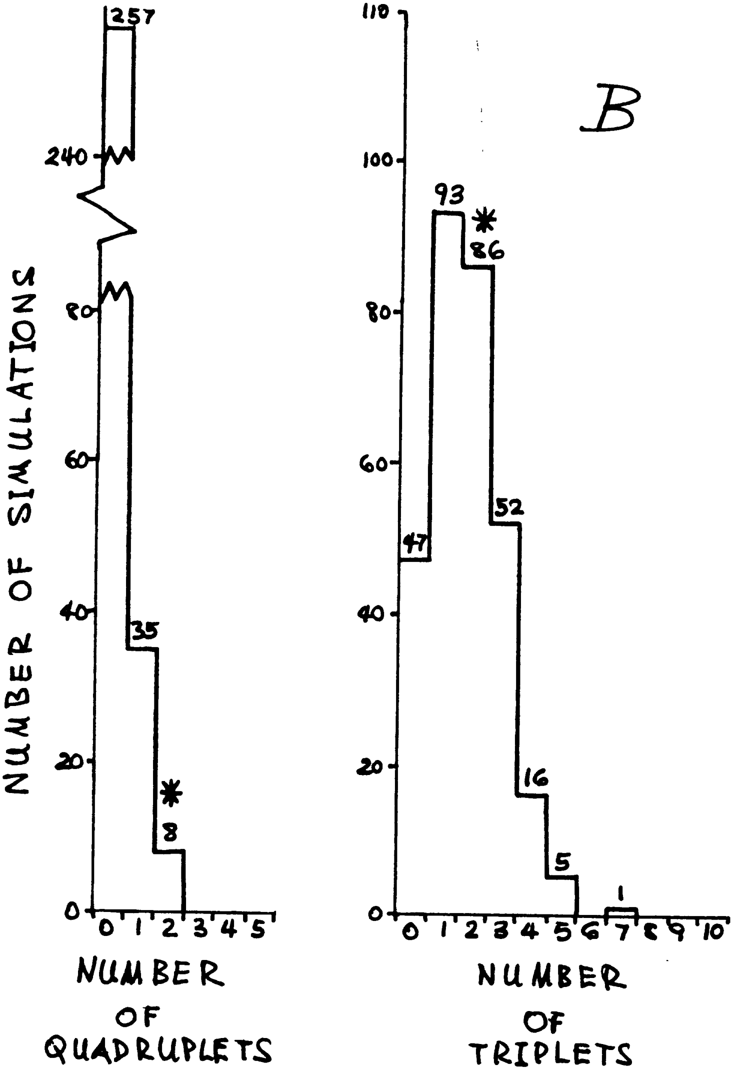
B
NUMBER OF SIMULATIONS
0
20
40
60
80
240
257
35
*
8
0
1
2
3
4
5
NUMBER OF QUADRUPLETS
110
100
80
60
40
20
0
47
93
*
86
52
16
5
1
0
1
2
3
4
5
6
7
8
9
10
NUMBER OF TRIPLETS

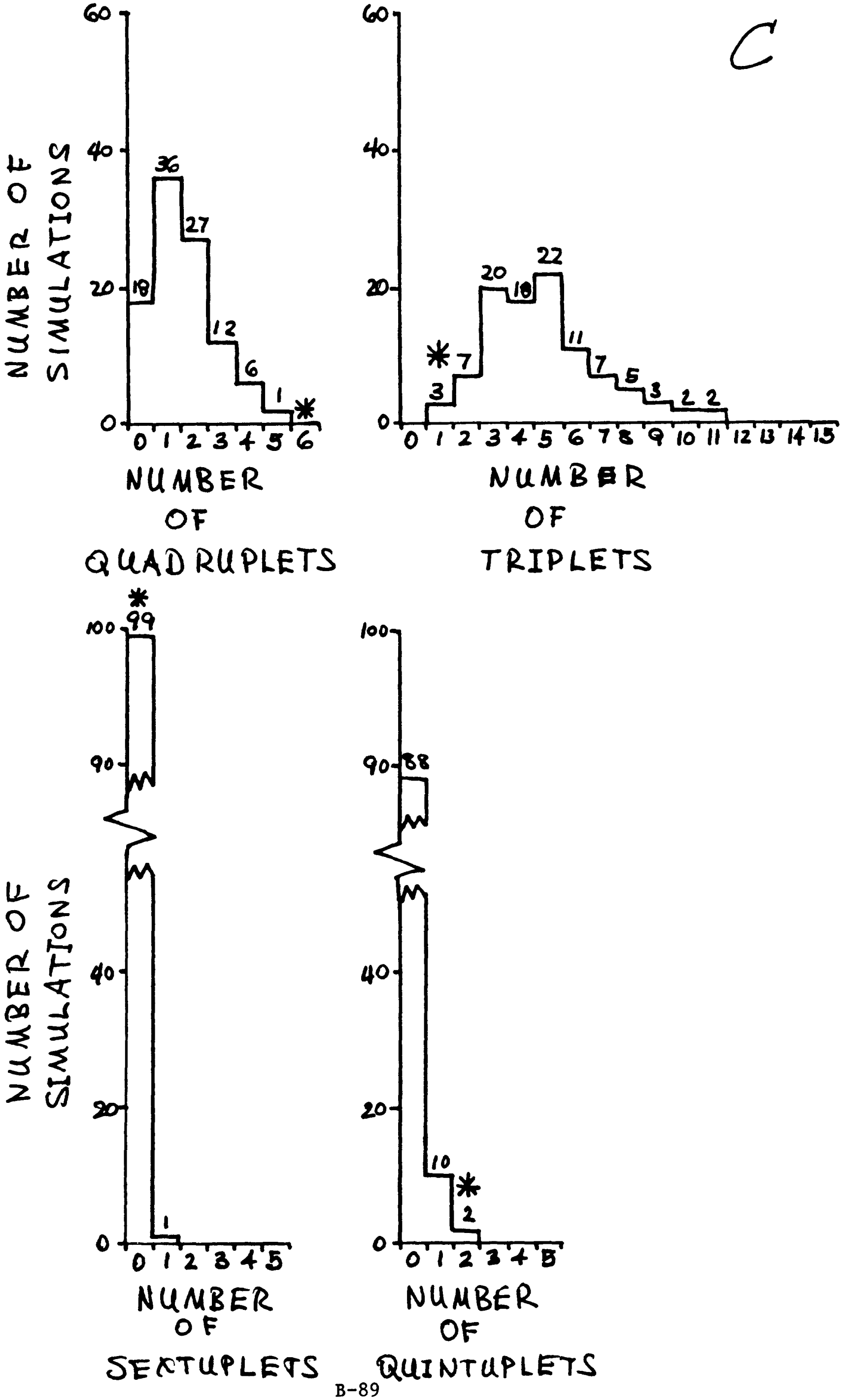
C
NUMBER OF SIMULATIONS
60
40
20
0
36
27
18
12
6
1
*
0 1 2 3 4 5 6
NUMBER OF QUADRUPLETS
60
40
20
0
22
20
18
11
*
7
7
5
3
3
2 2
0 1 2 3 4 5 6 7 8 9 10 11 12 13 14 15
NUMBER OF TRIPLETS
NUMBER OF SIMULATIONS
100
90
40
20
0
*
99
1
0 1 2 3 4 5
NUMBER OF SEXTUPLETS
100
90
40
20
0
88
10
*
2
0 1 2 3 4 5
NUMBER OF QUINTUPLETS

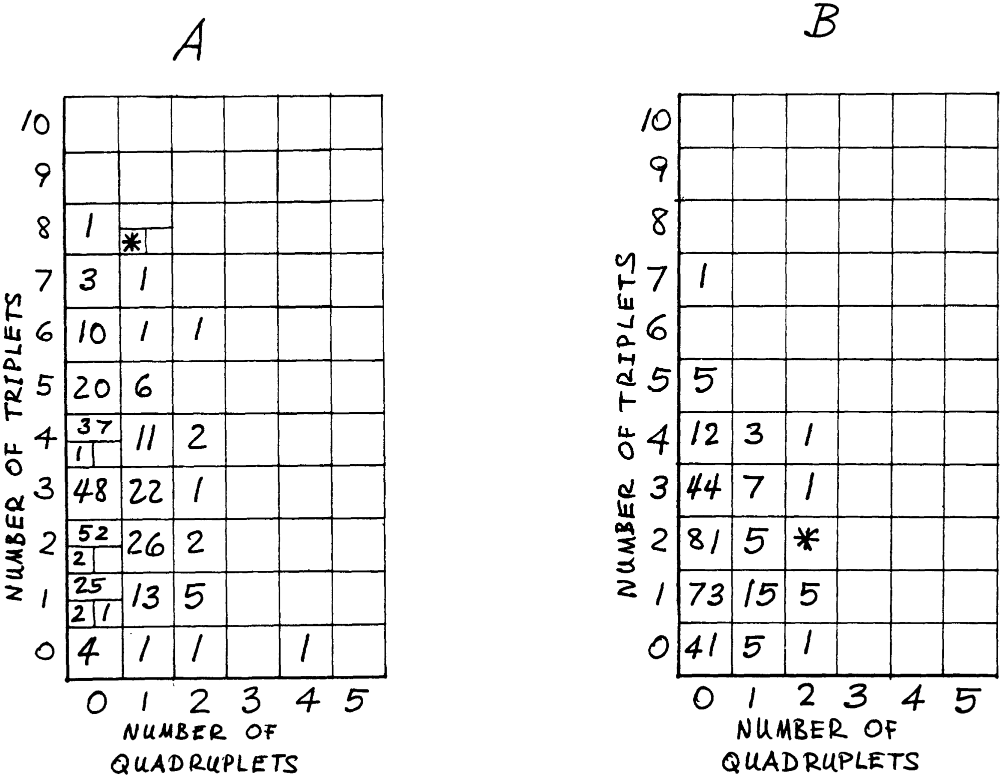

FIGURE 12.--Diagrams comparing numbers of m-tuplets in observed and simulated patterns. Asterisks represent observed pattern. Numerical entries are the numbers of simulated patterns that have the indicated numbers of triplets and quadruplets. Cells that are divided into three subcells record patterns with quintuplets. Upper, lower left, and lower right subcells give numbers of patterns with zero, one, and two quintuplets, respectively. Zero-valued entries are omitted for clarity. Imagine that numbers of quintuplets are plotted along a third axis that rises perpendicularly out of the page. For example, in A 28 simulated patterns have one triplet but no quadruplets, and of these patterns, 25 lack quintuplets and plot in the plane of the page, two have one quintuplet each and plot one unit above the page, and one has two quintuplets and plots two units above the page. A, Measured anomaly widths. 300 simulations. B, Minimum widths that are allowed by locational uncertainties of anomaly edges. 300 simulations. C, Maximum allowable widths. 100 simulations. Circled entry at (1,2) indicates that one of these two simulated patterns also has a sextuplet.

C

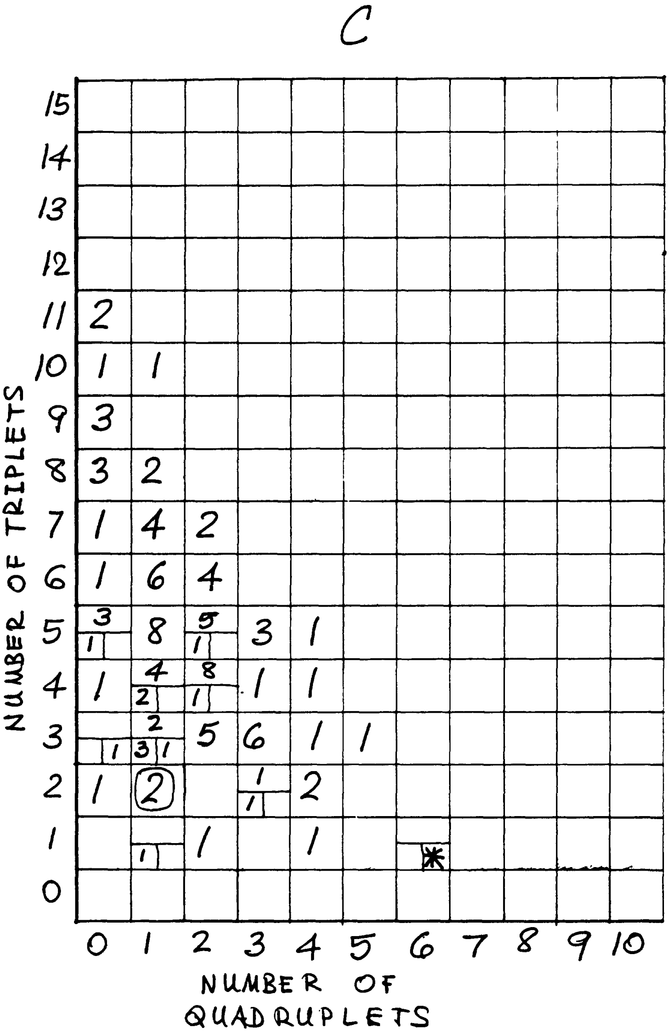

NUMBER OF TRIPLETS	0	1	2	3	4	5	6	7	8	9	10
15											
14											
13											
12											
11	2										
10	1	1									
9	3										
8	3	2									
7	1	4	2								
6	1	6	4								
5	3 1	8	5 1	3	1						
4	1	4 2	8 1	1	1						
3	1	2 3 1	5	6	1	1					
2	1	2		1 1	2						
1		1	1		1		*				
0											

NUMBER OF QUADRUPLETS

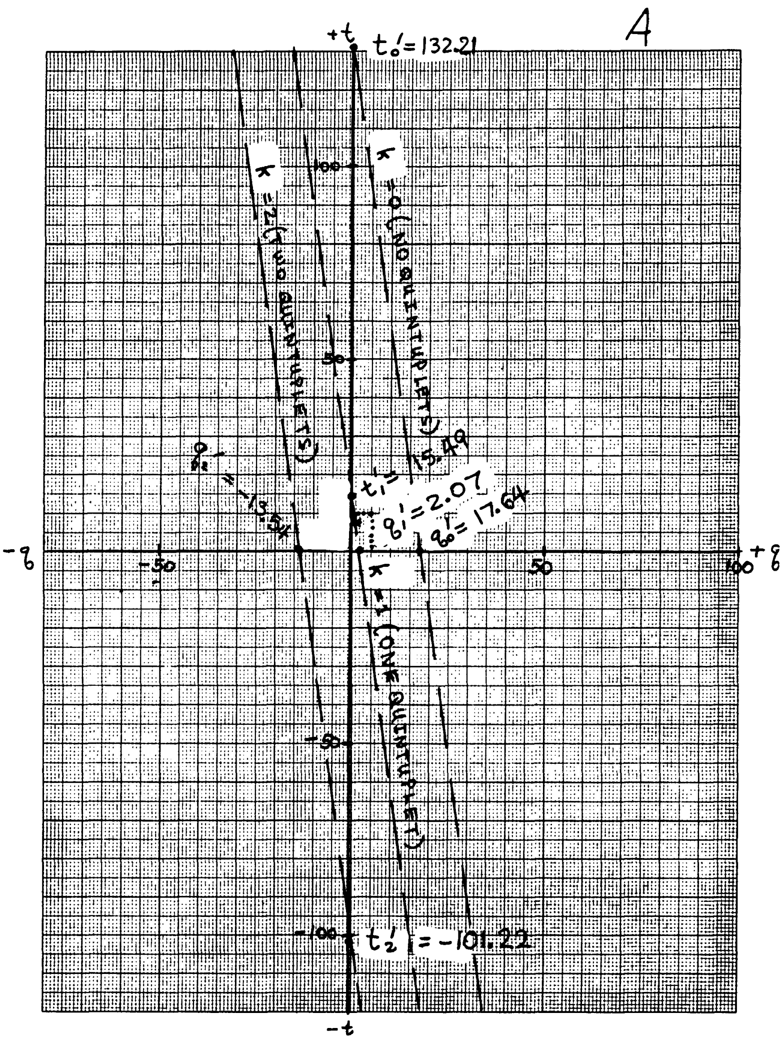

FIGURE 13.--Summaries of serial sections like that of figure 4. In notation similar to that of Wheeler and Krystinik (in press a), the number of quadruplets per pattern is q, number of triplets is t. Dashed lines are traces of significance plane S' (fig. 4), for various numbers (k) of quintuplets per anomaly pattern. Locations of intercepts q'_k and t'_k are shown by large dots. To aid comparisons with figure 12, values of intercepts are written near the large dots, asterisks represent observed pattern, and top and right edges of corresponding parts of figure 12 are shown by dotted lines. A, Measured anomaly widths. Compare to figure 12A. Observed pattern has eight triplets, one quadruplet, one quintuplet. B, Minimum widths that are allowed by locational uncertainties of anomaly edges. Compare to figure 12B. Observed pattern has two triplets and two quadruplets. No simulated or observed pattern has any quintuplets, so only the dashed line for k = 0 is shown. C, Maximum allowable widths. Compare to figure 12C. Observed pattern has one triplet, six quadruplets, two quintuplets.

7AS

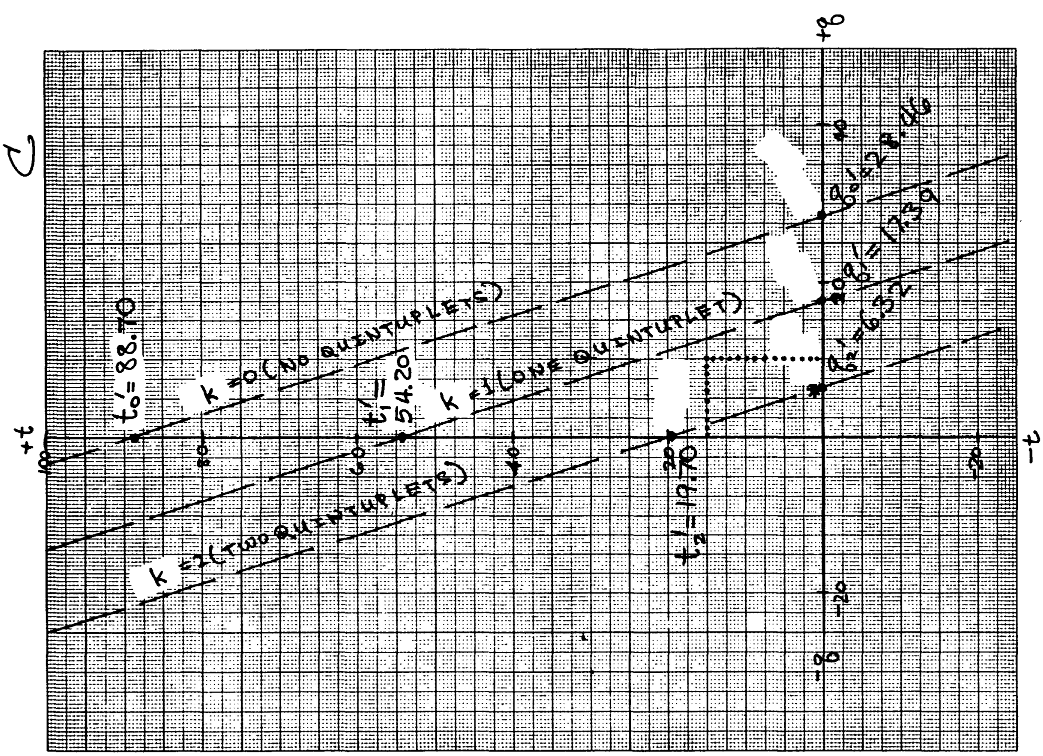
C
+θ
θ'0 = 28.46
θ'1 = 17.39
θ'2 = 6.32
t'0 = 88.70
t'1 = 54.20
t'2 = 19.70
k = 0 (NO QUINTUPLETS)
k = 1 (ONE QUINTUPLET)
k = 2 (TWO QUINTUPLETS)
+t
-t
-θ
100
80
60
40
20
-20
10
-20

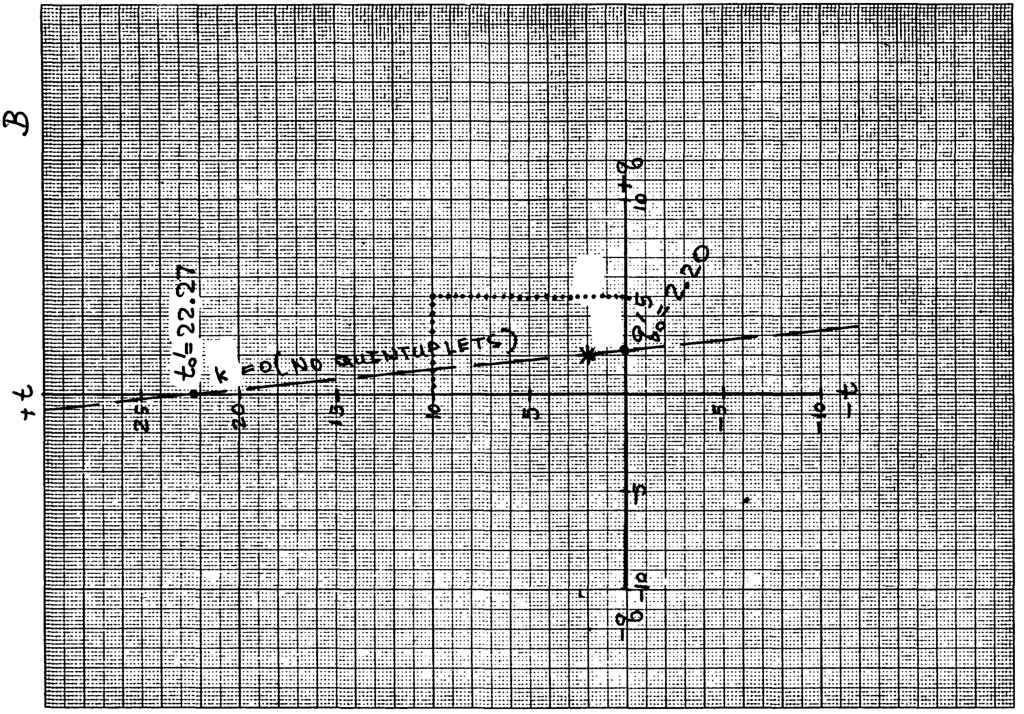
B
+θ
10
t'0 = 22.27
θ'0 = 2.20
k = 0 (NO QUINTUPLETS)
+t
-t
25
20
15
10
5
-5
-10
-5
-10
-θ

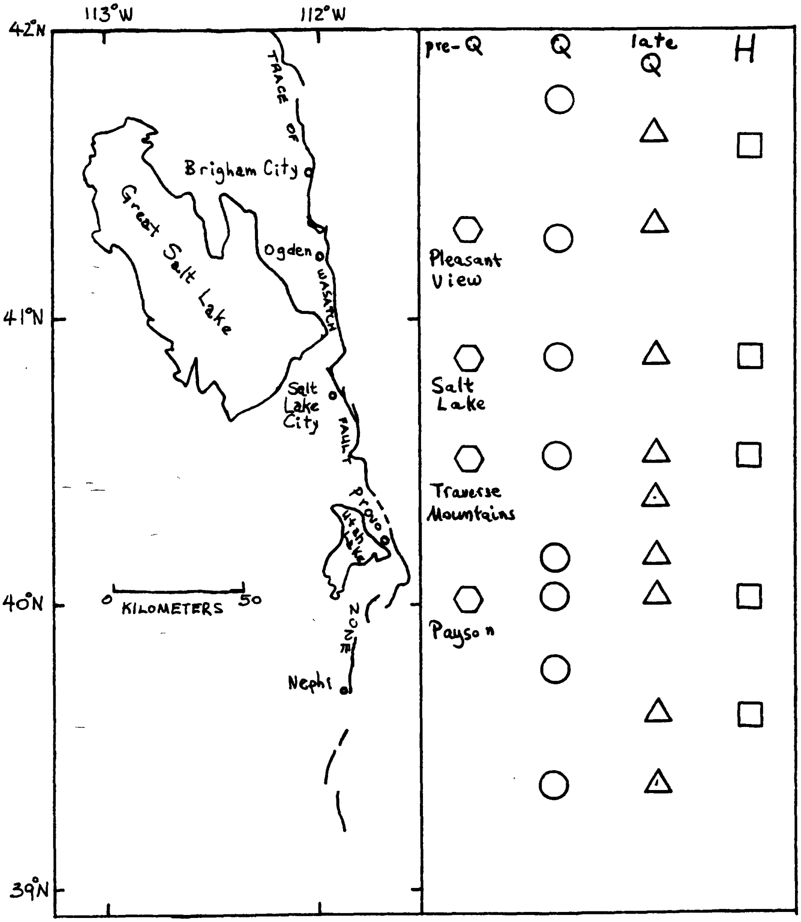

FIGURE 14.--Four sets of segment boundaries for the Wasstch fault zone, derived from different parts of the geologic record. In right half of figure, different symbols show latitudes of the suggested boundaries. Four hexagons show named boundaries of this report. The geologic record that we examined to define these boundaries is mostly pre-Quaternary (pre-Q), although we also used earthquake epicenters from 1962-1986. Eight circles show segment boundaries of Maclean (1985) and Mayer and Maclean (1986), which are based on the Quaternary (Q) record. Nine triangles locate boundaries of M.N. Machette, A.R. Nelson, S.F. Personius, and W.E. Scott (written communs. in Anderson, 1985, 1986), Machette and others (1986, in press), Nelson and Personius (1987), Personius (1986), and M.N. Machette, S.F. Personius, W.E. Scott, and A.R. Nelson (written commun., July, 1986). These boundaries are based on the late Quaternary (late Q) record. Five squares show boundaries of Schwartz and Coppersmith (1984), which are based mostly on the Holocene (H) record.

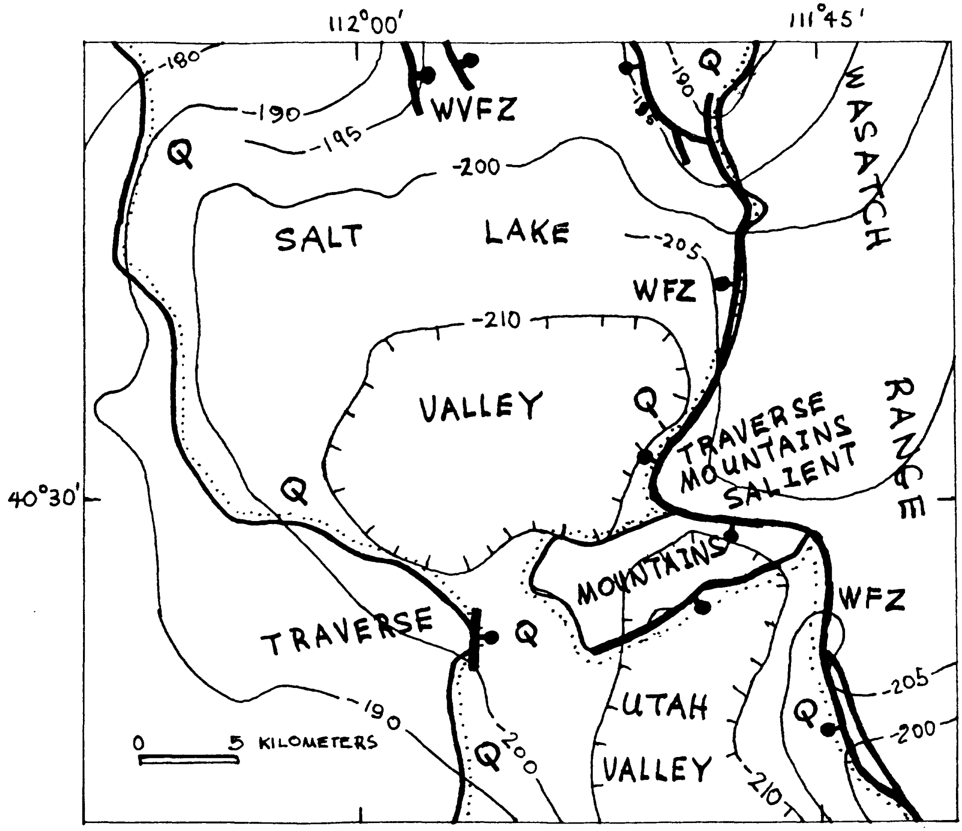

FIGURE 15.--Segment boundary at Traverse Mountains salient. Heavy lines represent traces of normal faults with Quaternary or probable Quaternary slip, simplified from Davis (1983b), Scott and Shroba (1985), Keaton and others (1987), and M.N. Machette (oral and written communs., 1987). Bar and ball are on downthrown side of each fault. Medium-weight dotted lines show contact between Quaternary valley-filling sediments (Q) and pre-Quaternary bedrock, with dots on Quaternary side of contact; simplified from Hintze (1980) and Zoback (1983, fig. 4). Light lines with numerals represent selected isogals of Bouguer gravity field, traced from Zoback (1983, fig. 4). Contour interval is 5 mgal near north and east edges of map, 10 mgal elsewhere. Single hachures point inward on lowest contours around local gravity minima. WFZ, Wasatch fault zone. WVFZ, south end of West Valley fault zone of Keaton and others (1987).

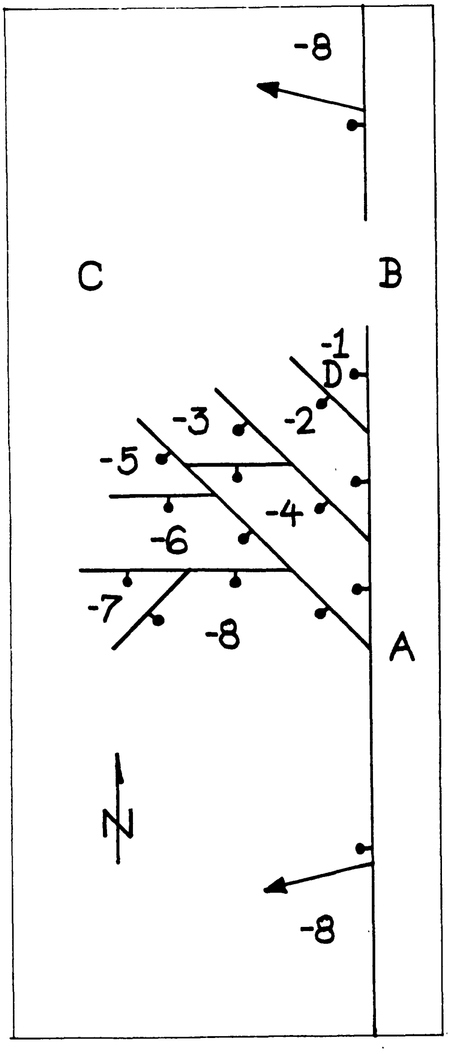

FIGURE 16.--Sketch map of the fault network (process zone) in a hypothetical nonconservative barrier on a normal fault. Solid lines represent traces of faults, with bars and balls on downthrown sides. Arrows show trends of slip vectors. Numerals give structural elevations, in arbitrary units, with respect to zero elevation of east wall of main (north-striking) fault strand. Letters identify locations discussed in text.

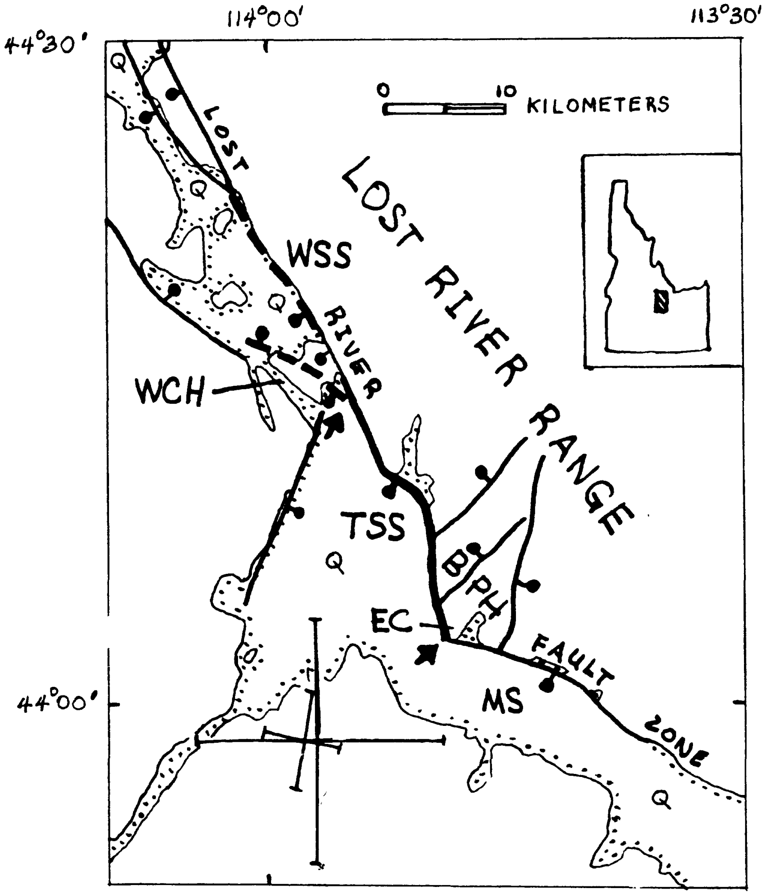

FIGURE 17.--Sketch map of October 28, 1983, Borah Peak earthquake. Heavy lines show ground ruptures from the normal-faulting earthquake, with bars and balls on downthrown sides. Solid line shows continuous surface ruptures, dashed lines show discontinuous ruptures. Medium-weight lines represent older normal faults. Light lines show contact between Quaternary sediments (Q) in valleys and pre-Quaternary bedrock, with dots on Quaternary side of contact. Two crosses show epicentral locations of main shock and locational uncertainties of two independent workers. Large cross is from results of Richins and others (1987, table 2 and p. 704), small cross from results of Dewey (1987, table 1). WSS, Warm Spring segment of Lost River fault; TSS, Thousand Springs segment; MS, Mackay segment; WCH, Willow Creek Hills; EC, Elkhorn Creek; BPH, Borah Peak horst; two small arrows, boundaries of TSS. Inset shows location of map area within Idaho. Simplified from Bond (1978), Skipp and Harding (1985), and Crone and others (1987).

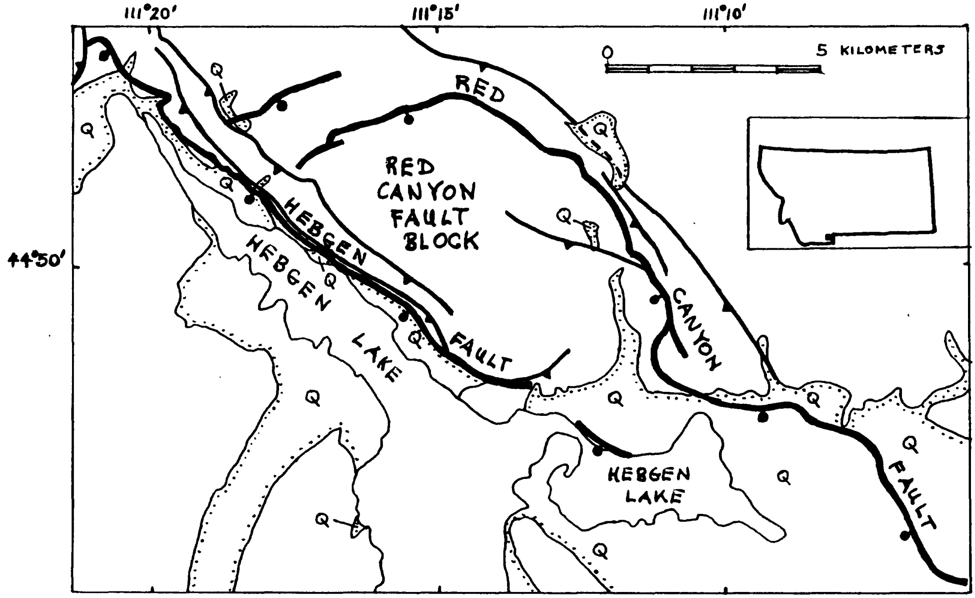

FIGURE 18.--Sketch map of August 17, 1959, Hebgen Lake earthquake. Heavy lines show main ground ruptures from the normal-faulting earthquake, with bars and balls on downthrown sides. Medium-weight lines show traces of reverse faults, with teeth on upthrown sides. Light lines show shoreline of Hebgen Lake, and contact between Quaternary glacial, landslide, and other deposits (Q) and underlying pre-Quaternary bedrock, with dots on Quaternary side of contact. Inset shows location of map area in southwestern Montana. Simplified from Myers and Hamilton (1964, plate 2) and Witkind and others (1964, plate 5).

FIGURE 19.--Sketch maps of July-December, 1954, Rainbow Mountain, Fairview Peak, and Dixie Valley earthquakes. A, normal faults and epicenters. Heavy lines show main surface faulting from 1954, with bars and balls on downthrown sides: DVF, Dixie Valley fault; FF, Fairview fault; GKF, Gold King fault (hachured part also had ground rupture in 1903); RMF, Rainbow Mountain fault; WGF, West Gate fault. Light lines with bars and balls represent other late Quaternary faults. Light lines with dots show contact between Quaternary valley fillings (Q) and pre-Quaternary bedrock, wherever the contact is not a late Quaternary normal fault. Dots identify Quaternary side of contact. Large filled circles locate epicenters of 1954 main shocks, using identifying letters of Doser (1986): A, Rainbow Mountain earthquake, M6.6, July 6, locational precision about 20 km; C, Rainbow Mountain earthquake, M6.8, August 24, precision also about 20 km; F, Fairview Peak earthquake, December 16, M7.1, precision about 8 km (Doser (1986) used this as a master event to locate the other three, but did not include the effect of its locational uncertainty in the precision of the other locations); G, Dixie Valley earthquake, also December 16, M6.8, precision about 40 km. P shows Pirouette Mountain, R locates Rainbow Mountain. Inset shows location of map area within Nevada. Simplified from Slemmons (1956, 1957), Tocher (1956), Slemmons and others (1959), Stewart and Carlson (1978), and Doser (1986). B, Bouguer gravity contours. Dashed lines show Quaternary - pre-Quaternary contact from A, both faulted and unfaulted, with dots identifying Quaternary side. Solid lines represent isogals at 10 mgal contour interval. Simplified from Erwin and Bittleston (1977) and Erwin and Berg (1977), who used a contour interval of 5 mgal.

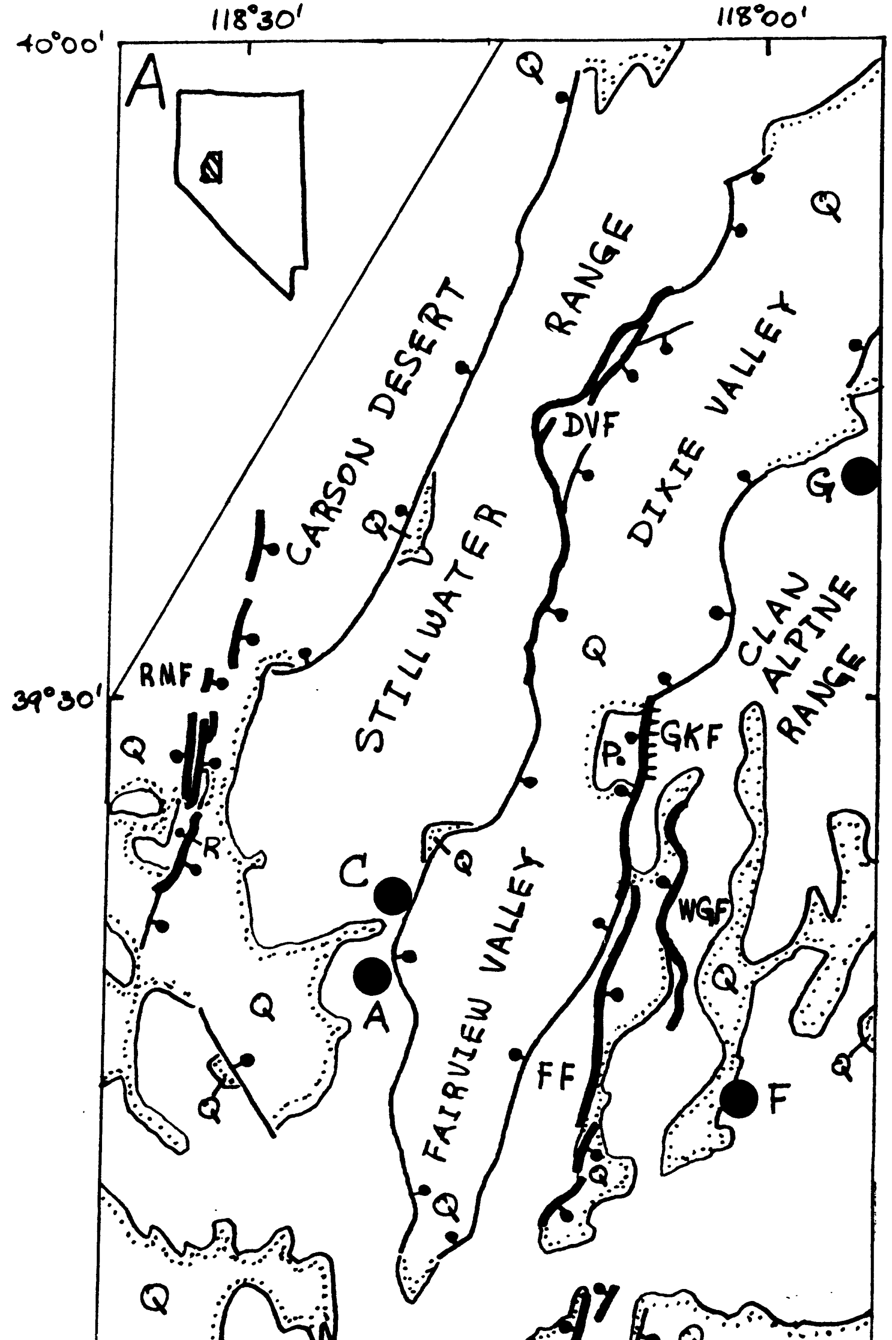
118°30'
118°00'
40°00'
39°30'
39°00'
A
CARSON DESERT
STILLWATER RANGE
RANGE
DIXIE VALLEY
CLAN ALPINE RANGE
FAIRVIEW VALLEY
DVF
RMF
R
GKF
P
WGF
FF
C
A
G
F
Q
0
20 KILOMETERS

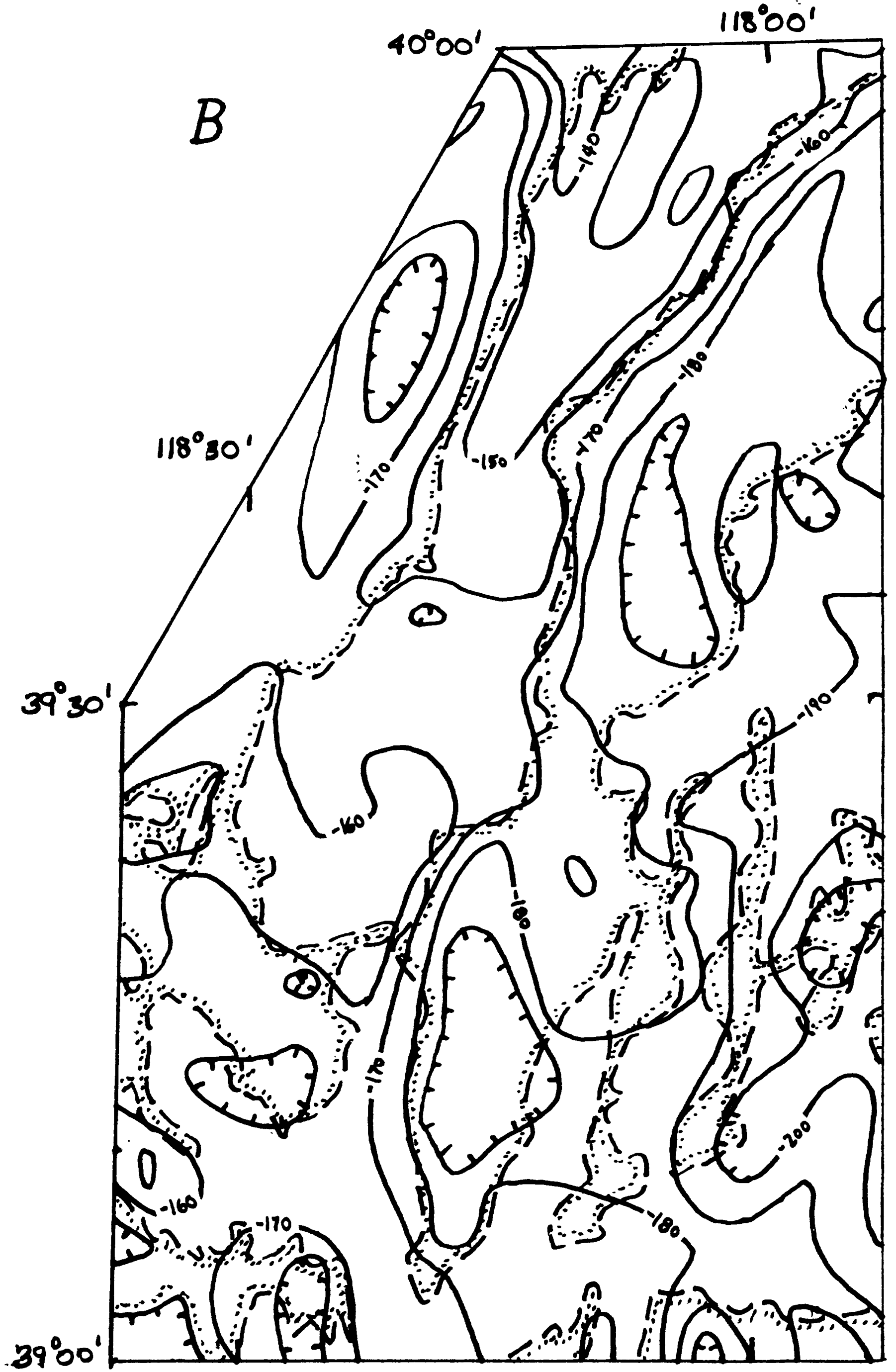
B
118°00'
40°00'
118°30'
39°30'
39°00'
-140
-160
-150
-170
-180
-190
-160
-180
-170
-200
-160
-170
-180
0
20 KILOMETERS

FIGURE 20.--Sketch map of October 2, 1915, Pleasant Valley earthquake. A, Normal faults. Heavy lines show main surface faulting from 1915, with bars and balls on downthrown sides: CMS, China Mountain scarp; TS, Tobin scarp; PS, Pearce scarp; SHS, Sou Hills scarp; SS, Stillwater scarp. Light lines with bars and balls represent other Quaternary faults. Bars and balls are omitted where slip sense is not known. Light lines with dots show contact between Quaternary valley fillings (Q) and pre-Quaternary bedrock, wherever the contact is not a Quaternary fault. Dots identify Quaternary side of contact. Inset shows location of map area within Nevada. Simplified from Muller and others (1951), Speed (1976), Stewart and Carlson (1978), Wallace (1984), and Wallace and Whitney (1984). B, Bouguer gravity contours. Dashed lines show Quaternary - pre-Quaternary contact from part A, both faulted and unfaulted, with dots identifying Quaternary side. Solid lines represent selected isogals. Contour interval is 5 mgal near gravity saddles A-C, 10 mgal elsewhere. Simplified from Erwin (1974).

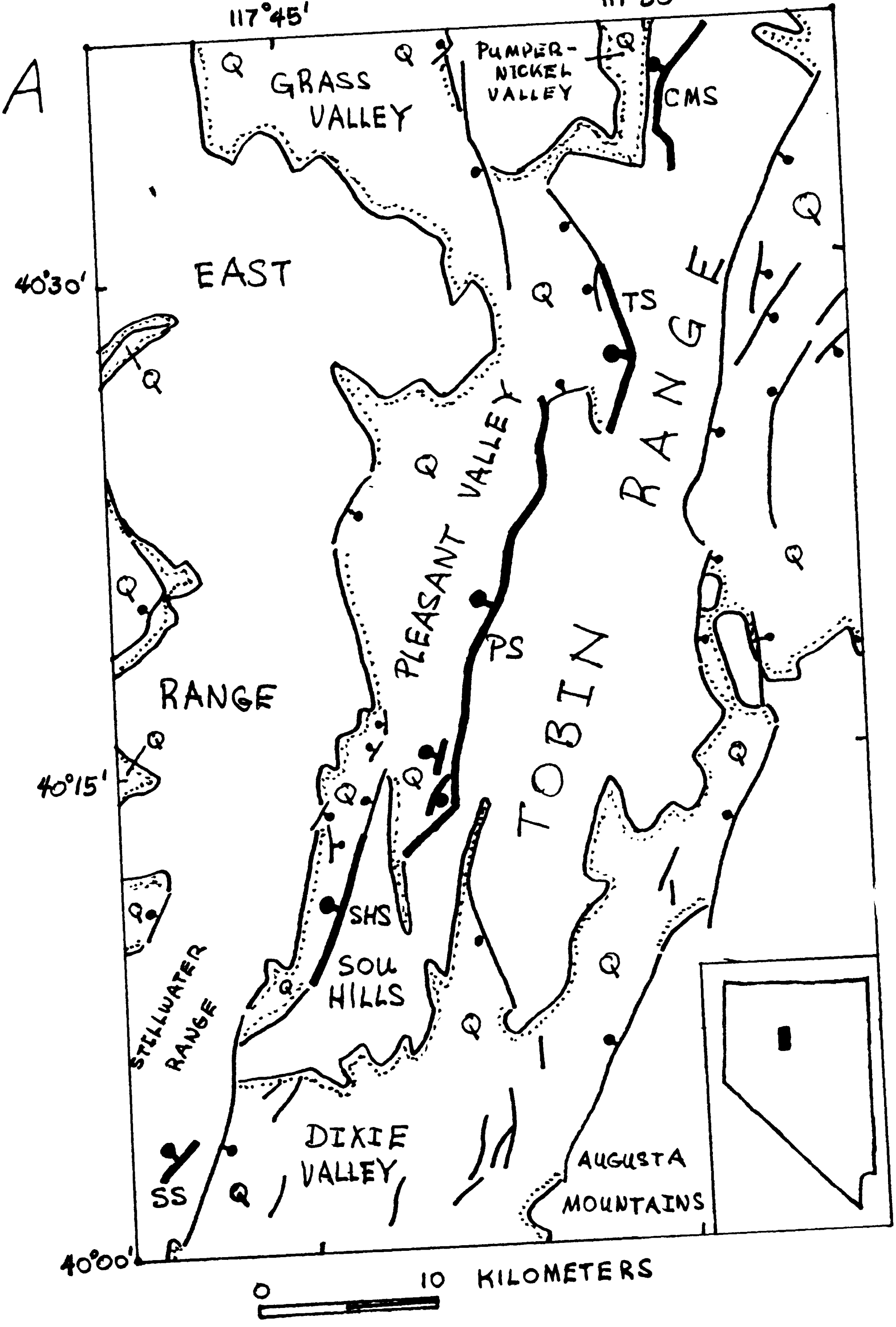
A
117°45'
117°30'
40°30'
40°15'
40°00'
GRASS VALLEY
PUMPER-NICKEL VALLEY
CMS
EAST RANGE
TS
TOBIN RANGE
PLEASANT VALLEY
PS
SHS
SOU HILLS
STILLWATER RANGE
DIXIE VALLEY
SS
AUGUSTA MOUNTAINS
Q
0
10 KILOMETERS

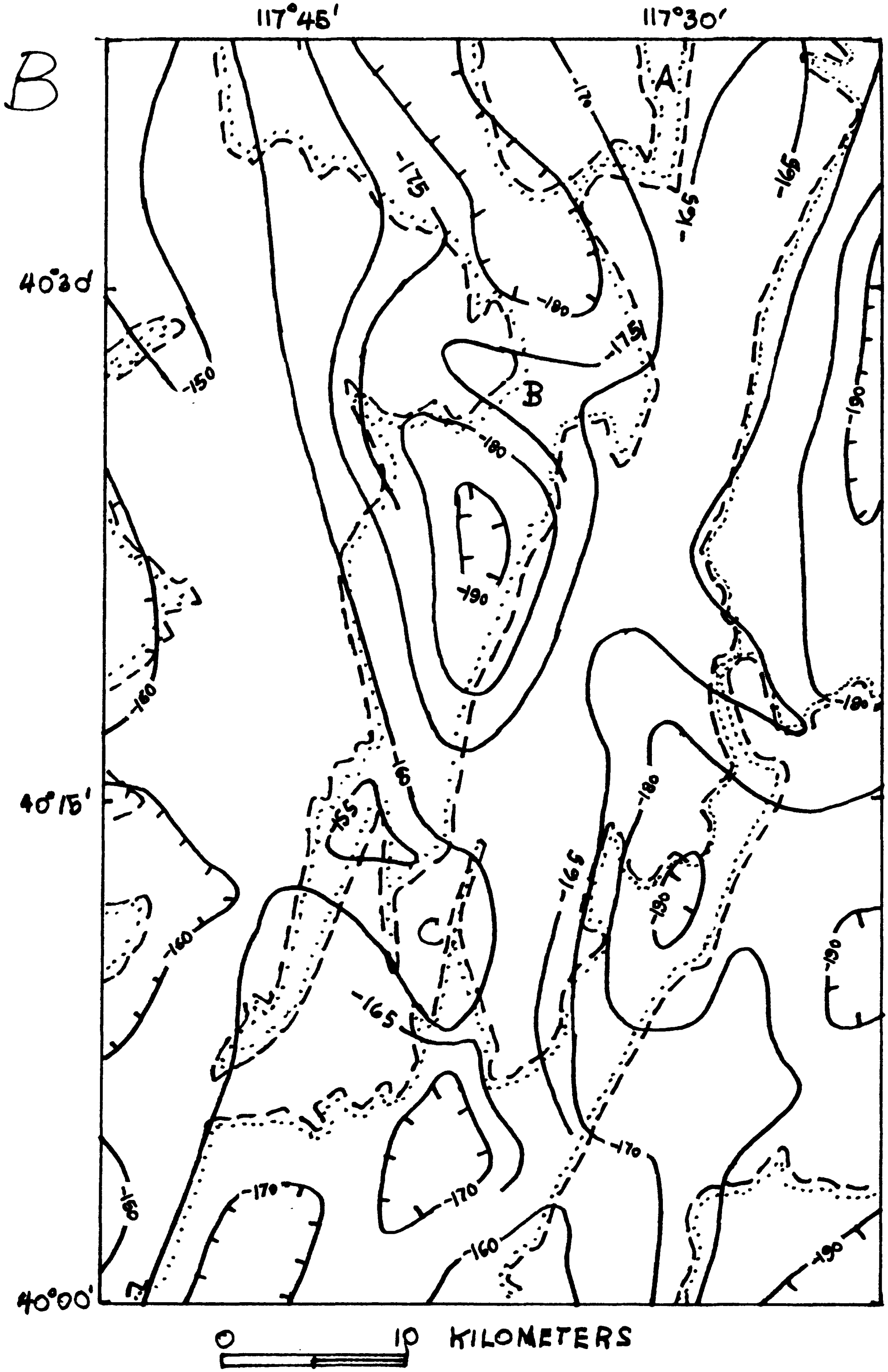
B
117°45'
117°30'
40°30'
40°15'
40°00'
A
B
C
-170
-175
-165
-165
-180
-175
-150
-180
-190
-190
-190
-180
-190
-160
-160
-16
-55
-180
-190
-165
-165
-190
-170
-170
-170
-180
-160
-190
0
10 KILOMETERS

REFERENCES

Algermissen, S.T., Perkins, D.M., Thenhaus, P.C., Hanson, S.L., and Bender, B.L., 1982, Probabilistic estimates of maximum acceleration and velocity in rock in the contiguous United States: U.S. Geological Survey Open-File Report 82-1033, 99 p., 6 folded pl.

Anderson, R.E., 1985, Regional and local hazards mapping in the eastern Great Basin, in Jacobsen, M.L., and Rodriguez, T.R., compilers, National Earthquake Hazards Reduction Program, Summaries of Technical Reports Volume XXI: U.S. Geological Survey Open-File Report 86-31, p. 472-478.

-----1986, Regional and local hazards mapping in the eastern Great Basin, in Jacobsen, M.L., and Rodriguez, T.R., compilers, National Earthquake Hazards Reduction Program, Summaries of Technical Reports Volume XXII: U.S. Geological Survey Open-File Report 86-383, p. 480-483.

Arabasz, W.J., 1984, Earthquake behavior in the Wasatch Front area: Association with geologic structure, space-time occurrence, and stress state, in Hays, W.W., and Gori, P.L., eds., Workshop on "Evaluation of regional and urban earthquake hazards and risk in Utah", Salt Lake City, Utah, August 14-16, 1984, Proceedings: U.S. Geological Survey Open-File Report 84-763, p. 310-339.

Arabasz, W.J., and Julander, D.R., 1986, Geometry of seismically active faults and crustal deformation within the Basin and Range-Colorado Plateau transition in Utah: Geological Society of America Special Paper 208, p.

43-74.

Arabasz, W.J., Smith, R.B., and Richins, W.D., 1980, Earthquake studies along the Wasatch Front, Utah: Network monitoring, seismicity, and seismic hazards: Bulletin of the Seismological Society of America, v. 70, p. 1479-1499.

Armstrong, R.C., and Oriel, S.S., 1965, Tectonic development of Idaho-Wyoming thrust belt: Bulletin of the American Association of Petroleum Geologists, v. 49, p. 1847-1866.

Armstrong, R.L., 1968, Sevier orogenic belt in Nevada and Utah: Geological Society of America Bulletin, v. 79, p. 429-458.

Barrientos, S.E., Stein, R.S., and Ward, S.N., 1987, Comparison of the 1959 Hebgen Lake, Montana and the 1983 Borah Peak, Idaho earthquakes from geodetic observations: Bulletin of the Seismological Society of America, v. 77, p. 784-808.

Boatwright, John, 1985, Characteristics of the aftershock sequence of the Borah Peak, Idaho, earthquake determined from digital recordings of the events: Bulletin of the Seismological Society of America, v. 75, p. 1265-1284.

Bond, J.G., 1978, Geologic map of Idaho: Moscow, Idaho, Idaho Bureau of Mines and Geology, 1 sheet, scale 1:500,000.

Bonilla, M.G., Villalobos, H.A., and Wallace, R.E., 1984, Exploratory trench across the Pleasant Valley fault, Nevada: U.S. Geological Survey Professional Paper 1274-B, p. B1-B14, 1 folded plate.

Bruhn, R.L., Gibler, P.R., Houghton, Wendy, and Parry, W.T., in press, a, Structure of the Salt Lake segment, Wasatch normal fault zone: Implications for rupture propagation during normal faulting, in Hays, W.W., and Gori, P.L., eds., Evaluation of urban and regional earthquake hazards and risk in Utah: U.S. Geological Survey Professional Paper.

Bruhn, R.L., Gibler, P.R., and Parry, W.T., in press, b, Rupture characteristics of normal faults: An example from the Wasatch fault zone, Utah, in Dewey, J.F., Coward, M.P., and Hancock, P.H., eds., Continental extensional tectonics: Journal of the Geological Society of London.

Bruhn, R.L., Picard, M.D., and Beck, S.L., 1983, Mesozoic and early Tertiary structure and sedimentology of the central Wasatch Mountains, Uinta Mountains and Uinta Basin, in Gurgel, K.D., ed., Geologic excursions in the overthrust belt and metamorphic core complexes of the Intermountain region: Utah Geological and Mineral Survey Special Studies 59, p. 63-105.

Bryant, Bruce, 1984, Reconnaissance geologic map of the Precambrian Farmington Canyon Complex and surrounding rocks in the Wasatch Mountains between Ogden and Bountiful, Utah: U.S. Geological Survey Miscellaneous Investigations Map I-1447, scale 1:50,000, 1 sheet.

-----1985, Structural ancestry of the Uinta Mountains, in Picard, M.D., ed., Geology and energy resources, Uintah basin of Utah: Utah Geological Association Publication 12, p. 115-120.

Bryant, Bruce, and Nichols, D.J., in press, Late Mesozoic and early Tertiary reactivation of an ancient zone of crustal weakness along the Uinta arch and its interaction with the Sevier orogenic belt, in Schmidt, C.J., and Perry, W.J., Jr., eds., Interaction of the Rocky Mountain foreland and the frontal Cordilleran thrust belt: Geological Society of America Special Paper.

Burke, Kevin, and Dewey, J.F., 1973, Plume-generated triple junctions: Key indicators in applying plate tectonics to old rocks: Journal of Geology, v. 81, p. 406-433.

Cheetham, A.H., and Hazel, J.E., 1969, Binary (presence-absence) similarity coefficients: Journal of Paleontology, v. 43, p. 1130-1136.

Crittenden, M.D., Jr., 1961, Magnitude of thrust faulting in northern Utah: U.S. Geological Survey Professional Paper 424-D, art. 35, p. D128-D131.

-----1965, Geology of the Dromedary Peak quadrangle, Utah: U.S. Geological Survey Geologic Quadrangle Map GQ-378, scale 1:24,000, 1 sheet.

-----1972, Willard thrust and the Cache allochthon, Utah: Geological Society of America Bulletin, v. 83, p. 2871-2880.

-----1974, Regional extent and age of thrusts near Rockport Reservoir and relation to possible exploration targets in northern Utah: American Association of Petroleum Geologists Bulletin, v. 58, p. 2428-2435.

Crittenden, M.D., Jr., and Sorensen, M.L., 1985, Geologic map of the North Ogden quadrangle and part of the Ogden and Plain City quadrangles, Box Elder and Weber Counties, Utah: U.S. Geological Survey Miscellaneous Investigations Series Map I-1606, 1 sheet, scale 1:24,000.

Crittenden, M.D., Jr., Stuckless, J.S., Kistler, R.W., and Stern, T.W., 1973, Radiometric dating of intrusive rocks in the Cottonwood area, Utah: Journal of Research of the U.S. Geological Survey, v. 1, p. 173-178.

Crone, A.J., Haller, K.M., Guo, Shunmin, Liao, Yuhua, Li, Yulong, and Vincent, K.R., 1985, Late Quaternary faulting along the Mackay segment of the Lost River fault, central Idaho [abs.]: Transactions of the American Geophysical Union, v. 66, no. 46, p. 1067.

Crone, A.J., and Machette, M.N., 1984, Surface faulting accompanying the Borah Peak earthquake, central Idaho: Geology, v. 12, p. 664-667.

Crone, A.J., Machette, M.N., Bonilla, M.G., Lienkaemper, J.J., Pierce, K.L., Scott, W.E., and Bucknam, R.C., 1987, Surface faulting accompanying the Borah Peak earthquake and segmentation of the Lost River fault, central Idaho: Bulletin of the Seismological Society of America, v. 77, p. 739-770.

Davis, F.D., compiler, 1983a, Geologic map of the central Wasatch Front, Utah: Utah Geological and Mineral Survey Map 54-A, scale 1:100,000, 2 sheets.

-----1983b, Geologic map of the southern Wasatch Front, Utah: Utah Geological and Mineral Survey Map 55-A, scale 1:100,000, 2 sheets.

-----1985, Geologic map of the northern Wasatch Front, Utah: Utah Geological and Mineral Survey Map 53-A, scale 1:100,000, 2 sheets.

Dewey, J.W., 1987, Instrumental seismicity of central Idaho: Bulletin of the Seismological Society of America, v. 77, p. 819-836.

Doser, D.I., 1985a, The 1983 Borah Peak, Idaho and 1959 Hebgen Lake, Montana earthquakes, in Stein, R.S., and Bucknam, R.C., eds., Workshop XXVIII On the Borah Peak, Idaho, earthquake, 3-6 October, 1984, Proceedings, v. A: U.S. Geological Survey Open-File Report 85-290, p. 368-384.

-----1985b, Source parameters and faulting processes of the 1959 Hebgen Lake, Montana, earthquake sequence: Journal of Geophysical Research, v. 90, no. B6, p. 4537-4555.

-----1986, Earthquake processes in the Rainbow Mountain-Fairview Peak-Dixie Valley, Nevada, region 1954-1959: Journal of Geophysical Research, v. 91, no. B12, p. 12572-12586.

Doser, D.I., and Smith, R.B., 1985, Source parameters of the 28 October 1983 Borah Peak, Idaho, earthquake from body wave analysis: Bulletin of the

Seismological Society of America, v. 75, p. 1041-1051.

Erwin, J.W., 1974, Bouguer gravity map of Nevada--Winnemucca sheet: Nevada Bureau of Mines and Geology Map 47, 1 sheet, scale 1:250,000, 4 p. pamphlet.

Erwin, J.W., and Berg, J.C., 1977, Bouguer gravity map of Nevada--Reno sheet: Nevada Bureau of Mines and Geology Map 58, 1 sheet, scale 1:250,000.

Erwin, J.W., and Bittleston, E.W., 1977, Complete Bouguer gravity map of Nevada--Millett sheet: Nevada Bureau of Mines and Geology Map 53, 1 sheet, scale 1:250,000.

Fonseca, J.E., 1985, Barriers to faulting in the Basin-Range province--Evidence from the Sou Hills transverse block: Geological Society of America Abstracts with Programs, v. 17, no. 7, p. 585.

Forrester, J.D., 1937, Structure of the Uinta Mountains: Geological Society of America Bulletin, v. 48, p. 631-666.

Glass, C.E., and Slemmons, D.B., 1969, Restudy of surface faulting from the October 2, 1915, Pleasant Valley area earthquake, Nevada: Geological Society of America Abstracts with Programs, v. 1, no. 5, p. 28.

Gries, Robbie, 1983, North-south compression of Rocky Mountain foreland structures, <u>in</u> Lowell, J.D., and Gries, Robbie, eds., Rocky Mountain foreland basins and uplifts: Denver, Colorado, Rocky Mountain Association of Geologists, p. 9-32.

Hanks, R.C., and Schwartz, D.P., 1987, Morphologic dating of the pre-1983 fault scarp on the Lost River fault at Doublespring Pass Road, Custer County, Idaho: Bulletin of the Seismological Society of America, v. 77, p. 837-846.

Hansen, W.R., 1965, Geology of the Flaming Gorge area, Utah-Colorado-Wyoming: U.S. Geological Survey Professional Paper 490, 196 p.

Hazel, J.E., 1970, Binary coefficients and clustering in biostratigraphy: Geological Society of America Bulletin, v. 81, p. 3237-3252.

Hintze, L.F., 1980, compiler, Geologic map of Utah: Salt Lake City, Utah, Utah Geological and Mineral Survey, scale 1:500,000, 2 sheets.

Houghton, W.P., 1986, Structural analysis of the Salt Lake-Provo segment boundary of the Wasatch fault zone: M.S. thesis, University of Utah, 64 p.

Keaton, J.R., Currey, D.R., and Olig, S.J., 1987, Paleoseismicity and earthquake hazards evaluation of the West Valley fault zone, Salt Lake City urban area, Utah: Salt Lake City, Utah, Report to U.S. Geological Survey for contract no. 14-08-0001-22048, 93 p.

King, Geoffrey, 1983, The accomodation of large strains in the upper lithosphere of the Earth and other solids by self-similar fault systems: The geometrical origin of b-value: Pure and Applied Geophysics, v. 121, p. 761-815.

King, G.C.P., 1986, Speculations on the geometry of the initiation and termination processes of earthquake rupture and its relation to morphology and geological structure: Pageoph, v. 124, p. 567-585.

King, Geoffrey, and Nabelek, John, 1985, Role of fault bends in the initiation and termination of earthquake rupture: Science, v. 228, p. 984-987.

King, Geoffrey, and Yielding, Graham, 1983, The evolution of a thrust fault system: Processes of rupture initiation, propagation and termination in the 1980 El Asnam (Algeria) earthquake: Geophysical Journal of the Royal Astronomical Society, v. 77, p. 915-933.

Larson, E.R., 1957, Minor features of the Fairview fault, Nevada: Bulletin of the Seismological Society of America, v. 47, p. 377-386.

Lawton, T.F., 1985, Style and timing of frontal structures, thrust belt, central Utah: American Association of Petroleum Geologists Bulletin, v. 69, p. 1145-1159.

Mabey, D.R., in press, Subsurface geology along the Wasatch Front, _in_ Hays, W.W., and Gori, P.L., eds., Evaluation of urban and regional earthquake hazards and risk in Utah: U.S. Geological Survey Professional Paper.

Mabey, D.R., Crittenden, M.D., Jr., Morris, H.T., Roberts, R.J., and Tooker, E.W., 1964, Aeromagnetic and generalized geologic map of part of north-central Utah: U.S. Geological Survey Geophysical Investigations Map GP-422, scale 1:250,000, 1 sheet.

Machette, M.N., 1984, Preliminary investigations of late Quaternary slip rates along the southern part of the Wasatch fault zone, central Utah, in Hays, W.W., and Gori, P.L., eds., Workshop on "Evaluation of regional and urban earthquake hazards and risk in Utah", Salt Lake City, Utah, August 14-16, 1984, Proceedings: U.S. Geological Survey Open-File Report 84-763, p. 391-406.

Machette, M.N., Personius, S.F., and Nelson, A.R., 1986, Late Quaternary segmentation and slip-rate history of the Wasatch fault zone, Utah [abs.]: Transactions of the American Geophysical Union, v. 67, no. 44, p. 1107.

-----in press, Quaternary geology along the Wasatch fault zone--Segmentation, recent investigations, and preliminary conclusions, in Hays, W.W., and Gori, P.L., eds., Evaluation of urban and regional earthquake hazards and risk in Utah: U.S. Geological Survey Open-File Report, 64 ms. p.

Maclean, A. F., 1985, Quaternary segmentation of the Wasatch fault zone, Utah, as studied by morphometric discriminant analysis: Oxford, Ohio, Miami University M. S. thesis, 200 p.

Mattick, R.E., 1970, Thickness of unconsolidated to semiconsolidated sediments in Jordan Valley, Utah: U.S. Geological Survey Professional Paper 700-C, p. C119-C124.

Mayer, Larry, and Maclean, Alison, 1986, Tectonic geomorphology of the Wasatch Front, Utah, using morphologic discriminant analysis--Preliminary implications for Quaternary segmentation of the Wasatch fault zone [abs.]: Geological Society of America Abstracts with Programs, v. 18, no. 2, p. 155.

Meister, L.J., 1967, Seismic refraction study of Dixie Valley, Nevada, <u>in</u> Thompson, G.A., Meister, L.J., Herring, A.T., Smith, T.E., Burke, D.B., Kovach, R.L., Burford, R.O., Salehi, I.A., and Wood, M.D., Geophysical study of Basin-Range structure, Dixie Valley region, Nevada: Bedford, Massachusetts, U.S. Air Force Cambridge Research Laboratories, Final Scientific Report, contract no. AF 19(628)-3867, part I, 80 p.

Miller, R.G., Jr., 1981, Simultaneous statistical inference, 2d. ed.: New York, Springer-Verlag, 299 p.

Muller, S.W., Ferguson, H.G., and Roberts, R.J., 1951, Geology of the Mount Tobin quadrangle, Nevada: U.S. Geological Survey Geologic Quadrangle Maps GQ-7, 4 folio p., including map of 1 sheet, scale 1:125,000.

Myers, W.B., and Hamilton, Warren, 1964, Deformation accompanying the Hebgen Lake earthquake of August 17, 1959--The Hebgen Lake, Montana, earthquake of August 17, 1959: U.S. Geological Survey Professional Paper 435-I, p. 55-98, 2 folded plates.

Nelson, A.R., and Personius, S.F., 1987, A nonconservative barrier to Holocene rupture propagation in the northern Wasatch fault zone, Utah [abs.]: International Union for Quaternary Research, 12th International Congress, Ottawa, Canada, July 31-August 9, 1987, Programme with Abstracts, p. 231.

Naeser, C.W., Bryant, Bruce, Crittenden, M.D., Jr., and Sorensen, M.L., 1983, Fission-track ages of apatite in the Wasatch Mountains, Utah: An uplift study, in Miller, D.M., Todd, V.R., and Howard, K.A., eds., Tectonic and stratigraphic studies in the eastern Great Basin: Geological Society of America Memoir 157, p. 29-36.

Okaya, D.A., and Thompson, G.A., 1985, Geometry of Cenozoic extensional faulting: Dixie Valley, Nevada: Tectonics, v. 4, p. 107-125.

Oriel, S.S., and Armstrong, F.C., 1966, Times of thrusting in Idaho-Wyoming thrust belt: Reply: Bulletin of the American Association of Petroleum Geologists, v. 50, p. 2614-2621.

Personius, S.F., 1985, Preliminary assessment of late Quaternary displacement along the Wasatch fault zone near Brigham City, Utah [abs.]: Geological Society of America Abstracts with Programs, v. 17, no. 4, p. 261.

-----1986, The Brigham City segment--A new segment of the Wasatch fault zone, northern Utah [abs.]: Geological Society of America Abstracts with Programs, v. 18, no. 5, p. 402.

Richins, W.D., Pechmann, J.C., Smith, R.B., Langer, C.J., Goter, S.K., Zollweg, J.E., and King, J.J., 1987, The Borah Peak, Idaho, earthquake and its aftershocks: Bulletin of the Seismological Society of America, v. 77, p. 694-723.

Ryall, Alan, 1962, The Hebgen Lake, Montana, earthquake of August 18, 1959--*P* waves: Bulletin of the Seismological Society of America, v. 52, p. 235-271.

Ryall, Alan, and Malone, S.D., 1971, Earthquake distribution and mechanism of faulting in the Rainbow Mountain-Dixie Valley-Fairview Peak area, central Nevada: Journal of Geophysical Research, v. 76, no. 29, p. 7241-7248.

Salyards, S.L., 1985, Patterns of offset associated with the 1983 Borah Peak, Idaho, earthquake and previous events, *in* Stein, R.S., and Bucknam, R.C., eds., Workshop XXVIII On the Borah Peak, Idaho, earthquake, 3-6 October, 1984, Proceedings, v. A: U.S. Geological Survey Open-File Report 85-290, p. 59-75.

Schirmer, T.W., 1985, Basement thrusting in north-central Utah: A model for the development of the northern Utah highland, *in* Kerns, G.J., and Kerns, R.L., Jr., eds., Orogenic patterns and stratigraphy of north-central Utah and southeastern Idaho: Utah Geological Association Publication 14, p. 129-143.

Schwartz, D.P., and Coppersmith, K.J., 1984, Fault behavior and characteristic earthquakes: Examples from the Wasatch and San Andreas fault zones:

Journal of Geophysical Research, v. 89, p. 5681-5698.

Schwartz, D.P., and Crone, A.J., 1985, The 1983 Borah Peak earthquake--A calibration event for quantifying earthquake recurrence and fault behavior on Great Basin normal faults, in Stein, R.S., and Bucknam, R.C., eds., Workshop XXVIII On the Borah Peak, Idaho, earthquake, 3-6 October, 1984, Proceedings, v. A: U.S. Geological Survey Open-File Report 85-290, p. 153-160.

Scott, W.E., and Shroba, R.R., 1985, Surficial geologic map of an area along the Wasatch fault zone in the Salt Lake Valley, Utah: U.S. Geological Survey Open-File Report 85-448, 18 p., 1 folded plate of 2 sheets.

Skipp, Betty, and Harding, S.T., 1985, Preliminary report on geology of Borah Peak area, Idaho, including interpretation of seismic and gravity data, in Stein, R.S., and Bucknam, R.C., eds., Workshop XXVIII On the Borah Peak, Idaho, earthquake, 3-6 October, 1984, Proceedings, v. A: U.S. Geological Survey Open-File Report 85-290, p. 657-671.

Slemmons, D.B., 1956, Geologic setting for the Fallon-Stillwater earthquakes of 1954: Bulletin of the Seismological Society of America, v. 46, p. 4-9.

-----1957, Geological effects of the Dixie Valley-Fairview Peak, Nevada, earthquakes of December 16, 1954: Bulletin of the Seismological Society of America, v. 47, p. 353-375, 1 folded plate.

Slemmons, D.B., McDonald, R.L., and Cluff, Lloyd, 1969, Surface faulting from the December 16, 1954, earthquake in Dixie Valley, Nevada: Geological Society of America Abstracts with Programs, v. 1, no. 5, p. 73-74.

Slemmons, D.B., Steinbrugge, K.V., Tocher, Don, Oakeshott, G.B., and Gianella, V.P., 1959, Wonder, Nevada, earthquake of 1903: Bulletin of the Seismological Society of America, v. 49, p. 251-265, 2 folded plates.

Smith, R.B., and Bruhn, R.L., 1984, Intraplate extensional tectonics of the eastern Basin-Range: Inferences on structural style from seismic reflection data, regional tectonics, and thermal-mechanical models of brittle-ductile deformation: Journal of Geophysical Research, v. 89, p. 5733-5762.

Smith, R.B., and Richins, W.D., 1984, Seismicity and earthquake hazards of Utah and the Wasatch Front: Paradigm and paradox, in Hays, W.W., and Gori, P.L., eds., Workshop on "Evaluation of regional and urban earthquake hazards and risk in Utah", Salt Lake City, Utah, August 14-16, 1984, Proceedings: U.S. Geological Survey Open-File Report 84-763, p. 73-112.

Snay, R.A., Cline, M.W., and Timmerman, E.L., 1985, Dislocation models for the 1954 earthquake sequence in Nevada, in Stein, R.S., and Bucknam, R.C., eds., Workshop XXVIII On the Borah Peak, Idaho, earthquake, 3-6 October, 1984, Proceedings, v. A: U.S. Geological Survey Open-File Report 85-290, p. 531-555.

Speed, R.C., 1976, Geologic map of the Humboldt lopolith and surrounding terrane, Nevada: Geological Society of America Map and Chart Series MC-

14, 1 sheet, scale 1:81,000, 6 p. pamphlet.

Stauder, William, and Ryall, Alan, 1967, Spatial distribution and source mechanism of microearthquakes in central Nevada: Bulletin of the Seismological Society of America, v. 57, p. 1317-1345.

Stewart, J.H., and Carlson, J.E., 1978, Geologic map of Nevada: U.S. Geological Survey and Nevada Bureau of Mines and Geology, 3 sheets, scale 1:500,000.

Stewart, S.W., Hofmann, R.B., and Diment, W.H., 1964, Some aftershocks of the Hebgen Lake earthquake--The Hebgen Lake, Montana, earthquake of August 17, 1959: U.S. Geological Survey Professional Paper 435-D, p. 19-24.

Stone, D.S., 1986, Seismic and borehole evidence for important pre-Laramide faulting along the Axial Arch in northwest Colorado, <u>in</u> Stone, D.S., ed., New interpretations of northwest Colorado geology: Denver, Colorado, Rocky Mountain Association of Geologists, p. 19-36.

Susong, D.D., and Bruhn, R.L., 1986, Structure of an earthquake rupture segment boundary in the Lost River fault zone, Idaho--Implications for rupture propagation during the 1983 Borah Peak earthquake [abs.]: Transactions of the American Geophysical Union, v. 67, no. 44, p. 1107.

Swan, F.H., III, Schwartz, D.P., and Cluff, L.S., 1980, Recurrence of moderate to large magnitude earthquakes produced by surface faulting on the Wasatch fault zone, Utah: Bulletin of the Seismological Society of America, v.

70, p. 1431-1462.

Thenhaus, P.C., ed., 1983, Summary of workshops concerning regional seismic source zones of parts of the conterminous United States, convened by the U.S. Geological Survey 1979-1980, Golden, Colorado: U.S. Geological Survey Circular 898, 36 p.

Tocher, Don, 1956, Movement on the Rainbow Mountain fault: Bulletin of the Seismological Society of America, v. 46, p. 10-14, 3 unnumbered folded plates.

Trimble, A.B., and Smith, R.B., 1975, Seismicity and contemporary tectonics of the Hebgen Lake-Yellowstone Park region: Journal of Geophysical Research, v. 80, no. 5, p. 733-741.

Vincent, K.R., 1985, Measurement of vertical tectonic offset using longitudinal profiles of faulted geomorphic surfaces near Borah Peak, Idaho--A preliminary report, _in_ Stein, R.S., and Bucknam, R.C., eds., Workshop XXVIII On the Borah Peak, Idaho, earthquake, 3-6 October, 1984, Proceedings, v. A: U.S. Geological Survey Open-File Report 85-290, p. 76-96.

Wallace, R.E., 1984, Fault scarps formed during the earthquakes of October 2, 1915, in Pleasant Valley, Nevada, and some tectonic implications: U.S. Geological Survey Professional Paper 1274-A, p. A1-A33, 1 folded plate.

Wallace, R.E., and Whitney, R.A., 1984, Late Quaternary history of the

Stillwater seismic gap, Nevada: Bulletin of the Seismological Society of America, v. 74, p. 301-314.

Wallace, C.A., and Crittenden, M.D., Jr., 1969, The stratigraphy, depositional environment and correlation of the Precambrian Uinta Mountain Group, western Uinta Mountains, Utah, in Lindsay, J.B., ed., Geologic guidebook of the Uinta Mountains, Utah's maverick range: Intermountain Association of Geologists, Annual field conference, 16th, September 4-6, 1969, Guidebook, p. 127-141.

Westphal, W.H., and Lange, A.L., 1967, Local seismic monitoring--Fairview Peak area, Nevada: Bulletin of the Seismological Society of America, v. 57, p. 1279-1298.

Wheeler, R.L., 1984, A plan for evaluating hypothesized segmentation of the Wasatch fault, in Hays, W.W., and Gori, P.L., eds., A workshop on "Evaluation of regional and urban earthquake hazards and risk in Utah", Salt Lake City, August 1984, Proceedings: U.S. Geological Survey Open-File Report 84-763, p. 576-605.

Wheeler, R.L., and Krystinik, K.B., 1987a, Persistent and nonpersistent segment boundaries on the Wasatch fault, central Utah [abs.]: Seismological Research Letters, v. 58, no. 1, p. 31.

-----1987b, Persistent and nonpersistent seismic segmentation of the Wasatch fault zone, Utah [abs.]: Geological Society of America Abstracts with Programs, v. 19, no. 5, p. 342.

-----in press a, Evaluating coinciding anomalies along a fault trace or other traverse--Simulations and statistical procedures: U.S. Geological Survey Bulletin.

-----in press b, Segmentation of the Wasatch fault zone, Utah--Summaries, analyses, and interpretations of geological and geophysical data: U.S. Geological Survey Bulletin.

Whitten, C.A., 1957, Geodetic measurements in the Dixie Valley area: Bulletin of the Seismological Society of America, v. 47, p. 321-325.

Witkind, I.J., Hadley, J.B., and Nelson, W.H., 1964, Pre-Tertiary stratigraphy and structure of the Hebgen Lake area--The Hebgen Lake, Montana, earthquake of August 17, 1959: U.S. Geological Survey Professional Paper 435-R, p. 199-207, 1 folded plate.

Witkind, I.J., Myers, W.B., Hadley, J.B., Hamilton, Warren, and Fraser, G.D., 1962, Geologic features of the earthquake at Hebgen Lake, Montana, August 17, 1959: Bulletin of the Seismological Society of America, v. 52, p. 163-180.

Zietz, Isidore, Shuey, Ralph, and Kirby, J.R., Jr., 1976, Aeromagnetic map of Utah: U.S. Geophysical Investigations Map GP-907, scale 1:1,000,000, 1 sheet.

Zoback, M.L., 1983, Structure and Cenozoic tectonism along the Wasatch fault zone, Utah, in Miller, D.M., Todd, V.R., and Howard, K.A., eds., Tectonics and stratigraphy of the eastern Great Basin: Geological Society of America Memoir 157, p. 3-27.

Zollweg, J.E., and Richins, W.D., 1985, Later aftershocks of the 1983 Borah Peak, Idaho, earthquake and related activity in central Idaho, in Stein, R.S., and Bucknam, R.C., eds., Workshop XXVIII On the Borah Peak, Idaho, earthquake, 3-6 October, 1984, Proceedings, v. A: U.S. Geological Survey Open-File Report 85-290, p. 345-384.

SUBSURFACE GEOLOGY ALONG THE WASATCH FRONT

by

Don R. Mabey

Utah Geological and Mineral Survey

Salt Lake City, Utah

ABSTRACT

Most of the life and property at risk from an earthquake on the Wasatch fault are in the valley areas west of the fault where a complete cover of Quaternary sediments obscures the pre-Quaternary geology. A compilation of drill holes in the valley that provide significant information on the subsurface aeolian has been used with regional gravity and magnetic data supplemented locally by more detailed geophysical surveys in a study of the subsurface geology of the Wasatch Front area. Bouguer gravity lows are produced by low-density sediment in a string of Cenozoic basins along the Wasatch Front. These sediments, which are primarily Miocene and Pliocene in age, are up to 4 km thick in grabens that underlie the valleys. Major normal faults are reflected by large linear gravity gradients. Detailed quantitative interpretations of the gravity anomalies requires information on the lateral and vertical variations in the density of the Cenozoic sediments. The large eastward decrease in regional Bouguer gravity anomalies across the Wasatch Front reflects isostatic compensation for the high elevations of the Wasatch Range and areas to the east. Individual basins and ranges to the west are not in isostatic equilibrium. The segmentation of the gravity lows and blocks of contrasting basement lithology indicated by the magnetic data suggest segment boundaries of the Wasatch fault zone that are generally consistent with segment boundaries inferred from surface mapping of the fault zone.

INTRODUCTION

The Wasatch fault zone lies between the north-trending Wasatch Range on the east and a near-continuous string of valleys on the west. At two locations Tertiary and older rocks occur in transverse zones extending between the Wasatch Range and parallel ranges to the west. Elsewhere, Quaternary sediments cover the valley areas. Most of the population and property at risk from an earthquake on the Wasatch fault zone is in these valleys. Knowledge of the subsurface structure of these valleys and the physical properties of the rocks underlying the valley floors is important to both an understanding the geologic structure of the Wasatch Front and to predicting the ground response and deformation that will occur with an earthquake along the Wasatch fault zone. Most pre-Cenozoic rocks that are exposed in the Wasatch Range and the parallel ranges to the west are in thrust sheets that moved tens of kilometers eastward relative to underlying rocks, during the Sevier orogeny . Exposures of autochthonous pre-Cenozoic rock are not adequate to reveal the deep subsurface geology or to define major crustal blocks along the Wasatch Front. The primary purpose of the investigations reported here is to examine the data relating to the subsurface geology of the Wasatch Front and to interpret the data in terms of regional subsurface geology related to the earthquake hazard of the area and to indicate how geophysical data can be used in more detailed studies.

The name Wasatch Front as generally used by the residents of Utah refers to a loosely defined area along the west side of the Wasatch Range where most of Utah's population resides. In 1983, the National Board of Geographic names (NBGN) upon recommendation of the Utah State Committee on Place Names defined the Wasatch Range as extending from Collinston on the north to Nephi on the south and being the westernmost of the several north-trending mountain masses in the Middle Rocky Mountain physiographic province. Wasatch Mountains is not recognized as a geographic name by the NBGN. Stokes (1977) defined the "Wasatch Front valleys" physiographic subdivision as the valley area west of the Wasatch Range (as later defined by the NBGN), excluding the area of maximum historic extent of Great Salt Lake but including Utah Lake, and including the valley area to the north on the west side of Clarkston Mountain. In this study the eastern part of the Great Salt Lake is included as part of the Wasatch Front valleys. Cache Valley and the other valleys lying immediately east of the Wasatch Range are not normally considered part of the Wasatch Front. Local concentrations of population and development exist in Cache Valley and a significant earthquake hazard exists there. Several lifelines into the Wasatch Front valleys extend through the Wasatch Range and water storage reservoirs in the Wasatch Range are upstream from major population centers of the Wasatch Front. For these reasons the Wasatch Range and Cache Valley are included in this study.

Information on the subsurface geology along the Wasatch Front can be obtained from geophysical and drill hole data. As part of the Wasatch Front Earthquake Hazards Reduction Program, the Utah Geological and Mineral Survey (UGMS) has compiled geophysical data along the Wasatch Front and assembled information on drill holes in the valley areas along the front. The primary sets of geophysical data are regional gravity and magnetic surveys that cover the entire study area, and a few refraction and reflection seismic profiles. Thousands of wells have been drilled in the valleys but only a small percent provide geologic data of use in this study. All available drill hole logs were examined and a computer file developed using 267 drill holes that either (1) were over 300 m deep, (2) encountered bedrock (usually pre-Tertiary rock or Tertiary volcanic rock) or (3) had complete and accurate lithologic logs (Case, 1985). The geophysical data, drill hole data, and surface geology were then interpreted to define (1) the thickness, structure and composition of the Cenozoic rocks underlying the valley areas, (2) blocks of crust with contrasting lithology and, (3) other regional crustal anomalies that might relate to current seismicity.

This study is built upon numerous other studies that usually involved only one of the data sets used or examined only part of the Wasatch Front. The earliest, published regional geophysical studies of a major part of the Wasatch Front were the gravity survey by Cook and Berg (1961) and the aeromagnetic survey by Mabey and others (1964). These two studies defined the major regional gravity and magnetic anomalies along the Wasatch Front from Nephi to Farmington and established the sources of the larger regional anomalies. Zoback (1983) used gravity data as the foundation of a study of structure and Cenozoic tectonism of north central Utah. Arnow and Mattick

(1968) reported on a seismic refraction profile to determine the thickness of valley fill in Salt Lake Valley. (Several reports by the USGS and others prior to 1983 used the name Jordan Valley for the valley area between the Oquirrh Mountains and the Wasatch Range. In 1983 the NBGN rejected the name Jordan Valley in favor of Salt Lake Valley) Mattick (1970) used the seismic refraction data along with gravity, magnetic and drill hole data in a study of the thickness of unconsolidated to semiconsolidated sediments in Salt Lake Valley. Resistivity soundings have been used locally to determine the thickness and resistivity of the sediments in the valleys (Zohdy and Jackson, 1969). Seismic reflection profiling has been used extensively by commercial companies in the exploration for petroleum in the Cenozoic basins and underlying older rocks but most of these data are not available to the public. Cook and others (1967) presented an interpretive geologic cross section along an east-west profile between Little Mountain and the Wasatch Range in the Ogden area based on a refraction and reflection seismic survey and detailed gravity data. Smith and Bruhn (1984) presented data from several reflection profiles obtained in petroleum exploration and Glenn and others (1980) report on one profile across Hill Air Force Base. Recently high-resolution refraction seismic profiles have been used to study near-surface fault geometry (Crone and Harding, 1984). Several other investigators have used geophysical data, most commonly gravity data, in studies of the subsurface geology of individual valleys or parts of the valleys.

The surface geology of the Wasatch Front has been the subject of study by numerous investigators for over a century. Regional geologic maps that were particularly useful to this study were the Geologic Map of Utah (Hintz, 1980), geologic maps of the northern, central and southern Wasatch Front (Davis, 1985, 1983a and 1983b) and the geologic map of the Farmington Canyon complex and surrounding rocks (Bryant, 1984).

GEOPHYSICAL DATA

Gravity Data

Zoback (1983) compiled a gravity map of the Wasatch Front region based on data in the U.S. Geological Survey (USGS) files. This data set includes gravity stations from numerous surveys by the USGS and others. This compilation was used to prepare a gravity map for this study (fig. 1). A new complete Bouguer gravity anomaly map of Utah is being prepared by the USGS and the UGMS. This map, which will be published by the UGMS at a scale of 1:500,000 will be based on a new data set which includes many gravity stations from the 30-year compilation of K.L. Cook and his students at the University of Utah not previously available to the public. The new data set will better define the gravity field throughout Utah and provide data for detailed interpretation of gravity anomalies in the area of the study reported here. The new data will not significantly alter the 5-mgal contours presented in Figure 1 or the regional interpretation based on the data used to prepare that map.

The Wasatch Front is coincident with a steep regional Bouguer gravity anomaly gradient between the regional gravity high over the topographic low of the Lake Bonneville basin and the higher terrain of the Middle Rocky Mountain province to the east. At its maximum, east of Great Salt Lake this gradient averages over 1 mgal/km for a distance of 100 km. This 100 mgal regional Bouguer gravity relief correlates well with the inverse of the regional topography, which involves a change in average elevation of about 800 to 1100 m (depending on how the average elevation is determined). This correlation of

Figure 1. Complete Bouguer gravity anomaly map of the Wasatch Front area and surface trace of Wasatch and East Cache fault zones. Contours interval is 5 mgal. Gravity map is modified from Zoback (1983).

0.09 to 0.13 mgal/m is approximately equal to the Bouguer correction of 0.11 mgal/m used to compute the Bouguer anomaly and indicates that the regional topography across the Wasatch Front is in approximate isostatic equilibrium. A major part of the mass deficiency under the Wasatch Range and the area to the east relative to the Basin and Range province to the west is likely due to a thicker crust, but part of the deficiency may be due to a less dense crust. The steepest part of the regional gravity gradient is coincident with the western front of the Wasatch Range and indicates that the relief across the range front is, at least in part, an isostatic response. This gravity feature is in marked contrast to most ranges in the Basin and Range province to the west where the ranges of average size appear to be supported by the strength of the crust (Eaton and others, 1978). Any explanation of the structure of the west front of the Wasatch Range must involve both the extension associated with basin and range structure and the isostatic response to the contrasting crust on the two sides of the front.

Superimposed on the large regional gravity gradient along the Wasatch Front are more local anomalies typical of the Basin and Range province that are produced by the relatively low-density rocks of Cenozoic age that underlie the valley areas and by generally smaller amplitude anomalies produced by density variations within pre-Cenozoic rocks. Before a quantitative interpretation of the local anomalies can be made they must be isolated from the regional anomaly.

In the Wasatch Front valleys is a zone of north-trending gravity lows produced by the Cenozoic rocks. The range in amplitude and form of these anomalies indicates the complexity of the structure underlying the valleys. Although the gravity data have been used by several investigators to infer the structure of the valleys and the thickness of the Cenozoic rocks, important uncertainties exist relative to the interpretation of the gravity data. The two most important uncertainties are: (1) the amplitude and form of the regional gravity anomaly produced by deeper sources which must be inferred before the anomaly caused by the Cenozoic rocks can be analyzed and (2) the variations in the density of the Cenozoic rocks.

Several methods can be used to isolate the gravity effect of the Cenozoic rocks. A regional gravity anomaly can be computed by fitting a relatively low-order surface to the Bouguer gravity amonaly values, and removing that regional anomaly from the Bouguer gravity anomaly. The application of this technique is compromised because the local anomalies of interest are so large in both extent and amplitude that they are an important factor in controlling the computed surface. The most commonly used method has been to assume a regional anomaly based on the anomaly values for stations on pre-Cenozoic rock. This technique is often highly subjective particular in the area immediately west of the Wasatch Range. A regional gravity anomaly can be computed that correlates with regional elevation. This can be done by assuming either an isostatic model or a correlation function between the regional gravity anomaly and the average elevation. The computed regional gravity anomaly is strongly influenced by the isostatic model or correlation function assumed. A technique that works well for two-dimensional modeling of profiles is to model the total Bouguer gravity anomaly including the regional component. With this technique all mass anomalies that contribute to the

Bouguer gravity profile are considered in one model and the uncertainties of all assumptions are apparent to the interpreter.

In computing the Bouguer gravity anomaly and in interpreting the gravity anomalies, the rocks of pre-Cenozoic age in the Wasatch Front area are generally assumed to have a density of 2.67 g/cc. The density of the Cenozoic rocks ranges from less than 2.0 g/cc for some of the unconsolidated, fine, well-sorted sediments to over 2.5 g/cc for some of the volcanic rocks and the well consolidated sedimentary rocks. In general the older, more deeply buried Cenozoic sedimentary rocks and the volcanic rocks, are more dense than the younger sedimentary rocks, but another important factor determining density is sedimentary rock type. The coarse, poorly sorted, fluvial sediments along the margins of the local basins are significantly more dense than the fine, well sorted, lacustrine sediments in the central part of the basins. This systematic decrease in density toward the centers of Cenozoic basins in the Basin and Range province was described by Kane and Pakiser (1960) and Mabey (1960) for California basins and by Mabey and Morris (1967) for a Utah basin, but most intrepretations of gravity anomalies along the Wasatch Front have assumed a single density contrast for sediments of the same age or depth within a basin. This assumption is valid when the gravity data are used only to indicate the general configuration and thickness of the Cenozoic basins but can lead to incorrect conclusions when modeling details of basin margins including location and dip of normal faults bounding the basins.

Magnetic Data

The magnetic map of Utah (Zietz and others, 1976) was prepared by mosaicing magnetic contour maps based on several independent surveys. A new magnetic map of Utah based on a merging of digital data sets to a common datum and projecting the data to a common level is being prepared and will be published by the UGMS at a scale of 1:500,000. As with the new gravity data set, the new magnetic data set will facilitate a more detailed quantitative analysis of the data than is attempted here. The magnetic map of the Wasatch Front area presented here (fig. 2) is modified only slightly from that of Zietz and others (1976). The two surveys that were used to compile this part of the State map were both flown at 3700 m above sea level; thus, no flight level problem exists within the data. The survey in the northern part of the area is based on north-south flight lines 8 km apart and the survey to the south on east-west flight lines 3.2 km apart.

The regional residual magnetic field in the Wasatch Front area is dominated by magnetic anomalies from two prinicipal sources: Tertiary igneous rock and Precambrian crystalline rock (Mabey and others, 1964). Two west-trending zones of Tertiary igneous rock are indicated by bands of magnetic highs south of Salt Lake City. The northern zone is here called the Bingham-Park City magnetic zone and the southern the Tintic magnetic zone. The major cause of these magnetic highs are Tertiary plutons although Tertiary volcanic rock locally contributes to the magnetic anomalies. The magnetic anomalies over Antelope Island and Wasatch Range north of Salt Lake City are produced by rocks in the Archean Farmington Canyon Complex. Over these Archean rocks magnetic highs are associated with the quartz monzonite granite

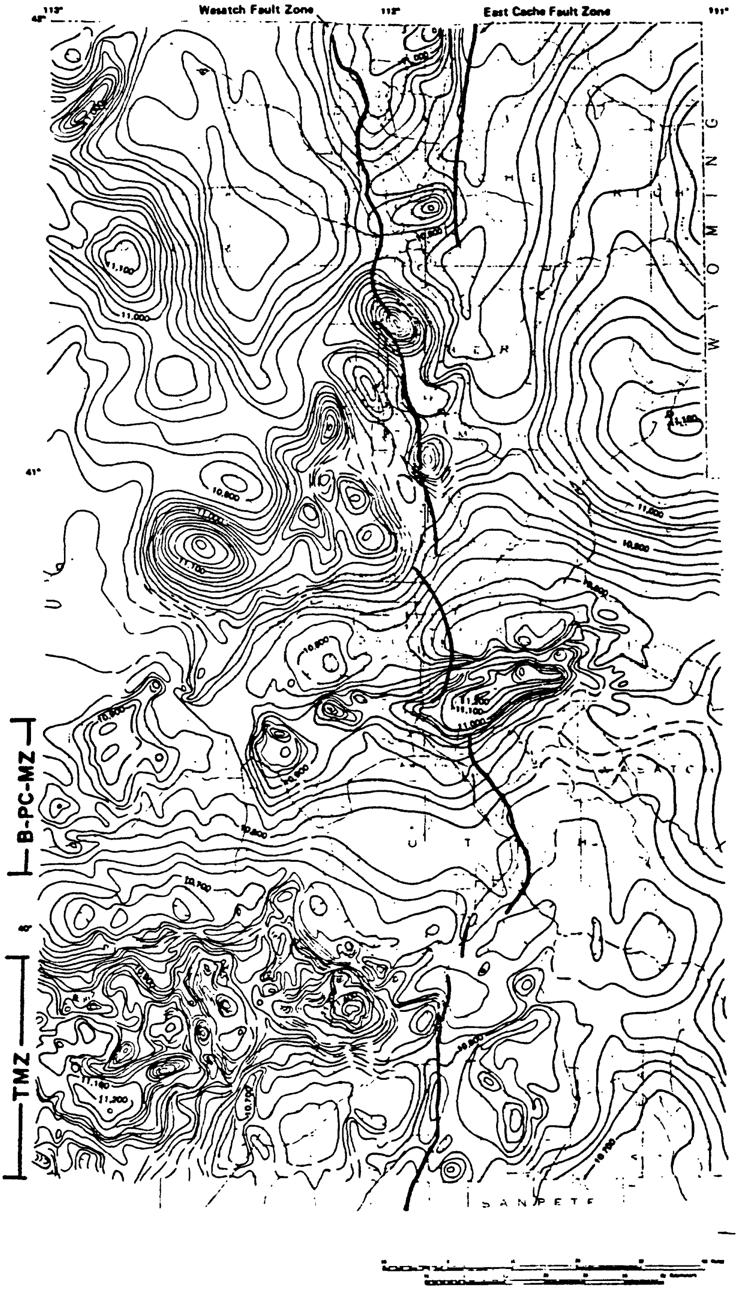

Figure 2. Residual total intensity magnetic map of the Wasatch Front area and surface trace of Wasatch and East Cache fault zones. B-PCMZ is the Bingham - Park City Magnetic Zone and TMZ is Tintic Magnetic Zone. Contour interval is 20 gammas. Magnetic map is modified from Zietz and others 1976.

gneiss, and migmatite mapped by Bryant (1984). There is little magnetic expression of the schist and gneiss as mapped by Bryant. A broad magnetic high in Cache Valley and over the range to the west is also probably produced primarily by Precambrian rock, but Cenozoic volcanic rock in northeast Cache Valley appears to be contributing to the anomaly (Scheu, 1985).

INTERPRETATIONS

Cenozoic Sediments

The Wasatch Formation of Eocene and Paleocene age is exposed in the central Wasatch Range and areas to the east but does not crop out west of the Wasatch fault zone. The sedimentary rocks exposed over much of the Salt Lake salient were once thought to be Wasatch Formation but now appear to be younger (Bryant, 1984). THe Wasatch Formation is over 1000 m thick in the Wasatch Range and may extend west under the Wasatch Front valleys. Sedimentary rocks encountered in several wells in valleys west of the Wasatch fault have been identified as Wasatch Formation primarily on the basis of color (Case, 1985). Some of these rocks may be younger or older than the Wasatch Formation. Paleocene and Eocene rocks of the North Horn, Flagstaff, and Colton Formations occur in the southern Wasatch Range and may occur under adjacent valleys.

Volcanic rock of upper Eocene and Oligocene age are widespread in the ranges over the Wasatch Front area and are reported in some drill holes in the valleys (Case, 1985). The Norwood Tuff, which includes tuff, tuffaceous sandstone, conglomerate and clay, is over 1000 m thick in the central Wasatch Range and underlies some of the valley areas. Latite, andesite and rhyolite flows and tuffs were erupted in the igneous belts producing the Bingham-Park City, and Tintic magnetic zones. These rocks are exposed in the ranges and are known to extend under the valleys in the area of these belts.

The pattern of basin and range topography in the Wasatch Front region appears to have developed in Miocene time in response to regional extension (Stewart, 1978). In the Wasatch Front area Miocene and Pliocene rocks are extensively exposed only around Cache Valley and the City Creek spur; however, they are encountered in most deeper wells in the valleys (Case, 1985) and appear to be the major low-density rock causing the gravity lows in the valleys.

The Miocene and Pliocene history of the Wasatch Front valleys is poorly known, but it appears that local basins of deposition began to subside in Miocene time and have continued subsiding to the present. As the basins evolved, the area, location of maximum subsidence, style of deformation, climate and source of sediments likely changed producing a complex distribution of sedimentary rock types in the basins. Igneous flows and sills occur interbedded with Miocene and Pliocene sedimentary rocks in northern Cache Valley (Scheu, 1985) and in the area of Great Salt Lake.

The subsurface contact between the Tertiary and Quaternary sediments under the valleys often cannot be identified with confidence. In northern Salt Lake County Arnow and Mattick (1968) correlated a downward increase in resistivity and an increase in seismic velocity with the Tertiary-Quaternary contact. P-wave velocities above this contact were less than 1.8 km/s. They attributed P-wave velocities as high as 3.8 km/s to Tertiary rock and velocities greater than 4.6 km/s to consolidated rocks of several ages. They interpreted a seismic refraction profile across the valley north of Salt Lake City and data from three drill holes as indicating that the thickness of the Quaternary sediments ranges from 180 to 770 m and the thickness of Tertiary rock from 0 to 1040 m. The maximum thickness of the combined Cenozoic units along the profiles is 1470 m. They reported that one well penetrated volcanic rock, possibly andesite, between 700 and 850 m below the surface. Arnow and others (1970) prepared a contour map (at 500-ft contour interval) of the base of the Quaternary deposits in Salt Lake Valley south of this profile. This map was based on drillers logs; and the top of the Tertiary deposits was selected at the first reported beds of lava, conglomerate, hardpan, or various types of cemented or hard materials that were more than 3 ft (1 m) thick. Nowhere did they find Quaternary deposits thicker than along the seismic profile; and over most the valley Quaternary sediments were less than 300 m thick.

Hunt and others (1953) interpreted well logs in northern Utah Valley as indicating that the Quaternary sediments thickened southward to the Geneva Steel plant where they were about 150 m thick. Dustin and Merritt (1980), also using well logs, concluded that the Quaternary deposits at the north end of Utah Valley were approximately 50 to 60 m thick and at the south end 135 to 150 m thick. Feth and others (1966), in a study of the Weber and Davis County area, reported that a well near Farmington appears to have penetrated the base of the Quaternary at 248 m but that Quaternary sediments are less than 60 m thick at most places in their study area. Williams (1962) reports that most wells in southern Cache Valley do not penetrate the base of the Quaternary sediments but that one well did at about 150 m. In northern Cache Valley Stanley (1971) found an increase in resistivity at depths ranging from 90 to 150 m. He concluded that this horizon was probably the top of pre-Lake Bonneville sediments of Pleistocene age; however, this horizon could also be interpreted as the base of the Quaternary sediments. Bjorklund and McGreevy

(1971) examined the logs of five deep wells in Cache Valley and concluded it was difficult to distinguish the Quaternary-Tertiary contact, but they placed the contact at the top of a thick conglomerate at depths of about 335 to 400 m.

Only in one local area of the Wasatch Front valleys, northern Salt Lake County, are Quaternary sediments in excess of 400 m thick indicated and as will be discussed later, this is an area of anomalous structure. In most of the valley areas the Quaternary sediments are reported to be less than 200 m thick. Where seismic velocity and resistivity data are available the base of the assumed Quaternary deposits appears to correlate with a significant increase in seismic velocity and resistivity. The inferred subsurface boundary between the Quaternary and Tertiary sediments in the Wasatch Front valleys has not been dated in most areas. The horizon at which the degree of consolidation of the sediments increases may not everywhere correspond to a time boundary. It is, however, a boundary significant to predicting ground response in an earthquake. Either seismic refraction or resistivity soundings have proven to be practical geophysical techniques for mapping this boundary.

Quaternary and Paleogene rocks do contribute to the large gravity lows under the Wasatch Front valleys but in areas where borehole data are available the largest contribution is from the Miocene and Pliocene sedimentary rocks. Locally these rocks are very thick. Nearly 4000 m of these rocks were penetrated in the Gulf Energy and Minerals well in southern Utah Valley and the base of these rocks was not reached (Davis and Cook, 1983).

If the assumption is made that all of the residual Bouguer gravity lows over the Wasatch Front valleys are produced by the density contrast between the Miocene and younger sediments and the more dense older rocks, then the gravity anomaly can be analyzed to determine the thickness of the low-density rocks required to produce the gravity low. A computer program was used to determine the thickness of low-density sediments that would produce the Bouguer gravity low along 26 profiles across the Wasatch Front valleys. The computation assumes that the prism of sediments is normal to the profile and extends to considerable distances on each side of the profile. Because of the elongation of the gravity lows and the locations and orientations of the profiles the assumption does not induce large errors. A density contrast of -0.4 g/cc was assumed. The resulting inversion of the gravity data is shown as a contour map of sediment thickness in Figure 3. Zoback (1983), Peterson (1974), Peterson and Oriel (1970), Davis and Cook (1983) and others have interpreted gravity profiles to infer the thickness of low-density sediments along profiles in the same area. Their procedures involved assuming a density model and modifying the model until a model was produced that satisfied the geologic constraints they chose to apply and also produced an acceptable match to the gravity anomaly. The technique used here differs in that the only geologic constraint is that the surface extent of the low-density sediments corresponds to the known geology, thus, it is an inversion of the gravity data. The thickness of sediments indicated in Figure 3 is generally greater than inferred by Zoback (1983), Peterson (1974), and Peterson and Oriel (1970) because they assumed a density contrast of -0.5 g/cc and here a contrast of -0.4 g/cc was assumed. The thicknesses are in general agreement with those of Davis and Cook (1983) who assumed a contrast decreasing with depth from -0.62 to -0.22 g/cc. The density of the Cenozoic sediments normally increases with

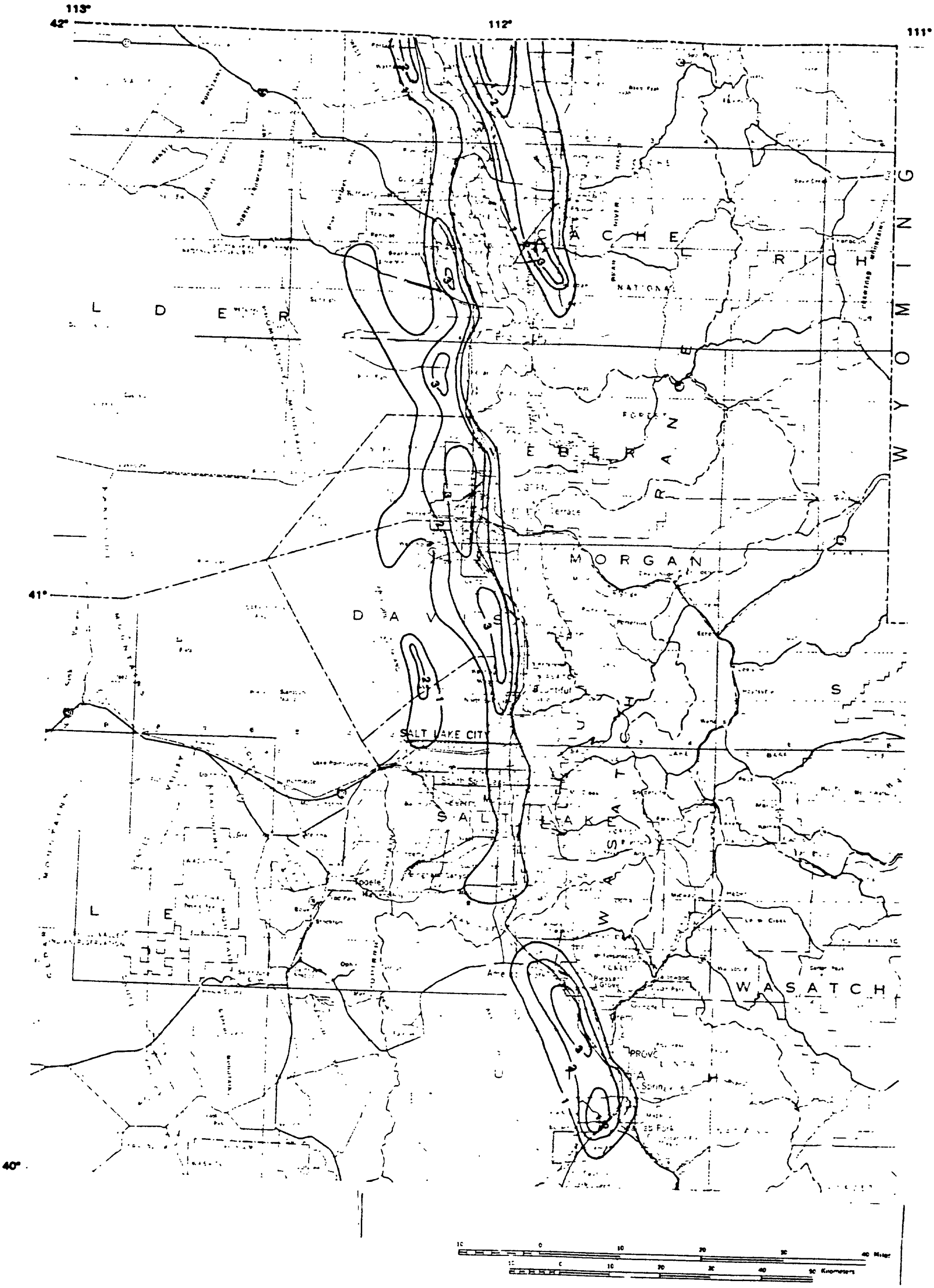

Figure 3. Thickness of low-density sedimentary rocks in Wasatch Front valleys and Cache Valley inferred from gravity data. Contour interval is 1 km.

depth and, at depths greater than 2 km, the density contrast with the older rocks is likely to be substantially less than the -0.4 g/cc assumed in the inversion of the gravity data. The result is that in the area of thickest sediments the calculated thickness may be substantially less than the actual thickness. This is the known situation at the south end of Utah Valley where a drill hole is reported to have bottomed at 4000 m in Cenozoic sediments at a location where the inversion of the gravity data indicates these sediments are less than 4000 m thick.

Throughout the Wasatch Front valleys the axis of the gravity low, and presumably the structural low, is east of the center of the valley. The topographic low is generally west of the axis of the valley. This suggests that movement along of the Wasatch fault zone on the east side of the valley tilts the valley floor eastward but debris derived from the Wasatch Range and highlands to the east is then deposited along the east side of the valley displacing the topographic low to the west. This is well illustrated in Utah Valley where the axis of the gravity low lies along the east shore of Utah Lake and on the east shore of Great Salt Lake where the axis of the gravity low is generally east of the lake. The gravity data support the conclusion that the gross structure of the valleys is eastward-tilting blocks.

Displacement Along the Wasatch Fault Zone

The crest of the Wasatch Range is generally 1.5 to 2 km above the valley floor to the west. This range of values is often accepted as the minimum vertical displacement of the Wasatch fault. The maximum vertical displacement can be estimated by adding to the range height the maximum depth to the base of the Miocene sediments under the valley - about 4 km - and the estimated thickness of rock removed from the range crest in Miocene and post-Miocene time, which is dificult to estimate but might be as much as 2 km. This process yields a maximum vertical displacement across the Wasatch fault zone of about 8 km. These calculations of maximum and minimum fault displacement both assume that warping has not made a major contribution to the structural relief across the Wasatch Front.

Although local evidence of lateral displacement along the Wasatch fault zone has been identified, there is no evidence that lateral displacement is an important component of total displacement and the character of the surface trace of the fault is inconsistent with major lateral movement. Displacement of magnetic features that extend across the fault can be used to estimate lateral movement. The Bingham-Park City magnetic zone is nearly normal to the Wasatch fault. If the Oligocene intrusive rock that is the major cause of the magnetic anomaly was once a continuous mass with linear sides, any post-Oligocene offset of the mass should be apparent in the magnetic data. No major offset is apparent. The approximately 5 km left-lateral offset of the crest of the magnetic high across the fault can be explained by the present topography of the top of the intrusive mass. The Tintic magnetic zone is best defined from the Tintic Mountains west and it is questionable if the large volumes of Oligocene intrusive rocks that produce the higher amplitude magnetic highs in the zone occur east of the Wasatch fault. Local magnetic highs in the Wasatch Range east of Nephi appear to be produced by outcropping

Tertiary volcanic rock. Therefore, this magnetic zone is of limited use in detecting lateral offset.

The magnetic anomalies north of Salt Lake City are not continuous but appear to define two zones; one trending north and one trending north-northwest. Over Antelope Island the adjacent valley area to the east three high magnetic closures form a north-northwest trending zone about 50 km long. A magnetic low over the structurally low part of the valley separates these anomalies from a magnetic high zone of similar length over the Wasatch Range. The left-lateral offset of these two zones is about 40 km. This is weak evidence of lateral offset of the Precambrian rocks. Even if it is real, the offset could have occurred long before the development of the Wasatch fault zone.

between contrasting density units but can be modeled with an interface sloping about 20 degrees to the west. An example is the East Bench fault in the eastern part of Salt Lake City. These relatively low gravity gradients can be interpreted as reflecting a series of step faults. The decrease in density of basin fill toward the center of the valley will also tend to extend the gravity gradient associated with the edge of a prism of valley fill over a greater distance than if fill was one density unit. If a single density contrast is assumed in interpreting such an anomaly, the inferred dip of the density interface will be lower than the actual dip. In some locations such as at the west end of spurs and parts of the range front steep gravity gradients approximately coincident with the surface fault trace indicate considerable concealed displacement along the exposed traces of the Wasatch fault zone. Because the gravity lows in the valleys west of the fault zone are in large part reflecting the distribution of Miocene and Pliocene sediments the lack of correlation between some of the structures indicated by the gravity data and the surfaces traces of the Wasatch fault may reflect changes of basin structure with time. The relatively low dip of most of the faults in the Wasatch fault zone and the lateral gradation of density in the basin fill are serious handicaps in using the gravity data to infer the geometry of the Wasatch fault zone.

Smith and Bruhn (1984) estimated the dip of the Wasatch fault at five locations using seismic reflection data. At depths from 0.8 to 2.0 km they estimated apparent dips ranging from 6° to 54° to the west with the average estimate 30°. At two locations the apparent dip at depths greater than 2.0 km was estimated to be 4° and 10°.

Dip of the Wasatch Fault

Gilbert (1928) measured the dip of the Wasatch fault at several locations and, excluding the dips on spurs and salients, determined an average dip of 33.4^{0}. Zoback (1983) questioned that some of the dips Gilbert measured were of the fault surface and she reported four new measurements, for the dip of the fault in bedrock, at locations not on spurs; here values of dip ranged from 44^{0} to 68^{0} Gilbert's and other measurements in the vicinity of the spurs and the Transverse Range indicate that individual faults of the Wasatch fault zone in near-surface bedrock dip about 70^{0} to the west. Away from the spurs the near-surface dips vary considerably but are generally less than 70^{0} and in some areas less than 30^{0}.

A Bouguer gravity anomaly gradient parallels the front of the Wasatch Range and the Wasatch fault zone for most of their lengths. Locally the steepest gradient is coincident with the active surface trace of the fault, but along portions of the fault the gravity data suggest that pre-Tertiary bedrock occurs at relatively shallow depths on the downthrown side of the mapped traces of the fault. In the Bountiful area, for example, the mapped fault traces are in the area of a gravity high that suggest that bedrock is at relative shallow depths on both sides of the fault. Here a large gravity gradient that is suggestive of faulting along the northern extension of the Warm Springs fault (Cook and Berg, 1961, plate 13) lies about 3 km west of the mapped traces. In some places where a gravity gradient occurs in the area of the fault zone, the gradient does not indicate a high-angle fault interface

The geophysical evidence available on the dip of the Wasatch fault zone indicates that the zone and major faults within the zone dip to the west. In the vicinity of the spurs and the Transverse Range individual faults dip steeply at least near the surface. Elsewhere the dips are considered less and commonly appear to decrease with increasing depth. Accurately determining the dip of the Wasatch fault zone or that of individual faults in the zone at depths of more than a few tens of meters is difficult. The most useful data have been obtained by reflection seismic profiling. Reflection seismic surveys designed to determine fault geometry and supplemented by other geophysical data and perhaps drilling appear to offer the most promise of providing detailed information on subsurface geology of the Wasatch fault zone. When the fault ruptures, measurements of deformation before, during and after the events, focal mechanism analysis, and the distribution in space of related earthquakes will likely provide information on fault geometry that cannot be obtained before the event.

Linear zones of steep gravity gradients occur on the west side of most of the major gravity lows in the Wasatch Front valleys. These gradients are generally interpreted as indicating normal faults or fault zones that are the west side of grabens within the valleys. These fault zones are usually not along mountain fronts but from 4 to 20 km east of the nearest mountains to the west. These gradients cannot usually be correlated with mapped surface faults but thermal springs coincident with these gradients suggest that they may reflect active fault zones. These gradients are in areas inundated by Lake Bonneville within the last 15,000 years and evidence of faulting older than this is difficult to identify in the unconsolidated sediments involved. The areas of lowest Bouguer gravity anomaly values in the Wasatch Front valleys can be interpreted as indicating grabens, but the individual grabens are generally significantly narrower than the valley. Only in a few locations such as at the ends of some of the spurs of the Wasatch Range does the inferred location of the faults bounding the grabens correspond to the mapped location of the surface trace of active faults.

In the Cache Valley area the area of thick low-density rocks extends beyond the valley over outcropping Tertiary sedimentary rocks. The gravity data suggest that all of southern Cache Valley is underlain by thick low-density sediments but in the north the area of thick sediments is confined to the west side of the valley. An appended area of thick sediments extends from Cache Valley into Clarkston Valley.

Spurs of the Wasatch Range

Gilbert (1928) studied the Wasatch fault and named the major spurs of the Wasatch Range and his names are used here. The gravity data provide some indication of the subsurface geology that was not available to Gilbert and geologic mapping since Gilbert's work has better defined the surface geology. Gilbert concluded that the spurs were separated from the main mass of the Wasatch Range and from the valleys by faults. He further concluded that the faults along the valley side of the spurs were likely to dip more steeply than those along the range front. He noted that hot springs occur along each of the major spurs and that only at two other locations along the Wasatch fault did hot springs occur. Gilbert concluded: "It may be that the outer faults of the spurs are peculiarly favorable for the conveyance of deep penetrating circulation because of the less perfect adjustment there of the fault walls" (Gilbert, 1928, p. 32). The geophysical data and recent geologic mapping generally support Gilbert's conclusion except as they relate to his Traverse spur.

Steep local gravity gradients are measured along the Wasatch fault zone at the west edge of the Madsen, Pleasant View and City Creek spurs. This supports Gilbert's conclusion that the faults here are dipping more steeply than is normal for the Wasatch fault zone. The faults on the west side of each of these spurs trend a few degrees west of north. Only at the City Creek spur do we have data on the thickness of Quaternary sediments under the valley west of the spur but here the 770 m thickness inferred by Arnow and Mattick (1968) is the thickest reported anywhere in the Wasatch Front valleys. The Tertiary sedimentary rocks in City Creek spur that had earlier been considered to be of Eocene age are now mapped as Miocene and Pliocene age (Bryant, 1984). If these sediments were deposited in the valley their presence on the spur supports Gilbert's conclusion that the spur blocks were once so associated with the valley block as to receive the same deposit and have since been lifted with reference to the balley block" (Gilert, 1928, p. 31). In addition, Gilbert (1928, p. 32) noted that the diversities in history of each spur "show that the conditions determining adhesion to the (Wasatch) range or to the sinking valley were local and variable." There is no evidence in the gravity data of a fault with major vertical displacement on the west side of the Traverse spur as defined by Gilbert. A concealed fault trending a few degrees north of east, west end, has been postulated along the hot springs in the area (Gilbert, 1928, p. 29; Cook and Berg, 1961, p. 81). The Tertiary rocks exposed on the spur are Oligocene volcanic rocks and do not provide evidence that the spur is an uplifted part of the valley. The Traverse spur as defined by Gilbert appears to be a part of the Traverse Range and not a spur of the Wasatch Range in the sense that the Madsen, Pleasant View and City Creek spurs are.

Fault Segments

The Wasatch fault zone consists of several segments and each segment behaves with some degree of independence from adjacent segments. Schwartz and Coppersmith (1984) defined six major rupture segments and propose that a rupture event will likely be confined to one segment. The gravity and magnetic data were analyzed independently to identify features that might relate to segment boundaries. These maps were then compared with the segments defined by Schwartz and Coppersmith (fig. 4). Schwartz and Coppersmith used the Zoback (1983) gravity data along with other data to define their segments; therefore, their segments are not completely independent of the geophysical data.

Five blocks of contrasting magnetic properties were identified (fig. 4a). Block I is the east end of the Tintic magnetic zone. To the west the zone is dominated by magnetic highs produced by Tertiary intrusive rocks but in the

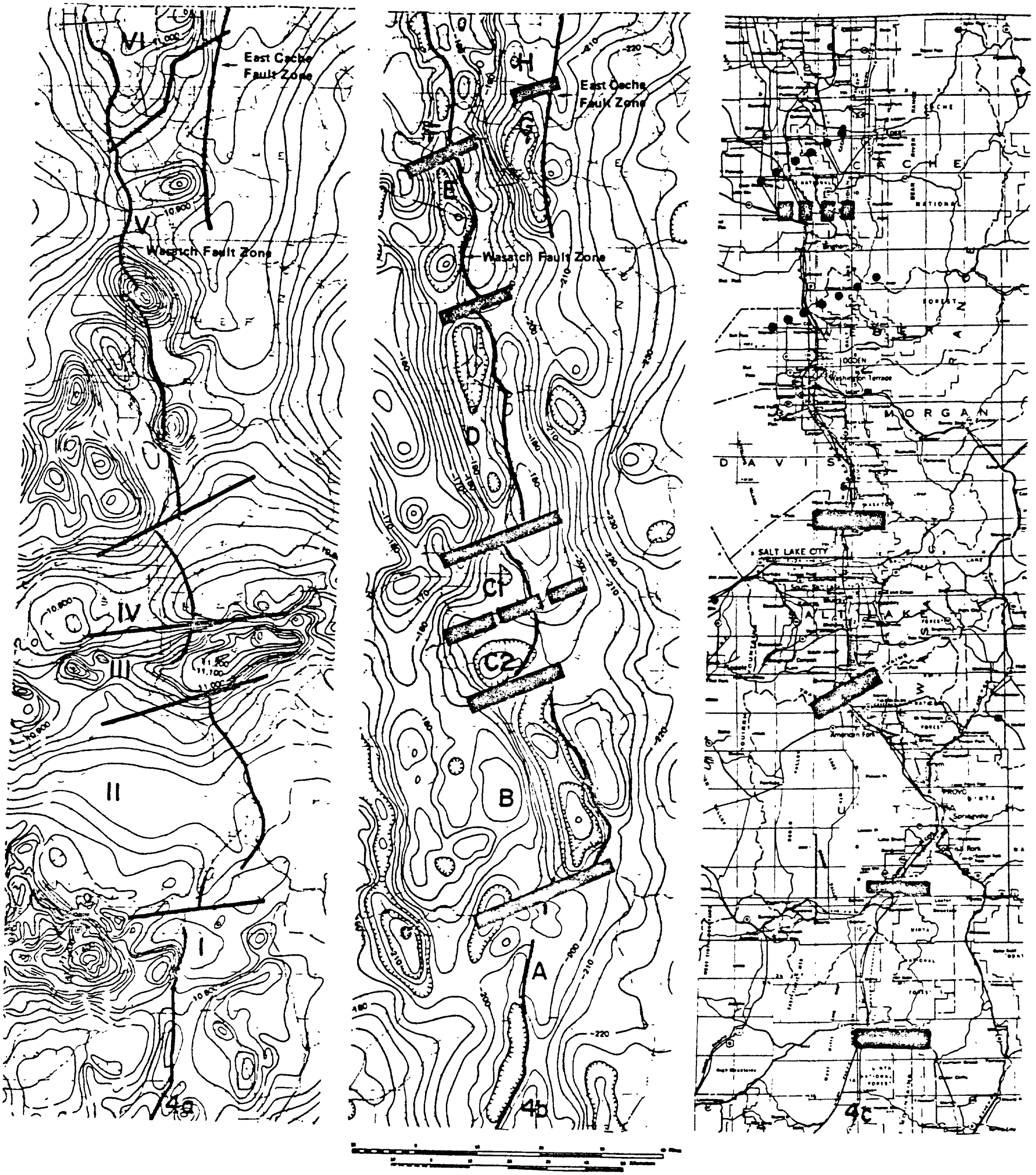

Figure 4. Map of the Wasatch Front showing (a) blocks of contrasting lithology inferred from magnetic anomalies, (b) boundaries of areas contrasting gravity anomalies and (c) fault rupture segment boundaries from Schwartz and Coppersmith (1984) as solid and dashed bars and additional boundaries inferred from geophysical data as dotted lines.

Wasatch Range the amplitude of the anomalies is lower and most individual magnetic highs relate to Tertiary volcanic rock. Block III is the Bingham-Park City magnetic zone. Here Tertiary intrusive rocks appear to make up much of the upper crust. In both of these blocks, but particularly in Block III, Tertiary igneous activity likely significantly modified the crust so that it now responds differently to regional strain than do the adjacent blocks. Blocks II and IV are characterized by generally low magnetic relief. In these blocks the Phanerozoic sedimentary rocks appear to be very thick and there is no evidence of an underlying, strongly magnetized, magnetic basement. Block V is characterized by magnetic highs produced by Precambrian crystalline rocks of the Farmington Canyon Complex. There is no indication in the magnetic data that these rocks are allochthonous. Block VI is a region of relative low magnetic relief except for two areas of high magnetic intensity in the Cache Valley area. The maximum intensity of the northern magnetic high in Cache Valley occurs a few kilometers north of the Utah-Idaho border in an area where intrusive and extrusive basalts crop out (Scheu, 1985). However, there is no evidence that these rocks underlie the central and southern parts of Cache Valley, and it seems unlikely that the entire area of high magnetic intensity is produced by Tertiary igneous rocks. This zone of high magnetic intensity continues north to the Pocatello area where Precambrian rock appear to be the primary cause of the anomaly. The magnetic data suggest that a block of anomalous magnetic basement rock underlies much of Cache Valley.

The gravity lows along the west side of the Wasatch fault are segmented and these segments reflect the total accumulation of sediment since the start of the subsidence of the structural lows, presumably in Miocene time (fig.

4b). The southern segment (A) is defined by a low-amplitude gravity low between Nephi and Santaquin. This is in Juab Valley, which is the valley area of thinnest sediment west of the range and also adjacent to the highest part of the Wasatch Range. Segment B is Utah Valley which contains the largest gravity low of any of the Wasatch Front valleys and probably the thickest sediments. This segment is bounded on the north by a high gravity trend approximately coincident with the Traverse Range. Segment C is Salt Lake Valley. The southern part of Salt Lake Valley (designated C-2) contains an approximately equal-dimensional gravity low that is different in shape from any other lows immediately west of the Wasatch fault zone. This low may be in part produced by Oligocene or older rocks. In northern Salt Lake Valley (C-1) there is a low-amplitude gravity low east of the axis of the valley. The two gravity segments of Salt Lake Valley are separated by a major gravity gradient that extends across the valley and into the ranges on each side of the valley. The north edge of segment C-1 is defined by a high-gravity trend coincident with the City Creek spur. Segment D is a pronounced gravity low in the eastern part of the valley area extending from Bountiful to a gravity high over the Pleasant View spur north of Ogden. Segment E is flanked by a relatively narrow gravity low along the front of the range between the Pleasant View spur and the largely concealed spur near Honeyville (Madsen spur). The northern segment (F) is a moderately complex low on the eastern side of the valley. Two segments of the East Cache fault zone on the east side of Cache Valley are suggested by the gravity data. In Cache Valley south of Smithfield, segment G is along a pronounced gravity low approximately coincident with the valley. North of Smithfield in segment H the gravity low is confined to the west side of the valley.

Combining the segments inferred from the gravity and magnetic data suggests six segments of the Wasatch fault zone between Nephi and the Utah-Idaho border. The three southern segments agree well with the segments defined by Schwartz and Coppersmith (1984) (fig. 4c). The geophysical data suggest that the Ogden segment as defined by Schwartz and Coppersmith may be terminated on the north by the Pleasant View spur. A division of the fault zone north of the Pleasant View spur into two segments is suggested by relatively subtle features in the gravity and magnetic anomalies. Rather than segment boundaries near Brigham City as concluded by Schwartz and Coppersmith (dashed bar in Figure 4c) the interpretations of the geophysical data suggest a segment boundary at the largely concealed Madsen spur near Honeyville. The boundaries proposed here reduce the length of the Ogden segment from over 80km to less than 60 km and leaves the Provo segment at about 60 km as the longest segment of the Wasatch fault zone.

CONCLUSIONS

Geophysical data combined with bore hole data and surface geologic mapping can make substantial contributions to understanding the Wasatch fault zone. Gravity data in the Wasatch Front valleys indicate that the valleys are underlain by low density sediments that are commonly more than 1000 m thick and locally more than 3000 m thick. Data from drill holes and from other geophysical surveys indicate that most of these rocks are Miocene or Pliocene in age. The thickest accumulation of these rocks are in grabens that are usually centered east of the center of the valleys. The geophysical data are generally consistent with the Wasatch fault dipping rather gently to the west except at the ends of spurs where the faults dip steeply to the west. Faults on the west side of the grabens within the valleys generally dip steeply to the east. The gravity and magnetic data can be used to define crustal blocks of contrasting lithology along the Wasatch fault and the boundaries of these blocks may correspond to segment boundaries of the fault. The Wasatch Range and adjacent highlands to the east are in approximate isostatic balance with the lower areas to the west. This contrast with normal ranges in the Basin and Range province suggests that isostatic forces are partly responsible for the uplift of the Wasatch Range.

References Cited

Arnow, T., and Mattick, R.E., 1968, Thickness of valley fill in the Jordan Valley east of the Great Salt Lake, Utah: U.S. Geol. Survey Prof. Paper 600-B, p. B79-82.

Arnow, T., Van Horn, R., and LaPray, R., 1970, The pre-Quaternary surface in the Jordan Valley, Utah: U.S. Geol. Survey Prof. Paper 700-D, p. D257-261.

Bjorklund, L.J., and McGreevy, L.J., 1971, Ground-water resources of Cache Valley, Utah and Idaho: Utah Department of Natural Resources Technical Publication No. 36, 72 p.

Bryant, Bruce, 1984, Reconnaissance geologic map of the Precambrian Farmington Cayon complex and surounding rocks in the Wasatch Mountains between Ogden and Bountiful, utah: U.S. Geol. Survey Miscellaneous Investigation Map I-1447, scale 1:50,000.

Case, W.F., 1985, Significant drill holes of the Wasatch Front Valleys including Cache Valley and Tooele Valley: Utah Geological and Mineral Survey Open File Report No. 82.

Cook, K.L., and Berg, J.W., Jr., 1961, Regional gravity survey along the central and southern Wasatch front, Utah: U.S. Geol. Survey Prof. Paper 316-E, p. 75-89.

Cook, K.L., and Berg, J.W., Jr., and Lum, Daniel, 1967, Seismic and gravity profile across the northern Wasatch trench, Utah: in Seismic Refraction Prospecting, editor A.W. Musgrave, Society of Exploration Geophysicists, Tulsa, Okalahoma, p. 539-549.

Crone, Anthony and Harding, Samuel, 1984, Near-surface faulting associated with Holocene fault scarps, Wasatch fault zone, Utah: in A workshop on evaluation of regional and urban earthquake hazards and risk, ed. Hays, W.W., and Gori, P.L., U.S. Geol. Survey Open-File Report 84-763, p. 242-268.

Davis, D.A., and Cook, K.L., 1983, Evaluation of low-temperature geothermal potential in Utah and Goshen Valleys and adjacent areas, Utah--Part I: Gravity Survey: Utah Geological and Mineral Survey Report of Investigation RI-179, 139 p.

Davis, F.D., 1983a, Geologic map of the southern Wasatch Front, Utah: Utah Geological and Mineral Survey Map 55-A, scale 1:100,000.

Davis, F.D., 1983b, Geologic map of the central Wasatch Front, Utah: Utah Geological and Mineral Survey Map 54-A, scale 1:100,000.

David, F.D., 1985, Geologic map of the northern Wasatch Front, Utah: Utah Geological and Mineral Survey Map 53-A, scale 1:100,000.

Dustin, J.D., and Merritt, L.B., 1980, Hydrogeology of Utah Lake with emphasis on Goshen Bay: Utah Geological and Mineral Survey Bulletin 23, 50 p.

Eaton, G.P., Wahl, R.R., Prostka, H.J., Mabey, D.R. and Kleinkopf, M.D., 1978, Regional gravity and tectonic patterns: Their relation to the late Cenozoic epeirogeny and lateral spreading in the western Cordillora: in Smith, R.B. and Eaton, J.P. eds, Cenozoic tectonics and regional geophysics of the western Cordillera: Geological Society of America Memoir 152, p. 51-91.

Feth, J.H., Barker, D.A., Brown, R.J., Moore, L.G., and Viers, C.E., 1966, Lake Bonneville: geology and hydrology of the Weber delta district, including Ogden, Utah: U.S. Geol. Survey Prof. Paper 518, 76 p.

Gilbert, G.K., 1928, Studies of basin-range structure: U.S. Geol. Survey Pro. Paper 153, 89 p.

Glenn, W.E., Chapman, D.S., Foley, Duncan, Capuano, R.M., Cole, D.R., Sibbett, Bruce, and Ward, S.H., 1980, Geothermal exploration program Hill Air Force Base, Davis and Weber Counties, Utah: Earth Science Laboratory, University of Utah Research Institute report no. 34, 77 p.

Hintze, L.F., 1980, Geologic map of Utah: Salt Lake City, Utah: Utah Geological and Mineralogical Survey Map, scale 1:500,000.

Hunt, C.B., Varnes, H.D., and Thomas, H.E., 1953, Lake Bonneville: Geology of northern Utah Valley, Utah: U.S. Geol. Survey Prof. Paper 257-A, 99 p.

Mabey, D.R., Crittenden, M.D., Jr., Morris, H.T., Roberts, R.J., and Tooker, E.W., 1964, Aeromagnetic and generalized geologic map of part of North-Central Utah: U.S. Geol. Survey Geophysical Investigations map GP-422.

Mabey, D.R., and Morris, H.T., 1967, Geologic interpretation of gravity and aeromagnetic maps of Tintic Valley and adjacent areas, Tooele and Juab counties, Utah: U.S. Geol. Survey Prof. Paper 516-D, p. 1-10.

Mattick, R.E., 1970, Thickness of unconsolidated to semiconsolidated sediments in Jordan Valley, Utah: U.S. Geol. Survey Prof. Paper 700-C, p. C119-124.

Peterson, D.L., 1974, Bouguer gravity map of part of northern Lake Bonneville basin, Utah and Idaho: U.S. Geol. Survey Miscellaneous Field Studies Map MF-627, scale 1:250,000.

Peterson, D.L., and Oriel, S.S., 1970, Gravity anomalies in Cache Valley, Cache and Box Elder Counties, Utah and Bannock and Franklin Counties, Idaho: U.S. Geol. Survey Prof. Paper 700-C, p. C114-118.

Scheu, S.R., 1985, A gravity and magnetic investigation east of Preston, Idaho: Idaho State University unpublished thesis, 77 p.

Schwartz, D.P. and Coppersmith, K.J., 1984, Fault behavior and characteristic earthquakes: examples from the Wasatch and San Andreas fault zones: Jour. of Geoph. Res. v. 89, n. B7, P. 5681-5698.

Smith, R.B., and Bruhn, R.L., 1984, Intraplate extensional tectonics of the eastern Basin-Range: inferences on structural style from seismic reflection data, regional tectonics, and thermal-mechanical models of brittle-ductile deformation: Jour. of Geoph. Res., v. 89, no. B7, p. 5733-5762.

Stanley, W.D., 1971, An integrated geophysical study related to ground-water conditions in Cache Valley, Utah and Idaho: University of Utah Ph.D. Thesis, 142 p.

Stewart, J.H., 1978, Basin-range structure in western North America: A review: in Smith, R.B., and Eaton, J.P. eds, Cenozoic tectonics and regional geophysics of the western Cordillera: Geological Society of America Memoir 152, p. 1-32.

Williams, J.S., 1962, Lake Bonneville: Geology of southern Cache Valley, Utah: U.S. Geol. Survey Prof. Paper 257-C, p. 131-152.

Zoback, M.L., 1983, Structure and Cenozoic tectonism along the Wasatch fault zone, Utah: Geological Society of America Mem. 157, p. 3-27.

Zohdy, A.A.R., and Jackson, D.B., 1969, Electrical resistivity profile east of the Jordan Narrows, Utah: U.S. Geol. Survey Prof. Paper, 650-C, p. C83-88.

Zietz, I., Shuey, R., and Kirby, J.R., Jr., 1976, Aeromagnetic map of Utah: U.S. Geol. Survey Geoph. Inv. Map GP-907, scale 1:1,000,000.

OBSERVATIONAL SEISMOLOGY AND THE EVALUATION OF EARTHQUAKE HAZARDS AND RISK IN THE WASATCH FRONT AREA, UTAH

By

W. J. Arabasz, J. C. Pechmann, and E. D. Brown
Department of Geology and Geophysics
University of Utah
Salt Lake City, Utah 84112

ABSTRACT

This paper presents and considers in a systematic way up-to-date information from observational seismology that is basic to evaluating earthquake hazards and risk in the Wasatch Front area. We present basic information relating to (a) the earthquake data base, (b) the seismotectonic framework, (c) seismic source zones and seismicity parameters, (d) ground-shaking hazard, and (e) current seismicity and the Wasatch fault.

Important features of the seismotectonic framework of the Wasatch Front include (1) the absence of any surface-faulting earthquakes on the Wasatch fault in historic time, (2) the notable paucity of contemporary earthquakes on the Wasatch fault, and (3) the problematic correlation of background seismicity with mapped Cenozoic faulting. Nonetheless, historical and instrumental earthquake data, combined with paleoseismological information, firmly establish the danger of earthquakes in Utah's Wasatch Front area.

Seismic hazards in the Wasatch Front region arise from two fundamental sources: first, the occurrence of infrequent large (magnitude 6.5 to 7.5±0.2) surface-faulting earthquakes on identifiable faults having evidence of late Quaternary displacement; and, second, small- to moderate-size (up to magnitude 6.5) earthquakes that are not constrained in location to mapped faults and may occur anywhere throughout the region. The small to moderate earthquakes dominate the historical earthquake record, and are the largest contributor to probabilistic ground-shaking hazard for exposure periods of 50 years or less. Recurrence modeling using the 25-year instrumental catalog predicts an average return period of 24±10 years for potentially damaging earthquakes of magnitude 5.5 or greater along the Wasatch Front.

INTRODUCTION

The record of earthquake activity since 1850, together with geological observations dating from more than a century ago, firmly establishes the danger of earthquakes in Utah's Wasatch Front area. A dual threat relates to the occurrence of large (magnitude 6-1/2 to 7-3/4) surface-faulting earthquakes, especially on the Wasatch fault, and to cumulative exposure to moderate-size (magnitude 5 to 6-1/2) earthquakes, perhaps below the threshold for surface rupture.[1] The purpose of this paper is to present and consider in a systematic way information from observational seismology that is basic to evaluating earthquake hazards and risk in the Wasatch Front area.

We follow usage urged by the Earthquake Engineering Research Institute and distinguish a seismic hazard from seismic risk in the following way. A seismic hazard is "any physical phenomenon...associated with an earthquake that may produce adverse effects on human activities," whereas seismic risk is the "probability that social or economic consequences of earthquakes will equal or exceed specified values at [one or more sites] during a specified exposure time" (EERI Committee on Seismic Risk, 1984). The most notable seismic hazards are the geological processes of ground shaking, ground failure, surface faulting, tectonic deformation, and inundation.

Insofar as the evaluation of earthquake hazards involves recognition of the location, frequency, and severity of those hazards, observational seismology is generally relied upon to characterize the space, time, and size distribution of earthquakes giving rise to those hazards. This might involve little more than a qualitative consideration of the available earthquake record and the spatial pattern of earthquake occurrence. On the other hand, more rigorous evaluations of seismic hazard and risk rely on observational seismology to specify quantitative models of earthquake behavior and mechanics so that the level either of a hazard (e.g., a non-exceedance value of ground motion) or the level of risk can be computed at one or more sites for some exposure time. Either a deterministic or a probabilistic approach may be used. In the former case, each independent variable has a single value and a model predicts a specific value for the dependent value. For example, the maximum ground shaking expectable at a site might be estimated from the comparative effects of nearby earthquake source zones, each of which is assigned a maximum-size event and minimum distance to the site—with a corresponding upper limit of predicted ground motion. In the case of a probabilistic approach, uncertainties arising from natural variations or incomplete knowledge are taken into account, and probability theory is used for the analysis (e.g., see Youngs and others, this volume).

A flowchart shown in figure 1 outlines the basic elements of a modern seismic hazard analysis—using as an example the objective of estimating the hazard of ground motion. (Seismological input to a risk analysis would be similar.) The sequence of necessary procedures is shown by steps 1 through 5 in the left-hand column; interrelated aspects of observational seismology are shown in the right-hand column. We use the figure as a useful guide for our presentation as we give an overview of fundamental information from observational

---

[1] (Unless otherwise specified, herein all magnitudes less than 6.5 are local Richter magnitude; those of 6.5 or greater, surface-wave magnitude.)

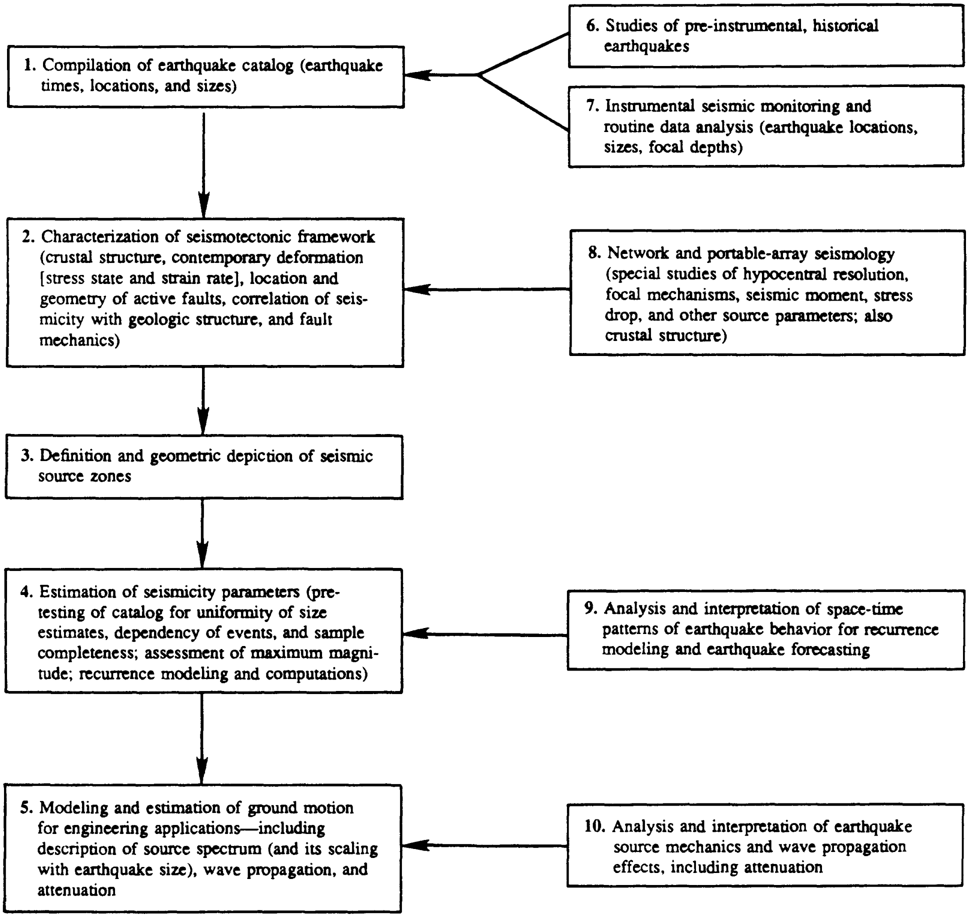

Figure 1. Flowchart outlining steps in a formalized earthquake hazard analysis (left column) and interrelated aspects of observational seismology (right column).

seismology in the Wasatch Front area contributing to steps 1 to 4. Sequentially we consider (a) the earthquake data base, (b) the seismotectonic framework, and (c) seismic source zones and seismicity parameters. We then discuss a selected aspect of ground-shaking hazard—referring the reader to Youngs and others (this volume) for an example of the fully completed process of step 5 in which probabilistic estimates of ground motion are made. In the final section we address the question, What does observational seismology tell us about the behavior of the Wasatch fault?

ACKNOWLEDGMENTS

The data in this manuscript implicitly reflect substantial efforts by numerous individuals associated with the University of Utah Seismograph Stations. We thank D. Veneziano of the Massachusetts Institute of Technology for providing data on independent main shocks for the recurrence modeling, and for assistance with the probabilistic hazard methodology. We also thank J.A. Barlow, L.B. Burnett, K.J. Quigley and J.E. Shemeta for assistance in the manuscript preparation. The research arises from ongoing support by the U.S. Geological Survey, Department of the Interior, currently under award numbers 14-08-0001-G1349 and 14-08-0001-A0265, and from support by the state of Utah.

EARTHQUAKE DATA BASE

The catalog of documented earthquakes in the Utah region (step 1, fig. 1), as elsewhere in the western United States, is a mixed one relying initially upon reports and newspaper accounts of felt earthquakes, and later upon seismographic recordings during several stages of evolving instrumental coverage (Arabasz and others, 1979, 1980; see fig. 2). (Our usage of "Utah region" is defined in fig. 2.) The historical earthquake record effectively dates from 1850 with the publication of the first newspaper in the region, shortly after settlement by Mormon pioneers beginning in 1847. Instrumental earthquake locations in the region, based on regional seismographic recordings in the western United States, with a few exceptions, date from about 1950.

The most prominent sources of earthquake data for the Utah region are (1) compilations made by the University of Utah Seismograph Stations (UUSS) (Arabasz and others, 1979; Richins and others, 1981, 1984; Brown and others, 1986; also, unpublished current data) and (2) data files of the National Geophysical Data Center, National Oceanic and Atmospheric Administration (NOAA). Other earthquake summaries include: (1) a recent compilation for the state of Utah by Stover and others (1986)[2], (2) a data file compiled by Askew and Algermissen (1983) for the Basin and Range province, (3) a western U. S. data file produced by Eddington and others (1987) for a study of Basin and Range geodynamics, and (4) a continental-scale data file produced by Engdahl and Rinehart (1986) for the Decade of North American Geology.

Ideally, the establishment of a master "consensus" catalog would involve the coordinated and formalized efforts of numerous individuals with relevant data and expertise, as was recently done for the entire central and eastern United States (EPRI, 1986). The required efforts relate to establishing catalog completeness, uniform estimates of earthquake size, preferred epicentral locations and origin times, and to documenting uncertainties. Similarly rigorous and formal scrutiny of a data base for the Utah region remains to be made. In this paper, we rely upon the University of Utah's data base, which represents the primary source of instrumental earthquake data since mid-1962 for the Utah region and which includes a comprehensive listing of historical seismicity for which only minor variance should be found with other catalogs. For 1962 to 1986, the UUSS catalog contains an order of magnitude more earthquakes than the NOAA data file for the Utah region (e.g., 6,994 versus 342 earthquakes for the Wasatch Front area).

Although seismographs were first installed on the University of Utah campus in 1907, contributions to the instrumental location of regional earthquakes postdate 1939 when photographic records from modern seismographs began to be routinely forwarded from Salt Lake City to the U.S. Coast and Geodetic Survey. Systematic computerized locations based on local seismographic coverage in the Utah region by the University of Utah date from mid-1962. Prior to late 1974, a skeletal statewide network of several widely-spaced stations was in operation (fig. 2, upper right). (Instrumental earthquake data for the 1962-1974 period were

---

[2] The published compilation of Stover and others (1986) omits at least four shocks of magnitude 5 or greater since 1959—presumably due to editorial error.

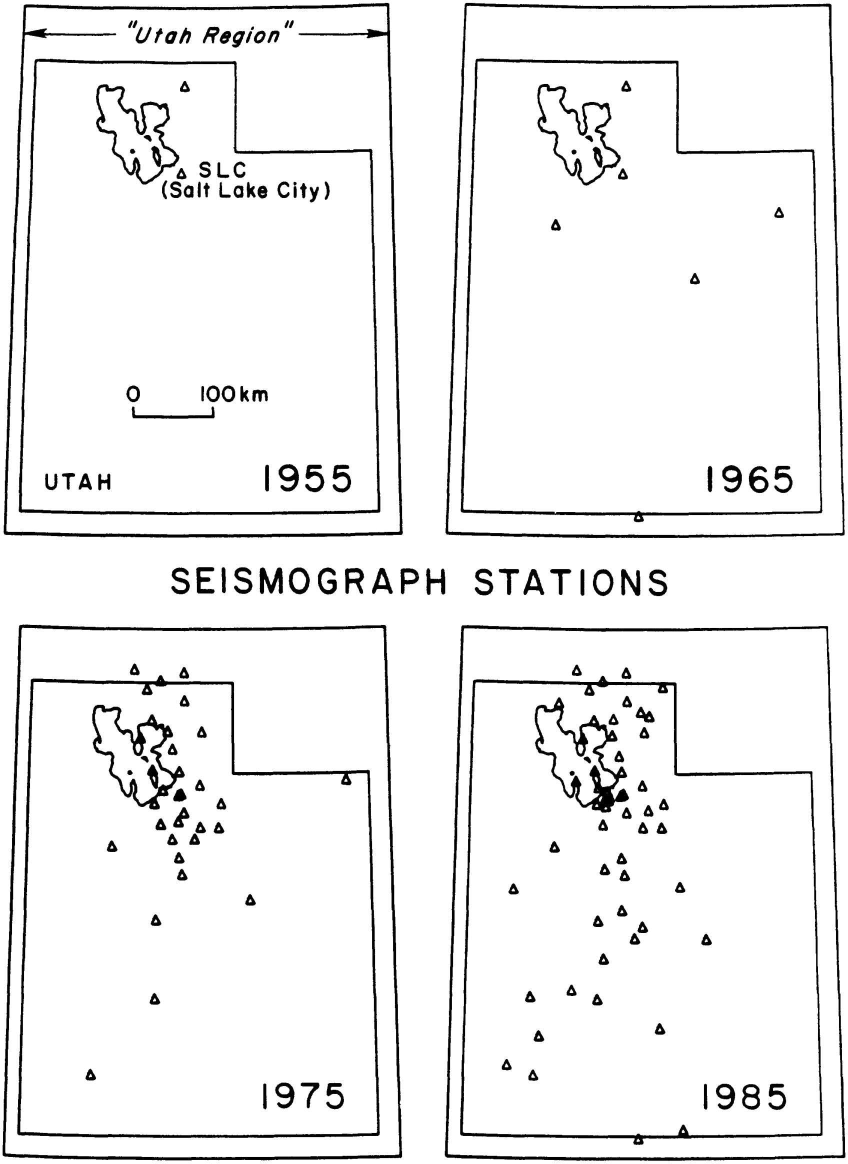

Figure 2. Maps of the Utah region showing distribution of seismograph stations (triangles) at four different times, 1955-1985. The "Utah region," corresponding to a specific domain of the University of Utah's earthquake catalog, extends from latitude 36°45'N to 42°30'N, and from longitude 108°45'W to 114°15'W.

systematically re-analyzed and revised in a major study by the UUSS [Arabasz and others, 1979].) Since late 1974, the University of Utah has operated a modern telemetered network of high-gain short-period seismographic stations in the Intermountain region. About two-thirds of the current network's 85 stations lie within the Utah region (fig. 2, lower right). The seismographic data are centrally recorded at the University of Utah in Salt Lake City. From 1974 through 1980 the recording was in analog form; since January 1, 1981, it has been in digital form.

The UUSS catalog for the Utah region currently contains 9,561 earthquakes for the period from 1850 through 1986. This includes 413 (chiefly non-instrumental) earthquake locations from 1850 through June 1962, and 9,148 (instrumental) locations from July 1, 1962 to December 31, 1986. Magnitudes given in the UUSS catalog are estimates of local Richter magnitude (M_L) based on systematic procedures described, for example, in Brown and others (1986). Such estimates may differ significantly from values of magnitude in the NOAA catalog, which are typically body-wave magnitude and known to be commonly as much as one magnitude unit larger than M_L for small ($m_b \leq 4.0$ earthquakes (Dewey, 1987). We refer the reader to special publications of the UUSS (e.g., Arabasz and others, 1979; Brown and others, 1986) for other details of the UUSS data base.

SEISMOTECTONIC FRAMEWORK

The characterization of the seismotectonic framework of any seismically active region (step 2, fig. 1) basically involves an understanding of its geological and geophysical makeup, its earthquake-generating structures, and the operative deformational processes that lead to earthquake occurrence. Some notable previous studies which have developed such a framework for the Wasatch Front area and its surrounding region include those by Smith and Sbar (1974), Smith (1978), Arabasz and others (1980), Zoback (1983), Smith and Bruhn (1984) and Arabasz and Julander (1986). We will not attempt a complete review. Our intent in this section is (1) to summarize some essential characteristics of the seismotectonic framework of the Wasatch Front area and (2) to emphasize relatively new information acquired from observational seismology by researchers at the University of Utah. Information from network and portable-array seismology (element 8, fig. 1) includes precise earthquake locations, earthquake focal mechanisms and source properties, strain-rate tensors from seismic-moment release, and models of crustal structure.

General Setting and Characteristics

The Wasatch Front area, synonymous herein with a rectangular area outlined in figure 3, is well known to encompass the physiographic boundary between the Basin and Range province and the Middle Rocky Mountains. The boundary coincides with a prominent west-facing topographic escarpment that follows the 370-km-long Wasatch normal fault zone.

Figure 3 shows the location of the Wasatch Front area with respect to the Intermountain seismic belt (ISB)—as depicted by Arabasz and Smith (1981). The ISB is a coherent belt of intraplate earthquake activity extending more than 1,300 km from southern Nevada and northern Arizona to northwestern Montana (Smith and Sbar, 1974; Smith, 1978; Stickney and Bartholomew, 1987). In general, the ISB is characterized by late Quaternary normal faulting, diffuse shallow seismicity (focal depths < 15-20 km), and episodic scarp-forming earthquakes (M~6.5-7.5) associated with the complex interaction of subplates within the western North American plate.

Since 1850, at least 16 independent earthquakes (aftershocks excluded) of magnitude 6.0 or greater have occurred within the ISB. Their locations and sizes are shown in figure 3. Three of these historical earthquakes were associated with documented surface faulting. Normal fault scarps with maximum surface displacements of 0.5 m, 5.5±0.3 m, and 2.7 m, respectively, were produced by the M_S6.6 Hansel Valley, Utah, earthquake of March 1934 (Shenon, 1936), the M_S7.5 Hebgen Lake, Montana, earthquake of August 1959 (Bonilla and others, 1984), and the M_S7.3 Borah Peak, Idaho, earthquake of October 1983 (Crone and others, 1987).

The ISB within the Utah region is notably characterized by: (1) a general predominance of normal faulting, reflecting an extensional stress regime—although contemporary strike-slip

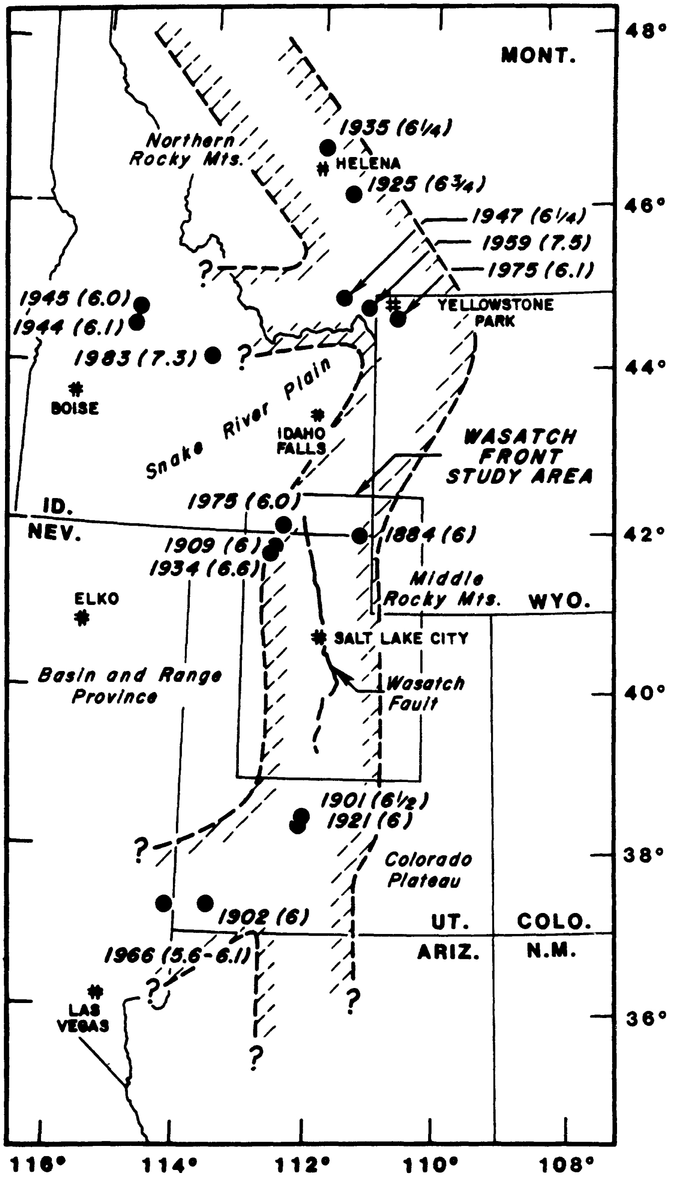

Figure 3. Map showing setting of the Wasatch Front study area with respect to the Intermountain seismic belt and historical earthquakes of magnitude 6.0 and greater (circles) (adapted and updated from Arabasz and Smith, 1981).

deformation has recently been recognized from earthquake studies in central Utah (Arabasz and Julander, 1986); (2) moderate background seismicity, which is lower by a factor of 4 to 6 than that along the western North American plate boundary (see Arabasz and Smith , 1981); (3) diffuse seismicity having weak correlation with major active faults, and with focal depths almost exclusively shallower than 15-20 km; (4) relatively long (~1,000 yrs or more), and perhaps temporally variable, average recurrence intervals for surface faulting on individual fault segments (Schwartz and Coppersmith, 1984; Wallace, 1987); (5) slip rates of late Quaternary faulting of about 1 mm/yr or less, one to two orders of magnitude lower than those on major plate-boundary faults (Schwartz, 1987); and (6) the historical absence of any surface-faulting earthquake larger than the M_S6.6 Hansel Valley earthquake of 1934—despite the presence of abundant late Quaternary and Holocene fault scarps.

Earthquake focal mechanisms in the Wasatch Front area (Smith and Lindh, 1978; Arabasz and others, 1980; see also Zoback, 1983) are known to reflect the predominance of roughly east-west crustal extension. Twenty-four single-event focal mechanisms recently determined by Bjarnason and Pechmann (1987), representing the best and most rigorously analyzed data to date for the Wasatch Front area, have an average tension-axis azimuth of 96°±12°. Zoback (1983) summarized various data on deformation in the Wasatch Front region that indicate an east-west to west-southwest-east-northeast (~N75°E) least principal stress/strain direction. Source properties for earthquakes in the Utah region appear to be comparable to those for other seismic zones in the western U.S., but moment-magnitude behavior may differ (Doser and Smith, 1982; Peinado, 1986) and Benz and Smith (1987) have shown that notable complexities can be expected in the near-field wave propagation from dip-slip normal faults.

Figure 4 illustrates in cartoon form some important aspects of the seismotectonic framework of the Wasatch Front area. (Letters in parentheses here are keyed to the figure.) There is an eastward increase in total crustal thickness (a) across the transitional boundary between the eastern Basin and Range and the Middle Rocky Mountain-Colorado Plateau provinces, and total lithospheric thickness similarly increases from about 65 km beneath the Basin and Range to more than 80 km beneath the Colorado Plateau (Smith and others, 1987). A wedge of material (b) with P-wave velocity of ~7.5 km/sec, formerly thought to be upwarped mantle, has been mapped by Pechmann and Loeb (Pechmann and others, 1984; Loeb, 1986) as lying above the 7.9 km/sec Moho—based on time-term inversion of travel times from local earthquakes recorded by the University of Utah's regional seismic network. The importance of horizontal detachments (c) and listric-fault geometries (d) in upper-crustal structure beneath the eastern Basin and Range appears well established from COCORP seismic reflection profiling (Allmendinger and others, 1983, 1987) and from intensive extensive interpretation of industry seismic reflection data at the University of Utah (Smith and Bruhn, 1984; see also Smith and others, 1987, for a summary of multiple studies).

The brittle-ductile transition (e) marking the base of the seismogenic layer has been modeled rheologically by Smith and Bruhn (1984) to be transitional, as shallow as ~8 km but probably about 10 to 15 km deep beneath the Wasatch Front area. Large surface faulting earthquakes in the Wasatch Front area will expectedly nucleate (f) at that depth on penetrative

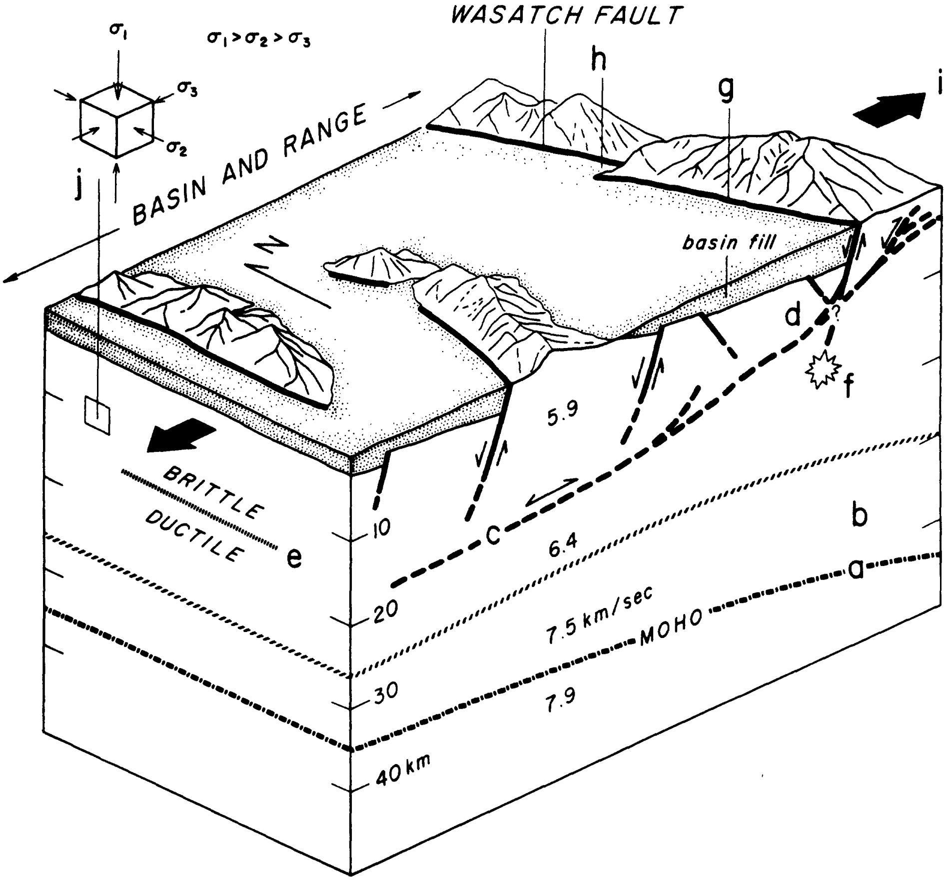

Figure 4. Cartoon block-diagram (vertical exaggeration ~1.0-1.5) illustrating selected aspects of the seismotectonic framework of the Wasatch Front area. Bold letters indicate elements discussed in the text. P-wave seismic velocities shown for reference.

planar faults of moderate dip (Smith and Richins, 1984; Doser, 1985a) somehow connected to surface fault scarps (g). As discussed later, most of the small to moderate-size background seismicity in the area does not associate simply with the first-order faults. Segmentation (h) of first-order faults such as the Wasatch fault (Machette and others, 1987; Schwartz and Coppersmith, 1984) places important constraints on rupture length, maximum earthquake size, and rupture dynamics.

We noted earlier that the Wasatch Front area is characterized by roughly east-west extensional deformation (i). Moment-tensor strain calculated by Eddington and others (1987) from historical earthquakes (see also Doser and Smith, 1982) implies an average strain rate of about 2×10^{-16}/sec for the Wasatch Front area and total extension of 1 to 2 mm/yr across the study area. Upper-crustal stress state (j) implied by earthquake focal mechanisms and other stress-indicator data (e.g., Zoback, 1983) is one in which the maximum principal stress is vertical and the intermediate and minimum principal stresses lie in the horizontal plane, with the latter oriented in an east-west to east-northeast-west-southwest direction. Zoback (1984) has argued that both horizontal principal stresses are approximately equal in magnitude along the Wasatch Front, implying the potential for slip on normal faults of varying strike. Earthquake focal mechanisms, however, continue to display strong clustering of tension axes in an east-west direction (Bjarnason and Pechmann, 1987).

Late Quaternary Faulting

In the absence of a definitive map of known and suspected active faults throughout the Wasatch Front area, efforts were made to compile a base map of late Quaternary faulting for comparison with instrumental seismicity. The resulting map shown in figure 5, which relies chiefly on published sources, includes the traces of fault displacements of Holocene (less than 10,000 yrs B.P.) and late Pleistocene (10,000 to about 500,000 yrs B.P.) age.

The following sources were used to compile the digitized base map of figure 6: The trace of the Wasatch fault is based chiefly on detailed mapping done by Cluff and others (1970, 1973, 1974) and was taken, in part, from subsequent compilations by Davis (1983a,b; 1985). Depiction of the West Valley fault zone near Salt Lake City is from unpublished mapping by S.J. Olig and J. Keaton of Dames and Moore (personal communication, 1987). Faulting to the east of the Wasatch fault in Utah is from detailed maps of Sullivan and others (1986) and Foley and others (1986); that in Wyoming, from Gibbons and Dickey (1983). The trace of the East Great Salt Lake fault, lying within the bounds of the Great Salt Lake, was taken from Cook and others (1980) and Viveiros (1986). West of 112°W, we relied heavily on maps of fault scarps in unconsolidated sediments published by Bucknam (1977) and Bucknam and Anderson (1979). Faulting identified by Anderson and Miller (1979) and not mapped by others in the "Western Desert" region of Utah was added for completeness. Finally, faulting to the north of 42°N in Idaho, other than the northern extension of the Wasatch fault, was taken from Witkind (1975).

There is some inhomogeneity in figure 6 in that some of the fault traces to the west of the Wasatch fault within the Basin and Range province reflect only the extent of mapped fault

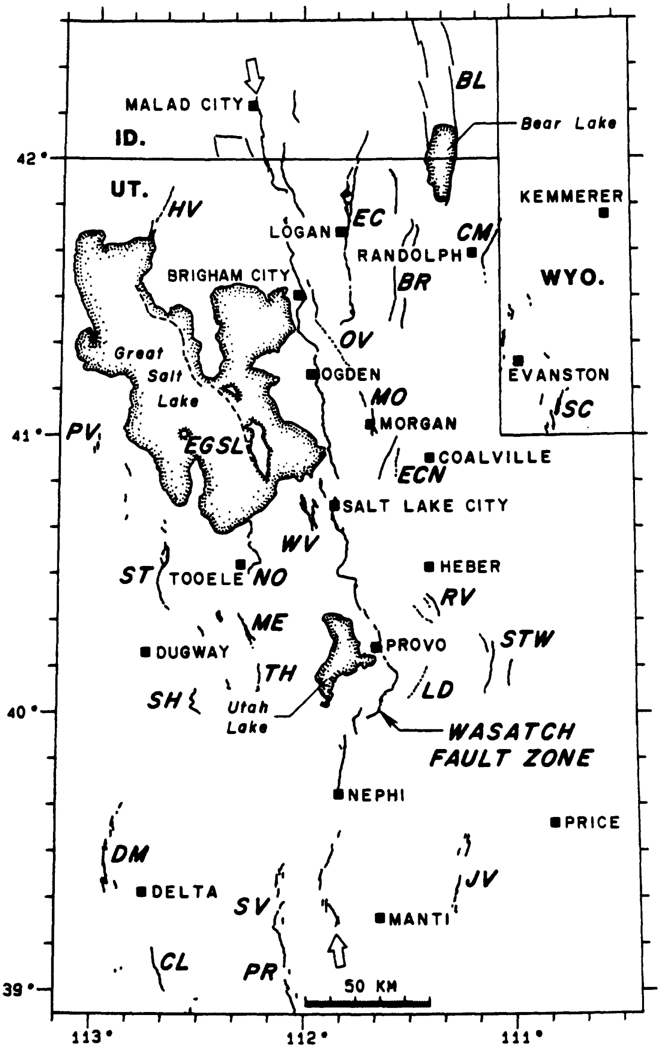

Figure 5. Index map of the Wasatch Front study area showing traces of late Quaternary faulting (see text for sources). Large arrows delimit the extent of the Wasatch fault zone. Other faults labeled for general orientation include: BL, Bear Lake; BR, Bear River Range; CL, Clear Lake; CM, Crawford Mts.; DM, Drum Mts.; EC, East Cache; ECN, East Canyon; EGSL, East Great Salt Lake; HV, Hansel Valley; JV, Joes Valley; LD, Little Diamond Creek; ME, Mercur; MO, Morgan; NO, Northern Oquirrh; OV, Ogden Valley; PR, Pavant Range; PV, Puddle Valley; RV, Round Valley; SC, Sulphur Creek; SH, Sheeprock Mts.; ST, Stansbury Mts.; STW, Strawberry Valley; SV, Scipio Valley; TH, Topliff Hill; WV, West Valley.

scarps in unconsolidated deposits and not necessarily the entire length of a seismogenic range-front fault. Fluctuation of ancient Lake Bonneville, especially between about 25,000 yrs and 13,000 yrs ago (Currey and others, 1984), could have obliterated evidence of late Quaternary surface faulting in many places.

The Wasatch fault is by far the best-studied fault depicted in figure 6. We refer the reader to other papers in this volume for summaries of up-to-date paleoseismological information on its segmentation, slip rate, and the timing and size of prehistoric earthquakes. A first-order active fault to which little attention has heretofore been paid is one beneath the Great Salt Lake that Cook and others named the "East Great Salt Lake fault zone" and whose slip rate and earthquake potential have recently been investigated by one of us (Pechmann, 1987; Pechmann and others, 1987). This fault zone can be clearly seen in seismic reflection profiles across the lake (Mikulich and Smith, 1974; Smith and Bruhn, 1984; Viveiros, 1986). Reflection data and well data indicate that the sedimentary basin underlying the lake deepens towards the east where it is bounded by the East Great Salt Lake fault. The deepest part of the basin contains more than 10,000 feet (3,048 m) of post-Miocene sedimentary rocks (Mikulich and Smith, 1974; Viveiros, 1986), indicating major subsidence during the past 25 million years.

The East Great Salt Lake fault cuts sediments identified as Quaternary on the basis of well data (Mikulich and Smith, 1974; Viveiros, 1986) and must be considered active. Seismic reflection data (Mikulich and Smith, 1974; Viveiros 1986) indicate that the East Great Salt Lake fault appears to offset sediments to within at least 0.015-0.025 sec two-way travel time beneath the lake bottom, corresponding to an approximate depth of less than 14-23 m , which implies that slip has occurred in the recent geologic past. Viveiros (1986, p. 72) estimated fault slip rates on the East Great Salt Lake fault of 0.96 mm/yr during the Pliocene and 1.48 mm/yr during the Quaternary from the thicknesses of sedimentary deposits—dependent upon an interpreted geometry of faulting. Pechmann and others (1987) interpret average Quaternary slip rates of 0.4 to 0.7 mm/yr, taking subsurface fault dip into account and assuming that rates of sedimentation adjacent to the fault are controlled by subsidence on the fault. These slip rates are about half the recent slip rates along central segments of the Wasatch fault (Schwartz and Coppersmith, 1984).

The 1959 Hebgen Lake and 1983 Borah Peak Earthquakes

The only historical earthquake in the Utah region known to have produced surface faulting occurred on March 12, 1934, in Hansel Valley just north of the Great Salt Lake (fig. 3). This earthquake was assigned a magnitude of 6.6 by Gutenberg and Richter (1954), and is the largest earthquake to have occurred in the Utah region since 1850. Because earthquakes with surface displacements much larger than the 0.5 m of the 1934 earthquake are expected to occur in Utah in the future, based on geologic evidence, information from large surface faulting earthquakes elsewhere in the Intermountain seismic belt and in the Basin and Range province is important for evaluating their likely magnitudes and other characteristics.

In the Intermountain seismic belt, there have been two large, historic normal faulting earthquakes over magnitude 7.0, both of which produced surface rupture: the October 28, 1983, M_S7.3 (NEIS determination) Borah Peak earthquake in central Idaho, and the August 18, 1959, (GMT), M_S7.5 Hebgen Lake earthquake in southern Montana (fig. 3). These two earthquakes are generally considered to be good models for future large earthquakes on the Wasatch fault and other major faults in Utah (Smith and Richins, 1984; Doser, 1985a). The surface wave magnitude (M_S) of 7.5 for the Hebgen Lake event is from Abe (1981), and is probably more accurate than a previous estimate of 7.1, attributed by Murphy and Brazee (1964) to Pasadena. The Hebgen Lake earthquake was accompanied by 35 km of surface faulting along the Red Canyon and Hebgen faults with vertical displacements of up to 5.5±0.3 m (Bonilla and others, 1984; Witkind, 1964) and an average displacement of 2.1 m (Hall and Sablock, 1985). The Borah Peak earthquake produced 36 km of surface faulting along the Lost River and Arentson Gulch faults with vertical displacements of up to 2.7 m and an average displacement of 0.8 m (Crone and Machette, 1984; Crone and others, 1987). Both earthquakes nucleated at depths of about 15-16 km and ruptured upward along faults dipping at 45°-60° (Doser, 1985a, b; Doser and Smith, 1985).

The most reliable and physically meaningful measurement of earthquake size is the seismic moment, M_o, (Aki, 1966) given by

$$M_o = \mu S d$$

where μ is the shear modulus, S is the area of the rupture surface, and d is the average displacement along the rupture surface. From the seismic moment, a moment magnitude, M_w (Kanamori, 1977; Hanks and Kanamori, 1979) can be calculated from the definition

$$M_w = (2/3)\log M_o - 10.7$$

M_w should be comparable to M_S for earthquakes of $5.0 \leq M_w \leq 7.5$ (Hanks and Kanamori, 1979). The Hebgen Lake earthquake had a seismic moment of 1.0×10^{27} dyne-cm (Doser, 1985b), which converts to a moment magnitude of 7.3. The Borah Peak earthquake had a moment of 2.1×10^{26} (Doser and Smith, 1985) to 3.1×10^{26} (Ekstrom and Dziewonski, 1985), which gives a moment magnitude of 6.8 to 7.0.

Threshold of Surface Faulting

Various authors (e.g. Arabasz, 1984; Arabasz and Julander, 1986; Doser, 1985a) have suggested that the threshold magnitude for surface faulting in Utah is approximately 6.0-6.5. This conclusion appears to be well founded based on the historical record of earthquakes in the Intermountain seismic belt and in the Basin and Range province. Bucknam and others (1980) note that all 7 historic earthquakes of M_L6.3 or greater in the Great Basin have produced surface faulting, including the 1934 M_L6.6 Hansel Valley, Utah event. In their tabulation of 11 earthquakes with historic surface faulting in the Basin and Range Province, all 5 events with $M_L \leq 6.8$ had maximum displacements of less than 1 meter. In the Intermountain seismic belt, Doser (1985a) points out that neither the 1975 M_L6.0 Pocatello Valley earthquake nor the 1975 M_L6.1 Yellowstone Park earthquake (fig. 3) had identifiable surface faulting, although both earthquakes were accompanied by an apparently coseismic subsidence of up to 12-13 cm (Bucknam, 1976; Pitt and others, 1979). The implication of the M_L6.0-6.5 threshold for surface faulting is that one can argue that earthquakes up to this size could occur anywhere in the Wasatch Front region within the main seismic belt, even where there is no geologic evidence for surface faulting. We elaborate in a later section.

Seismicity

Figure 6 shows the distribution of all historical main shocks of estimated Richter magnitude 4.0 or greater (or maximum Modified Mercalli intensity V or greater) in the Utah region. The historical sample includes at least fifteen independent main shocks that have had an estimated Richter magnitude of 5.5 or greater (or a Modified Mercalli intensity of VII or greater). These earthquakes are listed in table 1 and their epicenters are shown as solid circles in figure 6. At the scale of figure 6, apparent correlations of historical seismicity with specific faults must be considered with care. For example, many of the epicenters located along the Wasatch fault are non-instrumental and correspond to locations where felt effects were strongest for a particular shock, typically an established city or town. Hence, the coincidence of historical epicenters with the Wasatch fault reflects the locations of settlements along the Wasatch Front, not necessarily earthquake activity on the Wasatch fault itself. It is arguable whether the earthquakes of about magnitude 5-1/2 in 1910 near Salt Lake City and in 1914 near Ogden occurred directly on the Wasatch fault (Arabasz and others, 1980). Thus, as many as two--or perhaps no--earthquakes of magnitude 5 or greater have occurred on the Wasatch fault in historical time. The average inter-event time since 1884 of the moderate-to-large main shocks listed in table 1 is 6 to 7 years. There was, however, one unusually long 25-year interval between 1934 and 1959 without an earthquake of magnitude 5.5 or greater.

Figure 7 shows the pattern of instrumental seismicity for the Utah region determined from monitoring by the University of Utah since mid-1962 (element 7, fig. 1). The epicentral distribution of small- to moderate-size background earthquakes is generally similar to that in figure 6. The sample of figure 7 includes 9,148 earthquakes of all sizes up to magnitude 6.0, and 2,152 earthquakes of magnitude 2.0 or greater. Table 2 lists independent main shocks in the sample of magnitude 4.0 and greater. Focusing attention on the Wasatch Front study area, figures 8 and 9 show the patterns of instrumental seismicity respectively for October 1974 through June 1978 (2,480 events) and July 1978 through December 1986 (3,936 events). The first sample is the same as that described in detail by Arabasz and others (1980) for the first 3.75 years of detailed monitoring by the University of Utah's telemetered seismic network. The second sample allows an updated comparison for the subsequent 8.5-year period.

The patterns of seismicity shown in figures 8 and 9 are remarkably similar, and comparison with that for the period 1962-1974 (Arabasz and others, 1980, fig. 4) indicates general stability in the pattern of seismicity throughout the period of instrumental monitoring. One notable exception arises from aftershock activity following the 1975 M6.0 Pocatello Valley earthquake on the Idaho-Utah border (see upper left, figs. 8 and 9). The pattern of most recent seismicity in the Wasatch Front area illustrated in figure 9 includes several notable features, described from north to south:

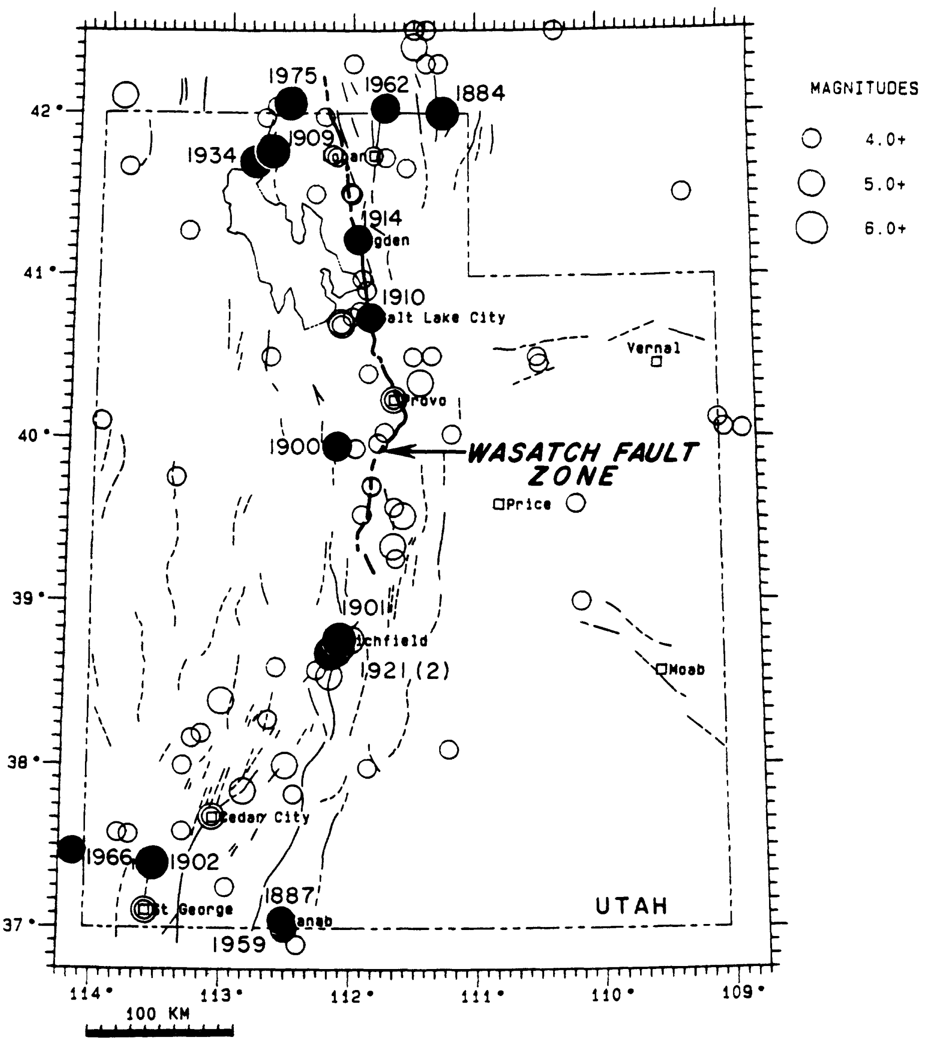

Figure 6. Epicenter map of the Utah region showing all independent main shocks of M_L 4.0 or greater (or Intensity V or greater), 1850-1986. Earthquakes of estimated M_L 5.5 or greater specially labeled. Data from University of Utah Seismograph Stations. Base map of young faults (from Arabasz et al., 1979) is superseded by the compilation shown in figure 5.

TABLE 1.—Largest earthquakes in the Utah region—1850 through June 1987[1] (modified from Arabasz et al., 1979)

Local Date	Lat(°N)	Long(°W)	Location	Intensity (MM)	Magnitude (M_L)	Moment[3] (x10^{24}dyne-cm)
1884 Nov 10	42.0	111.3	Bear Lake Valley	8	(6)	
1887 Dec 05	37.1	112.5	Kanab	7	(5½)	
1900 Aug 01	40.0	112.1	Eureka	7	(5½)	
1901 Nov 13	38.8	112.1	Richfield	9	(6½+)	
1902 Nov 17	37.4	113.5	Pine Valley	8	(6)	
1909 Oct 05	41.8	112.7	Hansel Valley	8	(6)	
1910 May 22	40.8	111.9	Salt Lake City	7	(5½)	
1914 May 13	41.2	112.0	Ogden	7	(5½)	
1921 Sep 29	38.7	112.2	Elsinore	8	(6)	
1921 Oct 01	38.7	112.2	Elsinore	8	(6)	
1934 Mar 12	41.7	112.8	Hansel Valley	9	6.6[2]	77.0
1959 Jul 21	37.0	112.5	Utah-Arizona border	6	5.5+	
1962 Aug 30	42.04	111.74	Cache Valley	7	5.7	7.0
1966 Aug 16	37.46	114.15	Nevada-Utah border	6	5.6	1.1
1975 Mar 27	42.10	112.52	Pocatello Valley	8	6.0	18.6

[1] Table includes earthquakes of maximum Modified Mercalli intensity of VII or greater, or of Richter magnitude 5.5 or greater. Magnitudes in parentheses are estimated from intensity. Sample area: 36°45'N - 42°30'N, 108°45'W - 114°15'W. Aftershocks excluded.

[2] Richter (1935, p. 24) estimated an M_L value of 7.0. The value of 6.6 comes from Gutenberg and Richter (1954) and appears to be a surface-wave magnitude.

[3] Doser and Smith (1982).

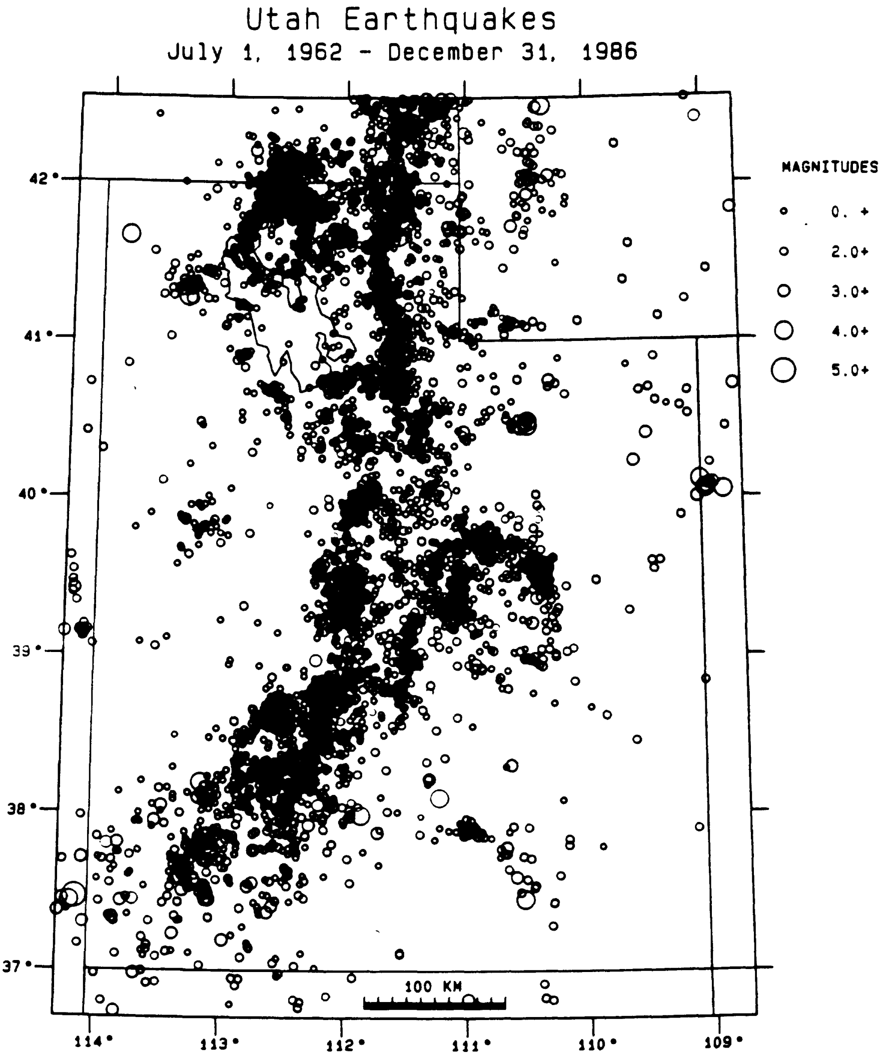

Figure 7. Epicenter map of all earthquakes located by the University of Utah Seismograph Stations in the Utah region, 1962-1986.

TABLE 2.—Earthquakes of magnitude (M_L) 4.0 or greater in the Utah region—1962 - December 1986

Local Date	Lat (N)	Long (W)	Magnitude (M_L)	Location
1962 Feb 15	36.90	112.40	4.5	Arizona-Utah border (Kanab)
1962 Aug 30	42.03	111.74	5.7	Cache Valley (Logan)—*damage*
1962 Sep 05	40.72	112.09	5.2	Magna—*damage*
1963 Jul 07	39.53	111.91	4.4	Juab Valley (Levan/Nephi)—*damage*
1963 Jul 09	40.03	111.19	4.0	Soldier Summit area
1963 Sep 30	38.10	111.22	4.3	Capitol Reef Area
1964 Oct 18	41.73	111.73	4.1	Cache Valley
1966 Mar 17	41.66	111.56	4.6	Logan
1966 May 20	37.98	111.87	4.1	Aquarius Plateau area
1966 Aug 16	37.46	114.15	5.6	Nevada-Utah border
1966 Oct 21	38.20	113.16	4.2	Escalante Valley
1967 Feb 14	40.11	109.05	4.0	Utah-Colorado border
1967 Feb 16	41.27	113.33	4.0	Newfoundland Mts. area
1967 Oct 04	38.54	112.16	5.2	Marysvale—*damage*
1970 Mar 29	41.66	113.84	4.7	Grouse Creek area
1970 Apr 21	40.06	109.01	4.0	Colorado-Utah border
1971 Dec 03	42.50	110.34	4.1	SW Wyoming
1972 Jan 03	38.65	112.17	4.4	Elsinore—*damage*
1972 Jun 01	38.67	112.07	4.0	SW Sevier County
1972 Oct 01	40.51	113.35	4.3	Heber City—*damage*
1973 Apr 13	42.04	112.63	4.2	Pocatello Valley
1975 Mar 27	42.07	112.53	6.0	Pocatello Valley—*damage*
1976 Nov 04	41.81	112.70	4.0	Hansel Valley
1977 Sep 30	40.46	110.48	4.5	NW Duchesne County—*damage*
1978 Nov 30	42.10	112.49	4.6	Pocatello Valley
1979 Mar 19	40.04	108.86	4.1	Colorado-Utah border
1980 May 24	39.94	111.96	4.4	Goshen Valley
1981 Apr 05	37.59	113.30	4.6	Kanarraville
1982 May 24	38.71	112.04	4.0	Sevier Valley (Annabella)
1983 Oct 08	40.75	111.99	4.3	N. Salt Lake Valley
1986 Mar 24	39.24	112.01	4.4	Japanese Valley
1986 Aug 22	37.45	110.53	4.0	SE Utah (near Bullfrog Basin)

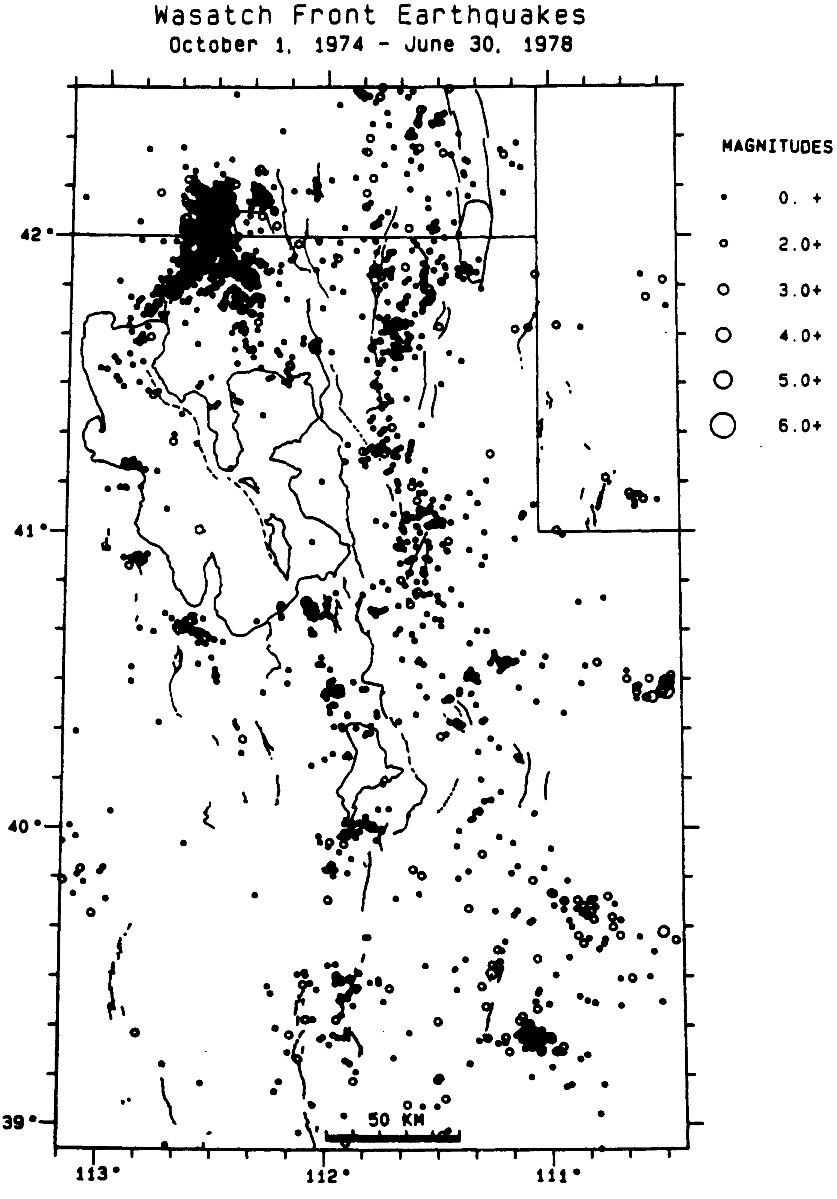

Figure 8. Epicenter map of all earthquakes located by the University of Utah Seismograph Stations in the Wasatch Front area, 1974-1978. Base map as in figure 5.

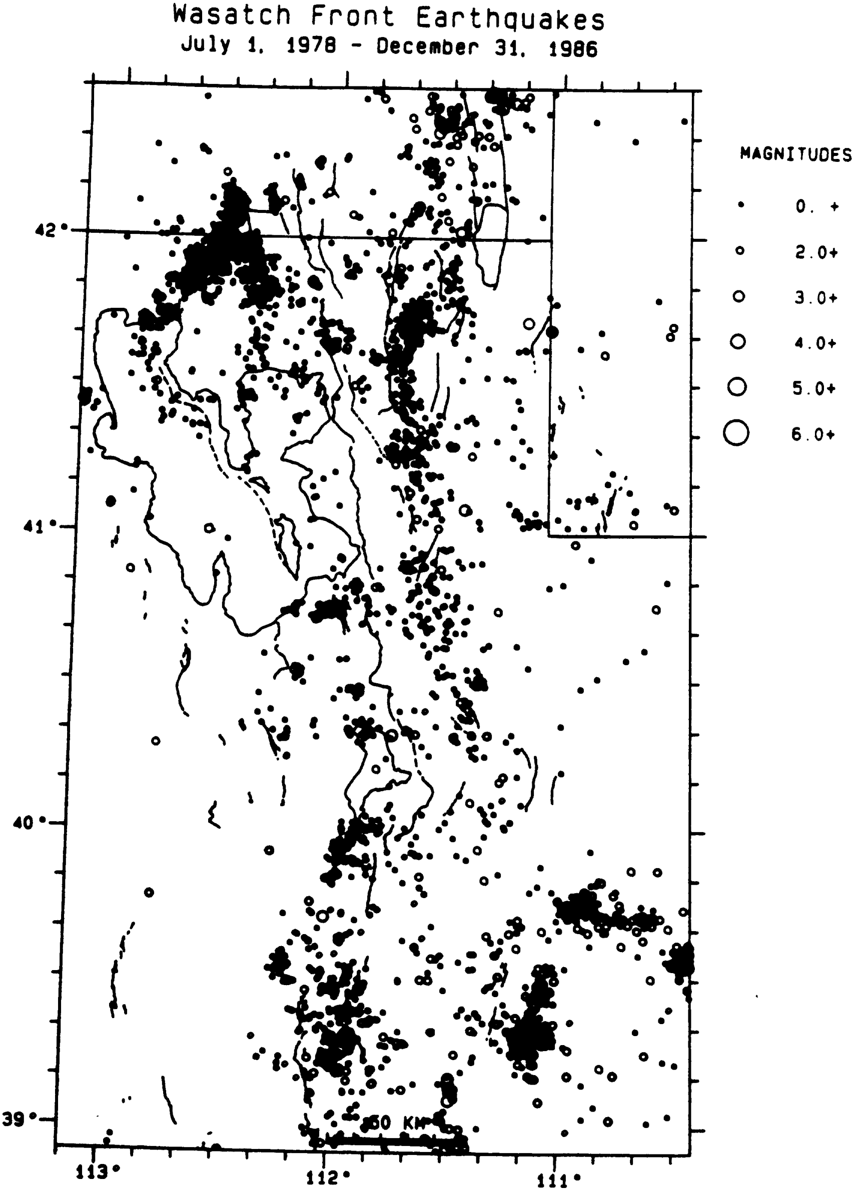

Figure 9. Epicenter map of all earthquakes located by the University of Utah Seismograph Stations in the Wasatch Front area, 1978-1986. Base map as in figure 5.

(1) At the northern extremity of figure 9, earthquake clusters are part of a northeast-trending belt of seismicity that continues to the Jackson-Yellowstone Park region. This includes episodic swarm seismicity in the Soda Springs, Idaho, area (approx. 42°30'N, 111°30'W). A swarm begining as early as December 1981 peaked with an M4.7 earthquake in October 1982 (Richins and others, 1983), and seismicity in that area continues to the present.

(2) Earthquake activity in the Idaho-Utah border area west of the Wasatch fault has been prominent ever since the 1975 M6.0 Pocatello Valley earthquake (Arabasz and others, 1981). Small- to moderate-size earthquakes extending from the state border southwest into Hansel Valley, and southeast into Blue Creek Valley, form an inverted "Y" pattern, which began to form several months after the March 1975 main shock and in which seismicity persists to the present. At the southwest extremity of the "Y" pattern, scattered small earthquakes beneath the northern part of the Great Salt Lake have previously appeared to be part of a broad northeast-trending belt. The sample of figure 9, however, suggests a northwest-trending epicentral pattern in the vicinity of the East Great Salt Lake fault.

(3) Densely-clustered earthquakes occurring roughly 20 to 40 km east of the Wasatch fault define a linear belt extending southward from about 41°50'N to at least 41°N--and perhaps as far south as 40°N. Earthquakes in the northern part of this belt lie east of the west-dipping East Cache and Wasatch faults and occur within a volumetric zone beneath the Bear River Range. To the south of 41°N, earthquake clusters within this belt to the east of the Wasatch fault follow a zone of northerly-trending valleys within the so-called Wasatch Hinterland (Sullivan and others, 1986).

(4) Clusters of seismicity appear close to or just west of the trace of the Wasatch fault near Honeyville at about 41°40'N, within the vicinity of Salt Lake City at about 40°45'N, at the northern end of Utah Valley at about 40°20'N, in the vicinity of Goshen Valley at about 40°00'N, and in a broadly scattered zone at the southern end of the Wasatch fault. We return to this seismicity when we consider the Wasatch fault in finer detail in a later section.

(5) In the lower right part of figure 9, a prominent feature of the seismicity of east-central Utah is a pattern of persistent shallow seismicity forming an inverted U-shape that corresponds with underground coal mining along the eastern side of the Wasatch Plateau and the arcuate Book Cliffs escarpment. The seismicity is well known to be mining-related and appears to correlate with mining areas where annual rates of extraction exceed 500,000 tons (see summary by Arabasz and Julander, 1986). Results of a recent study of mining-related seismicity in the eastern Wasatch Plateau are reported by Williams and Arabasz (1987).

Earthquake Focal Depths

The purpose of this section is to examine the seismic network data in the Wasatch Front region for focal-depth information. It is an unfortunate fact that computed focal depths of most earthquakes located with the regional seismic network are unreliable due to the large station spacings of 15-35 km in the immediate Wasatch Front area and 35-100 km elsewhere (fig. 2). As a partial solution to this problem, temporary arrays of portable seismographs are routinely deployed by the University of Utah in selected target areas and have provided some of the best data for correlating seismicity with structure (e.g., Arabasz and Julander, 1986). It remains useful, nontheless, to evaluate the regional network data for focal-depth information.

It is commonly assumed that the presence of a recording station within one focal depth of an earthquake's epicenter provides good depth control. To test this assumption, K. J. Quigley (Univ. of Utah, unpub. rept., 1986) performed numerical experiments on synthetic arrival-time data for the Wasatch Front seismic network to determine statistical criteria for focal-depth reliability. Based on his results, 485 earthquakes out of 6,416 from the post-1974 UUSS catalog for the Wasatch Front area were judged to have reliable focal depths, using the following criteria: (1) distance to the nearest station less than or equal to the focal depth or 5 km, whichever is larger, and (2) standard vertical hypocentral error (ERZ) of 2 km or less, as calculated by the location program HYPOELLIPSE (1974-1980) or HYPOINVERSE (1981-1986). Quigley's results verify that there is a 68% probability that the computed focal depth for such events is within 1.0 ERZ of the true focal depth, and 95% that it is within 2.4 ERZ.

Figure 10 shows the best-resolved foci in map and cross-section view. It should be noted that the selection criterion of having a close station may filter out shallow events in some areas, but deeper events will be less affected. In general, the east-west cross sections do not appear to be particularly informative in terms of significant variations in the east-west distribution of maximum focal depths or spatial association with the Wasatch fault. The north-south cross section, however, suggests that there may be significant variations in maximum earthquake depth along the Wasatch Front. For example, the maximum focal depths at the northern and southern ends of the cross section appear to be about 18-20 km, while the maximum focal depths in the central part, near the intersection of the east-west-trending Uinta Arch with the Wasatch Front, appear to be about 12-14 km. Maximum earthquake focal depths bear directly on crustal rheology, the depth of nucleation of large earthquakes, and maximum fault-rupture dimension. Accordingly, the north-south variations of maximum focal-depth suggested in figure 10 should be investigated further. Figure 10 emphasizes the sparseness of three-dimensional information available from the multi-thousands of earthquakes located by the permanent regional network. A consequence is that only limited information is available to address the association of seismicity with subsurface structure, as we discuss next.

Problematic Correlation of Seismicity with Geologic Structure

Fundamental problems in correlating diffuse seismicity with mapped Cenozoic faulting and subsurface geologic structure in the Utah region have been discussed at length by Arabasz (1984) and by Arabasz and Julander (1986). Discussion is repeated here because of its continued relevance. Problems include: (1) uncertain subsurface structure, which typically is more complex along the main seismic belt than apparent from the surface geology; (2) observations of discordance between surface fault patterns and seismic fault slip at depth (Arabasz and others, 1981; Zoback, 1983); (3) a paucity of historic surface faulting; and (4) inadequate focal-depth resolution from regional seismic monitoring.

Crustal structure along the eastern Great Basin is known to involve vertically stacked plates separated by low-angle detachments resulting from relict pre-Neogene thrustbelt structure

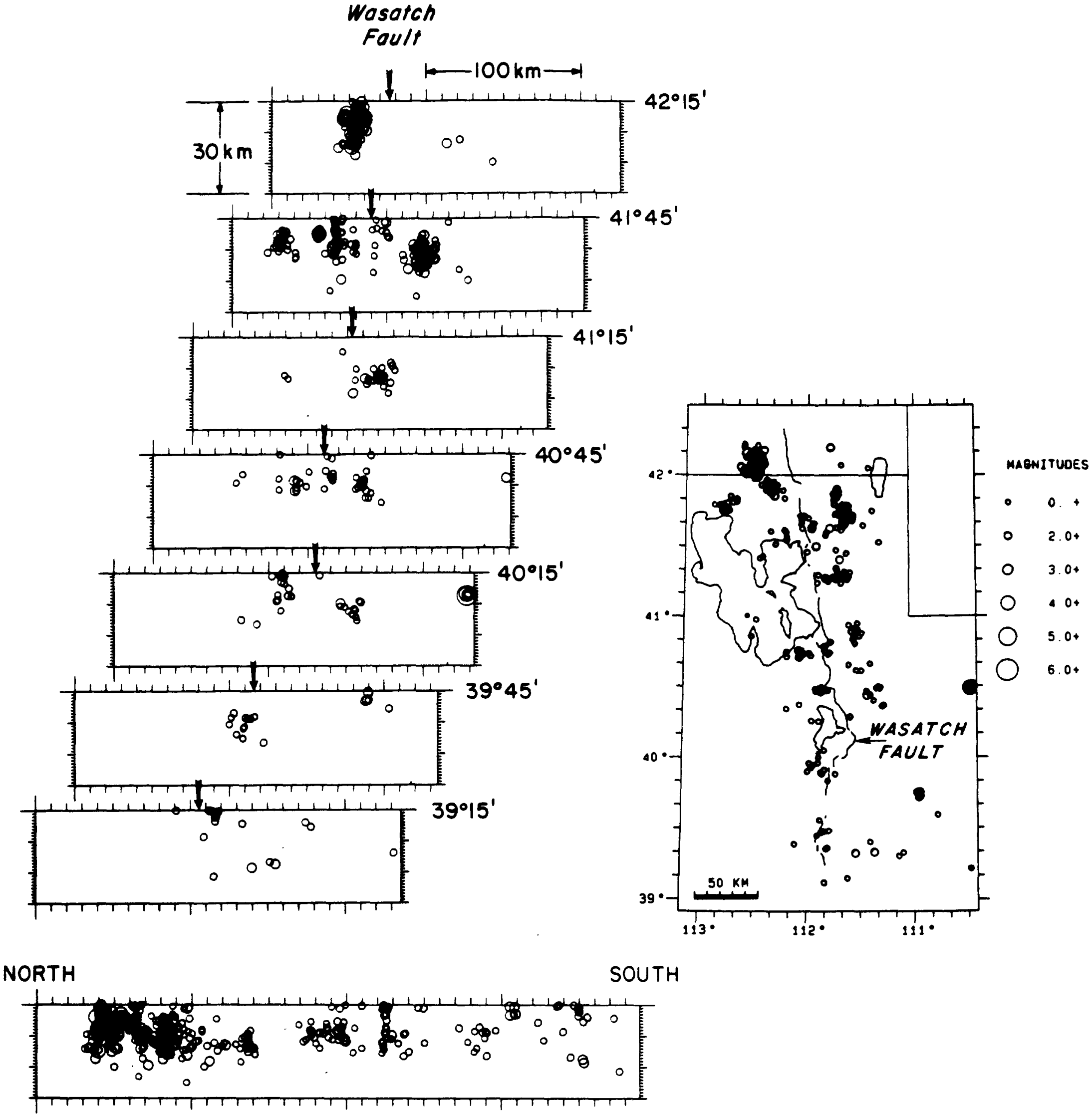

Figure 10. Epicenter map and corresponding vertical sections summarizing reliable earthquake focal-depth information for the Wasatch Front area, October 1974-December 1986.

and/or Neogene extension (Allmendinger and others, 1983; Smith and Bruhn, 1984; Smith and others, 1987). Smith and Bruhn (1984) present a summary of seismic-reflection data that indicate the widespread presence of low-angle and downward-flattening faults in the subsurface and an intimate relationship between pre-Neogene thrustbelt structure and young normal faults along the eastern Basin and Range margin. Seismological evidence to date indicates that, at least for small to moderate earthquakes, seismic slip in this region predominates on fault segments with moderate (≥30°) to high-angle dip (Zoback, 1983; Arabasz and Julander, 1986).

Given the relatively high threshold of surface faulting, and observations of discordance between surface fault patterns and seismic slip at depth, one can argue that—with the sole exception of the 1934 Hansel Valley earthquake—no other of Utah's 15 historical earthquakes of M_L 5.5 or greater (table 1) can be confidently associated with a mapped surface fault. Within the domain of Utah's main seismic belt, future seismicity below the threshold of surface faulting (M_L approx. 6 to 6½) thus cannot be confidently precluded by knowledge of the surface geology alone. Where subsurface structure is complex, moderate size earthquakes may occur on "blind" subsurface structures that have no direct surface expression.

On the basis of special earthquake studies in the southern Wasatch Front area, neighboring parts of central Utah, and southeastern Idaho, the following working hypothesis was offered by Arabasz (1984; see also Arabasz and Julander, 1986) to explain observations of diffuse background seismicity. Background seismicity, it was suggested, is fundamentally controlled by variable mechanical behavior and internal structure of individual horizontal plates within the seismogenic upper crust. Diffuse epicentral patterns may then result from the superposition of seismicity occurring within individual plates, and also perhaps from favorable conditions for block-interior rather than block-boundary microseismic slip. Figure 11 schematically shows some aspects of the working hypothesis.

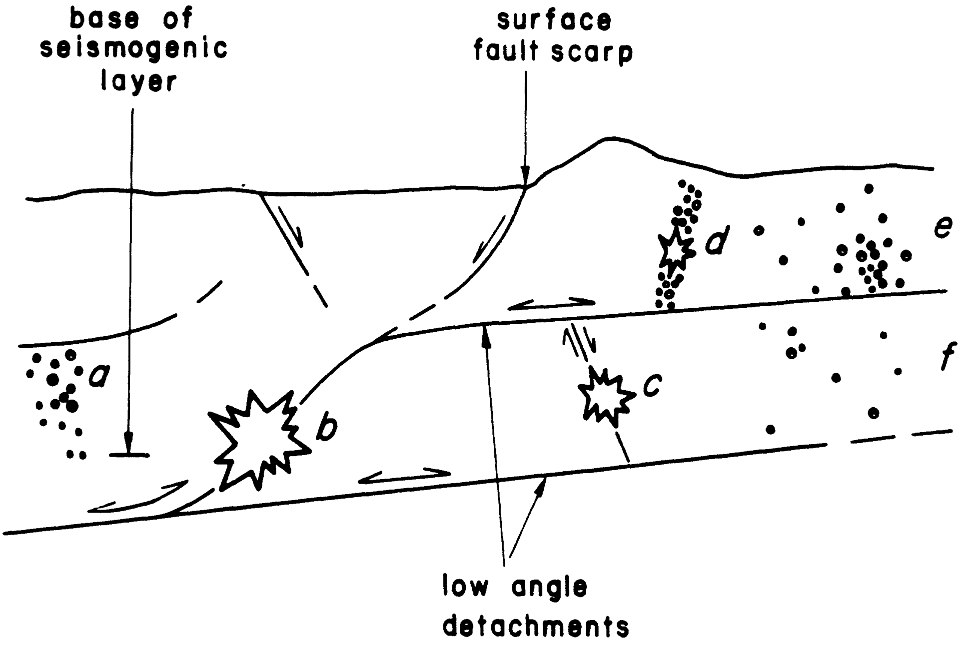

Figure 11. (a) Schematic geologic cross-section of the upper crust illustrating complex association of seismicity with geological structure in the Intermountain seismic belt (from Arabasz, 1984, and Arabasz and Julander, 1986). Starbursts indicate foci of moderate-to-large earthquakes; small circles, microseismicity; lines in subsurface, faults. Arrows indicate sense of slip on faults; two-directional arrows, extensional backsliding on pre-existing low-angle faults possibly formed as thrust faults. Base of seismogenic layer is approximately at 10-15 km depth. Letters identify aspects (not exhaustive) of observations and a working hypothesis relating seismicity to structure: (a) local predominance of seismicity within a lower plate; (b) nucleation of a large normal-faulting earthquake near the base of the seismogenic layer, hypothetically on an old thrust ramp, and with linkage or an established rupture pathway to a major surface fault; (c) occurrence of a moderate-size earthquake within a lower plate, without linkage to a shallow structure; (d) occurrence of a moderate-size earthquake and aftershocks on a secondary fault where an underlying detachment restricts deformation to the upper plate; (e) diffuse block-interior microseismicity predominating within an upper plate--perhaps responding to extension enhanced by gravitational backsliding on an underlying detachment; and (f) diffuse block-interior microseismicity within a lower plate where frequency of occurrence is markedly lower than in the overlying plate.

SEISMIC SOURCE ZONES AND SEISMICITY PARAMETERS

General Remarks

Two key steps in any analysis of earthquake hazards or risks are (1) the identification and geometric depiction of seismic source zones within which earthquakes are likely to originate (step 3, fig. 1), and (2) the estimation of seismicity parameters for these source zones (step 4, fig. 1). The important seismicity parameters are the maximum magnitude, the expected earthquake distribution as a function of size, and the rate of activity. Both earthquake catalog data and geologic data on active faults can be used to identify and characterize seismic source zones.

Our current understanding of the seismotectonic framework of the Wasatch Front region, as summarized above, leads to the position that seismic hazards arise from two fundamental classes of earthquakes: (1) infrequent, large (magnitude greater than 6.0 to 6.5) surface-faulting earthquakes on identifiable faults having evidence of late Quaternary displacement, and (2) small-to moderate-size (up to magnitude 6.5) earthquakes, below the threshold of surface faulting, that are not constrained in location to mapped faults and may occur randomly in space throughout broadly defined regions. This position is a consequence of detailed studies that show clear evidence for large, prehistoric earthquakes on faults in the region (e.g., Swan and others, 1980; Schwartz and others, 1984), the diffuse scatter of small-to moderate-size earthquakes illustrated in figures 7, 8, and 9, and the problematic correlation of seismicity and geologic structure discussed above. It therefore seems reasonable to distinguish two different types of seismic source zones: (1) fault-specific sources for which the evidence is primarily geological, and (2) areal source zones that are based upon the historical and instrumental earthquake record and have a maximum magnitude of 6.5. This approach has been used in several studies of seismic hazard in the Wasatch Front region, including the elaborate probabilistic analysis of ground shaking hazard by Youngs and others (1987), a study of the "Wasatch Hinterland" by Sullivan and others (1986), and a study by Arabasz and others (1987) of the region surrounding Utah's proposed sites for the Superconducting Supercollider, which are located southwest of the Great Salt Lake along the western boundary of the Wasatch Front region.

In this section, we treat the entire Wasatch Front study area as one areal source zone and use the instrumental earthquake record to model the recurrence of earthquakes up to magnitude 6.5 in this region. Although the available data suggest that seismicity rates may vary somewhat within this region, there are not enough earthquakes in the record to reliably estimate seismicity parameters for subsets of this region. Furthermore, the 25-year record of instrumental seismicity is simply too short to allow the extrapolation into the future of spatial variations of seismicity rate within the Wasatch Front region. We first present results from recurrence modeling for the Wasatch Front region, then briefly discuss the fault-specific sources in this region and the maximum earthquake size that can be expected to occur on them.

Recurrence Modeling

Earthquake catalog data provide the only means to determine the rate of occurrence and size distribution of earthquakes smaller than the threshold of surface faulting. The standard way to characterize seismicity in any seismically active region is with the Gutenberg-Richter exponential frequency-magnitude relationship given by

$$\log N = a - bM$$

where N is the average number of independent events per year of magnitude M or greater and a and b are constants appropriate for the particular region. The a-value is a measure of the overall rate of earthquake activity. The b-value is a measure of the relative proportion of small events to large events, with higher b-values indicating relatively more small events. If we define A as the average number of events per year of $M \geq 3.0$, then the above equation can be rewritten as

$$N = A\ 10^{-b(M - 3.0)}$$

In order to obtain meaningful estimates for the seismicity parameters a (or A) and b from earthquake catalog data, it is first necessary to remove from the catalog dependent events such as aftershocks, foreshocks, and secondary events in swarm sequences. Shimizu (1987) identified dependent and independent events in the University of Utah catalog for the time period July 1962 through December 1985 by applying the local clustering method of Veneziano and Van Dyck (1986). This is a statistically rigorous method that allows for variations in the space-time clustering of dependent events from one main shock to the next. Shimizu's listing of independent events of $M_L \geq 2.0$ in the catalog for this time period was supplied to us on computer tape by D. Veneziano. This listing contained 571 main shocks within the study area. The epicenters of these events are plotted in figure 12. For purposes of the recurrence modeling, we eliminated the 126 events in the study area south of 39°50'N and east of 111°15'W (dashed box, fig. 12), where the seismicity is predominantly mining-related. This left 445 independent main shocks of $2.0 \leq M_L \leq 6.0$ in the remaining 85,000 km^2 of the study area. These main shocks form the basic data set for our recurrence modeling of the Wasatch Front area.

Figure 13 is a cumulative recurrence plot (log N versus M) for the 445 independent main shocks (dots). Note that the observed number of $M_L \geq 2.0$ events per year is equal to or greater than the number expected from a linear extrapolation of the data for the larger magnitude cutoffs. In fact, the recurrence curve formed by connecting the dots in figure 13 even appears to have a steeper slope for $M_L \leq 3.0$. This observation suggests that the University of Utah catalog contains a reasonably complete listing of main shocks of $M_L \geq 2.0$ in the Wasatch Front region after July 1962.

The apparent change in slope of the recurrence curve near magnitude 3 may be an artifact of the way that magnitudes are assigned in the University of Utah catalog. The catalog magnitudes for most earthquakes in the Wasatch Front region over magnitude 3 are true local magnitudes calculated from peak amplitudes measured on seismograms from low-gain Wood-

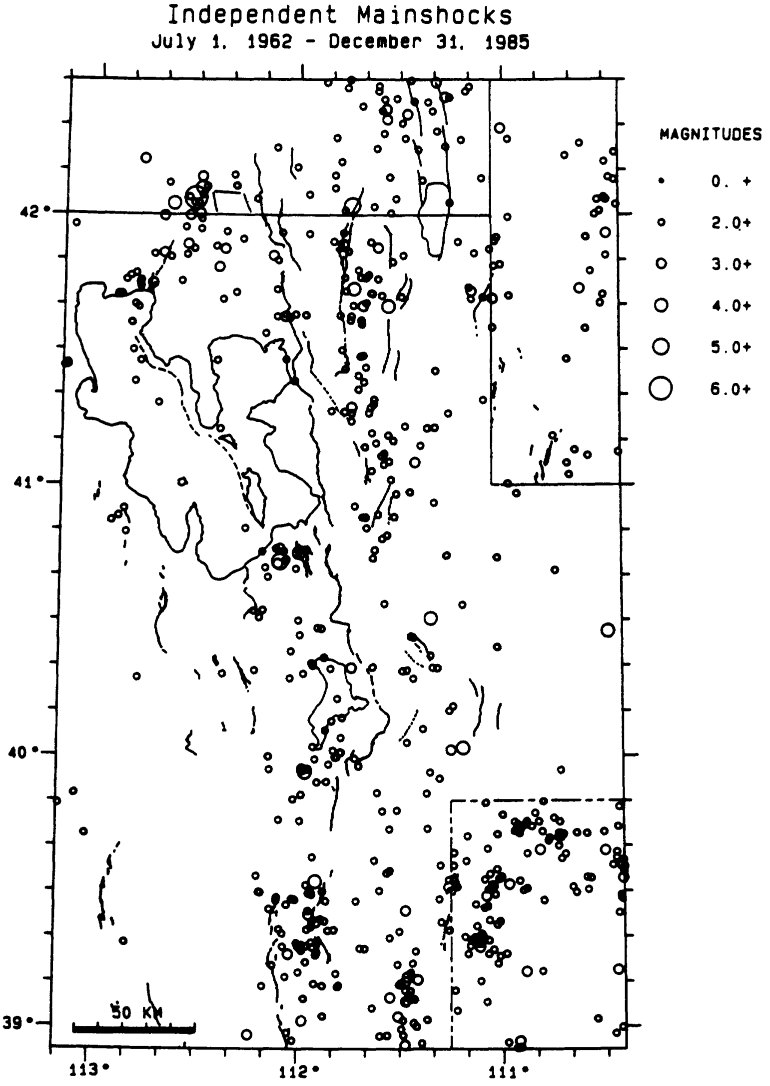

Figure 12. Epicenters of independent mainshocks in the Wasatch Front area from July 1962 through December 1985, plotted on the map of late Quaternary faulting shown in figure 5. Dashed box at lower right indicates area of mining-induced seismicity that was excluded from the recurrence analysis.

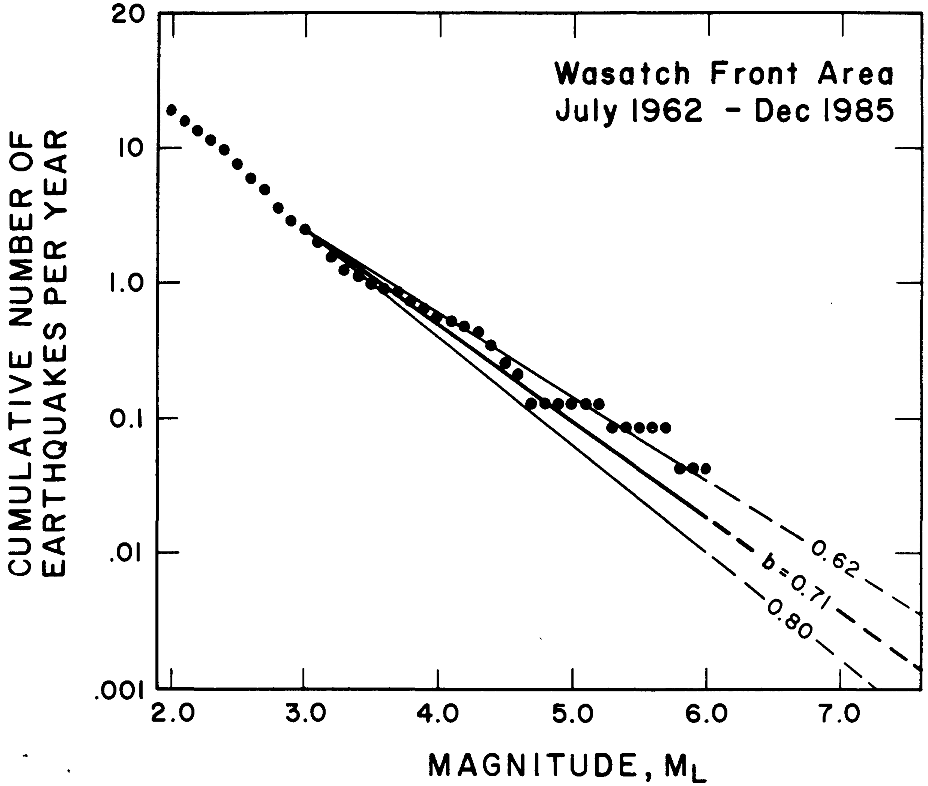

Figure 13. Recurrence data for independent main shocks in the Wasatch Front area from July 1962 through December 1985. The dots show the cumulative number of earthquakes per year greater than or equal to the local magnitude, M_L, given on the horizontal axis. The heavy line through the dots for $M_L \geq 3.0$ indicates the preferred maximum likelihood fit with a slope, b, of 0.71, calculated using the method of Weichert (1980). The lighter lines indicate the lower- and upper-bound slopes of 0.62 and 0.80. The area used for the recurrence modeling is 85,000 km^2 (area shown in fig. 12 minus the dashed box).

Anderson-type instruments. The magnitudes listed for most of the smaller earthquakes are coda magnitudes calculated from signal durations measured on records from various types of higher-gain instruments (for details, see Arabasz and others, 1979; Richins and others, 1981; Richins and others, 1984; and Brown and others, 1986). The coda magnitude scales were calibrated against Wood-Anderson M_L measurements, and should therefore give compatible results. Nevertheless, it is possible that there are some small, systematic differences between the two types of estimates. Research on refined methods of magnitude determination using digital waveform data is currently underway at the University of Utah.

The heavy line in figure 13 shows a straight-line fit to the recurrence data (dots) above M_L 3.0, determined by the maximum likelihood technique of Weichert (1980). The best-fit line has a slope of b = 0.71±0.09. The lighter lines are drawn with the lower-bound and upper-bound slopes of 0.62 and 0.80, respectively. Note that all three lines are constrained to pass through the data point for the minimum magnitude of 3.0. The lighter lines appear to bound the range of possible slopes quite well if a magnitude cutoff of 3.0 is used. However, the b-value is unfortunately very sensitive to the cutoff magnitude. Cutoff magnitudes of 2.0 and 2.5 give b-values of 0.82±0.04 and 0.88±0.07, respectively. We chose the cutoff magnitude of 3.0 because of the possible problems with the smaller magnitudes discussed above and because the lines calculated using this cutoff provide a better fit to the data for the larger earthquakes, which are the ones of primary concern for seismic hazards.

The recurrence relationship given by our preferred maximum likelihood fit to the data shown in figure 13 is

$$N = (2.51)10^{-(0.71\pm0.09)(M_L - 3.0)}$$

or, alternatively,

$$\log N = 2.53 - 0.71\ M_L$$

Table 3 lists average return periods for earthquakes in the Wasatch Front region calculated from the first of these equations. The preferred estimate is for the b-value of 0.71. The values in the right-hand column are lower and upper limits calculated using the limiting b-values of 0.62 and 0.80, respectively.

As a check on table 3, consider the number of earthquakes of magnitude 5.5 or greater (or Modified Mercalli intensity VII or greater) in the Wasatch Front region from 1850 to 1987. There have been eight such earthquakes (table 1, fig. 4), which gives an average inter-event time of 17 years. This falls within the lower end of our estimated range of return periods for $M_L \geq 5.5$ earthquakes, which is 14 to 40 years. If, following Arabasz and others (1980), we assume that the catalog is complete at the $M_L \geq 5.5$ level only since 1878, the average repeat time shortens to 14 years. The repeat times calculated for earthquakes greater than magnitude 6 represent an extrapolation beyond the limits of the data shown in figure 13. Nevertheless, the predicted return period for $M_L \geq 7.0$ events of 120 to 630 years (with a preferred estimate of 280 years) is consistent with the return period for $M_L \geq 7.0$ events on the Wasatch fault of 330±90 years determined by Youngs and others (1987), given that the Wasatch fault is the

TABLE 3.—Average return periods for earthquakes in the Wasatch Front region[1]

M_L	Average Return Period (years) Preferred Estimate	Range of Estimates
≥3.0	0.40	
≥3.5	0.90	0.81 - 1.0
≥4.0	2.0	1.7 - 2.5
≥4.5	4.6	3.4 - 6.3
≥5.0	10	7 - 16
≥5.5	24	14 - 40
≥6.0	54	29 - 100
≥6.5	120	60 - 250
≥7.0	280	120 - 630
3.0 - 3.5	0.71	.66 - .78
3.5 - 4.0	1.6	1.6 - 1.7
4.0 - 4.5	3.7	3.3 - 4.2
4.5 - 5.0	8.3	6.6 - 10
5.0 - 5.5	19	14 - 26
5.5 - 6.0	42	28 - 66
6.0 - 6.5	96	57 - 170
6.5 - 7.0	220	120 - 420
7.0 - 7.5	490	240 - 1000

[1] 38°55'N-42°30'N, 110°25'W-113°10'W, excluding mining-related seismicity in the southeast corner of the area. Area equals 85,000 km^2.

dominant source of magnitude 7 and greater earthquakes in the region.

Arabasz and others (1980) modeled earthquake recurrence for the Wasatch Front region using the entire University of Utah catalog of MM intensity V or greater (approximately $M_L \geq 4$) earthquakes from 1850 through 1978. They obtained the equation

$$\log N = 2.98 - 0.72M_L$$

Their b-value of 0.72 is essentially the same as our b-value of 0.71±0.09. However, their a-value of 2.98 is larger than our value of 2.53. This difference corresponds to a difference in seismicity rates of a factor of 2.8. Two possible explanations for this disparity are (1) the seismicity from 1962 through 1985 was low compared to the seismicity from 1850 through 1961, or (2) the magnitudes of the pre-1962 events are overestimated by about 0.6 magnitude units.

It should be pointed out that our preferred b-value of 0.71 is lower than the b-values obtained in most previous studies of earthquake recurrence along the Wasatch Front that made major or exclusive use of the post-1962 instrumental University of Utah catalog. Arabasz and others (1980) determined a b-value of 0.95±0.15 using the catalog data from July 1962 through June 1978 for a subset of the Wasatch Front region between 111°15'W and 112°15'W. Youngs and others (1987) obtained b-values ranging from 0.77 to 0.86 (depending on the criteria used to remove dependent events), using all catalog data from 1850 through March 1986 above the uniform detection thresholds that they estimated. The north-south extent of the study area of Youngs and others is from 39°N to 42°30'N, nearly the same as that of our study area, but their area has a narrower east-west extent. Finally, Shimizu (1987) obtained a b-value of 1.1 using data from July 1962 through December 1985 for a region extending from 39°N to 42.5°N and 108°45'W to 114°15'W, which he calls the "Central-Northern Utah" region.

The higher b-values obtained by Youngs and others (1987) and by Arabasz and others (1980) for the post-1962 data can be attributed primarily to the use of different methods for removing dependent events. The b-value of 1.1 obtained by Shimizu (1987) cannot be explained in this way, since we used his listing of independent events for our recurrence modeling. The higher b-value obtained by Shimizu results from his use of a minimum magnitude of 2.5 in his recurrence analysis, and, to a lesser extent, his use of the maximum likelihood method of Utsu (1965) to fit a straight line to the data. Utsu's method tends to give higher b-values than the method of Weichert (1980), which was used both by us and by Youngs and others (1987). Application of Utsu's method to the data in figure 13 for $M_L \geq 2.5$ gives a b-value of 0.97, which is in reasonable agreement with Shimizu's value considering that his calculation included data from a larger area.

Fault-Specific Sources

Although the 1934 M_S6.6 Hansel Valley earthquake is the largest historic earthquake to have occurred in the Wasatch Front region, there is good geologic evidence that larger earthquakes can be expected to occur on the Wasatch fault and other active faults in the region. All of the faults with evidence for late Quaternary (< 500,000 years) movement shown on the map in figure 5 are considered to be potential source of earthquakes larger than M_L 6.0-6.5, the threshold for surface faulting. Maximum earthquake magnitudes for these fault-specific sources can be assessed from estimates of the rupture length, area, and displacement for the maximum size event. Average return periods for surface-faulting events can, at least in some cases, be determined from geomorphic observations or from the stratigraphy of deposits near the fault trace exposed by trenching (see Allen, 1986, and Schwartz and Coppersmith, 1986, for reviews of these techniques). A detailed description of all the fault-specific sources shown in figure 6 is beyond the scope of this paper. We refer the reader to the paper by Youngs and others (1987) for a thorough summary of available information on the major faults in the Wasatch Front region and a determination of seismicity parameters for these faults. Here, we present information on four fault-specific sources that we use below in some probabilistic hazard calculations, consider the maximum probable earthquake for the whole Wasatch Front area, and briefly discuss the issue of frequency-magnitude relationships for individual faults.

Table 4 presents basic information for the four most prominent fault-specific sources near Salt Lake City: the Wasatch fault, West Valley fault zone, East Great Salt Lake fault, and North Oquirrh Mountains fault (figure 5). The faulting parameters for the Wasatch fault are taken from segmentation model B of Youngs and others (1987). This model has ten segments, and is very similar to the segmentation model proposed by Machette and others (1986). The maximum magnitude listed for each segment is a mean estimate calculated from the set of possible values and their assigned weights listed in table 1 of Youngs and others. The recurrence intervals for maximum earthquakes are mean estimates taken directly from table 3 of Youngs and others. For the West Valley fault zone the maximum magnitude of 6.5 is also a mean value calculated from table 1 of Youngs and others. The average return period of 2,000 years is inferred from the observation of 6 to 7 discrete faulting events on the fault zone within the last 13,000 years (S.J. Olig, written communication, 1987). The segmentation of the East Great Salt Lake fault is very uncertain, but it appears to be divided into at least two segments, each about 50 km long (fig. 5; Pechmann and others, 1987). The maximum magnitude of 7.2 assigned to each segment is based on a simple analogy with the Weber and Salt Lake City segments of the Wasatch fault, which are of comparable length. The average recurrence interval for maximum earthquakes on each segment is judged to be about 4,000 years, based on the fact that the observed slip rates are about half of those measured for the central segments of the Wasatch fault, which have recurrence intervals of about 2,000 years (Pechmann and others, 1987). For the North Oquirrh Mountains fault, the maximum magnitude of 7.0 is from table 1 of Youngs and others (1987). The average recurrence interval of about 10,000 years or more is inferred from the observation that the most recent surface-faulting event on this fault occurred between 8,000 and 13,500 years ago (Youngs and others, 1987), together with generic arguments made by Arabasz and others (1987). For all of the faults in table 4, the annual probability of the maximum earthquake is taken to be the inverse of the average time interval between maximum earthquakes, since in most cases the elapsed time since the last large earthquake is poorly known.

Estimates of the maximum earthquake size on any particular fault are subject to uncertainties inherent in both the prediction of future rupture characteristics and in the conversion of

TABLE 4.—Information for selected fault-specific sources

Fault Source	Approx. Length (km)	Maximum Magnitude (M_S)	Minimum Distance to Site (km)[1]	Interval for Max. Earthquake (years)	Annual Probability of Max. Earthquake
1. Wasatch fault (Youngs et al., 1987; Machette et al., 1986)					
Collinston segment	60	7.3	110	8,800	1.1×10^{-4}
Brigham City segment	40	7.1	70	7,250	1.4×10^{-4}
Weber segment	57	7.2	15	1,350	7.4×10^{-4}
Salt Lake City segment	45	7.2	0	2,550	3.9×10^{-4}
American Fork segment	18	6.8	25	1,900	5.3×10^{-4}
Provo segment	19	6.8	40	1,900	5.3×10^{-4}
Spanish Fork segment	32	7.0	60	2,050	4.9×10^{-4}
Nephi segment	40	7.1	80	1,750	5.7×10^{-4}
Levan segment	35	7.1	120	7,100	1.4×10^{-4}
Fayette segment	14	6.6	155	10,000	1.0×10^{-4}
2. West Valley fault zone (Young et al., 1987; S.J. Olig, written communication, 1987)	18	6.5	0	2,000	5.0×10^{-4}
3. East Great Salt Lake fault (Pechmann et al., 1987; Viveiros, 1986)					
Promontory segment	50	7.2	70	4,000	2.5×10^{-4}
Antelope Island segment	50	7.2	20	4,000	2.5×10^{-4}
4. N. Oquirrh Mts. fault (Youngs et al., 1987; T. Barnhard, personal communication, 1987)	35	7.0	30	10,000	1.0×10^{-4}

---

[1] The site used for the calculation of the hazard curves is the intersection of I-15 and I-80 in South Salt Lake, at approximately 40°43.1'N, 111°54.2'W.

these rupture characteristics to magnitude estimates. For this reason, it is useful to consider from a historic point of view the maximum earthquake size that is likely to occur anywhere within the Wasatch Front region.

The 1959 M_S7.5 Hebgen Lake earthquake is considered by some to represent the maximum earthquake for the Intermountain seismic belt (e.g. Doser, 1985a). However, it is worth noting that earthquakes larger than this have occurred in the western Basin and Range Province. Slemmons (1980) lists 13 historic surface faulting earthquakes in the western Great Basin. These include two events of magnitude greater than 7.5: the March 26, 1872 Owens Valley, California earthquake of estimated magnitude 8.0, and the October 3, 1915 Pleasant Valley, Nevada earthquake of magnitude 7.75. Slemmons (1980) lists a rupture length of 110 km for the Owens Valley event with a maximum displacement of 6.44 m, and a rupture length of 62 km with a maximum displacement of 5.6 m for the Pleasant Valley event. Thus, both of these earthquakes have a maximum displacement comparable to that of the Hebgen Lake event, but significantly longer rupture lengths. The magnitude of 7.75 for the Pleasant Valley event is from Gutenberg and Richter (1954), and is nearly identical to the surface wave magnitude of 7.7 calculated by Abe (1981). The magnitude of the Owens Valley event is more controversial, owing to the lack of seismographic instruments at the time. Magnitude estimates for this earthquake based on felt reports range from 8.3 (Oakeshott and others, 1972) to 7.2 (Evernden, 1975). From the surface faulting, Beanland and Clark (1987) estimate a moment magnitude of 7.5 to 7.7.

The slip that occurred during the 1872 Owens Valley earthquake had a large strike-slip component to it (Richter, 1958; Oakeshott and others, 1972) and may even have been dominantly strike-slip (Beanland and Clark, 1987). Faults in the Wasatch Front region show predominantly normal slip, although there is abundant evidence of strike-slip faulting in south-central Utah (Anderson and Barnhard, 1984). Thus, the Pleasant Valley and Hebgen Lake earthquakes may be better models for the maximum credible Wasatch Front earthquake than the Owens Valley earthquake. The characteristics of the Pleasant Valley and Hebgen Lake earthquakes suggest that future Wasatch Front earthquakes could have surface wave magnitudes of up to 7.5-7.7, rupture lengths of up to 35-65 km, and maximum vertical displacements of up to about 6 m.

One interesting question concerning fault-specific sources is to what extent they act as sources for small-to moderate-size earthquakes, excluding foreshocks and aftershocks of large events. The Gutenberg-Richter exponential frequency-magnitude relationship usually fits the size distribution of earthquakes over large regions quite well. However, in general, this relationship does not apply to individual faults (Wesnousky and others, 1983; Singh and others, 1983; Youngs and Coppersmith, 1985). Youngs and others (1987) modeled the magnitude distribution of independent earthquakes on individual faults in the Wasatch Front region in two different ways: (1) using a standard exponential magnitude distribution, and (2) using the "characteristic" magnitude distribution proposed by Youngs and Coppersmith (1975). In both cases, only earthquakes of $M_L \geq 6.0$ were included in their analysis. The characteristic distribution is a modification of the exponential distribution that incorporates a decrease in b-value at magnitudes approaching the maximum magnitude for the fault. Thus, the characteristic magnitude distribution includes relatively more larger earthquakes. A third possible model to consider is the "maximum magnitude" model, which holds that each fault or fault segment produces only maximum-size earthquakes, together with their associated aftershocks and possible foreshocks (Wesnousky and others, 1983; Wesnousky, 1986). In tectonic regions where the repeat time for large earthquakes is relatively short, the available data favor either the characteristic or the maximum magnitude model. In the Wasatch Front region, major faults such as the Wasatch fault have not been important sources of small to moderate background earthquakes over the 25-year record of instrumental seismicity. This observation tends to favor the characteristic and maximum magnitude earthquake models, but the period of observation is too short relative to the repeat times for large earthquakes to allow any definite conclusions to be drawn.

GROUND SHAKING HAZARD

The final step in the seismic hazard analysis outlined in figure 1 is the estimation of ground motion for engineering applications. Predictions of ground motions from future earthquakes can be arrived at in many different ways and presented in a variety of different forms. One especially popular approach to the problem is the probabilistic methodology for estimation of peak ground motions first outlined by Cornell (1968). Algermissen and others (1982) use this basic methodology to derive maps of probabilistic ground motion estimates for the contiguous United States, including Utah. Youngs and others (1987) use a similar methodology to carry out a detailed probabilistic analysis of ground shaking hazard for the Wasatch Front region. In this section, we use Cornell's method to perform some simple probabilistic calculations of maximum ground acceleration for a representative site in the Salt Lake Valley, halfway between the Wasatch and West Valley faults. Our intent here is not to duplicate the extensive work of Youngs and others (1987), but rather to illustrate the relative contributions of various seismic sources to the ground shaking hazard. In particular, we investigate the relative importance to seismic hazard of small to moderate ($M \leq 6.5$) earthquakes, which dominate the historical earthquake record.

The site that we chose for our calculation is the intersection of interstate highways 15 and 80 in the city of South Salt Lake at approximately 40°43.1'N, 111°54.2'W (fig. 5). Our calculation incorporated two fundamental types of earthquake sources, as discussed above: (1) moderate ($M_L \leq 6.5$) earthquakes within a circular source area of radius 100 km centered on the site, and (2) the fault-specific sources listed in table 4, which have maximum magnitudes of 6.5-7.3. Although we have not included all of the possible earthquake sources in the Wasatch Front region in our calculations, we believe that we have included all of the major contributors to ground shaking hazard in the Salt Lake Valley. Earthquakes within the circular source area are assumed to be independent in size and location, have a spatially uniform probability of occurrence, and have an exponential magnitude distribution. We used the seismicity parameters estimated in the recurrence modeling section above to characterize this source area. For the fault-specific sources, only the contribution of the maximum earthquake to the hazard was included in the computation. For these maximum earthquakes, the contribution to the annual probability of exceedance of a given peak acceleration value is the product of two factors: (1) the annual probability of occurrence of the earthquake, and (2) the probability that the given peak acceleration level will be exceeded if an earthquake of the specified magnitude and distance occurs.

Peak horizontal acceleration as a function of magnitude and distance was calculated using the constrained relationship of Campbell (1987). Campbell actually presents a range of median acceleration estimates to reflect uncertainties in how stress regime, fault type, anelastic attenuation, and local site conditions could affect ground motion in Utah. We performed our calculations using both his upper-bound curves and his lower-bound curves, which differ in their predictions of peak horizontal accelerations by about a factor of two. In both cases, the natural log of the peak acceleration was assumed to be normally distributed about the predicted median value with a standard deviation of 0.3, the standard error given by Campbell.

Some assumption about the depths of the earthquakes was necessary since Campbell defines source-to-site distance as the shortest distance between the site and the zone of seismogenic rupture. We assumed that the zone of seismogenic rupture penetrates to within 4 km of the surface for all earthquakes included in the computation. However, this assumed depth is important only for earthquakes very near the site. The site is located about 4 km east of the surface trace of the West Valley fault and 4 km west of the surface trace of the Wasatch fault. Since the West Valley fault dips to the east and the Wasatch fault dips to the west, both faults probably extend directly beneath the site. Assuming fault dips of 45° to 70°, the distance to the seismogenic rupture for a surface-faulting event on either fault would be about 3-4 km, which is consistent with the assumption we made about seismogenic depth.

Figure 14 presents four graphs of the probability of exceedance per year versus peak horizontal ground acceleration at our representative Salt Lake Valley site. The four graphs illustrate the contributions to the ground-shaking hazard from (1) background earthquakes, (2) earthquakes on the Wasatch fault, (3) earthquakes on the other three faults listed in table 4, and (4) all of these sources together. The solid curves bordering the shaded regions on each graph were calculated using Campbell's lower- and upper-bound peak acceleration relationships. The shaded regions between these curves indicate the range of annual probabilities for any given peak horizontal acceleration. On the graph for the background seismicity, the two dashed curves were calculated with the preferred b-value of 0.71 whereas the upper and lower solid curves were calculated with the lower- and upper-limit b-values of 0.62 and 0.80, respectively.

Assuming that earthquake occurrence is a Poisson process, peak acceleration values having a 90% probability of nonexceedance in 50 years have an annual probability of 0.0021 or a return period of 475 years (upper horizontal lines, fig. 14). On the graph that includes all of the sources, the acceleration value corresponding to this return period lies between 0.17 and 0.40 g, as indicated on the plot. For comparison, the value obtained by Algermissen and others (1982) is 0.20-0.28 g and the value obtained by Youngs and others (1987) is 0.3 g. Peak acceleration values having a 90% probability of nonexceedance in 250 years have an annual probability of 0.00042 or a return period of 2,373 years (lower horizontal lines, fig. 14). The acceleration value corresponding to this return period is 0.49 to 1.05 g on figure 14. For comparison, the value obtained by Algermissen and others (1982) is 0.60-0.70 g and the value obtained by Youngs and others (1987) is 0.7 g. Thus, the results of Algermissen and others (1982) and Youngs and others (1987) fall within the range of probabilistic acceleration values that we calculate for both the 475-year and the 2,373-year return periods.

Figure 14 implies that the background source is the largest contributor to the ground shaking hazard for return periods shorter than 600 years and accelerations less than 0.1 to 0.2 g, depending on the ground motion model used. The Wasatch fault is the largest contributor to the hazard at longer return periods and higher accelerations. However, other faults, particularly the West Valley faults, are also quite important. We note that our calculation assumes that earthquakes on the West Valley fault are independent earthquakes, even though there is some

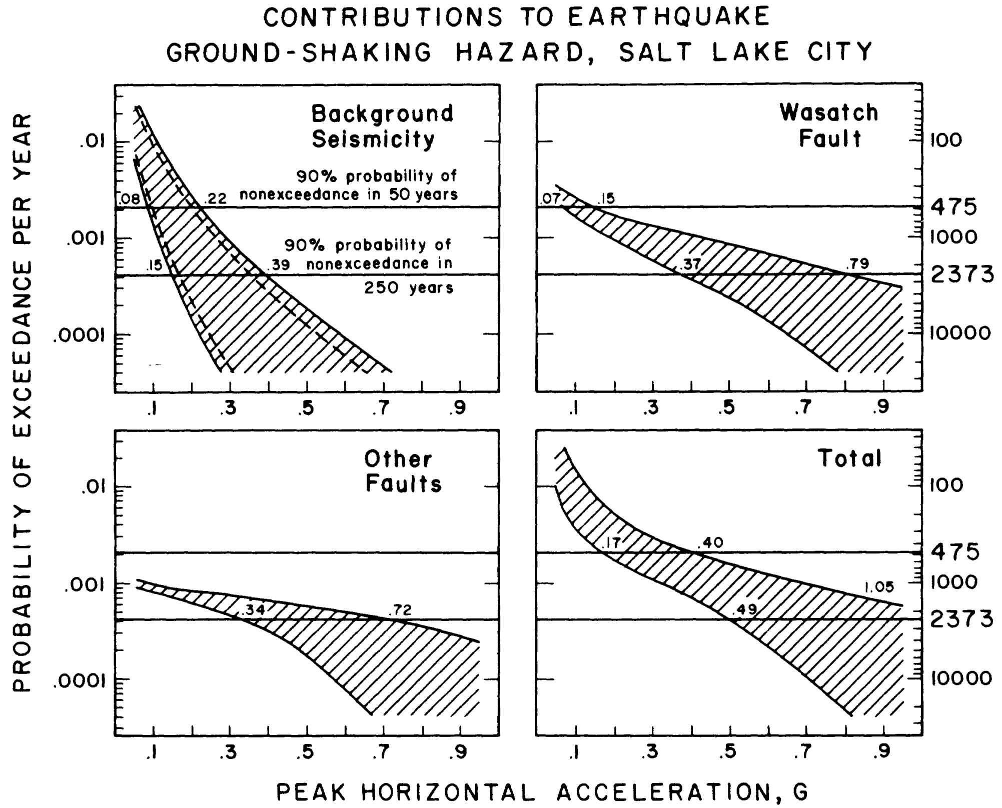

Figure 14. Graphs showing the probability of exceedance per year for peak horizontal ground accelerations on soil at the intersection of I-15 and I-80 in South Salt Lake at approximately 40°43.1'N, 111°54.2'W. The shaded zones represent the range of values calculated using the range of median attenuation curves for peak horizontal acceleration presented by Campbell (1987). The results of separate calculations for the background seismicity, the Wasatch fault, other faults (the West Valley, East Great Salt Lake, and North Oquirrh Mountains faults), and all of these sources together are shown. On the graph for the background seismicity, the dashed curves bound the range of values obtained using the preferred b-value of 0.71. The lower solid curve was calculated using the upper-bound b-value of 0.80 and Campbell's lower-bound acceleration estimates, whereas the upper solid curve was calculated using the lower-bound b-value of 0.62 and Campbell's upper-bound acceleration estimates. The vertical axes at the right show the average return period in years (the inverse of the annual probability).

possibility that they represent subsidiary fault movements associated with earthquakes on the Wasatch fault (S.J. Olig, personal communication, 1987). At locations farther away from the West Valley and Wasatch faults, the contribution of these faults to the ground shaking hazard will be less than is indicated by figure 14. The hazard curves for the background source, however, are applicable throughout most of the interior of the Wasatch Front region.

CURRENT SEISMICITY AND THE WASATCH FAULT

In this final section we wish to consider the question, separate from the systematics of a hazard or risk analysis, What does observational seismology tell us about the behavior of the Wasatch fault? We then summarize our perspective on evaluating earthquake hazards and risk in the Wasatch Front area from the viewpoint of observational seismology.

Let us first consider instrumental earthquake locations. Figure 15 shows a detailed plot of instrumental seismicity that might, on the basis of epicentral locations alone, be associated with the Wasatch fault zone. The data include 1,538 earthquake locations from the UUSS catalog for the period July 1962 through December 31 1986. The largest earthquake included is the magnitude 5.2 Magna earthquake of September 1962, located in the northwest corner of box B-B'. Earthquakes were sampled from 30-km-wide zones extending 10 km east of the surface trace of the Wasatch fault, to allow for epicentral errors, and 20 km west of the fault, to allow both for epicentral errors and reasonable down-dip projection of the fault. Figure 16 shows complementary cross-section views for those foci included in figure 15 that meet the rigorous criteria for focal-depth reliability specified for figure 10. Epicentral precision of ± 5 km would be conservative for the data of figure 15, but errors as large as ± 10 km cannot be ruled out for a very minor fraction of the sample. Insofar as the vast majority of the data post-date 1974, most of the epicenters probably have a precision of ± 2-3 km (Brown and others, 1986; Arabasz and Julander, 1986).

The cross sections of figure 16 suggest that well-located foci sampled from the vicinity of the Wasatch fault do not occur on the fault—if one believes that the fault is a planar penetrative structure of moderate dip. The best available data for addressing the question of whether small earthquakes are occurring on a listric subsurface projection of the Wasatch fault are those from portable-array studies reported by Arabasz and Julander (1986). At the southern end of the Wasatch fault, both in the northern and southern parts of box D-D', they show that earthquake foci and corresponding focal mechanisms are incompatible with seismic slip on either a listric or simple planar projection of the Wasatch fault. Rather, the background seismicity appears to be occurring on secondary structures of moderate (>30°) to high-angle dip. For the Wasatch fault near Nephi, Zoback (1987) interprets a planar, relatively steeply-dipping (50°-55°W) subsurface geometry. Elsewhere along the Wasatch fault, existing data for earthquakes down-dip of the fault are either inadequate or ambiguous (e.g., Pechmann and Thorbjarnardottir, 1984) for interpreting subsurface association with a listric projection of the fault.

Comparison of figure 15 with figures 8 and 9 indicates a remarkable paucity of microseismicity along the Wasatch fault within the broadly active earthquake belt of the Wasatch Front. Some specific features of small-earthquake occurrence in the vicinity of the fault are targets of ongoing investigation, such as epicentral clustering along the fault trace at the northern end of the Brigham City segment, and clustering to the west of the Collinston and Salt Lake City segments. The episodic nature of the earthquake activity, however, handicaps

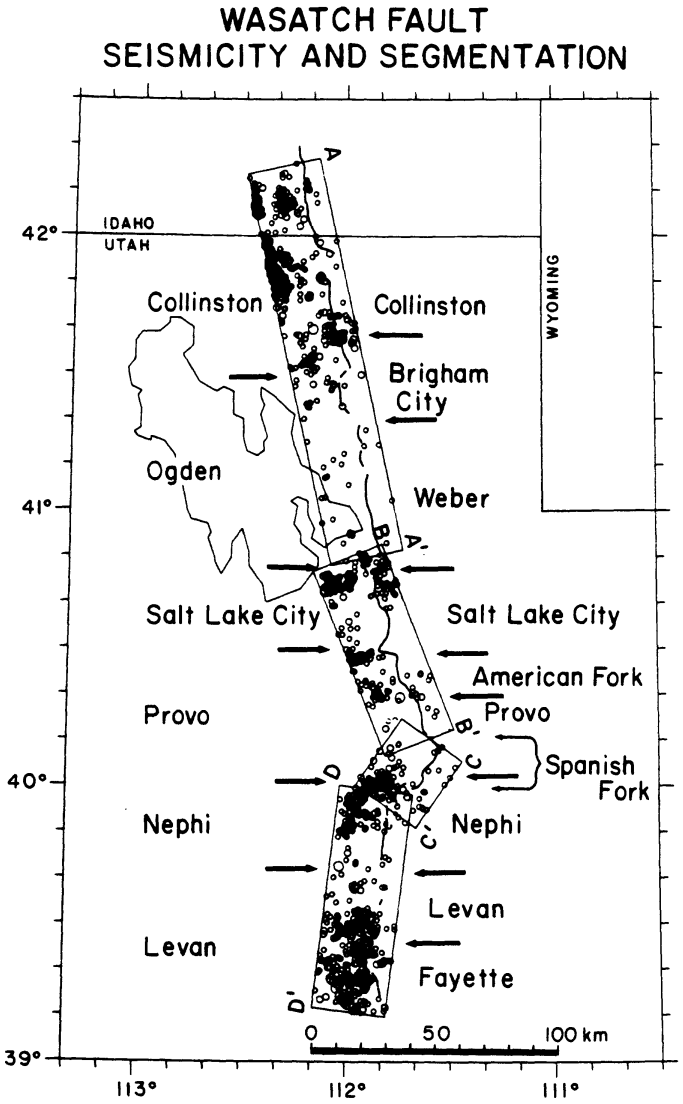

Figure 15. Strip map showing the Wasatch fault, segment boundaries (according to Machette and others, 1987, right-hand side; and Schwartz and Coppersmith, 1984, left-hand side), and all earthquakes located by the University of Utah Seismograph Stations during the period July 1962 through December 1986.

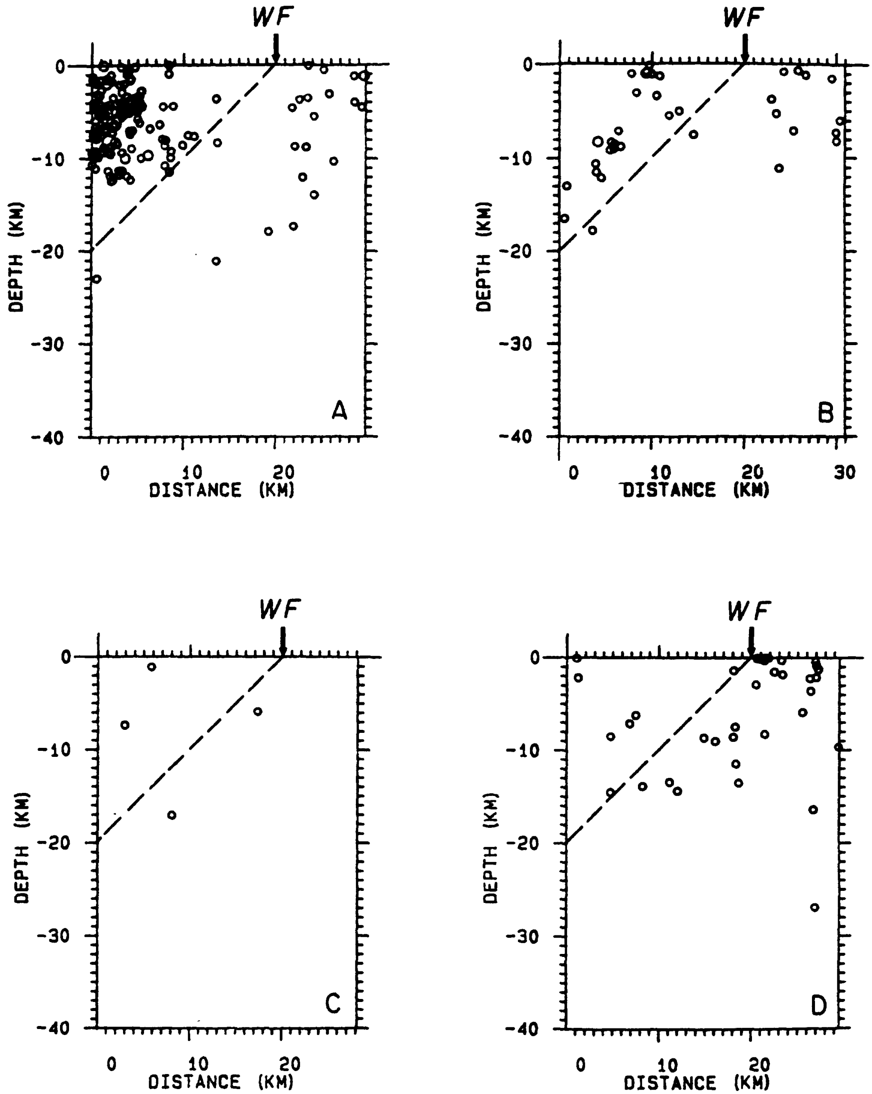

Figure 16. Composite figure of cross section keyed to the boxes in figure 15. WF marks the surface trace of the Wasatch fault, arbitrarily depicted by a plane dipping 45° to the west. Only foci meeting criteria for reliable focal depths are included.

the studies.

Figure 17 shows the space-time distribution of the earthquake sample included in figure 15. Such data might appear attractive for relating seismicity to segmentation and the sectional behavior of the Wasatch fault, but caution is clearly appropriate given the problematic relationship between the seismicity and the fault.

The following general observations can be made from figure 17: Seismicity north of Brigham City provides a clear contrast with that between Brigham City and Bountiful. Ironically, the northernmost segments of the Wasatch fault show no evidence of latest Quaternary movement (Machette and others, 1987). There is a clear onset of the northern seismicity at about 1975, which corresponds both to the timing of the 1975 M6.0 Pocatello Valley earthquake and the approximate beginning of operation of the UUSS telemetered seismic network. The case for seismic quiescence before the 1975 earthquake is made by Arabasz and Smith (1981). Activation of regional seismicity west of the Wasatch fault after the Pocatello Valley earthquake (discussed earlier) would be consistent with the interpretation that most of the northern seismicity in figure 17 is not on the Wasatch fault itself—although the episodic clustering of earthquakes near Honeyville at the boundary between the Brigham City and Collinston segments is indeed suggestive of at least partial association.

Seismicity near the northern end of the Salt Lake City segment (northern end of box B-B'), both west and east of the Wasatch fault, has long been recognized—as has quiescence to the south.

Other apparent features of the space-time diagrams of figure 17 are the post-1974 appearance of scattered earthquakes along the latitudes of the American Fork and Provo segments of the Wasatch fault, and temporally persistent seismicity near Santaquin and along the southernmost Wasatch fault. There is minimal microseismicity along a 30-km-long section of the Wasatch fault north of Levan. This includes at least the southern half of the Nephi segment, which has the youngest (<300-500 years) surface rupture known on the Wasatch fault (Schwartz and Coppersmith, 1984). However, depending on the structural association of earthquakes west of the Wasatch fault along much of its course, the Wasatch fault itself could conceivably be aseismic throughout most of the space-time diagram of figure 17 (see Arabasz and others, 1980).

As argued by Arabasz and Smith (1981), apparent seismicity gaps along the Wasatch fault are not necessarily indicative of a late (i.e., pre-earthquake) stage of a seismic cycle. Temporal decreases in seismicity ambiguously characterize both the early post-aftershock stage and the late premainshock stage of a seismic cycle (e.g., Ellsworth and others, 1981). Veneziano and others (1987) have recently analyzed the UUSS earthquake catalog between 1962 and 1985 for the identification of independent main events and for the hierarchical clustering of secondary events. One result of the statistical analysis was documentation that between roughly 39.5°N and 41.5°N—along an area encompassing most of the Wasatch fault—dependent events are systematically suppressed, compared with earthquake behavior in neighboring areas. The significance of this suppressed earthquake clustering is the subject of current study.

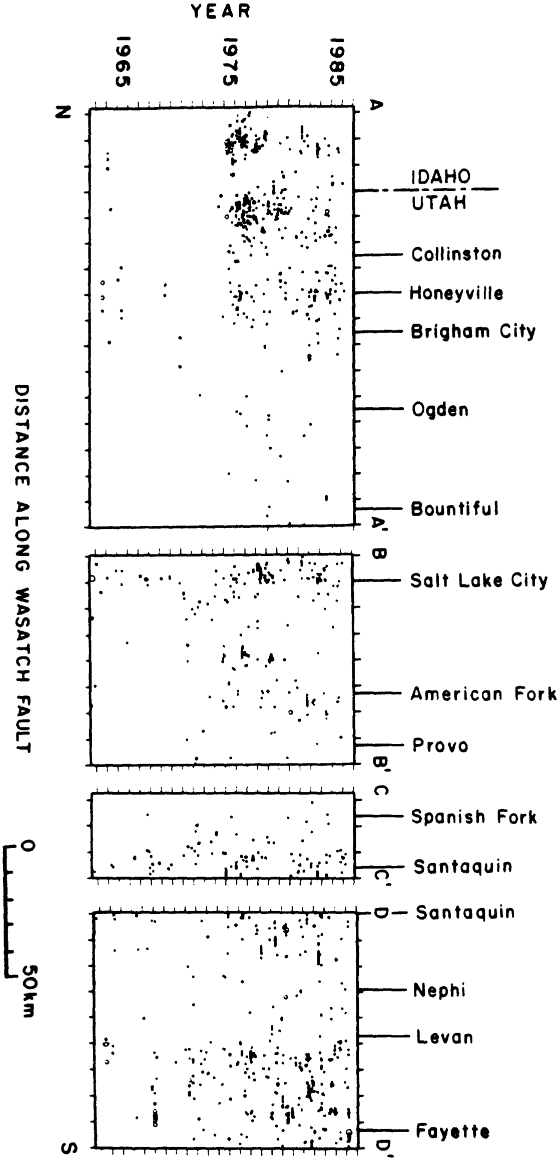

Figure 17. Composite figure of space-time diagrams keyed to figure 15.

The Wasatch Front area is a classic example of a seismically active region in which the historical and instrumental earthquake record provides an inadequate guide to assessing earthquake potential. The absence of any surface-faulting earthquakes on the Wasatch fault in historical time, the problematic correlation of background seismicity with mapped Cenozoic faulting, and the notable paucity of contemporary earthquakes with the Wasatch fault all combine to enhance the importance of paleoseismological information. The potential for large surface-faulting earthquakes effectively must be considered independently of observed seismicity. The occurrence of the 1983 M_S 7.3 Borah Peak, Idaho, surface-faulting earthquake in an area of low historical seismicity (Richins and others, 1987; Dewey, 1987)—but in an area of clearly recognizable late Quaternary faulting—is a case in point.

Our closing perspective is that observational seismology contributes essential information— much of it still to be refined—for accurate estimations of earthquake hazards and risk in the Wasatch Front area. Background seismicity currently predominates on second-order faults in the Wasatch Front area, and is the largest contributor to the probabilistic ground-shaking hazard for exposure periods of 50 years or less. From a seismotectonic point of view, background seismicity poses a major challenge in terms of understanding its association with geological structure and its information content about deformation on individual segments of the Wasatch fault. Beyond providing essential input to analyses of hazards and risk for engineering applications and decision-making, observational seismology remains a critical tool for probing the deformation state of segments of the Wasatch fault and for monitoring changes in their behavior.

REFERENCES

Abe, K., 1981, Magnitudes of large shallow earthquakes from 1904 to 1980: Phys. Earth Planet. Interiors, v. 27, p. 72-92.

Aki, K., 1966, Generation and propagation of G waves from the Niigata earthquake of June 16, 1964: Bulletin of the Earthquake Research Institute, Tokyo University, v. 44, p. 23-88

Algermissen, S. T., Perkins, D. M., Thenhaus, P. C., Hanson, S. L., and Bender, B. L., 1982, Probabilistic estimates of maximum acceleration and velocity in rock in the contiguous United States: U.S. Geological Survey Open-File Report 82-1033, 107 pp.

Allen, C. R., 1974, Geological criteria for evaluating seismicity: Geological Society of America Bulletin, v. 86, p. 1041-1057.

Allen, C. R., 1986, Seismological and paleoseismological techniques of research in active tectonics, *in* Active Tectonics, National Academy Press, Washington, D.C., p. 148-154.

Allmendinger, R. W., Sharp, J. W., Von Tish, D., Serpa, L., Brown, L., Kaufman, S., Oliver, J., and Smith, R. B., 1983, Cenozoic and Mesozoic structure of the eastern Basin and Range province, Utah, from COCORP seismic reflection data: Geology, v. 11, p. 532-536.

Allmendinger, R. W., Hauge, T. A., Hauser, E. C., Potter, C. J., Knuepfer, P., Nelson, K. D. and Oliver, J. E., 1987, Overview of the COCORP 40° N Transect western U.S.A.—The fabric of an orogenic belt: Geological Society of America Bulletin, v. 98, p. 308-319.

Anderson, R. E., and Miller, D. G., 1979, Quaternary fault map of Utah, Technical Report, Fugro, Inc., 35 pp.

Anderson, R. E., and Barnhard, T. P., 1984, Extensional and compressional paleostresses and their relationship to paleoseismicity and seismicity, central Sevier Valley, Utah: U.S. Geological Survey Open-File Report 84-763, p. 515-546.

Arabasz, W. J., Smith, R. B., and Richins, W. D., eds., 1979, Earthquake Studies in Utah, 1850 to 1978: Salt Lake City, Utah, University of Utah Seismograph Stations Special Publication, 552 pp.

Arabasz, W. J., Smith, R. B., and Richins, W. D., 1980, Earthquake studies along the Wasatch Front, Utah: Network monitoring, seismicity, and seismic hazards: Bulletin of the Seismological Society of America, v. 70, p. 1479-1499.

Arabasz, W. J., and Smith, R. B., 1981, Earthquake prediction in the Intermountain seismic belt—An intraplate extensional regime, *in* Earthquake Prediction—An International Review, Simpson, D. W., and Richards, P. G., eds., American Geophysical Union, Maurice Ewing Series, v. 4, 248-258.

Arabasz, W. J., Richins, W. D., and Langer, C. J., 1981, The Pocatello Valley (Idaho-Utah border) earthquake sequence of March to April 1975: Bulletin of the Seismological Society of America, v. 71, p. 803-826.

Arabasz, W. J., 1984, Earthquake behavior in the Wasatch Front area: Association with geologic structure, space-time occurrence, and stress state, *in* Proceedings of Conference XXVI, A Workshop on "Evaluation of Regional and Urban Earthquake Hazards and Risk in Utah," Hays, W. W., and Gori, P. L., eds., U.S. Geological Survey Open-File Report 84-763, p. 310-339.

Arabasz, W. J., and Julander, D. R., 1986, Geometry of seismically active faults and crustal deformation within the Basin and Range--Colorado Plateau transition in Utah, *in* Extensional Tectonics of the Southwestern United States: A Perspective on Processes and Kinematics, Mayer, L., ed., Geological Society of America Special Paper, v. 208, pp. 43-74.

Arabasz, W. J., Pechmann, J. C., and Brown, E. D., 1987, Evaluation of seismicity relevant to the proposed siting of a superconducting supercollider (SSC) in Tooele County, Utah: Unpublished Technical Report submitted to the Dames and Moore Utah SSC Proposal Team, 107 pp.

Askew, B., and Algermissen, S. T., 1983, An earthquake catalog for the Basin and Range province 1803-1977: U.S. Geological Survey Open-File Report 83-86.

Beanland, S., and Clark, M. M., 1987, The Owens Valley fault zone, eastern California, and surface rupture associated with the 1872 earthquake: Seismological Research Letters, v. 58, p. 32.

Benjamin, J.R., and C.A. Cornell (1970). *Probability, Statistics, and Decision for Civil Engineers,* McGraw-Hill Book Co., New York, 684 pp.

Benz, H. M., and Smith, R. B., 1987, Kinematic source modelling of normal-faulting earthquakes using the finite element method: Geophysical Journal of the Royal Astronomical Society, v. 90, p 305-325.

Bjarnason, I. T., and Pechmann, J. C., 1987, Contemporary tectonics of the Wasatch front region, Utah, from earthquake focal mechanisms: Bulletin of the Seismological Society of America, (submitted).

Bonilla, M. G., Mark, R. K., and Lienkaemper, J. J., 1984, Statistical relations among earthquake magnitudes, surface rupture length, and surface fault displacement: Bulletin of the Seismological Society of America, v. 74, p. 2379-2411.

Brown, E. D., Arabasz, W. J., Pechmann, J. C., McPherson, E., Hall, L. L., Oehmich, P. J., and Hathaway, G. M., 1986, Earthquake Data for the Utah Region—January 1, 1984 to December 31, 1985: Salt Lake City, Utah, University of Utah Seismograph Stations Special Publication, Utah, 83 pp.

Bucknam, R. C., 1976, Leveling data from the epicentral area of the March 27, 1975, earthquake in Pocatello Valley, Idaho: U.S. Geological Survey Open-File Report 76-52, 6 pp.

Bucknam, R. C., 1977, Map of suspected fault scarps in unconsolidated deposits, Tooele, 1° x 2° sheet, Utah: U.S. Geological Survey Open-File Report 77-495.

Bucknam, R. C., and Anderson, R. E., 1979, Map of fault scarps on unconsolidated sediments, Delta 1° x 2° sheet, Utah: U.S. Geological Survey Open-File Report 79-366, 21 pp.

Bucknam, R. C., Algermissen, S. T., and Anderson, R. E., 1980, Patterns of late Quaternary faulting in western Utah and an application in earthquake hazard evaluation, *in* Proceedings of Conference X, Earthquake Hazards along the Wasatch Sierra-Nevada Frontal Fault Zones, U.S. Geological Survey Open-File Report 80-801, p. 299-314.

Campbell, K. W., 1987, Predicting strong ground motion in Utah, *in* Assessment of Regional Earthquake Hazards and Risk Along the Wasatch Front, Utah, U.S. Geological Survey Professional Paper, in press.

Cluff, L.S., Brogan, G. E., and Glass, C. E., 1970, Wasatch fault, northern portion—earthquake fault investigation and evaluation: Report to Utah Geological and Mineral Survey, Woodward-Clyde and Associates, 27 pp.

Cluff, L. S., Brogan, G. E., and Glass, C. E., 1973, Wasatch fault, southern portion: Earthquake fault investigation and evaluation: Report to Utah Geological and Mineral Survey, Woodward-Lundgren and Associates, 79 pp.

Cluff, L. S., Brogan, G. E., and Glass, C. E., 1974, Investigation and evaluation of the Wasatch fault north of Brigham City and Cache Valley faults, Utah and Idaho—A guide to land-use planning with recommendations for seismic safety: Report to U.S. Geological Survey, Woodward-Lundgren and Associates, 147 pp.

Cook, K. L., Gray, E. F., Iverson, R. M., and Strohmeier, M. T., 1980, Bottom gravity meter regional survey of the Great Salt Lake, Utah, *in* Great Salt Lake, A Scientific, Historical, and Economic Overview, Gwynn, J. W., ed., Utah Geological and Mineral Survey Bulletin 116, p. 125-143.

Cornell, C. A., 1968, Engineering seismic risk analysis: Bulletin of the Seismological Society of America, v. 58, p.1583-1606.

Crone, A. J., and Machette, M. N., 1984, Surface faulting accompanying the Borah Peak earthquake, central Idaho: Geology, v. 12, p. 664-667.

Crone, A. J., Machette, M. N., Bonilla, M. G., Lienkaemper, J. J., Pierce, K. L., Scott, W. E., and Bucknam, R. C., 1987, Surface faulting accompanying the Borah Peak earthquake and segmentation of the Lost River fault, central Idaho: Bulletin of the Seismological Society of America, v. 77, p. 739-770.

Currey, D. R., Atwood, G., and Mabey, D. R., 1984, Major levels of Great Salt Lake and Lake Bonneville: Utah Geological and Mineral Survey Map 73, scale 1:750,000.

Davis, F. D., 1983a, Geologic map of the southern Wasatch Front, Utah: Utah Geol. and Min. Surv. Map 55-A, scale 1:100,000.

Davis, F. D., 1983b, Geologic map of the central Wasatch Front, Utah: Utah Geological and Mineral Survey Map 54-A, scale 1:100,000.

Davis, F. D., 1985, Geologic map of the northern Wasatch Front, Utah: Utah Geological and Mineral Survey Map 53-A, scale 1:100,000.

Dewey, J. W., 1987, Instrumental Seismicity of Central Idaho: Bulletin of the Seismological Society of America, v. 77, p. 819-836.

Doser, D. I., 1985a, The 1983 Borah Peak, Idaho and 1959 Hebgen Lake, Montana Earthquakes—Models for normal fault earthquakes in the Intermountain seismic belt, *in* Proceedings of Workshop XXVIII on the Borah Peak, Idaho, Earthquake, Stein, R. S., and Bucknam, R. C., eds., U.S. Geological Survey Open-File Report 85-290, p. 368-384.

Doser, D. I., 1985b, Source parameters and faulting processes of the 1959 Hebgen Lake, Montana, earthquake sequence: Journal of Geophysical Research 90, p. 4537-4555.

Doser, D. I., and Smith, R. B., 1982, Seismic moment rates in the Utah region: Bulletin of the Seismological Society of America, v. 72, p. 525-551.

Doser, D. I., and Smith, R. B., 1985, Source parameters of the 28 October 1983 Borah Peak, Idaho earthquake from body wave analysis: Bulletin of the Seismological Society of America, v. 75, p. 1041-1051.

Eddington, P. K., Smith, R. B., and Renggli, C., 1987, Kinematics of Basin-Range intraplate extension, *in* Continental Extensional Tectonics, Coward, M. P., Dewey, J. F., and Hancock, P. L., eds., Geological Society of London Special Publication, p. 371-392.

Ekstrom, G., and Dziewonski, A. M., 1985, Centroid-moment tensor solutions for 35 earthquakes in western North America (1977-1983): Bulletin of the Seismological Society of America, v. 75, p. 23-39.

Ellsworth, W. L., Lingh, A. G., Prescott, W. H., and Herd, D. G., 1981, The 1906 San Francisco earthquake and the seismic cycle: *in* Earthquake Prediction: An International Review, Simpson, D. W., and Richards, P. G., eds., Maurice Ewing Series 4, American Geophysical Union, Washington, D.C., p. 209-216.

Engdahl, E. R., and Rinehard, W. A., 1986, Seismicity map of the North America project [abs.]: Eos (American Geophysical Union Transactions), v. 67, p. 1235.

Evernden, J. F., 1975, Seismic intensities, "size" of earthquakes, and related matters: Bulletin of the Seismological Society of America, v. 65, p. 1287-1313.

Foley, L. L., Martin, R. A., and Sullivan, J. T., 1986, Seismotectonic study for Joes Valley, Scofield and Huntington, North Davis, Emery County and Scofield Project, Utah: U.S. Bureau of Reclamation Report 83-288.

Gibbons, A. B., and Dickey, D. D., 1983, Quaternary faults in Lincoln and Uinta Counties, Wyoming, and Rich County, Utah: U.S. Geological Survey Open-File Report 83-238.

Gutenberg, B., and Richter, C. F., 1954, Seismicity of the Earth and Associated Phenomena, Princeton University Press, Princeton, New Jersey, 2nd edn., 310 pp.

Hall, W. B., and Sablock, P. E., 1985, Comparison of the geomorphic and surficial fracturing effects of the 1983 Borah Peak, Idaho earthquake with those of the 1959 Hebgen Lake, Montana earthquake, *in* Proceedings of Workshop XXVIII on the Borah Peak, Idaho, Earthquake, Stein, R. S., and Bucknam, R. C., eds., U.S. Geological Survey Open-File Report 85-290, p. 141-152.

Hanks, T. C., and Kanamori, H., 1979, A moment magnitude scale: Journal of Geophysical Research, v. 84, p. 2348-2350.

Kanamori, H, 1977, The energy release in great earthquakes: Journal of Geophysical Research, v. 82, p. 2981-2987.

Loeb, D. T., 1986, The P-wave velocity structure of the crust-mantle boundary beneath Utah: Salt Lake City, Utah, University of Utah, M.S. thesis, 126 pp.

Machette, M. N, Personius, S. F., and Nelson, A. R., 1986, Late Quaternary segmentation and slip-rate history of the Wasatch fault zone, Utah [abs.]: Eos (American Geophysical Union Transactions), v. 67, p. 1107.

Mikulich, M., and Smith, R. B., 1974, Seismic reflection and aeromagnetic surveys of the Great Salt Lake, Utah: Geological Society of America Bulletin, v. 85, p. 991-1002.

Murphy, L. M., and Brazee, R. J., 1964, Seismological investigations of the Hebgen Lake earthquake: U.S. Geological Survey Professional Paper 435-C, p. 13-17.

Oakeshott, G. B., Greensfelder, R. W., and Kahle, J. E., 1972, The Owens Valley earthquake of 1872—One hundred years later: California Geology, v. 25, p. 55-62.

Pechmann, J.C., and Thorbjarnardottir, B., (1984), Investigations of an M_L 4.3 earthquake in the western Salt Lake Valley using digital seismic data, *in* Proceedings of Conference XXVI, A Workshop on "Evaluation of Regional and Urban Earthquake Hazards and Risk in Utah," W.W. Hays and P.L. Gori, Editors, U.S. Geol. Surv. Open-File Rept. 84-763, p. 340-365.

Pechmann, J. C., Richins, W. D. and Smith, R. B., 1984, Evidence for a double Moho beneath the Wasatch front, Utah: Eos (American Geophysical Union Transactions), v. 54, p. 988.

Pechmann, J. C., 1987, Earthquake design considerations for the inter-island diking project, Great Salt Lake, Utah: Unpublished Technical Report submitted to Rollins, Brown, and Gunnell, Provo, Utah, 40 pp.

Pechmann, J. C., Nash, W. P., Viveiros, J. J., and Smith, R. B., 1987, Slip rate and earthquake potential of the East Great Salt Lake fault, Utah [abs.]: Eos (American Geophysical Union Transactions), in press.

Peinado, J. F., 1986, Moment-magnitude relations in the Intermountain Seismic Belt from regional seismic data—applications of an indirect network calibration scheme: Salt Lake City, Utah, University of Utah, M.S. thesis, 96 pp.

Pitt, A. M., Weaver, C. S., and Spence, W., 1979, The Yellowstone Park earthquake of June 30, 1975: Bulletin of the Seismological Society of America, v. 69, n. 1, p. 187-205.

Richins, W. D., Arabasz, W. J., Hathaway, G. M., Oehmich, P. J., Sells, L. L., and Zandt, G., 1981, Earthquake Data for the Utah Region—January 1, 1978 to December 31, 1980: Salt Lake City, Utah, University of Utah Seismograph Stations Special Publication, 125 pp.

Richins, W. D., Arabasz, W. J., Hathaway, G. M., McPherson, E., Oehmich, P. J., and Sells, L. L., 1984, Earthquake Data for the Utah Region—January 1, 1981 to December 3, 1983: Salt Lake City, Utah, University of Utah Seismograph Stations Special Publication, 111 pp.

Richins, W.D., J.C. Pechmann, R.B. Smith, C.J. Langer, S.K. Goter, J.E. Zollweg, and J.J. King (1987). The 1983 Borah Peak, Idaho, earthquake and its aftershocks: Bulletin of the Seismological Society of America, v. 77, p. 694-723.

Richter, C. F., 1958, Elementary Seismology: W.H. Freeman and Co., San Francisco, Calif., 768 pp.

Schwartz, D. P., Swan, F. H., III, and Cluff, L. S., 1984, Fault behavior and earthquake recurrence along the Wasatch fault, *in* Hays, W. W., and Gori, P. L., eds., Proceedings of Conference XXVI, A Workshop on "Evaluation of Regional and Urban Earthquake Hazards and Risk in Utah," U.S. Geological Survey Open-File Rept. 84-763, p. 113-125.

Schwartz, D. P., and Coppersmith, K. J., 1984, Fault behavior and characteristic earthquakes—examples from the Wasatch and San Andreas fault zones: Journal of Geophysical Research, v. 89, p. 5681-5698.

Schwartz, D. P., and Coppersmith, K. J., 1986, Seismic hazards—New trends in analysis using geologic data, *in* Active Tectonics: National Academy Press, Washington, D.C., p. 215-230.

Schwartz, D. P., 1987, Earthquakes of the Holocene: Reviews of Geophysics, in press.

Shenon, P. J., 1936, The Utah earthquake of March 12, 1934 (extracts from unpublished report): *in* F. Neumann, *United States Earthquakes, 1943,* U.S. Coast and Geodetic Survey, serial 593, p. 43-48.

Shimizu, Y., 1987, Earthquake clustering in the Utah region: Cambridge, Massachusetts, Massachusetts Institute of Technology, M.S. thesis, 149 pp.

Singh, S. K., Rodriguez, M., and Esteva, L., 1983, Statistics of small earthquakes and frequency of occurrence of large earthquakes along the Mexican subduction zone: Bulletin of the Seismological Society of America, v. 73, p. 1779-1796.

Slemmons, D. B., 1980, Design earthquake magnitudes for the western Great Basin, *in* Proceedings of Conference X, Earthquake Hazards Along the Wasatch Sierra-Nevada Frontal Fault Zones: U.S. Geological Survey Open-File Report 80-801, p. 62-85.

Smith, R. B., 1978, Seismicity, crustal structure, and intraplate tectonics of the interior of the western Cordillera, *in* Cenozoic Tectonics and Regional Geophysics of the Western Cordillera, Smith, R. B., and Eaton, G. P., eds., Geological Society of America Memoir 152, p. 111-144.

Smith, R. B., and Lindh, A, 1978, A compilation of fault plane solutions of the western United States, *in* Cenozoic Tectonics and Regional Geophysics of the Western Cordillera, Smith, R. B., and Eaton, G. P., eds., Geologial Society of America Memoir 152, p. 107-110.

Smith, R. B., and Bruhn, R. L., 1984, Intraplate extensional tectonics of the eastern Basin-Range—Inferences on structural style from seismic reflection data, regional tectonics, and thermal-mechanical models of brittle-ductile deformation: Journal of Geophysical Research, v. 89, p. 5733-5762.

Smith, R. B., and Richins, W. D., 1984, Seismicity and earthquake hazards of Utah and the Wasatch Front—Paradigm and paradox, *in* Proceedings of Conference XXVI, A Workshop on "Evaluation of Regional and Urban Earthquake Hazards and Risk in Utah," Hays, W. W., and Gori, P. L., eds., U.S. Geological Survey Open-File Report 84-763, p. 73-112.

Smith, R. B., and Sbar, M. L., 1974, Contemporary tectonics and seismicity of the western United States with emphasis on the Intermountain seismic belt: Geological Society of America Bulletin, v. 85, p. 1205-1218.

Smith, R. B., Nagy, W. C., Julander, K. A., Viveiros, J. J., Barker, C. A., Bashore, W. W., and Gants, D. G., 1987, Geophysical and tectonic framework of the Basin Range Colorado Plateau-Rocky Mountain transition: Geophysical Framework of the Continental U.S.—Intermountain System, (in press).

Stickney, M. C., and Bartholomew, M. S., 1987, Seismicity and late Quaternary faulting of the northern Basin and Range province, Montana and Idaho: Bulletin of the Seismological Society of America, v. 77, in press.

Sullivan, J. T., Nelson, A. R., LaForge, R. C., Wood, C. K., and Hansen, R. A., 1986, Regional seismotectonic study for the back Valleys of the Wasatch mountains in northeastern Utah: Denver, Colorado, U.S. Bureau of Reclamation Technical Report, Seismotectonic Division.

Stover, C. W., Reagor, B. G., and Algermissen, S. T., 1986, Seismicity map of the state of Utah: U.S. Geological Survey Miscellaneous Field Studies Map MF-1856, scale 1:1,000,000.

Swan, F. H., III, Schwartz, D. P., and Cluff, L. S., 1980, Recurrence of moderate to large magnitude earthquakes produced by surface faulting on the Wasatch fault zone, Utah: Bulletin Seismological Society America, v. 70, p. 1431-1462.

Utsu, T., 1965, A method for determining the value of b in the formula log n = a – bM showing the magnitude-frequency relation for earthquakes: Hokkaido University, Japan, Geophysical Bulletin, v. 13, p. 99-103.

Veneziano, D., and Van Dyck, J., 1986, Statistical analysis of earthquake catalogs for seismic hazard, *in* Proceedings, International Symposium on Engineering Geology Problems in Seismic Areas, Bari, Italy.

Veneziano, D., Shimizu, Y., and Arabasz, W. J., 1987, Suppressed Earthquake Clustering in the Wasatch Front Region, Utah [abs.]: Eos (American Geophysical Union Transactions), v. 68, in press.

Viveiros, J. J., 1986, Cenzoic tectonics of the Great Salt Lake from seismic reflection data: Salt Lake City, Utah, University of Utah, M.S. thesis, 81 pp.

Wallace, R. E., 1981, Active faults, paleoseismology, and earthquake hazards in the western United States, *in* Earthquake Prediction: An International Review, Simpson, D. W., and Richards, P. G., eds., Maurice Ewing Series 4, American Geophysical Union, Washington, D.C., p. 209-216.

Wallace, R. E., 1987, Grouping and migration of surface faulting and variations in slip rates on faults in the Great Basin Province: Bulletin of the Seismological Society of America, v. 77, p. 868-876.

Weichert, D. H., 1980, Estimation of the earthquake recurrence parameters for unequal observation periods for different magnitudes: Bulletin Seismological Society America, v. 70, p. 1337-1346.

Wesnousky, S. G., Scholz, C. H., Shimazaki, K., and Matsuda, T., 1983, Earthquake frequency distribution and the mechanics of faulting: Journal of Geophysical Research, v. 88, p. 9331-9340.

Wesnousky, S. G., 1986, Earthquakes, Quaternary faults, and seismic hazard in California: Journal of Geophysical Research, v. 91, p. 12587-12631.

Williams, D. J., and Arabasz, W. J., 1987, Mining-related and tectonic seismicity in the east mountain area, Wasatch Plateau, Utah: Submitted to PAGEOPH Special Issue on Seismicity in Mines.

Witkind, I. J., 1964, Reactivated faults north of Hebgen Lake: U.S. Geological Survey Professional Paper 435-G, p. 37-50.

Witkind, I. J., 1975, Preliminary map showing known and suspected active faults in Idaho: U.S. Geological Survey Open File Report 75-278, 71 pp.

Youngs, R. R., and Coppersmith, K. J., 1985, Implications of fault slip rates and earthquake recurrence models to probabilistic seismic hazards estimates: Bulletin of the Seismological Society of America, v. 75, p. 939-964.

Youngs, R. R., Swan, F. H., III, Power, M. S., Schwartz, D. P., and Green, R. K., 1987, Probabilistic analysis of earthquake ground-shaking hazard along the Wasatch front, Utah: submitted to Assessment of Regional Earthquake Hazards and Risk Along the Wasatch Front, Utah, U.S. Geological Survey Professional Paper.

Zoback, M. L., 1983, Structure and Cenozoic tectonism along the Wasatch fault zone, Utah: Geological Society of America Memoir 157, p. 3-27.

Zoback, M. L., 1984, Constraints on the in-situ stress field along the Wasatch Front, *in* Proceedings of Conference XXVI A Workshop on "Evaluation of Regional and Urban Earthquake Hazards and Risk in Utah," Hays, W. W., and Gori, P. L., eds., U.S. Geological Survey Open-File Report 84-763, p. 286-310.

Zoback, M. L., 1987, Superimposed late Cenozoic, Mesozoic, and possible Proterozoic deformation along the Wasatch Fault zone in central Utah: (this volume).

Superimposed Late Cenozoic, Mesozoic, and Possible Proterozoic Deformation along the Wasatch Fault Zone in Central Utah

by

Mary Lou Zoback
U.S. Geological Survey
Menlo Park, CA 94025

ABSTRACT

Surface geology, gravity data, and information from petroleum exploration wells have been used to constrain the subsurface structure along a 30 km long seismic reflection profile across the Wasatch fault zone in central Utah near the town of Nephi. In this region, late Cenozoic normal faulting along the Wasatch fault zone is superimposed on the frontal portion of the Mesozoic Sevier fold and thrust belt. Juab Valley, which is bounded on the east by the Wasatch fault zone, is interpreted as an asymmetric sag, with beds on both sides tilting towards the axis of the valley and with a central graben defining the deepest part of the basin. Maximum valley thickness is about 1.60 km, based on a combined interpretation of the gravity and seismic reflection data. Possible displacement of a buried thrust(s), truncation of deep reflectors, and the absence of reverse drag in the basin sediments suggest a planar, relatively steeply-dipping (50-55°) geometry for the Wasatch fault zone at this locality. However, because of complex subsurface structure, the lack of reverse drag in the basin sediments is probably the strongest evidence against a listric geometry for the Wasatch. Within the study area both a major Sevier frontal thrust (the Nebo thrust) and possible deeper thrust(s) appear to ramp up in the vicinity of the Wasatch fault zone. A similar correlation of major thrust ramps occuring along several other segments of the Wasatch fault zone was noted by Smith and Bruhn (1984). It is speculatively suggested here that both the thrust ramping and late Cenozoic normal faulting may be localized by a major west-dipping normal fault zone formed during the early phases (pre-drift) of late Precambrian rifting of the western Cordillera.

INTRODUCTION

In central Utah late Cenozoic extensional faulting along the Wasatch and other normal fault zones is superimposed on the frontal portion of the Mesozoic Sevier fold and thrust belt (fig. 1) which deforms sediments deposited on a passive margin formed by late Precambrian rifting Stewart, 1972; (Stewart and Poole, 1974). Many of the rocks exposed in the modern range blocks are remanents of laterally extensive thrust sheets transported 100 km or more from the west during the Sevier orogeny (Crittenden, 1961).

In this paper gravity and well data, together with a 30-km-long seismic reflection profile across the Wasatch fault zone near its intersection with one of the frontal sole thrust faults, are used to detail the structural style of late Cenozoic extension superimposed on Mesozoic compressional deformation.

Particular emphasis is placed on understanding the subsurface geometry of Cenozoic normal faulting and its relationship, to earlier low-angle thrust faults, ramps, decollement surfaces, as well as possible normal faults in the crystalline basement formed during Precambrian rifting.

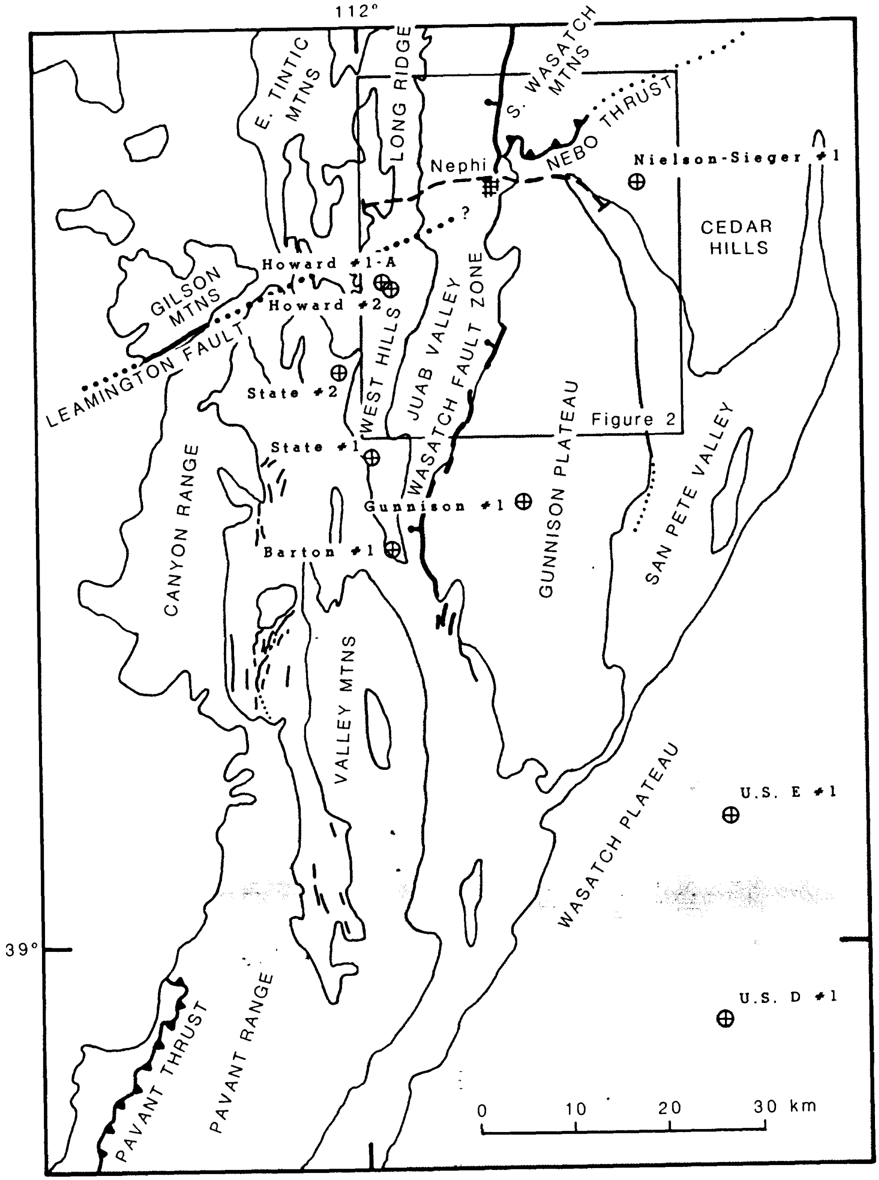

Figure 1. Index map of central Utah showing late Cenozoic normal faults (heavy lines with bar and ball on downthrown side) and Sevier frontal thrust faults (with barbs). Ranges are shaded. Locations of seismic reflection profiles near Nephi and to the south (Smith and Bruhn, 1984) are indicated by heavy dashed lines. Location of petroleum exploration wells also indicated. Box shows location of Figure 2.

LOCAL GEOLOGIC SETTING

The area of study is centered on the town of Nephi in central Utah, a region of complex, superimposed compressional and extensional deformation of several ages. The Wasatch fault zone separates the southern Wasatch Mountains and Gunnison Plateau on the east from Juab Valley on the west (fig. 2). Approximately 5 km wide, Juab Valley is bordered on the west by Long Ridge and West Hills.

A late Precambrian (< 850 m.y.) rifting event (Stewart, 1972) formed a north-trending, west-facing passive margin through western Utah and eastern Nevada (Stewart and Poole, 1974). The study area lies along the inferred hingeline (boundary between shelf and miogeocline) of this margin. In central Utah deposition on the passive margin continued until the inception of Sevier compressional deformation which started in latest Jurassic or possibly mid-Cretaceous and continued to at least Paleocene time (Standlee, 1982; Lawton, 1982; Heller and others, 1986). During this time interval, wide-spread low-angle eastward-directed thrusting occurred in central Utah with concurrent deposition of synorogenic clastic sediments. The Sevier frontal thrust system is considered the basal and most far-travelled thrust sheet and typically places Paleozoic rocks on Mesozoic rocks. Thrust relations interpreted as part of the frontal thrust zone have been mapped in the Mount Nebo area of the southern Wasatch Mountains, 3.5 km north of the seismic line (fig. 2). The Nebo thrust has been correlated with the

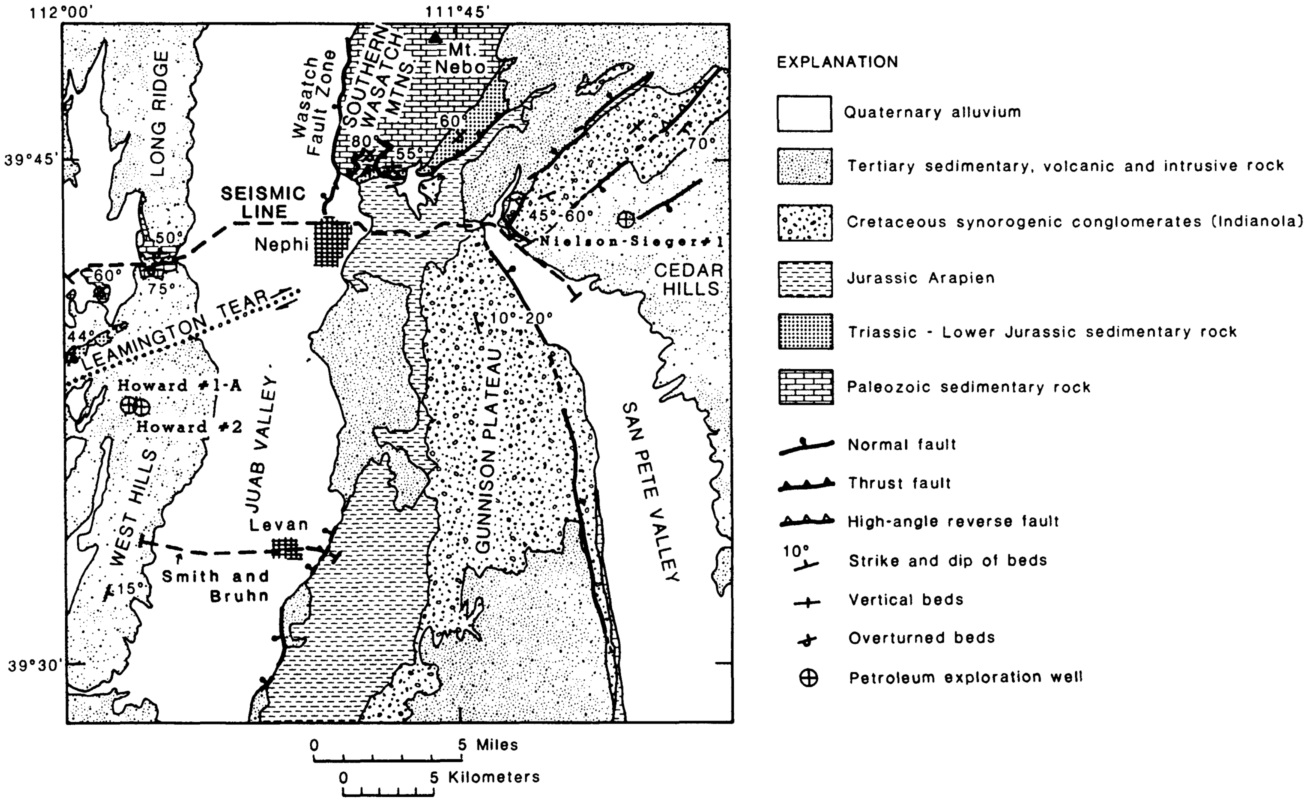

Figure 2. Generalized geologic map of the study area, see Figure 1 for location. Seismic reflection line indicated by heavy dashed line. Leamington tear fault is described in the text.

Charleston thrust to the north (Crittenden, 1961) and occupies a similar structural level as the Pavant thrust to the south (Burchfiel and Hickcox, 1972); however, Morris (1983) has inferred a major discontinuity in thrust sheet geometry between the Nebo and Pavant thrusts. Morris interprets a major tear fault, the Leamington fault, as separating these two frontal thrust systems.

The southern edge of the Nebo thrust which is exposed in the Mt. Nebo area contains steeply dipping Paleozoic through early Mesozoic rocks deformed into an overturned anticline (Black, 1965). The Nebo allocthon is thrust over the Jurassic Arapien Shale, a sequence of highly disturbed calcareous mudstone and siltstone units that locally contain significant quantities of salt and anhydrite. A lively controversy exists over the stratigraphic definition and nomenclature of Jurassic marine rocks in central Utah (Spieker, 1946; Hardy, 1952; Witkind, 1982, 1983; Sprinkel, 1982; Lawton, 1985). These disputes over nomenclature are of little importance here, hence an informal usage describing all the Jurassic shale, silt, limestone rocks above the Jurrassic-Triassic Navajo Sandstone as Arapien rocks or simply Arapien has been adopted. This usage includes all of the Arapien Shale as originally named and described by Spieker (1946) including his upper Twist Gulch Member and the underlying Twelve-Mile Canyon Member. Sprinkel (1982) subdivided the Jurassic rocks into two units on the basis of well log data: the Arapien Shale (calcareous mudstone, shaly siltstone, arenaceous limestone and evaporites) and the underlying Twin Creek Limestone (limestone with minor amounts of siltstone, sandstone, gypsum and anhydrite) which rests directly on Navajo Sandstone. The Twin creek Limestone has not been identified in surface exposure in central Utah. Twin Creek Limestone is used in this report as the lowermost part of Arapien rocks, as identified in well data.

The Wasatch fault zone truncates the Nebo allocthon along the western edge of the southern Wasatch Mountains and presumably has downdropped the thrust sheet beneath Juab Valley. Exposures of overturned Paleozoic and early Mesozoic rocks in the vicinity of and just south of where the seismic line crosses West Hills-Long Ridge probably represent the western continuation of the Nebo thrust (fig. 2).

The probable southern boundary of the Nebo thrust, the N 60°E-trending Leamington tear fault, is exposed 22 km SW of the end of the seismic line (fig. 1). Where exposed, the fault dips steeply and the dominant sense of motion is strike-slip (Morris, 1983). Its projected trace through the study area is constrained by the exposures of overturned Paleozoic and early Mesozoic rocks in the northern part of the West Hills and by two wells in West Hills drilled 8 km south of the seismic line (Placid Oil WXC-Howard #1-A and Howard #2--see figs. 1 and 2). Both wells penetrate a normal stratigraphic section of Tertiary through late Mesozoic sedimentary rocks, a section of Jurassic Arapien, and bottom in Jurassic - Triassic Navajo Sandstone (Howard 2, T.D. 3282 m) or Triassic Chinle (?) (Howard #1-A, T.D. 3704 m).

The eastern half of the seismic line crosses the Gunnison Plateau which composed primarily of Arapien rocks and overlying synorogenic conglomerates, the Cretaceous Indianola Formation, both of which are deformed into a broad asymmetric syncline whose axis generally parallels the modern range. Deformation of these synorogenic conglomerates, particularly along the steep eastern limb of this syncline, has been attributed to simple folding (Spieker, 1946), Laramide compression (Gilliland, 1963), and extensive salt diapirism (Witkind, 1983). However, recent mapping combined with extensive well data and seismic profiling indicate that much of the geometry of deformation within the Gunnison Plateau can be attributed to late-stage Sevier compression and superimposed Tertiary normal faulting. Specifically, the deformation has been related to thrusting beneath the Gunnison Plateau which culminates either in a complex system of west- and east-verging thrusts (Standlee, 1982) or in a triangular zone (Lawton, 1985) both along the eastern margin of the Gunnison Plateau. Well data indicate that the Arapien both beneath the Gunnision Plateau and areas to the west is complexly deformed and tectonically thickened, probably by bedding plane thrusts (Standlee, 1982; Lawton, 1985). The thrusting beneath the Gunnison Plateau probably has minor displacement and may not have reached the synorogenic erosion surface; Lawton (1985) estimates only 5-6 km of shortening in his interpreted triangular zone along the eastern margin on the Gunnison Plateau.

On the basis of repeated and overturned stratigraphic sections in wells along the western margin of the Gunnison Plateau, both Standlee (1982) and Lawton (1985) concluded that bedding plane thrusts within the Arapien ramped upward in the vicinity of the modern Wasatch fault. An increase in westward dip of the Nebo basal thrust from an essentially flat attitude on the eastern edge of its exposure in the southern Wasatch Mountains (fig. 2) to a dip of 23° W near the range-front fault also suggests a ramp structure near the Wasatch fault. Smith and Bruhn (1984) have presented evidence of similar structural styles within thrust sheets to the north that suggest the modern Wasatch fault is located near the sites of major ramps in Sevier-age thrust faults.

In summary, the seismic line is in a complex structural setting. The eastern part of the line crosses Arapien rocks that have been tectonically thickened by bedding-plane thrusts and folding and locally disturbed by salt diapirism. These bedding plane thrusts are below the "basal" Nebo thrust and probably involve only minor transport (~ 5 km). Upper plate rocks of the Nebo thrust are exposed on the westernmost part of the line, thus both the Nebo and the lower minor thrust(s) are likely present in the subsurface in this area. The line probably obliquely cuts the southern edge of the Nebo thrust beneath Juab Valley. Geologic and well data suggest a ramp in both the Nebo and the deeper, minor thrust(s) near the modern location of the Wasatch fault zone. Because of the complex subsurface structure, additional geophysical data were collected to aid in the interpretation of the seismic profile.

GRAVITY AND DENSITY DATA

Existing gravity data in the study area supplemented by over 200 new stations are shown in figure 3. As expected, a broad gravity low is associated with Juab Valley. The data suggest a maximum anomaly of about -20 mgal in the valley south of the town of Nephi.

Quantitative modelling of the observed gravity field requires information on the subsurface geometry of the basin and also the rock densities. Constraints on the subsurface geometry come from the seismic reflection profile and are described later in the interpretative section together with a quantitative model of valley fill in Juab Valley. Density data from density logs of significant wells in the region are summarized in Table 1. In general, rock density increases with age. Despite the complex internal structure of the Arapien and reported large lateral variations in lithology (particularly in salt/anhydrite content), this unit has only a moderate variation in density (2.54-2.64 g/cm^3). However, these values are substantially greater than Arapien density values reported by Brown and Cook (1982) from logs of the Phillips U.S. D #1 well located 90 km south of the

TABLE 1

Log-Determined Densities (g/cm^3)/Sonic Velocities (km/sec)

Location of wells on Figure 1.

	Howard #1-A	Niellson-Sieger #1	Dixel Res. Gunnison #1	WXC State #1		WXC State #2	WXC Barton #1	US. E#1
				above thrust^2	below thrust^2			
Tertiary volcanic rocks							-/2.93*	
Eocene Flagstaff Fm.		-/3.05*		2.55/3.93*				
Cretaceous Indianola	2.57*/4.88*	2.55/4.47*	2.68*/5.65*	2.54/4.97*				-/4.76*
Jurassic Arapien	2.54/5.04		2.59*/4.97	2.60*/5.72*	2.64*/5.61*	2.63*/4.27*	-/4.82	
Ja^1	2.54/4.95			---- /5.63	---- /5.23		-/4.70	
Jtc^1	2.54/5.40			---- /5.95*	---- /6.25*		-/5.54*	
Jurassic-Triassic Navajo Sandstone	2.60/5.12		2.58*/5.23*	2.60*/6.16*		2.56/4.97	-/5.09	2.53/-
Triassic shales	2.63*/5.44*					2.60/5.03	-/5.21*	2.65/-
Permian limestones						2.69*/5.35*		2.75/5.94
Paleozoic shelf section (Permian-Cambrian)								2.73*/5.95*

* Only part of the unit was sampled due to logging difficulties or structure encountered in well

1 - division of Arapien age rocks into Arapien (Ja) and Twin-Creek limestone (Jtc) equivalents after Sprinkel (1982)

2 - refers to a thrust fault believed to have been encountered in the well

seismic line (see fig. 1). Brown and Cook (1982) recognized three distinct lithologic units within the Arapien age rocks with mean densities of 2.11, 2.54, and 2.01 g/cm^3 with a weighted mean density of 2.41 g/cm^3. For this study a mean density for the Arapien age rocks (including the Twin Creek Limestone of Sprinkel, 1982) of 2.55 g/cm^3 is preferred because it is more representitive of the values in Table 1 from wells located close to the seismic profile, particularly Howard #1-A, State #1. and State #2 (fig. 1 and 2).

The Jurassic-Triassic Navajo Sandstone underlying the Arapien rocks has approximately the same mean density (2.55 g/cm^3) as the Arapien whereas, the Triassic rocks are slightly more dense (2.63 g/cm^3). Rock units within the Paleozoic have primarily limestone lithologies and a mean density of about 2.73 g/cm^3, resulting in a density contrast of +0.10 to +0.18 g/cm^3 with the overlying Triassic and Jurassic rocks.

In addition to the main basin fill anomaly, the gravity data also reveal a relative gravity high within the basin which separates the closed low directly southwest of Nephi from the closed low about 15 km to the north (fig. 3). The source of this relative gravity high may be due to a transverse structure separating a shallow basin to the north from a deeper basin to the south. Similar transverse structures have been interpreted from gravity and geologic data from many of the basins bounded by the Wasatch fault zone (Zoback, 1983). Alternately, since the E-W trending gravity high separating the two gravity lows generally coincides with the southern termination of the Nebo allochton in the range to the east, it is possible that the gravity high is due in part to lateral variations in bedrock density. In the latter case the gradient may define the buried extension of the Lemington tear fault which forms the southern edge of the Nebo thrust plate. The decrease in gravity values south of this gravity high would thus be attributed to the +0.10-0.18

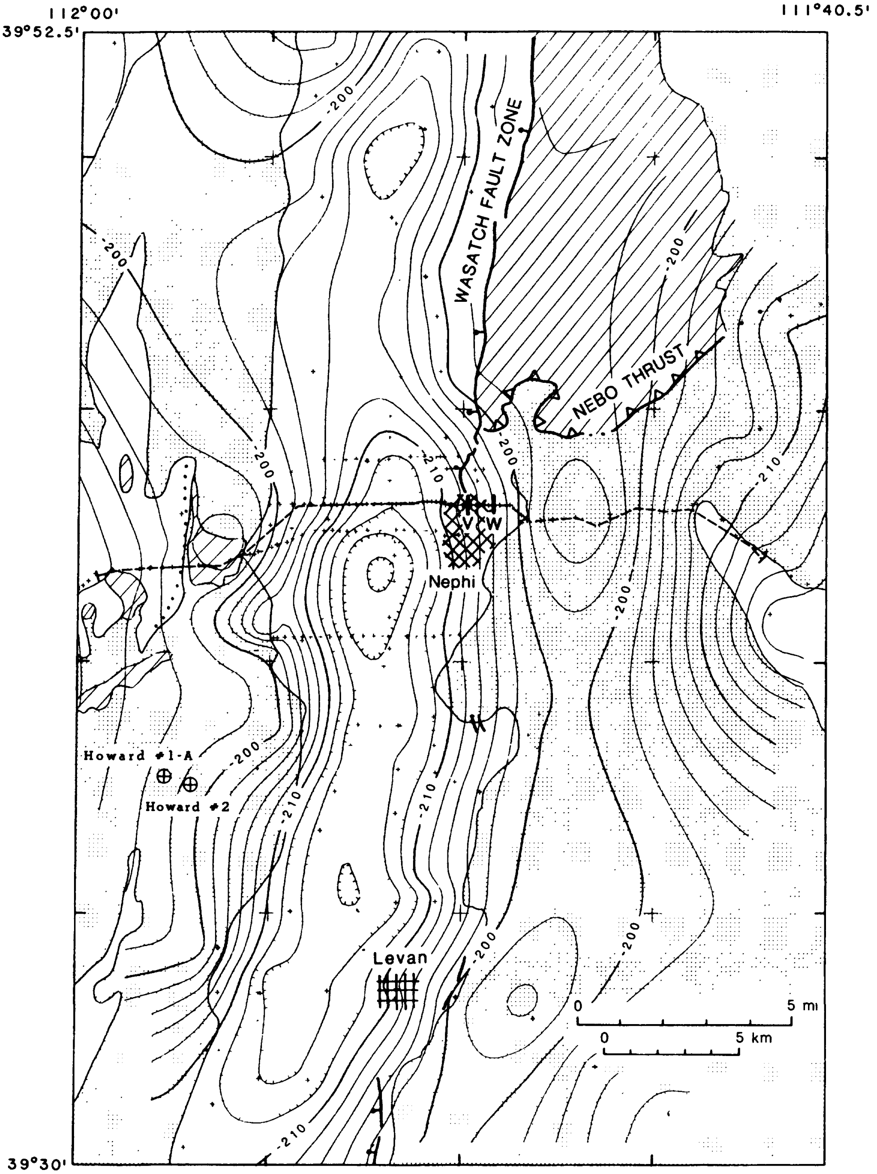

Figure 3. Complete Bouguer gravity map of the Nephi area, contour interval is 2 mgals. Gravity stations are shown by "+". Ranges are shaded. Rocks inferred to be part of the Nebo thrust sheet are cross-hatched. Heavy solid line is location of reflection profile.

g/cm^3 density contrast between the primarily limestone lithologies of Paleozoic rocks within the thrust plate and the predominantly shale and siltstones of the Arapien upon which it rests. This interpretation supports an inferred buried connection between the overturned Paleozoic rocks forming the Nebo allochthon and the overturned Paleozoic and Mesozoic rocks exposed in and just south of the pass between Long Ridge and West Hills (fig 2 and 3). The gentle slope of the gravity gradient may indicate that in this area the tear fault may have a shallow dip to the north. Wallace and Morris (1979) have reported that tear faults commonly flatten in dip to merge with the bounding thrust. The shape of the gravity gradient, particularty the closed low southwest of Nephi suggests that this transverse relative gravity high may be related to both effects described above, in which case the southern edge of the Nebo allochthon (Leaminton tear fault) may have acted to segment extensional fault structure in the hanging wall, producing a variaton in fill thickness between the north and southern portions of the basin.

SEISMIC REFLECTION AND VELOCITY DATA

A standard, 24-fold Vibroseis (trademark of Conoco, Inc.) profile was shot in 1975 across the Wasatch fault zone through the town of Nephi (fig. 2). The data were collected by a private contractor, United Geophysical, and purchased by the U.S. Geological Survey. Group and shot point intervals were 67.1 m (220 feet), and the data were recorded on a split spread with a near offset of 268 m (880 feet) and a far offset of 1811 m (5940 feet). The standard processing sequence included demultiplexing, velocity analysis, elevation and residual statics, stacking and filtering. The automatic residual statics produced a very poor quality record section with little continuity of reflectors. The contractor then used an "in-house" statics routine and hand picked of some of refraction arrivals which greatly improved the data quality and yielded the section shown in figure 4. A floating datum used to display the data is generally 30-70 m below the ground surface and has a constant value in the basin.

The 30-km-long profile begins in San Pete Valley on the east and follows the divide separating the southern Wasatch Mountains from the Gunnison Plateau (fig. 2). It crosses the Wasatch fault zone at Nephi and continues westward across Juab Valley, through the pass between Long Ridge and West Hills and ends in Dog Valley. There are several large data gaps on the section, the one in the western half of the section is due to a stream and the one near the center of the section because of a major highway and Nephi city streets. Despite folded, and steeply-dipping to overturned beds exposed in the ranges, the profile is dominated by horizontal and subhorizontal reflectors both beneath the basin and the ranges.

A line drawing of the prominent reflectors on the section is given in figure 5a. A discussion of the lettered reflectors and their geologic interpretation is presented later. First, velocity data are needed to estimate the depth and apparent dip of reflectors on the time section. Some velocity information is derived from the processing of the reflection data; these "stacking velocities" are best determined in areas of strong subhorizontal continuous reflectors. An additional source of velocity data is sonic logs of exploration wells. Sonic velocities and rock densities obtained from logs of nearby wells are summarized in Table 1.

The well-log velocities show a significant amount of scatter for individual

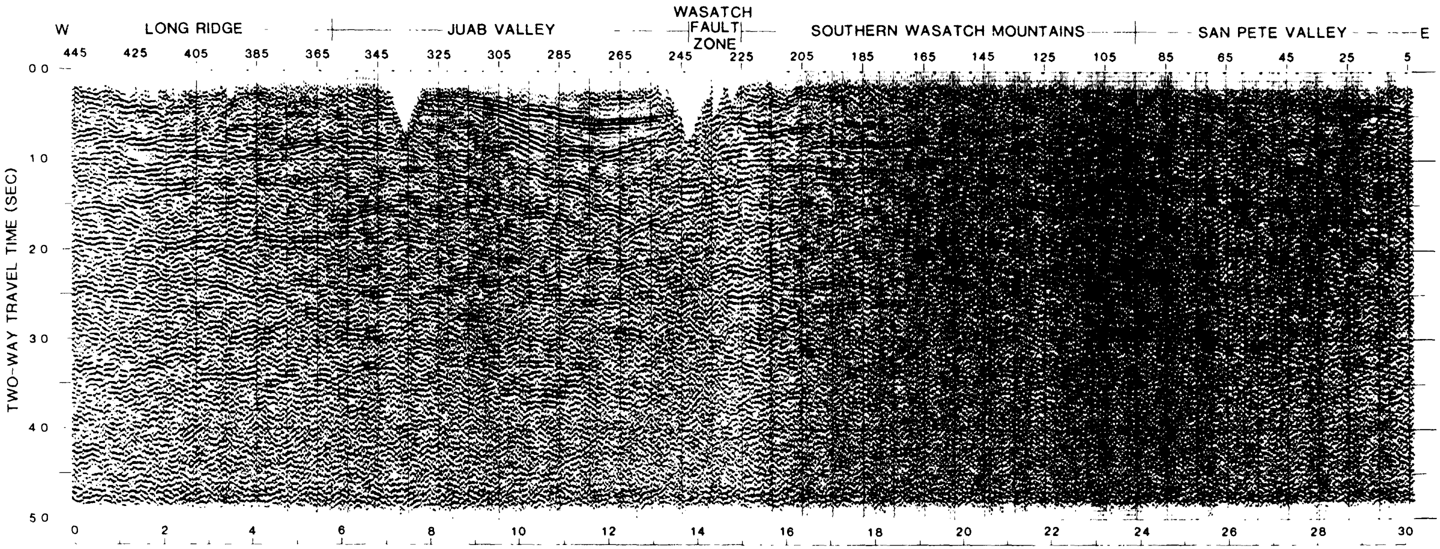

Figure 4. Seismic reflection profile, see Figure 2 for location. Vibrator points (VP) are indicated.

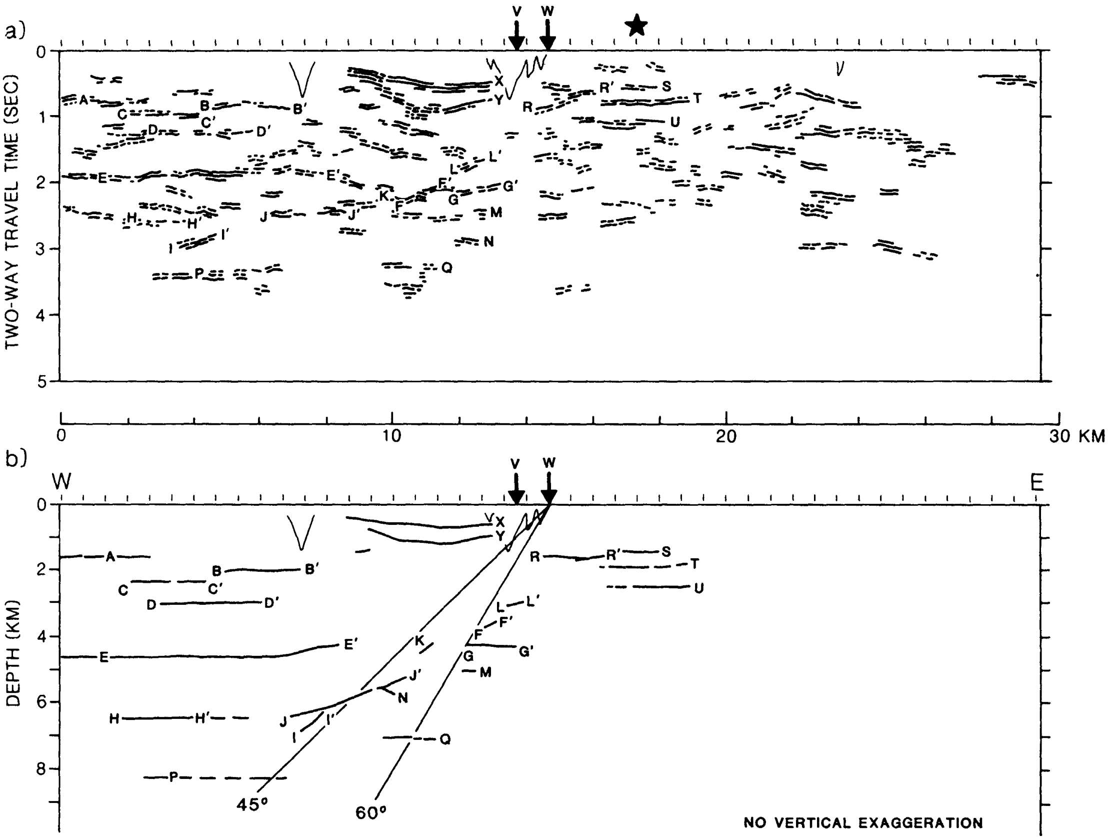

Figure 5a. Line drawing of seismic reflection profile. Reflectors discussed in the text are lettered.

b) True depth, migrated cross-section of selected reflectors on line drawing.

units; this scatter may reflect real variations in lithology between wells, or may be because of incomplete sampling of a unit due to poor log quality caused by borehole irregularities or geologic structure in the well. The velocity values in Table 1 represent reasonable ranges for the lithologies of the units of interest. The velocity ranges for the Mesozoic have considerable overlap units (Indianola 4.47-5.65 km/sec, Arapien 4.95-6.25 km/sec, Navajo 5.09-6.16 km/sec, and Triassic rocks 5.03-5.44 km/sec). In the wells in which Sprinkel (1982) sub-divided Arapien-age rocks into Arapien and Twin Creek equivalents there is generally a large velocity increase between the calcareous mudstones and shaly siltstones of the Arapien rocks and the limestones that dominate the underlying Twin-Creek equivalents.

Since seismic reflectance depends on impedance contrasts (velocity x density), the density and velocity data in Table 1 indicate numerous potential reflecting horizons throughout the section. Clearly the Mesozoic-Paleozoic boundary has a large impedance contrast. There is also a considerable impedance contrast between the Arapien shale and Twin Creek limestone in wells where these units are differentiated Sprinkel (1982). This impedance contrast within Arapien age rocks is greater than that between the base of the Twin Creek Limestone and underlying Navajo Sandstone. The velocity and density data from the Paleozoic shelf rocks drilled in the U.S. E # 1 well on the Wasatch Plateau (fig. 1) also indicate significant impedance contrasts between individual units in the Paleozoic section. Thus, numerous potential reflectors occur in the Mesozoic and Paleozoic rocks due to stratigraphic and lithologic contrasts. In addition, structural features, including thrust-juxtaposed units of high impedance contrast as well as low-angle fault zones (Jones and Nur, 1984) may produce some of the reflections.

Comparison of these well-log velocities with stacking velocities obtained during processing of the seismic section indicate that the stacking velocities in general are unrealistically low except for the basin fill region where the reflectors are strong and very continuous. In particular, the stacking velocities from a velocity analysis near the center of the Gunnison Plateau, where Arapien rocks are exposed and are probably at least 2000 m thick, indicate a velocity of 3.8 km/sec at 1.0 sec two-way travel time (TWTT) and a velocity of 4.27 km/sec at 2.0 sec TWTT. In contrast, the sonic log determined velocities for Arapien rocks, although variable, range between 4.95-6.25 km/sec (Table 1). Similarily, stacking velocities on the west end of the line where overturned Paleozoic limestones are exposed at the surface are low compared to sonic-log velocities. The log velocity of the Paleozoic rocks is quite high, ~ 5.95 km/sec, compared to several stacking velocities between 3.66-3.81 km/sec for the prominent reflector (E-E') at about 1.9 sec TWTT. The Paleozoic rocks at the surface are presumed to be part of the Nebo thrust which probably rests on Jurassic Arapien or older rocks, nonetheless, these stacking velocities are unrealistic even if there is only a thin plate of Paleozoic rocks and much of the section is lower plate Mesozoic rocks. Low stacking velocities may sometimes indicate the presence of multiple reflections in the section. The simplest multiple path predicts a second reflection at twice the two-way travel time and twice the dip with a stacking velocity one half of the true root-mean-square velocity. However, there are no obvious shallower reflectors which may have generated multiples, particularly in the case of the laterally continuous reflector, E-E'. Because of the inconsistencies between the sonic-log and stacking velocities the interpretation of the seismic reflection time section in the next section generally relies on the well-log velocities (except for within the basin fill section) to calculate depth to observed reflectors.

INTERPRETED SUBSURFACE STRUCTURE

Basin Geometry and Shallow Structure of the Wasatch fault zone

The most prominent and continuous reflectors on the seismic profile are from the late Cenozoic basin fill section (figs. 4 and 5). Figure 6a is a detailed view of this part of the seismic line with a possible interpretation of reflectors across minor faults within the basin. Figure 6b is a one-to-one schematic depth cross-section of several prominent reflectors showing inferred depth and dip of these reflectors based on stacking velocities. Stacking velocities within the basin fill section compare quite favorably with velocity data from other basins (e.g. Okaya and Thompson, 1985) and since the reflectors are so strong and continuous, the stacking velocities were considered valid for this part of the line. The best constrained reflectors are marked X and Y, three separate velocity analyses detail their depths. Depth of other reflectors shown on figure 6b were obtained by interpolation.

The Wasatch fault zone bounds the basin on the east and the internal structure of the basin is a gentle synclinal sag with dips of 7°-20° on the western flank and dips of 5-7° on the eastern flank. On the time section (fig. 6a), the basinward dips on the eastern flank are exaggerated because of a velocity increase (suggested by stacking velocities) eastward toward the Wasatch fault zone.

The base of the valley fill section is not marked by a single well-defined reflector. In the western half of the basin, the base of the valley fill is inferred to lie between the discontinuous basal synclinal sag (reflectors) and

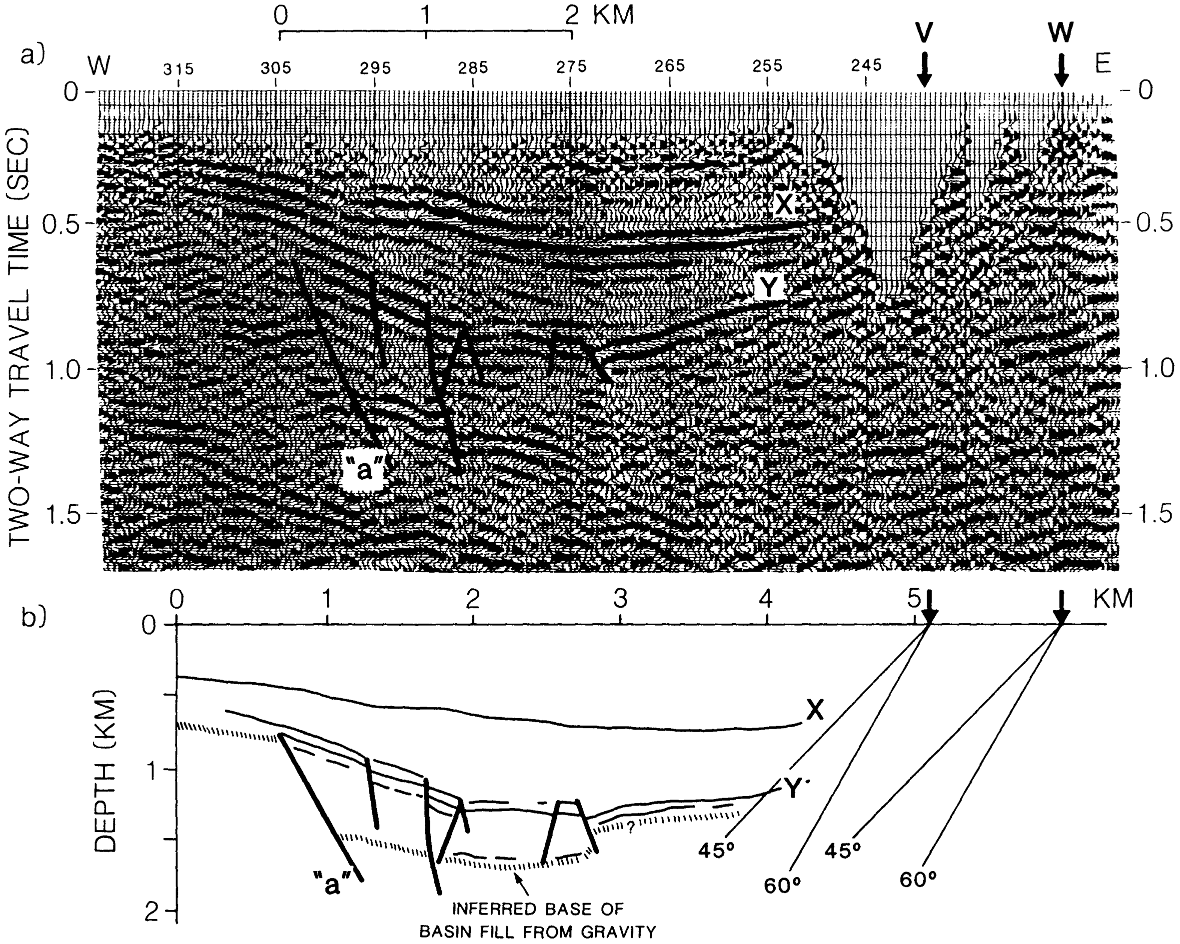

Figure 6. a) Detail of seismic reflection profile in Juab Valley showing basin fill. Positions W and V mark possible surface location of Wasatch fault zone described in text. Reflectors X and Y are discussed in the text. Heavy solid lines are interpreted faults.

b) True depth cross-section of prominent reflectors in basin. Projection of planar faults with dips of 45° and 60° that reach the surface at locations W and V are shown. Vertical and horizontal scales are equal.

the deeper discordant reflectors (fig. 5a). The deepest part of the basin has a graben-like structure, bounded on the west by a normal fault (fault "a" in fig. 5) with about 700 m of displacement. There are no obvious subjacent discordant reflectors directly beneath the eastern half of the basin so only a minimum thickness of valley fill can be determined there. Mean velocities for the basin fill obtained from three stacking velocity analyses on reflectors near the base of the synclinal sag vary between 2.74-2.97 km/sec with the lower velocity from the center of the valley and slightly higher values near the margins. Interval velocities between reflectors in the lower part of the basin fill exceed 3.2 km/sec, and may represent early Tertiary volcanic or sedimentary rocks (see Table 1). The thickest section of basin fill is interpreted to lie beneath VP 285, where the fill is estimated to be 1.60 km thick.

The eastern margin of the basin is marked by a broad zone of little or no reflectance. Interpretation of this part of the section is hampered by a data gap caused by cultural noise associated with the town of Nephi. The eastward termination of the basin reflectors in this region may be due to the data gap and reduction in fold as the gap is approached, but may also be due in part to a general decay in reflector continuity in the poorly sorted, poorly stratified coarse clastics which comprise the alluvial fans adjacent to major range front faults. This decay of coherent reflectors within the fan region (as opposed to the uniform reflectors from the finer-grainer basinal facies) is typical of many basins within the Basin and Range province (Anderson and others, 1983; Zoback and Anderson, 1983; and Okaya and Thompson, 1985).

Prominent multiple-event Holocene scarps mark the trace of the Wasatch fault zone directly north of the study area (Schwartz and Coppersmith, 1984, see figure 2); the scarps extend southward to within about 2 km of the seismic line. A curved scarp, located basinward of the main zone of range-front scarps has been identified by Cluff and others (1973) just north of the seismic profile (fig. 2). The surface location of the main Wasatch fault zone along the profile is believed to lie between the southerly projection of the large Holocene scarps to the north (marked W on figure 6) (Schwartz and Coppersmith, 1984) and young faulting with a net vertical displacement of 11 m at depths of about 150 m (marked V on figure 6) by a shallow high resolution seismic reflection profile run along the same road as the industry reflection profile (Crone and Harding, 1984). The zone of shallow faulting at V is near the southern end of the curved scarp of Cluff and others (1973). However, minor fault displacements were also observed by the high-resolution seismic survey near W, the southward projection of the range front scarp.

Projection of faults that dip between 45°-60° are shown on Figure 5b at localities V and W. Note that the eastward extent of reflector Y places a minimum dip of about 52° for a bounding fault with a surface trace at V. Locating the major bounding fault trace at V assumes that some coherent basin reflectors extend through any fan wedge that might have built up along such a bounding fault, it also assumes that there was no decay of the reflector signal by the data gap. Interestingly, high quality reflection data with good surface faulting control in a comparable basin, Dixie Valley, Nevada, indicate a 1.0-1.25 km fan wedge adjacent to the range-bounding fault (Okaya and Thompson, 1985); this would favor location W as the major bounding fault zone. Of course, there may well be a broad fault zone with displacement distributed across it, with apparently the youngest offset near V, as indicated by the high-resolution seismic data (Crone and Harding, 1984).

Gravity data can help to constrain the geometry of the basin margin. As described earlier, gravity data were collected at more than 200 stations in the vicinity of and along the seismic profile. Gravity measurements were made approximately every 170 m along most of the reflection line. These data are plotted in cross-section on Figure 7. Several two-dimensional gravity models were computed for the basin fill assuming a -0.4 g/cm^3 density contrast with adjacent bedrock. The only difference in the three models in Figure 6 is the location of the eastern margin of the basin. The maximum fill thickness in the center of the basin for all models is about 1.6 km, consistent with the interpretation of the reflection data. A notable feature of the models is a central graben, as inferred from the reflection data. The configuration of and vertical displacement on the fault bounding the western side of the graben are taken directly from the reflection data. The modelled base of the basin closely matches the base inferred from the seismic data except along the eastern margin of the basin.

In model 1 on figure 7 the Wasatch fault zone is located at W, along the southern projection of the range-front fault and has a dip of 60° W. This model matches the gravity gradient directly above the fault quite well but greatly over estimates the gravity values east of the fault. Model 2 places the main Wasatch fault zone at V, the most basinward position of young faulting inferred from the high resolution seismic reflection described by Crone and Harding (1984). This position for the bounding fault clearly provides a very poor fit to the observed gravity data for almost the entire eastern part of the basin.

In an attempt to model the low gravity values east of the fault zone an easternmost limit for faulting (model 3) was generated from the surface

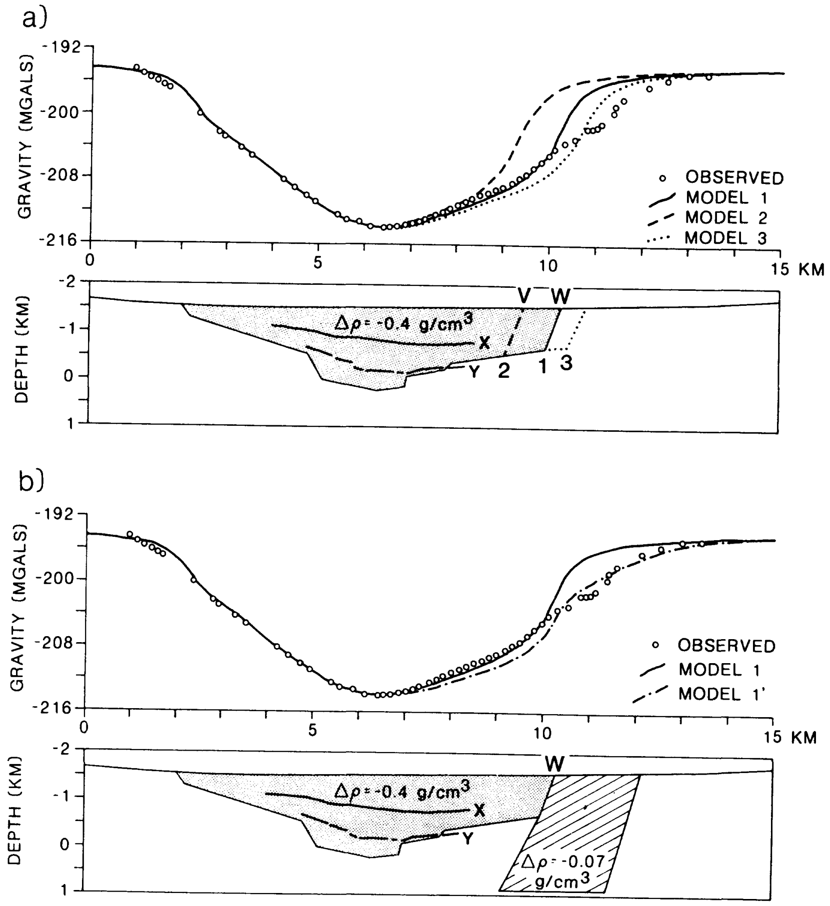

Figure 7. a) Gravity models of the basin fill in Juab Valley. Diamonds are observed gravity values; solid, dashed, and dotted lines give computed values based on the geometries indicated. A constant density contrast of -0.4 g/cm^3 between basin fill and surrounding bedrock was assumed for all models. Reflectors X and Y from Figure 6 are shown for reference.

b) Same as model 1 in (a) except a low density tabular body has been added to the footwall of the Wasatch zone.

location of bedrock in the range and from the western truncation of reflector R-R' on the footwall block (figure 5b). This model over-predicts the anomaly to the west of the fault (although the fit would improve if a higher density alluvial wedge were added to the model). Once again, while the fit to the gravity data east of the fault is improved, the computed values are still too large in a 2 km wide zone east of the easternmost possible fault location. This suggests that the source of the observed gravity low east of the fault is the result of less dense bedrock (Arapien rocks) of the footwall.

In all three models in figure 7a, the inferred base of the basin contradicts the position of the intrabasin reflector Y whose depth was determined from an Advanced Interpretative Modeling Systems (AIMS, trademark Geoquest) migration using stacking velocities on the seismic section. One explanation of this discrepancy between the gravity- and seismically-inferred basin geometry just west of the bounding fault zone may be the assumption of a single density contrast for the entire basin. As previously mentioned, alluvial fans along major basin-bounding normal faults produce in a wedge of higher velocity, higher density sediment adjacent to the fault zone. Okaya and Thompson (1985) used a fan wedge with a density 0.2-0.3 g/cm^3 higher than the rest of the basin to reconcile gravity and reflection data from Dixie Valley, Nevada. Use of a higher density fan wedge would increase the gravity values west of the fault (improving the fit in Model 3), however, it was not included in these simple models since its inclusion would not explain the low gravity values east of the fault zone. Because the initial objective in modelling the gravity data was to constrain both the location and shallow geometry of the Wasatch fault zone, several possible surface traces for the main bounding fault zone utilizing the simple but probably unrealistic assumption of a constant density for the basin were examined to determine the effects of different fault locations on the gravity field east of the fault.

Figure 7b shows a modified simple model that is generally consistent with the observed gravity values east of the fault data. Here the main Wasatch fault zone is positioned at W and a roughly 2-km-wide tabular low-density body has been included east of the fault zone. The geometry of the low density body was chosen simply to provide a reasonable fit to the gravity data. Inclusion of a higher density clastic wedge west of the fault zone (discussed above) could provide a near perfect fit to the data, however lacking additional constraints on the geometries of these bodies, any near-perfect fit would be non-unique, and not particularly instructive. The presence of a low density body just east of the Wasatch fault zone is supported by the geology along the western edge of the Wasatch Range in the area of the seismic line. Here the seismic line passes an open-pit mine where large quantities of gypsum have been removed from the Arapien. Possibly the low density body in the model represents a concentration of diapiric gypsum which rose along or just east of the Wasatch fault zone with the major bedrock offset.

Thus, because of complicated structure within the footwall the gravity data cannot tightly constrain the near surface location of the Wasatch fault zone. The gravity data do appear to exclude location V as the position of the main Wasatch fault. Based on the geology and high resolution seismic work, location W seems to be the most likely position for the main fault zone with the major bedrock offset.

Deep Structure

Prominent reflectors on the seismic profile are shown on the line drawing in Figure 5a. Each of the lettered reflectors in Figure 5a was represented by a straight line segment, or a series of straight line segments, and were migrated using a AIMS migration scheme and a very simple velocity model.

Velocities in Juab Valley were obtained from the stacking velocities and elsewhere a constant velocity of 5 km/sec was assumed since, as discussed earlier, stacking velocities were generally unrealistically low. A velocity of 5 km/sec is probably somewhat low for the deeper portions of the section where Paleozoic rocks are probably present, thus the depths given for the deep events are only minimum depths.

Figure 5b shows the approximate true depth positions (obtained from the AIMS migration) of the lettered reflectors on Figure 5a. The outline of the inferred basin structure (from the gravity and seismic interpretation in Figure 6b) is indicated as well as projections of planar faults dipping 45° and 60° from the preferred near-surface fault location W. The relationship and position of the lettered reflectors are discussed below and their geologic interpretation is described in the next section.

Subhorizontal reflectors are common throughout the profile to depths of 2.5-3.0 seconds, and there are several strong and relatively continuous reflectors (marked P and Q) at TWTT of 3.3-3.7 seconds on the western half of the profile. Using the velocity model described above, the depth to the top of the P reflectors is greater than 8.3 km. Relatively shallow reflectors in the western half of the seismic profile include the events marked A, B-B', C-C', and D-D'. These events are beneath the pass between Long Ridge and the West Hills where overturned steeply-dipping Paleozoic rocks believed to be part of the upper plate of the Nebo thrust are exposed at the surface. The complex band of reflectors marked A, B-B' and C-C' lacks significant lateral continuity. Events A and B-B' are at a depth of 1.65-2.0 km (assuming a mean near-surface velocity of 5.0 km/sec). Event C-C' occurs at a depth of about 2.3 km, and a slightly deeper, zone of subhorizontal reflectors (D-D'), laterally continuous for 6 km, is at a depth of about 3.0 km.

Where the Nebo thrust is exposed in the southern Wasatch Mountains on the eastern side of the basin, the Paleozoic limestones in the upper plate of the

Nebo thrust are emplaced on Arapien rocks which, based on velocities and densities in Table 1, should produce a significant impedance contrast. However, the lack of a single continuous well-defined reflector marking the Nebo thrust fault on the western half of the profile is not surprising, and is probably due to the complex structure of the overturned anticline forming the upper plate. At the surface the Paleozoic rocks are overturned, dipping to the north 50°-75°. An additional complicating structural feature along this portion of the line is the apparent eastward tilt of the entire Long Ridge-West Hills range complex. Oligocene volcanic and volcanic-sedimentary rocks capping these two ranges are rather uniformly tilted 15-30° to the east. The steeply-dipping, overturned Paleozoic limestones (inferred to be part of the Nebo thrust) which are exposed in the pass between these two ranges have presumably also been eastward tilted. However, none of the sub-horizontal reflectors A, B-B', C-C' or D-D' have eastward dips. Either structural accommodation of the tilting seen at the surface occurs at depths less than 1.5-2.0 km or else those shallow reflectors had a westward dip prior to tilting. Thus, because of the complex internal structure of the thrust sheet, post-thrust tilting of the range as well as the possibility of a ramp in the thrust near the Wasatch fault (discussed previously) not even an approximate thickness of the Nebo plate can be used to constrain which of the reflections A, B-B', C-C', or D-D' might be from the actual Nebo thrust plane.

The most continuous zone of deep reflectors are E-E', a nearly horizontal band of reflectors that extend across the western half of the section at 1.8-2.0 seconds TWTT (fig. 5a). These reflectors are lateral continuous for at least 10 km, and possibly as much as 15 km (to G-G'). An average (rms) velocity of about 5.0 km/sec for this part of the profile yields a depth of 4.7 km for this prominent reflector. The eastward continuation of reflector

E-E' which appears to exhibit velocity "pulldown" beneath the basin, is obscured by cross cutting events including west-dipping events K and F-F'. However, on the migrated depth section shown in Figure 5b, the eastern end of event E-E', when corrected for velocity pulldown, is actually dips to the west beneath the western part of the basin.

On the time section (Figure 5a) it appears that events E-E' and G-G' might be laterally continuous. However, on the migrated depth section the events appear unrelated. Reflector G-G' becomes subhorizontal, shifts eastward, and would be located in the footwall block of a 60° dipping fault with a surface trace at W. Significantly, west-dipping events L-L' and F-F', (which appear to cut events E-E' and G-G' on the time-section and could be interpreted as possible reflections from a listric fault plane) migrate, with the simple velocity model described above, up-dip and are located, along with G-G', in the foot-wall block of a 60° (or shallower dipping) fault plane. The apparent dips, in the plane of the profile, of reflectors L-L' and F-F' are 11°W and 30°W respectively (true dips may be steeper). Event M also appears to be in the foot-wall block of a 60° fault, whereas the top of the deep events marked Q would be within the foot-wall block of a west-dipping planar fault with a dip of 55° or less. Similarily, the top of the subhorizontal deep events, P, limits a planar fault dip to be greater than 47°.

The reflectors deeper than E-E', including those marked H-H', I-I', J-J', and K are rather complex, consisting of west-dipping, east-dipping and cross-cutting events. Westward-dipping, event J-J', beneath the western side of the basin moves considerably upon migration and has an apparent dip of 22°W. East-dipping event N migrates up-dip and appears to be truncated by event J-J'. Similarily, event I-I' also migrates to event J-J' and appears truncated. The migrated position and geometry of event J-J' is highly suggestive of a reflection from a listric fault plane possibly flattening and merging with event H-H'. However, there is no suggestion on the actual reflection data of continuity between J-J' and H-H'.

The general character of the seismic profile changes near the Wasatch fault zone. The eastern half of the profile, beneath the Gunnison Plateau, is characterized by a thick sequence of short discontinuous subhorizontal reflectors. With the exception of the reflectors marked R-R', S, T, and V on Figure 5a no attempt has been made to interpret these numerous discontinuous reflectors. Seismic reflection and well data along the western margin of the Gunnison Plateau 15-20 km south of the profile indicate a complicated structure within the Arapien rocks including multiple thrust faults and overturned to recumbent folds (Standlee, 1982 and Lawton, 1985). The west-dipping reflector R-R' on the time section is one of the stronger reflectors east of the Wasatch fault zone and appears to truncate overlying horizontal reflectors. Upon migration the western portion of event R-R' becomes subhorizontal and appears to be cut by the west-dipping, eastern limb of R-R'. This eastern limb may also truncate subhorizontal reflectors S, T, and U.

Prominent subhorizontal reflectors beneath the Gunnison Plateau argue against large-scale deep-seated salt diapirism along the axis of the Gunnison Plateau, as suggested by Witkind (1982, 1983). In fact, the axis of a proposed major diapiric fold interpreted to extend for at least 38 km along strike (Witkind, 1983) crosses the seismic line approximately at the location of the star on Figures 5a and 5b. Reflectors in the shallowest part of the time record (Figure 5a) here are slightly upwarped however, the deeper reflectors (S, T, and, U) at approximate depths of 1.5 km, 2.0 km, and 2.75 km respectively (assuming a velocity of 5.0 km/sec) are subhorizontal beneath this presumed anticlinal axis suggesting that the diapirism may be a localized, shallow phenomena, rather than a major deep-seated feature.

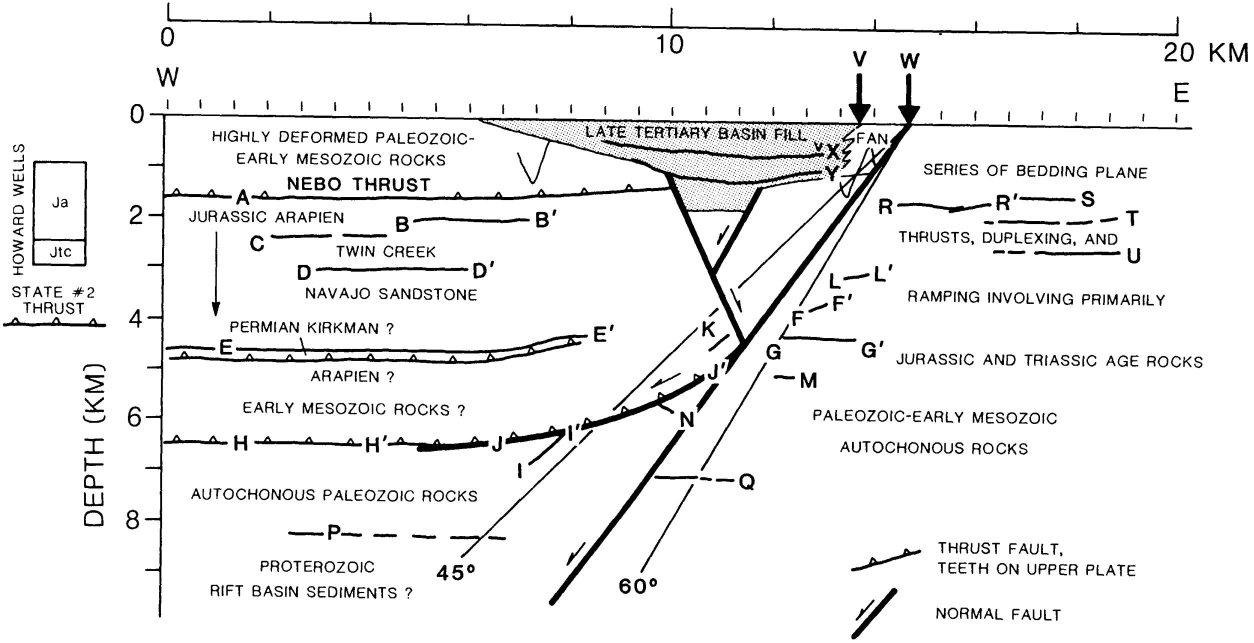

Figure 8. Geologic interpretation of western half of true depth line drawing shown in Figure 5b. Heavy lines are seismic reflections, inferred stratigraphic contacts are indicated.

Geologic Interpretation of Deep Structure

One possible geologic interpretation of the subsurface structure on the western half of the seismic profile consistent with subsurface data and regional geologic structure is shown on the true depth line drawing in Figure 8 and described below. Reflector A and short west-dipping reflectors located just west of graben fault "a" are interpreted to be the base of the Nebo thrust which rests on the lower part of the Arapien section. The seismic profile is interpreted to obliquely cut the southern edge of the Nebo thrust near a ramp in the thrust inferred from surface exposures of the thrust just east of the Wasatch fault zone. As discussed earlier none of the reflectors in this area display the west dip expected for a thrust fault ramping up to the east; however, the younger eastward tilt of the Long Ridge-West Hills range no doubt complicates and obscures the earlier thrust geometry.

Reflectors B-B', C-C', and D-D' are interpreted as a stratigraphic boundaries, possibly within Arapien rocks or from the base of Arapien rocks resting on Jurassic-Triassic Navajo Sandstone. This interpretation is based in part on well data from the Howard #1-A and Howard #2 wells drilled 8 km south of the seismic line (figs. 1 and 2). Both wells were positioned south of the southern edge of the Nebo thrust (Leamington tear fault) and were spud in Tertiary sedimentary rocks, drilled through Cretaceous synorogenic conglomerates into the Jurassic Arapien (thickness 2082 and 1977 m respectively) and bottomed in Jurassic and Triassic rocks. The absolute depth range that the Arapien rocks were encountered in these two wells is indicated on the left-hand side of fig. 8. Sprinkel (1982) designated the lower 431 m of the Arapien secton of Howard #1-A as the limestones of the Jurassic Twin Creek, he did not report on the data from Howard #2. Thus, interpretation of B-B', C-C', and D-D' as from within or from the base of the Jurassic rocks is consistent with the depth levels of Arapien rocks south of the Nebo thrust.

The State #2 well, located approximately 28 km south of the seismic line (fig. 1), drilled through a thin section of Arapien rocks and apparently a complete section (1383 m thick) of Jurassic-Triassic (Navajo Sandstone) and Triassic rocks testing on 672 m of Permian rocks (Diamond Creek and Kirkman Limestone) (D.A. Sprinkel, 1984, personal comm.). The Permian rocks were truncated by a thrust fault which emplaced the overlying rocks on the Navajo Sandstone. The absolute depth of this thrust of Permian over Jurassic-Triassic rocks was 2542 m below sea level which correspnds roughly to a depth (from the surface) along the seismic profile of about 4.15 km (see left hand side of fig. 8). Thus, if D-D' is interpreted as the top of the Navajo Sandstone, then the prominent, nearly horizontal reflector E-E' is in a similar position to the Permian Limstones encountered just above the thrust in in State # 2. Beneath the Cenozoic basin, reflector E-E' begins to dip westward and is interpreted to be part of a ramp anticline above this inferred blind thrust fault. The blind thrust is shown as emplacing Permian on early Mesoic, possibly Arapien rocks. The section between D'-D' and E-E' is about 1.58 km thick, comparable in thickness to the 1.38 km thick section of Jurassic-Triassic rocks beneath the Arapien and above the Permain in State # 2.

Reflectors H-H' are interpreted as a deeper blind thrust which ramps up (J-J') and possibly splays (K). Events I-I' and N appear truncated by J-J'. The section beneath E-E' and above H-H' probably represents Jurassic and Triassic rocks however, probably not a complete section, since Standlee (1982) estimates a 1702 m thickness of Arapien rocks alone beneath the Gunnison Plateau and the State #2 well encountered an additional 1.38 km of Jurassic and Triassic rocks beneath the Arapien. The impedance contrast at H-H' is interpreted to be due to the thrust juxtaposition of Lower Mesozoic rocks on

Paleozoic limestones. The 1.8 km thick section between H-H' and P is interprted as autochonous Paleozoic rocks. Nearly complete section of autochonous Paleozoic rocks (approximately 1280 m thick) was drilled in U.S. E #1, located approximately 30 km east of the western end of the seismic line. Along most of its length, the Wasatch fault zone is close to and generally parallels the "Wasatch line" (Kay, 1951), the hinge line which marks the transition from shelf to basinal facies of the Cordillera geosyncline, i.e. zone of dramatic westward thickening of strata deposited on the late Precambrian rifted margin (Stewart, 1972). Thus, the 1280 m encountered in U.S. E#1 probably represents a minimum thickness for the autochonous Paleozoic rocks. H-H' may mark a thrust occurring near the top of the Paleozoic section. Both of the inferred blind thrust (below E-E' and H-H') faults may be cut and offset by the Wasatch fault zone, and may be correlative to the bedding plane thrust(s) inferred beneath the southern Wasatch Mountains just north of the seismic profile by Jefferson (1982) and Lawton (1985).

The band of reflectors defined by P are speculatively interpreted as late Proterozoic sediments. Thrust ramps have been interpreted near the location of the modern Wasatch fault in several localties (e.g. Smith and Bruhn, 1984). These ramps may have developed over abrupt changes in basement geometry, i.e. pre-existing structural discontinuities. Specifically, it is proposed that the thrust ramps may have developed over west-dipping normal faults in the Precambrian crystalline basement which formed during the initial Precambrian rifting event. In this scenario, the reflectors marked by P may be sediments deposited in such a rift basin.

Well data along the westernmost edge of the Gunnison Plateau 25 km to the south (Gunnison #1, fig. 1 and other wells not shown) indicate a very complicated shallow structure beneath the Plateau including recumbent and overturned folds and numerous bedding plane thrusts involving Arapien and Jurassic-Triassic rocks (Standlee, 1982 and Lawton, 1985). The possible thrust splay K and reflectors R-R' and F-F' may be related to such deformation.

Two possible subsurface geometries for the Wasatch fault zone are indicated on fig. 8. The position and westward dip of both reflectors E-E' and J-J' beneath the Cenozoic basin strongly suggest a listric geometry for the main Wasatch fault zone. In particular, reflection J-J', which appears to flatten and merge with inferred blind thrust H-H', is an excellent candidate for listric backsliding on a pre-existing thrust. The symmetric, sag-like geometry of the Cenozoic basin and specifically the lack of growth faulting and reverse drag (e.g. Anderson and others, 1983) argues against such a sharply curved listric geometry (flattening at depths of only 4.5-6.5 km). The alternate interpretation, a planar dip of 54° for the main fault zone is constrained by the eastern end of reflectors J and the western truncation of reflector Q. The synclinal sag-like geometry of the basin is produced by beds dipping away from the boundary fault zone and appears related to the development of the small central graben. Analysis of a number of seismic reflection profiles in the Great Basin area led Anderson and others (1983) to suggest that the sag-like geometry is commonly associated with a steep, relatively planar bounding fault zone. Dixie Valley, Nevada is a well-documented example of such a basin and steep-planar fault geometry (Okaya and Thompson, 1985). Microearthquake studies in central Utah also support a high angle fault interpretation, indicating seismic strain release on relatively steep (~ 33°-90°) planes (Arabasz, 1983).

Distinguishing between the two alternate models for the Wastch fault geometry is complicated by a possible earlier episode of extensional tectonism responsible for the 15-30° eastward tilt of the Oligocene volcanic and desimentary rocks capping Long Ridge and West Hills. An inferred angular unconformity between these rocks and the oldest basin fill sediments on the western end of the seismic line (with maximum dips of 20°E) suggests possible listric or block-tilt faulting prior to the development of the modern basin.

As mentioned earlier the lack of east-tilted reflectors at depth may indicate a relatively shallow depth or complex geometry for accomodation of this earlier tilting.

Both the listric and planar fault model suggest a markedly asymmetric fault pattern for the development of Juab Valley. The west-dipping Wasatch fault zone is the master fault, and internal basin structure is related to formation of a cental graben. There is a net topographic decrease across the Wasatch fault zone as indicated by range heights on either side of Juab Valley (range height is also moderated by bedrock lithology of the ranges). Elevation of Long Ridge (1800-2130 m) and West Hills (1800-1900 m) are 500-800 m lower than the southern Wasatch Mountains (2440-3600 m) and the Gunnison Plateau (2440-2700 m) east of the Wastach fault zone. This net topographic offset could be accomodatd by either the listric or planar fault model.

DISCUSSION

It is apparent that there is no unique interpretation of the reflection section despite constraints imposed by the gravity data and the high-resolution seismic profiling of Crone and Harding (1984). The complex and superposed Mesozoic and Cenozoic deformation as well as the lack of any drill hole data along the profile permit only inferences on the subsurface thrust geometry. As noted above, if several of the reflectors are interpreted as thrust faults, simple listric back-sliding on these faults fails to explain the basin-fill geometry.

The steep-fault interpretation presented here contrasts with that of Smith and Bruhn (1984) for the Wasatch fault zone 18 km to the south near Levan. From a Vibroseis profile across the fault near Levan (see figure 1) Smith and Bruhn interpret a planar fault zone with a 34° dip penetrating only 5 km deep. Reverse drag and growth faulting are observed in the subsurface structure of the basin along their profile. Schwartz and Coppersmith (1984) have inferred a segment boundary along the Wasatch fault zone between the two reflection profiles, allowing the possibility that both subsurface geometries might be correct and applicable to different major fault segments.

As described in the section on geologic setting, within the study area the Nebo thrust and a deeper thrust(s) may ramp up in the vicinity of the Wasatch fault zone. Smith and Bruhn (1984) conclude that along several of the segments (including the segment in the study area) the Wasatch fault zone is located above inferred west-dipping Sevier thrust fault ramps. They suggest that along several segments the Wasatch fault may overlie and utilize the thrust fault ramps and merge with subhorizontal thrusts at depth. This conceptual model strongly influenced their and Standlee's (1982) interpretation of the subsurface geometry of the Wasatch fault zone for the Levan seismic profile mentioned above.

As suggested by Smith and Bruhn, the general correlation between the Wasatch fault zone and inferred thrust ramps in the subsurface can be used to argue for a relationship between the location of late Cenozoic normal faults and the geometry of older thrust faults. Alternately, an even older structure may have controlled both the development of the thrust ramps and the Wasatch fault zone. The location of thrust fault ramps can be controlled by facies changes along the decollement horizon or by interruptions of the decollement by basement offsets such as normal fault zones (Suppe, 1985, p. 282). It is suggested here that west-dipping normal fault zones in the Precambrian crystalline basement which formed during the early phases (pre-drift) of Precambrian rifting (Stewart, 1972) may have provided the structural relief responsible for the formation of the thrust ramps.

The modern passive margin along the Atlantic coast of the United States contains numerous examples of major Triassic basins which formed on the shelf near the contemporary hinge line (e.g. Klitgord and Behrendt, 1979, Hutchinson and others, 1986). Since the Wasatch fault zone developed near the Paleozoic hingeline, similar Precambrian rift basins may be located at depth near the trace of the modern Wasatch fault. Interestingly, the length of these Atlantic shelf basins similar to that of the basin structure along the modern Wasatch fault. Hence, it is suggested here that the location of both the thrust ramps and the modern Wasatch fault may have ultimately been controlled by the location of a Precambrian normal fault zone bounding a basin or series of rift basins along the developing continental shelf.

Wheeler and Krystinik (in press) independently suggests that Precambrian extensional faults may help localize the Wasatch fault zone and control its geometry. Wheeler and Krystinik (in press) discuss geologic and stratigraphic data that suggest the presence of these late Precambrian normal faults and cites several examples of reactivation of such sub-thrust faults. The critical test of this hypothesis would be to identify the sedimentary sections filling basins of Precambrian Z - early Paleozoic age which were bounded by these faults. Unfortunately, the thick cover of Mesozoic thrust sheets have deeply buried these basins and, as is obvious from the present study, the complex superposed Mesozoic and late Cenozoic structure makes it difficult to identify these older deeper structures. The identification here of reflectors P as a sequence of Proterozoic sediments is purely speculative and intended to provoke further studies.

CONCLUSIONS

Seismic reflection and gravity data suggest that the overall structure of Juab Valley near the town of Nephi is an asymmetric sag, with beds on both sides of the valley tilting towards the axis of the valley. A central graben defines the deepest part of the basin. Anderson and others (1983) and Zoback and Anderson (1983) have identified this type of basin as commonly being bounded by one or more major, planar, steep normal faults. The maximum valley fill thickness is about 1.60 km based on interpretation of both the reflection and gravity data (assuming a density contrast for basin sediments of -0.4 g/cm^3). Possible displacement of a buried thrust(s), truncation of deep reflectors, and absence of reverse drag in basin sediments sugest that the Wasatch fault zone has a planar, high-angle with a dip of 50°-55° (as opposed to a listric or low-angle geometry). However, the lack of reverse drag within basin sediments is the strongest evidence against a listric geometry.

On a more regional note, structural data suggest the presence of major ramps in the Mesozoic thrust system near the trace of the modern Wasatch fault at several localities along its length. One possible source for this ramping may be a major basement displacements on normal faults formed along a north-trending, west-facing passive margin that developed through the region in late Proterozoic time (Stewart, 1972). Thus the Wasatch fault zone may be localized by a zone of pre-existing extensional faulting in Precambrian crystalline rocks.

ACKNOWLEDGEMENTS

The manuscript was substantially improved by critical, thoughtful reviews by Tony Crone and Tom Brocher. Discussion with Doug Sprinkel, Tim Lawton, Bill Jefferson, and Hal Morris greatly increased my understanding of the structure and tectonics of the region. However, any shortcomings of the interpretations presented here are my own responsibility.

REFERENCES

Anderson, R. E., Zoback, M. L., and Thompson, G. A., 1983, Implication of selected subsurface data on the structural form and evolution of some basins in the northern Basin and Range Province, Nevada and Utah: Geological Society of America Bulletin, v. 94, p. 1055-1072.

Arabasz, W. J., 1983, Geometry of active faults and seismic deformation within the Basin and Range-Colorado Plateau transition, central and SW Utah: Earthquake Notes, v. 54, no. 1, p. 48.

Black, B. A., 1965, Nebo overthrust, southern Wasatch Mountains, Utah: Brigham Young University Geology Studies, v. 12, p. 55-89.

Brown, R. P., and Cook, K. L., 1982, A regional gravity of the Sanpete-Sevier Valley and adjacent areas in Utah, *in* Nielson, D. L., ed., Overthrust belt of Utah: Salt Lake City, Utah Geological Association Publication 10, p. 121-136.

Burchfield, B. C., and Hickcox, C. W., 1972, Structural development of central Utah, *in* J. L. Baer and E. Callaghan, eds., Plateau-Basin and Range transition zone, central Utah: Utah Geological Association Publication 2, p. 55-66.

Cluff, L. S., Brogan, G.E., and Glass, E.E., 1973, Wasatch fault, southern position, earthquake fault investigation and evaluation: Utah Geological and Mineralogical Survey, separate publicaton, 33 p.

Crittenden, M. D., Jr., 1961, Magnitude of thrust faulting in northern Utah: U.S. Geological Survey Professional Paper 424D, p. 128-131.

Crone, A. J., and Harding, S. T., 1984, Near-surface faulting associated with Holocene fault scarps, Wasatch Fault Zone, Utah-- A preliminary report, in Hays, W. W., and Gori, P. L., A workshop on "Evaluation of regional and urban earthquake hazards and risk in Utah", August 14-16, 1984, Salt Lake City, Utah: U.S. Geological Survey Open File report 84-763, p. 241-265.

Gilliland, W. N., 1963, Sanpete-Sevier Valley anticline of central Utah: Geological Society of America Bulletin, v. 74, p. 115-124.

Hardy, C. T., 1952, Eastern Sevier Valley, Sevier and Sanpete Counties, Utah with reference to formations of Jurassic age: Utah Geological and Mineral Survey Bulletin 43, 98 p.

Heller, P. L., Bowdler, S. S., Chambers, H. P., Coogan, J. C., Hagen, E. S., Shuster, M. W., Winslow, N. S., and Lawton, T. F., 1986, Time of initial thrusting in the Sevier orogenic belt, Idaho-Wyoming and Utah: Geology, v. 14, p. 388-391.

Hutchinson, D. R., Klitgord, K. D., Detrick, R. S., 1986, Rift basins of the Long Island platform: Geological Society of America Bulletin, v. 97, p. 688-702.

Jones, T.D., and Nur, A., 1984, The nature of seismic reflections from deep crustal fault zones: Journal of Geophysical Research, v. 89, p. 3153-3171.

Jefferson, W. S., 1982, Structural and stratigraphic relations of Upper Cretaceous to Lower Tertiary orogenic sediments in the Cedar Hills, Utah: Utah Geological Association Publication 10, p. 65-80.

Kay, M., 1951, North American geosynclines: Geological Society of America Memoir 48, 143 p.

Klitgord, K. D., and Behrendt, J. C., 1979, Basin structure of the U.S. Atlantic margin _in_ Watkins, J. S., Montadert, L., and Dickerson, P. W., eds.: Geological and geophysical investigations of continental margins: American Association of Petroleum Geologists Memoir 29, p. 85-112.

Lawton, T. F., 1985, Style and timing of frontal structures, thrust belt, central Utah: American Association of Petroleum Geologists Bulletin, v. 69, p. 1145-1159.

Lawton, T. F., 1982, Lithofacies correlations within the Upper Cretaceous Indianola Group, central Utah, in Nielson, D. L., ed., Overthrust belt of Utah: Salt Lake City, Utah Geological Association Publication 10, p. 199-213.

Morris, H. T., 1983, Interrelations of thrust and transcurrent faults in the central Sevier orogenic belt near Leamington, Utah, in Miller, D. M., Todd, V. R., and Howard, K. A., eds., Tectonic and stratigraphic studies in the Eastern Great Basin: Geological Society of America Memoir 157, p. 75-82.

Okaya, D. A., and Thompson, G. A., 1985, Geometry of Cenozoic extensional faulting: Dixie Valley, Nevada: Tectonics, v. 4, p. 107-126.

Schwartz, D. P., and Coppersmith, K. J., 1984, Fault behavior and characteristic earthquakes: Examples from the Wasatch and San Andreas fault zones: Journal of Geophysical Research, v. 89, p. 5681-5698.

Smith, R. B., and Bruhn, R. L., 1984, Intraplate extensional tectonics of the eastern Basin-Range: Inferences on structural style fron seismic reflection data, regional tectonics, and thermal-mechanical models of brittle-ductile deformation: Journal of Geophysical Research, v. 89, p. 5733-5762.

Spieker, E M., 1946, Late Mesozoic and early Cenozoic history of central Utah: U.S. Geological Survey Professional Paper 205-D, p. 117-161.

Sprinkel, D. A., 1982, in Nielson, D. L., ed., Overthrust belt of Utah: Salt Lake City, Utah Geological Association Publication 10, p. 169-180.

Standlee, L. A., 1982, Structure and stratigraphy of Jurassic rocks in central Utah: Their influence on tectonic development of the Cordilleran foreland thrust belt, in Powers, R. B., ed., Geologic studies of the Cordilleran thrust belt: Rocky Mountain Association of Geologists, p. 357-382.

Stewart, J. H., 1972, Initial deposits in the Cordilleran geosyncline: Evidence of a Late Precambrian (850 m.y.) continental separation: Geological Society of American Bulletin, v. 83, p. 1345-1360.

Stewart, J. H., and Poole, F. G., 1974, Lower Paleozoic and uppermost Precambrian Cordilleran Miogeocline, Great Basin, western United States: *in* Tectonics and Sedimentation, Society of Economic Paleotologists and Mineralogists Special Publication, no. 22, W. R. Dickinson, ed., p. 28-57.

Suppe, J., 1985, Principles of Structural Geology, Prentice-Hall, Inc., Englewood Cliffs, New Jersey, 537 p.

Wallace, R. E., and Morris, H. T., 1979, Characteristics of fault and shear zones as seen in mines at depths as much as 2.5 km below the surface, *in* Analysis of actual fault zones in bedrock: U.S. Geological Survey Open File Report 79-1239.

Wheeler, R. L. and Krystinik, K. B., 1987, Segmentation of the Wasatch Fault Zone, Utah--Summaries, analyses, and interpretations of geological and geophysical data: U.S. Geological Survey Bulletin, in prep.

Witkind, I. J., 1982, Salt diapirism in central Utah, *in* Nielson, D. L., ed., Overthrust belt of Utah: Salt Lake City, Utah Geological Association Publication 10, p. 13-30.

Witkind, I. J., 1983, Overthrusts and salt diapirs, central Utah: Geological Society of America Memoir 157, p. 45-59.

Zoback, M. L., 1983, Structure and Cenozoic tectonism along the Wasatch fault zone, Utah: Geological Society of America Memoir 157, p. 3-27.

Zoback, M. L., and Anderson, R. E., 1983, Style of Basin-Range faulting as inferred from seismic reflection data in the Great Basin, Nevada and Utah: Geothermal Resources Council, Special Report No. 13, p. 363-381.

Neotectonic framework of the central Sevier Valley area, Utah, and its relationship to seismicity

By R. Ernest Anderson and Theodore P. Barnhard

U.S. Geological Survey
Denver, Colorado

ABSTRACT

Central Sevier Valley is one of the most seismically active parts of the intermountain seismic belt. Two areas of concentrated seismicity in central Sevier Valley coincide with anomalous concentrations of late Quaternary deformation suggesting a genetic relationship. Both areas contain late Quaternary fault scarps suggestive of normal faulting and microseismicity suggestive of strike-slip faulting, and each is broadly consistent with east-west extension. Both areas are located at complex structural junctures where the geometry and vergence directions of major structures show dramatic on-strike contrast. Transverse zones of structural accommodation in which stress is likely concentrated are required in both areas and probably explain the concentration of seismicity and late Quaternary deformation. Strain rates, faulting histories, rupture lengths and other deformational aspects of these zones that might be relevant to earthquake hazards assessments are not characteristic of the major structures that extend away from them and are therefore of little value in regional assessments. Geologic mapping and detailed fault-slip studies of areas directly adjacent to the areas of concentrated seismicity show that the youngest deformation is dominated by strike-slip faulting and associated folding of apparent compressional origin in one, extreme extension and structural attenuation in another, and mixtures

of strike-slip and normal faulting with or without monoclinal flexuring in still others. Thus, the areas of concentrated seismicity are not only localized at complex structural junctures they are surrounded by complexly variable neotectonic structures.

Major features of the seismicity include (1) a mixture of strike-slip and normal faulting focal mechanisms in the transition zone, (2) a predominance of strike-slip microseismal focal mechanisms with a conspicuous element of slip incompatibility, P axes of some mechanisms being parallel to T axes of other mechanisms, and (3) hypocenter frequencies that fall off sharply at depths of 5-6 km, suggesting deformation above planes of structural compensation. To explain the mechanics and kinematics of neotectonic deformation in central Sevier Valley and how that deformation relates to the neotectonic framework of the region requires not only the integration of these major features of the seismicity but also the integration of an extremely varied and complex group of structures including folds of contrasting orientation; conjugate, nonconjugate, and incompatible types of strike-slip faults, normal faults, mixtures of normal and strike-slip faults, and known or inferred attenuation-type detachment faults. These structures must be understood in the contextual framework of an extensional tectonic regime superposed on an area with a long and complex history of earlier deformation and a strong preexisting northeast-trending structural fabric. Though it appears impossible to develop a tectonic model capable of explaining all these complexities, one that seems to satisfy most has five critical elements: (1) Extensional deformaiton with σ_3 oriented approximately east-west is distributed very unevenly in space and ranges in magnitude from extreme local attenuation to mountain-size blocks with less than 5 percent internal extension. (2) Either complimentary to or in competition with the extension there is an element of lateral tectonic transport resulting either from interchanges in the position of σ_1 and σ_2 or from shear tractions applied to the base of structural blocks at a high angle to the direction of extension (aproximately north-south). (3) There is a strong element of strain gatherng by preexisting steeply dipping northeast-trending zones of structural weakness and by gently dipping mechanically weak clay-rich or evaporite-rich strata or preexisting thrust faults. The former results in zones of concentrated extension or strike-slip faulting and the latter in detachment or decoupling of the internally deformed plates. (4) Mechanically resistant structural entities such as the Marysvale volcanic pile and its plutonic root interfere with and produce internal deformation within laterally migrating thin-skinned sructural plates. (5) Facing monoclinal folds of the type bordering Sevier Valley result from extension superposed on lateral shear and resemble divergent strike-slip and oblique-slip mobile zones.

The inferred structural style of extension applied to laterally displaced blocks bounded by strike-slip faults and driven by tractions or drag on their basal detachments is consistent with seismic evidence for strike-slip faulting, slip incompatibility, and hypocenters above distinct planes of structual compensation. Because the deformational style is basically thin skinned detachment, the potential for large earthquakes on faults in the upper plate is low. Our recognition that some of the largest and youngest exposed faults in the area are strike-slip faults does not significantly increase seismic hazard above that which would be estimated for normal faults. Normal faults such as the Sevier fault, because they bound 15- to 20-km-wide blocks that are uniformly tilted, probably cut one or more levels of potential structural detachment and penetrate to the base of the seismogenic part of the crust. Such faults are more likely to be the source of infrequent large earthquakes than are faults in the complex structural junctures where late Quaternary deformation is concentrated.

INTRODUCTION

The central Sevier Valley study area is located in the High Plateaus subprovince of the Colorado Plateau in a structural and physiographic transition zone between the Basin and Range on the west and the Colorado Plateaus on the east (fig. 1). The area straddles the intermountain seismic belt (ISB) as shown in figure 2. Though most of the study is focused in the central Sevier Valley, the study extends westward to Dog Valley (fig. 3).

This report has a threefold purpose: (1) to present the results of a study of fault-slip characteristics and associated folding in the central Sevier Valley area, (2) to interpret those results in the context of the diverse structural history and historic earthquake record of the region, and (3) to evaluate their relevance to the neotectonic framework and their impact on earthquake hazards. The initial scope of the investigation was to search for geologic evidence of strike-slip faulting in areas where W. J. Arabasz and his students from the University of Utah had provided us with advance reports of earthquakes with a strike-slip mode. The search was successful and it is now clear that the geologic record contains abundant evidence of Neogene (includes Pleistocene and Holocene as used herein) late Cenozoic strike-slip faulting in the region. The success of our search (Anderson and Barnhard, 1984, 1985) resulted in expanding the scope to include a synthesis of Pliocene-Pleistocene deformation in the area. The range margins along the central Sevier Valley were examined for geologic evidence of late Tertiary and Quaternary deformation, and we herein integrate those findings with our earlier results.

FIGURES 1, 2, and 3 FOLLOW TEXT

Fault-slip data were collected from parts of the Pavant Range, Tushar Mountains, Antelope Range, Sevier Plateau, and Sanpete-Sevier anticline, all of which flank the Sevier Valley (fig. 3). The comprehensiveness of our investigation varies greatly from area to area. Accordingly, only a general description of fault slip is given for some areas, quantitative fault orientation and fault-slip data are given for others, and a comprehensive account of paleoslip, and where the data are sufficiently coherent the results of paleostress analysis are given for still others. Only from the Clear Creek area do the fault-slip data provide paleostress results that can be confidently related to mapped structural patterns. However, data from the other areas provide valuable insight into the distribution of strike-slip faulting as well as an opportunity for qualitative comparison with the results from the Clear Creek area.

A long and complex structural history has been recognized in the study area. It includes compressional thrusting and folding and related foreland deposition ranging in age from latest Jurassic to Paleocene (Standlee, 1982), block uplift and basin formation of Paleocene and Eocene age (Stanley and Collinson, 1979), igneous activity and associated intense volcano-tectonic activity of Oligocene and Miocene age (Rowley and others, 1979), basin development and associated sedimentation of late Miocene age (Callaghan and Parker, 1962, Rowley and others, 1979), and the Pliocene-Pleistocene deformation, volcanism, and landsliding that have shaped some of the most conspicuous structural and physiographic features of the area. Though it is the last part of this structural history that is of central importance to this study, the possible influence of old structures on young structures must be considered. We therefore include a section on structural history and setting in which we review what is known about the early deformations--especially those events that left a major imprint on the structural fabric of the area.

We do not discuss the stratigraphy or provide detailed information about the lithology of the deformed rocks. The stratigraphic sequence is summarized in figure 4.

FIGURE 4 FOLLOWS TEXT

ACKNOWLEDGEMENTS

We are grateful to Walter Arabasz for providing us with prepublication drafts of reports in which the ocurrence of strike-slip focal mechanisms in cental Sevier Valley was highlighted, and for taking the time to visit us in the field. Field visits by Grant Willis and Peter Rowley helped us understand some stratigraphic relationships. We thank Jacques Angelier for providing us with computer programs for paleostress analysis, Mary Lou Zoback for help in using the programs, and Steve Harmsen for help in developing computer graphics. The report was improved substantally as a result of critical reviews by Dwight Schmidt and Peter Rowley.

PROCEDURE

Field procedure for this study consisted of measuring the orientation of fault surfaces and movement-related striae on those surfaces and determining the slip sense for motions parallel to those striae. These fault measurements were made in specific small sample areas within the Sevier Valley study area. Each sample area is either named for a nearby geographic locality or identified by a locality letter (fig. 3). In the absence of evidence to the contrary, the striae are assumed to represent the youngest deformation on a fault. On some faults, polyphase slip is indicated by two or more sets of striae, and for some of these sets it is possible to determine their sequence of development. The sequential aspects of faulting can also be determined by studying fault intersections or by inferring the angular relationship that faults of contrasting orientation and slip make with bedding-tilt directions. The data are classified according to the displacement amount and the certainty with which the sense of slip was determined. Data analysis consists of a preliminary separation into faulting mode, with faults whose rake angles exceed 45° separated into a dip-slip mode and those less than 45° into a strike-slip mode. For most data sets, oblique-slip faults are relatively uncommon so computations can be performed without treating them separately. Paleostress orientations and various paleostress parameters are computated utilizing methods similar to those described by Angelier (1979) and are performed on data representing both strike-slip and dip-slip modes.

Displacement amount in this report is classified as follows: small-displacement faults have known or estimated offsets from a few centimeters to a few meters, large-displacement faults have known or inferred displacements greater than 30 m, and the remainder are referred to as intermediate-displacement faults. Many of the large- and intermediate-displacement faults are shown on figure 3, small displacement faults cannot be shown at the scale of figure 3. In each of the sample areas investigated, we attempted to determine the orientation and sense of slip on mapped faults. This strategy leads inevitably to gathering large amounts of data from small faults with small displacement, and this report is based in large part on data from these small-displacement faults.

Three large-displacement north- to norhteast-striking faults were previously named and interpreted as normal faults--Sevier, Dry Wash, and Elsinore (Callaghan and Parker, 1961, 1962; Cunningham and others, 1983). Of these, only the Sevier and Dry Wash faults are shown on figure 3. Except for the southern part of the Dry Wash fault, these two faults are buried by range-flanking alluvium. The strategy used to evaluate slip characteristics of the large-displacement faults is to search for clues on small- and intermediate-scale faults in the bedrock adjacent to the large faults.

Large-displacement faults in a sample area possibly reflect stress states of a different vintage, more fundamental rank or order, more regional extent, or more deeply penetrating tectonic realm than do small-displacement faults. Because of these possibilities, in each sample area where paleostress studies are conducted, small-displacement faults must be determined to have orientations and slip characteristics similar to those of large-displacement faults. To do this, two separate computations are generally performed--one on the raw data and one on data that are weighted according to the amount of displacement on each fault as described by Angelier and others (1985). The numerical weights given in table 1 represent a crudely logarithmic scale from 1 to 9 with category-1 displacements less than 10 cm or unknown and category-9 displacements greater than 100 m. Because exposures of large faults are uncommon in nature, most data sets reported herein consist only of small-displacement faults or contain a very small sample of larger faults, thus precluding a direct evaluation of the effect of fault size on paleostress. As an exception, however, slip data gathered from many moderate- and large-displacement faults in the Clear Creek area provide an excellent opportunity to test for the effect of fault size on paleostress. The test shows no significant shift in position of the paleostress axes or quality of the limited tensor (table 1). Paleostress computations using data from sample areas where only small faults were found yield results similar to those using the Clear Creek data, suggesting that fault size is not an important factor in determining paleostress in the central Sevier Valley study area.

TABLE 1 FOLLOWS TEXT

STRUCTURAL HISTORY AND SETTING

The oldest structural feature in the study area is the Cordilleran hingeline that separates upper Precambrian to Triassic Cordilleran miogeoclinal rocks on the west from platform-facies rocks on the east (Armstrong, 1968; Burchfiel and Hickcox, 1972). Though the hinge, probably initially a zone several tens of kilometers wide, is tectonically and depositionally covered in the study area by thrusts and sediments, it probably trended northeasterly through the area and could have exerted a control on subsequent fold and thrust structures. Deposition in the miogeocline was interrupted by compressional deformation of the Sevier orogeny possibly as early as latest Jurassic and extending through late Cretaceous (Campanian) (Armstrong, 1968). The northeast-trending Pavant thrusts shown in the western part of the Pavant Range (fig. 3) were formed during this compressional deformation. The principal compressional structure is a thrust-faulted recumbant fold formed in the Paleozoic miogeoclinal or shelf carbonate rocks and Mesozoic clastic rocks. Associated tear faults suggest thrusting to the southeast (Davis, 1982). A total of 10 km of displacement is inferred for the exposed thrusts (Baer and others, 1982). A buried thrust of unknown displacement is inferred beneath the Pavant thrust at a depth of 4-5 km from seismic reflection data referred to by W. J. Arabasz and B. R. Julander (in prep.). On the basis of drill-hole data, thrusts and folds that developed during the Sevier orogeny are interpreted to extend east of the Pavant Range beneath Sevier Valley and probably beneath the northernmost Sevier Plateau (Standlee, 1982). They may also extend southward beneath the thick volcanic cover of the Tushar Mountains but that is less certain (Richard Kennedy, oral commun., 1984; T. A. Steven, oral commun., 1985).

The folds and thrusts of the Sevier orogeny were erosionally truncated and depositionally overlain by thick continental clastic and chemical (lacustrine) strata and some marine strata ranging in age from latest Cretaceous (Price River Formation, Speiker, 1946) through late middle Eocene (Green River Formation, Willis, 1985) to late Eocene (Crazy Hollow and Bald Knoll Formations, Willis, 1985). The distribution and depositional history of the latest Cretaceous through early Eocene strata in the region reflect the trend and location of the Cordilleran hingeline and the Sevier fold and thrust belt but are considered by some to be post-orogenic (Stanley and Collinson, 1979). Conglomeratic and other coarse clastic facies in these strata are related, instead, to localized uplifts resembling those of the Laramide orogeny. In central Utah, and especially along the Sanpete and Sevier Valleys, many deformational events, some perhaps very localized, were spread over much of the latest Cretaceous through late Eocene depositional interval (Spieker, 1949, Gilliland, 1963, Standlee, 1982). The regional state of stress accompanying this "post-orogenic" deformation is not obvious. A long-standing controversy concerns the relative roles of vertical tectonics versus compressional tectonics in shaping early Tertiary structures in much of central Utah (see Witkind, 1982, and Standlee, 1982 for dramatically differing interpretations). The area of controversy extends southward into central Sevier Valley at least as far south as Richfield (fig. 3). Structural trends involved are predominantly northeast and thus parallel the Cordilleran hingeline as well as the Sevier thrust front-foreland boundary. The potential for influencing young structural patterns via inheritance is high in this area.

The late Eocene Crazy Hollow and Bald Knoll Formations (fig. 4) contain lithologic evidence of syndepositional volcanism probably to the north of the area of figure 3 (Willis, 1985). As part of the province-wide southerly progression of mid-Tertiary volcanism (Stewart and others, 1977) the Tushar Mountains area became the locus of major volcanic activity beginning about 35 Ma ago (the Marysvale volcanic field of Rowley and others, 1979). Airfall tuffs in the Dipping Vat Formation in the central Sevier Valley dated isotopically at 34.2 Ma apparently record volcanism that occurred in the Marysvale field in the southern part of and south of the area of figure 3 (Willis, 1985). The calc-alkaline volcanic rocks of the Marysvale field--mostly lava flows, volcaniclastic sedimentary rocks, and ash-flow tuffs--thin northward through the area and lap onto lower Tertiary and pre-Cenozoic sedimentary rocks (fig. 3). They range to as young as 16 Ma (Rowley and others, 1979). Volcano-tectonic structures such as domes, sags, and caldera walls related to their eruption are recognized in the southern part of and south of the area covered in figure 3 (Cunningham and others, 1983). Those structures are largely or completely older than the faults we studied, and we therefore do not show their outlines on figure 3.

Neogene deformation that included faulting and folding occurred along the flanks of the Sanpete-Sevier anticline form Glenwood northeastward (Spieker, 1949; Gilliland, 1963) contemporaneously with and outlasting the volcanism. The paleostress conditions that existed during this Neogene deformation are as uncertain as those that deformed the same area on similar trends during the early Tertiary. Gilliland (1963) studied the part of the anticline that extends into the area we studied (from Glenwood to Salina, fig. 3). He suggested that it formed no later than during upper Cretaceous time under lateral compressional stresses and that those stresses played a role in its long history of deformation, presumably extending well into the Neogene.

The southern Pavant Range is separated from the structurally elevated volcanic edifice of the Tushar Mountains to the south by a broad open east-trending synclinal sag named the Clear Creek downwarp (fig. 3) by Callaghan and Parker (1962). The youngest stratigraphic unit that appears to be fully involved with the formation of the downwarp is a 19-Ma ash-flow tuff, the Joe Lott Tuff Member of the Mount Belkamp volcanics (Callaghan and Parker, 1962; Stevens and others, 1979). That unit crosses the downwarp with no conspicuous thickening in the axial part of the downwarp. It exhibits almost 2 km of structural relief where it crosses the downwarp (Callaghan and Parker, 1962), and we assume that to be an approximation of the magnitude of downwarping.

Between 16 and 14 m.y. ago conditions in the south part of the area changed from predominantly volcanic to basin-fill sedimentation (Callaghan and Parker, 1962, Steven and others, 1979). Callaghan and Parker referred to the sediments as Sevier River Formation, and their general distribution is shown on figure 3. These strata range from basin-margin coarse conglomeratic facies to basin-medial silt and clay and are as young as 5.6 Ma on the basis of a K-Ar age from a tuff bed exposed east of Annabella (H. H. Mehnert and P. D. Rowley, written commun., 1982).

The Clear Creek downwarp may have influenced the depositional history and distribution of the Sevier River Formation, but to a large extent those strata are involved in the downwarping and in subsidiary parallel folding on the south flank of the downwarp (fig. 3).

Over a stratigraphic interval of several tens of meters, the middle part of the Sevier River Formation directly southwest of Joseph Flats contains an upward transition from pale salmon fluvial coarse to medium sand and gravel to a sequence of pastel yellowish-gray and yellowish-green fluviolacustrine beds. A strikingly similar transitional sequence is exposed 30 km northeast in the area south of Glenwood, suggesting deposition in a single basin of unknown size or shape. In neither area does the lithology of the transitional sequence suggest close proximity to a rising mountain flank. The paleogeographic implication is that neither the Pavant Range, Sevier Plateau, nor the Sevier Valley existed when those beds were deposited. The tectonic implication is that the present system of structurally controlled mountains and valleys had not yet formed, and, by our definition, the neotectonic realm had not yet begun.

Because the Sevier River Formation represents the youngest well-exposed deformed strata in the area, we concentrated much of our study on the neotectonic structures that deform them. We emphasize that the basalt-rhyolite Black Rock volcanics in the western part of the study area are generally younger than the Sevier River Formation and are highly faulted (Clark, 1977), but they provide little opportunity for gathering fault-slip data and have not been studied for this report.

The study area is located in the structural transition zone between the Basin and Range and Colorado Plateaus provinces--a location that we infer is fundamental to any understanding of neotectonic deformation. Three major transition-zone faults are reported in the area. The Sevier fault, with a conspicuous zigzag trace and an overall northerly trend, separates Sevier Valley from the uplifted Sevier Plateau. The fault is one of several major plateau-margin faults between which approximately 30-km-wide structural blocks are tilted gently eastward within the regional extend of the transition zone. The Dry Wash fault strikes northeast and is located at the northwestern base of the topographically subdued northern part of the Antelope range from where it extends southwestward into the northern flank of the Tushar Mountains. Callaghan and Parker (1961, 1962) and Cunningham and others (1983) map it as a normal fault in that area. As it is traced to the southwest, striations on it show that it is chiefly a sinistral strike-slip fault. The third major fault (not shown on fig. 3), the Elsinore fault, is essentially a northeast extension of the Dry Wash fault. Callaghan and Parker (1961) map it as a major buried northeast-trending normal fault separating Sevier Valley from the Pavant Range in the Elsinore area.

Rowley and others (1979) concluded that the major faulting in the Clear Creek downwarp took place after 7 Ma and Rowley and others (1981a) concluded that the main uplift of the Sevier Plateau (about 1.5 km) took place in less than 2.5 m.y. between 7.6 and 4.8 Ma. Anderson and Bucknam (1979) noted fault scarps of probable late Pleistocene age along the Sevier fault near Anabella and along the Elsinore fault near Elsinore. Callaghan and Parker (1961) noted that Quaternary river terraces northeast of Joseph appear to be tilted eastward by displacement on the Dry Wash fault. Thus, the major faulting probably extends from latest Miocene through Pleistocene.

RESULTS FROM FAULT-SLIP SAMPLE AREAS

Presentation of results of our fault-slip studies is arranged geographically in sample areas and begins in the Clear Creek downwarp where we collected our most homogeneous and interpretable data. The next sample areas discussed are located northward along the east margin of the Pavant Range where we have evidence of diachronous Neogene deformation, then eastward to the margin of the Sevier Plateau where our study relies heavily on minor structures, and from there northeastward along the Sanpete-Sevier anticline where Neogene rocks are mildly to strongly tilted. We present last the results from a reconnaissance in the northern Antelope Range where we collected our most inhomogeneous and uninterpretable data.

CLEAR CREEK DOWNWARP

Field studies of exposed structures were made in four sample areas along the Clear Creek downwarp. The easternmost is referred to as the Clear Creek sample area containing the specific locality A (fig. 3). Westward other sample areas are designated B through D (fig. 3).

In the Clear Creek sample area, deep erosion by Clear Creek and its tributaries has produced excellent exposures of the Joe Lott Tuff Member and overlying Sevier River Formation. Callaghan and Parker (1962) mapped several upright open east-trending folds in those rocks on the south flank of the downwarp. These folds have very narrow hinge zones, amplitudes of about 200 m, and wavelengths of about 2 km (cross section, fig. 3). Callaghan and Parker (1962, 1961) also mapped several northeast-striking faults, the largest of which is the Dry Wash fault. The Dry Wash fault is a critical structure because the Clear Creek downwarp and the subsidiary folds on its south flank terminate against it showing a genetic and mechanical interrelationship between folding and faulting. Our study shows that where it cuts the axis of the Clear Creek downwarp the Dry Wash fault has major sinistral slip, as indicated by common subhorizontal striations and corrugations and the geometry and stratigraphic position of rock slabs that are distributed along it (fig. 5). Net displacement on the fault in that area could be several kilometers on the basis of structural and stratigraphic terminations (Cunningham and others, 1983) and stratigraphic contrasts across it (T. A. Steven, oral commun., 1983). In the vicinity of Joseph Flat it has important dip-slip displacement. Directly northwest of the Dry Wash fault, two additional northeast-striking map-scale faults display abundant evidence of sinsitral slip and have net slip of as much as 1 km (fig. 6, 7). Some of their displacement is probably accommodated by the east-trending folds that are located near their southwestern terminations (fig. 3).

FIGURES 5, 6 and 7 FOLLOW TEXT

The east-trending folds also are cut by many small-displacement steep strike-slip faults many of which are well exposed in cliffs held up by the Joe Lott Tuff Member (fig. 8). In the welded ash-flow tuffs of the Joe Lott, many of these faults utilized preexisting cooling joints and represent displacements of a few centimeters or less. Detailed study of 81 of these faults in axial and opposed-limb positions in the folded Joe Lott Tuff and Sevier River Formation show that they comprise northeast-striking sinistral (N=33) and northwest-striking dextral (N=48) sets that (1) offset one another, (2) have broad ranges in strike with no overlap, and (3) contain striations whose rake angles are independent of position on the fold (fig. 9). These relationships indicate that the sinistral and dextral sets are conjugate. Mohr-Coulomb theory (Anderson, 1951) would predict that they formed under conditions of north-south compression. The relationship of their striae to position on the folds (fig. 9) suggests that the last motion on them occurred late in the folding history or perhaps after folding.

FIGURES 8 AND 9 FOLLOW TEXT

We also identified sparse small-displacement dextral faults adjacent to the sinistral Dry Wash fault. They have the same range of strike as those that cut the folds, and exhibit similar mutually offsetting characteristics with the larger displacement sinistral faults of the Dry Wash system. These small dextral faults are clearly synthetic to the Dry Wash fault.

Fault-slip data were gathered from 209 faults in the Clear Creek sample area. The determination of sense of slip is classified as certain or probable on 89 percent of the faults and 16 percent of the faults have displacements of a meter or more. The sample is large but by no means represents all faults in the sample area. We arbitrarily omit data from a northeast-striking oblique dextral fault zone southwest of Joseph Flats (specifically at locality A, fig. 3) because the slip sense is obviously discordant to that of the other northeast-trending faults in the area. The possible structural significance of the oblique-dextral fault at locality A is discussed in the second paragraph below. For the 209 faults, dips are distributed in a remarkably tight, steep pattern (fig. 10) and rakes show a strong bimodal distribution with a predominance of low values (strike-slip faulting). Strikes show a bimodal distribution with a complete separation of dextral and sinistral fields. The separation would, of course, be incomplete if data from the omitted dextral fault were included. The bimodal rake distribution provides a rationale for separating the data into strike-slip and dip-slip subsets for computational purposes. For the strike-slip subset, north-south maximum compressive stress is indicated (fig. 10) consistent with the stress state inferred for the east-west folds and the small faults that cut them. The value for Φ of 0.16 suggests that σ_1 is well constrained and σ_2 and σ_3 are moderately well constrained. Mapped structures show that the deformation is strongly asymmetric and dominated by sinistral slip on northeast-striking faults and by folding. The analysis of small-displacement faults does not explain the strain asymmetry but shows that it is consistent with north-south compression.

FIGURE 10 FOLLOWS TEXT

Dip-slip striations were measured on 60 small-displacement faults in the Clear Creek sample area (fig. 10). Five of these faults show evidence of polydirectional slip. Of those, the dip slip is younger than the strike slip on three and older on two. Thus, no evidence is provided for a temporal separation of strike-slip and dip-slip faulting.

Dip-slip faults that dip greater than 80° and less than 20° are not as compatible with a normal faulting regime as are those with dips between 80° and 20°. Also, faults with moderate and shallow rake angles are not likely to contribute as much to extensional deformation as are faults with steep rakes. In order to test the importance of normal faulting in the Clear Creek sample area we eliminated steep- and shallow-dipping faults and those with moderate and shallow rakes and computed the paleostress characteristics from the remaining data (31 of the original 60 faults). We do not report the computational results because they do not reflect a lessening of angular discordance between the measured striae and the theoretical maximum shear stress nor does the value of Φ (0.05) indicate a significantly better-constrained σ_3 axis than that computed from all dip-slip data (0.04, table 1). We conclude from these relationships, together with the overwhelming evidence that in the Clear Creek area the dominant faulting mode is strike slip, that dip-slip faulting in the area is not of first-order structural significance. Alternatively, the dip-slip faulting may provide weak evidence of a temporal interchanging of σ_1 and σ_2 in a field with σ_3 oriented east-northeast to east-west and dominated by north-south compression.

The northeast-trending oblique-dextral fault at locality A (fig. 3) that is eliminated from the Clear Creek area computations dips 80°-85° southeast, is sharp and planar (fig. 11), and juxtaposes contrasting facies of basin-fill sediments of the Miocene-Pliocene Sevier River Formation (Callaghan and Parker, 1962). It strikes transverse to bedding which dips 20°-30° northeast (figs. 11, 12). Stratigraphic offset and sense of drag show that throw is down to the southeast, and the net displacement is more than 100 m. Fault-slip data were collected from the main fault and 16 additional northeast-striking surfaces with displacements as little as 20 cm. The main fault and adjacent small-displacement faults presumably constitute a single fault zone. Twelve of the 17 faults have a dextral-slip component and 11 of those plot within 30° of the pole to bedding (fig. 12). This predominantly oblique dextral slip probably represents the principal displacement on this fault zone. Because the slip direction is consistently about parallel to the pole to bedding, the striae on the fault planes presumably was caused by rotation of a fault block containing the tilted beds. This can be called a block-boundary displacement related to stratal tilting and not directly related to paleostress. For this fault zone the data set does not meet the criterion of independence required for the paleostress inversion procedure (Angelier, 1979). However, not all of the data are consistent with such an interpretation. Five of the northeast-striking minor faults have sinistral-slip components that suggest an incompatible element of slip in the fault zone. Similar slip incompatibility is seen in other fault-slip data samples from the central Sevier Valley study area and suggests that slip incompatibility is a common feature. It could be related to block motions driven by a system of tractional forces applied to the base of the blocks.

FIGURES 11 and 12 FOLLOW TEXT

At sample area B (fig. 3) sedimentary strata of the Sevier River Formation are down faulted to the east against Miocene ash-flow tuffs on a well-exposed striated surface with a local attitude of 345°, 72° NE (fig. 13). An average rake of about 90° indicates normal faulting. Over a distance of 5 km to the north along the same fault zone striae on 19 subparallel subsidiary faults have rake angles that range from 68° to 90° and average 82° and provide confirmation that the last major movement on this fault zone is normal dip slip. South of locality B, bedrock in the footwall block is cut by numerous striated small-displacement faults exhibiting dextral slip with rake angles as low as 3°. One of those fault surfaces contains intersecting striae indicating both dextral and normal displacements of which the normal motion is the youngest. These relationships suggest that rocks in this fault zone experienced an early episode of Neogene strike-slip displacement, but that the youngest and principal displacement is dip slip.

FIGURE 13 FOLLOWS TEXT

At sample area C, several roadcuts along a 1.5-km stretch of Interstate 70 (I-70) provide good exposures of transversely faulted Oligocene and Miocene volcanic and sedimentary rocks. The faulted rocks consist of tuffaceous sandstone and gravel, sandstone and cobbly sandstone of probable fluvial origin, ash-flow tuff, and dacite and andesite flows. They dip east to southeast 15°-30° and are cut by numerous steep northeast-striking faults. At and around locality C, bedding repetition and physiography suggest simple normal faulting (Cunningham and others, 1983), but the fault-plane striae tell a much different story. Slip orientations and senses were measured on 20 faults ranging in displacement from about 20 cm to more than 100 m. One fault strikes north and is dextral. The remaining 19 faults strike northeast; 17 of these are sinistral and two are normal (fig. 14A). The degree of certainty of the sense of slip was determined as certain on 14 and probably for the remainder of the faults. The large-displacement faults have gouge zones as wide as 50 cm. The gouge has a strong internal shear fabric whose geometry and orientation are consistent with the orientation and sense of displacement measured on the planar walls of the shear zone, suggesting an unusually high degree of uniformity of fault motion. Eight of the 20 faults have measured or estimated displacements of 10 m or more. The cumulative displacement is not known but could easily be more than 1 km. These excellent exposures show that fault deformation along the 1.5 km of cross-strike distance is predominantly on northeast-striking sinistral faults and that no significant difference exists between the slip on large- and small-displacement faults. The contrast in paleoslip of the youngest observed striae between sample areas B and C is dramatic.

FIGURE 14 FOLLOWS TEXT

Sample area D is along the northbound and southbound lanes of I-15 about 6 km north of the junction with I-70; this area is a few kilometers west of the Basin and Range boundary. Roadcuts along I-70 expose strongly fractured Oligocene volcanic rocks which strike west-northwest and dip gently south-southwest. The average strike of faults in the area is 015° (Cunningham and others, 1983). Because the faults strike at a high angle to the strike of the beds, the faults are either unrelated to and presumably younger than the stratal tilting or are transverse block-bounding structures that were active during stratal tilting. In either case, we infer that the youngest movement on these faults is late Quaternary because the faults are coextensive with faults that cut nearby volcanic rocks dated radiometrically at about 0.5 Ma (Steven and Morris, 1983; Best and others, 1980). The amount of displacement on an individual fault is not known but is assumed, on the basis of fracture appearances, to range from a few centimeters to a few meters. Steven and Morris (1983) map a fault striking 045° along I-15 between the two roadcuts, and unpublished mapping by one of us (R. E. Anderson) shows that the rocks in the eastern cut are displaced in an oblique sinistral sense at least 150 m relative to the rocks in the western cut. The orientation and sense of slip were measured on six faults in the eastern cut and nine in the western cut. These faults, which range in strike from 345° through 0° to 085° and in dip from 28° to 85°, are probably representative of the range of principal fault orientations near the cuts. Polyphase slip is indicated on 4 of the 15 faults we studied. Of the 15 faults, 3 northward-striking ones are predominantly dextral, 9 northeastward-striking ones are predominantly sinistral, and the remaining 3 show a predominance of dip slip (fig. 14B). These faults, inferred by us to reflect neotectonic deformation, are similar to those in the Clear Creek sample area because they display a mixture of strike slip and dip slip with a preference for sinistral strike slip on northeasterly striking planes. They indicate that the style of faulting in the Clear Creek area extends westward into the Basin and Range. A limited stress tensor computed from the 15 faults (using the youngest motions on those with two sets of striae) is shown on figure 14B.

In summary, our study of four sample areas along the Clear Creek downwarp on both sides of the boundary between the Basin and Range and transition zone illustrates that the neotectonic deformational mode differs greatly from the extensional mode generally assumed for the late Cenozoic deformation in this part of Utah. In two of the four sample areas we studied, if it were not for highway-related excavations neither the presence nor predominance of young compression-related structures would be known. One of these areas is, at first glance, an excellent structural and physiographic candidate for simple late Cenozoic extension. A high probability of error exists for determining the sense of slip of faults shown on geologic maps of this region unless specific data on the orientation and sense of slip are available. In particular, we suspect that several faults mapped as scissors faults in nearby parts of the Pavant Range, Tushar Mountains, and Sevier Plateau (see Cunningham and others, 1983, for example) are actually faults with a high proportion of strike-slip displacement and that the scissors mode is an apparent feature arising from juxtapositioning of strata that are gently to moderately deformed prior to strike-slip faulting. Nevertheless, we emphasize that late Cenozoic dip-slip faulting does exist in the Clear Creek area, and we describe a good example at and north of sample area B. Also, in a highway excavation near Cove Fort at least 20 m of late Pleistocene dip slip is indicated on the principal east-bounding normal fault of the Cove Fort graben (Anderson, 1980). The presence of dip-slip faults, some of large displacement, intermixed with strike-slip faults of similar orientation suggests that paleostress was not distributed homogeneously in time or space or both.

Studies along the Clear Creek downwarp show that strike-slip faulting is genetically and mechanically associated with east-trending folds whose axes parallel that of the downwarp. Faults and folds in this area give the appearance of having formed in response to late Miocene and (or) younger subhorizontal maximum compressive stress oriented approximately north-south. Because sinistral slip on northeast-striking faults dominates, the overall displacement of blocks bounded by these faults is southwesterly, and, if the entire fault system could be imagined to be simultaneously active, the result would be a positive velocity gradient from east to west. The integrated fault-fold system in the eastern part of the Clear Creek downwarp probably reflects a resistance to this southerly motion by the buttressing effect of the enormous Marysvale volcanic field and its plutonic root that is inferred from gravity modeling (Halliday and Cook, 1980). Structures produced by such a resistance could appear to result from simple, local north-south compression.

Structures along the Clear Creek downwarp may have resulted from a thin-skinned deformational mode because available geologic maps provide no evidence that the large cumulative horizontal deformation in the downwarp can be projected northeast along strike into the pre-Cenozoic rocks of the Pavant Range. The apparent dramatic Neogene strain contrast between the two areas of contrasting rock types requires some form of structural detachment at a stratigraphic level near the base of the Neogene volcanogenic sedimentary rocks. Detachment would also explain the strong contrast in faulting mode northeast and southwest of Richfield noted in a subsequent section. We infer low-angle fault detachment with the traces of main faults largely masked by the large areas mapped as landslide at or near the contact between the Neogene volcanic rocks and older rocks in the Pavant Range (fig. 3). Within the landslides southwest of Richfield we recognize major attenuation of stratigraphic sequences above the Flagstaff Formation. We suspect that much of the attenuation there and to the southwest results from tectonic processes that left the area highly susceptible to landsliding or is simply the direct result of landsliding. One possible interpretation is that the Clear Creek downwarp, with its structural relief of about 2 km, provided the gravitational potential for producing the detachment and southward sliding, whereas the volcanic-plutonic Tushar complex served to buttress the southerly motion of the detached mass, thereby producing the east-west folds and associated faults. This interpretation embodies the unlikely gravitational transport of rocks across the axis of the downwarp where they crumpled into folds on the south limb (cross section, fig. 3). In a second possible interpretation, the south- and southeast-directed transport results from subhorizontal shear tractions applied to the base of the block at some unspecified depth. This possibility is developed more fully in the summary and conclusions.

PAVANT RANGE

The folds and thrusts of the Sevier orogeny in the southern Pavant Range are onlapped along a northeast-trending uncomformity by southeast-dipping fluvial, lacustrine, and volcanic rocks ranging in age from Paleocene to Oligocene (Callaghan and Parker, 1962; Hickcox, 1971). The southeastward dip of the unconformity, of the strata above the unconformity, and of the Pavant thrust beneath the unconformity is caused by southeastward rotational uplift of the Pavant Range block during Neogene time. Concentration of maximum uplift along the west side of the range may result from structural rebound associated with tectonic unloading in the breakaway zone of the west-vergent late Cenozoic Sevier Desert detachment fault (Almendinger and others, 1983; Wernicke, 1985). Map-scale high-angle faults are conspicuously sparse in the western part of the range (fig. 3) suggesting that the block remained intact during uplift and tilting. We conducted a reconnaissance study of the slip characteristics of large- to small-displacement high-angle faults and measured numerous stratal attitudes along the eastern flank of the range. For purposes of discussion, the results from the northern and southern part of the eastern flank are presented separately, with the division made approximately at the latitude of Richfield (fig. 3). This division has structural significance because north-northeast of Richfield vertical displacement of the Pavant Range relative to Sevier Valley was accomplished by a combination of monoclinal flexing and normal faulting whereas south-southwest of Richfield we recognize no evidence of range-bounding normal faulting.

PAVANT RANGE BETWEEN JOSEPH FLAT AND RICHFIELD

The Pavant Range between Joseph Flat and Richfield consists of ash-flow tuff and lava flows of Oligocene age sandwiched between variegated sandstone, siltstone, shale, and limestone below and basin-fill clastic strata belonging to the Sevier River Formation above. Structural complications make it difficult to assess stratigraphic thicknesses but the volcanic rocks are at least 400 m thick. Their stratigraphic relationship to regionally distributed volcanic rocks is shown by Cunningham and others (1983). Callaghan and Parker (1961) show that the structure of this part of the range is a northeast-trending syncline-anticline pair in the area south of the latitude of Elsinore grading toward Richfield into a single east-southeast-facing monocline. In detail, the structure is complex and includes a few small-scale folds and many previously unmapped faults. To document it adequately would require detailed mapping at a scale of no less than 1:12,000. Our approach, instead, was to measure many stratal, fault, and striation orientations, record them on aerial photographs, and use the photogeologic compilation as an adjunct to interpreting the published geologic maps. The abundant small structures are too small to depict in figure 3. Instead, figure 3 emphasizes the anticline-syncline pair and southeast dips in the monocline. Figure 3 shows, as does the map of Callaghan and Parker (1961), that the Miocene-Pliocene Sevier River Formation is involved in the folding.

The complex structure of the Joseph Flat to Richfield segment of the range flank led Cunningham and others (1983) to depict it as dominated by the effects of landsliding. Though landsliding is a factor in shaping the complexity, we conclude that most of it is caused by at least two superposed episodes of deformation, each including faulting and stratal tilting.

Data gathered from 59 intermediate and small-displacement faults (fig. 15) show that most have moderate to steep dips and strike north to northwest. Their strikes are transverse or acute to that of the range margin which trends about N. 35° E. Directly west and northwest of Elsinore ash-flow tuffs correlated with the Needles Range Group of Oligocene age (Steven, 1979) strike chiefly northwest and are repeated by numerous northwest-striking faults. The average angle between bedding and faults is about 90°, suggesting that the faults formed as tension fractures before the strata were tilted. Most fault-plane striae show dip slip. The tension fractures were probably reactivated as normal faults and were rotated as the beds rotated similar to the faulting history described by Angelier and Colletta (1983). The exposed bedding and fault pattern suggests northeast-southwest extension. Some striae on these same faults or on parallel faults have low-angle rakes, possibly suggesting late-stage reactivation as strike-slip faults. In Flat Canyon directly north of Elsinore (locality G, fig. 3), the Bald Knoll Formation of late Eocene age is cut by conjugate sets of northwest-trending normal faults with a symmetry axis normal to bedding. These faults also suggest northeast-southwest extension. These strata are also cut by steep north- and northeast-trending strike-slip faults (fig. 16), some of which have large displacements, and by small-displacement reverse faults that offset the conjugate normal faults. The reverse faults are apparently associated with east tilting of the early conjugate normal faults. We infer that the north to northeast-striking strike-slip faults formed in response to the same forces that produced similar faulting in the Clear Creek sample area and at sample area C described on earlier pages (see also fig. 16). We also infer that these faults postdate the early normal faulting in the area. This inference is strongly supported at a few localities between Joseph Flat and Richfield where fault-tilted northwest-striking strata can be traced to the edge of the range where they bend sharply into the southeast-dipping monocline and strike northeast--indicating that the monocline is superposed on the previously block-faulted strata. This superposed deformation is reflected in figure 17 by the concentration of northwest-plunging poles to bedding. Also, the northeast- and southwest-plunging poles to bedding do not lie along a vertical northeast-striking plane (fig. 17). Instead, they are displaced slightly to the northwest probably as a result of superposed moderate southeast tilting in the monocline.

FIGURES 15, 16, and 17 FOLLOW TEXT

Several faults in the Joseph Flat to Richfield sample area have striae with a bewildering variety of rake angles and polyphase slip. Qualitative analysis of the oblique-slip and strike-slip motions on similarly oriented faults shows slip incompatibility. The data are not uniquely consistent with either a landslide interpretation or an interpretation based on a compressional stress field analogous to the one that controlled late Cenozoic structural development in the Clear Creek sample area. Though the cause of the slip complexity and incompatibility is not known, we suspect that much of it results from polyphase deformations in a tectonic regime where uplift caused by tectonic unloading competes with lateral shearing caused either by north-south compression, wrench faulting, or tectonic rafting of structural blocks in a highly mobile shear zone. Unfortunately, the fault-slip data we gathered are too few and heterogeneous to use as a basis for paleostress computations.

Of the 59 small- and intermediate-displacement faults observed along the range front between Joseph Flats and Richfield, only 6 strike within ±20° of the N. 35° E. trend of the range front, and, of those, only 3 dip southeast--the dip direction that one would expect if the faults are part of a range-front fault system. Of the three, two show sinistral strike-slip striae and one shows normal slip. Thus, only 1 of 59 faults has an orientation and slip sense similar to what would be expected for a range-front normal fault system that might be implied from the geology and present-day physiography.

Previous workers have inferred a major normal fault, the Elsinore fault, to be the range-front structure along the Joseph Flat to Richfield segment of the range front (Callaghan and Parker, 1961; Cunningham and others, 1983). Our identification of the chief range-front structure as a monocline and, more specifically, our failure to identify minor structures related to a range-front normal fault suggests that if a fault exists, it is either (1) buried beneath the monocline and genetically related to it, (2) buried beneath alluvium at some distance east of the range front, or (3) a continuation of the sinistral-slip Dry Wash fault which, if projected northeastward, should lie along the range front (fig. 3).

PAVANT RANGE, RICHFIELD TO WILLOW CREEK

The east part of the Pavant Range between a line extending southwest from Richfield northward to Willow Creek (fig. 3) is underlain by early Tertiary sedimentary rocks. In that area, the east margin of the main range block extends northeast from Richfield to approximately the locality marked by H in figure 3. From there it bends sharply northwest toward Willow Creek where it is marked by a fault scarp of probable Holocene age (Anderson and Bucknam, 1979).

The lobe of bedrock that extends toward Aurora from the main range block is dominated by a series of northeast-tilted fault-repeated blocks of Green River Formation but also contains a major and controversial fold structure that wraps around the northeastern extreme of the range and involves the Green River and younger Tertiary rocks (fig. 18_A_). Our early reconnaissance mapping of that area led us to interpret the faulting and tilting on northwest trends as an early episode of deformation related to northeast-southwest extension and the wrap-around fold as a subsequent episode of monoclinal fold deformation related to formation of Sevier Valley--a structural history very analagous to that described in the previous section for the Elsinore area. On the basis of 1:24,000-scale quadrangle mapping, C. G. Willis (written commun, 1987) interprets all major folding and faulting in that area to be genetically and temporally related to a single deformational episode and suggests that the deformation could be as young as Pliocene. His interpretation is strongly influenced by mapping that indicates that most of the northwest-striking faults terminate southeastward at the Elsinore fault, thus making them contemporaneous with or younger than the Elsinore fault. We maintain that the quality of exposures and lack of marker beds east of the northeast-striking Elsinore fault do not preclude small faults extending into that area and suggest that some large faults do, based on Willis' mapping (fig. 18A). We therefore adhere to our initial interpretation of diachronous deformation.

Along Sevier Valley between Richfield and Aurora, a few hills of dark-colored volcanic rocks of Oligocene age protrude through the alluvium. Most of these volcanic rocks dip moderately to steeply toward the valley, showing that Neogene monoclinal flexing plays an important role in producing the vertical structural relief of that part of the range front. Along some segments displacements on subvertical northeast-striking faults also contribute to or, in some places, dominate the vertical structural relief. Mapping by G. C. Willis (written commun., 1987) shows that the fault system can be traced northeast to the latitude of Aurora northeast of which displacement transfers to a southeast-facing monocline (fig. 18A). We interpret the entire wrap-around fold as part of that monocline.

Directly west of Richfield, well-exposed monoclinally flexed rocks belonging to the Flagstaff, Colton, and Green River Formations in the upthrown block of the range-front fault are cut by numerous small- to intermediate-displacement down-to-the-mountain normal faults. About 6 km north of Richfield, similarly flexed equivalent strata with valleyward dips ranging from 15° to 60° on the downthrown side of the range-front fault are cut by intermediate- to large-displacement down-to-the-mountain normal faults. We infer from an anomalously large breadth of outcrop and steep valleyward dips reported by G. C. Willis (written commun., 1987) that the Tertiary volcanic rocks southwest of Aurora are displaced by as yet unrecognized down-to-the-mountain faults (fig. 18A). The exposures west of Richfield reveal that the down-to-the-mountain faults tend to cut the tilted strata at approximately 90° to bedding, whereas faults of the main range-front system are subvertical (fig. 18B). Rocks of the Flagstaff Formation in the upthrown block of the northwest-striking main range front in the vicinity of Willow Creek also form a faulted monocline with a cross sectional form very similar to that west of Richfield (fig. 18*B*) but with dramatically different orientation. Despite their different orientation, we infer that these structures are coeval and that, together with the structures of the downthrown block, they adequately characterize the style of range-margin deformation. Little, if any, net extension can be attributed to the near-vertical down-to-valley faults. Stratal flexing tends to subtract from, and may completely negate, extension on down-to-range faults. Therefore, there may be little or no net extension associated with the uplift across these range-margin structures. If so, the range margins are very different from the bedrock lobe west of Aurora where faulted repetition suggests moderate northeast-southwest extension.

FIGURE 18 FOLLOWS TEXT

Fault-slip data were gathered from 33 small-, intermediate-, and large-displacement faults belonging to the range-margin system, 20 from the northeast-trending segment west of Richfield, and 13 from the northwest-trending segment near Willow Creek. Strike distributions presented in figure 19 show the contrasting northeast and northwest trends of the range-margin segments.

FIGURE 19 FOLLOWS TEXT

A paleostress computation using the 20 faults from the northeast-trending segment yields almost the same orientation for σ_3 (316°) as a computation using all 33 faults (315°). At first this seems inconsistent with the contrasting strikes of the range-margin structures. We note, however, that most of the northwest-striking faults in the Willow Creek area, instead of being pure dip-slip faults, are actually oblique-slip faults with rakes consistently to the northwest as shown in the stereoplot on figure 19.

We have no direct evidence of strike-slip faulting along the Richfield to Aurora segment of the Pav~~e~~ant Range margin. This contrasts greatly with the abundant evidence of strike-slip faults in the volcanic rocks from Richfield southwest. This dramatic contrast may result from structural decoupling or detachment of the volcanic rocks from the underlying sediments as outlined in the summary and conclusions section.

SEVIER FAULT

The Sevier fault is one of the major structures of the transition zone. It forms the west boundary of the 25-30 km-wide east-tilted Sevier Plateau block, and locally has at least 1.5 km of down-to-the-west throw. In most places, uplift of the Sevier Plateau is probably distributed over a broad zone of faults that we collectively refer to as the Sevier fault. The Sevier fault extends from near Annabella south about 120 km to near Panguitch, Utah, but consists of several north-, northeast- and northwest-striking segments that give the fault a conspicuous zigzag trace (Rowley, 1968, Rowley and others, 1979, Cunningham and others, 1983). The northern Sevier fault is well defined, though buried, south of Monroe where it apparently controls the N. 5° E. trend of the range for about 6 km (fig. 3). Its trace north of Monroe is conjectural because the range-front escarpment bends sharply eastward and it is uncertain whether the main trace of the Sevier fault follows that bend or, as indicated by Callaghan and Parker (1961), strikes 035°. beneath a thick mantle of landslide and alluvial debris to reemerge at the west base of the Bull Claim Hills northeast of Annabella. Whether its main trace north of Monroe strikes northeast or east-northeast (fig. 3), its contrast in strike north and south of Monroe serves as a basis for discussing those segments separately.

SEVIER FAULT, MONROE SEGMENT

The Monroe segment of the Sevier fault is defined as the 6-km-long northerly trending part south of Monroe (fig. 3). Though modeling of detailed geophysical data and interpretation of drill-hole data at the Monroe geothermal area yield conflicting results, together they indicate that the Sevier fault is a zone of several major northerly trending step faults that dip valleyward 80° (Mase and others, 1978; Chapman and Harrison 1978). In our study, the Sevier fault was observed at only one exposure (directly northeast of locality E, fig. 3). At this locality, a fault with an attitude 007°, 70° W. cuts sharply through conspicuously unbrecciated and unfractured Oligocene andesite and is marked by a 1- to 2-m-wide rib of massive silica that has been prospected locally. Striations on and within the secondary silica have gentle north plunges indicating late-stage strike-slip motion. Neither the sense nor amount of displacement is known. Directly northwest of locality E the mapped trace of a fault that separates calc-alkalic andesite of Oligocene age from downdropped rhyolitic ash-flow tuffs of Miocene age strikes N. 55° E., dips steeply northwest, and has a stratigraphic separation of at least 1 km (Cunningham and others, 1983). Six steeply dipping gouge-coated surfaces hand-excavated in fractured andesite breccia of the footwall block strike within ±15° of that of the mapped fault and show normal dip slip. Though this fault is not part of the Monroe segment as defined herein, it is a main strand of the Sevier fault. On the basis of these limited data we infer that the Sevier fault, though predominantly dip slip, has some strike-slip components of displacement along northerly striking segments. This is consistent with observations of bimodal dip-slip and strike-slip striae seen on the southernmost part of the Sevier fault (R. Krantz, written commun., 1986).

Stratal strikes in Oligocene volcanic rocks along the 005°-striking Monroe segment are varied and dips average only about 10°. Study of 62 small- and intermediate-displacement faults in these gently tilted and faulted rocks shows fault strikes with northeast and northwest maxima and no tendency for fault strikes to parallel the range front (fig. 20). Of 14 faults whose strikes fall within 20° of the range-front trend, only three dip toward the valley and show normal displacement. Of the 62 faults, 36 have rakes less than 45° and 26 have rakes greater than 45°. The data indicate heterogenous slip on faults that have attitudes conspicuously different from that of the Monroe segment of the Sevier fault. Because they contribute little to extension, dip-slip faults with dips greater than 80° were eliminated for computational purposes. The remaining subset of dip-slip faults (N-13), table 1) is of marginally small size for paleostress computation. The dip-slip and strike-slip subsets yield paleostress axes, as expected, with subvertical σ_1 and σ_2 respectively (fig. 20). Subhorizontal σ_3 axes from the dip-slip and strike-slip subsets are within 12° of one another, suggesting that the two modes of faulting are parts of a single deformational process. The computational results as well as the data distributions are quantitatively similar to those from the Clear Creek sample area. We find this similarity astonishing in view of the very strong contrast in local structural setting of the two areas. However, we emphasize that the determination of slip sense for strike-slip faults along the Monroe segment are very poorly constrained (table 1).

FIGURE 20 FOLLOWS TEXT

SEVIER FAULT, ANNABELLA SEGMENT

The Annabella segment of the Sevier fault is herein defined as the range-front fault extending east-northeast from the Thompson Creek landslide (fig. 3). For 2.2 km east of the landslide, the trace of the Annabella segment is clearly marked by a precipitous straight bedrock escarpment trending 075°. Stratal attitudes of volcanic and sedimentary bedrock in the escarpment are highly variable and dips are mostly less than 30° (figs. 21, 22). The escarpment projects eastward toward the lower reaches of Cliff Canyon where excellent exposures reveal that volcanic rocks in the hanging wall block are downbent toward the north, suggesting a large drape fold or possibly normal drag (fig. 22). The Annabella segment extends up Cliff Canyon with possibly as much as 400 m of down-to-the-north stratigraphic offset of Oligocene volcanic rocks (Rowley and others, 1981a). A thick sequence of well-exposed Oligocene volcanic rocks in the plateau block south of that part of the fault is very mildly deformed. The rocks are horizontal to gently southeast dipping and are cut by sparse small-displacement faults (fig. 22).

FIGURES 21 AND 22 FOLLOW TEXT

A total of 235 fault-slip measurements were made on moderately to steeply dipping faults in the upthrown and downthrown blocks along the approximately 4-km-long trace of the Annabella segment (fig. 23). Fault strikes in this sample area are varied and the histogram of strike distributions shows a minor concentration in the 30° sector centered on the 075° average trend of the Annabella segment. Dip directions for these faults, however, are skewed to the southern hemisphere; that is, toward the uplifted plateau block. Oblique slip is common. The histogram of rake distributions shows a clearly defined minimum at 30°. Dip-slip and oblique-slip faults predominate over strike-slip faults.

FIGURE 23 FOLLOWS TEXT

In order to evaluate the role of dip-slip faulting in plateau uplift, we present in figure 23 data-distribution histograms for dip-slip faults with rakes greater than 60° (90 faults). As for the entire data set, this subsample shows varied strikes and a strongly skewed pattern of dip directions toward the southern hemisphere. Of particular significance is the paucity of dip directions toward the 330°-360° sector; that is, toward the downdropped block of the Annabella segment. This paucity cannot be ascribed to post-faulting rotation in the draped or folded hanging wall block because much of the data is from the uplifted footwall block which shows no consistent pattern of stratal rotation (fig. 21). We did not observe the main fault of the Annabella segment and, therefore, do not know its true dip. We emphasize that many of our measurements were taken from faulted rocks within a few meters of the main fault. The data suggest that the main fault is a sharp break and that normal faults associated with it drop strata down toward the uplifted plateau. The data show that most of the dip-slip faults in this sample area are not part of a range-front fault system and may not contribute significantly to plateau uplift. In this respect, the Annabella segment is similar to the Monroe segment as well as to the eastern margin of the Pavant range.

The sense of slip was determined with certainty or reasonable probability on only about 15 percent of the oblique-slip and strike-slip faults along the Annabella segment. A lower-hemisphere stereographic plot of faults in this 15 percent subsample is shown in figure 24. For predominantly strike-slip faults the subsample shows an unusually wide range of attitudes (especially dip values). Despite the attitude variability, slip lines show a strong preference for dispersion around a north-south azimuth, but sinistral and dextral faults are <u>not</u> concentrated in separate strike sectors as they are for the Clear Creek sample area. We infer from the dip variability, north-south dispersed slip lines, and the lack of sinistral-dextral partitioning, that faulting with a predominantly strike-slip mode does not represent a conjugate-shear response to remote stress. Therefore, quantitative attempts to resolve paleostress characteristics using strike-slip faults should not be made.

FIGURE 24 FOLLOWS TEXT

We computed a pleostress orientation from the dip-slip faults with rakes greater than 60° (N=90). It shows σ_3 at 282°, but the value of Φ is low (0.03, table 1). This low value suggests that moderately to steeply dipping faults of any strike are appropriately oriented for dip-slip movement. Though the computed σ_3 orientation is clearly not a reflection of principal extension normal to the Annabella segment of the range front, the low value of Φ and the fact that oblique-slip and strike-slip faults are excluded in its computation, lessens its paleostress significance. The dip-slip faulting may be analogous to the strike-slip faulting and may not represent a response to applied remote stresses. Alternatively, a complex and unresolvable history of polyphase deformation could be recorded by the striae we measured.

ANTICLINE SAMPLE

The southern part of the Sanpete-Sevier anticline, cored by mechanically weak rocks of the Arapien Formation, is an important structural element in the central Sevier Valley area. For about 20 km south-southwest of Salina a 5-km-wide core zone of Arapien rocks is exposed, and the adjacent Tertiary rocks tend to dip moderately to steeply (locally overturned) away from the core rocks. By contrast, in the area east of Glenwood and northeast of Annabella Arapien rocks are only locally exposed in a narrow band and Tertiary rocks dip uniformly westward as depicted in cross section (fig. 22). We conducted reconnaissance fault-slip studies in Tertiary rocks at and above the contact with the Arapien. Those rocks contain abundant evidence of extensional deformation and structural attenuation at widely ranging scales and magnitudes. In may places, structural attenuation is so extreme that hundreds of meters of strata are reduced to broken or shattered layers a few meters thick. The ultimate contact with the Arapien is shown on published maps as depositional. We recognize it as a fault in most places. Though it ranges widely in dip direction and magnitude, it dips gently and is discordant to bedding in overlying rocks in many places and over wide areas.

Though we gathered fault-slip data as far north as Salina, the area of greatest interest is to the south where it is clear that the late Miocene and Pliocene basin-fill sediments of the Sevier River Formation are intensely involved in the deformation. Our studies in that area are extremely important for they are the first to demonstrate that extensional deformation, locally of large magnitude and including severe structural attenuation, dominates the late Cenozoic structural record. Our results preclude a major role for compressional tectonics and suggest that diapirism is not the first-order deformational mode. In this regard, they contribute significantly to resolving the long-standing controversy concerning the relative importance of vertical (diapiric) and horizontal (regional compression) motions in shaping the late Tertiary structure of the anticline. Neither appear to be important.

A total of 72 fault-slip measurements were made on 69 faults in rocks at and above the contact between Arapien rocks and cover rocks. Though most faults strike northeast, parallel to the Sanpete-Sevier anticline, many have a more northerly strike (fig. 25). Rake angles are varied but mostly steep, and the faults dip more moderately than in any of the other areas we sampled. The moderate dips probably result from rotation of faults during extension. On faults with polyphase slip, striae with the shallowest rake angles are the youngest on two of the 69 faults, providing insufficient data for establishing whether dip-slip faulting is older or younger than strike-slip faulting.

FIGURE 25 FOLLOWS TEXT

In order to separately evaluate the significance of dip-slip faulting, we present in figure 25 strike- and dip-direction histograms for a subsample of 49 normal faults taken from the entire 69-fault sample. The data distributions are similar to those of the entire sample and show that many normal faults strike more northerly than the anticline and that there is a strong tendency for the faults to dip easterly, consistent with our qualitative field observation that Tertiary rocks dip uniformly westward and are downdropped uniformly eastward across the southernmost part of the anticline. Taken together, these relationships suggest that some process other than anticlinal folding was active during extension and that the anticline did not exert a strong influence on fault kinematics during the extension. This suggestion is supported by a weakly constrained least principal stress direction of 282° computed from the subsample of 49 normal faults (fig. 25, table 1). This orientation is closer to those computed from other sample areas than it is to a direction perpendicular to the anticline. It is almost identical to that computed for the Annabella segment to the south (also weakly constrained) though the two sample areas have dramatically differing structural settings. We conclude that regionally significant extensional faulting and associated structural attenuation is the dominant deformational mode in the cover rocks of the southern part of the anticline. Where the Sevier River formation is exposed, it is involved in the full range of this deformation leading us to conclude that the deformation is neotectonic.

In order to separately evaluate the significance of gently raking fault motions in the area of the anticline sample we present in figure 26 A a lower-hemisphere stereographic plot of those faults and striations. This subsample of 29 faults shows orientation diversity similar to that seen in the strike-slip subsample of faults from the Annabella segment directly to the south (fig 24). This similarity is remarkable in light of the highly contrasting structural setting of the two areas. In particular, there is no tendancy of the diversely dipping north- to northeast-striking faults to divide into sinistral and dextral fields as would be expected if they were conjugate faults. On the basis of data gathered from individual exposures (fig. 26 B, C), faults that have generally east-west stirkes are probably block-bounding structures genetically linked to systems of predominantly normal faults whose motions are a response to generally east-west extension. Neither these faults, because of their lack of slip independance (Angelier, 1979) nor the north- to northeast-striking ones, because of their slip incompatibility, are candidates for paleostress analysis. Perhaps the components of strike-slip motion on north- and northeast-trending faults is a response to tractions imparted to the base of the extending slab by lateral flowage of subjacent rock. This concept will be elaborated on in a subsequent section.

FIGURE 26 FOLLOWS TEXT

NORTHERN ANTELOPE RANGE

The part of the Antelope Range adjacent to the Dry Wash fault consists of a fault-repeated sequence of Oligocene and Miocene flows and tuffs with east to northeast dips ranging from 5° to 45° (Cunningham and others, 1983). Mapped faults strike mostly north to northeast and drop strata down to the west. No evidence was found for easterly trending folds such as are common in the Clear Creek area across the Dry Wash fault. Because the northern Antelope Range consists of a more orderly arrangement of fault-tilted blocks than most other areas in the region, it was hoped that a straightforward relationship between fault slip, block tilting, and extensional deformation consistent with the mapped structural pattern could be discerned. Instead, a reconnaissance of fault slip reveals a complex mixture of strike slip, oblique slip, and dip slip that cannot be understood in terms of a single deformational event or any simple structural pattern.

Paleoslip was measured on 135 faults. Displacement on 108 of them are known or estimated to be less than a meter and on the remaining 27 it ranges from a meter to more than 100 m. Most measurements were made within 3 km of the trace of the Dry Wash fault. Of the 135 faults, 17 contain polydirectional striae and on all but one the older slip event has the lowest rake. This indication that dip-slip faulting is consistently younger than strike-slip faulting agrees with observations near locality B in the Clear Creek downwarp but is not a feature recognized in all other areas we studied.

Some major dip-slip faults in the northern Antelope Range displace the sparcely preserved Sevier River Formation by at least 100 m. We assume that the strike-slip displacements also postdate the Sevier River Formation because they do so in the adjacent Clear Creek area.

Fault strikes are mostly north and northeast, and sinistral slip predominates over dextral slip in the strike-slip subset, similar to the faults in the Clear Creek sample area (figs. 27, 10). A larger proportion of the faults with rake angles greater than 30° have a component of reverse slip than for the other sample areas. As with a major, steeply north-dipping, east-striking sinistral and reverse-sinistral fault at locality F (near the south boundary of fig. 3), a distinction between true reverse faults and subsequent rotation by later faulting is generally not possible (fig. 28). Of the 92 measurements with rake angles greater than 30°, the slip sense on 17 indicates reverse slip. Neither these 17 measurements nor the 56 measurements of strike-slip striae with rake angles of 30° or less are qualitatively consistent with the mapped pattern of fault-repeated and fault-tilted blocks.

FIGURE 27 AND 28 FOLLOW TEXT

In summary, a reconnaissance investigation of fault slip in the northern Antelope Range reveals complex data distributions, many aspects of which are qualitatively inconsistent with what would be expected from the mapped structural patterns. The structural significance of the complexities are not understood. Also, the data provide no basis for meaningful paleostress computations. Nevertheless, from the common occurrence of reverse-slip and strike-slip displacements represented by the striae we observed, the faults clearly did not result from straightforward application of extensional stresses with σ_1 always in an approximate vertical position. As with the other areas we studied, a horizontal maximum compression or lateral tectonic transport of blocks, possibly caused by tractional forces applied from below, or both is required to produce some of the deformation.

SEISMICITY AND LATE QUATERNARY DEFORMATION

Seismicity studies in the Intermountain Seismic Belt (ISB) by W. Arabasz and his students at the University of Utah, using a combination of permanent regional and temporary local seismic networks, have established the distribution of earthquake epicenters and have resulted in an extensive sample of earthquake hypocenters and fault-plane solutions (Arabasz and Julander, 1985). Earthquake epicenters in western Utah tend to form clusters and there is, in general, no clear-cut spatial association between the clusters and fault scarps formed on Quaternary alluvium. In central Sevier Valley, however, two areas of concentrated seismicity do coincide with areas of late Quaternary surface deformation. One is a magnitude-4.0 main shock and aftershock sequence that occurred in 1982 in the area northeast of Annabella where late Quaternary fault scarps are common. (All magnitudes reported herein are local Richter magnitudes taken from Arabasz and Julander, 1985.) The other is directly southwest of Elsinore, where we recognize tilted Quaternary geomorphic surfaces, late Quaternary fault scarps, and possible deformation-related anomalies in the channel pattern of the Sevier River. In both areas, complex junctures between major mapped structures are logical candidates for localization of the seismicity--the Sevier fault system east of Annabella and the northeasternmost extent of the Dry Wash fault in the Elsinore area. These two coincidences are very unusual in the ISB where generally an association between seismicity and known mapped structures is not possible (Smith, 1978; Arabasz and Smith, 1981). Because the coincidence of seismicity with mapped faults offers an opportunity for improving understanding of the relationship between mapped faults, surface deformation, and seismicity, we discuss each area in some detail. But first, some general comments on seismicity of the region are given.

Analysis of 53 fault-plane solutions by Arabasz and Julander (1985) shows that seismic slip in the transition zone is characterized by a mixture of strike-slip and normal faulting as shown in the summary of those results in figure 29. They suggest that this mixture results from interchanges in the positions of σ_1 and σ_2 whereas σ_3 remains stationary and approximately horizontal at about 102°.

FIGURE 29 FOLLOWS TEXT

In three areas in the ISB, Arabasz and Julander (1985) recognized that horizontally bounded zones of microearthquake hypocenters correlate with known or inferred subhorizontal thrust faults. On the basis of this correlation, they hypothesized that the depth distribution of background seismicity is controlled by the internal structure and variable mechanical behavior of horizontal plates bounded by major low-angle faults within the seismogenic upper crust (fig. 29). This heterogeneity that influences the depth distribution of earthquakes, they state, was produced by vertical stacking of thrust plates during Sevier-age overthrusting. Seismic slip on the bounding low-angle faults in any of the three areas or elsewhere in the ISB is not evident and led Arabasz and Julander to speculate that such faults may move aseismically. The central Sevier Valley, including the concentrated seismicity in the Annabella and Elsinore areas, is one of the three areas for which the correlation between horizontal seismicity zones and low-angle faults was suggested by those writers (fig. 29).

AREA NORTHEAST OF ANNABELLA

The part of the Sevier Plateau bounded on the west by the Monroe segment and on the north by the Annabella segment of the Sevier fault is best characterized as a weakly deformed generally east-tilted relatively intact structural block of Tertiary igneous rocks uplifted 0.5-2 km above its surroundings. In sharp contrast, the part of the Sevier Plateau north of the Annabella segment, including the Bull Claim Hills, is best characterized as a highly deformed series of west-tilted blocks of volcanic and sedimentary rocks that are repeated eastward by faults that drop strata down toward the east and southeast (toward the uplifted Sevier Plateau) (fig. 22). That area is also characterized by strong structural attenuation of the stratigraphic section, especially in the vicinity of the exposed Arapien rocks. The tilting, stratal repetition, and attentuation involve strata of the late Tertiary Sevier River Formation to the same extent as older Tertiary rocks, suggesting that the deformation is neotectonic. Between the two areas of highly contrasting internal structure and neotectonic structural vergence, and tucked into the large physiographic embayment in the plateau margin, is a northeast-trending graben that we refer to as the Annabella graben (fig. 22). Downdropped strata of the Sevier River Formation are preserved in the graben and are overlain unconformably by Quaternary landslides, debris flows, and coarse alluvial deposits that accumulated during graben formation. The Sevier River Formation in this area predates graben formation and plateau uplift. A K-Ar age of 5.6±0.4 Ma was determined by H. H. Mehnert on a sample of volcanic ash from the Sevier River Formation east of Annabella (H. H. Mehnert and P. D. Rowley, written commun., 1982).

An anomalous concentration of northeast-trending fault scarps ranging in height from less than 1 m to more than 100 m is formed on the Quaternary deposits of the Annabella graben. These scarps are concentrated in an area of only 15 km^2. Individual fault-scarp lengths are less than 5 km. Some of the scarps are high and contain evidence for recurrent movement as late as the time of the Pleistocene-Holocene boundary (Anderson and Bucknam, 1979). The main fault in this area appears to be the fault labeled MS in figure 22. This fault bounds the graben on the southeast. The surface scarp that marks the trace of this fault not only reveals strong evidence of recurrent late Quaternary movement, but it also has a large cumulative displacement of late(?) Quaternary deposits of about 109 m, making it one of the highest fault scarps in alluvial deposits in Utah (figs. 30, 31). It has a 90-m-long midslope section with a slope of about 35°. To maintain such a large steep slope resulting from slip events equivalent in size to the youngest event (fig. 30) requires about 25 small slip events spaced close in time. Though it is uncertain how this fault connects with the Annabella segment of the Sevier fault (fig. 22), it must at least intersect that fault.

FIGURE 30 AND 31 FOLLOW TEXT

A magnitude 4.0 main shock and extensive aftershock sequence in 1982 is centered on the Annabella graben (Arabasz and Julander, 1985). First-motion data for the mainshock are inconsistent with the focal-mechanism characteristics of and planar distribution of the aftershock sequence (fig. 32). Of several nodal planes allowed by main-shock first-motion data, a northeast-striking southeast-dipping plane with predominantly normal slip would correspond well with the fault that bounds the Annabella graben on the northwest. Alternatively, hypocenter distributions resulting from detailed aftershock studies define a northeast-trending envelope dipping about 75° NW. (fig. 32). The envelope is only about 5 km long by 3 km wide and 5 km deep (fig. 32). Though such an envelope agrees well with any of several similarly oriented faults marked by Quaternary scarps in the Annabella graben, the aftershocks that define it yield focal mechanisms indicating predominantly strike slip on steeply dipping faults and the envelope does not match any of the main-shock nodal planes. Thus, the faulting kinematics indicated by this seismicity are internally enegmatic and their relationship to mapped faults is unresolved. Nevertheless, the spatial coincidence of this seismicity with the area of anomalously disrupted late Quaternary deposits suggests to us a genetic relationship between the seismicity and scarp-producing faults.

FIGURE 32 FOLLOWS TEXT

The aftershocks of the 1982 seismicity define two types of focal mechanisms with approximately interchangeable pressure (P) and tension (T) axes (Arabasz and Julander, 1985). The preferred orientation for the T axes is approximately east-west similar to that indicated by the main shock (Arabasz and Julander, 1985). If the T axes are inferred to be colinear with the extension direction, a simple interchange between σ_1 and σ_2 positions analagous to that suggested for the entire transition zone satisfies most of the data. The internally incompatible strike-slip events can be related to the oblique-slip main shock by assuming that release of extensional stress creates a secondary compensatory motion of blocks parallel to the preexisting northeast-trending dominant structural fabric. In the case of the 1982 aftershocks, we would choose the northeast-striking dextral and sinistral nodal planes and would assume a southwest-directed tectonic transport of blocks bounded by faults analagous to these nodal planes. Such deformation would have to result from some secondary system of basal tractions or horizontally layered stress gradients felt by the blocks as extension progresses. This is consistent with our fault-slip data that indicate a mixture of dip slip and strike slip and, in particular, with the tectonic transport parallel to the axis of the Sanpete-Sevier anticline indicated by the incompatible strike-slip striae from the Annabella segment and the southern Sanpete-Sevier anticline. We return to this notion of basal tractions in the Summary and Conclusions section.

The late Quaternary faulting and seismicity may be concentrated in the Annabella graben because a structural juncture exists here between the down-to-the-west and northwest faults related to the Sevier fault and the dramatically different set of down-to-the-east structures along the north and northeast projection of the Sevier fault. An east-northeast-trending transverse zone of structural accommodation seems to be required beneath the graben. Concentration of stress in such a zone would be expected. The short length of fault scarps, the fact that they do not rupture contemporaneously, and the small size of the area containing them does not portend large-magnitude (6.5-7.5) earthquakes associated with their development. In particular, there is no justification for assuming that the concentrated young deformation is characteristic of the Sevier fault. Slip events on the Sevier fault from the graben southward are likely to be associated with larger earthquakes with much longer return periods than those that produced the scarps.

AREA SOUTHWEST OF ELSINORE

The Elsinore area is one of the most seismically active in Utah. Five earthquakes of magnitude 5 or greater are assigned to the area--two in 1910 and three in 1921 (Williams and Tapper, 1952, Arabasz and McKee, 1979). An intense cluster of microseisms ($M \leq 1.9$) was recorded in 1981 about 4 km southwest of Elsinore (Julander, 1983). The cluster is centered at the alluviated gap connecting Joseph Flats with the broad Sevier Valley. The envelope containing the densest part of the cluster dips steeply and has an east-west strike. Eight focal mechanisms, all indicate predominantly strike-slip faulting (Julander, 1983). As with the aftershocks northeast of Annabella, the focal mechanisms divide into two types with approximately interchangeable P and T axes, and are indicative of strong slip inhomogeneity and incompatibility.

North of the alluvial gap at Joseph Flat, at a locality marked X on figure 31, faulted and tilted Sevier River Formation is unconformably overlain by Quaternary alluvium. A fault at this locality with attitude 054°, 76° SE and an estimated displacement of 30 m contains striated clay suggesting a 34° rake to the southwest. The predominately strike-slip component is dextral. Although we have no direct evidence of the direction and sense of slip on the Dry Wash fault in the vicinity of the alluvial gap, elsewhere its strike-slip component is known to be sinistral. Therefore, the geologic record suggests incompatible strike slip on northeast-striking faults; this suggestion is geometrically and mechanically consistent with the microseismic data. As with the faults northeast of Annabella, our preference is to interpret such incompatible slip as an indication of lateral block motion.

A northwest-southeast gravity profile across Joseph Flat and the Dry Wash fault shows no significant anomaly at the fault (Halliday and Cook, 1978). Instead, a 10-mGal gravity low is located beneath Joseph Flat with its axis about 2 km northwest of the fault trace. These data are consistent with our interpretation that the Dry Wash is primarily a strike-slip fault and that the alluvial basin beneath Joseph Flat results mainly from the southerly projection of an open south-southwest-plunging syncline (fig. 3).

Steven (1979) mapped north- to northeast-striking faults whose traces are well marked by scarps in Quaternary alluvium on the north and south flanks of the alluviated gap separating Joseph Flat from Sevier Valley. A northeast-trending fault scarp about 3 m high is formed on a gently inclined river terrace (terrace 4, fig. 33), south of which are remnants of three additional geomorphic surfaces that show southward-increasing erosional dissection and southward-increasing eastward inclinations (fig. 34). The relationships suggest increasing eastward tilts on increasingly older Quaternary surfaces. The faulting, which appears to be mostly normal sense, and the tilting, which may be on the east flank of an anticline, paired with the syncline beneath Joseph Flat, seems to represent higher rates of Quaternary deformation than those seen along major structures extending away from the alluviated gap.

FIGURE 33 AND 34 FOLLOW TEXT

Witkind (1983) noted the colinearity of the Sanpete-Sevier Valley anticline and the Sevier fault and suggested a genetic relationship between the two. Within this same context we suggest an alternative interpretation for the concentration of seismicity and young deformtion. The concentration could be related to lateral movement of the relatively ductile rocks of the Arapien Formation. The southernmost exposures of the Arapien are directly northeast of the graben, and equivalent rocks could exist in the shallow subsurface beneath the graben. Perhaps Arapien rocks have flowed into the extensional regime of the northeasterly projection of the Sevier fault where, because of a reduction in confining pressure, they tend to spread laterally. As suggested by Witkind (1983) movement of the Arapien could be stimulated by displacements on buried faults. Arapien rocks could be supplied to the fault zone from beneath the Sevier Plateau. This is consistent with our observations in the vicinity of exposed Arapien rocks where there is an indication that these rocks have been drawn out from beneath the Sevier Plateau (fig. 22). Such flowage would tend to remove most or all surface and near-surface traces of the Sevier fault. Though this is an attractive alternative for explaining the thin-skinned extensional attenuation in rocks above the Arapien, it does not explain fault-slip and seismicity data that indicate that strike-slip motions are common on north and northeast-trending faults and that lateral motions have occurred parallel to the principal fault-fold trend. These factors introduce complexities that seem to require competing deformational processes.

Within the alluviated gap, the channel pattern of the Sevier River appears to have responded to young deformation. Along the 3.5-km reach downstream from Joseph, the channel pattern changes from sinuous to reticulate. Where the river crosses the projection of the Dry Wash fault (fig. 35A), the pattern changes abruptly from reticulate to a sinuous or island-braided pattern. This abrupt change is analagous to an experimentally supported model of a meandering river carrying a combination of suspended- and bed-load sediment (like the Sevier River) that has had to adjust to an anticlinal uplift across its course (fig. 35B; Ouchi, 1985). The east-side-up fault displacement in the alluviated gap is analagous to an uplift axis at the fault trace. The reticulate pattern results from the damming effects of the uplift which enhances flood-plain deposition upstream. The sinuous or island-braided pattern downstream of the the uplift axis is a feature that results from cutoff of intensified meander loops that develop first as the river attemps to lengthen its course to maintain its gradient across the oversteepened terrain. Though sufficient time has presumably lapsed since deformation for the Sevier River to reach this stage, the lapsed time is insufficient for the river to reestablish an equilibrium channel pattern analagous to the final stage in figure 35B. Though it is not possible to estimate these lapsed times, the fluvial patterns clearly support late Quaternary displacement on the Dry Wash fault system in this area. About 90 km northwest of Elsinore we recognize an analogous anomaly in the channel pattern of the Sevier River where it flows southwest across the southern projection of the Drum Mountains fault scarp system of Holocene age southwest of Delta, Utah. There the young deformation appears to have affected a 35 km-long reach of the river suggesting a basin-range-scale structural disturbance.

FIGURE 35 FOLLOWS TEXT

The displacement sense inferred from the stream-pattern anomaly near Elsinore is consistent with the pattern of east to northeast tilting of geomorphic surfaces and underlying Sevier River Formation in the area east of the northernmost Dry Wash fault (figs. 33, 34). If a range of ages is assigned to these east-tilted elements and a specific size and geometry assigned to the structural block containing them it is possible to compute a range of rates of uplift of the terrace-bearing block. The computed range can then be compared with ~~slip~~ uplift rates on faults in the eastern Great Basin region. We assume that the slope angles shown in figure 31 represent structural tilts of a block with a minimum width of 2 km and that the block is bounded by the gravity step beneath Joseph Flat on the west and is hinged along its east edge. We assign age ranges of 2-5X10^4 years for the 0.5°-tilted surface, 2-5X10^5 years for the 5.5°-tilted surface, and 1-5X10^6 years for the duration of tilting of the 15°-tilted Sevier River strata. The rate of uplift required to produce those tilts in the assumed time slots ranges from about 0.4 to 1.0 mm/yr for the two geomorphic surfaces and 0.1 to 0.6 mm/yr for the Sevier River Formation. The range of lower rates (0.1 to 0.4 mm/yr) seems to us to be more reasonable than the range of higher rates because it falls below the approximately 0.4 mm/yr long-term rates of uplift on the Wasatch and Hurricane faults (Anderson and Mehnert, 1979).

Because of large uncertainties in the epicentral locations of the magnitude-5 or greater 1910 and 1921 earthquakes near Elsinore, no direct association can be made between the known Quaternary surface deformation and those earthquakes. Also, only a spatial association can be made between the known Quaternary surface deformation and the microseismic record.

The geologic setting of the surface scarps and seismicity near Elsinore is complex. Northeastward projection of the Dry Wash fault (and the inferred flexure cut by it) beyond the alluvial gap between Joseph Flat and Sevier Valley encounters the monoclinal flexure along the southeast base of the Pavant Range. These two structures have opposite senses of vertical displacement suggesting that such a projection is not reasonable in terms of dip-slip components. If both structures terminate in the vicinity of the alluvial gap, there is a need for a transverse structural zone to accommodate the dramatically contrasting along-strike deformational styles. As in the area east of Annabella, stress is likely to be concentrated in such a transverse zone. Though we see no exposed transverse structures, we infer a blind transverse fracture zone in the subsurface. We also infer that the concentration of seismicity and Quaternary surface deformation is related to this structural juncture. If the predominantly sinistral slip Dry Wash fault terminates at the alluvial gap, sagging might be expected in an area of extension northwest of the terminal segment and uplift might be expected in an area of compression southeast of the terminal segment (Segall and Pollard, 1980). Uplift of the block containing the tilted terraces and depression of the the block containing Joseph Flats could represent a highly imperfect distribution of extensional and compressional deformation related to the fault termination.

In summary, concentrations of seismicity and Quaternary deformation in the Elsinore and Annabella areas appear to be related to strong along-strike disparities in the geometry and vergence of major structures. These disparities are probably sites of transverse zones of structural accommodation and stress concentration. They are located on opposite sides of Sevier Valley and could, in fact, be parts of a single transverse zone. Strain rates, displacement histories, or other features that are relevant to earthquake hazards in those zones should not be assumed to be typical of the major structures extending from them or of the central Sevier Valley in general.

SUMMARY AND CONCLUSIONS

Multiphase deformation possibly beginning with events related to evolution of the Paleozoic miogeocline and extending through the compressional events of the Mesozoic and early Cenozoic Sevier and Laramide orogenies fashioned a strong northeast-trending structural fabric in the central Sevier Valley study area. The compressional events probably also left the crust of the area structuraly layered as a result of thrusting. The control that these early structures exerted on the location, trend, and form of late Cenozoic structures is least in the southern part of the study area, probably because of crustal welding associated with large middle- and late-Cenozoic volcanic centers and their inferred subjacent plutons. Subsequent to the igneous activity and a phase of basin-fill sedimentation, the entire area became the structural transition zone between the Basin and Range and the Colorado Plateaus--an event that we identify as ushering in the neotectonic regime. Our structural studies, chiefly in the part of the area where the potential for control by preexisting structure is high, reveal the previously unappreciated importance of late Cenozoic folding, strike-slip faulting, and, locally, structural attenuation within this part of the transition zone. Thus, the fundamentally extensional neotectonic framework of the central Sevier Valley area must be examined not only in terms of the long and complex and sometimes controversial history of early events occurring in diverse tectonic settings but also in terms of the newly revealed evidence for neotectonic folding, strike-slip faulting, and detachment faulting.

The magnitude and style of neotectonic deformation varies dramatically in the central Sevier Valley area. The main aspects of the variations are shown in figure 36. They include sharp constrasts in (1) the amount of extension and structural attenuation, (2) the amount of strike-slip faulting, (3) the amount of monoclinal flexing associated with block-bounding structures, and (4) the vergence direction of on-strike range-bounding structures. Each of these is considered in the the paragraphs that follow, and their relevance to seismicity and seismic hazards are considered.

FIGURE 36 FOLLOWS TEXT

The main Pavant Range block is divided into a northern part lacking evidence of significant internal deformation and a deformed southern part. The deformed southern part is further divided into a northern (updip) area of structural(?) attenuation and landsliding and a southern (downdip) area deformed in apparent north-south compression that produced mechanically coupled neotectonic folds and strike-slip faults (fig. 36). Horizontal deformation is concentrated on northeast-striking sinistral-slip faults on which displacements range from a few centimeters to a few kilometers. The abundance of these faults in excavations and excellent natural exposures suggests localized sinistral shear strain approaching unity, much greater than in any other part of the study area. The net sinistral-slip displacement could approach 10 km. This concentration of horizontal displacement reflects either (1) regionally significant simple shear in the upper crust, (2) north-south compression with strong strain asymmetry resulting from the strain-gathering effect of preexisting steep zones of structural weakness, or (3) inhomogeneously distributed block motions associated with either gravity-driven thin-skin tectonic denudation or detachment or with lateral motion of mass at depth and resultant tractional shear stresses imparted to a structurally layered uppermost crust. Deformation in the updip area may result from updip attachment and that in the downdip area from downdip buttressing analogous to similar attributes of landslides (Kehle, 1970). Such analogy has serious implications regarding earthquake hazards because the class of large-displacement strike-slip faults forming lateral boundaries to the area of compressional buttressing would have minimal depth penetration in comparison to the plateau-bounding normal faults. Accordingly, the strike-slip faults would constitute a lesser hazard than the large normal faults. This contradicts a conclusion we reached earlier (Anderson and Barnhard, p. 543, 1984).

The chief element of structural consistency in the Pavant Range is the lack of evidence of significant neotectonic extensional deformation even in the deformed southern part and along the range-bounding structures on its east flank. Evidence for an earlier episode of extension is found in restricted areas west of Aurora and near Elsinore (fig. 36). As with the main Pavant Range structural block, the part of the Sevier Plateau we studied south of the Annabella segment of the Sevier fault lacks evidence of significant extensional deformation even in areas within a few meters of the main "extensional" plateau-bounding faults. These faults are, by definition, neotectonic structures. Because they bound broad evenly tilted blocks with little internal deformation we assume that they extend to the base of the seismogenic crust.

In sharp contrast to the large blocks of weak internal extension, rocks adjoining and lying atop the Arapien-cored Sanpete-Sevier anticline are highly extended and, locally, severely attenuated. The southernmost exposures reveal persistent down-to-the-east throw across the anticline and a strong tendency for the extensional strain to be absorbed at the contact zone with the mechanically weak underlying Arapien Formation. Deformational kinematics suggest that Arapien rocks are withdrawn from beneath the northernmost part of the Sevier Plateau as an integral part of the extensional and attenuation process. As with the deformed southern part of the Pavant Range, this deformation has strong thin-skinned attributes. The Arapien apparently serves as a decollement zone characterized by relatively low-viscosity rock flowage below a cover-rock sequence that deforms by brittle failure. Such a zone is capable of vertically partitioning deformation and providing the kind of mechanical layering in the upper crust that gives rise to depth partitioning of small and moderate earthquakes (Arabasz, 1984; Arabasz and Julander, 1986). The inferred detachment fault in the Clear Creek area is capable of similar partitioning. Seismic-hazards assessments in the central Sevier Valley area are closely linked to our understanding of the depth of penetration of faults. We believe that very few of the mapped faults in the central Sevier Valley area penetrate more than a few kilometers and that only range-bounding faults such as the Sevier fault have the potential of large damaging earthquakes related to their probable penetration to the base of the seismogenic crust.

The northerly trending Monroe segment of the Sevier fault appears to break cleanly through gently east-tilted Tertiary strata with no suggestion of monoclinal flexing toward Sevier Valley. Apart from this example, our studies show that the margins of uplifted blocks in the central Sevier Valley area are mostly or partly monoclinal flexures cut by one class of faults that displace rocks down toward the uplifted block and another class of very steep faults that displace rocks down toward the valley. The net extension may be small in some monoclines. Where well developed in range-margin structural settings, such as in the Pavant Range, the possibility exists that this deformational style reflects draping over major buried faults that dip toward the valley at steep or moderate angles. The steep dip of these faults measured at the surface may result from refraction as they approach the zero-stress environment at the air-rock interface. There may be an additional component of lateral spreading or mushrooming as blocks loose lateral confinement during uplift. Such spreading may be a factor in the large-scale extension and structural thinning seen in the southernmost part of the Sanpete-Sevier anticline. As such, the deformational style of the monoclines qualifies as thin skinned, though it may portend deeply penetrating buried structures. Because it is common, it is important that it be understood and that it be integrated with our understanding of seismicity. This is a vital topic for future research.

Clustered seismicity and surface deformation in the central Sevier Valley area coincide, and the coincidence can be explained in terms of localized zones of high stress that develop where there is a need to compensate for strongly contrasting along-strike style and vergence of range-front structures. We make no claim to understanding the dynamics of faulting and seismicity in these zones. We assert, however, that fault recurrence times and slip rates estimated from the high-stress zones do not characterize the major structures that extend away from them and therefore should not be used to characterize earthquake hazards beyond the zones themselves.

In the central Sevier Valley area, geologic fault-slip and earthquake focal-mechanism data are generally similar in (1) an approximate east-west orientation of inferred least compressive stress (figs. 29, 36), (2) the widespread distribution of mixed-mode dip-slip and strike-slip faulting (figs., 29, 36), and (3) the common presence of slip incompatibility for strike-slip faults. The slip incompatability indicates significant amounts of block-boundary faulting that cannot be interpreted in terms of applied remote stress. Unfortunately, we know of no straightforward way to separate block-bounding strike-slip faults from other strike-slip faults. In addition to the slip incompatibility, there is a paradox inherent in the results of our fault-slip studies. Four of the five Φ values for dip-slip faulting (table 1) are very low (<0.1) and the other is low (2.6). If, for the purpose of discussion, strike-slip faulting is disregarded, the low Φ values suggest that σ_2 and σ_3 are close in value and that moderately dipping faults of any orientation are favorably oriented for dip slip. If strike-slip faulting <u>is</u> regarded, its intermixture with dip-slip faulting suggests that σ_1 and σ_2 are capable of interchanging their positions and are therefore close in value. We make no attempt to resolve this paradox.

Gilliland (1963) suggested that repeated folding in the Sanpete-Sevier Valley anticline resulted from a combination of compression and geostatic pressure anomalies. We rule out lateral compression directed normal to the northeast-trending folds as the principal cause of Neogene folding because of the widespread evidence for coeval extensional faulting in the Neogene rocks that form the sheath of the southern part of the fold.

Witkind (1982) suggested that Cenozoic folding resulted from episodes of salt diapirism triggered by movement on deep-seated faults. Diapirism has great appeal because either compressional or extensional regional stresses acting on deep-seated faults will produce the same deformational style associated with diapirism. It explains how, in an extensional enviornment, Neogene folds can form parallel to or superposed on and with similar geometry to earlier folds resulting from compression. It does not seem adequate to explain the uniform down-to-the-plateau faulting in the southern part of the anticline unless the diapiric process is extended to include the lateral withdrawal of rock from beneath the northern Sevier Plateau. Also, the fault contact between the Arapien and superjacent rocks in that area is approximately planar and dips at moderate to low angles over large areas. Diapiric upwelling would be expected to produce a highly irregular and steep to overturned contact (Witkind, 1982).

On the basis of geologic mapping G. C. Willis (written commun., 1987; 1986)and on an unpublished cross-valley reflection profile by S. T. Harding (written commun, 1986), the part of Sevier Valley bordering the Sanpete-Sevier anticline from Salina to Annabella is underlain by a relatively symmetrical Neogene syncline. Diapirism does not seem adequate to explain the northeast-trending folding and faulting along the Pavant Range-Sevier Valley margin where the folded rocks are far above the Arapien Formation which is the causitive rock that has been identified for the diapiric process. Because fold-fault patterns involving Neogene rocks are so similar on both limbs of the syncline beneath Sevier Valley, we believe they result from a single process that is not likely to be diapirism.

With special reference to thrusts and thrust-related structures, Standlee (1982) emphasized that major blind (unexposed) structures exist in the region and that tectonic interpretations based on surface geology along can be very equivocal. We further recognize that in areas where deformation is thin skinned and dominated either by lateral spreading of rock at the margins of or from beneath uplifted blocks or by detachment faulting such as that inferred in the Clear Creek area the location, geometry, and kinematics of major deeply penetrating neotectonic structures could be masked. The alluvial fill of Sevier Valley also masks deep structure. Despite these conditions fostering equivocation regarding deep structure, it is worthwhile to speculate how the earthquake record, subsurface geology, and surface geology, especially that pertaining to widespread neotectonic folding and strike-slip faulting, factor into the regional picture of crustal-scale deformation.

In the Basin and Range, the principal deformational mode is reasonable assumed to be extensional and the strike-slip faulting either results from extension or is superposed on it from a competing deformational process. In the western part of the Basin and Range, right-lateral shear associated with the plate-margin transform fault system (San Andreas) has been suggested as a deformational process that competes with east-west extension (Atwater, 1970).

Based on results from the present study and other studies to the southwest (Anderson, 1973, 1980; Bohannon, 1983), the principal horizontal shearing along the southwestern margin of the northern Basin and Range is sinistral on northeast-striking faults. Because such shear cannot be caused by distributed plate-margin transform interaction other explanations must be sought. The orientation of active extension in the Basin and Range and transition zone of west-central and central Utah is interpreted to be about 285°-105° (Zoback and Aoback, 1980; Arabasz and Julander, 1986). Anderson and Barnhard (1986) determined an identical neotectonic paleostress orientation from the eastern part of the transition zone and similar poorly constrained average paleostress is inferred from the present study (fig.) for the western part of the transition zone. These orientations are all approximately normal to the Basin and Range-Colorado Plateau boundary. Extension and accompanying crustal thinning leads to lateral transfer of material at depth either by simple shear or ductile flow. For the central Utah transition zone it is reasonable to assume west-to-east transfer of material within the semiductile or quasiplastic zone of upper crustal (7-15 km) low velocity (Smith and others, 1975; Gants and Smith, 1983) and possibly also at deeper levels. Rocks at these levels are warm and thermally weakened relative to equivalent-depth lithosphere of the adjacent Colorado Plateau (Thompson and

Zoback, 1979). Lateral transfer of thermally weakened material could be significantly retarded by the mechanical resistance of the thicker cooler lithosphere beneath the Plateau interior. The retardation could translate some of the outward (west to east) material transfer into movement parallel to the boundary in the direction of least resistance to such movement (Anderson, 1973). If an avenue of escape exists along the trend of the transition zone, the material would tend to flow or be translated in that direction; that is, subparallel to the province boundary. Specific directions of such translation could be strongly influenced by preexisting structural weakenesses. The result is a local rafting of surficial crustal blocks parallel to the flow direction. If coeval extension on the Basin and Range side of the boundary is uniformly distributed over extensive areas, the rate and magnitude of tectonic transport would increase in the direction of escape because the required compensation for the retardation would be cumulative. Very large and episodic motions, such as the 65 km of southwesterly tectonic transport of the Frenchman Mountain block near Las Vegas (Anderson, 1973; Bohannon, 1979), could be predicted as one progressed southwestward from the central Sevier Valley. This tectonic model combines a fundamental aspect of approximately east-west extension with tectonic rafting imposed by a system of basal tractions propagated upward from deep lateral flow of material.

Direct evidence for large-scale strike-slip faulting beneath Sevier Valley does not exist. The presence of folds that strike approximately parallel to a principal set of strike-slip faults such as the Dry Wash and subparallel faults is not an uncommon feature in strike-slip structural settings, though it eludes understanding through structural modeling. For example, Aydin and Page (1984) studied the distribution, geometry, and orientation of folds and other structures related to strike-slip faults in the San Francisco Bay region. They found that the diverse structures collectively are more compatible with a simple shear model than with a Mohr-Coulomb model of remote compressive stress. However, even after allowances for structural inhomogeneities, transient influences, and varied degrees of rotation are made, the simple shear model fails to account for folds that commonly parallel the principal shear direction (Aydin and Page, 1984). In the Mercury quadrangle, Nevada, Barnes and others (1982) mapped Neogene folds that parallel the principal northeast-trending sinistral-shear direction. In southern Nevada Bohannon (1983) mapped Neogene folds that parallel the sinistral-slip Lake Mead shear zone. In the Death Valley area Cemen (1984) reported folds that developed parallel to late Cenozoic northwest-striking dextral faults. Those maps and reports show that such Neogene folds exist along strike-slip faults in the Basin and Range and give confidence to an assumption of a similar association in central Sevier Valley. In the Andaman Sea area, Harding (1985) showed that drape folds, interpreted to be caused by dip-slip components of displacement on predominantly strike-slip faults, have axes that parallel the main wrench faults. In addition, he noted that divergent wrench faults commonly have a pair of drape folds that face one another and parallel the main wrench fault. On the basis of seismic reflection, profiles Howell and others (1980) described synclinal troughs paralleling major faults in the divergent wrench-fault regime off coastal California. Basin-margin unconformities attest to repeated tectonism during basin development possibly analagous to the late-stage unconformities described along Sevier Valley by Spieker (1946). We interpret the facing monoclinal folds bordering Sevier Valley as resulting from the superpositioning on the system of east-west extension of a competing system of southwest-directed basal tractions and associated strike-slip faults. Although this model is highly speculative it is consistent with the slip incompatibility seen in the earthquake and geologic fault-slip records, as well as with observed major components of strike slip on some of the deepest earthquakes of the region (Arabasz and Julander, 1986).

Future geologic studies in this area should focus on evaluating the role of detachment faults in the localization and dynamics of lateral block motions, compressional folding, and shear folding. Because the style of deformation in the central Sevier Valley is dramatically different from that along the Wasatch Front, an effort should be made to locate and characterize the deformational boundary between these two on-strike terrains.

REFERENCES

Allmendinger, R. W., Sharp, J. W., Von Tish, D., Serpa, L., Brown, L., Kaufman, S., Oliver, J., and Smith, R. B., 1983, Cenozoic and Mesozoic structure of the eastern basin and Range province, Utah, from COCORP seismic-reflection data: Geology, v. 11, p. 532-536.

Anderson, E. M., 1951, The dynamics of faulting: Edinburg, Scotland, Oliver and Boyd, 2nd edition, 206 p. (1st edition, 1962).

Anderson, R. E., 1973, Large magnitude late Tertiary strike-slip faulting north of Lake Mead, Nevada: U.S. Geological Survey Professional Paper 794, 18 p.

______1980, The status of seismotectonic studies of southwestern Utah: U.S. Geological Survey Open-File Report 80-801, p. 519-547.

______1980a, Structural ties between the Great Basin and Sonoran Desert sections of the Basin and Range province: U.S. Geological Survey Open-File Report 81-503, p. 4-6.

Anderson, R. E., and Barnhard, T. P., 1984, Extensional and compressional paleostress and their relationship to paleoseismicity and seismicity, central Sevier Valley, Utah: U.S. Geological Survey Open-File Report 84-763, p. 515-546.

______1984, Late Cenozoic fault and fold patterns in Sevier County, Utah, and their relationships to seismicity in the area [abs.]: Geological Society of America Abstracts with Programs, v. 16, no. 6, p. 430.

______1986, Genetic relationship between faults and folds and determination of Laramide and neotectonic paleostress, western Colorado Plateau-transition zone, central Utah: Tectonics, v. 5, no. 2, p. 335-357.

Anderson, R. E., and Bucknam, R. C., 1979, Map of fault scarps on unconcolidated sediments, Richfield 1°X2° quadrangle, Utah: U.S. Geological Survey Open-File Report 79-1239, 15 p., 1 sheet, scale 1:250,000.

Anderson, R. E., and Mehnert, H., 1979, Reinterpretation of the history of the Hurricane fault in Utah: Rocky Mountain Association of Geologists--Utah Geological Association, 1979 Basin nd Range Symposium, p. 145-173.

Angelier, Jacques, 1979, Determination of the mean principal stress for a given fault population: Tectonophysics, v. 56, p. T17-T26.

Angelier, Jacques, and Colletta, Bernard, 1983, Tension fractures and extensional tectonics: Nature, v. 301, no. 5895, p. 49-51.

Angelier, Jacques, Colletta, Bernard, and Anderson, R.E., 1985, Neogene paleostress changes in the Basin and Range--a cast study at Hoover Dam, Nevada-Arizona: Geological Society of America Bulletin, v. 96, p.347-361

Arabasz, W.J., 1984, Earthquake behavior in the Wasatch Front area: Association with geologic structure, space-time occurrence, and stress state: U.S. Geological Survey Open-File Report 84-763, p. 310-339.

Arabasz, W.J., and Julander, D.R., 1986, Geometry of seismically active faults and crustal deformation within the Basin and Range-Colorado Plateau transition in Utah: Geological Society of America Special Paper 208, p. 43-73.

Arabasz, W.J., and McKee, M.E., 1979, Utah earthquake catalog 1850-June 1962, _in_ Arabasz, W.J., Smith, R.B., and Richins, W.D., eds., Earthquake Studies in Utah 1850 to 1978: Special publication of the University of Utah Seismograph Stations, Department of Geology and Geophysics, University of Utah, p. 548.

Arabasz, W.J., and Smith, R.B., 1981, Earthquake prediction in the intermountain seismic belt--An intraplate extensional regime, in Simpson, D.W., and Richards, P.G., eds., Earthquake prediction--An international review: American Geophysical Union, Maurice Ewing Series, v. 4, p. 238-258.

Armstrong, R.L., 1968, Sevier orogenic belt in Nevada and Utah: Geological Society of America Bulletin, v. 79, no. 4, p. 429-458.

Atwater, Tanya, 1970, Implications of plate tectonics for the Cenozoic tectonic evolution of western North America: Geological Society of America Bulletin, v. 81, p. 3513-3536.

Aydin, A., and Page, B.M., 1984, Diverse Pliocene-Quaternary tectonics in a transform environment, San Francisco Bay region, California: Geological Society of America Bulletin, v. 95, p. 1303-1317.

Baer, J.L., Davis, R.L., and George, S.E., 1982, Structure and stratigraphy of the Pavant Range, central Utan, in Neilson, D.L., ed., Overthrust belt of Utah: Utah Geological Association Publication 10, p. 31-48.

Barnes, Harley, Ekren, E.B., Rodgers, C.L., and Hedlund, D.C., 1982, Geologic and tectonic maps of the Mercury quadrangle, Nye and Clark Counties, Nevada: U.S. Geological Survey Miscellaneous Investigations Map I-1197, scale 1:24,000.

Best, M.G., McKee, E.H., and Damon, P.E., 1980, Space-time-composition patterns of late Cenozoic mafic volcanism, southwestern Utah and adjoining areas: American Journal of Science, v. 280. p. 1035-1050.

Bohannon, R.G., 1979, Strike-slip faults of the Lake Mead region of southern Nevada, in Armentrout, J. M., Cole, M. R., and TerBest, Harry, eds., Cenozoic paleogeography of the Western United States: Pacific Coast Paleogeography Sumposium 3: Los Angeles, Pacific Section, Society of Economic Paleontologists and Mineralogists, p. 129-139.

______1983, Geologic map, tectonic map and structure sections of the Muddy and northern Black Mountains, Clark County, Nevada: U.S. Geological Survey Miscellaneous Investigations Map I-1406.

Burchfiel, B.C., and Hickcox, C.W., 1972, Structural development of central Utah, in Baer, J. L., and Callaghan, E., eds., Plateau-Basin and Range transition zone, central Utah, 1972: Salt Lake City, Utah Geological Association Publication 2, p. 55-66.

Callaghan, Eugene, Parker, R.L., 1961, Geology of the Monroe quadrangle, Utah: U.S. Geological Survey Geologic Quadrangle Map GQ-155, scale 1:62,500.

______1962, Geology of the Sevier quadrangle, Utah: U.S. Geological Survey Geologic Quadrangle Map GQ-156, scale 1:62,500.

Cemen, I., Pickens, T.B., Wright, L.A., Drake, R.E., and Johnson, F.C., 1984, Cenozoic deformation and sedimatation, south easternmost part of the Furnace Creek fault zone, Death Valley, California: Geolgogical Society of America Abstracts with program, v. 16, no. 6, p.466.

Chapman, D.S., and Harrison, R., 1978, Monroe, Utah, hydrothermal system: results from the drilling of test wells MC-1 and MC-2: University of Utah, Department of Geology and Geophysics Topical Report, DOE/DGE Contract EY-76-S-07-1601.

Clark, E.E., 1977, Late Cenozoic volcanic and tectonic activity along the eastern margin of the Great Basin, in the proximity of Cove Fort, Utah: Brigham Young University Geology Studies, v. 24, pt. 1, p. 87-114.

Cunningham, C.G., Steven, T.A., Rowley, P.D., Glassgold, L.B., and Anderson, J.J., 1983, Geologic map of the Tushar Mountains and adjoining areas, Marysvale volcanic field, Utah: U.S. Geological Survey Miscellaneous Investigations Map I-1430-A, scale 1:50,000.

Davis, R.L., 1982, Geology of the Dog Valley-Red Ridge area, Southern Pavant Mountains, Millard County, Utah: Brigham Young University Geology Studies, v. 30, no. 1, p. 19-36.

Gants, D.L., and Smith, R.B., 1983, Joint interpretation of refraction and reflection data for an area of low-angle faulting in the eastern Basin-Range: EOS [Transactions of the American Geophysical Union], v. 64, p. 763.

Gilliland, W.N., 1963, Sanpete-Sevier Valley anticline of central Utah: Geological Society of America Bulletin, v. 74, p. 15-124.

Halliday, M.E., and Cook, K.L., 1978, Gravity and ground magnetic surveys in the Monroe and Joseph KGRA's and surrounding region, south-central Utah: University of Utah, Department of Geology and Geophysics Report, DOE/DGE Contract EY-76-S-07-1601.

______1980, Regional gravity survey, northern Marysvale volcanic field, south-central Utah: Geological Society of America Bulletin, v. 91 p. 502-508.

Harding, T.P., 1985, Seismic characteristics and identification of negative flower structures, positive flower structures, and positive structural inversion: American Association of Petroleum Geologists Bulletin, v. 69, no. 4, p. 582-600.

Hardy, C.T., 1952, Eastern Sevier Valley, Sevier and Sanpete Counties, Utah: Utah Geological and Mineralogical Survey, Bulletin 43, 93 p.

Hickcox, C.W., 1971, The geology of a portion of the Pavant Range allochthon, Millard County, Utah: Ph.D. dissertation, Rice University, Houston, Texas, 67 p.

Hill, D.P., 1982, Contemporary block tectonics: California and Nevada: Journal Geophysical Research, v. 87, no. B7, p. 5433-5450.

Howell, D.G., Crouch, J.K., Greene, H.G., McCulloch, D.S., and Vedder, J.G., 1980, Basin development along the late Mesozoic and Cenozoic California margin: a plate tectonic margin of subduction, oblique subduction and transform tectonics: in Sedimentation in oblique-slip mobile zones, P.F. Ballance and H.G., Reading eds, International Association of Sedimentologists Special Publications, 4, p. 43-62.

Julander, D.R., 1983, Seismicity and correlation with fine structures in the Sevier Valley area of the Basin and Range-Colorado Plateau transition, south-central Utah: Salt Lake City, Utah, University of Utah, M.S. thesis, 142 p.Nabelek,

Kehle, R.O., 1970, Analysis of gravity sliding and orogenic translation: Geological Society of America Bulletin, v. 81, p. 1641-1664.

Lawton, T.F., 1985, Style and timing of frontal structures, thrust belt, central Utah: American Association of Petroleum Geologists Bulletin, v. 69, no. 7, p. 1145-1159.

Mase, C.W., Chapman, D.S., and Ward, S.H., 1978, Geophysical study of the Monroe-Red Hill geothermal system: University of Utah, Department of Geology and Geophysics Topical Report, DOE/DGE Contract 78-C-07-1701.

Ouchi, Shunji, 1985, Response of alluvial rivers to slow active tectonic movement: Geological Society of America Bulletin. v. 96, no. 4, p. 504-515.

Rowley, P.D., 1968, Geology of the southern Sevier Plateau, Utah: Ph.D. Thesis, Univeristy of Texas, Austin, Texas, 385 p.

Rowley, P.D., Steven, T.A., Anderson, J.J., and Cunningham, C.G., 1979, Cenozoic stratigraphic and structural framework of southwestern Utah: U.S. Geological Survey Professional Paper 1149, 22 p.

Rowley, P.D., Steven, T.A., and Kaplan, A.M., 1981a, Geologic map of the Monroe NE quadrangle, Sevier County, Utah: U.S. Geological Sruvey Miscellaneous Field Studies Map MF-1330, 1 sheet, scale 1:24,000.

Rowley, P.D., Steven, T.A., and Mehnert, H.H., 1981b, Origin and structural implications of upper Miocene rhyolites in Kingston Canyon, Piute County, Utah: Geological Society of America Bulletin, v. 92, p. 590-602.

Segall, P., and Pollard, D.D., 1980, Mechanics of discontinuous faults: Journal of Geophysical Research, v. 85, p. 4337-4350.

Smith, R.B., 1978, Seismicity, crustal structure, and intraplate tectonics of the Western Cordillera: Geological Society of America Memoir 152, p. 111-144.

Smith, R.B., Braile, L.W., and Keller, G.R., 1975, Crustal low velocity layers: Possible implications of high temperature at the Basin and Range-Colorado Palteau transition: Earth Planetary Science Letters, v. 28, p. 197-204.

Spieker, E.M., 1946, Late Mesozoic and early Cenozoic history of central Utah: U.S. Geological Survey Professional Paper 205-D, p. 117-161.

______1949, The transition between the Colorado Plateaus and the Great Basin in central Utah: Salt Lake City, Utah Geological Society, no. 4, 106 p.

Standlee, L.A., 1982, Structure and stratigraphy of Jurassic rocks in central Utah: Their influence on tectonic development of the Cordilleran foreland and thrust belt, in Powers, R. B., ed., Geologic studies of the Cordilleran thrust belt: Denver, Rocky Mountain Association of Geologists, v. 1, p. 357-382.

Stanley, K.O., and Collinson, J.W., 1979, Depositional history of Paleocene-lower Eocene Flagstaff Limestone and coeval rocks, central Utah: American Association of Petroleum Geologists Bulletin, v. 63, p. 311-323.

Steven, T.A., 1979, Geologic map of the Monroe NW quadrangle, west-central Utah: U.S. Geological Survey Miscellaneous Field Studies Map MF-107, 1:24,000.

Steven, T.A., Cunningham, C.G., Naeser, C.W., and Mehnert, H.H., 1979, Revised stratigraphy and radiometric ages of volcanic rocks and mineral deposits in the Marysvale area, west-central Utah: U.S. Geological Sruvey Bulletin 1469, p. 1-40.

Steven, T.A., and Morris, H.T., 1983, Geologic map of the Cove Fort quadrangle, west-central Utah: U.S. Geological Survey Miscellaneous Investigations Map I-1481, 1 sheet, scale 1:50,000.

______1983, Geologic map of the Richfield 1°X2° quadrangle, west-central Utah: U.S. Geological Survey Open-File Report 83-583.

Stewart, J.H., Moore, W.J., and Zietz, Isidore, 1977, East-west patterns of Cenozoic igneous rocks, aeromagnetic anomalies, and mineral deposits, Nevada and Utah: Geological Society of America Bulletin, v. 88, p. 67-77.

Thompson, G.A., and White, D.E., 1964, Regional geology of the Steamboat Springs area, Washoe County, Nevada: U.S. Geological Survey Professional Paper 458-A, 52 p.

Wernicke, B., 1985, Uniform-sense normal simple shear of the continental lithosphere: Canadian Journal of Earth Sciences, v. 22, no. 1, p. 108-125.

Williams, J.S., and Tapper, M.L., 1953, Earthquake history of Utah, 1850-1949: Seismological Society of America Bulletin, v. 43, p. 191-218.

Williams, P.L., and Hackman, R.J., 1971, Geology, structure, and uranium deposits of the Salina quadrangle, Utah: U.S. Geological Survey Miscellaneous Geologic Investigations Map I-591.

Willis, G.C., 1985, Revisions to the geochronology and source areas of Early Tertiary formations in the Salina area of Sevier Valley, central Utah [abs.]: Geological Society of America Abstracts with Programs, v. 17, no. 4, p. 272.

______1986, Geology of the Salina quadrangle, Sevier County, Utah: Utah Geological and Mineral Survey, Map 83.

Witkind, I.J., 1982, Salt diapirism in central Utah, in Nielson, D.L., ed., Overthrust belt of Utah: Salt Lake City, Utah Geological Association Publication 10, p. 13-30.

Zoback, M.L., and Zoback, M.D., 1980, State of stress in the conterminous United States: Journal of Geophysical Research, v. 85, p. 6113-6156.

				SEVIER FAULT			
	Clear Creek Area		Richfield Willow Creek	Monroe Segment		Annabella segment	Anticline Sample
	SS	DS		SS	DS	DS	
N	149(251)	60	33 (66)	36	13 (25)	90	49 (109)
σ_1	4, 3	265, 84	147, 88	173, 3	183, 73	166, 86	170, 87
σ_2	163, 87	170, 1	45, 1	24, 87	347, 17	13, 4	12, 3
σ_3	274, 1	80, 6	315, 2	263, 2	79, 4	282, 2	282, 1
Φ	0.16	0.04	0.06	0.12	0.26	0.03	0.05
Δ	23°	23°	12°	19°	15°	20°	15°
discordant data	5	4	1	1	1	2	0
weight	1=116 3=25 5=3 9=5	1=59 3=1	1=25 2=1 3=1 3=3 7=3	1=34 5=2	1=10 5=3	1=86 4=1 5=2 9=1	1=31 2=4 3=3 5=9 7=1 9=1
Sense of Slip	D=58 S=91			D=20 S=16			
D+S Strike Ranges	D 275°-000° S 001°-85°			D 279°-352° S 358°-065°			
Degree of Certainty	C=57 P=75 S=17	C=15 P=40 S=4	C=12 P=21 S=0	C=2 P=0 S=34	C=4 P=8 S=1	C=7 P=60 S=23	C=24 P=24 S=1

TABLE 1.-- Fault-slip data and computational results

SS indicates strike-slip, DS indicates dip slip, Φ is the stress ratio, described in text. The mean angular difference (Δ) is the difference between actual striae and the theoretical maximum shear stress on the fault plane. Discordant data are identified as striae that form an angle >45° with the theoretical maximum shear stress. Weight is a crudely logarithmic function of fault displacement (1= 50 cm, 3=2-5 m, 5=10-20 m, 7=50-75 m, 9=100-200 m,); weight is followed by the number of faults in each weight category. Sense of slip gives the number of dextral and sinistral strike-slip faults. The azimuthal range of strikes of dextral and sinistral faults is also shown. The degree of certainty refers to the determination of the sense of slip (C, certain; P, probable; S, supposed; and is followed by the number of faults in each category).

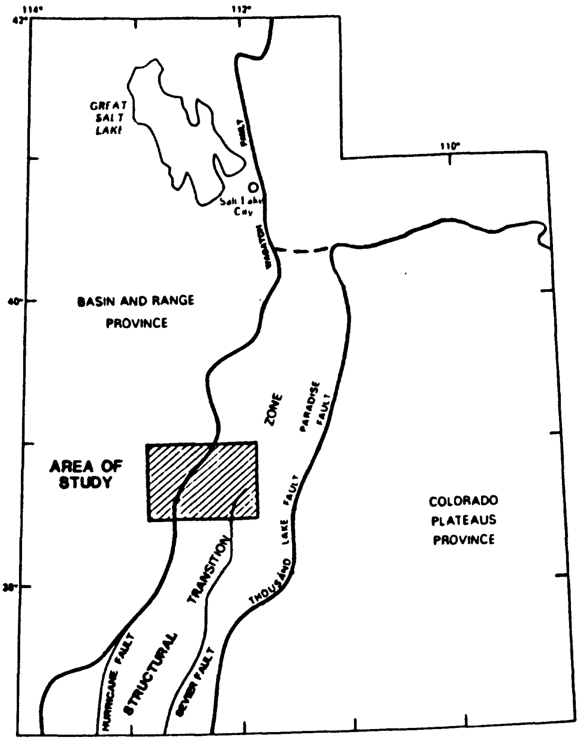

FIGURE 1.--Index map showing location of the central Sevier Valley study area relative to the structural transition zone and bordering provinces. Hurricane and Sevier faults shown with hachures on downthrown side.

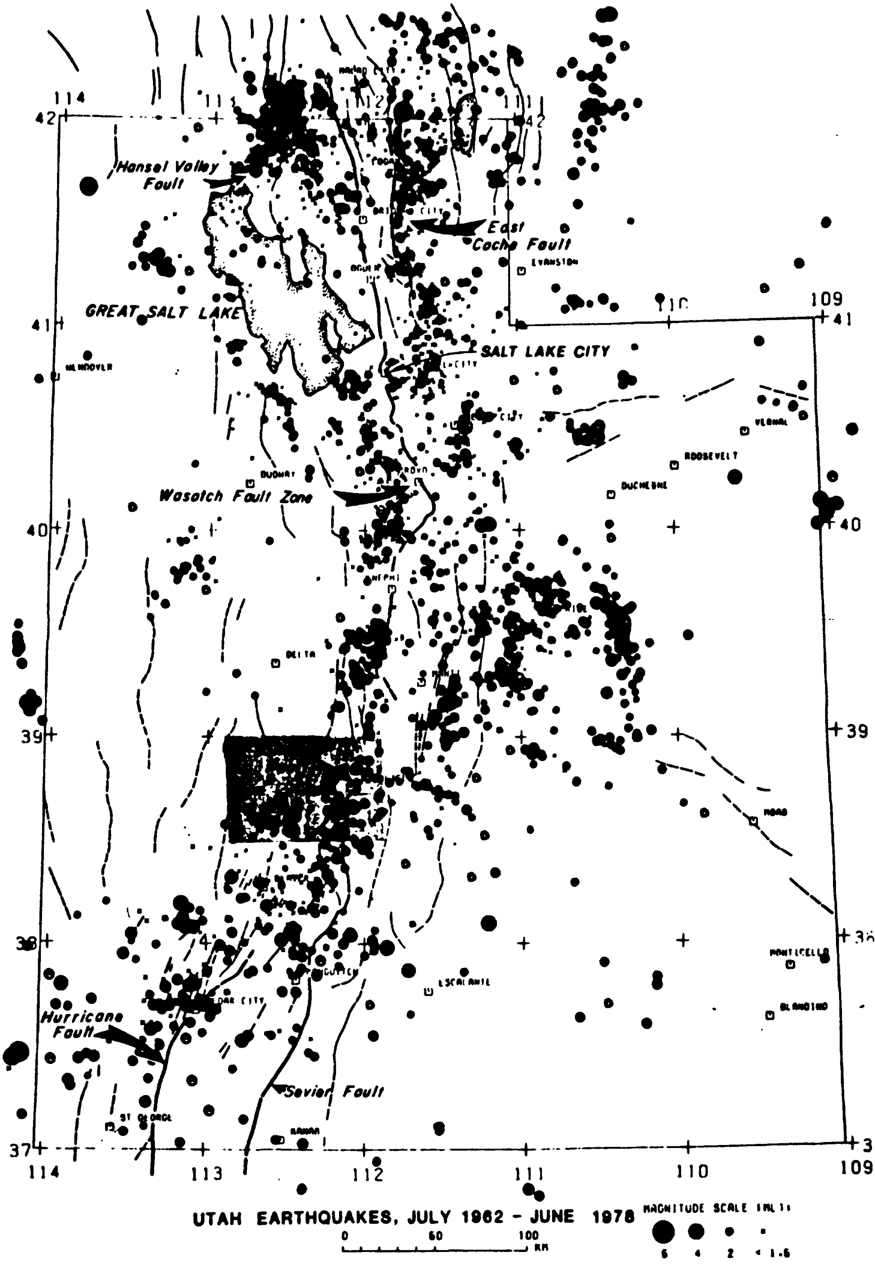

FIGURE 2.--Map showing distribution of earthquake epicenters in Utah for the period July 1962-September, 1984 (from Smith and Richins, 1984). The central north-south zone of abundant seismicity is called the Intermountain Seismic Belt. Shading shows area covered by figure 3.

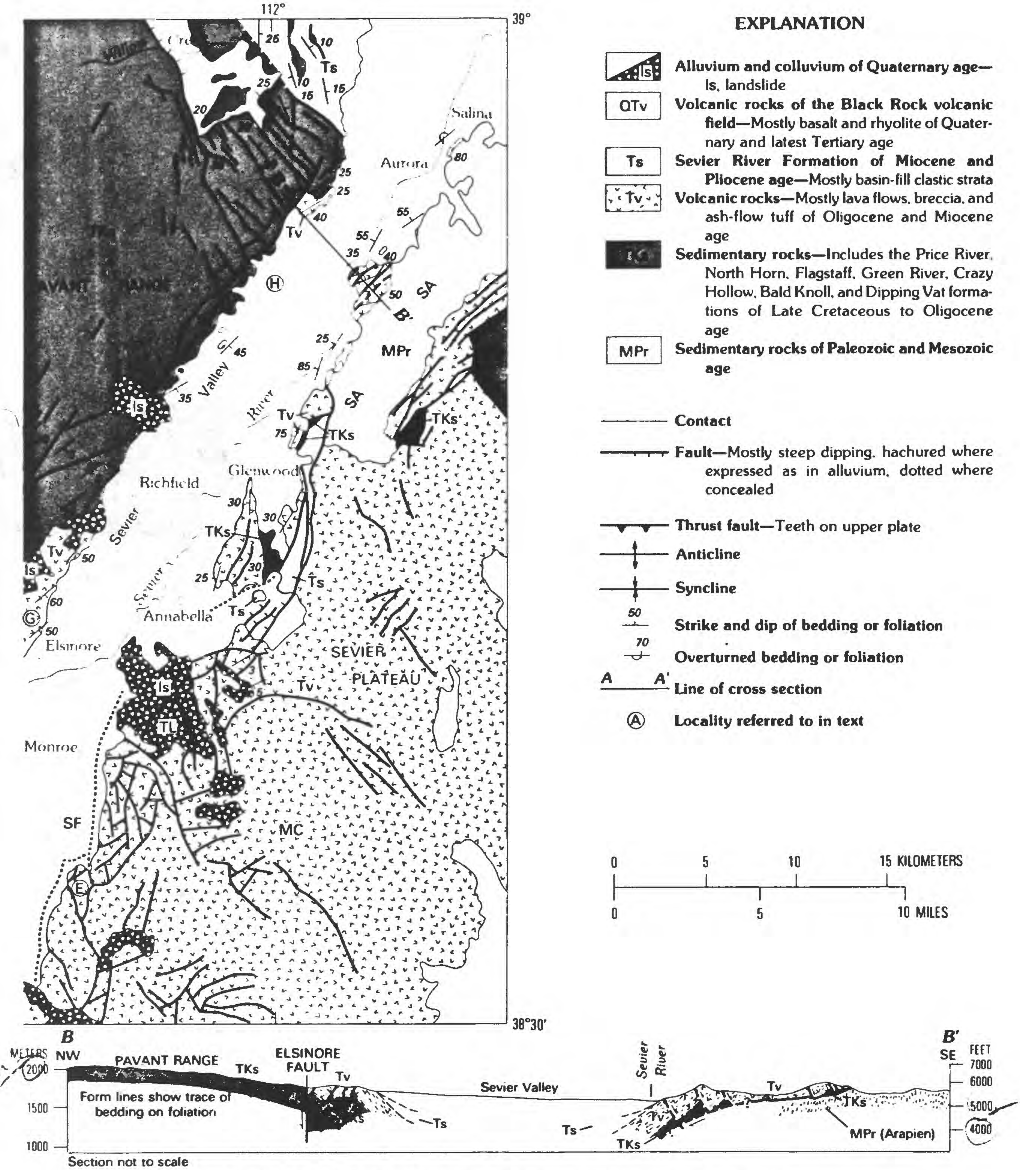

FIGURE 3.--Geologic map and section of the central Sevier Valley area, Utah after Cunningham and others, 1983, Steven and Morris, 1983a, and Williams and Hackman, 1971. BV, Black Rock volcanic field, CD, Clear Creek downwarp; CG, Cove Fort graben; DF, Dry Wash fault; MC, Monroe Peak caldera; PT, Pavant thrust; SA, Sanpete-Sevier Valley anticline; SF, Sevier fault; TC, Three Creeka caldera; J. Joseph. Approximate line of section shown by hachures in Clear Creek area. Circled letters are localities referred to in text

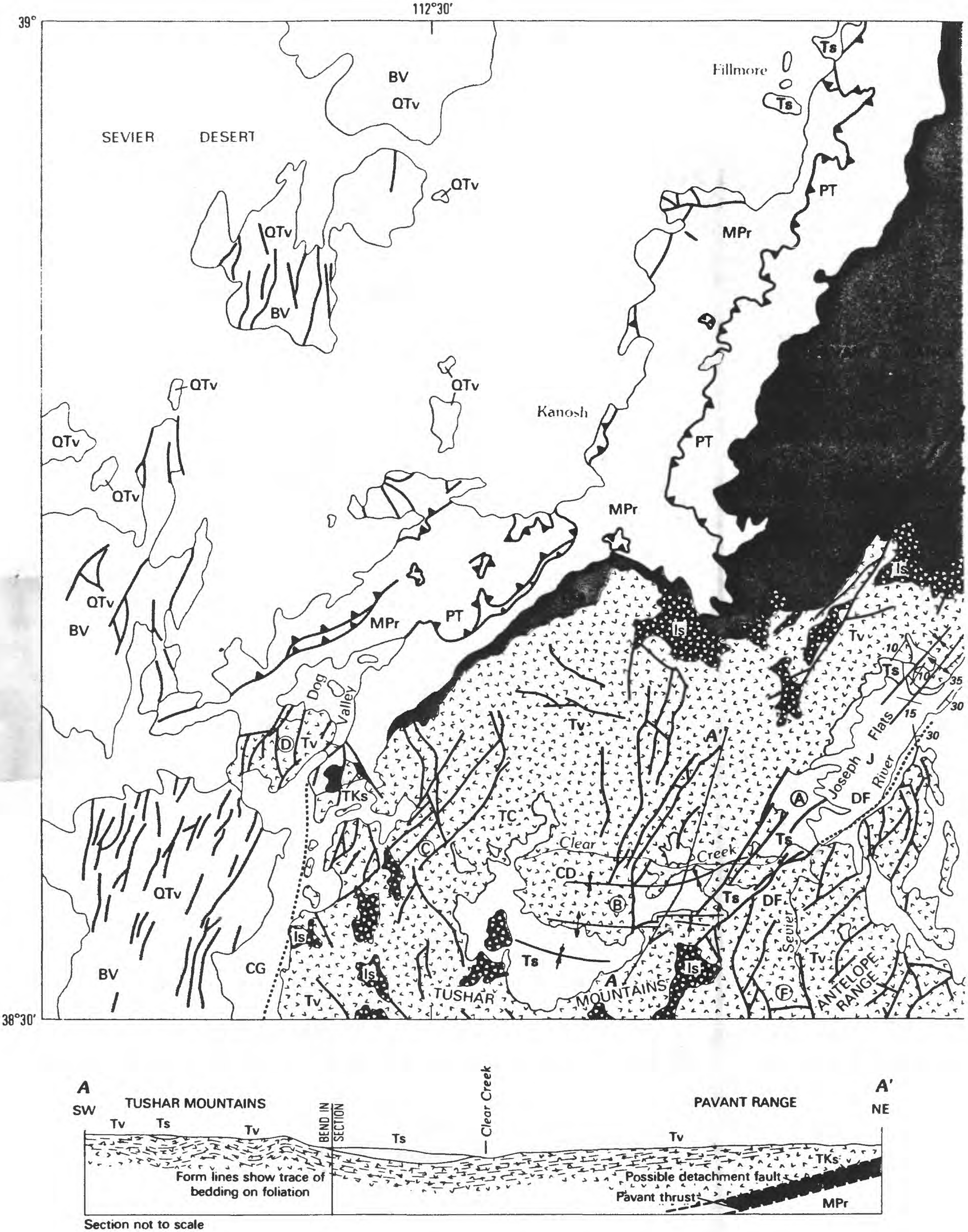
112°30′
39°
38°30′
SEVIER DESERT
Fillmore
Kanosh
BV
QTv
Ts
PT
MPr
Is
Tv
TKs
TC
CD
CG
DF
Dog Valley
Clear Creek
Joseph Flats
J
Sevier River
TUSHAR MOUNTAINS
ANTELOPE RANGE
A
A′
Ⓐ
Ⓑ
Ⓒ
Ⓓ
Ⓕ
10
35
30
15
A
A′
SW
NE
TUSHAR MOUNTAINS
PAVANT RANGE
BEND IN SECTION
Clear Creek
Form lines show trace of bedding on foliation
Possible detachment fault
Pavant thrust
Section not to scale

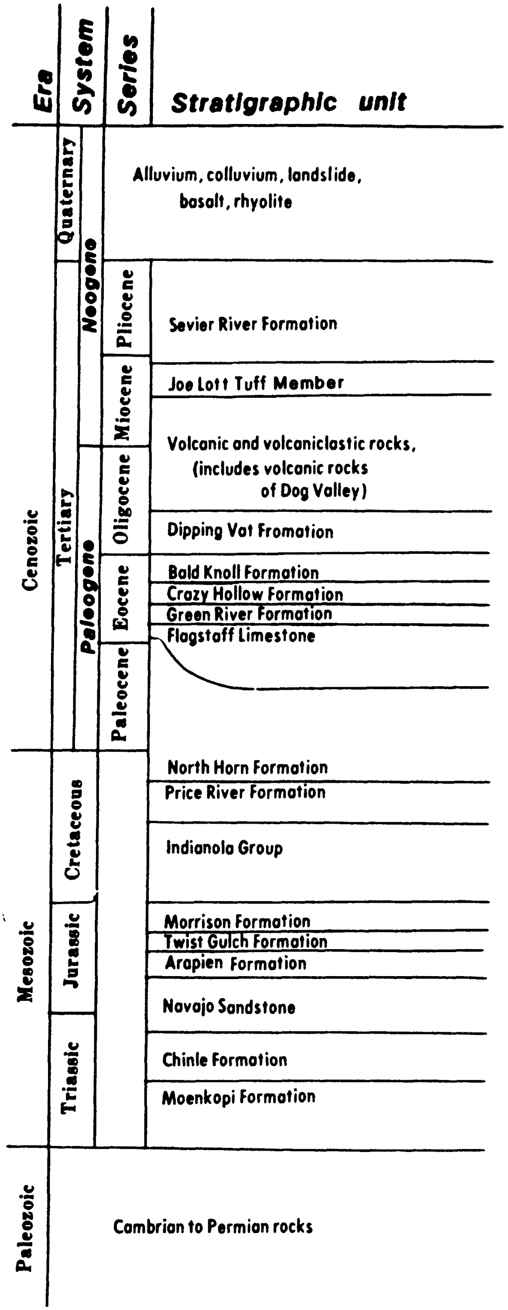

FIGURE 4.--Generalized stratigraphic column for the central Sevier Valley area.

FIGURE 5.--Photographs of Dry Wash fault. A, View looking northeast along trace of fault showing slivers of Joe Lott Tuff Member (at and beyond man at arrow) displaced to exotic positions and separating younger coarse clastic sediments of the Sevier River formation (exposed beds to left of man and unexposed beds in covered slope to right of man). The clastic strata dip about 35° away from the camera so the slivers of tuff that mark the trace of the fault resemble dikes that crosscut the sediments. The dikelike juxtapositioning results from strike-slip displacement of a previously fault-tilted and fault-repeated sequence of strata. B, View looking southeast at location marked by man in A showing horizontally striated fault surface on Joe Lott Tuff Member where the cemented gravel of the Sevier River Formation of the hanging wall (lower part of photo) has spalled away along the fault plane. C, View looking southwest along main trace of Dry Wash fault showing gently plunging striations developed on brecciated Joe Lott Tuff Member. Note man at arrow for scale to left and below the center of photo.

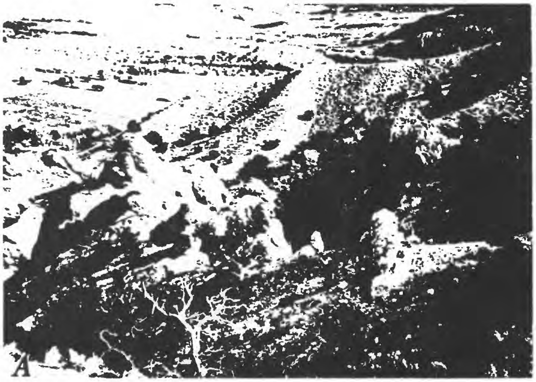

A

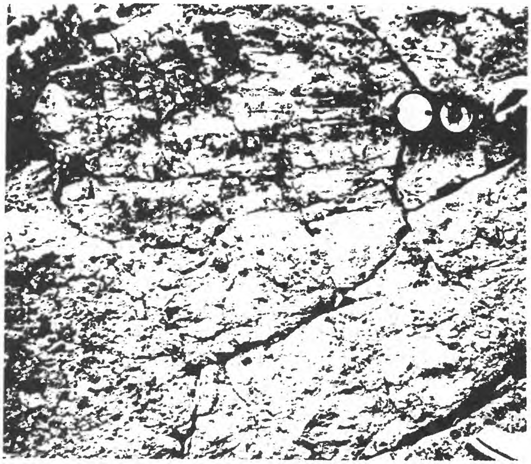

B

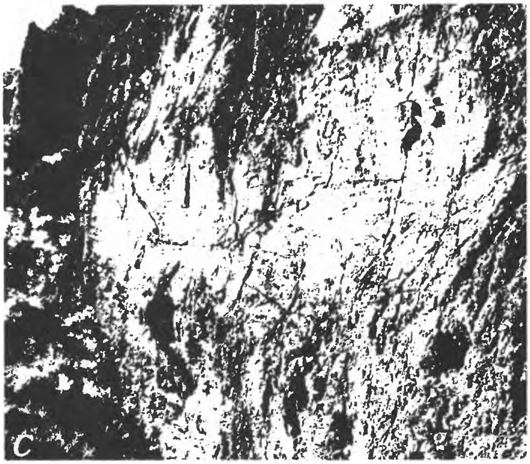

C

FIGURE 6.--Photograph looking northwest from Dry Wash fault across Clear Creek in foreground to trace of sinistral strike-slip fault in middle distance (scar between arrow and heavy line, labeled FT). Fault parallels the Dry Wash fault and juxtaposes south-dipping rocks of the north flank of the Clear Creek downwarp beyond trace against north-dipping rocks of the south flank of the downwarp on camerman's side of trace. Tj, Joe Lott Tuff Member; Ts, Sevier River Formation; light-weight continuous lines are contacts, light-weight dashed lines accentuate bedding traces. Linear skyline elements and vegetation stripes below skyline show extent of south-dipping flank of downwarp. See figure 7 for closeup views of fault which is very well exposed in area of scar (labeled X).

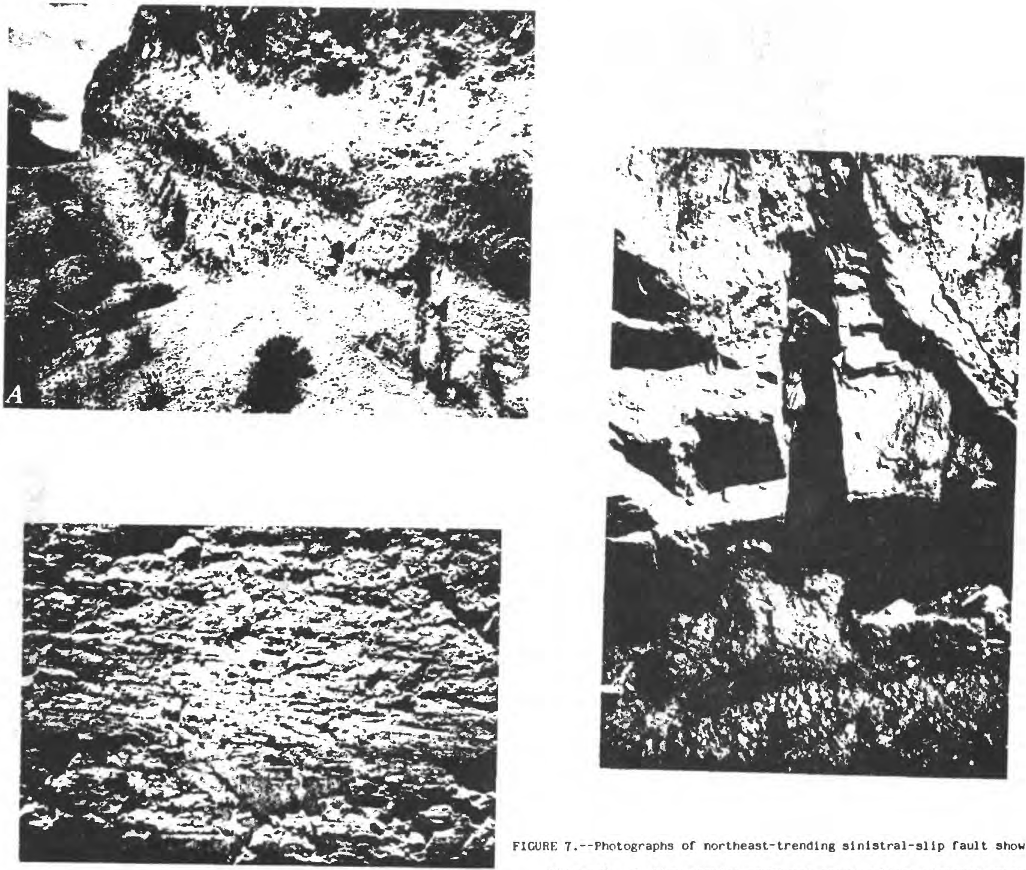

FIGURE 7.--Photographs of northeast-trending sinistral-slip fault shown in figure 6. A, View looking southwest showing large striated grooves on Joe Lott Tuff Member where coarse cemented gravels of the Sevier River Formation (visible in lower part of scarp) have spalled away from fault surface. B, Close-up view of striations on large groove shown in A. Arrow drawn on fault surface in center of view is 3 cm long and shows motion direction of block as required by streamlining of gouge deposits to right of small mechanically resistant lithic inclusions in tuff above arrow. C, View looking down at fault surface (in shade) separating clayey sands of the Sevier River Formation in foreground from Joe Lott Tuff Member. The mechanically weak clayey sands are squeezed like toothpaste into a conspicuous tension gash about 20 cm wide in the mechanically resistant Joe Lott Tuff. Though not visible, the shaded fault surface is conspicuously striated, showing that the Joe Lott block moved to the left (sinistral).

FIGURE 8.--Well-exposed large smooth striated surface of small sinistral-slip fault in Joe Lott Tuff Member. Rough surfaces (near top of photo) that extend out from and offset the large smooth surface also contain gently plunging striae (not obvious in photo). Displacement on the rough-surface fractures is dextral, showing that they are conjugate to the large smooth surface.

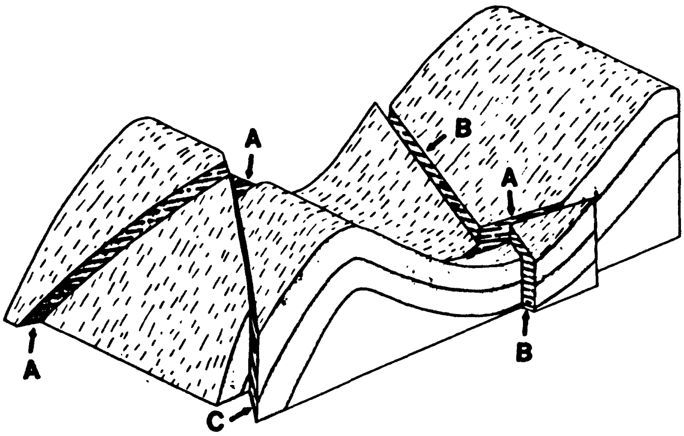

FIGURE 9.--Schematic representation in block-diagram form showing a fold cut by a sinistral fault (A) and two dextral faults (B, C). Heavy lines symbolize striae on fault surfaces. Fault C offsets fault A and fault A offsets fault B as indication of conjugate behavior. Also, rake of striae on faults is independent of position in fold.

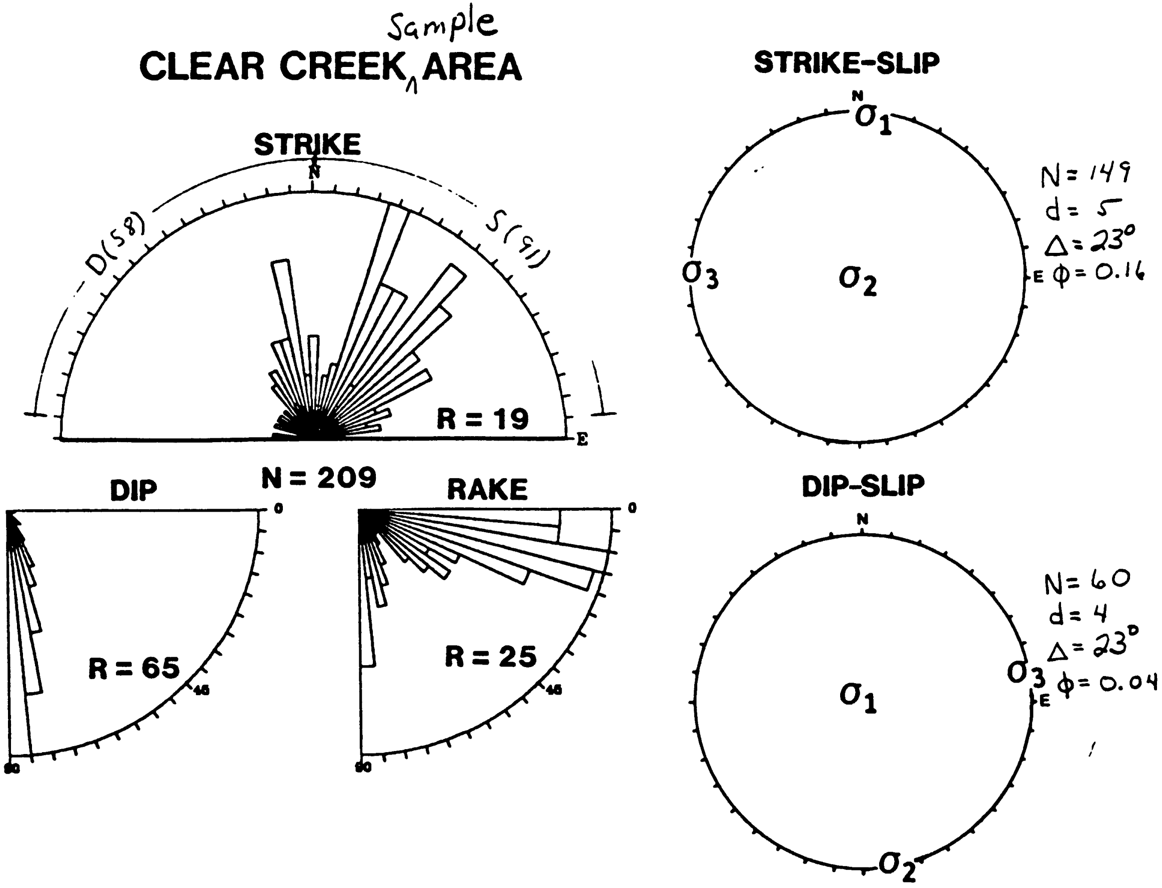

FIGURE 10.--Histograms of strike, dip, and rake and lower hemisphere stereographic plots of computed paleostress axes for faults from the Clear Creek sample area in the easternmost part of the Clear Creek downwarp. R, radius of histogram in number of measurements; N, sample size; D, azimuthal range of dextral faults with number of faults in parentheses; S, same for sinistral faults; σ_1, σ_2, and σ_3 are the maximum, intermediate, and minimum principal compressional stresses; d, the number of striae that form an angle >45° with the theoretical maximum shear stress; Δ, the mean angular difference between the actual striae and the theoretical maximum shear stress on the fault plane; $\phi=(\sigma_2-\sigma_3)/(\sigma_1-\sigma_3)$.

FIGURE 11.--Photograph looking northwest at excavated surface of steep planar fault that cuts transversely through northeast-tilted beds of the Sevier River Formation at locality A on figure 3. See figure 12 for stereographic plot of fault and other data. Cameraman is standing on clayey and sandy sediments (not visible) that are downthrown by oblique dextral slip against coarse clastic gravel and conglomerate across the fault.

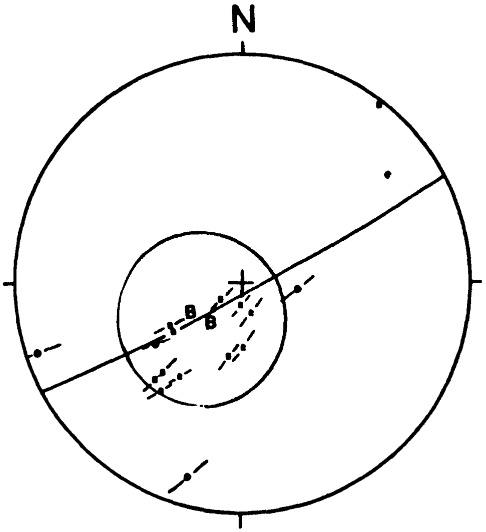

FIGURE 12.--Lower hemisphere stereographic plot of the main fault (great circle arc) and 16 subsidiary northeast-trending faults (segments of great circles) at locality A, figure 3. Striae on fault planes shown as squares for those with dextral components and dots for those with sinistral components. Poles to bedding indicated by symbol B. Circle shows 30° cone with an axis near the poles to bedding. The concentration of striae within the cone is consistent with an interpretation that most of the faulting is caused by transverse block-boundary displacements related to stratal tilting.

FIGURE 13.--View looking north along well-exposed Joe Lott Tuff Member in footwall (left and center) of north-northwest-striking normal fault at locality B on figure 3. Hanging wall block (right edge of photo) consists of poorly exposed Sevier River Formation.

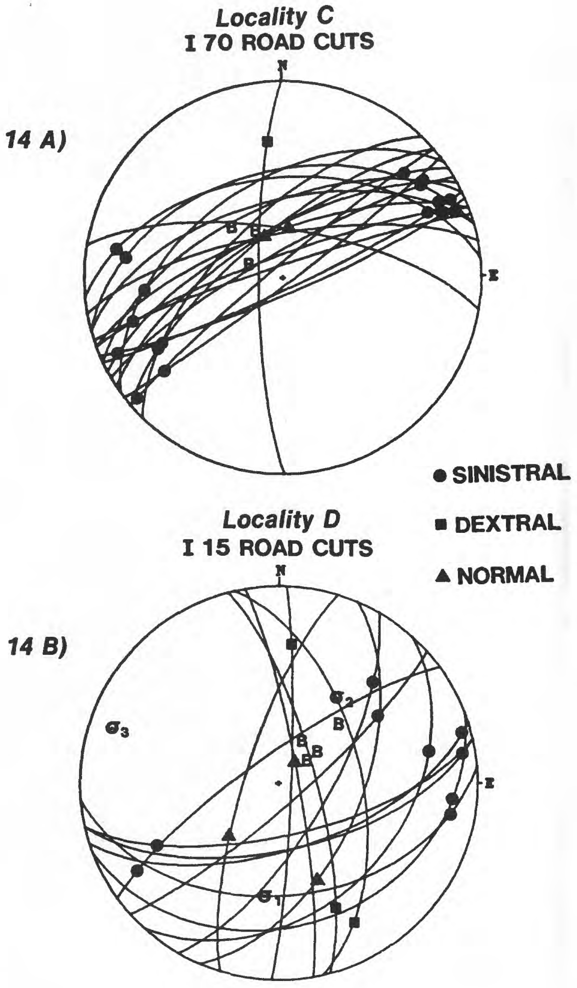

FIGURE 14.-- Lower-hemisphere plots of faults as great-circle arcs and striae in those faults as filled symbols distinguished according to type of slip. Poles to bedding are shown by the symbol B. A, Faults to locality C (I-70 roadcuts). Most are sinistral except for one north-trending dextral and two dip-slip faults. Note that the poles to bedding plot near the normal-faulting striae suggesting an association between the stratal tilting and the dip-slip components of faulting. B, Faults at locality D (I-15) roadcuts). Those that strike between 015° and 085° are all sinistral or normal sinistral. The remaining are dextral except for a normal fault with a steep rake. The faults do not appear to have any simple genetic relationship to stratal tilting. The computed stress axes are poorly constrained because of the small sample size and predominance of sinistral slip. Nevertheless, the position of σ_3 is reasonable when compared with other computed orientations reported herein (table 1). The moderate inclination of σ_1 could result from late-stage rotation of the faults and bedding.

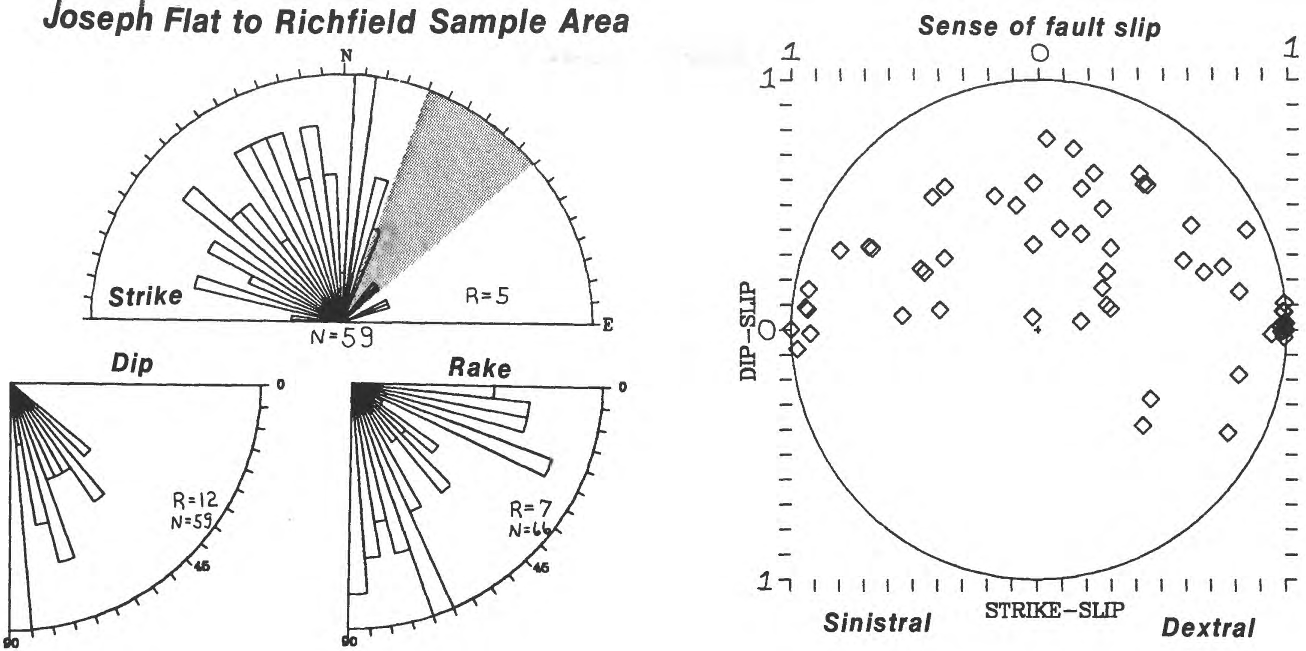

FIGURE 15.--Histograms of strike, dip, and rake, and plot of dip-slip versus strike-slip components of fault slip for faults along the southeast margin of the Pavant Range between Joseph Flats and Richfield. For the sense of fault-slip diagram, the ratio of the strike-slip to net slip is plotted along abscissae and the ratio of the dip slip component to net slip is plotted along ordinate. This plot reveals the complex mixture of strike-slip, dip-slip, and oblique-slip faulting that characterizes this sample area. Compare this fault-slip diagram with the simple pattern of dip-slip faulting along the same range front to the northeast of Richfield (fig. 19). The patterned sector on the strike plot shows the average trend, 35° ± 15°, of the Pavant range front. Symbols are the same as for figure 10.

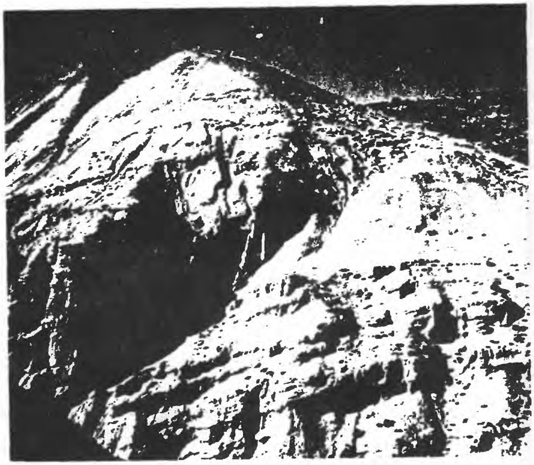

FIGURE 16.--View looking west in Flat Canyon north of Elsinore showing offset contact between smooth- and rough-weathering beds of gently southwest-dipping sandstone, siltstone, and claystone belonging to the Bald Knoll Formation of Eocene age. The fault that separates the offset sections is approximately vertical, strikes 005°, and has an estimated down-to-the-east throw of 10 m. At first glance this fault, and another nearby fault of similar orientation and displacement but out of camera view appear to be steep dip-slip faults that repeat the strata by down-to-the-east (lower right) displacements. However, as with the faults at locality C along the Clear Creek downwarp, these faults are sinistral strike-slip faults having rakes of 3° and 13° to the south.

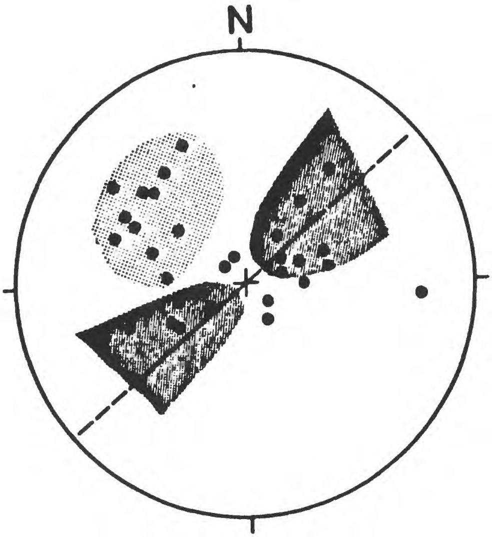

FIGURE 17.--Lower Hemisphere stereographic plot of poles to bedding along the flank of the Pavant Range between Joseph Flats and Richfield. Dark pattern embraces poles that represent first-phase stratal tilting to the northeast and southwest on generally northwest-trending faults. Light pattern embraces poles representing second-phase monoclinal tilting to the southeast. Locally the northeast-dipping block-faulted strata in the range can be traced continuously into the monocline.

FIGURE 18A.--Map showing generalized geology of the northwest part of the Aurora 7½-minute quadrangle. With the exception of the highly interpretive fault-and-fold pattern in volcanic rocks southwest of Aurora, the data are taken from an unpublished map by G. C. Willis. The Elsinore fault terminates near point marked by A where its displacement is transferred to a southeast-facing monocline which, in turn, bends westward and looses expression near point marked by B. Loss of expression is in large part due to its mergence with the homoclinally northeast-tilted Eocene strata. To the west of the Elsinore fault and its coextensive monocline, the Eocene and Oligocene sedimentary rocks and overlying volcanic rocks wrap neatly around the northwest-trending series of fault-repeated blocks of Eocene sedimentary rocks. This wrap-around structure is herein interpreted to postdate the faulting and tilting on northwest trends whereas G. C. Willis (written commun., 1987) interprets all structures in that area as coeval. The down-to-the-northwest series of inferred faults shown cutting the volcanic rocks southwest of Aurora represents a stylized attempt to resolve an anomalously great stratal thickness of volcanic rocks suggested by the moderate to steep dips over a cross-strike distance of more than 1 km. The faulting style follows that seen to the southwest in the downthrown block of the Elsinore fault. The folds are based on stratal strike variations mapped by Willis.

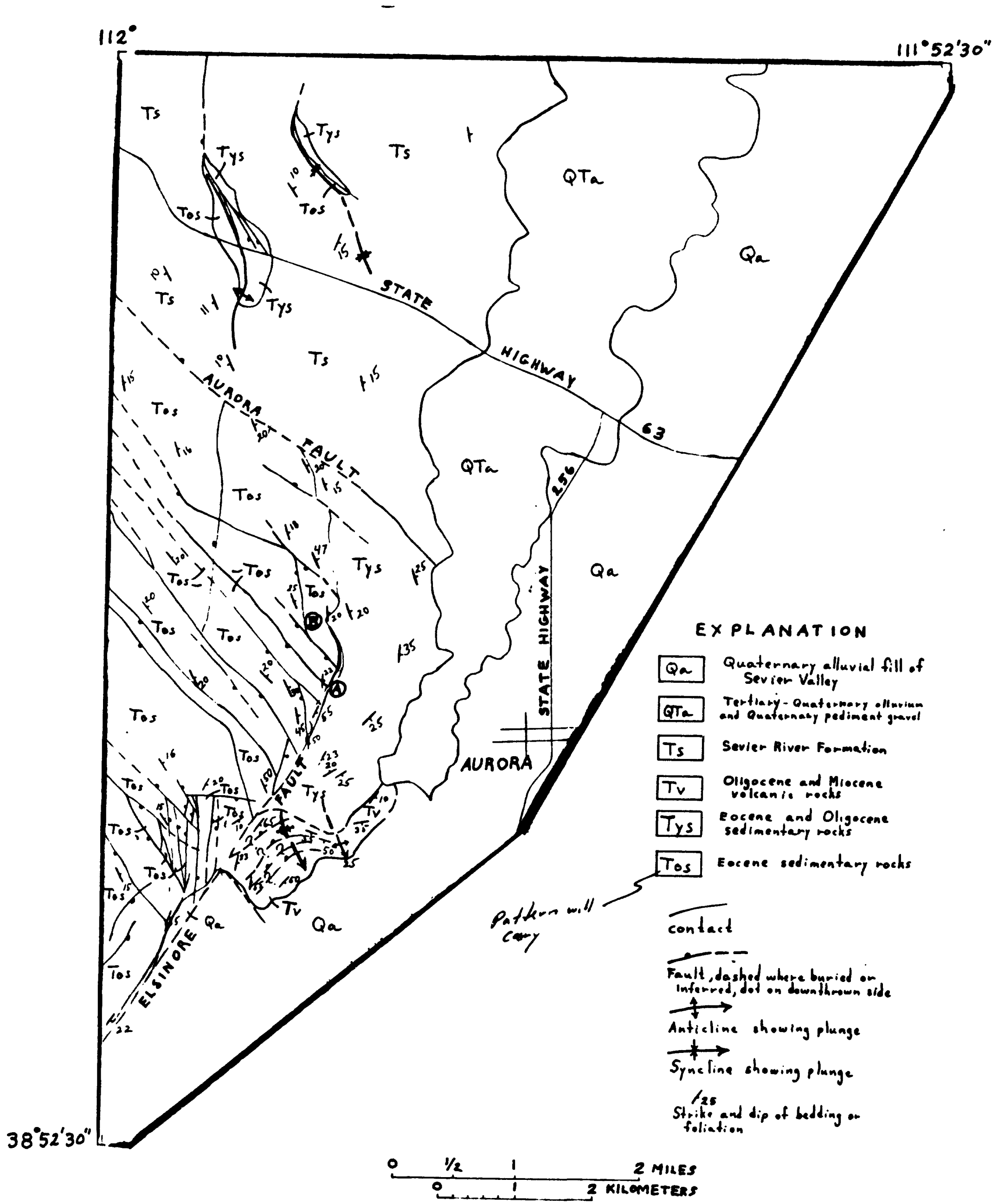
112°
111°52'30"
38°52'30"
Ts
Tys
Tos
QTa
Qa
Tv
STATE HIGHWAY 63
256
STATE HIGHWAY
AURORA FAULT
ELSINORE FAULT
AURORA
A
B
EXPLANATION
Qa Quaternary alluvial fill of Sevier Valley
QTa Tertiary-Quaternary alluvium and Quaternary pediment gravel
Ts Sevier River Formation
Tv Oligocene and Miocene volcanic rocks
Tys Eocene and Oligocene sedimentary rocks
Tos Eocene sedimentary rocks
Pattern will copy
contact
Fault, dashed where buried or inferred, dot on downthrown side
Anticline showing plunge
Syncline showing plunge
25
Strike and dip of bedding or foliation
0 1/2 1 2 MILES
0 1 2 KILOMETERS

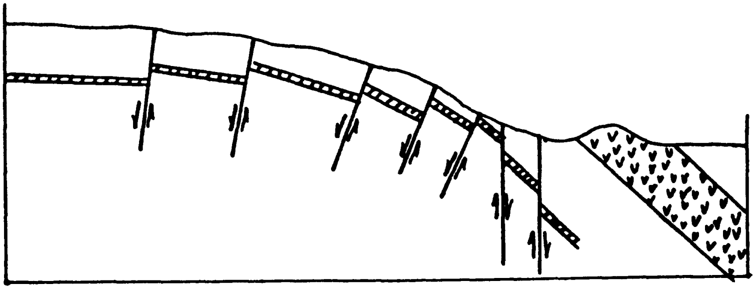

FIGURE 18B.--Cross sectional sketch showing the typical fault pattern seen in the monoclinally flexed margin of the Pavant Range. Note that down-to-range faults cut bedding at approximately right angles and that bedding is not rotated by the steep down-to-valley faults.

FIGURE 19.--Histograms of strike, dip, and rake; lower hemisphere stereographic plot of faults, striae, and computed paleostress axes; and plot of dip-slip versus strike-slip components of fault slip for faults along the eastern margin of the Pavant Range between Richfield and Willow Creek. Note strong contrast in strike and rake distributions between these data and the data shown in figure 16. The dip distribution shows two maxima--the 85°-90° spike represnts mostly down-to-valley faults and the 65°-70° node represents mostly down-to-mountain faults. Two types of striae are differentiated in the stereographic plot of the fault planes (lower left)--crosses for normal sinistral and squares for normal dextral. For the fault-slip plot the ratio of strike slip to net slip is plotted along abscissae and the ratio of the horizontal component of the dip slip to net slip is plotted along ordinate. This plot shows a clear preference for oblique dextral slip on the predominently northwest-striking faults in the Aurora to Willow Creek segment of the range front (filled squares) and normal dip slip on the predominantly northeast-striking faults in the Aurora to Richfield segment (open squares). The oblique dextral separations are mostly on northwest-striking faults believed to have been early dip-slip faults reactivated in the stress field shown on the stereographic plot. Symbols are the same as for figure 10.

Richfield to Willow Creek Sample Area

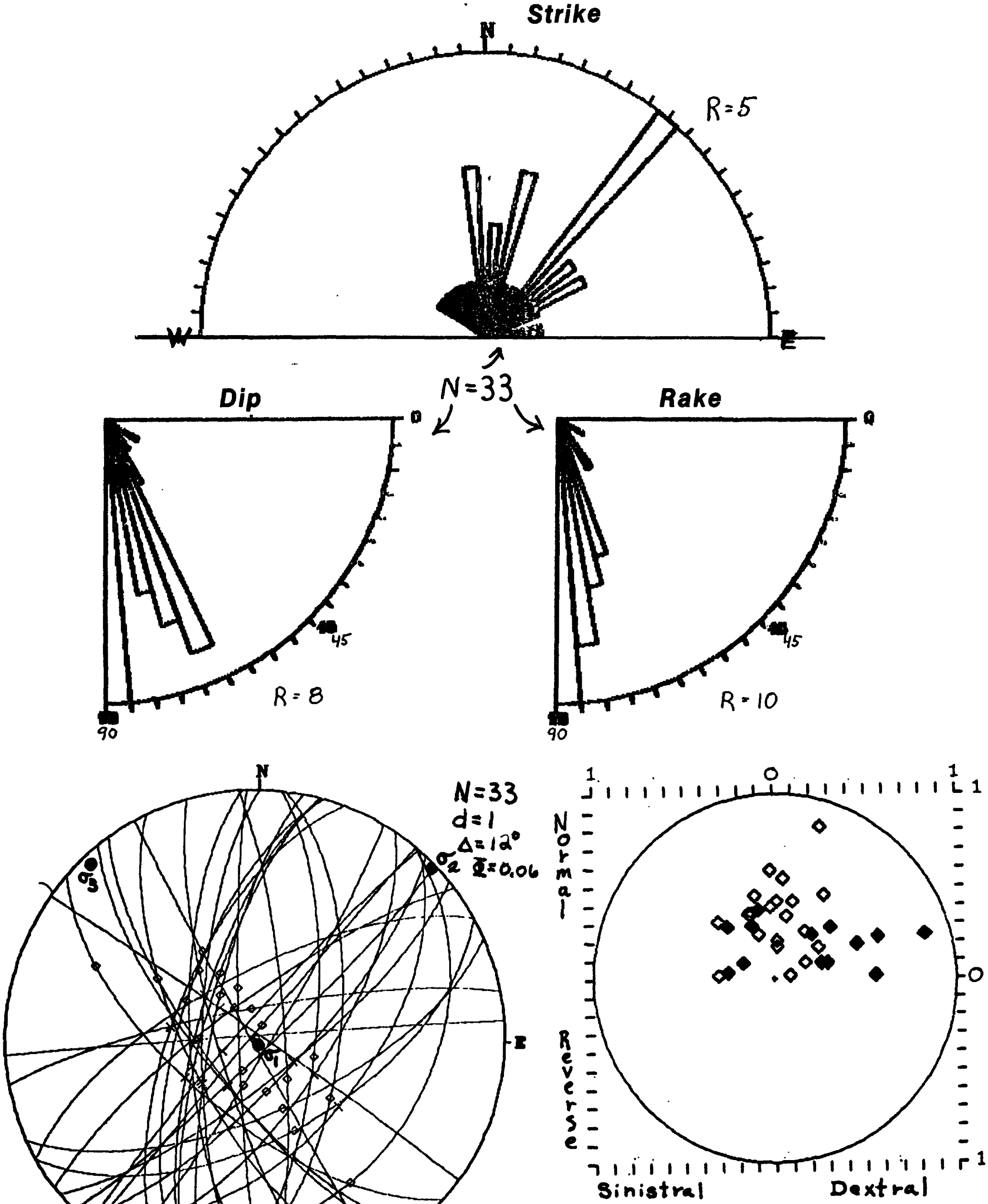

Faults, striae, and paleostress axes

Figure 19.

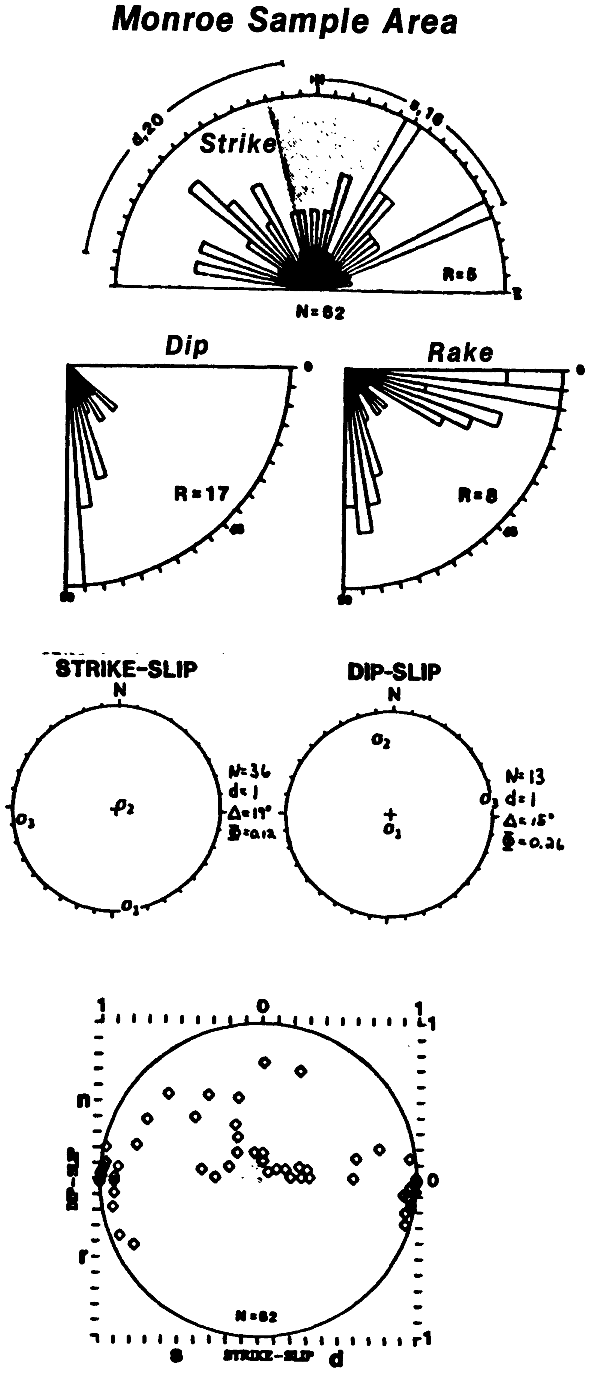

FIGURE 20. -- Histograms of strike, dip, and rake; lower hemisphere stereographic plots of computed paleostress axes; and plot of dip-slip versus strike-slip components of fault slip for faults in the western margin of the Sevier Plateau in the Monroe area. Patterned sector on strike plot is average range-front trend 005°± 20°. Symbols are the same as in Figure 10.

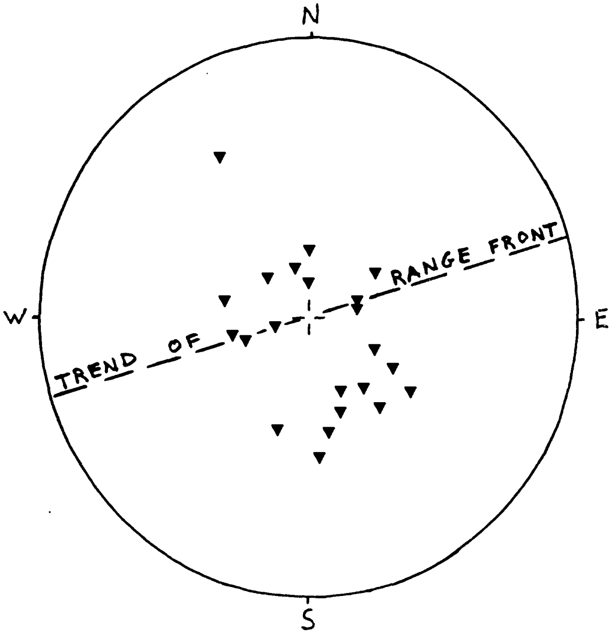

FIGURE 21.--Lower-hemisphere plot of poles to bedding in bedrock along the Annabella segment of the Sevier fault. Poles that plot in southeast sector mostly represent rocks in the monoclinally flexed or fault-dragged beds of the hanging-wall block where flexing is away from the range trend (dashed line).

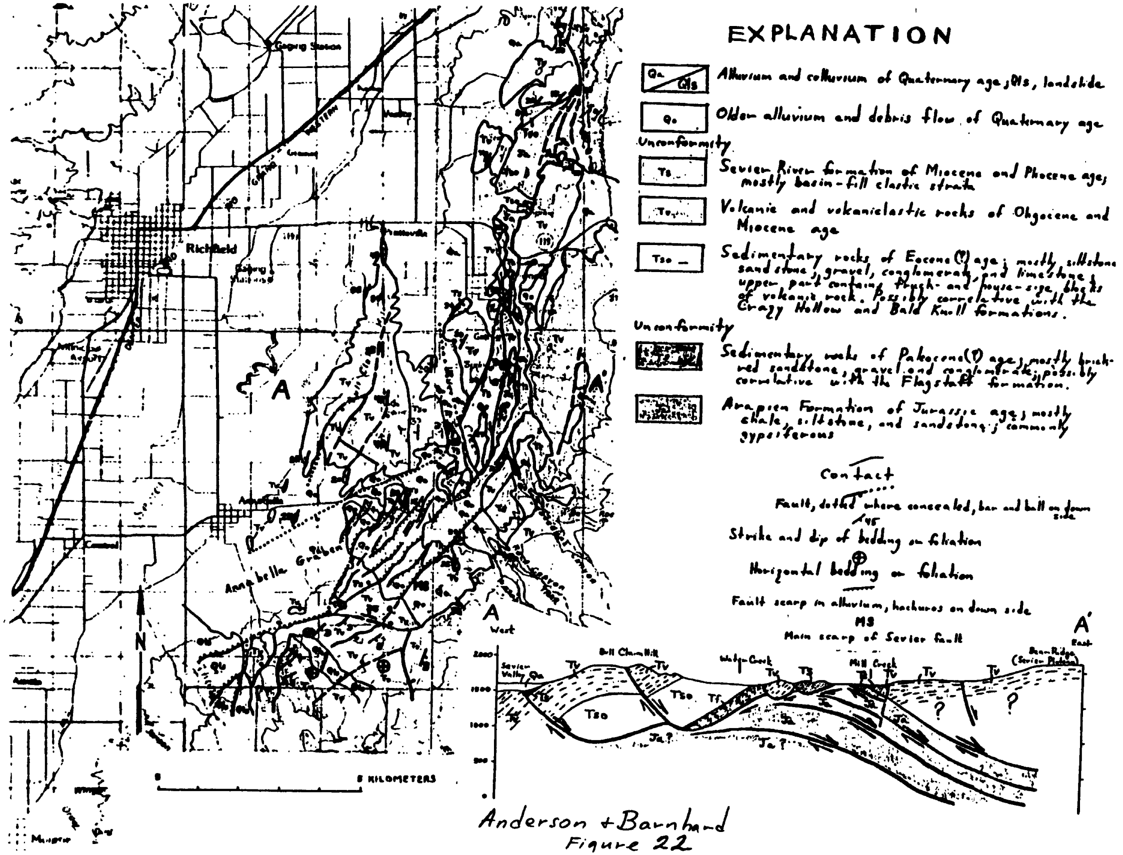

Anderson + Barnhard
Figure 22

FIGURE 22.--Geologic map and cross section (between points A + A' on map) of the Annabella area. Dotted and dashed lines in section are form lines indicating bedding traces. Low-angle faults in Arapien Formation in section schematically depict semiductile "flowage" of that mechanically incompetent unit out from beneath the Sevier Plateau. Note that a large down-to-the-west fault analagous to the Sevier fault at latitude of cross section is not required. Except for beneath Sevier Valley, areas underlain by Quaternary deposits are not shown on the cross section.

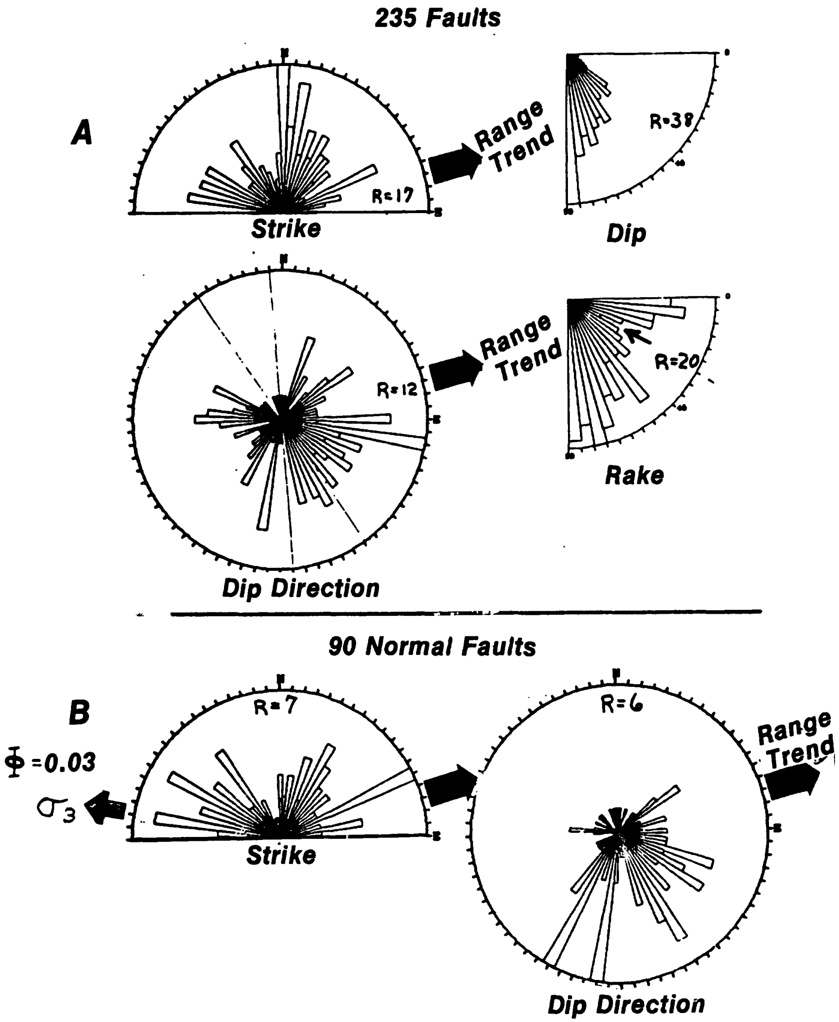

FIGURE 23.--Histograms of faults and striations from Tertiary volcanic and sedimentary rocks along the Annabella segment of the Sevier fault (Annabella sample area). A, Strike, dip, rake, and dip-direction distributions for 235 faults; R is radius value of histogram; heavy arrow marks approximate strike of the Annabell segment. B, Strike and dip-direction distributions for a subsample of 90 normal faults derived from sample represented in A. Small arrow shows computed azimuth of σ_3; Φ is stress ratio computed for the subset; other symbols as in A.

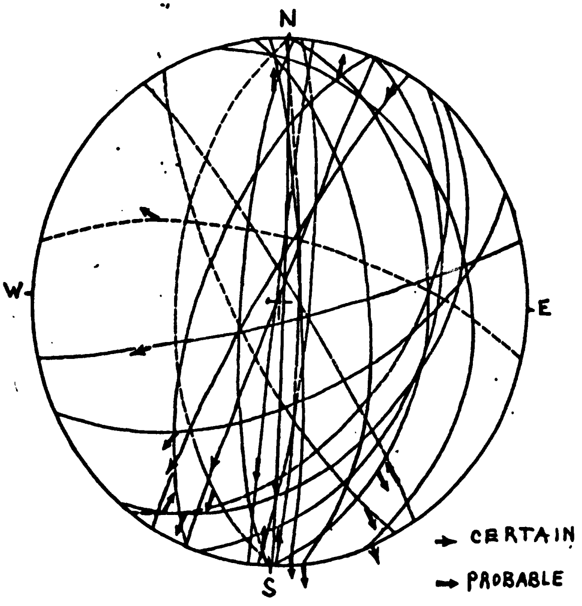

FIGURE 24.--Lower-hemisphere stereographic plot of a subsample of predominantly strike-slip faults derived from the sample shown in figure 23A. Only faults with certain and probable slip-sense determinations are shown, and those are discriminated by different types of arrows. Base of arrow shafts mark lineations, and arrows point in direction of motion of hanging-wall block. Solid lines are dextral faults, dashed lines are sinistral faults.

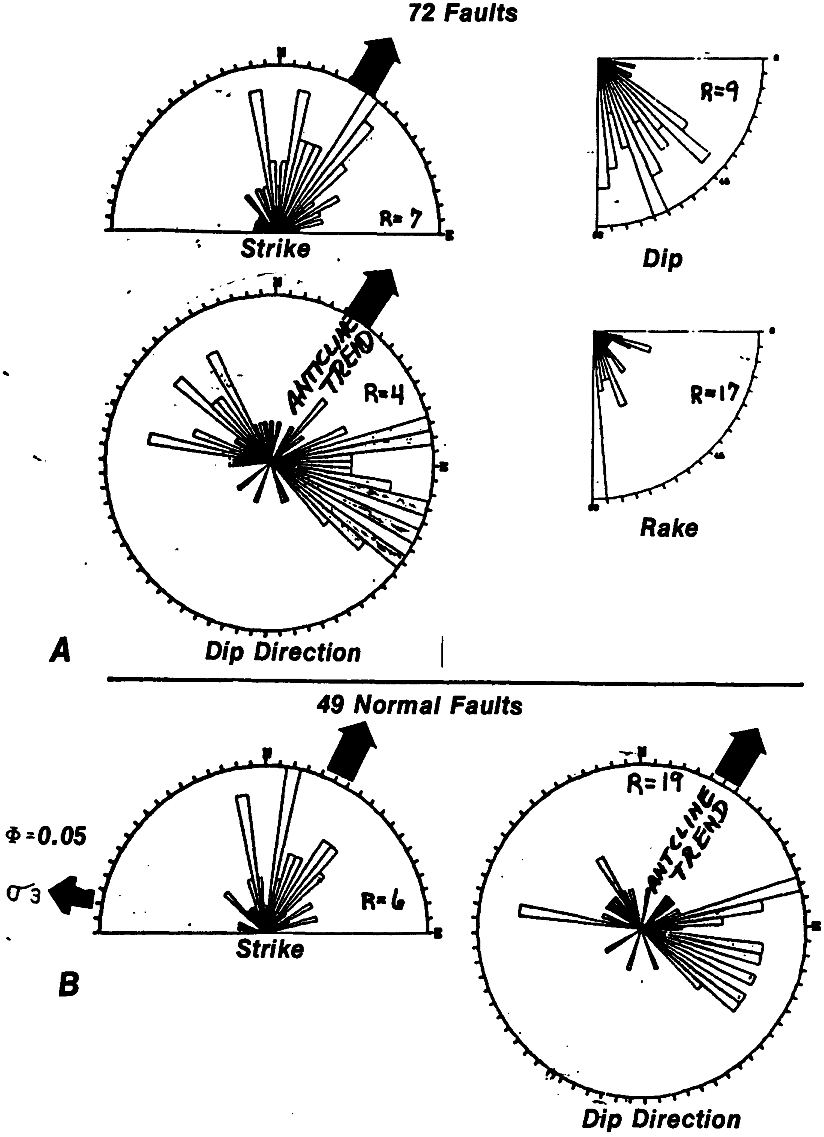

FIGURE 25.--Histograms of faults and striations from the Tertiary cover rocks of the Sanpete-Sevier anticline (anticline sample). A, Strike, dip, rake, and dip-direction distributions for 72 faults; R is radius value of histogram; heavy arrow marks approximate strike of the Sanpete-Sevier anticline. B, Strike and dip-direction distributions for a subset of 49 normal faults derived from sample represented in A. Small arrow shows computed azimuth of σ_3; Φ is stress ratio computed for the subset; other symbols as in A.

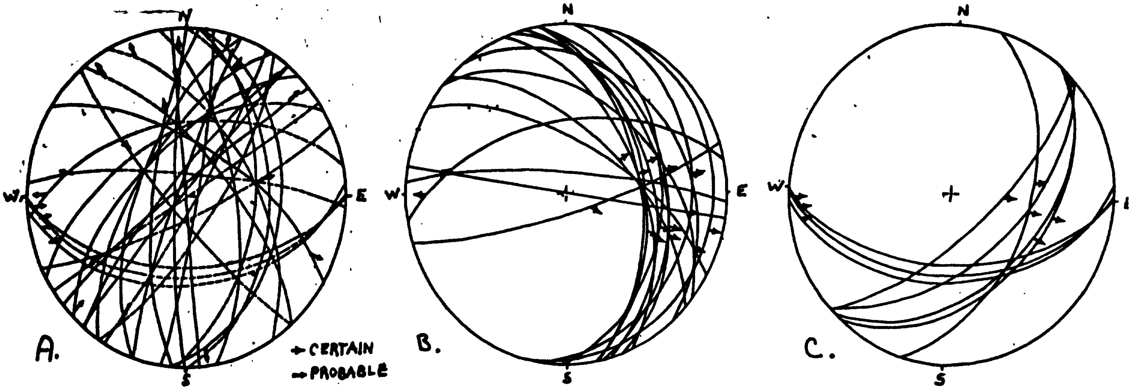

FIGURE 26.--Sterographic plots of faults that cut Tertiary rocks at or above the contact with the mechanically weak Arapien Formation along the southern part of the Sanpete-Sevier anticline. A, Subsample of predominantly strike-slip faults derived from sample shown in figure 25A. Significance of arrows and solid and dashed lines same as in figure 25. B, Faults and striae from a group of closely spaced exposures of highly fractured welded ash-flow tuffs on the east flank of the anticline. Base of arrow shafts mark lineations, and arrows point in direction of motion of hanging-wall block. C, Faults and striae from an exposure on the west flank of the anticline. Arrows same as in B. Note that strike-slip faults in B and C are also in diagram A. That group of strike-slip faults is interpreted as block-boundary structures genetically and mechanically related to the dip-slip and oblique-slip motions represented by the easterly directed clusters of arrows in B and C.

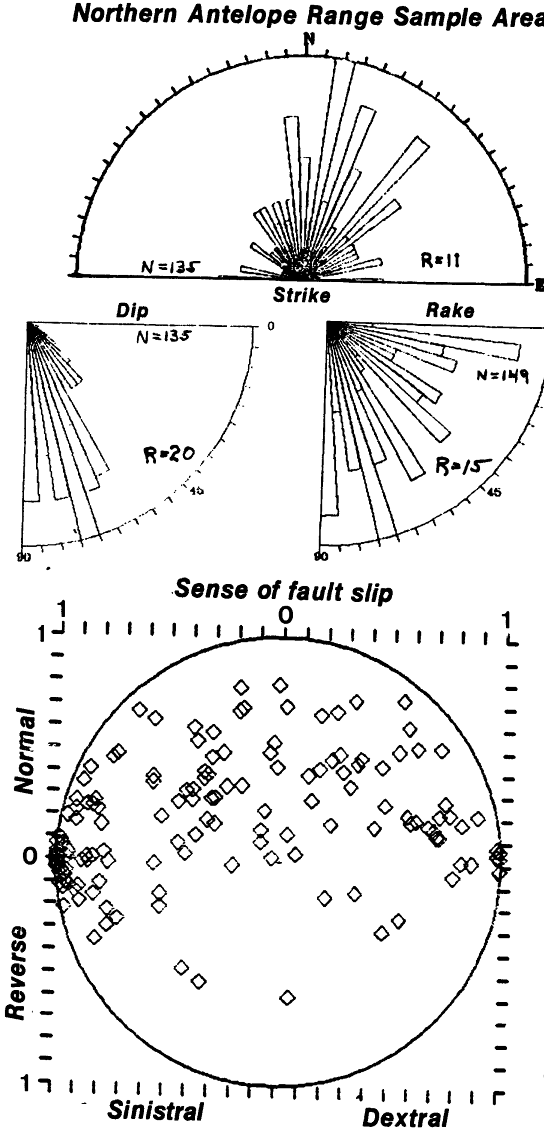

Figure 27.

FIGURE 27.--Histograms of strike, dip, and rake and plot of dip-slip versus strike-slip components of fault slip for faults in the northern part of the Antelope Range. Note the wide distribution of rake angles, the significant number of reverse-slip faults, and the strong bias for sinistral slip. Only in the distribution of strike and the bias for sinistral slip do these data distributions resemble those from the adjacent Clear Creek sample area (fig. 10). Symbols are the same as in figure 10.

FIGURE 28.--View looking west at surface trace of a high-angle fault at locality F in Antelope Range, (figure 3). Hydrothermally altered and fractured rocks of the Bullion Canyon volcanics form the upthrown hanging wall on right and stratigraphically higher unaltered volcanic sediments in the lower part of the Mount Belknap Volcanics (Cunningham and others, 1983) form the footwall block. Bedding in the footwall dips about 40° south whereas the fault dips 60°-80° north. Striations and stratigraphic separation indicate reverse and reverse sinistral movement on the fault. However, it is not known whether the bedding and the fault were tilted after faulting, thus making the structure a tilted normal-sinistral fault.

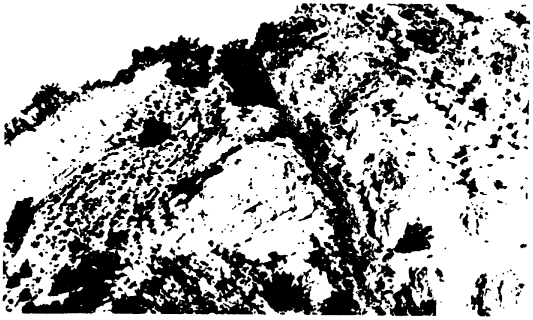

FIGURE 29.--Aspects of seismicity in the transition zone from Arabasz 1984. A, Map showing sample of current stress orientations inferred from earthquake focal mechanisms for the transition zone (from Julander, 1983). The single outward-directed arrows are least-compressive-stress directions inferred from dip-slip focal mechanisms; the combined inward- and outward-directed arrows are maximum- and least-compressive-stress directions inferred from strike-slip focal mechanisms. B, Lower part shows depth distribution of microseisms in Elsinore and Annbella areas and upper part shows the correlation in schematic cross section between the seismic discontinuites suggested by the depth distributions and detachment faults inferred from reflection seismicity. pc, Precambrian rocks; Pz, Paleozoic rocks; JK, Jurassic and Cretaceous, and Tertary rocks; KT, Cretaceous and Tertary rocks; Tv, Tertary volcanic rocks; QT, Tertary and Quaternary basin-fill sedimentary rocks.

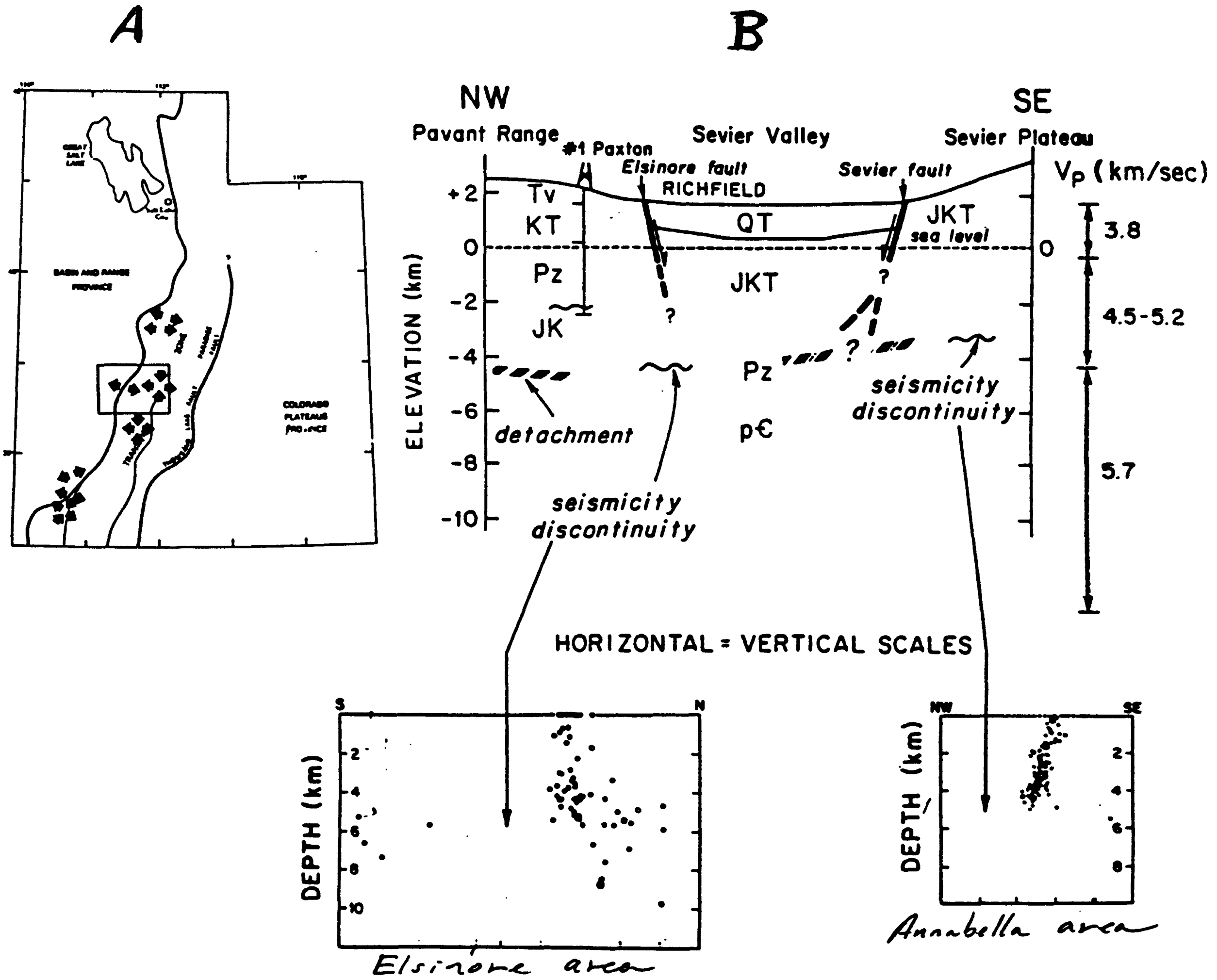
A
B
GREAT SALT LAKE
BASIN AND RANGE PROVINCE
ZONE
FAULT
COLORADO PLATEAUS PROVINCE
NW
SE
Pavant Range
#1 Paxton
Sevier Valley
Sevier Plateau
Elsinore fault
RICHFIELD
Sevier fault
Tv
KT
QT
JKT
sea level
Pz
JKT
JK
?
?
Pz
?
pЄ
detachment
seismicity discontinuity
seismicity discontinuity
ELEVATION (km)
+2
0
-2
-4
-6
-8
-10
0
V_P (km/sec)
3.8
4.5-5.2
5.7
HORIZONTAL = VERTICAL SCALES
S
N
DEPTH (km)
2
4
6
8
10
Elsinore area
NW
SE
DEPTH (km)
2
4
6
8
Annabella area

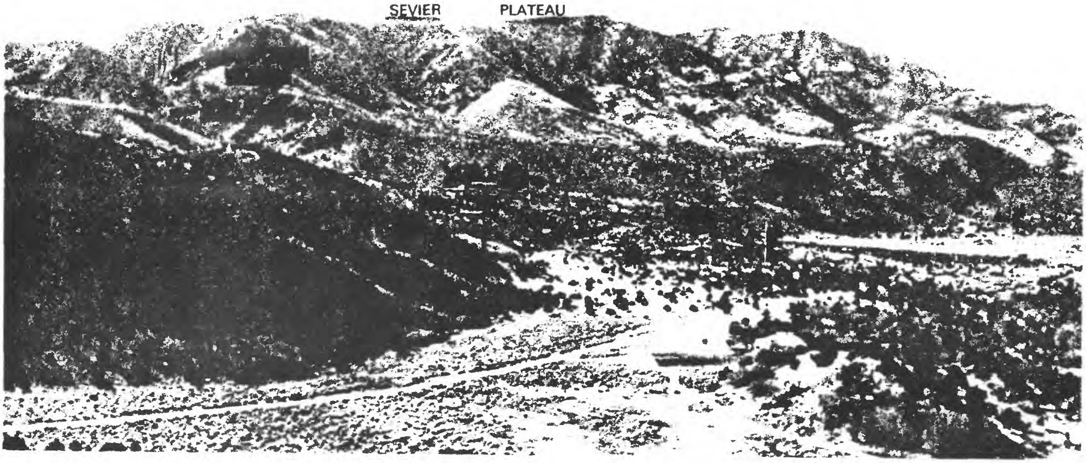

FIGURE 30.--Photograph looking south across northeast-trending main strand of the Sevier fault toward the Glenwood Mountain part of the western Sevier Plateau. Geomorphic surfaces labeled A, B, and C terminate to the northwest against conspicuous scarps that mark the trace of the Sevier fault. Lettered arrows A, B, and C below the respective surfaces point to localities where scarp profiles shown in figure 29 are measured. Irregularly forested area beneath scarps is part of a structurally complex graben containing clastic sediments of Miocene to Quaternary age. In contrast, linear elements of the Glenwood Mountain skyline as well as crudely banded vegetation patterns beneath skyline reflect the structural simplicity of that structural block. The uplifted remnants of surface C that are found on both sides of Water Creek Canyon are interpreted to be parts of a once-continuous surface that predates cutting of the canyon. That surface is smoothly graded across the alluvium-bedrock contact high in the plateau margin, with no suggestion there of displacements by young faults.

FIGURE 31.--Profiles across scarps formed on late Quaternary alluvium and debris flows in the Annabella area. Profiles A, B, and C cross the main strand of the Sevier fault at localities identified by corresponding letters in figure 21. Profiles A and B were measured with a clinometer. At profile A, the fault offsets the youngest terrace above the modern stream bed at the mouth of Water Creek Canyon, whereas at profile B the same fault offsets an older and higher terrace a short distance to the south of A. The young surface faulting event represented by profile A produced a surface offset of 5.2 m. That surface faulting event, which probably occurred close in time to the Holocene-Pleistocene boundary, is seen in profile B by a 20-m-long scarp midsegment with an average slope near the angle of repose at 35°. This oversteepened part of the compound scarp yields a young surface offset of about 4.7 m, similar to that of the single-event scarp at A. This young faulting event is probably also expressed in the high compound scarp at locality C (note tenfold scale difference) but it cannot be discriminated because that profile was constructed from data on the 1:24,000 topographic map (Water Creek Canyon, Utah) and therefore only approximates the true surface profile. A remarkably large planar part of the scarp at C stands approximately at the angle of repose (compare profile C with photograph in fig. 21), indicating numerous late Quaternary faulting events. With a surface offset of about 130 m, it is probably the highest late Quaternary fault scarp in alluvial deposits in Utah. Profile D was measured with clinometer on a northeast-striking fault scarp 1.5 km northwest of the scarp at locality C. It is included to show that other scarps in the Annabella area do not reflect the same high rates of activity as on the main strand of the Sevier fault.

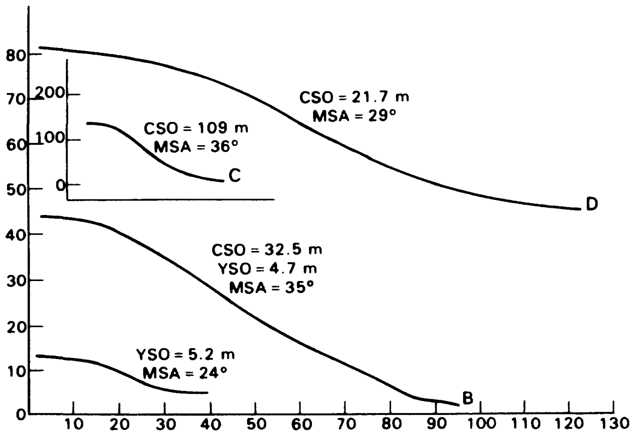

Scales are in meters

CSO, cumulative surface offset
YSO, young surface offset
MSA, maximum slope angle

Figure 31.

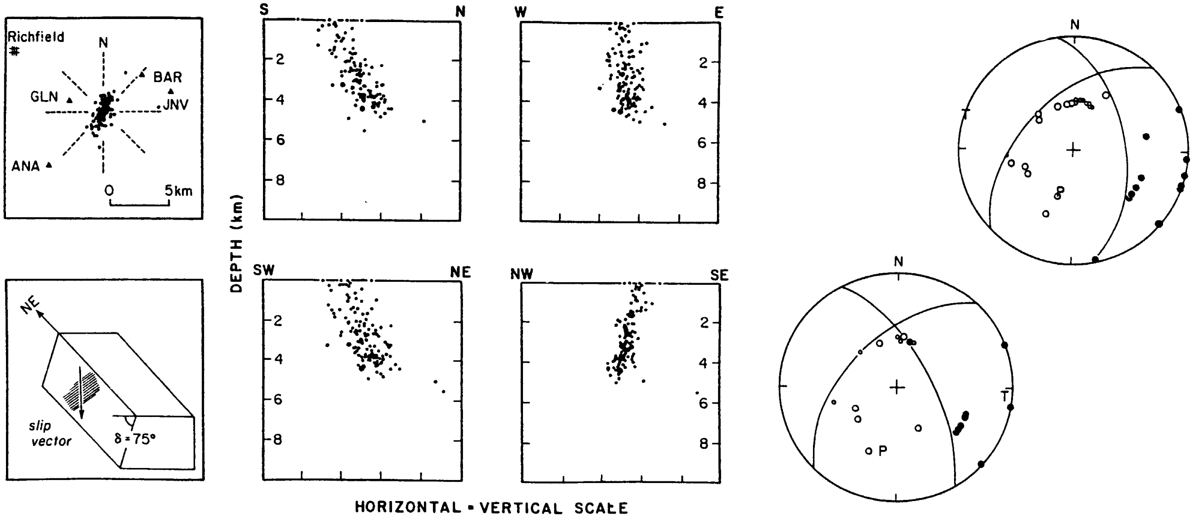

FIGURE 32.--Spatial distributions of aftershock foci in the Annabella area (squares) and focal mechanisms for the 1982 magnitude 4.0 main shock (upper sterogram) and magnitude 2.7 aftershock (lower sterogram) (from Julander, 1983). The earthquake foci are shown in map view (upper left square) and cross section (center and right squares). Block diagram (lower left) shows planar orientation of clustered foci and slip direction from main shock. For focal mechanisms, the solid circles represent compression and open circles represent tension. P and T are pressure and tension axes.

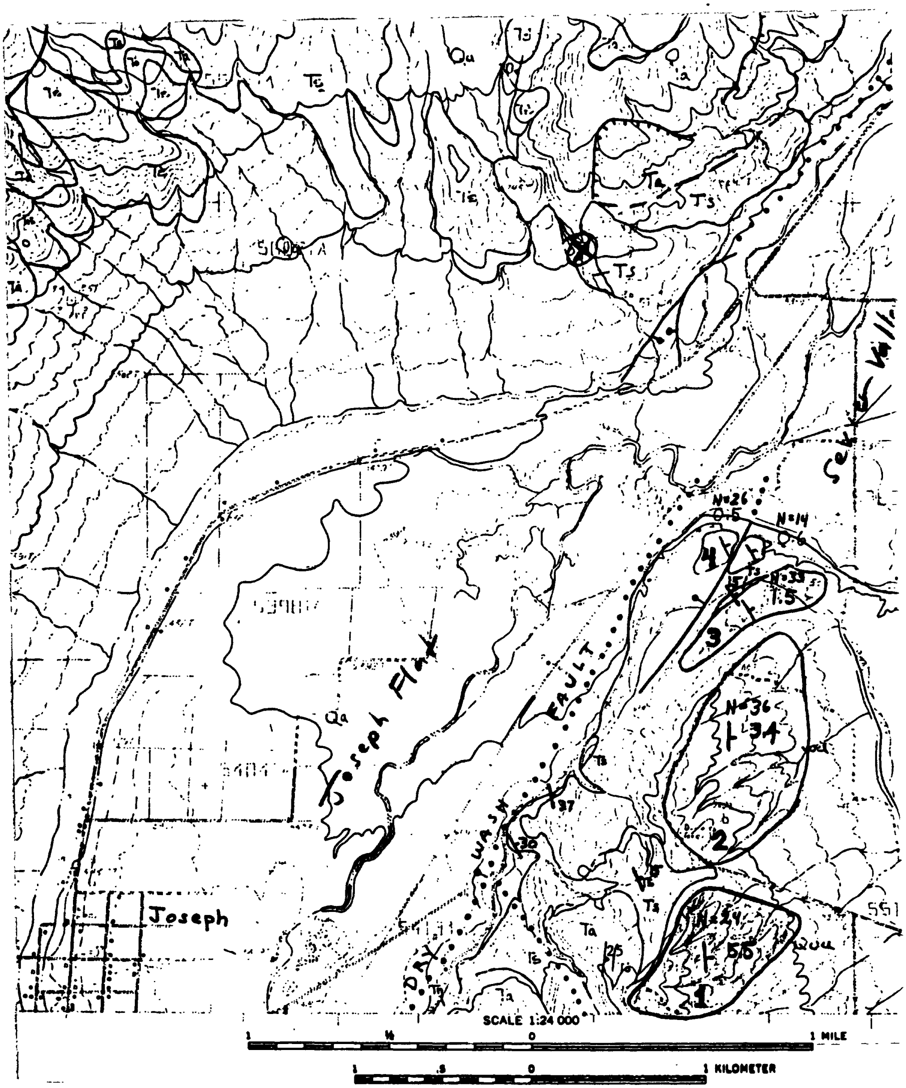

MONROE NW QUADRANGLE

FIGURE 33. South-central part of the geologic map of the Monroe NW quadrangle (Steven, 1979) and showing the average slopes of four terraces first identified by Callighan and Parker (1961). The slopes (in degrees shown adjacent to dip symbol) were determined by best-fit planes through a series of highest possible points on the terraces or dissected ridge crests within the four outlined areas (N=number of points). A computer assisted stereometric procedure was used to calculate slope. The northern terrace (number 4) is represented by two areas separated by a fault scsrp. A representative sample of attitudes in the Sevier River Formation (Ts) shows that the geomorphic surfaces are unconformable underlain by tilted and erosionally truncated Sevier River strata. The three high terraces (1 through 3), fault scarp, and two low terrace elements (4) are identified in a south-looking photograph in Figure 34. Young deformation in this ares is probably responsible for an anomaly in the channel pattern of the Sevier River as shown in Figure 35. X indicates locality referred to in text.

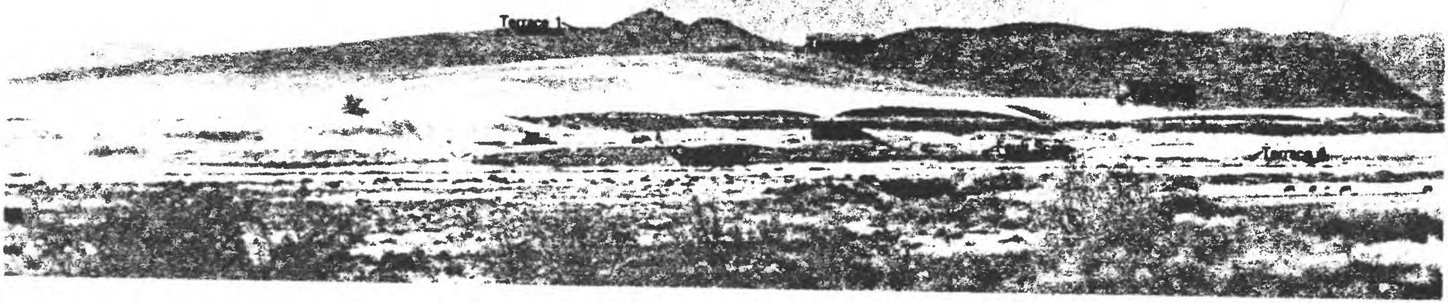

FIGURE 34.--View looking south showing terraces (numbers) that have progressively greater height and greater eastward tilts with greater age. Age is inferred from height above grade of Sevier River and degree of erosional dissection. The conspicuous shaded scarps below terrace 3 are excavations for an irrigation ditch; those below terrace 4 result from erosional trimming by Sevier River. Slopes of the terraces are given in figure 33. Access was denied to area where fault scarp could be studied. Only relative ages of terraces are known.

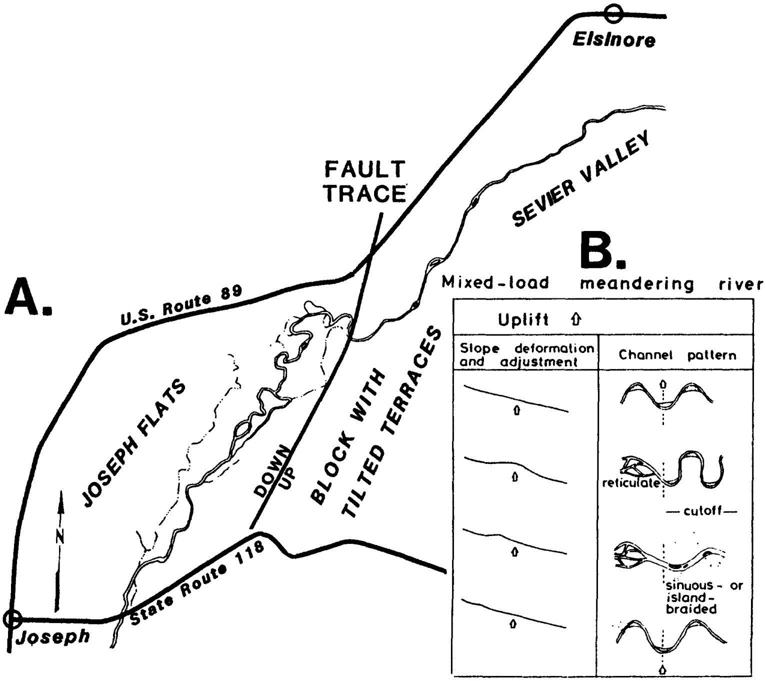

FIGURE 35.--Channel pattern of Sevier River between Joseph and Elsinore (from Monroe quadrangle, 1:62,500, 1940) in relationship to an axis of relative uplift. Inset shows hypothetical model of time-sequential response (age increases downward) of the slope and channel pattern to uplift across the course of a mixed-load (bed-load and suspended-load sediments) meandering river (from Ouchi, 1985). Note similarity between channel pattern of Sevier River and the third stage of channel-pattern response.

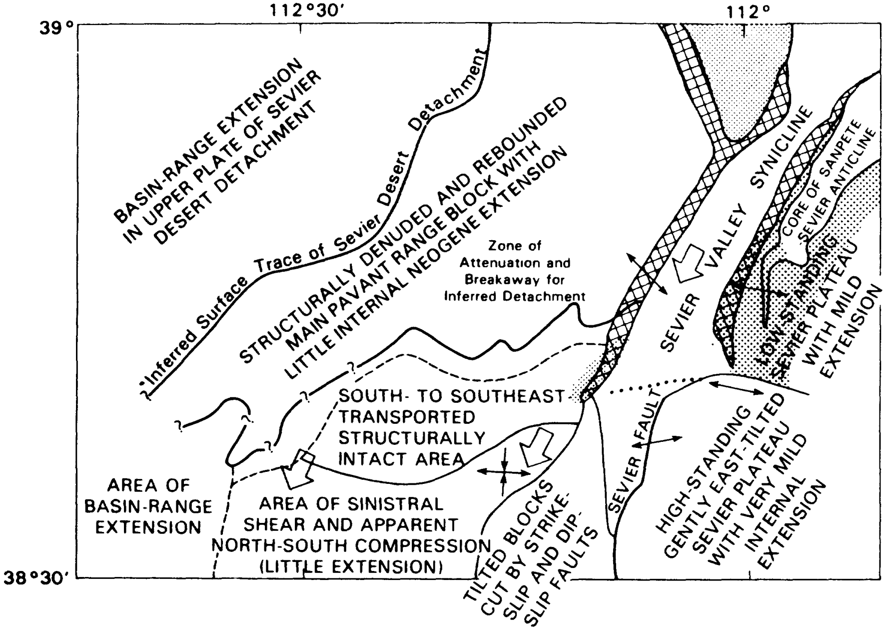

FIGURE 36.--Map showing structural characterizations of central Sevier Valley area; resolved paleostress directions (outward-pointing double-headed arrows show σ_3 for dip-slip solutions, inward- and outward-pointing arrows show σ_1 and σ_3, respectively, for strike-slip solution); directions of principal tectonic transport (large open arrows, inferred for Sevier Valley); possible cross-valley transverse structure (dotted line); faulted monoclines bordering uplifted blocks (cross ruled); area of major extension and structural attenuation (stipple); areas of northwest-striking faults interpreted to represent a preneotectonic stage of northeast-southwest extension (shaded); and sites of coincident earthquake clustering and anomalously intense late Quaternary surface deformation (stars).

NEOTECTONICS OF THE HANSEL VALLEY-POCATELLO VALLEY CORRIDOR, NORTHERN UTAH AND SOUTHERN IDAHO

by

James McCalpin, Robert M. Robison, and John D. Garr
Utah State University
Logan, Utah

ABSTRACT

The Hansel Valley-Pocatello Valley corridor on the Utah-Idaho border has experienced intense historic earthquake activity, including damaging earthquakes in 1934 (M_L6.6) and in 1975 (M_L6.0). Range fronts flanking both valleys display youthful morphology, yet valleys contain few well-preserved fault scarps in Quaternary deposits which might allow reconstruction of fault histories. Range-front trenching, pluvial lake shoreline surveying, and arroyo wall mapping were used to reconstruct the neotectonic history of each valley. In Pocatello Valley 15 ka shorelines are locally warped vertically as much as 6.4 m where they cross en-echelon splays of the eastern range front fault but no scarps in unconsolidated deposits are found. A trench at the range front exposes unfaulted colluvial wedges up to 95 ka old which may have been rotated down toward the valley center and locally warped. The absence of either fault scarps or liquefaction features in late Quaternary deposits implies that displacement on the range front fault in eastern Pocatello Valley occurs by creep or by small displacements which do not propagate as discrete fractures to the surface.

Two short fault scarps on the eastern range front fault of Hansel Valley indicate that 4-5 surface-faulting events have occurred in the last 65 to 140 ka. A splay fault in an Interstate 84 roadcut shows only one recent 2.6 m displacement in the last 100 ka, not compatible with the scarp evidence. Along the southwestern valley margin one of several scarps created by the 1934 earthquake merges with an 8 km long prehistoric scarp up to 9 m high which displaces Lake Bonneville shoreline gravels. Scarp profiles and geomorphic relations with shorelines indicate the scarp was formed by one or two subaqueous displacements totalling 1.3-2.5 m during the period 26-12 ka. Supporting evidence of recurrent faulting based on gully exposures and five thermoluminescence dates show that deposits have been multiply faulted between 138 and 72 ka, with no events from 72-58 ka, one event between 58 and 26 ka (nearer the latter), one event around 15-21 ka, and a possible event at 13 ka. Displacements of up to 2.5 m seemed to be clustered in time when large pluvial lakes existed in the basin (oxygen isotope stages 6 and 2) rather than when either no lake or only shallow lakes existed (stages 5,4 and 3). We suggest the 1934 M_L 6.6 earthquake may be a typical interpluvial maximum event (long recurrence time, small displacement) compared to the larger, more frequent surface-faulting events presumably triggered by pluvial lake water loading.

INTRODUCTION

The Hansel Valley-Pocatello Valley corridor on the Utah-Idaho Border has been the site of intense historic seismicity, including the 1934 M6.6 and the 1975 M6.0 earthquakes (Fig. 1). The 1934 event, largest in Utah's history, is one of only

FIGURE 1 FOLLOWING PAGE

three historic earthquakes in the Intermountain Seismic Belt (ISB) to rupture the surface and produce a fault scarp. The high rate of historic seismicity in the corridor contrasts with a scarcity of pre-historic fault scarps offsetting late Quaternary deposits, in spite of the youthful range-front morphology of bounding mountain ranges. The primary objective of this research was to determine why such a seismically active area lacked abundant geologic evidence of late Quaternary surface faulting. A second objective was to compare earthquake frequency-magnitude relations deduced from geological evidence with those of historic time, to help assess the current potential of this region to generate large, damaging earthquakes. Finally, if damaging earthquakes could occur without leaving significant geologic evidence, do the methods currently used on the Wasatch Fault need to be modified for estimating earthquake potential.

The study area is located within the Hansel Mountains-West Hills Section of the Basin and Range physiographic province (Stokes, 1977) and is composed of north to northeast-trending valleys separated by linear mountain ranges (Fig. 2). The

FIGURE 2 FOLLOWING PAGE

Hansel, North Hansel, and North Promontory Mountains are primarily composed of Permo-Pennsylvanian Oquirrh Formation (Adams, 1962; Allmendinger, 1983; Jordan, 1985), while Samaria Mountain contains carbonates and clastic rocks of Ordovician through Pennsylvanian age (Beus, 1968; Platt, 1977). In the valleys, Lake

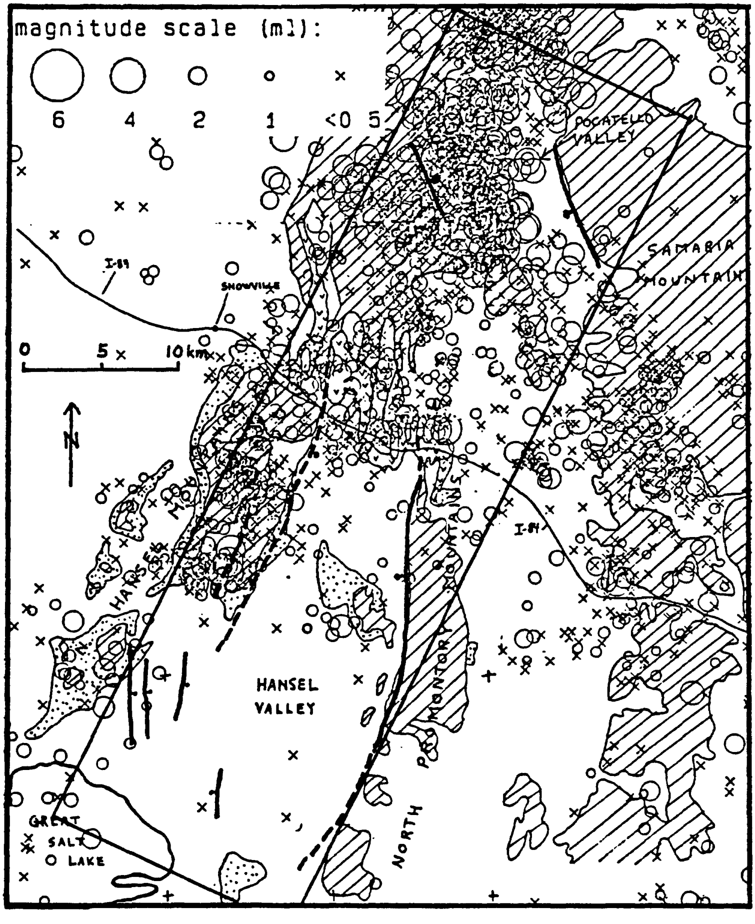

Figure 1. Earthquake epicenter map of the Hansel Valley-Pocatello Valley corridor for the period March 28, 1975 to June 30, 1985. Data provided by the University of Utah Seismograph Station.

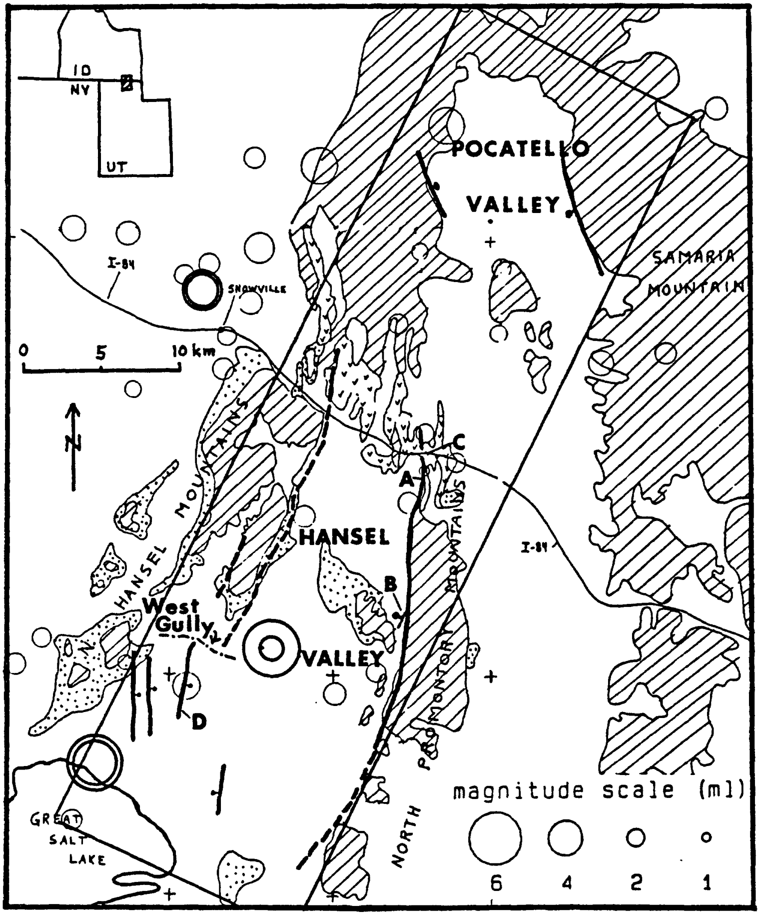

Figure 2. Location and general geologic map of the Hansel Valley-Pocatello Valley corridor (rectangle). marginal normal faults discussed in text are shown by heavy lines, with bar-and-ball on downthrown side. Earthquake epicenters from 1850-June, 1962 are shown by heavy circles; epicenters from June, 1962-March 27, 1975 are shown by lighter circles. General geology: Paleozoic rocks (ruled pattern), Tertiary volcanic rocks (small v's), Quaternary shoreline gravels (stippled), Quaternary lake bottom deposits and alluvium (no pattern). Capital letters A through D locate faults discussed in text.

Bonneville sediments occur below about 1585 m; higher valley margins are covered by alluvial fans. The valley fill beneath Lake Bonneville sediments is as much as 570 m thick in Pocatello Valley (estimated from gravity data by Harr and Mabey, 1976, p. 6-7), presumably composed mainly of pre-Bonnevile Quaternary deposits and the Tertiary Salt Lake Group, the latter of which outcrops on valley margins. Fill in Hansel Valley is considerably thinner, based on smaller gravity anomalies (Fig. 3; from Peterson, 1974) and on outcrops of Paleozoic rock within the valley (Hood, 1971, p. 5).

FIGURE 3 FOLLOWING PAGE

NEOTECTONIC FEATURES IN POCATELLO VALLEY

Tectonic Setting

Pocatello Valley is a topographic and structural depression, bounded on the east by Samaria Mountain, on the west by the North Hansel Mountains, and on the north and south by low hills (Fig. 4). Cenozoic normal faults bound the east side of the valley (Beus, 1968, Platt, 1977) and part of the west side (Allmendinger, 1983). Platt (1975, 1976) inferred late Quaternary activity on the eastern margin fault from indirect geomorphic evidence such as steepness of faceted spurs. Both gravity data and tilt of strata suggest that this fault forms the boundary between two east-tilted blocks. Another inferred north-trending fault may bound the west side of a gravity high in the center of the valley (Fig. 3). Cenozoic displacement on the eastern margin fault may be up to 1420 m, based on the elevation difference between the top of Samaria Mountain (2440 m) and the bottom of inferred valley fill (1020 m; Harr and Mabey, 1976). A shorter (8 km long) normal fault of lesser displacement bounds the central western margin of Pocatello

FIGURE 4 FOLLOWING PAGE

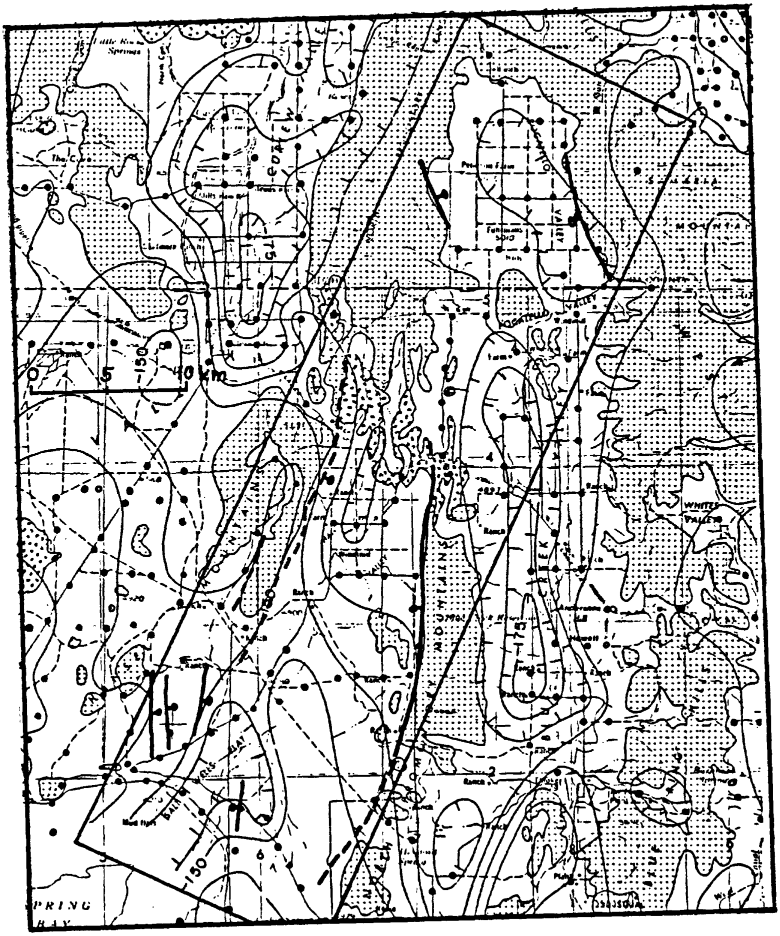

Figure 3. Bouger gravity map of the Hansel Valley-Pocatello Valley corridor (rectangle) and adjacent areas (from Peterson, 1974). Stippled areas represent mountain blocks; heavy lines represent Quaternary faults. The gravity low of Pocatello Valley seems to continue southward to Blue Creek Valley rather than southwestward to Hansel Valley.

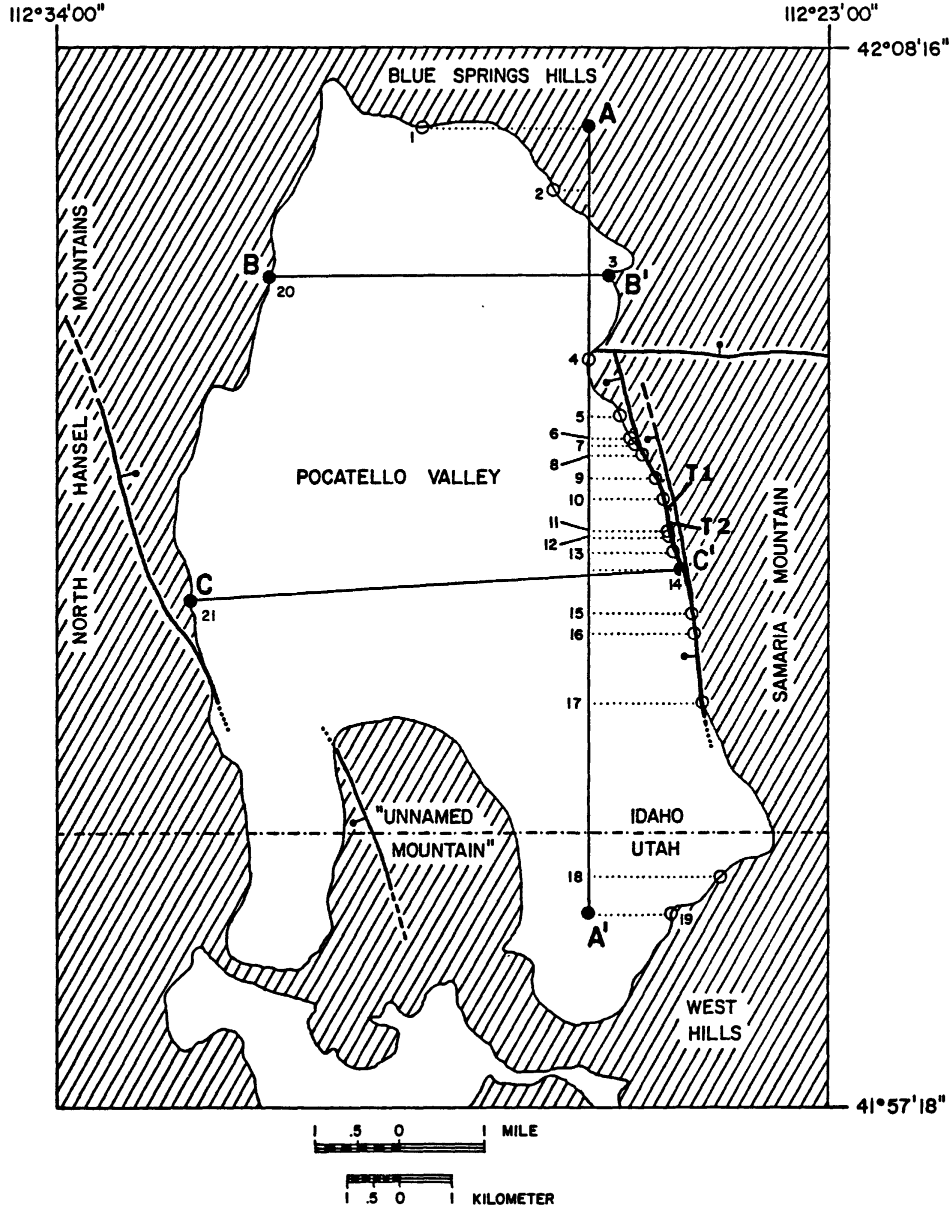

Figure 4. Index map of the Pocatello Valley area, Idaho-Utah. Diagonal lines indicate highlands above the Lake Utaho and lake Bonneville shorelines. Open circles are shoreline elevation data points, closed circles are data points and/or endpoints of profiles shown on Fig. 9. Dotted lines indicate the position of shoreline elevation data points used in profile A-A' (Fig. 9). Normal faults are shown by heavy lines, with bar-and-ball on downthrown side.

Valley. Where it offsets Paleozoic rocks on its northern end, Allmendinger (1983, Section C-C') shows a down-to-the-east displacement of about 122 m. The smooth gravity gradients and lack of large range-front spurs suggest that the western valley margin is dominantly a dip slope of an east tilted block (Allmendinger and Platt, 1983, Fig. 3) with a few short, low displacement normal faults. In late Quaternary time this topographic depression was occupied by pluvial Lake Utaho (Currey, 1981), a small water body contemporaneous with but physically separate from Lake Bonneville.

Eastern Margin Fault

The youthful range-front morphology cited by Platt (1977) as evidence of late Quaternary activity was quantified using mountain front sinuosity ratios (S) and valley floor width-valley height ratios (Vf) (after Bull and McFadden, 1977). S is the ratio of the length of the mountain-piedmont junction to the overall length of the mountain front. Tectonically inactive fronts have high (3.0 to 7.0) S values due to extensive embayment and pedimentation, while tectonically active fronts have lower values (1.2 to 1.6). The eastern margin range front has a sinuosity ratio of 1.7, suggestive of slightly-active to active tectonism.

The valley floor width-valley height ratio (Vf) gives a general indication of whether streams draining the mountain block are engaged in channel downcutting (high rate of tectonic base level fall, low value of V_f), or lateral erosion (low rate of base level fall, high value of V_f). The width of a canyon floor is compared to the mean height of the canyon at a given distance (0.5 km in this study) upstream from the mountain front. Canyons and valleys in several ranges in the northern Mojave desert have V_f values ranging from 0.055 to 47.0 (Bull and McFadden, 1977). Only two canyons along the eastern margin of Pocatello Valley have stream channels long enough for use in valley floor width-valley height calculation; these yielded values of 0.22 and 0.24. The mountain front sinuosity

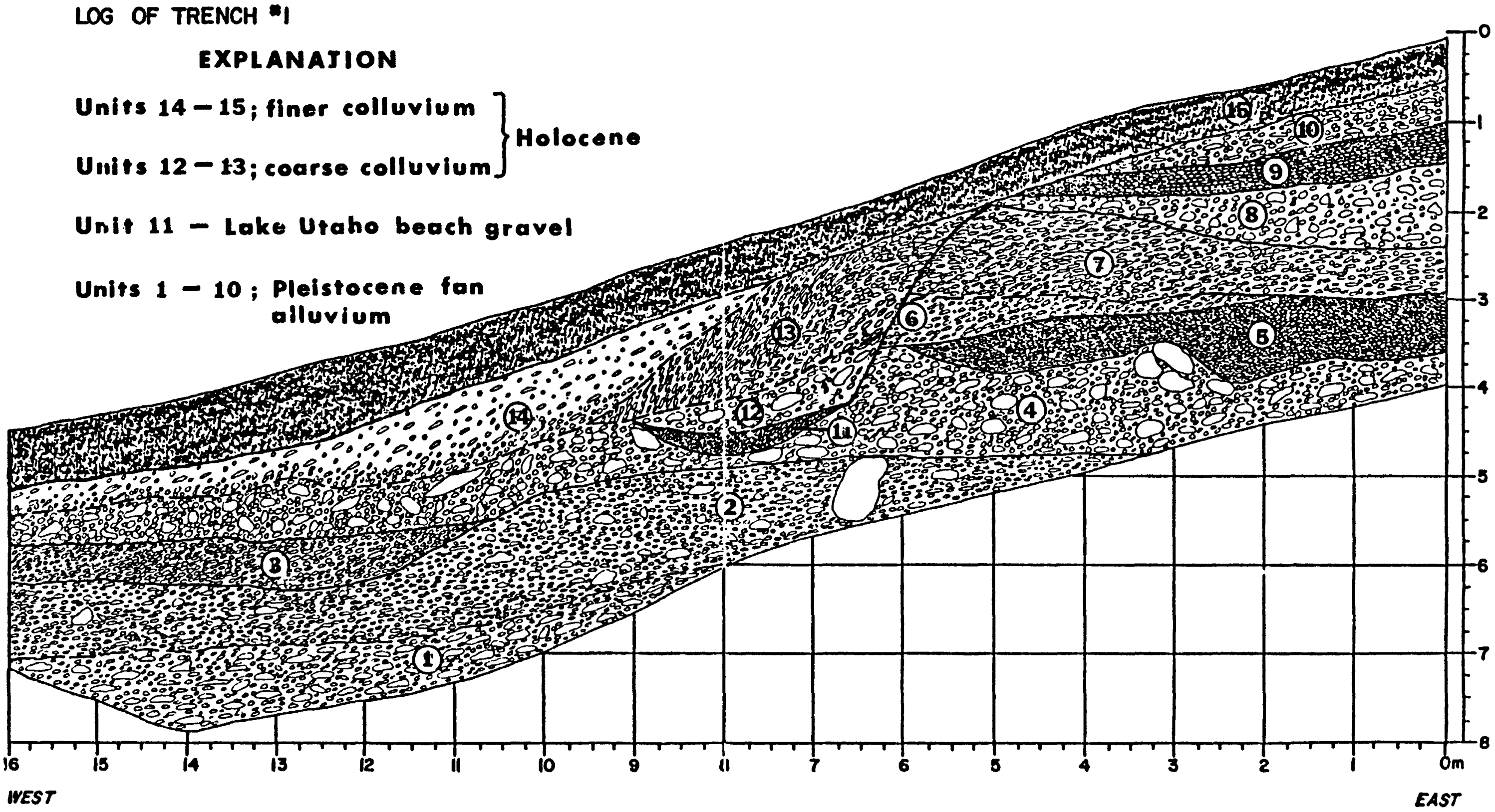

Figure 5. Log of Trench 1 excavated across the Lake Utaho shoreline on the eastern valley margin (T1 in Fig. 4). Lenticular late Pleistocene alluvial fan gravels (units 1-10) are truncated by an erosional scarp, at the base of which lies Lake Utaho highstand beach gravels (unit 11). Bouldery scarp-derived colluvium (unit 12) is overlain by a wedge of gravelly colluvium with a fabric dipping 35o W (unit 13), suggesting a growing colluvial wedge. Finer colluvial unit 14 appears to be mixed with loess (early Holocene?), while unit 15 contains a weak A/Cca soil profile. Alluvial fan strata beneath the buried scarp face (units 1-4) are not displaced, proving no surface faulting at this location in roughly the last 15 ka.

ratio and valley floor width-valley height ratios quantify what can be seen in the field: the mountain front is steep, the canyons are deeply incised and strongly V-shaped, and embayment and pedimentation are minimal, suggesting a young, active mountain front. In addition Platt (1976) infers that subsidence of the valley floor near the base of Samaria Mountain has resulted in alluvial fans of much smaller volume than would be expected, considering the size of the canyons from which the alluvium originated.

According to gravity data (Harr and Mabey, 1976) the deepest depocenter within the valley (570 m of fill) is adjacent to the southern portion of the Samaria Mountain front. The gravity gradient from the mountain to the depocenter is approximately 3mgals/km, almost double the gradient around most of the valley margin. Despite this indirect evidence for Quaternary fault activity, no fault scarps displacing Quaternary deposits could be located at the range front, either by earlier workers (Rogers and others, 1976) or in this study.

Stratigraphy at the Range Front

Two trenches were excavated with a large track-mounted backhoe to look for evidence of Quaternary faulting at the range front. Trench 1 was cut across the most prominent scarp in Quaternary deposits along the range front (T1 on Fig. 4). This scarp was located at the same elevation as the Lake Utaho shoreline and could have been: 1) a fault scarp, 2) an abnormally well-developed pluvial lake-shoreline scarp, or 3) a fault scarp later occupied and reworked by a shoreline. Trench logging revealed a thin lens of beach gravels at the base of the buried scarp free face, overlain by a fining-upward colluvial wedge (Fig. 5). Moderately well-stratified alluvial fan gravels beneath the beach gravel were continuous across the entire length of the trench, indicating no tectonic offset beneath the

FIGURE 5 FOLLOWING PAGE

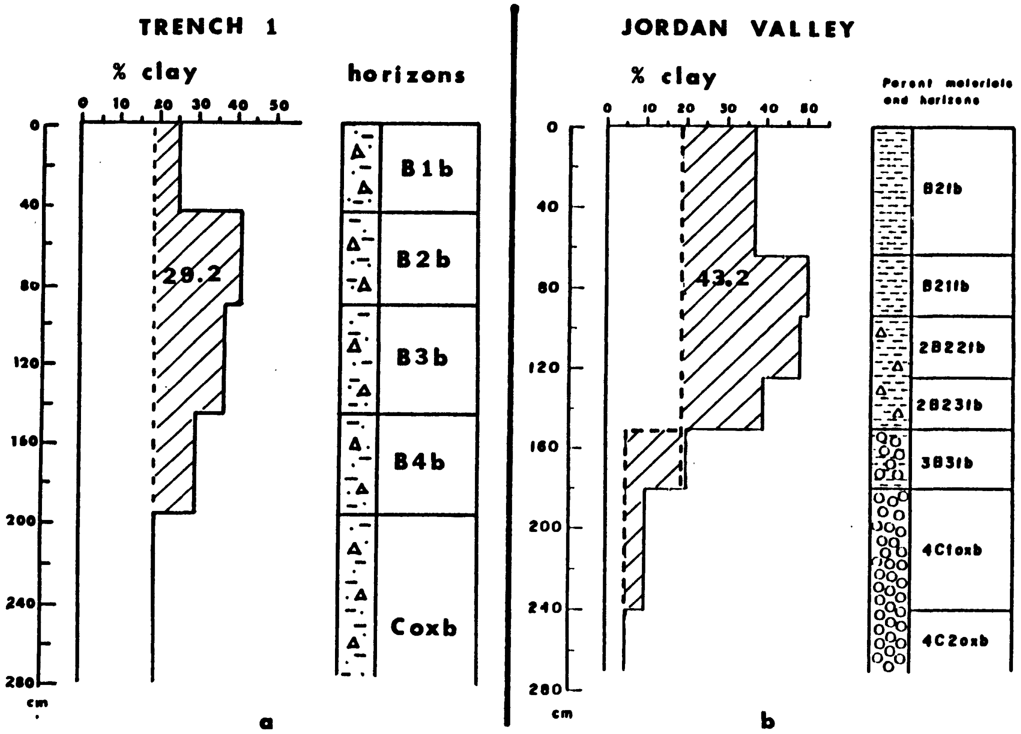

Figure 7. Comparison of soil profile properties between: a)the Trench 1 paleosol developed on unit 1, and b)a buried non-calcareous soil developed on Little Valley-cycle lacustrine gravel and loess in the Pioneer gravel pit in Kearns, Jordan Valley, UT. Scott and others (1982, Table 5 and p. 42) estimate the duration of soil formation of the calcareous facies of soil b as 94+22 ka, based on calcium carbonate content. The total pedogenic clay in soils a and b is represented by the ruled area. If bulk densities are similar, then the Trench 1 soil has about 67% as much pedogenic clay as does the Jordan Valley soil. Assuming clay formation rates are constant through time, this implies that the Trench 1 soil represents roughly 63+15 ka of soil formation.

considerably lower (8°-25°; Wallace, 1977, Fig. 3, stage E). Buried soil horizons within unit I must have required slope stability to form, but now dip 35° to 49° west downslope of the tilt axis in Fig. 6. The unit II/unit IV contact is bent slightly along this axis, while younger units are unbent. The amount of angular change on the unit I/unit II contact (8°; age ≃32 ka if deposited early during the Utaho transgression) versus that on the unconformity between units II and IV (4°; age 15-17 ka) suggests progressive monoclinal flexure with time (0.25°/ka). If this rate is applied to the even steeper dipping buried soil horizons B3b and B4b, an age of approximately 88 ka is obtained. This date is roughly compatible with an age of 95 ± 15 ka for unit 2 estimated from degree of soil development (Fig. 7). There are no discrete faults or shears within the colluvial wedge.

Monoclinal flexure of surficial materials in narrow (2-5 m wide) zones overlying fault traces has been previously described by Clark and others (1972, p. 118) and by Bonilla (1982, p. 18). Although the evidence in Trench 2 is not conclusive, it suggests that some kind of progressive flexure has occurred over the last 95 ka within 20 m downslope of the inferred range front fault in bedrock, unaccompanied by any surface faulting. It is unknown whether the warping resulted from syntectonic deformation or aseismic creep, but the absence of fractures supports the latter explanation.

Warped shorelines

The elevation of the Lake Utaho shoreline was determined at 46 points around the margin of Pocatello Valley to detect indirect evidence of tectonic deformation. Survey points were concentrated along suspected fault zones at the base of steep mountain fronts, to look for anomalous warps or tilts in the originally-horizontal shorelines. Surveying was performed with a Leitz TM10E theodolite and Leitz RED-2 electronic distance meter (EDM). The EDM and theodolite were set up over a benchmark or spot elevation on the valley floor, while the tripod-mounted reflecting prism was placed at the base of the shoreline scarp. While measurements were taken at the instrument station, an assistant measured a profile of the shoreline scarp using a 4.5 m rod and Abney level (after Bucknam and Anderson, 1979, p.12). In most instances the profile measurement was made from 30 m above to 30 m below the shoreline scarp. Typically, three distinct slope components were evident: a beach platform (3°-4°), a colluvial wedge (8°-12°), and a wave-cut scarp (18°-28°) (Fig. 8).

FIGURE 8 FOLLOWING PAGE

Because the Pleistocene lake shorelines were developed in unconsolidated deposits in all but a few locations around the valley margin, the shoreline angle has been covered by Holocene colluvium. The amount of colluvial cover varies depending on slope, aspect, deposit grain size, and local drainage patterns. To eliminate the effect of colluvial deposition from the surveyed shoreline scarp elevations, the beach platform and wave-cut scarp angles were projected under the colluvial wedge component on the profiles (Fig. 8). The intersection of the two angles is assumed to be a more accurate approximation of the shoreline angle. Because trenches 1 and 2 were excavated after the shoreline surveying phase of the study they provided a means of checking the accuracy of the method; in both instances the projected beach platform and wave-cut scarp angles intersected within 30 cm of the tops of Lake Utaho beach gravel lenses.

Although the water surface at the Lake Utaho highstand was horizontal, shorelines could have been superelevated, coincident, or subelevated with respect to the formative water plane (Currey, 1982, p. 21-22). All survey points along the eastern range front were in similar drift-aligned gravel beaches; data from Rose (1981, Table 5.6) shows that the shoreline angle of such beaches is usually within 0.5 m of the mean water surface. Large waves which might deposit gravel

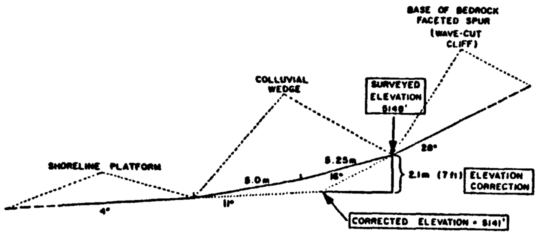

Figure 8. Diagram showing the method used in estimating actual elevations of pluvial lake shorelines covered by Holocene colluvium. The shoreline platform and wave-cut cliff components are projected beneath the colluvial wedge. The resulting intersection is presumed to be a more accurate representation of the actual shoreline angle.

far above the mean water surface would be hard to generate in Lake Utaho, which was only 10 km in diameter at its maximum extent.

The precision of the instrumentation used in this study was calculated to be ± 13.1 cm of elevation per kilometer of horizontal distance. The longest survey shot made was 1.5 km, and most were less than 0.5 km long. The combined uncertainties of surveyed elevation (0.13 m), projected shoreline angle (0.3 m), and relation to water surface (0.5 m) yield a ±0.93 m (3.05 ft.) uncertainty for each measured shoreline point (Table 1).

TABLE 1 FOLLOWING PAGE

Figure 9 (Transect A-A') shows shoreline elevations that deviate as much as 6.4 m from each other and up to 4.5 m from elevations predicted by Crittenden (1963) based on basin-scale isostatic rebound. The most significant deviations from a smooth profile occur where the north-northwest trending shoreline crosses the more northerly-trending faults at the base of Samaria Mountain. The shoreline at the southern end of the transect (point 17) is cut onto a faceted spur on the upthrown side of the fault, while at points 4,5, and 6 the shoreline is clearly on the downthrown side of the two parallel range front faults (Fig. 4). Point 17 falls at almost the exact elevation predicted for the Bonneville shoreline by Crittenden (1963, Fig. 3) while points 4-6 on the downthrown block plot 4.2-4.5 m too low in relation to their expected post-rebound elevation. Highly variable shoreline elevations between points 16 and 7 probably result from the sinuous shoreline repeatedly crossing from the upthrown to downthrown side of a more linear but buried fault or fold hinge line. For example, point 9 is a shoreline cut onto bedrock at the base of a spur, while the shoreline at points 8 and 10 is

FIGURE 9 FOLLOWING PAGE

Table 1. Surveyed elevation data for the Lake Utaho shoreline, Pocatello Valley

Reference Elevation[1] (ft. asl)	Shoreline Elevation Point[2]	Height of Shoreline above Reference Elevation (ft)[3]	Calculated Shoreline Elevation (ft)[4]	Colluvial Wedge Correction (ft)[5]	Corrected Shoreline Elevation (ft. asl)[6]
5032[a]	1	110	5142	-3	5139
5022[b]	2	111	5133	+3	5136
"	3	105	5127	+2	5129
"	4	113	5135	-2	5133
4977[c]	5	157	5134	0	5134
"	6	161	5138	-3	5135
"	7	168	5145	-3	5142
"	8	166	5143	-2	5141
"	9	182	5159	-3	5156
"	10	164	5141	0	5141
"	11	174	5151	0	5151
"	12	176	5153	-3	5150
"	13	172	5149	0	5149
4994[d]	14	148.5	5142.5	-1.5	5141
"	15	149	5143	-1.5	5141.5
"	16	146.5	5140.5	-4	5136.5
5063[e]	17	88	5151	-2	5149
"	18	98.5	5159.5	-13	5148.5
"	19	96.5	5159.5	-10	5149.5
5006[f]	20	127	5133	0	5133
4997[g]	21	160	5157	+9.5	5166.5

---

[1] Reference points of known elevation where the surveying base station was located: a, SW corner, Sec.16 T15S, R34E; b, BM O'FNL, Sec.26, T15S, R34E; c, SW corner, Sec.1, T16S, R34E; d, SW corner, Sec.13, T16S, R34E; e, SW corner, Sec.30, T16S, R34E; f, BM SE corner, Sec.20, T15S, R34E; g, NW corner, Sec.17, T16S, R34E.

[2] Shoreline points located on Figures 4 and 9.

[3] Calculated by trigonometric leveling from reference elevation; precision= 0.5 ft.

[4] Calculated by adding column 3 to column 1.

[5] The elevation difference between:a)the projected shoreline angle (see Fig.8), and b)the point where the shoreline elevation was measured; precision= 1.0 ft.

[6] Calculated by adding or subtracting column 5 from column 4. This elevation should be within 1.6 ft of the mean elevation of the formative water plane (Rose, 1981, Table 5.6)

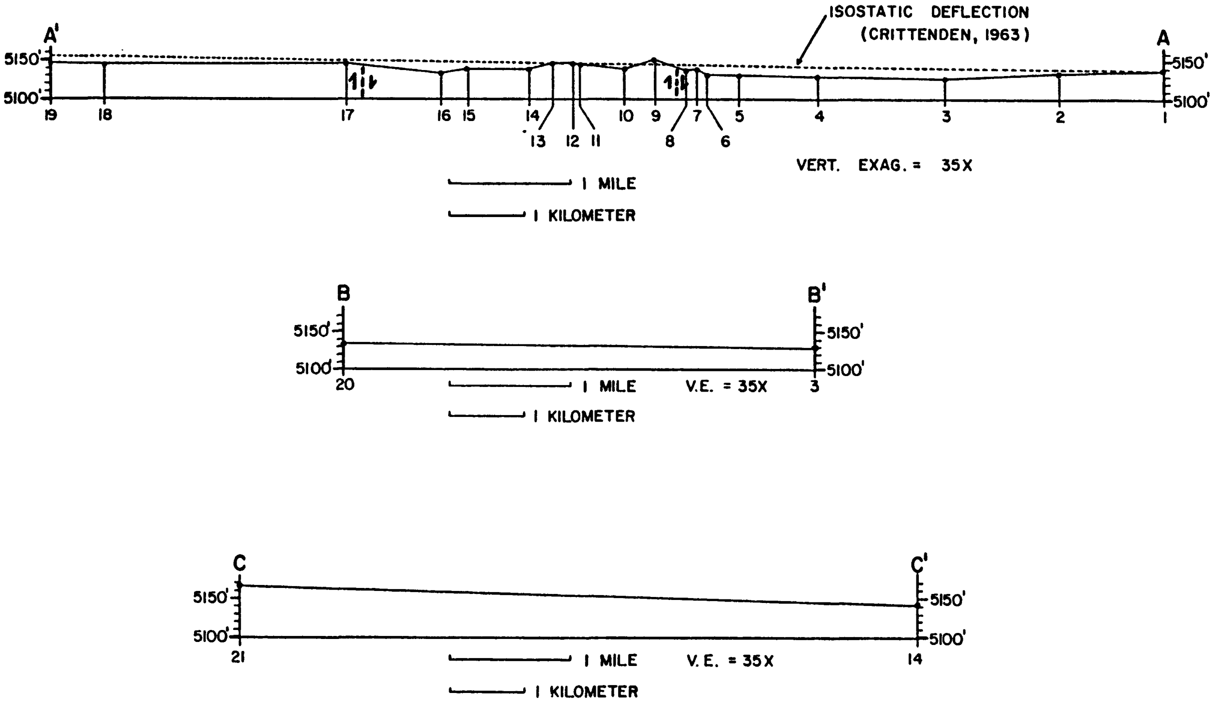

Figure 9. Lake Utaho shoreline elevation profiles. Location of profiles is shown in Fig. 4. The amount of error due to instrument inaccuracies and projecting of the shoreline angle is approximately represented by the width of the profile line (0.4m). Significant deviations from the expected elevation occur where the shoreline crosses inferred branches of the range-front fault (points 17-16, points 9-6).

cut into colluvium farther valleyward. The position of a linear fault paralleling the range front would cross between point 9 and points 8 and 10. Farther north, a parallel branch of the north-trending range front fault intersects the north-northwest-trending Utaho shoreline somewhere between points 6 and 9 (Fig. 9). Within this area the shoreline loses 6.4 m of elevation in a horizontal distance of 900 m. All shoreline profiles are very similar suggesting that they were formed with a constant relation to the mean water plane. Importantly, there are no fault scarps visible in this area.

East-west profiles suggest the Utaho shoreline has been tilled eastward from 1.8 m (Fig. 9, B-B'), to as much as 7.4 m (Fig. 8, C-C') in the most active-appearing range front area. Crittenden (1963, Fig. 3), shows an expected west to east shoreline elevation drop of approximately 1 m across Pocatello Valley resulting from differential isostatic rebound. The small residual displacement on transect B-B' (1.8 m-1.0 m = 0.8 m) is within the range of surveying error and suggests no significant tectonic eastward rotation has occurred north of the mapped eastern margin fault. The 6.4 m residual down-to-the-east displacment along transect C-C' strongly argues for post-Utaho slip along the central range front.

The overall implication is that late Quaternary slip on the range front fault has resulted in very little absolute elevation change of the upthrown block, but points on the downthrown block have been lowered 4.5-6.4 m, presumably by subsidence of the Pocatello Valley block. Geodetic data collected by Bucknam (1976) after the 1975 M6.0 earthquake showed no absolute uplift of surrounding mountain blocks, but a maximum of 13 cm of valley floor subsidence near the epicenter in western Pocatello Valley. The closed topography of the valley suggests that subsidence has been the dominant long-term tectonic trend during the Quaternary, as previously suggested for the late Cenozoic by Harr and Mabey

(1976).

Western Margin Fault

Over 30 normal faults have been mapped by Allmendinger (1983) in the portion of the North Hansel Mountains in our study area. The longest fault strikes N20W, is 8 km long (Fig. 4), and displaces older Quaternary pediment gravels by at least 55 m down to the east. The S value for the southern portion of the fault is 2.33, indicative of moderate-to-slightly active tectonism (Bull and McFadden, 1977). The V_f ratios of two gullies along the western margin fault are 5.0 and 4.0, values which are approximately 20 times those calculated for the eastern margin fault. The difference in V_f values suggests the western margin is less active than the eastern margin fault.

NEOTECTONIC FEATURES IN HANSEL VALLEY

Tectonic Setting

Hansel Valley, UT lies southeast of Pocatello Valley and is bounded on the east by the North Promontory Range, and on the west by the Hansel (or Summer Ranch) Mountains (Fig. 2). The fault at the west base of the North Promontory Mountains has created an extremely linear north-trending range front, complete with faceted spurs, about 25 km long. Strata of the Oquirrh Formation on either side of the fault near Bull's Pass are tilted eastward, suggesting eastward rotation of fault blocks (Jordan, 1985). The inferred Cenozoic throw on this fault near Bull's Pass (425 m; Jordan, 1985, Section A-A') is considerably less than the 1420 m inferred for the eastern fault of Pocatello Valley. The linear range front at the eastern base of the Hansel Mountains is inferred to be underlain by a normal fault (Adams, 1962, Plate 1; Doelling, 1980, Plate 1 and Plate 3, Section G-G'). However, the fault does not offset Quaternary deposits and has not created the sharp faceted spurs which exist on the eastern valley margin. Outcrops of Oquirrh Formation on the valley floor suggest that the throw on this fault is no greater than that on the eastern margin fault; it may be a minor fault on a hinged valley side, similar to the western margin fault in Pocatello Valley. The southwestern margin of Hansel Valley is a subdued and irregular range front veneered by Lake Bonneville deposits. The east-facing 1934 fault scarp and a pre-historic scarp up to 9 m high trend northerly across this zone. Very low gravity gradients in this region (Fig. 3) and the lack of appreciable topographic relief suggest that this fault has a low Cenozoic slip rate. Early Pleistocene and Tertiary sediments exposed in arroyos on the valley floor are extensively faulted. These faults usually have displacements of less than 5 m and do not displace overlying Lake Bonneville bottom sediments. The segmented linear nature of arroyos in northern Hansel Valley may be controlled by these north to northeast-trending faults in underlying Tertiary sandstones (Salt Lake Formation). Normal faults of similar strike offset Tertiary basalts immediately north of Interstate 84 and tilt them into a series of east-dipping blocks (Adams, 1962).

Eastern Margin Fault

Fault scarps occur at only two locations along the eastern margin fault, where the trace is not covered by Holocene talus. At the northern location (A on Fig. 2) a 13 m-high scarp offsets a delta graded to the Bonneville shoreline. Farther south a branch fault (B on Fig. 2) diverges southwesterly from the range front, creating a scarp up to 12.9 m high across pre-Bonneville alluvial fans. Both scarps are probably the result of multiple events; because each is limited to a single geomorphic surface and displays no multiple crests, reliable evidence of recurrent movement is lacking. Two profiles across the northern scarp, and three across the southern scarp yield scarp heights and maximum scarp slope angles which can be compared to those of dated single-event scarps elsewhere in Utah (Fig. 10).

FIGURE 10 FOLLOWING PAGE

The sparse data suggest the scarps are roughly comparable in age to the Bonneville shoreline (15.5-17 ka; Scott and others, 1983).

A graben bounded by two high-angle faults in Quaternary deposits is exposed on the southern roadcut of Interstate highway 84 across Rattlesnake Pass (C on Fig. 1). The faults offset seven distinct units of locally derived alluvium and colluvium deposited in a broad swale cut into Tertiary basalts (Fig. 11). Of the

FIGURE 11 FOLLOWING PAGE

four paleosols within the sequence, the lowest one is better developed than 140 ka-old non-calcareous soils developed elsewhere in the Bonneville Basin (Scott and other, 1982, p. 42), while soils 2, 3, and 4 each resemble calcareous soils developed elsewhere on 17 ka deposits (Scott and others, 1982, p. 36). Units I through V are clearly faulted: Unit VI may be faulted, while soil K_1 is clearly superposed across the fault, indicating faulting occurred between the deposition of unit V and the formation of soil K_1 (latest Pleistocene - early Holocene?).

Northwestern Margin Fault

The northwestern margin fault flanks the eastern margin on the Hansel Mountains (Fig. 2). The range front is linear and exhibits subdued talus-covered faceted spurs. Bonneville cycle shoreline deposits abut the range front, but no evidence of surface faulting exists in these sediments. Any fault scarps that may have been formed prior to the transgression of Lake Bonneville were presumably completely eroded. A shorter fault, about 4 km in length, parallels the northwest margin fault along the east side of a small valley at the southern end of the Hansel Mountains (Fig. 2; Adams, 1962; Doelling, 1980). This fault forms a horst at the southern end of the mountain, and decreases in displacement toward the

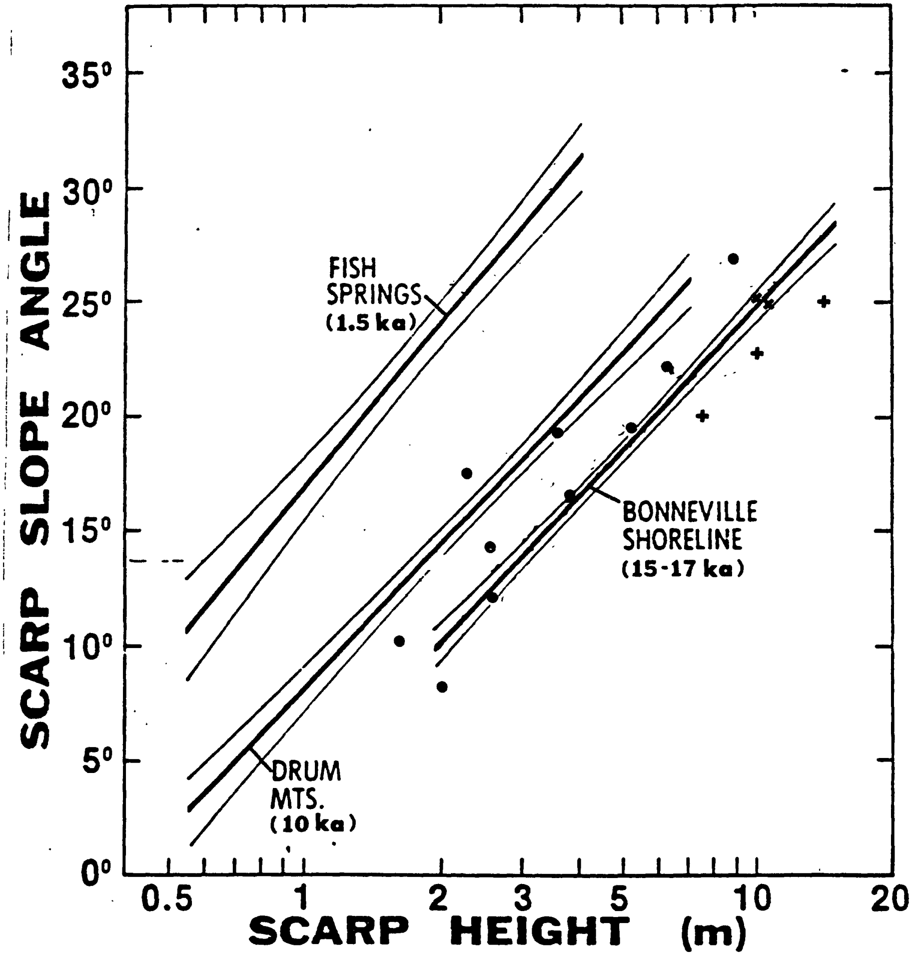

Figure 10. Graph of scarp surface offset versus the tangent of maximum scarp slope angle for Hansel Valley fault scarps and other dated scarps within Utah (modified from Hanks and others, 1984). Solid circles = scarps of the southwestern margin fault (D in Fig. 2) Profile numbers correspond to those on Fig. 12; Triangles = scarps of the eastern margin fault in pre-Bonneville alluvial fans (B in Fig. 2); Squares = scarps of the eastern margin fault in a Bonneville delta (A in Fig. 2). FS = Fish Springs; DM = Drum Mountains; BS = Bonneville Shoreline; OM = Oquirrh Mountains.

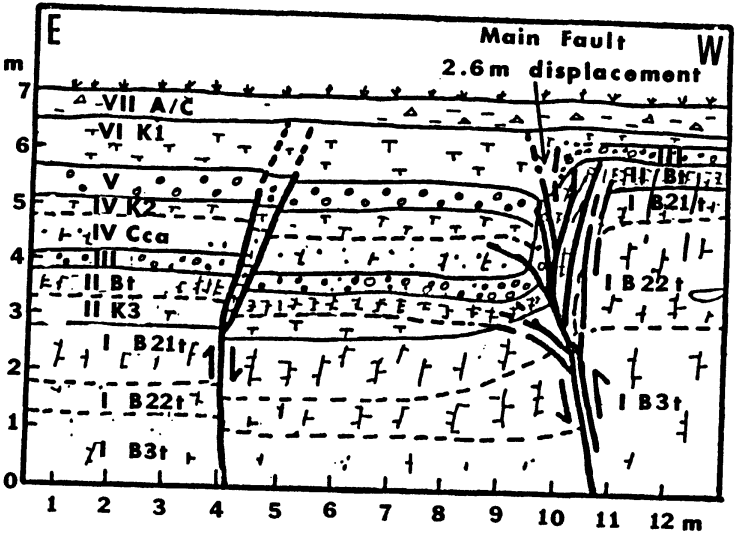

Figure 11. Sketch showing the fault exposed on the south side of the Rattlesnake Pass (I-84) roadcut (C in Fig. 2). The main fault displaces units I-III by 2.6m. Units IV and V do not appear on the upthrown block, while VI is considerably thinner on the upthrown side. Unit VII (Holocene? colluvium) is not faulted. Pattern intensity indicates the degree of secondary carbonate or clay enrichment in soil horizons.

north. This smaller fault is aligned with the trace of the 1934 scarp, and may be an extension of that fault zone.

Southwestern Margin Fault

The fault on the southwestern margin of Hansel Valley is markedly different from the valley-bounding faults previously described. Here the mountain block is located 3-4 km west of a 8 km-long, east facing fault scarp offsetting Bonneville-cycle shoreline gravels. Eleven profiles across the scarp (Fig. 12) reveal an increase in scarp height from 1.2 m to 9.0 m along the central part of the scarp where it ascends a 60 m-high bedrock-cored escarpment. The increased scarp heights probably result from the addition of a fault scarp plus a landslide scarp produced by syntectonic sliding (Fig. 13), based on the arcuate plan shape of the scarp.

FIGURE 12 FOLLOWING PAGE

FIGURE 13 FOLLOWING PAGE

Because the material involved in the sliding (beach gravel) is not particularly susceptible to landsliding when unsaturated, we infer that pore pressures were very high at the time faulting and sliding occurred, either from ground water saturation or from submersion under Lake Bonneville.

Geomorphic relations (described below) between the fault scarp and shorelines indicate that the scarp must have formed after the Bonneville transgression rose above 1402 m (about 26 ka; Scott and others, 1983, Fig. 5) but before the post-Provo regression fell below 1326 m (about 12 ka). Our reasoning is explained as follows. The timing of surface faulting events in relation to the timing of a pluvial lake cycle can occur: 1) before the lake rose, 2) during the transgression, 3) during the lake highstand, 4) during the regression, or 5) after the lake had completely receded. Small fault scarps (1-2 m high) which formed

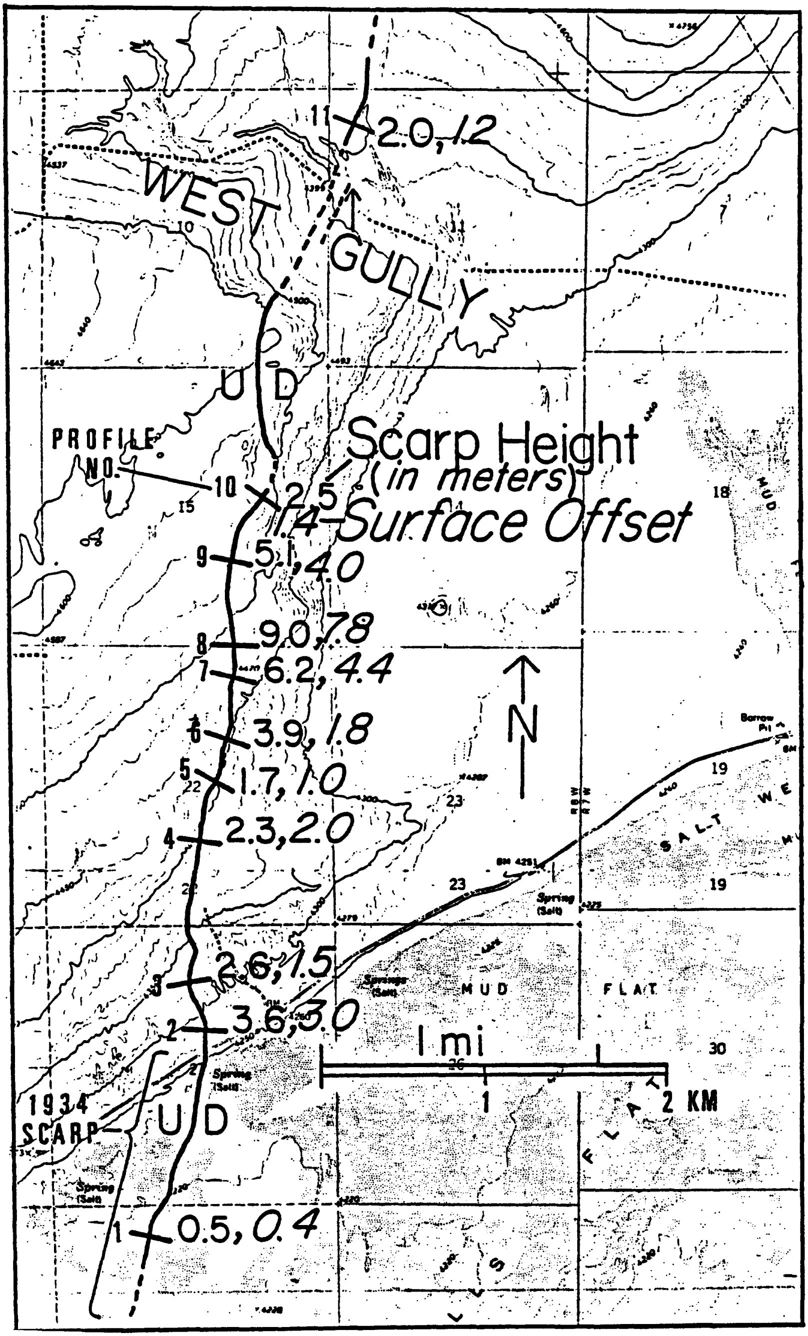

Figure 12. Map showing profile locations, scarp heights, and surface offsets on the Hansel Valley southwestern margin fault (D in Fig. 2). The 1934 scarp appears on the southern end of the prehistoric scarp. Scarp heights increase as the scarp ascends a larger escarpment; arcuate scarp plan shape strongly indicates syntectonic slumping (Fig. 13). Disregarding slump effects, most surface offsets are in the 1.0-2.0 m range.

before a major transgression would be reworked and destroyed, judging from the thickness (>5 m) and coarseness of Bonneville transgressive bars. Surface faulting during a transgression would displace submerged shorelines already formed; this scarp might be preserved if below effective wave base. That part of the scarp above the shoreline would be destroyed during the continued transgression. A scarp formed during a transgression therefore should displace all shorelines below the one occupied at the time of faulting and terminate at that shoreline, being obscured at higher elevations by wave reworking and longshore deposition (Fig. 14a). Any fault scarp formed during the lake highstand will displace all transgressive shorelines which it intersects. If faulting occurs during a regression, small regressive shorelines already formed as the lake receded should be displaced. The position of later (lower elevation) regressive shorelines would be controlled by the position of the fault scarp, because only minor deposition (<1 m) accompanies regression (except for the Provo shoreline) in the Bonneville Basin. In this case, a scarp would displace regressive shorelines above a certain elevation; below that elevation, shorelines would wrap around or abut a modified scarp of similar height (Fig. 14b). The elevation of this transition in morphology marks the position of the shoreline at the time of surface faulting. Surface faulting after the lake had completely receded would result in displacement of all transgressive and regressive shorelines.

FIGURE 14 FOLLOWING PAGE

Most fault scarps in the Bonneville Basin trend parallel to shorelines near range fronts, and therefore are not in a favorable orientation for intersecting multiple shorelines. The Hansel Valley scarp, however, displaces numerous shorelines as it ascends from the valley floor (1286 m) to 1402 m (Fig. 12). All transgressive shorelines up to 1402 m are displaced, indicating that surface

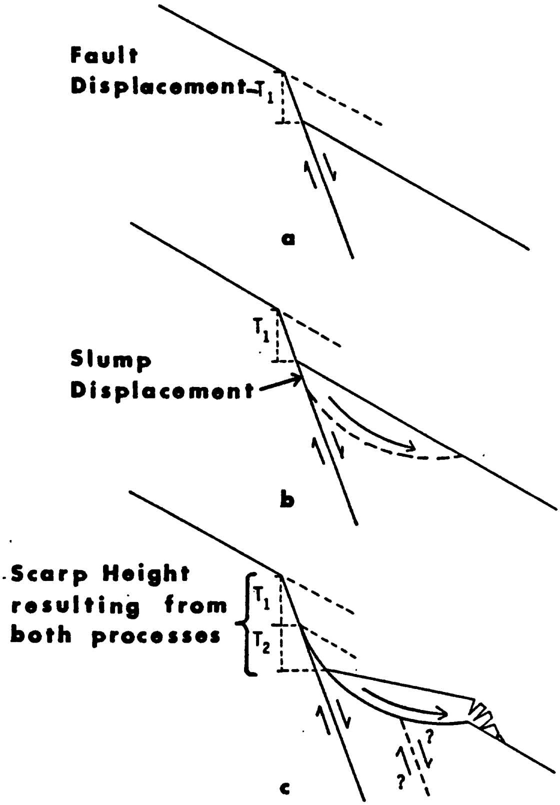

Figure 13. Diagram of a fault scarp heightened by a syntectonic rotational slump. a. Fault displacement (T1) would be increased by the addition (b) of a slump head scarp (T2). The exact location of the fault plane beneath the slump may be obscured. Theoretically, surface offset would not be affected if scarp profiles were extended beyond the toe of the slump mass on a uniformly dipping surface.

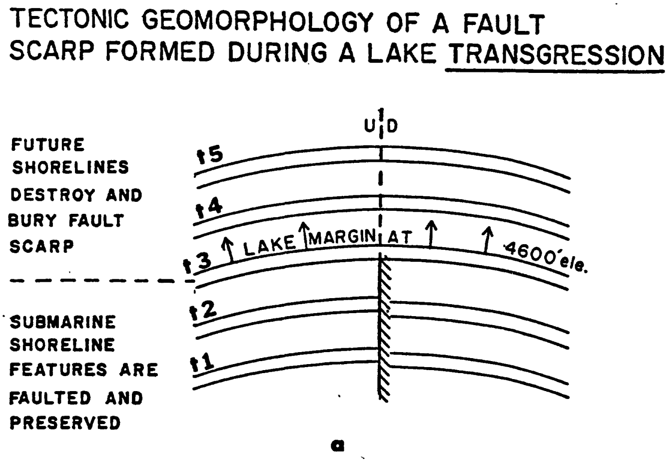

TECTONIC GEOMORPHOLOGY OF A FAULT SCARP FORMED DURING A LAKE TRANSGRESSION

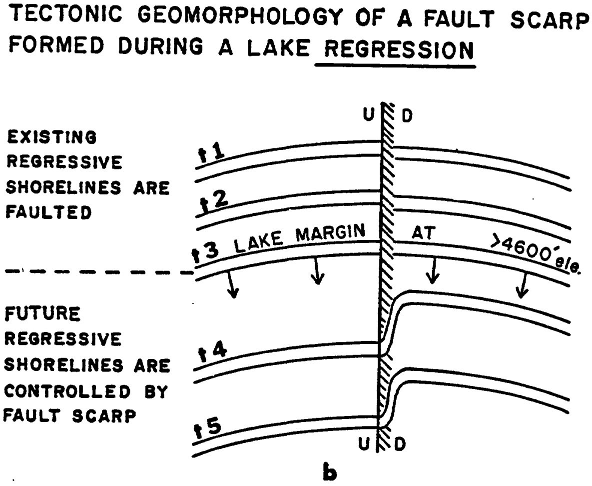

TECTONIC GEOMORPHOLOGY OF A FAULT SCARP FORMED DURING A LAKE REGRESSION

Figure 14. Sketches showing the geomorphic setting of a fault scarp formed during a lacustrine transgression (a) and regression (b). Time of shoreline occupation is shown by t, with time progressing from t1 to t5. In both instances, hypothetical faulting occurs when the shoreline is at t3.

faulting occurred after the Bonneville transgression had risen to this elevation (about 26 ka; Scott and others, 1983, Fig. 5). Small regressive bars at 1326 m terminate against the scarp, indicating that the scarp was already formed by the time the post-Provo regression reached that elevation (about 12 ka). Therefore, the scarp must have formed after 26 ka but before 12 ka. Scarp height-versus-slope angle data suggest the latest surface rupture event occurred between roughly 15 ka and 10 ka (Fig. 10; from Bucknam and Anderson, 1979), although scarps formed underwater are not strictly comparable to subaerial scarps. The overlap between these age estimates (12 ka-15 ka) probably closely dates the latest faulting event.

Near its north end the prehistoric scarp is intersected by a 10-15 m deep arroyo (informally termed the West Gully; Fig. 2). Two deformation zones are well exposed on arroyo walls; 1) the main fault zone, consisting of 11 normal faults defining a 90 m-wide graben, (Fig. 15) and 2) a subsidiary fault zone approximately 100 m to the east, composed of three major normal faults. Detailed logging and sampling of 200 m of arroyo walls revealed that the faults offset a stratigraphic section 19 m thick composed of 11 lacustrine units (Fig. 16) from three lake cycles. Physical stratigraphy, sedimentology, ostracod assemblages, and thermoluminescence (TL) dating (described in McCalpin, 1986) indicate that deposits of two pre-Bonneville ages are present. The older deposit (unit 1, Fig. 16) appears discontinuously in arroyo bottoms, consists of very compact, laminated silt and clay beds, and is disrupted by numerous high-angle fractures and faults of small displacement. Ostracod fauna and a TL date of 138 ka suggest this lower

FIGURE 15 FOLLOWING PAGE

FIGURE 16 FOLLOWING PAGE

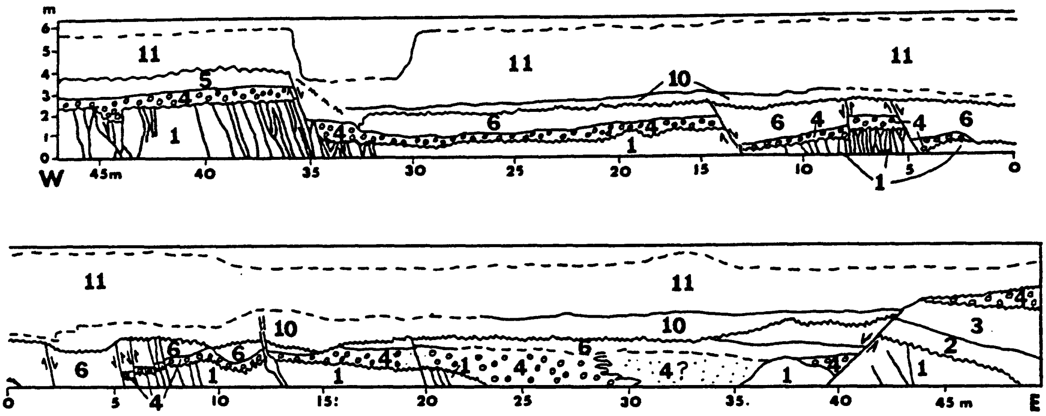

Figure 15. Wall log of the West Gully showing fault patterns. Numbered units refer to stratigraphic section of Fig. 16. The zero point on the horizontal scale is the Sec.10 - Sec.11 boundary which crosses the arroyo (Fig. 12). The chronology of faulting deduced from this log is discussed in the text.

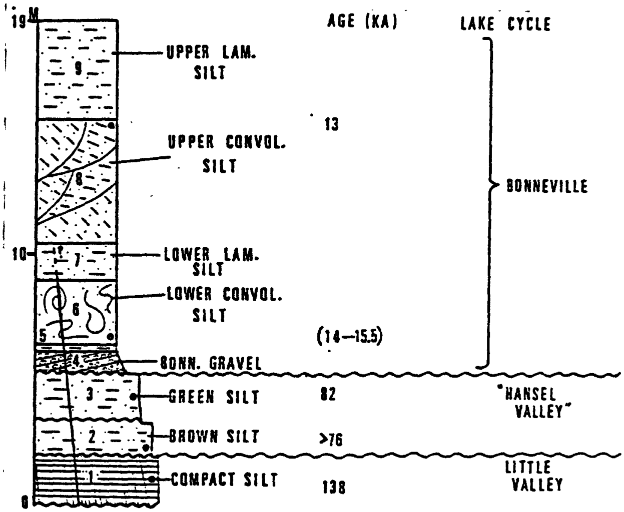

Figure 16. Composite stratigraphic section of Quaternary deposits exposed in the West Gully. Numbers correspond to those on Fig. 15, except that post-Bonneville alluvium (units 10 and 11) is not shown. Ages are from thermoluminescence dates on bulk sediment (McCalpin, 1986) or from 14C dates on gastropod shells (in parentheses).

unit is correlative with the Little Valley deposits described by Scott and others (1983). Unconformably overlying this unit are shoreline gravels and lake-marginal marsh sediments (units 2 and 3) which are also faulted (Fig. 15; 40-45 m E). TL dates of 76 ka and 82 ka indicate these units were deposited during a previously undated lake cycle (informally termed the Hansel Valley cycle) in late oxygen-isotope stage 5 or early stage 4 (Morley and Hays, 1981). A lake cycle of similar inferred age has been recently postulated by Oviatt and others (1985). Deposits of the Bonneville cycle (units 4-9) include the transgressive gravel, and lake bottom silts and clays. Lake bottom beds (unit 6) approximately 1.5 m above the transgressive gravel date at 14 ka by amino acids and 15.5 ka by ^{14}C on gastropod shells. Strata 4 m below the top of the stratigraphic section (upper unit 8) date at 13 ka by TL. These dates are roughly correlative with the Bonneville-cycle lake elevation curve of Scott and others (1983, Fig. 5).

Although not shown on Fig. 15, faults extend through unit 6, but cannot be traced through units 7 or 8. Both units 6 and 8 are internally deformed, the former by diapirs, roll structures and convolutions, the latter by rotational faulting of intact blocks along listric faults (lateral spreading?). Although such deformation could be caused by non-tectonic mechanisms, the coincidence of discrete deformed beds with a known, multiple-event Quaternary fault suggests earthquake-induced liquefaction. The difference in deformation styles may be due to great difference in water depths (and pore pressures) between the time when unit 6 was deformed (roughly 245 m) versus when unit 8 was deformed (less than 60 m).

Post-Bonneville alluvium (units 10 and 11) truncates all faults exposed in the West Gully, demonstrating that no Holocene events (not even the 1934 earthquake) have induced surface rupture at this location. Although the prehistoric scarp cannot be traced to the edge of the West Gully (due to agricultural disturbances), the net displacement of the transgressive gravel (unit 4) across the graben (1.3 m, down to the east) is similar to scarp heights north and south of the arroyo.

LATE QUATERNARY TECTONIC HISTORY

Pocatello Valley

Three lines of indirect evidence suggest a small but measurable amount of late Quaternary displacement on the eastern margin of Pocatello Valley: 1) lack of fault scarps in 15 ka deposits, 2) rapid elevation changes (up to 6.4 m) of a 15 ka shoreline, and 3) tilted, but unfaulted, Quaternary colluvium at the range front. Shoreline elevation data further suggest that deformation has been dominated by valley subsidence along the 7 km-long central segment of the eastern margin fault. Compilations by Bonilla (1982) and Slemmons (1983) show the threshold of surface rupture for shallow-focus earthquakes on normal faults is roughly M_L 6.2-6.3. Therefore, it appears that no earthquakes of this magnitude or larger have occurred anywhere along the range front fault in the last 15 ka. Within 20 m of the inferred range front fault, no tectonic displacements have disrupted 95 ka colluvium, suggesting no earthquakes of M_L>6.2-6.3 since that time. If this 7 km-long fault segment is capable of generating surface-faulting earthquakes, then recurrence times between them must be at least 15 ka, and possibly as much as 95 ka.

The cause of the rapid 4.5 m-6.4 m vertical changes in shoreline elevation is not fully understood. The magnitude of change appears to be significantly greater than the combined surveying errors, while the locations of greatest change coincide with shoreline-fault intersections. However, the calculated post-Utaho subsidence rate (4.5 m in 15 ka, or 0.3 mm/yr) seems excessive in light of the overall structural relief and age of the valley. At that rate, the 1420 m inferred displacement across the fault could be created in only 475 ka. The presence of Salt Lake Formation (Miocene-Pliocene?) within the downthrown block shows that inception of block faulting must be at least this old, so the inferred late Quaternary rate must be much higher than the post-Miocene average. This inference is compatible with the observed high rates of historic seismicity.

The 1975 M_L 6.0 earthquake we tentatively assign to the western margin fault, based on epicentral location and focal mechanisms derived by Arabasz and others (1979). Like the eastern margin fault, this fault does not displace any Lake Utaho deposits, indicating no $\overline{M_L >}$6.2-6.3 events in the last 15 ka. An early (?) Quaternary pediment (500 ka?) is displaced at least 55 m down to the east, yielding a slip rate of 0.11 mm/yr. This rate is roughly one-third of the slip rate calculated for the eastern margin fault, which is compatible with the differences in their tectonic geomorphology values quoted earlier.

Hansel Valley

Paleoseismic recurrence and magnitude data from the eastern margin fault are scanty and somewhat contradictory. The scarp with 8 m surface offset across a 15 ka delta implies multiple ruptures (3-4 if displacements per event were 2.0-2.5 m) in the last 15 ka. The resulting recurrence times (3.7-5.0 ka) seem too short in view of the total range front relief and tectonic geomorphology, compared to nearby normal faults such as the Wasatch Fault (Machette and others, this volume). Evidence of only a single recent 2.6 m displacement on the Rattlesnake Pass splay fault within the last 100 ka is not compatible with 3-4 events on the main trace in 15 ka, unless the main fault has ruptured many times without involving this particular splay. However, multiple post-Bonneville displacements are seen nowhere else along the length of the eastern margin, although the inferred fault trace emerges from under its talus cover for several long stretches. Only a single branch fault farther south offsets pre-Bonneville (stage 4 or stage 6) alluvial fans 9.5 m. Depending on the age assigned to these fans (roughly 65 ka or 140 ka) the recurrence intervals for 2.0-2.5 m events are between 16 ka to 35 ka, although not every main trace rupture may have involved this branch. Considering the poor geomorphic evidence, all that can be stated with certainty is that this fault has sustained surface rupture at least once since Bonneville time, and several times since either stage 4 or 6.

Although the temporal control is better for the well-exposed faulted strata in the West Gully, the inability to trace any subsurface faults to the surface (and thus connect them to the surface scarp) poses a large obstacle to fault history reconstruction. The older history of faulting is ambiguous; multiple events of unknown displacement along many traces, some of which were truncated by the stage 4 transgression about 72 ka. On blocks rotated by post-26 ka faulting, there is no angular unconformity between stage 6 and 4 deposits, indicating no tectonic rotation there in the period 72 ka-58 ka (see Fig. 15, 35 m E). The 26 ka Bonneville transgression truncates many small-displacement fractures of unknown age in unit 1, but also fills in an open tectonic fissure (Fig. 15, 42 m W) which could not have remained open for too long after its creation; this implies an event not far in advance of 26 ka. Units 4, 5, and 6 are displaced along major faults, but these faults cannot be traced through overlying units due to poor exposures. The only later evidence of tectonism is the rotated blocks of unit 8, which could be a result of either tectonic or non-tectonic lateral spreading. Taken together, the evidence argues for multiple events between roughly 140 and 72 ka, no events from 72-58 ka, at least one event between 58 ka and 26 ka (nearer the latter), an event around 14-15 ka (the age of unit 6), possibly another at 13 ka (unit 8), and a M_L 6.6 event in 1934 A.D.

This history implies widely varying recurrence intervals, from 1 event from 72-26 ka (RI=46 ka) to 2 events at 14-15 ka and 13 ka (RI=1-2 ka). Although the field evidence is ambiguous, it appears that recurrence times have been shorter when large lakes existed in the Bonneville Basin (stages 6 and 2) than during times of small or no lakes (stages 5,4,3). An exception is the 1934 M6.6 earthquake, which occurred in the middle of an interpluvial episode. However, its small maximum displacement (0.5 m) compared to those seen in stage 2 time (2.2-2.6 m, in either one or two events) may indicate that interpluvial earthquakes are limited to smaller size than pluvial earthquakes. The rapid crustal stresses imposed by filling and draining pluvial lakes (especially the catastrophic drop from Bonneville to Provo shorelines) may be the main triggering mechanism for the Quaternary surface faulting events experienced by the southwestern margin fault, as suggested by others (Swan and others, 1983; Machette and others, this volume) for the nearby Wasatch Fault.

CONCLUSIONS

Quaternary geologic mapping, shoreline surveying, arroyo wall logging, and trenching indicate that late Quaternary displacements have occurred on both margin faults in Pocatello and Hansel Valleys. The lack of fault scarps in pluvial lake deposits in Pocatello Valley suggests no surface faulting has occurred in the last 15 ka, yet shorelines and colluvium at the range front appear warped. The 6.4 m maximum vertical shoreline warping may be caused by monoclinal flexure over a buried fault trace; examples of similar warping of surficial deposits near faults are given by Bonilla (1983, p. 18), although none are for normal faults. Colluvium in a range-front trench appeared warped but unfractured, suggestive of creep flexure rather than flexure around an upward-propagating rupture. Recent trenching on the West Valley Fault Zone, Salt Lake County, by Keaton and others (this volume) has exposed monoclinal warps along Quaternary normal faults. With the limited data on hand, it appears that surface flexure could occur from creep or from earthquakes slightly below the threshold magnitude necessary to create a fault scarp. Geomorphic evidence from Pocatello Valley suggests that significant

REFERENCES CITED

Adams, O.C., 1962, Geology of the Summer Ranch and North Promontory Mountains, Utah: M.S. Thesis, Utah State University, Logan, Utah 57 p.

Allmendinger, R.W., 1983, Geologic map of the North Hansel Mountains, Idaho and Utah: U.S. Geological Survey Map MF-1643, 1:24,000.

Allmendinger, R.W. and Platt, L.B., 1983, Stratigraphic variation and low-angle faulting in the North Hansel Mountains and Samaria Mountain, Southern Idaho: Geological Society of America, Memoir 157, p. 149-163.

Arabasz, W.J. and McKee, M.E. (comp.) 1979, Utah Earthquake Catalog, 1850-June-1962, in Arabasz, W. J., Smith, R.B. and Richins, W.D. (eds.), Earthquake Studies in Utah, 1850-1978, Special Publication, University of Utah Seismograph Station, Salt Lake City, UT, p.

Beus, S.S., 1968, Paleozoic stratigraphy of Samaria Mountain, Idaho-Utah: Bulletin of the American Association of Petroleum Geologists, V. 52, no. 5, p. 782-808.

Bonilla, M.G., 1982, Evaluation of potential surface faulting and other tectonic deformation: U.S. Geological Survey Open-File Report 82-0732, 91 p.

Bucknam, R.C., 1976, Leveling data from the epicentral area of the March 27, 1975, earthquake in Pocatello Valley, Idaho: U.S. Geological Survey Open-File Report 76-52, 6 p.

Bucknam, R.C., and Anderson, R.E., 1979, Estimation of fault-scarp ages from a scarp-height-slope-angle relationship: Geology, v. 7, p. 11-14.

Bull, W.B. and McFadden, L.D., 1977, Tectonic geomorphology, north and south of the Garlock Fault, California, in Doehring, D.O. (ed.), Geomorphology in Arid Regions, 8th Annual Binghampton Geomorphology Symposium, Allen and Unwin, p. 115-138.

Clark, M.M., Grantz, Arthur, and Rubin, Meyer, 1972, Holocene activity of the Coyote Creek Fault as recorded in sediments of Lake Cahuilla: U.S. Geological Survey Professional Paper 787, p. 112-130.

Crittenden, M.D., Jr., 1963, New data on the isostatic deformation of Lake Bonneville: U.S. Geological Survey Professional Paper 454-E, 31 p.

Curry, D.R., 1981, Late Quaternary Lake Utaho in southern Idaho-northern Utah: Association of American Geographers, Program Abstracts, 1981, p. 166-167, Denver, CO.

Currey, D.R., 1982, Lake Bonneville: selected features of relevance to neotectonic analysis: U.S. Geological Survey Open File Report 82-1070, 30 p.

Doelling, H.H., 1980, Geology and mineral resources of Box Elder County, Utah: Utah Geological and Mineralogical Survey Bulletin 115, 251 p.

when large lakes existed in the Bonneville Basin (stages 6 and 2) than during times of small or no lakes (stages 5,4,3). An exception is the 1934 M6.6 earthquake, which occurred in the middle of an interpluvial episode. However, its small maximum displacement (0.5 m) compared to those seen in stage 2 time (2.2-2.6 m, in either one or two events) may indicate that interpluvial earthquakes are limited to smaller size than pluvial earthquakes. The rapid crustal stresses imposed by filling and draining pluvial lakes (especially the catastrophic drop from Bonneville to Provo shorelines) may be the main triggering mechanism for the Quaternary surface faulting events experienced by the southwestern margin fault, as suggested by others (Swan and others, 1983; Machette and others, this volume) for the nearby Wasatch Fault.

CONCLUSIONS

Quaternary geologic mapping, shoreline surveying, arroyo wall logging, and trenching indicate that late Quaternary displacements have occurred on both margin faults in Pocatello and Hansel Valleys. The lack of fault scarps in pluvial lake deposits in Pocatello Valley suggests no surface faulting has occurred in the last 15 ka, yet shorelines and colluvium at the range front appear warped. The 6.4 m maximum vertical shoreline warping may be caused by monoclinal flexure over a buried fault trace; examples of similar warping of surficial deposits near faults are given by Bonilla (1983, p. 18), although none are for normal faults. Colluvium in a range-front trench appeared warped but unfractured, suggestive of creep flexure rather than flexure around an upward-propagating rupture. Recent trenching on the West Valley Fault Zone, Salt Lake County, by Keaton and others (this volume) has exposed monoclinal warps along Quaternary normal faults. With the limited data on hand, it appears that surface flexure could occur from creep or from earthquakes slightly below the threshold magnitude necessary to create a fault scarp. Geomorphic evidence from Pocatello Valley suggests that significant vertical displacements may occur without the creation of fault scarps, over horizontal distances of hundreds of meters, and that these displacements are not detectable in the field without careful surveying. Such a conclusion has implications for displacement studies on the Wasatch Fault, where it has been assumed that most (if not all) of cumulative net vertical tectonic displacement can be measured solely by fault scarp profiling.

Marginal faults bounding Hansel Valley have generated multiple surface-faulting earthquakes in the late Quaternary, despite the seemingly small structural relief of this valley compared to Pocatello Valley. While a few short scarps occur on the steep eastern margin, the best record of activity is on the southwestern margin where an 8 km-long scarp is intersected by a 15 m-deep arroyo. The multiple events deduced from logging a 90 m-wide complex graben which displaces lacustrine sediments 138 ka to 13 ka old show that even faults with minimal topographic and structural expression can have complex recurrence histories. Thermoluminescence dating of silty lacustrine deposits in the graben yielded ages compatible with stratigraphic and paleoecologic evidence, and showed that this dating technique holds promise for dating non-carbonaceous, non-fossiliferous lake beds. Finally, the concentration of deformation in the oldest lacustrine deposit (oxygen isotope stage 6) and in the deposits of the Bonneville cycle (oxygen isotope stage 2) suggest that surface faulting is enhanced when deep pluvial lakes occupied Hansel Valley, as opposed to when no lakes (stages 3 and 5) or shallow lakes (stage 4) existed. This temporal clustering has been described by others (Swan and others, 1983) and may result from increased pore pressures and water loading of the crust.

ACKNOWLEDGEMENTS

Rick Forester, U.S. Geological Survey, interpreted the ostracod faunas from the West Gully. Jerry Stipp, Alpha Analytic Inc., provided the TL dates and valuable advice, while Bill McCoy, University of Massachusetts, contributed TL dates from type localities at Promontory Point. The manuscript benefitted from reviews by Alan Nelson and Bob Bucknam, U.S. Geological Survey. Field work was supported by U.S. Geological Survey Contract 13-08-001-21899.

REFERENCES CITED

Adams, O.C., 1962, Geology of the Summer Ranch and North Promontory Mountains, Utah: M.S. Thesis, Utah State University, Logan, Utah 57 p.

Allmendinger, R.W., 1983, Geologic map of the North Hansel Mountains, Idaho and Utah: U.S. Geological Survey Map MF-1643, 1:24,000.

Allmendinger, R.W. and Platt, L.B., 1983, Stratigraphic variation and low-angle faulting in the North Hansel Mountains and Samaria Mountain, Southern Idaho: Geological Society of America, Memoir 157, p. 149-163.

Arabasz, W.J. and McKee, M.E. (comp.) 1979, Utah Earthquake Catalog, 1850-June-1962, in Arabasz, W. J., Smith, R.B. and Richins, W.D. (eds.), Earthquake Studies in Utah, 1850-1978, Special Publication, University of Utah Seismograph Station, Salt Lake City, UT, p.

Beus, S.S., 1968, Paleozoic stratigraphy of Samaria Mountain, Idaho-Utah: Bulletin of the American Association of Petroleum Geologists, V. 52, no. 5, p. 782-808.

Bonilla, M.G., 1982, Evaluation of potential surface faulting and other tectonic deformation: U.S. Geological Survey Open-File Report 82-0732, 91 p.

Bucknam, R.C., 1976, Leveling data from the epicentral area of the March 27, 1975, earthquake in Pocatello Valley, Idaho: U.S. Geological Survey Open-File Report 76-52, 6 p.

Bucknam, R.C., and Anderson, R.E., 1979, Estimation of fault-scarp ages from a scarp-height-slope-angle relationship: Geology, v. 7, p. 11-14.

Bull, W.B. and McFadden, L.D., 1977, Tectonic geomorphology, north and south of the Garlock Fault, California, in Doehring, D.O. (ed.), Geomorphology in Arid Regions, 8th Annual Binghampton Geomorphology Symposium, Allen and Unwin, p. 115-138.

Clark, M.M., Grantz, Arthur, and Rubin, Meyer, 1972, Holocene activity of the Coyote Creek Fault as recorded in sediments of Lake Cahuilla: U.S. Geological Survey Professional Paper 787, p. 112-130.

Crittenden, M.D., Jr., 1963, New data on the isostatic deformation of Lake Bonneville: U.S. Geological Survey Professional Paper 454-E, 31 p.

Curry, D.R., 1981, Late Quaternary Lake Utaho in southern Idaho-northern Utah: Association of American Geographers, Program Abstracts, 1981, p. 166-167, Denver, CO.

Currey, D.R., 1982, Lake Bonneville: selected features of relevance to neotectonic analysis: U.S. Geological Survey Open File Report 82-1070, 30 p.

Doelling, H.H., 1980, Geology and mineral resources of Box Elder County, Utah: Utah Geological and Mineralogical Survey Bulletin 115, 251 p.

Harr, C.J. and Mabey, D.R., 1976. Gravity survey of Pocatello Valley, Idaho and Utah: U.S. Geological Survey Open-File Report 76-766, 12 p.

Hood, J.W., 1971, Hydrologic reconnaissance of Hansel Valley and Northern Rozel Flat, Box Elder County, Utah: Technical Publication No. 33, Utah Department of Natural Resources, 41 p.

Jordan, T.E., 1985 Geologic map of the Bull's Pass quadrangle, Box Elder County, Utah: U.S. Geological Survey Map MF-1491, 1:24,000.

McCalpin, James, 1986, Thermoluminescence (TL) dating in seismic hazard evaluations; an example from the Bonneville Basin, Utah: Proceeding of the 22nd Annual Engineering Geology and Soils Engineering Symposium, Boise, ID, p. 156-176.

Morley, J.J. and Hays, J.D., 1981, Towards a high-resolution, global, deep sea chronology for the last 750,000 years: Earth and Planetary Science Letters, v. 15, p. 279-295.

Oviatt, C.G., McCoy, W.D. and Reider, R.G., 1985, Quaternary lacustrine stratigraphy along the lower Bear River, UT: Evidence for a shallow early Wisconsin lake in the Bonneville Basin: Geological Society of America, Abstracts with Programs, v. 17, no. 4, p. 260.

Peterson, D.L., 1974, Bouger gravity map of part of the northern Lake Bonneville Basin Utah and Idaho: U.S. Geological Survey Map MF 627, 1:250,000.

Platt, L.B., 1975, Recent faulting at Samaria Mountain, Southeastern Idaho: Geological Society of America, Abstracts with Programs, v. 7, p. 1224-1230.

__________, 1976, Geologic mapping and earthquakes in Southeastern Idaho: Earthquake Information Bulletin, v. 8, p. 8-12.

__________, 1977, Geologic map of the Ireland Springs-Samaria area, southeastern Idaho and northern Utah: U.S. Geological Survey Map MF-890, 1:48,000.

Richins, W.D., 1979, The Hansel Valley, Utah, earthquake sequence of November, 1976, in Arabasz, W.J., Smith, R.B. and Richins, W.D. (eds.), Earthquake studies in Utah, 1850-1978: Special publication of the University of Utah Seismograph Stations, Salt Lake City, Utah, p. 409-421.

Rogers, A.M., Langer, C.J. and Bucknam, R.C., 1975, The Pocatello Valley, Idaho earthquake; Earthquake Information Bulletin, v. 7, no. 3 p. 16-18.

Rose, J., 1981, Raised shorelines, in Goudie, Andrew (ed.), Geomorphological Techniques, p. 327-341, Allen and Unwin, London.

Scott, W.E., Machette, M.N., Shroba, R.R., and McCoy, W.D., 1982, Guidebook for the 1982 Friends of the Pleistocene Rocky Mountain Cell Field Trip to Central Utah: Part I, Little Valley and Jordan Valley, Utah: U.S. Geological Survey Open File Report 82-845, 58 p.

Scott, W.E., McCoy, W.D., Shroba, R.R. Rubin, Meyer, 1983, Reinterpretation of the exposed record of the last two cycles of Lake Bonneville, Western United States: Quaternary Research, v. 20, p. 241-265.

Slemmons, D.B., 1982, Determination of design earthquakes magnitudes for microzonation: Proceedings of the Third International Earthquake Microzonation Conference, Seattle, WA; Earthquake Engineering Research Institute, v. 1, p. 110-130.

Stokes, W.L., 1977, Subdivisions of the major physiographic provinces in Utah: Utah Geology, v. 4, no. 1, p. 1-17.

Swan, F.H. III, Hanson, K.L., Schwartz, D.P. and Black, J.H., 1983, Study of earthquake recurrence intervals on the Wasatch Fault, Utah: 8th Semi-Annual Technical Report, U.S. Geological Survey Contract N. 14-08-0001-19842, May 1983, 20 p.

STRUCTURE OF THE SALT LAKE SEGMENT, WASATCH NORMAL FAULT ZONE; IMPLICATIONS FOR RUPTURE PROPAGATION DURING LARGE EARTHQUAKES

by

R.L. Bruhn, P.R. Gibler, W. Houghton and W.T. Parry
Department of Geology and Geophysics
University of Utah, Salt Lake City, Utah 84112

ABSTRACT

The Salt Lake fault segment is one of six, independent earthquake rupture segments in the Wasatch normal fault zone, Utah proposed by Schwartz and Coppersmith (1984). The Salt Lake segment is about 35 km long and capable of generating earthquakes of M = 7.0-7.5. The fault segment is defined by a series of Quaternary scarps that form a branched fault trace, with a narrow, single rupture zone that bifurcates into two, subparallel rupture zones in the northern half of the segment. The surface rupture trace is subdivided into several linear to curvilinear sections ≈3 to 12 km in length. The dips of these fault sections are modelled using information about characteristics of the paleo-slip directions and paleo-stress field. Estimated dips vary from 45° to 90° depending on the strike of individual fault sections.

A non-conservative rupture barrier is located at each end of the segment, and the zone of fault bifurcation forms a third, non-conservative barrier located in the center of the segment. The relative fracture toughness of barriers has been estimated based soley on their cross-sectional dimensions and by assuming that the barriers are mechanically equivalent to a "plastic tip" deformation zone in fracture mechanics theory.

Two potential sites of rupture initiation for large earthquakes are tenatively proposed based on considerations of the structural history and inferred mechanical characteristics of the Salt Lake segment. One site is the non-conservative barrier in the central part of the segment. A rupture

initiating there would propagate bilaterally to the north and south, possibly arresting in the two non-conservative barriers at the ends of the segment. The other likely rupture initiation site is within the non-conservative barrier at the southern end of the fault segment. An earthquake initiating there would rupture unilaterally towards the north, propagating into the bifurcated northern half of the fault segment in a manner similar to that of the Hebgen Lake, Montana (Ms = 7.3) and Borah Peak, Idaho (Ms = 7.3) earthquake ruptures. Evidence of significant lateral variations in the long-term deformation rate within the segment suggests that this latter site may have been the the most common position for repetitive rupture initiation during the last ≈17 m.y.

INTRODUCTION

Large fault zones are divided into sections that vary in geometry and rupture history. The intersections of adjacent fault sections may form geometrical barriers that strongly influence the history of rupturing within the fault zone, and play a fundamental role in determining the seismogenic characteristics of the crust (Aki, 1979; King, 1983; King and Yielding, 1984; King and Nabelek, 1985). A propagating rupture may exhibit several different types of behavior upon encountering a barrier. The rupture front may slow down or pause temporarily for periods of seconds or minutes, or become permanently arrested. In the latter case, new ruptures may nucleate and propagate into adjacent parts of the fault zone at later times. Consequently, geometrical barriers must be considered as potential sites of both rupture arrest and initiation (King, 1983; King and Yielding, 1984; King and Nabelek, 1985).

King and Yielding (1984) have defined two fundamental types of geometric barriers - the <u>conservative</u> and <u>non-conservative</u> barrier. Geometrical barriers represent jogs or bends in the main fault zone caused by offset in fault trace, and changes in strike and dip. A conservative barrier is one in which the fault slip vector is constant on both sides of the barrier and parallels the intersection line between the primary fault planes comprising the adjacent sections of the fault zone. That is, the adjacent sections form a cylindrical surface that can be generated by moving the slip vector parallel to itself Conversely, a non-conservative barrier develops in regions where the slip vectors differ between two adjacent sections of the fault zone. The structure of these two types of barriers differs significantly. Faulting in the conservative barrier may be accommodated within a narrow fault zone and does not require extensive fracturing of the adjacent country rock in order to transfer motion between two adjacent sections of the fault zone. Alternatively, rupturing through a non-conservative barrier requires the development of at least one new direction of primary faulting in addtion to that of the two intersecting fault sections comprising the main fault zone. This process will result in the formation of numerous subsidiary faults that must be activated to allow the transfer of motion between the fault sections. This network of subsidiary faults results in a broad, diffuse zone of deformation in the non-conservative barrier, which has the effect of "blunting" the tip zone of the propagating rupture and diffusing energy into a large volume of rock. Consequently, non-conservative barriers are likely sites for the permanent arrest of a propagating rupture. This process, in turn, may set the stage for the initiation of a subsequent rupture that will propagate into an adjacent section of the primary fault zone (King and Nabelek, 1985). The mutual interference and interlocking of numerous subsidiary faults in the barrier results in the development of asperities, which must be broken in order to establish the full length of the next rupture segment. Breaking of these asperities must be a time dependent process that is related to 1) rates of deformation that increase stress level through time, 2) fluid chemistry and pressure in the barrier, and 3) material properties of the barrier.

Several criteria exist for identifying geometrical barriers in fault zones

(King, 1983; King and Yielding, 1984; King and Nabelek, 1985). An abrupt offset, bend or geometrical branching in the trace of a primary fault zone is sufficient to identify the presence of a barrier. The presence of a non-conservative barrier is indicated by change in the amount or directions of slip on two adjacent sections of the primary fault zone. This phenomenon leads to 1) development of a third direction of faulting in the barrier, 2) break-up of the hanging wall above the barrier in normal fault zones, 3) abrupt changes in the amount of throw across the fault zone between the two primary sections, and 4) the possibility of diffuse seismicity associated with the failure of asperities within the barrier.

This paper presents our study of the geometry and paleo-stress field of the Salt Lake rupture segment in the Wasatch fault zone (Fig. 1). The Salt Lake segment (Fig. 2) is one of six, large rupture segments within the Wasatch fault zone that were proposed by Schwartz and Coppersmith (1984). This segment extends for about 35 km through the urban corridor of Salt Lake City, along the eastern edge of the Basin-Range Province. The fault zone is marked by prominent scarps in Quaternary deposits and has undergone at least two, and probably four, earthquakes of M = 7.0-7.5 that generated surface scarps during the last 8000 years (Schwartz and Coppersmith, 1984). Our goal is to determine the geometrical and mechanical characteristics of the segment in order to better understand the processes of crustal segmentation and the seismogenic characteristics of the Wasatch fault zone.

TECTONICS OF WASATCH FAULT ZONE

The Wasatch normal fault zone extends for 370 km along the eastern edge of the Basin-Range Province in southern Idaho and northern Utah. This major fault zone has a pronounced footwall escarpment, with up to 3 km of relief, that separates alluvial filled valleys of the Basin-Range to the west from the Wasatch Mountains to the east (Gilbert, 1928). Total

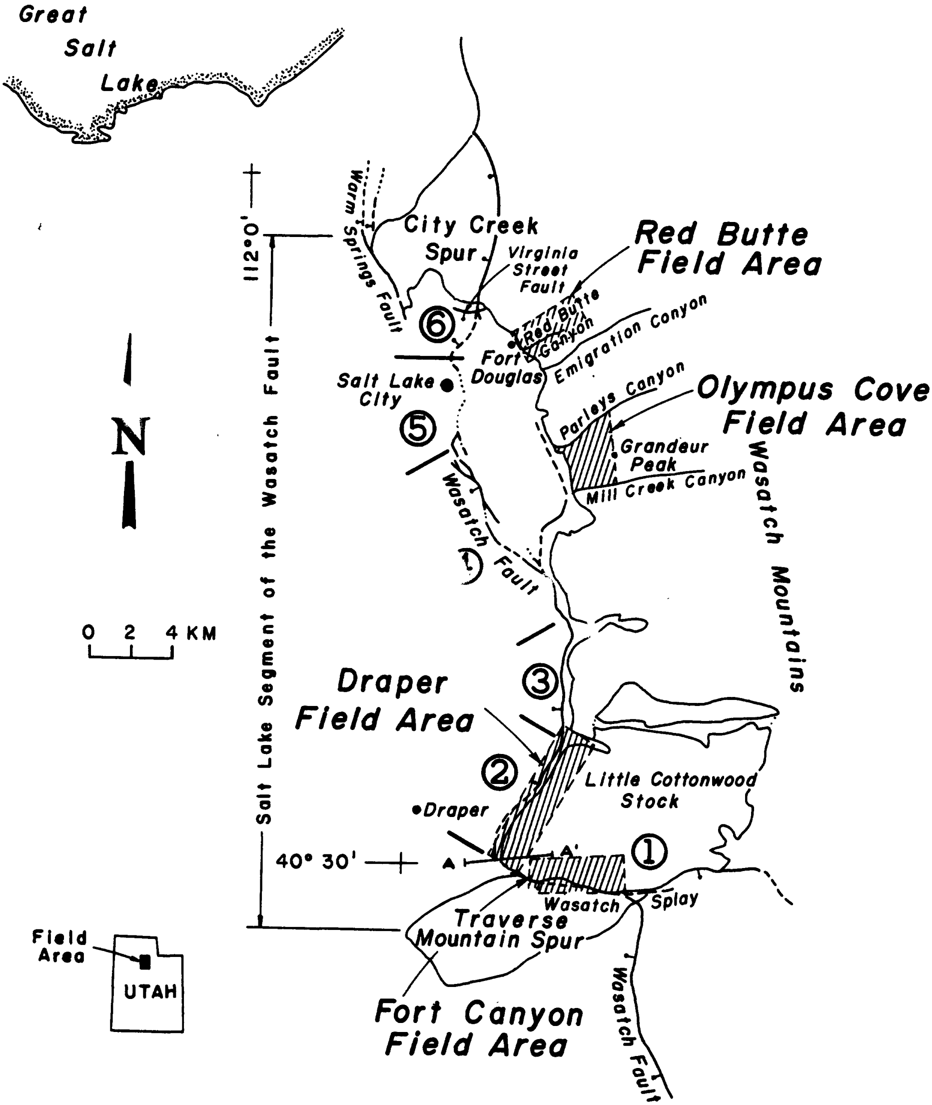

Figure 1: Tectonic map of the Salt Lake rupture segment, Wasatch normal fault zone, Utah. Structural domains for paleo-stress analysis indicated by cross hactures.

EXPLANATION

Tsv	Tertiary sedimentary and volcanic rock
J	Jurassic strata
Tr-J	Triassic-Jurassic strata
Tr	Triassic strata
Pu	Upper Paleozoic strata
Pl	Lower Paleozoic strata
P€s	Precambrian strata
P€m	Precambrian metamorphic rock
Tqm	Tertiary igneous intrusive

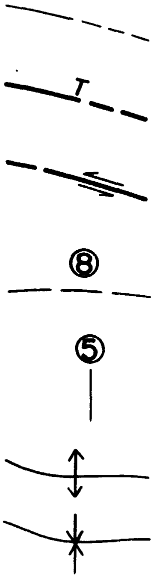

Lithologic contact, dashed in the subsurface

Thrust Fault, dashed in the subsurface

Normal Fault, dashed in the subsurface

Projection of barrier onto cross section

Projections of barrier (bend in Fault Zone) on cross section

Axial trace of anticline

Axial trace of syncline

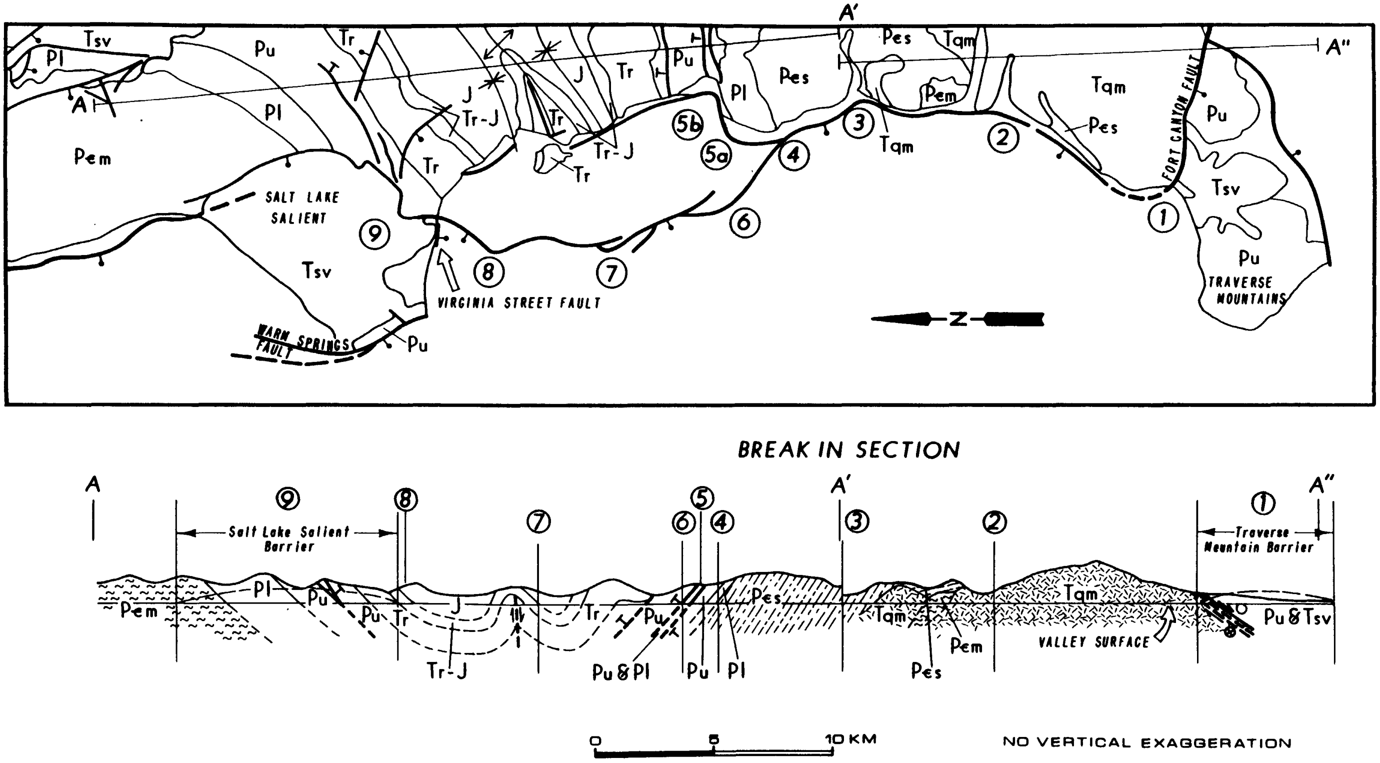

Figure 2: Geological map and cross section ofthe Wasatch front and Salt Lake rupture segment. Barriers in the fault zone are numbered and projected onto the footwall cross section. Geology from Davis (1983a,b) and Wasatch fault trace from Marsell (1969).

throw across the Wasatch fault zone varies along strike. Estimates from gravity modelling range from 2.6 to 4.0 km (Zoback, 1983). Throw across the fault zone may reach 11 km just south of Salt Lake City, Utah (Parry and Bruhn, 1984, 1986).

Schwartz and Coppersmith (1984) proposed that the Wasatch fault zone is divided into six structural segments defined by differences in the geometry of the fault trace, variations in footwall topography and earthquake rupture history. Individual segments have strike lengths of 35 to 70 km and their ends are marked by east-trending faults and basement ridges that subdivide basins in the hanging wall of the fault zone (Zoback, 1983; Schwartz and Coppersmith, 1984 Smith and Bruhn, 1984). Each segment has undergone multiple episodes of surface faulting during the Pleistocene and Holocene and is presumed capable of generating "characteristic" earthquakes of M = 7.0-7.5 based on fault displacements measured in trenches placed across Quaternary scarps. The recurrence interval of surface rupturing on individual segments is estimated to be as short as 4580 years with an average recurrence interval for characteristic earthquakes of 400 to 600 years for the entire Wasatch fault zone (Swan et al., 1980; Schwartz et al., 1983; Schwartz and Coppersmith, 1984).

The Wasatch fault zone is associated with a N-S zone of diffuse seismicity that generally does not show a strong spatial correlation with the Quaternary fault scarps (Arabasz et al., 1980; Zoback, 1983). Earthquake focal mechanisms, geodetic measurements and fault slip-vector data taken from Quaternary scarps indicate that regionally, the crust is extending in a west-southwest -- east-northeast direction, with an average orientation of the least principal stress (maximum extension axis) at 073° ±15° (Zoback, 1983).

STRUCTURE OF THE SALT LAKE SEGMENT

The Salt Lake segment of the Wasatch fault zone extends for 35 km from

Salt Lake salient on the north to Traverse Mountain spur on the south (Fig. 2; Gilbert, 1928; Schwartz and Coppersmith, 1984). The footwall of the Salt Lake segment is composed of Tertiary through Proterozoic sedimentary strata, Oligocene quartz monzonite and Precambrian schist and amphibolite. Mesozoic, Paleozoic and Precambrian strata generally strike eastward and are folded in the east-trending Uinta arch, a large anticlinorium that developed during the latest Cretaceous and earliest Tertiary (Crittenden, 1976). Quartz monzonite of the Little Cottonwood stock intruded Precambrian and Paleozoic rock along the southern part of the footwall during the Oligocene (Crittenden et al., 1973). The Wasatch fault cuts across these earlier structures at high angle to their strike.

The hanging wall of the Salt Lake segment contains a large Neogene basin with over a kilometer of sedimentary fill. The fill consists of Quarternary through Miocene strata and volcanics (Cook and Berg, 1961; Zoback, 1983). The hanging wall basin is structurally segmented by an east-trending basement step that separates the deeper southern part of the basin, which is about 1-1.5 km deep, from the northern section, where the thickness of the basin fill is generally less than 300 metres according to Zoback (1983).

The history of faulting on the Salt Lake segment is poorly constrained. Normal faulting post-dated intrusion of the Little Cottonwood stock, which was intruded 31.1 ± 0.9 m.y. ago (Crittenden et al., 1973). A muscovite concentrate from exhumed fault rock in the Wasatch fault zone along the southwestern margin of the stock was dated as 17.3 ± 0.7 m.y., and represents the age of the earliest observed, syntectonic hydrothermal alteration in the fault zone at that locale (Parry and Bruhn, 1986). Consequently, normal faulting in the Salt Lake segment began by latest Early Miocene. Relative uplift of the footwall at the southern end of the Salt Lake segment is about 11 km based on fluid pressure estimates from fluid inclusions trapped in cataclasite in the fault zone (Parry and Bruhn, 1984; Parry and Bruhn, 1986). A minimum estimate for throw at the northern end of the segment is 2.5 km based on the maximum topographic elevation of the footwall and an estimated 300 m of fill in the hanging wall basin (Zoback, 1983).

The Quaternary surface trace of the Salt Lake segment consists of several linear to curvilinear fault sections that vary in orientation and range in length from as little as 3 km to as much as 12 km (Fig. 2). These sections are separated by significant bends in the trace of the fault zone that define geometrical barriers. The bends are classified as either conservative or non-conservative barriers based on the criteria listed in Table 1. Several barriers can be readily identified, and of these, three are classified as non-conservative barriers; one at each end of the Salt Lake segment (#1 & 9; Table 1), and another, a composite barrier associated with a branch point in the fault trace located in the central part of the segment (#4, 5a and 5b).

The fundamental characteristics of a non-conservative barrier are that the slip directions on the adjacent sections of the primary fault zone are different in orientation or magnitude, or both, and that at least a third direction of faulting is required to accommodate displacement within the primary fault zone (King, 1983; King and Yielding, 1984). The direction of slip on a series of variably oriented fault sections will depend on the geometry of the sections, and the orientation and relative magnitudes of the principal stresses operating across the fault planes. We first consider the nature of the paleo- and contemporary stress fields in the Salt Lake segment, and then continue by discussing the geometrical characteristics of the individual fault sections and barriers. Finally, we speculate on the rupture characteristics of the Salt Lake segment.

PALEO-STRESS ANALYSIS

The orientation of the paleo-stress field in the Salt Lake segment was determined based on a stress tensor inversion analysis of mesoscopic

TABLE 1: BARRIER CLASSIFICATION

STRUCTURAL CHARACTERISTICS

B - BEND IN TRACE
BR - BRANCHING OF FAULT TRACE
OF - LATERAL OFFSET OF TWO PRIMARY RUPTURE TRACES
TF - THREE DIRECTIONS OF LARGE SCALE FAULTING
HB - HANGING WALL BREAKUP OR BASEMENT RIDGE
TH - ABRUPT DIFFERENCE IN PRIMARY FAULT THROW
ID - DIP INCOMPATIBLE WITH CONSERVATION OF SLIP ON ADJACENT FAULT SECTION
SE - DIFFUSE SEISMICITY

BARRIER *	STRUCTURAL CHARACTERISTICS	BARRIER TYPE
1	TF,HB,TH,SE, OF	NON-CONSERVATIVE
2	B	CONSERVATIVE
3	B	CONSERVATIVE
4*	BR,TF,HB	NON-CONSERVATIVE
5a*	B, ID	NON-CONSERVATIVE
5b*	B,TF(?),ID	NON-CONSERVATIVE
6	B	CONSERVATIVE (?)
7	B	CONSERVATIVE (?)
8	B	CONSERVATIVE (?)
9	TF,BR,HB,SE, OF	NON-CONSERVATIVE

*** this branch point and two bends considered as one composite, non-conservative barrier.**

fault populations in the Wasatch fault zone and adjacent parts of the footwall. Four structural domains were chosen for analysis (Fig. 1). Each domain was chosen because of excellent exposure and because of structural position within the fault segment. The Red Butte Canyon and Olympus Cove domains were located in Mesozoic and Paleozoic strata in the northern and central parts of the segment. The Draper and Fort Canyon domains were located in exhumed fault rock within the Wasatch fault zone on the western and southern margins of the Little Cottonwood stock. The latter two domains were chosen to provide information about paleo-stress orientations in the Traverse Mountain barrier at the southern end of the Salt Lake segment.

Faults within each domain form several sets that permeate the rock on the meter to centimeter scale (Fig. 3). The age of faulting is not well constrained. The Draper and Fort Canyon domains are located in a structural carapace of cataclastic and phyllonitic quartz monzonite that varies from a few meters to about a hundred meters in thickness. This fault rock formed at depth within the Wasatch fault zone beginning about 17 m.y. ago and continued to form during uplift of the footwall relative to the hanging wall of the fault zone (Parry and Bruhn, 1984; Parry and Bruhn, 1986).

Faults in Red Butte Canyon and Olympus Cove cut Mesozoic and Paleozoic strata in the footwall of the Wasatch fault zone (Figs. 1,2). They are part of a large population of normal to normal-oblique slip faults that occur in the footwall block and increase in number as the Holocene scarps of the Wasatch fault zone are approached. The Red Butte and Olympus Cove domains are both located about 2.5 km east of the youngest Holocene scarp system, but lie directly adjacent to an older system of Quaternary scarps along the Wasatch Mountain front (Fig. 1; Van Horn, 1972).

Slickenlines for fault populations from each domain are plotted in Figure 3 and, with the exception of the Fort Canyon domain, the slickenlines generally form two or more maxima. In the Fort Canyon domain the

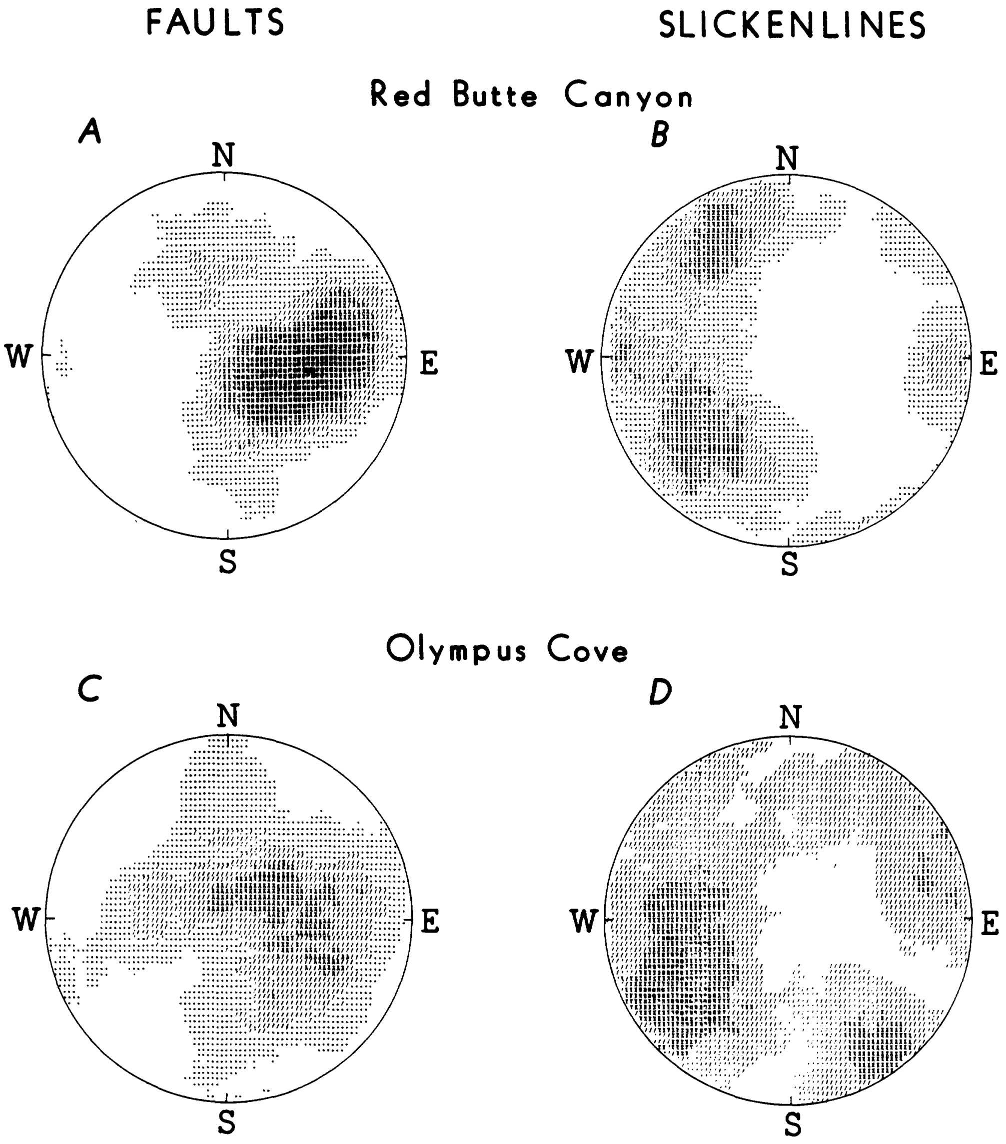
FAULTS
SLICKENLINES
Red Butte Canyon
A
B
Olympus Cove
C
D
N
S
E
W

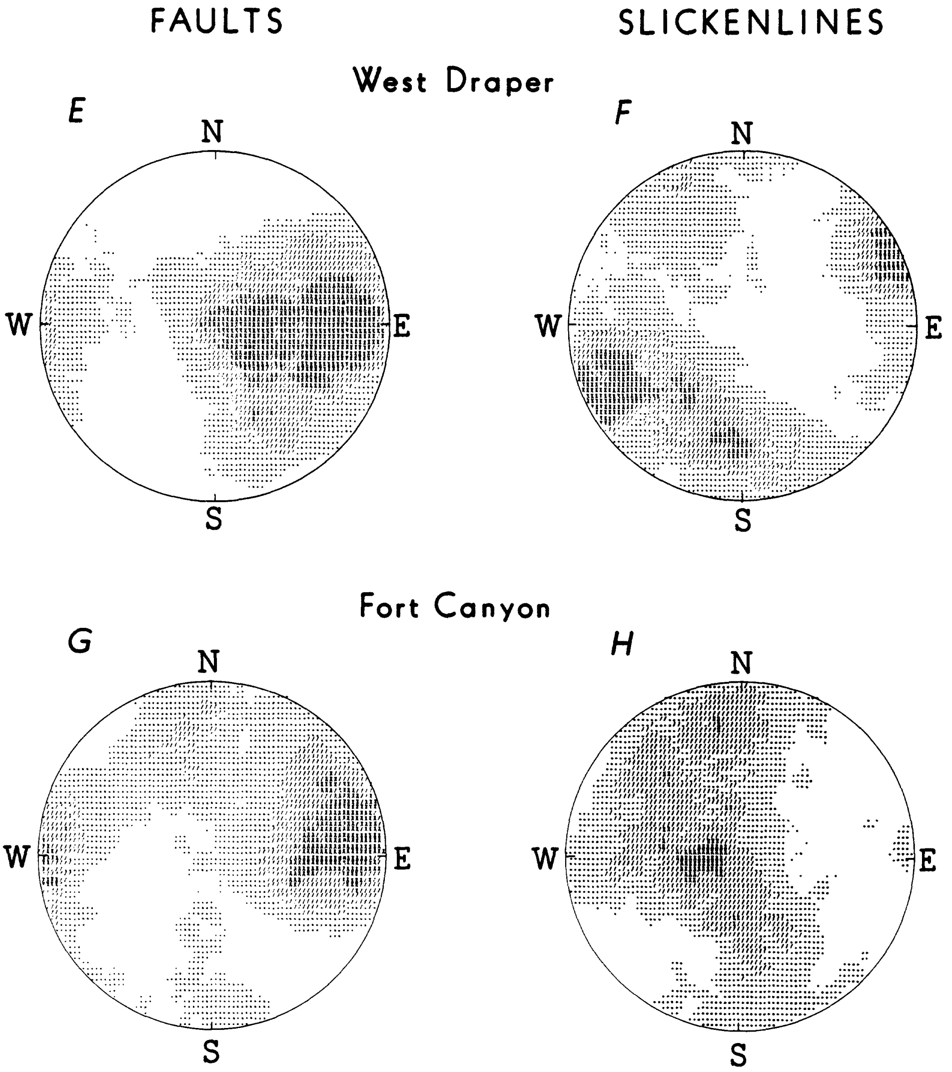

Figure 3: Contoured orientations of poles to fault planes and slickenlines for fault populations in each domain of Figure 1. Red Butte Canyon - 129 measurements of faults (A) and slickenlines (B); Olympus Cove - 105 measurements, faults (C) and slickenlines (D); West Draper - 110 measurements, faults (E) and slickenlines (F); Fort Canyon - 106 measurements, faults (G) and slickenlines (H). Contour intervals are 0,2,4,6 and 8 standard deviations above a random distribution plotted on lower hemisphere, equal area projections.

slickenlines form a broad partial girdle in the stereoplot, indicating a diffuse spatial distribution of slip directions. The dominant spatial concentrations in the other domains trend between 230° and 250°, with subsidiary maxima plunging at moderate angles into either the northern or southern quadrants. The fault populations are composed of a mixture of fault types, with slip varying from purely normal, through oblique-slip to almost pure strike-slip motion on faults of various orientations.

Slip directions on bedrock fault surfaces, against which Quaternary gravels were faulted, were reported by Pavlis and Smith (1980) from two faults exposed at the northern end of the segment, in the Salt Lake salient (Fig. 2). Exposures of the Warm Springs fault, which strikes N45°W and dips 70°W contained two sets of slickenlines. The older set trended 288° and the younger 239°. The Virginian Street fault located a few kilometers to the southeast, strikes N80°E and dips 68°S. Slickenlines on this fault formed two maxima plunging towards the west-southwest. The average trend of the northern maximum was 255° and that of the southern was 233°. The relative age of the two slickenline sets on the Virginia Street fault could not be determined from field observations.

The slip directions determined by Pavlis and Smith (1979) for Quaternary faulting at the northernmost end of the Salt Lake segment are consistent with the slip directions of the most prominent slickenline maxima from the paleo-fault populations in the Red Butte Canyon, Olympus Cove and West Draper domains. This observation does not imply that all of the paleo-fault populations are Quaternary in age, but rather, raises the contention that extension across the Salt Lake segment may have been oriented consistently toward the west-southwest over an extended period of time. The oldest set of slickenlines on the Warm Springs fault provides an exception, in that this set trends about 20° north of west, while the prominent maxima in the paleo-fault populations trend south of west. However, the remainder of the Quaternary slickenline sets lie within the general trend of the prominent set in each of the paleo-fault population domains.

The paleo-stress directions in each domain were determined using a linear stress tensor inversion method like that discussed by Michael (1984). This technique provides an estimate of the trend and plunge of the paleo-principal deviatoric stresses (S1 ≥ S2 ≥ S3) and the stress parameter ϕ = (S2 - S3)/S1 - S3) for a population of faults. The data input into the inversion routine include the orientation of each fault and the fault's slip direction and sense of slip. The following assumptions are required to generate a system of linear equations for solution. 1) The paleo-stress tensor remained constant in orientation and magnitude during the deformation event. 2) Slip on an individual fault plane was parallel to the maximum resolved shear stress vector ($\tilde{\tau}$), which paralleled the slickenline directions. 3) Each fault slipped when $\tilde{\tau}$ reached a specific magnitude, which was assumed constant for each fault in the population. These assumptions allow construction of a system of linear equations of form

$$\hat{\tau}i = \overset{\approx}{S}\,\hat{n}i - ((\overset{\approx}{S}\,\hat{n}i) \cdot \hat{n}i) \cdot \hat{n}i$$

where $\hat{\tau}i$ = unit shear stress vector parallel to $\tilde{\tau}$ on fault "i", $\overset{\approx}{S}$ = normalized deviatoric paleo-stress tensor and $\hat{n}i$ = unit normal vector to the ith fault plane. This set of "i" linear equations is then solved for S using a singular value decomposition procedure described by Lawson and Hanson (subroutine SVA, 1974). The normalized principal deviatoric stresses (S1 ≥ S2 ≥ S3) and their orientations are then found as the eigenvalues and eigenvectors of $\overset{\approx}{S}$. The procedure is discussed in

The principal stress directions determined for each domain indicate that the maximum principal stress (S1) dipped steeply and that the least principal stress (S3) plunged gently and trended east-northeast (Fig. 4; Table 2). The preferred trend of S3 between the four domains varied only 11°, and the average for the set of measurements was 050° ± 5°. ϕ values for the domains varied from a high of 0.54 in Red Butte Canyon to a low of 0.21 at Fort Canyon (Table 2).

TABLE2: PRINCIPAL STRESS DATA

FIELD DOMAIN	S-1	S 2	S 3	ϕ^*	# OF FAULTS
A. Red Butte	095°/83°	324°/07°	054°/00°	0.54	130
B. Olympus Cove	180°/82°	314°/06°	044°/07°	0.50	105
C. Draper	113°/77°	317°/12°	227°/04°	0.42	110
D. Fort Canyon	301°/66°	146°/21°	056°/10°	0.21	106

$$^*\phi = \frac{S_2 - S_3}{S_1 - S_3}$$

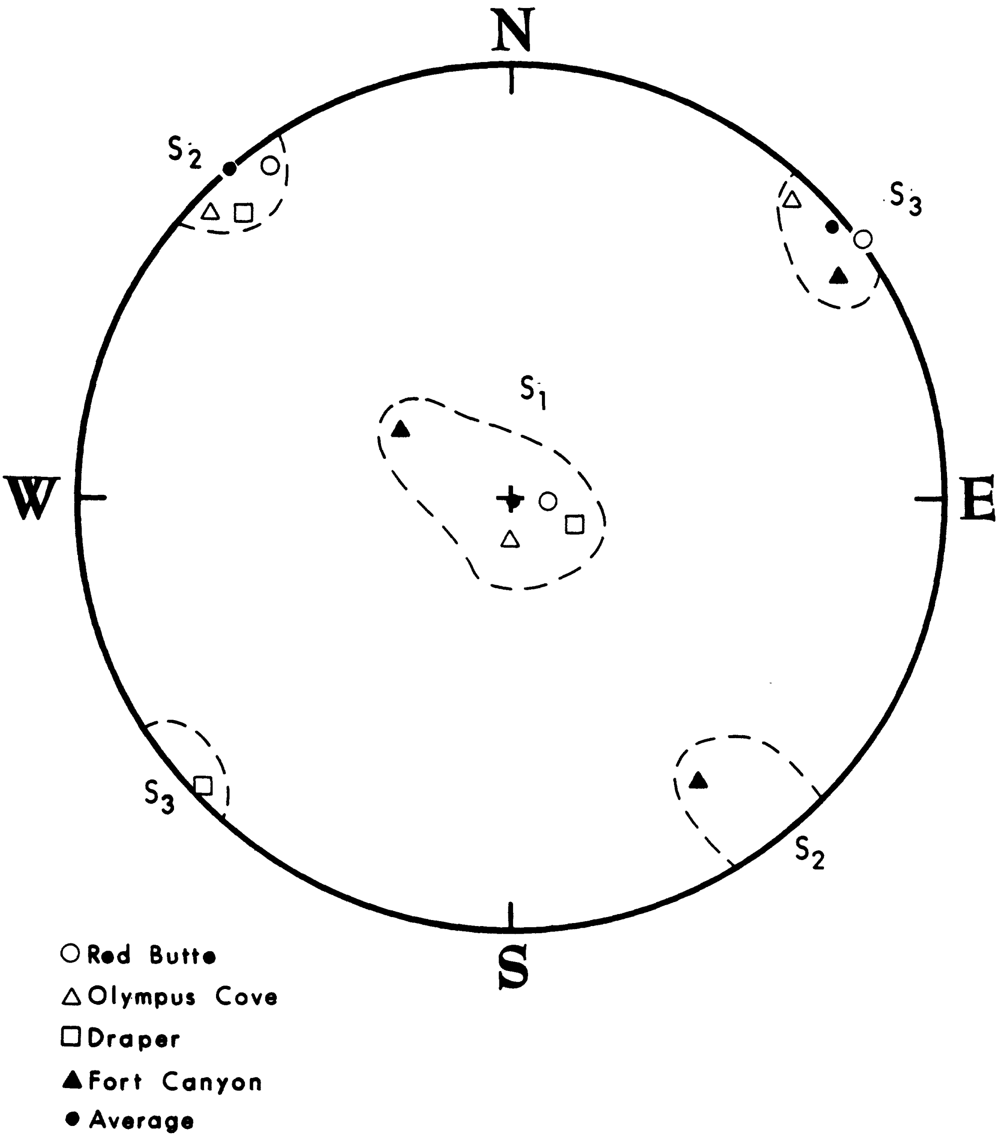

Figure 4: Paleo-principal deviatoric stress orientations from each of four domains in Figure 1 based on inversion of fault plane and slickenline data. S1 - maximum principal compressive stress, S2 - intermediate principal stress, S3 - least prinicpal stress. Trend and plunge of each stress axis are recorded in Table 2.

The solutions for the paleo-principal deviatoric stress directions and relative magnitudes must be considered as an approximation to the true characteristics of the stress tensor because of assumptions concerning the temporal and mechanical characteristics of faulting and potential errors in field measurement. The assumption that faults within the population slipped at the same resolved shear stress is a fundamental mechanical constraint on fault behavior that may not be justified, particularly in a volume of rock occupied by numerous, intersecting, and potentially interlocking faults. However, Michael (1984) compared the results of the linear inversion technique with the non-linear inversion method of Angelier (1979) and Angelier and others (1982) and found the results to be similar. The non-linear inversion method does not require the assumption of equal shear strength on each fault plane in the population.

Potential measurement errors include the following: 1) Inadvertently including faults of several different deformational events in the fault population. This was a potential problem, particularly in the Red Butte Canyon and Olympus Cove domains, where Mesozoic and Paleozoic strata were deformed in folds and thrust sheets during the Mesozoic and Early Tertiary. However, measurements were confined to faults within zones of extensive north-south trending normal faulting adjacent to the Wasatch fault zone. This sampling problem was considered less serious for the southern domains, which were located in the Little Cottonwood stock. There, the mesoscopic faults slipped either during or subsequent to the high temperature hydrothermal alteration event dated at 17.3 ± 0.7 m.y. ago (Parry and Bruhn, 1986). Consequently, faults in these latter two domains must reflect movement in the Wasatch fault zone, although the history of faulting could be protracted, and there is no a priori reason to assume that the stress tensor remained constant in either magnitude or orientation. 2) Random errors in fault plane and slickenline orientation may have been introduced as the result of field measurement. Our measurements were reproducable to within ± 5°, and such errors should not affect the results of the analysis because of their random nature, which would cancel out this effect in the inversion routine. 3) The stress tensor was implicitly assumed to be constant in direction and magnitude throughout the volume of rock occupying a domain. This assumption was verified in a subjective manner only, by noting that faults formed consistently oriented sets with consistent slip directions throughout the domain as the measurements were made in the field.

The results of the inversion analysis appear reasonable based on several independent lines of evidence. First, the steeply dipping S1 attitude is to be expected in the vicinity of a normal fault zone, and the attitude of the least principal stress (S3), which trends to the west-southwest is consistent with the trend of the prominent slickenline maxima in each domain except Fort Canyon, where no strong maxima occur in the slickenline orientation data. The trend of S3 is also consistent with the Quaternary slip directions determined by Pavlis and Smith (1979) on the Warm Spring and Virginia Street faults in the northern end of the Salt Lake segment. Finally, notice that the paleo-stress orientations are very similar in each of the four domains even though the fault populations vary considerably in their overall geometrical characteristics, and are located in rocks of different ages and lithologies. Qualitatively, the mixture of normal, oblique and strike slip faults in the populations from each domain are consistent with $\phi > 0$, which supports the results of the inversion analysis. If $\phi = 0$, then S2 = S3 (Table 3) and the slickenlines should plunge down dip on all faults within the population, given a nearly vertical S1. This is clearly not the case in each of the domains. However, other than this qualitative evaluation based on the geometrical characteristics of fault populations, we have no independent means of quantatively evaluating the accuracy of ϕ as determined in the paleo-stress inversion analysis.

The average paleo-S3 trend determined from the stress tensor inversion of fault populations is about 23° north (clockwise) of the regional, contemporary S3 orientation of 073° ± 15° determined for the entire Wasatch Front region by Zoback (1983) based on her analysis of earthquake focal mechanisms, geodetic measurements, insitu stress measurements and Quaternary fault surfaces. The ϕ -value for the contemporary stresses is near zero according to Zoback (1985) based on stress magnitudes and directions determined from hydrofracture stress tests and well bore breakouts in areas south of the Salt Lake segment, in the region surrounding the three southernmost rupture segments defined by Schwartz and Coppersmith (1984). Alternatively, Arabasz (1985) and Arabasz and Julander, in press) concluded that ϕ is close to 1 based on their analysis of earthquake focal mechanisms and hydrofracture tests from the southernmost segment of the Wasatch fault zone and the adjacent Basin-Range - Colorado Plateau Province transition zone. Consequently, the contemporary ϕ - parameter of the regional stress field remains controversial and poorly defined.

FAULT ZONE STRUCTURE

Traverse Mountain Barrier: A complex zone of faulting forms a non-conservative barrier at the southern end of the Salt Lake fault segment, that we have informally named Traverse Mountain barrier (Barrier #1, Table 1). The Traverse Mountains are located at the intersection of the Provo and Salt Lake rupture segments as defined by Schwartz and Coppersmith (1984). Here we consider only the northern part of the Traverse Mountains structure. Further work is required to establish the structural relations between the Traverse Mountains and the Ogden segment. This barrier is composed of three primary fault sections that form a triple junction comprised of the southern end of the Salt Lake segment, the Fort Canyon section of the Wasatch fault zone, and the west-southwest trending fault zone along the northern edge of the Traverse Mountains (Fig. 5). The southern end of the Salt Lake segment is marked by a major jog in the trace of the Wasatch fault zone, where the

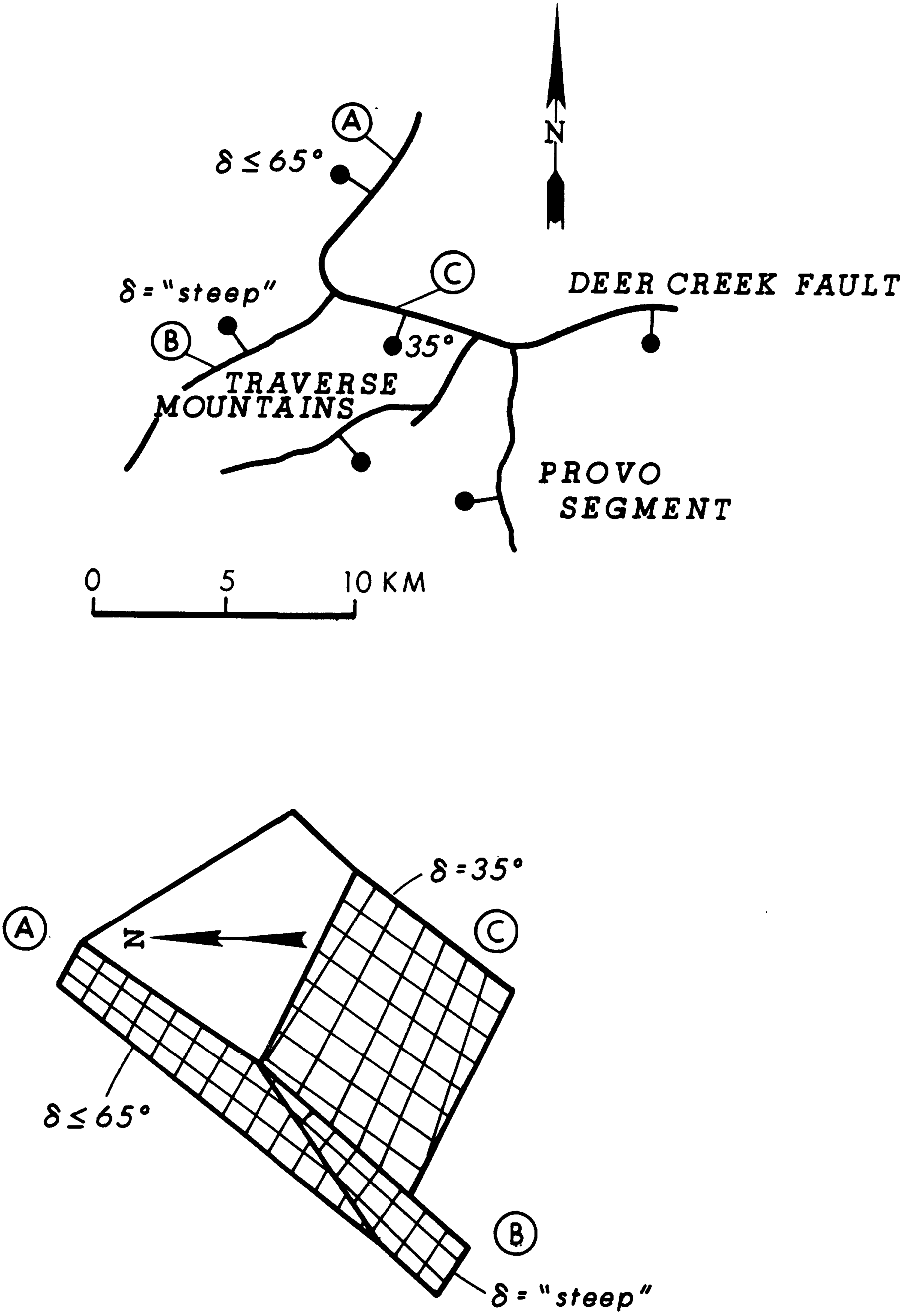

Figure 5: Geometry of faulting at Traverse Mountain barrier (top) and block diagram of tripartite fault array (bottom). Fault A = Draper fault section, B = Fort Canyon fault section, C = Traverse Mountain fault section. δ = fault dip angle. Ball on hanging wall of normal-oblique slip faults.

Salt Lake and Provo segments are offset about 7.5 km and connected by an east-trending fault zone along the southern margins of the Little Cottonwood igneous stock. We informally refer to this east-trending section of the Wasatch fault zone as the Fort Canyon fault. The Fort Canyon fault zone lies along the westward projection of the Deer Creek normal fault, which is located in the footwall of the Wasatch fault zone and can be traced eastward through the Wasatch Mountains for a distance of at least 20 km (Baker and Crittenden, 19 61). The eastern part of the Traverse Mountains are in the hanging wall of the southward dipping Fort Canyon fault section, while the western part of the mountains form the footwall of a north-dipping, west-southwest trending normal fault zone at the southern end of Jordan Valley, informally named the Traverse Mountain fault section (Fig. 5).

The southern part of the Salt Lake segment (Draper Fault Section) can be traced as a series of south-southwest trending scarps that strike 035° in unconsolidated deposits (Gilbert, 1928). These scarps project southward into the exhumed bedrock fault zone along the western edge of the Little Cottonwood quartz monzonite stock. Here the fault zone curves southward to join the east-trending Fort Canyon normal fault section along the southern margins of the stock and intersects the southwest striking Traverse Mountains fault.

The exhumed, bedrock fault zone consists of a cataclastic carapace of faulted quartz monzonite that extends along the western and southern edges of the Little Cottonwood stock (Fig. 6; Gilbert, 1928; Bullock, 1954). The carapace varies in thickness from several tens of meters to hundreds of meters. Progressive uplift of the footwall relative to the hanging wall resulted in overprinting of higher temperature-pressure alteration mineral assemblages by lower temperature-pressure assemblages during faulting (Parry and Bruhn, 1984; 1986). The oldest , and highest temperature alteration mineral assemblage in the faulted carapace consists of chlorite, epidote and muscovite, which occur in relict patches of

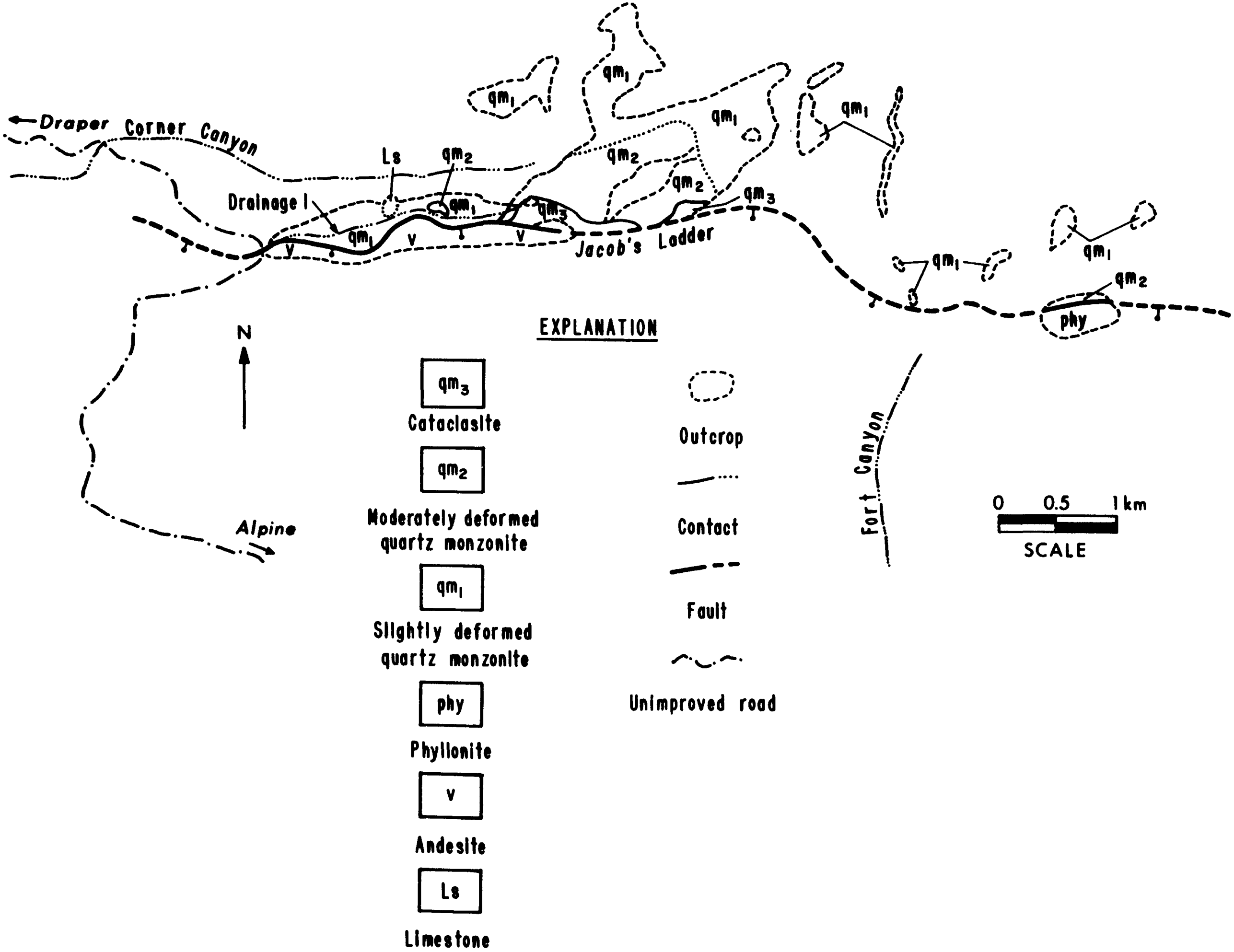

Figure 6: Geological map of the Fort Canyon fault zone in the Fort Canyon structural domain indicated on Figure 1.

phyllonite and younger, more broadly distributed cataclasite. Fluid inclusions trapped in microcracks within deformed quartz grains in the cataclasite yield paleo-fluid temperatures as high as 350°C and pressures up to 280 MPa, indicating that this faulted rock originated at depths ≥ 11 km in the crust in a fault zone where transient fluid pressures were nearly lithostatic (Parry and Bruhn, 1984; 1986). This high temperature alteration formed in the cataclasite about 17 m.y. ago based on a K/Ar date on hydrothermal muscovite from the fault zone (Parry and Bruhn, 1986). The high temperature mineral alteration assemblage was subsequently faulted and overprinted by a younger, lower temperature laumontite-prehnite assemblage that is also faulted, suggesting that fluid temperature and pressure decreased during progressive uplift and exhumation of the footwall.

The attitude of the Fort Canyon fault section has been determined by detailed mapping of the fault zone along the southern margins of the Little Cottonwood stock. Here, Oligocene volcanics and Paleozoic strata in the hangingwall are faulted directly against the cataclastic carapace on the margin of the igneous stock, where the fault zone dips 30° to 40° southward (Fig. 6). Direct measurement of the dip of the cataclastic carapace in the footwall can be made in Fort Canyon, where there is an abrupt transition from essentially undeformed quartz monzonite in the interior of the Little Cottonwood stock into overlying phyllonite and cataclasite in the fault zone. Here, we measured the dip as 30° to 35° south and Gilbert (1928) estimated the dip as 29°. We will use a strike of N80°W and dip of 35° south as a best estimate for the attitude of the Fort Canyon fault section based on the mapping and direct field measurements.

The paleo-slip direction on the Fort Canyon fault section has been estimated using the results of the paleo-stress tensor analysis on mesoscopic faults within the cataclastic carapace on the southern margin of the Little Cottonwood stock (Fort Canyon Domain, Table 2). The slip direction on the fault zone was assumed to coincide with the trace of the maximum resolved shear stress vector in the plane of the fault zone (Angelier, 1979). This trace is the projection of the total stress vector ($\tilde{S}$) onto the fault plane, and the orientation of this trace is uniquely determined by the orientation of the fault, the directions of the principal stresses and the stress parameter (ϕ) (Angelier, 1979). Knowledge of the actual magnitudes of the principal stresses is not required. The range of possible paleo-slip vectors in the plane of the fault zone was determined graphically on a steronet using a construction proposed by Angelier (1979). If $\phi = 0$ then S2 = S3 and the slip direction is defined by the projected trace of S1 on the fault plane. Conversely, if $\phi = 1$ then S1 = S2 and the predicted slip direction coincides with the trace of S3 on the fault plane. Slip directions for $0 < \phi < 1$ lie in the plane of the fault zone between these two slip directions (Fig. 7). The slip direction limits estimated for the Fort Canyon fault zone are 24°/238° for $\phi = 0$ to 18°/252° for $\phi = 1$. The paleo-stress tensor inversion estimated $\phi \approx 0.2$, which defines the preferred estimate for the slip direction as 22°/242°. This slip direction requires dextral-normal movement on the Fort Canyon fault zone.

Structural fabrics of relic phyllonite preserved in the fault zone are also consistent with a component of dextral slip. These fabrics pre-date the cataclastic deformation (Parry and Bruhn, 1986) that resulted in development of the mesoscopic fault populations used in the stress tensor inversion analysis. The oldest fault rock preserved in the faulted carapace in Fort Canyon consists of the isolated outcrops of phyllonite which contain a penetrative foliation and, in some locales, an extension lineation. Locally these rocks also contain a mesoscopic, shear band fabric (S-C bands, Simpson and Schmidt, 1983) in which the primary foliation is deflected into planar, mm-wide zones of intensive shearing. The sense of slip on these S-C bands as measured in outcrop is consistent with dextral normal movement on the fault zone with the slip directions plunging 20°-30° to 210°-230° (Parry and Bruhn, 1986). Slip directions

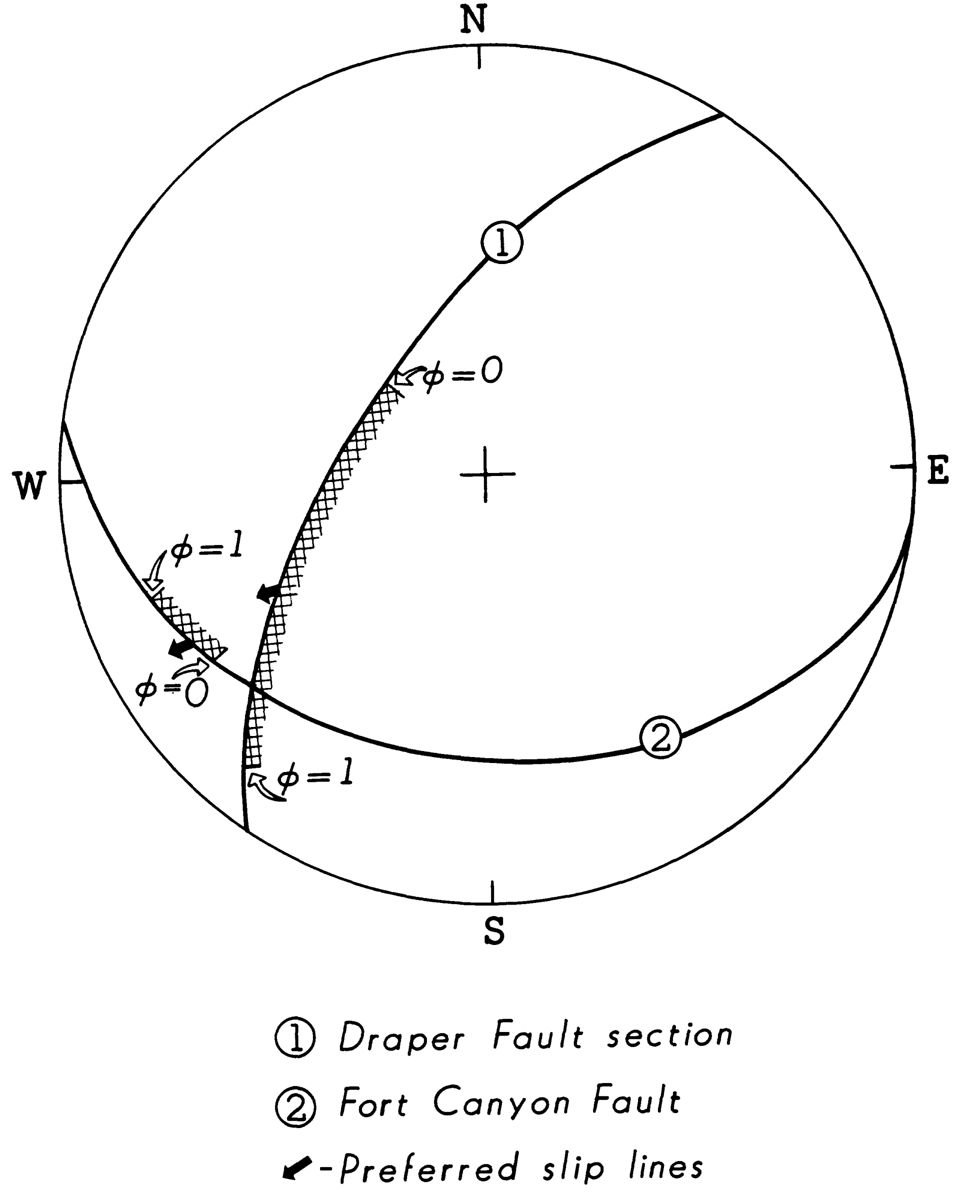

Figure 7: Stereo-projection showing orientation of Fort Canyon fault, preferred orientation of Draper fault section at southern end of Salt Lake segment and slip directions for various ϕ- values of paleostress field Preferred slip direction on Draper section is 240° on a fault plane dipping about 65° to the northwest. Lower hemisphere, equal area projection. See Figure 5 for a geometrical model of these faults in Traverse Mountain barrier

determined from S-C bands and asymmetric augen in oriented thin sections from the phyllonite also indicate dextral to dextral-normal movement in the fault zone (Houghton, 1986).

The southernmost section (Draper section) of the Salt Lake segment of the Wasatch fault zone is marked by a discontinuous series of scarps in Quaternary deposits that strike 035° for a distance of about 7 km along the western edge of Little Cottonwood stock. The fault zone is not exposed in bedrock in this area, although numerous, discrete normal faults occur in the margins of the stock and presumably represent subsidiary normal faulting associated with the Wasatch fault zone. We have attempted to constrain possible dip angles for this section of the fault zone based on the geometry of faulting within the Traverse Mountain barrier. The approach is based on finding possible slip directions on the Draper section that are consistent with slip directions on the other two primary fault zones in the barrier - namely, the Fort Canyon fault zone and the north-dipping Traverse Mountain fault zone that extends in the subsurface of Jordan Valley along the northwestern edge of the Traverse Mountains. The paleo-slip direction on the Fort Canyon fault zone has been estimated as about 22°/242°. We have no data bearing on the slip direction on the fault bounding the northern edge of the Traverse Mountains other than the strike of the fault zone, which is ~N60E (240°) and drill data and gravity modelling indicating that the fault zone dips steeply northward, with a minimum throw of about 1 km (Cook and Berg, 1961; Zoback, 1983). This latter evidence indicates that the fault zone has a normal component of slip, requiring an unknown component of extension perpendicular to its strike. This observation, taken in conjunction with the slip direction across the Fort Canyon fault zone is sufficient to constrain a maximum probable dip on the Draper section of the Wasatch fault zone.

The primary faults in Traverse Mountain barrier form a tripartite fault array. We do not have complete information concerning the magnitudes of the three slip vectors, but we do know the slip direction on the Fort Canyon section and require that the slip direction across the northern Traverse Mountain fault zone have a normal component of movement. This latter criterion constrains the slip direction on the Draper fault section in that the resultant slip vector between the Fort Canyon and Draper fault sections cannot cause convergence across the Traverse Mountain fault. Consequently, we seek acceptable solutions for slip directions on the Draper fault section by assuming various dip angles and applying the paleo-principal stress orientations and $\phi \approx 0.4$ determined from stress tensor inversion of the mesoscopic fault populations at the southern most end of the Draper section.

This approach is shown graphically in Figure 7. The maximum dip angle (δ) on the Draper fault section that meets the criterion for extension across the fault zone along the northern edge of the Traverse Mountains is δ=65°. In this case, the difference vector between the Fort Canyon and Draper fault sections is parallel to the trend of the Traverse Mountain fault zone. Lesser dip angles on the Draper section are also satisfactory, in that the difference vector across Traverse Mountain fault zone requires extension. Steeper dips on the Draper fault section require convergence across the northern edge of Traverse Mountains, and are therefore unacceptable solutions to the slip direction analysis. Further refinement of the dip estimate of the Draper fault section would require more information on the dip angle and slip vector in the fault zone along the northern edge of Traverse Mountains.

The structural model for Traverse Mountains barrier consists of a triple junction formed by a tripartite array of primary fault zones (Fig. 5). The northern arm, consisting of the Draper fault section dips ≈ 65° or less toward the west-northwest, the eastern arm, comprised of the Fort Canyon fault sections dips ≈ 35° south and the third, western arm dips steeply northward. The difference in slip between the Draper and Fort Canyon fault sections is presumably accommodated by sinistral-normal faulting on this latter, third arm of the triple junction. The barrier must plunge towards the southwest into the crust, presumably paralleling the intersection line between the Draper and Fort Canyon fault sections. This line plunges ≈ 28° to 230°, subparallel to the strike (240°) of the third arm of the triple junction. This structure is clearly a non-conservative barrier, representing a likely site for the arrest and/or initiation of seismic ruptures within the Wasatch normal fault zone.

Southern Fault Sections: The surface trace of the Wasatch fault zone consists of three rectilinear sections between Traverse Mountain barrier (#1) and the bifurcation of the fault trace at branch point #4 (Fig. 2). These rectilinear sections are separated by two bends (#2 & 3, Fig. 2) that mark significant changes in the strike of the fault zone. These bends are classified as conservative barriers because there is no apparent developmment of a major third direction of faulting in either the hanging or footwalls of the fault zone in the regions of the bends. This implies that the slip direction on the Draper fault section parallels that on the two sections to the north, and that the fault zone in this area can be modelled as a cylindrical surface. Consequently, one can use the dip estimate and slip direction (≈240° trend) on the Draper fault section to model the dip of these two adjacent sections. The requirement is that the intersection lines between the fault sections parallel the plunge and trends of the slip vector in the Draper fault section. This problem can be solved on a stereonet using a geometrical construction and results in an estimated dip angle of 55° for the fault section between barriers #2 and #3 and 45° for the section between barriers #3 and #4 (Fig. 8). These solutions are directly dependent on our estimate of the dip of the Draper fault section. If the 65° dip estimate in this section is too great, then the remaining sections would have more gentle dips, conversely, if the estimate for the Draper section is too low, the other sections would dip more steeply. A similar type of error would be introduced by the estimated slip direction in the Draper fault section, in that too shallow a

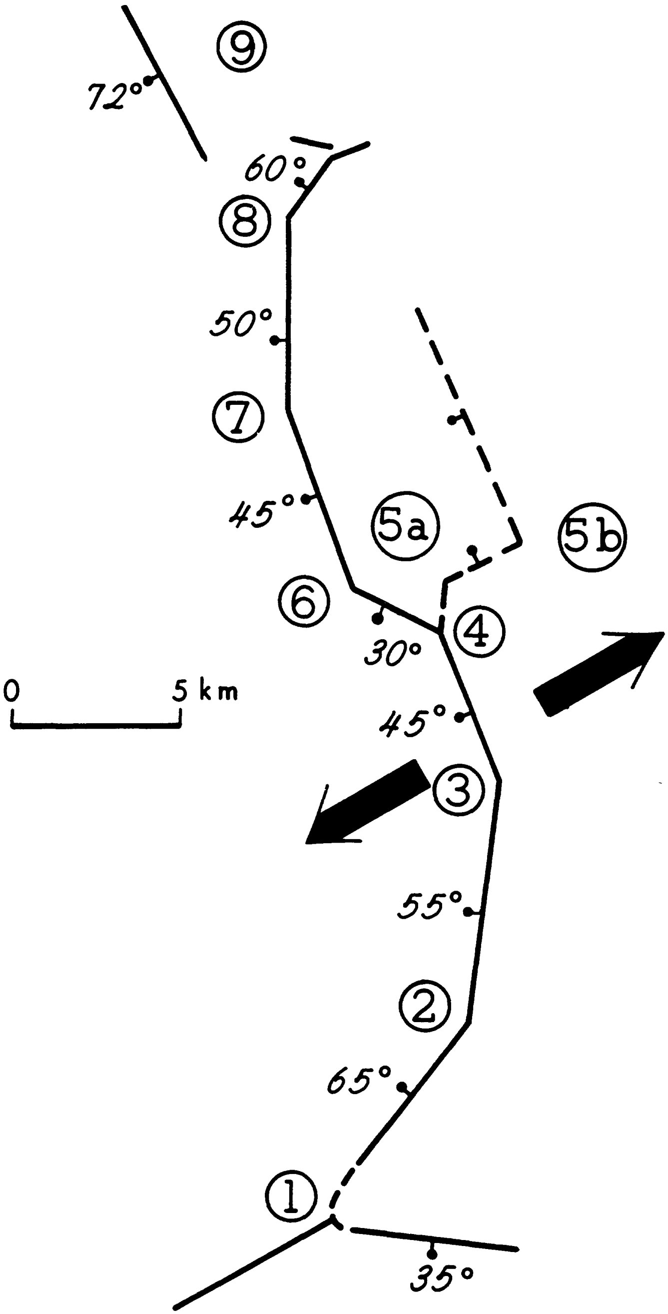

Figure 8: Map of surface fault traces in the Salt Lake segment with preferred dip angles based on geometrical modelling. Numbers of barriers the same as those in Figure 2 and Table 1. See text for discussion.

plunge would result in underestimating the dip angle of the adjacent fault sections and too steep a plunge would cause an overestimation of the fault dip angles.

An unreversed seismic refraction/reflection profile across the fault zone in the section between barriers *2 and *3 by Bashore and others (1981) provides an independent check on our fault zone modeling in this area. The fault zone was modelled using two-dimensional synthetic seismograms and gravity data as dipping about 60° west near the surface and decreasing in dip to between 40° and 50° at a depth of 4-5 km. Their result is generally consistent with the 55° westward dip in our model, which is based on a totally different approach and set of data than used by Bashore et al. (1981).

Northern Fault Sections: The geometry of the northern half of the Salt Lake fault segment is different than the southern part, where the fault zone is delineated by a narrow zone of surface scarps along the Wasatch mountain front. The northern part of the segment, in contrast to the southern part, is characteried by a major bifurcation of the Quaternary fault trace into a zone about 12 km long by 6 km wide (Fig. 2; Marsell, 1969; Van Horn, 1972) beginning at branch point *4 . This zone extends northward, terminating in the Salt Lake salient, a bedrock ridge that separates the proposed Ogden rupture segment to the north from the Salt Lake segment to the south (Schwartz and Coppersmith, 1984). Two zones of surface scarps delineate an eastern branch extending along the mountain front for 10 km north of the branch point, and a western branch that extends about 15 km northward until it curves abruptly eastward and intersects the mountain front at the southern end of the Salt Lake salient (bend *8). Each of these branches is composed of discontinuous, mostly linear zones of surface scarps separated by bends in the fault zone trace (Figs. 2, 8).

According to Van Horn (1972) surface scarps in the eastern branch are older than most of those in the western branch. The eastern scarps presumably formed between 5000 and 3 million years ago, while most scarps in the western branch formed during the last 5000 years. Greater activity on the western branch of the fault is also indicated by the distribution of Quaternary sediments, which thicken abruptly westward across the western branch of the fault zone while the area in between the two branches is underlain by only a thin veneer of Quaternary deposits overlying bedrock (Marsell, 1969; Crone and Harding, 1985).

The zone of bifurcation in the fault zone between branch point (#4) and bends #6 and #5b apparently represents a non-conservative barrier. There are two lines of evidence for this conclusion. First, this region lies along a major east-northeast trending basement ridge beneath Jordan Valley (Cook and Berg, 1961; Zoback, 1983). This ridge separates Jordan graben into a deeper southern part and more shallow northern half according to the gravity modelling of Zoback (1983). Presumably, this ridge reflects structural accommodation of the hanging wall to changes in slip vector direction and/or magnitude in the vicinity of branch point #4. Secondly, the fault section between bends 5a and 5b dips steeply northward and trends between 240°-245°, sub-parallel to the 240° average slip vector for the Salt Lake segment as a whole. A north-dipping fault section with this strike cannot link with the fault section immediately to the south and conserve a slip vector orientation of 240° around bend 5a. Consequently, bend 5a must be a non-conservative barrier.

The dips of the fault sections between branch point #4 and bend #9 along the western branch of surface faulting have been estimated by assuming that each of these bends represent conservative barriers. The only support for this assumption is that no major structures have been inferred from the gravity data in Jordan Valley between the basement ridge near branchpoint #4 and Salt Lake salient barrier (Cook and Berg, 1961; Zoback, 1983). The preferred dip of the north-trending section between bends #7 and #8 was first found by assuming a slip vector trending 240° and using the paleo-stress data from the Red Butte domain, where $\phi = 0.5$. The solution for the preferred fault plane dip is shown in the stereoplot of Figure 9 where the orientation of the maximum shear stress vector for this paleo-stress system is plotted as a series of three curves for $\phi = 0$.. 0.5 and 1.0 on faults dipping between 20° and 80° westward. Notice that the 240° slip line does not intersect the $\phi = 0.5$ shear stress vector curve, but lies a few degrees to the north of it at the closest point of approach. A fault plane dipping 50° west lies closest to this maximum resolved shear stress vector, and therefore, $\delta = 50°$ is the preferred dip estimate for the north-dipping fault section. The dip angles of the remaining fault sections in the western branch of surface rupturing were then found assuming a cylindrical fault zone surface. These angles vary between 45° and 75° , as shown on Figure 8.

Salt Lake Salient: The Salt Lake salient is a ridge of Tertiary and Paleozoic bedrock that extends west of the Wasatch Mountain front at the northern end of the Salt Lake rupture segment (Gilbert, 1928; Schwartz and Coppersmith, 1984). A large, west dipping normal fault with a total throw of about 1.5 km forms the eastern boundary of the salient, where Tertiary strata are faulted against Precambrian metamorphic and Paleozoic sedimentary rock in the footwall (Fig. 2; Gilbert, 1928). The western boundary of the salient is formed by the Warm Springs fault, a north-trending normal fault that dips ≈70° west (Gilbert, 1928). Quaternary strata in the hanging wall are faulted directly against Paleozoic rocks in the footwall of the normal fault. We have not mapped the intermal structure of the salient in this study, but 1:24000 scale mapping by Van Horn (1981) shows a number of north-northwest and northeast trending normal faults that post-date Oligocene deposits and were probably formed during the Late Tertiary.

The geometry of linkage between the main rupture zones in the Salt Lake segment and faults in the interior of the Salt Lake salient is not clear. Surface scarps at the southern margin of the salient are discontinuous, but apparently extend into the large normal fault along the eastern boundary of

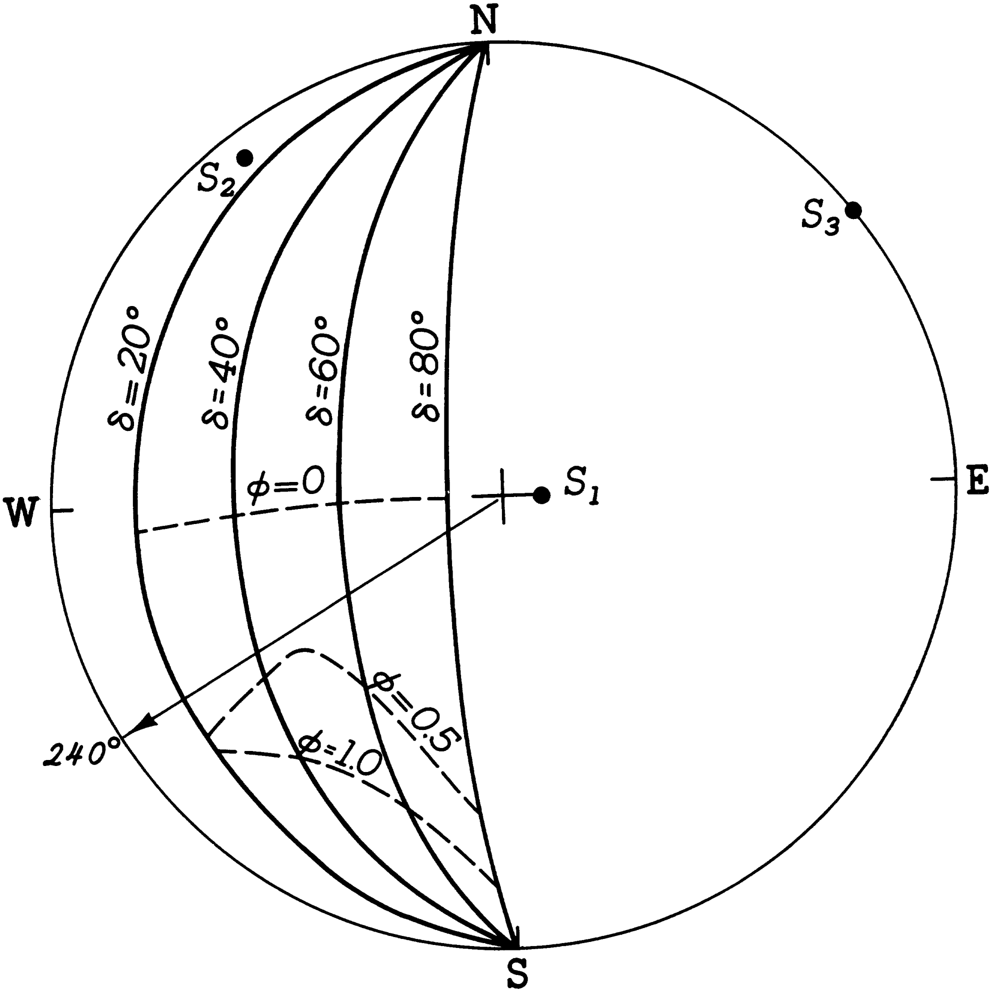

Figure 9: Stereo-plot of north-striking faults with dips (δ) between 20° and 80° west and sliplines for paleo-stress field in the Red Butte Canyon domain (Fig. 1; Table 2). Slip directions for φ = 0.0, 0.5, and 1.0 are defined by intersections of great circles defining fault planes with lines of constant φ. Best estimate for slip in a 240° direction is a fault plane dipping 50°. See text for discussion.

the segment. There is no evidence reported for Quaternary movement on this fault in the interior of the salient, so presumably the Quaternary ruptures have not reactivated this fault. The Virginia Street fault trends westward along the southern margin of the salient, and conceivably represents an offset of the rupture zone, in which displacement is transferred onto the Warm Springs fault at the western boundary of the salient (Pavlis and Smith, 1979; Zoback, 1983).

Gravity and drill data from the valley west of the Salt Lake salient indicate that it forms part of a major, west-trending basement high that extends across the entire width of the valley (Cook and Berg, 1961; Zoback, 1983). This basement ridge is reflected in an elongate gravity high at the northern end of Jordan Valley and by a significant change in the thickness of Tertiary valley fill based on drill data and gravity modelling. The fill in the northern end of Jordan Valley is only several hundred meters thick, while immediately north of the basement ridge, the fill is in exess of 1 km according to Zoback (1983).

The structure of Salt Lake salient indicates that it marks the site of a large, non-conservative barrier in the Wasatch fault zone. The salient is marked by three primary fault systems, the Salt Lake rupture segment on the south, the Ogden rupture segment to the north, and the inferred west-trending fault zone associated with the gravity saddle and modelled basement ridge at the northern end of Jordan Valley. The structure of the Ogden fault segment has not been mapped in this study, but the observaton that the Tertiary valley fill is thicker immediately north of the salient relative to the area to the south indicates that throw across the Ogden segment may be greater than that in the northern part of the Salt Lake segment. This could be due to several factors, the most likely being 1) steeper dip on the Ogden fault segment than in the adjacent Salt Lake segment, or 2) greater extension across the Ogden segment. The resolution of this problem requires further mapping and detailed gravity studies in the Salt Lake salient and southern part of the Ogden fault segment.

DISCUSSION

Geometry of Fault Sections: Our modelling of dips for fault sections in the Salt Lake segment is based on the premise that traces of surface ruptures forming linear to slightly curvilinear patterns 3 km or more in length reflect the strike of fault sections in the subsurface. This premise is supported by (1) the physiography of the Wasatch front, and (2) by the overall shape of gravity contours in the hanging wall basin, both of which partly mimic the geometrical pattern of the fault zone (Cook and Berg, 1961; Zoback, 1983).

The estimated dip angles are steeper than those reported by Gilbert (1928) based on measurements of bedrock fault exposures on the southwestern edge of the Little Cottonwood stock at the southern end of our Draper Structural domain (Fig. 1) and at Mill Creek Canyon in the Olympus Cove domain. He estimated the dip of the fault zone as 35° in the Draper Domain, and we agree that the cataclastic carapace in the fault zone dips 35°-45° southwest in the same area. However, this area is located in the curvilinear zone of intersection between the Fort Canyon fault and Draper fault sections, it is not representative of the main part of the north-east trending Draper fault section. Our work predicts a 20°-30° southwest dip at this locale because of the intersection of the Fort Canyon fault, which dips 35° south and the Draper section which dips ≈65° or less to the northwest (Fig. 5).

We have not estimated the dip of the eastern rupture zone in the Olympus Cove area because of the non-conservative barrier at bends 5a-5b. We prefer a dip of about 45°-50° for the fault section about 6 km west of the mountain front (Fig. 8). This dip is ≈10° greater than that measured in the bedrock by Gilbert (1928)

Fault scarps in Quaternary deposits, which define almost all of the rupture traces in the Salt Lake segment dip steeply between 60° and 70°

(Gilbert, 1926). Our model of the fault zone predicts that these dips do not extend into bedrock at depth in some of the fault sections, but are probably confined to the surficial deposits. This conclusion is similar to that reached by Bashore et al. (1981) based on their seismic reflection/refraction experiment in the southern part of the fault segment. We do not have any evidence as to whether or not the fault zone is listric, or remains planar at depth.

Directional Characteristics of Rupture Propagation: Predicting the direction of rupture propagation during a large earthquake in the Salt Lake segment is an important goal in earthquake hazards mitigation. If the position of rupture nucleation within the fault segment can be predicted, then this region should be selectively monitored for precursory phenomena . Also, the distribution of strong ground motion during a large earthquake depends on the direction of rupture propagation, which is in turn related to the position of rupture nucleation in the fault segment.

Three types of evidence are considered in discussing the possible directions of large earthquake rupture propagation within the Salt Lake segment; long-term deformation rates, dimensions of non-conservative barriers and overall geometry of Quaternary rupture traces. Here we focus our attention only on large earthquakes of $M \approx 7.0$-7.5, the "characteristic earthquakes" defined by Schwartz and Coppersmith (1984), which would presumably rupture most, if not all, of the segment during a single event. We do not consider the effects of large earthquake ruptures that could originate in adjacent segments and propagate into the Salt Lake segment. These types of events are beyond the scope of this study.

Large, kilometer-scale variations in total displacement along the strike of a normal fault zone provide evidence that average rates of deformation have varied systematically along the length of the zone over extended periods of time. The rationale for relating long-term deformation rates to rupture nucleation is as follows: 1) An increase in deformation rate within a fault zone raises ambient shear stress levels, and 2) enhances the transition from quasi-plastic to cataclastic (frictional) deformation. This latter effect may increase the permeability of the fault zone leading to greater fluid access. Increased shear stress levels and the chemical and physical effects of fluids enhance the nucleation and growth of quasi-static ruptures, which may in turn become unstable and trigger earthquakes (Das and Scholz, 1981). Consequently, we suggest that large variations in displacement along the strike of a rupture segment is one criterion for identifying potential sites of rupture nucleation. This criterion is not necessarily valid for predicting the site of rupture nucleation for each large earthquake, but must be used in a long-term statistical sense. That is, by assuming that the greatest frequency of nucleation events, when considered over a large number of M = 7.0 - 7.5 earthquakes, is likely to occur in the area with greatest long-term rates of deformation.

Differential displacement data from the footwall of the Salt Lake segment indicate that the greatest long-term deformation rate has occurred at the southern end. The amount of net-slip across the Salt Lake segment is difficult to quantify because Mesozoic and Paleozoic rocks in the hanging wall are buried beneath late Cenozoic sedimentary deposits in Jordan Valley (Cook and Berg, 1961; Mattick, 1970; Zoback, 1983). However, there is evidence that the footwall has been warped on a regional scale, with a minimum of 5 km and perhaps as much as ≈ 9 km uplift of the southern end of the footwall with respect to the northern end. The evidence consists of the following: (1) The unconformity at the base of the Paleocene-Eocene Wasatch Formation in the northern part of the segment provides a geological dataum - this unconformity marked the surface during Paleocene to Eocene time. This formation is in turn overlain by the Norwodd Tuff, Oligocene volcaniclastic deposits that were coeval with emplacement of the Little Cottonwood and Alta stocks at the southern end of the Salt Lake segment (Hintze, 1973). Our studies of fluid inclusions

(Parry and Bruhn, 1986) and geobarometry on Oligocene skarn deposits on the margins of the Alta stock (Parry and Bruhn, under review) in the southern part of the footwall indicate fault rock now exposed at about 1515 meters elevation originated at depths of ≈ 11 km, while the skarns at 3 km elevation formed at depths of ≈ 5 km. The skarn deposits are now at the same elevation as the projected base of the Oligocene tuffaceous deposits (Norwood Tuff) at the northern end of the segment, indicating differential warping of the footwall, with the southern end uplifted a minimum of 5 km with respect to the northern end. The maximum value of ≈ 9 km is obtained by subtracting the elevation of the Oligocene-Eocene unconformity (≈3 km) from the estimated depth of origin of the fault rock (≈ 11 km) now at an elevation of 1515 m.

Fission track and K/Ar dating of the uplift history and time of origin of fault rock at the southern end of the segment indicate that faulting began by ≈ 17 m.y. ago. The differential uplift rate between the southern and northern ends of footwall is ≈ 0.3 to 0. 5 mm/yr averaged over this time interval. In fact, the fission track dating of Evans et al. (in press) suggests that the greatest rates of footwall uplift occurred in the last 10 m.y. Notably, the long-term average differential uplift or "north-south warping" rate of the footwall is a significant fraction of estimated net slip rates across the fault zone. These latter rates are between 0.6 and 1.4 mm/yr during the last 19,000 years based on trenching studies done by Swan et al. (1980). Clearly, the southern end of the segment meets our criterion as a probable site for repetitive rupture nucleation based on long-term differential displacement rates.

The dimensions of non-conservative barriers within the fault segment may be an additional factor in controlling the direction of rupture propagation during large earthquakes (M ≈7.0-7.5). King and Yielding (1984) suggest that fracture toughness is a geometrical property of the fault zone, and can be crudely estimated by considering the barrier as a zone of plastic deformation. If several non-conservative barriers are present in a fault zone, then rupture nucleation may be favored in the barrier with least fracture toughness.

The length of a plastic deformation zone can be estimated for an ideal elastic-plastic material from simple fracture mechanics considerations. The length (Db) of the plastic deformation zone at the tip of a Mode III (anti-plane shear) crack is given by the Bilby-Cottrell-Swinden model:

$$Db = \pi/8 \, (K^*/Sy) \qquad (1)$$

where K* = fracture toughness and Sy = plastic yield stress (Knott, 1973, p. 70-71). The fracture toughness (K*) is a stress intensity factor, which reflects the stress concentration at the tip of a Mode III rupture due to (1) the regional stress field, and (2) crack size. K* is that stress intensity factor at which the crack can undergo self-extension in the zone of plastic deformation at its tip. Notice that K* increases with increased plastic zone length (Db). The plastic deformation zone effectively "blunts" the tip of the popagating crack, reducing the stress concentration below that for an identical crack without a plastic tip zone.

King and Yielding (1984) suggested that non-conservative barriers act as regions of plastic deformation in fault zones and applied an equation like (1) in a study of rupture propagation in the Al Asnam fault zone, Algeria. Here, plastic deformation is used in only an approximate sense, implying distortion of a volume of material by contemporaneous movement on a population of broadly distributed fault planes that mutually interfere and interlock. In this sense, a barrier is considered mechanically equivalent to a plastic yield zone in an ideal elastic-plastic material.

The magnitude Sy of the yield stress in equation (1) is unknown. King and Yielding (1984) used a maximum value of 200 MPa, a typical shear strength of intact rock, and a minimum of 20 MPa, a nominal stress drop for large earthquakes in their study of the Al Asnam, Algeria earthquake fault zone.

Two large earthquakes within the Rocky Mountain region have recently occurred in fault segments with similar geometries and dimensions to that of the Salt Lake segment. The Ms = 7.5 Hebgen Lake, Montana earthquake had a stress drop of ≈11 MPa while the stress drop estimated for the Borah Peak, Idaho earthquake (Ms = 7.3) was ≈ 1 Mpa (Dozer, 1985a). These stress drops are significantly lower than the nominal values used by King and Yielding (1984).

Here, we tentatively evade the problem of the magnitude of Sy by comparing the relative fracture toughness of any two non-conservative barriers. The relationship, derived directly from equation (1) is simply

$$\frac{K^*_1}{K^*_2} = \left[\frac{Db}{Db}\right]^{\frac{1}{2}} \qquad (2)$$

where the numerical subscripts refer to barrier #1 and #2, respectively. Use of equation (2) implys that the yield stress (Sy) is the same in all non-conservative barriers within the fault zone. This assumption is partly supported by rock friction experiments, where the static coefficent of sliding friction is essentially constant over a large range of temperature, strain rate and effective confining pressure for rocks of many different lithologies (Byerlee, 1968). This is similar to the situation in a large barrier, where highly fractured rocks of different lithologies extend to depth within the fault zone. However, other factors, such as the geometry of the fault population and fluid pressures and chemistry, may differ significantly between barriers, strongly influencing relative yield stresses. Presently, we do not have sufficient data to determine differences in overall fault population geometries between barriers, or whether or not major differences in fluid pressure or chemistry may occur. These features of barriers are important parameters for further research.

Three large, non-conservative barriers have been identified within the Salt Lake segment (#1,#9 and the composite barrier at #4). The lengths of these barriers can be determined from geological mapping (Fig. 2, 10). Db for Traverse Mountain barrier is ≈ 8 km, while that for Salt Lake salient is ≈ 10 km (Fig.10). The difference in relative fracture toughness between the Salt Lake and Traverse Mountain barriers based on equation (2) is only 10%, and in our opinion it is not at all certain that such a small difference is meaningful given the assumptions required in the use of equation (2).

The structural characteristics of the northern half of the Salt Lake segment, between Salt Lake salient and branch point #4 can be interpreted in two fundamentally different ways. The zone of branching between branch point #4 and bends #6 on the west, and 5b on the east, may represent a separate, non-conservative barrier. The size of this barrier is estimated by assuming that it can be approximated as a right, circular cylinder, with an axis dipping 45° westward. The estimated diameter of this cylinder is 4 km, and is taken to be the effective length (Db) of the non-conservative barrier. The relative fracture toughness of this barrier is ≈60% less than that of the Salt Lake salient and ≈40% less than Traverse Mountain barrier. Consequently, in this interpretation, the barrier in the center of the segment has the least fracture toughness, and according to the model of King and Yielding (1984), a large earthquake rupture is most likely to nucleate from the central part of the segment.

The alternative interpretation of the mechanical characteristics is that the entire northern half of the segment (north of branch point #4) may act as a large non-conservative barrier with length Db ≈ 24 km (Fig. 10). This interpretation is based on speculation about the geometrical and mechanical characteristics of the region between the two primary fault traces north of the branch point (#4). Mapping in the footwall of the fault zone shows that the footwall is extensively faulted for a distance of about 1 to 2 km from the trace of the primary fault zone (Fig. 11). These faults form a conjugate system of east and west-dipping normal to oblique-slip

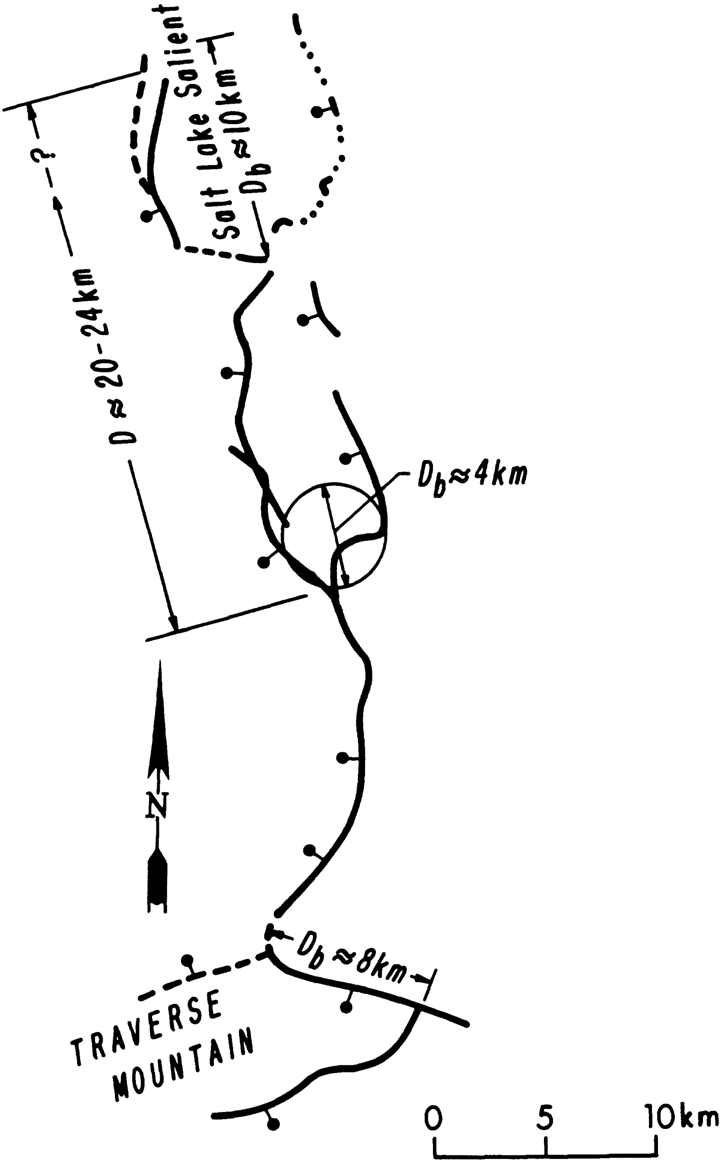

Figure 10: Trace map of Salt Lake fault segment showing estimated dimensions Db of barriers modelled as equivalent "plastic" deformation zones.

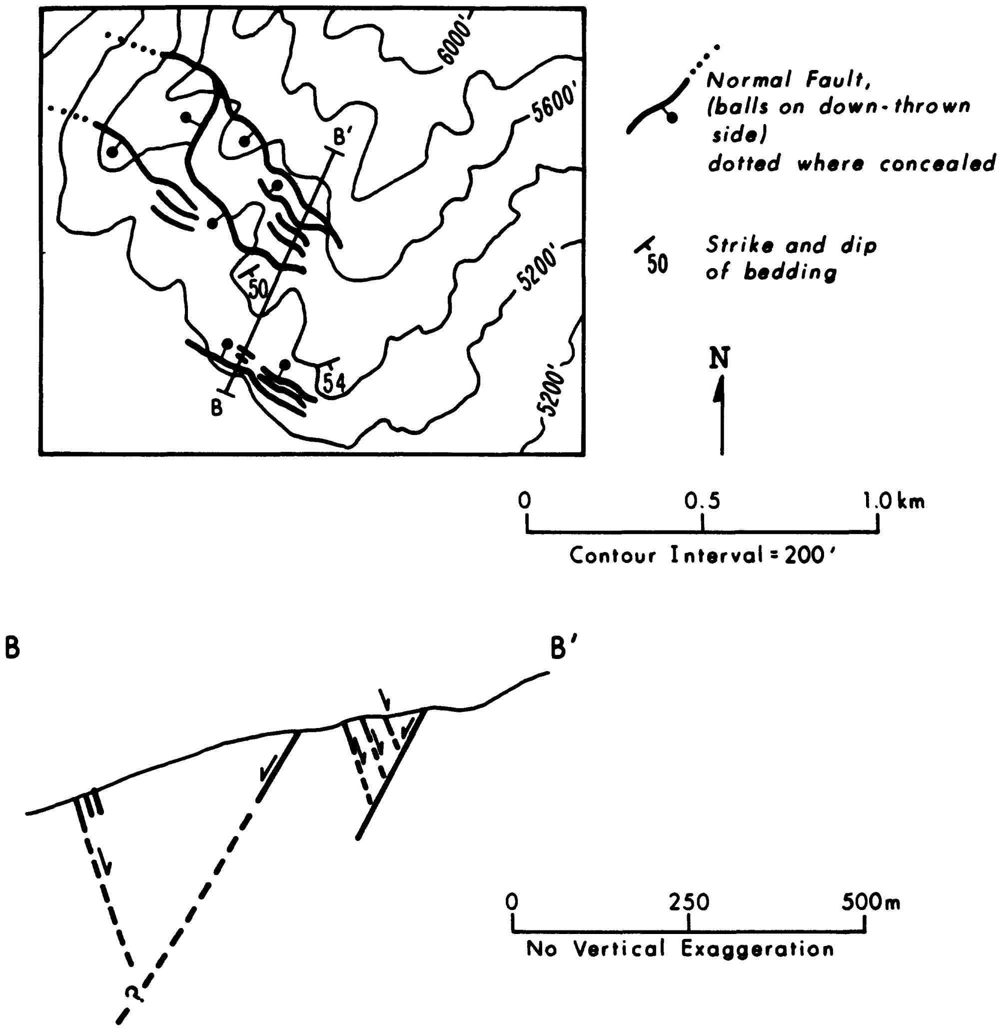

Figure 11: A. Map of normal faults in the northern half of Red Butte Canyon structural domain (Fig. 1). B. Cross section b-b' illustrating the conjugate geometry of faulting in the footwall.

faults. We suspect that the region between the two primary fault zones in the northern half of the segment is pervaded by conjugate fault systems like those exhumed in the footwall. This region may then approximate a large, "plastic" deformation zone comprised of numerous interlocking and mutually interfering conjugate faults. Two schematic cross-sections of this zone are shown in Figure 12, in one the two primary fault traces are shown as parallel fault planes, while in the other, the two primary fault planes intersect at depth. Presently, there is insufficent evidence to choose one section over the other. In either case, the zone of highly faulted rock between the two primary faults presumably forms an elongate plastic deformation zone. This zone, when combined with Salt Lake salient immediately to the north, has a length Db ≈ 24 km, much larger than Db = 8 km estimated for Traverse Mountain barrier. The large length of the former barrier invalidates the small tip zone approximation inherent in derivation of equation 1, and therefore one cannot use equation 2 to estimate relative fracture toughness between this and other barriers. Clearly, the fracture toughness of the northern half of the fault segment is greater than Traverse Mountain barrier. This interpretation of the mechanical characteristics of the Salt Lake segment implies that large earthquake ruptures are most likely to nucleate at the southern end of the segment and propagate northward.

The geometry of two other seismogenic fault zones in the Basin and Range - Rocky Mountain Province transition zone supports the contention that geologic structure may provide information about directions of rupture propagation during large earthquakes. Ruptures in the Hebgen Lake, Montana (Ms = 7.5, 1959) and Borah Peak, Idaho (Ms = 7.3, 1983) earthquakes propagated unilaterally in both events, rupturing towards points of structural bifurcation in the fault zone (Smith et al., 1985; Dozer, 1985a,b; Fig. 13). At Borah Peak, the bifurcation zone was marked by a major bedrock ridge that extends northwest of the main mountain front (Crone and Machette, 1984), while at Hebgen Lake the fault zone

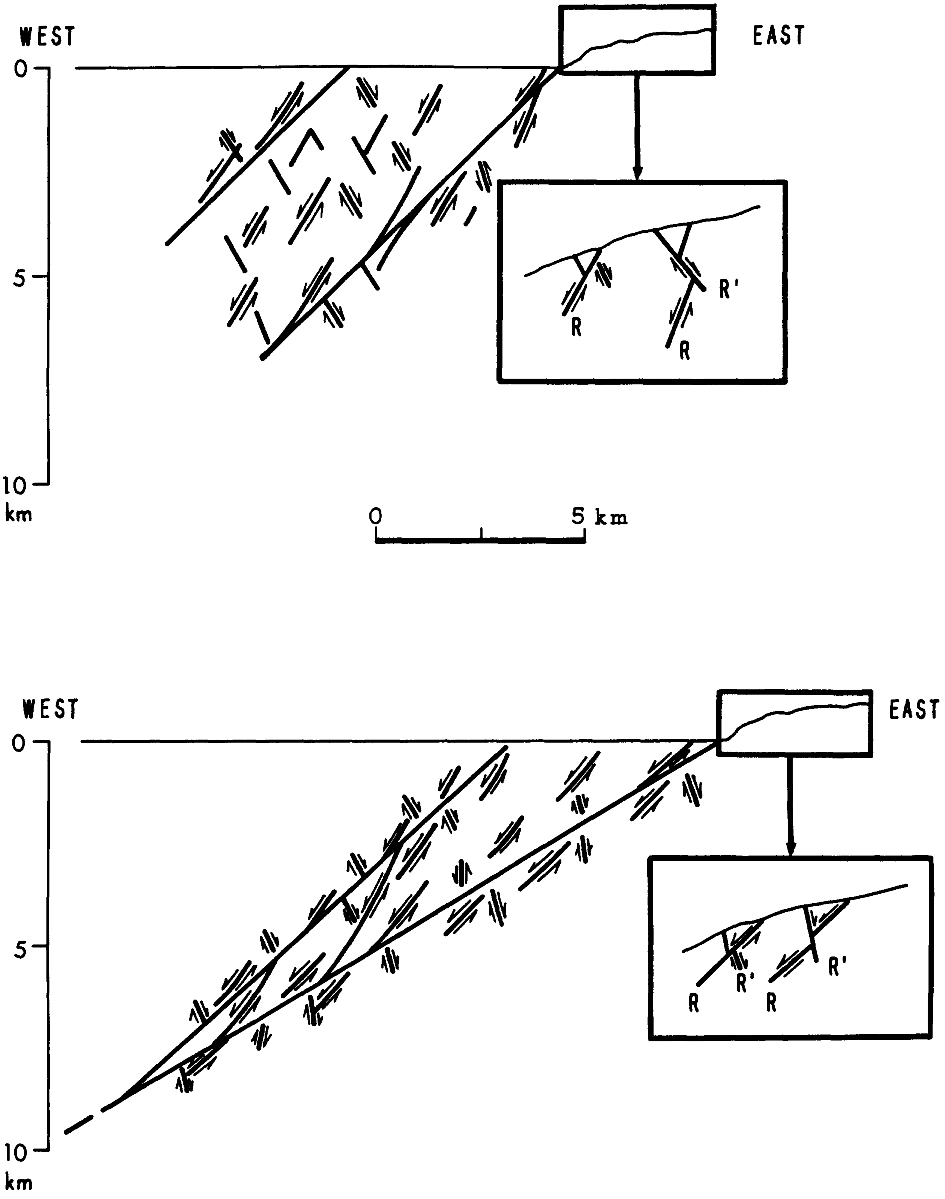

Figure 12: Schematic cross sections illustrating possible structure of the branched fault zone in the northern half of the Salt Lake segment. Conjugate faults like those in Figure 11 are interpreted to pervade the region between the eastern and western primary fault planes. A. The two primary fault branches are assumed to dip at the same angle. B. The two primary fault branches are assumed to intersect at a depth of several kilometers.

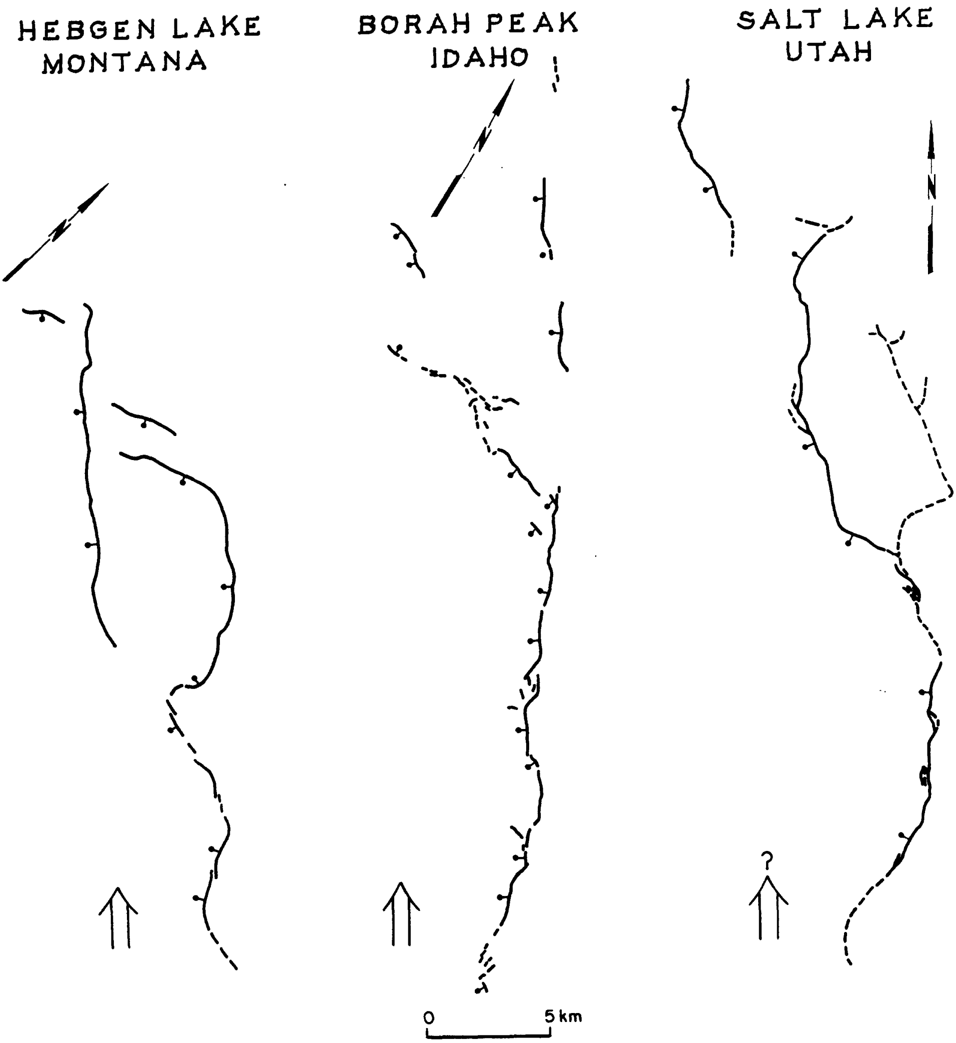

Figure 13: Rupture traces of the Borah Peak, Idaho and Hebgen Lake, Montana earthquake rupture zones compared with the Quaternary trace of the Salt Lake rupture segment. The large arrows indicate the directions of unilateral rupture propagation for the Borah Peak and Hebgen Lake events. Borah Peak rupture trace after Crone and Machette (1984), Hebgen Lake trace after Myers and Hamilton (1964).

bifurcated into two normal fault zones, one of which extended well into the main mountain range while the other paralleled, and locally cut into, the main mountain front along the edge of the hanging wall valley (Myers and Hamilton, 1961). The structural geometry of both fault zones clearly developed over an extended period of time, presumably reflecting the summation of numerous large earthquakes.

The branch-like structure of the Borah Peak and Hebgen earthquake fault zones is characteristic of bifurcated cracks in experiments on crack branching. That is, the direction of propagation in experiments is towards the direction of bifurcation (Broek, 1983), implying that the geometrical characteristics of an earthquake fault zone developed as the result of numerous rupturing events may reflect a consistent directionality of rupture propagation. This rationale is particularly applicable to normal fault zones, where the hanging and footwalls remain essentially stationary along the strike of the fault zone during numerous rupturing events. In strike-slip zones, on the other hand, such evidence is likely to be destroyed as the opposite walls of the fault zone are translated into adjacent regions of changing rupture characteristics.

The overall geologic structure of the Salt Lake segment is comparable with that of the Borah Peak and Hebgen earthquake fault zones in that it also contains a bifurcation point, where the fault zone divides into two primary branches. However, caution must be taken in making direct comparisons in that there currently is no reported evidence for simultaneous surface rupturing on both fault branches in the northern half of the Salt Lake segment (Van Horn, 1972). That is, there is a possibility that the eastern branch, with scarps beteen 5000 and 3 million years age , may have become inactive and earthquake rupturing may now be confined to the western branch, which has the youngest scarps. Alternatively, slip may have occurred at depth on the eastern fault branch during the youngest earthquakes without propagation of the rupture to the surface.

Two fundamentally different, but equally important, views of the structural comparison between the Borah Peak, Hebgen and Salt Lake rupture segments arise from the previous discussion. On one hand, the bifurcated geometry of the Salt Lake segment may still control seismic ruptures, even though the youngest surface scarps are located on only one branch. In this case, the geometry of the Borah Peak and Hebgen earthquake scarp systems may provide direct analogies for expected directionality of rupturing within the Salt Lake segment. Notably, the direction of inferred rupture direction would agree with that implied from arguments concerning 1) long-term displacements and 2) the effective fracture toughness model in which the bifurcated, northern half of the fault segment is considered as a large, plastic deformation zone . Alternatively, the fact that the youngest surface scarps apparently occur only on the western fault branch of the Salt Lake segment may indicate that the bifurcated fault geometry has been bypassed during the Holocene, as the fault zone continued to evolve structurally. In this latter case, comparative studies of the three earthquake fault zones may further knowledge of barrier evolution within seismically active normal fault zones, an important topic in itself.

CONCLUSIONS

The Salt Lake rupture segment (Schwartz and Coppersmith, 1984) is composed of several, linear to slightly curivilinear fault sections that intersect in geometrical barriers defined by bends and branch points in the trace of the fault zone. The dips of these fault sections vary with the strike of the fault zone, with estimated dips ranging between 45° and 90°.

Extension across the normal fault zone was to the southwest, averaging $\approx 240°$. This extension direction superimposed a component of sinistral slip on individual sections of the rupture segment; this slip, that varied as a function of the strike and dip of each fault section. The stress parameter (ϕ) varied from a low of ≈ 0.2 to in the Fort Canyon fault section at Traverse Mountain barrier to ≈ 0.5 in the remainder of the rupture segment.

The Salt Lake segment is bounded on its northern and southern ends by two large non-conservative barriers. A third non-conservative barrier occurs in the central part of the segment, located at the point of bifurcation in the trace of surface ruptures. The mechanical characteristics of this third barrier may be interpreted in two ways. (*1) The barrier may be considered as the smallest non-conservative barrier in the segment, with the corresponding least effective fracture toughness (K*). Alternatively, (*2) this barrier may be viewed as part of a much larger, elongate zone of effective "plastic" deformation comprising the entire northern, bifurcated half of the rupture segment. In this case, Traverse Mountain barrier, at the southern end of the segment, would be the non-conservative barrier with least K*.

Long term deformation rates have been highest at the southern end of the Salt Lake segment, providing a rationale for selecting this part of the rupture segment as the most likely site for repetitive initiation of large earthquake (M ≈ 7.0-7.5) ruptures. This hypothesis is consistent with the alternative (*2) interpretation of fault zone fracture toughness and, possibly, with observed directions of rupture propagation in the Borah Peak, Idaho and Hebgen Lake earthquakes. These latter earthquakes occurred in fault zones with an overall, bifurcated geometry similar to that of the Salt Lake segment, although the latest earthquakes in the Salt Lake segment apparently did not produce surface scarps on both primary fault branches, as they did at Borah Peak and Hebgen Lake. Whether or not this represents a fundamental difference in the mechanical characteristics of the Salt Lake rupture segment relative to those at Borah Peak and Hebgen lake remains an important and fundamental problem

ACKNOWLEDGEMENTS

This work is part of a program of structural and geochemical studies of the Wasatch fault zone undertaken by R.L. Bruhn and W.T. Parry. P.R. Gibler wrote the stress tensor inversion programs and collected field data for the paleo-stress analysis. W. Houghton mapped the Fort Canyon fault zone and studied petro-fabrics of the fault rock. This work represented part of Gibler's and Houghtons's M.S. theses at the University of Utah. Financial support was provided by U.S. Geological Survey Earthquake Hazards Program grant #14-08-0001-G-886 to R.L. Bruhn and W.T. Parry and American Chemical Society Grant #14179AC to R.L. Bruhn, and the Intergrated Tectonics and Seismology Program. We thank W.J. Arabasz, J. Pechmann, R.B. Smith and D.P. Schwartz for discussions concerning the structural and seismogenic characteristics of normal faulting. Thorough reviews of a draft version of the manuscript by P.C. Thenhaus and R. L. Wheeler were very helpful.

REFERENCES

Aki, K., 1979 , Characteristics of barriers on earthquake faults: J. Geophys. Res., v. 84, p. 6140-6148.

Angelier, J., 1979, Determination of the mean principal directions of stresses for a given fault population: Tectonophysics, v. 56, p. T17-T26.

Angelier, J., A. Tarantola, B. Valette, and S. Manoussis,1982, Inversion of field data in fault tectonics to obtain the regional stress, I, single phase fault populations: a new method of computing the stress tensor: Geophys. J.R. Astron. Soc.,v. 69, p. 607-621.

Arabasz, W., 1985, Earthquake behavior in the Wasatch front area: association with geologic structure, space-time occurrence and stress state: Proceedings of conference XXVI, A workshop on "evaluation of regional and urban earthquake hazards and risk in Utah": U.S. Geol. Surv. Open-file Report 84-763, p. 310-339 .

Arabasz, W.J., R.B. Smith and W.D. Richins,1980, Earthquake studies along the Wasatch front, Utah: Network monitoring, seismicity, and seismic hazards: Bull. Seismol. Soc. Am., v. 70, p.1479-1500.

Arabasz, W.J., and D.R. Julander,in press, Geometry of seismically active faults and crustal deformation within the Basin and Range - Colorado Plateau transition in Utah, Geol. Soc. Amer. Spec. Paper on Extensional Tectonics.

Baker, A.A. and M.D. Crittenden Jr., 1961, Geology of the Timpanogos Cave quadrangle, Utah: U.S. Geological Survey Geologic Quadrangle Map GQ-132, Scale 1:24,000.

Bashore, W.M., R.B. Smith, G. Zandt and J. Ansorge,1981, Upper crustal structure of the Salt Lake Valley and the Wasatch Front from seismic modelling: EOS Trans. A.G.U., v. 62, p. 961.

Broek, D.,1983, Elementary engineering fracture mechanics (Martinus Nijhoff Publishers, Boston, 469 p.).

Bruhn, R.L., M.D. Picard and J. Isby, in press, Tectonics and sedimentology of Uinta Arch, western Uinta Mountains and Uinta Basin: Amer. Assoc. Pet. Geol. Mem. "Paleotectonics and sedimentation in Rocky Mountain Region, U.S.."

Bullock, R..L., 1954, The geology of Lehi quadrangle, Utah: unpublished M.S. thesis, Brigham Young University.

Byerlee, J.D., 1968, Brittle-ductile transition in rocks: J. Geophys. Res., v. 73, p. 4741-4750.

Cook, K.L. and J.W. Berg Jr., 1961, Regional gravity survey along the central and southern Wasatch front, Utah: U.S. Geol. Surv. Prof. Paper 316-E, p. 75-89.

Crittenden, M.D. Jr., 1976, Stratigraphic and structural setting of the Cottonwood area, Utah: in Hill, J.G., ed.; Geology of the Cordilleran Hingeline: Rocky Mountain Assoc. of Geologists, Denver, p. 281-317.

Crittenden, M.D. Jr., J.S. Stuckless, R.W. Kistler and T.W. Stern, 1973, Radiometric dating of intrusive rocks in the Cottonwood area, Utah: U.S. Geol. Survey Jour. Res., v. 1, p. 173-178.

Crone, A.J. and M.N. Machette, 1984, Surface faulting accompanying the Borah Peak earthquake, central Idaho: Geology, v. 12, p. 664-667.

Crone, A.J. and S.T. Harding, 1985, Near-surface faulting associated with Holocene fault scarps, Wasatch fault zone, Utah: a preliminary report, Proceedings of Conference XXVI, a workshop on "evaluation of regional and urban earthquake hazards and risk in Utah, U.S. Geol. Surv. Open-file Report 84-763, p. 241-268.

Das, S. and C.H. Scholz, 1981, Theory of time-dependent rupture in the earth: J. Geophys. Res., v. 86, p. 6039-6051.

Davis, F.D., 1983, Geologic map of the central Wasatch front, Utah: Utah Geological and Mineralogical Survey, Mapp 55-A, scale 1:100,000.

Davis, F.D., 1983, Geologic map of the southern Wasatch front, Utah: Utah Geological and Mineralogical Survey, Mapp 55-A, Scale 1:100,000.

Doser D.I., 1985a, The 1983 Borah Peak, Idaho and 1959 Hebgen Lake, Montana earthquakes: models for normal fault earthquakes in the Intermountain Seismic Belt: Proceedings of Workshop XXVIII on the Borah Peak, Idaho, Earthquake, U.S. Geol. Surv. Open-file Report, 85- 29, 368-384.

Doser, D.I., 1985b, Source parameters and faulting processes of the 1959 Hebgen Lake, Montana earthquake sequence : J. Geophys. Res., v. 90, p. 4537-4556.

Evans, S.H., Parry, W.T. and Bruhn, R.L., in press, Thermal, mechanical and chemical history of Wasatch fault cataclasite and phyllonite, Traverse Mountains area, Salt Lake City, Utah: age and uplift rates from K/Ar and fission track measurements: Progress Report for U.S. Geological Survey Earthquake Hazards Reduction Program contract #14-08-001-G-886, U.S. Geol. Surv. Open - File Report.

Gibler, P.R., 1985, Bedrock deformation along the Salt Lake segment of the Wasatch fault: implications for stress magnitudes, stress directions and seismicity; University of Utah M.S. thesis.

Gilbert, G.K., 1928, Studies of Basin-range structure: U.S. Geol. Surv. Prof. Paper, 153, 92p.

Hintze, L.F., 1973, Geologic history of Utah: Brigham Young University Geology Studies, v. 20, p. 1-181.

Houghton, W., 1986, Structural geology of the Deer Creek and Wasatch fault: Univerity of Utah M.S. thesis.

King, G., 1983, The accommodation of large strains in the upper lithosphere of the earth and other solids by self-similar fault systems: the geometrical origin of b-value: Pageoph., v. 121, p. 761-814.

King, G. and G. Yielding, 1984, The evolution of a thrust fault system: processes of rupture initiation, propagation and termination in the 1980 El Asnam (Algeria) earthquake: Geophys. J.R. Astr. Soc., v. 7, p. 915-933 .

King, G and Nabelek, 1985, Role of fault bends in the initiation and termination of earthquake rupture: Science, v. 228, p. 987.

Knott, J.F., 1973, Fundamentals of Fracture Mechanics (Butterworth and Co., London), 273 pp.

Lawson, D.L. and R.J. Hanson, 1974, Solving Least Squares Problems, Prentice-Hall, New Jersey, 340 p.

Marsell, R.E., 1969, The Wasatch fault zone in north central Utah: in Jensen, M.L., Ed., Guidebook of northern Utah, Utah Geological and Mineralogical

Survey Bull., v. 82, p. 125-139

Mattick, R.E., 1970, Thickness of unconcolidated to semiconsolidated sediments in Jordan Valley, Utah: U.S. Geological Survey Professional Paper 700-C, p. c119-c124.

Michael, A.J., 1984, Determination of stress from slip-data; faults and folds: J. Geophys. Res., v. 89, p. 11,517-526.

Myers, W.B. and W. Hamilton, 1961, Deformation accompanying the Hebgen Lake earthquake of August 17, 1959: U.S. Geol. Surv. Prof. Paper 316-E, p. 75-89.

Parry, W.T. and R.L. Bruhn, 1984, Pore fluid and seismogenic characteristics of fault rock at depth on the Wasatch fault, Utah: EOS.

Parry, W.T. and R.L. Bruhn, 1986, Pore fluid and seismogenic characteristics of fault rock at depth on the Wasatch fault, Utah: J.Geophys. Res.,v. 91, p. 730-744.

Parry, W.T., and Bruhn, R.L., Geochemical evidence for 11 km vertical offset on the Wasatch fault, Utah: Geology (under review).

Pavlis, T.L. and R.B. Smith, 1980, Slip vectors from faults near Salt Lake City from Quaternary displacement and seismicity: in Earthquake Studies in Utah 1850 to 1978, ed. W.J. Arabasz, R.B. Smith and W.D. Richins, p. 378-382.

Schwartz, D.P. and K.J. Coppersmith, 1984, Fault behavior and characteristic earthquake: examples from the Wasatch and San Andreas fault zone: J. Geophys. Res., p. 5681-5698.

Schwartz, D.P., K.L. Hanson and F.H. Swann III, 1983, Paleoseismic investigations along the Wasatch fault zone: an update: in Geologic Excursions in Neotectonics and Engineering Geology in Utah, Guidebook, Part IV, p. 45-48, Geol. Soc. Am., Salt Lake City, Utah.

Smith, R.B. and R.L. Bruhn, 1984, Intra-plate extensional tectonics of the eastern Basin-Range; inferences of structural style from seismic reflection data regional tectonics and thermal-mechanical models of brittle-ductile deformation: J. Geophys. Res.,v. 89, p. 5733-5762.

Smith, R.B., W.D. Richins, D.I. Dozer, J.C. Pechmann and C. Langer, 1984, The 1983 M 7.3 Borah Peak, Idaho earthquake: a model for active crustal extension: Geol. Soc. Am. Abstracts with Progs., p.16.

Swan, F.H., III, D.P. Schwartz and L.S. Cluff, 1980, Recurrence of moderate-to-large magnitude earthquakes produced by surface faulting on the Wasatch fault zone: Bull. Seis. Soc. Am., v. 70, p. 1431-1462.

Van Horn, R., 1972, Map showing relative ages of faults in the Sugarhouse Quadrangle, Salt Lake Country, Utah: U.S. Geol. Sur. Map GQ-1-7667-B, 1:24,000.

Van Horn, R., 1981, Geologic map of pre-Quaternary rocks of the Salt Lake City North Quadrangle: U.S. Geol. Surv. Map 1-1330, 1:24,000.

Zoback, M.L., 1983, Structure and Cenozoic tectonism along the Wasatch fault zone, Utah: Mem. Geol. Soc. Am., v. 157, p. 3-27.

Zoback, M.L., 1985, Constraints on in-situ stress field along the Wasatch front: Proceedings of Conference XXVI, a workshop on "evaluation of regional and urban earthquake hazards and risk in Utah": U.S. Geol. Sur. Open-file Report 84-763, p. 286-309.

QUATERNARY DISPLACEMENT ON THE MORGAN FAULT, A BACK VALLEY FAULT IN THE WASATCH RANGE OF NORTHEASTERN UTAH

by

J. Timothy Sullivan
U.S. Bureau of Reclamation
Denver, CO 80225

and

Alan R. Nelson
U.S. Bureau of Reclamation
and U.S. Geological Survey
Denver, CO

ABSTRACT

The Morgan fault is a 16-km-long, north-trending normal fault bounding the east side of Morgan Valley, one of the back valleys of the Wasatch Range. A history of late Cenozoic surface displacements on the Morgan fault is suggested by triangular facets preserved on the footwall escarpment of the fault, back-tilted erosion surfaces adjacent to the fault, and the preservation of a 1000-m-thick fanglomerate in the hanging wall of the fault. Trenches across the Morgan fault show that middle Pleistocene colluvial deposits are displaced about 4 m and Holocene deposits are displaced about 1 m. Amino-acid ratio minimum age estimates on shells, radiocarbon dating of peat deposits, soil development indices, displacement data, and stratigraphic correlations of Quaternary deposits among the trenches suggest an average middle to late Pleistocene slip rate of about 0.01 to 0.02 mm/yr for the Morgan fault. Stratigraphic relations in one of the trenches suggest that repeated surface displacements on the fault have been about one meter or less, suggesting that paleoearthquakes with magnitudes in the range 6-1/2 to 7 have occurred on the fault.

INTRODUCTION

Most neotectonic studies in Utah have emphasized the hazard posed by the occurrence of large-magnitude earthquakes on the Wasatch fault (Swan and others, 1980; Schwartz and Coppersmith, 1984), but fault maps (Anderson and Miller, 1979; Nakata and others, 1982) and other studies show late Quaternary (<125 ka) faults east of the Wasatch fault. These faults include those in Cache Valley (Swan and others, 1983; Nelson and Sullivan, this volume), Bear Lake Valley (Williams and others, 1962), the Bear River fault zone (West, 1986), and Strawberry Valley (southeast of Kamas Valley on figure 1) (Nelson and Martin, 1982; Nelson and Van Arsdale, 1986). A diffuse band of contemporary seismicity including earthquakes as large as magnitude 5.7 extends through this area about 20 km east of the Wasatch fault (Arabasz and others, 1980; this volume) suggesting additional late Quaternary faults may be present.

FIGURE 1.-- FOLLOWING PAGE

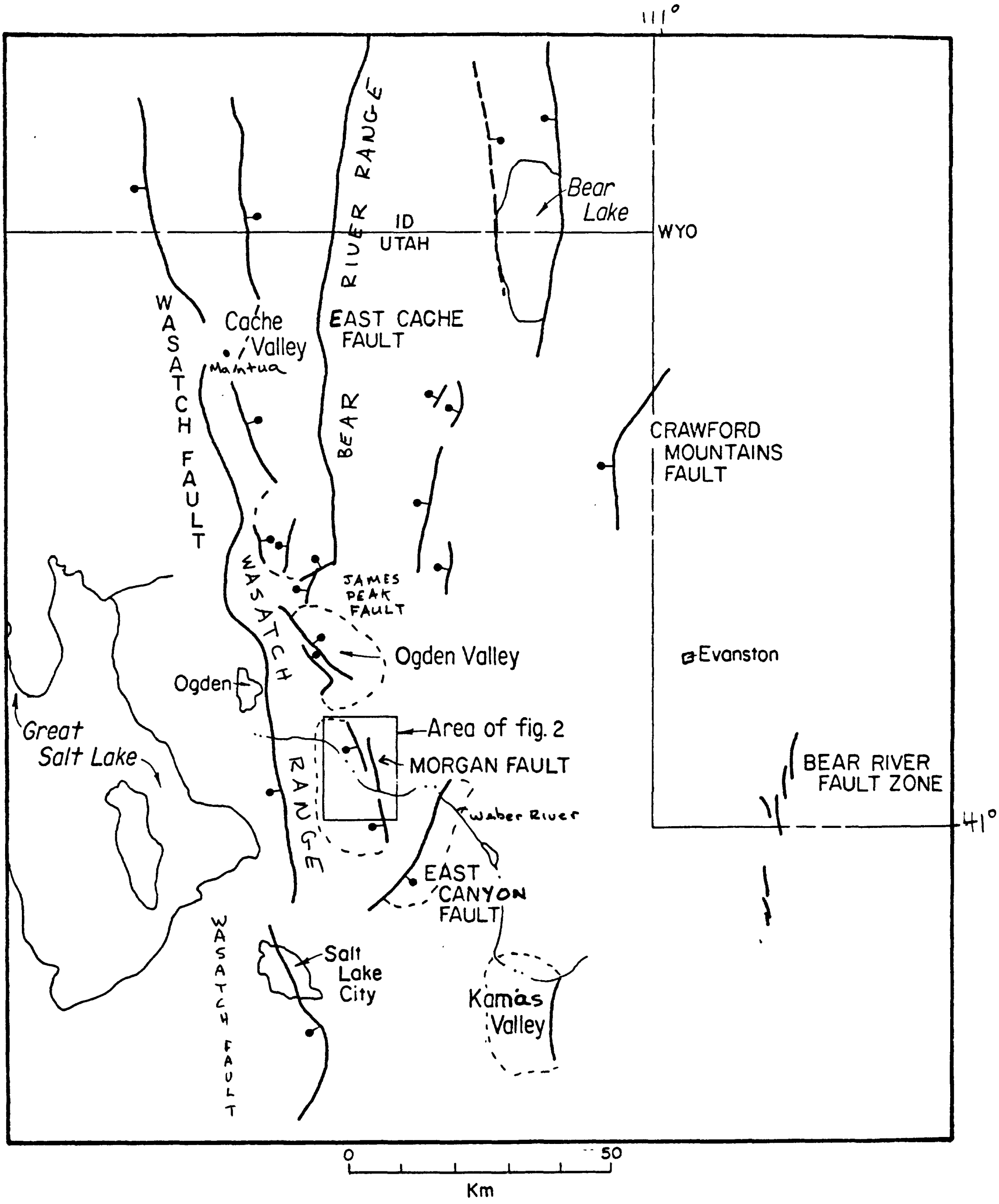

Figure 1.--Location map showing the Morgan fault, the Wasatch fault, and other middle or late Quaternary faults in northeastern Utah. The back valleys of the northern Wasatch Range are outlined by dashed lines. The Wasatch Range extends east of the Wasatch fault from Cache Valley to south of Kamas Valley. Area of figure 2 is shown.

THE BACK VALLEYS OF THE WASATCH RANGE

The back valleys of the northern Wasatch Range are in the transition zone between the eastern Basin and Range Province and Middle Rocky Range and Colorado Plateau provinces. This zone is coincident with late Cretaceous and early Paleogene thrust faults of the Sevier Thrust Belt (Armstrong, 1968). Seismic reflection data generated for oil and gas exploration, locally detailed surface mapping, and seismologic investigations in the transition zone indicate a complex interaction between these stacked thrust faults and younger normal faults (Royse and others, 1975; Lamerson, 1982; McKee and Arabasz, 1982; Smith and Bruhn, 1984). The back valleys are structural and physiographic basins with less late Cenozoic structural relief than morphologically similar basins in the Basin and Range (Zoback, 1983; Sullivan and others, 1986). Gilbert (1928) suggested recent displacement on some faults in Cache Valley, Ogden Valley, Morgan Valley, and Kamas Valley, structural basins in the Wasatch Range he termed "back valleys" (fig. 1). Late Quaternary displacement has been inferred on faults in Ogden Valley, near Mantua, and on the East Canyon fault (Sullivan and others, 1986). Other unstudied late Cenozoic normal faults that may have Quaternary displacement are the Crawford Mountains fault and faults in the Bear River Range (Sullivan and others, 1986).

MORGAN VALLEY

Morgan Valley is a 25-km-long, 10 to 15 km wide, northwest-trending back valley, located 20 km east of the Wasatch fault, that was described by Gilbert (1928) as a structural trough similar to Ogden and Cache Valleys to the north. Eardley (1944) later described Morgan Valley as a syncline, but subsequently recognized the role of normal faulting in the development of the valley (Eardley, 1955). Most recently, Morgan Valley has been interpreted as an asymmetric graben bounded on the east by the Morgan fault (Hopkins, 1982; Hopkins and Bruhn, 1983).

Cenozoic deposits of three ages, separated by angular unconformities, are present in Morgan Valley and suggest a deformational history dating from the Eocene. The conglomerates of the Eocene Wasatch Formation, dipping 40 to 65° to the east and northeast, are exposed on the west margin of the valley unconformably overlying Mesozoic and Paleozoic sedimentary rocks (Mullens and Laraway, 1973; Bryant, 1984). The overlying tuffaceous sandstones and conglomerates of the Norwood Tuff, described and dated as late Eocene to early Oligocene by Eardley (1944), are exposed throughout the valley dipping 10 to 40° to the northeast. Schick (1955) and Coody (1957) mapped a fanglomerate unconformably overlying the Norwood Tuff on the east side of the valley (Thv on fig. 2) that they informally correlated with the Huntsville fanglomerate, which is mapped in Ogden Valley and near the East Canyon fault (fig 1).

FIGURE 2.-- FOLLOWING PAGE

Figure 2.--Cenozoic Geology of Morgan Valley modified from Mullens and Laraway (1973). Reversely magnetized samples of a silty clay from the B horizon of a soil on an erosion surface west of the Weber River (site W-16) indicate that this soil, the underlying deposits, and higher erosion surfaces in the valley are >730 ka (Sullivan and others, 1986). Most younger alluvium post-dates the fall of Lake Bonneville from the Provo shoreline (14 ka). Fluvial terraces are all of Pleistocene age, but several ages are represented, including a terrace graded to the Provo shoreline (Qtp). Area of figure 4 is shown.

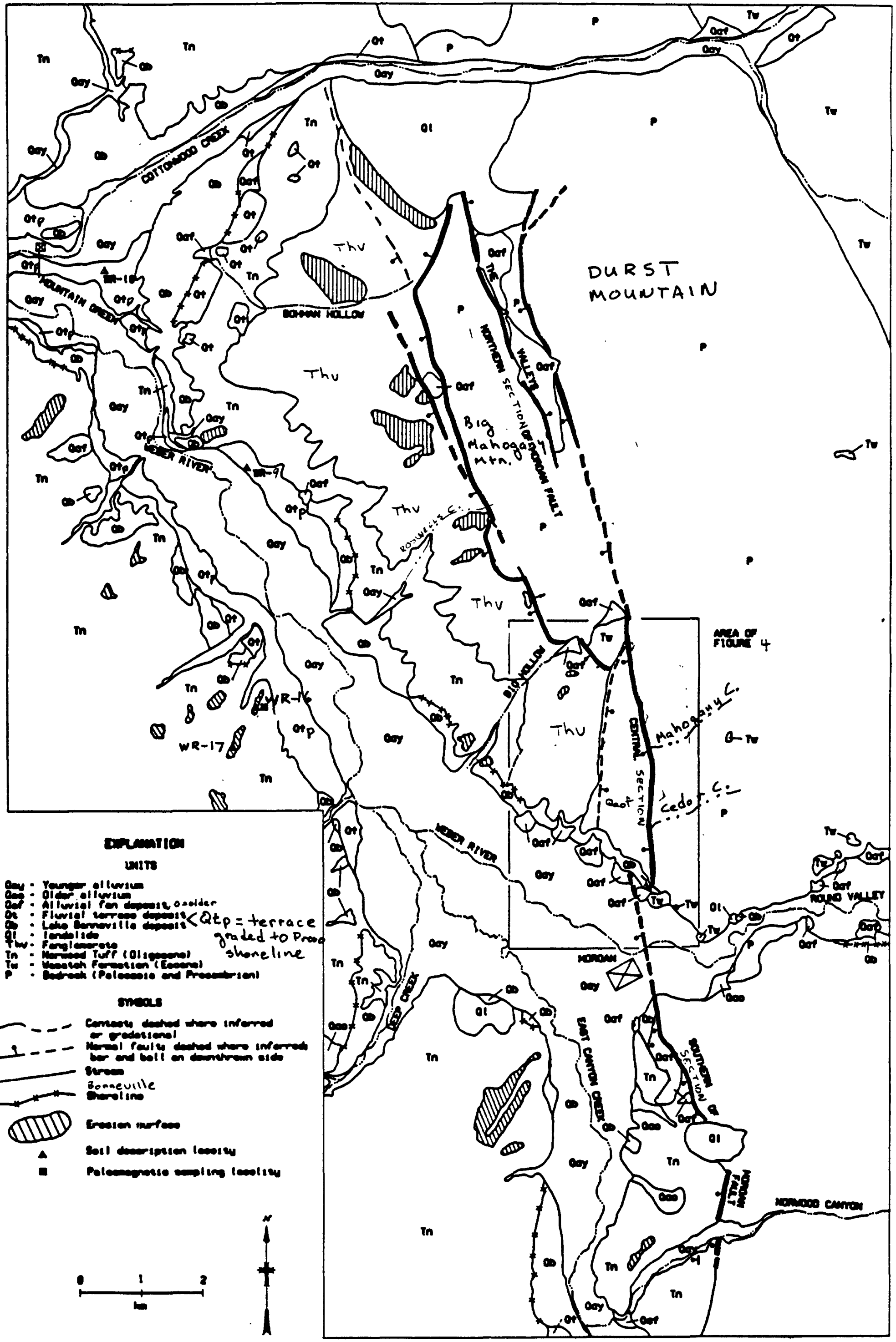
DURST MOUNTAIN
Big Mahogany Mtn.
NORTHERN SECTION OF MORGAN FAULT
THE VALLEYS
COTTONWOOD CREEK
MOUNTAIN GREEN
BOHMAN HOLLOW
WEBER RIVER
Roswells C.
BIG HOLLOW
AREA OF FIGURE 4
CENTRAL SECTION
Mahogany C.
Cedar C.
ROUND VALLEY
MORGAN
DEEP CREEK
EAST CANYON CREEK
SOUTHERN SECTION OF
MORGAN FAULT
NORWOOD CANYON
WR-18
WR-9
WR-16
WR-17
Qay
Qao
Qaf
Qaof
Qt
Qtp
Qb
Ql
Thv
Thu
Tn
Tw
P
EXPLANATION
UNITS
QUATERNARY
TERTIARY
Qay - Younger alluvium
Qao - Older alluvium
Qaf - Alluvial fan deposit, Qaof = older
Qt - Fluvial terrace deposit < Qtp = terrace graded to Provo shoreline
Qb - Lake Bonneville deposit
Ql - landslide
Thv - Fanglomerate
Tn - Norwood Tuff (Oligocene)
Tw - Wasatch Formation (Eocene)
P - Bedrock (Paleozoic and Precambrian)
SYMBOLS
Contact, dashed where inferred or gradational
Normal fault, dashed where inferred, bar and ball on downthrown side
Stream
Bonneville Shoreline
Erosion surface
Soil description locality
Paleomagnetic sampling locality
0
1
2
km
N

FIGURE 2

THE MORGAN FAULT

The Morgan fault is mapped on the east side of Morgan Valley at the base of an escarpment formed in Paleozoic rocks (Mullens and Laraway, 1973). The escarpment consists of three linear, 5- to 8-km-long sections that correspond with en-echelon steps in the trace of the fault and with differences in escarpment height and the elevation of hanging wall deposits (figs. 2 and 3). There are no fault scarps in unconsolidated deposits along the three sections of the fault. However, triangular facets along the base of the escarpment that are 100 to 250 m high and slope 20 to 25° suggest that Quaternary displacements have occurred on all sections of the fault.

FIGURE 3.-- FOLLOWING PAGE

Evidence suggests that Cenozoic displacement may be greatest on the northern section of the fault. Based on correlation of thrust faults mapped on Durst Mountain in the footwall of the Morgan fault and those exposed on the west side of the valley and on the thickness of Cenozoic deposits in the valley, Hopkins (1982) concludes that 6800 m of Cenozoic normal displacement has occurred on the northern section of the fault. Along this section of the fault, tilted late Cenozoic erosion surfaces are cut on the Huntsville fanglomerate (fig. 2) which overlies the Norwood Tuff in the hanging wall of the fault. Schick (1955) concludes this fanglomerate is of Pliocene (?) age and suggests it was displaced by the Morgan fault. Recent mapping (Mullens and Laraway, 1973; Hopkins, 1982) indicates that this fanglomerate dips 5 to 38° into the fault and also suggests that the fanglomerate is faulted. Although triangular facets are also present on the southern section of the

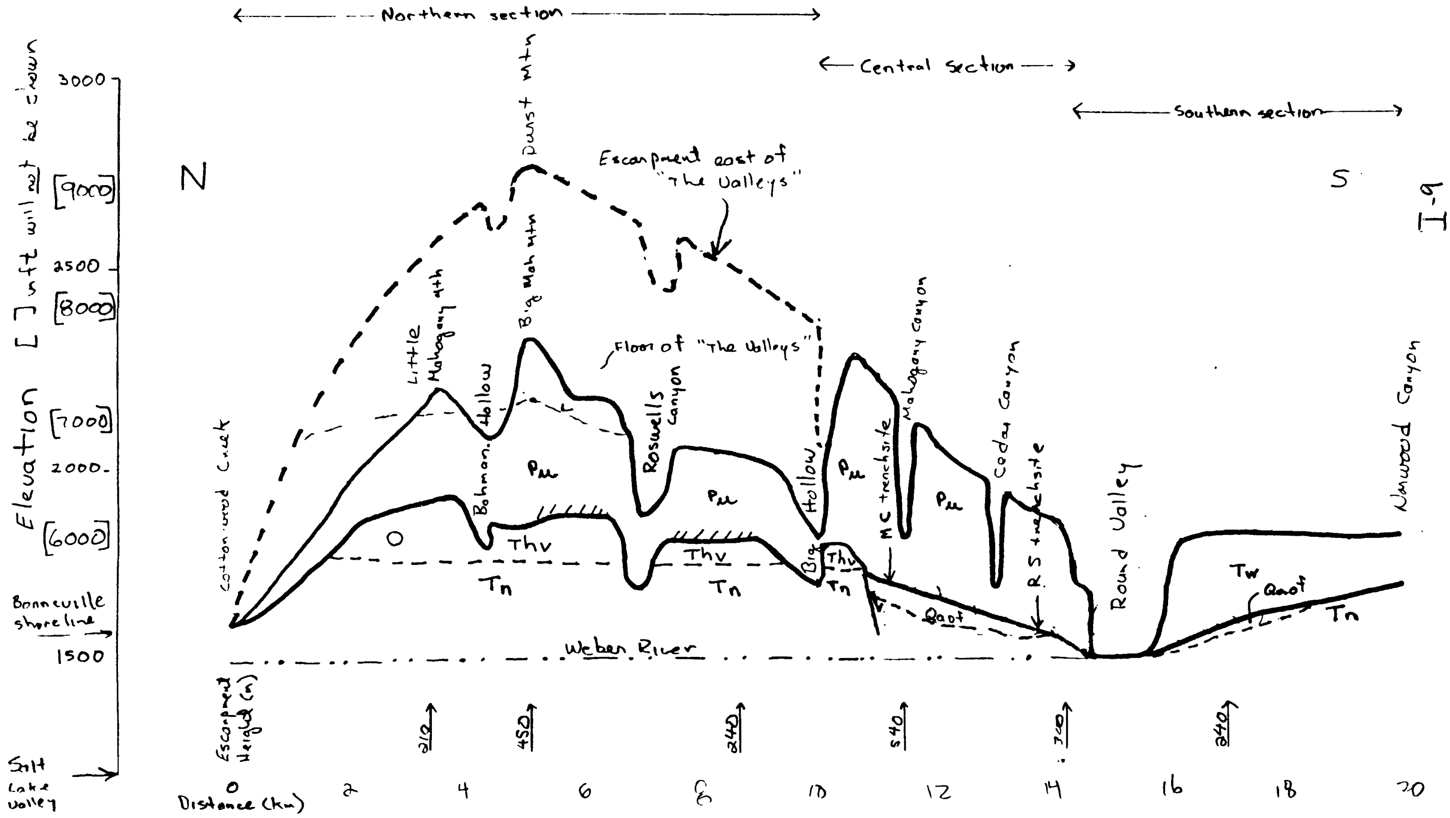

Figure 3.--Generalized topographic profiles (solid lines) and geologic section parallel to the Morgan fault drawn along the crest of the footwall escarpment and along the hanging wall at the base of the escarpment. Profiles from 1:62,500 map with vertical exaggeration of 6:1. A generalized profile (dashed line) of "The Valleys" is projected from about 1 km east of the section. The modern profile of the Weber River, escarpment heights (arrows) and the locations of erosion surfaces (hachured lines) are also shown. Geologic units are the same as figure 2.

fault, Cenozoic displacement appears to be less than on the northern section (Hopkins, 1982, p. 35).

Our investigation of the Morgan fault focused on the central section of the fault, for along this section Quaternary alluvial fans (Qaof), are inset into the Huntsville fanglomerate, suggesting that they have been displaced by the Morgan fault (figs. 2, 3, and 4). We infer this topographic low on the hanging wall of the fault to be a 0.5- to 1-km-wide graben filled with alluvial fan deposits that is bounded on the east by the main scarp of the Morgan fault and on the west by an inferred east-facing antithetic fault (figs. 3 and 4). Dissected alluvial fan deposits (Qaof) slope 6-9° to the southwest within this inferred graben. The lower 50 m of some of the facets slope 1 to 3° more steeply than their upper portions. Thus, we infer the surface trace of the fault to be at the 50 to 100 m wide break in slope between the facets and the fans. Although a few small, discontinuous, Holocene fans along the break in slope in the larger drainages are undissected, channels (some up to 20 m deep) are incised into the surfaces of all the larger alluvial fans along the central section (fig. 4). Longitudinal profiles down these channels show they are graded to the Bonneville shoreline along all but their lowest reaches. Knickpoints in the profiles due to the fall of the lake (dated at 15 ka by Scott and others, 1983) do not appear to have migrated more than 100 m up the fan channels. Holocene alluvial fans have been deposited where the channels reach the floodplain of the Weber River. Thus, we conclude that most of the sediment derived from the footwall of the fault is being carried beyond the hanging wall fan surfaces. Distinguishing tectonic from climatic or changing baselevel responses in alluvial fan systems is difficult at best (for example, Funk, 1976; Bull, 1977), but the dissection of older fans along the central section suggests fault slip rates are lower than stream downcutting rates.

FIGURE 4. -- FOLLOWING PAGE

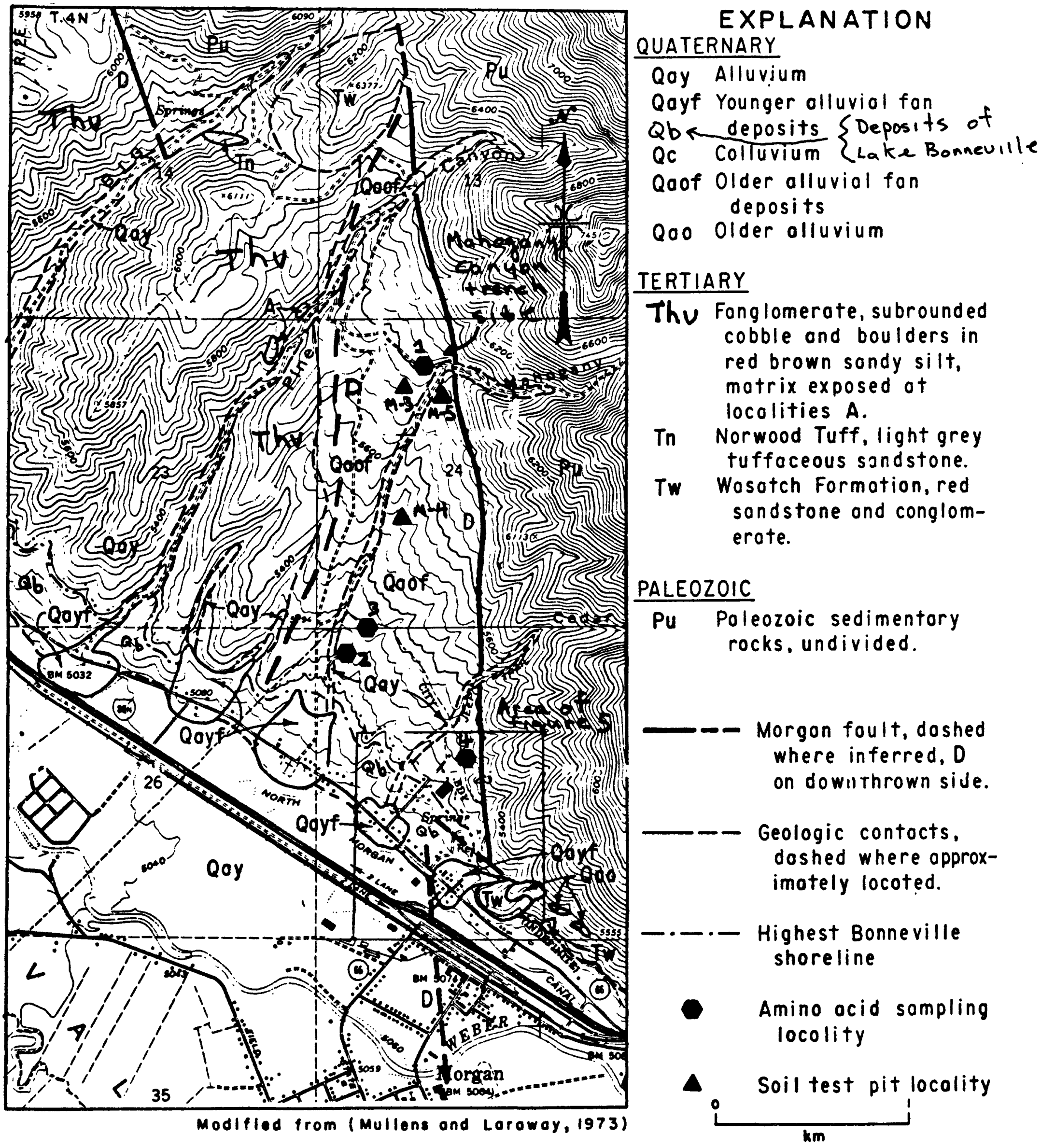

Modified from (Mullens and Laraway, 1973)

Figure 4.--Surficial geologic map of the central section of the Morgan fault, modified from Mullens and Laraway (1973). See figure 2 for location. Older alluvial fan deposits have an estimated age of >400 ka and colluvial deposits, shown only at the southern end of the central section, are inferred to range in age from Holocene to >400 ka. The upslope inflections in contour lines on unit Qaof mark channels incised into the older alluvial fan deposits. Younger alluvium and alluvial fan deposits post-date Lake Bonneville deposits (16-14 ka) in the valley. Sampling localities and the area of figure 5 at southern end of the central section are shown.

AGE OF QUATERNARY DEPOSITS ADJACENT TO THE CENTRAL SECTION OF THE MORGAN FAULT

The Quaternary deposits along the central section of the Morgan fault consist of Holocene alluvium in the major drainages, deposits of Lake Bonneville, and older colluvial and alluvial deposits at elevations above the Bonneville shoreline (fig. 4). Soils developed in the alluvium in the larger drainages (Qay on figs. 4 and 5) and in the fans (Qayf) deposited where the drainages reach the floor of Morgan Valley are weakly developed without argillic B horizons. Comparison of these soils with the Holocene soils described by Shroba (1982) indicates that the alluvium is of Holocene age. Soils began forming on the buff-colored sands and silts between the present floodplain and the highest stand of Lake Bonneville in the valley following the fall of the lake about 14 to 15 ka. A soil developed on these deposits near Robeson Springs (M-2, Table 1 and fig. 5) lacks an argillic horizon, but contains substantial amounts of pedogenic carbonate. A sequence of older fan deposits (Qaof on figs. 3, 4, and 5) derived from the mountains to the east are exposed above the Bonneville shoreline. These deposits are overlain by thin (1- to 3-m-thick) hillslope colluvium (not shown on fig. 4 except south of Cedar Creek) that thickens to 7 m adjacent to the Morgan fault near Mahogany Canyon. Exposures and test pits (all sampling localities on fig. 4) show thick calcium carbonate soil horizons (stages II and III of Gile and others, 1966) on both the colluvial and alluvial deposits; a 1-m-thick petrocalcic horizon (stage IV) in fan deposits was exposed beneath about 3 m of colluvium near Mahogany Canyon (locality 1, fig. 4). Thus, based on comparisons with similar soils developed in similar deposits elsewhere in the region (Machette, 1985a), many of these alluvial and colluvial sediments are probably of middle Quaternary age (125 to 730 ka). However, the differing degree of carbonate development in units of similar lithology, unconformities between most alluvial and overlying colluvial units, and uncertainty in correlating individual alluvial units between isolated exposures suggests units deposited during a number of episodes during the Pleistocene may be present.

TABLE 1. -- FOLLOWING PAGE

FIGURE 5 -- FOLLOWING PAGE

We used three relative dating methods to attempt to more accurately estimate the ages of the older colluvial and alluvial sediments along the central section of the Morgan fault -- two measures of the degree of soil development and amino-acid ratios measured on fossil gastropod shells in the deposits.

Soil development indices (Harden and Taylor, 1983) provide an objective way of comparing the degree of soil development on deposits of unknown age with the degree of soil development on deposits of similar lithology in areas where numerical ages are available (Birkeland, 1984). Several calibrated (independently dated) soil profiles are available from Morgan Valley (discussed in Sullivan and others, 1986): 1) soil M-6 which overlies a peat dated at 8.3 ka in a trench near Robeson Springs (table 1 and fig. 5), 2) soils (M-2, table 1; W-9, W-18, fig. 2) on both fine and coarse materials younger than the Bonneville shoreline (14-15 ka), and profile W-16 with a reversely-magnetized B horizon that shows it to be >730 ka (fig. 2). Unfortunately, the variable but high carbonate content of the soils described

TABLE 1.--Selected properties of soils on alluvial, colluvial, and lacustrine sediments along the Morgan fault, Morgan Valley, north-central Utah

[Leaders (----) indicate no detectable carbonate]

Profile	Horizon[1]	Average depth (cm)	Parent material	Munsell dry	Estimated percent by volume			Percent by weight[2]			Percent organic matter[3]	Percent carbonate[4]	Soil profile index[5]	Total pedogenic carbonate[6] (g/cm²)
					Pebbles (0.2-8 cm)	Cobbles (8-25 cm)	Boulders (>25 cm)	Sand (2-0.5 mm)	Silt (50-2 um)	Clay (<2 um)				
M-1	A	0- 10	Slopewash colluvium	10 YR 6/2	5	0	0	27	56	18	1.7	16.5	15	63
	Bwk	10- 23	----do-------------	10 YR 5/3	5	0	0	28	52	21	1.2	24.9		
	Bkm	23- 50	----do-------------	10 YR 8/0	5	0	0	28	58	15	.5	43.7		
	Bk1	50- 84	----do-------------	7.5 YR 8/2	5	0	0	18	75	7	.4	48.9		
	Bk2	84-161	----do-------------	7.5 YR 7/3	2	0	0	14	79	7	.3	35.6		
	C	161-228+	----do-------------	7.5 YR 7/3	2	0	0	28	62	11	3.3	----		
M-2	Ap	0- 9	Loess and lake sediments.	7.5 YR 5/3	0	0	0	21	73	6	1.5	----	15	19
	A	9- 20	----do-------------	7.5 YR 5/3	0	0	0	22	70	9	1.1	----		
	Bw	20- 42	Lake sediments-----	7.5 YR 6/4	0	0	0	44	43	13	.3	----		
	Cox1	42- 50	----do-------------	7.5 YR 7/4	0	0	0	50	40	11	.1	5.5		
	Bk1	50- 61	----do-------------	7.5 YR 7/4	0	0	0	44	45	11	.2	13.9		
	Bk2	61- 71	----do-------------	7.5 YR 8/3	0	0	0	39	47	15	.4	35.5		
	Bk3	71-107	----do-------------	7.5 YR 8/3	0	0	0	6	81	14	.1	21.7		
	Cox2	107-155+	----do-------------	7.5 YR 7/3	0	0	0	6	82	12	.1	13.0		
M-3	Ap	0- 10	Loess and alluvium-	7.5 YR 5/3	10	10	2	28	57	15	6.5	----	19	35
	Bt	10- 32	----do-------------	7.5 YR 5/3	10	10	2	20	52	28	3.4	14.3		
	2Bkm	32- 35	Alluvium-----------	7.5 YR 8/0	20	5	2	17	66	17	1.2	50.4		
	2Bk	35- 73	----do-------------	7.5 YR 8/3	20	5	2	20	66	14	.4	56.0		
	2Bt	73-128	----do-------------	7.5 YR 6/3	5	0	0	19	73	7	.2	21.6		
	3Ckm	128-135+	----do-------------	7.5 YR 8/1	20	10	2	27	41	32	.3	51.0		
M-4	A1	0- 13	Loess and colluvium	7.5 YR 4/3	10	5	1	22	57	20	4.5	21.6	12	49
	A2	13- 37	----do-------------	7.5 YR 4/3	10	5	1	22	62	16	3.2	28.0		
	2BA	37- 50	Alluvium-----------	7.5 YR 7/3	30	1	0	36	50	15	1.3	53.8		
	2Bk	50- 71	----do-------------	7.5 YR 7/4	30	1	0	31	43	26	.7	54.6		
	3Ck	71-120	----do-------------	7.5 YR 8/3	10	5	2	17	73	10	.4	47.6		
	3C	120-140+	----do-------------	7.5 YR 7/3	10	5	2	19	53	29	.2	39.8		
M-5	Ap	0- 9	Loess and colluvium	7.5 YR 5/3	15	10	1	24	58	18	4.7	----	14	40
	A	9- 30	----do-------------	7.5 YR 5/4	15	10	1	21	53	26	2.7	12.8		
	BA	30- 44	----do-------------	7.5 YR 7/4	15	10	1	29	48	23	1.4	46.1		
	2Bkm	44- 52	Alluvium-----------	7.5 YR 8/2	20	10	0	32	48	20	.4	47.9		
	2Bk	52- 88	----do-------------	7.5 YR 8/3	20	10	0	38	43	19	.4	46.6		
	3CB	88-138	----do-------------	7.5 YR 7/4	40	1	0	31	48	21	.2	41.6		
	4C	138-149+	----do-------------	7.5 YR 7/4	5	0	0	34	48	18	.2	46.0		
M-6	Ap	0- 16	Slopewash colluvium	7.5 YR 4/2	5	0	0	31	56	13	9.8	10.7	16	7
	A	16- 37	Colluvium----------	7.5 YR 4/3	5	0	0	28	55	17	3.4	19.8		
	Bt	37- 69	----do-------------	7.5 YR 5/3	5	0	0	30	55	14	2.2	25.0		
	Ck	69- 98	----do-------------	7.5 YR 7/3	5	0	0	33	57	10	1.4	12.4		
	2C1	98-135	----do-------------	10 YR 7/3	10	0	0	28	49	23	.9	36.4		
	2C2	135-175+	----do-------------	10 YR 7/3	5	2	0	23	50	27	1.0	11.6		

---

[1] Horizon nomenclature of Guthrie and Witty (1982) and Birkeland (1984) except that master K horizon is not used.

[2] Particle-size distribution of <2 mm fraction using sieve-pipette methods (for example, Carver, 1971) and a Sedigraph for some silt-clay fractions with prior removal of carbonates and organic matter using methods of Jackson (1956).

[3] Percent organic matter by method of Walkley and Black (1934).

[4] Percent carbonate by method of Allison and Moodie (1965, p. 1387).

[5] Nonarid index of Harden and Taylor (1983).

[6] Method of Machette (1985a).

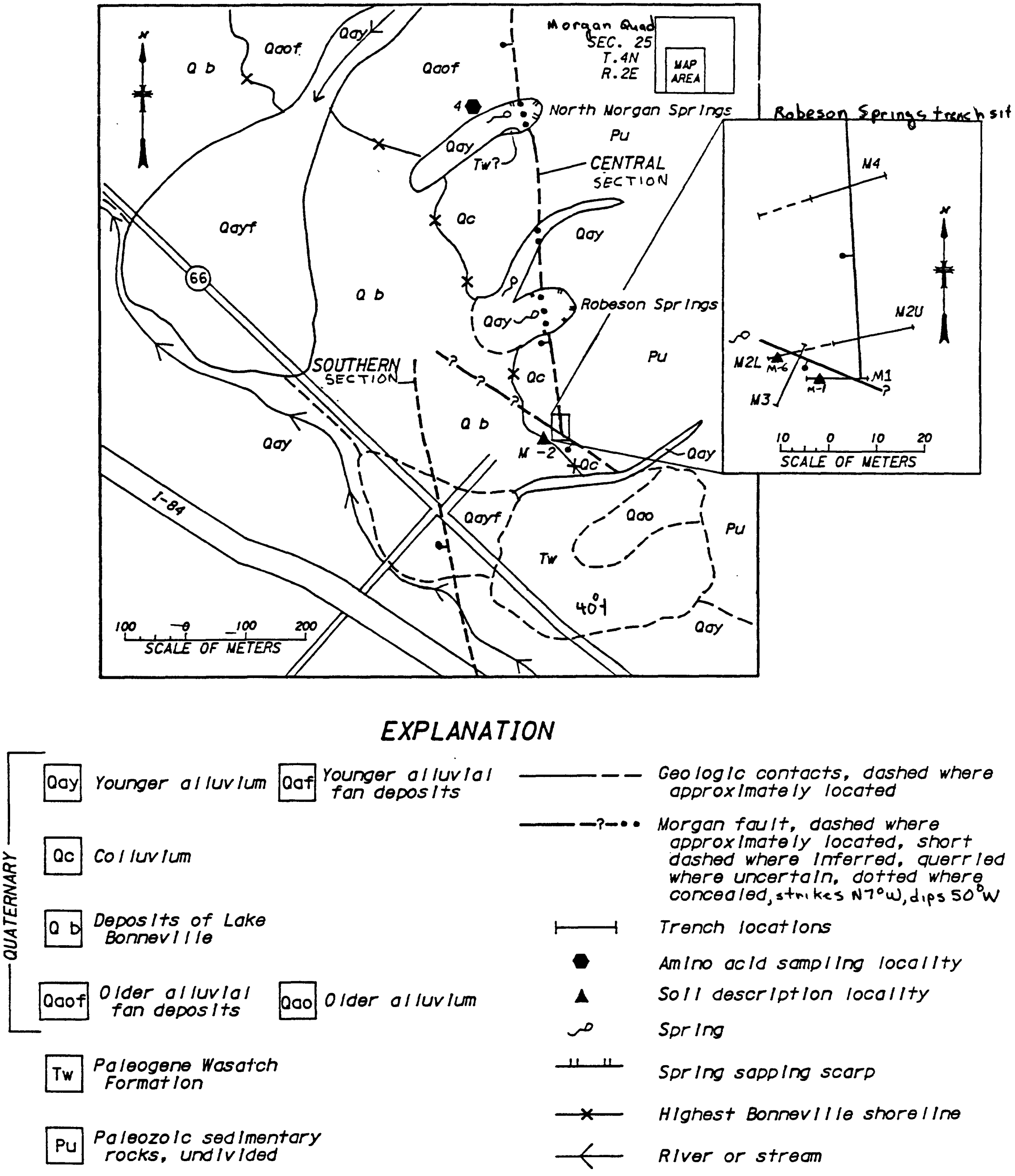

Figure 5.--Geologic map of the south end of the central section of the Morgan fault showing locations of trenches at the Robeson Springs trench site and sampling sites.

on alluvial and colluvial deposits along the central section of the Morgan fault (Table 1, fig. 4) makes the indices of Harden and Taylor (1983) (Table 1) less useful in estimating the age of these soils than the ages of many of the soils elsewhere in the Wasatch Range (Sullivan and others, 1986).

Rates of total pedogenic carbonate accumulation in soils is another method that has proven useful in estimating the age of soils in a number of areas in the arid and semi-arid western United States (Machette, 1985a). Age estimates based on total carbonate values cannot be relied on for soils significantly younger than the last interglacial (125 ka) (unless many independent age estimates for similar soils in the region are available) because of the probable major changes in carbonate accumulation rates over this period. However, over longer time spans, multiple cycles of climate change tend to attenuate accumulation rate changes and this results in relatively more accurate age estimates for older soils (Machette, 1985b; Colman and others, in press).

Using the methods of Machette (1985a) amounts of carbonate in g/cm^2 in the total profile were calculated for the Morgan soils and compared with values for carbonate-rich soils in the northern Wasatch Range with some independent age control. Sullivan and others (1986) calculated latest Pleistocene-Holocene (0 to 15 ka) carbonate accumulation rates as high as 1 g/cm^2/kyr using two soils (M-2 and M-6, table 2) in Morgan Valley and one soil in Heber Valley (about 65 km to the south). However, groundwater may have added carbonate to soil M-2 and primary carbonate values are difficult to estimate for all soils. The longer-term (0-150 ka) rate of Sullivan and others, (1986) is 0.5 g/cm^2/kyr (again based on only 3 soils along the Weber River, fig. 1) is roughly half the latest Pleistocene-Holocene rate. Based on their locations east of the crest of the Wasatch Range, it is unlikely that latest Pleistocene-Holocene carbonate accumulation rates for the back valley soils are higher than the 0.5 g/cm^2/kyr calculated by Scott and others (1982) for soils of similar age near Salt Lake City. Based on rates of about 0.15 g/cm^2/kyr for Fisher Valley (Colman and others, in press), 0.14 g/cm^2/kyr for the Beaver area (Machette, 1985b), and maximum rates of 0.14-0.26 g/cm^2/kyr for Spanish Valley (Harden and others, 1985) elsewhere in Utah, middle and late Quaternary rates in the eastern Wasatch Range may well have been <0.2 g/cm^2/kyr. We use 0.5 g/cm^2/kyr as a maximum rate to estimate minimum ages of 70 to 100 ka for soils M-3, M-4, and M-5 (Table 1). These calculations suggest soils on the alluvial fans (unit Qaof on fig. 4) are certainly >50 ka and probably of pre-last interglacial age (>125 ka). Because the fans are being eroded even finite soil ages would be minimum ages for the fan sediments.

Amino-acid ratios derived from the analysis of the organic matrix within carbonate fossils have proven useful in the relative dating and correlation of a variety of Quaternary stratigraphic units worldwide (Wehmiller, 1982). This methodology, termed aminostratigraphy by Miller and Hare (1980), is valid within a region as long as all samples have had very similar temperature histories and if the amino acids in the species analyzed racemize at about the same rate (Williams and Smith, 1977). Although most studies have used marine mollusks (Wehmiller, 1982), recent work indicates amino acid ratios from non-marine gastropods are useful for relative dating (Miller and others, 1982; Scott and others, 1983; Nelson and others, 1984; Barnes and others, 1986). The Paleozoic carbonates and alluvial fan surfaces with carbonate-rich soils along the central section of the Morgan fault provide a favorable environment for lime-loving terrestrial gastropods. The large terrestrial gastropod Oreohelix cf. strigosa is abundant in the surface litter along the trace of the fault and fragments and whole shells of this species were found in the older alluvial fan sediments (Qaof) and overlying colluvium (Qc) at four sites (fig. 4 and table 2). Ratios of D-alloisoleucine to L-isoleucine in these samples in the alluvium are >0.4 while those in the colluvial units range from 0.20 to 0.57, suggesting the shells are of several ages.

TABLE 2.-- FOLLOWING PAGE

Accurate numerical-age estimates are difficult to obtain from amino-acid ratios. These estimates require accurate kinetic models of amino-acid racemization in the mollusk genera of interest along with estimates of the temperature histories of the fossil samples. A +/- 1^{o} uncertainty in the effective diagenetic temperature (EDT) (integrated chemical effect of the sample's temperature history) results in a 20% uncertainty in the age estimate and we have no way of estimating the uncertainty in our EDTs. The diagenetic models we used were developed using different genera (table 2), but the models for many genera differ little and at the present time there is no reason to think these models do not apply to Oreohelix shells in Morgan Valley.

We used two kinetic models to calculate ages (minimum ages) for the samples (table 2). The linear model assumes a constant rate for the isoleucine racemization reaction in shells, but it probably only applies to our younger

TABLE 2. - D-alloisoleucine/L-isoleucine ratios in the total (free + peptide-bound) amino acid fraction and calculated ages for Oreohelix cf. strigosa from alluvial and colluvial sediments along the Morgan fault, Morgan Valley, Utah

[Leaders (---) indicate age not calculated]

INSTAAR lab no. (Univ. of Colo.)	Depth below surface (meters)	Number of sample preparations	Mean total alle/Ile ratio[1]	Minimum age estimate (ka)		Location[4]	
				Linear kinetic model[2]	Nonlinear model[3]	Site	Unit
			Modern surface float (MAT=7.2-7.7 °C)				
DAN-194	0	8	0.025+0.005	---	---	1	----
			North Morgan Springs				
DAN-190	>4	3	.61+ .05	709-777	1511-1660	4	Qaof
			Gravel pit				
DAN-207	2.3	3	.27+ .06	317-289	---	2	Qc
DAN-209	.7	3	.35+ .06	422-386	---	2	Qc
DAN-189	3	2	.41+ .06	456-503	---	2	Qaof
DAN-208	5.5	3	.43+ .04	485-530	---	3	Qaof
			Mahogony Canyon roadcut				
DAN-198	>1.6	3	.30+ .04	337-369	---	1	Qc
DAN-193, 195,196 197,199	>2	8	.49+ .06	582-637	861- 942	1	Qaof
			Trench M6, Mahogony Canyon[5]				
DAN-206	1.7	3	.20+ .01	214-234	---	1	Qc
DAN-201	5.0	3	.35+ .05	400-438	---	1	Qc
OAN-200	5.1	3	.57+ .03	691-757	1350-1478	1	Qc
DAN-203	6.0	3	.40+ .05	463-508	---	1	Qc
DAN-204	4.8	3	.44+ .03	515-564	---	1	Qaof
DAN-205	5.8	3	.46+ .03	542-593	677- 740	1	Qaof

[1] Alle/Ile ratio (peak area) measured using methods of Miller and Hare (1980). Mean ratios include one standard deviation. Extraneous values rejected using methods of Dixon (1965).

[2] Age calculated using a linear kinetic model of isoleucine racemization (equation 18 in Williams and Smith (1977)) with k = 0.77, a modern ratio of 0.025 for Oreohelix (Nelson, unpub. data), Arrhenius parameters determined for Vallonia by Nelson and others (1984), values of constants in Arrhenius equation (no. 9 in Williams and Smith, 1977), and an EDT for the late Quaternary in this region of 8 °C less than present mean annual temperature (Nelson and others, 1984) (for example, Wehmiller and Belknap, 1982). Age range calculated using +/-0.25 °C range in estimated EDT.

[3] Age calculated using a nonlinear model and Quaternary EDT (see footnote 2) (for example, Wehmiller, 1982) with the same relationships as for the linear model except that the reaction rate is assummed to decrease to one-fifth the initial rate for samples with alle/Ile ratios >0.4.

[4] As seen on figure 4.

[5] Trench discussed in detail in Sullivan and others (1986).

samples because the reaction rate has been shown to decrease markedly in older samples (Wehmiller, 1982). One of several possible non-linear models suggests much greater ages for the older samples. A few of the samples which were collected <2 m below the surface may have been affected by seasonal temperature changes (which would increase their apparent age), but because the alluvial fan sediments are being eroded most samples must have been buried more deeply during most of their burial history. If the shallower samples were <2 m deep for their entire burial history, the maximum possible surface heating effect would reduce our calculated ages by about half (for example, Wehmiller, 1977). Because of the large uncertainties in sample temperature histories and appropriate kinetic models only the linear-model age estimates (table 2) are used, which provide only minimum age estimates. However, enough is known about EDTs in the region and the reaction rate in gastropods to suggest that the samples from the colluvium with ratios of 0.20 and 0.27 are < 400 ka and <500 ka respectively.

Thus, based on 6 samples (table 2), the older alluvial fan deposits are >400 ka. The colluvial deposits overlie these older fan deposits at all the sampling sites. The lowest ratio obtained from colluvium, in the trench near Mahogany Canyon, suggests an age of >200 ka. Higher ratios from other colluvial units indicate that either these units are older or that shells in the slope colluvium are reworked from the older fan deposits. The minimum age estimates from the soil carbonate data are consistent with these age estimates from amino-acid ratios.

TRENCH INVESTIGATIONS OF QUATERNARY FAULTING ON THE CENTRAL SECTION OF THE MORGAN FAULT

The Morgan fault is exposed at the base of the escarpment in 2-m-high exposures at Robeson Springs (fig. 5) as a planar, N7°W striking, 65° west-dipping sheared contact between Paleozoic carbonates and light brown, silty colluvium. Sheared and altered dolomite is exposed for a distance of about 15 m to the east in the footwall of the fault, but no other shears are evident in the colluvial deposits in the exposure that extends about 25 m west of the fault. This exposure and additional exposures at North Morgan Springs (fig. 5) showed that unconsolidated deposits, exposed above the Bonneville shoreline, were displaced by the Morgan fault in a narrow zone at the base of the triangular facets on the escarpment.

The Robeson Springs trench site is located at the southern end of the central section of the Morgan fault (fig. 5). The linear trace of the footwall escarpment ends at a small, east-trending ephemeral drainage south of the trench site. South of this drainage red sandstone and conglomerate of the Wasatch Formation are exposed dipping 40° to the west and extending across the projection of the central section of the fault. Projection of the southern section of the fault north across the Weber River indicates that the Morgan fault steps westward about 200 m between the southern and central sections (figs. 2 and 5).

At the Robeson Springs site four trenches were excavated at or near the break-in-slope at the base of the footwall escarpment of the Morgan fault (fig. 5). Two of these trenches (M2U and M4) exposed the main trace of the Morgan fault. Another normal fault trending northwest between the central and southern sections of the Morgan fault is exposed in trenches M2U, M1, and M3. The Devonian and Cambrian dolomite which forms the escarpment is exposed in all the trenches. To the east it is overlain by Devonian and Mississippian sedimentary rocks that generally dip to the west, but that have been complexly folded and faulted (Mullens and Laraway, 1973). In trenches (M2U and M4) colluvial deposits overlie the dolomite in the hanging wall of the fault, but in the exposures at North Morgan Springs the colluvial deposits overlie older alluvial fan deposits that are correlated with similar deposits exposed at four locations north of the Robeson Springs site (figs. 4 and 5).

Stratigraphy in Trench M4

In trench M4 the Morgan fault is clearly expressed as a zone of sheared dolomite and fault gouge from within a meter of the ground surface to the base of the trench (fig 6). The fault zone juxtaposes colluvial deposits and bedrock along a N7°W striking, 50° west-dipping planar contact. The east boundary of the fault zone is an abrupt planar shear separating fractured bedrock (unit 1) from rock flour (unit 1b) which is interpreted to be a fine-grained fault breccia derived from the bedrock. Near the base of the trench a plastic clay gouge (unit 1c) forms part of the fault zone.

FIGURE 6.-- FOLLOWING PAGE

On the west margin of the fault zone a 4-m-thick sequence of colluvial deposits have been displaced by the fault (fig 6, units 3, 6, 7a, and 7b). The colluvial deposits are all of similar lithology--clayey silts with variable but small (<15%) amounts of dispersed, angular pebbles of dolomite. Using slight differences in color, clay content, carbonate content and induration, three main colluvial units (unit 3, unit 6, and unit 7) have been mapped and separate facies within each unit (small letters) have been identified. Unit 3 is massive, well-indurated, and contains upper and lower zones of pedogenic carbonate (stage II). Unit 6 is siltier, lacks carbonate, and is loose and unconsolidated. The modern soil is developed in unit 7, including a the cambic B-horizon with weak stage II carbonate in some parts (unit 7a).

Discrete, downslope-thinning, colluvial wedges that are derived from erosion

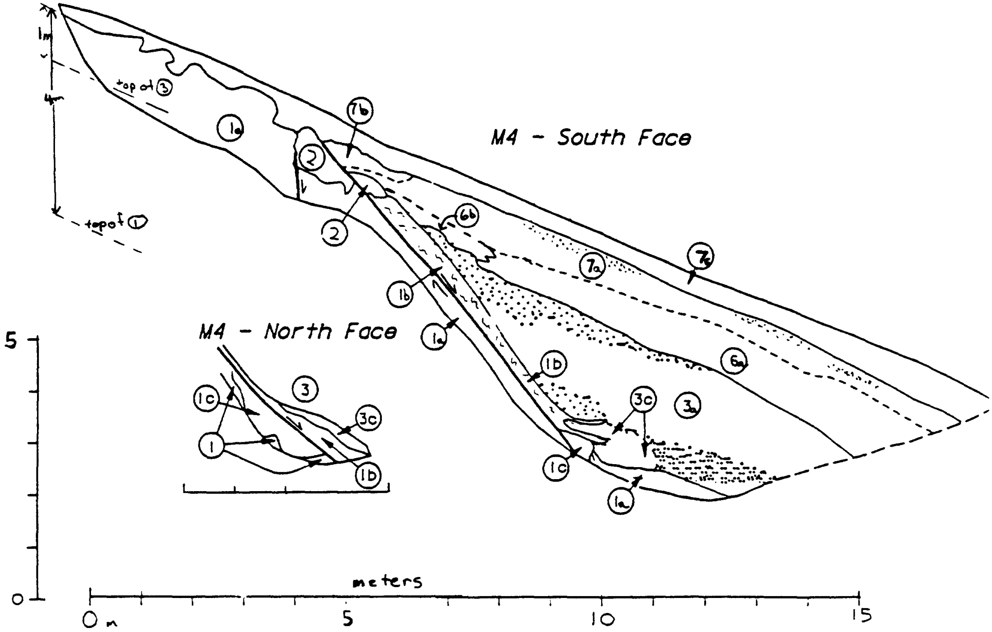

UNIT DESCRIPTIONS

7c	Colluvium - dark brown (10YR 3/3 to 7.5 YR 3/4), loose, pebbly, silt with organic material, A-horizon. (HOLOCENE)
7b	Colluvium - dark brown (10YR 3/3 to 7.5YR 3/4), loose, pebbly silt. (HOLOCENE)
7a	Colluvium - light brown (7.5 YR 7/4), moderately indurated, pebbly silt with calcic B and BCa horizon. (HOLOCENE)
6b	Colluvium and loess - brown (7.5 YR 8/4 to 6/6), firm, pebbly, clayey silt (HOLOCENE)
6a	Colluvium and loess - brown (7.5 YR 8/4 to 6/6), loose, clayey silt. (HOLOCENE)
3c	Colluvium - yellowish-brown (10 YR 6/6), well-indurated, pebbly clay (MID-PLEISTOCENE)
3a	Colluvium - light brown (10 YR 6/4), moderately-indurated, pebbly, clayey silt. (MIDDLE AND LATE PLEISTOCENE)
2	Colluvium - yellow (10 YR 7/4), well-indurated, sandy silt. (MID-PLEISTOCENE)
1a	Dolomite - dark grey (2.5 Y 4/2), moderately weathered with no recognizable bedding, DCd of Mullens and Laraway (1973). (PALEOZOIC)
1b	Fault breccia - dark grey (2.5 Y 4/2), uncemented silt-size dolomite fragments.
1c	Fault gouge - yellow (2.5 Y 7/8) plastic clay.

—— contacts, dashed where indistinct

⁖ zones of carbonate accumulation

⇊ fault

⟆⟆ fault zone

Figure 6.--Log of trench M4 at the Robeson Springs trench site showing faulted middle and late Quaternary colluvial deposits at the southern end of the central section of the Morgan fault. Dashed lines at the left are projections of displaced surfaces with the amount of the displacement indicated. Units 3b, 4, and 5, which are not exposed in this trench, are exposed in trenches M1, M2, and M3 (fig. 5) and are discussed in Sullivan and others (1986).

of the free face of a fault scarp are typically found adjacent to faults with scarps more than a meter high in unconsolidated deposits. The stratigraphy and thickness of these colluvial wedges have been used to estimate the size of the individual surface displacements on faults (for example, Schwartz and Coppersmith, 1984). Near the floor of trench M4, two 0.1-m-thick, 0.5- to 0.8-m-long fingers of fault breccia (unit 1b) are interbedded with colluvial unit 3c (fig. 6). This interbedding of fault breccia and colluvium appears to have resulted from the erosion of fault breccia from the free face of a scarp that was formed during two separate surface displacements on the fault. The colluvium between these fingers of fault breccia is 0.4 m thick, and 0.5 m of colluvium is preserved between the lower finger and the underlying bedrock. These thicknesses provide minimum estimates of the height of the scarp and the vertical displacement that produced it.

The lack of discrete horizons within unit 3a suggests that it did not accumulate as a succession of scarp-derived colluvial wedges. Unit 3a consists of 2 m of massive pebbly, clayey silt deposited by surface wash aand creep from above the trench site. The uniform thickness of fault breccia preserved adjacent to this unit along a planar 50° west-dipping contact indicates that unit 3a has been faulted into its present position. We interpret this unit to consist of multiple, indistinguishable colluvial units that have been downdropped along the fault during successive small surface displacements and subsequently buried by continuing deposition from the escarpment above the fault. These colluvial units inferred to comprise unit 3 are lithologically identical; unconformities between them or any differences in soil development from one unit to another have apparently been masked by carbonate accumulation. Based on the depth of carbonate in the modern soil (unit 7a) the pedogenic carbonate zones of unit 3 probably developed 1 to 2 m below the ground surface. The lack of interbedding within unit 3 (other than at the floor of the trench where fingers of fault breccia divide portions of unit 3c) indicates that the displacements did not expose the fault breccia in the scarp free face. This indicates that the individual surface displacements were not significantly greater than the present thickness of slope colluvium (unit 7c), about 0.5 m, on the footwall of the fault. Thus, the displacements were probably about the size of the minimum displacements inferred from the thickness of colluvium preserved below the fingers of fault breccia near the floor of the trench.

The total displacement since the deposition of unit 3c has been estimated by projecting the base of the unit 3 to the footwall of the fault using the same slope as the ground surface (fig. 6). The measured vertical displacement between the bedrock surface and the top of unit 3 is about 4.0 m.

In the upper portion of trench M4 the apparent displacement of the base of unit 6a records the most recent displacement event on the fault at this locality. Unit 6b is a slightly pebblier upslope facies of unit 6a, a key stratigraphic unit which is present in all of the trenches at the site and which overlies a dated peat deposit in trenches M2 and M3 (discussed below). The amount of this displacement has been estimated by projecting the base of unit 6a to the footwall of the fault using the same slope as that of the present ground surface (fig. 6). The measured vertical displacement between the bedrock surface and the base of unit 6a is about 1.0 m. The fault plane on which this displacement occurred is preserved in unit 2, a lighter colored, well-indurated, pocket of colluvium, as a carbonate-impregnated plane dipping 50° to the west.

Estimated displacements of 0.5 to 1 m per event are small compared with those estimated for other Quaternary faults in Utah (for example, Schwartz and Coppersmith, 1984; Nelson and Van Arsdale, 1986; Nelson and Sullivan, this volume). These small displacements and empirical relationships (for example, Bonilla and others, 1984) between earthquake magnitude and the amount of surface displacement suggest paleoearthquake magnitudes of 6 1/2 to 7 for the Morgan fault. Similar relationships between earthquake magnitude and fault rupture length also suggest paleoearthquake magnitudes of 6 1/2 to 7 for the 16 km-long Morgan fault.

The preservation of unit 2 directly above the main fault appears to be related to an earlier displacement. A near-vertical carbonate-filled shear extends from the base of unit 2 to the floor of the trench in the bedrock east of the main fault and strikes N8°E across the trench. Unit 7a and its more pebbly upslope facies, unit 7b, are interpreted to be parts of a horizon of slope colluvium downdropped to its present position by the most recent displacement event on the main fault zone. Unit 6b thins upslope to its contact with unit 2 in the hanging wall of the fault and it is not clear if it ever extended across the fault. The predominance of silt and the lack of induration in unit 6 suggest that it consists principally of loess (or loess redeposited by surface wash) rather than slope colluvium eroded from the escarpment. It is the only colluvial unit in this and other trenches that thickens downslope suggesting that it was deposited only on the lower parts of the slope and may not have extended across the fault zone.

Ages of faulted deposits

Estimates of the ages of displaced colluvial deposits at the Robeson Springs trench site are based on radiocarbon dates on peat interbedded with colluvial deposits in trenches M2L and M3, and on amino-acid ratios from snails in colluvial and alluvial fan deposits exposed in four other locations along the central segment of the Morgan fault. In trenches M2L and M3 a small (3 m by 6 m) bog deposit of peat is exposed that underlies colluvial unit 6 and overlies bedrock in the hanging wall of the Morgan fault. Unit 6 is correlated between trench M4 and the other trenches, 32 m to the south (fig. 5), on the basis of similar lithology and stratigraphic and geomorphic position (Sullivan and others, 1986). Radiocarbon dates of 8.3 ka on peat (Beta-9244) and 9.1 ka on wood (Beta-9244) from this deposit indicate an early Holocene age for the bog and an early or middle Holocene age for the overlying colluvial unit 6.

A post-early Holocene displacement event of 1 m might be expected to have produced scarps along the central section of the fault that would still be visible today. Scarps 1 m high on gently sloping alluvial fans probably would be preserved for tens of thousands of years (Hanks and others, 1984). However, the Morgan fault is mapped at the base of a 20 to 25° sloping escarpment and figure 6 shows that the 1-m-high scarp has been completely covered since the deposition and faulting of unit 6. Erosion and deposition of younger alluvial deposits apparently obliterated the scarp in drainages crossing the escarpment.

We infer a middle to late Pleistocene age for the older colluvial deposits (unit 3) in trench M4 by using their similar lithology, degree of carbonate development, stratigraphic position, depth, and position adjacent to the fault to correlate them with the sequence at Mahogony Creek for which we have amino-acid age estimates (table 2). At Mahogany Creek about 2.5 km north of the Robeson Springs trench site (fig. 4), a similar sequence of colluvial deposits varies in thickness from 7 m in a trench at the mountain front to about 1 m in a roadcut 180 m to the west. In the trench at Mahogany Canyon this colluvium overlies older alluvial fan deposits in which a petrocalcic horizon with stage IV carbonate is developed. This degree of pedogenic carbonate development suggests that the fan deposits are at least 200 to 300 ka and probably >500 ka. Snails from this colluvium at depths of 1 to 5 m, and from other sites at similar depths have estimated ages of 200 to 400 ka or greater (discussed above, table 2). However, the upper parts of unit 3 may date from the late Pleistocene (10-125 ka), for individual units can not be correlated from Mahogany Creek to Robeson Springs.

Events in trench M4

On the basis of the stratigraphic relations in trench M4 and our estimates of the age of the colluvial deposits we have interpreted the following sequence of events:

1) During the middle and late Pleistocene units 3a and 3c were deposited as a series of 0.5 to 1.0 m thick horizons of slopewash that were downdropped and preserved by a series of small displacement events comprising a total of 3 m of displacement on the Morgan fault. Prior to or during this period unit 2 was deposited as slopewash across the fault zone, and displaced about 1 m on a near vertical shear which resulted in its preservation from erosion above the main fault zone.

2) Following an interval of non-deposition of unknown duration, a depression in in the hanging wall of the fault exposed in trench M2L (fig. 5) was filled with bog deposits (radiocarbon dates of 8.3 and 9.1 ka).

3) Unit 6 was deposited above unit 3 and the bog deposits principally as loess that may have been derived from exposed Lake Bonneville sediments in the valley.

4) Units 7a and 7b were deposited by surface wash across the fault zone.

5) Units 2, 7a, and 7b were displaced about 1.0 m along the main fault zone.

6) Modern surface wash continued to deposit colluvium (unit 7c) on the slope.

Other trenches

In trench M2, about 30 m south of M4 (fig. 5), vertical relief on the bedrock surface across the projection of the fault exposed in M4 is about 3.5 m, although the fault plane is not distinct. A 1.5-m-high, near vertical displacement of the bedrock surface striking N7°W marks the Morgan fault in this trench. This step is overlain by about 1.0 m of undisplaced colluvium with the same lithology and in the same stratigraphic position as units 7 and 7a in trench M4 (Sullivan and others, 1986). Below this horizon, massive colluvium about 1.5 m thick, equivalent to unit 3 in trench M4, is also interpreted to have been displaced during small (<1 m) faulting events (Sullivan and others, 1986).

About 10 m south and west of trench M2, a normal fault striking N65°W and dipping about 50° to the southwest that is exposed in trenches M1, M3, and the lower portion of M2 (M2L), displaces fine-grained colluvial deposits equivalent to unit 3 (figs. 5 and 6), but overlying colluvial units are not displaced. Trench M1 crosses the projection of the N7°W striking fault exposed in trenches M2U and M4 and shows that the main trace of the Morgan fault has been terminated by this northwest-striking fault, as suggested by the bedrock relationships at the trench site (discussed earlier). The base of the colluvium was not exposed in the hanging wall of the fault in trench M1 precluding an estimate of the amount of displacement since the deposition of the colluvial deposits.

SLIP RATES ON THE MORGAN FAULT

Quaternary slip rates

Mapping and trench investigations on the central section of the Morgan fault provided evidence that middle to late Pleistocene and Holocene displacements have occurred on this back valley fault. At the Robeson Springs trench site, two faults were identified: 1) the north-trending central section of the main fault that displaces middle to late Pleistocene and Holocene colluvial deposits 4 m, and 2) a northwest-trending trace of a subsidiary fault that displaces similar middle to late Pleistocene colluvial deposits. Radiocarbon dates of 8.3 and 9.1 ka provide a maximum age for the younger colluvium that has been displaced about 1 m by the main fault in trench M4. Assuming the lower part of the underlying sequence of colluvial deposits in trench M4 is 200-400 ka, 4 m of displacement yields a middle to late Pleistocene slip rate of 0.01 to 0.02 mm/yr. Because only 1 event is recorded an Holocene slip rate can not be calculated. These Pleistocene slip rates are an order of magnitude lower than long-term Pleistocene rates on the Wasatch fault (Machette and others, this volume), but some other faults in the region may have rates nearly this low (Nelson and Van Arsdale, 1986; McCalpin and others, this volume; Nelson and Sullivan, this volume).

We interpret the colluvial stratigraphy in trench M4 as suggesting recurrent Quaternary surface displacements of 0.5 to 1.0 m. If 0.5 m most nearly represents the average size of the surface displacement events that are represented by the 4 m of displacement in at least the last 200 to 400 ka as suggested by the lack of discrete scarp-derived colluvial wedges in the trench, about 8 individual events have occurred. These estimates yield a minimum average middle to late Quaternary event recurrence interval of 25 to 50 kyr. If only four events of 1 m displacement have occurred, the minimum average recurrence interval would be 50 to 100 kyr.

Cenozoic slip rates

The effect of the late Cenozoic uplift of the Wasatch Range on the evolution of landforms in Morgan Valley partly depends on the distribution of late Cenozoic faults. Naeser and others (1983) estimate uplift rates of 0.8 mm/yr over the last 5 Ma and 0.4 mm/yr over the last 10 Ma for the north-central Wasatch Range west of Morgan Valley. As shown in a section across the northern section of Morgan Valley constructed by Hopkins (1982, her fig. 5), the faults bounding the west side of Morgan Valley mapped by Bryant (1984) have limited displacement and the structural relief in the valley is primarily due to Cenozoic displacement on the Morgan fault. If the late Cenozoic slip rate on the Wasatch fault is much greater than that of the Morgan fault, the effect of this relative uplift of the Wasatch Range would be to accelerate late Cenozoic erosion in Morgan Valley. The Weber River has incised the Norwood Tuff more than 300 m in Morgan Valley (fig. 3) indicating that this is the case and suggesting that the average late Cenozoic slip rate on the Morgan fault is much lower than that of the Wasatch fault.

The thickness and attitude of the Huntsville fanglomerate adjacent to the northern section of the Morgan fault provide an estimate of the average Cenozoic slip rate on the fault. In the cross section of Hopkins (1982), the Huntsville fanglomerate overlies the late Eocene-early Oligocene Norwood Tuff and dips 13° to the east with an estimated maximum thickness of 1000 m adjacent to the Morgan fault which provides a minimum estimate of displacement since deposition of the fanglomerate. The age of this deposit is poorly constrained; the previous workers have suggested it is of Pliocene age (Eardley, 1944; Coody, 1957). However, similar unconsolidated gravel deposits of Oligocene age have been mapped further south in the Wasatch Range overlying and interbedded with the Oligocene Keetley volcanics (Bromfield and Crittenden, 1971; Sullivan and others, 1986). Using an age range of 5 - 35 Ma for the Huntsville fanglomerate and a minimum displacement estimate of 1000 m yields an estimated average middle and late Cenozoic slip rate of 0.03 to 0.2 mm/yr.

The tilting of late Cenozoic erosion surfaces adjacent to the northern section of the fault also provides a crude estimate of the average late Cenozoic slip rate on the fault. In this area locally well-preserved, gently (0.5 - 1.7°) east-dipping erosion surfaces, cut on the Huntsville fanglomerate, slope up to 1.7° northeast, into the fault (fig 2). Based on our observations in less dissected terrains of the Weber River drainage, these surfaces probably once sloped at least 3° towards the center of the valley; therefore, we interpret the back tilting of these surfaces to have resulted from displacement on the Morgan fault. If the most steeply tilted surface, south of Bohman Hollow and 1.7 km west of the main trace of the fault, has been uniformly rotated from a 3° westerly dip to its present 1.7° easterly dip, then projection of this surface to the fault indicates about 150 m of displacement. If the erosion surface has been down dropped relative to the footwall as well as rotated, total displacement would be greater. These erosion surfaces are probably significantly older than a much lower erosion surface on the west side of the valley paleomagnetically dated at >730 ka (fig. 2). Assuming an age of 1 to 5 Ma for this surface yields an average latest Cenozoic slip rate of 0.03 to 0.15 mm/yr for this section of the fault, which is consistent with the rate estimated from the thickness and age of the Huntsville fanglomerate.

These slip rate values are poorly constrained and do not take into account probable significant variations in slip rates during the late Cenozoic. Estimates of 0.01 to 0.02 mm/yr determined at the Robeson Springs trench site for the middle to late Quaternary are at the low end of the ranges of late Cenozoic slip rates. Because we infer only one Holocene event and our estimates of average minimum recurrence intervals range from 25-100 ka, we have no way of judging whether the Holocene slip rate or recurrence differs from our estimates for the middle to late Quaternary, as has been suggested for the Great Basin by Wallace (1984) and for the Wasatch fault by Machette and others (1986). Our dating control is too imprecise to determine whether there has been a significant change in slip rates during the late Cenozoic. If there is a difference in rates, middle to late Quaternary rates on the Morgan fault are probably lower than for earlier periods.

CONCLUSIONS

Mapping and trenching of the central section of the Morgan fault demonstrates that surface displacements have occurred on the fault during the middle Pleistocene and Holocene. Colluvial deposits, estimated from amino-acid ratios on gastropods found in correlative deposits to be at least 200 - 400 ka, are displaced 4.0 m at the Robeson Springs trench site. These data yield an average middle to late Pleistocene slip rate of 0.01 to 0.02 mm/yr. These rates are near the low end of the range of estimates of the late Cenozoic slip rate on the Morgan fault based on the tilting of late Cenozoic erosion surfaces and estimates of the displacement of a Cenozoic fanglomerate. Radiocarbon dates of 8.3 ka and 9.1 ka on bog deposits beneath Holocene alluvial units show that the most recent surface displacement event (approximately 1 meter) post-dates deposition of the bog deposits. The colluvial stratigraphy in one trench at the site is interpreted as showing that individual surface displacements on the fault have been small (0.5 to 1 m). These small displacements, the limited length of the fault, and empirical displacement-earthquake magnitude relationships suggest that paleoearthquakes in the magnitude range 6 1/2 to 7 have occurred on the Morgan fault.

ACKNOWLEDGEMENTS

This study is part of a regional seismotectonic study for assessment of seismic hazards to U. S. Bureau of Reclamation dams in the Wasatch Range in central Utah (Sullivan and others, 1986). The staff of the Bonneville Construction Office, U. S. Bureau of Reclamation, provided the logistic support essential to completion of this work. We especially thank Mr. Leyland Kippen and the Union Pacific Railroad for permission to excavate on their properties. Ed Baltzer and Carol Krinsky assisted in the trench logging. Dean Ostenaa reviewed early drafts of this manuscript. Soils analyses by Rolf Kihl, INSTARR, University of Colorado, are appreciated. Nelson determined amino acid ratios in the Amino Acid Geochronology Laboratory, INSTARR, with the help of Dan Goter, under the direction of Gifford Miller.

REFERENCES CITED

Allison, L. E., and Moodie, C. D., 1965, Carbonate, in Black, C. A., Methods of soil analysis, part 2, Chemical and microbiological properties: Madison, Wisconsin, American Society of Agronomy, p. 1379-1396.

Anderson, L. W., and Miller, D. G., 1979, Quaternary fault map of Utah: Long Beach, California, Fugro, Inc., 39 p., scale 1:1,000,000.

Arabasz, W. J., Smith, R. B., and Richins, W. D., 1980, Earthquake studies along the Wasatch front, Utah--Network monitoring, seismicity, and seismic hazards: Bulletin of Seismological Society of America, v. 70, p. 1479-1500.

Arabasz, W. J., Observational seismology and earthquake hazards evaluation in the Wasatch Front area, in Hays, W. W., and Gori, Paula, eds., Assessment of regional earthquake hazards and risk along the Wasatch Front, Utah: U.S. Geological Survey Professional Paper, this volume.

Armstrong, R. L., 1968, Sevier orogenic belt in Nevada and Utah: Geological Society of America Bulletin, v. 79, p. 429-459.

Barnes, D. A., Clark, P. U., and Nelson, A. R., 1986, Preliminary aminostratigraphy of Mississippi Valley loess: Programs and abstracts of the 9th biennial meeting, American Quaternary Association, University of Illinois, Champaign-Urbana, p. 117.

Birkeland, P. W., 1984, Soils and Geomorphology: New York, Oxford University Press, 372 p.

Bonilla, M. G., Mark, R. K., and Lienkaemper, J. J., 1984, Statistical relations among earthquake magnitude, surface rupture length, and surface fault displacement: Bulletin of Seismological Society of America, v. 74, p. 2379-2411.

Bromfield, C. S., and Crittenden, M. D., 1971, Geologic map of the Park City East quadrangle, Summit and Wasatch Counties, Utah, U.S. Geological Survey Geologic Quadrangle Map GQ-852, scale 1:24000.

Bryant, Bruce, 1984, Reconnaissance geologic map of the Precambrian Farmington Canyon Complex and surrounding rocks in the Wasatch Mountains between Ogden and Bountiful, Utah: U. S. Geological Survey Miscellaneous Investigations Map I-1447, scale 1:50,000.

Bull, W. B., 1977, The alluvial-fan environment: Progress in Physical Geography, v. 1, p. 222-270.

Campbell, J. A., 1978, Cenozoic structural and geomorphic evolution of the Canyon Range, central Utah: Salt Lake City, University of Utah, Ph.D. thesis, 158 p.

Carver, R. E., ed., 1971, Procedures in Sedimentary Petrology: New York, Wiley-Interscience, 653 p.

Colman, S. M., Choquette, A. F., Hawkins, F. F., Physical, soil, and paleomagnetic stratigraphy of the upper Cenozoic sediments in Fisher Valley, southeastern Utah: U.S. Geological Survey Bulletin, (in press).

Coody, G. L., 1957, Geology of the Durst Mountain-Huntsville area: Salt Lake City, University of Utah, M.S.thesis, 63 p.

Dixon, W. J., 1965, Extraneous values, in Black, C. A., Methods of soil analysis, part 2, Chemical and microbiological properties: Madison, Wisconsin, American Society of Agronomy, p. 43-49.

Eardley, A. J., 1944, Geology of the north-central Wasatch Mountains, Utah: Geological Society of America Bulletin, v. 55, p. 819-894.

Eardley, A. J., 1955, Tertiary history of north central Utah, in Eardley, A. J., ed., Tertiary and Quaternary geology of the eastern Bonneville Basin: Utah Geological Society, Guidebook to the Geology of Utah, No. 10, p. 37-44.

Funk, J. W., 1976, Climatic and tectonic effects on alluvial fan systems, Birch Creek Valley, east central Idaho: Lawrence, University of Kansas, Ph.D. thesis, 246 p.

Gilbert, G. K., 1928, Studies of Basin and Range structure: U.S. Geological Survey Professional Paper 153, 89 p.

Gile, L. H., Peterson, F. F., and Grossman, R. B., 1966, Morphological and genetic sequences of carbonate accumulation in desert soils: Soil Science, v. 101, p. 347-360.

Guthrie, R. L., and Witty, J. E., 1982, New designations for soil horizons and layers and the new Soil Survey Manual: Soil Science Society of America Journal, v. 46, p. 443-444.

Hanks, T. C., Bucknam, R. C., Lajoie, K. R., and Wallace, R. E., 1984, Modification of wave-cut and faulting-controlled landforms: Journal of Geophysical Research, v. 89, no. B7, p. 5771-5790.

Harden, D. R., Biggar, N. E., and Gillam, M. L., 1985, Quaternary deposits and soils in and around Spanish Valley, Utah, in Weide, D. L., ed., Soils and Quaternary geology of the southwestern United States: Geological Society of America Special Paper 203, p. 43-64.

Harden, J. W., and Taylor, E. M., 1983, A quantitative comparison of soil development in four climatic regimes: Quaternary Research, v. 20, no. 3, p. 342-359.

Hopkins, D. L., 1982, A structural study of Durst Mountain and the north central Wasatch Mountains, Utah: Salt Lake City, University of Utah, M.S. thesis, 50 p.

Hopkins, D. L., and Bruhn, R. L., 1983, Extensional faulting in the Wasatch Mountains, Utah [abs.]: Geological Society of America, Abstracts with Programs, v. 15, n. 5, p. 402.

Hunt, C. B., 1982, The anomalous transverse canyons of the Wasatch Range, in Nielson, D. L., ed., Overthrust belt of Utah: Salt Lake City, Utah Geological Association Publication No. 10, p. 81-89.

Jackson, M. L., 1956, Soil Chemical Analysis, Advanced Course : Madison, University of Wisconsin, Department of Soil Science [unpublished], 656 p.

Lamerson, P. R., 1982, Fossil Basin area and its relation to the Absaroka thrust system, in Powers, R. B., ed., Geological studies of the Cordilleran thrustbelt: Denver, Rocky Mountain Assocation of Geologists, p. 279-340.

Machette, M. N., 1985a, Calcic soils of the southwestern United States in Weide, D. L., ed., Soils and Quaternary geology of the southwestern United States: Geological Society of America Special Paper 203, p. 1-23.

Machette, M. N., 1985b, Late Cenozoic geology of the Beaver Basin, southwestern Utah: Brigham Young University Studies in Geology, v. 32, part 1, p. 19-37.

Machette, M. N., Personius, S. F., Scott, W. E., and Nelson, A. R., Quaternary geology along the Wasatch Front--Evidence for ten fault segments and large-scale changes in slip rate along the Wasatch fault zone, in Hays, W. W., and Gori, Paula, eds., Assessment of regional earthquake hazards and risk along the Wasatch Front, Utah: U.S. Geological Survey Professional Paper, this volume.

McCalpin, James, Robison, R. M., and Garr, J. D., Neotectonics of the Hansel Valley-Pocatello Valley Corridor, northern Utah and southern Idaho, in Hays, W. W., and Gori, Paula, eds., Assessment of regional earthquake hazards and risk along the Wasatch Front, Utah: U.S. Geological Survey Professional Paper, this volume.

McKee, M. E., and Arabasz, W. J., 1982, Microearthquake studies across the Basin and Range-Colorado Plateau transition zone in central Utah, in Nielson, D. L., ed., Overthrust belt of Utah: Salt Lake City, Utah Geological Association Publication No. 10, p. 137-149.

Miller, G. H., and Hare, P. E., 1980, Amino acid geochronology: Integrity of the carbonate matrix and potential of molluscan fossils, in Hare, P. E., Hoering, T. C., and King, K., Jr., eds., Biogeochemistry of Amino Acids: New York, John Wiley, p. 415-443.

Miller, G. H., McCoy, W. D., and Nelson, A. R., 1982, Environmental controls in the amino acid racemization rate from continental-interior deposits: Geological Society of America, Abstracts with Programs, v. 14, no. 7, p. 565.

Mullens, T. E., and Laraway, W. H., 1973, Geologic map of the Morgan 7.5-minute quadrangle, Morgan County, Utah: U.S. Geological Survey Miscellaneous Field Studies Map MF-318, scale 1:24,000.

Nakata, J. K., Wentworth, C. M., and Machette, M. N., 1982, Quaternary fault map of the Basin and Range and Rio Grande Rift provinces, western United States: U.S. Geological Survey Open-File Report 82-579, scale 1:2,500,000.

Naeser, C. W., Bryant, Bruce, Crittenden, M. D., and Sorenson, M. L., 1983, Fission-track ages of apatite in the Wasatch Mountains, Utah--An uplift study, _in_ Miller, D. M., Todd, V. R., and Howard, K. A., eds., Tectonic and stratigraphic studies in the eastern Great Basin: Geological Society of America Memoir 157, p. 29-36.

Nelson, A. R., and Martin, R. A., 1982, Seismotectonic study for Soldier Creek Dam, Central Utah Project: Seismotectonic Report 82-1, Engineering and Research Center, U.S. Bureau of Reclamation, Denver, CO, 115 p.

Nelson, A. R., Madole, R. F., Evanoff, Emmett, Piety, L. A., Scott, G. R., 1984, Quaternary paleotemperature estimates using amino-acid ratios measured on terrestrial gastropods from fluvial sequences in Colorado: Boulder, CO, American Quaternary Association, 8th biennial meeting, Program and Abstracts, p. 92.

Nelson, A. R., and Sullivan, J. T., Late Quaternary slip rates on the James Peak fault, southernmost Cache Valley, north-central Utah, in Hays, W. W., and Gori, Paula, eds., Assessment of regional earthquake hazards and risk along the Wasatch Front, Utah: U.S. Geological Survey Professional Paper, this volume.

Nelson, A. R., and VanArsdale, R. B., 1986, Recurrent late Quaternary movement on the Strawberry normal fault, Basin and Range -- Colorado Plateau transition zone, Utah: Neotectonics, v. 1, p. 1-30.

Royse, Frank, Jr. Warner, M. A., Reese, D. L., 1975, Thrust belt structural geometry and related stratigraphic problems, Wyoming-Idaho-northern Utah, in Bolyard, D. W., ed., Symposium on deep drilling frontiers of the central Rocky Mountains: Denver, Colorado, Rocky Mountain Association of Geologists, p. 41-54.

Schick, R. B., 1955, Geology of the Morgan-Heneter Area, Morgan and Summit Counties, Utah: Salt Lake City, University of Utah, M.S. thesis, 54 p.

Scott, W. E., Shroba, R. R., and McCoy, W. D., 1982, Guidebook for the 1982 Friends of the Pleistocene, Rocky Mountain Cell, field trip to Little Valley and Jordan Valley, Utah: U.S. Geological Survey Open-File Report 82-845, 58 p.

Scott, W. E., McCoy, W. D., Shroba, R. R., and Rubin, Meyer, 1983, Reinterpretation of the exposed record of the last two cycles of Lake Bonneville, western United States: Quaternary Research, v. 20, p. 241-265.

Schwartz, D. P., and Coppersmith, K. J., 1984, Fault behavior and characteristic earthquakes--examples from the Wasatch and San Andreas fault zones: Journal of Geophysical Research, v. 89, no. B7, p. 5681-5698.

Shroba, R. R., 1982, Soil B-horizon properties as age indicators for late Quaternary deposits along the Wasatch Front, north-central Utah [abs.]: Geological Society of America Abstracts with Programs, v. 14, no. 4, p. 233.

Smith, R. B., and Bruhn, R. L., 1984, Intraplate extensional tectonics of the eastern Basin and Range--Inferences on structural style from seismic reflection data, regional tectonics, and thermal-mechanical models of brittle-ductile deformation: Journal of Geophysical Research, v. 89, no. B7, p. 5733-5762.

Sullivan, J. T., and Nelson, A. R., 1983, Late Cenozoic faulting in Heber and Keetley valleys, northeastern Utah, _in_ Crone, A. J., ed., Paleoseismicity along the Wasatch front and adjacent areas, central Utah, _in_ Geologic excursions in neotectonics and engineering geology in Utah, Geological Society of America, Fieldtrip guidebook for Rocky Mountain and Cordilleran Section Meeting - Part IV: Utah Geologic and Mineral Survey Special Studies 62, p. 55-61.

Sullivan, J. T., Nelson, A. R., Martin, R.A., Jr., Foley, L. L., Baltzer, E. M., and Krinsky, C. M., 1986, Regional seismotectonic study for the Central Utah Project, Utah: Seismotectonic Section Report 86-3 [unpublished], U. S. Bureau of Reclamation, Denver, Colorado, (in press).

Swan, F. H., III, Schwartz, D. P., and Cluff, L. S., 1980, Recurrence of moderate to large magnitude earthquakes produced by surface faulting on the Wasatch fault zone, Utah: Bulletin Seismological Society of America, v. 70, no. 5, p. 1431-1462.

Swan, F. H., III, Hanson, K. L., Schwartz, D. P., and Black, J. H., 1983, Study of earthquake recurrence intervals on the Wasatch fault, Utah: 8th semi-annual technical report: U.S. Geological Survey Contract No. 14-08-0001-19842, Woodward-Clyde Consultants, San Franciso, CA, 36 p.

Threet, R. L., 1959, Geomorphology of the Wasatch-Uinta Mountains junction, Utah-Wyoming, _in_ Guidebook to the geology of the Wasatch and Uinta Mountains transition area, 10th annual field conference: Salt Lake City, Intermountain Association of Petroleum Geologists, p. 24-33.

Walkley, A., and Black, I. A., 1934, An examination of the Degtjareff method for determining soil organic matter, and a proposed modification of the chromic acid titration method: Soil Science, v. 34, p. 29-38.

Wehmiller, J. F., 1977, Amino acid studies of the Del Mar, California midden site: apparent rate constants, ground temperature models, and chronological implications: Earth and Planetary Science Letters, v. 37, p. 184-196.

Wehmiller, J. F., 1982, A review of amino acid racemization studies in Quaternary mollusks--stratigraphic and chronologic applications in coastal and interglacial sites, Pacific and Atlantic coasts United States, United Kingdom, Baffin Island, and Tropical Islands: Quaternary Science Reviews, v. 1, p. 82-120.

Wehmiller, J. F., and Belknap, D. F., 1982, Amino acid age estimates, Quaternary Atlantic coastal plain--Comparison with U-series dates, biostratigraphy, and paleomagnetic control: Quaternary Research, v. 18, n. 3, p 311-336.

West, M. W., 1986, Quaternary extensional reactivation of the Darby and Absaroka thrusts, southwestern Wyoming and north-central Utah: Geological Society of America Abstracts with Porgrams, v. 18, no. 5, p. 422.

Williams, J. S., Willard, A. D., and Parker, Verlyn, 1962, Recent history of Bear Lake Valley, Utah-Idaho: American Journal of Science, v. 260, p. 24-36.

Williams, K. M., and Smith, G. G., 1977, A critical evaluation of the application of amino acid racemization to geochronology and geothermometry: Origins of Life, v. 8, p. 91-144.

Zoback, M. L., 1983, Structure and Cenozoic tectonism along the Wasatch fault zone, Utah; in Miller, D. M., Todd, V. R., and Howard, K. A., eds., Tectonic and stratigraphic studies in the eastern Great Basin: Geological Society of America Memoir 157, p. 3-29.

LATE QUATERNARY HISTORY OF THE JAMES PEAK FAULT, SOUTHERNMOST CACHE VALLEY, NORTH-CENTRAL UTAH

by

Alan R. Nelson
U.S. Bureau of Reclamation
and U.S. Geological Survey
Denver, CO

and

J. Timothy Sullivan
U.S. Bureau of Reclamation
Denver, CO 80225

ABSTRACT

The James Peak normal fault is marked by a northeasterly trending, 7-m-high scarp that cuts outwash fans of Bull Lake age on the north flank of James Peak. Two surface faulting events, each with about 2 m of displacement, have occurred on the fault in the last 140 ka indicating a late Quaternary slip rate of about 0.03 m/kyr. The degree of soil development on the outwash fans and on fault-related colluvial wedges provides only limited control on the timing of events. Average event recurrence intervals are at least 50 kyr, but recurrence may be nonuniform and the most recent event may be as young as 30 ka. The amount of displacement during each event suggests that surface breaks may have extended north, rupturing the southern portion of the East Cache fault. If so, the James Peak fault may be a westerly splay of the East Cache fault rather than a separate valley-bounding fault.

INTRODUCTION

Comparing Quaternary fault-slip rates is a widely used means of assessing the earthquake potential of geologically young faults. The Wasatch fault poses the greatest hazard to population centers in north-central Utah because it may have a slip rate several times greater and a recurrence of surface faulting 3-10 times greater than for other faults in the Wasatch Mountain region (Schwartz and Coppersmith, 1984). However, other faults in the region may still pose a significant earthquake hazard, but their histories and slip rates have been documented in only a few cases (Nelson and VanArsdale, 1986; Sullivan and Nelson, this volume; McCalpin and others, this volume). Anderson and Miller (1979) and Nakata and others (1982) mapped a number of faults with significant Quaternary slip, but other faults in the eastern Wasatch Mountains (some with late Quaternary (<125 ka) slip) have only recently been identified (Sullivan and Nelson, 1983; Sullivan and others, 1986). One such fault, the James Peak normal fault, is marked by scarps in bedrock, outwash fans, and other alluvium on the north flank of James Peak. It extends west-southwesterly from the southern tip of the East Cache fault in southern Cache Valley almost to Ogden Valley (fig. 1). Here we summarize trench data used to estimate a slip rate on the James Peak fault and suggest how surfaces breaks on the fault may relate to ruptures on the adjacent East Cache fault, which is recognized to pose a significant earthquake hazard (Swan and others, 1983).

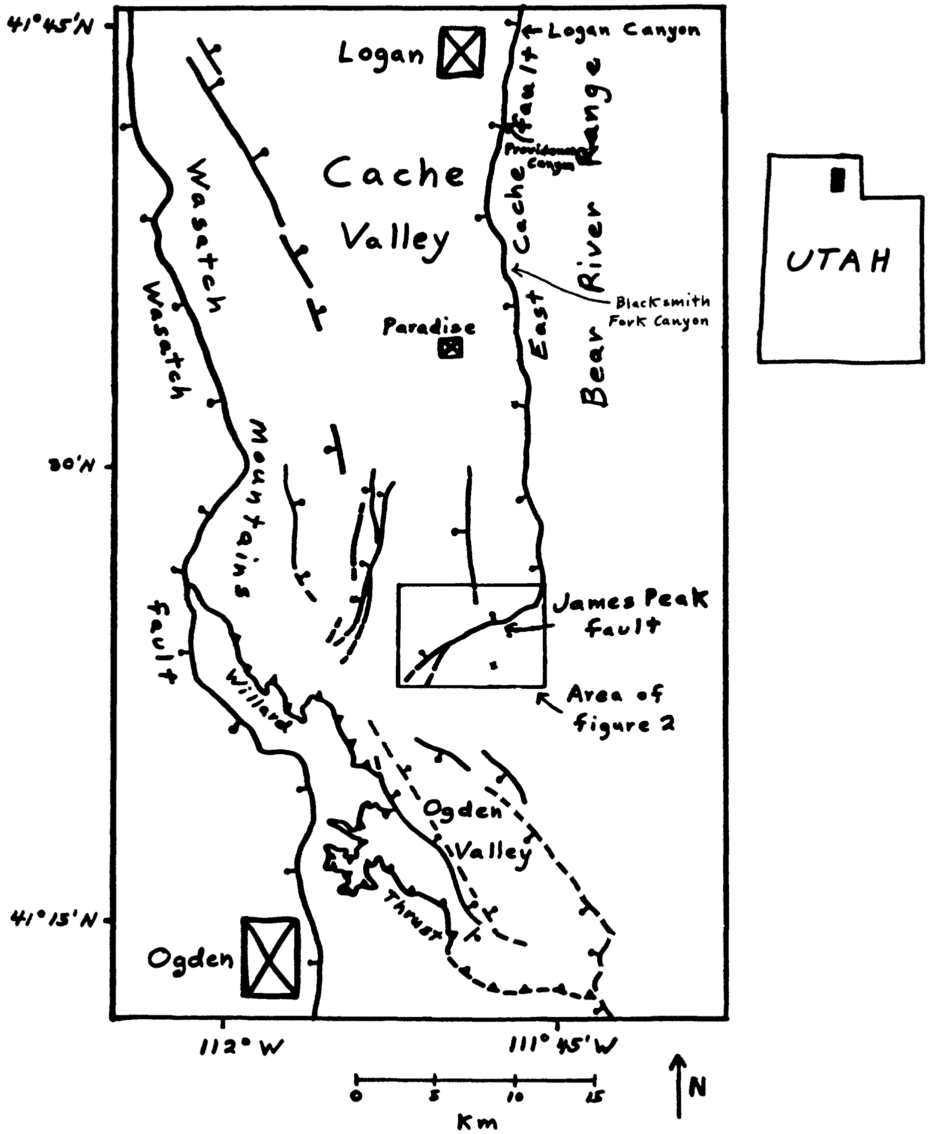

FIGURE 1.--Location of the southern Cache Valley region. Selected late Cenozoic normal faults (modified from Crittenden and Sorensen, 1985a, b) are heavy lines with bar and ball on downthrown side. Edge of the Willard thrust is heavy barbed line.

GEOLOGIC SETTING

Our review of 1:58,000-scale color infra-red and 1:15,000-1:40,000 black-and-white aerial photographs shows that the scarp of the James Peak normal fault is the only previously unreported fault scarp in unconsolidated deposits in the eastern Wasatch Mountains. The scarp marks the southern edge of an unnamed structural and topographic basin between James Peak and Middle Mountain at the southern end of Cache Valley and 5 km north of Ogden Valley (figs. 1, 2). The basin, about 3 km wide and 9 km long, contains Tertiary Salt Lake Formation with a cover of Quaternary colluvium and alluvium (Blau, 1975; Hintze, 1980). The basin is bounded on the north by highly dissected Paleozoic limestones, shales, dolomites, and quartzites and on the south by Paleozoic and Precambrian orthoquartzites, argillites, and volcanics that make up the highlands around James Peak (King, 1965; Blau, 1975; Davis, 1983).

STRUCTURE

Cenozoic structural basins termed "back valleys" occur throughout the Wasatch Mountains east of the Wasatch fault (Gilbert, 1928). Cache Valley is a late Cenozoic structural and topographic basin, bounded by normal faults, that developed in the Cache Allocthon, the upper plate of the Willard and Woodruff thrusts (Bjorkland and McGreevy, 1971; Crittenden, 1972; Hintze, 1980) (fig. 1). The East Cache fault, the principal fault in the valley, is marked by triangular facets cut on the east-dipping Precambrian and Paleozoic rocks at the western base of the Bear River Range. Geophysical data (Stanley, 1972; Petersen, 1974) complied by Zoback (1983) suggest that the late Cenozoic basin fill in the valley is 1.7-2.1 km thick. A seismic reflection profile across the East Cache fault shows that Cache Valley is an asymmetric basin, deepest on the east margin adjacent to the East Cache fault (Smith and Bruhn, 1984). Consistent east dips of reflectors in the late Tertiary basin fill suggest a listric geometry for the East Cache fault although the fault plane cannot be resolved from the available data.

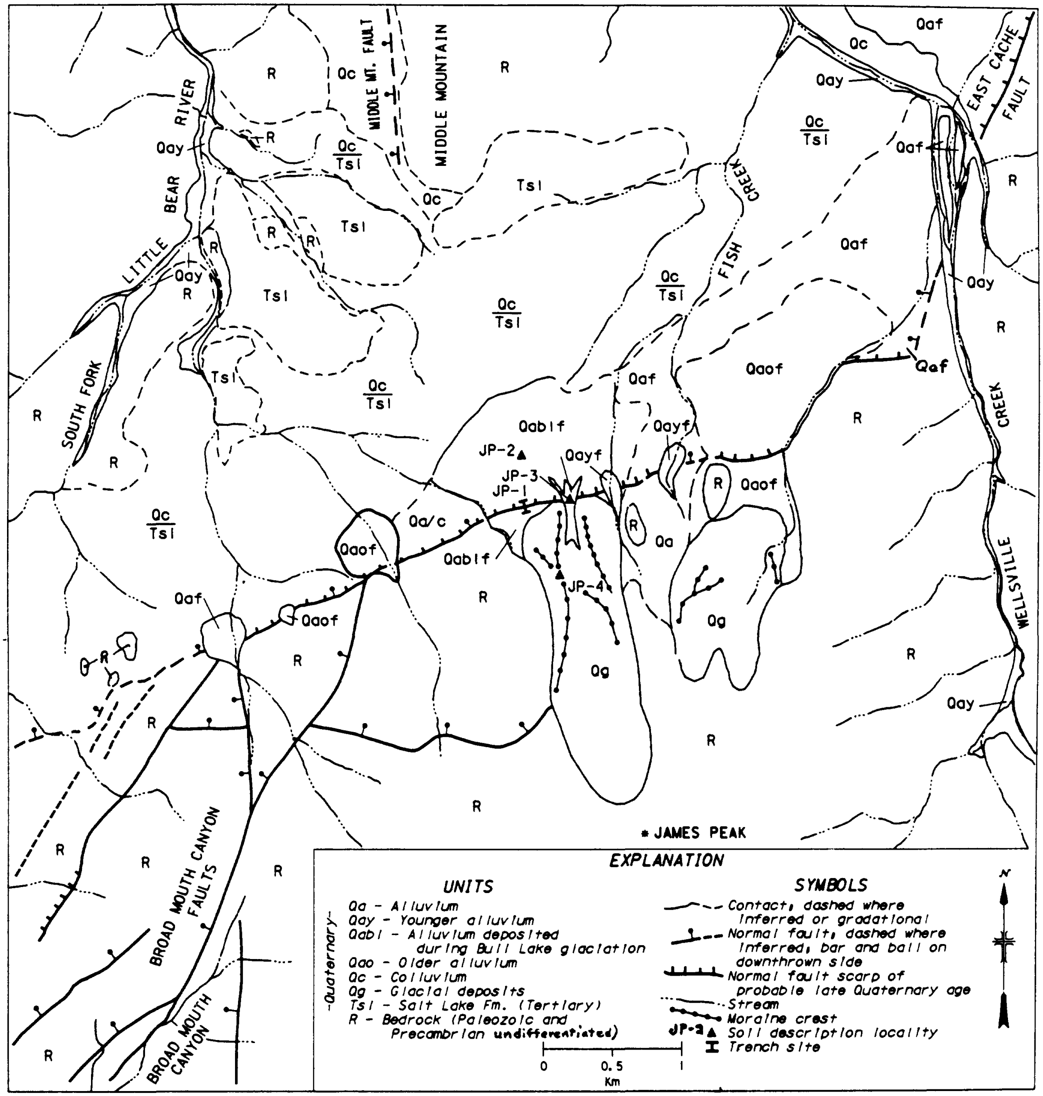

FIGURE 2.--Generalized Quaternary geologic map of the area north of James Peak. The James Peak fault scarp trends northeast-southwest in the middle of the figure. Surficial units with "f" following the unit symbol have alluvial fan morphology. Slash within a unit symbol shows a deposit of multiple genesis (Qa/c = alluvium and colluvium). Qay deposits are primarily of Holocene and latest Pinedale age (<15 ka). Most Qao (Qaof) units are pre-Pinedale (>30 ka). Qa and Qc units are undifferentiated on the basis of age. Qc/Tsl marks thin deposits of colluvium over Tertiary Salt Lake Formation. Most faults in bedrock south of the James Peak fault scarp are from Blau (1975). Many units (such as Qablf) contain smaller areas of younger and older deposits.

The James Peak normal fault, at the base of the escarpment in Paleozoic and Precambrian rocks on the north side of James Peak, marks the southern boundary of the east-west-trending basin at the southern end of Cache Valley (fig. 2). Isolated outcrops of Paleozoic sedimentary rocks suggest that the Salt Lake Formation may be <100 m thick in the basin indicating cumulative subsidence is much less here than in Cache Valley. North of the basin, north-dipping, lower Paleozoic rocks are cut by north-trending normal faults including the Middle Mountain fault. Near Broadmouth Canyon on the west side of James Peak, Blau (1975) maps north-trending normal faults with estimated displacements of about 1500 m that are about on trend with the Middle Mountain fault. Escarpments in bedrock mark these north-trending faults, but north-trending scarps are not developed in the sediments in the basin. No east-west-trending faults are mapped along the northern edge of the basin where fluvial dissection has produced extensive outcrops of the Salt Lake Formation. Thus, the basin appears to be a shallow half-graben connecting the larger and deeper grabens at the southern end of Cache Valley and the northwest end of Ogden Valley (Zoback, 1983; Sullivan and others, 1986).

QUATERNARY DEPOSITS

Quaternary deposits in the basin consist of locally-derived, bouldery, colluvial deposits (unit Qc/Tsl on fig. 2) in the central and northern portions which thicken and are interbedded with fan alluvium to the south. Alluvial fan deposits (Qaf), including two large, bouldery outwash fans (Qaof and Qablf) derived from the quartzites exposed on James Peak, occur along the southern edge of the basin. These fans become larger and appear to thicken from west to east; if so, this thickening may indicate downfaulting, tilting, or deeper erosion of the eastern part of the basin near Wellsville Creek and the East Cache fault. Sandy till (Qg) makes up the high, steep moraines built by the glaciers that deposited the outwash fans in two of the unnamed drainages on the north flank of James Peak.

SCARP AND MOUNTAIN FRONT MORPHOLOGY

Mountain front slopes developed in bedrock along the James Peak fault are steep, especially on James Peak (26°), despite the fact that this side of the peak has been extensively eroded by glaciers. On the lower half of the mountain eroded spurs (ridge crests) are faceted. Three breaks in slope on the spurs, as well as the north-facing faceted spur (25° slope) just west of Wellsville Creek at the east end of the basin (fig. 2), suggest a history of recurrent Quaternary displacements on the fault (for example, Gilbert, 1928; Hamblin, 1976). To the east, the mountain front is lower and more dissected with gentler slopes, although here, as elsewhere, the steepest facets are at the base of the slopes along the fault. However, by comparison, the facets along the fault are smaller, less continuous, and less steep than those along the East Cache and Wasatch faults. The short (<7 km) mountain front along the James Peak fault makes quantitative comparisons with other mountain fronts (for example, Bull and MacFadden, 1977) of little value. Overall, the mountain-front morphology of the north flank of James Peak suggests much lower Quaternary slip rates than that on major nearby faults such as the East Cache and Wasatch faults.

The James Peak fault scarp is expressed primarily as a scarp in bedrock over much of its length, but along the central part of the fault the scarp cuts alluvial and colluvial deposits and the large alluvial fans (units Qablf and Qaof, fig. 2) issuing from the glaciated drainages on the north flank of the mountain. The scarp is generally higher (10-30 m) and steeper (20°-35° maximum slope angle) in bedrock (or thin colluvium over bedrock) than in fan sediments (1-4 m; 15°-30°). Where the scarp is in alluvium undissected by small drainages, it is uniformly 3-4 m high.

An en echelon offset at the east end of the scarp forms a junction with the prominent scarp at the southern end of the East Cache fault; the scarps join at about a 110° angle. The eastern half of the scarp is subdued (<2 m high, 20° maximum slope angle) where it crosses the apex of the easternmost alluvial fan (Qaof on fig. 2), but the scarp is steeper (20°-25°) in the Cambrian quartzite on the en echelon segment (500 m west of Wellsville Creek). The lower slopes of the Paleozoic limestone and sandstone bedrock facets, 2.7 km to the north on the East Cache fault, are steeper still (25°-30°). Just west of the large alluvial fans, the western half of the scarp is steep (22°-30° maximum slope angle) near the base of dissected facets in quartzite, but farther west the scarp is indistinct because the bedrock hills west of James Peak are lower and more rounded than the faceted mountain flanks to the east.

Just south of the western end of the basin, the Broadmouth Canyon normal faults trend about N. 30° E. through low, dissected bedrock hills (Blau, 1975). A major topographic boundary between the west flank of James Peak and the lower hills to the west marks the largest normal fault, with 1,500 m of throw, that extends into Broadmouth Canyon. One large (120 m difference in elevation) and several smaller topographic steps (most down-to-the-northwest) (fig. 2) that parallel the largest fault are interpreted as related subsidiary faults.

AGE OF FAULTED DEPOSITS

Our chronology of Quaternary deposits and the scarps bounding or cutting them near James Peak is based on the morphology and relative position of fans, moraines, and scarps, and data from four soils developed on deposits in the largest glaciated drainage. Most mapped Quaternary deposits are undifferentiated as to age (fig. 2), but even the oldest are probably no more than a few hundred thousand years old.

The height of topographic scarps along the Broadmouth Canyon faults suggests Pliocene to Quaternary, but not necessarily late Quaternary displacement. Most of the faults cannot be traced into the Salt Lake Formation in the basin to the north and thus, they appear to be buried by Tertiary sediments. However, in two areas where the Broadmouth Canyon faults meet the James Peak fault faint lineaments extend into dissected Salt Lake Formation sediments; exposures are not sufficient to resolve the relationships between the lineaments and the faults. Although the Broadmouth Canyon faults may join the James Peak fault, the young scarp on the latter fault indicates the Broadmouth Canyon faults have been displaced by it.

The steep, continuous scarp in the alluvial fans along the central part of the James Peak fault suggests late Quaternary displacement on the fault. However, except for the smallest, youngest fans, which lack scarps where the fault crosses them, fans of significantly different ages (in which to compare scarp heights) were not identified. Topographic profiling across the scarp was difficult because of the thick alder-aspen forest and the soft, loose organic-rich soil on the surface of the scarp. For this reason, profiling to obtain displacement and relative-age estimates (for example, Bucknam and Anderson, 1979) was not attempted.

Most Quaternary chronology studies in the Rocky Mountain region have subdivided deposits of the most recent major glaciations into those deposited during the Bull Lake glaciation and the Pinedale glaciation and designated older deposits as pre-Bull Lake (Madole, 1976; Pierce, 1979). These groupings are usually based on relative-age data such as relative position in the landform sequence, landform morphology, the degree of soil development, and surface weathering characteristics (Birkeland and others, 1979). Because the data used to subdivide these deposits into these relative-age groups are usually only compared for sites within a single mountain range or drainage basin, deposits in different ranges or basins elsewhere in the region that have been assigned to the same relative-age group may not be the same age (Pierce, 1979; Porter and others, 1983). Colman and Pierce (1981) have identified moraines in Idaho probably dating from about 60-70 ka, intermediate in age between the accepted ages of 15-25 ka for most Pinedale deposits and 130-150 ka for Bull Lake deposits. Thus, deposits placed in the Bull Lake relative-age group in some drainages might be as young as 60-70 ka. Following Pierce (1979) and Porter and others (1983) we use "Pinedale" and "Bull Lake" to name the more recent major Quaternary glaciations in the Rocky Mountains and assume ages for the deposits of each glaciation by comparing our soils data with similar data from numerically-dated glacial deposits (Pierce and others, 1976; Porter and others, 1983; Colman and Pierce, 1986).

Soil development indices are an objective way of comparing the degree of development of soils (Birkeland, 1984). The soil properties that vary the most systematically with time in the Rocky Mountain region include horizon thickness, color, texture, and calcium carbonate accumulation (Shroba and Birkeland, 1983). Ways to express changes in these properties include simple, widely-used soil development indices (for example, depth to base of observable oxidized parent material and maximum percent clay increase), profile summations (Machette, 1985), and the indices of Harden (1982) and Harden and Taylor (1983). Harden's indices refine those of Bilizi and Ciolkosz (1977) and incorporate, in a quantitative way, most of the concepts represented by development indices used previously in the western United States. The profile development index (Harden, 1982; fig. 3) is particularly useful because the degree of development of all selected properties can be objectively summarized by a single value.

We followed Harden and Taylor (1983) in using X-Y plots to compare indices for the soils we described and sampled near the trench site (table 1; fig. 2) with soils of known age elsewhere in the Wasatch Mountains (fig. 3). Soils on a lateral moraine (JP-4) and on the outwash fan in front of it (JP-2) were described to determine whether these were Bull Lake or Pinedale deposits. For comparison, a Holocene soil (JP-)3 was described on very coarse, bouldery alluvium in a narrow channel where the moraines are narrowly breached. The thick soil developed on the colluvial wedges in the trench (JP-1) was also described to help estimate their age. Soils JP-1 and JP-2 are developed in deposits of more than one age. To help estimate the time interval represented by the degree of soil development in the younger deposits as well as by the whole soil we calculated soil indices for each depositional unit of these two soils (table 1; fig. 3).

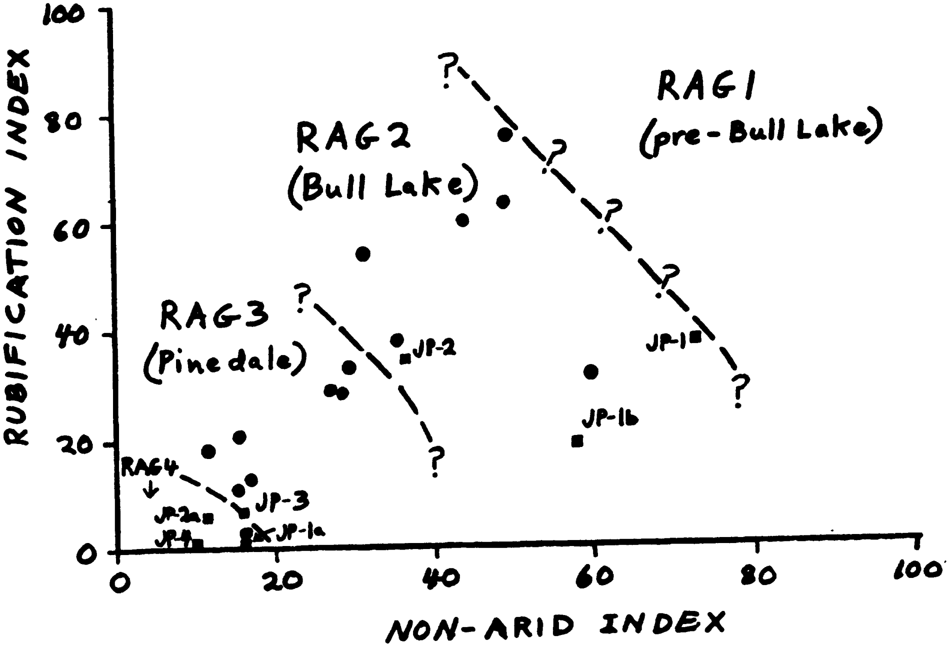

FIGURE 3.--Plot of rubification and nonarid soil-development indices (squares) (after Harden, 1982, and Harden and Taylor, 1983) for soils in pits near the trench site (fig. 2, table 1). Point Jp-1a is a plot of indices for the upper 83 cm of soil JP-1 (unit 4, fig. 4), JP-1b is for the upper 205 cm of the same soil (units 3 and 4), JP-2a is for the upper 53 cm of soil JP-2, and JP-1, JP-2, JP-3, and JP-4 are indices for the entire profiles. Dashed lines divide the diagram into four relative-age groups (RAGs) defined by indices from soils of known age (marked by dots) elsewhere in the eastern Wasatch Mountains (Nelson and Krinsky, 1982; Nelson, unpub. data, 1984). Comparison of the degree of development of soils in these RAGs with soils on glacial deposits elsewhere in the Rocky Mountain region (Madole, 1976; Pierce, 1979; Shroba and Birkeland, 1983; Colman and Pierce, 1986) suggest soils in RAG 4 are of Holocene age or a little older (<12 ka), those in RAG 3 correlate with glacial deposits of Pinedale age (15-25 ka), those in RAG 2 may be of Bull Lake age (130-150 ka), and those in RAG 1 are older than Bull Lake.

TABLE 1.--Selected properties of soils on the north flank of James Peak, north-central Utah

Profile	Trench log unit	Horizon[1]	Average depth (cm)	Parent material	Munsell dry color	Estimated percent by volume: Pebbles (0.2-8 cm)	Estimated percent by volume: Cobbles (8-25 cm)	Estimated percent by volume: Boulders (>25 cm)	Percent by weight[2]: Sand (2-0.5 mm)	Percent by weight[2]: Silt (50-2 um)	Percent by weight[2]: Clay (<2 um)	Percent organic matter[3]
JP-1	4b	A1	0- 10	Colluvium-loess	7.5YR 2/2	10	2	0	20	57	23	9.4
	4b	A2	10- 46	----do---------	7.5YR 3/2	10	2	0	22	54	24	8.8
	4a	Bw	46- 83	----do---------	7.5YR 5/3	10	5	0	28	51	21	3.2
	3bB	2Bt1	83-100	----do---------	7.5YR 5/4	10	5	0	26	53	21	2
	3aB	2Bt2	100-205	----do---------	7.5YR 6/4	25	15	0	28	48	24	.7
	2	3Cox/3Bt	205-248	Scarp colluvium	7.5YR 7/4	20	20	2	33	45	23	.6
	1B	4Bt	248-278	Outwash--------	5YR 4/6	30	30	10	54	18	28	.3
	1	4Cox	278-390+	----do---------	7.5YR 7/3	30	30	10	90	8	3	.2
Extra	2b	3C	260	Scarp colluvium	7.5YR 7/4	10	15	25	36	45	19	.9
samples[4]	2a	3C	355	----do---------	7.5YR 6/4	10	20	20	21	39	40	.4
JP-2		Ap	0- 10	Sheetwash-loess	10YR 6/3	20	25	0	29	52	19	5.2
		A	10- 20	----do---------	7.5YR 6/4	20	25	0	28	52	20	3.7
		Bt	20- 53	----do---------	7.5YR 6/4	20	25	0	37	37	26	1.4
		2Bt	53- 85	Outwash--------	2.5YR 4/6	50	25	0	72	17	11	.6
		2BC	85-114	----do---------	5YR 7/4	50	25	0	88	7	5	.2
		2Cox	114-136+	----do---------	5YR 7/4	40	35	1	84	11	5	.3
JP-3		A1	0- 16	Loess-alluvium-	7.5YR 4/3	15	20	25	35	53	12	13.4
		A2	16- 41	----do---------	7.5YR 5/3	15	20	25	41	41	19	5.2
		Bt	41- 85	----do---------	7.5YR 5/4	15	20	25	63	27	10	1.2
		2C	85-132+	Alluvium-------	7.5YR 7/3	25	20	30	82	13	5	.4
JP-4		A1	0- 13	Sheetwash-till-	7.5YR 3/3	20	5	10	62	31	8	10.4
		A2	13- 48	----do---------	7.5YR 4/3	10	20	10	66	27	6	3.6
		2Bt	48- 72	Till-----------	7.5YR 8/1	20	10	10	72	20	9	.4
		2C	72-105+	----do---------	7.5YR 8/0	20	15	10	81	15	4	.4

[1] Horizon nomenclature of Guthrie and Witty (1982) and Birkeland (1984).

[2] Particle-size distribution of <2 mm fraction using sieve-pipette methods (for example, Carver, 1971) and a Sedigraph for some silt-clay fractions with prior removal of organic matter using methods of Jackson (1956). No samples contained carbonate.

[3] Percent organic matter by method of Walkley and Black (1934).

[4] From center of units 2a and 2b at station 21 (fig. 4).

Soil development indices (fig. 3) calculated using field and laboratory data shows that the outwash gravels (unit Qablf on fig. 2) in the lower parts of soils JP-1 and JP-2 are in RAG 2 (relative-age group 2) and are probably chronocorrelative with outwash from the Bull Lake glaciation. Although it is possible that this outwash significantly post-dates the last interglacial (125 ka) (discussed above), the reddish, clay-rich argillic horizons of these soils suggest they began forming about 140 ka.

Soil JP-4 on the steep, high, left lateral moraine (fig. 2) is poorly developed with soil indices lower than those for most soils on tills and outwash of the Pinedale glaciation (fig. 3). However, the till on which the soil is developed is derived entirely from quartzites, which do not weather easily. In addition, the steep slopes and narrow crests of the moraines indicate this soil may have been partially stripped by erosion on the moraine crest. Thus, both because soil development proceeds so slowly in quartzite-derived tills and because of erosion the moraine is probably much older than the soil indices suggest.

The bouldery surfaces, narrow crests, and steep slopes of the moraines on the north flank suggest they were built during the Pinedale glaciation, but the indices for soils developed on the outwash apron in front of the moraines suggest an older, probably pre-last interglacial age (>125 ka). The most probable interpretation of the age of the moraines is that Pinedale and Bull Lake glaciers extended the same distance downvalley, but that during the Pinedale glaciation, high Bull Lake lateral moraines protected all but the center of the fan surfaces from burial by younger outwash. Thus, the outwash fans that are displaced by the James Peak fault (Qablf and Qaof on fig. 2) are probably primarily of Bull Lake age (130-150 ka).

Soil JP-3 and the upper parts of JP-1 and JP-2 are only weakly developed, falling in RAG 4 (fig. 3). Cambic and weak argillic B horizons have developed in the mixed, fine-grained sheetwash and loess deposits in the upper parts of soils JP-1 and JP-2. Soil JP-3 has a weak argillic horizon, but no increase in hue or chroma to bright reddish colors (table 1). Soil indices suggest a Holocene or very latest Pleistocene age for this soil, and this soil's position near the main stream channel of the largest drainage basin on the north flank also suggests it is of Holocene (probably late Holocene) age. Argillic horizon development in deposits this young is probably due to a locally high rate of eolian dust influx (fine silt as well as clay) from the large areas of exposed Bonneville lake sediments in southern Cache Valley. Shroba (1980) has also described argillic horizons from deposits of mid- to early Holocene age along the Wasatch fault.

FAULT DISPLACEMENT HISTORY

To estimate the size, number, and age of the more recent surface displacement events on the James Peak fault a single trench was excavated across the 7-m-high scarp on the outwash fan 200 m west of the left lateral moraine (fig. 2). Dense aspen forest and soft soils prevented access to all other promising trench sites. The trench exposed white, coarse sandy, quartzite-derived outwash (unit 1; fig. 4) with a reddish, argillic horizon developed on it (unit 1B) overlain by bouldery, silty colluvial wedges (unit 2). The wedges were overlain by silty colluvial units (3 and 4) with thick cambic and argillic B horizons. Despite the slumping and raveling of the very loose, unconsolidated outwash in the lower trench walls we were able to expose the fault zone and former free face of the scarp at the south end of the trench. A topographic profile across the scarp indicates the fan has been displaced about 4.2 +0.6/-0.2 m at this site. The stratigraphic relationships, unit contacts, lithologies of the outwash and the colluvial wedges, and the soils developed on them do not clearly show whether one event of about 4-m displacement or two events of about 2-m displacement have occurred on the same fault in the trench. As discussed below, we favor a two-event interpretation.

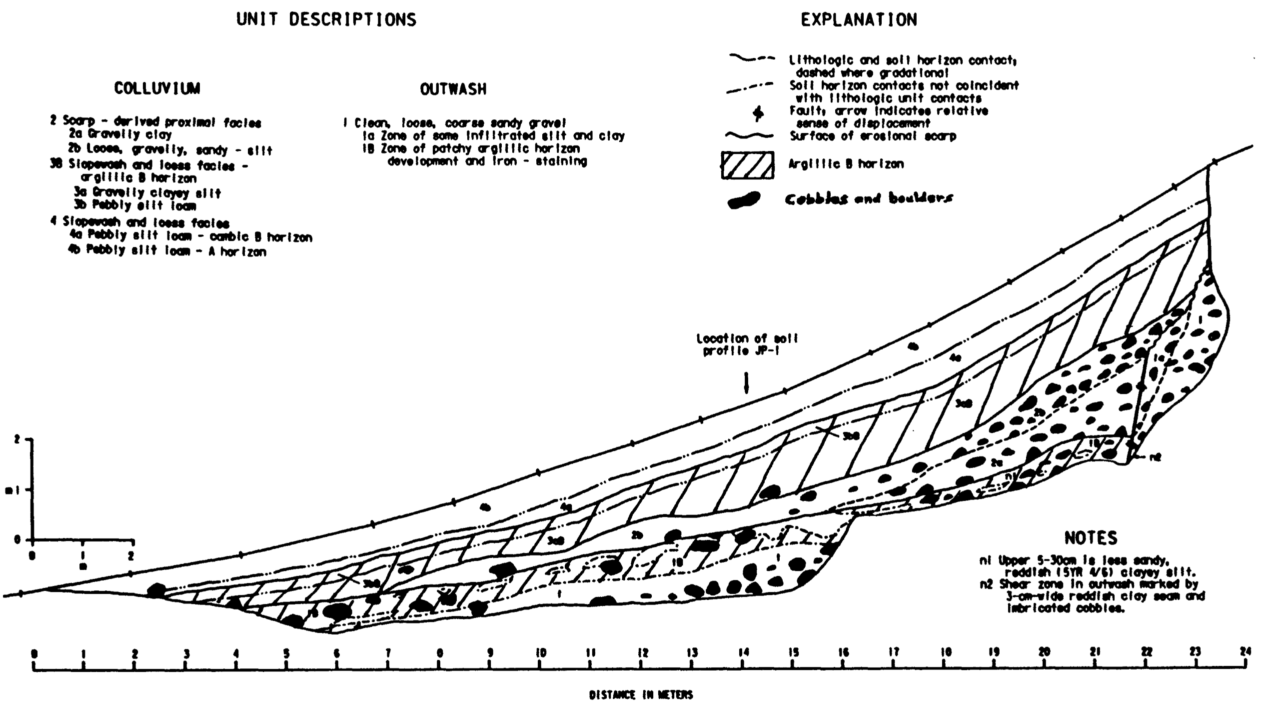

UNIT DESCRIPTIONS

COLLUVIUM

2 Scarp - derived proximal facies
  2a Gravelly clay
  2b Loose, gravelly, sandy - silt
3B Slopewash and loess facies - argillic B horizon
  3a Gravelly clayey silt
  3b Pebbly silt loam
4 Slopewash and loess facies
  4a Pebbly silt loam - cambic B horizon
  4b Pebbly silt loam - A horizon

OUTWASH

1 Clean, loose, coarse sandy gravel
  1a Zone of some infiltrated silt and clay
  1B Zone of patchy argillic horizon development and iron - staining

EXPLANATION

Lithologic and soil horizon contact; dashed where gradational
Soil horizon contacts not coincident with lithologic unit contacts
Fault; arrow indicates relative sense of displacement
Surface of erosional scarp
▨ Argillic B horizon
● Cobbles and boulders

NOTES

n1 Upper 5-30cm is less sandy, reddish (5YR 4/6) clayey silt.
n2 Shear zone in outwash marked by 3-cm-wide reddish clay seam and imbricated cobbles.

FIGURE 4.--Log of the east wall of the trench across scarp of the James Peak fault (fig. 2). The segmented line at the top of the log is the central portion of a topographic profile measured across the site using the methods of Bucknam and Anderson (1979). In order to trench as high as possible on the scarp the trench was dug in two stages; stage 1 (station 0-12) was backfilled before stage 2 (station 12-19) was dug. Note that small letters in unit symbols indicate sublithofacies and "B" marks argillic B horizons. The lithology of the proximal colluvial wedges, units 2a and 2b, suggests that the scarp was formed by two surface faulting events (see text).

Based on regional correlation of map and trench units (fig. 3), we infer the following sequence of events:

1. Moraines and an extensive outwash fan were deposited on the north flank of James Peak, probably during the Bull Lake glaciation (about 130-150 ka). Soils developed on stable areas of moraines and outwash, but gradual erosion prevented well-developed soils from forming on moraine crests. The length of time required to develop the reddish argillic B horizons on the outwash is difficult to estimate, partly because the soil north of the trench site (JP-2) appears to have been stripped. The fact that the argillic horizon and the fine-grained units overlying it are thin suggests soil JP-2 has been eroded, perhaps by meltwater in braided, outwash channels (which did not reach the trench site) during the later Pinedale glaciation. These horizons may have developed rapidly because of high dust influx rates due to the silt and clay from lake sediments exposed in Cache Valley to the north. Because the B horizons on these deposits are much more strongly developed than the B horizons on late Pinedale or Holocene deposits, these horizons must have taken at least a few tens of thousands of years to develop, perhaps as many as 70 kyr.

2. Surface faulting vertically displaced the outwash (unit 1, fig. 4) about 1.6-2.2 m, down-to-the-north. A proximal, colluvial debris wedge (unit 2a), formed by spall, slump, and slopewash, rapidly buried the argillic horizon developed on the outwash (unit 1B) and the lower part of the free face of the scarp. The source of the bouldery debris wedge, with a matrix of silty clay (table 1), must have been the surface colluvium of similar lithology overlying the outwash on top of the scarp (not exposed in our trench). Although it is mapped as part of the soil developed on unit 1, the thickening of the reddish, clayey silt near the top of outwash unit 1B adjacent to the fault (note n1, fig. 4) and the inclusion of reddish clayey peds in the matrix of less-reddish clayey silt near the base of unit 2a suggest that material along the unit 1B-unit 2a contact may be fragments of the argillic horizon eroded from the scarp right after this event. We infer that none of the loose, sandy outwash (unit 1) was exposed in the free face by this event; if it had been the free face would have slumped almost immediately after faulting, contributing much coarse sand to the debris wedge. Equilibrium scarp degradation models at gently sloping sites suggest the maximum fault displacement is about two times the maximum colluvial wedge thickness (for example, Nash, 1981). However, the steep slope above the site and the inferred active surface transport processes (discussed below) suggest the amount of vertical displacement during this event was probably not much greater than the wedge thickness (1.6 m).

3. After the argillic horizons had formed and probably after the first fault event, soil development on the lower part of the outwash fan continued. However, the steep (20°-25°) slope of the fan above the trench site, the lack of well-developed B horizons on the proximal wedges, and the high clay content of surface colluvium above the scarp suggest that creep and solifluction may have been the dominant slope processes during periods of cold, moist climate (onset of Pinedale glaciation, about 75 ka?) during or after the deposition of the first proximal wedge. These processes may have eroded existing soils or prevented well-developed soils from forming at and above the site.

4. A second displacement event on the same fault moved unit 2a down against the outwash. The looser, sandier lithology of the proximal debris wedge (unit 2b) produced following this event indicates that some outwash was exposed in the free face in addition to the bouldery, clayey silt (not exposed in the trench) overlying the outwash. Erosion of the scarp following the first event also probably reduced the proportion of bouldery silt to outwash exposed in the free face during the second event, resulting in a sandier wedge. Slumping of the outwash in the lower part of the free face helped to spread loose debris downslope and buried the debris wedge from the first event. The loose debris produced a thinner wedge (unit 2b) that extended farther downslope than the first wedge (unit 2a); this geometry is typical of debris wedges produced by later events on multiple-event scarps (Ostenaa, 1984). Displacement during the second event is more difficult to estimate from the thickness of the debris wedge; it must be close to the difference between total topographic displacement across the scarp and the displacement of the first event (4.2 m - (1.6-2.2 m)) = 2.0-2.6 m). We could not measure total throw because the top of the outwash unit in the footwall was not exposed in the trench. The lack of any evidence of soil development on the debris wedge resulting from the first event suggests that the two events may have occurred less than a few tens of thousands of years apart. However, the active surface processes on the steep fan (discussed above) could also have eroded a moderately-developed soil or prevented one from forming. It is also possible that weak soil development near the top of wedge 2a is masked by later development of more strongly developed soils on units 2b and 3aB (fig. 4).

An alternate interpretation that must be considered is that both units 2a and 2b are proximal debris wedges produced following a single displacement event of about 4 m. This would explain the absence of 1) an abrupt contact between units 2a and 2b, 2) any evidence of soil development on unit 2a, and 3) deformation of the first debris wedge (2a) during the second event. The apparent overlap of the time estimates for pre-first-event and post-second-event soil-forming intervals (discussed below) would also be explained by a single event. Clear evidence of shearing along the contact between units 2a and 1a was not observed, but three cobbles were imbricated parallel with the contact near the base of unit 1a and the outwash is so unconsolidated that evidence of shearing may not have been preserved. Possibly, unit 1a is a fissure which filled with outwash that slumped from the free face after a second event. In any case, the stratigraphic relationships near the fault show that most of unit 2a must have been deposited immediately after faulting and its lithology shows this unit was derived from units which contained little sand. Because we find it difficult to explain how a thick, proximal debris wedge could be deposited adjacent to a several-meter-high, almost vertical free face of loose, sandy outwash without the outwash contributing any sediment to the wedge, we favor a two-event fault history. In addition, 2-m displacement events are much more typical of faults in the region, even faults that are much longer than the James Peak fault (Schwartz and Coppersmith, 1984).

5. A silty colluvial wedge (unit 3) was deposited over the proximal debris wedges by wash erosion of the scarp crest and by rill and wash transport of fines from above the site. The thickness and high silt content of the wedge (table 1) suggests it has a strong eolian component, probably due to exposed lake sediments in Cache Valley. As the deposition rate of the colluvial wedge decreased, B horizon development in the upper part of the wedge became more distinct, culminating in a 122-cm-thick, argillic horizon (table 1) on the wedge. Because of its position on the scarp slope, this soil is not directly comparable to soils in more stable landscape positions whose age is better known. We interpret this soil as forming in a climate not greatly different from the present; thus, it must either pre-date the main Pinedale glaciation (18-25 ka) or postdate the fall of Lake Bonneville from its high stand (15 ka, Scott and others, 1983). The total amount of clay in this soil (9 g/cm^2) compared with regional rates of clay accumulation (for example, Colman and others, 1986) and most other soil indices for this part of the soil on unit 3 (fig. 3) suggest an age as great as 100-150 ka because these horizons are so thick. However, the (1) limited soil reddening and weak B horizon structure, (2) probable high dust influx rate during part of the history of the site, and (3) likelihood of some of unit 3 being derived from clay-rich soils upslope all suggest a much younger age. Thus, we estimate this soil, which post-dates both fault events, developed over 30-70 kyr.

6. Finally, an episode of rapid slopewash deposition, probably with some eolian influx, produced a silty colluvial unit (4) which is very similar to unit 3. A weak cambic B horizon (4B) and a thick, silty A horizon (4A) on this unit, indicate a Holocene age (soil JP-1a, fig. 3). Deposition during the warmer, and probably drier Altithermal of the mid-Holocene (Baker, 1983) is likely.

SLIP RATES AND RECURRENCE

The topographic profile across the scarp at the trench site (fig. 4) shows the outwash, most likely about 140 ka, is displaced about 4.2 m for an average late Quaternary vertical-slip rate of 0.03 m/kyr on the James Peak fault.

Because the soils developed on the outwash and on the colluvium overlying the faulting-related wedges provide only maximum and minimum age estimates for the wedges, the true recurrence of surface faulting events is difficult to estimate. Displacement data for each of the two fault events is uncertain, but scarp erosion models that consider the position of the scarp at the foot of a steep slope, the thickness of the first colluvial wedge, and the volumes and lithologies of both wedges suggest the second event may have been larger than the first. We estimate average displacements of about 1.8 +0.4/-0.2 m for the first event and 2.4 +0.8/-0.6 m for the second event. The reddish argillic horizon on the outwash beneath the colluvial wedges probably required at least several tens of thousands of years (we assume >30 kyr) to develop before burial, perhaps even 70 kyr. This well-developed soil adjacent to the fault shows that no significant displacement occurred on the fault for a long period of time after outwash deposition ceased. Thus, the first event could have occurred as early as 110 ka (140-30 ka) or as late as 70 ka (140-70 ka). The thick argillic horizon on unit 3, which post-dates the second displacement event, also suggests a soil forming interval of at least 30 kyr and perhaps 70 kyr. With these broad constraints, a time interval of 80 kyr (from 110 ka to 30 ka) is available in which the two events could have occurred. If we take the mean of possible times at which each event occurred (first event, x = 90 ka, second event, x = 50 ka) the events are separated by 40 kyr (90-50 ka). Because the maximum estimates of the length of the soil forming intervals following each event overlap, no minimum estimate of the length of this period can be made. If the two events were separated by 40 kyr, the recurrence interval between these events and earlier and future events would be >50 kyr (50 + 40 + 50 = 140 kyr). Thus, the average recurrence interval for the two events since 140 ka is at least 50 kyr, but the lack of a soil between the two debris wedges suggests non-uniform recurrence. However, if there was only one event (discussed above), it probably occurred about 70 ka.

RELATIONSHIP TO THE EAST CACHE FAULT

The location of the James Peak fault at the southern end of the East Cache fault suggests their surface rupture histories may be related. Blau's (1975) mapping shows that the East Cache fault is abruptly terminated at its high-angle intersection with the James Peak fault (fig. 2) because no north-trending fault extends up Wellsville Creek . The James Peak fault is also oriented at near right angles to the contemporary regional extensional stress field (Zoback and Zoback, 1980). However, portions of the Wasatch fault which intersect at high angles have ruptured concurrently during the Holocene (Nelson and Personius, 1986) and similar fault patterns are found along late Quaternary fault zones elsewhere in the Basin and Range (for example, Wallace, 1979). The morphology of the bedrock scarps on the Broadmouth Canyon faults (fig. 2) does not suggest recurrent late Quaternary displacement, but also does not preclude some Quaternary slip. These scarps trend southwesterly, nearly parallel to the southern part of the East Cache fault. We speculate that the Broadmouth Canyon faults may be the southernmost part of a Quaternary rupture zone encompassing all three faults.

Some of the larger surface displacement events on the James Peak fault may have ruptured part of the East Cache fault. Empirical relationships between the amount of surface displacement and fault rupture length (Bonilla and others, 1984) suggest that more than 7 km of surface faulting is associated with events that produce the 2 m of displacement that we infer from our trench stratigraphy. On the Wasatch fault, surface displacements of 1.6-2.6 m are thought to be associated with ruptures on fault segments 30-60 km long (Schwartz and Coppersmith, 1984). The 1983 Borah Peak earthquake had a maximum displacement of about 2.5 m and a total rupture length of 36±3 km (Crone and Machette, 1984). Thus, even if small, unrecognized ruptures occurred on the Broadmouth Canyon faults during the events recorded at James Peak, at least 15 to 20 km of the southern part of the East Cache fault may also have ruptured. Near the southern end of the East Cache fault, Swan and others (1983) could not determine the age of most recent displacement because the main trace of the fault is well above the Bonneville shoreline at the range front, and because scarps along the fault are almost completely masked by younger (post-Provo shoreline, <14 ka, Scott and others, 1983) alluvial fans. Mullens and Izett (1964) also did not find evidence of surface faulting in the Paradise area (fig. 1). Thus, any scarps along the East Cache fault related to the James Peak events are probably covered by younger deposits. Farther north along the East Cache fault near Logan (fig. 1), Swan and others (1983) concluded that two, 1- to 2-m, post-Bonneville surface displacement events have occurred on this part of the East Cache fault for a slip rate of 0.10 to 0.2 m/kyr for the last 15 kyr. The first event occurred between the high stand of Lake Bonneville (15-16 ka, Scott and others, 1983) and its catastrophic fall to the Provo shoreline (14-15 ka). The second event post-dates the Provo level of the lake and pre-dates alluvial fans thought to be about 6-10 ka. Excavations at several places along the East Cache fault have also revealed post-Bonneville displacements (B.N. Kaliser, oral commun., 1981), but these investigations are undocumented. Thus, average recurrence on the section of the East Cache fault marked by the post-Provo scarps near Logan since the high stand of Lake Bonneville appears to be about 7 kyr, but the actual interval between events could be as short as 2-3 kyr (Swan and others, 1983).

Estimates of the thickness of basin-fill in southern Cache Valley (Zoback, 1983) and topographic relief on the bedrock escarpment of the East Cache fault both decrease south of Logan suggesting that total displacement on the fault also diminishes to the south. Late Pleistocene scarps are mapped along the fault at least as far south as Blacksmith Fork Canyon (Cluff and others, 1974; Swan and others, 1983), but Swan and others (1983) speculate that the rupture near Logan may die out south of Providence Canyon.

Site-specific fault slip data indicate differing histories for the East Cache and James Peak faults, but little reliable information on the southern half of the East Cache fault is available to distinguish among several possible relationships. One possibility is that displacements on the James Peak fault occur near the end of surface ruptures produced by very large, but infrequent (average recurrence of >50 kyr) earthquakes which break a large part of the East Cache fault (>50 km). The length of these ruptures and the fact that the amount of displacement is likely to be greater near the center than near the end of the rupture segment indicate these earthquakes would be as large as or larger than those inferred on the central segments of the Wasatch fault (Bonilla and others, 1984; Schwartz and Coppersmith, 1984), which seems very unlikely. Alternatively, the East Cache fault may consist of unrecognized segments, with the southern part of the fault (and the James Peak fault) having an order of magnitude longer recurrence than the East Cache fault near Logan. The southern part of the East Cache fault could also have a slip rate and recurrence similar to that for the central part of the fault; if displacements were occurring near the base of the facets along the range front, on faults buried by the post-Provo alluvial fans along the range front, or on faults basinward of the alluvial fans, scarps on these unrecognized faults would be either buried or quickly eroded.

Although the apparent slip rates on the East Cache and James Peak faults differ by a factor of 3-6, it should be emphasized that the age of the datums used to estimate the rates differ by almost an order of magnitude. A similar situation is reported by Machette and others (this volume) whose mapping suggests that the high slip rates and short recurrence intervals on the central segments of the Wasatch fault zone may only apply to the latest Pleistocene and Holocene; longer term, late Quaternary rates appear to be much lower, closer to those estimated for other faults in the region (for example, Nelson and VanArsdale, 1986; Sullivan and Nelson, this volume). The rapid changes in subsurface pore pressures and isostatic loading and unloading accompanying the rise and fall of Lake Bonneville about 15 ka may have triggered many earthquakes on the Wasatch and East Cache faults resulting in a latest Pleistocene and Holocene recurrence rate several times that for the late Quaternary (Swan and others, 1983; Machette and others, this volume). Thus, we speculate that late Quaternary slip rates on the East Cache fault and the James Peak fault, and perhaps recurrence as well, do not differ nearly as much as suggested by the apparent slip rates above.

CONCLUSIONS

Two surface-displacement events of about 2 m each have occurred on the James Peak fault in the last 140 ka indicating a late Quaternary slip rate of about 0.03 m/kyr. Surface-faulting recurrence intervals are difficult to estimate because of poor age control, but the average recurrence between events is at least 50 kyr. The fault may be a westerly splay of the East Cache fault rather than a separate valley-bounding fault like those to the south. The lack of detailed slip and recurrence data from the southern half of the East Cache fault precludes determining whether the central part of the East Cache fault behaves independently from the southernmost part of the fault and from the James Peak fault or whether all parts of both faults have had a similar late Quaternary history.

ACKNOWLEDGMENTS

This study is part of a regional seismotectonic study for assessment of seismic hazards to large dams in the Wasatch Mountains supported by the U.S. Bureau of Reclamation (Sullivan and others, 1986). The staff of the Bonneville Construction Office, U.S. Bureau of Reclamation, Provo, Utah, provided considerable logistical support. We especially thank Karl A. Jensen, Tremonton, Utah, for permission to excavate on his property. Ed Baltzer assisted in mapping and logging the trench. Soil analyses by Rolf Kihl, INSTAAR, University of Colorado, are appreciated. Dean Ostenaa reviewed earlier drafts of the manuscript and Tony Crone and Jim McCalpin substantially improved this draft.

REFERENCES CITED

Anderson, L. W., and Miller, D. G., 1979, Quaternary fault map of Utah: Long Beach, Calif., Fugro, Inc., 39 p.

Baker, R. G., 1983, Holocene vegetational history of the western United States, _in_, Wright, H. E., Jr., Late-Quaternary environments of the United States, Wright, H. E., Jr., ed., The Holocene, v. 2: Minneapolis, Minnesota, University of Minnesota Press, p. 109-127.

Bilzi, A. F., and Ciolkosz, E. J., 1977, Time as a factor in the genesis of four soils developed in recent alluvium in Pennsylvania: Soil Science Society of America Journal, v. 41, p. 122-127.

Birkeland, P. W., 1984, Soils and Geomorphology: New York, Oxford University Press, 372 p.

Birkeland, P. W., Colman, S. M., Burke, R. M., Shroba, R. R., and Meierding, T. C., 1979, Nomenclature of alpine glacial deposits--or what's in a name?: Geology, v. 7, p. 532-536.

Bjorkland, C. J., and McGreevy, C. J., 1971, Geologic map and section of Cache Valley, Utah and Idaho: Utah Department of Natural Resources Publication No. 36, 1 pl.

Blau, J. C., 1975, Geology of the southern part of the James Peak quadrangle [unpub. M.S. thesis]: Logan, Utah, Utah State University, 55 p.

Bonilla, M. G., Mark, R. K., and Lienkaemper, J. J., 1984, Statistical relations among earthquake magnitude, surface rupture length, and surface fault displacement: Bulletin of Seismological Society of America, v. 74, p. 2379-2411.

Bucknam, R. C., and Anderson, R. E., 1979, Estimation of fault-scarp ages from a scarp-height-slope-angle relationship: Geology, v. 7, p. 11-14.

Bull, W. B., and McFadden, L. D., 1977, Tectonic geomorphology north and south of the Garlock fault, California, in, Doehring, D. O., ed., Geomorphology in arid regions: Proceedings, 8th Annual Geomorphology Symposium, State University of New York, Binghamton, NY, p. 115-138.

Carver, R. E., ed., 1971, Procedures in Sedimentary Petrology: New York, Wiley-Interscience, 653 p.

Cluff, L. S., Glass, C. E., and Brogan, G. E., 1974, Investigation and evaluation of the Wasatch fault north of Brigham City and Cache Valley faults, Utah and Idaho; A guide to land use planning with recommendations for seismic safety [unpub. report, U.S. Geological Survey contract no. 14-08-001-13665]: Oakland, CA, Woodward-Lundgren and Associates, 146 p.

Colman, S. M., and Pierce, K. L., 1981, Weathering rinds on andesitic and basaltic stones as a Quaternary age indicator, western United States: U.S. Geological Survey Professional Paper 1210, 56 p.

______1986, Glacial sequence near McCall, Idaho: Weathering rinds, soil development, morphology, and other relative-age criteria: Quaternary Research, v. 25, p. 25-42.

Colman, S. M., Choquette, A. F., Hawkins, F. F., 1986, Physical, soil, and paleomagnetic stratigraphy of the upper Cenozoic sediments in Fisher Valley, southeastern Utah: U.S. Geological Survey Bulletin, (in press).

Crittenden, M. D., Jr., 1972, Willard thrust and Cache Allochthon, Utah: Geological Society of America Bulletin, v. 83, p. 2871-2880.

Crittenden, M. D., Jr., and Sorensen, M. L., 1985a, Geologic map of the North Ogden quadrangle and part of the Ogden and Plain City quadrangles, Box Elder and Weber Counties, Utah: U.S. Geological Survey Miscellaneous Investigations Map I-1606, 1 pl., scale 1:24,000.

______1985b, Geologic map of the Mantua quadrangle and part of the Willard quadrangle, Box Elder, Weber, and Cache Counties, Utah: U.S. Geological Survey Miscellaneous Investigations Map I-1605, 1 pl., scale 1:24,000.

Crone, A. J., and M. N. Machette, 1984, Surface faulting accompanying the Borah Peak earthquake, central Idaho: Geology, v. 12, p. 664-667.

Davis, F. D., 1983, Geologic map of the central Wasatch Front, Utah: Utah Geological and Mineral Survey Map 54-A, 2 pls., scale 1:100,000.

Gilbert, G. K., 1890, Lake Bonneville: U.S. Geological Survey Monograph No. 1, 438 p.

______1928, Studies of Basin and Range structure: U.S. Geological Survey Professional Paper 153, 89 p.

Guthrie, R. L., and Witty, J. E., 1982, New designations for soil horizons and layers and the new Soil Survey Manual: Soil Science Society America Journal, v. 46, p. 443-444.

Hamblin, W. K., 1976, Patterns of displacement along the Wasatch fault: Geology, v. 4, p. 619-622.

Harden, J. W., 1982, A quantitative index of soil development from field descriptions--Examples from a chronosequence in central California: Geoderma, v. 28, p. 1-28.

Harden, J. W., and Taylor, E. M., 1983, A quantitative comparison of soil development in four climatic regimes: Quaternary Research, v. 20, p. 342-359.

Hintze, L. F., 1980, Geologic map of Utah: Utah Geological and Mineral Survey, 2 pls., scale 1:500,000.

Jackson, M. L., 1956, Soil Chemical Analysis, Advanced Course: [unpublished laboratory manual] Madison, Wis., University of Wisconsin, Department of Soil Science, 656 p.

King, H. D., 1965, Paleozoic stratigraphy of the James Peak quadrangle, Utah: [unpub. M.S. thesis] Logan, Utah, Utah State University, 47 p.

Machette, M. N., 1985, Calcic soils of the southwestern United States: Geological Society of America Special Paper 203, p. 1-21.

Machette, M. N., Personius, S. F., and Nelson, A. R., Quaternary geologic and tectonic history of the Wasatch fault zone, Utah, in, Hays, W. W., and Gori, Paula, eds., Assessment of regional earthquake hazards and risk along the Wasatch Front, Utah: U.S. Geological Survey Professional Paper, this volume.

Madole, R. F., 1976, Glacial geology of the Front Range, Colorado, in, Mahaney, W. C., ed., Quaternary Stratigraphy of North America: Stroudsburg, Pa., Dowden, Hutchinson, and Ross, p. 297-318.

McCalpin, James, Robison, R. M., and Garr, J. D., Neotectonics of the Hansel Valley-Pocatello Valley Corridor, northern Utah and southern Idaho, in, Hays, W. W., and Gori, Paula, eds., Assessment of regional earthquake hazards and risk along the Wasatch Front, Utah: U.S. Geological Survey Professional Paper, this volume.

Mullens, T. E., and Izett, G. A., 1964, Geology of the Paradise Quadrangle, Utah: U.S. Geological Survey Geologic Quadrangle Map GQ-185, 1 pl., scale 1:24,000.

Nakata, J. K., Wentworth, C. M., and Machette, M. N., 1982, Quaternary fault map of the Basin and Range and Rio Grande Rift provinces, western United States: U.S. Geological Survey Open-File Report 82-579, 2 pls., 1:2,500,000 scale.

Nash, D. B., 1981, Fault--A Fortran program for modeling the degradation of active normal fault scarps: Computers and Geosciences, v. 7, p. 249-266.

Nelson, A. R., and Krinsky, C. K., 1982, Late Cenozoic history of the upper Weber and Provo Rivers, NE. Utah [abs.]: Geological Society of America, Abstracts with Programs, v. 14, no. 3, p. 344.

Nelson, A. R., and Personius, S. F., 1986, Surficial geology map of the Kaysville segment of the Wasatch fault zone, Davis and Weber Counties, Utah: U.S. Geological Survey Map MF- (in preparation).

Nelson, A. R., and VanArsdale, R. B., 1986, Recurrent late Quaternary movement on the Strawberry normal fault, Basin and Range--Colorado Plateau transition zone, Utah: Neotectonics, v. 1, p. 1-30.

Ostenaa, D. A., 1984, Relationships affecting estimates of surface fault displacements based on scarp-derived colluvial deposits [abs.]: Geological Society of America, Abstracts with Programs, v. 16, no. 5, p. 327.

Peterson, D. L., 1974, Bouger gravity map of part of the northern Lake Bonneville Basin, Utah and Idaho: U.S. Geological Survey Map MF-627, 1 pl., scale 1:250,000.

Pierce, K. L., 1979, History and dynamics of glaciation in the northern Yellowstone National Park area: U.S. Geological Survey Professional Paper 729-F, 90 p.

Pierce, K. L., Obradovich, J. D., Friedman, I., 1976, Obsidian hydration dating and correlation of Bull Lake and Pinedale glaciations near West Yellowstone, Montana: Geological Society of America Bulletin, v. 87, p. 703-710.

Porter, S. C., Pierce, K. L., and Hamilton, T. D., 1983, Late Wisconsin mountain glaciation in the western United States, *in*, Wright, H. E., Jr., Late-Quaternary environments of the United States, Porter, S. C., ed., The Late Pleistocene, v. 1: Minneapolis, Minn., University of Minnesota Press, p. 71-111.

Scott, W. E., McCoy, W. D., Shroba, R. R., and Rubin, Meyer, 1983, Reinterpretation of the exposed record of the last two cycles of Lake Bonneville, western United States: Quaternary Research, v. 20, p. 241-265.

Schwartz, D. P., and Coppersmith, K. J., 1984, Fault behavior and characteristic earthquakes--Examples from the Wasatch and San Andreas fault zones: Journal of Geophysical Research, v. 89, no. B7, p. 5681-5698.

Shroba, R. R., 1980, Influence of parent material, climate, and time on soils formed in Bonneville-shoreline and younger deposits near Salt Lake City and Ogden, Utah [abs.]: Geological Society of America, Abstracts with Programs, v. 12, no. 6, p. 304.

Shroba, R. R., and Birkeland, P. W., 1983, Trends in late-Quaternary soil development in the Rocky Mountains and Sierra Nevada of the western United States, *in*, Wright, H. E., Jr., ed., Late-Quaternary environments the United States, Porter, S. C., ed., The late Pleistocene, v. 1: Minneapolis, Minn., University of Minnesota Press, p. 145-156.

Smith, R. B., and Bruhn, R. L., 1984, Intraplate extensional tectonics of the eastern Basin and Range--Inferences on structural style from seismic reflection data, regional tectonics, and thermal-mechanical models of brittle-ductile deformation: Journal of Geophysical Research, v. 89, no. B7, p. 5733-5762.

Stanley, W. D., 1972, Geophysical study of unconsolidated sediments and basin structure in Cache Valley, Utah and Idaho: Geological Society of America Bulletin, v. 83, p. 1817-1830.

Sullivan, J. T., and Nelson, A. R., 1983, Late Cenozoic faulting in Heber and Keetley valleys, northeastern Utah, in, Crone, A. J., ed., Paleoseismicity along the Wasatch front and adjacent areas, central Utah, in, Geologic excursions in neotectonics and engineering geology in Utah, Geological Society of America, Fieldtrip guidebook for Rocky Mountain and Cordilleran Section Meeting - Part IV: Utah Geologic and Mineral Survey Special Studies 62, p. 55-61.

______ Recurrent late Quaternary displacement on the Morgan fault, Morgan Valley, north-central Utah, in, Hays, W. W., and Gori, Paula, eds., Assessment of regional earthquake hazards and risk along the Wasatch Front, Utah: U.S. Geological Survey Professional Paper, this volume.

Sullivan, J. T., Nelson, A. R., Martin, R. A., Jr., Foley, L. L., Baltzer, E. M., and Krinsky, C. M., 1986, Regional seismotectonic study for the Central Utah Project, Utah [unpub. report]: Denver, Colo., Seismotectonic Section Report 86-3, U. S. Bureau of Reclamation, (in press).

Swan, F. H., III, Hanson, K. L., Schwartz, D. P., and Black, J. H., 1983, Study of earthquake recurrence intervals on the Wasatch fault, Utah [unpub. 8th semiannual technical report for U.S. Geological Survey Contract No. 14-08-0001-19842]: San Francisco, Calif., Woodward-Clyde Consultants, 36 p.

Walkley, A., and Black, I. A., 1934, An examination of the Degtjareff method for determining soil organic matter, and a proposed modification of the chromic acid titration method: Soil Science, v. 34, p. 29-38.

Wallace, R. E., 1979, Map of young fault scarps related to earthquakes in north-central Nevada: U.S. Geological Survey Open-File Report 79-1554, 2 pls., scale 1:125,000.

Zoback, M. L., 1983, Structure and Cenozoic tectonism along the Wasatch fault zone, Utah, in, Miller, D. M., Todd, V. R., and Howard, K. A., eds., Tectonic and stratigraphic studies in the eastern Great Basin: Geological Society of America Memoir 157, p. 3-29.

Zoback, M. L., and M. D. Zoback, 1980, State of stress in the conterminous United States: Journal of Geophysical Research, v. 85, no. B, pp. 6113-6156.

UNITED STATES
DEPARTMENT OF THE INTERIOR
GEOLOGICAL SURVEY

ASSESSMENT OF REGIONAL EARTHQUAKE HAZARDS AND RISK ALONG THE WASATCH FRONT, UTAH

VOLUME II

Editors
Paula L. Gori and Walter W. Hays

Contributions from:

UTAH GEOLOGICAL AND MINERAL SURVEY
UTAH DIVISION OF COMPREHENSIVE EMERGENCY MANAGEMENT
UNIVERSITY OF UTAH
UTAH STATE UNIVERSITY

Open File Report 87-585

Reston, Virginia
1987

FOREWORD

This report represents an ongoing U.S. Geological Survey effort to transfer accurate earth science information about earthquake hazards along the Wasatch front, Utah to researchers, public officials, design professionals, land-use planners, and emergency managers in an effort to mitigate the effects of earthquake hazards. This report is a preview of the future U.S. Geological Survey professional paper on regional earthquake hazards and risk along the Wasatch front.

Currently State and local governments, private institutions, and individuals are implementing earthquake hazards reduction measures in Utah. The success of their efforts will depend, in part, on the availability of accurate earth science information. The timeliness and importance of the multidisciplinary research contained in this report and the need for its utilization has made it imperative to release the information in the form of an open-file report while the process of publishing the professional paper is being completed.

The report is organized into 2 volumes. Volume I contains chapters on the tectonic framework and earthquake potential of the Wasatch front area. Volume II contains chapters on the ground shaking hazards and aspects of loss estimation, as well as, chapters on the use of hazards information for urban and regional planning and development. Many of the chapters are in draft format and, therefore, the figures follow the text.

The information contained in this report is the latest and most accurate information available on earthquake hazards along the Wasatch front and may be used and cited until such time as the Professional Paper on "Regional earthquake hazards and risk along the Wasatch front," is published.

Paula L. Gori
Walter W. Hays
Editors

ASSESSMENT OF REGIONAL EARTHQUAKE HAZARDS AND RISK ALONG THE WASATCH FRONT, UTAH

Table of Contents

VOLUME I

INTRODUCTION TO ASSESSMENT OF REGIONAL EARTHQUAKE HAZARDS AND RISK ALONG THE WASATCH FRONT, UTAH

THE TECTONIC FRAMEWORK AND EARTHQUAKE POTENTIAL OF THE WASATCH FRONT AREA

VOLUME II

THE GROUND-SHAKING HAZARDS AND ASPECTS OF LOSS ESTIMATION IN THE WASATCH FRONT AREA

THE USE OF EARTHQUAKE HAZARDS INFORMATION FOR URBAN AND REGIONAL PLANNING AND DEVELOPMENT IN THE WASATCH FRONT AREA

SITE AMPLIFICATION IN THE SALT LAKE CITY-OGDEN-PROVO URBAN CORRIDOR AND THE IMPLICATIONS FOR EARTHQUAKE-RESISTANT DESIGN

By

Walter W. Hays
U.S. Geological Survey
Reston, Virginia 22092

Abstract

Like many other urban areas in the United States, the Salt Lake City-Ogden-Provo urban corridor is underlain by soil deposits that will amplify earthquake ground motions in narrow period bands under certain conditions. When soil amplification occurs, the demand on the structure can exceed its capacity to resist the enhanced ground shaking in the narrow period band. In that case, the structure may experience severe damage or collapse.

Estimating the level of surface ground shaking in the Salt Lake City-Ogden-Provo urban corridor is complex because the cities are founded on soils of differing thickness, softness, and spatial extent. Also, no empirical data from past earthquakes in Utah have been recorded on these soil deposits to demonstrate the effects they have on the amplitude and spectral composition of the surface ground motion. This gap in knowledge makes it difficult to estimate the level and variability of ground motion expected from future moderate- to large-magnitude earthquakes occurring along the Wasatch front.

In terms of bedrock motions, analysis by Algermissen and others (1982) indicates that earthquakes along the Wasatch front could, in a 50-year exposure time, generate bedrock ground motions having peak amplitudes of horizontal acceleration and velocity that reach 0.28 g and 16 cm/s, respectively. Ordinates of spectral velocity for 5-percent damping are expected to reach 100 cm/s at sites underlain by bedrock and even higher values at sites underlain by soil.

The amplitude and spectral characteristics of the surface ground motions at sites in the urban corridor underlain by soil are difficult to quantify precisely, because one must consider the magnitude and epicentral distance of the earthquake; the propagation paths of the body and surface seismic waves; and variations in the thickness, softness, and geometry of the near-surface soil deposits. To aid the analysis, small-amplitude nuclear-explosion ground-motion data, representative of the low-strain environment were recorded at 71 sites in the urban corridor underlain by soil and rock. These data have provided new insight, especially in the period band 0.2 to 0.7 s. This period band corresponds to the fundamental mode of response of 2 to 7 story buildings, a dominant category in the Salt Lake City-Ogden-Provo urban corridor. These data combined with observations of site amplification throughout the World, indicate that the ground-shaking hazard in Salt Lake City-Ogden-Provo area is worst for sites in the centers of the valleys underlain by thick, soft silts and clays deposited in connection with the filling of the Great Salt Lake in the Pleistocene Epoch. These soft soil deposits cause frequency-dependent amplification of ground motion relative to a bedrock site on the Wasatch front with soil-to-rock amplification factors that can reach 10 (1,000 percent) in the period band 0.2 to 0.7 s under conditions of low (0.0001 to 0.1 percent) levels of shear strain. The soil-to-rock amplification factors in this period band are about 2 (200 percent) when the soil deposits are thin gravels and sands near the Wasatch front. Because the thickness of the silts and clays increases toward the valley centers, the soil-to-rock amplification factors also increase as distance from the Wasatch fault zone increases out to a distance of about 35 km, the valley centers.

Evaluation of site-amplification effects in Utah in the context of results obtained from worldwide postearthquake investigations and other regional studies, indicates unequivocally that the soil deposits in the Salt Lake City-Ogden-Provo urban corridor should be expected to amplify earthquake ground motions, especially when the level of shear strain induced in the soil column is less than about 0.5 percent. This level of strain would be expected to occur either in large-magnitude earthquakes located tens of kilometers or more from the site or in small-to-moderate magnitude earthquakes having epicenters located as close as a few kilometers from the site. Also, such an evaluation indicates that a high potential exists for the occurrence of damaging resonance in some 2-7 story buildings at some locations in the Salt Lake City-Ogden-Provo urban corridor during future earthquakes. Data from the September 19, 1985, Mexico earthquake are the best example of what might happen in Utah; they showed that "surprising" damage can occur at great epicentral distances (e.g., 400 km) when the frequency response of a soft soil column and the building are the same or almost the same.

The technical concern along the Wasatch front is how to account for the nonlinear soil response in future moderate- to large-magnitude earthquakes that might nucleate directly under one of the cities. Accurate depiction of the nonlinear response of soil to ground shaking in the near-source area is still a controversial issue that will remain unresolved in Utah until adequate near-source ground-motion data can be acquired to define the bounds on the effect.

The potential for site amplification of ground motion and the matched responses of some soil columns and buildings (resonance) are the most important future implications for earthquake-resistant design of buildings along the Wasatch front. The seismic-design provisions of the Uniform Building Code need to be evaluated to determine if the level of ground motion (that is, peak ground acceleration, peak ground velocity, spectral velocity) expected in a given exposure time and the soil-to-rock amplification factors defined by the soil-structure interaction factor in the code are adequate for designing buildings and other facilities in the Salt Lake City-Ogden-Provo urban corridor.

INTRODUCTION

Background

This paper presents information on site amplification in the Salt Lake City-Ogden-Provo urban corridor located adjacent to the Wasatch fault zone (Fig. 1) and suggests ways to incorporate this information in earthquake-resistant design and land use practices. The Wasatch fault zone is a 370-km-long zone of active, normal faulting within the Intermountain Seismic Belt. In Utah, the largest growth in population is occurring in this urban corridor where approximately 1,000,000 people (almost 80 percent of the population of Utah) now live. The building stock in this urban corridor is quite varied and includes low-, medium-, and high-rise buildings; schools; hospitals; the capital; government command centers; and lifeline systems (energy, water, communication, and transportation systems). The Wasatch fault zone has the potential for generating moderate- to large-magnitude earthquakes (Schwartz and Coopersmith, 1984). Ground shaking, surface fault rupture, and earthquake-induced landslides and liquefaction generated in such earthquakes could cause serious social and economic disruption throughout the State unless

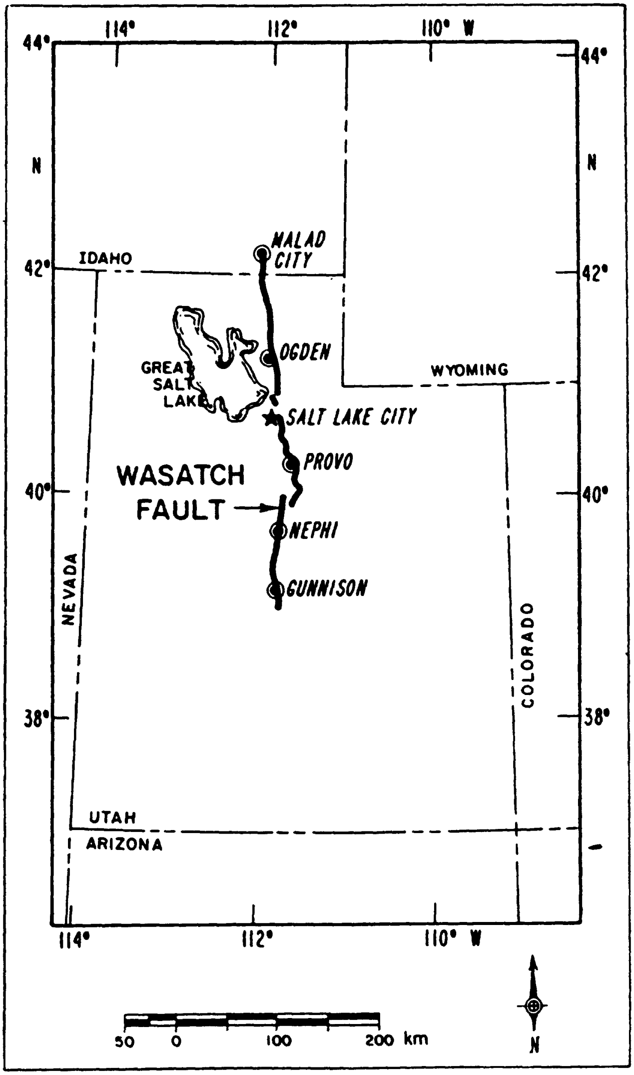

Figure 1.--Map showing the Wasatch fault zone, a major zone of active, normal faulting. The largest urban centers of Utah are located along the fault zone. Geologic and geomorphic evidence acquired primarily from paleoseismicity studies show that earthquakes having magnitudes of 7 or greater have occurred on the fault in the past 8,000 years.

realistic mitigation measures are devised and implemented before these earthquakes occur.

The Salt Lake City-Ogden-Provo urban corridor, like many other urban areas in the United States, is underlain by soil deposits that have the potential for amplifying earthquake ground motions in narrow period bands (Table 1). However, before elaborating further, some of the terminology will be reviewed to facilitate understanding.

Several terms (for example, site response, soil response, ground response, ground-motion response) are used interchangeable with site amplification in the ground-motion literature. All of these terms generally carry the same meaning as the term "site amplification" which is used in this report. Amplification is always defined relative to a rock site. (Figure 2 and 3). Site amplification refers to the frequency- and strain-dependent physical processes that occur when an overlying soil deposit responds to bedrock ground shaking. These physical processes can modify the peak amplitudes of acceleration, velocity, and displacement recorded at the ground surface, but these effects are small and relatively insignificant compared to the effects that occur in a discrete period band of the response spectrum. The result is that the spectral composition of the ground motions recorded at the surface of a soil deposit will differ from that for the subsurface bedrock ground motions or the ground motion recorded on surface outcrops of bedrock. Whether or not the peak amplitude of surface acceleration is increased or decreased by the soil column and the amount are the most controversial aspect of site amplification and the subject of continuing debate.

TABLE 1: SITE AMPLIFICATION EFFECTS IN VARIOUS URBAN AREAS

	PERIOD BAND OF DOMINANT RESPONSE		
LOCATION	SHORT (0.05-0.5 s)	INTERMEDIATE (0.5-3.0 s)	LONG (3.0-10 s)
California San Francisco Region (References: Wood, 1908; Reid, 1910; Steinbrugge, 1968; Idriss, and Seed, 1968; Borcherdt, 1975; Borcherdt and others, 1975; 1978; Joyner and others, 1981).	x	x	x
Los Angles Region (References: Murphy and others, 1971a; Boore, 1973; Davis and West, 1973; Hanks, 1976, Hays, 1977; Hays and others, 1979; Rogers and others, 1979; Rogers and others, 1985a)	x	x	x
Nevada Las Vegas Region (References: Murphy and others, 1971b; Bennett, 1974; Murphy and Hewlett, 1975).	x	x	x
Tonopah Region (References: Murphy and others, 1971b; Murphy and Hewlett, 1975)	x		
Beatty Region (References: Murphy and others, 1971b; Murphy and West, 1974)	x		
Washington Seattle Region (References: Ihmen and Hadley, 1987)			
Illinois Chicago Region (References: Peck and Reed, 1954)	x	x	x
Tennessee Memphis Region (References: Sharma and Kovacs, 1980)	x	x	
Massachusetts Boston Region (References: Whitman, 1983)	x	x	
South Carolina Charleston Region (References: Elton and Martin, 1986	x	x	
Puerto Rico San Juan Region (References: Molinelli, 1985)	x	x	

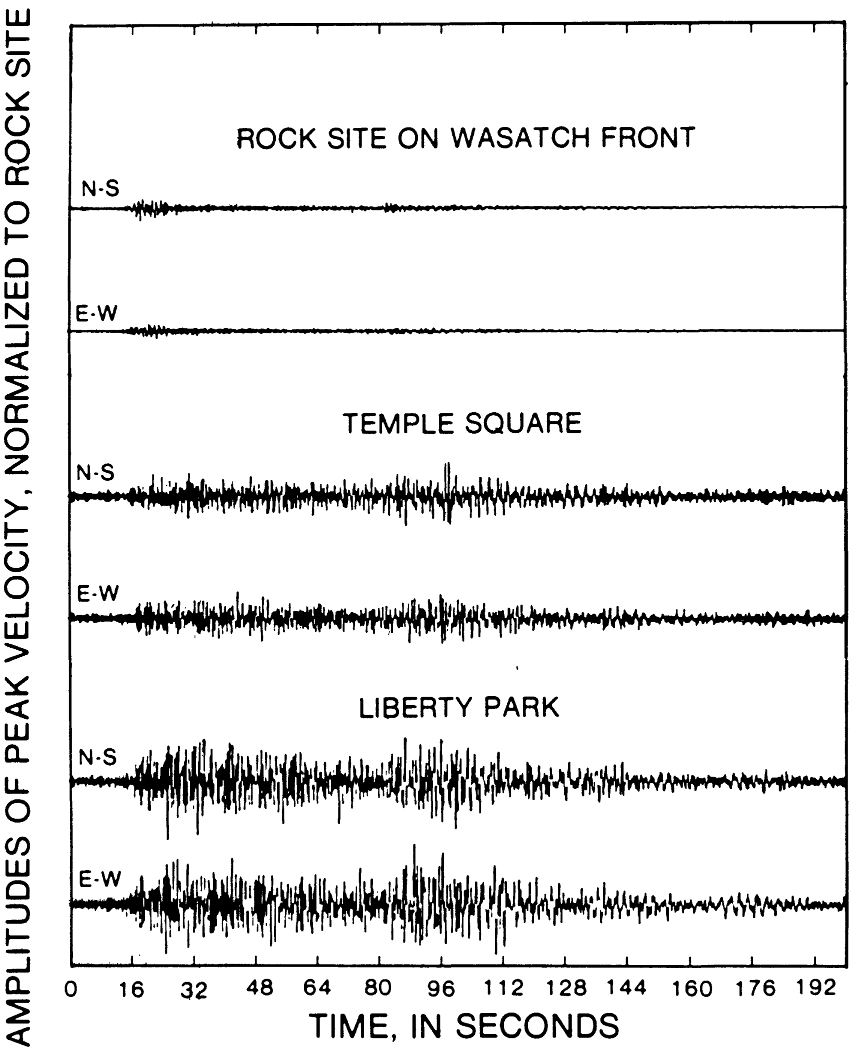

Figure 2.—Example of site amplification in Salt Lake City. The velocity time histories depict low-amplitude ground motions representing a low-strain environment which causes essentially elastic response. The potential for site amplification in the Salt lake City-Ogden-Provo urban corridor was recognized in the 1960's when ground motion records at sites underlain by deep soft soil exhibited higher levels of ground motion than records at nearby sites underlain by rock or thinner soil deposits.

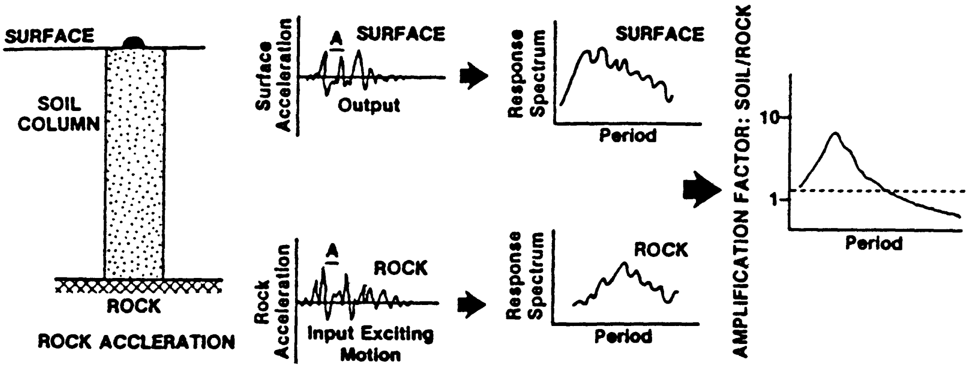

Figure 3.--Schematic illustration showing (from left to right) the soil-rock column, the bedrock and surface acceleration time histories, the corresponding response spectra derived from them, and the transfer function. The peak amplitude of acceleration is read from the acceleration time histories. The soil-to-rock amplification factor for a discrete period band is read from the transfter function.

The soil-to-rock amplification factor is a multiplicative factor ranging from a fraction (deamplification) to values of about 10 (1,000 percent). The multiplicative factor is related to a specific part (period band) of the spectrum. A typical description is that the amplification factor is a factor of 5 (500 percent) for the period band 0.2 to 0.7 s. Unless noted, the soil-to-rock amplification factor describes a frequency-domain effect for the horizontal component of ground motion, rather than a time-domain effect. The factor describes empirically what happened at the site underlain by soil relative to the reference site underlain by rock and is described in terms of a specific period, or a period band, or the period where the maximum or dominant response occurred (Figure 4) A factor of 5 in the frequency domain does not correspond to a factor of 5 in the time domain. The extent to which the peak amplitude of ground acceleration is increased or decreased depends on what happens physically at zero period (i.e., the very high frequencies).

The concept of a transfer function comes from the theory of linear operators (i.e., Fourier and Laplace transforms). In this paper, the transfer function is used to describe site amplification in the frequency domain, and, unless noted, the soil-to-rock transfer function is always derived. For a site underlain by a soil deposit, the procedure for estimating the transfer function is to divide the response spectrum by the corresponding response spectrum for a nearby site that is underlain by rock. The distance between the two sites must be small in comparison with the epicentral distance to each site. The soil-to-rock amplification factor for a discrete period band is determined from the transfer function. In the Fourier analysis of ground-motion data, the typical procedure until recently was to use the amplitude spectrum (which is a display of the amplitudes of the sinusoids composing the

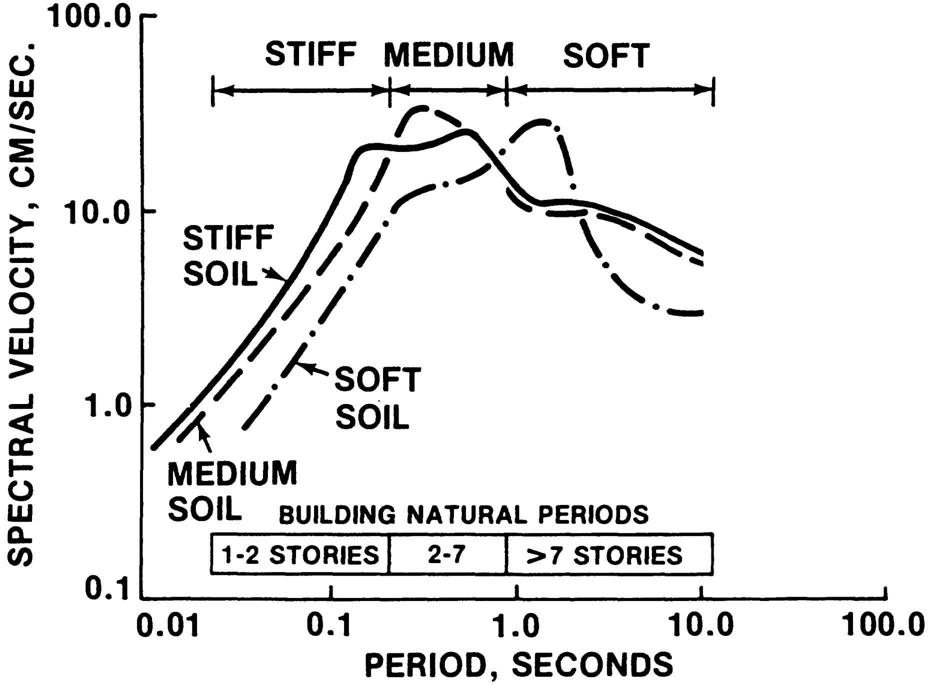

Figure 4.--Graph showing the effect of different types of soil columns on the spectral composition of ground motion. The general correlation with the height of the building is also shown for comparison. The soil column in the lake-bed zone of Mexico City caused a dominant response centered at 2 s. The period band 0.2 to 0.7 s. is emphasized in this paper because 2 to 7 story buildings are a dominant category.

time history as a function of frequency) and to neglect the phase spectrum (which is a display of the phase lead or lag of the sinusoids making up the time history as a function of frequency). One advantage of using the transfer function is that the source terms (for example, the nuclear-explosion forcing function) can be eliminated when analyzing site-amplification effects. This process makes the result essentially independent of the energy source (Rogers and Hays, 1978). Thus, nuclear-explosion sources can be used to add to the ground-motion data sample in an urban area if proper judgment is used.

Evaluation of the Bedrock Ground-Shaking Hazard in Utah

The bedrock ground-shaking hazard for a community is usually presented in a map format and the soil effects are considered in separate analyses. Such a map displays the spatial variation and relative severity of a physical parameter (such as peak bedrock ground acceleration or bedrock spectral velocity) and provides a basis for dividing a region into geographic zones, each region or zone having a similar relative severity throughout its extent to earthquake-generated ground-acceleration (or some other ground-motion parameters such as ground velocity or spectral acceleration). Once the level and extent of ground shaking have been defined for all zones in a region, public policy can be devised to mitigate the potential effects through implementation of appropriate actions such as avoidance, land-use planning, engineering design, and distribution of losses through insurance (Hays, 1981). Each mitigation strategy requires some sort of map to zone the ground-shaking hazard. The most familiar zoning map is contained in the Uniform Building Code (UBC). Soil amplification is not a part of the UBC zone map, but is considered separately in the analysis.

Algermissen and Perkins (1976) and Algermissen and others (1982) constructed the first probabilistic maps that could be used to define the bedrock ground-shaking hazard in Utah. Later, Youngs and others (see paper in this report) constructed a probabilistic ground-shaking hazard map for Utah which included consideration of the surface soil type through the attenuation relation. These maps were based on an integrated analysis of the following types of data:

1. seismicity,
2. earthquake source (seismogenic) zones, and
3. attenuation of peak acceleration (or another ground-motion parameter), holding bedrock or a soil type constant and allowing magnitude to vary.

The maps prepared by Algermissen and others (1982) were national maps; the portion for Utah is shown in Figures 5 and 6. These maps represent a 90 percent probability of nonexceedance in an exposure time of 50 years. They display bedrock ground shaking with levels as high as 0.28 g and 16 cm/s.

METHODOLOGY FOR EVALUATING SITE AMPLIFICATION

Evaluation of the ground-shaking hazard, including soil effects, in the Salt Lake City-Ogden-Provo urban corridor has proceeded slowly. The reasons include the need to acquire and analyze scientific and geotechnical data along the Wasatch fault zone, to integrate these data with other relevant worldwide data, and to resolve a number of technical problems (Hays and Gori, 1984).

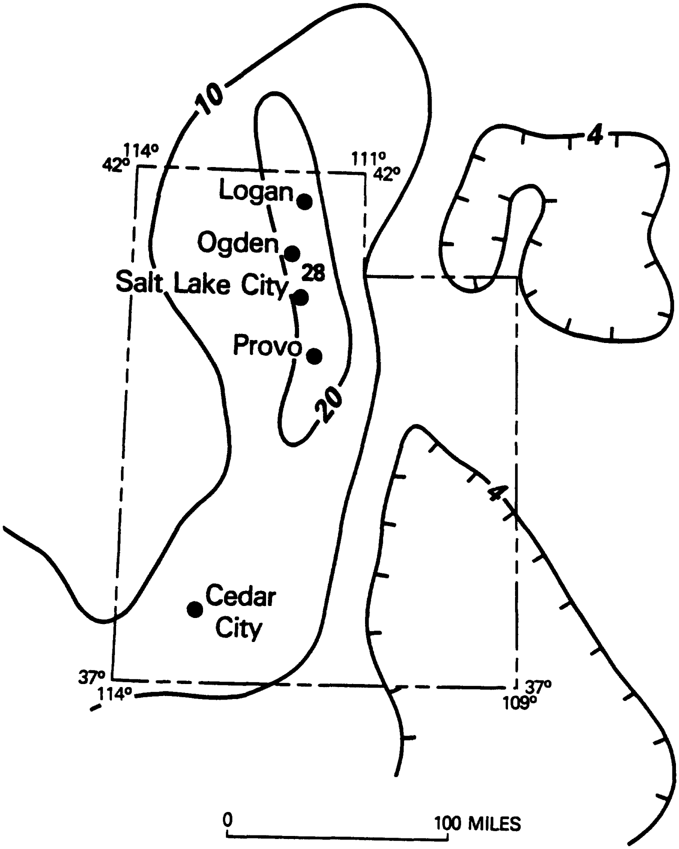

Figure 5.--Map of the probabilistic bedrock peak horizontal ground acceleration in Utah. The map is a portion of the national map (scale 1:7,500,000). It represents a 90 percent probability of nonexceedance in a 50 year exposure time (from Algermissen and others, 1982). The contours are expressed in terms of a percentage of the force of gravity. The effects of soil amplification are considered separately.

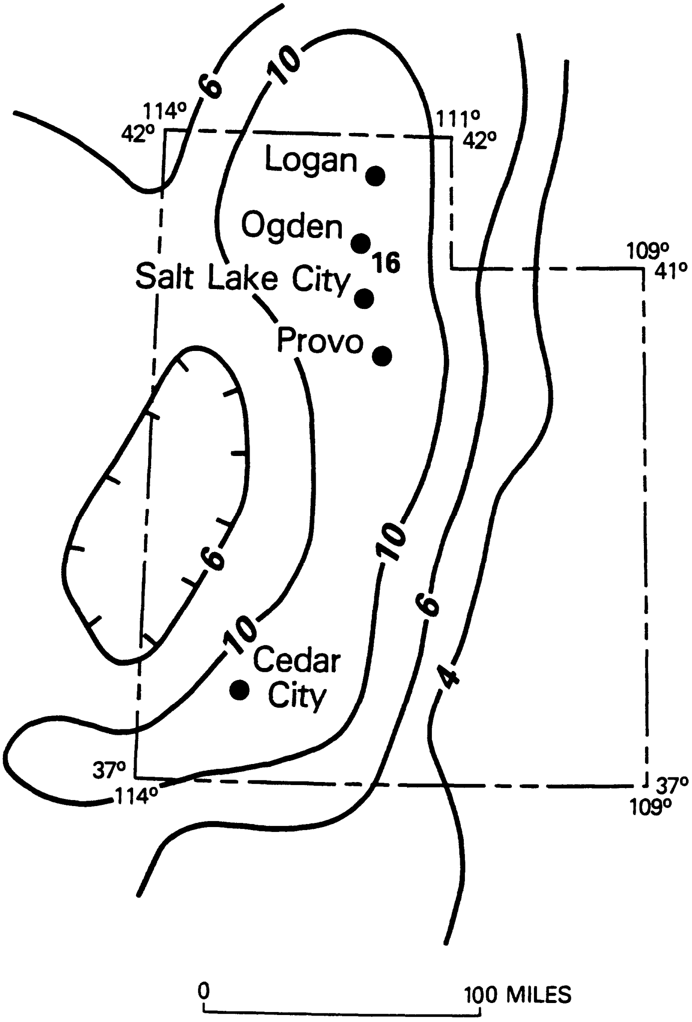

Figure 6.--Map of the probabilistic bedrock peak horizontal ground velocity in Utah. The map is a portion of the national map (scale 1:7,500,000). The map represents a 90 percent probability of nonexceedance in a 50 year exposure time (From Algermissen and others, 1982). The contours are expressed in centimeters per second. The effects of soil amplification are considered separately.

Evidence from seismic reflection lines shows that individual faults in the Wasatch fault zone dip at low angles and that they probably become listric at a depth of about 8 km, the depth above which earthquakes having magnitudes less than about 5.5 occur. Moderate- to large-magnitude (i.e., magnitudes (M_s) of about 6.5-7.5) earthquakes, although completely absent in the record of historical seismicity dating from 1847, appear to nucleate at depths of 10-15 km in or near the zone of brittle-ductile transition (Smith and others, 1985). When the frequency-magnitude plots of the recent instrumental seismicity data in Utah are extrapolated linearly, the frequency of small earthquakes is underestimated and the frequency of large earthquakes is over estimated (Schwartz and Coppersmith, 1984). Geologic data from trenching (i.e., fault-offset distances) show that the Wasatch fault zone is segmented and that repeated large-magnitude earthquakes have occurred in the past 8,000 years with average recurrence intervals of several hundred years (Schwartz and Coppersmith, 1984) The geologic and seismological data also suggest that the Wasatch fault zone may generate characteristic earthquakes of magnitudes (Ms) 7.0 to 7.5 and that the standard $\log N = a - bM$ relation does not apply in the strict sense (Schwartz and Coppersmith, 1984).

The estimated regional attenuation relation must be based on and constrained by California strong ground-motion data, not Utah data. No acceleration-attenuation relation exists for Utah earthquakes because strong ground-motion data have been recorded from only one earthquake in Utah, the 1962 magnitude 5.7 Cache Valley earthquake.

Empirical strong-motion data from past Utah earthquakes that show the frequency-dependent characteristics of ground response under low- to high-strain ground shaking are completely lacking along the Wasatch front. Data on building response in Utah earthquakes are also lacking.

Special studies performed to overcome these limitations and to evaluate the potential for site amplification are described below.

Soils data - A special effort was made in the 1970's (Miller, 1980) to quantify the physical properties of unconsolidated materials along the Wasatch front so that the response of the various soil deposits to earthquake ground shaking could be determined. Miller's work gave the following information. Salt Lake City, Ogden, and Provo are founded on several different types of soil deposits. These deposits are from several lakes that filled the Great Salt Lake Basin during the Pleistocene Epoch and can be grouped into three depositional types: onshore, nearshore, and offshore. Onshore deposits are primarily fluvial gravels and coarse sands that form a parallel band along the major mountain fronts. In contrast, nearshore and offshore deposits are lacustrine. Nearshore sediments were deposited on beaches, long shore spits and bars, deltas, and marshes. Offshore deposits consist of very fine sands, silts, and clays that accumulated in quiet, relatively deep water, and probably represent the finer portion of debris being carried into the lake from the mountains.

The soil columns in the Salt Lake City area range in thickness from about 100 m near the Wasatch front to 900 m in the deepest part of the Jordan River valley. In the Jordan River valley, the surficial materials have shear-wave velocities averaging about 200 m/s and have a natural moisture content by weight of about 43 percent (Miller, 1980). The available information in Ogden and Provo, although less than in Salt Lake City, suggests that the physical properties of the soil columns underlying Ogden and Provos are similar to those underlying the Salt Lake City area. A borehole in the Provo area indicates a shear-wave velocity of about 155 m/s for the surficial materials (Miller, 1980). To provide a comparison with another urban area having soils that vary in thickness and softness, the range of values of shear-wave velocities determined for soils in the San Francisco Bay region are given below (Gibbs and others, 1976) and are shown graphically in Figure 7:

1. 55 to 115 m/s - very soft to soft clay and silty clay.
2. 160 to 190 m/s - medium stiff clay to silty clay.
3. 170 to 305 m/s - very stiff to hard clay and silty clay.
4. 210 to 310 m/s - sandy clay and silty loam.
5. 240 to 270 m/s - interbedded sandy gravels and silty clay.
6. 150 to 250 m/s - loose to dense sand
7. 250 to 400 m/s - dense to very dense near-surface sand 0-12 m thick.
8. 250 to 570 m/s - dense to very dense sand 12 to 30 m thick.
9. 400 to 500 m/s - near-surface gravel.
10. 420 to 750 m/s - deep gravel.

Site amplification data - Two strategies were used to offset the limitations posed by the lack of ground-motion data from past Utah earthquakes (Hays and others, 1978; Hays, 1980). They are: 1) use nuclear-explosion ground-motion data recorded simultaneously at selected sites (Table 2) underlain by soil and rock in each city as a basis for deriving soil transfer functions to give a bound on site amplification under low-strain conditions, and 2) relate soil transfer functions to the depositional environment and physical properties

Table 2.--Locations of portable broadband seismograph stations in Utah that recorded nuclear explosions

Station	Location	Lat N. (degrees)	Long W. (degrees)
	Logan Area		
1	Logan Airport	41.846	111.894
3	Young Ward	41.708	111.909
4	90 S. Main, Providence	41.707	111.816
5	Utah State University	41.745	111.813
[1]6	Logan Canyon	41.741	111.786
	Ogden Area		
1	2095 N 100 E	41.288	111.983
2	1049 Kiesel	41.246	111.974
3	4376 W 2350 N	41.303	112.086
4	Rainbow Bowling Lanes	41.236	111.928
5	Rogers Poultry Farm	41.253	111.969
6	Weber Main Library	41.221	111.964
7	4463 Forrest Green Dr.	41.180	111.942
8	Syracuse Fire Dept.	41.092	112.055
11	4725 S 300 W	41.180	111.970
12	2550 S 4476 W; Taylor	41.235	112.087
13	Hooper Post Office	41.164	112.123
16	6675 900 S; West Warren	41.266	112.152
20	100 N 844 W; Farmington	39.989	111.912
	Salt Lake City Area		
1	West Bank of Jordan River	40.652	111.929
2	1663 Mt. View	40.639	111.844
[1]3	Rotary Park	40.826	111.801
4	Liberty Park	40.749	111.870
[1]5	Georges Hollow, Ft. Douglas	40.768	111.809
6	Utah Geol. & Min. Survey	40.755	111.827
[1]7	3100 Kennedy Dr.	40.757	111.791
8	So. Side of Parleys Creek	40.708	111.809
[1]9	Mill Creek Canyon	40.692	111.770
11	Castro Springs	40.673	111.809
10	4500 South Street	40.679	111.801

[1] Sites underlain by rock; other sites underlain by unconsolidated sediments.

Table 2.--Locations of portable broadband seismograph stations--Continued

Station	Location	Lat N. (degrees)	Long W. (degrees)
	Salt Lake City Area		
12	North Bank of Dry Creek	40.569	111.821
[1]13	Little Cottonwood Canyon	40.573	111.763
14	1932 Parkridge	40.616	111.839
15	Sandy City Fire Station	40.580	111.872
16	Murray City	40.639	111.892
17	Salt Lake Int'l. Airport	40.785	111.955
18	Saltair	40.769	112.101
19	SLC Airport-Fire Station	40.783	111.979
20	Hidden Valley G. C.	40.556	111.839
21	12000 S 1700 E	40.536	111.830
22	Bateman Dairy Farm	40.612	111.927
23	10875 S 12 W	40.554	111.922
24	North Jordan Park	40.752	111.918
25	SLC Fire Station #7	40.776	111.920
26	Capitol Building	40.777	111.887
27	University of Utah	40.776	111.847
28	Taylorsville	40.663	111.949
29	4060 S 725 W	40.683	111.910
30	Sugar House Library	40.721	111.866
31	3702 S 645 E	40.691	111.872
32	2838 Imperial	40.709	111.843
33	6100 S 700 W	40.641	111.917
34	4130 S 1221 E	40.682	111.856
35	2270 E. Evergreen St.	40.699	111.832
36	1560 Industrial Road	40.773	112.011
37	4036 So. Golden Cir.	40.684	111.852
38	3915 Brooklane Dr.	40.687	111.848
39	1759 Mt. View	40.691	111.841
41	1964 E. Evergreen St.	40.697	111.832
	Provo Area		
1	Olmstead Office Bldg.	40.315	111.655
[1]2	Olmstead	40.326	111.639
3	Orem Fire Station	30.314	111.695
4	Orem City Offices	40.299	111.693
5	Cherry Hill Farm	40.264	111.717

[1] Sites underlain by rock; other sites underlain by unconsolidated sediments.

Table 2.--Locations of portable broadband seismograph stations--Continued

Station	Location	Lat N. (degrees)	Long W. (degrees)
	Provo Area		
6	Provo Airport	40.221	111.718
7	Boat House, Utah Lake	40.236	111.736
8	Provo City offices	40.238	111.671
9	K-96 Radio Station	40.213	111.671
10	Youd Farm 40.133	111.730	
11	Springville Fire Station	40.167	111.610
	Cedar City Area		
1	Three Peaks 37.717	113.225	
[1]2	Coal Canyon 37.679	113.050	
3	Rush Lake 37.864	113.064	
4	Stevensville 37.786	113.092	
5	College of Southern Utah	37.675	113.067
6	SUSC Football Field	37.676	113.077
7	Highway 14 Trailer Park	37.678	113.055
8	Cemetery 37.689	113.063	
9	Settling Pond	37.656	113.068
10	Imperial 400 Motel	37.673	113.061

[1] Sites underlain by rock; other sites underlain by uncolidated sediments.

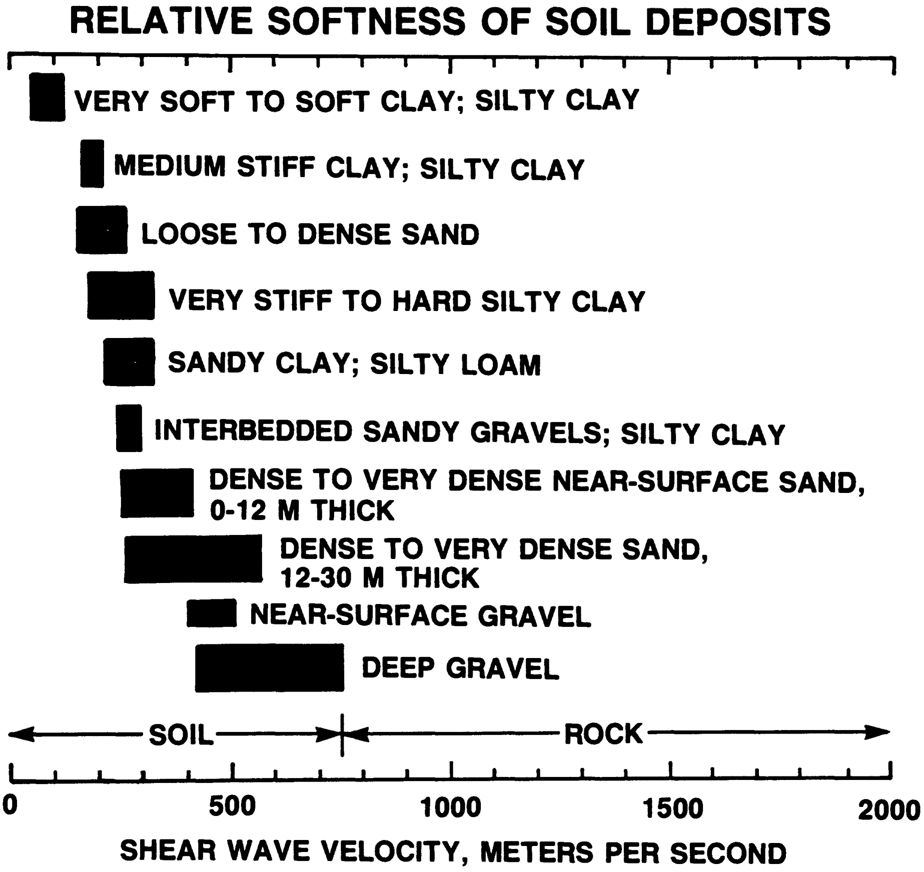

Figure 7.--Graph showing the range of shear-wave velocities of surficial soils in the San Francisco Bay Region. The relative softness increases from right to left. For comparison, the thick, soft clay and silt deposits in the Salt Lake City-Ogden-Provo urban corridor have an average shear-wave velocity of 200m/s. (After Gibbs and others, 1976).

(e.g., shear-wave velocity, bulk density, lithology and water content) of the 71 recording sites in the Salt Lake City-Ogden-Provo urban corridor. Ground-motion measurements from a dozen nuclear explosions at the Nevada Test Site were made simultaneously at sites underlain by soil and rock in each city as well as at sites in Logan and Cedar City to provide some comparison of effects. Recording sites underlain by rock on the Wasatch front encompassed limestone, quartz monozonite, shale, and sandstone. Portable broadband velocity seismographs were deployed at each location. Acceleration and displacement time histories were derived from the velocity records along with 5-percent damped response spectra. These data provide complete information on the amplitude and spectral composition of the ground motion recorded at each site, but they are representative only of the small-amplitude, low-strain environment.

A brief discussion of the response spectrum is provided below to facilitate understanding. The response spectrum is the most common representation of the spectral composition of earthquake and ground motion. The response spectrum (Figure 8) depicts graphically the peak amplitude of each time history representing the individual response of each one of a series of damped, simple harmonic oscillators to the acceleration time history input at the base of the oscillator. The structural engineering uses the response spectrum having 2 to 5 percent damping as a tool to correlate characteristics of ground motion with the elastic response of buildings of various heights and types. The concepts of the response spectrum are also incorporated in the UBC and other building codes.

GROUND MOTION AND THE RESPONSE SPECTRUM

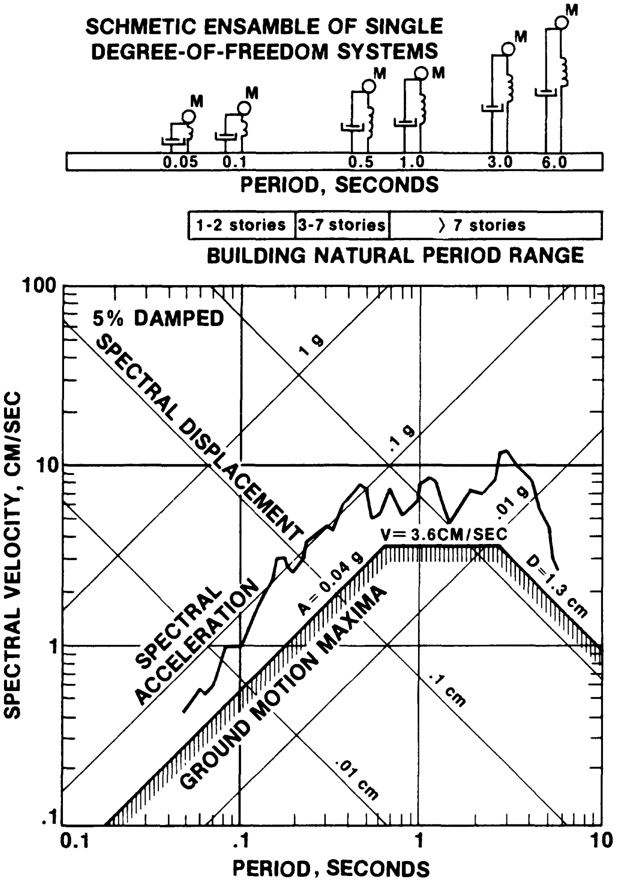

Figure 8.--Schematic illustration showing the correlation of the response spectrum derived froma stong-motion accelerogram with a series of clamped, signt degree-of-freedom, harmonic oscillators. The peak amplitude of acceleration is the zero-period asymptote t the spectrum and the peak amplitude of displacmeent is the infinite-period asymptote. The ground motion can be correlated with building response through the response spectrum.

Soil transfer functions were derived in each city from the response spectra (Figures 9, 10, 11, 12, 13). Many investigators (for example, Borcherdt, 1975; Rogers and Hays, 1978; Hays and others, 1978, 1979; Hays, 1980) have shown that the transfer function, defined as the average ratio of the 5-percent damped, horizontal, velocity response spectra for a pair of soil-rock sites, is a sensitive function of the properties of the soil columns underlying the sites. Rogers and Hays (1978) showed that a transfer function can be determined reasonably well from either earthquake or nuclear-explosion ground-motion data because the source effects are essentially eliminated when taking the ratios, though there may be a significant difference in the levels of peak ground accelerations and dynamic shear strain (defined approximately by the ratio of the peak particle velocity to the shear-wave velocity of the soil). Hays and others (1978) concluded from the lack of dependence of site amplification on amplitude that the response of some soil deposits in Nevada is probably linear up to about 0.5 percent strain. However, this conclusion can not be verified for the Salt Lake City-Ogden-Provo urban corridor until earthquake data have been recorded.

MAPS OF THE SITE AMPLIFICATION FACTORS FOR SALT SALE CITY, OGDEN, AND PROVO

Maps showing the spatial variation of soil-to-rock amplification factors were prepared for Salt Lake City, Ogden, and Provo (Figures 14, 15, and 16). These maps were based on the mean value of the soil transfer function in a specific period band, 0.2 to 0.7 s, derived from the small-amplitude nuclear-explosion data (Hays and King, 1982, 1984). This period band was selected because the signal-to-noise ratio is best for this band and it correlates roughly with the

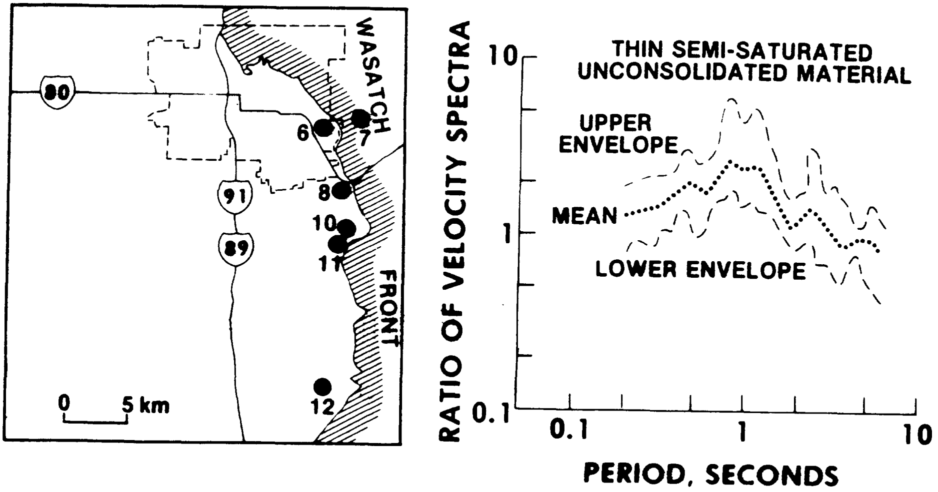

Figure 9.--Range of transfer functions showing horizontal ground response of sites underlain by thin (150 m or less) deposits of sands and gravels (stations 6, 8, 10, 11, 12) relative to a rock site (station 7) on the Wasatch front, Salt Lake City area. Ground response is shown in terms of a mean transfer function. These data represent a low-strain environment.

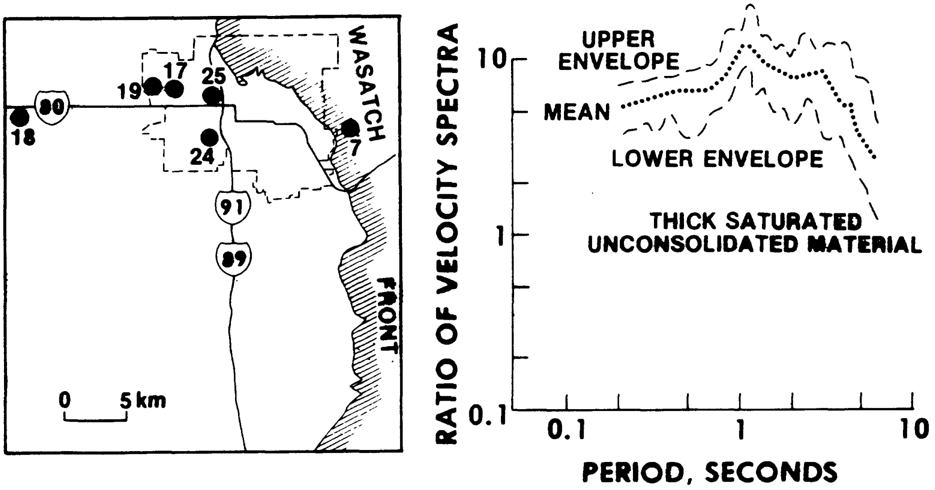

Figure 10.--Range of transfer functions showing horizontal ground response of sites underlain by thick (450-750 m), soft deposits of silts and clays (station 17, 18, 19, 24, 25) relative to a rock site (station 7) on the Wasatch front, Salt Lake City area. Ground response is shown in terms of a mean transfer function. These data represent a low-strain environment.

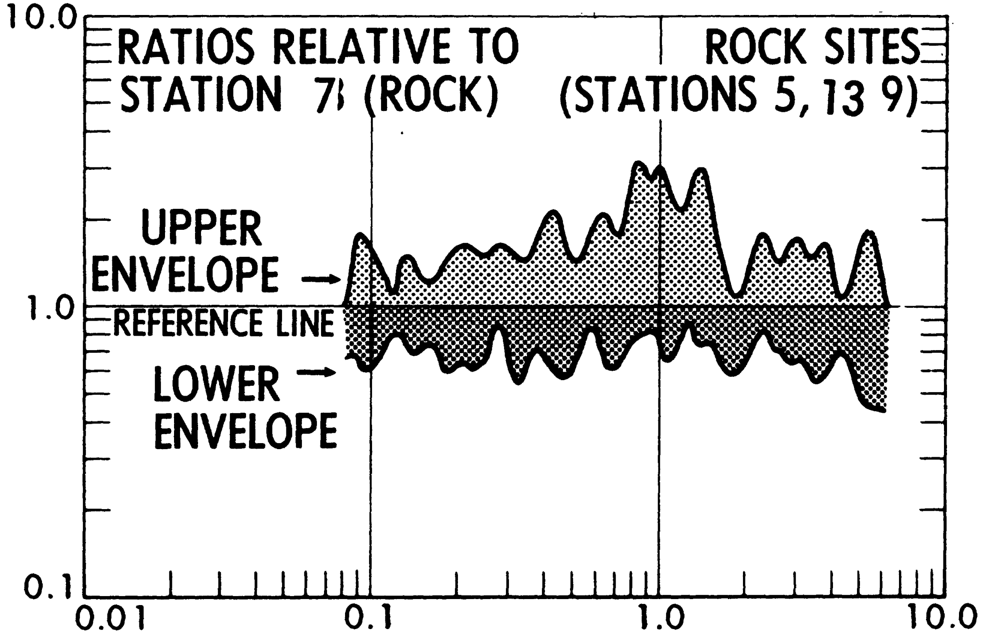

Figure 11.--Range of transfer functions showing horizontal ground response of sites underlain by rock. The reference station is station 7 on the Wasatch front, Salt Lake City area.

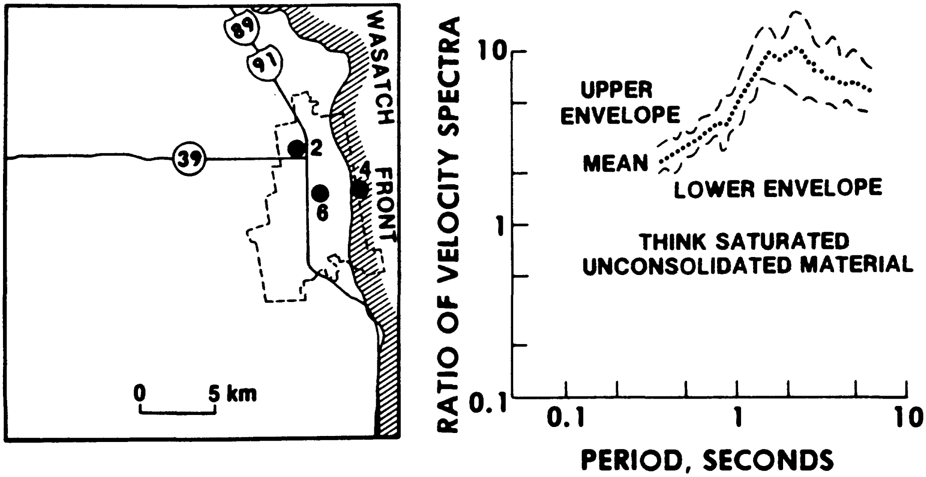

Figure 12.--Range of transfer functions showing horizontal ground response of sites underlain by thick soft silts and clays (station 2 and 6) relative to a rock site (station 4) on the Wasatch front, Ogden area. These data represent a low-strain environment.

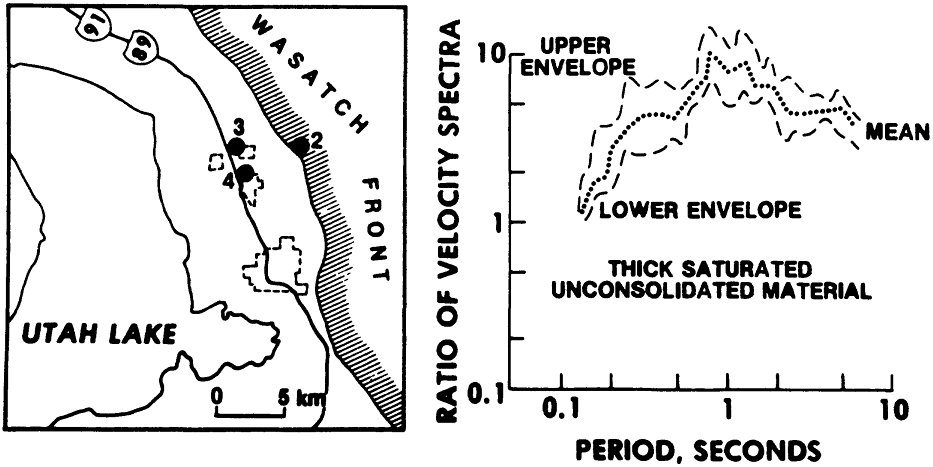

Figure 13.--Range of transfer functions showing horizontal ground response of sites underlain by thick soft silts and clays (station 3 and 4) relative to a rock site (station 2) on the Wasatch front, Provo area. Station 3 and 4 are located in Orem. These data represent a low-strain environment.

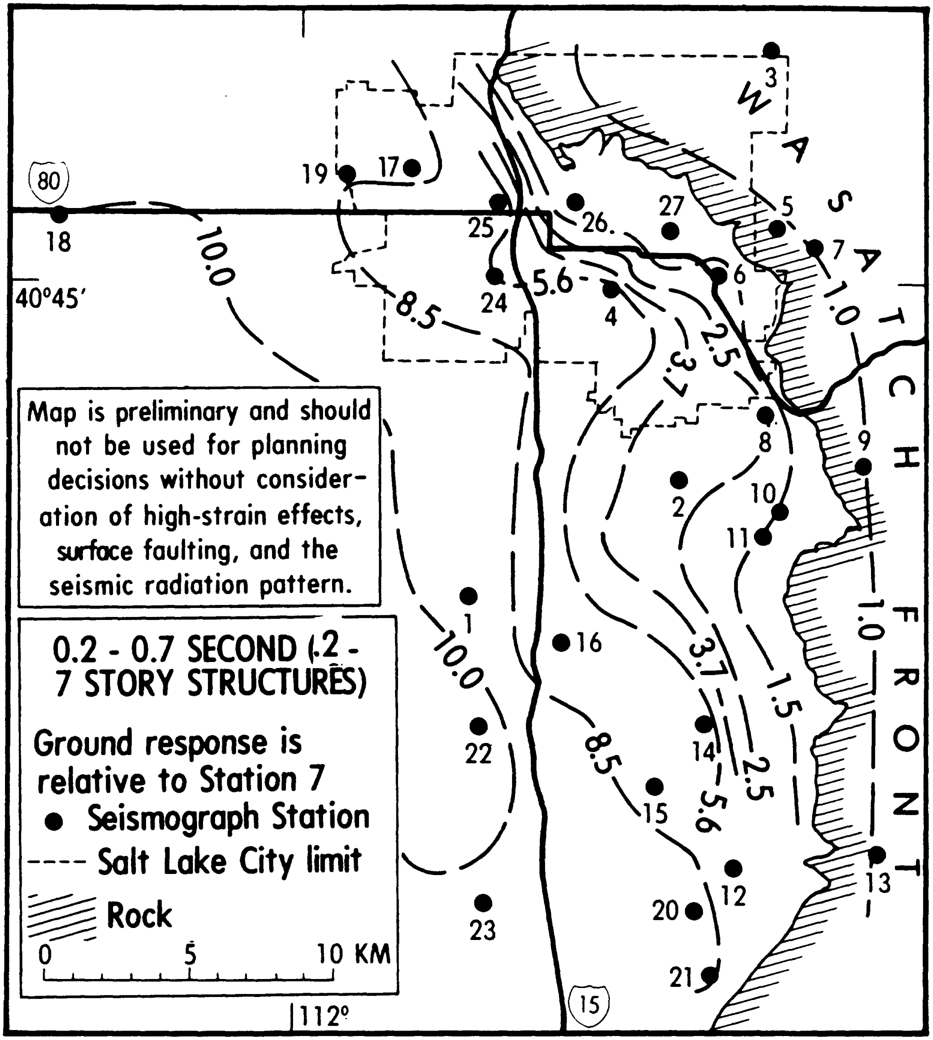

Figure 14. Map showing the spatial variation of site-amplification factors for the period band 0.2 to 0.7 s, Salt Lake City area. Values on contours indicate the ratios of velocity response spectra that would be expected at underlain by soil relative that experienced at sites underlain by rock on the Wasatch Front. These values provide an estimate of the spatial variation of ground motion in the period band for which 2 to 7 story buildings have their fundamental natural period of vibration (from Hays and King, 1982). These data represent a low-strain environment. Repeatability would be least certain when a moderate-to large-magnitude earthquake nucleates underneath the city.

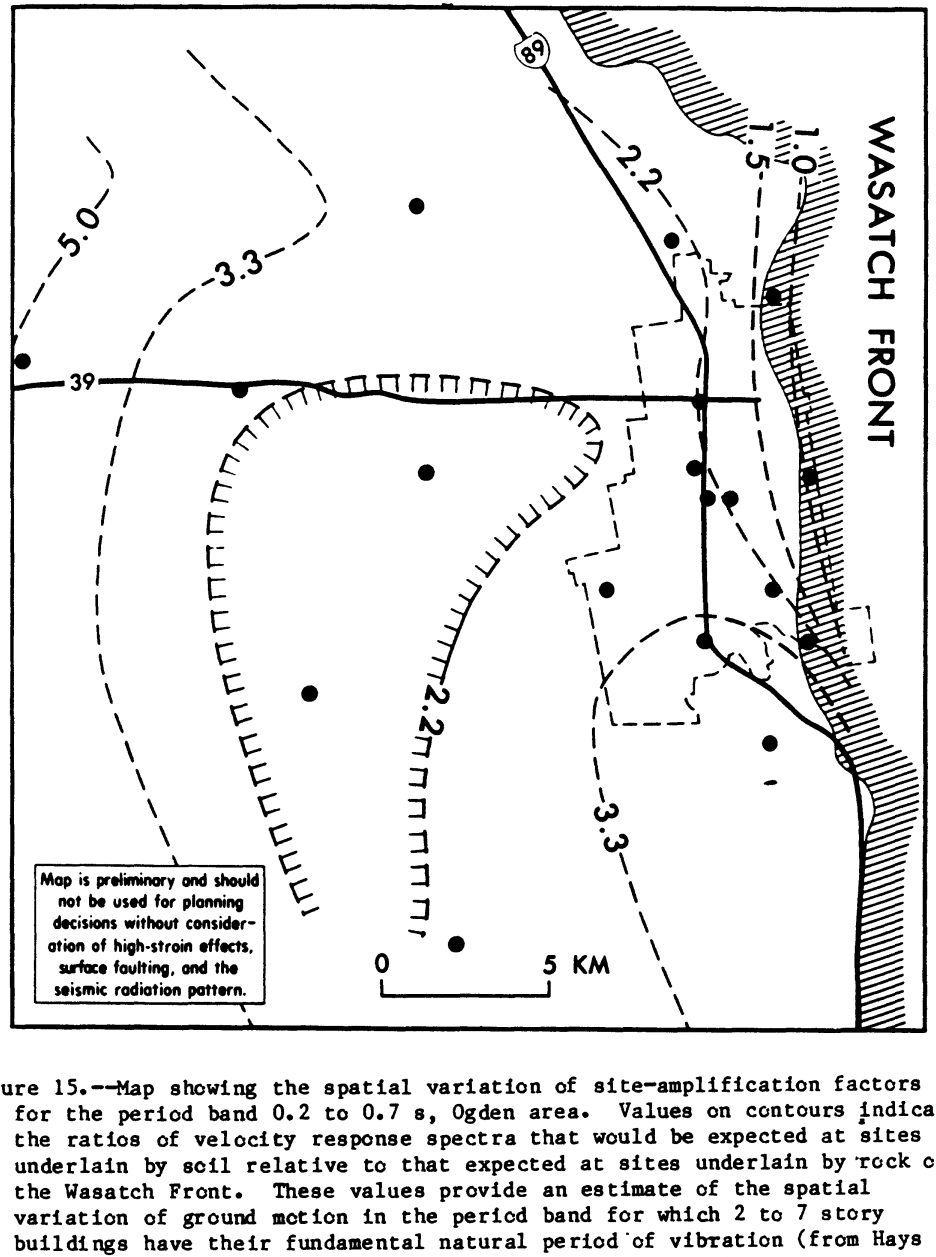

Figure 15.—Map showing the spatial variation of site-amplification factors for the period band 0.2 to 0.7 s, Ogden area. Values on contours indicate the ratios of velocity response spectra that would be expected at sites underlain by soil relative to that expected at sites underlain by rock on the Wasatch Front. These values provide an estimate of the spatial variation of ground motion in the period band for which 2 to 7 story buildings have their fundamental natural period of vibration (from Hays and King, 1982). These data represent a low-strain environment. Repeatability would be least certain when a moderate- to large-magnitude earthquake nucleates underneath the city.

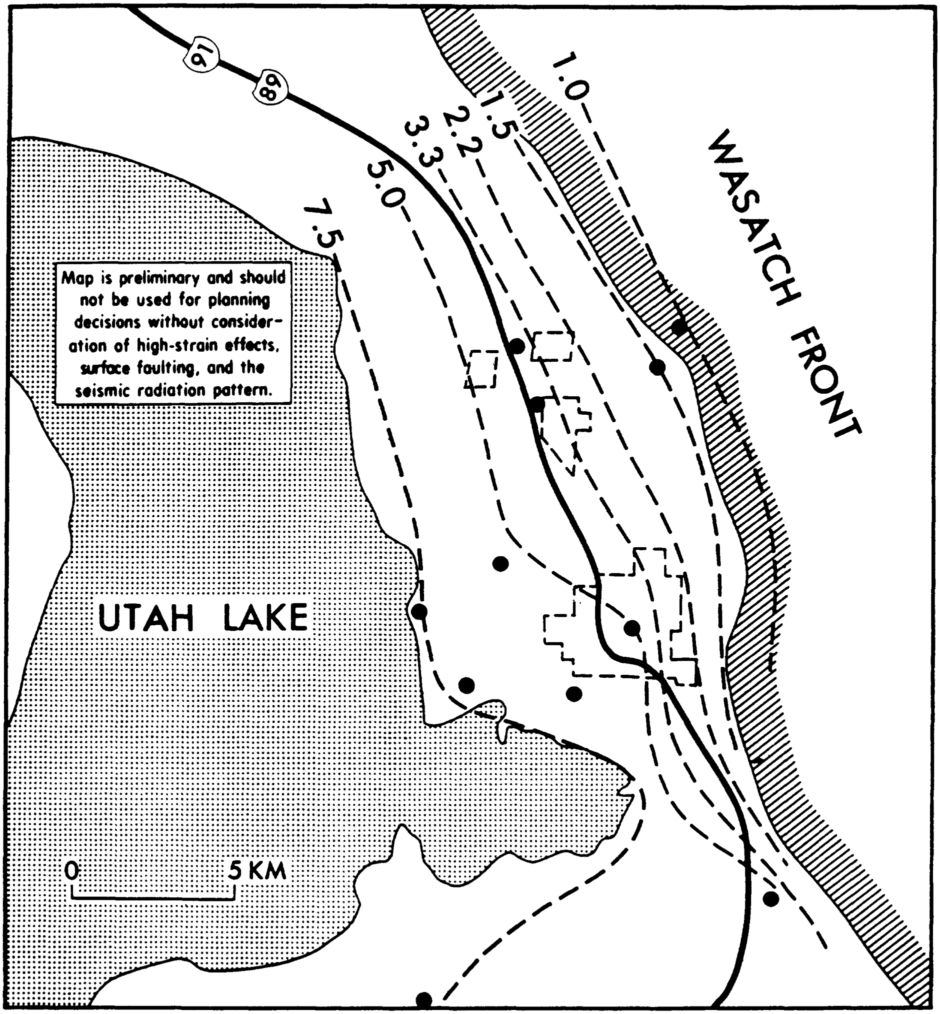

Figure 16.—Map showing the spatial variation of site amplification factors for the period band 0.2 to 0.7 s, Provo area. Values on contours indicate the ratios of velocity response spectra that would be expected at sites underlain by soil relative to that expected at sites underlain by rock on the Wasatch Front. These values provide an estimate of the spatial variation of ground motion in the period band for which 2 to 7 story buildings have their fundamental natural period of vibration (from Hays and King, 1982). These data represent a low strain environment. Repeatability would be least certain when a moderate- to large-magnitude earthquake nucleates underneath the city.

fundamental response mode of 2 to 7 story buildings, a dominant group in this urban corridor.

Salt Lake City region

Soil-to-rock or site amplification factors in the Salt Lake region for the period band 0.2 to 0.7 s are shown in Figure 14. For this period band these data indicate the following:

- Site-amplification factors vary from 1 to 10 within the corporate limits of the city.

- Site-amplification factors (relative to a site underlain by rock on the Wasatch front) increase to the west with increasing distance from the Wasatch fault zone. This effect, which correlates with the transition from stiff soils near the Wasatch front to thick, soft soils in the valley center, offsets to some degree the normal decay of the peak amplitudes and spectral ordinates of ground motion with distance from the fault zone. The effect would be most important when the hypocenters are 20-50 km from Salt Lake City.

- Site-amplification factors are as much as 10 (1,000 percent) at sites underlain by the thick (500-900 m), soft deposits of clays and silts in the center of the valley; whereas, they are about 2 (200 percent) at sites underlain by the relatively thinner (150 m) deposits of sand and gravels near the Wasatch front. These data suggest a high damage potential for to 2 to 7 story buildings in parts of Salt Lake City when the response of the soil column and the response of the building are closely matched.

Ogden region

The site amplification factors for the period band 0.2 to 0.7 s are shown in Figure 15. For this period band, these data show the following:

- The spatial variation of the site-amplification factors is rapid, but not as rapid as in the Salt Lake City (and Provo) areas.
- The site-amplification factors (relative to a rock site on the Wasatch front) are as great as 5 (500 percent) and are greatest for the thick, soft deposits of clays and silts located in the valley center some distance from the Wasatch front. Except for one zone, the factors also increase with increasing distance from the surface trace of the fault zone. The explanation for the zone of low site amplification is unknown at present, but a local soil deposit having a higher value of shear-wave velocity than normal is suspected as the cause.

Provo region

The site-amplification factors (relative to a rock site on the Wasatch front) in the Provo area are shown in Figure 16 for the period band 0.2 to 0.7 s. These data lead to the following conclusions:

- The site-amplification factors vary from 1 to 7 over a distance of only 10 km and increase with increasing distance westward from the surface trace of the Wasatch fault zone, as in Salt Lake City and Ogden.

- The greatest site-amplification factors (Figures 14, 15, 16) correlate with thick, soft deposits of clays and silts located some distance from the surface trace of the fault zone, and the smallest site-amplification factors correlate with relatively thin deposits of gravel and sand near the Wasatch front.

POSSIBLE USES OF THE SITE-AMPLIFICATION DATA AND MAPS

Uniform Building Code

In Utah, considerable new knowledge is becoming available on the earthquake potential of specific faults, the bedrock ground-shaking hazard, soil amplification, earthquake-induced ground failures, and other earthquake-related phenomena. Also, recent damaging earthquakes (for example, the September 19, 1985, Mexico earthquake) have provided engineers with important information on earthquake-resistant design. This new knowledge has not yet been incorporated in the Uniform Building Code (UBC) nor in design of structures in Utah.

The UBC, the most widely used standard for earthquake-resistant design, contains the following commentary about seismic design.

Basically, the problem is that the entire phenomenon, from the earthquake ground motion to the realistic response of structures to this ground motion, is very complex. Codes, of necessity, are generalized simplifications. Complex mathematical analyses have been made on simple and idealized structures subjected to past earthquake ground motions. These have been helpful in improving our understanding of the phenomenon. However, for purposes of design of the vast majority of structures, it is necessary to reduce this complex, dynamic problem to one of equivalent static lateral forces. These can be related to the dynamic characteristics of the structure. They provide the basic code criteria, applied with stresses within the elastic limit. However, in applying these simplified concepts, the structural engineer must do this with sound judgment that can only be developed with experience, observation, and study of the earthquake phenomenon. He must be especially aware of the nature of the response of the particular structure under design and he must evaluate the capabilities of the structure to perform satisfactorily beyond the elastic-code-stipulated stresses.

The Uniform Building Code is a minimum standard to assure public safety. The requirements are intended to safeguard against major failures and loss of life. The aim of the code is to provide structures that will:

1. Resist minor earthquakes without damage;

2. Resist moderate earthquakes without structural damage, but with some nonstructural damage;

3. Resist major earthquakes without collapse, but with some structural and nonstructural damage.

The basic formula used in the UBC is:

$$V = ZIKCSW \tag{1}$$

where the terms in the equation are defined below:

V is the base shear or total lateral force at the base of the structure,

Z is zone factor, the numerical coefficient that depends on the seismic risk zone. California is in a zones 3 and 4; the Salt Lake City-Ogden-Provo urban corridor is in zone 2.

I is the occupancy importance factor for the building.

K is an arbitrary horizontal force factor that, in effect, is a safety factor adjustment. It is based on an arbitrary classification of the type of construction. It recognizes that different degrees of risk for collapse are inherent in different types of construction.

C is a numerical coefficient based on the fundamental period of the building. A plot of C against period represents a response spectrum and roughly parallels the spectrum derived from the accelerogram of the Imperial Valley, California, earthquake recorded at El Centro, California in 1940.

S is the soil-structure interaction factor that incorporates the potential for site-structure resonance. The values of s range form 1 to 1.5 with the highest value occurring when the fundamental periods of vibration of the building and soil column are equal.

W is the total dead load of the building.

A strategy for incorporating the new information on earthquake hazards along the Wasatch front should include the following activities:

1. Update the seismic risk zone map that gives the Z factor to reflect the latest information on the ground-shaking hazard, as depicted probabilistically. (For example, use the map of Utah that gives the peak horizontal bedrock acceleration for a 50-year exposure time (the useful life of ordinary buildings) and a 90 percent probability of nonexceedance.)

2. Review the soil-structure interaction factor that is prescribed in the building code to determine if Utah soils are represented adequately, especially the thick, soft clays and silts in the valley centers.

Since the UBC undergoes vigorous evaluation and recommendations for change every three years, a mechanism already exists to implement changes that are relevant for Utah.

Applications in Utah

Maps of the bedrock ground-shaking hazard (for example, those produced by Algermissen and others, 1982) and soil-to-rock amplification factors can be applied in building codes; land-use guidelines; construction practices; and criteria for repair, strengthening, and retrofit of existing buildings. Implementation of these kinds of loss-reduction applications in Utah would involve the following technical tasks:

1. Evaluation of the Uniform Building Code (UBC) - The need for modifying the current edition of the UBC to provide design criteria that are realistic in terms of the current knowledge of both the earthquake potential and the ground-shaking hazard in the Salt Lake City-Ogden-Provo urban corridor should be evaluated carefully. In addition, the best available data on soil-structure interaction should be incorporated into recommended code changes to ensure that poor site-structure combinations are either avoided or appropriate engineering is performed to develop adequate structural capacity.

2. Evaluation of regional and urban land-use practices - Alternatives to current practices should be identified that will reduce the probability of constructing at sites having poor site-structure combinations (i.e., siting of buildings on soil-rock columns where the natural period of the soil column, t_s, is the same as the natural period, T_b, of the building). When there is no viable alternative, appropriate engineering can reduce the chance for severe damage.

3. Evaluation of construction practices for new buildings - Alternatives to current practices should be specified that will ensure a higher level of quality of materials, workmanship, and inspection.

4. Evaluation of the current practices to repair and strengthen existing buildings - Alternatives to current practices should be identified to increase the seismic resistance of buildings designed and built to an earlier standard of earthquake resistance.

Arguments to Minimize or Eliminate Controversy in the Application of these Data.

The most important requirement for maps of the earthquake ground-shaking hazard (including site-amplification effects) is that they be useful for guiding engineering, social, and political decisions. From a scientific viewpoint, such a map must encompass all possible earthquake source-path-site combinations, for a given exposure time, or the scale must be such that variations in source and path effects cause negligible changes in the expected values. The repeatability of site amplification must be reasonably consistent from earthquake to earthquake, especially for the larger magnitude earthquakes used to set design and construction practice and to guide response planning.

The results in the Salt Lake City-Ogden-Provo urban corridor are unequivocal except for considerations involving near-source locations. At these locations, the source effects dominate the site effects. The trends of site amplification in the Salt Lake City, Ogden, and Provo areas shown in Figures 14, 15, and 16 can be expected to recur in small- to moderate-magnitude earthquakes occurring along the Wasatch fault zone and producing small-amplitude, low-strain ground motion causing essentially elastic response. The most significant implication of these results is that ground motion may be amplified by as much as a factor of 10 (1,000 percent) at some sites in the 0.2 to 0.7s period band corresponding with the natural periods of vibration of 2 to 7 story buildings. This type of elastic or essentially elastic response could also be realized in a large, distant earthquake (occurring as far away as 100 km), which could cause unusual damage to some buildings, (for example, in a similar manner as in the September 19, 1985, Mexico earthquake).

Significant differences in the trends of site amplification shown by these data should be expected in the case of a moderate- to large-magnitude earthquake occurring at a depth of 10-15 km directly under one of the cities and causing a peak bedrock acceleration of 0.2 g or greater. This would be the worst case of the near-source problem for listric fault. The variability of ground motion can be expected to be greatest at sites closest to and aligned with the fault rupture. In such a case, the effects of the source and the path are both important; they are also difficult to separate. The amplification of ground motion expected to occur in the period band 0.2 to 0.7 s at sites underlain by thick, soft clays and silts and located at distances ranging from the epicenter to 35 km of the zone of earthquake nucleation would tend to offset the normal attenuation of ground motion with increasing distance from the hypocenter. The most likely outcome in this case is that locations in a broad area in each city within about 35 km of the hypocenter would experience about the same level of ground shaking, as represented by peak ground acceleration or peak ground velocity, but exhibit considerable variability as represented by the response spectrum. The range, represented on the smooth response spectrum, is shown in Figure 17. The effect of strain dependence on site amplification in the near-source area is the primary unknown (Figure 18). This question will not be completely resolved for Utah until ground motions near the fault are recorded in large-magnitude earthquakes either in Utah, or in other parts of the World having a similar seismotectonic setting.

TECHNICAL ASPECTS OF SITE AMPLIFICATION

Because site amplification of earthquake ground motion is a controversial subject and the limited earthquake data in Utah required utilization of small-amplitude nuclear-explosion data, a brief review of worldwide site-amplification data will be given in the next section to provide a broader framework of understanding. Such understanding is needed for interpreting and using the site-amplification data obtained in Utah until a more complete data set is available.

Scientists and engineers throughout the world have recognized and documented since the 1800's that site amplification commonly occurs in earthquakes (MacMurdo, 1824; Idriss and Seed, 1968; Seed and Idriss, 1969; Seed and others, 1972; Tezcan and others, 1977; Joyner and others, 1981; Rosenblueth, 1986; Savy and others, 1986). Many earthquakes have shown scientists and engineers that two frequency-dependent phenomena, site response and structural response, must be considered explicitly in earthquake-resistant design. A number of factual statements such as the following can now be made about various aspects of these phenomena:

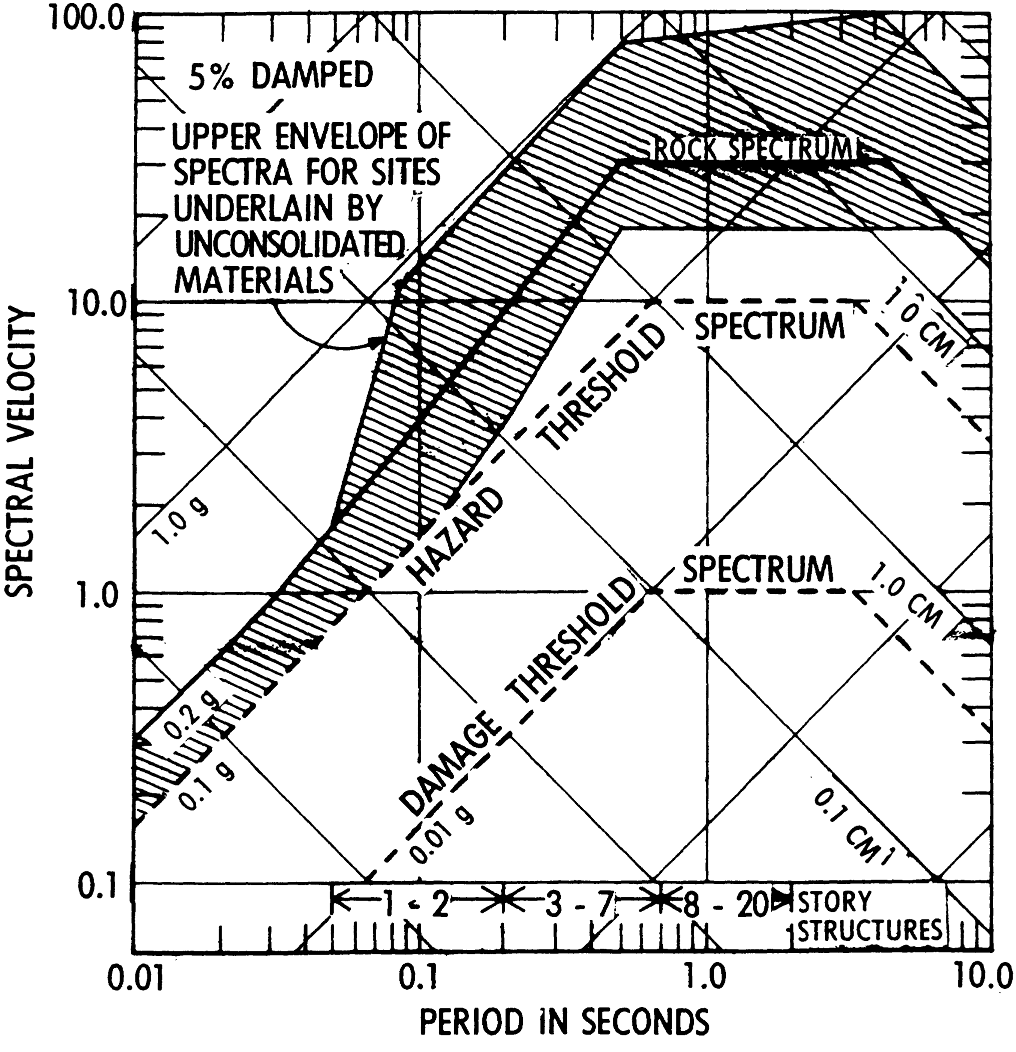

Figure 17.--Graph showing the estimated range of values of horizontal spectral velocity that might be expected in Salt Lake City, Ogden, or Provo within about 35 km of a large (Ms of 7.5) earthquake on the Wasatch fault zone. Such an earthquake is currently estimated to produce a peak bedrock velocity of 16 cm/s (Algermissen and others, 1982). The greatest controversy is over the question of strain dependency and whether or not the peak bedrock acceleration (zero-period asymptote of the response spectrum) would be increased or decreased at sites underlain by soil. The period band 0.2 to 0.7 s emphasized in this paper is shown on the graph.

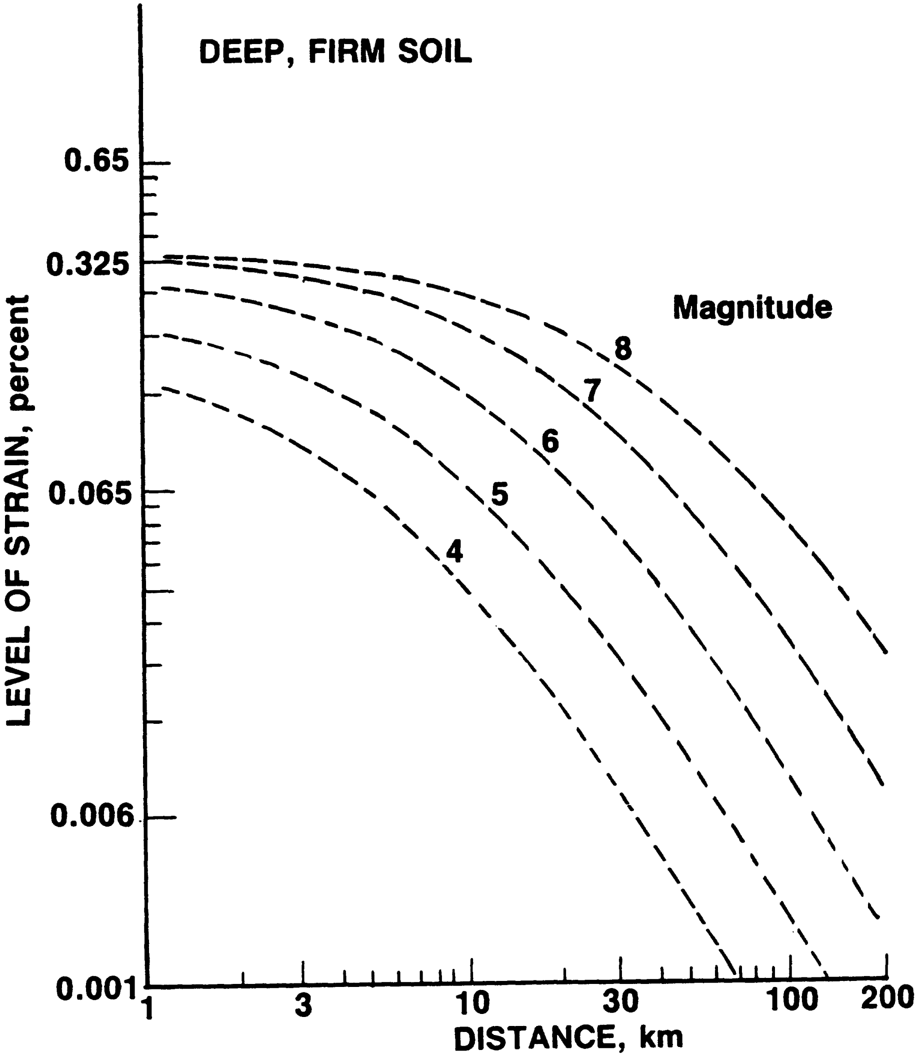

Figure 18.--Graph showing an estimate of the level of dynamic shear strain as a function of epicentral distance and magnitude. A deep soil column having a near-surface shear-wave velocity of about 200 m/s is modeled.

1. During an earthquake, the characteristics of the earthquake ground motion in any city will vary widely depending on a) thickness, softness, and geometry of the local soil-rock columns and b) source phenomena causing directivity and focusing of energy (Earthquake Engineering Research Institute, 1986). This observation means that there probably will be some "surprises" in the Salt Lake City-Ogden-Provo urban corridor in that some ground motion phenomena in future earthquakes will not be able to be explained except in terms of site-amplification phenomena.

2. Damage to a structure at a particular site in an earthquake is complexly related to the dynamic frequency-dependent properties of the earthquake source, the low-pass filtering characteristics of the wave propagation path, and the band-pass filtering characteristics of both the soil-rock column underlying the structure and the structure. The physical parameters of the earthquake and the earth that cause the soil-rock column and the structure to vibrate at the same period increase the potential for damage (Yamahara, 1970). These parameters are not completely known yet in the Salt Lake City-Ogden-Provo urban corridor. Additional geologic investigations needed to improve basic understanding are underway.

3. The level of dynamic shear strain and its effects on soil properties are the most controversial aspects of site amplification. The level of shear strain induced in the soil column by the input bedrock motion increases as the magnitude of the earthquake increases and decreases as the distance from the center of energy release increases (see Figure 18).

4. The response of the site to ground shaking depends strongly on the strain-dependent properties of the soil-rock column underlying the site, The level of dynamic shear strain and the contrast in physical properties of the soil and rock determine whether the soil acts to transmit or to dissipate energy. As an energy transmitter, the soil column acts as a band-pass filter by modifying the amplitude and phase spectra of the incident body and surface seismic waves in selected periods (Murphy and others, 1971b) and increasing the duration of shaking (Hays, 1975). As an energy dissipator, the soil column can damp the earthquake ground motion reducing the level of peak acceleration. As a soil-structure system, part of the vibrational energy of both the soil column and the structure can be transmitted back into the Earth, which permits vertical movement, rocking, and side-to-side movement of the structure on its base (Wolf, 1985).

5. Site amplification (the frequency- and strain-dependent response of the soil-rock column to body and surface seismic waves) increases the amplitude of the surface ground motion in a narrow-period band that can be related to the thickness, softness, shear-wave velocity, bulk density, and geometry of the soil column (Seed and others, 1976). The transfer function is one way to categorize the dominant spectral response in terms of the period band where it occurs. Although the response can be related to many discrete period bands, three period bands are typically used to categorize the effect: a) short period (0.05-0.5 s, b) intermediate period (0.5-3 s), and c) long period (3-10 s). Each period band correlates approximately with the fundamental made of response of buildings of increasing heights and decreasing stiffness.

6. The structure also acts as a band-pass filter as it responds to the ground shaking at its base. The spectral response of the structure can be increased or decreased in selected period bands that depend on the type of structure, the construction materials used in the lateral-force-resisting system, the lateral and vertical dimensions, the physical properties of the soil-rock column, and the wavelengths and amplitudes of the incident seismic waves. The demand on the structure is greatest when the dominant period of the bedrock motion, the fundamental natural period of vibration of the structure, and the natural period of the soil column are the same. a case which creates a condition for site-structure resonance (Figures 3 and 4).

Site and building periods - Earthquake-resistant design must take into account the conditions that cause site amplification of ground motion and damaging soil-structure resonance. In an urban area, careful evaluation is required to identify the wide range of soil-rock columns and their physical properties, the various types of buildings, and the physical conditions that cause the soil and building responses to occur at or close to the same period. A soil column, like a building or structure (see Figure 13), has a natural period of vibration, T_s, given by the relation

$$T_s = \frac{4H}{V_s} \tag{2}$$

where H is the thickness of the soil column and V_s is the shear-wave velocity measured at low levels (0.0001 percent) of strain. Soils, depending on their physical properties, typically have shear-wave velocities ranging from 50 to 600 m/s; whereas, rock-like material and rock have shear-wave velocities greater that about 750 m/s.

One of the characteristics of site amplification in the Salt Lake City-Ogden-Provo urban corridor is that the response is not dominated by a specific period or period band. The entire spectrum at sites underlain by soil exceeds that for site underlain by rock.

Soils clearly exhibit strain-dependent properties in laboratory tests (Seed and Idriss, 1969). Tests on "undisturbed" samples have shown that as the level of dynamic shear strain increases the material damping increases and the shear modulus decreases. The result is that T_s increases as the level of shear strain increases. The basic empirical relation has been given by Seed (1975) as:

$$T_s = \frac{4H}{RV_s} \tag{3}$$

where R is an empirical factor having the following values:

1. 0.9 for a magnitude 6 earthquake producing a peak effective acceleration of 0.1 g.

2. 0.8 for a magnitude 6 earthquake producing a peak effective acceleration of 0.2 g.

3. 0.67 for a magnitude 7 earthquake producing a peak effective acceleration of 0.3 to 0.4 g.

The fundamental natural period of vibration T_b of a building is given approximately by the relation

$$T_b = \frac{N}{10} \qquad (4)$$

where N is the number of stories. However, the stiffness and flexibility of a building (design parameters controlled by the structural engineer and architect) can make its actual fundamental natural period shorter or longer. Observations from postearthquake investigations have shown that T_b lengthens as the thresholds of various states of damage are reached. In an earthquake, the "worst" case for damage is when the value of T_s coincides with that of T_b. This situation causes resonance of the building and can result in severe damage or collapse unless the building has been designed to withstand the forces generated by this phenomenon.

The type of structure being sited controls the scope of the evaluation. For example, amplification of surface waves is not typically considered in siting a nuclear power plant, which is more sensitive to short-period vibrations of body waves than to long-period vibrations of surface waves. On the other hand, potential site amplification of long-period Rayleigh waves is an important consideration when siting a high-rise building, especially if the building is founded on a deep, soft soil deposit like those in the Salt Lake City-Ogden-Provo urban corridor.

Level of dynamic shear strain - Assessing the level of dynamic shear strain and its effects on the physical properties of the soil column requires laboratory tests and good technical judgment. Laboratory measurements have demonstrated that soils have shear moduli and damping characteristics that depend on the level of strain, which suggests that, under certain conditions, nonlinearities and inelasticities in the soil will attenuate rather than amplify the peak amplitudes of surface ground motion at sites underlain by soil. Current understanding is limited because the high levels of strain produced in the laboratory have not been duplicated in the in situ environment by actual strong motion records of past earthquakes. For example, the greatest value of peak ground velocity ever recorded (in the 1971 San Fernando, California, and 1979 Imperial Valley, California, earthquakes) is 110 cm/s. The empirical rule that

$$\text{strain} = \frac{\text{peak velocity recorded at the site}}{\text{shear wave velocity of the soil column at the site}} \quad (5)$$

leads to the conclusion that the greatest level of strain induced in situ in soil columns in past earthquakes has reached only about 0.5 percent, much less than the level of strain developed in the laboratory environment.

Some researchers (for example, Hays and others, 1979; Hays and King, 1982) have shown that site response is essentially linear up to in situ strain levels of about 0.5 percent for some soil-rock columns. The epicentral distance to the strain level of 0.5 percent is only a few kilometers for soil columns like those in Salt Lake City having a shear-wave velocity of 200 m/s. The epicentral distance to 0.5 percent decreases as the shear-wave velocity of the soil approaches the shear wave velocity of the bedrock.

The complexity in the specification of the dynamic properties of the soil is directly related to the differences in the laboratory and in situ environments and the problem of obtaining an "undisturbed" sample. The complexity increases below depths of 30 m because of the difficulty and expense of sampling.

Thickness of the soil column - Two different points of view have been used to define the critical thickness of the soil column, the physical parameter that strongly affects the period of the dominant site amplification. One view (Seed, 1975) considers that the soil column includes only near-surface material having a shear-wave velocity less than 765 m/s. The other view (Kobayashi and Nagahashi, 1982) considers that the soil column extends to bedrock having a compressional wave velocity of at least 3,600 m/s. In the first case, surface ground motions are assumed to be affected mainly by a short soil column, typically about 30 m thick; whereas, in the second case surface ground motions are assumed to be affected by a much thicker soil column. The short soil column will mainly affect the short periods and the peak amplitudes of acceleration; whereas, the thick soil column will mainly affect the intermediate- and long-period bands and the peak amplitudes of velocity and displacement. In the Salt Lake City-Ogden-Provo urban corridor, the effects of both short and deep soil columns are present because the thickness of the soil deposits adjacent to the Wasatch front vary from about 150 to 900 m.

Near field - The near field (or near source) of an earthquake is the most complex area to evaluate for potential site amplification. The site is defined as being in the far field (or "far-source" region) of an earthquake when it is located sufficiently far from the physical extent of the earthquake source that the solid angle subtended by the source and the site is very small. In the far field, estimation of the characteristics of ground motion is much easier than in the near field where seismic energy arrives nearly simultaneously from many different directions. The difference is essentially one of using a point-source (the far field) or a line source (the near field) approximation. In Utah, the near-field problem is complicated because of the listric nature of the Wasatch fault zone which makes it plausable for earthquakes to nucleate directly under any of the three cities. Analyses of strong-ground-motion data close to the causative fault have been made by a number of investigators (for example, Idriss, 1978; Hays, 1980; Singh, 1985). For the near field, these analyses indicate the following:

1. Analytical separation of the frequency-dependent effects of the source from the effects of the soil-rock column is very difficult. Near the fault, the source tends to dominate the path and site effects. The directivity of the source can cause considerable variability in the values of the peak amplitudes of ground acceleration, velocity and displacement, and the ordinates of spectral velocity (Singh, 1985).

2. A "killer pulse," a pulse of approximately one second duration that typically does not have the greatest peak amplitude of acceleration but which has the greatest kinetic energy, is generated in some cases in the near field (for example, in the 1971 San Fernando, California earthquake) as a consequence of the "fling" of the fault (Bertero and others, 1978). Breakout and stopping phases of the fault rupture can also affect the near-field ground motion and complicate the analysis.

Bedrock Motions - Estimating bedrock ground motions is also a difficult task in evaluating site-amplification effects. The frequency-dependent characteristics of the bedrock motion that is input to the soil column depend on the details of the geology of the propagation path. These details are usually imprecise. Therefore, analytical calculations must be bounded, using a suite of strong-motion accelerograms acquired in past earthquakes at sites underlain by rock to constrain the analyses. The ideal data are from sites underlain by the same type of rock, located at about the same distance from the zone of energy release, and having the same geology underlying the propagation path as for the site being evaluated. An adequate analog having the appropriate source-path-site characteristics does not yet exist for the Salt Lake City-Ogden-Provo urban corridor.

Variability in site-amplification effects - Several investigators (for example, Murphy and others, 1971b; Hays, 1980) have shown that site-amplification effects for some soils are fairly repeatable if the soil is soft relative to the bedrock, the level of strain is low (e.g., 0.0001 to 0.1 percent), and the site is not near the fault zone. The degree of repeatability of the site transfer function is currently unknown everywhere for sites near the fault when the shear strain approaches and exceeds 0.5 percent.

Worldwide data - Four examples of site amplification of ground motions representing a low-strain environment are described below because of the relevance to the Salt Lake City-Ogden-Provo urban corridor:

1. The 1967 Caracas, Venezuela earthquake - Soil-structure resonance occurred in Caracas, 56 km from the epicenter of this moderate (Ms 6.4) earthquake. Severe damage was mainly restricted to tall buildings (buildings greater than 12 stories) sited on thick, soft soil columns that

were at least 160 m thick. The dominant site response occurred in the intermediate period band, centered around 1.4 s (Seed and others, 1972).

2. The 1970 Gediz, Turkey earthquake - Soil-structure resonance under small-amplitude ground motions caused the collapse of a one-story garage and paint workshop (a part of the Tofias automobile factory) located 225 km from the epicenter of this large (Ms 7.0) earthquake. The cause was the similarity of the predominant periods of: a) the bedrock motions, b) the response of the 120-135 m column of alluvium, and c) the response of the building. The resonance occurred in the intermediate-period band and was centered around 1.2 s (Tezcan and others, 1977).

3. The 1976 Friuli, Italy earthquake - Site amplification of a factor of 4 (400 percent) occurred in the short- to intermediate-period band (0.2-0.7 s) for a site underlain by 15 m of alluvium located 25 km from the epicenter. The peak amplitude of bedrock accelerations ranged from 0.10 to 0.53 g (Savy and others, 1986). The magnitude (Ms) of the main shock was 6.9.

4. The 1985 Mexico earthquake - This great (Ms 8.1) earthquake produced two surprises: a) the low value of the peak amplitude of acceleration (0.18 g) in the epicentral region, and b) the high (0.18 g) value of the peak amplitude of acceleration in certain parts of Mexico City located 400 km from the epicenter (Figure 19). Extensive damage occurred in 5- to 20-story buildings sited in the lake-bed zone of Mexico City underlain by soft lake-bed deposits (Rosenblueth, 1986). These deposits had been recognized in the 1960's (Zeevaert, 1964) as a 2-second band-pass

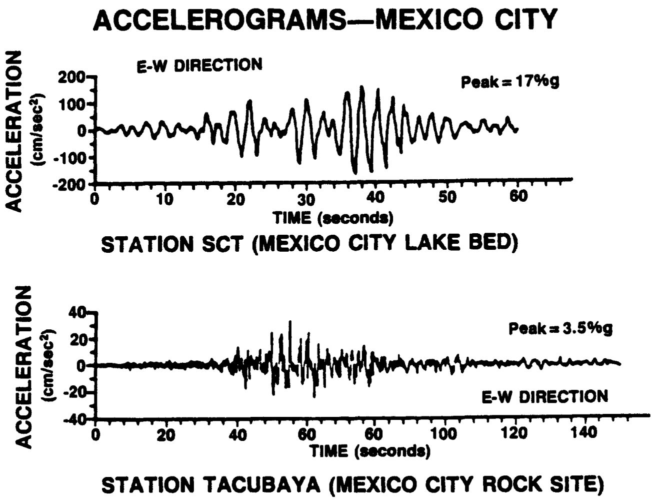

Figure 19.—Comparison of the strong-motion accelerogams in a low-strain environment recorded on firm soil and in the soft soil (of the lake-bed zone) in the September 19, 1985, Mexico earthquake. The soft soil in the lake-bed zone OF Mexico City located 400 km from the epicenter amplified the ground motion in a period band centered around 2 s. The records were privided by Universidad Nacional Autonoma de Mexico.

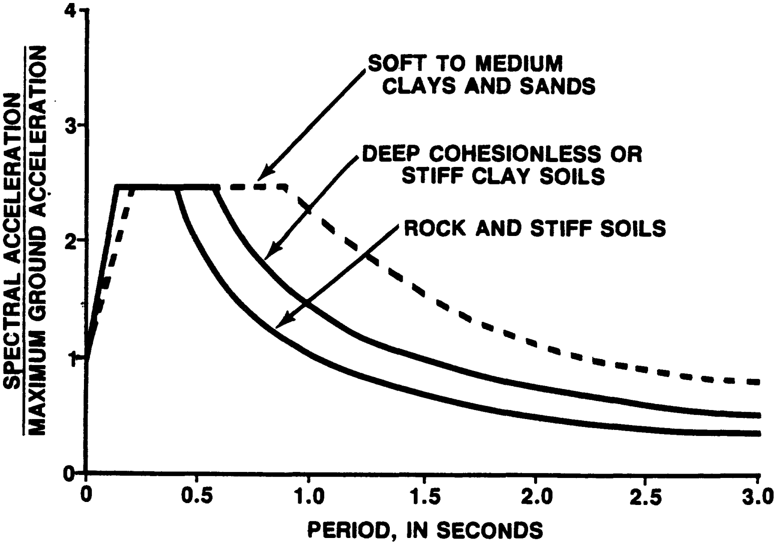

Figure 20.—Graph showing the shape of normalized response spectra for 3 different soil columns proposed in 1985 by the Seismology Committee of the Structural Engineers Association of California. These curves are based mainly on ground motion data recorded in California. A relevant question is, "to what degree do they represent soil colümns in the Salt Lake City-Ogden-Provo corridor?" The assertion of this paper is that the amplifying effects for soft-to-medium clays may be underestimated except for the near-source, high-strain environment, the rarest case.

filter. The largest ground motions in Mexico City occurred at sites underlain by 35 to 50 m of soft lake-bed deposits having a shear-wave velocity of about 100 m/s. The dominant period of the accelerogram recorded in the lake-bed zone was 2 s. The response of the lake-bed deposits was essentially elastic. They amplified the peak amplitude of acceleration (caused by Rayleigh waves) by about a factor of 5 (500 percent) relative to the level of peak acceleration observed at nearby sites underlain by stiffer, rock-like material (Rosenblueth, 1986). The ordinate of 5 percent damped spectral acceleration at 2 s reached 1 g. The similarity of the soil response and the building response at many locations in the lake-bed zone caused resonance that was a major cause of severe damage and collapse of about 400 engineered buildings. These buildings generally had fundamental natural periods ranging from 0.5 to about 2 s. The number of severely damaged and collapsed buildings represented less than one percent of the total number of engineered buildings in Mexico City, which indicates that buildings constructed according to the Mexican building code performed well everywhere but in the lake-bed zone.

CONCLUSIONS, UNRESOLVED TECHNICAL ISSUES, AND RECOMMENDATIONS

Research on the ground-shaking hazard in the Salt Lake City-Ogden-Provo urban corridor has provided technical information that can be incorporated into the process of improving building codes, land-use regulations, and construction practices in Utah. The soil columns underlying this urban corridor cause distinctive characteristics of site amplification depending on their softness, thickness, and location relative to the zone of energy release. Observations at 71 sites in Utah, augmented by observations in other parts of the world, suggest that 2 to 7 story buildings sited on thick, soft deposits of clays and silts in the Salt Lake City-Ogden-Provo urban corridor may face a demand that exceeds their capacity in moderate- to large-magnitude earthquakes. The hazard is less for structures sited on thin deposits of gravel and sand near the Wasatch front. In the case of a large earthquake (e.g. the characteristic-earthquake having a magnitude (M_s of 7.0 to 7.5) nucleating at a depth of 10-15 km on the listric Wasatch fault zone directly under one of the cities, a large portion of the city within about 35 km of the surface trace of the fault zone could possibly experience severe ground shaking and buildings could suffer extensive damage or possibly collapse. In this case, the characteristics of the ground motion will probably be controlled mainly by parameters of the earthquake source, and directivity effects could be large, causing considerable variability in the distribution of ground motion and damage patterns. The trends indicated by the maps in this report would not be expected to be closely replicated because of lower soil-to-rock amplification factors and a shift to longer periods of dominant response, the primary results of high-strain effects. The trends shown by the maps would be replicated best when the hypocenter of a magnitude 7.0 to 7.5 earthquake is 50 km or more from any one of the principal cities, causing a low-strain environment.

Technical Issues Needing Resolution

Additional data and research on site-amplification will aid in understanding and quantifying the following technical issues in Utah:

1) Do the characteristics of site-amplification in the Salt Lake City-Ogden-Provo area derived from distant nuclear-explosion ground-motion data adequately represent what will happen in future earthquakes on the Wasatch front?

2) How different will the characteristics of site amplification be in earthquakes having magnitudes of 7.0 to 7.5 for a site close to the source? For the same site far from the source?

3) What levels of dynamic shear strain will be generated in the in situ environment at sites near the source in moderate-to-large-magnitude earthquakes? How will these levels of strain compare with strain produced in the laboratory environment?

4) Are the soil-to-rock amplification factors in current building codes and practices used in Utah adequate for earthquake-resistant design in the Salt Lake City-Ogden-Provo urban corridor (Figure 20)?

Recommendations

More detailed geologic investigations are needed to determine the controlling factors at each site, especially in the valley centers. Also integration of the empirical ground-motion data and results of analytical models are needed. Additional ground-motion data from earthquakes in the Intermountain Seismic Belt or in other parts of the World having analogous seismotectonic settings and soil-rock columns must be acquired and analyzed to quantify the ground-shaking hazard for the near-source and far-source environments of the Salt Lake City-Ogden-Provo urban corridor.

Although current research on site amplification in Utah is incomplete, and gaps in knowledge exist, the results of this research can be implemented as preliminary design criteria that will probably have a 5-10 year useful life because of the slowness of data acquisition to address the issues described above. Appropriate uses include:

1) Risk maps (zoning maps) for inclusion in the 1991 edition of the Uniform Building Code.
2) Maps of site-amplification factors for discrete period bands that correspond to the full range of new and existing buildings in Utah.
3) Preliminary seismic microzonation studies and products that identify the parts of the Salt Lake City-Ogden-Provo urban corridor that are best suited for certain types of construction and land use.
4) Studies of potential vulnerability of existing 2-7 story buildings as well as other categories of existing buildings, lifelines, and other facilities.

Acknowledgments

The technical contributions of Kenneth King and Robert Miller, USGS, are gratefully acknowledged. Both individuals contributed substantially to the acquisition of ground-motion data and surficial geology data along the Wasatch front and assisted in the analysis of the integrated data. Randy Jibson and Steve Obermeier, USGS, provided valuable suggestions for improving the paper.

References

Algermissen, S. T., and Perkins, D. M., 1976, A probabilistic estimate of maximum acceleration in rock in the contiguous United States: U.S. Geological Survey Open-File Report 76-416, 45 p.

Algermissen, S. T., Perkins, D. M., Thenhaus, P. C., Hanson, S. L., and Bender, B. L., 1982, Probabilistic estimates of maximum acceleration and velocity in rock in the contiguous United States: U.S. Geological Survey Open-File Report 82-1033, 99 p.

Algermissen, S. T., 1969, Seismic risk studies in the United States: World Conference on Earthquake Engineering, 4th, Santiago, Chile, Proceedings, v. 1, 14 p.

Bennett, T. J., 1974, Amplitude and propagation characteristics o short-period seismic surface waves in the Las Vegas valley: Environmental Research Corporation Report NVO-1163-242, 75p.

Bertero, V. V., Mahin, S. A., and Herrera, R. A., 1978, Aseismic design implications of near-field San Fernando records: Journal of Earthquake Engineering and Structural Dynamics, v. 6, pp. 31-42.

Boore, D. M., 1973, The effect of simple topography on seismic waves: implications for the acceleration recorded at Pacoima Dam, San Fernando Valley, California: Seismological Society of America Bulletin, v. 63, pp.

1603-1610.

Borcherdt, R. D., (Editor) 1975, Studies of seismic zonation of the San Francisco Bay region: U.S. Geological Survey Professional Paper 941-A, 102 p.

Borcherdt, R. D., Gibbs, J. R., and Fumal, T. E., 1978, Progress on Ground Motion Predictions for the San Francisco Bay Region: International Conference on Microzonation for Safer Construction Research and Applications (2nd) Proceedings, v. 1, p. 241-254.

Borcherdt, R. D., Joyner, W. D., Warrick, R. E., and Gibbs, J. F., 1975, Response of local geologic units to ground shaking, <u>in</u> Borcherdt, R. D., (Editor), Studies for Seismic Zonation of the San Francisco Bay Region: U.S. Geological Survey Professional Paper 941-A, pp. 52-67.

Davis, L. L., and West, L. R., 1973, Observed effects of topography on ground motion: Seismological Society of American, Bull, v., 63.

Earthquake Engineering Research Institute, 1986, Reducting Earthquake Hazards: Lessons Learned from Earthquakes: Earthquake Engineering Research Institute Publication 86-02, El Cerrito, California, 108 p.

Elton, D. J., and Martin, J. R., 1986, Site Period Study for Charleston, S.C.: 3rd U.S. Conference on Earthquake Engineering, Proceedings, Charleston, S.C., v. 1, pp. 497-504.

Gibbs, J. F., Fumal, T. E., and Borcherdt, R. D., 1976, In situ measurements of seismic velocities in San Francisco Bay Region: U.S. Geological Survey Open-File Report 76-731, 145 p.

Hanks, T. C., 1976, Observations and estimation of long period strong ground motion in the Los Angles Basin: International Journal of Earthquake Engineering and Structural Dynamics, v. 4, pp. 473-488.

Hays, W. W., 1975, A note on the duration of earthquake and nuclear explosion ground motions: Seismological Society of America Bulletin, v. 65, pp. 875-844.

Hays, W. W., 1977, Evaluation of the seismic response in the Sylmar-San Fernando area, California, from the 1971 San Fernando earthquake: American Society of Civil Engineers, Mechanics Division Specialty Conference on Dynamic Response of Structures, Los Angles, Proceedings, pp. 502-511.

Hays, W. W., 1986, The importance of post earthquake investigations: Earthquake Spectra, v. 2, pp. 653-668.

Hays, W. W., 1980, Procedures for estimating earthquake ground motions: U.S. Geological Survey Professional Paper 1114, 77 p.

Hays, W. W., Algermissen, S. T., Miller, R. D., and King, K. W., 1978, Preliminary ground response maps for the Salt Lake City area: International Conference on Microzonation, 2nd, San Francisco California, Proceedings, v. 2. pp. 487-508.

Hays, W. W., Editor, 1981, Facing Geologic and Hydrologic Hazards: Earth Science Considerations: U.S. Geological Survey Professional Paper 1240-B, 90 p.

Hays, W. W., 1978, Ground response maps for Tonopah, Nevada: Seismological Society of America Bulleting, v. 68, p. 451-469.

Hays, W. W., and Gori, P. L., Editors, 1984, Evaluation of regional and urban earthquake hazards and risk in Utah: U.S. Geological Survey Open-File Report 84-763, 687 p.

Hays, W. W., and King, K. W., 1984, Seismic microzoning along the Wasatch fault zone, Utah: World Conference on Earthquake Engineering, 8th, Proceedings, v. 1, pp. 1-12.

Hays, W. W., and King, K. W., 1982, Zoning of the earthquake ground-shaking hazard along the Wasatch fault zone, Utah: International Conference on Microzonation, 3rd, Seattle, Washington, Proceedings, v. 3, pp. 1307-1317.

Hays, W. W., Rogers, A. M., and King, K. W., 1979, Empirical data about local ground response: Earthquake Engineering Research Institute, National Conference on Earthquake Engineering, 2nd, Stanford, California, Proceedings, pp. 223-232.

Idriss, I. M., 1978, Characteristics of earthquake ground motions: Earthquake Engineering and Soil Dynamics, Proceedings of Specialty Conference, American Society of Civil Engineers, v. 3, pp. 1151-1267.

Idriss, I. M., and Seed, H. B., 1968, Analysis of ground motions during the 1957 San Francisco earthquake: Seismological Society of America Bulletin, v. 58, pp. 2013-2032.

Ihnen, Steven, and Hadley, D. M., 1987, Seismic hazard maps for Puget Sound, Washington: Seismological Society of American Bulletin, v. 77, p. 1091-1109.

Joyner, W. B., Warrick, R. E., and Fumal, T. E., 1981, The Effects of Quaternary Alluvium on Strong Ground Motion in the Coyote Lake, California Earthquake of 1979: Seismological Society of American Bull., v., 71, pp. 1333-1349.

Kobayaski, Hiroyoshi, and Nagahashi, Sumio, 1982, Response spectra on seismic bedrock during earthquakes: Engineering Seismology, Tokoyo Institute of Technology, pp. 22-27.

MacMurdo, J., 1824, Papers relating to the earthquake which occurred in India in 1819, Philadelphia Magazine, v. 63, pp. 105-177.

Miller, R. D., 1980, Surficial geologic map along part of the Wasatch Front, Salt Lake Valley, Utah: Miscellaneous Field Studies Map, MS-1198, (scale: 1:100,000).

Molinelli, Jose, 1985, Earthquake Vulnerability Study for the Metropolitan Area of San Juan, Puerto Rico: in Hays, W. W., and Gori, P. L., (Editors), A Workshop on Reducing Potential Losses from Earthquakes in Puerto Rico, Proceedings of Conference XXX, U.S. Geological Survey, Open-File Report 85-731, p. 211-277.

Murphy, J. R., and Hewlett, R. A., 1975, Analysis of seismic response in the city of Las Vegas, Nevada: A preliminary microzonation: Seismological Society of America Bulletin, v. 65, pp. 1575-1598.

Murphy, J. R., Lynch, R. D., and O'Brien, L. J., 1971a, Predicted San Fernando earthquake spectra: Environmental Research Corporation Report NVO-1163-TM30, to U.S. Atomic Energy Commission, 38 p.

Murphy, J. R., and West, L. R., 1974, An analysis of surface and subsurface seismic measurements demonstrating the amplification effect of near-surface geology: Environmental Research Corporation Report NVO-1163-TM41 to U.S. Atomic Energy Commission, 21 p.

Murphy, J. R., Weaver, N. L., and Davis, A. H., 1971b, Amplification of seismic body waves by low-velocity layers: Seismological Society of America Bulletin, v. 61, pp. 109-146.

Peak, R. B., and Reed, W. C., 1954, Engineering Properties of Chicago Subsoils: University of Illinois Engineering Experiment Station bulleting 423, 43 p.

Reid, H. F., 1910, The California earthquake of April 18, 1906, in The mechanics of the earthquake, v.2: Report of the State Earthquake Investigation, Commission, Carnegie Institute of Washington, Publication 87, Washington, D.C., 500 p.

Rogers, A. M., and Hays, W. W., 1978, Preliminary evaluation of site transfer functions developed from nuclear explosions and earthquakes: International Conference on Microzonation, 2nd, San Francisco, California, Proceedings, v. 2., p. 753-764.

Rogers, A. M., Tinsley, J. C., and Borcherdt, R. D., 1985, Predicting relative ground response, in Ziony, J. F., (Editor), Evaluating earthquake hazards in the Los Angles region--An earthquake science perspective: U.S. Geological Survey Professional Paper 1360, pp. 221-248.

Rogers, A. M., Tinsley, J. C., Hays W. W., King, K. W., 1979, Evaluation of the relation between near-surface goelogical units and ground response in the vicinity of Long Beach, California: Seismological society of America Bulletin, v. 69, p. 1603-1622.

Rosenblueth, Emilio, 1986, The Mexican earthquake: A first-hand report: Civil Enginering, American Society of Civil Engineers, New York, January, pp. 38-40.

Savy, Jean, Bernreuter, Don, and Chen, J. C., 1986, Site effects: A generic method for modeling site effects in seismic hazard analyses, in Hays, W. W., (Editor), Proceedings of Conference XXXIV, U.S. Geological Survey Open File Report 86-185, pp. 249-284 35 p.

Schwartz, D. P., and Coppersmith, K. J., 1984, Fault behavior and characteristic earthquakes: examples from the Wasatch and San Andreas faults: Journal of Geophysical Research, v. 89, no B7, pp. 5681-5698.

Seed, H. B., and Lysmer, John, 1986, Site response - A critical problem in soil-structure interaction analyses for embedded structures: Workshop on Soil-structure Interaction, Brookhaven National Laboratory and U.S. Nuclear Regulatory Commission, Proceedings, pp. 233-250.

Seed, H. B., 1975, Design provisions for assessing the effects of local geology and soil conditions on ground and building response during earthquakes, in New earthquake design provisions: Proceedings of seminar sponsored by Professional Development Committee of Structural Engineers Association of Northern California and San Francisco Section of America Society of Civil Engineers, pp. 38-63.

Seed, H. B., and Idriss, I. M., 1969, Influence of soil conditions on ground motions during earthquakes: Journal on Soil Mechanics and Foundations Division of America Society of Civil Engineers, v. 95, pp. 1199-1218.

Seed, H. B., Murarka, R., Lysmer, John, and Idriss, I. M., 1976, Relationships of maximum acceleration, maximum velocity, distance from source, and local site conditions for moderately strong earthquakes: Seismological Society of America Bulletin, v. 66, pp. 1323-1342.

Seed, H. B., Whitman, R. v., Dezfulian, H., Dobry, R., and Idriss, I. M., 1972, Soil Conditions and building damage in the 1967 Caracas earthquake, Journal of the Soil Mechanics Foundations Division, America Society of Civil Engineers, v. 98, pp. 787-806.

Singh, J. P., 1985, Earthquake ground motions: Implications for designing structures and reconciling structural damage: Earthquake Spectra, v. 1, pp. 239-270.

Sharma, S., and Kovacs, W. D., 1980, The Microzonation of the Memphis, Tennesseee Area: U.S. Geological Survey Open-File Report 80-914, 129 p.

Smith, R. B., Richins, W. D., and Dose, D. I., 1985, The 1983 Borah Peak, Idaho Earthquake: Regional seismicity, kinematics of faulting, and tectonic mechanics <u>in</u> Stein, R. S, and Bucknam, R. C., (Editors), On the Borah Peak, Idaho, earthquake: U.S. Geological Survey Open-File Report 85-290, p. 236-263.

Steinbrugge, K. V. (Chairman), 1968, the Safety of Fills: Report prepared for the San Francsico Bay Conservation and Development Commission, San Francisco, CA., 33 p.

Structural Engineers Association of California, 1985, Tentative lateral force requirements: Report of Seismology Committee, Sacramento, California, 76 p.

Tezcan, S. S., Seed, H. B., Whitman, R. v., Serff, N., Christian, J. T., Durgunoglu, H. T., and Yegian, M., 1977, Resonant period effects in the Gediz, Turkey earthquake of 1970: Earthquake Engineering and Structural Dynamics, v. 5, pp. 157-179.

Whitman, R. v., 1983, An Engineer's Perspective on the Cape Anne, Massachusetts Earthquake of 1755: Earthquake Notes, v. 54, no. 1, p. 8 (Abstract).

Wolf, J. P., 1985, Dynamic Soil-Structure Interaction, Prentice-Hall Publishing Company, Englewood Cliffs, New Jersey, 466 p.

Wood, H. O., 1908, Distribution of Apparent Intensity in San Francisco, in The California Earthquake of April 18, 1906: Report of the State Earthquake Investigation Commission, Carnegie Institution of Washington, Washington, D.C., pp. 220-245.

Yamahara, H., 1970, The interrelation between frequency characteristics of ground motion and earthquake damage to structure: Soils and Foundations, v. 10, pp. 57-74.

Youngs, R. R., Swan, F. H., Power, M. S., Schwartz, D. P., and Green, R. K., 1987, Probabilistic analysis of earthquake ground shaking hazard along the Wasatch front, Utah, _in_ Gori, P. L., and Hays, editors: Evaluating Earthquake Hazards in the Los Angeles Region - An Earth Science Perspective, U.S. Geological Professional Paper _______, p. ________

Zeevaert, L., 1964, Strong ground motions recorded during earthquakes of May 11 and 19th, 1962 in Mexico City: Seismological Society of America Bulletin, v. 54, pp. 209-232.

PREDICTING STRONG GROUND MOTION IN UTAH

by

Kenneth W. Campbell
U.S. Geological Survey
Denver, Colorado

ABSTRACT

Near-source attenuation relationships for predicting peak horizontal acceleration and velocity in terms of earthquake magnitude, source-to-site distance, and several source and site parameters are used to estimate strong ground motion in northcentral Utah. A range of estimates are provided reflecting uncertainty in the state of knowledge regarding the effects of stress regime, fault type, anelastic attenuation, and local site conditions. Regional data were used to quantify these effects when possible. For a site located directly above the rupture zone of an hypothesized M_S=7.5 earthquake on the Wasatch fault (a distance of approximately 5 km), median estimates of peak horizontal acceleration and velocity range from 0.55-1.1 g and 45-120 cm/sec, respectively. These ground-motion estimates, when translated into median estimates of 5-percent-damped response spectral values using the Newmark-Hall procedure, result in estimates of pseudo-absolute acceleration for the 0.1-0.5-sec period band that range from 1.05-2.1 g and estimates of pseudo-relative velocity for the 0.5-3.0-sec period band that range from 70-200 cm/sec.

INTRODUCTION

Near-source attenuation relationships for predicting peak horizontal acceleration (PHA) and peak horizontal velocity (PHV) from earthquake magnitude, source-to-site distance, and various source and site parameters are developed from strong-motion recordings of worldwide earthquakes with magnitudes ranging from 5.0-7.7. The study revises several previous studies (Campbell, 1981a, 1981b, 1982a, 1982b, 1983, 1984a). Major revisions include changes in the definition of parameters representing source-to-site distance, site geology, and building size and embedment.

Two types of attenuation relationship are developed. The first, a near-source relationship, is empirically derived from a set of near-source strong-motion recordings with no constraint on its far-field behavior. It is similar to the *unconstrained* model of Campbell (1981a). The second relationship includes an anelastic attenuation term as a means of extrapolating the model beyond the near-source region. This latter relationship, similar to the *constrained* model of Campbell (1981a), provides a means of incorporating regional differences in anelastic attenuation when predicting strong ground motion.

THE GROUND-MOTION MODEL

The equation used to model the attenuation and magnitude-scaling haracteristics of PHA and PHV is given by the expression (Campbell, 1984a)

$$\mathrm{Ln}\ Y=a+bM-d\ \ln[R+c_1\exp(c_2M)]-\gamma R+\Sigma e_iK_i+\varepsilon \qquad (1)$$

ere Y is the ground-motion parameter being predicted, M is earthquake gnitude, R is source-to-site distance, K_i are variables representing source d site effects, γ is the coefficient of anelastic attenuation, and is a random error term with zero mean and standard deviation equal to the ndard error of regression. The coefficients a through e are parameters to determined from the data. All logarithms in equation 1 are given in terms the natural logarithm.

The nonlinear from of equation 1 was selected to accommodate any turation of PHA and PHV with magnitude and distance if supported by the ta. The far-field properties of the model are characterized by the itude scaling coefficient b, the coefficient of geometrical attenuation d, the coefficient of anelastic attenuation γ . The near-source properties the model are characterized by the coefficients c_1, and c_2. The form of e term in brackets was first proposed by Esteva (1970) and later used by ley and others (1982) to model the near-source attenuation of simulated ound motions. For $c_1>0$, the strong-motion parameter saturates with ecreasing distance, approaching a finite value at R=0. For $c_2>0$, the strong-otion parameter saturates with increasing magnitude at short distances until $c_2=-b/d$, when it becomes totally independent of magnitude at R=0.

The parameters Y, M, R, and K_i were defined according to guidelines set forth by Campbell (1985a). Brief definitions of these parameters follow.

STRONG-MOTION PARAMETERS

PHA and PHV were defined as the arithmatic mean of the peak horizontal values of acceleration and velocity, respectively. This mean, referred to as the mean peak horizontal component, was chosen because (1) it tends to minimize the variability associated with the near-random azmuthal orientation of the two orthogonal horizontal components and, thus, is statistically superior to the largest horizontal component (Campbell, 1982a), and (2) it avoids the error associated with using both peak horizontal components as independent observations (Campbell, 1985a).

Item 2 is particularly important because it has been common practice in the past for investigators to use both peak horizontal components as independent observations. This practice artificially increases the number of degrees of freedom, thereby invalidating the statistical interpretation of the results. This is also true for analyses that use one of the horizontal components as an independent variable. The only correct use of both horizontal components as individual variables is by means of multivariate multiple regression (Johnson and Wichern, 1982)--a technique which properly accounts for statistical correlation between dependent variables.

The mean peak horizontal component of acceleration has been found to be approximately 12 percent less, and the mean peak horizontal component of velocity approximately 17 percent less, than the largest peak horizontal component (Campbell, 1981a; Joyner and Fumal, 1985). On the other hand, median predictions of ground-motion parameters based on the mean peak horizontal component have been found to be virtually identical to those based on the use of both peak horizontal components (Campbell, 1982a). The above factors may be used to compare median predictions of ground-motion parameters between the current study and other studies available from the literature.

Peak accelerations were scaled from either uncorrected[1] time series or copies of the original accelerograms to avoid the reduction in amplitude caused by decimation and low-pass filtering of the records during routine processing. Peak velocities were scaled directly from the processed velocity time series.

---

[1] This refers to the first stage of routine processing in which the accelerogram is digitized and baseline corrected. Unequal time intervals are used to preserve the peak amplitudes of the original accelerogram.

MAGNITUDE

Magnitude was defined as surface-wave magnitude (M_S), when both local magnitude (M_L) and M_S were greater than or equal to 6.0, or as M_L, when both M_S and M_L were less than 6.0. The use of the M_S scale for the larger earthquakes serves as a uniform basis for characterizing the size of worldwide events, avoiding saturation of the m_b and M_L scales (see fig. 2 of Campbell, 1985a).

Bakun (1984) and Hanks and Boore (1984) have found M_L and moment magnitude, the magnitude measure recommended by Joyner and Boore (1981), to be roughly equivalent for $5.0 \leq M_L \leq 6.0$, and Hanks and Kanamori (1979) cite a similar equivalence between moment magnitude and M_S for $5.0 \leq M_S \leq 7.5$. Furthermore, Nuttli (1979) has interpreted the commonly cited Richter-magnitude scale, used in many previous ground-motion attenuation relationships, to represent M_L for earthquakes less than about magnitude 6.0 and M_S for larger earthquakes. Thus, the magnitude scale used in the current study is considered to be consistent with both the moment-magnitude and Richter-magnitude scales for the range of magnitudes used in this study and, thus, does not constitute a significant departure from the magnitude scales used in previous ground-motion studies.

SOURCE-TO-SITE DISTANCE

Source-to-site distance was defined as the shortest distance between the recording station and the zone of seismogenic rupture. This zone was identified, when possible, from aftershocks of the earthquake. When the aftershock distribution was too diffuse, too inaccurate, or too limited to reliably define this zone, then modeling studies, past seismicity, geodetic data, refraction experiments, and geologic information--particularly the depth to basement-rock contact on the fault zone--were used to infer its spatial extent. By adopting this distance measure, it is implicitly assumed that dynamic stresses within the upper sediments are too small to be seismogenic, even if significant displacement occurs within these sediments.

The current definition of distance is a revision of that used in the writer's previous studies. The former distance measure--defined as the shortest distance between the site and the rupture zone--was found to be difficult to determine for many moderate-size earthquakes. For large earthquakes ($M \geq 6.5$), where surface rupture was clearly identified, the former distance was measured from the surface trace of the fault. For small-to-moderate earthquakes ($M \leq 5.5$), where it could be reasonably assumed that rupture was confined to basement rock beneath the sediments, the former distance was measured from the inferred fault rupture at depth. However, for moderate-size earthquakes ($M \approx 5.5-6.5$), where the surface expression of rupture was identified only by a zone of small, discontinuous ground cracks in the vicinity of the fault trace, it was not clear whether rupture was confined to basement rock, whether it terminated somewhere within the sediments, or whether it propagated to the surface of the sediments. The revised definition of distance avoids these ambiguities, and in the opinion of the writer, represents a more physically sound basis for modelling wave propagation characteristics of strong ground motion.

The strongest phase of shaking recorded at a site may not always come from the closest part of the seismogenic rupture zone. In fact, Shakal and Bernreuter (1981) suggest that ground-motion predictions made using attenuation relationships based on closest-distance measures will "at best be accurate and at worst may significantly underpredict ground-motion levels." This would be true only if the relationships were developed in terms of closest distance to seismogenic rupture and then applied in terms of distance to the actual source of the strongest phase of shaking--the distance measure preferred by Shakal and Bernreuter. Since it is not known in advance where the true source of the strongest ground motion will come from, it is not feasible in practice to make predictions in terms of the latter distance measure. The distance measure used in the current study can be reliably estimated for both actual and hypothesized earthquakes, and if consistently applied, will appropriately account for uncertainty in the location of the actual source of the strongest recorded ground motion by including it as inherent variability.

DATA BASE

The data consists of peak horizontal acceleration and velocity parameters obtained from accelerograms recorded in the near-source region of selected worldwide earthquakes. The study was not restricted to earthquakes occurring only in western North America as has been common practice in the past. Several factors have minimized the potential bias of the foreign data used in the analyses. The restriction to the near-source regime has made any regional differences in anelastic attenuation negligible compared to the inherent scatter from other factors. In addition, the foreign data used in this investigation come from events occurring within active tectonic provinces generally similar to the seismotectonic regime of western North America. Deep subduction events were excluded from the analyses because of potential significant differences in travel paths and tectonic stress conditions for such earthquakes as compared to the shallow events used in the current study. All the foreign data were recorded on instruments having dynamic characteristics similar to those commonly used in the United States to avoid a potential instrument bias.

The data base was assembled using criteria designed to select only consistent and reliable data over a range of magnitudes and distances of greatest interest to engineers and engineering seismologists. Data were selected if (1) the largest horizontal component of peak acceleration was at least 0.02 g; (2) the accelerograph triggered early enough to record the strong phase of shaking; (3) the magnitude of the earthquake was 5.0 or larger; (4) the closest distance to seismogenic rupture was less than 30 or 50 km, depending on whether the magnitude of the earthquake was less than or greater than 6.25; (5) the shallowest extent of seismogenic rupture was no deeper than 25 km; and (6) the recording site was located on unconsolidated deposits.

Rock sites--sites located on sedimentary or crystalline rock--were excluded from the analyses because of their potentially significant and extremely variable site effects (Campbell, 1983; Tucker and others, 1984; Cranswick and others, 1985). Such sites are typically located in areas of significant topographic relief, such as near the abutments of dams, or founded on rock having a large degree of weathering. In addition, the limited number of near-source recordings on rock makes it virtually impossible to empirically quantify any significant site effects for such sites.

Ideally, it would be desirable to restrict the analyses to strong-motion records obtained in the free field. However, as Campbell (1986) points out, there are very few true free-field recordings. Therefore, it was necessary to include records obtained at the foundation level of buildings in order to have a sufficient number of recordings for analysis. In accordance with the recommendations of Campbell (1984b, 1985a, 1986), the analyses were carefully evaluated for potential soil-structure interaction effects, and these effects were modeled when found to be significant. Accelerograms recorded on instruments located on the abutments and toes of dams were excluded because of the potential effects of the dam.

The earthquakes selected for analysis, together with their magnitudes and type of faulting, are listed in table 1; the peak accelerations, peak velocities, and source-to-site distances for each recording site are given in table 2; and table 3 gives a description of each recording site. Figure 1 shows the distribution of recordings with respect to magnitude and distance. This figure indicates that there is little correlation between magnitude and distance for either PHA or PHV, a positive attribute in regression analyses that treat these parameters as independent variables. The final data base contains 134 acceleration values, 107 velocity values, 130 recording stations, and 21 earthquakes that meet the criteria presented above.

TABLE 1.--NEAR HERE

TABLE 2.--NEAR HERE

TABLE 3.--NEAR HERE

FIGURE 1.--NEAR HERE

TABLE 1.--Earthquake data

Earthquake	Date yy-mm-dd	M	Fault type	No. of recordings Accel.	Vel.
Long Beach, Calif.........	33-03-11	6.2	Strike-slip	2	2
Imperial Valley, Calif....	40-05-19	7.1	Strike-slip	1	1
Kern County, Calif........	52-07-21	7.7	Reverse	1	1
Daly City, Calif..........	57-03-22	5.3	Strike-slip	4	4
Parkfield, Calif..........	66-06-28	6.0	Strike-slip	5	4
Borrego Mtn., Calif.......	68-04-09	6.7	Strike-slip	1	1
Lytle Creek, Calif........	70-09-12	5.4	Reverse	5	4
San Fernando, Calif.......	71-02-09	6.6	Reverse	53	44
Managua, Nicaragua........	72-12-23	6.2	Strike-slip	1	1
Point Mugu, Calif.........	73-02-21	5.9	Reverse	1	0
Hollister, Calif..........	74-11-28	5.1	Strike-slip	3	3
Oroville, Calif...........	75-08-01	5.7	Normal	1	0
Kalapana, Hawaii..........	75-11-21	7.1	Thrust	1	0
Gazli, U.S.S.R............	76-05-17	7.0	Reverse	1	1
Santa Barbara, Calif......	78-08-13	5.7	Reverse	5	3
Tabas, Iran...............	78-09-16	7.4	Reverse	1	1
Bishop, Calif.............	78-10-04	5.8	Strike-slip	2	0
Malibu, Calif.............	79-01-01	5.0	Reverse	4	0
St. Elias, Alaska.........	79-02-28	7.2	Thrust	1	1
Coyote Lake, Calif........	79-08-06	5.9	Strike-slip	6	5
Imperial Valley, Calif....	79-10-15	6.9	Strike-slip	35	31

TABLE 2.--Strong-motion data

Earthquake	Station no.	Distance (km)	Peak horizontal acceleration (g)	Peak horizontal velocity (cm/sec)
Long Beach, 1933..........	131	6.4	0.180	22.6
	288	22.0	0.140	22.9
Imperial Valley, 1940.....	117	8.3	0.292	34.4
Kern County, 1952.........	1095	48.4	0.186	16.7
Daly City, 1957...........	1080	12.9	0.083	4.6
	1065	14.8	0.053	2.2
	1078	14.8	0.047	3.8
	1049	24.6	0.038	1.6
Parkfield, 1966...........	1013	3.0	0.400	61.2
	1014	6.3	0.435	24.0
	1015	10.1	0.275	11.3
	1438	11.0	0.350	--
	1016	15.2	0.066	7.5
Borrego Mtn., 1968........	117	45.0	0.102	20.3
Lytle Creek, 1970.........	290	12.4	0.175	8.8
	116	17.9	0.175	--
	112	20.0	0.068	3.5
	274	28.3	0.090	4.3
	113	28.8	0.043	2.2

Table 2.--Strong-motion data--Continued

Earthquake	Station no.	Distance (km)	Peak horizontal acceleration (g)	Peak horizontal velocity (cm/sec)
San Fernando, 1971........	241	13.8	0.205	26.8
	458	16.0	0.115	30.1
	267	18.1	0.195	11.6
	128	18.7	0.325	--
	461	20.5	0.140	19.2
	253	21.6	0.225	21.6
	466	21.6	0.185	25.6
	127	22.6	0.155	--
	264	25.0	0.195	13.1
	232	25.4	0.165	18.8
	235	25.4	0.115	17.4
	238	25.5	0.105	13.0
	446	25.5	0.145	12.1
	475	25.7	0.105	11.1
	133	26.7	0.130	18.2
	135	26.7	0.205	18.8
	262	27.6	0.120	11.8
	145	28.3	0.135	--
	148	28.3	0.185	--
	142	28.6	0.090	17.4
	199	28.7	0.180	--
	208	28.7	0.135	20.4

Table 2.--Strong-motion data--Continued

Earthquake	Station no.	Distance (km)	Peak horizontal acceleration (g)	Peak horizontal velocity (cm/sec)
San Fernando, 1971--Continued				
	211	28.7	0.155	19.4
	223	28.7	0.105	21.2
	431	28.7	0.105	--
	452	28.7	0.075	14.1
	449	28.8	0.100	--
	482	29.0	0.120	13.7
	160	29.1	0.220	18.6
	455	29.1	0.185	15.7
	163	29.3	0.105	16.4
	166	29.3	0.235	20.2
	125	29.6	0.145	16.7
	416	29.9	0.140	17.9
	437	30.0	0.105	19.1
	469	30.0	0.205	19.2
	428	30.1	0.084	26.8
	443	30.1	0.130	22.1
	140	31.0	0.095	8.4
	175	31.0	0.135	20.8
	413	31.0	0.115	14.6
	425	31.1	0.090	13.5
	181	31.3	0.140	16.9

Table 2.--Strong-motion data--Continued

Earthquake	Station no.	Distance (km)	Peak horizontal acceleration (g)	Peak horizontal velocity (cm/sec)
San Fernando, 1971--Continued				
	184	31.3	0.090	13.0
	187	31.3	0.145	13.2
	121	32.1	0.160	--
	205	33.1	0.070	17.6
	288	34.8	0.100	16.3
	269	35.5	0.125	--
	229	42.2	0.060	14.0
	244	42.2	0.040	10.5
	247	42.2	0.030	12.1
	1052	48.2	0.090	7.3
Managua, 1972.............	3501	5.4	0.365	32.7
Point Mugu, 1973..........	272	24.0	0.105	--
Hollister, 1974...........	1377	8.9	0.085	5.0
	1028	10.8	0.135	8.6
	1250	10.8	0.120	3.7
Oroville, 1975............	1291	30.0	0.065	--
Kalapana, 1975............	2808	37.9	0.165	--
Gazli, 1976...............	9110	3.5	0.666	74.5

Table 2.--Strong-motion data--Continued

Earthquake	Station no.	Distance (km)	Peak horizontal acceleration (g)	Peak horizontal velocity (cm/sec)
Santa Barbara, 1978.......	5093	12.7	0.353	--
	885	12.9	0.331	32.9
	283	14.6	0.154	10.9
	5137	14.6	0.176	13.8
	9022	16.3	0.267	--
Tabas, 1978...............	9124	5.4	0.755	98.2
Bishop, 1978..............	1008	30.7	0.045	--
	1490	30.8	0.060	--
Malibu, 1979..............	5081	18.1	0.080	--
	5079	20.2	0.065	--
	657	20.7	0.040	--
	757	23.7	0.045	--
St. Elias, 1979...........	2734	36.4	0.136	27.3
Coyote Lake, 1979.........	1411	5.4	0.243	28.7
	1410	6.6	0.256	23.2
	1409	8.4	0.225	21.1
	1377	14.4	0.109	6.3
	1492	16.2	0.106	6.5
	1422	28.0	0.045	--

Table 2.--Strong-motion data--Continued

Earthquake	Station no.	Distance (km)	Peak horizontal acceleration (g)	Peak horizontal velocity (cm/sec)
Imperial Valley, 1979.....	6618	5.0	0.254	31.7
	6616	5.2	0.278	--
	6617	5.2	0.310	34.6
	5028	5.5	0.440	76.4
	5155	5.5	0.307	81.3
	942	5.6	0.585	85.9
	952	5.6	0.480	65.3
	958	6.7	0.570	50.6
	5054	6.8	0.735	43.9
	955	6.9	0.495	57.4
	6621	7.3	0.265	27.4
	5060	7.5	0.195	36.2
	5165	7.5	0.440	55.2
	9034	7.5	0.352	36.4
	117	8.3	0.335	--
	5055	9.3	0.240	46.6
	5154	9.4	0.240	48.7
	6619	9.8	0.385	--
	412	10.1	0.215	43.3
	5057	10.9	0.245	41.6
	5053	11.9	0.250	17.8
	5115	12.3	0.380	28.9

Table 2.--Strong-motion data--Continued

Earthquake	Station no.	Distance (km)	Peak horizontal acceleration (g)	Peak horizontal velocity (cm/sec)
Imperial Valley, 1979--Continued				
	5058	13.8	0.380	37.1
	6622	14.6	0.169	12.4
	5051	15.0	0.155	15.9
	5056	16.0	0.150	12.9
	5169	16.0	0.094	20.5
	931	18.8	0.130	18.5
	6605	21.7	0.292	27.0
	5059	22.7	0.135	14.4
	5061	23.7	0.110	13.7
	5062	29.5	0.060	--
	6610	30.8	0.142	7.0
	5052	32.5	0.060	4.5
	724	36.4	0.087	10.1

TABLE 3.--Station data

Sta. No.	Description	Housing	No. of stories	Level	Sediment depth (km)	Geology*
112	Cedar Springs, Pump House	Building	1	Ground	0.092	A
113	Colton, SCE Substation	do	1	do	0.18	A
116	Devil Canyon, Fiter Plant	do	1	do	--	E
117	El Centro Array Sta. 9	do	2	Basement	5.0	A
121	Fairmont Reservoir	do	1	Ground	--	E
125	Lake Hughes Array Sta. 1	do	1	do	3.0	A
127	Lake Hughes Array Sta. 9	do	1	do	--	E
128	Lake Hughes Array Sta. 12	do	1	do	--	E
131	Long Beach, Public Utilities Bldg.	do	4	Basement	2.6	B
133	L.A., Hollywood Storage Bldg.	do	14	do	3.7	A
135	L.A., Hollywood Storage PE Lot	Shelter	--	Ground	3.7	A
140	L.A., UCLA Math Science Bldg.	Building	7	Basement	0.91	B
142	L.A., 120 N. Robertson	do	9	do	3.4	A
145	L.A., 222 Figueroa	do	19	Ground	--	A
148	L.A., 234 Figueroa	do	19	do	--	A
160	L.A., 533 S. Fremont	do	10	Basement	3.0	B
163	L.A., 611 W. Sixth St.	do	42	do	3.0	A
166	L.A., 646 S. Olive	do	7	Ground	3.0	A
175	L.A., 808 S. Olive	do	8	do	2.9	A
181	L.A., 1640 Marengo	do	7	do	3.4	B

Table 3.--Station data--Continued

Sta. No.	Description	Housing	No. of stories	Level	Sediment depth (km)	Geology*
184	L.A., 1900 Ave. of the Stars	Building	27	Basement	3.7	B
187	L.A., 1901 Ave. of the Stars	do	20	do	--	B
199	L.A., 3407 W. Sixth St.	do	8	Ground	--	A
205	L.A., USC Phillips Hall	do	12	Basement	4.6	A
208	L.A., 3470 Wilshire	do	12	do	2.9	B
211	L.A., 3550 Wilshire	do	20	do	2.9	A
223	L.A., 4680 Wilshire	do	6	do	3.0	B
229	L.A., 5250 Century	do	7	Ground	2.4	B
232	L.A., 6430 Sunset	do	15	do	2.9	A
235	L.A., 6464 Sunset	do	11	Basement	2.9	A
238	L.A., 7080 Hollywood	do	11	do	2.9	A
241	L.A., 8244 Orion	do	7	Ground	4.2	A
244	L.A., 8639 Lincoln	do	12	Basement	2.4	B
247	L.A., 9841 Airport	do	14	do	2.4	B
253	L.A., 14724 Ventura	do	14	Ground	1.8	A
262	Palmdale, Fire Station	do	1	do	0.20	A
264	Pasadena, CIT Millikan Library	do	9	Basement	0.91	B
267	Pasadena, JPL Bldg. 180	do	9	do	0.027	B
269	Pearblossom, Pumping Plant	Shelter	--	Ground	--	E
272	Port Hueneme, Naval Lab	Building	1	do	--	A
274	San Bernardino, Hall of Records	do	6	Basement	1.1	A

TABLE 3.--Station data--Continued

Sta. No.	Description	Housing	No. of stories	Level	Sediment depth (km)	Geology*
283	Santa Barbara, Courthouse	Building	2	Basement	8.5	B
288	Vernon, CMD Terminal Bldg.	do	6	do	6.7	A
290	Wrightwood, 6074 Park Dr.	do	2	Ground	0.068	B
412	El Centro Array Sta. 10	do	1	do	4.5	A
413	L.A., 1177 S. Beverly Dr.	do	7	Basement	4.1	B
416	Beverly Hills, 9100 Wilshire	do	10	do	3.7	A
425	L.A., 1800 Century Park East	do	15	do	3.7	B
428	L.A., 5900 Wilshire	do	31	do	3.5	B
431	L.A., 616 S. Normandie	do	16	do	--	A
437	L.A., 1150 S. Hill	do	10	do	2.6	A
443	L.A., 6200 Wilshire	do	17	Ground	3.5	A
446	L.A., 1760 N. Orchid	do	23	do	2.9	A
449	L.A., 2500 Wilshire	do	13	Basement	--	A
452	Beverly Hills, 435 N. Oakhurst	do	10	do	3.8	A
455	Beverly Hills, 450 N. Roxbury	do	10	Ground	3.7	A
458	L.A., 15107 Van Owen	do	7	Basement	2.9	A
461	L.A., 15910 Ventura	do	16	do	1.8	A
466	L.A., 15250 Ventura	do	12	do	1.8	A
469	L.A., 1625 W. Olympic	do	10	Ground	2.9	B
475	Pasadena, CIT Athenaeum	do	2	Basement	0.91	B
482	Alhambra, 900 S. Fremont	do	12	do	1.2	B

TABLE 3.--Station data--Continued

Sta. No.	Description	Housing	No. of stories	Level	Sediment depth (km)	Geology*
657	Santa Monica, 201 Ocean	Building	18	Basement	--	B
724	Niland, 8071 Luxor	do	1	Ground	4.1	A
757	Sepulveda Canyon Control Facility	do	9	Basement	--	B
885	Santa Barbara, UCSB Physical Plant	do	1	Ground	8.4	A
931	El Centro Array Sta. 12	Shelter	--	do	4.4	A
942	El Centro Array Sta. 6	do	--	do	5.3	A
952	El Centro Array Sta. 5	do	--	do	5.5	A
955	El Centro Array Sta. 4	do	--	do	5.7	A
958	El Centro Array Sta. 8	do	--	do	5.1	A
1008	Bishop, L.A. Water Dept.	do	--	do	--	A
1013	Cholame-Shandon Array Sta. 2	do	--	do	1.7	A
1014	Cholame-Shandon Array Sta. 5	do	--	do	1.7	A
1015	Cholame-Shandon Array Sta. 8	Building	1	do	1.7	B
1016	Cholame-Shandon Array Sta. 12	Shelter	--	do	1.7	A
1028	Hollister, City Hall	Building	1	Basement	1.4	A
1049	Oakland, City Hall	do	15	do	0.3	B
1052	Oso Pumping Plant	Shelter	--	Ground	3.0	A
1065	San Francisco, Alexander Bldg.	Building	15	Basement	0.043	A
1078	San Francisco, So. Pacific Bldg.	do	12	do	0.087	F

TABLE 3.--Station data--Continued

Sta. No.	Description	Housing	No. of stories	Level	Sediment depth (km)	Geology*
1080	San Francisco, State Bldg.	Building	6	Basement	0.062	A
1095	Taft, Lincoln School	do	1	Tunnel	6.4	A
1250	Gilroy, Gavilan College	do	1	Ground	0.020	B
1291	Marysville, CDOT Maintenance Bldg.	do	1	do	--	A
1377	San Juan Bautista, 24 Polk	do	1	do	1.2	A
1409	Gilroy Array Sta. 2	Shelter	--	do	4.0	A
1410	Gilroy Array Sta. 3	do	--	do	4.0	A
1411	Gilroy Array Sta. 4	Building	1	do	4.0	A
1422	Halls Valley, Grant Ranch	Shelter	--	do	--	A
1438	Cholame-Shandon Array, Temblor	do	--	do	--	E
1490	Mammoth Lakes, High School	Building	1	do	--	B
1492	San Juan Bautista, 101/156 Overpass	Shelter	--	do	0.015	B
2734	Icy Bay, Gulf Timber Co.	Building	1	do	6.1	F
2808	Hilo, UH Cloud Physics Lab	do	1	do	--	E
3501	Nicaragua, Managua, ESSO Refinery	do	1	do	2.0	A
5028	El Centro Array Sta. 7	do	1	do	5.2	A
5051	El Centro, Parachute Test Site	do	1	do	3.4	A
5052	Plaster City	do	1	do	2.0	A
5053	Calexico, Fire Station	do	1	do	4.3	A
5054	Bonds Corner	do	1	do	5.7	A

TABLE 3.--Station data--Continued

Sta. No.	Description	Housing	No. of stories	Level	Sediment depth (km)	Geology*
5055	Holtville, Post Office	Building	1	Ground	5.6	A
5056	El Centro Array Sta. 1	do	1	do	5.1	A
5057	El Centro Array Sta. 3	do	1	do	5.7	A
5058	El Centro Array Sta. 11	do	1	do	4.5	A
5059	El Centro Array Sta. 13	Shelter	--	do	3.8	A
5060	Brawley, Airport	Building	1	do	5.2	A
5061	Calipatria, Fire Station	do	2	do	5.0	A
5062	Salton Sea Wildlife Refuge	do	1	do	--	A
5079	Malibu, Kilpatrick Boy's School	do	1	do	--	E
5081	Topanga, Fire Station	do	1	do	--	E
5093	Santa Barbara, UCSB North Hall	do	3	do	--	E
5115	El Centro Array Sta. 2	Shelter	--	do	5.5	A
5137	Santa Barbara, Freitas Bldg.	Building	4	Basement	8.5	B
5154	El Centro, Imperial Co. Center	Shelter	--	Ground	4.8	A
5155	El Centro, Meloland Overpass	Vault	--	do	5.1	A
5165	El Centro, Differential Array SMA-1	Shelter	--	do	5.0	A
5169	Westmorland, Fire Station	Building	2	do	5.1	A
6605	Mexico, Delta	Shelter	--	do	7.5	A
6610	Mexico, Victoria	do	--	do	8.0	A
6616	Mexico, Aeropuerto	do	--	do	--	A

TABLE 3.--Station data--Continued

Sta. No.	Description	Housing	No. of stories	Level	Sediment depth (km)	Geology*
6617	Mexico, Cucapah	Shelter	--	Ground	7.0	A
6618	Mexico, Agrarias	do	--	do	5.5	A
6619	Mexico, Mexicali, SAHOP	Building	1	do	--	A
6621	Mexico, Chihuahua	Shelter	--	do	7.0	A
6622	Mexico, Compuertas	do	--	do	5.5	A
9022	Goleta, SCE Substation	do	--	do	--	E
9034	El Centro, Differential Array	Vault	--	do	5.0	A
9110	U.S.S.R., Karakyr	Building	1	do	1.4	A
9124	Iran, Tabas	do	1	do	2.0	A

*Geology code adopted from Campbell (1981a)

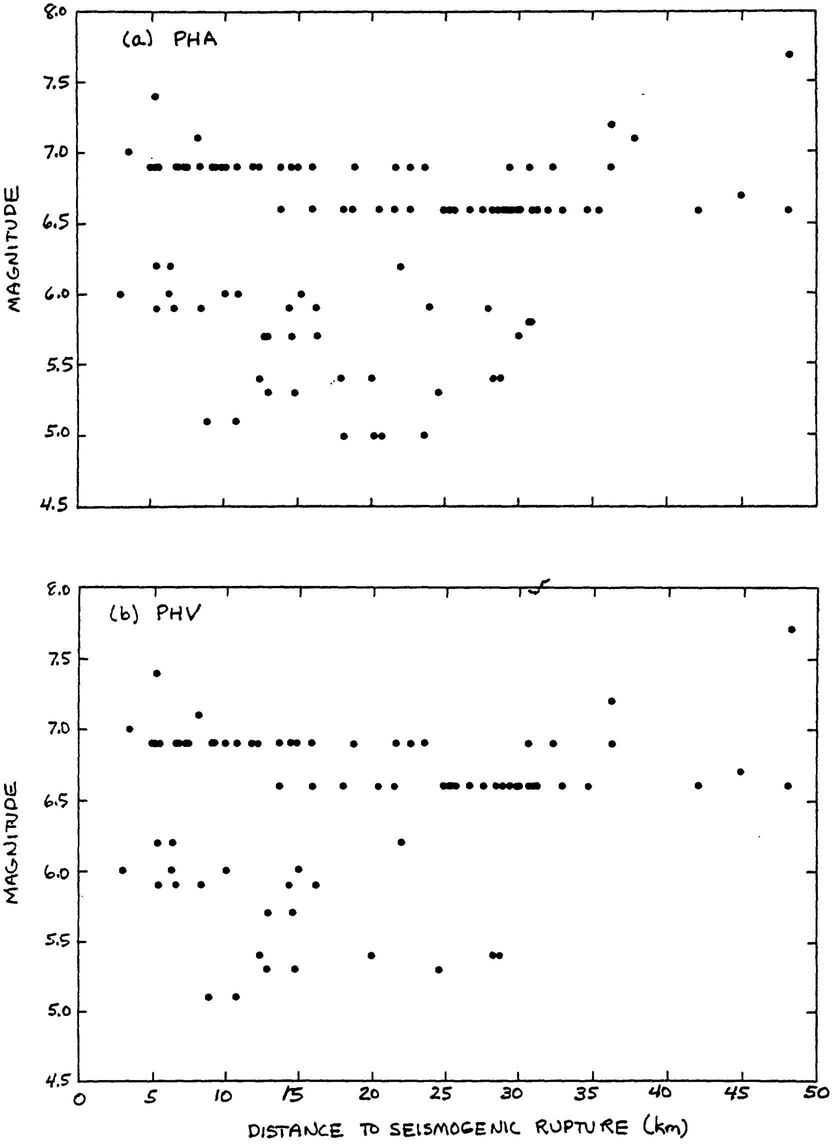

FIGURE 1.--Distribution of strong-motion recordings with respect to magnitude and distance: (a) peak horizontal acceleration; (b) peak horizontal velocity.

REGRESSION ANALYSIS

The coefficients *a* through *e* of equation 1 were estimated using a nonlinear least-squares regression routine developed by More and others (1980). The method was modified to incorporate weights used to control the influence of those earthquakes having a large number of recordings. The weighting scheme is identical to that described by Campbell (1981a, 1982a). It is designed to give each earthquake an equal weight in the analysis in each of nine distance intervals, thereby balancing the information on magnitude scaling contributed by earthquakes whose recordings are poorly distributed with respect to distance with the information on distance scaling contributed by earthquakes whose recordings are well distributed with respect to distance. The distance intervals were selected to be roughly equal in logarithmic increments between 0 and 56.6 km.

The weight of each recording was computed from the expression

$$w_i = \frac{n}{n_i} \left. \sum_{j=1}^{n} \frac{1}{n_j} \right.^{-1} \qquad (2)$$

where n is the total number of recordings used in the analysis and n_i is the number of recordings associated with the specific earthquake and distance interval containing the ith recording. Note that the quantity n_i is not unique to a single recording, rather it is the same for all recordings of the same earthquake whose distance falls within the specified distance interval. The above expression assures that the sum of the weights equals n, thus preserving the correct number of degrees of freedom. Table 4 gives the distribution of recordings with respect to the nine distance intervals used in the analyses.

TABLE 4.--NEAR HERE

TABLE 4.--Distribution of recordings by distance

Distance range (km)	Earthquake	No. of recordings Accel.	Vel.
0-2.4	---	0	0
2.5-4.9	Parkfield, 1966	1	1
	Gazli, 1976	1	1
5.0-7.4	Long Beach, 1933	1	1
	Parkfield, 1966	1	1
	Managua, 1972	1	1
	Tabas, 1978	1	1
	Coyote Lake, 1979	2	2
	Imperial Valley, 1979	11	10
7.5-9.9	Imperial Valley, 1940	1	1
	Hollister, 1974	1	1
	Santa Barbara, 1978	2	1
	Coyote Lake, 1979	1	1
	Imperial Valley, 1979	7	5
10.0-14.0	Daly City, 1957	1	1
	Parkfield, 1966	2	1
	Lytle Creek, 1970	1	1
	San Fernando, 1971	1	1
	Hollister, 1974	2	2
	Imperial Valley, 1979	5	5

TABLE 4.--Distribution of recordings by distance--Continued

Distance range (km)	Earthquake	No. of recordings Accel.	Vel.
14.1-19.9	Daly City, 1957	2	2
	Parkfield, 1966	1	1
	Lytle Creek, 1970	1	0
	San Fernando, 1971	3	2
	Santa Barbara, 1978	3	2
	Malibu, 1979	1	0
	Coyote Lake, 1979	2	2
	Imperial Valley, 1979	5	5
20.0-28.2	Long Beach, 1933	1	1
	Daly City, 1957	1	1
	Lytle Creek, 1970	1	1
	San Fernando, 1971	13	12
	Point Mugu, 1973	1	0
	Malibu, 1979	3	0
	Coyote Lake, 1979	1	0
	Imperial Valley, 1979	3	3
28.3-40.0	Lytle Creek, 1970	2	2
	San Fernando, 1971	32	25
	Oroville, 1975	1	0
	Kalapana, 1975	1	0
	Bishop, 1978	2	0

TABLE 4.--Distribution of recordings by distance--Continued

Distance range (km)	Earthquake	No. of recordings Accel.	Vel.
28.3-40.0	St. Elias, 1979	1	1
	Imperial Valley, 1979	4	3
40.1-56.6	Kern County, 1952	1	1
	Borrego Mtn., 1968	1	1
	San Fernando, 1971	4	4

Other investigators have proposed alternate methods for compensating for the bias associated with the erratic distribution of distances and numbers of recordings between earthquakes. The two most notable are the two-step regression procedure suggested by Joyner and Boore (1981) and the random-effects procedure suggested by Brillinger and Preisler (1984). Although the latter technique may be more mathematically rigorous, all three techniques are fundamentally similar in their results. Therefore, the weighted regression procedure has been retained for the current study to be consistent with the writer's previous analyses.

For peak horizontal acceleration, the weighted nonlinear regression analysis resulted in the following unconstrained relationship:

$$\ln \mathrm{PHA}=-2.817+0.702M-1.20\ \ln[R+0.0921\ \exp(0.584M)]+f(e_i,K_i,R) \qquad (3)$$

and for peak horizontal velocity,

$$\ln \mathrm{PHV}=-0.798+1.02M-1.26\ \ln[R+0.0150\ \exp(0.812M)]+f(e_i,K_i,D) \qquad (4)$$

where acceleration, velocity, and distance have units of g, centimeters per second, and kilometers, respectively. Magnitude and distance are as defined previously and D is the depth of sediments beneath the recording site in kilometers. The coefficients e_i, parameters K_i, and functions $f(e_i, K_i, R)$ and $f(e_i, K_i, D)$ are summarized in tables 5 and 6; the relationships are plotted in figures 2-5. The standard errors of regression are 0.30 and 0.26 for equations 3 and 4, respectively.

TABLE 5.--NEAR HERE

TABLE 6.--NEAR HERE

FIGURE 2.--NEAR HERE

TABLE 5.--Definitions of K_i, $f(e_i, K_i, R)$, and $f(e_i, K_i, D)$*

Parameter	Definition	
	Peak horizontal acceleration	Peak horizontal velocity
Fault type	$K_1 =$ 0 strike-slip 1 reverse and thrust	$K_1 =$ 0 strike-slip 1 reverse and thrust
Source directivity	$K_2 =$ 0 all other rupture geometries 1 rupture towards site	$K_2 =$ 0 all other rupture geometries 1 rupture towards site
Shallow soil	$K_3 =$ 0 soils >10-m deep 1 soils ≤10-m deep	---
Building size	---	$K_3 =$ 0 buildings ≥5 stories 1 shelters and buildings <5 stories
Embedment	$K_4 =$ 0 all other recordings 1 basements of 3-9 story buildings	---
	$K_5 =$ 0 all other recordings 1 basements of ≥10-story buildings	---

*$f(e_i, K_i, R) = e_1K_1 + e_2K_2 + e_3K_3 + e_4K_4 + e_5K_5 + e_6[K_4 + K_5]\tanh(e_7R)$ [Peak horizontal acceleration]

$f(e_i, K_i, D) = e_1K_1 + e_2K_2 + e_3K_3\tanh(e_4D) + e_5[1 - K_3]\tanh(e_6D)$ [Peak horizontal velocity]

TABLE 6.--Summary of regression coefficients, e_i[*]

Coefficient	Peak horizontal acceleration Equation 3	 Equation 4	Peak horizontal velocity Equation 5	 Equation 6
e_1	0.32	0.34	0.47	0.49
e_2	0.52	0.53	0.95	0.99
e_3	0.41	0.41	0.63	0.53
e_4	-0.85	-0.86	0.39	0.41
e_5	-1.14	-1.12	0.72	0.60
e_6	0.87	0.89	0.75	0.88
e_7	0.068	0.065	--	

[*] The functions involving e_i are defined in the footnote of table 5.

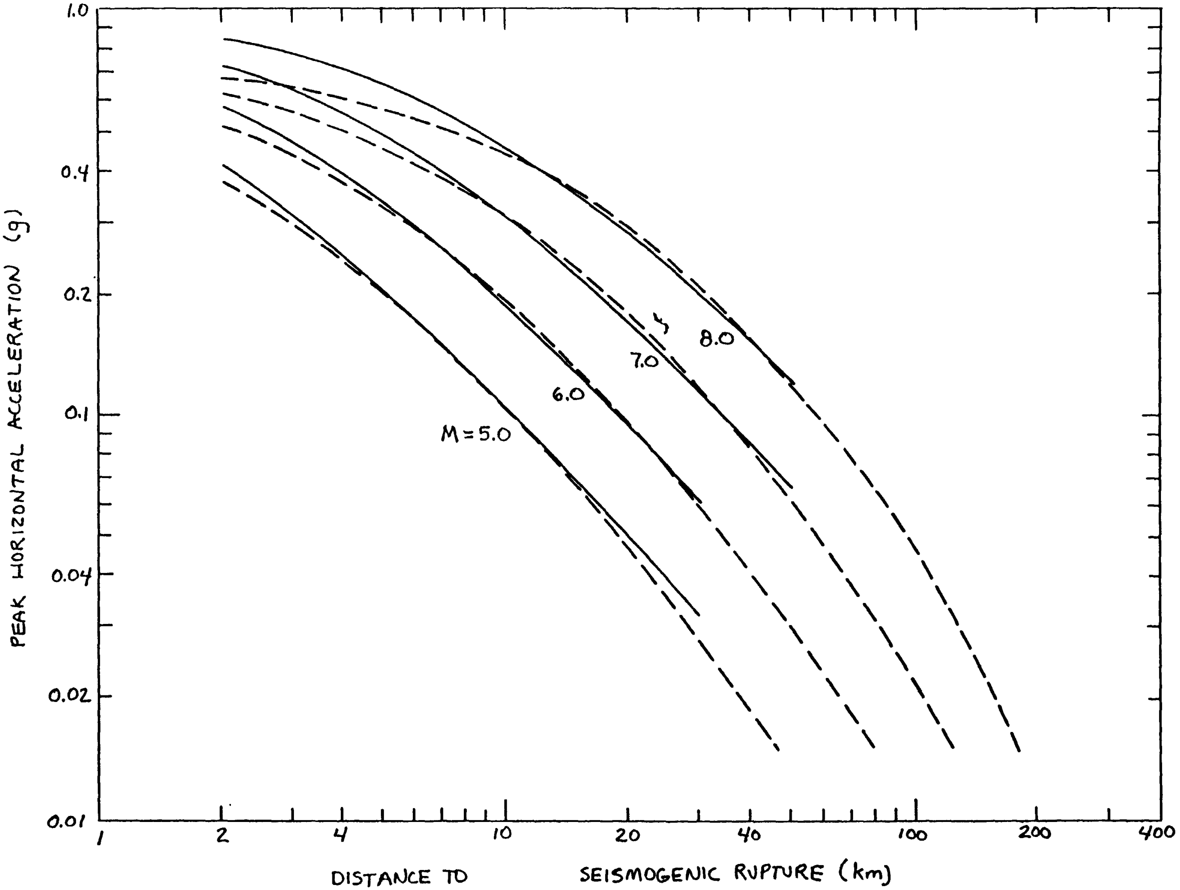

FIGURE 2.--Attenuation relationships of peak horizontal acceleration for magnitudes of 5.0, 6.0, 7.0, and 8.0: solid line--unconstrained model (equation 3); dashed line--constrained model with Y=0.0059 (equation 5). Relationships are plotted for K_1=0.

FIGURE 3.--NEAR HERE

FIGURE 4.--NEAR HERE

FIGURE 5.--NEAR HERE

The definitions and functional relationships for K_i were determined from an analysis of residuals described later in the text. Because of the nonlinear form of equation 1, rigorous statistical tests to determine the significance of coefficients $\underline{a}$ through $\underline{e}$ require Monte Carlo simulation (Gallant, 1975), beyond the scope of this study. Therefore, the statistical significance of these coefficients are not precisely known. A visual inspection of the residuals did indicate a very strong need for all coefficients except possibly $\underline{c}_2$, suggesting that these coefficients are statistically significant at least at the 90-percent confidence level. $\underline{c}_2$ is controlled by too few recordings to be judged solely on visual inspection. It should be noted, however, that the regression analyses for both strong-motion parameters resulted in a value for $\underline{c}_2$ at its practical upper limit, $c_2=-b/d$. This represents complete saturation of PHA and PHV at the source of an earthquake in accordance with some geophysicists' interpretations of earthquake rupture mechanics (Campbell, 1985a). Confirmation of the statistical significance of $\underline{c}_2$ will have to await the outcome of Monte Carlo simulations.

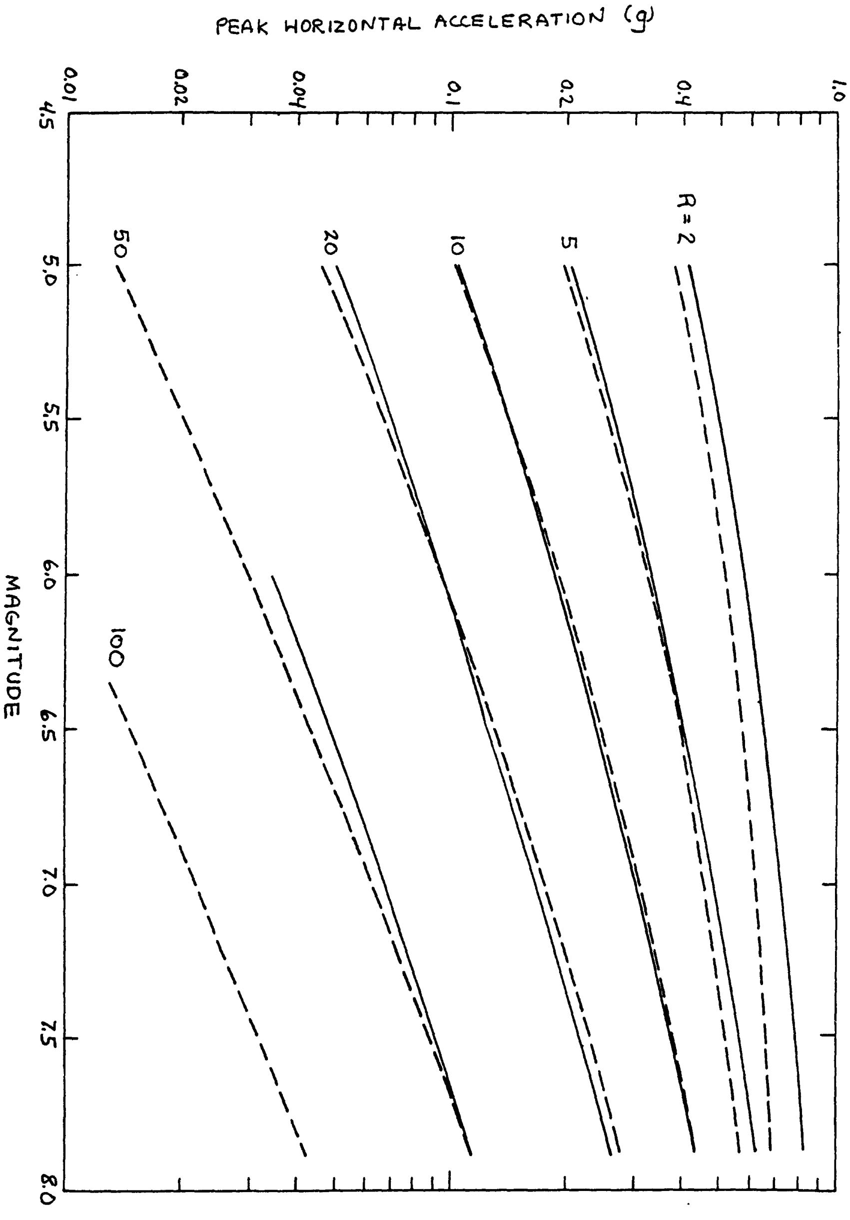

FIGURE 3.--Predicted magnitude scaling of peak horizontal acceleration for distances of 2, 5, 10, 20, 50, and 100 km: solid line--unconstrained model (equation 3); dashed line--constrained model with γ=0.0059 (equation 5). Relationships are plotted for K_1=0.

FIGURE 4.--Attenuation relationships of peak horizontal velocity for magnitudes of 5.0, 6.0, 7.0, and 8.0: solid line--unconstrained model (equation 4); dashed line--constrained model with γ=0.0059 (equation 6). Relationships are plotted for K_i=0.

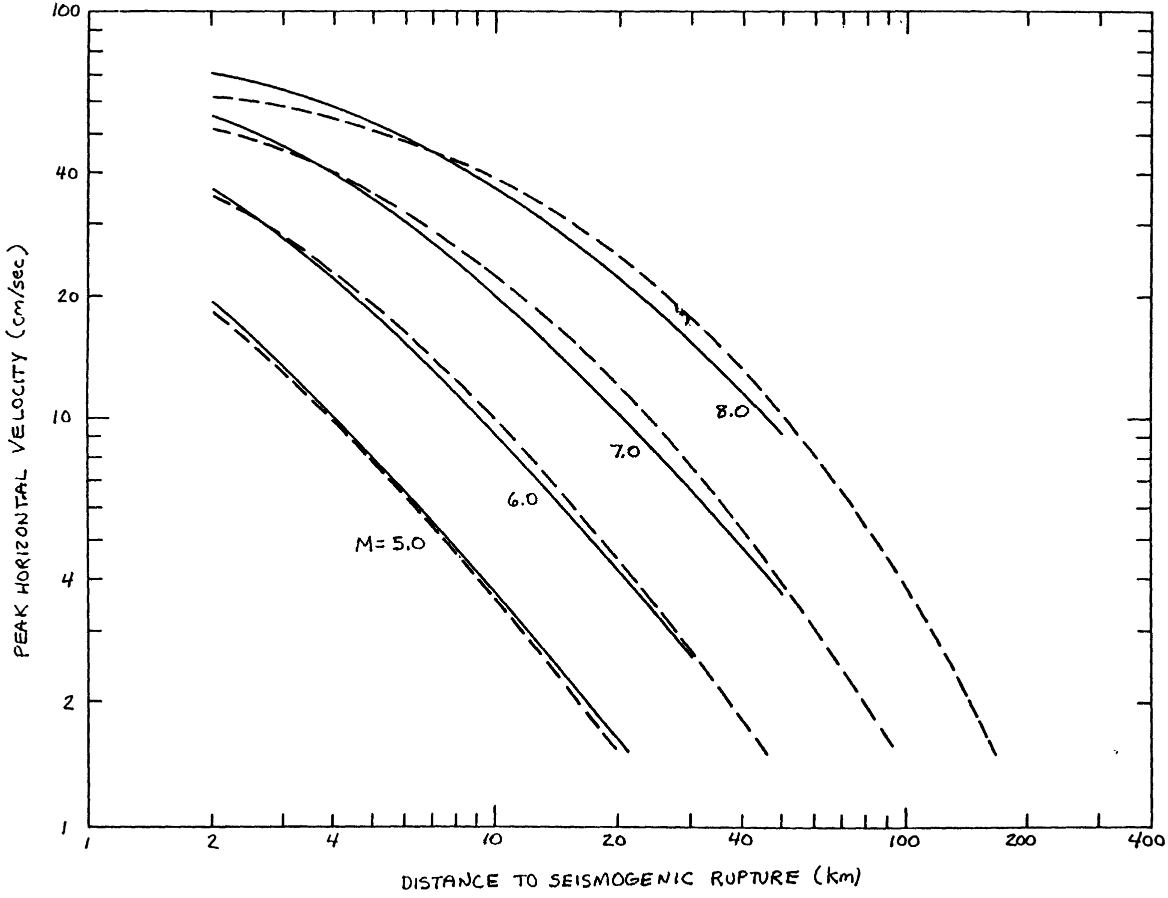

FIGURE 5.--Predicted magnitude scaling of peak horizontal velocity for distances of 2, 5, 10, 20, 50, and 100 km: solid line--unconstrained model (equation 4); dashed line--constrained model with γ=0.0059 (equation 6). Relationships are plotted for K_i=0.

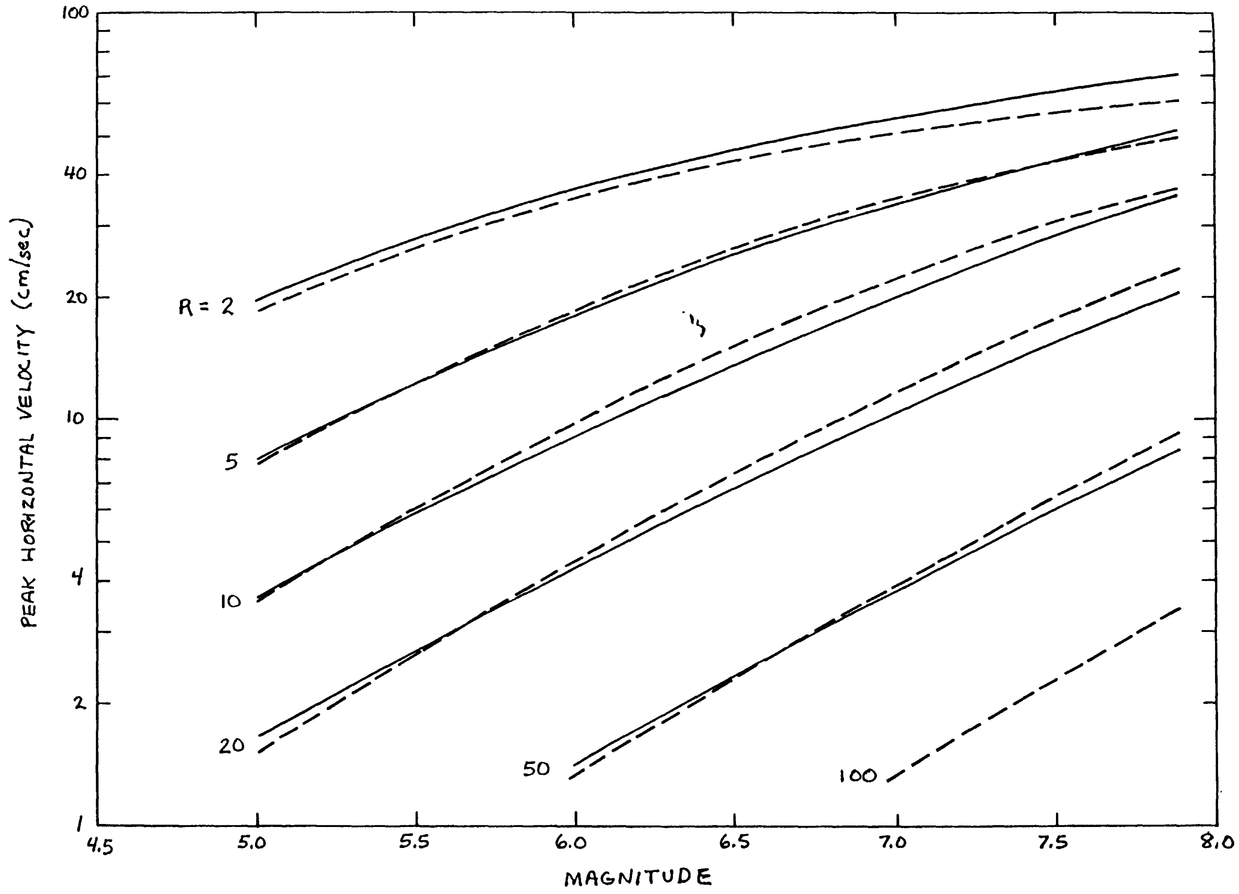

The results presented in tables 5 and 6 indicate that PHA is systematically high when recorded on ground-level instruments located on shallow soils, and that it is systematically low when recorded in basements of buildings greater than 3 stories high. Shallow soils are defined as unconsolidated deposits less than about 10 m in depth which overlie sedimentary or crystalline rock (Campbell, 1981a). The reduction in PHA due to embedment was found to be dependent on building size and distance, with buildings 10 stories and higher having lower accelerations than 3- to 9-story buildings, and buildings further from the source having smaller reductions than those closer in. This distance dependence was adequately modeled by a hyperbolic tangent function, where distance is expressed in kilometers. This function is plotted in figure 6.

FIGURE 6.--NEAR HERE

The results given in tables 5 and 6 indicate that PHV is dependent on sediment depth (i.e., depth to crystalline basement rock), increasing rapidly with depth at relatively shallow depths and becoming virtually independent of depth at depths of 5-6 km. This dependence was found to be dependent on building size with buildings 5 stories and higher having peak velocities that increase faster with depth than smaller buildings and instrument shelters. For depths greater than about 5 km, at which point the effect of sediment depth remains relatively constant, the effect of building size is less than about 10 percent. The depth dependence was adequately modeled by a hyperbolic tanget function, where sediment depth is expressed in kilometers. This function is plotted in figure 7. No amplification due to shallow soils nor any reduction as a result of building embedment was observed for peak velocity.

FIGURE 6.--Dependence of peak horizontal acceleration on building embedment: solid line--<u>unconstrained</u> model (equation 3); dashed line--<u>constrained</u> model (equation 5). The embedment factor is a multiplicative factor given by the expression $\exp[e_4K_4+e_5K_5+e_6(K_4+K_5)\tanh(e_7R)]$ where e_i and K_i are defined in tables 5 and 6.

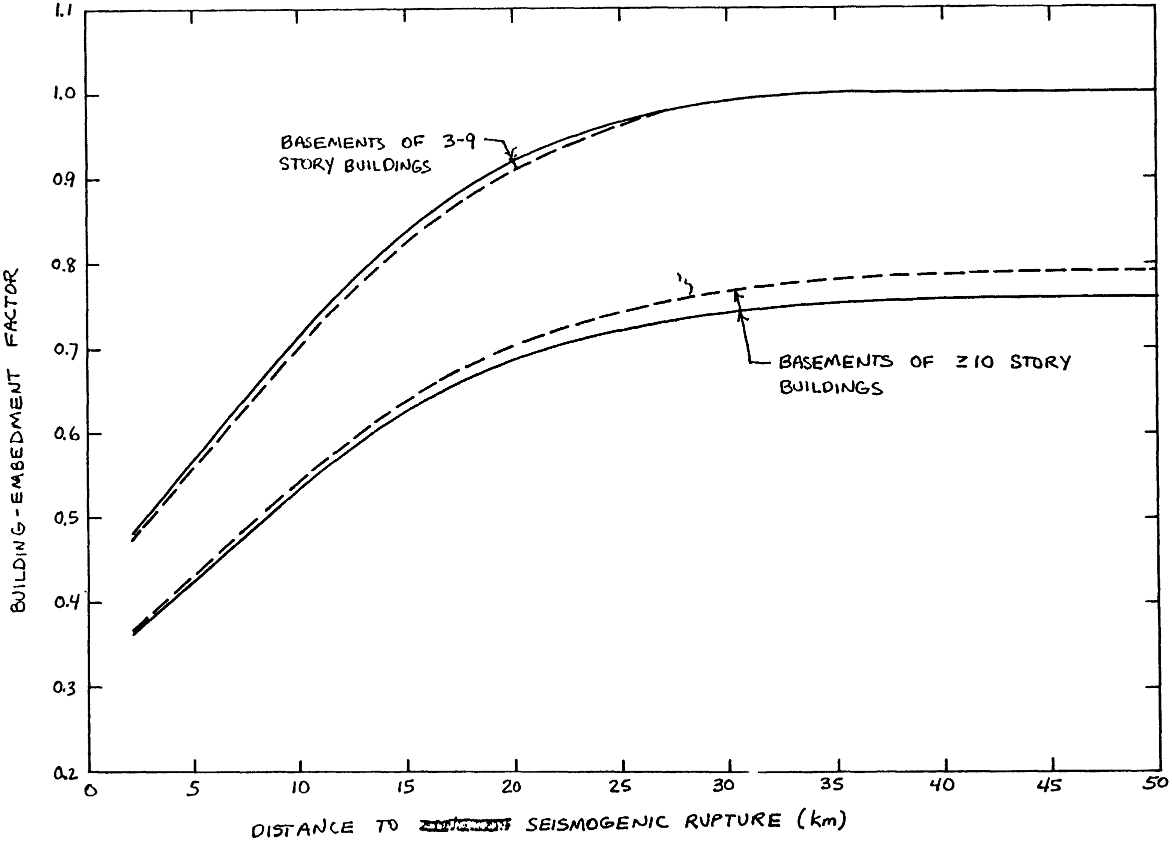

FIGURE 7.--NEAR HERE

Both PHA and PHV were found to be influenced by fault type, being higher for reverse and thrust faults than for strike-slip faults. The effect is somewhat larger for velocity than for acceleration, but the difference may not be statistically significant.

During the analysis of residuals for both PHA and PHV, three recordings were found to have such large positive residuals that they appeared to be outliers. All three recordings had weighted residuals exceeding 4 standard errors. Upon further investigation, it was discovered that all three recordings had three factors in common: (1) they were associated with earthquakes exhibiting unilateral rupture towards the site, (2) their azimuths with respect to the source were within 5-10 degrees of the direction of rupture, and (3) they were sited on sediments at least 5-km deep. These results appeared to indicate a directivity effect, possibly enhanced by the thickness of the sediments. The effect was so strong, especially for peak velocity, that it was decided to include it as a parameter, even though it was represented only by three recordings. This is not to say that other recordings in the data base are not also affected to some degree by directivity, only that these three recordings may represent a combination of factors that lead to a near-maximum effect of this phenomenon. A more thorough investigation of directivity effects is beyond the scope of the current study.

FIGURE 7.--Dependence of peak horizontal velocity on sediment depth: solid line--unconstrained model (equation 4); dashed line--constrained model (equation 6). The sediment-depth factor is a multiplicative factor given by the expression $\exp[e_3K_3\tanh(e_4D)+e_5(1-K_3)\tanh(e_6D)]$ where e_i and K_i are defined in tables 5 and 6.

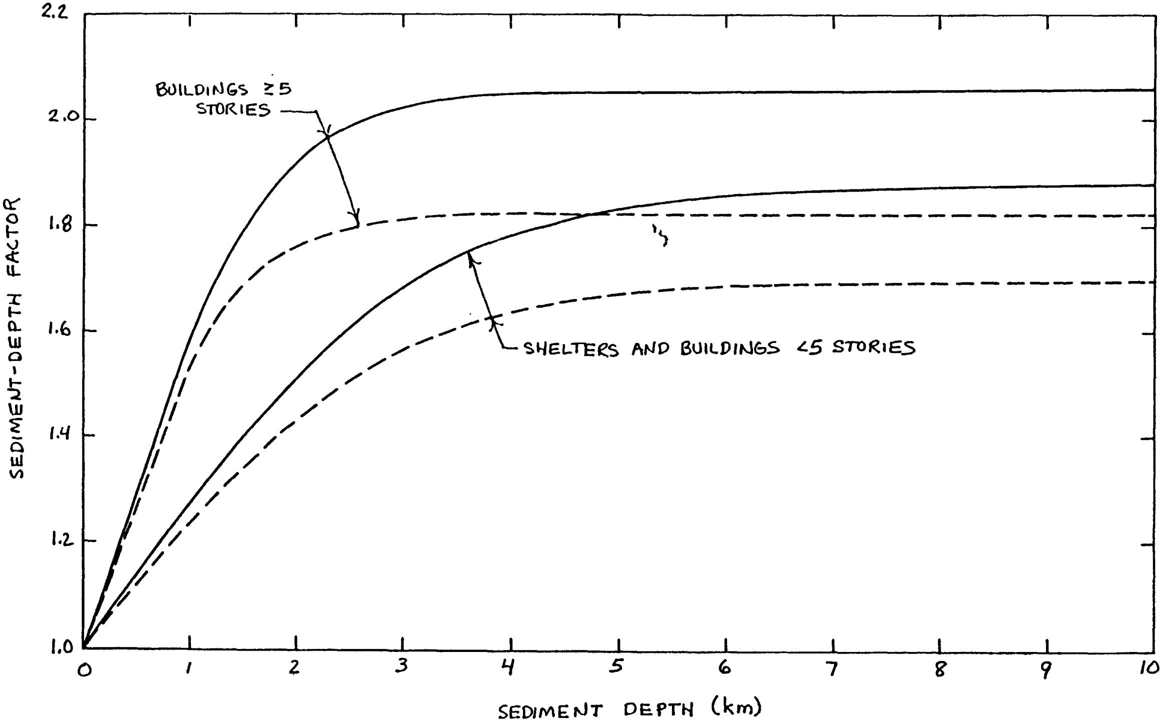

FAR-FIELD CONSTRAINTS

Because this study was not directly concerned with predicting far-field ground motion, accelerograms recorded further than 30-50 km from seismogenic rupture were not included in the analyses. In order to develop attenuation relationships that could be extrapolated to larger distances, a second analysis was performed where Υ, the coefficient of anelastic attenuation in equation 1, was constrained to values appropriate for the majority of data making up the data base.

Because of the similarity in the regional makeup of the current data base and that of Joyner and Boore (1981), we adopted their statistically determined values of Υ for our constrained analyses. Repeating the weighted nonlinear regression analyses using $\Upsilon=0.0059$ resulted in the following constrained relationships[2]:

$$\ln PHA=-3.303+0.850M-1.25\ \ln[R+0.0872\ \exp(0.678M)]-\Upsilon R+f(e_i,K_i,R) \qquad (5)$$

$$\ln PHV=-1.584+1.18M-1.24\ \ln[R+0.00907\ \exp(0.951M)]-\Upsilon R+f(e_i,K_i,D) \qquad (6)$$

where all parameters are defined as in equations 3 and 4. The coefficients e_i, parameters K_i, and functions $f(e_i, K_i, R)$ and $f(e_i, K_i, D)$ are summarized in tables 5 and 6; the relationships are plotted in figures 2-5. The standard errors of regression for equations 5 and 6 are 0.30 and 0.27, respectively.

---

[2] The analyses of Joyner and Boore (1981) resulted in the same value of Υ for both peak acceleration and peak velocity, suggesting that anelastic attenuation is nearly independent of frequency in California.

Equations 5 and 6 were compared to the attenuation relationships of Joyner and Boore (1981) to verify that the attenuation characteristics were similar beyond distances of 30-50 km as originally intended. The comparison was made for $M=6.5$ and $R \geq 30$ km after modification to account for differences in the definition of parameters between the two studies. The magnitude was chosen to be near the median magnitude of both studies. Comparisons were restricted to $R \geq 30$ km to minimize the impact of differences in the near-source behavior of the two functional forms. Close agreement in the attenuation rates of both studies suggested that the extrapolation of equations 5 and 6 beyond 30-50 km using $Y=0.0059$ was valid to distances of at least several hundred kilometers.

Coefficients derived for the *constrained* relationships are generally consistent with those derived for the *unconstrained* relationships. This indicates that relatively small adjustments were required to accommodate the constraint on anelastic attenuation imposed during the second analysis. It should be noted, however, that the coefficients presented in tables 5 and 6 are constrained only by near-source recordings and may not be valid for distances greater than 30-50 km. This is especially true for the shallow-soil and building-embedment parameters, which may become less important as distance and, hence, wave period, increases.

ANALYSIS OF RESIDUALS

An analysis of residuals was used to (1) select and define the parameters used in the attenuation relationships and (2) check the adequacy of the final elationships. For convenience, the analysis used the normalized weighted esidual,

$$NWR_i = \frac{w_i(y_i - \hat{y}_i) - MWR}{\sigma} \qquad (7)$$

where i is the index of the recording, w_i is the weight assigned to the ecording, y_i is the observed value of ln Y, $\hat{y}_i$ is the predicted value of ln Y, σ is the standard error of the regression, and MWR is the mean weighted esidual, defined by the expression

$$MWR = \frac{1}{n} \sum_{i=1}^{n} w_i(y_i - \hat{y}_i) \qquad (8)$$

The definition and functional form of the parameters listed in table 5 were developed by an iterative procedure. First, a list of candidate parameters were selected from theoretical considerations of source, site, and soil-structure interaction effects available from the literature. Second, regression analyses were used to establish attenuation relationships in terms of M and R by setting $K_i=0$ in equation 1. In the case of continuous parameters such as sediment depth, the normalized weighted residuals were then plotted against the candidate parameters. In the case of classification or so-called "dummy" parameters such as fault type, the normalized weighted residuals associated with each class were plotted against M and R. When visually perceptible trends were identified from the residual plots, those parameters were added to the model. The process was repeated until all significant parameters and their proper functional relationships were identified and included in the model. From a purely scientific point of view, the above procedure might be criticized for its strong empirical basis; though from a statistical standpoint such procedures are accepted as standard model-building techniques (Draper and Smith, 1971; Tukey, 1977).

The adequacy of the final attenuation relationships was assessed by plotting the normalized weighted residuals against each dependent and independent variable included in the models. The residual plots against magnitude, distance, and predicted value are given in figures 8-10 for the unconstrained relationships, equations 3 and 4. A lack of any significant trend indicated that the models were statistically adequate. Similar results were found for equations 5 and 6 as well as for other independent variables included in the relationships.

FIGURE 8.--NEAR HERE

FIGURE 9.--NEAR HERE

FIGURE 10.--NEAR HERE

GROUND-MOTION ESTIMATES FOR NORTHCENTRAL UTAH

The region of northcentral Utah contains the major population centers of Ogden, Provo, and Salt Lake City. The dominant feature of this region is the Wasatch Front--a massive 370-km-long scarp extending along the western margin of the Wasatch Mountains from Gunnison, Utah, to Malad City, Idaho. The scarp is a result of normal faulting along the Wasatch fault, which marks the boundary between the Basin and Range and Middle Rocky Mountain Physiographic Provinces (Fenneman, 1946). The boundary marks the transition from a northwest-southeast extensional stress regime on the west to a northwest-southeast compressional stress regime on the east (Zoback and Zoback, 1981).

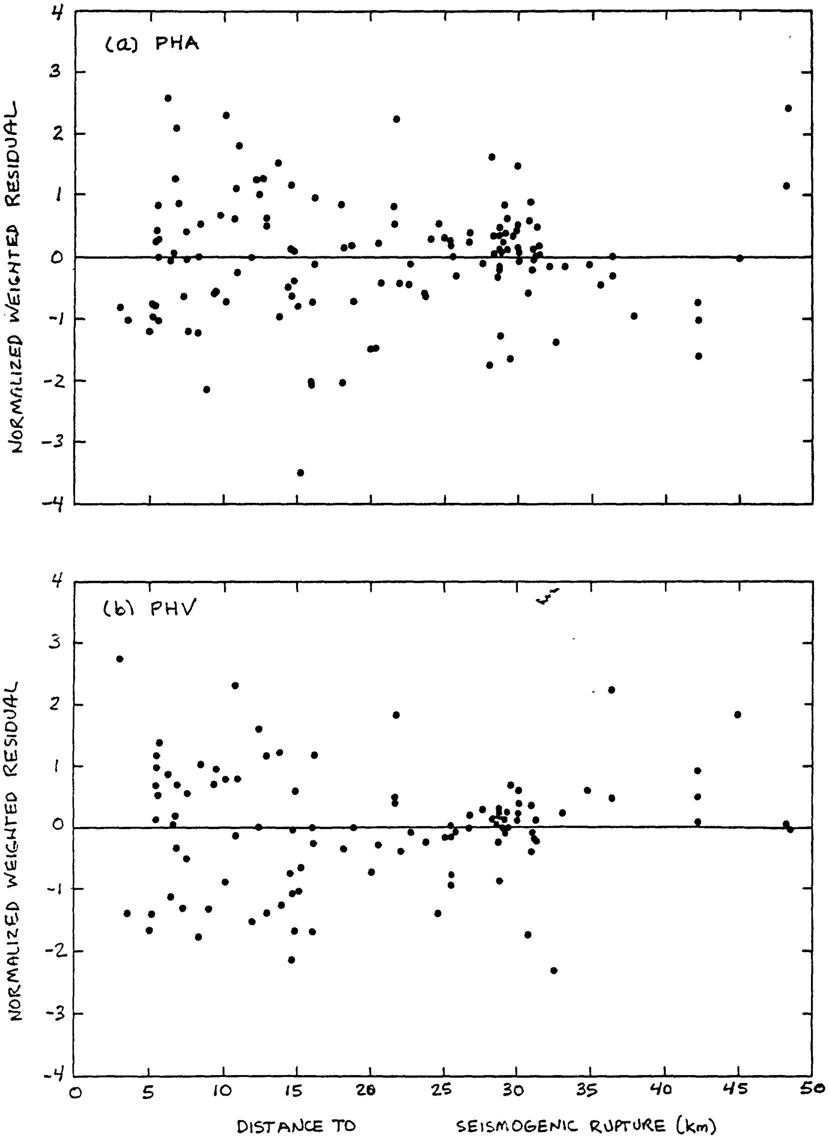

FIGURE 8.--Normalized weighted residuals plotted as a function of distance: (a) peak horizontal acceleration; (b) peak horizontal velocity. Plots are shown for the unconstrained models (equations 3 and 5). Similar distributions were found for the constrained models.

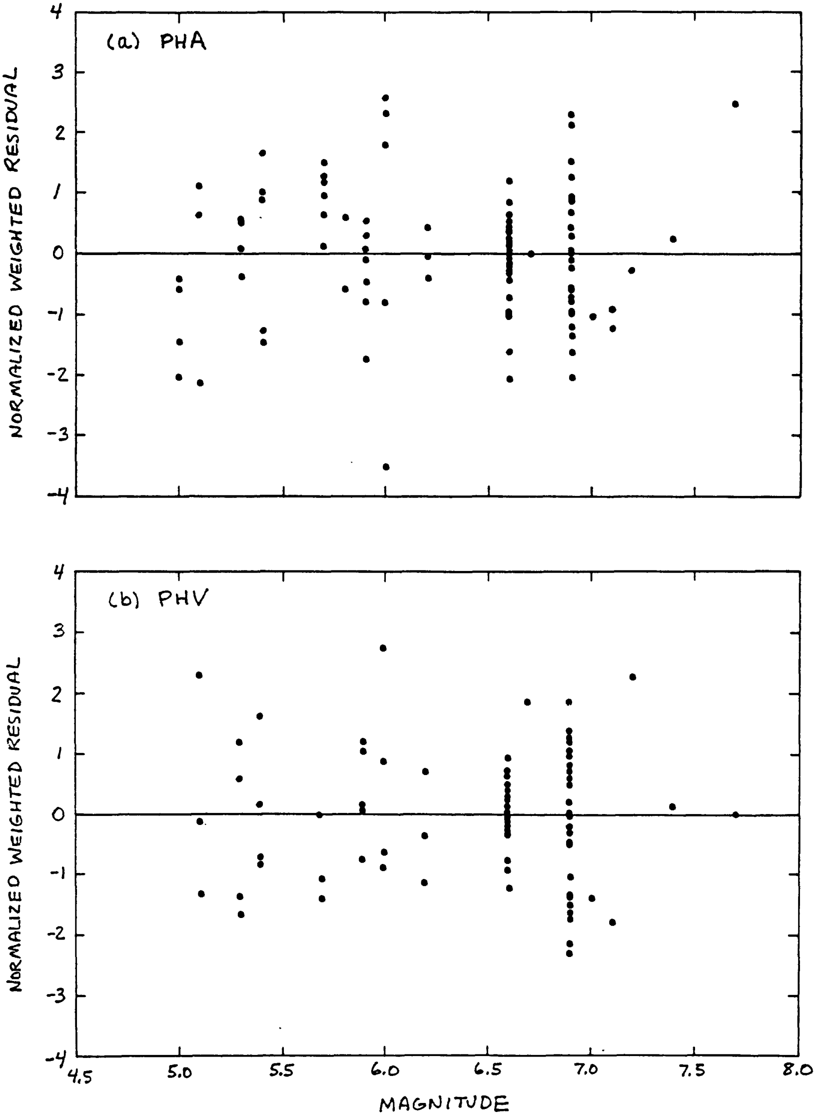

FIGURE 9.--Normalized weighted residuals plotted as a function of magnitude: (a) peak horizontal acceleration; (b) peak horizontal velocity. Plots are unconstrained distributions were found for the constrained models.

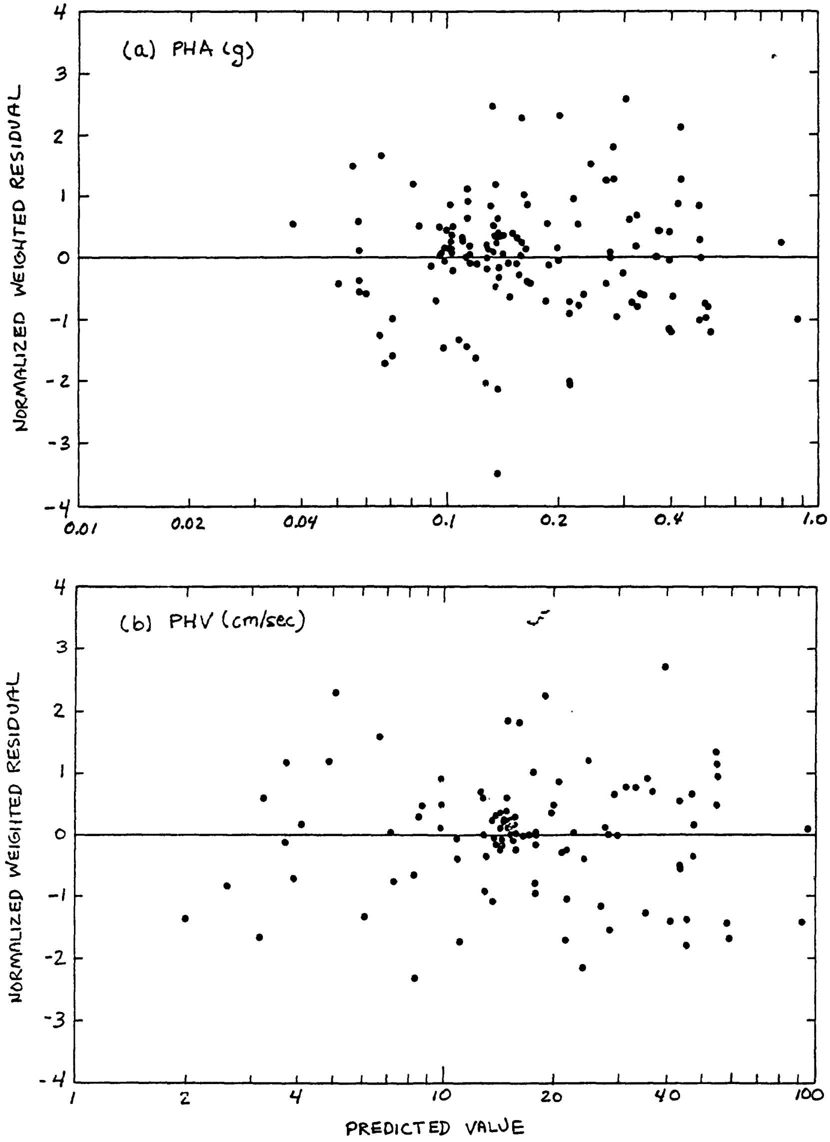

FIGURE 10.--Normalized weighted residuals plotted as a function of predicted values: (a) peak horizontal acceleration; (b) peak horizontal velocity. Plots are shown for the unconstrained models (equations 3 and 5). Similar distributions were found for the constrained models.

The Wasatch fault poses the greatest seismic threat from major earthquakes in this region. Geologic evidence indicates that surface faulting associated with earthquakes of magnitude 6.5-7.5 has occurred repeatedly along several segments of this fault at an average rate of one event every 444 yr (Swann and others, 1980). In contrast, the greatest seismic threat in the next 100 yr, assuming a Poisson model of earthquake occurrences, comes from small-to-moderate earthquakes located in the historically more active regions of the state (Powers and others, this volume).

There are several important issues that need to be addressed before attempting to estimate strong-motion parameters in northcentral Utah. These issues are discussed below.

STRESS REGIME

McGarr (1984) presents theoretical and empirical results indicating that peak acceleration and peak velocity are strongly dependent on stress state and focal depth. He contends that, for a given seismic moment, both parameters are smaller for earthquakes occurring in an extensional stress regime than those occurring in a compressional stress regime, and that both parameters increase with focal depth. Differences due to stress regime are quite large, being as great as a factor of three for peak acceleration and a factor of two for peak velocity at a given depth.

Taken at face value, McGarr's results would have a considerable impact on the estimation of ground motion in the region of Utah west of the Wasatch Front. This region, including the Wasatch fault, is characterized by Basin and Range extensional tectonics. In contrast, the majority of the strong-motion data used to develop the attenuation relationships in this study come from coastal California--a region undergoing predominantly north-south compression (Zoback and Zoback, 1981). Thus, if McGarr is correct, one would expect substantially smaller ground motion in western Utah than would be predicted from equations 3-6. However, McGarr's results are not consistent with other empirical observations.

McGarr's results appear to be contradicted by the writer's own study of peak acceleration data from near-source recordings in California (Campbell, 1985b). Campbell analyzed strong-motion data recorded within 20 km of earthquakes of M_L=2.5-5.0, which occurred in Oroville, Calif., Imperial Valley, Calif., and coastal California in an attempt to identify regional differences in peak acceleration scaling relations. The Oroville region falls along the western margin of the Sierra Nevada Physiographic Province (Fenneman, 1946)--a region characterized by east-to-northeast extension (Zoback and Zoback, 1981). Focal mechanisms in this area are predominantly normal. The other two areas are within the San Andreas Physiographic Province (Fenneman, 1946)--a region characterized by north-south compression (Zoback and Zoback, 1981). Focal mechanisms in this region are predominantly strike-slip on northwest-trending faults and reverse or reverse-oblique on west-trending faults.

Campbell's regression analyses demonstrated only minor regional differences in magnitude and distance scaling. For magnitudes ranging from 3.5-4.5 and epicentral distances ranging from 5-10 km (about 1-2 focal depths), the scaling relations predict peak accelerations that vary by less than 10-15 percent between regions. Furthermore, the study found no significant dependence of peak acceleration on focal depth for depths in the range 4-10 km. These depths represent the major seismogenic portion of the crust in California. Similar results were found whether hypocentral distance or epicentral distance was used in the analyses.

The reasons for the discrepancy between the above results and those of McGarr are largely speculation. One major difference between the two studies that may help to explain this discrepancy is a difference in magnitude scaling. McGarr assumed that at relatively short distances peak acceleration should be relatively independent of seismic moment. On the other hand, the near-source regression analyses of Campbell (1985b) indicate a strong correlation between peak acceleration and M_L and, hence, seismic moment with ln PHA being proportional to $0.5-0.7M_L$. The latter dependence is generally consistent with magnitude scaling of peak acceleration from $M_L \geq 5.0$ earthquakes (Campbell, 1981a, 1984a; Joyner and Boore, 1981). In fact, Campbell (1985b) found that when an estimate of closest distance to fault rupture was used as the distance metric in his regression analyses, the near-source magnitude and distance scaling properties of peak acceleration for $M_L \leq 5.0$ earthquakes were remarkably consistent with the extrapolation of the near-source attenuation relationships for $M_L \geq 5.0$ earthquakes developed by Campbell (1984a). Thus, either McGarr's assumption of magnitude independence of PHA for hypocentral distances on the order of 10 km is wrong, or M_L scales with seismic moment, state of stress, and focal depth in a manner similar to his proposed scaling relationship for PHA.

The hypothesis that M_L and PHA might have similar dependencies on stress state and focal depth is important because, if correct, it would infer that scaling relations between the two parameters are relatively independent of stress state and, thus, tectonic regime. There is some empirical evidence to suggest that this hypothesis may be correct. It stems from an observation by Boore (1980) that western United States' strong-motion records show a direct relationship between peak horizontal velocity and Wood-Anderson amplitude and, hence, M_L. Combining Boore's findings with McGarr's observation that both PHA and PHV are dependent on stress state and focal depth suggests that M_L is also dependent on stress state and focal depth.

A further implication of the above hypothesis is that the relationship between seismic moment and M_L should be dependent on stress state. Such a relationship has been proposed by Thatcher and Hanks (1973) from source-parameter relations developed for Southern California. Their proposed relationship,

$$\text{Log } M_o = 2.0M_L + 14.2 - \log \Delta\sigma \quad (9)$$

suggests that the relationship between seismic moment and M_L is dependent on stress drop, $\Delta\sigma$. The hypothesis is then validated if $\Delta\sigma$ can be considered dependent on stress state. McGarr uses just such a proposed dependence to give theoretical credibility to his observations by inferring a direct relationship between localized stress drop and crustal strength and between crustal strength and stress state. From considerations of tectonic stress, he suggests that crustal strength and, thus, stress drop is nearly a factor of 4 greater in compressional tectonic regimes than in extensional tectonic regimes, and that stress deop is expected to increase linearly with depth. It is interesting to note that regional variations in stress drop and moment-magnitude relationships in Southern California and northern Baja, California, have also been attributed to regional differences in tectonic stresses by Thatcher (1972) and Thatcher and Hanks (1973).

All things considered, it would seem that McGarr's results may be irrelevant with respect to the estimation of strong-motion amplitudes, at least when magnitude is used as the measure of source strength. If his hypothesis is wrong, as suggested from the analyses of Campbell (1985b), then there is no need to consider stress regime as being important. If his hypothesis is correct, then there is evidence to suggest that scaling relations between ground-motion parameters and magnitude are relatively independent of stress state. Since there is no clear empirical evidence to the contrary, any attempt to account for hypothesized differences in ground motion due to stress state appears to be unwarranted at this time. This issue is not totally resolved, however, and should be reevaluated as new results become available.

FAULT TYPE

In this study, as well as in previous studies (Campbell, 1983, 1984a), fault type has been found to be a significant factor in predicting strong ground motion. Its importance has been confirmed theoretically by studies of Anderson and Luco (1983) and Boore and Boatwright (1984). Boore and Boatwright computed average radiation coefficients for three types of faulting: a vertical strike-slip fault, a 30°-dipping dip-slip fault, and a 45°-dipping oblique-slip fault. They found that the average radiation coefficients for dipping faults were 14-28 percent higher than those for vertical strike-slip faults for distances within about a focal depth of the source. At regional distances (tens to hundreds of kilometers) the opposite was found, with dipping faults having average radiation coefficients 14-20 percent smaller than vertical strike-slip faults. These results suggest that, on average, near-source amplitudes of ground motion from dipping faults will start off higher but attenuate more rapidly than those from near-vertical faults, the transition occurring at a distance of approximately one focal depth. Indeed, such a result was observed in the analyses of the Oroville and Imperial Valley strong-motion recordings described in the preceding section.

Boore and Boatwright's results would seem to indicate that the effects of fault type should be negligible, on average, over the range of distances used in this study if differences in attenuation rate between different fault types are neglected. Yet, the current study found significantly higher ground motions for dipping faults. The most plausible explanation for these results is offered by the ground-motion simulation studies of Anderson and Luco (1983). They found that sites located directly above the rupture surface of dipping faults had the highest amplitudes of any other rupture configuration. Since the data in the present study include several such sites (such as the 1976 Gazli and 1978 Tabas recordings), it is possible that these sites are largely responsible for the observed results. These results can have serious implications for cities like Ogden, Provo, and Salt Lake City that are located directly above the Wasatch fault. For this reason, we have chosen to incorporate the uncertainty associated with the potential effect of fault type by estimating ground motions for a range of fault types (K_2=0, K_2=1 from table 5).

ANELASTIC ATTENUATION

There have been a number of attenuation studies conducted in the Basin and Range in the past with widely varying results. The closest study geographically was that conducted by King and Hays (1977). They measured ground motions from four aftershocks of the March 27, 1975 Pocatello Valley, Idaho earthquake (M_s=6.0) along a 150-km linear array extending from southern Idaho to Salt Lake City. They concluded that this region exhibits higher attenuation of 1-10 Hz pseudo-relative velocity (PSRV) response spectra than either California or Southern Nevada. This conclusion, however, is in direct contradiction to the results of Singh and Herrmann (1983).

Singh and Herrmann quantified the regional attenuation of Lg coda waves throughout the United States through the relationship

$$Q=Q_o f^n \tag{10}$$

where Q is a measure of anelastic attenuation referred to as the quality factor, Q_o is a measure of Q at 1 Hz, and f is frequency. Their maps indicate that attenuation in northcentral Utah is represented by $Q_o \approx 400$ and $n \approx 0.2$, substantially higher than attenuation in coastal California for which $Q_o < 200$ and $n \approx 0.5$.

There is similar controversy regarding regional attenuation elsewhere in the Basin and Range. For example, in the southern Great Basin, Rogers and others (1986) found $Q_o=600$ and $n=0.1$ from vertical peak-amplitude earthquake data, $Q_o=143$ and $n=0.84$ from vertical coda-amplitude earthquake data, and $Q_o=188$ and $n=1.05$ from vertical coda-amplitude nuclear-explosion data. In this same region, Singh and Herrmann (1983) found $Q_o \approx 200$ and $n \approx 0.4$, and King and Hays (1977) present attenuation rates for PSRV spectra from nuclear explosions that are similar to earthquake attenuation rates in California over a broad range of frequencies. In the northern Great Basin, Chavez and Priestley (1985) found $Q_o=125-280$ from synthetic Wood-Anderson earthquake amplitudes, Chavez and Priestley (1986) found $Q_o=130$ and $n=0.85$ from nuclear-explosion Lg amplitudes, and Singh and Herrmann (1983) found $Q_o=200-300$ and $n \approx 0.4$ from Lg-coda amplitudes.

The above results would seem to imply that there are large regional variations of attenuation characteristics throughout the Basin and Range and that the computed attenuation rates for the region are highly method and data dependent. Large regional variations in attenuation is supported by Taylor and Patton (1986) who found that structural inversions of regionalized Rayleigh-wave dispersion curves indicate significant lateral variations in the crust and upper-mantle structure of the Basin and Range and transition areas. The uncertainty in computed attenuation rates is supported by the extreme variability in attenuation characteristics derived for the same area by different investigators and different techniques.

Singh and Herrmann's maps also suggest that there is significant azimuthal variation in attenuation in northcentral Utah; though this variation is no larger than the variability associated with estimates of Q in the Basin and Range provided by various investigators. Until a definitive study of attenuation in northcentral Utah becomes available, it is necessary to estimate ground motion using a range of attenuation rates that can be assumed to reasonably bracket the true attenuation rate of the region.

In order to incorporate anelastic attenuation in the prediction of ground-motion amplitudes in northcentral Utah, the predictions were derived from equations 5 and 6, where γ is estimated from the relationship

$$\gamma=\frac{\pi f^{1-n}}{Q_o U} \qquad (11)$$

where Q_o and n are as defined in equation 10 and U is the group velocity of the particular phase amplitude used to derive Q in kilometers per second. According to Singh and Herrmann (1983), the group velocity of Lg waves is approximately equal to 3.5 km/sec.

For $n \neq 1$, γ will be different for PHA and PHV, since these parameters sample different parts of the frequency spectrum. For the present study, PHA and PHV are assumed to have fundamental frequencies on the order of 5 Hz and 1 Hz, respectively (Nuttli, 1979). In actuality, these strong-motion parameters should be magnitude and frequency dependent (Seed and others, 1969), but such a refinement seems unwarranted at this time in light of the large variability associated with Q_o and n. The various studies of attenuation in the Basin and Range cited above were used to bracket estimates of γ. The largest values were derived from the assumption of California-type attenuation, for which $\gamma=0.0059$ and $Q=152$ for both PHA and PHV. Recall that this value of γ was used to quantify anelastic attenuation for the purposes of deriving equations 5 and 6. The smallest values of γ were obtained from the study of Rogers and others (1986) for the southern Great Basin. Their nuclear-explosion, vertical coda-amplitude study resulted in estimates of $Q=1020$ and $\gamma=0.0044$ for 5-Hz waves, and their vertical peak-amplitude earthquake study resulted in estimates of $Q=600$ and $\gamma=0.0015$ for 1-Hz waves. Therefore, for the purposes of the present study, PHA was evaluated using $\gamma=0.0044$-0.0059 and PHV was evaluated using $\gamma=0.0015$-0.0059.

SITE EFFECTS

Recordings of nuclear explosions in Ogden, Provo, and Salt Lake City (Hays and others, 1978; Hays and King, 1982, 1984, this volume) show significant amplification of PSRV spectra on valley sediments as compared to rock over a wide range of frequencies. In Salt Lake City, average amplifications as high as a factor of 10 were observed in the 5-10 Hz and 1.4-5 Hz frequency bands, with even higher amplifications observed at specific frequencies. Areal contours of amplification show a rapid increase along profiles extending west from the range front out into the valley, with maximum amplification obtained within distances as little as 5-10 km. Similar results for Modified Mercalli intensities based on a study of damage in Salt Lake City from six historical earthquakes are presented by Oaks and Algermissen (this volume). The 5-10 Hz contours appear to correlate with the depth of unconsolidated deposits, obtaining maximum amplification for depths exceeding approximately 300 m (Hays and others, 1978). The 1.4-5 Hz contours appear to correlate more with the depth of low-density sedimentary rock, which obtains depths as great as 4 km along the range front valleys (Mabey, this volume).

The correlation of site amplification with subsurface geology, especially sediment depth, is well documented in the literature (Seed and others, 1976; Trifunac and Lee, 1978, 1979; Campbell, 1984a, this study; Joyner and Fumal, 1984, 1985; Rogers and others, 1984, 1985). However, simple relationships between ground-motion parameters and sediment depth appear to significantly underestimate the observed amplification of ground motion in Salt Lake valley. For example, the maximum amplification observed in Salt Lake City in the 1.4-5 Hz frequency band is larger by a factor of 2 or more than that estimated from Trifunac and Lee (1978) or Rogers and others (1985) using reasonable estimates of sediment depth in Salt Lake valley (Mabey, this volume). For low-to-intermediate frequencies this discrepancy may be due to the rather large depth-to-width ratio of the range front valleys, which have the potential to amplify these ground motions by 2-3 times over valleys having relatively small aspect ratios (Bard and Bouchon, 1985). For intermediate-to-high frequencies, this discrepancy may be the result of seismic resonance within the unconsolidated deposits.

The phenomenon of seismic resonance is well documented in the literature (Campbell, 1981a, 1983, 1984a; Chiaruttini and Siro, 1981; Faccioli, 1981; Mueller and others, 1982; Prince, 1984; Rogers and others, 1984, 1985; Anderson and others, 1986). Resonance occurs when upward propagating waves are trapped in a surface layer of relatively low velocity. For vertically incident seismic waves, the maximum amplification of ground motion at the surface ignoring free-surface effects is proportional to ρ_2V_2/ρ_1V_1, which is reached when the frequency of the incidence waves coincides with the natural frequency of the surface layer, $V_1/4H$ ($V_1$and V_2 are the propagation velocities of the surface layer and underlying layer, respectively, and H is the thickness of the surface layer). ρ_2V_2/ρ_1V_1 is referred to as the seismic impedance ratio. Theoretically, resonance can occur within a deposit of any thickness, as long as the impedance is large enough to overcome the effects of attenuation within the deposit. This condition becomes more difficult to meet as the deposits become thicker. The phenomenon is most commonly observed in relatively shallow deposits, where seismic impedances are more likely to be relatively large; for example, as in the saturated unconsolidated deposits of the range-front valleys of northcentral Utah.

A recent example of the potentially devastating effects of seismic resonance is the destruction that beset Mexico City on September 19, 1985 as a result of the M_s=8.1 Michoacan, Mexico, earthquake (Anderson and others, 1986). The earthquake occurred off the western coast of Mexico some 350 km from Mexico City. The central portion of the city lies on lakebed deposits as much as 500-m thick. These deposits, composed of soft saturated clays, were known to resonate at a natural freuqency of about 0.5 Hz from ground motions recorded from previous earthquakes. During the September 19 earthquake, 5-percent-damped absolute acceleration response spectra recorded on the lakebed deposits were again observed to peak near 0.5 Hz with amplitudes as much as a factor of 10 larger than those recorded on a nearby rock site located south of the central portion of the city. In contrast, peak horizontal accelerations and spectral accelerations at nonresonant frequencies showed amplifications of a factor of three or less. The amplification due to resonance at the surface of the lakebed deposits was large enough to literally destroy hundreds of buildings whose natural frequencies coincided with the natural frequency of these deposits. Similar phenomena have been observed in Caracas, Venezuela (Seed and Idriss, 1981) and in Japan (Kanai, 1983).

The Mexico City experience is extremely relevant to northcentral Utah. The average amplification of 5-percent-damped PSRV spectra from nuclear explosions recorded in Salt Lake valley reaches values at least as large as those observed in Mexico City for frequencies of 1.4-10 Hz (Hays and others, 1978; Hays and King, 1982, 1984, this volume). Thus, buildings having natural frequencies in this range are potentially vulnerable to damage from ground motions of even moderate strength depending on their location within the valley. High-frequency resonance is also possible along the margins of the range-front valleys where shallow unconsolidated deposits and high impedance ratios are likely to be found. Large amplifications are also possible at frequencies greater than 1.4 Hz in the deepest parts of the valleys.

It must be emphasized that the observed amplification of PSRV spectra in Ogden, Provo, and Salt Lake City are for low-amplitude, low-strain ground motions. It is possible that high-amplitude ground motions from a large nearby earthquake on the Wasatch fault would induce strains large enough to significantly reduce the amount of amplification (Prakash, 1981); though, this effect has been documented only from laboratory tests on disturbed soil samples. In any event, this effect would be restricted only to those sites located very near the source of the seismic waves. The only exception would be those sites susceptible to strong nonlinear behavior such as loose saturated sands and soft sensitive clays where large strains could be induced by relatively small amplitudes.

The spectral amplification data for Utah are not directly applicable to the estimation of peak horizontal acceleration and velocity. However, these data may be used to develop relative spectral amplification factors between Utah and California which can be used to infer relative ratios of peak ground-motion parameters between the two regions. Since the attenuation relationships developed in this study are based on California strong-motion recordings and, thus, represent California site conditions, the relative ratios of peak ground-motion parameters between the two regions can be used to approximately adjust these relationships for Utah site conditions. The technique is admittedly crude, but it will have to suffice until attenuation relationships for response spectra are developed.

Spectral amplification factors for thick (450-750 m) saturated unconsolidated sediments in Salt Lake valley (Hays and King, 1982) were used to establish site response for Utah. These factors represent an upperbound to those found for shallower deposits in Salt Lake valley as well as for those found in the Provo and Ogden areas. Spectral amplification factors developed for the Los Angeles region (Rogers and others, 1985) were used to establish site response for California. The Rogers' study developed average spectral amplification factors for three frequency bands: 0.1-0.3, 0.3-1.0, and 1.0-5.0 Hz. The data consisted of recordings of nuclear explosions and accelerograms recorded during the 1971 San Fernando earthquake. Spectral amplification factors were computed in terms of Fourier spectra ratios with a crystalline rock site in Pasadena, California, serving as the reference site. For the current study, only the intermediate- and high-frequency bands are of interest, since these roughly coincide with the assumed predominant frequencies of peak velocity and peak acceleration, respectively.

For the deeper parts of the Los Angeles basin, Rogers found average spectral amplification factors ranging from 3.6-4.5 for the intermediate-frequency band and 3.6-6.5 for the high-frequency band. Hays and King (1982) found spectral amplification factors of roughly 9.0 and 7.0 for these same frequency bands for thick unconsolidated sediments in Salt Lake valley. Thus, site amplification in Salt Lake valley appears to be roughly a factor of 2 times higher at intermediate frequencies and roughly a factor of 1.5 times higher at high frequencies as compared to the Los Angeles basin. The larger amplification in Salt Lake valley may reflect the two-dimensional resonance of the valley as suggested by Bard and Bouchon (1985), or it may simply be the result of geotechnical factors such as soft soils, a shallow water table, and large velocity gradients that lead to larger amplifications.

Based on the preceding discussion, equation 5 with $K_3=0$ was used to establish a lowerbound median estimate of PHA with respect to site effects for northcentral Utah. This estimate is believed to be appropriate for sites located in Provo and Ogden and those located on relatively shallow (<150 m) unconsolidated sediments in Salt Lake valley. This estimate is probably also appropriate for rock, at least for sources within about 50 km of the site; though the actual values could be somewhat smaller or larger than this estimate depending on such factors as the type of rock, degree of weathering, and local topography (Campbell, 1983; Tucker and others, 1984). For very shallow unconsolidated deposits near the range front, the shallow soil factor in table 5 ($K_3=1$) was used to establish an upperbound median estimate for PHA. This multiplicative factor of 1.5 was also used to account for the additional amplification expected at high frequencies at sites underlain by thick unconsolidated deposits in Salt Lake valley.

Equation 6 with $K_3=1$, $D=0$ was used to establish a lowerbound median estimate for PHV with respect to site effects. This estimate is appropriate for sites located on hard rock. The soil-depth factor in table 5 ($K_3=1$, $D \rightarrow \infty$) augmented with an additional factor of 2 to represent the additional amplification at intermediate frequencies expected at sites underlain by thick unconsolidated sediments was used to establish an upperbound median estimate for PHV.

SOURCE DIRECTIVITY

Source directivity is the focusing or defocusing of seismic energy as rupture propagates towards or away from a site. The current study has shown that rupture towards a site can lead to substantial amplification of ground motion in some cases (see tables 5 and 6). Similar effects have been observed by Boatwright and Boore (1982) and Singh (1985). The cities of Ogden, Provo, and Salt Lake City are particularly vulnerable to this phenomenon because they lie directly above the Wasatch fault. Because of their locations, they lie at relatively small azimuths with respect to the fault plane and would probably be subject to some kind of focusing for almost any rupture configuration. The only configuration that would tend to defocus ground motions would be unilateral rupture away from one of these cities.

Though potentially important, directivity was not taken into account in the prediction of ground motion in northcentral Utah for several reasons. First, there is no definitive empirical study on which to base the selection of appropriate amplification factors. Second, directivity effects have never been known to result in peak horizontal accelerations and velocities in excess of about 1.3 g and 100 cm/sec, respectively--these values being within the upperbounds estimated for an M_S=7.5 earthquake in northcentral Utah. If one is concerned about the potential effects of directivity, it is recommended that estimates of ground motion presented in the next section be multiplied by an additional factor to account for these effects. However, one should be careful not to exceed reasonable upperbound values for PHA and PHV. What constitutes reasonable upperbound limits of these parameters is a subject of some controversy. Practically speaking, median estimates that exceed the maximum near-source estimates of PHA and PHV for the M_S=7.5 earthquake presented below might be considered reasonable upper limits. A rough estimate of what may be considered near-maximum directivity effects may be obtained from the factors in tables 5 and 6. These factors suggest that amplification due to directivity may be as large as a factor of 1.7 for PHA and 2.7 for PHV.

GROUND MOTION ESTIMATES

Ground-motion attenuation curves for northcentral Utah are presented in figures 11 and 12. The range of values reflect variability associated with fault type, anelastic attenuation, and site response as discussed in the preceding sections. This variability can only be reduced with regional studies designed to better define and quantity these effects. Until such studies become available, it is believed that a range of estimates is the only reasonable means of quantifying this variability.

The development of attenuation relationships for PSRV response spectra is currently in progress. Until these relationships become available, it is recommended that response spectra be estimated from estimates of peak acceleration and velocity using the procedures proposed by Newmark and Hall (1983). This method is preferred over the use of attenuation relationships available in the literature (Joyner and Fumal, 1985) because regional uncertainties in fault type, anelastic attenuation, and site effects included in estimates of PHA and PHV are readily incorporated in the spectra.

As an example of the procedure, figure 13 displays a median estimate of a 5-percent-damped PSRV spectrum for a site located approximately 5 km from the zone of seismogenic rupture of an M_S=7.5 earthquake. This scenario probably represents the largest ground motion that can be expected anywhere in Utah. It is roughly equivalent to the level of ground motion that might be expected in Ogden, Provo, or Salt Lake City as a result of the largest earthquake that has been geologically inferred on the Wasatch fault (Swann and others, 1980).

FIGURE 11.--NEAR HERE

FIGURE 12.--NEAR HERE

FIGURE 11.--Estimates of peak horizontal acceleration for northcentral Utah. The shaded zone represents the range in median estimates of acceleration due to variability in fault type, site amplification, and anelastic attenuation (see text).

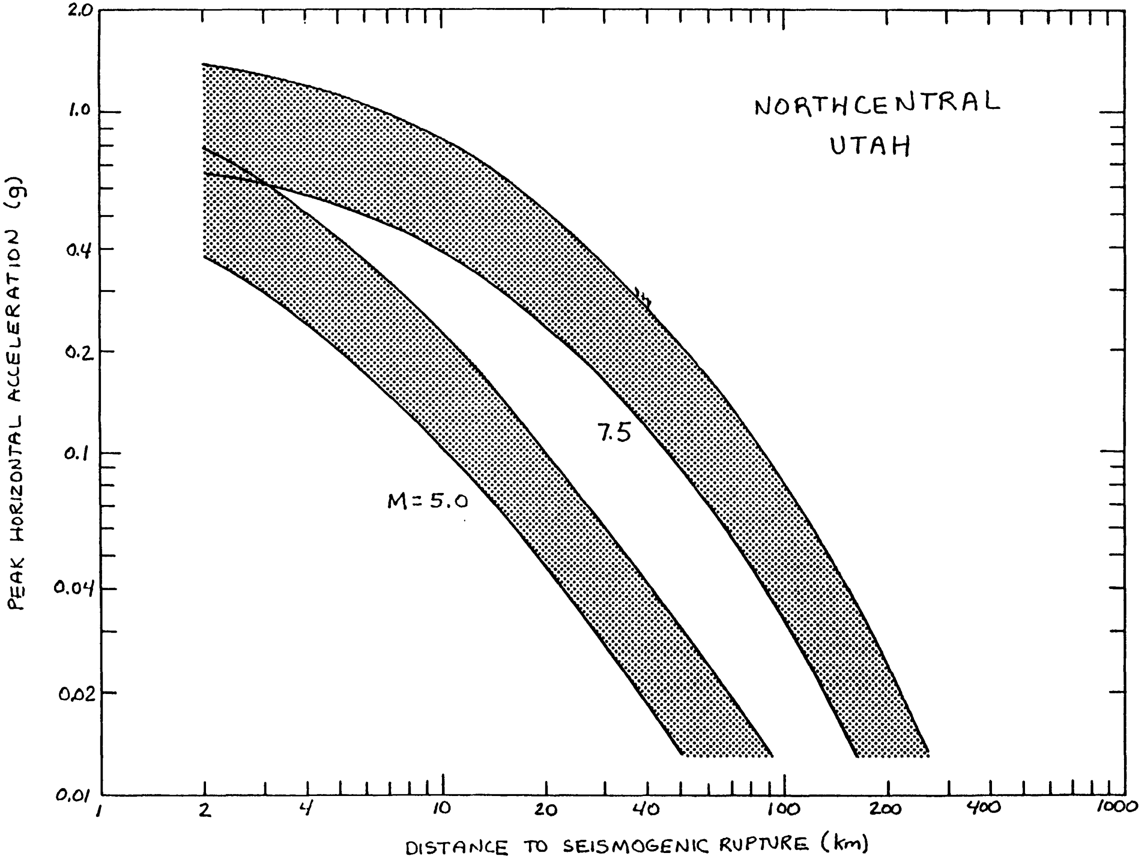

FIGURE 12.--Estimates of peak horizontal velocity for northcentral Utah. The shaded zone represents the range in median estimates of velocity due to variability in fault type, site amplification, and anelastic attenuation (see text).

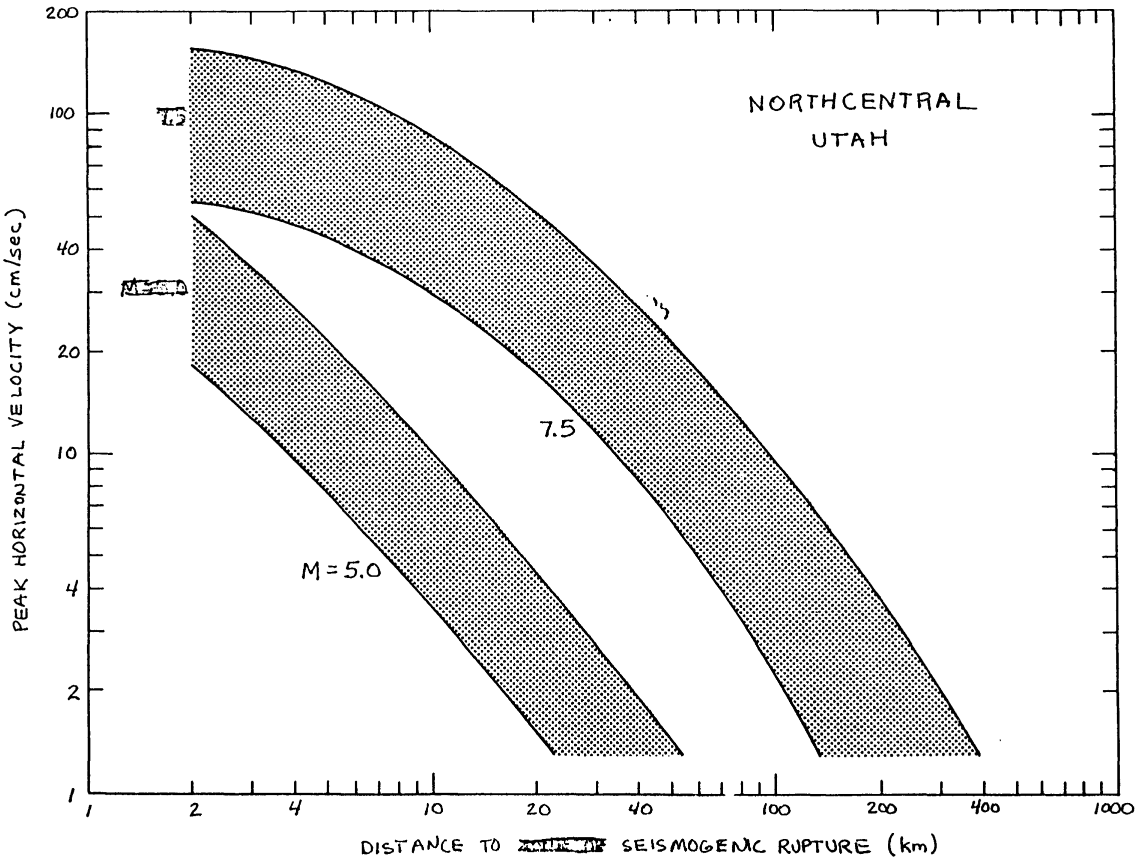

Figures 11-13 present median estimates of ground motion. If some other percentile is desired, then it should be estimated from the expression (Draper and Smith, 1981)

$$y_\alpha = \hat{y} + t_{\alpha,\nu}\left[\frac{\sigma^2}{n_o} + (\sigma_{\hat{y}})^2\right]^{1/2} \tag{11}$$

where y represents ln PHA or ln PHV, y_α is the α-percentile value of y, $\hat{y}$ is the median or predicted value of y, $t_{\alpha,\nu}$ is the t-statistic associated with a cumulative probability α and $\nu=n-p-1$ degrees of freedom, n is the number of observations used in the analysis, p is the number of coefficients in the model, n_o is the number of future observations (usually 1), σ is the standard error of regression, and $\sigma_{\hat{y}}$ is the standard deviation of $\hat{y}$.

FIGURE 13.--NEAR HERE

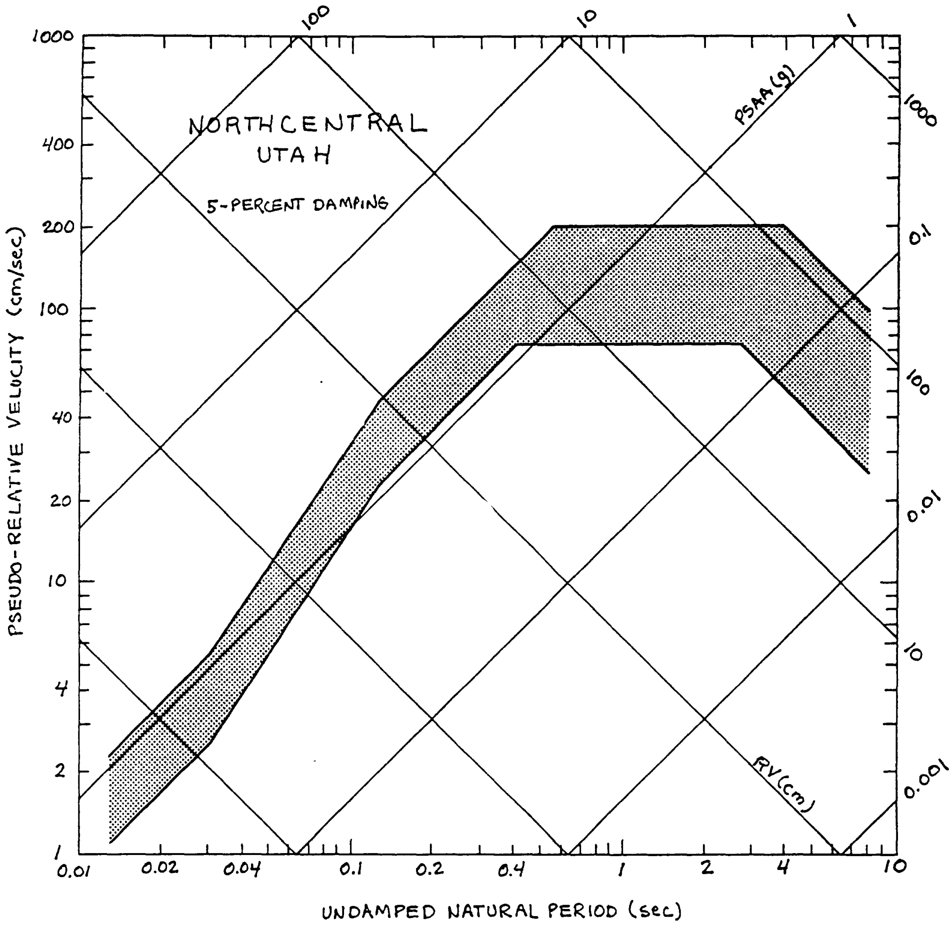

FIGURE 13.--An estimate of a 5-percent-damped PSRV spectrum for a site in northcentral Utah located approximately 5 km from the zone of seismogenic rupture of an M_s=7.5 earthquake. The shaded zone represents the range in the median estimate of PSRV due to variability in fault type and site amplification (see text).

For large ν, $t_{\alpha,\nu}$ can be replaced by z_{α}, the standard normal variable, and because one is usually interested in the prediction of a single future observation, $n_0=1$. Thus, the only quantity that is not known is $\sigma_{\hat{y}}$, which because of the nonlinear form of equations 5 and 6 can only be estimated by Monte Carlo simulation. This is beyond the scope of this study. For estimates near the centroid of the data (i.e., near the middle of the scattergrams in figure 1), $\sigma_{\hat{y}}$ is very small and can be neglected. In this case equation 11 becomes

$$y_{\alpha}=\hat{y}+z_{\alpha}\sigma \tag{12}$$

For estimates involving an extrapolation of the model, $\sigma_{\hat{y}}$ cannot be neglected and equation 12 will substantially underestimate the value of y_{α} for $\alpha>0.5$.

SUMMARY

In this study, empirical attenuation relationships for horizontal components of peak acceleration and peak velocity have been developed using as many as 134 near-source strong-motion recordings. These records were obtained within 30-50 km of 21 worldwide earthquakes whose magnitudes range from 5.0-7.7. All recordings come from sites located on relatively low-velocity unconsolidated deposits, thus avoiding limitations associated with the small number of available rock recordings. These attenuation relationships provide models for predicting peak acceleration and peak velocity from a suite of parameters characterizing source, propagation, and site effects--the most important being earthquake magnitude and distance to the zone of seismogenic rupture. Empirical analyses indicated that factors such as fault type, building size, building embedment, and shallow soil influence the prediction of peak acceleration, whereas factors such as fault type, building size, and depth of sediments influence peak velocity.

Two types of attenuation relationships were developed in the study: an unconstrained relationship, whose coefficients were all derived directly from regression analyses, and a constrained relationship, whose anelastic attenuation term was constrained to provide a relationship that could be reliably extrapolated beyond the near-source limit of the strong-motion data. Both types of relationship provide virtually identical estimates of ground motion within about 30-50 km of the source, but only the constrained relationship provides reliable estimates of ground motion to distances of several hundred kilometers. A significant advantage of the constrained relationship is its ability to provide estimates of ground motion in regions whose attenuation characteristics are different from those of California.

A striking feature of all four attenuation relationships developed in this study is the empirical constraint that peak ground-motion amplitudes be independent of magnitude at the earthquake source. This characteristic, referred to as saturation, has been proposed by many geophysicists as a fundamental property of the earthquake source. Its empirical basis, however, has been the subject of great controversy in the past (Campbell, 1985a).

The constrained attenuation relationships developed in this study were used to provide median estimates of strong ground motion for northcentral Utah. A range of estimates was provided to reflect uncertainties in the state of knowledge and regional variability associated with the potential effects of fault type, anelastic attenuation, and site effects. A range of values for anelastic attenuation believed to be appropriate for the Basin and Range were taken from the literature. Regional studies of site effects were used to modify the estimates for local site conditions. The range of estimates for a given value of magnitude and distance was found to be quite large, suggesting that regional studies of ground motion should be undertaken to better define the effects of fault type and anelastic attenuation.

A method developed by Newmark and Hall (1982) for estimating response spectra from estimates of peak ground-motion values was used to provide a median 5-percent-damped PSRV spectrum for an M_S=7.5 earthquake hypothesized to occur on the Wasatch fault approximately 5 km from a site located within one of the range front valleys. This scenario leads to what may be the largest ground motion that can be expected to occur in the cities of Ogden, Provo, and Salt Lake City.

REFERENCES

Anderson, J.G., Bodin, P., Brune, J.N., Prince, J., Singh, S.K., Quaas, R., and Onate, M., 1986, Strong ground motion from the Michoacan, Mexico, earthquake: Science, v. 233, p. 1043-1049.

Anderson, J.G., and Luco, J.E., 1983, Parametric study of near-field ground motions for oblique-slip and dip-slip dislocation models: Seismological Society of America Bulletin, v. 73, p. 45-57.

Bakun, W.H., 1984, Seismic moments, local magnitudes, and coda-duration magnitudes for earthquakes in central California: Seismological Society of America Bulletin, v. 74, p. 439-458.

Bard, P.-Y., and Bouchon, M., 1985, The two-dimensional resonance of sediment-filled valleys: Seismological Society of America Bulletin, v. 75, p. 519-541.

Boatwright, J.A., and Boore, D.M., 1982, Analysis of the ground accelerations radiated by the 1980 Livermore Valley earthquakes for directivity and dynamic source characteristics: Seismological Society of America Bulletin, v. 72, p. 1843-1865.

Boore, D.M., 1980, On the attenuation of peak velocity: Proceedings, Seventh World Conference on Earthquake Engineering, Instanbul, Turkey, 1980, v. II, p. 577-584.

Boore, D.M., and Boatwright, J.A., 1984, Average body-wave radiation coefficients: Seismological Society of America Bulletin, v. 74, p. 1615-1621.

Brillinger, D.R., and Preisler, H.K., 1984, An exploratory analysis of the Joyner-Boore attenuation data: Seismological Society of America Bulletin, v. 74, p. 1441-1450.

Campbell, K.W., 1981a, Near-source attenuation of peak horizontal acceleration: Seismological Society of America Bulletin, v. 71, p. 2039-2070.

______1981b, A ground motion model for the Central United States based on near-source acceleration data: Proceedings, Conference on Earthquakes and Earthquake Engineering: The Eastern U.S., Knoxville, Tenn., 1981, v. 1, p. 213-232.

______1982a, Near-source scaling characteristics of peak horizontal acceleration for moderate-to-large earthquakes, _in_ Proceedings, Conference XVI--A workshop on the dynamic characteristics of faulting inferred from recordings of strong ground motion, Incline Village, Calif., 1981: U.S. Geological Survey Open-File Report 82-591, v. 1, p. 120-184.

______1982b, A preliminary methodology for the regional zonation of peak acceleration: Proceedings, Third International Conference on Earthquake Microzonation, Seattle, Wash., 1982, v. I, p. 365-376.

______1983, The effects of site characteristics on near-source recordings of strong ground motion, _in_ Proceedings, Conference XXII--A workshop on site specific effects of soil and rock on ground motion and their implications for earthquake-resistant design, Santa Fe, N.M., 1983: U.S. Geological Survey Open-File Report 83-845, p. 280-309.

______1984a, Near-source attenuation of strong ground motion for moderate to large earthquakes--an update and suggested application to the Wasatch fault zone of north-central Utah, _in_ Proceedings, Conference XXVI--A workshop on the evaluation of regional and urban earthquake hazards and risk in Utah, Salt Lake City, Utah, 1984: U.S. Geological Survey Open-File Report 84-763, p. 483-499.

______1984b, Observed structural modification of recorded strong ground motion, in Critical aspects of earthquake ground motion potential: Applied Technology Council Report ATC-10-1, Palo Alto, Calif., p. 43-52.

______1985a, Strong motion attenuation relations: a ten-year perspective: Earthquake Spectra, v. 1, p. 759-804.

______1985b, Near-source estimation of strong ground motion for the eastern United States: Second-Quarter Progress Report to the U.S. Nuclear Regulatory Commission, Washington, D.C.

______1986, Empirical prediction of free-field ground motion using statistical regression models, in Proceedings, Workshop on soil-structure interaction, Bethesda, Maryland, 1986: Brookhaven National Laboratory, 30 p. [in press].

Chavez, D.E., and Priestley, K.F., 1985, M_L observations in the Great Basin and M_O versus M_L relationships for the 1980 Mammoth Lakes, California, earthquake sequence: Seismological Society of America Bulletin, v. 75, p. 1583-1598.

______1986, Attenuation of regional crustal phases in the Great Basin [abs.]: Earthquake Notes, v. 57, no. 1, p. 9.

Chiaruttini, C., and Siro, L., 1981, The correlation of peak ground horizontal acceleration with magnitude, distance, and seismic intensity for Friuli and Ancona, Italy, and the Alpide Belt: Seismological Society of America Bulletin, v. 71, p. 1993-2009.

Cranswick, E., Wetmiller, R., and Boatwright, J., 1985, High-frequency observations and source parameters of microearthquakes recorded at hard-rock sites: Seismological Society of America Bulletin, v. 75, p. 1535-1567.

Draper, N.R., and Smith, H., 1981, Applied regression analysis, second edition: New York, John Wiley and Sons.

Esteva, L., 1970, Seismic risk and seismic design decisions, in Hanson, R.J., ed., Seismic design for nuclear power plants: Cambridge, Mass., M.I.T. Press, p. 142-182.

Faccioli, E., 1981, The use of RMS acceleration as a measure of soil amplification in strong earthquakes, in Erguray, O., and Erdik, M., eds., State-of-the-art in earthquake engineering, 1981: Ankara, Turkey, Turkish National Committee on Earthquake Engineering, p. 98-105.

Fenneman, N.M., 1946, Physiographic divisions of the United States: U.S. Geological Survey Map, 1:7 million.

Gallant, A.R., 1975, Nonlinear regression: The American Statistician, v. 29, p. 73-81.

Hadley, D.M., Helmberger, D.V., and Orcutt, J.A., 1982, Peak acceleration scaling studies: Seismological Society of America Bulletin, v. 72, p. 959-979.

Hanks, T.C., and Boore, D.M., 1984, Moment-magnitude relations in theory and practice: Journal of Geophysical Research, v. 89, p. 6229-6235.

Hanks, T.C., and Kanamori, H., 1979, A moment magnitude scale: Journal of Geophysical Research, v. 84, p. 2348-2350.

Hays, W.W., Algermissen, S.T., Miller, R.D., and King, K.W., 1978, Preliminary ground response maps for the Salt Lake City area: Proceedings, Second International Earthquake Microzonation Conference, San Francisco, Calif., 1978, v. 2, p. 497-508.

Hays, W.W., and King, K.W., 1982, Zoning of the earthquake ground-shaking hazard along the Wasatch fault zone, Utah: Proceedings, Third International Earthquake Microzonation Conference, Seattle, Wash., 1982, v. III, p. 1307-1318.

______1984, The ground-shaking hazard along the Wasatch fault zone, Utah, in Proceedings, Conference XXVI--A workshop on the evaluation of regional and urban earthquake hazards and risk in Utah, Salt Lake City, Utah, 1984: U.S. Geological Survey Open-File Report 84-763, p. 133-147.

Johnson, R.A., and Wichern, D.W., 1982, Applied multivariate statistical analysis: Englewood Cliffs, New Jersey, Prentice-Hall, Inc.

Joyner, W.B., and Boore, D.M., 1981, Peak horizontal acceleration and velocity from strong-motion records including records from the 1979 Imperial Valley, California, earthquake: Seismological Society of America Bulletin, v. 71, p. 2011-2038.

Joyner, W.B., and Fumal, T.E., 1984, Use of measured shear-wave velocity for predicting geologic site effects on strong ground motion: Proceedings, Eighth World Conference on Earthquake Engineering, San Francisco, Calif., 1984, v. II, p. 777-784.

______1985, Predictive mapping of earthquake ground motion, in Ziony, J.I., ed., Evaluating earthquake hazards in the Los Angeles region--an earth science perspective: U.S. Geological Survey Professional Paper 1360, p. 203-220.

Kanai, K., 1983, Engineering seismology: Tokyo, Japan, University of Tokyo Press, 251 p.

King, K.W., and Hays, W.W., 1977, Comparison of seismic attenuation in northern Utah with attenuation in four other regions of the western United States: Seismological Society of America Bulletin, v. 67, p. 781-792.

McGarr, A., 1984, Scaling of ground motion parameters, state of stress, and focal depth: Journal of Geophysical Research, v. 89, p. 6969-6979.

More, J.J., Garbow, B.S., and Hillstrom, K.E., 1980, User guide for MINPACK-1: Argonne, Illinois, Argonne National Laboratory Report ANL-80-74.

Mueller, C.S., Boore, D.M., and Porcella, R.L., 1982, Detailed study of site amplification at El Centro strong-motion array station no. 6: Proceedings, Third International Earthquake Microzonation Conference, Seattle, Wash., 1982, v. I, p. 413-424.

Newmark, N.M., and Hall, W.J., 1982, Earthquake spectra and design: Berkeley, Calif., Earthquake Engineering Research Institute Monograph.

Nuttli, O.W., 1979, The relation of sustained maximum ground acceleration and velocity to earthquake intensity and magnitude, <u>in</u> State-of-the art for assessing earthquake hazards in the United States: Vicksburg, Miss., U.S. Army Engineer Waterways Experiment Station Miscellaneous Paper S-73-1, Report 16.

Prakash, S., 1981, Soil dynamics: New York, McGraw-Hill, 426 p.

Prince, J., 1984, Influence of the number of response maxima on the observed seismic behavior of structures, <u>in</u> Critical aspects of earthquake ground motion and building damage potential: Palo Alto, Calif., Applied Technology Council Report ATC-10-1, p. 57-66.

Richter, C.F., 1958, Elementary seismology: San Francisco, Calif., W.H. Freeman and Company.

Rogers, A.M., Tinsley, J.C., and Borcherdt, R.D., 1984, Geographic variation in ground shaking as a function of changes in near-surface properties and geologic structure near Los Angeles, California: Proceedings, Eighth World Conference on Earthquake Engineering, San Francisco, Calif., 1984, v. II, p. 737-744.

______1985, Predicting relative ground response, in Ziony, J.E., ed., Evaluating earthquake hazards in the Los Angeles region--an earth science perspective: U.S. Geological Survey Professional Paper 1360, p. 221-247.

Rogers, A.M., Harmsen, S.C., Herrmann, R.B., Meremonte, M.E., 1986, A study of ground motion attenuation in the southern Great Basin, Nevada-California, using several techniques for estimates of Q_s, log A_o, and coda Q: Journal of Geophysical Research [in press].

Seed, H.B., and Idriss, I.M., 1982, Ground motions and soil liquefaction during earthquakes: Berkeley, Calif., Earthquake Engineering Research Institute Monograph, 134 p.

Seed, H.B., Idriss, I.M., and Keifer, F.W., 1969, Characteristics of rock motions during earthquakes: Journal of the Soil Mechanics and Foundations Division, v. 95, p. 1199-1218.

Seed, H.B., Ugas, C., and Lysmer, J., 1976, Site-dependent spectra for earthquake-resistant design: Seismological Society of America Bulletin, v. 66, p. 221-243.

Shakal, A.F., and Bernreuter, D.L., 1981, Empirical analysis of near-source ground motion: Washington, D.C., U.S. Nuclear Regulatory Commission Report NUREG/CR-2095.

Singh, J.P., 1985, Earthquake ground motions: implications for designing structures and reconciling structural damage: Earthquake Spectra, v. 1, p. 239-270.

Singh, S., Herrmann, R.B., 1983, Regionalization of crustal Q in the continental United States: Journal of Geophysical Research, v. 88, p. 527-538.

Swann, F.H., Schwartz, D.P., and Cluff, L.S., 1980, Recurrence of moderate-to-large magnitude earthquakes produced by surface faulting on the Wasatch fault zone: Seismological Society of America Bulletin, v. 70, p. 1431-1478.

Taylor, S.R., and Patton, H.J., 1986, Shear-wave velocity structure from regionalized surface-wave dispersion in the Basin and Range: Geophysical Research Letters, v. 13, p. 30-33.

Thatcher, W., 1972, Regional variations of seismic source parameters in the northern Baja, California, area: Journal of Geophysical Research, v. 77, p. 1549-1565.

Thatcher, W., and Hanks, T.C., 1973, Source parameters of Southern California earthquakes: Journal of Geophysical Research, v. 78, p. 8547-8576.

Trifunac, M.D., and Lee, V.W., 1978, Dependence of the Fourier amplitude spectra of strong motion acceleration on the depth of sedimentary deposits: Los Angeles, Calif., University of Southern California Department of Civil Engineering Report CE78-14.

______1979, Dependence of pseudo-relative velocity spectra of strong motion acceleration on the depth of sedimentary deposits: Los Angeles, Calif., University of Southern California Department of Civil Engineering Report CE79-02.

Tucker, B.E., King, J.L., Hatzfeld, D., and Nersesov, I.L., 1984, Observations of hard rock site effects: Seismological Society of America Bulletin, v. 74, p. 121-136.

Tukey, J.W., 1977, Exploratory data analysis: Reading, Mass., Addison-Wesley Publishing Company.

Zoback, M.L., and Zoback, M.D., 1981, State of stress in the conterminous United States: Journal of Geophysical Research, v. 86, p. 4981-4998.

PROBABILISTIC ANALYSIS OF EARTHQUAKE GROUND SHAKING HAZARD ALONG THE WASATCH FRONT, UTAH

by

R. R. Youngs, F. H. Swan, and M. S. Power
Geomatrix Consultants, Inc.
San Francisco, California

D. P. Schwartz
U.S. Geological Survey
Menlo Park, California

R. K. Green
Woodward Clyde Consultants
Walnut Creek, California

ABSTRACT

This paper presents a probabilistic assessment of the ground shaking hazard along the Wasatch Front urban corridor utilizing the extensive geological and seismological data base that has been developed for the region. Using a logic tree methodology, the approach formally incorporates uncertainty in earthquake source geometry and fault segmentation, maximum earthquake magnitude, earthquake recurrence rate, ground motion attenuation, and other parameters and model components. The analysis results are presented in terms of maps showing contours of peak ground acceleration on soil site conditions for probabilities of exceedance of 10 percent in 10 years, 10 percent in 50 years, and 10 percent in 250 years. The major contributions to uncertainty in the hazard are uncertainties in selecting the appropriate models for earthquake recurrence on the faults and ground motion attenuation. By repeating the analyses using rock site attenuation relationships, it is concluded that rock site peak accelerations can be obtained by multiplying the soil site accelerations by a factor of 1.1 for a probability of exceedance of 10 percent in 10 years and by a factor of 1.2 for probabilities of exceedance of 10 percent in 50 years and 10 percent in 250 years.

Response spectral shapes for soil and rock site conditions are presented for the probability of exceedance levels used in mapping peak ground acceleration. Absolute response spectra can be obtained by multiplying these spectral shapes by the corresponding values of peak ground acceleration. A preliminary estimate is presented for the additional spectral amplification that might occur in areas of soft lake deposits.

INTRODUCTION

The urban corridor along the Wasatch Front, which includes more than 85 percent of Utah's population, is considered one of the highest risk areas within the conterminous United States with respect to earthquake hazards. The seismic hazards of this region are related primarily to the presence of the Wasatch fault zone, which extends for more than 370 km along the western front of the Wasatch Range. Paleoseismicity studies (Swan and others, 1980; Hanson and others, 1981; Schwartz and others, 1984; Schwartz and Coppersmith, 1984) have demonstrated that the Wasatch fault zone has repeatedly produced large magnitude earthquakes throughout the Holocene and that it is likely to be the source of future damaging earthquakes. In addition, the region may be affected by earthquakes originating on other faults with Quaternary movement, including the Oquirrh Mountains fault zone, the East Cache fault, the West Valley fault, the Hansel Valley fault, and the East Bear Lake fault. As indicated in Figure 1, Logan, Brigham City, Ogden, Salt Lake City, and Provo, the largest cities in Utah, all lie along active faults capable of producing damaging earthquakes.

During the past two decades geological studies have been conducted for the specific purpose of identifying and evaluating the potential earthquake hazards along the Wasatch Front (Utah Geological Association, 1972; U.S. Geological Survey, 1980, 1984). Extensive telemetered seismic arrays have been operating to assess the earthquake hazard along the Intermountain Seismic Belt since 1974. Prior to that, instrumental monitoring of the Wasatch Front only dates back to 1962 (Arabasz and others, 1980).

In this study, a quantitative assessment is made of the ground shaking hazard along the Wasatch Front urban corridor (Figure 1) utilizing the the extensive geological and seismological data base that has been assembled for the region. The ground shaking hazard is related to: 1) the location and geometry of the earthquake sources relative to the urban areas; 2) the recurrence of earthquakes of various magnitudes on these sources; and 3) the attenuation of ground motions from the sources to various locations within the study area. A probabilistic approach is used to formally incorporate the uncertainty in modeling the regional seismicity and

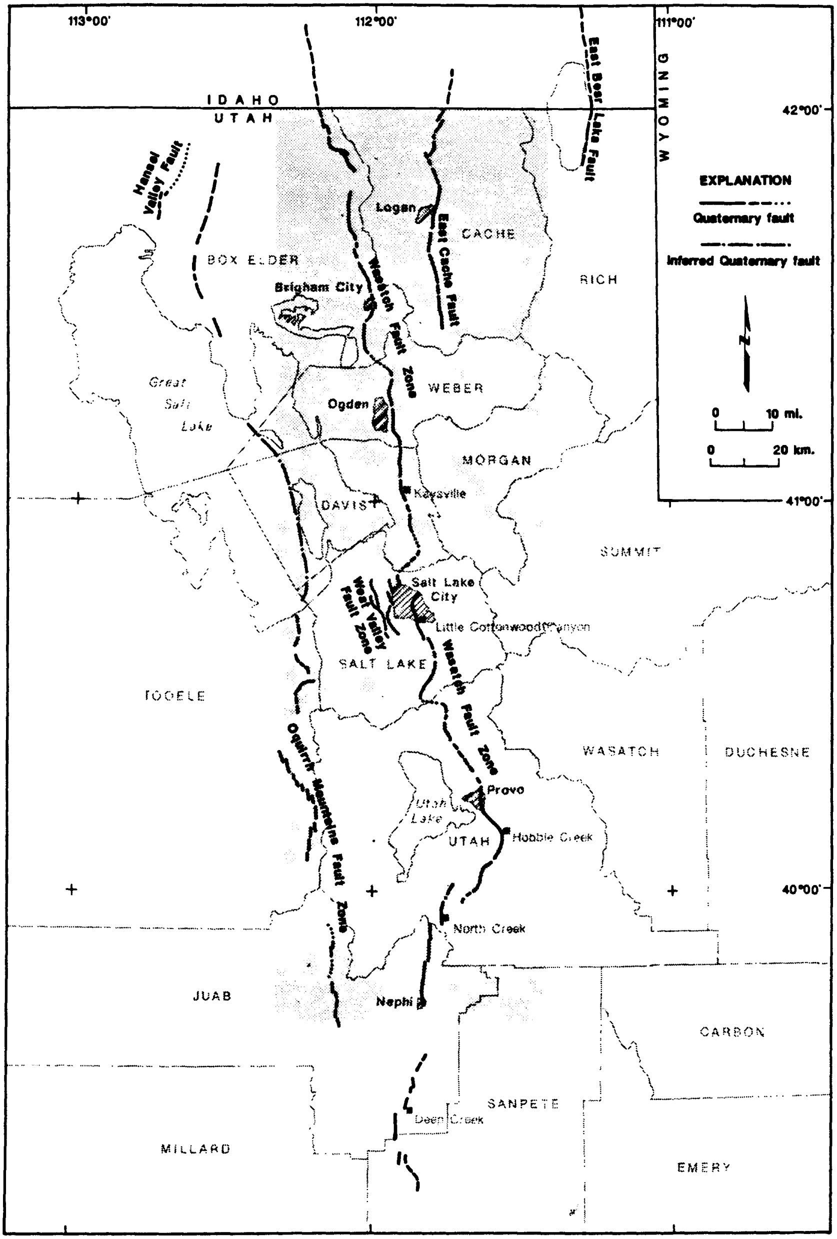

Figure 1 - Map showing location of the study area for ground shaking hazard mapping (shaded region) and the Quaternary faults modeled in the seismic hazard analysis.

attenuation characteristics into the hazard assessment. In this approach, distributions of values for source geometry, maximum earthquake magnitude, earthquake recurrence rate, characteristics of ground motion attenuation, and other parameters that are not known with certainty are selected to reflect the best understanding of the available data. The seismic hazard analysis integrates these data on source characteristics and ground motion attenuation to evaluate the probability of exceeding specified levels of ground motion within designated time intervals. The ground motion parameters addressed include both horizontal peak acceleration and horizontal spectral accelerations on soil and rock site conditions. A principal product of the study consists of maps showing the spatial variation of peak horizontal acceleration levels for three selected probability of exceedance levels. The uncertainty in the estimated hazard is analyzed and discussed with respect to the uncertainty in the various input parameters and sensitivity to models incorporated in the analysis. These analyses provide a means of evaluating the impact of new information on the results presented in this paper.

APPROACH

In probabilistic terms seismic hazard is defined as the likelihood that various levels of ground motion will be exceeded at a site during a specified time period. It is commonly assumed that the occurrence of individual main shocks can be represented as a Poisson process. Following the approach developed by Cornell (1968), the probability that at a given site a ground motion parameter, Z, will exceed a specified level, z, during a specified time period, t, is given by the expression:

$$P(Z>z|t) = 1 - e^{-\nu(z)\cdot t} \leq \nu(z)\cdot t \qquad (1)$$

where $\nu(z)$ is the average frequency during time period t at which the level of ground motion parameter Z exceeds z at the site resulting from earthquakes on all sources in the region. The inequality at the right of Equation 1 is valid regardless of the appropriate probability model for earthquake occurrence, and $\nu(z)\cdot t$ provides an accurate and slightly conservative estimate of the hazard for probabilities of 0.1 or less provided $\nu(z)$ is the appropriate value for the time period of interest.

The frequency of exceedance, $\nu(z)$, is a function of the uncertainty in the time, size and location of future earthquakes and uncertainty in the level of ground motions they may produce at the site. It is computed by the expression

$$\nu(z) = \sum_n \alpha_n(m^o) \int_{m^o}^{m^u} \int_{r=0}^{r=\infty} f(m)\cdot f(r)\cdot P(Z>z|m,r)\ dr\ dm \qquad (2)$$

where $\alpha_n(m^o)$ is the frequency of earthquakes on source n above a minimum magnitude of engineering significance, m^o; $f(m)$ is the probability density function for event size between m^o and a maximum event size for the source, m^u; $f(r)$ is the probability density function for distance to the earthquake rupture; and $P(Z>z|m,r)$ is the probability that, given a magnitude m earthquake at a distance r from the site, the ground motion exceeds level z.

The probability functions contained in Equations 1 and 2 represent the uncertainties inherent in the natural phenomena of earthquake generation and seismic wave propagation. For the north-central Utah region (as is usually the case in any region) one is faced with considerable uncertainty in selecting the appropriate models and model parameters required to apply Equation 2 arising from limited data and/or alternative interpretations of the available data. The approach used in this study explicitly incorporates these additional uncertainties into the analysis to assess their impact on the estimate of the expected level of seismic hazard as well as the uncertainty in that estimate.

The uncertainty in modeling the natural phenomena is incorporated into the hazard analysis through the use of logic trees. The logic tree formulation for seismic hazard analysis (Power and others, 1981; Kulkarni and others, 1984; Youngs and others, 1985; Coppersmith and Youngs, 1986; EPRI, 1987) involves specifying discrete alternatives for states of nature or parameter values and specifying the relative likelihood that each discrete alternative is the correct value or state of the input parameter. The relative likelihoods of the different parameter values are typically based on subjective judgment because the available data are too limited to allow an objective statistical analysis.

Figure 2 displays the logic tree representing the seismic hazard model developed for this study. The logic tree is laid out to provide a logical progression from general aspects/hypotheses regarding the characteristics of seismicity and seismic wave propagation in the region to specific input parameters for individual faults and fault segments. The rationale for developing the various levels of the logic tree is discussed below. The bases for selecting the parameter values and assigning relative weights are presented in the following sections of this paper.

The first node of the logic tree represents the uncertainty in selecting the appropriate strong ground motion attenuation relationship. Attenuation was placed first in the tree because it is felt that a single relationship (whichever relationship may be "correct") is applicable to all earthquake sources in the region. Alternative recently developed attenuation relationships are used in the analysis. As indicated in Figure 2, three attenuation relationships developed for soil site conditions were used. Four attenuation relationships were used to evaluate peak accelerations for rock site conditions. Response spectral values were evaluated using two published relationships for soil sites and two for rock sites.

The second node of the logic tree represents the uncertainty in selecting the appropriate form of the recurrence relationship for modeling the distribution of earthquake size for events occurring on faults. While the exponential model has been commonly used in hazard analyses, it was derived on the basis of large regional seismicity catalogs (Gutenberg and Richter, 1954). Recent studies (e.g. Schwartz and Coppersmith, 1984) suggest that the size distribution for individual faults and fault segments may be better represented by a "characteristic" model that implies relatively more frequent large events than intermediate size events. In modeling the magnitude-frequency distribution for the regional background seismicity only the exponential model is assumed to be applicable.

At this point the logic tree is expanded into subtrees, one for each of the seismic sources included in the analysis to model the additive hazard from multiple sources. Seven seismic sources were included in the analysis. Six sources consist for mapped fault zones having Quaternary displacement

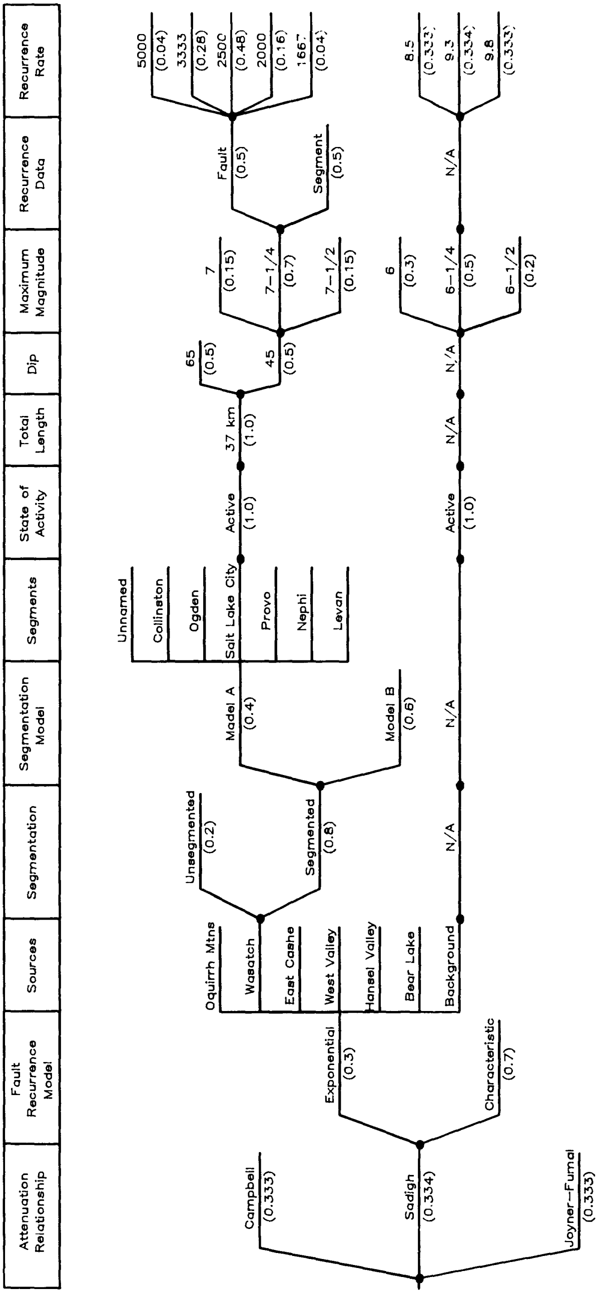

Figure 2 - Hazard model logic tree used for evaluating seismic hazards in the study. Parameter values are shown above the branches and assessed probabilities are shown in parentheses below the branches. (Note not all branches for all sources are shown.)

that have the potential of generating large magnitude events (Figure 1). In addition, a regional background zone was included in the analysis to model possible (random) locations for small to moderate magnitude events, reflecting the diffuse zone of seismic activity observed in the region (Figures 3 and 4). The historical seismicity and its implications to modeling earthquake occurrence is discussed in following sections. To the right of this node of the logic tree each source is considered to be acting independently, and the distribution in the total computed hazard is obtained by convolving the independent distributions obtained for each seismic source.

The first two nodes of the logic tree for each fault represent the uncertainty in whether or not a fault zone is segmented and, if segmented, what is the appropriate segmentation model. Segmentation affects both the assessment of maximum earthquake magnitude and the distribution of seismicity along the fault zone. If the fault is segmented the logic tree is again expanded into subtrees, one for each segment identified for a particular segmentation model. As was the case for the expansion at the seismic source level, each segment is considered to be acting independently and the distribution in the computed hazard for the fault as a whole is obtained by convolving the independent distributions obtained for each segment.

The remaining nodes of the logic tree for faults address specific parameters used in the hazard computation: whether or not the fault or fault segment is currently active, affecting whether or not it contributes to the hazard; uncertainty in the fault geometry in terms of total fault length and fault plane dip, affecting the distribution of distance to fault rupture, the assessment of maximum magnitude, and earthquake recurrence rate based on seismic moment rate; uncertainty in maximum magnitude; and uncertainty in estimating earthquake recurrence. The development of the conditional maximum magnitude distribution incorporates additional variables that are not shown in the overall logic tree of Figure 2. This is discussed further in the Seismic Source Characterization section of this paper.

The logic tree branches shown in Figure 2 are representative of the type of input parameters developed at each level for the seven seismic sources. As shown, many of the levels of the logic tree are not applicable to the background zone, and only uncertainty in maximum magnitude and recurrence rate (shown in Figure 2 as the return period for a magnitude 5 or greater event within the zone) are incorporated.

REGIONAL SEISMICITY

Earthquake Catalog

A comprehensive earthquake catalog for the State of Utah has been developed by researchers at the University of Utah Seismograph Stations. Their published catalog (Richins, 1979) together with recent updates through March 1986 (E. Brown, personal communication) were utilized in this study. The catalog can be divided into two primary periods of reporting, pre-instrumental and instrumental. The pre-instrumental catalog covers the time period from 1850, when the first newspaper was published in Utah, to July, 1962, when the first state-wide seismograph network was established. The assigned location for most events occurring prior to 1950 is that of the population center where the event was most strongly felt and the location error is estimated to be 25 to 50 km (Richins, 1979). Nearly all of the magnitudes reported in the catalog for events occurring before July 1962 were obtained from epicentral intensity using the relationship $M_L = 2/3I_o + 1$ developed by Gutenberg and Richter (1956). Earthquake recurrence estimates for the study region were found to be relatively insensitive to the use of other intensity-magnitude conversions. Figure 3 displays the locations of events in the pre-instrumental catalog for the region longitude 110.5°W to 113.5°W, latitude 39°N to 42.5°N.

The instrumental catalog used extends from July 1, 1962 to March 31, 1986. Events occurring in the period July, 1962 to October, 1974, were located with the focal depth fixed at 7.0 km and the size of the horizontal error elipsoid is 10 km or greater for most of the events (Richins, 1979). From 1974 to 1978 a statewide telemetered network was deployed, resulting in improved seismic monitoring. The size of the horizontal error elipsoid for events occurring after 1974 is generally less than 5 km (Richins, 1979).

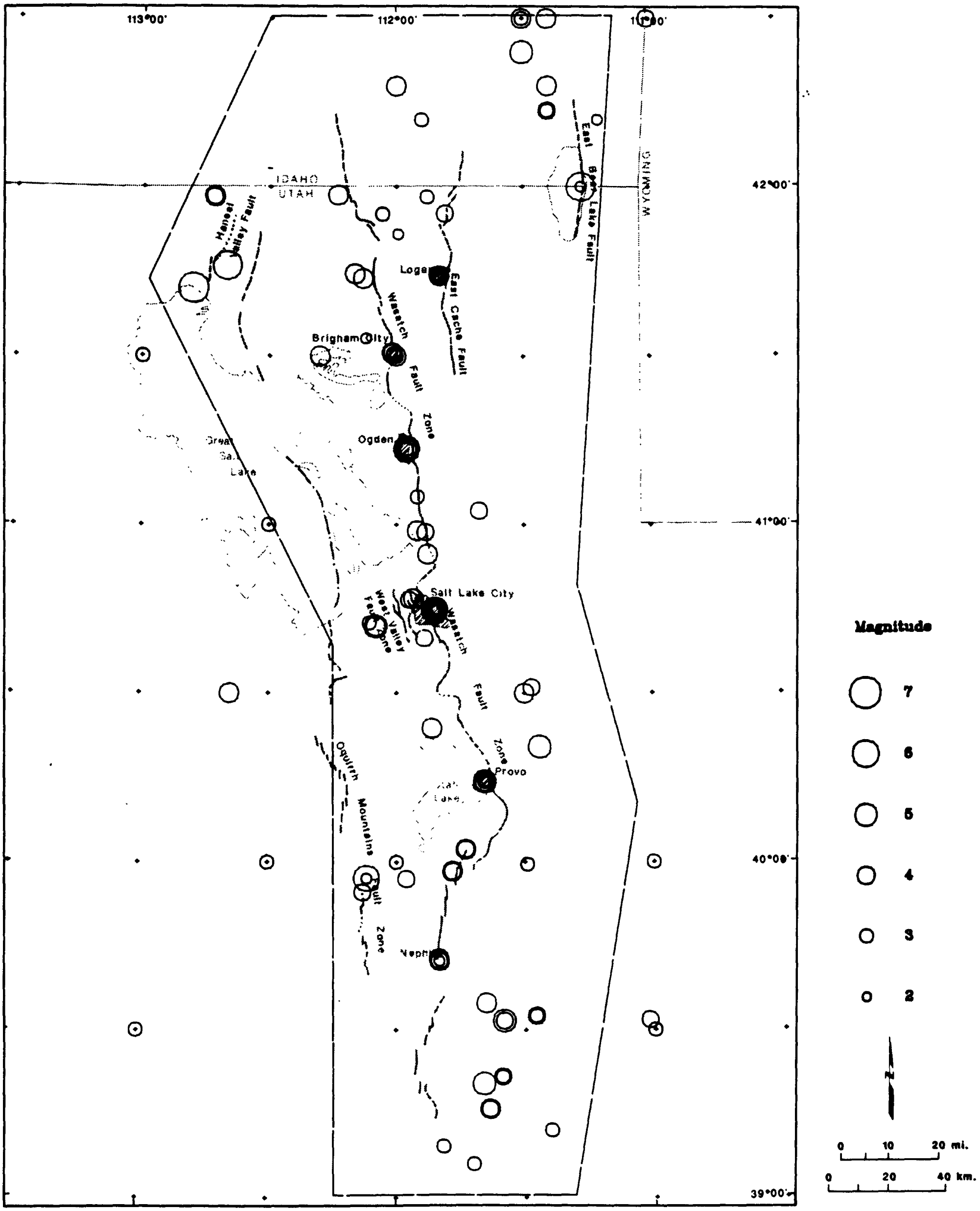

Figure 3 - Earthquake catalog of independent events of magnitude $M_L \geq 2$ occurring prior to July 1, 1962. Magnitudes represent either instrumentally determined values or values obtained from epicentral intensity using the relationship $M_L = 2/3I_o + 1$. Boundary defines limits of background seismic source.

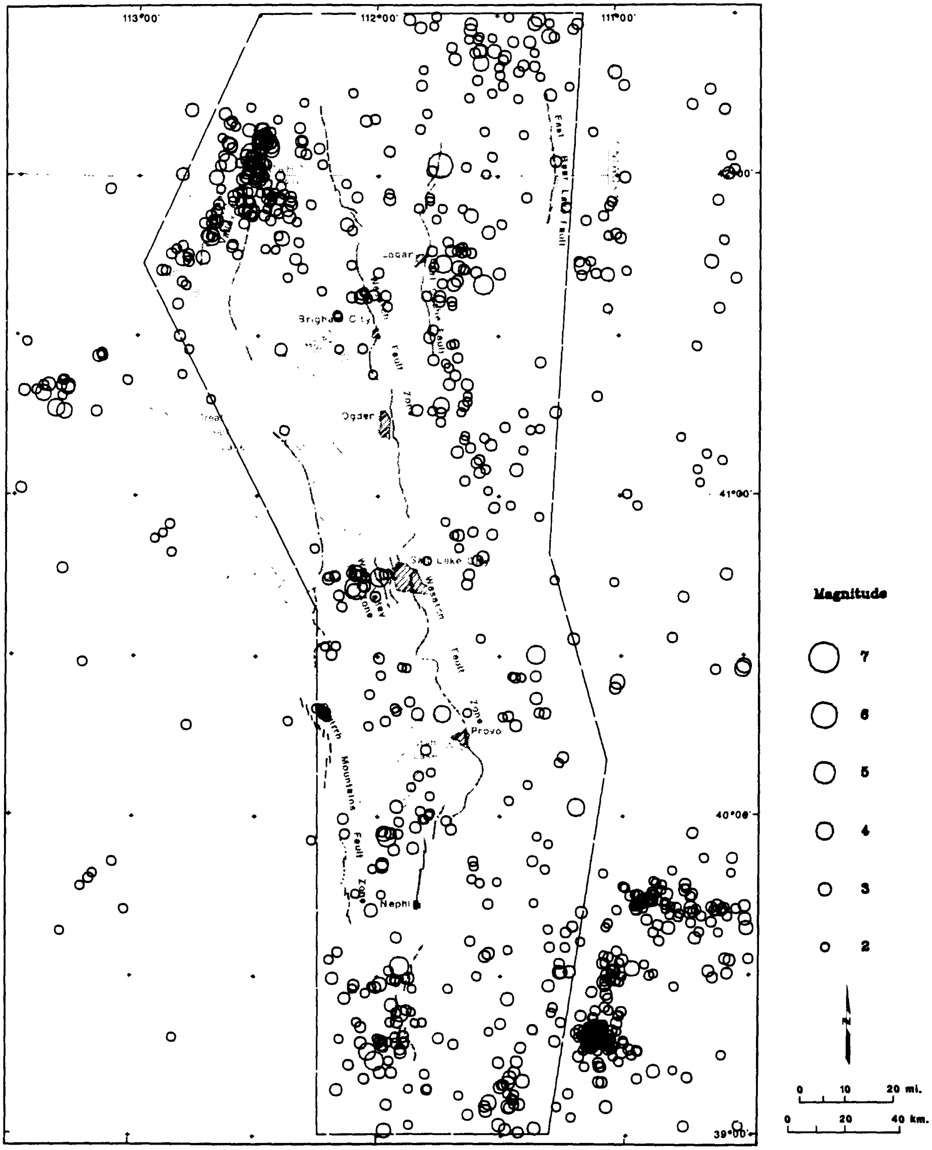

Figure 4 - Instrumental earthquake catalog of independent events of magnitude $M_L \geq 2$ occurring in time period July 1, 1962 to April 1, 1986. Boundary defines limits of background seismic source.

The focal depths are less well determined due to the regional station spacing of the network (Arabasz, 1984). Magnitudes are reported in terms of local magnitude, M_L. Figure 4 displays the locations of earthquakes contained in the instrumental catalog for the region.

Identification of Dependent Events

The mathematical formulation used in this (and most) hazard analysis is based on an assessment of the frequency of occurrence of independent earthquakes. It has been shown that the inclusion of dependent events (e.g. foreshocks and aftershocks) in the analysis results in only a minor increase in the computed hazard (Mertz and Cornell, 1973; Veneziano and Van Dyke, 1985). For this study, dependent events in the earthquake catalog were identified using the following procedure. The largest event in the catalog was identified and a spatial and temporal window was specified based on empirical criteria for the size of foreshock-aftershock sequences as a function of earthquake magnitude. All events falling within the window were flagged as dependent events. The next largest unflagged event was then selected and the process repeated down to the smallest magnitude event.

Three sets of empirical criteria for foreshock-aftershock sequence size were used: Gardner and Knopoff's (1974) criteria for southern California; Uhrhammer's (1986) criteria for California; and the time window developed by Arabasz and Robinson (1976) from California and New Zealand data combined with a multiple of earthquake rupture size evaluated from data presented by Wyss (1979). These three sets of criteria for window size are shown graphically in Figure 5. The time window for aftershocks was used to identify foreshocks. The three criteria were judged to perform equally well in identifying aftershocks as they all: 1) identified as dependent events nearly all of the earthquakes labeled as aftershocks by Arabasz and McKee (1979) in the pre-instrumental catalog; 2) yielded instrumental catalogs of independent events that pass the Kolmogorov-Smirnov goodness-of-fit test for a Poisson process at similar levels of significance; and 3) yielded identical catalogs of events of magnitude $M_L \geq 4$. The number of independent events in the magnitude range of 2 to 4 varies by about 25 percent depending on which set of window criteria is used. As discussed

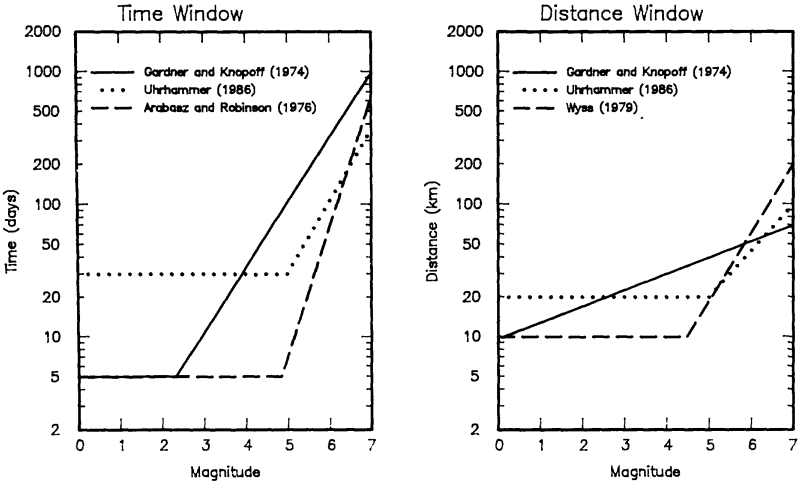

Figure 5 - Criteria used for time and distance windows in identifying independent events.

below, this variation results in differences in the **b**-value computed for the region. The uncertainty in identifying a catalog of independent events was incorporated in the earthquake recurrence estimates used in the hazard analysis. The catalog data shown in Figures 3 and 4 are for independent earthquakes of magnitude $\mathbf{M_L} \geq 2$.

Catalog Completeness

To estimate earthquake recurrence frequencies, the time periods over which independent events of various magnitudes can be considered completely reported in the catalog must be estimated. These time periods were estimated by plotting the observed frequency of occurrence of independent events in different magnitude intervals as a function of time before April 1, 1986, with the observed frequency equal to the number of events observed in the last **T** years divided by **T**. Assuming the earthquake occurrence rate on a regional scale is stationary in time, the time when the observed frequency begins to steadily decrease with increasing time represents the date before which the catalog cannot be considered complete. This approach to evaluating catalog completeness is similar to the method proposed by Stepp (1972).

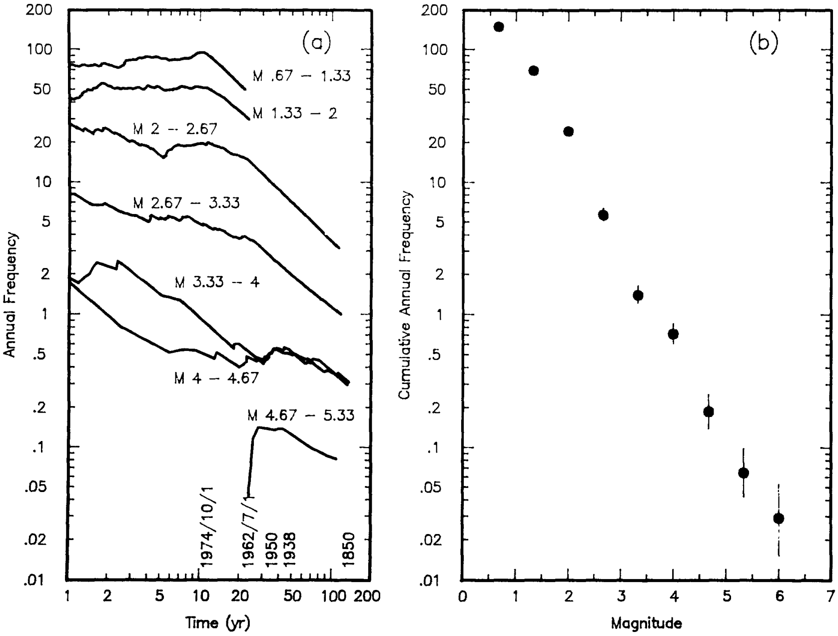

Figure 6 - Estimates of catalog completeness and regional recurrence for North-central Utah. Plotted in (a) are curves showing the frequency of occurrence for events in different magnitude intervals as a function of time prior to April 1, 1986. Plotted in (b) are the cumulative event frequencies obtained for the periods of completeness indicated in (a). The vertical lines denote the 68% confidence interval (16th percentile to 84th percentile) on the cumulative frequency.

Figure 6a presents a plot of the frequency of earthquakes as a function of time for earthquakes within the region outlined in Figures 3 and 4. This region was defined to encompass the seismic activity along the Intermountain seismic belt from latitude 39°N to 42.5°N. The region around Price, Utah (area of concentrated seismicity in the southeast corner of Figure 4) was excluded because it contains a significant level of mining-induced seismicity (Arabasz, 1984). The events are sorted into magnitude intervals two-thirds of a magnitude unit wide centered on the magnitudes obtained from the Gutenberg and Richter (1956) relationship given above using unit intensities. The periods of catalog completeness for the study region estimated from the results shown in Figure 6a are:

Magnitude Range	Period of Completeness
1.3 - 4.0	October 1974 - March 1986
4.0 - 5.3	January 1938 - March 1986

The numerical results presented in Figure 6a do not lend themselves to precise estimates of periods of completeness. The dates tabulated above were selected to correspond with known major changes in seismicity reporting in the Utah region: the initial operation of a telemetered network in October 1974 and the development of a cooperative agreement between the University of Utah and the US Coast and Geodetic Survey for routine transmission of seismographic information in 1938 (Arabasz, 1979). For earthquakes larger than magnitude M_L 5.3 (epicentral intensity VII or greater) there are too few events to make an estimate of completeness using the above method and the completeness periods estimated by Arabasz and others (1979) of 1875 for events of intensity VII and 1850 for intensity VIII were used in the analysis. These dates correspond to the start of the Townley and Allen (1939) catalog for Utah in 1875 and the first routinely published newspaper in 1850.

Figure 6b shows cumulative recurrence rates based on the data in Figure 6a for periods of complete reporting. The error bars represent 16th to 84th cumulative rates computed using the formulation given by Weichert (1980). The data indicates that there may not be complete reporting at present for events smaller than magnitude 2.0. The regional **b**-value for independent events computed using the Weichert (1980) maximum likelihood technique ranges from 0.75(±0.03) to 0.83(±0.03) depending on the choice of aftershock window criteria. Within the zone outlined in Figure 4, the frequency of events of magnitude M_L 4 or larger is one event every 1.3 years.

SEISMIC SOURCE CHARACTERIZATION

Active Quaternary faults along the Wasatch fault and in the adjacent areas have long been recognized as potential earthquakes sources (e.g. Gilbert, 1890). Numerous studies have been made in recent years to identify the locations of, and assess the seismic potential of faults having Quaternary displacement in the study area. At a regional scale, the concentration of earthquakes in the Intermountain Seismic Belt appears to align with the

Quaternary active faults (Figure 4), but, when examined in detail, many of the small- to moderate-magnitude events cannot be directly associated with mapped Quaternary faults (Arabasz and others, 1980; Arabasz, 1984). It should be noted that the apparent concentration of historical seismicity along the Wasatch fault indicated in Figure 3 reflects the fact that non-instrumental epicenters were assigned to the location reporting the strongest felt effects and that the established communities are concentrated along the Wasatch Front (Arabasz and others, 1980).

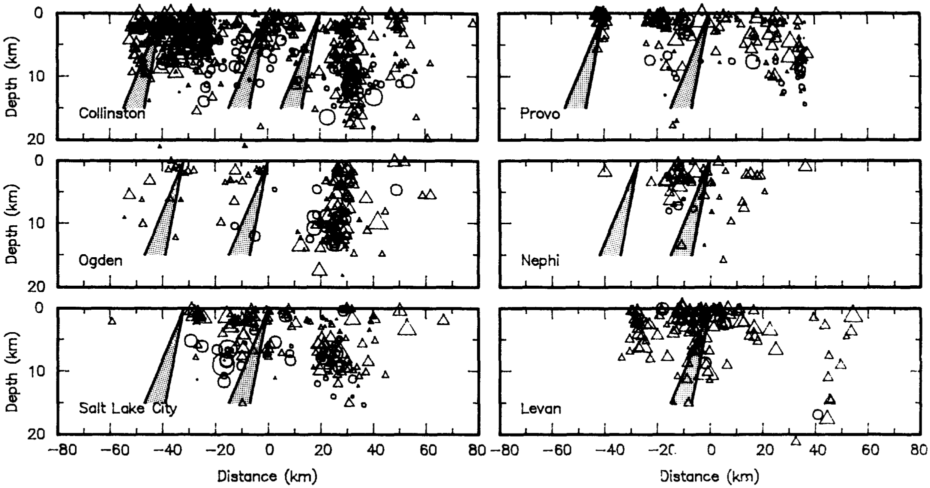

Figure 7 - Cross sections through six segments (segment locations shown in Figure 13a) of the Wasatch fault. Location and range of dip for Quaternary faults indicated by slanted lines. The Wasatch fault is located at distance 0. Circles denote location quality B events (horizontal error 2.5 km; vertical error 5 km) and triangles denote location quality C events (horizontal error 5 km; vertical error not specified).

The lack of signature of the Quaternary faults in the instrumental seismicity is illustrated in Figure 7. Shown are approximately east-west cross sections of the instrumental seismicity recorded in the period October 1974 to April 1986. The circles denote events with location quality B (horizontal error 2.5 km; vertical error 5 km) and the triangles denote events with location quality C (horizontal error 5 km; vertical error not specified). In each cross section the events occurring along the length of one of the segments of the Wasatch fault identified by Schwartz and Coppersmith (1984) are projected onto a plane normal to the fault trace. The locations and estimated range of dips of the identified Quaternary faults are shown, with the Wasatch fault located at distance zero in the plots. As can be seen, there is a poor correlation of instrumental seismicity with the identified faults.

Because of the poor correlation of smaller magnitude seismicity with mapped Quaternary surface faulting, two types of earthquake sources are included in the seismic hazard model: fault-specific sources representing the mapped active faults that may be the source of moderate-to-large magnitude earthquakes ($M_L \geq 6$); and an area source that models the background seismicity of smaller-magnitude earthquakes that may be occurring on unknown faults or faults that are not mapped as active in the Quaternary. On the fault-specific sources only the occurrence of events of magnitude 6 or larger was modeled. While smaller magnitude events may also occur on the mapped active faults, they do not appear to occur with a frequency discernible from the background rate. Therefore, the background source was used to model the occurrence of all smaller magnitude events.

Area Source Model for Background Seismicity

Conceivably there could be many faults within the region capable of generating small to moderate earthquakes that do not rupture to the surface. For this analysis the spatial distribution of future small to moderate magnitude seismicity is assumed to be uniform within the zone outlined in Figures 3 and 4. Seismicity occurring in areas to the east and west of the source zone shown in Figures 3 and 4 was not modeled in the analysis because small to moderate earthquakes occurring in these areas would be too far from the study area defined in Figure 1 to contribute significantly to the ground shaking hazard.

The maximum magnitude for events in the background zone is constrained by threshold for surface faulting events, which has typically been considered to be about magnitude 6 to 6-1/2. Surface faulting was reported for the 1934 M_L 6.6 Hansel Valley earthquake while no surface faulting was found for the 1962 M_L 5.7 Cache Valley and 1975 M_L 6.0 Pocatello Valley earthquakes. It is very unlikely that there are faults along the Wasatch Front long enough to generate earthquakes larger than about magnitude 6-1/2 that have not been mapped. Accordingly, the maximum magnitude for events in the background source was judged to lie in the range of 6 to 6-1/2. The maximum magnitude and assigned weights are: magnitude 6 (0.3); magnitude 6-1/4 (0.5); and magnitude 6-1/2 (0.2).

Earthquake recurrence for the background zone was based on the recorded seismicity located within the zone shown in Figures 3 and 4. As discussed previously, three different criteria were used to identify aftershocks in the catalog, resulting in a difference of about 25 percent in the number of events of magnitude 2 to 4. Figure 8a shows the cumulative frequency plot for the three catalogs of independent events and the associated recurrence relationships obtained using Weichert's (1980) maximum likelihood technique. The three recurrence curves shown in Figure 8a were used in the hazard analysis with equal weight. The mean annual frequency of events of magnitude $\mathbf{M}_L \geq 5$ ranges from 0.10 to 0.12 with associated **b**-values of 0.75 to 0.83. The uncertainty in the regional recurrence estimates was incorporated into the analysis by constructing a joint distribution for cumulative earthquake frequency and **b**-value using relative likelihoods for various parameter combinations (e.g. Bender, 1983). Figure 8b shows the resulting 90-percent confidence interval estimates of earthquake recurrence utilizing the joint distributions of recurrence relationship parameters.

Quaternary Faulting

The major faults having Quaternary displacement in the region that are close enough to the study area to be significant to the seismic hazard evaluation of the study area are shown in Figure 1. These include: the Wasatch fault zone; a discontinuous zone of faults along the west side of the East Tintic and Oquirrh Mountains referred to here as the Oquirrh Mountains fault zone; the East Cache fault; the West Valley fault; the Hansel Valley fault; and the East Bear Lake fault. The Quaternary active back-valley faults east of the Wasatch, such as the Strawberry Valley fault, are not specifically included in the seismic source model because of their distance from the urban areas and their low recurrence rate (Nelson and Van Arsdale, 1986).

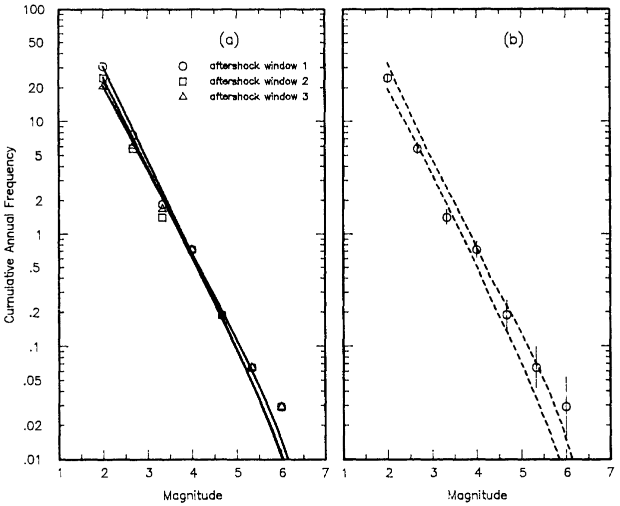

Figure 8 - Recurrence estimates for background seismicity source delineated in Figures 3 and 4. Shown in (a) are the recurrence relationships resulting from use of the three aftershock window criteria shown in Figure 5. Shown in (b) is the 90-percent confidence interval including uncertainty in cumulative frequency and **b**-value.

Fault-specific parameters that can significantly affect seismic hazard are shown in the overall logic tree for the study in Figure 2. Certain elements of the seismic hazard logic tree are common to all the faults, either because all the faults are believed to have certain characteristics that are shared in common or because, for some characteristic (e.g., dip and maximum depth of faulting) there are insufficient data to discriminate among the different faults. Elements that are common for all the faults include: the form of the earthquake magnitude distribution and methods used to assess recurrence; whether or not a fault consists of separate segments; fault dip and maximum depth of rupture; and the techniques used to assess maximum earthquake magnitude. These factors are discussed below.

Earthquake Magnitude Distribution and Recurrence Assessment: While the exponential magnitude distribution generally fits regional seismicity data, as evidenced by the data shown in Figure 6b, recent studies (e.g. Schwartz and Coppersmith, 1984) have suggested that the magnitude distribution for individual faults and fault segments may be better represented by a "characteristic" size that implies relatively more frequent large events than intermediate size events. The characteristic model of Schwartz and Coppersmith (1984) was developed on the basis of data from the Wasatch fault zone and the San Andreas fault in California. For this study, both the exponential magnitude distribution and the characteristic magnitude distribution, the latter as developed by Youngs and Coppersmith (1985a,b), were used to model earthquake recurrence for the faults. The characteristic model was favored over the exponential model (probability 0.7 versus 0.3) as comparisons of the geologic and seismicity data from the Wasatch fault zone originally formed the basis for the model.

Recurrence estimates for the fault-specific sources were based on two approaches. Where displacement data for individual past events were available, they were used to estimate the recurrence rate for the characteristic or maximum event and the form of the characteristic or exponential magnitude distribution was used to define the frequency of events down to magnitude 6.0. If only slip rate data were available for a fault or fault segment, then a moment rate approach was used with the seismicity rate defined by the relationship given by Anderson (1979) for the exponential model and by the relationship given by Youngs and Coppersmith (1985a,b) for the characteristic model. In these approaches the recurrence estimates for individual faults are anchored to the mean repeat times of the largest events estimated from geological evidence rather than an extrapolation of the observed frequency of small events. The geological based estimates of recurrence of large magnitude events are considered more reliable than the extrapolation of small magnitude seismicity rates because of the difficulty in attributing seismicity to specific faults.

In applying Youngs and Coppersmith's (1985a,b) characteristic magnitude distribution, the maximum magnitude assessed for the fault, $\mathbf{m}_{\mathbf{max}}$, is taken to be the expected magnitude for the characteristic size event, with individual events uniformly distributed in the range of $\mathbf{m}_{\mathbf{max}} \pm 1/4$ magnitude units. The cumulative frequency for earthquakes of magnitude $\mathbf{m}_{\mathbf{max}}-1/4$ is then set equal to the annual frequency of maximum events assessed for the fault and the upper bound magnitude, $\mathbf{m}^{\mathbf{u}}$, in Equation 2 is equal to $\mathbf{m}_{\mathbf{max}}+1/4$. To provide a consistent interpretation for the exponential model, the standard truncated exponential distribution (Cornell and Van Marke, 1969) was modified to treat the upperbound magnitude in the density function as uniformly distributed over the range of $\mathbf{m}_{\mathbf{max}} \pm 1/4$ magnitude units. The effect is to smear out the upper boundary of the magnitude distribution without altering the general shape of the recurrence relationship. The cumulative frequency for earthquakes of magnitude $\mathbf{m}_{\mathbf{max}}-1/4$ is again set equal to the annual frequency of maximum events assessed for the fault and the upper bound magnitude, $\mathbf{m}^{\mathbf{u}}$, is equal to $\mathbf{m}_{\mathbf{max}}+1/4$. In this modified form the distribution of events in the range $\mathbf{m}_{\mathbf{max}} \pm 1/4$ remains nearly exponential.

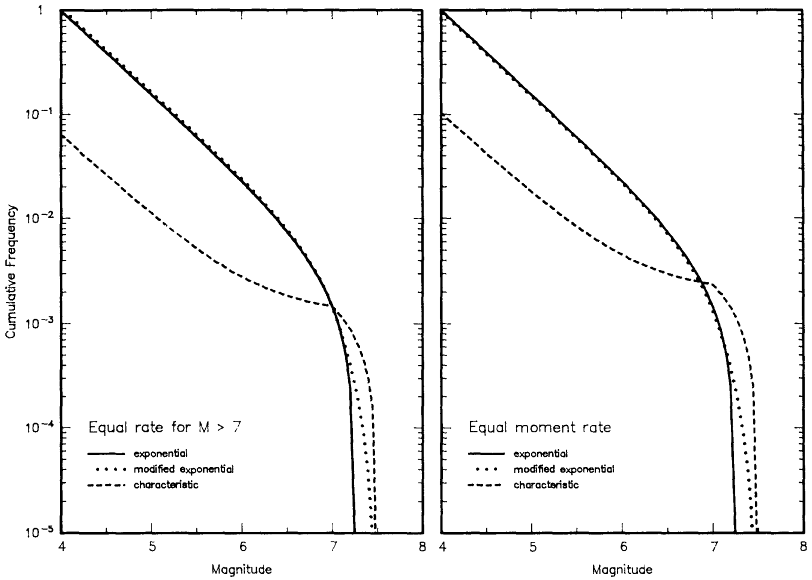

Figure 9 - Comparison of recurrence models used in the analysis for equal recurrence rate of maximum events and equal rate of seismic moment release. Curves are constructed with a **b**-value of 0.8.

Figure 9 compares the shape of the exponential, modified exponential, and characteristic magnitude distributions. Shown on the left are the three distributions developed for an assessed fault $\mathbf{m}_{\mathbf{max}}$ of 7.25 with the frequency of events larger than magnitude 7 held constant in all three models. Shown on the right in Figure 9 are the magnitude distributions developed on the basis of equal rate of seismic moment release. As can be seen, the modified exponential distribution is essentially equal to the exponential distribution except at the upper bound. The characteristic magnitude distribution results in about a factor of 10 reduction in the frequency of small magnitude events compared to the exponential model when the absolute level of the distribution is fixed by either the frequency of the largest events or by the rate of moment release.

Application of the two models requires specification of a **b**-value for the fault in order to be able to define the frequency of smaller magnitude events. Figure 10 presents frequency data for independent events from a 15-km wide corridor representing the surface projection of the west dipping Wasatch fault between latitudes 40°N and 41.5°N, which encompasses the more active central portion of the fault zone. The earthquake frequencies for the small magnitude events are based on instrumental seismicity and the frequency of large magnitude events is based on the paleoseismic data

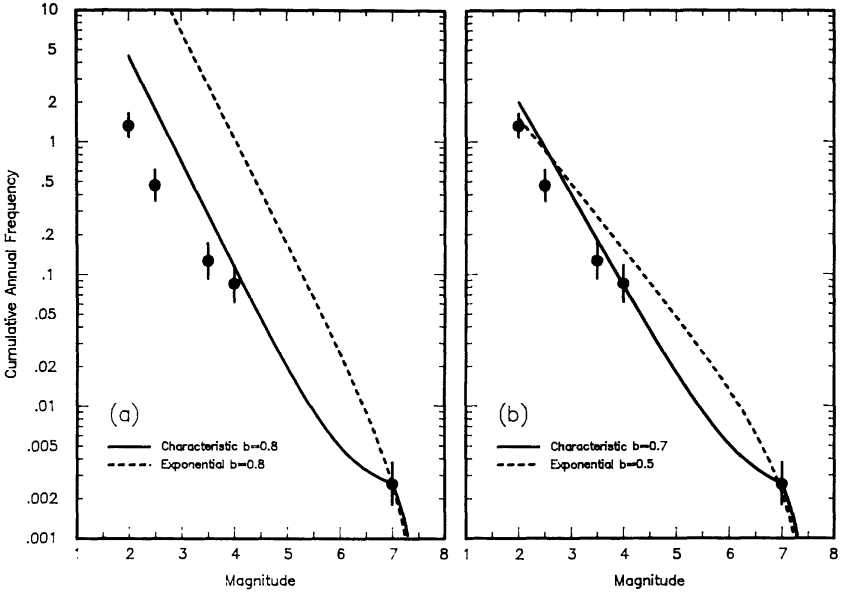

Figure 10 - Wasatch fault-specific **b**-values. (a) Recurrence curves using regional **b**-values. (b) Recurrence curves using selected fault-specific **b**-values. Note that in modeling the fault-specific sources for the hazard analysis, only events of magnitude greater than 6 are modeled, smaller events occurring in the background source.

described later in this paper. In Figure 10a characteristic and exponential magnitude distributions are anchored to the frequency of large magnitude events and then extended to smaller magnitudes using the **b**-value of 0.8 obtained for the regional seismicity. As can be seen, the frequency of smaller magnitude events that may be occurring on the fault is over estimated, especially by the exponential model. To provide more reasonable estimates of the frequency of smaller magnitude events occurring on the faults, fault-specific **b**-values were developed. Figure 10b shows that the recurrence curves obtained using a **b**-value of 0.7 with the characteristic model and a **b**-value of 0.5 with the exponential model provide a much better fit to the observed frequencies of small magnitude events. These two fault-specific **b**-values were used to model earthquake recurrence for all of the fault-specific sources. As discussed above, only the fault-specific recurrence estimates for events of magnitude 6 or greater are included in the analysis.

Use of the moment rate approach requires a relationship between earthquake magnitude and seismic moment. Doser and Smith (1982) analyzed the relationship between seismic moment and magnitude for the Utah region and concluded that the relationship was significantly different from that developed for California earthquakes. Doser and Smith's preferred relationship estimates seismic moment, $\mathbf{M}_\mathbf{o}$, as a function of $\mathbf{M}_\mathbf{L}$ magnitude and was developed on the basis of events of $\mathbf{M}_\mathbf{L}$ magnitude 3.7 to 6.0. This study requires a seismic moment-magnitude relationship applicable to events as large as $\mathbf{M}_\mathbf{S}$ 7-3/4 and one that is consistent with the attenuation relationships used in the hazard analysis. These relationships were derived largely on the basis of strong motion data from California, where the moment magnitude scale as defined by Hanks and Kanamori (1979) is equivalent to $\mathbf{M}_\mathbf{L}$ in the range of 3 to 7 and equivalent to $\mathbf{M}_\mathbf{S}$ in the range of 5 to 7.5. To apply these relationships in Utah we have made the assumption that ground motions are more directly correlated with magnitude than seismic moment. This assumption is supported by the theoretical model of ground motion developed by Hanks and McGuire (1979) in which ground motion levels are fixed by both seismic moment and stress drop. Boore (1983) has shown that this model can be used to simulate the characteristics of both strong motion attenuation and measurement of $\mathbf{M}_\mathbf{L}$ in California. Regional

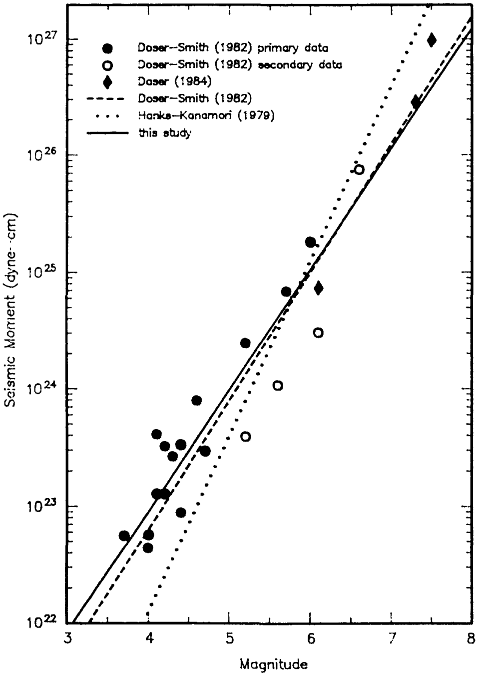

Figure 11 - Relationship between seismic moment and earthquake magnitude. Points denoted primary data from Doser and Smith (1982) were used by them to develop their preferred relationship shown in the figure.

differences in the seismic moment and stress drop should thus have similar effects on strong ground motion and on measured magnitude. We have made the assumption that events with similar measured magnitudes in Utah and California will have similar levels of strong ground motion, though the total seismic moment release may be different in the two regions.

For this study we have developed a modified form of the Doser and Smith relationship by including data for large M_s magnitude events reported by Doser and Smith (1982) and by Doser (1984). These events include the 1959 Hebgen Lake and 1983 Borah Peak earthquakes. The resulting data set is plotted in Figure 11. A least squares fit to the data yields the relationship $\log(M_o)=1.04M+18.8$, which is only slightly different from Doser and Smith's (1982) preferred relationship. This modified Doser-Smith relationship was used for all moment rate constrained recurrence estimates.

Also shown in Figure 11 for comparison is the relationship proposed by Hanks and Kanamori (1979), which clearly does not fit the trend of the data. As the Hanks and Kanamori relationship predicts larger seismic moments for earthquakes of magnitude 6 or greater, its use would result in somewhat lower earthquake frequencies estimated on the basis of the moment rate approach.

Application of the moment rate approach requires an estimate of the average slip rate for the fault or fault segment. Slip rates estimated from data for a single or only a few locations may not reflect the average slip rate along the entire fault because the locations selected for detailed study are usually where the fault is well-expressed topographically, and hence may represent points where the slip rate is somewhat greater than the average over the whole fault or segment length. Accordingly, the distributions of possible values of the average slip rate assessed for the faults were derived reflecting the uncertainty in the point estimates of slip rate together with a possible bias in the point estimate. The amount of possible bias was judged to range from 1.0 (no bias) to 0.5 (point estimate twice the average rate) with the expected amount of bias in the point estimates set to 0.8.

Unsegmented Versus Segmented Fault-Rupture Model: The formulation used in this study (and in most other seismic hazard analyses) treats the location of future earthquake rupture on a seismic source as a random process, usually a uniform distribution. For fault zones modeled as a single fault-specific source this would result in earthquake ruptures uniformly distributed along the length of the fault. However, based on the results of paleoseismic investigations, Schwartz and Coppersmith (1984) propose that faults may consist of separate segments that appear to rupture completely and independently during successive earthquakes of characteristic sizes, implying that the individual segments of a fault should be modeled as separate sources in the hazard analysis. The segmentation model not only affects the distribution of ruptures along the fault, it provides constraints on the maximum rupture length and, therefore, on maximum earthquake magnitude, and may also affect recurrence estimates.

Convincing arguments supporting fault segmentation have been presented by Schwartz and Coppersmith (1984, 1986), Aki (1979, 1984) and Slemmons and Depolo (1986). Studies by several investigators (Schwartz and Coppersmith, 1984; Mayer and MacLean, 1986; Machette and others ,1986; Personius, 1986) report evidence for distinct segments along the Wasatch fault zone. However, detailed analysis of some historical surface-faulting earthquakes suggests that faulting can rupture across and/or skip over barriers between adjacent segments. For example, the 10 October 1980 El Asnam, Algeria earthquake appears to have been produced by rupture of two or three adjacent segments (Deschamps and others, 1982; King and Yielding, 1984). Similarly, surface faulting during the 28 October 1983 Borah Peak, Idaho earthquake ruptured across the bedrock hills east of Willow Creek Summit, which may represent a major segment boundary along the Lost River fault separating the Warm Springs Valley segment from the Thousand Springs Valley segment (Crone and Machette, 1985).

To account for the uncertainty in the fault-rupture behavior, both an unsegmented model and a segmented model were included for each fault. The unsegmented model allows for rupture across the segment boundaries during events and for the simultaneous rupture of two or more adjacent segments. Rupture during successive earthquakes is assumed to be uniformly distributed along the entire length of the fault zone and the maximum length of rupture is not necessarily constrained by boundaries between segments. The segmented model assumes that rupture will not occur across the segment boundaries and that the segments behave independently with the maximum length of rupture on a given segment equal to the segment length. Based on the results of paleoseismic investigations, the segmented fault model is considered to be more representative of fault-rupture behavior of normal slip Basin and Range faults. Accordingly, the unsegmented and segmented conditions for all the faults are assigned weights of 0.2 and 0.8, respectively. For the Wasatch fault zone two segmented fault models are included to account for uncertainty in the actual number of segments, as discussed later.

Fault Dip and Depth: The down-dip geometry of the fault plane affects the seismic hazard computation in several ways. For nearby faults it can affect distribution for distance to earthquake rupture. It is a factor in determining fault-rupture area used in the assessment of maximum earthquake magnitudes and earthquake recurrence estimates based on seismic moment rate.

All the faults included in the seismic source model are high-angle normal faults. There are insufficient data on the down-dip geometry of these faults to discriminate among them. Therefore, the down-dip geometry is treated the same way for all the faults.

Nearly all the microseismicity along the Wasatch Front occurs at depths of about 15 Km or less (Figure 7). Based on microseismicity and aftershock data, the 6 July 1954 Fallon Stillwater, Nevada earthquake ($\mathbf{M}_s$ 7.1), the 18 August 1959 Hebgen Lake earthquake ($\mathbf{M}_s$ 7.5), and the 28 October 1983 Borah Peak, Idaho earthquake ($\mathbf{M}_s$ 7.3), are all interpreted to have occurred on 45 to 65 degree dipping normal faults that nucleated at depths of about 15 Km (Smith and others, 1985). Accordingly, all faults are assumed to have dips ranging between 45 and 65 degrees with a maximum depth of 15 Km. In the analysis dips of 45 and 65 were used with equal likelihood.

Maximum Earthquake Magnitude Assessment Techniques: Maximum earthquake magnitudes for the fault-specific sources are assessed by estimating the physical parameters of length, area, and displacement for the maximum size event and then relating these parameters to earthquake magnitude using published correlations for magnitude as a function of rupture length, **RL**, [Slemmons, 1982, $\mathbf{M} = 0.819 + 1.341\log_{10}(\mathbf{RL} \text{ in m})$; Bonilla and others, 1984, $\mathbf{M} = 5.17 + 1.237\log_{10}(\mathbf{RL} \text{ in km})$], rupture area, **RA**, [Wyss, 1979, $\mathbf{M} = 4.15 + \log_{10}(\mathbf{RA} \text{ in km}^2)$], and seismic moment. The relationship used to estimate magnitude from seismic moment, $\mathbf{M}_o$, was developed utilizing the data presented by Doser and Smith (1982) and Doser (1984) and shown in Figure 11. A least squares fit to the data shown in Figure 11 yielded the relationship $\mathbf{M} = -16.22 + 0.885\log_{10}(\mathbf{M}_o \text{ in dyne-cm})$ where **M** is assumed to be equivalent to $\mathbf{M}_L$ in the range of 3 to 7 and $\mathbf{M}_s$ in the range of 5 to 7.5. The distribution of possible values for the physical parameters of maximum rupture length, maximum rupture area, and average displacement in a maximum event are developed by extending the logic tree formulation shown in Figure 2.

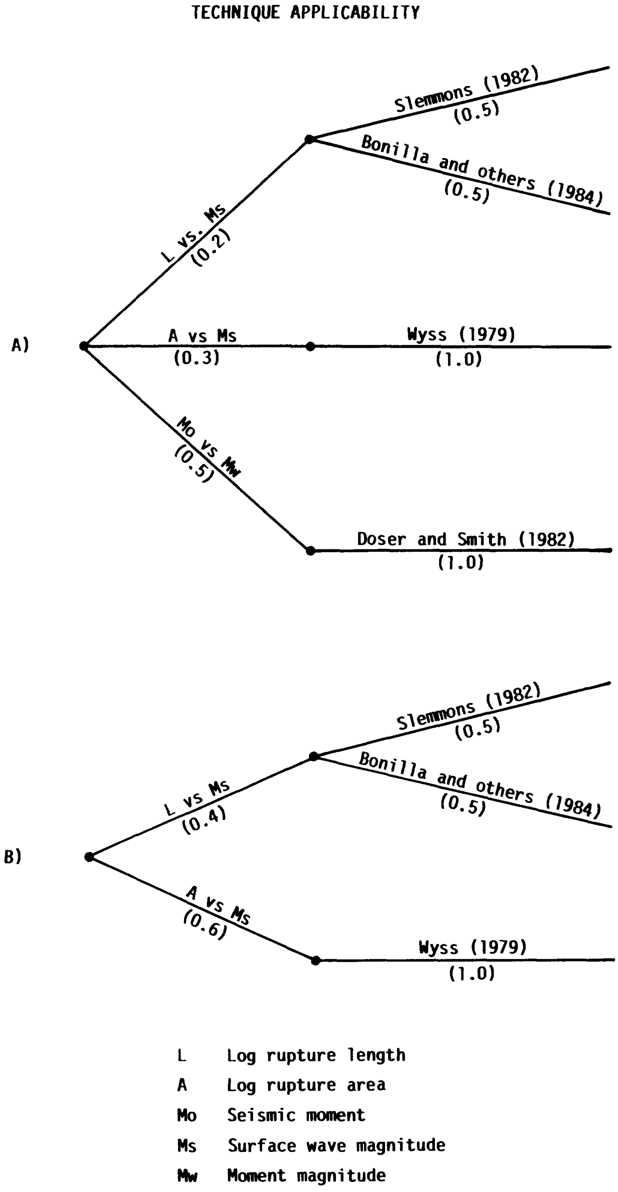

Figure 12 - Weighting factors for maximum magnitude assessment techniques for case: (a) data on displacement per event available and (b) data on displacement per event not available.

Completion of the assessment of maximum magnitude requires selection of the appropriate relationship between rupture parameters for a maximum event and earthquake magnitude. The relative weights assigned to the various techniques used to estimate the maximum earthquake magnitude for each fault and fault segment are illustrated in Figure 12. Where three techniques could be used (i.e., length versus magnitude, area versus magnitude, and moment versus magnitude), the greatest weight, 0.5, is assigned to magnitudes based on seismic moment, because this relationship incorporates essentially all the physical factors controlling earthquake size (fault rupture area, amount of slip and rigidity of the rock). The lowest weight, 0.2, is assigned to the length-versus-magnitude relationship because it incorporates the least number of these controlling factors. The balance, 0.3, is assigned to the area-versus-magnitude relationship.

The Wasatch and East Cache faults are the only faults having sufficient data to estimate the average fault displacement. Therefore, the moment-versus-magnitude technique could not be used for the other faults. Where only length-versus-magnitude and area-versus-magnitude relations were used, the techniques are assigned relative weights of 0.4 and 0.6 respectively. Given the length-versus-magnitude relationship, Slemmons (1982) and Bonilla and others (1984) relationships are assigned equal probability of reflecting the correct value. After maximum magnitude distributions are obtained from the logic trees such as illustrated in Figure 12, these distributions are rediscretized into quarter-magnitude intervals for use in the analysis.

The remaining parameters incorporated in the analysis (Figure 2) include: choices among different segmentation models; whether a fault is active (i.e. capable of independently producing earthquakes); total fault length; maximum earthquake magnitude; and earthquake recurrence rate. The assessed fault-specific parameter values and associated weights are summarized in Table 1 and are discussed below for each source. Table 2 lists the fault parameters and probability weights used for assessing maximum magnitude for each of the faults.

TABLE 1
SUMMARY OF FAULT CHARACTERIZATION PARAMETERS AND ASSOCIATED WEIGHTS FOR SEISMIC HAZARD MODEL

Fault and Segment	State of Activity	Total Length, Km	Dip, degrees	Maximum Magnitude	Recurrence Basis[1]	Slip Rate (mm/year)[1]	Recurrence Interval for Maximum Event (years)[1]
WASATCH FAULT							
Unsegmented Model (.2)	Active (1.0)	360(1.0)	45(.5) 65(.5)	7(.09); 7.25(.53), 7.5(.37); 7.75(.01) 7(.22); 7.25(.62), 7.5(.15); 7.75(01)	--	0.3(.02), 0 4(.1), 0.5(.1); 0.6(.42); 0 7(.12); 0.8(.18), 1.0(06)	-- --
Segmented Model (.8)							
Segments, Model A (.4):							
Unnamed	Active (1.0)	48(1.0)	45(.5) 65(.5)	7(.1); 7.25(.75); 7 5(.15) 7(.45); 7.25(.55)	Segment (1.0)	0.05(.05); 0.075(3); 0 1(2); 0.15(3); 0.2(.15)	--
Collinston	Active (1.0)	30(1.0)	45(.5) 65(.5)	6.75(.1), 7(.75); 7 25(.15) 6.75(.45), 7(4), 7 25(15)	Segment (1 0)	0 05(02); 0 1(26); 0.15(66); 0 2(.06)	--
Ogden	Active (1.0)	78(1.0)	45(5) 65(.5)	7 25(45); 7.5(55) 7.25(.45); 7.5(.55)	Segment (.5) Zone (.5)	-- --	1670(.04); 1430(.24); 1250(.55); 1110(.08); 1000(.04); 910(.04); 830(.01) 3030(.2); 1920(.6); 1390(.2)
Salt Lake City	Active (1 0)	45(1.0)	45(.5) 65(.5)	7(.15); 7 25(7); 7.5(.15) 7(45); 7.25(.55)	Segment(.5) Zone (.5)	-- --	5000(.04); 3330(.28); 2500(.48); 2000(.16); 1670(.04) 3030(.2); 1920(.6); 1390(.2)
Provo	Active (1.0)	70(1.0)	45(.5) 65(.5)	7.25(.45); 7.5(.55) 7.25(.75); 7.5(.25)	Segment (.5) Zone (.5)	-- --	2500(.32); 2000(.52); 1670(.16) 3030(.2); 1920(.6); 1390(.2)
Nephi	Active (1.0)	40(1.0)	45(.5) 65(.5)	7(.45); 7 25(.55) 7(.45); 7.25(.55)	Segment (0.5) Zone (.5)	-- --	2000(.28); 1670(.68); 1430(.04) 3030(.2); 1920(.6); 1390(.2)
Levan	Active (1.0)	49(1.0)	45(.5) 65(.5)	7(.1); 7.25(.75); 7.5(.15) 7(.45); 7.25(.55)	Segment (1.0)	--	9090(.04); 8330(.12); 7690(.16); 7140(.36); 6670(.16); 6250(.12); 5880(.04)
Segments, Model B (.6):							
Collinston	Active (1.0)	60(1.0)	45(.5) 65(.5)	7.25(.55); 7.5(.45) 7.25(.85); 7.5(.15)	Segment (1.0)	0.05(.05); 0.075(.3); 0.1(.2); 0.15(.3); 0.2(.15)	--
Brigham City	Active (1.0)	40(1.0)	45(.5) 65(.5)	7(.45); 7.25(.55) 7(.45); 7.25(.55)	Segment (1.0)	0.1(.02); 0.2(.56); 0.3(.42)	--
Weber	Active (1.0)	57(1.0)	45(.5) 65(.5)	7.25(.85); 7.5(1.15) 7(.35); 7.25(.65)	Segment (.5) Zone (.5)	-- --	1670(.04); 1430(.24); 1250(.55); 1110(.08); 1000(.04); 910(.04); 830(.01) 3570(.2); 1920(.6); 1320(.2)
Salt Lake City	Active (1.0)	45(1.0)	45(.5) 65(.5)	7(.15); 7.25(.7); 7.5(.15) 7(.45); 7.25(.55)	Segment(.5) Zone (.5)	-- --	5000(.04); 3330(.28); 2500(.48); 2000(.16); 1670(.04) 3570(.2); 1920(.6); 1320(.2)
American Fork	Active (1.0)	18(1.0)	45(.5) 65(.5)	6.5(.1); 6.75(.45); 7(.45) 6.5(.4); 6.75(.45); 7(.15)	Zone (1.0)	--	3570(.2); 1920(.6); 1320(.2)

TABLE 1
SUMMARY OF FAULT CHARACTERIZATION PARAMETERS AND ASSOCIATED WEIGHTS FOR SEISMIC HAZARD MODEL
(Continued)

Fault and Segment	State of Activity	Total Length, Km	Dip, degrees	Maximum Magnitude	Recurrence Basis[1]	Slip Rate (mm/year)[1]	Recurrence Interval for Maximum Event (years)[1]
WASATCH FAULT							
Segments, Model B (.6) (cont.):							
Provo	Active (1.0)	19(1.0)	45(.5) 65(.5)	6.5(.1); 6.75(45); 7(.45) 6.5(.1); 6.75(.75); 7(.15)	Zone (1.0)	--	3570(.2); 1920(.6); 1320(.2)
Spanish Fork	Active (1 0)	32(1.0)	45(.5) 65(.5)	6.75(.1); 7(.45); 7 25(.45) 6.75(.4); 7(45); 7.25(.15)	Segment (.5) Zone (.5)	-- --	2500(.32); 2000(.52); 1670(.16) 3570(.2); 1920(.6); 1320(.2)
Nephi	Active (1.0)	40(1.0)	45(.5) 65(5)	7(.45); 7 25(55) 7(.45); 7.25(.55)	Segment (.5) Zone (.5)	-- --	2000(.28); 1670(.68); 1430(.04) 3570(.2); 1920(.6); 1320(.2)
Levan	Active (1.0)	35(1 0)	45(.5) 65(.5)	7(.55); 7.25(.45) 7(85); 7.25(.15)	Segment (1.0)	--	9090(.04); 8330(.12); 7690(.16); 7140(.36); 6670(.16) 6250(.12); 5880(.04)
Fayette	Active (1.0)	14(1.0)	45(.5) 65(.5)	6.25(.1); 6.5(.4); 6.75(.35); 7(.15) 6.25(.1); 6.5(.45); 6.75(.45)	Segment (1.0)	--	10,000(1.0)
OQUIRRH MOUNTAINS FAULT							
Unsegmented Model (.2)	Active (1.0)	180(.35)	45(.5) 65(.5)	7(.13); 7.25(.72); 7.5(.14); 7.75(.01) 7(.37); 7.25(.51); 7.5(.11); 7.75(.01)	--	0.08(.03); 0.1(.23); 0.15(.41); 0.2(.27); 0.3(.06)	--
		250(.05)	45(.5) 65(.5)	7(.13); 7.25(.72); 7.5(.14); 7.75(.01) 7(.37); 7.25(.51); 7.5(.11); 7.75(.01)	--	0.08(.03); 0.1(.23); 0.15(.41); 0.2(.27); 0.3(.06)	--
Segmented Model (.8)							
Segments:							
East Tintic	Active (1.0)	35(1.0)	45(.5) 65(.5)	7(1.0) 7(1.0)	--	0.08(.03); 0.1(.23); 0.15(.41); 0.2(.27); 0.3(0.06)	--
Oquirrh Marginal	Active (1.0)	50(1.0)	45(.5) 65(.5)	7(.2); 7.25(.8) 7(.8); 7.25(.2)	--	0.08(.03); 0.1(.23); 0.15(.41); 0.2(.27); 0.3(0.06)	--
Northern Oquirrh Mountain	Active (1.0)	35(1.0)	45(.5) 65(.5)	7(1.0) 7(1.0)	--	0.08(.03); 0.1(.23); 0.15(.41); 0.2(.27); 0.3(0.06)	--
Great Salt Lake	Active (1.0)	60(1.0)	45(.5) 65(.5)	7.25(1.0) 7.25(1.0)	--	0.08(.03); 0.1(.23); 0.15(.41); 0.2(.27); 0.3(0.06)	--
Promonotory Mountain	Active (.5) Inactive (.5)	70(1.0)	45(.5) 65(.5)	7.25(.8); 7.5(.2) 7.25(.8); 7.5(.2)	--	0.08(.03); 0.1(.23); 0.15(.41); 0.2(.27); 0.3(0.06)	--

TABLE 1
SUMMARY OF FAULT CHARACTERIZATION PARAMETERS AND ASSOCIATED WEIGHTS FOR SEISMIC HAZARD MODEL
(Continued)

Fault and Segment	State of Activity	Total Length, Km	Dip, degrees	Maximum Magnitude	Recurrence Basis[1]	Slip Rate (mm/year)[1]	Recurrence Interval for Maximum Event (years)[1]
EAST CACHE FAULT							
Unsegmented Model (.2)	Active (1.0)	72(1.0)	45(.5) 65(.5)	7(.24); 7.25(.66); 7.5(.10) 7(.57); 7.25(.43)	--	0.05(.05); 0.075(.3); 0.1(.2); 0.15(.3); 0.2(.15)	--
Segmented Model (.8)							
Segments:							
Logan	Active (1.0)	47(1.0)	45(.5) 65(.5)	7(.1); 7.25(.75); 7.5(.15) 7(.45); 7.25(.55)	--	0.05(.05); 0.075(.3); 0.1(.2); 0.15(.3); 0.2(.15)	--
Richmond	Active (1.0)	25(1.0)	45(.5) 65(.5)	6.75(.4); 7(.45); 7.25(.15) 6.75(.45); 7(.55)	--	0.05(.05); 0.075(.3); 0.1(.2); 0.15(.3); 0.2(.15)	--
WEST VALLEY FAULT							
Unsegmented Model (1.0)	Independent (0.6) Sympathetic (0.4)	18(1.0)	45(.5) 65(.5)	6.25(.6); 6.5(.2); 6.75(.2) 6.5(.8); 6.75(.2)	--	0.3(.5); 0.5(.5)	--
HANSEL VALLEY FAULT							
Unsegmented Model (.6)	Active (1.0)	25(1.0)	45(.5) 65(.5)	6.75(.8); 7(.2) 6.75(.8); 7(.2)	--	0.05(.5); 0.1(.5)	--
Segmented Model (.4)							
Segments:							
North Hansel Mountains	Active (0.5) Inactive (0.5)	14(1.0)	45(.5) 65(.5)	6.25(.2); 6.5(.8) 6.25(.2); 6.5(.8)	--	0.01(.5); 0.05(.25); 0.1(.25)	--
South Hansel Mountains	Active (1.0)	11(1.0)	45(.5) 65(.5)	6.5(1.0) 6.5(1.0)	--	--	12,000(.5); 8,700(.5)
EAST BEAR LAKE FAULT							
Unsegmented Model (.2)	Active (1.0)	50(1.0)	45(.5) 65(.5)	6.75(.12); 7(.56); 7.25(.32) 6.75(.48); 7(.44); 7.25(.08)	--	0.05(.5); 0.1(.5)	--
Segmented Model (.8)							
Segments:							
Montpelier	Active (1.0)	23(1.0)	45(.5) 65(.5)	6.75(1.0) 6.75(1.0)	--	--	8,000(1.0)
Bear Lake	Active (1.0)	27(1.0)	45(.5) 65(.5)	6.75(.2); 7(.8) 6.75(.8); 7(.2)	--	--	15,000(1.0)

Note: 1 - Recurrence basis, slip rate, and recurrence interval characterizations are applicable to both sets of fault dips and maximum magnitudes.

TABLE 2

SUMMARY OF PARAMETERS AND RELATIONSHIPS USED TO ESTIMATE MAXIMUM MAGNITUDE AND ASSOCIATED WEIGHTS

	Rupture Length, Km	Dip, degrees	Average Displacement, meters	Estimation Technique	Estimation Relationship*
WASATCH FAULT					
Unsegmented Model (.2)	35(.05);45(.4); 65(.5);100(.05)	45(.5); 65(.5)	1(.1);1.5(.6); 2(.3)	L vs M (.2); A vs M (.3); M_o vs M (.5)	1(.5);2(.5) 3 (1.0) 4 (1.0)
Segmented Model (.8)	Segment Lengths (1.0)	"	"	"	"
OQUIRRH MOUNTAINS FAULT					
Unsegmented Model (.2):					
Fault Length 250 Km (.5)	35(.05);45(.4); 65(.5);100(.05)	45(.5); 65(.5)	—	L vs M (.4); A vs M (.6);	1(.5);2(.5) 3 (1.0)
Fault Length 180 Km (.5)	35(.5);65(.5)	"	—	"	"
Segmented Model (.8)	Segment Lengths (1.0)	"	—	"	"
EAST CACHE FAULT					
Unsegmented Model (.2)	36(.3);47(.7)	45(.5); 65(.5)	1(.1);1.5(.6); 2(.3)	L vs M (.2); A vs M (.3); M_o vs M (.5)	1(.5);2(.5) 3 (1.0) 4 (1.0)
Segmented Model (.8)	Segment Lengths (1.0)	"	"	"	"
WEST VALLEY FAULT					
Unsegmented Model (1.0)	16(1.0)	45(.5); 65(.5)	—	L vs M (.4); A vs M (.6);	1(.5);2(.5) 3 (1.0)
HANSEL VALLEY FAULT					
Unsegmented Model (.6)	25 (1.0)	45(.5); 65(.5)	—	L vs M (.4); A vs M (.6);	1(.5);2(.5) 3 (1.0)
Segmented Model (.4)	Segment Lengths (1.0)	"	—	"	"
EAST BEAR LAKE FAULT					
Unsegmented Model (.2)	50 (.4);27(.6)	45(.5); 65(.5)	—	L vs M (.4); A vs M (.6);	1(.5);2(.5) 3 (1.0)
Segmented Model (.8)	Segment Lengths (1.0)	"	—	"	"

* Relationships:

1. Slemmons (1982) (L vs M)
2. Bonilla and others (1984) (L vs. M)
3. Wyss (1979) (A vs. M)
4. Doser and Smith (1982) (M_o vs. M)

Wasatch Fault Zone: The Wasatch fault zone is an active westward-dipping normal fault (Figures 1 and 13). Paleoseismic studies demonstrate that there have been repeated large-magnitude earthquakes on most segments of this fault zone throughout the Holocene (Swan and others, 1980, 1981, 1982; Hanson and others, 1981; Schwartz and Coppersmith, 1984). These data are incorporated in the seismic hazard model in the following manner.

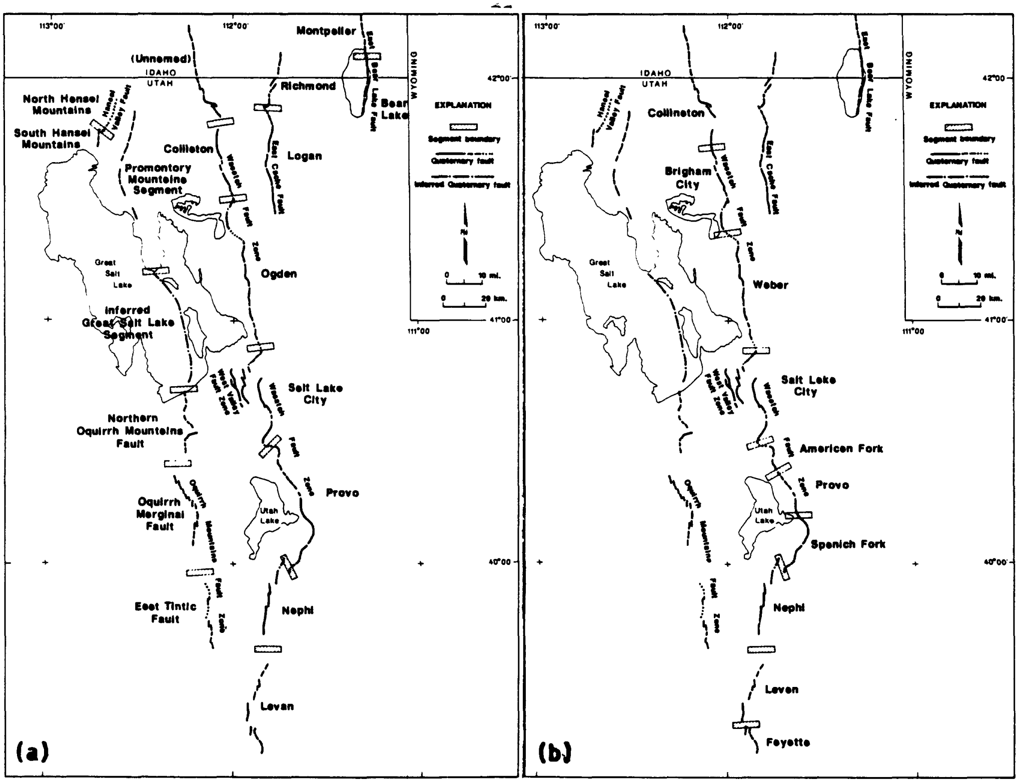

Figure 13 - Segmentation models for fault-specific sources. (a) Wasatch fault Model A and all other faults, and (b) Wasatch fault Model B.

Segmentation: In addition to the question of whether or not the fault-rupture process is characterized by unsegmented or segmented behavior, discussed above, there is uncertainty regarding the actual number of fault segments along the Wasatch fault zone. Schwartz and Coppersmith (1984) propose that the fault zone south of Collinston, Utah consists of six separate segments. They do not discuss the fault zone north of Collinston, which may comprise a seventh unnamed segment (Figure 13a).

Based on morphological discriminant analysis of selected geomorphic parameters (drainage basin shape, mountain front sinuousity, steepness of trunk streams, locations of steep sections of stream channels and valley shape), Mayer and MacLean (1986) have proposed that the zone may consist of nine separate segments. Machette and others (1986) suggest that the zone consists of at least ten segments.

At present, there are insufficient data to conclusively define the actual number of segments (Wheeler, 1984). Therefore, two segmentation models are included in the hazard analysis (Figure 13 and Table 1). The minimum number of segments proposed along the Wasatch fault zone is seven (segmentation model A on Figure 13a); the maximum number proposed is ten (segmentation model B on Figure 13b). The actual number of segments probably lies within this range. Model A and Model B were assigned relative weights of 0.4 and 0.6 respectively, reflecting our judgment that Model B is slightly more likely. Both models are conditional on the fault being segmented (Figure 2).

Maximum Earthquake Magnitude: Figure 14 presents the logic tree used to assess maximum magnitude for the Wasatch fault zone. Given an unsegmented fault model for the Wasatch fault, the rupture length likely to be associated with the maximum earthquake may be significantly longer than the length of individual mapped segments. Bonilla and others (1984) have developed a relationship relating displacement to rupture length for normal faults. The maximum net vertical displacement reported from paleoseismic investigations along the Wasatch fault zone is 4.75 m at Dry Creek (Lund and Schwartz, 1986). Using Bonilla and other's relationship relating rupture length to maximum displacement for normal faults and displacements of 4.75 m yields an expected rupture length (mean value) of 53 km. The longest historical surface fault rupture reported from the Basin and Range is 61 km associated with the 3 October 1915 Pleasant Valley, Nevada earthquake. However, if two or three of the identified fault segments were to rupture simultaneously (e.g., the Ogden and Salt Lake city segments or the Provo, Spanish Fork and Nephi segments), a maximum rupture length of about 100 km might be expected. This, however, is considered to be a very unlikely case. To account for the uncertainty in the maximum rupture length, values ranging from 45 km to 100 km are considered in the hazard analysis. Table 2 summarizes the assessed maximum rupture lengths and the relative weights assigned to each value for the unsegmented fault model. Given the segmented fault models, the maximum rupture lengths are assumed to be the lengths of the individual segments as shown in Table 1 and Figure 14.

Schwartz and others, (1983), and Schwartz and Coppersmith (1984; 1986) summarize the available displacement data from five locations along the Wasatch fault zone based on the paleoseismic investigations. The values,

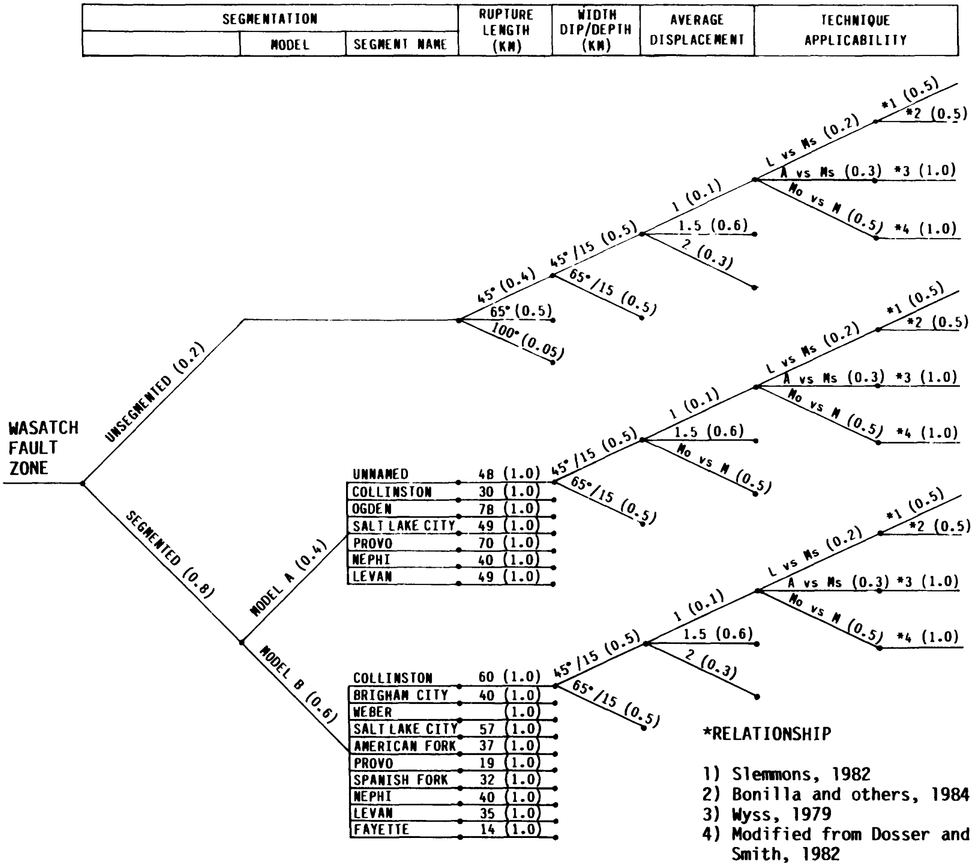

Figure 14 - Maximum magnitude logic tree for Wasatch fault zone.

which have been corrected for distortions due to effects of graben formation and backtilting, represent net vertical tectonic slip at specific locations along the fault zone. The values range from 1.6 to 2.7 m per event and average about 2 m per event. It is not known where these measurements are located with respect to the maximum displacement during the individual rupture events or how they relate to the average displacement along these surface ruptures.

Detailed measurements of recent surface faulting events show that there is a great deal of variability in the displacement along the length of the surface rupture. For example, the maximum displacement of 2.7 m during the 28 October 1983 Borah Peak earthquake occurred along less than 1 km of the 34 km-long rupture. Only 49 percent of the rupture was characterized by displacements equal to or greater than the average displacement of 0.8 m (Crone and Machette, 1984). Therefore, it is unlikely that the measured displacements along the Wasatch fault represent the maximum displacement along the surface rupture. If the locations where measurements were made had been randomly selected, it would be reasonable to assume that the average of all the displacements, which is about 2 m, would approximate the average displacement per event for past surface faulting events. However, the locations were selected where the fault is well-expressed topographically. This may bias the results towards values that are too large.

To account for the uncertainties in the displacement data, a range of values for the average displacement associated with the maximum earthquake is included in the probabilistic assessment of the maximum earthquake magnitude. Values of 1 m, 1.5 m and 2 m are assigned probabilities of 0.1, 0.6 and 0.3 respectively (Figure 14 and Table 2). Given the unsegmented model, the expected maximum earthquake on the Wasatch fault zone is about $\mathbf{M}_S$ 7-1/4. If the fault is segmented, the expected maximum magnitudes for the segments range from $\mathbf{M}_S$ 6-1/2 to 7-1/2 (Table 1).

Earthquake Recurrence Rate: The slip rate and displacement per event data presented in Table 3 are used to assess the earthquake recurrence rate of major surface faulting events on the various segments of the Wasatch fault zone and for the zone as whole. In addition to incorporating the

Table 3

	Recurrence Basis	SEGMENT		Site	Cumulative Vertical Displacement (m)	Age (1000's of years B.P.)	Point Estimate of Slip Rate (mm per year)	Vertical Displacement Per Event (m)[1]	Mean Recurrence Interval for Maximum Earthquake (years)	Comments and Sources of Data
		Model A	Model B							
Segmented Fault Rupture Model	--	Unnamed	Collinston	--	--	--	0.15	--	8,800	Slip rate assumed to be comparable to or less than East Cache fault; Swan and others, 1983. Slip rate assumed to be accurate to within about 30 percent.
	--	Collinston	Brigham City	Wellsville Mtns. Near Honeyville	26	150	0.17	--	7,250	Recurrence estimata based on seismic moment rate. Scott, 1980. Slip rate assumed to be accurate to within ebout 30 percent.
	Segment	Ogden	Weber	Kaysville	10. (.5) 11 (.5)	6 (.1) 8 (.7) 9 (.2)	1.3	1.6 [2]	1,350	Swen and others, 1980; Schwartz and others, 1984.
	Segment	Salt Lake City	Salt Lake City	Little Cottonwood Canyon	11.5 (.2) 14.5 (.7) 24.5 (.1)	17 (.2) 19 (.6) 21 (.2)	0.76	2.0 [2]	2,550	Swan and others, 1981b; Schwartz and Coppersmith, 1984.
			American Fork	--	--	--	--	--	1,900	"Zone" recurrence basis only.
			Provo	--	--	--	--	--	1,900	"Zone" recurrence basis only.
	Segment	Provo	Spanish Fork	Hobble Creek	11.5 (.5) 13.5 (.5)	11 (.2) 13.5 (.7) 15. (.1)	0.93	1.9 [6-7]	2,050	Swen end others, 1980, 1981c.
	Segment	Nephi	Nephi	North Creek	6.5 (.2) 7.0 (.6) 7.5 (.2)	5.1 (.5) 5.5 (.5)	1.3	2.3 [3]	1,750	Hanson and others 1981a; Hanson and Schwartz, 1982; Schwartz and Coppersmith, 1984.
	Segment	Levan	Levan	Deep Creek	2.5 (1)	6.3 (.2) 7.3 (.6) 8.3 (.2)	0.35	2.5 [1]	7,100	Hanson and others, 1981b; Schwartz end Coppersmith, 1984
			Fayette	--	--	--	0.20	--	10,000	This report. Slip rate assumed to be accurate to within ebout 50 percent.
	"Zone"	Central part of Zone (Brigham City to Nephi)		--	--	--	1.1	2.1	1,900 per segment	Average of data from Kaysville, Little Cottonwood Cenyon, Hobble Creek, North Creek and Deep Creek sites.
	WASATCH FAULT ZONE Unsegmented Model			--	--	--	0.80	--	280	
	WASATCH FAULT ZONE Combined Models			--	--	--	--	--	330	

---

[1] Standard Deviation of mean assumed to be 0.15. Number of events averaged is shown in brackets.

Table 3. Summary of geologic parameters used to characterize earthquake recurrence rate for the Wasatch fault zone

uncertainly in the correct recurrence model, described previously, the seismic hazard model also includes the uncertainty in the primary data, namely the uncertainties in the measured cumulative displacement, in the age of the displaced strata and the average displacement per event. Quantifying the uncertainty in each of these parameters allows the calculation of the probability distributions for the slip rate. The resulting probability distributions are presented on Table 1.

Given the unsegmented fault model the earthquake recurrence rate was calculated based on the seismic moment rate obtained from the estimated average slip rate. To arrive at an average rate, the slip rate data on Table 3 were weighted to reflect the segment lengths for model A. Model A was used because there are no independent slip rate data for the American Fork and Provo segments of model B. The overall average slip rate (weighted by segment length) is 0.8 mm/yr. The slip rate was distributed along the fault so as to produce a slip rate of 1.1 mm/yr in the central part of the fault consistent with the observed variation in rate.

Given the segmented fault model, the earthquake recurrence rate for the segments north of Brigham City and south of Nephi were estimated using the seismic moment rate approach because there are no data on the slip per event or on the timing of individual events for these segments.

For the central part of the fault zone, where there are slip-rate and displacement-per-event data from several localities, the recurrence rate for maximum events is estimated by dividing the slip rate by the average displacement per event. Uncertainty in these parameters was incorporated in the analysis as indicated by the distribution for recurrence rate shown in Table 1. Two bases were used to estimate the average slip rate and displacement per event. In one case (i.e. the "zone" recurrence basis in Table 1 and Figure 2), the segments along the central part of the fault between Brigham City and Nephi are considered to have the same rate of activity and the recurrence basis for these segments was calculated based on the average of the slip-rate and displacement-per-event data from the five sites located along this stretch of the fault (Table 1). The slip rate for the central part of the zone is 1.1 (±0.15) mm/yr based on data summarized by Schwartz and others (1984). The average displacement per event reported for paleoseismic events identified at the five sites along the central segments of the Wasatch fault zone is 2.1 (±0.1) m. These values were used to calculate the distribution for the recurrence interval for the maximum event shown in Table 1 for the "zone" recurrence basis. In the second case (i.e. the "segment" recurrence basis in Table 1), the slip rate and displacement data from each site shown in Table 3 were used to characterize the earthquake recurrence for the specific segments. In some cases (e.g. the American Fork and Provo segments of segmentation model B) only the "zone" recurrence basis could be used. Where both the "zone" recurrence basis and the "segment" recurrence basis were used, they were given equal weight.

The activity on the fault north of about Brigham City is significantly less active than the central part of the zone (Personius, 1987). Based on the subdued geomorphic expression of the northernmost part of the zone (i.e. the Unnamed segment in Figure 13a), it is assumed that the long term slip rate on this part of the fault is comparable to or less than the rate on the East Cache fault (see discussion below), and a nominal slip rate of 0.15 mm/yr was assigned to this part of the fault zone.

Immediately north of Honeyville, Utah (latitude 41° 33'N; i.e. the Collinston segment on Figure 13a and the Brigham City segment on Figure 13b), Scott (1980) reports that an alluvial fan, which he estimates to be about 150,000 years old, is displaced 26 m. This suggests an average slip rate of 0.17 mm/yr. This is comparable to the rate inferred for the northernmost part of the zone. There is insufficient information to directly assess the accuracy of these slip rates. In estimating the uncertainty in the earthquake recurrence rate on these segments of the fault, it is assumed that these slip rate values are only accurate to within about 30 percent.

The basis for slip-rate and the displacement-per-event data at the Kaysville, Little Cottonwood Canyon, Hobble Creek, North Creek and Deep Creek sites (Figure 1 and Table 3) are well documented in several papers and U.S. Geological Survey Open File Reports by Swan and others (1980, 1981a, 1981b, 1981c) and have been summarized by Schwartz and others (1984) and Schwartz and Coppersmith (1984, 1986). To quantify the uncertainty in the earthquake recurrence rates, distributions have been assigned to displacement and age data to reflect the uncertainty in these primary data. For example, at the Kaysville site, the cumulative vertical displacement is reported as 10 to 11 m since deposition of an alluvial fan estimated to be 8000 (+1000, -2000) years old. The actual displacement is equally likely to be anywhere within the 10 to 11 m range so these values are assigned equal weight (Table 3). The preferred age is assigned the highest probability weight (0.7). Ages of 6000 years and 9000 years were assigned weights of 0.1 and 0.2 respectively to reflect the judgement that it is unlikely that the fan is as young as 6,000 years and that it could be as old as 9,000 years (Schwartz and Coppersmith, 1984). Where the age of the displaced unit is based on radiocarbon dates, e.g. the age of 7,300 (±1000) ^{14}C years B.P. for the age of the displaced alluvium at the Deep Creek site, the reported error for this date is assumed to be within about one standard deviation of the actual age.

The available data indicate that the activity on the Wasatch fault zone dies out south of Levan. There are no reports on the rate of slip on the Fayette segment (Model B). This segment was assigned a nominal slip rate of 0.2 mm/yr based on the assumption of an event about every 10,000 years.

Table 3 presents the mean recurrence times for major surface faulting events on each of the fault segments. These are interpreted to represent the average repeat time for the maximum earthquake. Table 1 shows the distribution in the earthquake recurrence rates reflecting the uncertainty in the slip rate and recurrence data. Figure 14 presents the predicted recurrence rate for the entire zone. Based on the hazard model, the estimated return period for magnitude 7 or greater events is 330 (±90) years for the entire zone. This value compares favorably with an earlier estimate of 400 to 666 years based on the number of paleoseismic events inferred to have occurred on the central segments (Brigham City to Nephi) during approximately the past 8,000 years (Schwartz and Coppersmith, 1984). The shorter return period predicted by the model developed here is due to the inclusion of additional segments within the central part of the fault zone in the alternative segmentation model and contributions from the northern and southern segments of the fault zone which were not included in the Schwartz and Coppersmith estimate.

Oquirrh Mountains Fault Zone: The Oquirrh Mountains fault zone lies 25 km to 50 km west of the Wasatch Front (Figures 1 and 13). The fault zone consists of an alignment of late Pleistocene fault scarps at or near the boundary between the alluvial basin fill and the bedrock along the western side of the East Tintic and Oquirrh Mountains (Anderson and Miller, 1979) that indicates the presence of active westward dipping normal faults along this trend. This fault zone is discontinuous and is shown as two faults by Everitt and Kaliser (1979). These are the Oquirrh marginal fault along the eastern margin of Tooele Valley and the Oquirrh-Boulter-Tintic fault zone along the eastern margin of Rush Valley. The mapped onland faults extend northward along the western flank of Antelope Island beneath the Great Salt Lake (Figure 13a). The northern limit of Quaternary faulting is uncertain, similar faults may exist along the western flank of the Promontory Mountains.

Segmentation: Both unsegmented and segmented fault models are used in the seismic hazard model to characterize the fault rupture behavior of the Oquirrh Mountains fault zone. Figure 13a shows the locations of the five segments considered if the zone is segmented. Additional studies would undoubtedly result in a refinement of these somewhat arbitrarily defined segments, but comparison of the results from the alternative segmentation models used to characterize the Wasatch fault zone suggests that further refinement would not significantly affect the overall results of the hazard analysis.

Activity: Quaternary faulting has been recognized along all segments of the Oquirrh Mountains fault zone except the Promontory Mountains segment. Given the segmented fault model, a probability of 0.5 that the fault is an active seismogenic fault was assigned to the Promontory Mountains segment to account for the uncertainty regarding the existence of Quaternary faulting along this part of the zone.

Total Length: Uncertainty in the total length of an unsegmented Oquirrh Mountains fault zone was modeled to account for the uncertainty concerning the existence of active faulting north of the Great Salt Lake. Two values ranging from 180 km to 250 km are considered: 180 km is the combined lengths of the mapped traces along the four southern segments; and 250 km is the combined length if the zone extends to the northern end of the Promontory Mountains (Figure 13a). The two values were assigned equal weight.

Maximum Earthquake Magnitude: As there are insufficient paleoseismic data on the amount of displacement during past surface faulting events on this fault, the assessment of earthquake magnitude was based on rupture length and rupture area only (Figure 12b and Table 2). If the fault zone is unsegmented and 250 km long, the distribution on rupture length was assumed to be the same as for the unsegmented Wasatch fault (Table 3). If the fault zone length is 180 km, a 100 km rupture length is not considered credible, and weights were assessed for the remaining rupture lengths (Table 2). Given the segmented model, the maximum rupture lengths are assumed to be equal to the segment lengths (Table 1).

Table 1 presents the results of the maximum earthquake magnitude assessment for the Oquirrh Mountains fault zone. If the fault zone is unsegmented the most likely maximum earthquake is about magnitude 7-1/4. If the fault zone is segmented the most likely maximum earthquakes on the individual segments range from about magnitude 7 to 7-1/4.

Earthquake Recurrence Rate: The available data do not tightly constrain the time since the most recent surface faulting event or the recurrence interval between events on the Oquirrh Mountain fault zone. Along the northern part of the Oquirrh Marginal fault (Figure 13a) a series of recessional shorelines below the Provo level (younger than about 13,500 years B.P.) appear to be displaced across a prominent curvilinear fault scarp. The fault scarp just north of Bates Canyon is about 9m high. It consists of an upper slope 4.6 to 6m high that has been modified by shoreline or sub-lacustrine wave erosion and a lower steeper slope, 3.6 to 4.6 m high, that appears unaffected by lake processes and, therefore, represents a post-Provo surface faulting earthquake (Everitt and Kaliser, 1979; Woodward-Clyde Consultants, 1982). Based on the geomorphic expression of the fault and the absence of faulting in younger alluvial fans, Swan and Schwartz estimate that this event occurred between about 8,000 to 10,000 years ago and the recession of the lake from the Provo level about 13,500 years ago (Woodward-Clyde Consultants, 1982).

Most of the faulting along the East Tintic fault occurs within pre-Bonneville alluvial fan deposits (older than about 15,000 to 14,000 years B.P.) that lie above the Bonneville shoreline and, therefore, provides little information on the recency of faulting. Locally Everitt and Kaliser (1979) have mapped 0.6 m-high to 3 m-high scarps in strandline and alluvial fan deposits just below the Bonneville shoreline. Although the field relationships are not unequivocal, there seems to have been at least one major post-Bonneville surface faulting earthquake along the East Tintic fault (Woodward-Clyde Consultants, 1982).

The slip rate on the Oquirrh Mountain fault zone is very poorly constrained. The scarp heights reported above suggest a post-Povo slip rate of about 0.3 mm/yr on the Oquirrh Marginal fault and a post-Bonneville slip rate of about 0.04 mm/yr to 0.2 mm/yr on the East Tintic fault. The assessed distribution for average slip rate shown in Table 1 was based on the uncertainty in these point estimates of slip rate together with possible biases (described previously). Because of the limited data, no attempt was made to discriminate between the unsegmented and segmented models and all segments are assumed to have slip rates within this range. Based on the fault characterization parameters presented in Table 1, the estimated return period for magnitude 7 or greater earthquakes on the Oquirrh Mountains fault zone is 2200 (±800) years.

East Cache Fault: The East Cache fault lies on the east side of Cache Valley along the western base of the Bear River Range approximately 20 km to 40 km east of the Wasatch Front (Figures 1 and 13). It extends as a zone of westward-dipping Quaternary normal faults in a north-south direction for a distance of about 72 km from just north of James Peak in Utah, to Preston, Idaho (Cluff and others, 1974). Late Quaternary fault scarps along the East Cache fault are discontinuous and in many locations are subdued due to erosion or are buried by Holocene alluvial fans. Paleoseismic investigations (Swan and others, 1983; McCalpin, 1987) show that there have been repeated late Pleistocene surface faulting events and at least one Holocene event on the East Cache fault near Logan, Utah.

Segmentation: Both unsegmented and segmented fault models are used to characterize the rupture behavior of the East Cache fault. In this analysis the fault was divided into two segments, the Logan segment, which is 47 km long and the Richmond segment, which is 25 km long (Figure 13a). A salient in the range front immediately north of Smithfield Canyon is interpreted to reflect a structural barrier between these segments. McCalpin (1987) proposes a three segment model suggesting the possibility of shorter segments. This model, however, has not been explicitly incorporated into the analysis.

Maximum Earthquake Magnitude: The maximum magnitude logic tree for the East Cache fault is similar to that for the Wasatch fault shown in Figure 14. If the fault is assumed to be unsegmented, two rupture lengths are considered (Table 3). These are a rupture length of 36 km, which is 50 percent of the total fault length; and 47 km, which is equivalent to the longest segment included in the seismic source model. There are insufficient paleoseismic data along the East Cache fault to assess the average displacement per event. Swan and others (1983) and McCalpin (1987) report displacements for individual events on the fault near the mouth of Logan Canyon of 1.4 m to possibly as much 2.4 m. These values are comparable to the fault displacements observed along the Wasatch fault zone (Swan and others, 1984; Schwartz and Coppersmith, 1986). Therefore, the range of values and assigned probabilities used to characterize the average displacement per event during a maximum earthquake on the Wasatch fault zone were also assumed to be representative of the East Cache fault. If the East Cache fault is unsegmented, the most likely maximum earthquake is about magnitude 7-1/4. If the fault is segmented, the most likely maximum earthquake on the Logan and Richmond segments are about magnitude 7-1/4 and 7 respectively (Table 2).

Earthquake Recurrence Rate: The slip rate and recurrence data for the East Cache fault are not well constrained. Two surface faulting events that post date the recession of Lake Bonneville from the Bonneville shoreline 14,000 to 15,000 years ago have been identified near the mouth of Logan Canyon (Swan and others, 1983). This suggests an average recurrence rate of about 7,250 (±250) years for maximum events. The second most recent event occurred post 15,000 years B.P. and before formation of the Provo delta about 13,500 years ago. The age of the most recent post Provo displacement is not well constrained so the actual interval between these events is not known.

At the mouth of Logan Canyon, the cumulative displacement of the Bonneville shoreline deposits is about 2.8 m and the displacement of the Provo delta is 1.4 m, suggesting average slip rates of about 0.2 mm/yr and 0.1 mm/yr respectively. These rates are about four to 13 time slower that the rates reported for the Wasatch fault zone between Brigham City and Nephi (Table 3).

Slip rates ranging from 0.05 mm/yr to 0.2 mm/yr were included in the source model for the East Cache fault (Table 1) reflecting possible bias in the single point estimate as well as the fact that the slip rates are calculated based on only two slip events and the timing of the next event could have a significant impact on the calculated slip rates. Most of the weight is assigned to values close to the rates observed near Logan. The average slip rate is assumed to be the same on both segments of the East Cache fault. Based on the seismic hazard analysis the average recurrence interval for magnitude 7 or greater earthquakes on the whole East Cache fault zone is 7,500 (±2,700) years.

West Valley Fault Zone: The West Valley fault zone, originally called the Jordan Valley fault zone and subsequently renamed by Keaton and others (1986), consists of a series of mostly east-dipping normal faults that displace late Quaternary lake deposits in Salt Lake Valley. West facing scarps form graben locally. As mapped by Keaton and others (1986) the total length of the zone is about 18 km. The fault zone is within about 5 km of downtown Salt Lake City (Figures 1 and 13).

Activity: The relation of the West Valley fault zone to the Wasatch fault zone is not clear. The short length relative to the height of the fault scarps, the discontinuous nature of the fault and its close proximity to the Wasatch fault indicate that the West Valley fault zone may represent sympathetic faulting due to large earthquakes on the Wasatch fault zone. Keaton and others (1986) argue that the size of the fault scarps, the location of earthquake epicenters in the central part of Salt Lake Valley, and the evidence for repeated Holocene displacements strongly suggest that the West Valley fault zone is a seismogenic structure that operates independently of the Wasatch fault zone. Both of these interpretations are included in the analysis with equal probability.

Maximum Earthquake Magnitude: Given that the West Valley is an independently active source, it is modeled as a single fault segment because its overall length is so short. The maximum rupture length is assumed to be equal to the total length of the zone (18 km). The probability distribution for the maximum earthquake magnitude on the West Valley fault was calculated based on a rupture length of 18 km. The range of down-dip geometries considered included the effect of truncation of the fault by the west dipping Wasatch fault. The maximum earthquake magnitude probability distribution is presented in Table 1. The available data indicate the most likely maximum magnitude on the West Valley fault zone is about magnitude 6-1/2 if the fault is an independent seismogenic structure.

Earthquake Recurrence Rate: The earthquake recurrence on the West Valley fault zone is estimated based Holocene slip-rate data from on Keaton and others (1986). Based on the ranges of values that they calculated for different post-Lake Bonneville marker horizons (12,000 years old and younger), the Holocene slip rate is likely to be in the range of 0.3 mm/yr to 0.5 mm/yr. The actual slip rate is judged to be equally likely to be anywhere within this range, therefore both values are assigned equal weights (Table 1). Assuming the West Valley fault zone is independently generating earthquakes, these values yield a repeat time for magnitude 6-1/2 or greater earthquakes of about 8,000 years. This is within the range of Keaton and others preliminary estimates for the recurrence of surface faulting events based on their displacement data.

Hansel Valley Fault Zone: Hansel Valley was the source of the 12 March 1934 Hansel Valley earthquake (M_L 6.6). Surface fault rupture occurred along the west side of Hansel Valley for a distance of about 11 km producing a series of scarps up to half a meter high in an area of older Holocene fault scarps (Anderson and Miller, 1979). Slemmons (1977) reports a maximum displacement of 1.2 m for this event. The zone of Quaternary faulting is inferred to extend northwards along the west flank of the Hansel Mountains (Anderson and Miller, 1979), suggesting a total fault length of about 25 km. The activity of the northern part of the zone is not known.

Segmentation: Despite the short length of the fault, both an unsegmented and a segmented model are included in the source model for the Hansel Valley fault because of the apparent differences in the Quaternary displacements along the fault. Nonetheless, because of the short overall length of the fault, it seems less likely that the segmented model would define the maximum earthquake. Accordingly, the unsegmented model is assigned slightly higher weight, 0.6, than the segmented model, 0.4 (Table 1).

Activity: If the fault is unsegmented, the entire length of the fault is assumed to be active. In the segmented model, the fault is divided into two segments. The southern segment coincides with the 1934 surface rupture. The northern segment consists of the 14 km-long inferred extension to the north. The segment boundary coincides with a marked change in the character of the range and a large saddle along the crest of the range. The northern segment is assumed to have a fifty-fifty chance of being active (Table 1).

Maximum Magnitude: Given the unsegmented model, it is assumed that the entire 25 km-long fault could rupture during the maximum earthquake; given the segmented model, the maximum rupture lengths are assumed to be equal to the segment lengths (Table 1). Table 1 shows the discretized distribution resulting from the maximum earthquake magnitude logic tree. Given the unsegmented model, the expected maximum magnitude is about 6-3/4. Given the segmented model, the expected value is about magnitude 6-1/2 for both segments. In this case, the 1934 Hansel Valley earthquake would represent a maximum event.

Earthquake Recurrence Rate: For the unsegmented fault model and for the North Hansel Mountains segment of the zone given the segmented model, the rate of earthquake recurrence is estimated based on slip rate. The rate on the South Hansel Mountains segment also incorporates the results of McCalpin's (1985) study of the Quaternary history of faulting of the Hansel Valley area.

Slip rate data on the Hansel Valley fault are not well constrained. McCalpin (1985) reports that the probable tectonic throw during the past 26,000 years ranges from 1.2 m to 2.5 m. This suggests a slip rate of from 0.05 mm/yr to 0.1 mm/yr. These values were used to characterize the average slip rate on the Hansel Mountains segment and for the entire fault for the unsegmented model (Table 1). The values were assigned equal weight.

McCalpin infers that there have been three surface faulting events in Hansel Valley during about the past 26,000 years. This suggests an average recurrence interval of about 8,700 years. He reports that the most recent event prior to the 1934 earthquake occurred about 12,000 years ago, indicating an interval of about 12,000 years between events. These two estimates of the recurrence rate were assigned equal weight (Table 1).

Given the segmented model, there are no available data to constrain the timing of past events or the slip rate on the North Hansel Mountains segment. Based on the lack of evidence for late Quaternary faulting and the subdued geomorphic expression of the fault, it is assumed that the slip rate on the North Hansel Mountains segment is comparable to, or less than, the slip rate on the South Hansel Mountains segment. Slip rates ranging from 0.01 mm/yr to 0.1 mm/yr were assigned for the North Hansel Mountains segment. The recurrence interval for magnitude 6 1/2 or greater earthquakes on the Hansel Valley fault zone is 11,000 (±5,000) years.

East Bear Lake Fault: The East Bear Lake fault is approximately 65 km to 75 km east of the Wasatch Front (Figures 1 and 13). It is an approximately 50 km-long, westward-dipping normal fault that lies along the east side of Bear Lake and Bear Lake Valley separating the valley to the west from the Bear Lake Plateau and the southern part of the Aspen Range to the east (Figure 1).

Segmentation: Both unsegmented and segmented fault rupture models are included in the source model for the East Bear Lake fault. Preliminary reconnaissance of the East Bear Lake fault by the U.S. Geological Survey suggests that the late Quaternary history of faulting is different for the northern and southern parts of the fault (A. Crone and M. Machette, 1986, personal communications). North of Bear Lake the fault appears to have had very recent displacement. Where the fault crosses the alluvial terraces along Bear River, the fault scarps appear to displace all but the youngest meander scars suggesting late Holocene faulting. To the south, no evidence of Holocene faulting has been observed. Wave cut scarps associated with higher mid-Holocene(?) lake levels post-date the most recent faulting. The youngest deposit, displaced by the fault where it crosses North Eden Canyon and South Eden Canyon, is estimated by A. Crone (1986, personal communication) to be late Pleistocene in age (approximately 15,000 years old). It is possible that the recent faulting observed to the north also occurs to the south on a fault trace that might be beneath the lake west of the mapped trace of the fault. Accordingly, two models are considered: an unsegmented model where the fault is treated as a single 50 km-long fault; and a segmented model that treats the 23 km-long Montpelier segment to the north and the 27 km long Bear Lake segment to the south as independent sources characterized by different fault behavior. The available data suggest that the fault is segmented and the unsegmented model is assigned a weight of only 0.2 (Tables 2 and 3).

Maximum Earthquake Magnitude: Except for the lack of data on the amount of displacement per event, the approach used to estimate the probability distribution for the maximum earthquake magnitude is the same as that used for the Wasatch fault zone. If the East Bear Lake fault is unsegmented, two maximum rupture lengths are considered. Because there have been historic surface fault ruptures in the Basin and Range up to 61 km, 100 percent rupture of the 50 km-long East Bear Lake fault is considered as a possible maximum rupture length. Twenty seven kilometers, which is the length of the longest segment and is approximately equivalent to 50 percent of the mapped length of the fault, is considered to be a slightly more likely maximum rupture length (Table 2). Regardless of the segmentation model, the most likely maximum earthquake on the East Bear Lake fault is 6-3/4 to 7 (Table 1).

Earthquake Recurrence Rate: The available data indicate a long interval between surface faulting events on the East Bear Lake fault. The rate of activity is probably less than the rate of activity on the East Cache fault. Based on their limited reconnaissance investigations of the fault, M. Machette and A. Crone (personal communications, 1987) estimate that there has only been one surface faulting event on the Montpelier segment during approximately the past 8000 years. Based on the freshness of the fault scarp, this event, which had a displacement of about 2 m, appears to have occurred fairly recently. There do not appear to have been any faulting events on the Bear Lake segment for about the past 15,000 years. Despite the poor constraints on the recurrence interval for the East Bear Lake fault, the available evidence clearly indicates that the fault is significantly less active than the Wasatch fault. Intervals of 8,000 years and 15,000 years are assumed to characterize the recurrence of surface faulting events on the Montpelier and Bear Lake segments respectively and the slip rate is assumed to be on the order of 0.05 to 0.1 mm/yr (Table 1). The seismic hazard model gives a return period for maximum events of 7200 (±2000) years for the fault zone.

Comparison of Predicted and Observed Earthquake Frequency

The hazard model developed above can be used to predict the regional earthquake recurrence rates. Figure 15 compares the predicted earthquake cumulative frequencies with the observed seismicity rate. Figure 15a shows the mean recurrence estimates for the individual sources and the sum of the recurrence for all sources. The recurrence estimates for the West Valley fault and the Oquirrh Mountains fault zone have been weighted by the probabilities of activity assigned to the various segments. Figure 15b

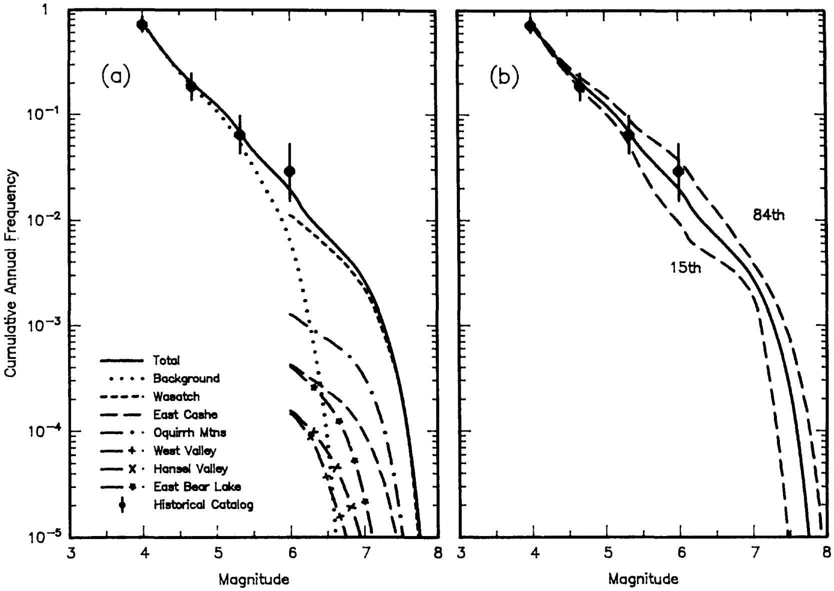

Figure 15 - Comparison of predicted recurrence rates for seismic sources with observed frequency of earthquakes. (a) Mean recurrence estimates for individual sources and total of all sources. (b) Fractiles of predicted distributions of earthquake recurrence compared with one standard deviation error bars for regional recurrence rate based on observed seismicity.

compares the fractiles of the distribution for earthquake recurrence obtained from the distribution in source parameters with the one standard deviation error bars on the regional seismicity rate. As can be seen, the sum of the predicted rates for all sources yields an estimated rate consistent with the historical record. The wider distribution in the estimated frequence of events near magnitude 6 results from the uncertainty in the appropriate form of the magnitude distribution. The Wasatch fault zone represents the dominate source of potential future large magnitude events in the region.

ATTENUATION RELATIONSHIPS

Attenuation relationships define the values of a ground motion parameter, such as peak ground acceleration, velocity, displacement, or response spectral values, as a function of earthquake magnitude and distance. For this study, attenuation relationships for peak ground acceleration and response spectral accelerations are required as inputs to the probabilistic ground motion analysis.

Attenuation relationships in the U.S. that are well constrained by strong motion data have been developed based on statistical analyses of data that are largely from California. To date, only one strong motion recording has been obtained in Utah, in Logan at a distance of about 30 Km from the 1962 $\mathbf{M}_L$ 5.7 Cache Valley earthquake. During the 1983 $\mathbf{M}_s$ 7.3 Borah Peak, Idaho earthquake, several recordings were obtained in Idaho at distances of about 90 to 100 Km. Aftershocks of the Borah Peak earthquake produced recordings at closer distances. The Appendix to this paper provides comparisons of ground motion data recorded during these earthquakes with recently developed attenuation relationships that are based largely on data from California. From the comparisons presented in the Appendix, it is concluded that the Cache Valley and the Borah Peak data exhibit the degree of scatter relative to the attenuation curves that is typically observed in strong motion data. The data are too limited to either strongly support or refute the applicability of California attenuation relationships to Utah.

In general, the earthquake ground motion recorded at a site can be viewed as the product of the earthquake source characteristics, the attenuation characteristics along the travel path between the earthquake source and the site, and the local site effects. Each of these factors may influence the attenuation relationships appropriate for a given region. Evidence regarding similarities or differences of these factors between Utah and California are briefly reviewed below.

Earthquake Source Characteristics

McGarr (1982, 1984) has suggested that normal faulting, the type of faulting expected for major earthquakes along the Wasatch front, results in lower ground motion than strike-slip faulting or reverse faulting for a given size event. Because California-type attenuation relationships are based on strong motion data predominantly from strike-slip and reverse faulting earthquakes, McGarr's studies suggest that the normal faulting environment in Utah might result in lower ground motion than in California. On the other hand, studies by Campbell reported in Campbell (1987) indicated only minor differences in ground motion attenuation between extensional and compressive stress environments within California. Campbell (1987) also found significantly higher ground motions for dip-slip faulting than for vertical strike-slip faulting. However, his results for dip-slip faulting are based on data almost entirely from reverse and thrust faulting earthquakes. Analysis of a sufficiently large strong motion data base to support and quantify the influence of a normal faulting environment is lacking at present.

Source-to-site Attenuation Characteristics

Several studies have addressed regional attenuation characteristics in Utah and in adjacent and broader regions of the Western U.S. King and Hays (1977) analyzed velocity seismograph data in northern Utah from four aftershocks (M_L 2.9 to 4.1) of the 1975 Pocatello Valley, Idaho earthquake. They concluded that higher-frequency (greater than 1 Hz) response spectral values attenuated at a faster rate in northern Utah than in California.

Griscom and Arabasz (1979) examined regional attenuation in Utah from a study of Wood-Anderson seismograph data. They concluded that the rate of attenuation in Utah might be greater than the rate of attenuation in southern California. Griscom (1980) analyzed Wood-Anderson seismograph data for Utah and also analyzed the attenuation of Modified Mercalli intensities for five Utah earthquakes. On the basis of both these analyses, she concluded that attenuation in Utah may be slightly greater than in coastal California.

McGuire (1983) analyzed the attenuation of Modified Mercalli intensities for five northern Utah earthquakes and four other earthquakes from the Rocky Mountain region. He combined results of his analyses of intensity attenuation with ground motion versus intensity relationships (the latter relationships based largely on California strong motion data) to derive ground motion attenuation relationships for northern Utah. By comparing his derived expression for velocity attenuation with the attenuation relationships for Wood-Anderson seismograph standard amplitudes for California, McGuire concluded that the rate of velocity attenuation could be slightly lower in Utah than in California, but that given the uncertainties in the analysis, the differences were not resolvable.

Several studies have examined Modified Mercalli intensity attenuation in broad regions of the U.S. As they pertain to evaluating attenuation along the Wasatch Front in northern Utah, all of these studies have the limitation that the regions considered are much larger than the specific region of the Wasatch Front. The studies by Everndon (1975), Howell and Schultz (1975), Chandra (1979),and Brazee (1980) all indicate a somewhat lower rate of intensity attenuation in the western mountain states than in California.

Recent studies have also been conducted of the intrinsic attenuation properties of the crust in different regions of the U.S. Singh and Herrmann (1983) present a regionalization of Q throughout the U.S., which indicates a lower rate of attenuation in Utah than in California. Chavez and Priestly (1985) found that the rate of attenuation at the Wood-Anderson instrument frequency (approximately 1.25 Hz) in Nevada was greater than in southern California and equal to or slightly less than in central California. On the other hand, Rogers and others (1986) concluded that the rate of attenuation was lower in the southern Great Basin, Nevada- California, than in central and southern California. Although these studies address intrinsic crustal attenuation over broad regions of the U.S. including Utah and in other parts of the Great Basin, they have the limitation of not specifically addressing attenuation in Utah.

The available evidence summarized above is equivocal. The studies that have focused specifically on Utah (King and Hays, 1977; Griscom and Arabasz, 1979; Griscom, 1980; and McGuire, 1983) suggest that the rate of attenuation in Utah is comparable to, or perhaps greater than, the rate of attenuation in California. On the other hand, some broad regional studies suggest that the rate of attenuation in Utah may be less than in California.

Local Site Effects

Local site conditions can also influence attenuation relationships. With the possible exception of areas underlain by lake deposits, the subsurface soil and rock conditions along the Wasatch Front are considered to be comparable to the range of conditions in California where ground motions have been recorded. Therefore, except for the lake deposits, site effects are not expected to lead to significant differences in attenuation relationships between Utah and California.

It is possible that the lake clays and silts along the Wasatch Front represent softer soil conditions than the soil conditions at ground motion recording sites in California. This could lead to differences in attenuation relationships between the two regions. The soil parameter that most directly characterizes soil stiffness from a site response standpoint is shear wave velocity. Shear wave velocity data for the lake deposits are in the process of being obtained and interpreted by the U.S. Geological Survey (Tinsley, 1987, personal communication), but are sparse at present. When such data become available, they will provide information on the stiffness of the lake deposits relative to soils at locations where ground motions have been recorded.

If the lake deposits are softer than typical soil conditions at strong motion recording sites, the potential effects on attenuation relationships would be greater for longer-period ground motion parameters (peak ground velocity and longer-period response spectral values) than for peak ground acceleration. Previous studies have indicated that peak ground acceleration attenuation is relatively insensitive to subsurface conditions (Joyner and Boore, 1981, 1982; Campbell 1981; Sadigh, 1983; Sadigh and others, 1986). Seed and others (1976a) and Seed and Idriss (1982) indicate that for acceleration levels greater than about 0.1 g, peak ground acceleration tends to decrease with decreasing soil stiffness and increasing soil depth; they also indicate the opposite trend for accelerations less than about 0.1 g. Attenuation relationships of Sadigh (1983) and Sadigh and others (1986) indicate somewhat lower peak ground accelerations for soil sites than for rock sites for higher acceleration levels and the opposite for lower acceleration levels, indicating a trend similar to that found by Seed and others (1976a) and Idriss (1978) for variations in peak acceleration with stiffness of a geologic deposit.

Hays and King (1982, 1984a, 1984b), King and others (1983), and Rogers and others (1984) have investigated site response effects on response spectral values along the Wasatch Front during very small amplitude motions produced mainly by distant underground nuclear blasts at the Nevada Test Site. Their studies indicate large spectral values for ground motions on the lake deposits relative to rock or to shallower, coarser-grained soils along the Wasatch Front. Also, comparison of their results with similar data for younger soil deposits in the Los Angeles, California region (Rogers and others, 1985) indicates that soil-to-rock spectral ratios are significantly larger for the lake deposits than for the California soil deposits. The results of studies by Hays and King (1982, 1984a, 1984b), King and others (1983), and Rogers and others (1984) provide an excellent guide to the relative soil amplification hazard of different geologic conditions along the Wasatch Front during future earthquakes. At present, it is difficult to use these results to quantify absolute levels of response spectral attenuation relationships for the lake deposits for strong ground shaking conditions because of potentially significant differences in the values of the spectral ratios for strong earthquake shaking as compared to small amplitude shaking. The potential differences arise from nonlinear (amplitude dependent) soil response effects and possibly from differences in the duration and frequency content of motions from local earthquakes and distant nuclear blasts.

Another factor that could influence ground motion along the Wasatch Front is the valley subsurface geometry (two and three-dimensional wave propagation effects). The influence of this factor has not been studied to date.

Based on the presently available data and evaluations discussed above, we conclude that, for peak ground acceleration, it is reasonable to assume that California attenuation relationships are applicable for the soil and rock conditions along the Wasatch front. Response spectral values at longer periods (greater than about 0.3 to 0.4 seconds) are more sensitive to soil conditions than peak ground acceleration. For areas along the Wasatch front underlain by rock and stiffer, denser soils such as predominantly sandy and gravelly fluvial and deltaic deposits, California attenuation relationships for response spectral values can reasonably be assumed to be applicable. The applicability of these relationships to areas of lake clays and silts is questionable, but alternative relationships are not available at present. The relationships used in the analysis may underestimate response spectra of longer-period motions in areas of soft lake deposits. The possible influence of soft soil conditions on response spectra obtained from the analysis is discussed later.

The attenuation relationships selected for the basic analyses are summarized below. Also summarized is a modified peak acceleration attenuation relationship that exhibits a lower rate of attenuation than the relationships used in the basic analyses. This relationship was developed and used in a sensitivity analysis to test the sensitivity of the results to a possibly lower rate of crustal intrinsic attenuation in Utah than in California.

Selected Attenuation Relationships for Peak Ground Acceleration

Two sets of peak acceleration attenuation relationships have been used in the basic analyses: one set for soil site conditions; and the second set for rock site conditions. The soil site set of relationships are the relationships of Joyner and Boore (1982), Sadigh and others (1986), and Campbell (1987). Joyner and Boore's (1982) relationship was modified by Joyner and Fumal (1985) to be applicable to the random horizontal component rather than the larger component of ground motion. The modified relationship, which is consistent in this respect with Sadigh and others (1986) and Campbell (1987), was used. Sadigh and others' (1986) relationship is summarized in Table 4. Campbell's (1987) relationship incorporates an anelastic attenuation term; his value of anelastic attenuation for California was used. Sadigh and others (1986) and Campbell (1987) distinguish the effect of the type of faulting (whether strike slip or reverse) in their attenuation relationships. Their relationships for strike-slip faulting, which give lower peak accelerations than those for reverse faulting, were used. As noted earlier, whether a normal faulting environment would lead to higher or lower ground motions than a strike-slip environment is not clear at present.

McGuire's (1983) attenuation relationships were not used in the analysis because of the large uncertainties involved in deriving peak acceleration attenuation relationships from intensity data. McGuire's relationships

TABLE 4

Values of Coefficients for the Attenuation Relationships of Sadigh and Others (1986) for Horizontal Peak Ground Acceleration and Pseudo Absolute Spectral Accelerations

Ground Motion	Period	Coefficient							
Parameter, y	(Sec)	b_1	b_2	b_3	b_4	b_5	b_6	b_7	σ_y
				Soil Site Conditions					
Peak Ground Acceleration	--	-2.611	1.1	0	2.5	-1.75	0.8217* 0.3157**	0.4814* 0.6286**	1.26-0.14M* 0.35**
Pseudo Absolute Spectral Acceleration (5% Damping)	0.1	-2.024	1.1	0.007	2.5	-1.75	0.8217* 0.3157**	0.4814* 0.6286**	1.332-0.148M* 0.37**
"	0.2	-1.696	1.1	0	2.5	-1.75	0.8217* 0.3157**	0.4814* 0.6286**	1.453-0.162M* 0.40**
"	0.3	-1.638	1.1	-0.008	2.5	-1.75	0.8217* 0.3157**	0.4814* 0.6286**	1.486-0.164M* 0.42**
"	0.5	-1.659	1.1	-0.025	2.5	-1.75	0.8217* 0.3157**	0.4814* 0.6286**	1.584-0.176M* 0.44**
"	1.0	-1.975	1.1	-0.060	2.5	-1.75	0.8217* 0.3157**	0.4814* 0.6286**	1.62-0.18M* 0.45**
"	2.0	-2.414	1.1	-0.105	2.5	-1.75	0.8217* 0.3157**	0.4814* 0.6286**	1.62-0.18M* 0.45**
	4.0	-3.068	1.1	-0.160	2.5	-1.75	0.8217* 0.3157**	0.4814* 0.6286**	1.62-0.18M* 0.45**
						Rock Site Conditions			
Peak Ground Acceleration	--	-1.406	1.1	0	2.5	-2.05	1.353* 0.579**	0.406* 0.537**	1.26-0.14M* 0.35**
Pseudo Absolute Spectral Acceleration (5% Damping)	0.1	-0.688	1.1	0.007	2.5	-2.05	1.353* 0.579**	0.406* 0.537**	1.332-0.148M* 0.37**
"	0.2	-0.479	1.1	-0.008	2.5	-2.05	1.353* 0.579**	0.406* 0.537**	1.453-0.162M* 0.40**
"	0.3	-0.543	1.1	-0.018	2.5	-2.05	1.353* 0.579**	0.406* 0.537**	1.486-0.164M* 0.42**
"	0.5	-0.793	1.1	-0.036	2.5	-2.05	1.353* 0.579**	0.406* 0.537**	1.584-0.176M* 0.44**
"	1.0	-1.376	1.1	-0.065	2.5	-2.05	1.353* 0.579**	0.406* 0.537**	1.62-0.18M* 0.45**
"	2.0	-2.142	1.1	-0.100	2.5	-2.05	1.353* 0.579**	0.406* 0.537**	1.62-0.18M* 0.45**
"	4.0	-3.177	1.1	-0.150	2.5	-2.05	1.353* 0.579**	0.406* 0.537**	1.62-0.18M* 0.45**

Notes:

* Magnitude <6.5
** Magnitude ≥6.5

General Note: Coefficients b_1 through b_7 are for use in the relationship: $\ln y = b_1 + b_2 M + b_3 (8.5-M)^{b_4} + b_5 \ln (R + b_6 e^{b_7 M})$ where M is moment magnitude. σ_y is the standard error of estimate of the relationship. The relationships are those derived for strike-slip faulting earthquakes.

show about the same rate of attenuation as those selected for use and differ significantly in amplitude (give higher amplitudes) only for events of magnitude less than about M_L 6.

The median attenuation curves for the selected relationships are compared in Figure 16 for earthquake magnitudes of 5.5, 6.5, and 7.5. The relationships were developed using magnitude definitions that are equivalent to M_L magnitude in the range of 3 to 7 and M_s magnitude in the range of 5 to 7.5. As discussed earlier, it is assumed that the relationship between strong ground motion and M_L and M_s magnitudes in Utah is similar to that observed in California.

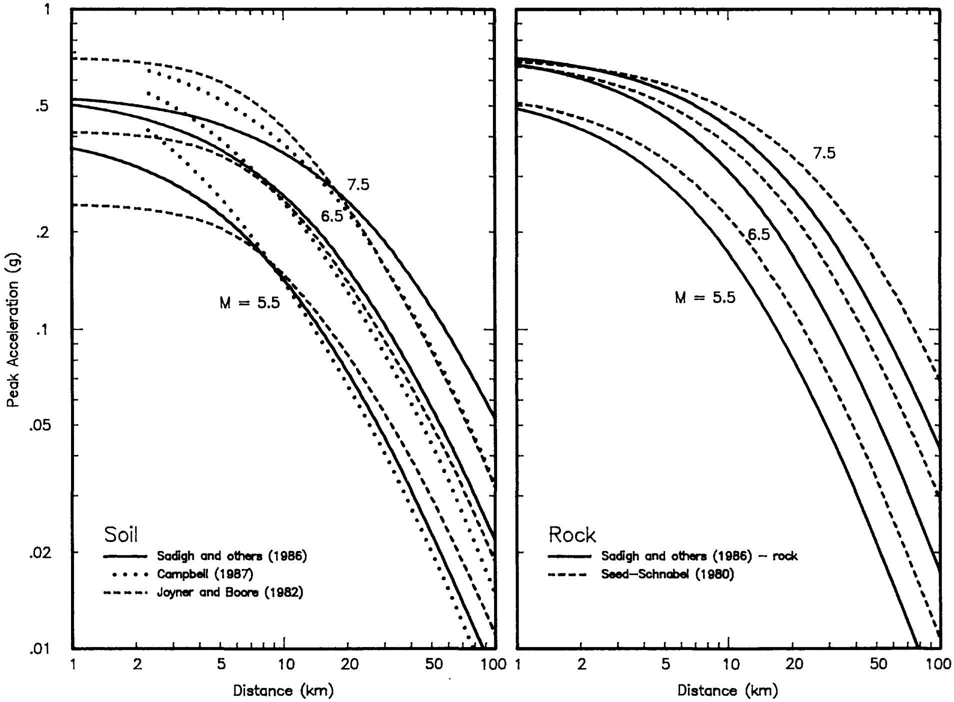

Figure 16 - Peak horizontal acceleration attenuation relationships used in the seismic hazard analysis.

Distance definitions for the attenuation relationships differ. For purposes of the comparisons shown in Figure 16, distance is as defined by each investigator (closest distance to fault rupture surface for Sadigh and others, 1986; closest distance to fault rupture surface in the seismogenic zone for Campbell, 1987; and closest horizontal distance to the vertical projection of fault rupture to the ground surface for Joyner and Boore, 1982). In using Campbell's (1987) relationship, a depth to the seismogenic zone of 2 km has been assumed. Therefore in Figure 16, acceleration values are not plotted for distances less than 2 km for Campbell's relationship. In the probabilistic seismic hazard analysis, distances have been used in each case that are consistent with the definitions for the respective relationships.

The rock site set of relationships selected for the analysis include two of the above-mentioned relationships, Joyner and Boore (1982) and Campbell (1987), and two additional relationships, those of Seed and Schnabel (1980) and Sadigh and others (1986) (the latter relationship summarized in Table 4). The relationships of Seed and Schnabel (1980) and Sadigh and others (1986) shown in Figure 16 were specifically developed for rock-site conditions. The relationship of Joyner and Boore (1982) does not distinguish between peak ground accelerations on soil and rock. The relationship of Campbell (1987) was developed using data from soil sites only; however, Campbell (1987) indicates that the ground motion estimates obtained therefrom are probably also appropriate for rock, at least for source-to-site distances of about 50 km or less. Campbell (1987, personal communication) indicates that prediction of peak accelerations on rock and soil may be little different at small distances, but that at large distances, predictions on rock may be substantially lower than on soil, indicating that use of his relationship for rock-site conditions may be conservative. On an overall basis, the four rock site relationships used in the analysis describe median peak accelerations averaging about 15 percent higher than the three soil site relationships within a distance of 50 km, decreasing to about 5 percent higher at a distance of 200 km.

The standard deviations in the predicted accelerations recommended by the developers of each attenuation relationship are incorporated into the seismic hazard analysis through the evaluation of the term $P(Z>z|m,r)$ in Equation 2. It is noted that the standard deviations differ significantly among the three relationships, being lowest for the relationship of Campbell (1987) and highest for that of Joyner and Boore (1982). Seed and Schnabel (1980) do not report a standard deviation for their attenuation curves. For their curves, the standard deviations defined by Sadigh and others (1986) were used.

Separate sets of probabilistic ground motion analyses were made using the soil-site set and the rock-site set of attenuation relationships described above. In each set of analyses, the different attenuation relationships were given equal weight in the logic tree formulation (Figure 2).

For the sensitivity analyses conducted for a lesser rate of attenuation, the following equation was derived to modify the attenuation relationships used in the basic analyses:

$$\mathbf{a}_s = \mathbf{a}\,(1 + 0.00675\mathbf{R}) \qquad (3)$$

where $\mathbf{a}_s$ is the peak acceleration adjusted for the lesser degree of attenuation used in the sensitivity analysis, $\mathbf{a}$ is the peak acceleration defined by each attenuation relationship used in the basic analyses, and $\mathbf{R}$ is source-to-site distance in km. The effect of this modifying relationship on attenuation is illustrated in Figure 17 for an attenuation curve for magnitude 6.5 constructed based on Sadigh and others (1986).

Equation (3) was derived in the following manner: Due to differences in anelastic attenuation between regions, the ratio of peak acceleration in a region with a slower rate of attenuation to peak acceleration in a region with a faster rate of attenuation can be expressed as

$$\mathbf{a}_s/\mathbf{a} = e^{\mathbf{R}(\gamma_f - \gamma_s)} \qquad (4)$$

where γ_f and γ_s are the coefficients of anelastic attenuation for the regions of faster and slower attenuation, respectively. Campbell (1982) evaluated the values of the coefficient of anelastic attenuation for California and Utah based on the regionalization of crustal $\mathbf{Q}$ in the U.S.

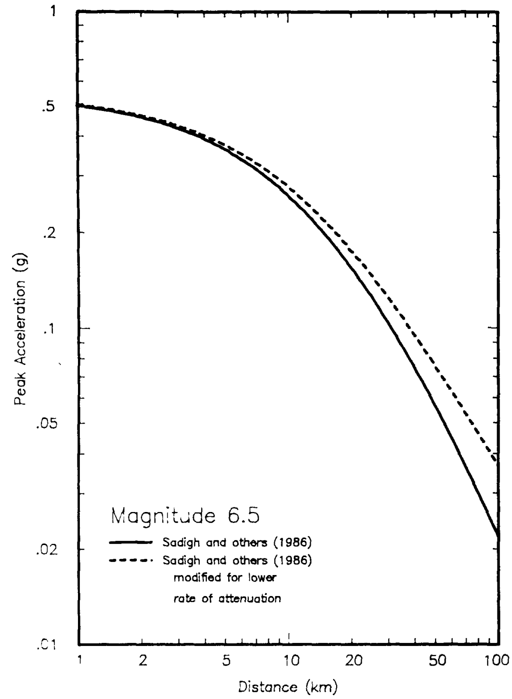

Figure 17 - Illustration of peak horizontal acceleration relationship modified for slower rate of attenuation.

by Singh (1981) (see also Singh and Herrmann, 1983) and the recommendations for predominant periods of ground motion developed by Seed and others (1969). The values of γ derived by Campbell (1982) are higher for California than for Utah. Equation (3) is a close approximation to Equation (4) using Campbell's (1982) results over the magnitude range 5.5 to 7.5 and the distance range 0 to 100 km.

Rogers and others (1986) estimated **Q** in the southern Great Basin to be nearly frequency independent and in the range of about 700 to 900. The corresponding value of γ may be evaluated from the expression, $\gamma = \pi f/vQ$, where **f** is frequency and **v** is the seismic wave velocity. Taking **v** = 3.5 km/sec, as assumed by Rogers and others (1986), and **Q** = 800, leads to the following approximate expression for γ:

$$\gamma = 0.0011f \qquad (5)$$

If it is assumed that Rogers and others' (1986) results are applicable to Utah, then the ratio of acceleration between Utah and California can be obtained by: evaluating γ for Utah as a function of frequency using Equation (5); taking γ for California equal to 0.0059 (incorporated in Campbell's 1987 acceleration attenuation relationship); and applying Equation (4). The results of this analysis are that for frequencies equal to or higher than about 5 Hz, γ Utah > γ California. For frequencies in the range of about 1 Hz to 5 Hz, γ Utah < γ California, but the effect of a lower γ for Utah would result in modifications to the basic attenuation relationships less than defined by Equation (3). Within source-to-site distances of 50 km, it is likely that the frequencies associated with peak accelerations exceed 1 Hz, indicating that Equation (3) would provide a conservative assessment of possible modifications to the basic attenuation relationships for peak acceleration. However, for ground motions occurring at low frequencies (such as response spectral values at frequencies less than 1 Hz), Rogers and others' (1986) results, if applicable to Utah, would indicate an effect on the attenuation rate greater than defined by Equation (3).

Selected Attenuation Relationships for Response Spectral Values

Sadigh and others (1986) and Joyner and Boore (1982) have developed attenuation relationships for response spectral values for 5 percent damping for a number of periods of vibration, for both soil site and rock site conditions. Sadigh and others' (1986) relationships are summarized in Table 4. Joyner and Boore's (1982) relationships are also summarized in Joyner and Fumal (1985). The relationships of Sadigh and others (1986) and Joyner and Boore (1982), equally weighted, were used in separate sets of analyses for soil and rock site conditions in the study. Examples of the attenuation curves defined by both relationships for soil site conditions are illustrated in Figure 18 for periods of vibration of 0.2 seconds and 2 seconds.

or soil site conditions, Joyner and Fumal (1985) extend the work of Joyner and Boore (1982) by presenting response spectral attenuation relationships that are a function of the soil shear wave velocity. Because of present lack of data on the shear wave velocity of the soils along the Wasatch front, just the single set of relationships for "soil" has been used in the analysis.

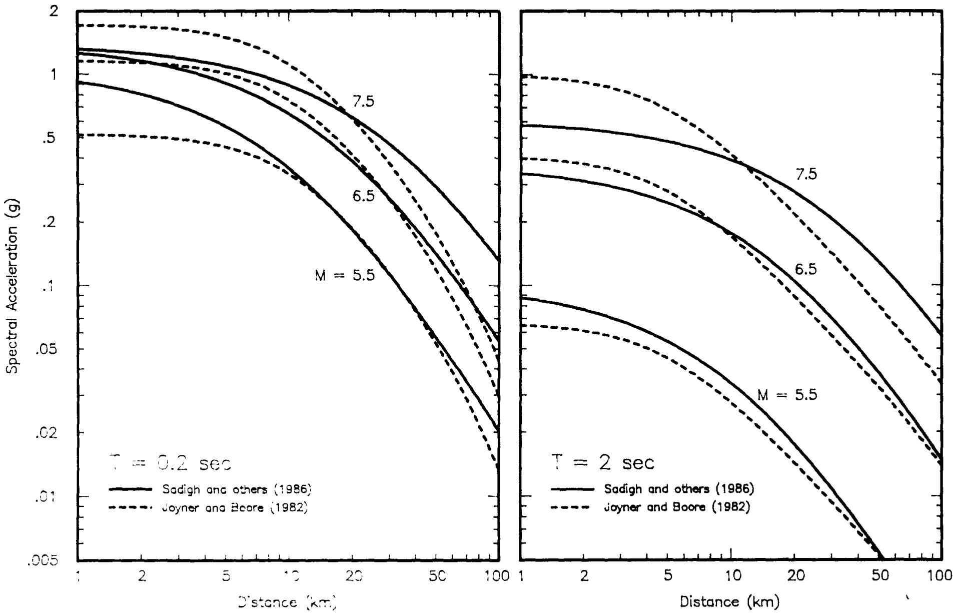

Figure 18 - Typical response spectral acceleration attenuation relationships (5% damping) for soil-site conditions used in seismic hazard analysis.

ANALYSIS RESULTS AND SENSITIVITY

Computed Hazard

The seismic hazard was mapped by performing hazard computations at 80 points located on an irregular grid throughout the study region defined in Figure 1. For hazard computations, the individual faults were modeled as segmented planer surfaces and the background zone was modeled as a set of closely spaced parallel fault planes occupying the background source region outlined in Figures 3 and 4. The probability density function for distance to earthquake rupture for each source was computed assuming earthquake ruptures were uniformly distributed horizontally along the fault and the focal depths were distributed according to the observed depth distribution for the region independent of magnitude (see Figure 7). The distance density functions were computed consistent with the distance measure used in each of the attenuation relationships. The rupture size of an event was specified by the relationship ln(rupture area) = 2.146M - 8.139 developed from the data presented by Wyss (1979). This relationship gives the mean rupture area for a specific magnitude rather than the median (mean log) rupture area. Studies by Bender (1984) have shown that the use of mean estimates of rupture size in the computation of hazard yields results nearly equal to those obtained when the statistical uncertainty in the size of individual ruptures is incorporated in the analysis.

The hazard was computed considering the contributions of earthquakes of magnitude M_L 5 and larger. Engineering experience has shown that even though relatively high peak accelerations have been recorded for earthquakes smaller than magnitude 5, generally events of this size have not caused structural damage to engineered buildings. Certain facilities may be sensitive to the effects of high frequency motions from smaller magnitude events so sensitivity analyses were made in which the contributions to hazard from earthquakes in the magnitude 4 to 5 range were included.

At each point in the study region distributions for the annual frequency of exceeding various levels of peak ground acceleration were developed by performing hazard computations using Equation 2 with the input parameters defined by each end branch of the logic tree shown in Figure 2. At each acceleration level, the complete set of computed results forms a discrete distribution for frequency of exceedance. Figure 19 shows the computed distributions of frequency of exceedance at three locations for a range of peak accelerations on soil sites. The selected acceleration levels correspond to the hazard levels used for regional hazard mapping discussed below and the identified return periods represent the mean frequency of exceedance for the distributions shown. The results shown are representative of the range in the computed hazard obtained for the study area. At all locations the computed distributions span approximately one order of magnitude in frequency of exceedance. The factors contributing to the uncertainty in the computed frequencies are discussed later in this section.

The computed distributions were used to obtain the mean frequency of exceeding various levels of peak ground acceleration (mean hazard curve) as

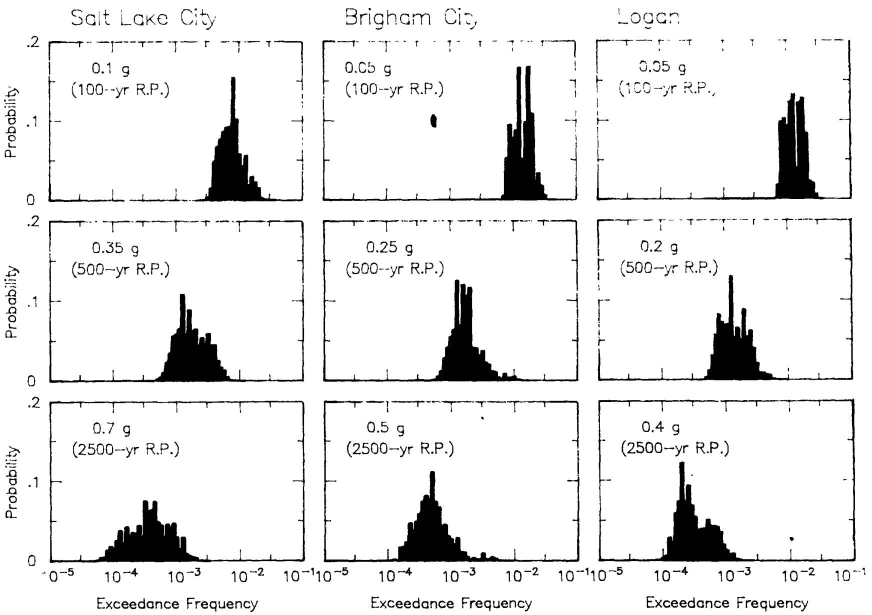

Figure 19 - Computed distributions for frequency of exceeding various levels of peak ground acceleration on soil at three locations. The top row of plots are for ground motion levels with a mean frequency of exceedance corresponding to a return period of approximately 100 years, the middle row to a return period of 500 years, and the bottom row to a return period of 2500 years.

well as hazard curves representing various percentiles. Figure 20 shows the resulting hazard curves for points at Salt Lake City, Brigham City and Logan. These results are for peak horizontal acceleration on soil sites. As indicated in the figure, the distributions in frequency of exceedance are somewhat skewed about the mean value, with the mean hazard curve located at about the 60th percentile of the distributions. The 90-percent confidence interval (5th to 95th percentile levels) in peak acceleration at a given frequency of exceedance typically represent a variation of ±50 percent about the level given by the mean hazard curve.

The computed hazard distributions represent our best judgement as to the uncertainty in defining the input parameters and thus represent our confidence in the estimated hazard. As indicated in Tables 1 through 3, extensive distributions are used to model the input parameters in the

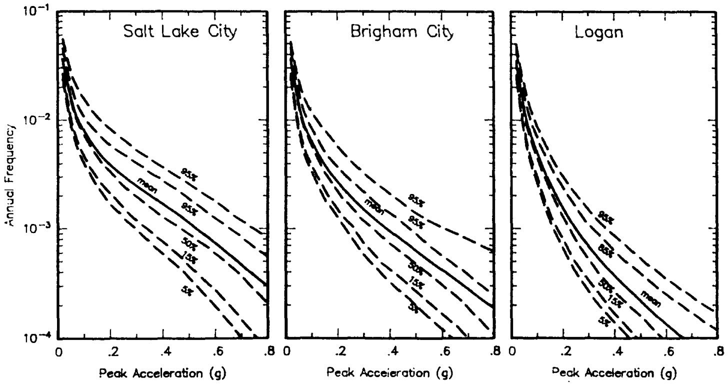

Figure 20 - Peak ground acceleration hazard curves for three locations. Shown are the mean hazard curves and hazard curves corresponding to the 5th, 15th, 50th, 85th, and 95th percentiles of the distributions for frequency of exceeding various levels of peak acceleration obtained at each site.

hazard model logic tree resulting in several thousand end branches. Limited sensitivity analyses conducted to investigate the effect of including more detained modeling of the individual parameter distributions showed no significant change in the computed fractiles. However, the more extreme fractiles should be considered to be less precisely defined than the central estimates.

The results shown in Figure 20 yield similar levels of peak acceleration at the three sites for return periods on the order of 100 years, but substantially different peak accelerations for longer return periods. The increased variation in acceleration level at longer return periods results from changes in the relative contribution of various earthquake sources to the hazard as a function of acceleration level and return period. Figure 21 shows the contributions of various sources to the hazard at six sites. The top row of plots presents the source contributions for the three sites illustrated in Figure 20. At each of the sites the hazard at low acceleration levels is dominated by the background seismicity. As the rate of occurrence of moderate magnitude events is assumed to be uniform throughout the background zone of seismicity, similar hazard levels are obtained at all three sites. For longer return periods the hazard is dominated by contributions from the identified faults, and their relative rates of seismic activity result in differences in the computed hazard depending on the proximity to the fault. This pattern was generally observed throughout

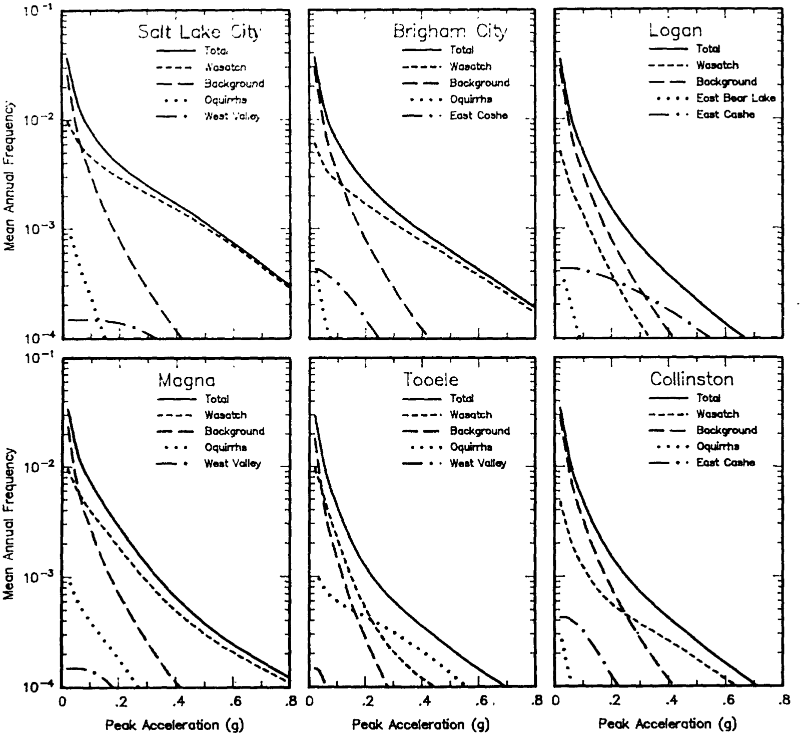

Figure 21 - Contributions of various sources to the computed mean hazard for six locations. Shown for each location are the mean hazard curves for various sources and the total mean hazard curve.

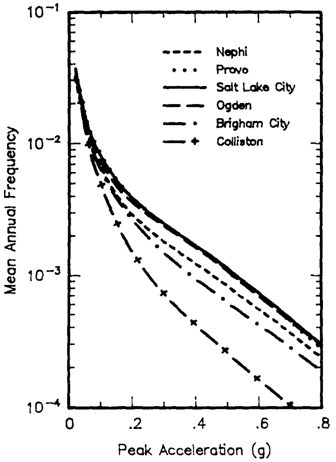

Figure 22 - Variation in the computed mean hazard along the length of the Wasatch fault zone from Nephi to Collinston.

the study area, as indicated by the results for additional sites shown in the bottom row of plots in Figure 21.

The differences between the computed hazard at Salt Lake City and at Brigham City reflect the modeled variations in the rate of activity along the length of the Wasatch fault zone. Figure 22 illustrates the variation in the computed hazard along the zone from Nephi to Collinston. As indicated in the figure, nearly identical results are obtained for sites along the central, active portion of the fault (latitude 40°N to 41.5°N). The hazard decreases slightly to the south as Nephi is approached and decreases significantly to the north beyond Brigham City where geologic evidence indicates a substantial decrease in the rate of fault movement. The spatial variation of seismic hazard throughout the study region is mapped in terms of contours of peak ground acceleration on soil sites for three return periods. These hazard maps are presented later in Figure 37.

Figure 23 illustrates the relative contribution of events in different magnitude and distance intervals to the computed mean hazard. Each plot in the figure presents a histogram of the percent contributions of events in 0.25 magnitude wide intervals. The histograms are in turn divided into the contributions from distance ranges of 0 to 10 km, 10 to 25 km, and greater than 25 km. As indicated by Figure 23, at higher probabilities of exceedance (short return periods) the contributions to hazard come from events in a wide range of magnitudes and distances. As the probability of exceedance decreases (return period increases), the hazard becomes increasingly dominated by the larger and closer events. The magnitude and distance range of contributions also narrows as the more active portion of the Wasatch fault is approached, indicating the increasing dominance of the fault contributions to the hazard as illustrated in Figure 21.

Contributions to Uncertainty

The distributions in the computed hazard shown in Figures 19 and 20 represent the cumulative effect of all levels of parameter uncertainty included in the hazard model (Figure 2). The relative contribution of various components of the model to the overall uncertainty can be identified readily from the logic tree formulation by computing the hazard holding

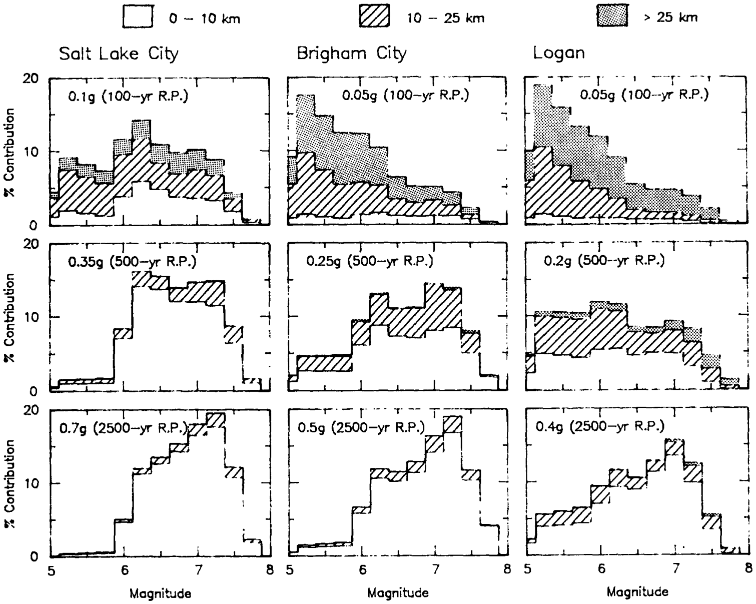

Figure 23 - Contributions of different magnitude events to total frequency of exceeding various levels of peak ground acceleration at three locations. The top row of plots correspond to a return period of approximately 100 years, the middle row to 500 years, and the bottom row to 2500 years. Contributions from different distance ranges are indicated by the three shaded region in each plot.

individual parameters fixed at specific values. For example, the contribution of uncertainty in soil site attenuation relationship can be obtained by computing the mean hazard assuming each of the three attenuation relationships is, in turn, the "correct" relationship, with weight of 1.0, and the other two have zero weight. The resulting hazard curves are shown in Figure 24 for three sites. In each plot the solid curve corresponds to the mean hazard and the heavy dashed curves to the 5th and 95th percentiles of the distribution in exceedance frequency shown in Figure 20. The three labeled curves are the resulting mean hazard for each of the soil site attenuation relationships and the differences between them represent the uncertainty in the computed hazard due to uncertainty in selecting the appropriate attenuation relationship.

The results shown in Figure 24 indicate that uncertainty in selecting the appropriate attenuation relationship generally has less significance at sites having higher hazard near the more active portion of the Wasatch fault than at sites having lower hazard away from the fault. The reason for this can be found by examining the contributions of events from various magnitude and distance ranges and the comparisons of the median attenuation relationships used in the analysis. At sites of lower hazard, such as Logan, there is a substantial contribution from events in the magnitude range of 5 to 6 (Figure 23). The differences in the hazard computed using the three attenuation relationships are greatest for this range of magnitudes and result from greater variability in the predicted median accelerations (Figure 16) enhanced by differences in the standard deviation about the median. For events at distances beyond 10 km, which have a large contribution to the hazard at Logan, Campbell's (1987) relationship has the lowest median values and the lowest standard deviation (0.30) while Joyner and Boore's (1982) relationship has the highest median values and the highest standard deviation (0.62). The smallest variability between the hazard curves is obtained for a return period of 500 years at Salt Lake City (similar results were observed at other sites along the more active part of the Wasatch fault). The contributions to hazard are largely from events of magnitude 6 to 7 occurring at distances of 10 km or less. The best agreement between the median attenuation curves shown in Figure 15 is

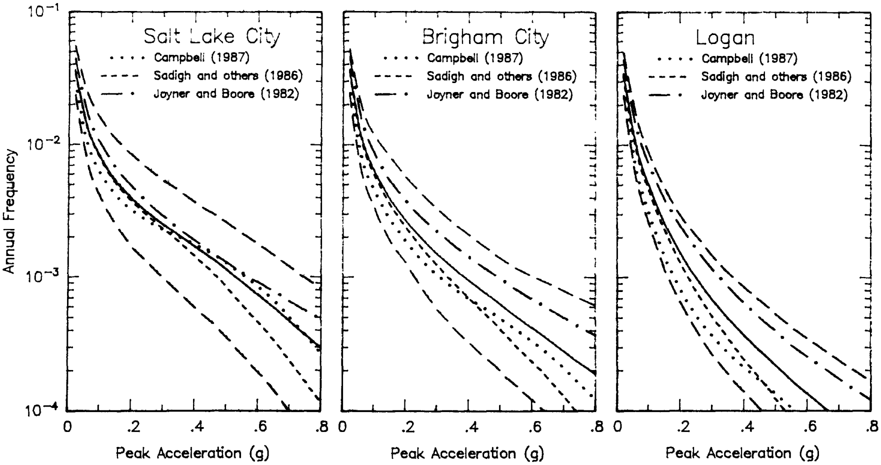

Figure 24 - Contribution to uncertainty in exceedance frequency from uncertainty in selecting the appropriate soil-site attenuation relationship. Solid curves are the computed mean hazard for each site and the long dashed curves are the 5th and 95th percentile hazard curves (see Figure 20). Conditional mean hazard curves obtained using each of the three attenuation relationships used in the analysis are labeled.

for events of magnitude 6.5 and the differences in the median curves at distances less than 10 km are partly compensated for by the differences in the standard deviation. In this magnitude and distance range, Campbell's relationship has the highest median values but the lowest standard deviation, while Joyner and Boore's relationship has the lowest median and the highest standard deviation. In general, as the range of magnitudes that contribute to the hazard increases, more variability between the median estimates of the three relationships is introduced into the analysis and the variability in computed hazard increases.

The results shown in Figure 24 also indicate that in areas of lower hazard, such as Logan, the uncertainty in hazard due to uncertainty in selecting the appropriate attenuation relationship becomes a major part of the total uncertainty in the hazard. At such sites, the computed hazard is largely dominated by the background seismicity (Figure 21) which has been modeled with a relatively smaller amount of uncertainty in the source parameters compared with the fault-specific sources (Figure 2). Thus, at such sites, the choice of attenuation relationship provides a relatively large proportion of the total uncertainty in the computed hazard.

The impact of uncertainty in recurrence model on the overall uncertainty in the frequency of exceedance is shown in Figure 25. Here the effect is opposite that shown in Figure 24, with greater variation obtained at locations of higher hazard. At sites where the hazard is largely due to events in the background source, such as at Logan, there is little uncertainty in the hazard as there is little uncertainty modeled for the earthquake recurrence rate in the background source. The variability increases as the dominance of the hazard by contributions from the faults increases (Figure 21) and reflects the large differences in the rate of magnitude 6 to 6.5 events predicted by the two recurrence models used for the faults (Figure 10). The percentage variability from the mean curve is somewhat lower at the highest acceleration levels because of the increasing contribution by the largest magnitude events whose predicted rate is insensitive to the choice of recurrence model. The overall mean hazard is skewed toward the characteristic hazard curve reflecting the greater weight assigned to this model in the hazard logic tree (Figure 2).

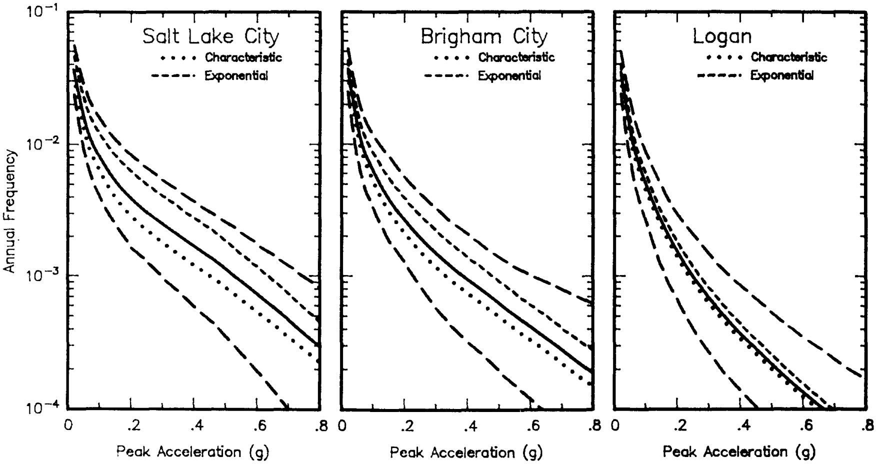

Figure 25 - Contribution to uncertainty in exceedance frequency from uncertainty in recurrence model. Conditional mean hazard curves obtained using the two recurrence models are labeled.

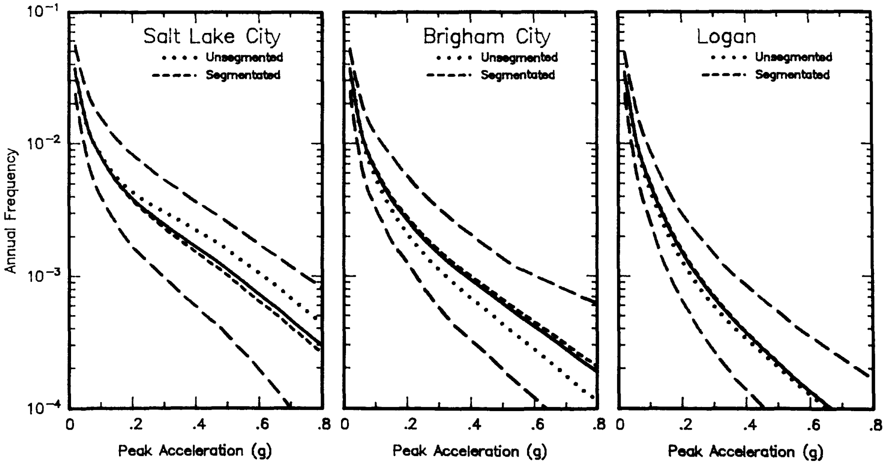

Figure 26 - Contribution to uncertainty in exceedance frequency from uncertainty in source segmentation. Conditional mean hazard curves obtained for unsegmented and segmented faults are labeled.

Figure 26 presents the influence of uncertainty in whether the faults are segmented or not. As indicated, the contribution to the total uncertainty is relatively small, being greatest where the contribution to hazard from the fault sources is greatest (and where the differences in recurrence estimates between the segmented and unsegmented models is the greatest). The opposite effects obtained at Salt Lake City and Brigham City reflect the difference between the recurrence estimate for individual segments versus the average recurrence rate assigned to the unsegmented model. Examination of the recurrence data presented in Table 1 indicates that the Wasatch fault segments near Brigham City (Ogden segment for Segmentation Model A; Weber segment for Segmentation Model B) have the highest recurrence rate relative to the average for the central active portion of the Wasatch, while the Salt Lake City segment has the lowest recurrence rate relative to the average.

For the Wasatch fault, two models of segmentation were considered, given that the fault is segmented. Figure 27 shows the effect of uncertainty in segmentation model at six locations along the fault. The two segmentation models produce significantly different results only in the vicinity of Brigham City. These differences arise due to differences in the northern extent of the most active portion of the Wasatch between the two models, extending to Brigham City in Segmentation Model A and extending to approximately 15 km south of Brigham City in Model B.

The variation in hazard due to uncertainty in fault activity is shown in Figure 28. On the left is shown the effect of uncertainty in the existence of a tectonically active extension of the Oquirrh Mountain fault zone to the north of the Great Salt Lake. This uncertainty was modeled in terms of uncertainty in the total length conditional on the Oquirrh Mountain fault zone being unsegmented or in terms of the state of activity of the northernmost segment (Figure 2 and Table 1). The combined effect of these two models is shown in the figure. The curve labeled "active northern extension" corresponds to an active Promontory segment for a segmented fault zone or a total length of 250 km for an unsegmented fault zone. The curve labeled "inactive northern extension" corresponds to an inactive Promontory segment for a segmented fault zone or a total length of 180 km for an

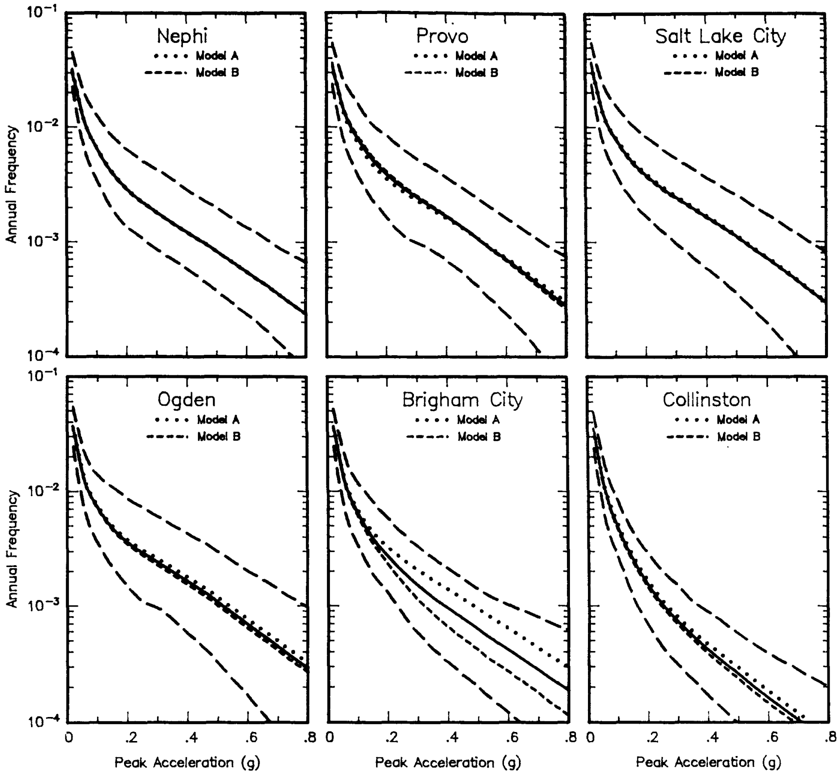

Figure 27 - Contribution to uncertainty in exceedance frequency from uncertainty in segmentation model at six locations along the Wasatch fault. Conditional mean hazard curves obtained using Segmentation Models A and B are labeled.

unsegmented fault zone. As can be seen, only at locations near the postulated northern extension of the fault zone, such as Promontory Point, is there any noticeable effect on the hazard; and even at this location the effect is small, due to the dominance of the hazard by the background source the more active Wasatch fault.

The hazard model also included uncertainty in whether or not the West Valley fault is an independent active source. As shown on the right in Figure 28, the effect on the computed hazard in the vicinity of Salt Lake City was very small because the West Valley fault has only a small contribution to the total hazard (see Figure 21) due to its limited extent, both in terms of length and downdip width.

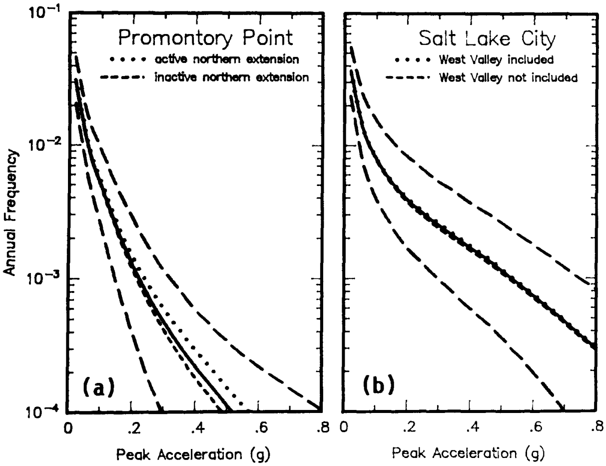

Figure 28 - Contribution to uncertainty in exceedance frequency from uncertainty in source activity. (a) shows the effect of uncertainty as to the existence of a northern extension of Oquirrh Mountains fault zone. Curves labeled "active northern extension" corresponds to active Promontory segment for a segmented fault zone or a total length of 250 km for an unsegmented fault zone. Curves labeled "inactive northern extension" corresponds to inactive Promontory segment for a segmented fault zone or a total length of 180 km for an unsegmented fault zone. (b) shows the effect of in whether or not West Valley fault zone is includes as an independent earthquake source.

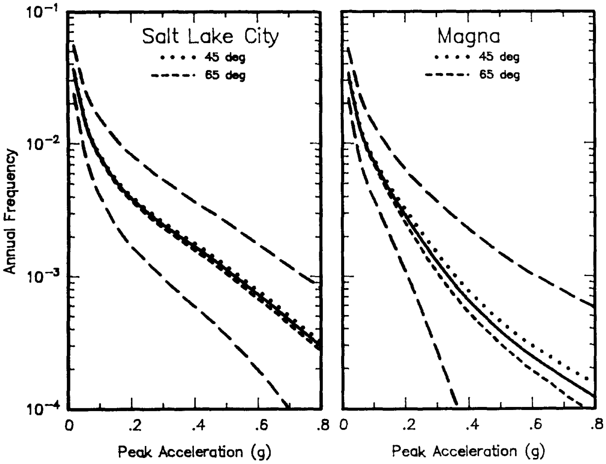

Figure 29 - Contribution to uncertainty in exceedance frequency from uncertainty in fault dip. Conditional mean hazard curves for each dip are labeled.

The impact of uncertainty in fault dip is illustrated in Figure 29. Uncertainty in fault dip is greatest at locations, such as Magna, that lie approximately 10 to 25 km west of the surface trace of the Wasatch fault zone. At these locations variations in fault dip produce the maximum relative change in the distribution for distance to earthquake rupture. However, as shown, even at these locations the effect of uncertainty in fault dip is small.

Figure 30 shows the effect of the choice of combining data from all segments or using only the data from an individual segment for modeling earthquake recurrence for the segments in the central portion of the Wasatch fault zone. As can be seen, the effect is variable along the fault, primarily reflecting differences between the data for an individual segment and the average behavior of the central segments of the fault zone.

For the remaining two parameters in the hazard model, maximum magnitude and recurrence rate, the contributions to total uncertainty were evaluated by computing the 5th and 95th percentile hazard curves considering only the

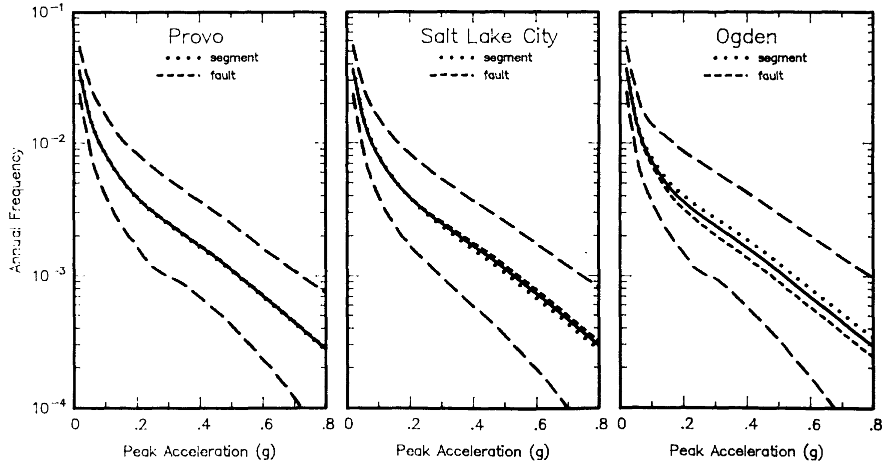

Figure 30 - Contribution to uncertainty in exceedance frequency along the Wasatch fault from use of recurrence data from either the segment only, denoted "segment" or an average value for the central segments of the fault zone, denoted "fault", in modeling earthquake recurrence for the fault segments.

uncertainty in the individual parameter. Figures 31 and 32 show the influence of uncertainty in maximum magnitude and recurrence rate, respectively. The variability in the computed hazard due to uncertainty in these two parameters is generally similar throughout the study region, tending to be smaller at locations where the background source has a greater contribution to the computed hazard.

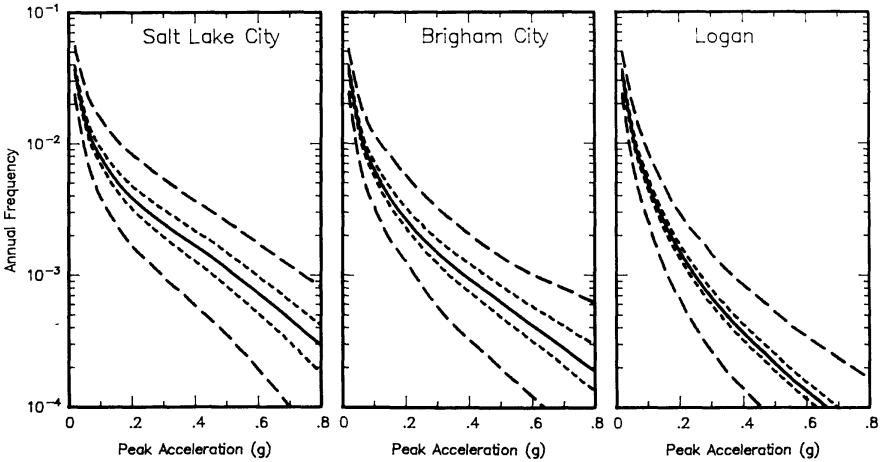

Figure 31 - Contribution to uncertainty in exceedance frequency from uncertainty in maximum magnitude. The long dashed curves are the 5th and 95th percentiles considering uncertainty in all parameters (see Figure 20) and the short dashed curves are the 5th and 95th percentiles considering only uncertainty in maximum magnitude.

In summary, for sites near the Wasatch fault zone south of Collinston, the uncertainty in the selection of the appropriate recurrence model is the largest contributor to uncertainty in the hazard, followed by uncertainty in selecting the appropriate attenuation relationship. For sites in areas of lower hazard, the uncertainty in selecting the appropriate attenuation relationship is the major contributor to uncertainty in the hazard. The uncertainties in the remaining parameters in general have relatively small contributions to the uncertainty in the hazard, although locally they may have more impact.

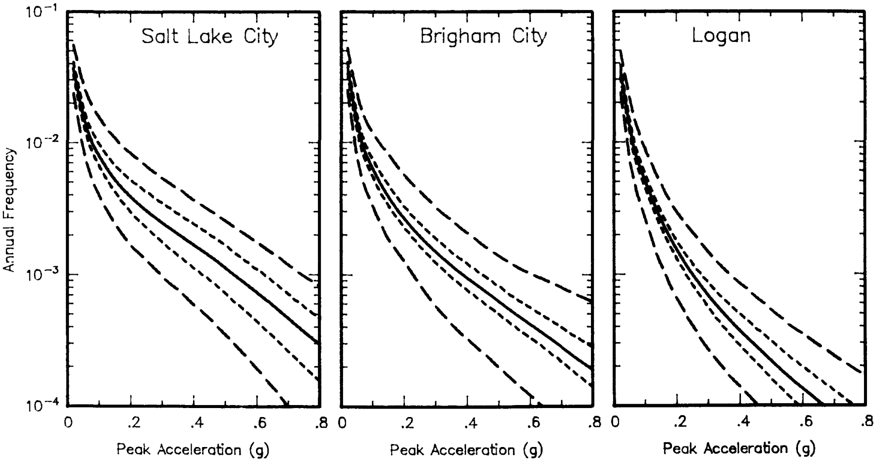

Figure 32 - Contribution to uncertainty in exceedance frequency from uncertainty in recurrence rate. The long dashed curves are the 5th and 95th percentiles considering uncertainty in all parameters and the short dashed curves are the 5th and 95th percentiles considering only uncertainty in recurrence rate.

Additional Sensitivity Analyses

Additional analyses were performed to evaluate the sensitivity of the results to local site conditions, possible lower rates of ground motion attenuation, alternative lower magnitude cutoff, and use of real time estimates of earthquake occurrence.

The hazard results presented above are applicable to locations underlain by soil deposits. As discussed previously, three published attenuation relationships were used for estimating peak ground accelerations on soil sites and four published relationships were used for rock sites. To evaluate differences between ground motions on soil and rock sites, the hazard computations were repeated using the four rock site attenuation relationships, equally weighted. Figure 33 compares the resulting rock site hazard curves with the soil site hazard curves for three locations. Similar comparisons made throughout the study region indicate that peak accelerations on rock should be about 10 percent greater than on soil for return periods of about 100 years and about 20 percent greater for return periods of 500 years or longer. These factors can be used to obtain accelerations on rock from accelerations on soil.

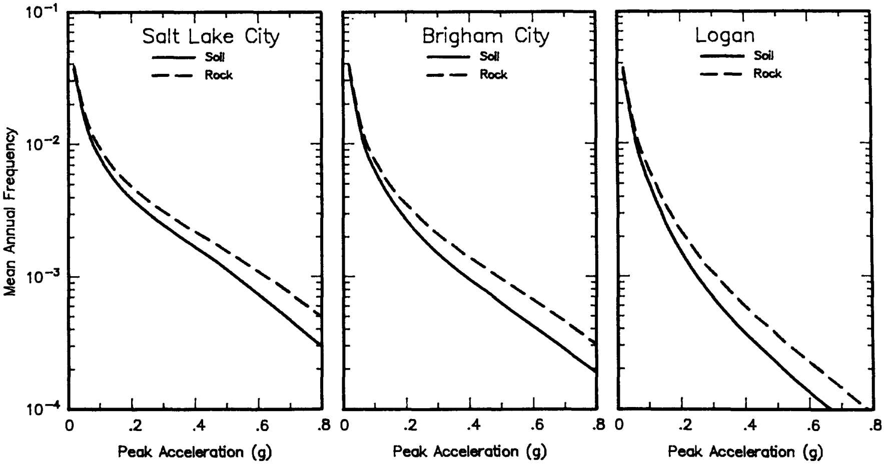

Figure 33 - Comparison of mean hazard curves for soil and rock sites at three locations.

Sensitivity analyses were performed to evaluate the effect of a possible lower rate of ground motion attenuation in Utah as compared to that observed in California. The modeled lower attenuation rate is described in the previous section and shown in Figure 17. Figure 34 compares the mean hazard curves obtained using the modified attenuation relationships with those used in the basic analysis. As can be seen, there is very little effect on the hazard, primarily because the hazard is dominated by the contributions from nearby events, either occurring on adjacent faults or within the background seismicity source. The largest percentage differences occur at lower acceleration levels where the contributions from more distant events is the greatest (see Figure 23).

It is noted that the uncertainty in rate of attenuation could have been directly included in the primary analysis as additional branches in the logic tree. If this were done, it would be necessary to incorporate an alternative for a higher, as well as a lower, rate of attenuation. The effect of a greater rate of attenuation in Utah as compared to California is expected to be a slight reduction in the computed hazard similar in magnitude to the increase shown in Figure 34. Based on the small effect on the results from the sensitivity study using a lower rate of attenuation

(Figure 34), it is concluded that the inclusion of this source of uncertainty has a negligible effect on the mean hazard. Its inclusion would slightly increase the dispersion about the mean hazard shown in Figure 20.

The results in Figure 34 can be viewed as showing the sensitivity to any factor that would result in an effect on the rate of attenuation of the order of magnitude given by Equation 3 and shown in Figure 17. Although the effect was specifically derived to model possibly lower crustal anelastic attenuation in Utah than in California, it could also be considered to model the possible influence of soft lake deposits on attenuation. As described in the previous section, Seed and others (1976a) and Seed and Idriss (1982) indicates that the influence of decreasing soil stiffness is to increase peak accelerations at low amplitudes and decrease them at high amplitudes. The tendency for increasing accelerations at low amplitudes results in an effect on attenuation similar to that shown in Figure 17. However, the offsetting tendency for decreasing accelerations of high amplitudes is not modeled by the relationship shown in Figure 17.

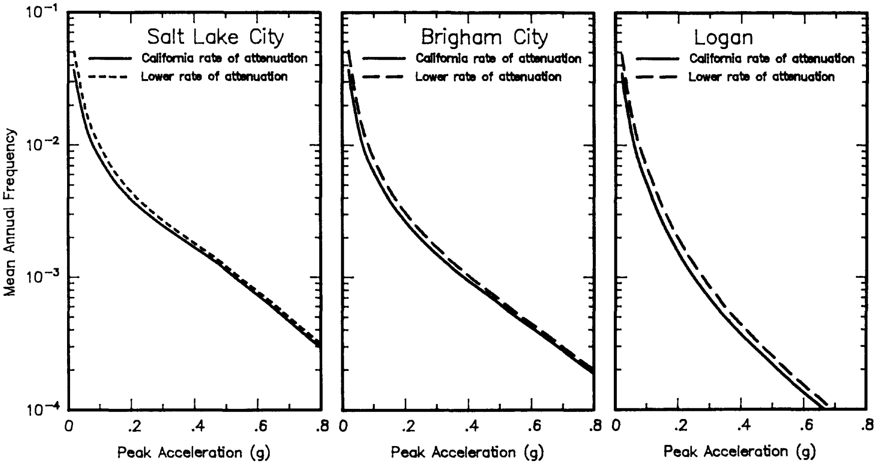

Figure 34 - Effect of postulated lower rate of attenuation in Utah as compared to California on computed hazard at three locations.

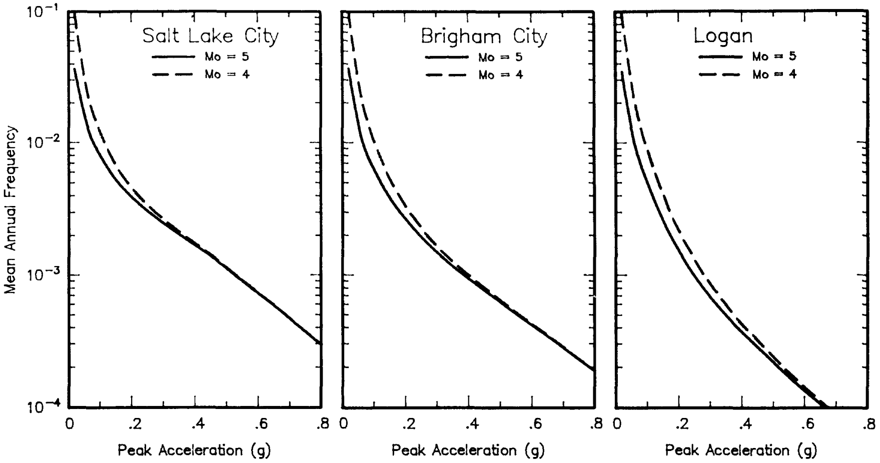

Figure 35 - Effect of choice of lower bound magnitude cutoff on computed hazard at three locations.

The hazard curves were computed considering the contributions to hazard from events of magnitude 5 or greater because it is judged that the ground shaking from smaller magnitude events poses little risk to engineered structures. The effect of including the contributions from events in the magnitude range of 4 to 5 on the computed hazard is shown in Figure 35. As can be seen, there is a small increase in the frequency of exceedance only at low acceleration levels for which smaller magnitude events contribute relatively more to the hazard. The increase in the computed hazard is greater at Logan than at Salt Lake City for the same reason. When considering longer-period ground motions the effect of including smaller magnitude events will be even less than the effect shown in Figure 35.

The hazard analyses were conducted using a memoryless, or Poisson, model for earthquake recurrence, that is the frequency of events in the near future (e.g. the expected number of events in the next 50 years) is a function of the long term earthquake recurrence rate without consideration of the elapsed time since the most recent event. While the Poisson model is almost exclusively used in seismic hazard analyses, it is at odds with the generally accepted physical model that earthquake occurrence on a fault is a process of the gradual accumulation of strain, followed by sudden release. The physical model implies that for individual faults undergoing relatively constant loading, the repeat time for those events that release the builtup stress should be more or less cyclic in nature. However, on a regional basis, the Poisson model for earthquake occurrence has been shown to be appropriate both on the basis of observation (e.g. Gardner and Knopoff, 1974) and on the basis of theory as the limiting result of a number of independent or nearly independent processes of whatever type on individual features (e.g. Brillinger, 1982). In addition, Cornell and Winterstein (1986) have shown that the Poisson model is conservative as long as the elapsed time since the most recent renewing event is less than the mean repeat time.

The renewal model provides the simplest approach for making real time estimates of earthquake occurrence. The renewal model specifies that, neglecting the occurrence of multiple events, the probability of a renewing event in the next $\mathbf{t}$ years given $\mathbf{t_o}$ years since the last renewing event is given by the expression:

$$P(\text{event in } \mathbf{t} \mid \mathbf{t_o}) = \frac{F(\mathbf{t}+\mathbf{t_o}) - F(\mathbf{t_o})}{1 - F(\mathbf{t_o})} \tag{6}$$

where F() is the cumulative density function for interarrival time of events. Investigators have employed different models for the distribution of interarrival times, such as the normal, lognormal, gamma, and Weibull distributions. Cornell and Winterstein (1986) indicate that the Weibull distribution provides the desired characteristics of a simple analytical form and a hazard function that increases monotonically with increasing $\mathbf{t_o}$. (The hazard function is a measure of the likelihood of an event in the next increment of time, dt, given no events in time $\mathbf{t_o}$.) They give a simple approximation for the Weibull distribution as:

$$F(\mathbf{t}) \approx 1 - e^{-\lambda \mathbf{t}^{1/V[\mathbf{T}]}} \tag{7}$$

in which

$$\lambda \approx \frac{1 - 0.5V[\mathbf{T}](1-V[\mathbf{T}])}{E[\mathbf{T}]} \tag{8}$$

with $E[\mathbf{T}]$ and $V[\mathbf{T}]$ being the mean and coefficient of variation of interarrival times, respectively. Equations (7) and (8) are good approximations for $0 \le V[\mathbf{T}] \le 1$ and have the advantage of degenerating to the Poisson model when $V[\mathbf{T}]=1$ (Cornell and Winterstein, 1986).

Equations (6) through (8) were used to obtain real time estimates of the frequency of future large events at the six locations along the Wasatch fault zone for which data are available for time since the most recent event (Schwartz and others, 1984). The coefficient of variation of interarrival time, $V[\mathbf{T}]$, was assumed to be 0.7, reflecting the large variations observed in the limited data for interarrival times for large earthquake on the Wasatch fault zone. The ratios of the estimated number of renewing events in the next 50 years to that given by the Poisson model at the six location are as follows:

Location	Mean Repeat Time (years)	Elapsed Time Since Most Recent Event (years)	Ratio Renewal/Poisson of Expected Number Events in 50 years:
Kaysville	1300	≤500	<0.83
Little Cottonwood Canyon	2600	>1000*	>0.82
Hobble Creek	2100	>1000	>0.90
North Creek	1800	300-500	0.67
Deep Creek	7000	<1750	<0.68

* assumed to be similar to the Hobble Creek site

The above ratios are all less than 1.0 reflecting the fact that the estimated elapsed times are less than the estimated mean repeat times at all locations. The above ratios are assumed to apply only to the largest or characteristic events on the appropriate fault segments. Smaller events are not likely to result in substantial stress release and are considered to occur randomly (Poisson) in time. The effect of the real time estimates of the near future rate of large events on the computed hazard along the Wasatch fault zone is shown in Figure 36. The effect is a minor decrease in hazard, with the largest decrease at long return periods where the hazard is dominated by contributions from the largest events (Figure 23).

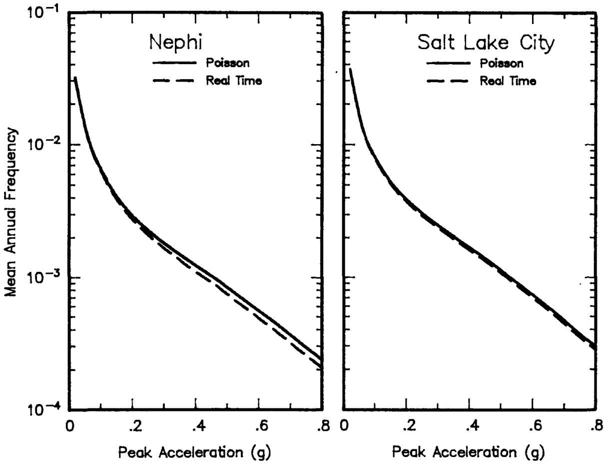

Figure 36 - Effect of use of real time estimates of earthquake occurrence probabilities on computed hazard at two locations along the Wasatch fault zone.

Peak Acceleration Hazard Maps

The variation in seismic hazard throughout the study region is shown in Figure 37 in terms of contours of peak ground acceleration level corresponding to 10 percent probability of exceedance in time periods of 10, 50, and 250 years. These probability levels span the range of probabilities typically considered in evaluating seismic hazard at commercial and industrial sites and also correspond to the levels used by the U.S. Geological Survey in their national maps of seismic hazard (Algermissen and others, 1982). Assuming that earthquake occurrence is a Poisson process, the three probability levels can be related to the mean frequencies of exceedance (and their inverse, return period) by applying Equation 1:

10% Probability of Exceedance in: (years)	Equivalent Exceedance Frequency (events/year)	Return Period (years)
10	0.0105	95
50	0.0021	475
250	0.00042	2373

Hazard computations were made for 80 points located on a grid in the study region. Peak accelerations corresponding to the above frequencies of exceedance were interpolated from the computed mean hazard curves, and the resulting values contoured to produce the maps shown in Figure 37. As indicated by the exceedance frequency fractiles shown in Figure 20, the mean hazard curves are somewhat higher than the median (50^{th} percentile) hazard curves and thus represent a more conservative estimate of the hazard. Peak accelerations obtained from the median hazard curves are about 10 percent less than those presented on the hazard maps. The computed 90-percent confidence intervals for peak ground acceleration at a given return period typically range from minus 40 percent to plus 60 percent about the values shown in Figure 37.

The hazard maps further illustrate the spatial trends shown in Figure 21. The spatial variation in hazard increases with decreasing probability of exceedance (increasing return period), reflecting the increased dominance of the hazard by contributions from the individual faults as the probability of exceedance decreases. This is particularly so for the central portion of the Wasatch fault zone as it has by far the highest estimated rate of activity for large events.

The hazard maps shown in Figure 37 are for peak accelerations on soil site conditions. Repeating the analysis for all locations using rock site attenuation relationships indicates that rock site acceleration levels can be obtained by increasing the soil site acceleration levels shown in Figure 37 by about 10 percent for 10 percent probability of exceedance in 10 years, and by about 20 percent for 10 percent probability of exceedance in 50 and 250 years, respectively.

In those areas underlain by soil, the peak accelerations in Figure 37 apply directly. Soil sites are considered to be sites where the depth to bedrock is 20 m or greater. In those areas of shallow soil or underlain directly by rock, it is recommended that the peak accelerations shown in Figure 37 be adjusted upward as described in the preceding paragraph.

Response Spectra

Response spectral accelerations appropriate for use with the mapped peak acceleration levels were evaluated by developing equal-hazard response spectra for a number of locations in the study region. The equal-hazard

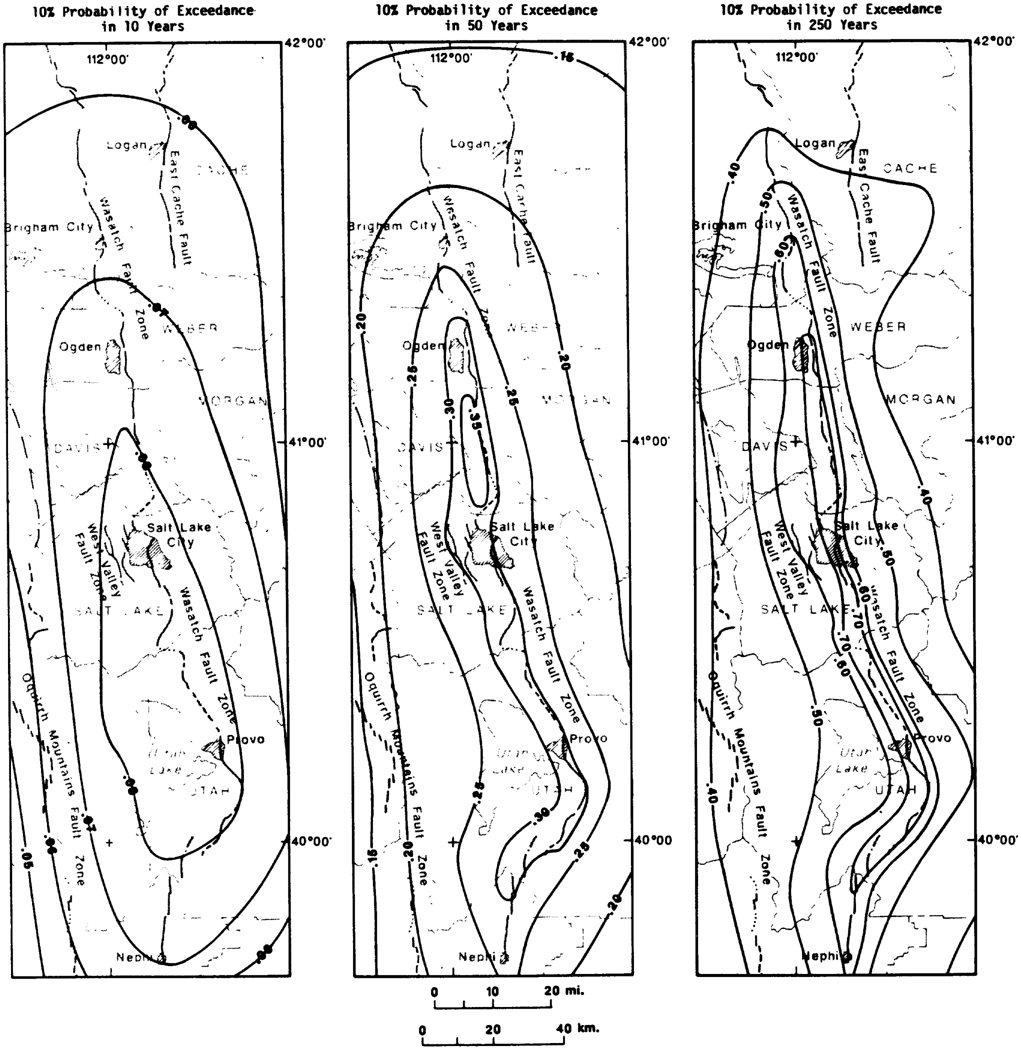

10% Probability of Exceedance in 10 Years

10% Probability of Exceedance in 50 Years

10% Probability of Exceedance in 250 Years

Figure 37 - Contours of peak ground acceleration on soil sites with 10 percent probability of being exceeded in 10 years, 50 years and 250 years. Peak accelerations on rock sites are expected to be approximately 10 percent higher than the values shown on the map for 10 percent probability of exceedance in 10 years and approximately 20 percent higher than the values shown on the maps for 50 and 250 years.

response spectra were developed by conducting hazard analyses using response spectral attenuation relationships described previously in this paper for periods of vibration between 0.04 and 4 seconds. The levels of spectral acceleration corresponding to the three probability levels used in the hazard maps were then interpolated from the hazard curves for each period of vibration and smooth response spectra were drawn through the computed points to construct equal-hazard spectra.

Figure 38 shows the resulting soil and rock equal-hazard spectra for three geographical locations. The plotted points indicate the computed spectral acceleration levels for the three probability levels. Use of the Sadigh and others (1986) and Joyner and Boore (1982) response spectra attenuation

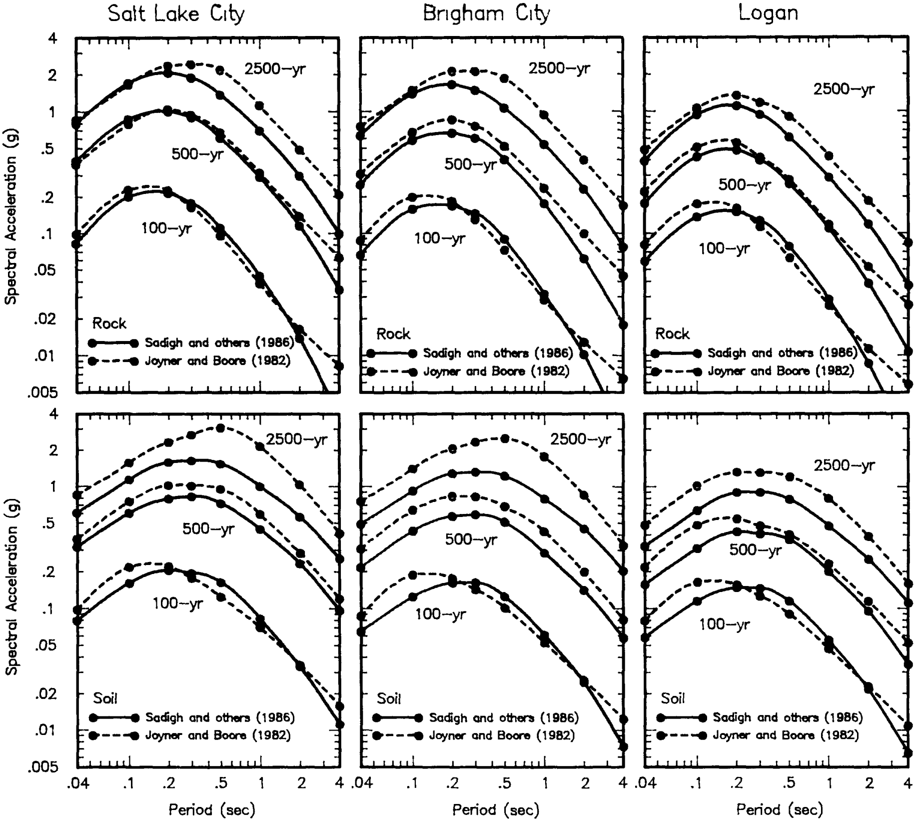

Figure 38 - Computed equal hazard response spectra (5% damping) for soil and rock sites at three locations using two attenuation relationships. Each plot shows the spectra for three return periods.

relationships yield similar results except for low probability levels on soil sites where the Joyner and Boore (1982) relationship gives spectral accelerations that are about 1-1/2 to 2 times higher than those obtained using the Sadigh and others (1986) relationships.

To directly compare the relative frequency content of the various equal-hazard spectra, the absolute spectra were normalized by their corresponding peak ground acceleration levels. The resulting spectral shapes are shown in Figures 39 and 40 for soil and rock sites, respectively. In

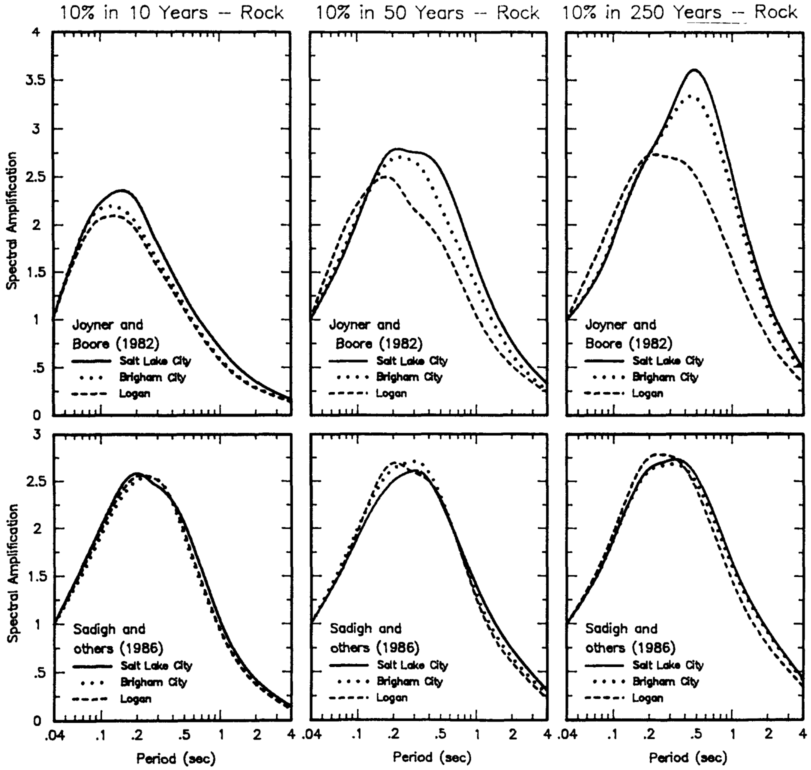

Figure 39 - Computed equal hazard response spectral shapes (5% damping) at three locations for soil sites. The upper row of plots show the spectral amplifications computed using the Joyner and Boore (1982) attenuation relationships and the lower row of plots show the spectral amplifications computed using the Sadigh and others (1986) attenuation relationships.

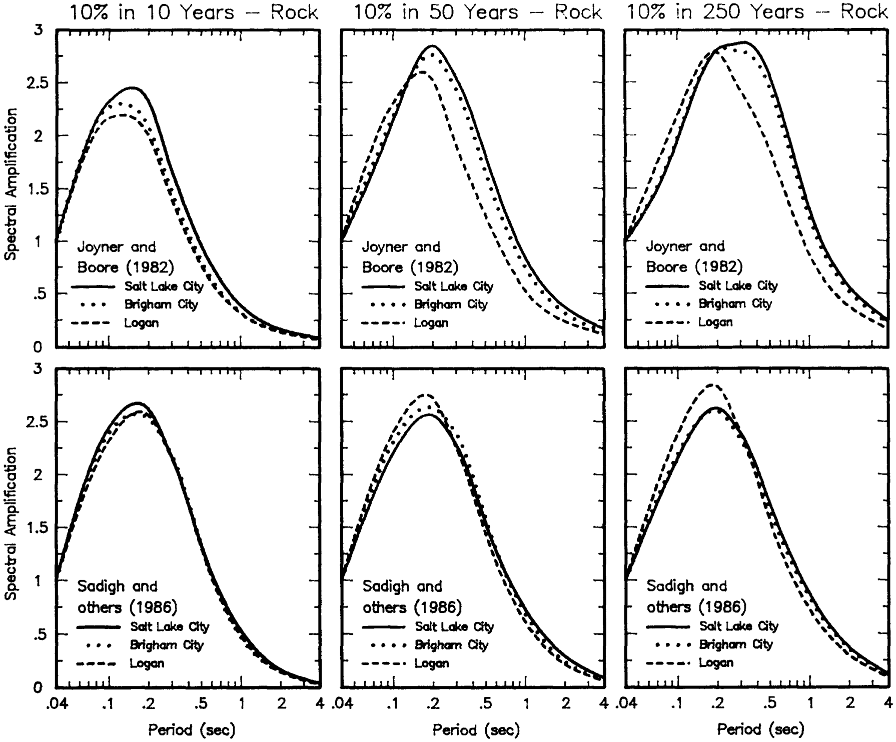

Figure 40 - Computed equal hazard response spectral shapes (5% damping) at three locations for rock sites. The upper row of plots show the spectral amplifications computed using the Joyner and Boore (1982) attenuation relationships and the lower row of plots show the spectral amplifications computed using the Sadigh and others (1986) attenuation relationships.

general, the computed spectral shape for a particular site classification, probability level and attenuation relationship is similar at all three geographical locations. Average spectral shapes for each probability level and site classification were obtained by averaging the six shapes computed using the Sadigh and others (1986) and Joyner and Boore (1982) relationships at the three locations. These spectral shapes are shown in Figure 41. The average spectral shapes differ by a maximum of 20 percent from the spectral shapes obtained at any given location. Consequently, we propose that the spectral shapes shown in Figure 41 be used for the respective probability level and site classifications, regardless of location within the study area.

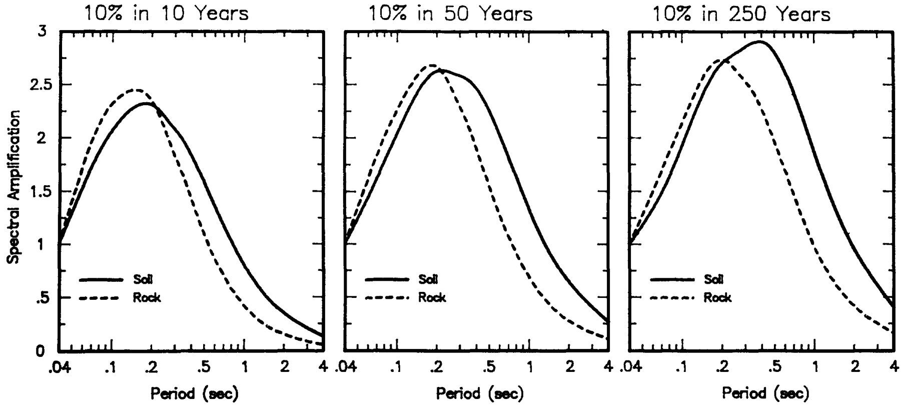

Figure 41 - Proposed spectral shapes (5% damping) for developing equal hazard response spectra. For soil sites, equal hazard spectra are developed by multiplying the soil spectral amplifications shown above by the appropriate peak ground acceleration obtained from the soil hazard maps shown in Figure 37. For rock sites, the appropriate peak acceleration to use with the above rock spectral amplifications is obtained by multiplying the peak ground accelerations shown on the soil hazard maps by a factor of 1.1 for a probability of exceedance of 10% in 10 years and by a factor of 1.2 for 10% probability of exceedance in 50 and 250 years.

It can be seen in Figures 39 through 41 that the response spectral shapes broaden significantly with decreasing probability level. This broadening reflects the increasing contribution of large magnitude events as the probability level decreases. It is therefore not appropriate to use a single spectral shape for all probability levels.

Absolute acceleration equal-hazard spectra for soil sites can be obtained by multiplying the soil spectral shapes shown in Figure 41 by the appropriate peak ground acceleration obtained from the hazard maps for the sample probability level (Figure 37). Absolute acceleration equal-hazard spectra for rock sites can be obtained by first estimating the peak acceleration on rock by multiplying the soil acceleration levels by a factor of 1.1 for 10 percent probability of exceedance in 10 years or a factor of 1.2 for lower probability levels and then multiplying by the appropriate rock spectral shapes shown in Figure 41.

As an example application, Figure 42 presents the equal-hazard response spectra that would be developed for rock and soil sites in the vicinity of

Magna corresponding to a 10 percent probability of exceedance in 50 years. The hazard map shown in Figure 37 indicates that the appropriate peak ground acceleration on soil sites is 0.25g. Using a factor of 1.2, the corresponding peak acceleration on rock would be 0.30g. The absolute acceleration spectra shown in Figure 42 were obtained by multiplying the appropriate spectral shapes in Figure 41 by these two acceleration levels.

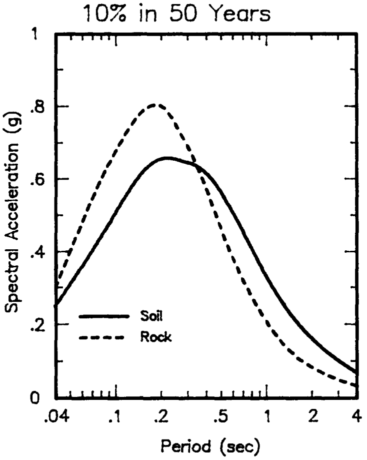

Figure 42 - Example development of equal hazard response spectra (5% damping) for a 10% probability of exceedance in 10 in 50 years for soil and rock sites near Magna.

The soil site spectra shown in Figure 41 are considered appropriate for firm soil conditions. Firm soils are considered to consist of medium dense to dense sands and gravels and stiff silts and clays. As discussed in the section of the paper describing attenuation relationships, there is uncertainty as to the relative amplitudes of ground motions at longer periods of vibration (periods greater than about 0.4 seconds) on softer lake deposits (soft clays and silts), especially in light of the observed effects in Mexico City from the September 19, 1985 earthquake. At present there is insufficient information to evaluate to what degree the lake deposits could further amplify longer period motions above the levels indicated by the soil response spectra presented in Figure 41.

A preliminary indication of the possible additional spectral amplification in areas of soft lake deposits can be obtained from the response spectral shapes developed by Seed and others (1976b) for different generalized categories of subsurface conditions. Seed and others (1976b) found that response spectral amplifications for "soft to medium clay and sand" exceeded the amplifications for "deep cohesionless" and "stiff" soils for periods greater than about 0.4 seconds and were less than the amplifications for "deep cohesionless" and "stiff" soils at shorter periods. The average increase in amplification in the period range of about 0.75 to 1.5 seconds corresponded to a factor of about 1.6. Using this factor with the response spectral curve for soil shown in Figure 41 and neglecting any possible decrease in amplification at periods less than 0.4 seconds, we obtained the ranges in response spectral shapes shown in Figure 43. The lower curves correspond to the shapes for soil shown in Figure 41 and are for firm soil conditions. The upper curves are preliminary estimates of response spectral shapes applicable to soft lake deposits. These curves can be multiplied by the appropriate peak acceleration values in Figure 37 to obtain preliminary estimates of absolute response spectra on soft lake deposits.

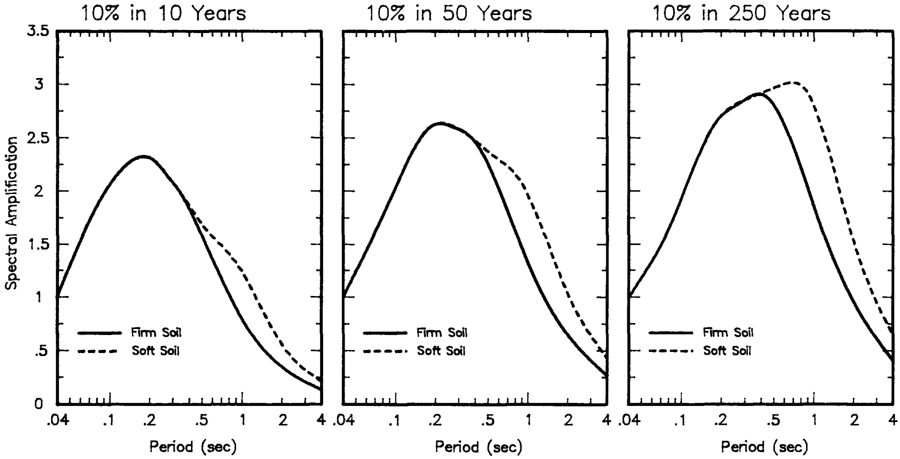

Figure 43 - Preliminary estimate of ranges of response spectral shapes (5% damping) for lake deposits. Lower curves are soil curves in Figure 41 and are intended for firm soil conditions. Upper curves in the ranges are preliminary estimates for soft lake silts and clays.

SUMMARY

A quantitative assessment has been made of the ground shaking hazard along the Wasatch Front urban corridor utilizing the extensive geological and seismological data base that has been developed for the region. A probabilistic approach was used to express levels of ground motion as a function of their probability of exceedance. Using a logic tree methodology, the approach formally incorporates variations in values for earthquake source geometry and fault segmentation, maximum earthquake magnitude, earthquake recurrence rate, ground motion attenuation, and other parameters and model components that are not known with certainty (Table 1).

Based on probabilistic analyses conducted at a 80 points located on a grid in the study area, maps were prepared showing contours of peak ground acceleration for probabilities of exceedance of 10 percent in 10 years, 10 percent in 50 years, and 10 percent in 250 years (Figure 37). These maps are for peak acceleration on soil site conditions, considered to be sites with a depth to bedrock of 20 m or more. By repeating the analyses using rock site attenuation relationships, it is concluded that rock site peak accelerations can be obtained by multiplying the soil site accelerations by a factor of 1.1 for a probability of exceedance of 10 percent in 10 years and by a factor of 1.2 for probabilities of exceedance of 10 percent in 50 years and 10 percent in 250 years.

Response spectra were also developed from the probabilistic analyses. Response spectral shapes (for a damping ratio of 0.05) for firm soil conditions and for rock site conditions were developed for the same probability of exceedance levels used in mapping peak ground acceleration (Figure 41). Absolute response spectra can be obtained by multiplying these spectral shapes by the corresponding values of peak ground acceleration. In areas underlain by soft lake silts and clays, considerable uncertainty exists regarding the spectral shapes. A preliminary estimate is presented for the additional spectral amplification that might occur in areas of soft lake deposits (Figure 43).

Extensive analyses were conducted to examine the sensitivity and uncertainty of the results of this study with respect to variations in the various

input parameters and models. The computed 90-percent confidence intervals for peak ground acceleration represent a range of minus 40 percent to plus 60 percent about the values shown on the hazard maps (Figure 37). The two biggest contributors to uncertainty in the results were uncertainties in selecting the appropriate models for earthquake recurrence on the faults and ground motion attenuation.

APPENDIX - COMPARISON OF STRONG MOTION DATA FROM STUDY REGION WITH SELECTED ATTENUATION RELATIONSHIPS

This appendix presents a comparison of strong ground motion data from recordings of earthquakes in the study region with recently developed attenuation relationships that are based primarily on data from California. The regional data include one recording in Logan, Utah, at a distance of about 30 km from the 1962 M_L 5.7 Cache Valley earthquake; several recordings at distances of about 90 to 100 km from the 1983 M_S 7.3 Borah Peak, Idaho earthquake; and many recordings in the distance range of about 2 to 50 km during aftershocks of the 1983 Borah Peak earthquake. For Borah Peak earthquake aftershocks, only data for earthquakes of M_L greater than 4 are included. The ground motion data from the study region are compared to the relationships of Joyner and Boore (1982), Sadigh and others (1986), and Campbell (1987).

Figure A-1 compares the peak ground accelerations of the only strong motion recording to date in Utah (i.e. the Logan recording obtained on a soil site during the 1962 M_L 5.7 Cache Valley earthquake) with the median attenuation curves from the three attenuation relationships. The data are higher than the curves. However, they are within the range of variation about the median curves typically found in strong motion data, with the average of the two data points being approximately 0.8, 1.3 and 2.6 standard deviations above the median relationships of Joyner and Boore (1982), Sadigh and others (1986), and Campbell (1987), respectively (using the standard deviations presented by the authors for their respective relationships).

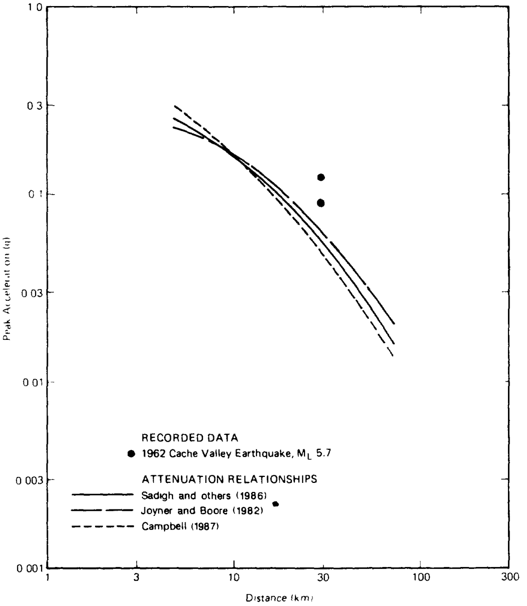

Figure A-1 - Comparison of peak ground accelerations recorded at Logan during 1962 Cache Valley, Utah earthquake with median attenuation relationships.

Figure A-2 compares response spectra of the Logan recording with median and 84th percentile spectra predicted by the relationships of Sadigh and others (1986) and Joyner and Boore (1982). The spectra of the recorded motions range from the median to well above the 84th percentile (median-plus-one standard-deviation) of the two relationships.

Peak acceleration data recorded during the M_s 7.3 Borah Peak, Idaho earthquake are compared with the respective attenuation relationships in Figure A-3. Because most of the data are from soil sites, Sadigh and others' (1986) relationship for soil sites rather than for rock sites was used. The recorded data, particularly those recorded in the free field rather than in basements as indicated in the figure, tend to be somewhat higher overall than two of the attenuation curves and about equal to or lower than the third curve. A moment magnitude of 7.1 was calculated for this earthquake using the moment vs. magnitude relationship adopted for this study (as described in the main text of this paper) and the seismic moment

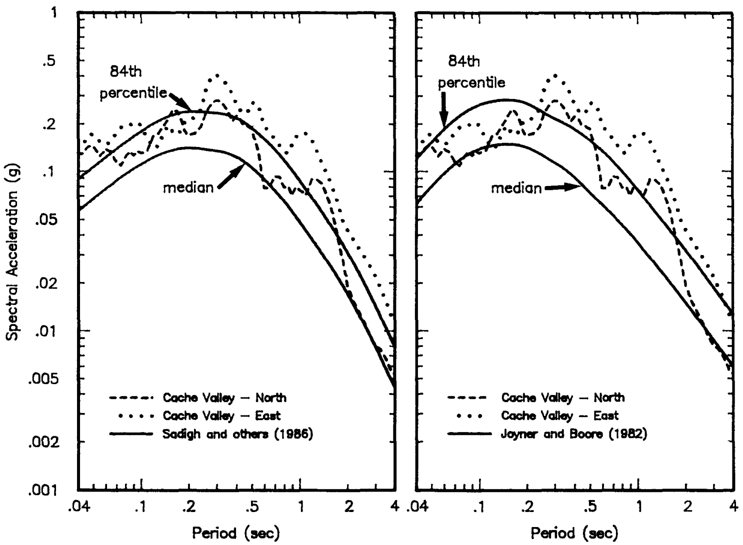

Figure A-2 - Comparison of response spectra (5% damping) of ground motions of motions recorded during the 1962 Cache Valley, Utah earthquake with median and 84th percentile spectra from attenuation relationships.

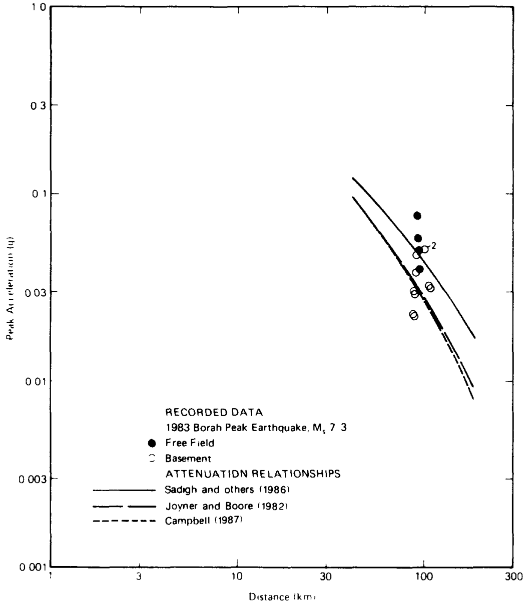

Figure A-3 - Comparison of peak ground accelerations recorded during the 1983 Borah Peak, Idaho earthquake with median attenuation relationships.

reported by Jackson and Boatwright (1985). The attenuation curves for magnitude 7.1 would be slightly lower that those for $\mathbf{M}_S$ 7.3 shown in Figure A-3, which would emphasize the overall trend for the recorded data for this earthquake to be slightly above the California attenuation curves.

Figure A-4 compares peak accelerations from the 1986 Borah Peak earthquake aftershocks (magnitudes greater then 4) with the respective attenuation curves. As is the case for the main shock, most of the aftershock data were recorded on soil sites, so Sadigh and others' (1986) soil-site relationship was used for the comparisons. The data are compared with the Joyner and Boore (1982) attenuation curves separately from the Sadigh and others and the Campbell (1987) curves because of significant differences in hypocentral and epicentral distances for some of the records. Hypocentral distance is most consistent with the distance definitions used by Sadigh and others and by Campbell, and epicentral difference most consistent with the distance definition used by Joyner and Boore (see main text for these distance definitions). However, for magnitudes less than 5, only comparisons with the Sadigh and others and the Campbell curves are presented because the Joyner and Boore's relationships are restricted to magnitudes equal to or greater than 5. (In fact, Campbell relationships were also developed for magnitudes equal to or greater than 5, but can be reasonably be used for magnitudes in the range of 4 to 5 [Campbell, 1986, personal communication]). For some of the aftershocks, significant differences exist between the $\mathbf{M}_L$ magnitudes reported by the University of Utah Seismograph Station and the moment magnitudes obtained by Boatwright (1985). Therefore, the data are compared with the curves for both sets of magnitudes. Regardless of whether the data are compared with the curves for $\mathbf{M}_L$ or moment magnitude, it can be concluded from Figure A-4 that the data tend to lie below the attenuation curves, and substantially so for some of the aftershocks.

For the Borah Peak mainshock and aftershock ground motion data, observations similar to those stated above have been made by Jackson and Boatwright (1985).

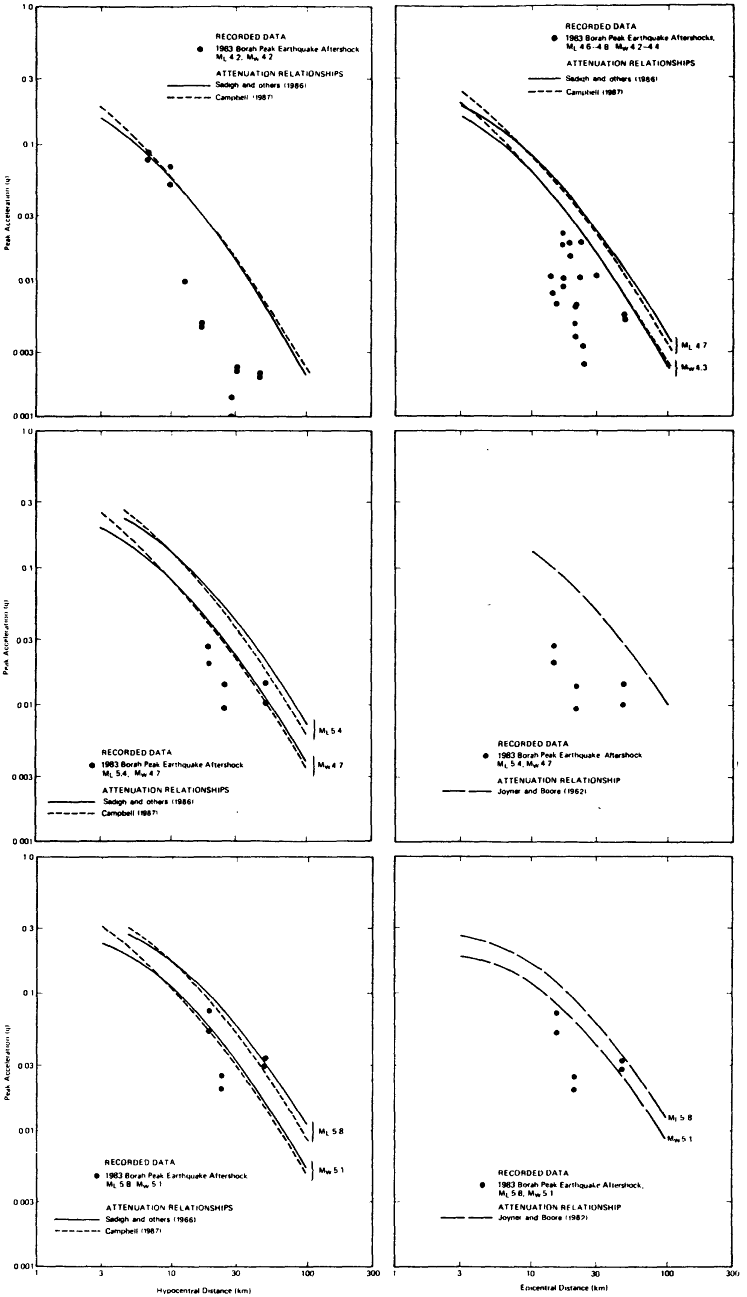

Figure A-4 - Comparison of peak ground accelerations recorded during 1983 Borah Peak, Idaho aftershocks with median attenuation relationships.

Our overall conclusion from these comparisons is that the data are too few to either strongly support or refute the applicability of California attenuation relationships to Utah. The data do not have a consistent trend to lie above or below the values predicted by the attenuation relationships.

ACKNOWLEDGEMENTS

The work presented in this paper was carried out under USGS contracts 14-08-0001-2194 and 14-08-0001-G1189. The authors wish to thank Walter Arabasz, Bernice Bender, Ken Campbell, Peter Knuepfer, and James Pechmann for their helpful review comments. We also appreciate the help of Ethan Brown in providing the earthquake catalog used in this study and Tony Crone and Michael Machette for providing unpublished data for the East Bear Lake fault zone.

REFERENCES

Aki, K., 1979, Characterization of barriers on an earthquake fault: Journal of Geophysical Research, vol. 84, pp. 6140-5148.

Aki, K., 1984, Asperities, barriers, and characteristic earthquakes: Journal of Geophysical Research, vol. 89, no B7, pp. 5867-5872.

Algermissen S.T., D.M. Perkins, P.C. Thenhaus, S.L. Hanson and B.L. Bender, 1982, Probabilistic estimates of maximum acceleration and velocity in rock in the contiguous United States: U.S. Geological Survey Open File Report OFR 82-1033, 99 pp.

Anderson, J.G., 1979, Estimating the seismicity from geological structure for seismic risk studies: Bulletin of the Seismological Society of America, vol. 69, no. 1, pp. 135-158.

Anderson, L.W., and D.G. Miller, 1979, Quaternary fault map of Utah: FUGRO, Inc., Long Beach, California, 35 pp.

Arabasz, W.J., 1979, Historical review of earthquake-related studies and seismographic recording in Utah: in Earthquake Studies in Utah 1850 to 1978, editors W.J. Arabasz, R.B. Smith and W.D. Richins, University of Utah Seismograph Stations, Department of Geology and Geophysics, University of Utah, July, 1979, pp. 33-56.

Arabasz, W.J., 1984, Earthquake behavior in the Wasatch front area: association with geologic structure, space-time occurrence, and stress state: in Proceedings of Conference XXVI - A Workshop on "Evaluation of Regional and Urban Earthquake Hazards and Risk in Utah," US Geological Survey Open-File Report 84-763, pp. 310-339.

Arabasz, W.J. and R. Robinson, 1976, Microseismicity and geologic structure in the northern South Island, New Zealand: New Zealand Journal of Geology and Geophysics, vol. 19, no. 2, pp. 561-601.

Arabasz, W.J. and M.E. McKee, 1979, Utah earthquake catalog 1850 - June 1962: in Earthquake Studies in Utah 1850 to 1978, editors W.J. Arabasz, R.B. Smith and W.D. Richins, University of Utah Seismograph Stations, Department of Geology and Geophysics, University of Utah, July, 1979, pp. 119-121.

Arabasz, W.J., R.B. Smith, and W.D. Richins, 1980, Earthquake studies along the Wasatch Front, Utah - network monitoring, seismicity, and seismic hazards: Bulletin of the Seismological Society of America, v. 70, No. 5, pp. 1479-1499.

Bender, B., 1983, Maximum likelihood estimation of b values for magnitude grouped data: Bulletin of the Seismological Society of America, v. 73, No. 3, pp. 831-851.

Bender, B., 1984, Seismic hazard estimation using a finite fault rupture model: Bulletin of the Seismological Society of America, v. 74, No. 5, pp. 1899-1923.

Bonilla, M.G., R.K. Mark, and J.J. Lienkaemper, 1984, Statistical relations among earthquake magnitude, surface rupture length, and surface fault displacement: Bulletin of the Seismological Society of America, vol. 74, no. 6, pp. 2379-2411.

Boore, D.M., 1983, Stochastic simulations of high-frequency ground motions based on seismological models of the radiated spectra: Bulletin of the Seismological Society of America, vol. 73, no. 5, pp. 1865-1894.

Brazee, R. J., 1980, An analysis of earthquake intensities with respect to attenuation, magnitude, and rate of recurrence - revised edition: U.S. Nuclear Regulatory Commission, NUREG/CR-1805, December.

Brillinger, D.R., 1982, Some bounds for seismic risk: Bulletin of the Seismological Society of America, vol. 72, no. 4, pp. 1403-1410.

Campbell, K.W., 1981, Near-source attenuation of peak horizontal acceleration: Bulletin of the Seismological Society of America, v. 71, No. 6, pp.

Campbell, K.W., 1982, A preliminary methodology for the regional zonation of peak ground acceleration: Third International Earthquake Microzonation Conference Proceedings, v. III, June 28-July 1, Seattle.

Campbell, K.W., 1987, Strong motion attenuation in Utah, in evaluation of urban and regional earthquake hazards and risk in Utah: U.S. Geological Survey Professional Paper (in press).

Chandra, U., 1979, Attenuation of intensities in the United States: Bulletin of the Seismological Society of America, v. 69, No. 6, pp. 2003-2024.

Chavez, D.E., and K.F. Priestly, 1985, M_L observations in the Great Basin and M_0 versus M_L relationships for the 1980 Mammoth Lakes, California earthquake sequence: Bulletin of the Seismological Society of America, v. 75, No. 6, pp. 1583-1598.

Cluff, L.S., G.E. Brogan, and C.E. Glass, 1970, Wasatch fault - northern portion - earthquake fault investigation and evaluation - a guide to land use planning: report prepared for Utah Geological and Mineralogical Survey by Woodward-Clyde and Associates, Oakland, California, 27 pp.

Cluff, L.S., G.E. Brogan, and C.E. Glass, 1973, Wasatch fault - southern portion - earthquake fault investigation and evaluation - a guide to land use planning: report prepared for Utah Geological and Mineralogical Survey by Woodward-Clyde and Associates, Oakland, California, 80 pp.

Cluff, L.S., C.E. Glass, and G.E. Brogan, 1974, Investigation and evaluation of the Wasatch fault north of Brigham City and Cache Valley faults, Utah and Idaho - a guide to land-use planning with recommendations for safety: report prepared for Utah Geological and Mineralogical Survey by Woodward-Lundgren and Associates, Oakland, California, 146 pp.

Coppersmith, K.C. and R.R. Youngs, 1986, Capturing uncertainty in probabilistic seismic hazard assessments within intraplate environments: in Proceedings of the 3rd National Conference on Earthquake Engineering, Charleston, South Carolina, August 24-28, vol I, pp. 301-312.

Cornell, C.A., 1968, Engineering seismic risk analysis: Bulletin of the Seismological Society of America, vol. 58, no. 5, pp. 1583-1606.

Cornell, C.A. and E.H. Van Marke, 1969, The major influences on seismic risk: in Proceedings of the Third World Conference on Earthquake Engineering, Santiago Chile, vol. A-1, pp. 69-93.

Cornell, C.A. and S.R. Winterstein, 1986, Applicability of the Poisson earthquake-occurrence model: EPRI NP-4770 Research Project P101-38 Final Report, August, see also The seismic hazard implications of non-Poissonian recurrence models (abs.): Earthquake Notes, vol. 57, no. 1, p. 25.

Crone, A.J., and M.N. Machette, 1984, Surface faulting accompanying the Borah Peak earthquake, central Idaho: Geology, vol. 12, pp. 664-667.

Deschamps, A., Y. Guademer, and A. Cisternas, 1982, The El Asnam, Algeria earthquake of 10 October 1980 - Multiple-source mechanism determined from long-period records: Bulletin Seismological Society of America, vol. 72, no. 4, pp. 1111-1128.

Doser, D.I., 1984, The 1983 Borah Peak, Idaho and 1959 Hebgen Lake, Montana earthquakes: models for normal fault earthquakes in the Intermountain Seismic Belt: in Proceedings of Workshop XXVIII - On the Borah Peak, Idaho, Earthquake, US Geological Survey Open-File Report 85-290, vol. A, pp. 368-384.

Doser, D.I. and R.B. Smith, 1982, Seismic moment rates in the Utah region: Bulletin of the Seismological Society of America, vol. 72, no. 2, pp. 525-551.

EPRI, 1987, Seismic hazard methodology for the central and eastern United States - Volume 1: Methodology: Report NP-4726, Volume 1, prepared for Seismicity Owners Group and Electric Power Research Institute under research projects P101-38, -45, -46, 2256-14, Revised, February, 1987.

Everitt, B.L., and B.N. Kaliser, 1979, Geology for assessment of seismic risk in the Tooele and Rush valleys, Tooele County, Utah: Utah Geological and Mineral Survey, 33 pp.

Everndon, J. F., 1975, Seismic intensities, "size" of earthquakes, and related parameters: Bulletin of the Seismological Society of America, vol. 65, no. 5, pp. 1287-1313.

Gardner, J.K. and L. Knopoff, 1974, Is the sequence of earthquakes in Southern California, with aftershocks removed, Poissonian: Bulletin of the Seismological Society of America, vol. 64, no. 5, pp. 1363-1367.

Gilbert, G.K., 1890, Lake Bonneville: U.S. Geological Survey Monographs I, 438 p.p.

Griscom, M., 1980, Space-time seismicity patterns in the Utah Region and an evaluation of local magnitude as the basis of a uniform earthquake catalog: M.S. Thesis, University of Utah.

Griscom, M., and W.J. Arabasz, 1979, Local magnitude (M_L) in the Wasatch front and Utah region: Wood-Anderson calibration, coda-duration estimates of M_L, and M_L versus m_B. in Earthquake studies in Utah 1950-1978: University of Utah Seismograph Stations, pp. 433-443, July.

Gutenberg B. and C.F. Richter, 1954, Seismicity of the Earth and Associated Phenomena, 2nd ed., Princeton University Press, Princeton, New Jersey, 310 pp.

Gutenberg B. and C.F. Richter, 1956, Earthquake magnitude, intensity, energy, and acceleration: Bulletin of the Seismological Society of America, vol. 46, pp. 105-145.

Hanks, T.C., and H. Kanamori, 1979, A moment magnitude scale: Journal of Geophysical Research, vol. 84, no. B5, pp. 2348-2350.

Hanks, T.C., and R.K. McGuire, 1981, The character of high frequency ground motion: Bulletin of the Seismological Society of America, v. 71, No. 6, pp. 2071-2095.

Hanson, K.L., F.H. Swan, and D.P. Schwartz, 1981a, Study of earthquake recurrence intervals on the Wasatch fault, Utah (North Creek site): Sixth semiannual technical report prepared for the U.S. Geological Survey under Contract No. 14-07-0001-19842, 22 pp.

Hanson, K.L., F.H. Swan, and D.P. Schwartz, 1981b, Study of earthquake recurrence intervals on the Wasatch fault, Utah: Fifth semiannual technical report prepared for the U.S. Geological Survey under Contract No. 14-08-0001-19115, 15 pp.

Hanson, K.L. and D.P. Schwartz, 1982, Guidebook to late Pleistocene and Holocene faulting and the vicinity - Little Cottonwood Canyon to Scipio, Utah: American Geophysical Union Chapman Conference on Fault Behavior and the Earthquake Process, Snowbird, Utah, October 11-15, 1982.

Hays, W.W., and K.W. King, 1982, Zoning of the earthquake ground-shaking hazard along the Wasatch fault zone, Utah: Third International Earthquake Microzonation Conference Proceedings, v. III, June 28-July 1, Seattle.

Hays, W.W., and K.W. King, 1984a, The ground-shaking hazard along the Wasatch fault zone, Utah: Eighth World Conference on Earthquake Engineering Proceedings, v. 1, p. 7-14.

Hays, W.W., and K.W. King, 1984b, The ground-shaking hazard along the Wasatch fault zone, Utah, in Proceedings of conference XXVI, a workshop on "evaluation of regional and urban earthquake hazards and risk in Utah": U.S. Geological Survey Open-File Report 84-763, p. 143-147.

Howell, B.F., Jr., and T.R. Schultz, 1975, Attenuation of modified Mercalli intensity with distance from the epicenter: Bulletin of the Seismological Society of America, v. 65, No. 1, p. 641-665, June.

Jackson, S.M., and J. Boatwright, 1985, The Borah Peak, Idaho earthquake of October 28, 1983-Strong ground motion: Earthquake Spectra, Earthquake Engineering Research Institute, v. 2, No. 1, p. 51-69, November

Joyner, W.B., and D.M. Boore, 1981, Peak horizontal acceleration and velocity from strong-motion records including records from the 1979 Imperial Valley, California earthquake: Bulletin of the Seismological Society of America, v. 71, No. 6, pp. 2011-2038.

Joyner, W.B., and D.M. Boore, 1982, Prediction of earthquake response spectra: US. Geological Survey Open File Report 82-977.

Joyner, W.B., and T.E. Fumal, 1985, Predictive mapping of earthquake ground motion, in Evaluating earthquake hazards in the Los Angeles region: U.S. Geological Survey Professional Paper 1360.

Keaton, J., D.R. Curry, and S.J. Olig, 1986, Paleoseismicity and earthquake hazards evaluation of the West Valley fault zone, Salt Lake City urban area: contract report prepared for U.S. Geological Survey, Contract No. 14-08-0001-22048, 18 pp.

King, K.W., and W.W. Hays, 1977, Comparison of seismic attenuation in Northern Utah with attenuation in four other regions of the western United States: Bulletin of the Seismological Society of America, v. 67, No. 3, pp. 781-792, June.

King, K.W., W.W. Hays, and P.J. McDermott, 1983, Wasatch front urban area seismic response data report: U.S. Geological Survey Open-File Report 83-452.

King, G., and G. Yielding, 1984, The evolution of a thrust fault system - Process of rupture initiation, propagation and termination in the El Asnam (Algeria) earthquake: Geophysical Journal Royal Astronomical Society, vol. 77, pp.913-933.

Kulkarni, R.B., R.R. Youngs, and K.J. Coppersmith, 1984, Assessment of confidence intervals for results of seismic hazard analysis: in Proceedings of the Eight World Conference on Earthquake Engineering, San Francisco, California, Vol. 1, pp. 263-270.

Lund, W.R., and D.P. Schwartz, 1987, Fault behavior and earthquake recurrence at the Dry Creek site, Salt Lake segment, Wasatch Fault Zone, Utah: EOS, V. 67, No. 44, p. 1107.

Machette, M.N., S.F. Personius, W.E. Scott, and A.R. Nelson, 1986, Quaternary geology for ten fault segments and large-scale changes in slip rate along the Wasatch fault zone: Paper presented at Workshop on "Earthquake Hazards Along the Wasatch Front, Utah," Salt Lake City, Utah, July 14-18, 1986.

Mayer, L., and A. Maclean, 1986, Tectonic geomorphology of the Wasatch Front, Utah, using morphologic discriminant analysis - preliminary implications for Quaternary segmentation of the Wasatch fault zone: Geological Society of America, Abstracts with Programs, vol. 18, no. 2, pp. 155.

McCalpin, J., 1985, Quaternary fault history and earthquake potential of the Hansel Valley area, north central Utah: National Earthquake Hazards Reduction Program, Summaries of Technical Reports, vol. XX, U.S. Geological Survey Open-File Report 85-464, pp. 105-108.

McCalpin, J., 1987, Quaternary deformation along the East Cache fault, north-central Utah: Geological Society of America, Abstracts with Programs, V. 19, No. 5, p. 320.

McGarr, A., 1982, Upper bounds on near-source peak ground motion based on a model of inhomogeneous faulting: Bulletin of the Seismological Society of America, v. 72, No. 6, p. 1825-1841, December.

McGarr, A., 1984, Scaling of ground motion parameters, state of stress, and focal depth: Journal of Geophysical Research, v. 89, No. 8, pp. 6969-6979, August 10.

McGuire, R.K., 1983, Estimation of seismic ground motion in northern Utah: Report submitted to U.S. Geological Survey by Dames & Moore under contract 14-08-0001-19825.

Merz, H.A., and C.A. Cornell, 1973, Aftershocks in engineering seismic risk analysis: M.I.T. Department of Civil Engineering Research Report R73-25, Cambridge, Massachusetts.

Nelson, A.R. and R.B. Van Arsdale, 1986, Recurrent late Quaternary movement on the Strawberry normal fault, Basin and Range - Colorado Plateau transition zone, Utah: Neotectonics, V. 1, p. 7-37.

Personius, S.F., 1986, The Brigham City segment - A new segment of the Wasatch fault zone, northern Utah: Geological Society of America, Abstract with Programs, V. , No. , p. .

Power, M.S., K.J. Coppersmith, R.R. Youngs, D.P. Schwartz, and F.H. Swan III, 1981, Seismic exposure analysis for the WNP-2 and WNP-1/4 site: Appendix 2.5K to Amendment No. 18 Final Safety Analysis Report WNP-2, for Washington Public Power Supply System, Richland Washington, September.

Richins, W.J., 1979, Earthquake data for the Utah region: in Earthquake Studies in Utah 1850 to 1978, editors W.J. Arabasz, R.B. Smith and W.D. Richins, University of Utah Seismograph Stations, Department of Geology and Geophysics, University of Utah, July, 1979, pp. 57-251.

Rogers, A.M., D.L. Carver, W.W. Hays, K.W. King, and R.D. Miller, 1984, Preliminary estimates of geographic variation in relative ground shaking in the Wasatch front urban corridor, in proceedings of conference XXVI, workshop on "evaluation of regional and urban earthquake hazards and risk in Utah": U.S. Geological Survey Open-File report 84-763, p. 547-556.

Rogers, A. M., S.C. Harmsen, R.B. Herrmann, and M.E. Meremonte, 1986, A study of ground motion attenuation in the southern Great Basin, Nevada-California, using several techniques for estimates of Q_s, log A_o, and coda Q_1: Paper accepted for publication by the Journal of Geophysical Research.

Rogers, A.M., J.C. Tinsley, and R.D. Borcherdt, 1985, Predicting relative ground response, in Evaluating earthquake hazards in the Los Angeles region: U.S. Geological Survey Professional Paper 1360.

Sadigh, K., 1983, Considerations in the development of site-specific spectra, in proceedings of Conference XXII, site-specific effects of soil and rock on ground motion and the implications for earthquake resistant design: U.S. Geological Survey Open File Report 83-845.

Sadigh, K., J.A. Egan and R.R. Youngs, 1986, Specification of ground motion for seismic design of long period structures: Earthquake Notes, vol. 57, no. 1, p. 13.

Schwartz, D.P., and K.J. Coppersmith, 1984, Fault behavior and characteristic earthquakes from the Wasatch and San Andreas faults: Journal of Geophysical Research, vol. 89, no. B7, pp. 5681-5698.

Schwartz, D.P. and K.J. Coppersmith, 1986, Seismic hazards: new trends in analysis using geologic data: in Active Tectonics, Academic Press, Washington D.C., pp. 215-230.

Schwartz, D.P., K.L. Hanson, and F.H. Swan, 1983, Paleoseismic investigations along the Wasatch fault zone: An Update: in Crone, A.J., (ed) Paleoseismicity along the Wasatch Front and Adjacent Areas, Central Utah, Geological Society of America Rocky Mountain and Cordilleran Sections Meeting, Guidebook Part 2, Utah Geological and Mineral Survey Special Studies 62, pp. 45-40.

Schwartz, D.P., F.H. Swan, and L.S. Cluff, 1984, Fault behavior and earthquake recurrence along the Wasatch fault zone: in Proceedings of Conference XXVI - A Workshop on "Evaluation of Regional and Urban Earthquake Hazards and Risk in Utah," US Geological Survey Open-File Report 84-763, pp. 113-125.

Scott, W.E., 1980, Quaternary stratigraphy of the Wasatch Front: National Earthquake Hazards Reduction Program Summaries of Technical Reports, vol. IX, U.S. Geological Survey Open File Report 80-6, pp. 62-64.

Seed, H.B. and Idriss, I.M., 1982, Ground motions and soil liquefaction during earthquakes, V. 5 of a series entitled Engineering monographs on earthquake criteria, structural design, and strong motion records, Earthquake Engineering Research Institute.

Seed, H.B., Idriss, I.M., and Keifer, F. W, 1969, characteristics of rock motions during earthquakes, Journal of Soil Mechanics and Foundation Division, ASCE, 95: 1199-1218.

Seed, H.B., R. Murarka, J. Lysmer and Idriss, I.M., 1976a, Relationships of maximum accelerations, maximum velocity, distance a from source and local site conditions for moderately strong earthquakes, Bulletin of the Seismological Society of America, Vol. 66, No. 4, August.

Seed, H. B., and P. Schnabel, 1980, presented in Ground motions and soil liquefaction during earthquakes, v. 5 of a series titled Engineering monographs on earthquake criteria, structural design, and strong motion records, by Seed H. B. and I.M. Idriss (1982): Earthquake Engineering Research Institute.

Seed, H.B., C. Ugas, and J. Lysmer, 1976b, Site-dependent spectra for earthquake-resistant design, Bulletin of the Seismological Society of America, Vol. 66, No. 1, February, pp 221-244.

Singh, S., 1981, Regionalization of crustal Q in the continental United States: Ph.D Dissertation, St. Louis University, St. Louis, Missouri.

Singh, S., and R.B. Herrmann, 1983, Regionalization of crustal coda Q in the continental United States; Journal of Geophysical Research, v. 88, No. B1, pp. 527-538, January 10.

Slemmons, D.B., 1977, State-of-the-art for assessing earthquake hazards in the United States, Report 6 - Faults and earthquake magnitude: U.S. Army Corps of Engineers, Waterways Experiment Station, Miscellaneous Paper S-73, 129 pp.

Slemmons, D.B., 1982, Determination of design earthquake magnitudes for microzonation: in Proceedings of the Third International Earthquake Microzonation Conference, vol 1., pp 119-130.

Slemmons, D.B., and G.M. Depolo, 1986, Evaluation of active faulting and associated hazards: in National Research Council, Studies in Geophysics - Active Tectonics, Academic Press, Washington, D.C., pp. 45-62.

Smith, R.B., W.D. Richins, and D.I. Doser, 1985, The 1983 Borah Peak, Idaho earthquake - regional seismicity, kinematics of faulting, and tectonic mechanism: in Proceedings of Workshop XXVIII on the Borah Peak, Idaho, Earthquake, V.A., U.S. Geological Survey Open-File Report 85-290, pp. 236-263.

Stepp, J.C., 1972, Analysis of completeness of the earthquake sample in the Puget Sound area an its effect on statistical estimates of earthquake hazard: in Proceedings of the International Conference on Microzonation, vol. 2, pp. 897-910.

Swan, F.H., III, D.P. Schwartz, and L.S. Cluff, 1980, Recurrence of moderate to large magnitude earthquakes produced by surface faulting on the Wasatch fault, Utah: Bulletin of the Seismological Society of America, vol. 70, no. 5, pp. 1431-1462.

Swan, F.H., III, D.P. Schwartz, K.L. Hanson, P.L. Knuepfer, and L.S. Cluff, 1981a, Study of earthquake recurrence intervals on the Wasatch fault at the Kaysville site, Utah: U.S. Geological Survey, Open-File Report No. 81-0228, 52 pp.

Swan, F.H., III, K.L. Hanson, D.P. Schwartz, and P.L. Knuepfer, 1981b, Study of earthquake recurrence intervals on the Wasatch fault at the Little Cottonwood Canyon site, Utah: U.S. Geological Survey, Open-File Report No. 81-450, 30 p.

Swan, F.H., III, D.P. Schwartz, L.S. Cluff, K.L. Hanson, and P.L. Knuepfer, 1981c, Study of earthquake recurrence intervals on the Wasatch fault at the Hobble Creek site, Utah: U.S. Geological Survey, Open-File Report No. 81-0229, 58 pp.

Swan, F.H., III, K.L. Hanson, and D.P. Schwartz, 1983, Study of earthquake recurrence intervals on the Wasatch fault, Utah: Eighth semiannual technical report prepared for the U.S. Geological Survey under Contract No. 14-07-0001-19842 (East Cache fault).

Townley, S.D. and M.W. Allen, 1939, Descriptive catalog of earthquakes of the Pacific coast of the United States - 1769 to 1928: Bulletin of the Seismological Society of America, vol. 29, no. 1, pp. 1-297.

Uhrhammer, R.A., 1986, Characteristics of northern and central California seismicity (abs.): Earthquake Notes, vol. 57, no. 1, p. 21.

U.S. Geological Survey, 1980, Earthquake hazards along the Wasatch and Sierra-Nevada frontal fault zones: Proceedings of Conference X, National Earthquake Hazards Reduction Program, 29 July 1979 - 1 August 1979, U.S. Geological Survey Open-File Report 80-801, 679 pp.

U.S. Geological Survey, 1984, A workshop on "Evaluation of regional and urban earthquake hazards and risk in Utah": Proceedings of Conference XXVI, National Earthquake Hazards Reduction Program, U.S. Geological Survey Open-File Report 84-763, 674 pp.

Utah Geological Association, 1972, Environmental Geology of the Wasatch Front, 1971: Utah Geological Association Publication 1, Salt Lake City, Utah.

Veneziano, D. and J. Van Dyck, 1985, Analysis of earthquake catalogs for incompleteness and recurrence rates: Seismic Hazard Methodology for Nuclear Facilities in the Eastern United States, EPRI Research Project No. P101-29, EPRI/SOG Draft 85-1, vol. 2, Appendix A-6, April 30.

Weichert, D.H., 1980, Estimation of the earthquake recurrence parameters for unequal observation periods for different magnitudes: Bulletin of the Seismological Society of America, vol. 70, no. 4, pp. 1337-1346.

Wheeler, R., 1984, A plan for evaluating hypothesized segmentation of the Wasatch fault: in Proceedings of Conference XXVI, A Workshop on "Evaluation of Regional and Urban Earthquake Hazards and Risk in Utah", U.S. Geological Survey Open-File Report 84-763, p. 576-605.

Woodward-Clyde Consultants, 1982, Preliminary assessment of the seismic potential of the Oquirrh fault zone, Utah: Report prepared for Davy McKee Corporation, San Mateo, 16 pp.

Wyss, M., 1979, Estimating maximum expectable magnitude of earthquakes from fault dimensions: Geology, vol. 7, no. 7, pp. 336-340.

Youngs, R.R. and K.J. Coppersmith, 1985a, Development of a fault-specific recurrence model: Earthquake Notes (abs.), vol 56, no. 1, p. 16.

Youngs, R.R. and K.J. Coppersmith, 1985b, Implications of fault slip rates and earthquake recurrence models to probabilistic seismic hazard estimates: Bulletin of the Seismological Society of America, vol. 75, no. 4, pp. 939-964.

Youngs, R.R., K.J. Coppersmith, M.S. Power and F.H. Swan III, 1985, Seismic hazard assessment of the Hanford region, eastern Washington State: in Proceedings of the DOE Natural Phenomena Hazards Mitigation Conference, Las Vegas, Nevada, October 7-11, pp. 169-176.

RELATIVE GROUND RESPONSE IN SALT LAKE CITY AND AREAS OF SPRINGVILLE-SPANISH FORK, UTAH

By Kenneth W. King, Robert A. Williams, and David L. Carver
U.S. Geological Survey
Denver, Colorado

INTRODUCTION

The principal population and urban areas of Utah are located near the Wasatch fault zone. Although the Wasatch fault and associated faults have not produced an earthquake larger than a magnitude 6 since 1850 (Arabasz and others, 1979), the potential for a damaging and (or) life-threatening earthquake to occur within the next 100 years is very high (Swan and others, 1980). Structural damage and life risks from ground motions induced from earthquakes could be lessened if the ground shaking intensity potential for the urban areas could be accurately predicted. This study is a part of the U.S. Geological Survey/Utah Geological and Mineral Survey's program to assess the earthquake hazards in Utah's Wasatch Front urban areas.

The general objective of this study is to improve the understanding of how shallow underlying geology affects ground shaking. The study (1) compares the site response amplification factors of this study that are derived from Fourier amplitudes with those derived from pseudo relative velocity algorithms (PSRV) (Hays and King, 1982); (2) develops a detailed ground response map of the Salt Lake City urban area in the low- to medium-response areas of Hays and King (1982); and (3) examines the feasibility of correlating site response with geologic data which has been derived from high-resolution shallow seismic reflection profiles.

The study included analysis of ground-shaking data induced by distant nuclear explosions at the Nevada Test Site recorded at 14 sites in the Salt Lake City and Springville-Spanish Fork area (figs. 1, 2). The methodology was similar to that used by Borcherdt (1975), Rogers and Hays (1978), Hays and King (1982), and Rogers and others (1985). High-resolution shallow reflection profiles were acquired at five of the sites. In addition, a semipermanent network of strong-motion seismic instruments was deployed in the Salt Lake City-Ogden urban areas to record higher intensity ground shaking if local earthquakes should occur during these urban hazards studies.

PREVIOUS STUDIES

The variability of damage to structures caused by induced vibrations have been documented since the early 20th century (Milne, 1908; Reid, 1910). These authors observed that structures underlain by loose soil, marshy deposits, or filled land incurred greater amounts of damage during ground shaking induced by earthquakes than similar structures underlain by bedrock. Advances in seismic instrument technology permitted Kanai (1952) and Gutenberg (1957) to make quantitative studies of ground shaking induced by earthquakes at sites underlain by different materials. Their studies indicated that sites underlain by alluvium or filled land may experience earthquake ground shaking up to 10 times larger than at bedrock sites.

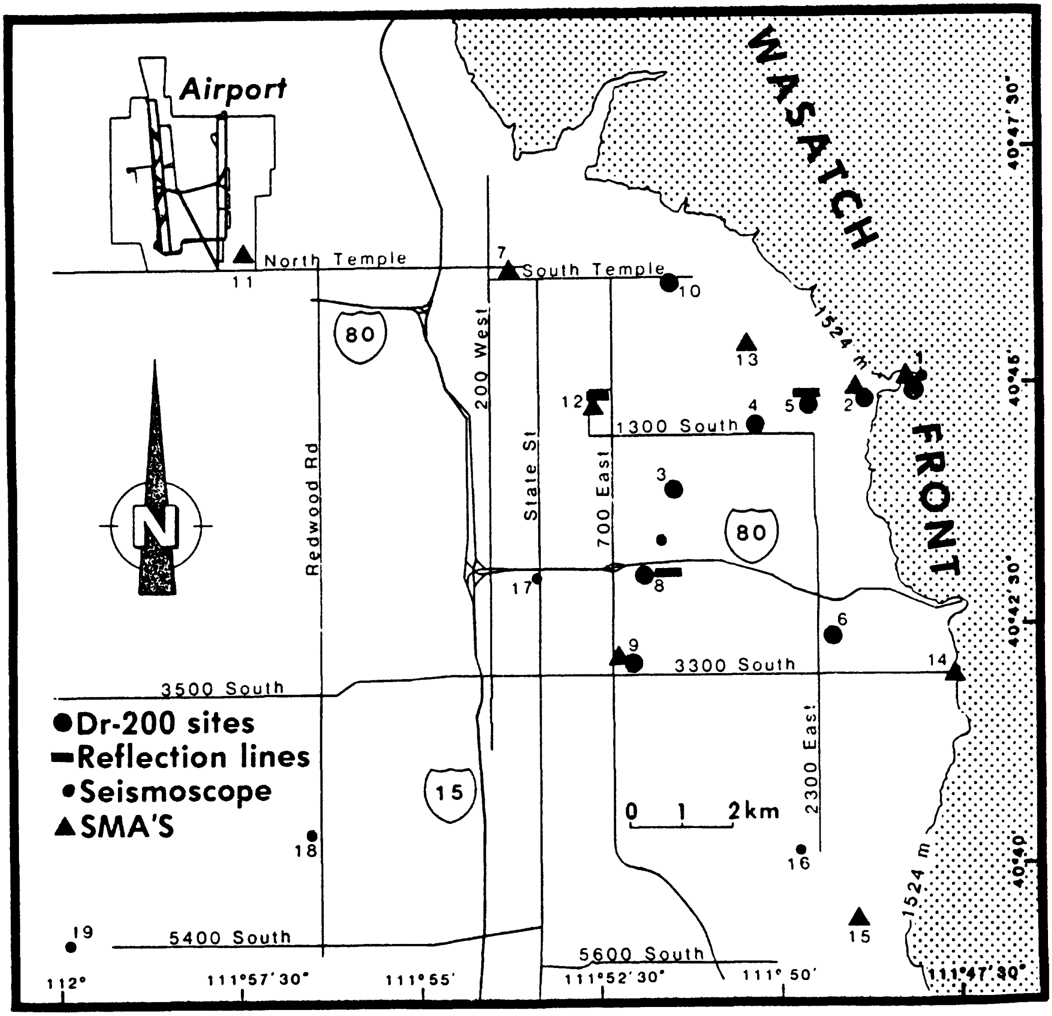

Figure 1.--Locations of sites, and their assigned station numbers, in Salt Lake City at which ground-motion recordings of nuclear explosions and shallow seismic reflection profiles were acquired. Seismoscope and SMA instrument sites are also shown.

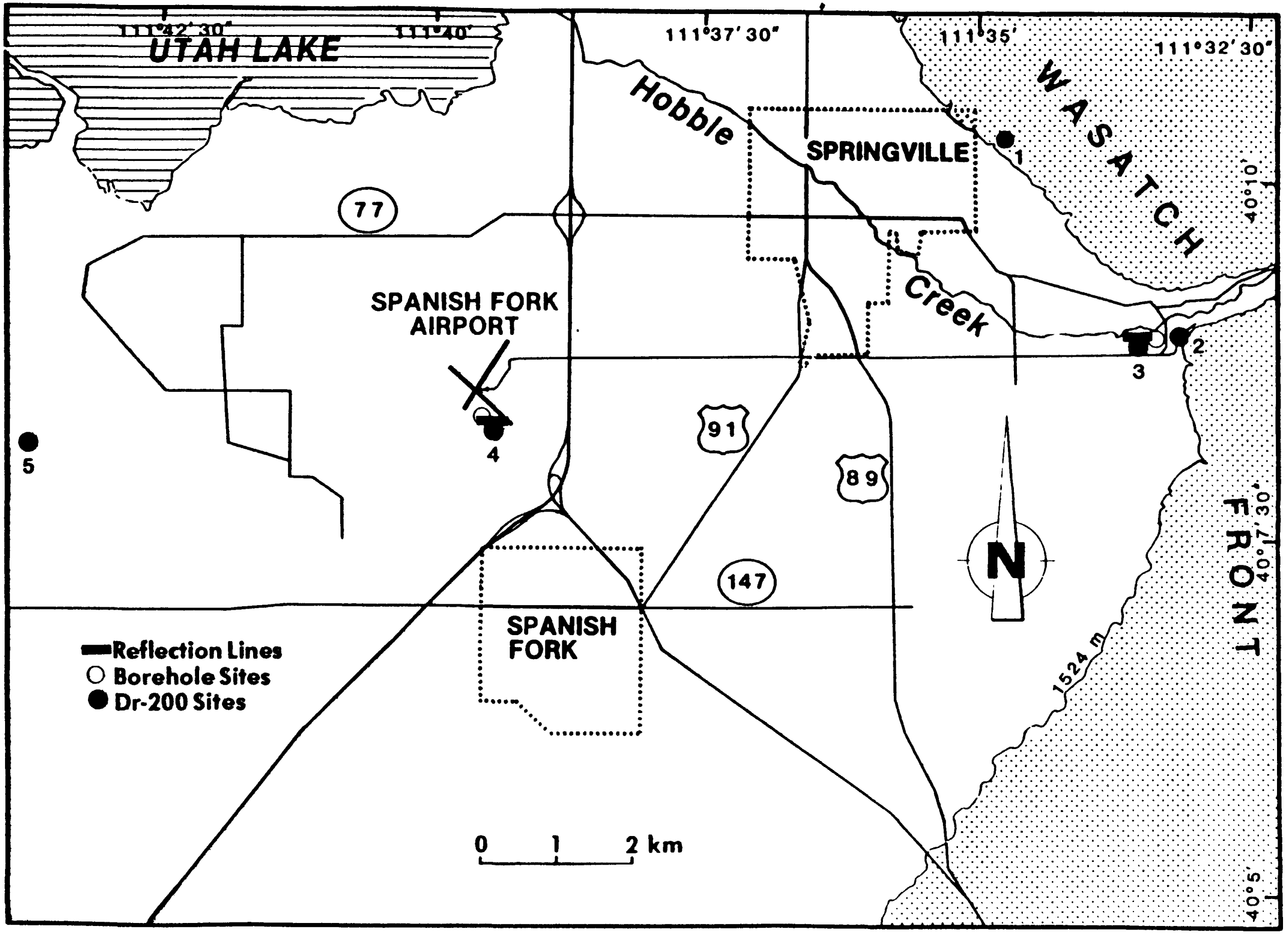

Figure 2.--Locations of sites, and their assigned station numbers, in the Springville-Spanish Fork areas at which ground-motion recordings of nuclear explosions and shallow seismic reflection profiles were acquired. Exploratory boreholes are also shown.

The testing of nuclear devices at the Nevada Test Site and the advancement of computer analysis has increased the sophistication in quantitative, detailed, and controlled empirical investigations of the variability of the frequency and amplitude of ground shaking at selected sites. Studies by Borcherdt (1970), Murphy and others (1971), Rogers and Hays (1978), and Hays and others (1978) have shown that realistic ground-shaking estimates for moderate-size earthquakes can be made by using ground-motion scaling laws derived from the analysis of low-strain nuclear explosion induced ground motions. The studies by Borcherdt and Gibbs (1976), Hays and King (1982), and Rogers and others (1985) show that the local site conditions have a greater influence on ground shaking than the effects of source azimuth, wave type, or angles of incidence. The ground-shaking study of the San Francisco Bay area (Borcherdt and Gibbs, 1976) showed an average spectral amplification for horizontal ground motions on bay mud sites to range between 3.7 and 11.3, relative to sites located on bedrock. A similar study in the Wasatch Front area (Hays and King, 1982) indicated that the greatest potential hazard from earthquake ground shaking in the Wasatch Front area would occur at sites underlain by thick, fine-grained, water-saturated, nearshore and offshore lacustrine deposits of silts and clays. The ground-response study of the Los Angeles area (Rogers and others, 1985) shows a ground-motion amplification factor of 4 to 6 (at certain frequencies) at sites that are underlain by Holocene and Pleistocene sediments compared with sites underlain by crystalline rock. The Los Angeles area study also indicated a correlation of ground-motion amplification with the mean void ratio of the near-surface materials when the ground-shaking period was 0.2-0.5 s.

GEOLOGY

The Salt Lake City and the Springville-Spanish Fork areas investigated in this study are located in similar geologic settings. The Wasatch Front borders both study areas on the east where Jurassic to Precambrian limestone, dolomite, shale, sandstone and quartzite are exposed (McGregor and others, 1974). These craton derived rocks are thought to underlie the alluvial sediments upon which the majority of the Wasatch Front urban areas are located. These sediments are unconsolidated fluvial and lacustrine materials deposited in and around Pleistocene lakes and alluvial fans of Pleistocene or younger age (Van Horn, 1972; Swan and others, 1980). McGregor and others (1974) divide the alluvial sequence beneath the Salt Lake City area into Quaternary alluvium at the surface underlain by Tertiary alluvial deposits which are underlain by Jurassic to Precambrian bedrock. Cumulative thickness of the alluvial stratum (Quaternary and Tertiary) increases westward as the distance from the Wasatch Front increases. The estimated range of total alluvial thickness underlying the Salt Lake study area is from 0 m to approximately 450 m (McGregor and others, 1974). Tertiary alluvium, varying in thickness from 0 to 200 m, rests on Jurassic and other bedrock in the Salt Lake City study area. The Tertiary deposits are generally semiconsolidated layers whose composition ranges from boulders to clay with some interbedded well-cemented layers. Information is included in this report where site-specific borehole and (or) reflection information are available at the study sites.

The unconsolidated sediment classification used in the study areas of Hays and King (1982) was adapted from Miller's (1980) study of the Salt Lake Valley surficial deposits. The Miller study divides the surficial deposits of the Salt Lake valley into three categories according to the environment of deposition: onshore, nearshore, and offshore. The study indicated that the deposits become more fine grained with increasing distance from the Wasatch Front. The onshore deposits are mostly fluvial in origin and generally form a narrow band along the base of the Wasatch Front and into the Salt Lake valley as terraces along the edges of the streams draining the Wasatch Range. The onshore deposits also are found as extensive flood-plain deposits overlying thick sequences of fine-grained lacustrine deposits. The onshore deposits consist mainly of sand, gravel, cobbles, and boulders and grade into the nearshore deposits which can be coarse grained and poorly sorted. The nearshore sediments were deposited chiefly in shallow water along the lakeshores and formed beaches, longshore spits and bars, deltas, and marsh deposits. The offshore deposits represent a quiet-water depositional environment and consist mainly of interbedded very fine sand, silt, and clay.

In the Salt Lake City area, the recording sites described in this report are located on the full range of surficial geological materials as defined by Miller (1980). Site 1 is located on Jurassic age limestone. Sites 2, 3, 9 and 10 are underlain by onshore deposits, sites 4 and 6 are underlain by nearshore deposits, and sites 5 and 8 are underlain by offshore deposits.

The geology of the Springville-Spanish Fork area is generally similar to that of the Salt Lake area. The thickness of alluvial deposits is less well known owing to sparse subsurface geotechnical information in the area. Site 1 in the Springville area is underlain by Pennsylvanian-Permian age quartzite. Geologic descriptions of surficial deposits near the Springville sites 2 and 3 (fig. 2) by Swan and others (1980), and a description of the subsurface material from a nearby borehole (J.C. Tinsley, written commun., 1986) indicate that the materials at this location are similar to the Salt Lake onshore deposits. A description of the material from a borehole at the Spanish Fork airport (site 4) and at the Youd farm (site 5) is similar to the descriptions of the Salt Lake City offshore deposits (J.C. Tinsley, unpub. data, 1986). The subsurface geology at these and other sites is being investigated.

DATA ACQUISITION

STRONG-MOTION NETWORK

Nine strong-motion accelerographs and seven strong-motion seismoscopes are deployed in the Salt Lake City/Ogden, Utah, areas. Three strong-motion accelerographs (SMA-1) are permanently located in the Salt Lake City area in standby operation mode. Six additional SMA-1 accelerographs have been added to the three-station network for the duration of the urban hazards investigation. These instruments were installed to give expanded recording of the ground shaking in the Salt Lake area if a medium to large earthquake should occur in or near the study area. The sites selected for the deployment of the six additional accelerographs followed criteria similar to those used for selecting site response station locations. One accelerograph is located on a hard-rock site near Salt Lake City (site 1) to establish a base against which to compare the other seismic data. The remaining five instruments were deployed at sites which are underlain by a variety of depths and types of alluvium. Two are located at sites occupied by Hays and King (1982), and two are located at sites investigated in this report (fig. 1).

Induced vibrations from large buildings during an earthquake could compromise the ground-shaking data recorded by the strong-motion instrument if the instrument is located near or in the structure. Therefore, the strong-motion instruments are located at a distance from the nearest large building by a distance greater than twice the building height. The strong-motion instruments begin recording when ground shaking exceeds 0.1 g acceleration in the 1.0-40 Hz bandwidth.

Seven seismoscopes were installed in the Salt Lake City area to supplement the strong-motion network. The seismoscopes will record the amplitudes of the ground shaking at the instrument's natural period (0.75 s) (Cloud and Hudson, 1961). The sites chosen for the seismoscopes represent different thicknesses of alluvium overlying the basement bedrock of the valley. The site locations (fig. 1) were selected from the Salt Lake valley gravity map data of Adhidjaja and others (1981). No earthquake large enough to trigger or record on the accelerographs or seismoscopes has occurred since the instruments were installed.

SITE RESPONSE

The site-response ground-shaking data presented in this report were recorded by portable digital seismographs. The seismometers are three-component velocity-sensing transducers that have a natural period of 0.62 s and are damped at 60 percent of critical. The data are digitally recorded on 1/4-inch magnetic tape at 50 samples per second per channel. Carver and others (1986) described the seismographs and their calibrations.

The sites at which response studies were conducted: (1) represent sites of the low-, medium-, and high-response areas described by Hays and King (1982); (2) are in the Salt Lake City area; (3) are at sites where additional geotechnical experiments could be done to reveal details of the underlying geology; (4) are in areas where major differences of surficial geology occur as described by Miller (1980); and (5) are in locations having sufficient open areas to be able to conduct high-resolution shallow reflection studies, drill a borehole, and conduct future experiments. The study did not include locations in Salt Lake City in high-response areas as described in Hays and King (1982), as most of those sites are now inundated by the rise of the Great Salt Lake. Site response sites selected in the Springville-Spanish Fork area (fig. 2) included two locations in the deeper parts of the basin which are believed to be similar to the high-response sites near Salt Lake City as reported by Hays and King (1982).

An underground nuclear test at the Nevada Test Site provided the seismic energy. Previous reports by Borcherdt (1970), Hays and King (1982) and Rogers and others (1985) have demonstrated the validity of using the ground motions from a Nevada Test Site nuclear test for a site response study. A minimum of 2 minutes of preevent seismic data was recorded for the tests. The preevent data at each site were used to establish the level of ambient seismic background noise at that station before the recording of the ground shaking from the nuclear event.

SHALLOW REFLECTION

High-resolution, shallow seismic reflection profiles were collected at five sites in the Salt Lake City and Springville-Spanish Fork area that coincided with the locations used to study relative ground shaking and site response (figs. 1, 2). The data for the reflection profiles were collected with a linear array that ranged from approximately 40 to 160 m in length. The arrays had station separations of 0.5-1.5 m which became the positions of the geophones and the reference location for the input source. The data were amplified, filtered, summed, converted to digital form with 0.5 ms sampling and stored on 1/2-inch magnetic tape by a high-resolution, 24-channel reflection system.

Single, 100 Hz (resonant frequency) vertical velocity sensing geophones with 15-cm ground coupling spikes were firmly planted in the ground surface at 0.5- to 1.5-m intervals to detect P-wave reflections. The -18 dB/octave rolloff of the 100-Hz geophones and a 80-Hz low-cut filter in the recording system help discriminate against the surface waves generated by the energy source. The seismic energy source was a 12-gauge shotgun which fired a 28-g lead slug vertically into the ground. The slug dissipated its energy quickly and usually penetrated less than 0.2 m into the ground. The high-resolution reflection system records the input from 24 different geophones for each shot location. The data from three shots at each shotpoint are summed and recorded. Summing of data from several shots at a single shotpoint improves the signal-to-noise ratio owing to enhancement of the coherent reflective seismic signal and by cancellation of some of the less coherent ambient seismic noise.

The shotpoints were located in the middle of the geophone array (split-spread). The distance from the source to the nearest geophone used for data input, and the distance from the source to the farthest geophone used for data input, remained constant (constant offsets) as the source locations were moved along the array in increments equal to the station (geophone) spacing distance. Figure 3 shows the source input shooting pattern, the station interval spacing, and the source-to-geophone distances used on each profile. The half interger source input configuration was used to achieve -3dB ambient seismic noise attenuation during the data processing (Knapp, 1985). The array also allows common-depth-point (CDP) processing of the data (Mayne, 1962). The array pattern and CDP processing achieve a summing of 12 different source-to-geophone raypath combinations for each subsurface point along the length of the profile (twelvefold coverage).

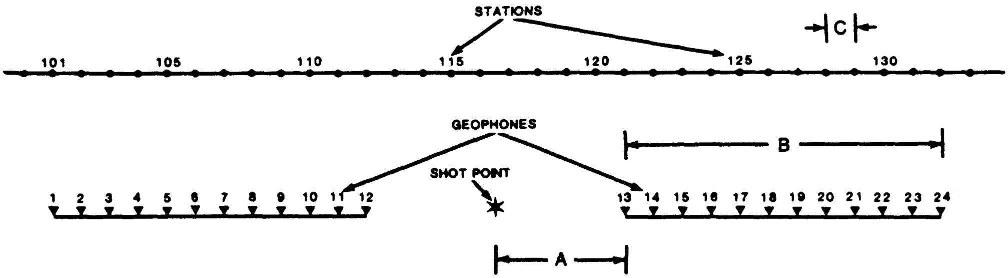

SLC 5-Bonneville Golf Course: A-9.1m, B-33.5m, C-3.0m

SLC 8-Forest Dale Golf Course: A-5.5m, B-13.4m, C-1.2m

SLC 12-Liberty Park: A-5.5m, B-13.4m, C-1.2m

SSF 3-Hobble Creek (Orchard): A-5.5m, B-13.4m, C-1.2m

SSF 5-Spanish Fork Airport: A-9.0m, B-33.0m, C-3.0m

Figure 3.--Seismic reflection profiling shooting pattern, (A) source-1st geophone distance, (B) geophone spread length, (C) geophone spacing used at each site. Shotpoint locations are half-way between stations. Station designations used in the reflection profiling are not related to site response station numbers.

DATA REDUCTION AND ANALYSIS

SITE RESPONSE

The ground motion due to a nuclear test in Nevada were digitally recorded at nine sites in the Salt Lake City area and at five sites in the Springville-Spanish Fork area. The data were recorded by wideband, digital-recording seismograph systems using three-component velocity-sensing seismometers (Carver and others, 1986). Approximately 2 minutes of preevent and 6 minutes of postevent seismic data from each site were preserved as time histories in digital form on VAX 11/750 files. These data were reduced to amplitude normalized time histories (figs. 4, 5), spectra (figs. 6, 7), spectral signal to spectral noise comparison (figs. 8, 9), and to spectral ratios (figs. 10, 11, 12). The data reduction methods were similar to those used by Hays and King (1982) and Rogers and others (1985). Spectral ratios (site transfer functions of sites on rock to sites underlain by alluvium) derived from nuclear test ground motions show reasonable agreement with site transfer functions similarly derived from earthquake-induced ground motions (Rogers and Hays, 1978). The results presented here are a reasonable estimate of the site effects from a damaging earthquake.

The time history data were low-pass filtered (10-Hz corner, -18dB/octave) to help eliminate the local ambient seismic noise. Rogers and others (1985) found that most of the seismic energy from the nuclear tests above 5 Hz is attenuated before reaching recording sites that are beyond approximately 400 km from the source. Therefore, the filtering was acceptable for this study as all the recording stations are over 500 km from the source.

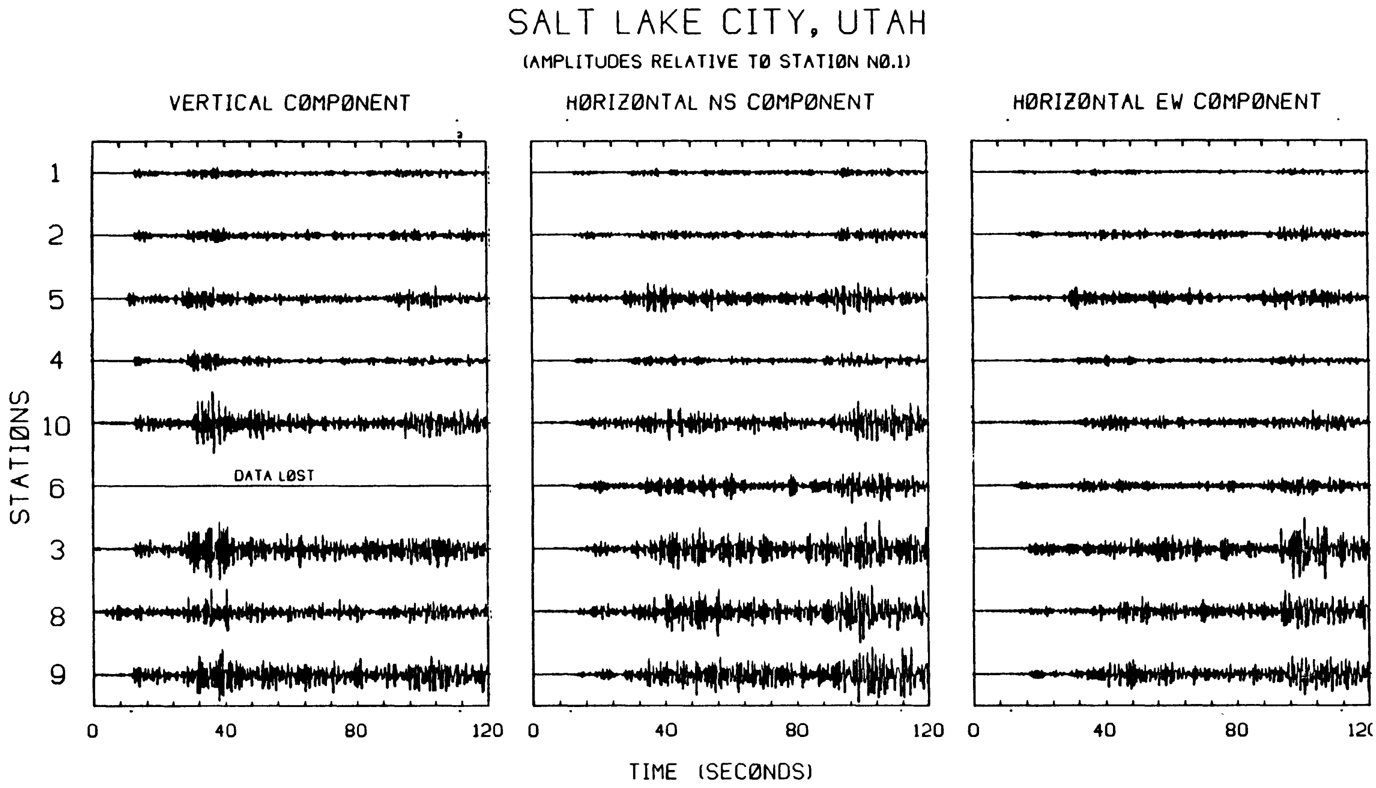

Figure 4.--Vertical, horizontal NS and EW component time-histories of ground motion from nuclear explosion Event B recorded simultaneously at 9 sites in Salt Lake City. Station numbers for each site are listed at the left of each record. Recording amplitudes are normalized to station 1 (hardrock).

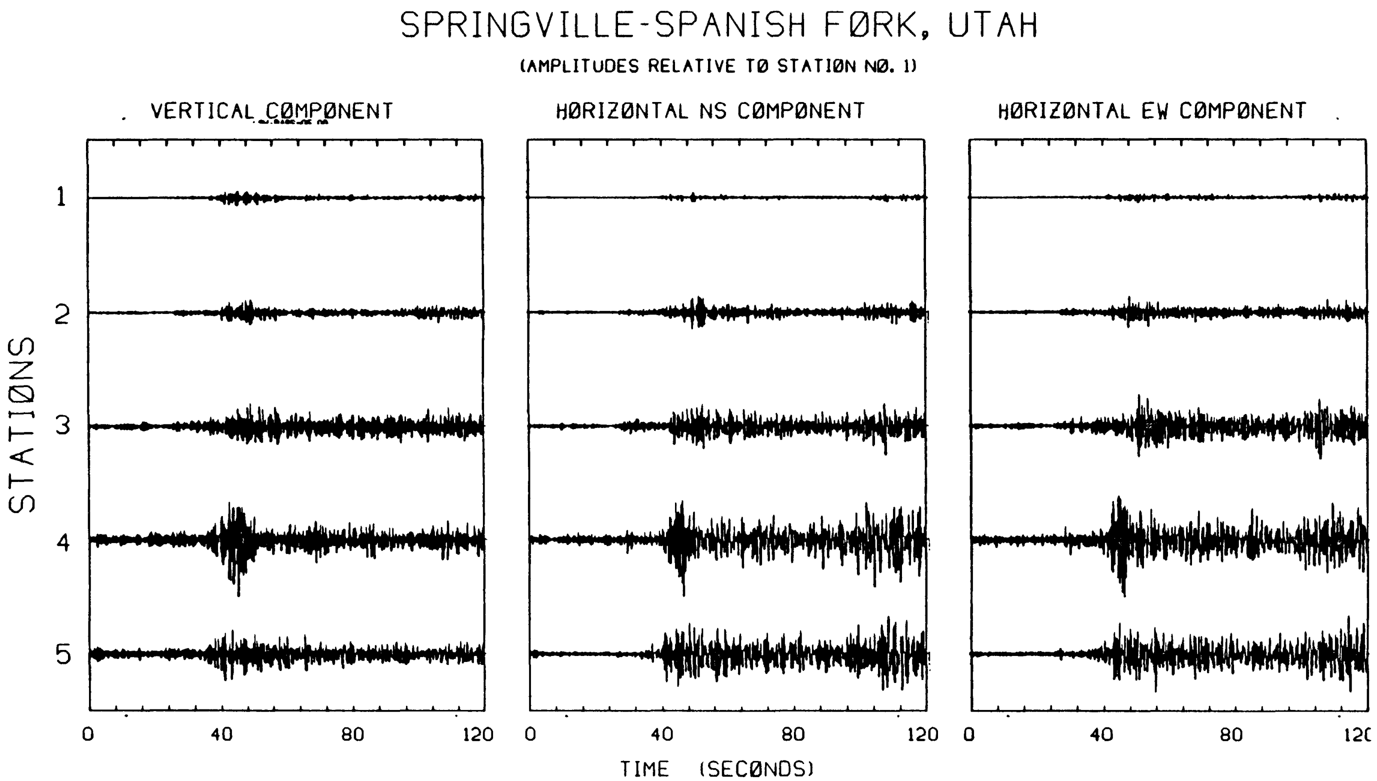

Figure 5.--Vertical, horizontal NS and EW component time-histories of ground motion from nuclear explosion Event A recorded simultaneously at 5 sites in the Springville-Spanish Fork areas. Station numbers for each site are listed at the left of each record. Recording amplitudes are normalized to station 1 (hardrock).

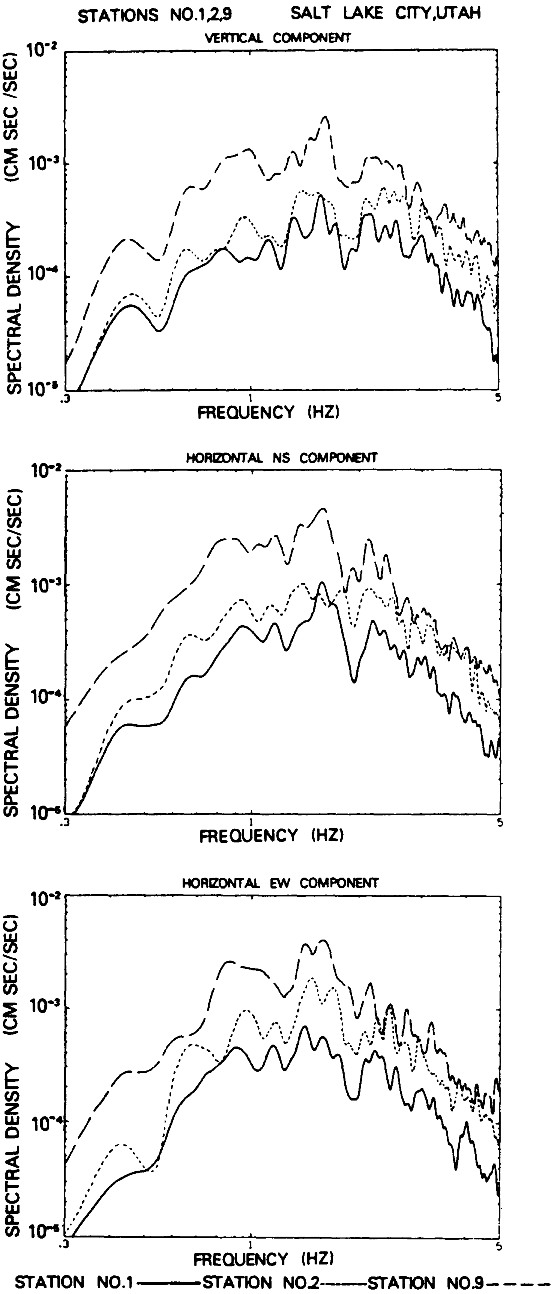

Figure 6.--Amplitude spectra computed from recordings of vertical and horizontal (NS and EW) ground motion generated by nuclear event B. The spectra are identified by station number location (see Figure 2) and arranged on the figure by increasing alluvial thickness. For this figure the thickness of alluvium increases as the station number increases. Spectra are plotted at frequencies for which the signal:noise ratio > 2.

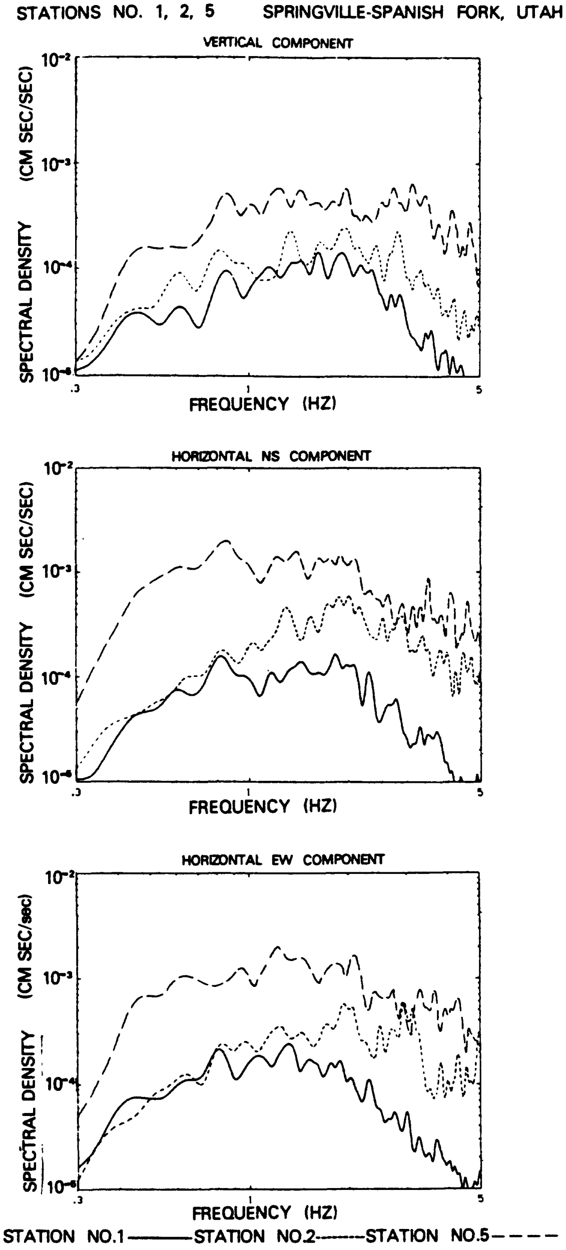

Figure 7.--Amplitude spectra comparison for three sites computed from recordings of vertical and horizontal (NS and EW) ground-motion generated by nuclear event A. The spectra are identified by the station number location (see Figure 3) and arranged on the figure in order of increasing alluvial thickness. For this figure the thickness of alluvium increases as the station number increases. Spectra are plotted at frequencies for which the signal:noise ratio > 2.

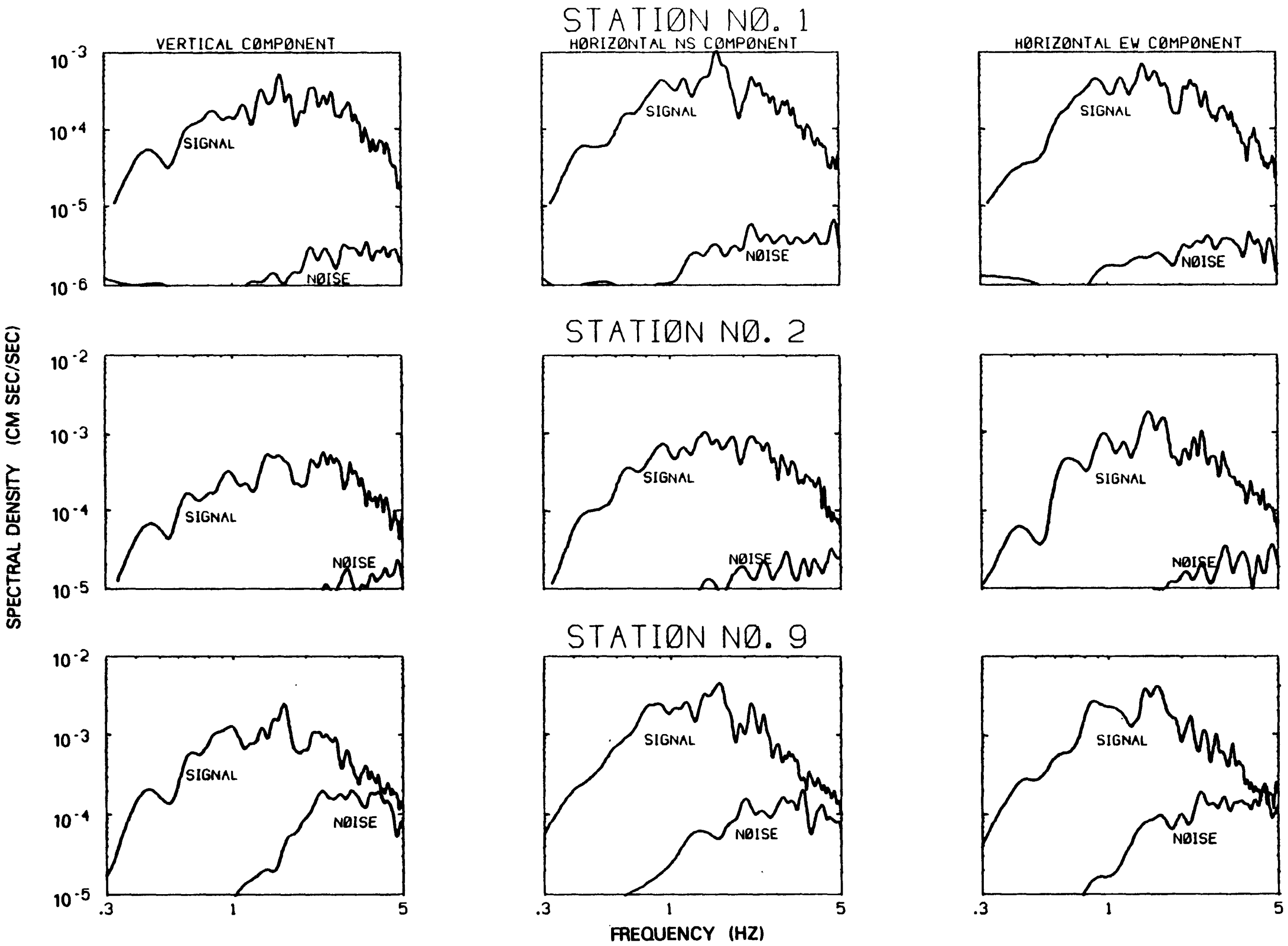

Figure 8.--Comparison of signal and noise amplitude spectra for three sites in Salt Lake City computed from ground motion generated by nuclear event B. Noise spectra calculated from analysis of a 50 s segment of data before the arrival of event B.

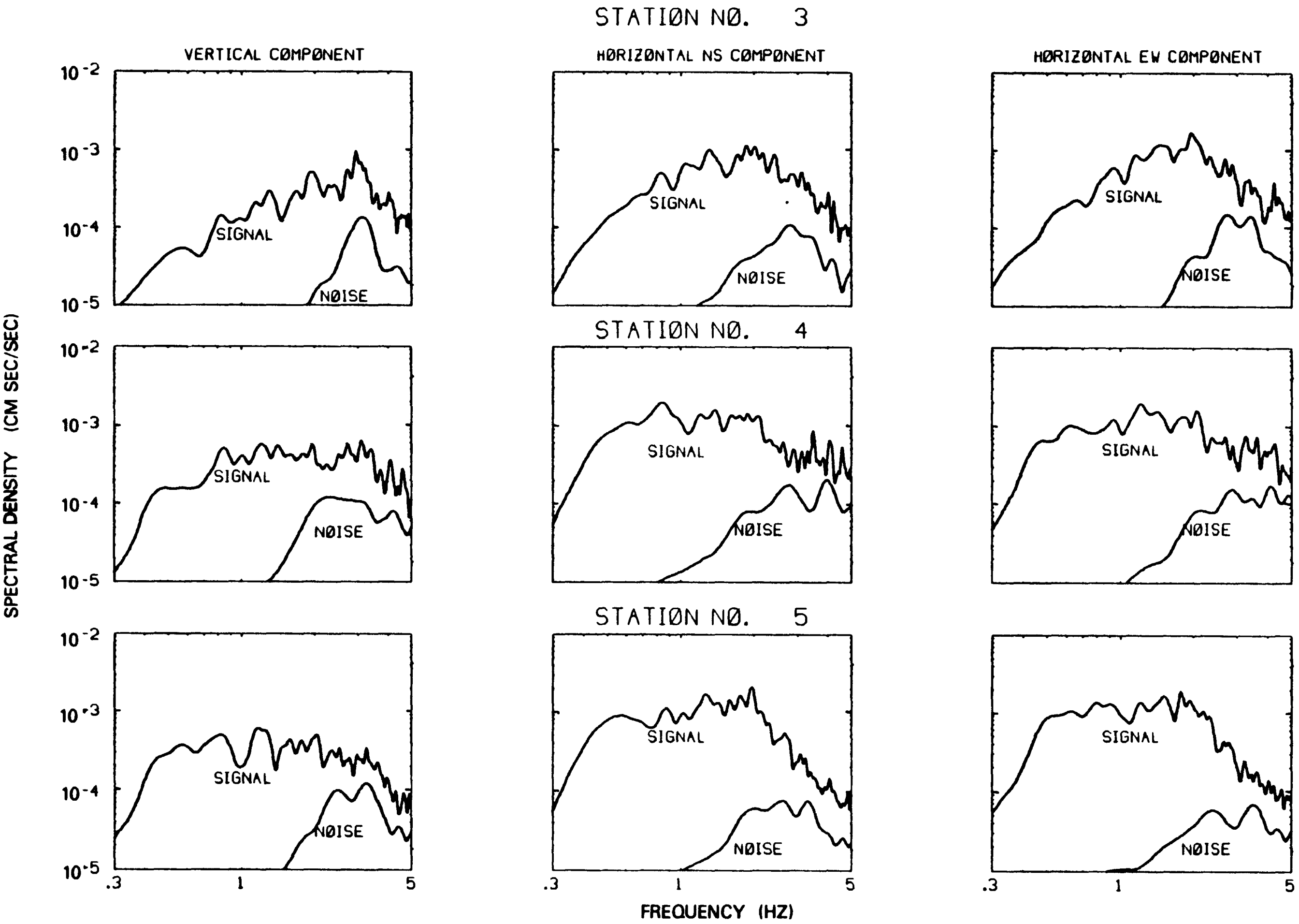

Figure 9.--Comparison of signal and noise amplitude spectra for three sites in the Springville-Spanish Fork area computed from ground motion generated by nuclear event A. Noise spectra calculated from analysis of a 50 s segment of data before the arrival of event A.

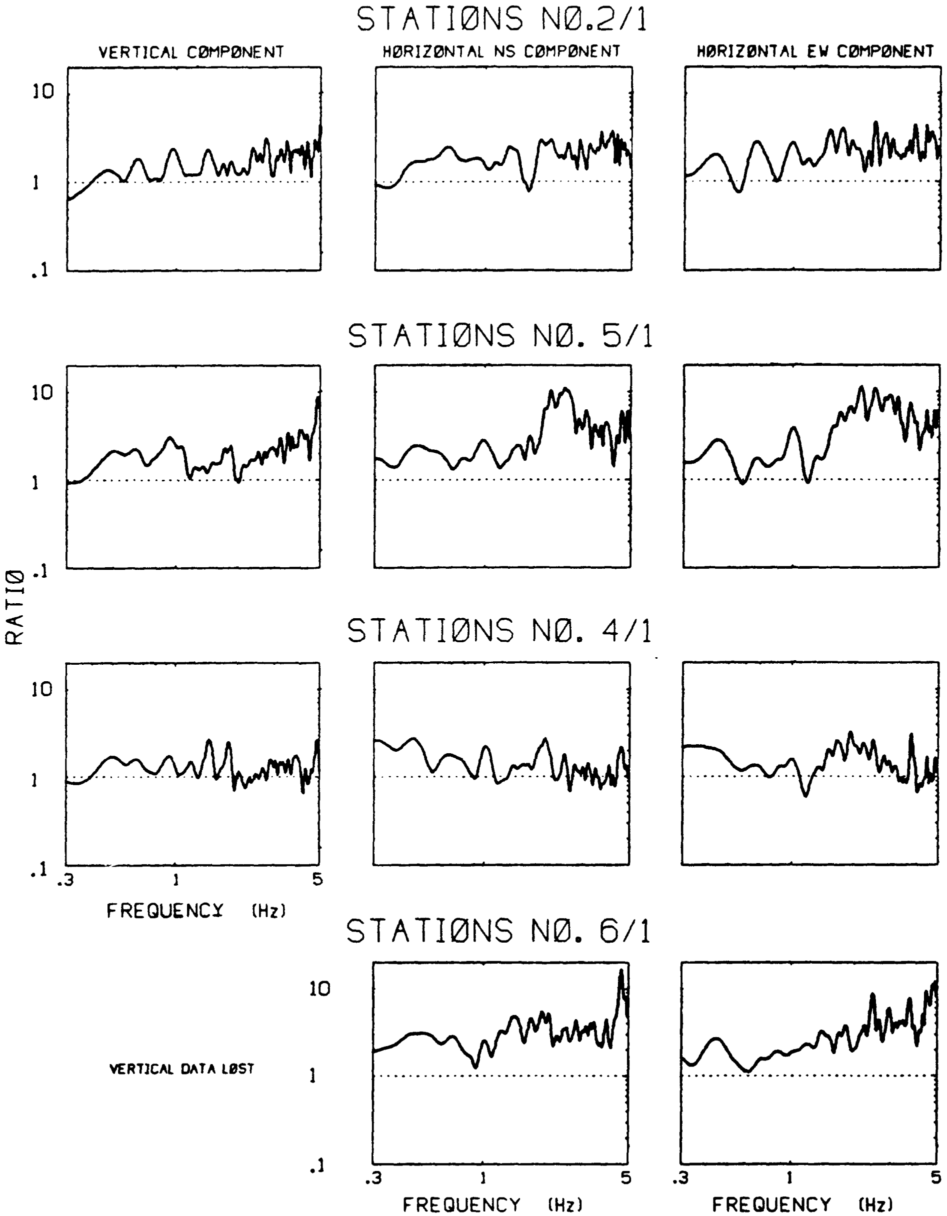

Figure 10.--Spectral ratios of vertical and horizontal (NS and EW) components of ground motion recorded on sites having geologic conditions different from the crystalline rock site (station 1) in Salt Lake City. Spectral ratios are not plotted for data with S/N < 2.

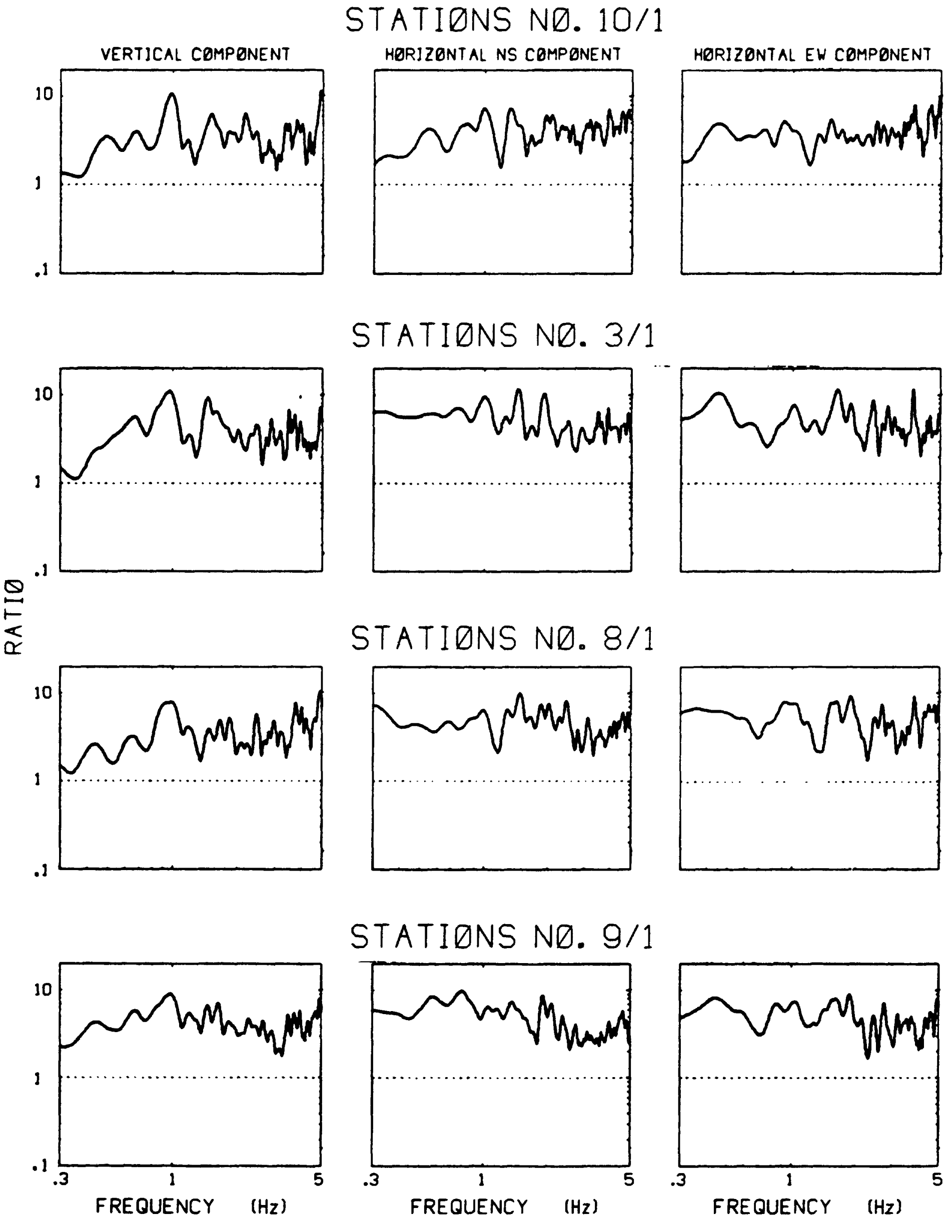

Figure 11.--Spectral ratios of vertical and horizontal (NS and EW) components of ground motion recorded on sites having geologic conditions different from the crystalline rock site (station 1) in Salt Lake City. Spectral ratios are not plotted for data with S/N < 2.

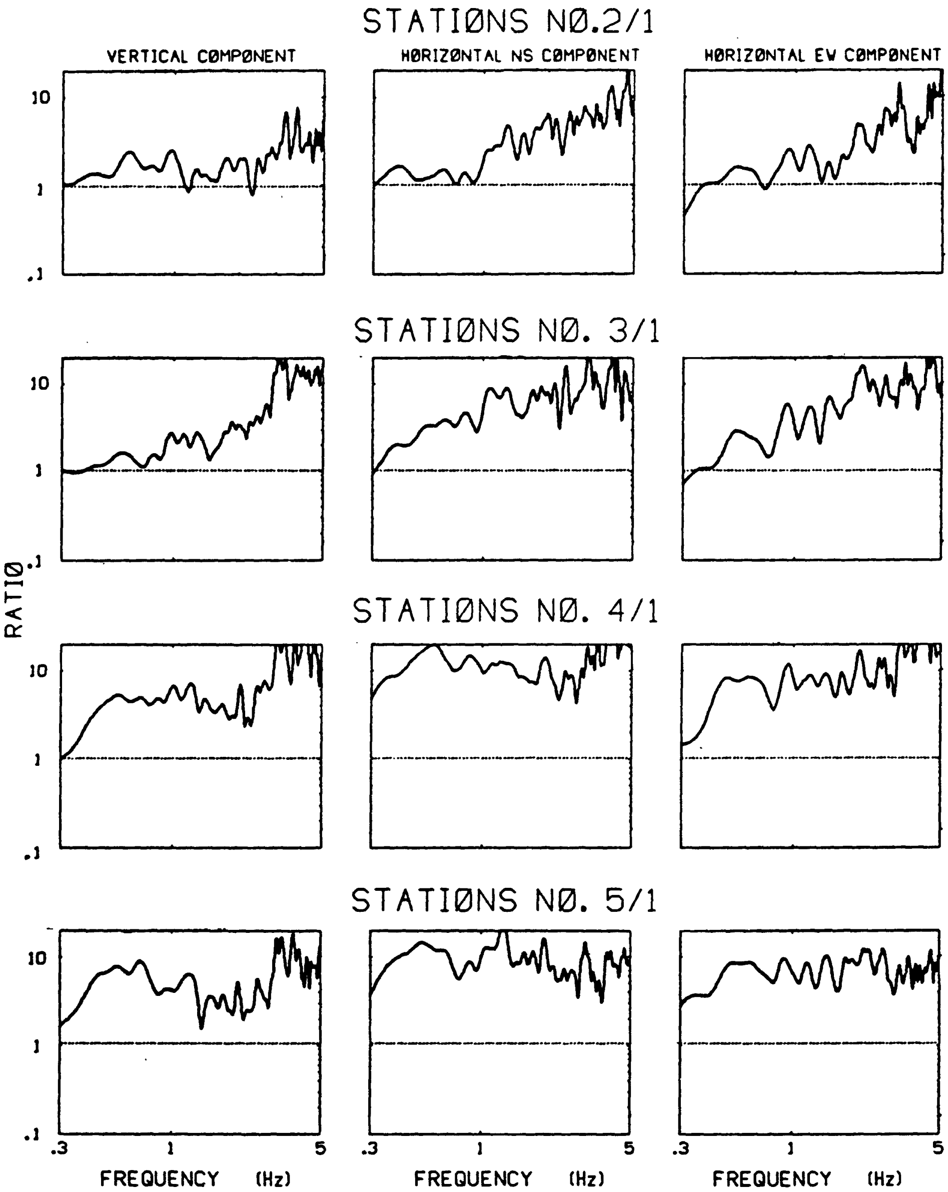

Figure 12.--Spectral ratios of vertical and horizontal (NS and EW) components of ground motion recorded on sites having geologic conditions different from the crystalline rock site in the Springville-Spanish Fork area. Spectral ratios not plotted where the S/N < 2.

Approximately 200 s of seismic signal was selected (windowed) to the nearest power-of-two of number of samples and tapered with a whole-cosine-bell (Hanning window) before being Fourier transformed by a Fast Fourier Transform (FFT) algorithm (A.C. Tarr and Edward Cranswick, unpub. data, 1986). A similar procedure was used on the preevent time history data to derive the spectra for ambient seismic noise at each site. None of the spectral amplitudes have been normalized by the window length because the spectra used for site-to-site comparisons are derived from time series of identical duration. The methods used by Rogers and others (1980) to estimate the reliability of the spectral estimates are not directly applicable to this study due to the absence of multiple observations (recordings) from each of the sites. The horizontal spectra were used to derive site transfer functions from the sites located on rock relative to the sites underlain by unconsolidated sediments. The site transfer function (STF) was calculated by the general formula of: STF=Sa/Sr where Sa is the derived spectrum of a site underlain by alluvium, Sr is the derived spectrum of the site underlain by rock and all spectra are in the frequency band between 0.3 and 5.0 Hz.

Rogers and others (1979) discuss the method of deriving the site transfer function in terms of spectral ratios. The site transfer functions of this study were calculated directly from the unsmoothed, independent spectral amplitudes. Similarly, the frequency band of the spectral ratios in this report represents the averages of the unsmoothed spectral ratios between the defined frequency limits (A.C. Tarr and Edward Cranswick, unpub. data, 1986). Only spectra with a signal-to-noise separation of greater than 6 dB were used for deriving the spectral ratios (figs. 8, 9). The absence of data or "holes" in some of the spectra ratios shown on figures 10, 11, and 12 are due to the elimination of the low signal to noise data. The frequency bands used to derive the average ratios in this report are the same as those used in the Hays and King (1982) report to enable a direct comparison of the spectral ratio numbers. The spectra and spectral ratios shown on the figures presented in this report are smoothed by convolving the derived spectra with a whole-cosine-bell of 16-samples width. The graphic smoothing is intended to emphasize what are judged to be the significant trends in the data; the reliability of these trends can be estimated by inspection of the composite signal and noise plots shown in figures 8 and 9.

SEISMIC-REFLECTION DATA PROCESSING

Five high-resolution shallow seismic-reflection profiles were completed for this report. The sites were chosen to coincide with site response locations, for variety of subsurface geology, and for the availability of a sufficient area in which an unobstructed reflection line could be obtained. Level sites were selected to eliminate the static corrections needed in the data processing. Correction for topography variations were needed, however, for Salt Lake City site 8. The field data are digitally recorded on magnetic tape. The field data tapes are processed by software on a VAX 11/780 computer. The data are first edited, sorted into CDP gathers, and plotted in preliminary form. The CDP gathers supply the two-way traveltime data to be used for further analysis. All seismic data with a two-way traveltime greater than 100 ms are eliminated. The data truncation (or data elimination) is necessary because the arrival of surface-wave seismic signals interferes with the reflection data after 100 ms. The truncated CDP data is then further analyzed by using a constant velocity search procedure to determine stacking velocities. The correct velocity will adjust traveltime differences in the CDP data which are due to the different source-to-receiver distances.

The velocity analysis procedure needs an input of a series of best-estimate traveltime velocities (V) likely to be encountered in the area. The following equation:

$$T_o = [T_x{}^2 - X^2/V^2]^{1/2},$$

where T_x is the actual two-way traveltime, X is the offset distance from the analyzed trace to the source position, and T_o is the zero-offset two-way traveltime for the given velocity, is used by the software program to automatically calculate a T_o on a sample by sample basis on each CDP trace for each velocity. A sequence of traveltime velocities are selected that will give CDP traces with the least amount of normal-moveout curvature. These selected traveltime velocities will also produce the maximum trace amplitude at the two-way traveltime of the reflection pulse when the CDP's are summed. The time corrected data are again edited to remove any interfering electrical noise, spikes or pre-first reflective pulse seismic signals that may have been moved into the desired data from the velocity-time corrections. The data are then filtered to help attenuate the seismic energy below 100 Hz. The final data are displayed in stacked CDP sections which show seismic-reflection amplitudes in a two-way traveltime versus horizontal distance format. The processing parameters are listed in table 1. The average spatial resolution for the profiles is 0.6 m calculated by using the 1/8-wavelength sensitivity on the velocities derived from the reflection data (Widess, 1973). All processed data were truncated to give a minimum of 800 percent (eightfold) or better coverage on the resultant profiles.

TABLE 1.--Seismic-reflection processing sequence

---

1. Reformat field data from modified SEG-Y.
2. Edit reformatted field data.
3. Reflection line geometry definition.
4. CDP sort of common-shot gathers.
5. Band-pass filter analysis of CDP gathers.
6. Seismic velocity analysis of CDP gathers.
7. Muting analysis of normal move out (nmo) corrected CDP gathers.
8. Preliminary stack.
9. Re-examine chosen velocities, filters, and mutes.
10. Amplitude scaling of final stack before plotting.
11. Final stack.

DISCUSSION

The time histories of the site response data for SLC (Salt Lake City) and SSF (Springville-Spanish Fork) areas are shown on figures 4 and 5. The data have been amplitude normalized to the sites underlain by rock and arranged from top to bottom on the illustration, according to general increase in thickness of underlying alluvium, and the increased distance west from the Wasatch Front toward the center of the valley. The sites on figures 4 and 5 are ordered according to thickness of underlying alluvium, this order owing to the limited amount of geologic information available at this time. The estimated depths to basement for the Salt Lake City sites shown on figure 4 are, from top to bottom: 0, 30, 80, 140, 140, 180, 190, 270, and 440 m (Richard Van Horn, unpub. data, 1986). The depths of alluvium at the SSF sites are less well known. The projection of the dip of an exposed outcropping of bedrock, approximately 50 m from SSF site 2, to a point at depth beneath SSF site 2, indicates that the underlying thickness of alluvium at that station probably does not exceed 30 m. Borehole tests near SSF site 3 and SSF site 4 did not penetrate bedrock at a 150-m total depth and borehole tests near SSF site 5 did not penetrate bedrock at a 300-m total depth (Richard Van Horn, unpub. data, 1986). Figures 4 and 5 show an increase in signal amplitude in both P-wave and surface-wave portions of the seismograms and an increase in the wave-train duration with the increasing alluvium depth and distance from the Wasatch Front (toward the center of the valley). Figure 6 shows the derived spectra from the data recorded at SLC site 1 (rock), SLC site 2 (30-m alluvium), and SLC site 9 (440-m alluvium). Figure 7 shows the derived spectra from the data recorded at SSF site 1 (rock), SSF site 2 (approximately 30-m alluvium) and SSF site 5 (approximately 300-m alluvium). The spectra show that an increased spectra amplification and a slight spectral peak shift toward the lower frequencies may correlate with increased thickness of alluvial deposits. Spectra from the stations underlain by alluvium were ratioed to the stations underlain by rock. The spectral ratios show that amplification occurs over most of the frequency band for which a good signal-to-noise ratio exists (figs. 10, 11, 12). Transfer functions, or averaged spectral ratios, were derived from unsmoothed spectra for bandwidths similar to those used in the Hays and King (1982) report. The average spectral amplification over four period bands, 0.2-0.7, 0.7-1.0, 1.0-2.0, and 2.0-3.33 s, are shown for SLC in figures 13 and 14 and for SSF in figures 15 and 16. The amplification factors range from approximately 1.5 to 3.0 for sites near the Wasatch Front, underlain by thinner sections of alluvium, to factors of 7-12 for sites in the SSF area that are located near the center of the valley and are underlain by more than 300 m of alluvium. The relatively high value of spectral ratio response numbers (7-12) in the Hays and King (1982) report, which were at locations near the middle of the Salt Lake valley, could not be reoccupied for direct comparison due to flooding from the rising of the Great Salt Lake level. However, data from sites in midvalley locations in the general Springville-Spanish Fork area, similar to the midvalley Salt Lake City locations, show site response in the 0.2- to 0.7-s period bandwidth to be higher than the rock site by a factor of 7-12 which compares well with Salt Lake City data in Hays and King (1982).

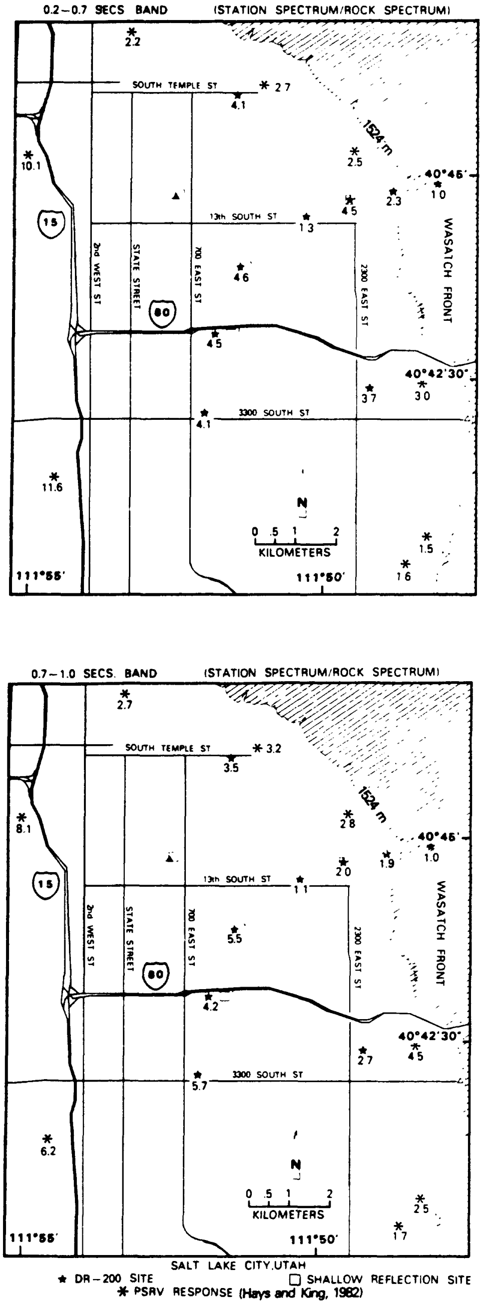

Figure 13.—Comparison of horizontal component average spectral ratios between Hays and King (1982) and this study for the Salt Lake City area. Top figure shows ratios for the period band 0.2 - 0.7 s. Bottom figure shows ratios for the period band 0.7 - 1.0 s.

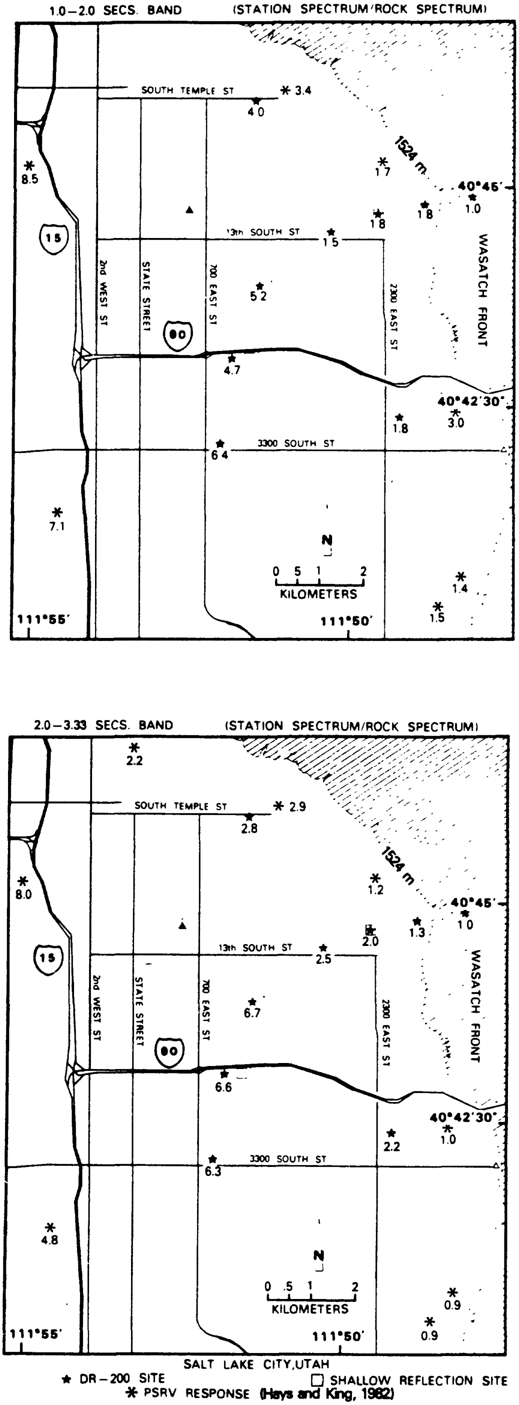

Figure 14.--Comparison of horizontal component average spectral ratios between Hays and King (1982) and this study for the Salt Lake City area. Top figure shows ratios for the period band 1.0 - 2.0 s. Bottom figure shows ratios for the period band 2.0 - 3.33 s.

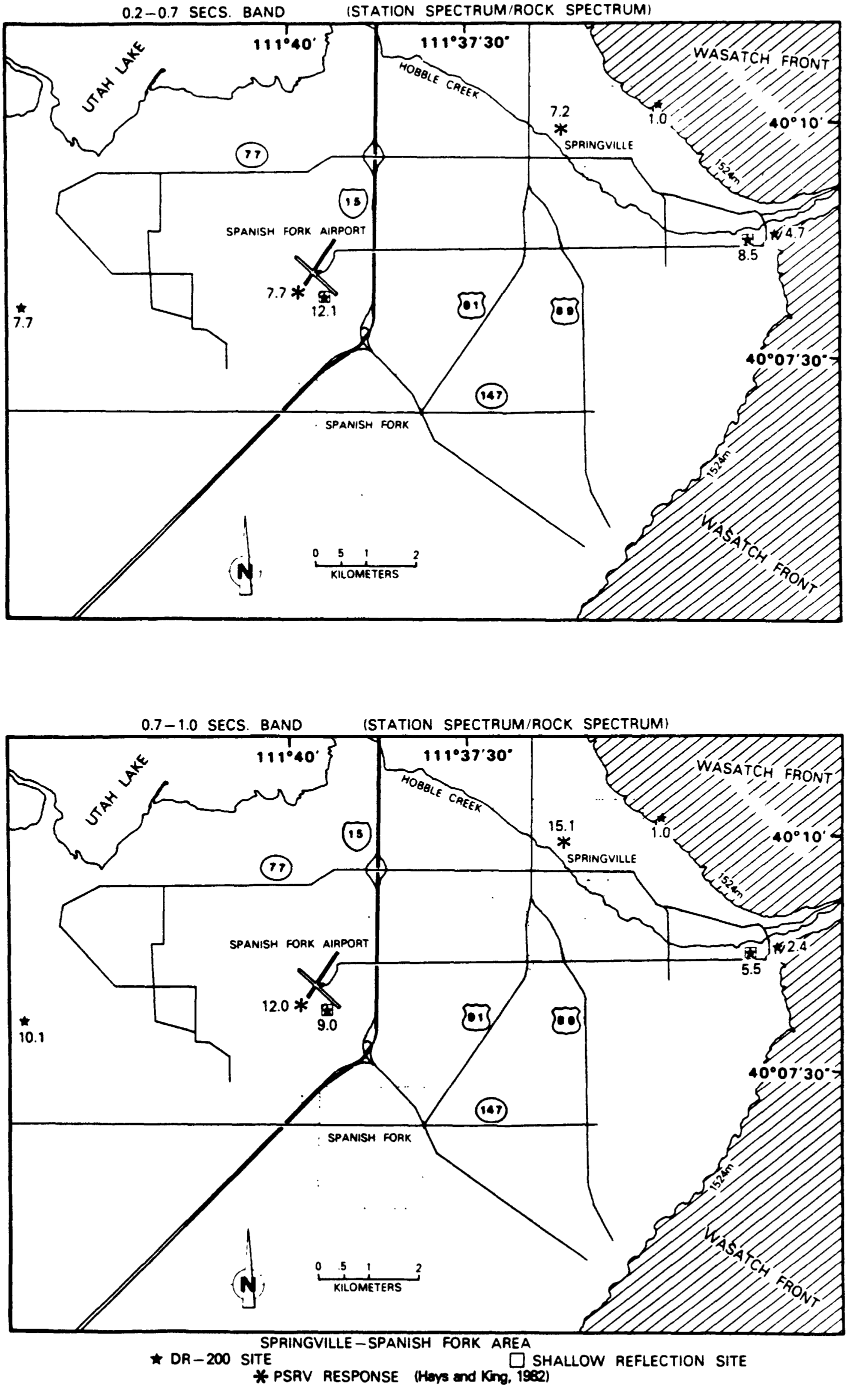

Figure 15.--Comparison of horizontal component average spectral ratios between Hays and King (1982) and this study for the Springville Spanish Fork area. Top figure shows ratios for the period band 0.2 - 0.7 s. Bottom figure shows ratios for the period band 0.7 - 1.0 s.

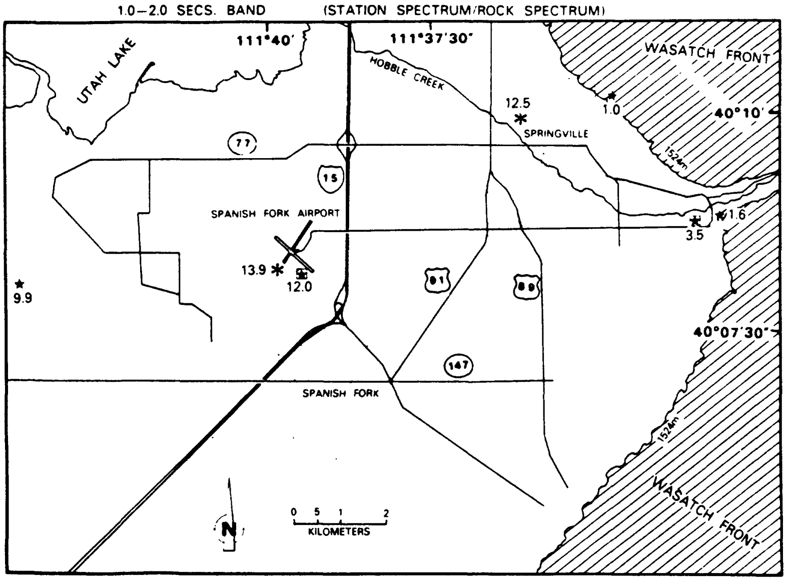

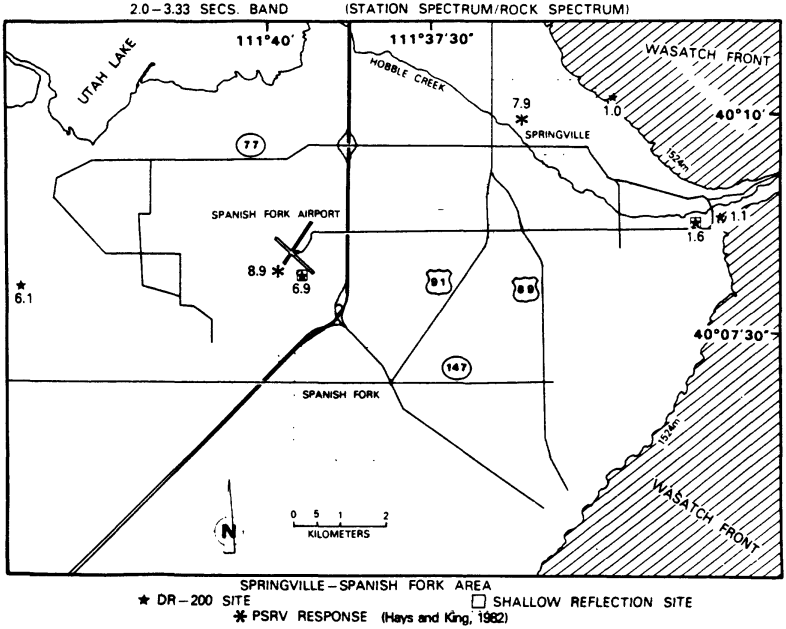

Figure 16.--Comparison of horizontal component average spectral ratios between Hays and King (1982) and this study for the Springville Spanish Fork area. Top figure shows ratios for the period band 1.0 - 2.0 s. Bottom figure shows ratios for the period band 2.0 - 3.33 s.

Figures 4 through 16 show a general trend in increased response as the depth of alluvium or distance from the Wasatch Front increases,, but anomalies in this trend are observed. For example, site 5 in the SLC array clearly shows more time history amplitude spectral energy and higher average spectral ratio factors in the 0.2- to 0.7- and the 0.7- to 1.0-s period bandwidths than site 4. Yet site 5 is located closer to the Wasatch Front and is underlain by a thinner alluvial sequence than site 4. Hays and King (1982) postulated the existence of such areas that would show high-ground shaking amplification in close proximity to sites with average ground response. An explanation for the anomalously high amplification observed at site 5 can be offered by the high-resolution shallow-reflection profile made at that site (fig. 17). The analysis of the data shown on the reflection profile gave seismic P-wave velocities of the near-surface layers that are much slower (550-600 m/s) than the deeper alluvium and underlying bedrock (4.5 km/s; Arnow and Mattick, 1968). Since the difference in impedance of vertically-adjacent layered media amplifies seismic waves in proportion to the contrast in impedances of these layers (Medvedev, 1962), then the slow near-surface velocities calculated for this site, contrasted with the deeper rocks with higher velocities may be producing the necessary impedance difference to generate the higher ground response. An aquifer at a 50-m depth is encountered in a well located 270 m northeast of the recording site but the aquifer was not detected on the reflection profile. This suggests either a very weak aquifer reflector, or more reasonably, a water table that is deeper than can be resolved with the reflection methods used (deeper than 75 m). Therefore, the presence of a shallow water table to explain the increased ground motion, as suggested by the work of Evernden and Thomson (1985), apparently does not exist at this site.

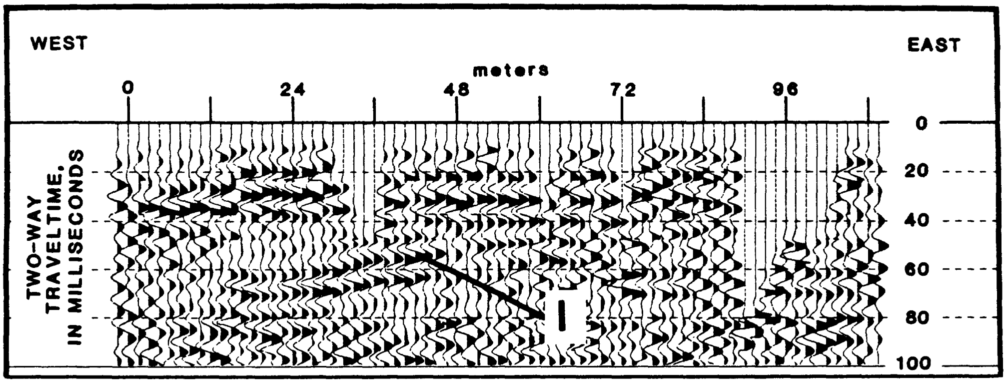

Figure 17.--Seismic reflection profile from SLC 5 (Bonneville Golf Course) showing reflection labeled I.

High-resolution shallow-reflection profiles were also run in Salt Lake City at sites 8 and 12. The near-surface P-wave velocities measured at site 12 (915-1650 m/s) were the highest observed among the three sites. The P-wave velocities at site 12 were calculated from the reflection two-way traveltimes of the three two-cycle reflections (labeled F, G, and H in fig. 18) shown in the stacked record section. A shallow depth to the water table (1-3 m; Mower and Van Horn, 1973) indicates the sediments are saturated which probably contributed to the increased seismic velocities calculated for this site. Additionally, the detection of three horizons in the subsurface, when compared to the high ground-response also recorded at this site and (using the principles defined by Medvedev, 1962) suggests that the three strong acoustic impedance contrasts, which produced the three reflections on the seismic profile, may be responsible for amplifying the upward propagating wave from the nuclear test.

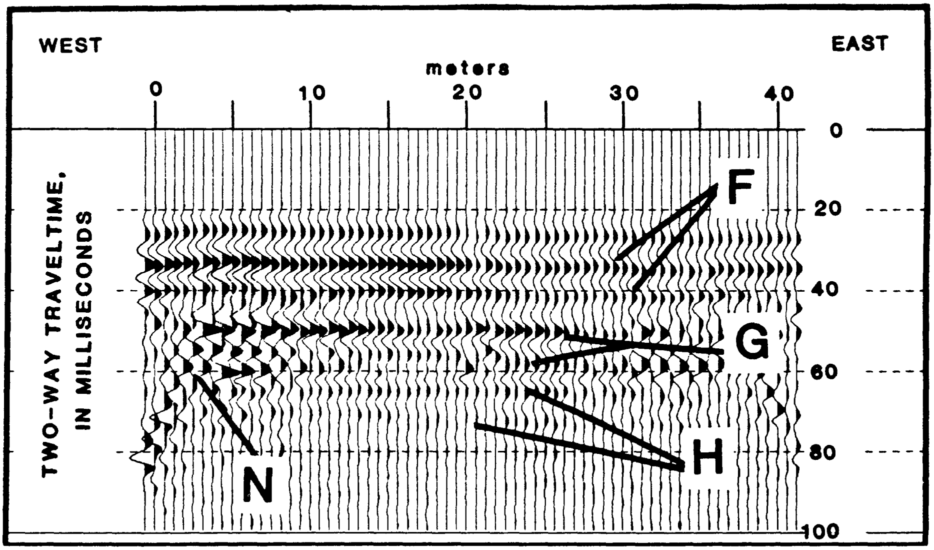

Figure 18.--Seismic reflection profile from SLC 12 (Liberty Park) showing reflections labeled F, G, and H. Ground roll dominates in the zone labeled N.

The P-wave velocities measured at site 8 (approximately 1000 m/s) were intermediate to velocities at sites 5 and 12. The velocities at this site were calculated from traveltime delays with increasing offsets for the reflections on the record section (fig. 19). The high-resolution reflection profile at this site crossed the East Bench Fault (labeled A, fig. 19) and shows a reflection downdropped to the west approximately 5 ms at position A. The profile also indicates considerable structure in the shallow unconsolidated sediments with several smaller west-dropped blocks, and a slight indication that beds between positions B and C may be backrotated toward the fault. The fault probably penetrates deeper into the section than shown; however, the surface wave and the shallower reflectors obscure later reflective arrivals from deeper structures. Ground response was also intermediate with average spectral ratio factors (ASRF) of 4.2-6.6 at this site, compared to SLC 5 (2-4.5) or SSF 5 12 (7.7-10.1).

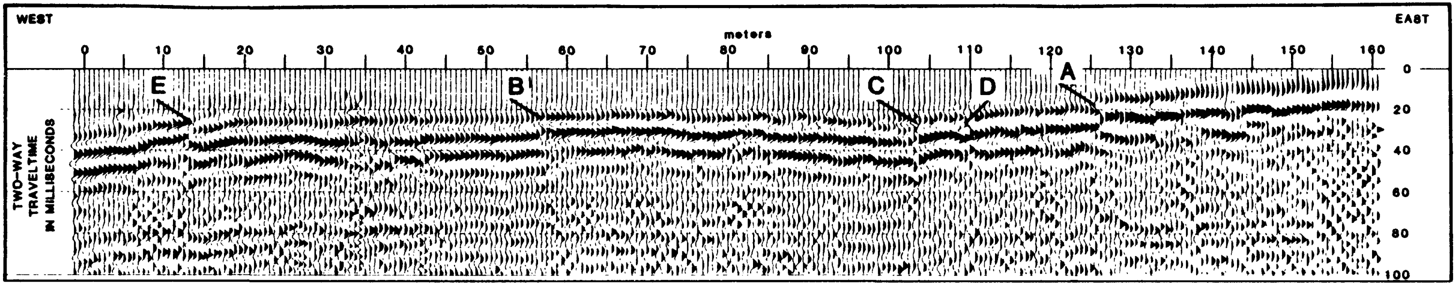

Figure 19.--Seismic reflection profile from SLC 8 (Forest Dale Golf Course) showing offset at position A where the profile crosses the East Bench Fault. Region between B and C shows possible backrotation toward the East Bench Fault. Position D and E mark other possible faults.

The seismic-reflection profile from site 3 in the Springville-Spanish Fork area is underlain by approximately 100 m of alluvium, and shows shallow reflections in the 20-50 ms two-way traveltime range (labeled J, K, and L, fig. 20). The origin of these undulating structures is unknown, but a possibilty is that they are due to the fluvial processes of nearby Hobble Creek. The seismic P-wave velocities computed for the labeled reflections in figure 20 are relatively slow: 550 m/s. Again, the slow seismic reflection velocities, calculated at this site for near-surface deposits, may be an indicator of an acoustic impedance contrast that would amplify upward traveling seismic waves into the intermediate ground-response range (ASRF between 4.0 and 8.0).

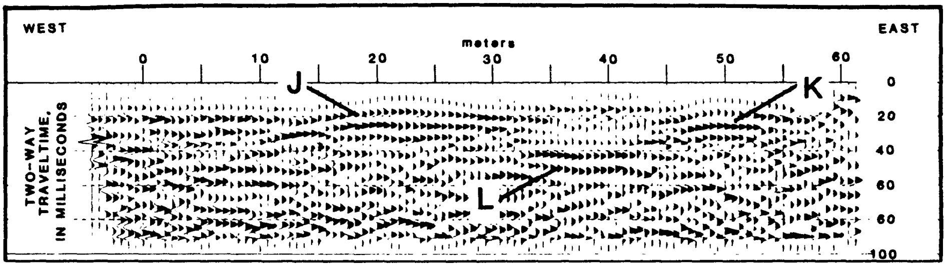

Figure 20.--Seismic reflection profile from SSF 3 (Hobble Creek) showing reflections labeled J, K, and L.

The reflection profile from SSF 4, a high ground-response site (ASRF between 8 and 12), shows a moderately deep (approximately 55 m) flat-lying two-cycle reflection at about 80-ms two-way traveltime (labeled M in fig. 21). A shallow water table depth (1.5 m), measured in the borehole at this site, probably improved the source coupling to the ground and therefore allowed deeper penetration of the seismic signal. Resolution of any horizons above this event was unsuccessful because the ground-roll and air-blast dominated this part of the record. Also, the absence of acoustic contrasts large enough to generate an observable reflection earlier in the record, may have contributed to the lack of reflections. Still, the reflection recorded in this profile is the latest event (in two-way traveltime) seen on any of the profiles. The seismic P-wave velocity determined for the reflection labeled M is 1370 m/s, which is significantly higher than the velocity determined for the reflections at Springville site 3.

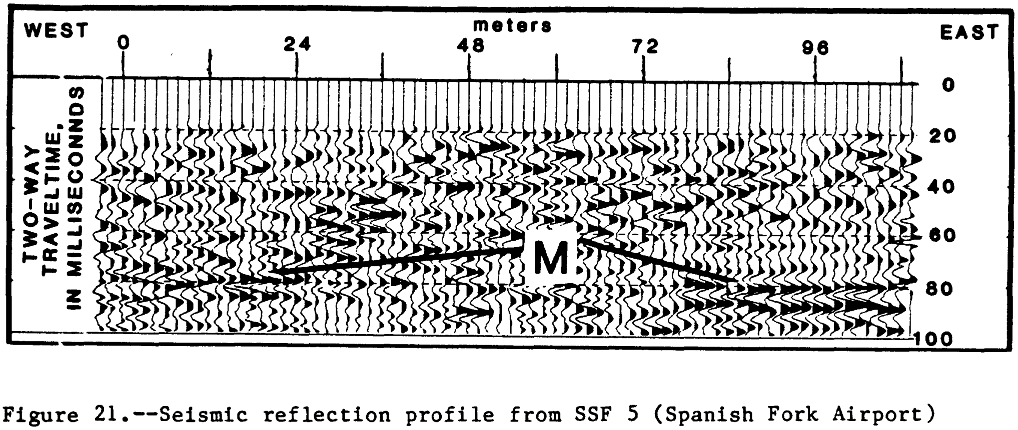

Figure 21.--Seismic reflection profile from SSF 5 (Spanish Fork Airport) showing reflection labeled M.

The data of table 2 suggest a weak correlation between ground response and the results of the seismic-reflection work. Two sites, SLC 12 and SSF 4, have high ground-response (ASRF 8 to 12); they were also the only two sites where seismic reflection data was collected, which showed a reflection arrival in the 70- to 80-ms range and 55- to 60-m depth range. Two other sites, SLC 8 and SSF 3, have intermediate ground-response (ASRF 4 to 8) and a reflector arrival at 30- to 45-ms range. The remaining reflection profile, SLC 5, does not fit into this pattern of ground-response versus depth and arrival time of reflections--it has low response (ASRF 1.5 to 5) and a moderately deep reflection (60 ms). It is possible that the calculated velocities for SLC 5 are in error or that different field methods would resolve more reflections that might fit the above pattern. However, the reflection depth versus ground-response data base is too small to be considered statistically significant at this time. Additional reflection profiles have been acquired and are being added to the data set.

TABLE 2.--Seismic-reflection and ground response data

	Bonneville Golf Course SLC 5	Forest Dale G.C. SLC 8	Liberty Park SLC 12	Hobble Creek SSF 3	Spanish Fork Airport SSF 4
Average spectral					
ratio factor	4.5	4.5	8.0	8.5	12.1
0.2 - 0.7 s					
0.7 - 1.0 s	2.0	4.2	9.0	5.5	9.0
1.0 - 2.0 s	1.8	4.7	8.5	3.5	12.0
2.0 - 3.3 s	2.0	6.6	6.0	1.6	6.9
No. of reflections					
on the profile	1	1	3	2	1
Reflection continuity	39	100	100	66	51
(in percent of	--	--	40	25	--
total profile)	--	--	40	--	--
Reflection two-way	60	30	30	20	80
traveltime	--	--	50	45	--
(in milliseconds)	--	--	70	--	--
Stacking velocity	600	1000	915	550	1370
for reflections	--	--	1475	600	--
(in meters/second)	--	--	1660	--	--
Depth to Reflection	18	15	14	8	55
	--	--	37	14	--
(in meters)	--	--	58	--	--

CONCLUSIONS

The comparison between results in Hays and King (1982), who developed a countoured site response map of the Salt Lake City area based on transfer functions derived from pseudo-velocity spectra ratios, and in this report, which used transfer functions derived from Fourier transformed spectra ratios, show good agreement (figs. 13-16). Both data sets show an increase in response as the distance westward from the Wasatch Front increases. Also, both data sets show that the average spectral ratio factors of SLC, at similar distances from the Wasatch Front, differ from those of SSF; for sites near the Wasatch Front in SLC the ASRF vary from 1.5 to 4, whereas for sites at similar distances from the Wasatch Front in SSF, the factors are 5-15. The good agreement in the results of this study with those of Hays and King (1982) demonstrates the repeatability of generating site response values and gives a sense of reliability to the overall procedure for mapping ground response and developing ground response predictions in urban areas, as used by Borcherdt and Gibbs (1976), Hays and King (1982), and Rogers and others (1985).

The analysis of the high-resolution shallow reflection profiles show that the technique is a viable means to map shallow structures in urban areas underlain by unconsolidated sedimentary sections. The profiles suggest promising correlations between the later arriving reflections (70-80 ms) and higher ground response, and, intermediate site response associated with earlier arriving reflections (30-45 ms). However, the high-resolution shallow reflection method will need a larger data base to show if a statistically significant correlation exists. Additional site-specific geologic studies and high-resolution shallow reflection studies are being conducted at the ground response sites used in this and the Hays and King (1982) report. The resultant geotechnical analysis and correlations among geologic factors and the site response factors are in progress.

REFERENCES

Adhidjaja, J.I., Cook, K.L., and Serpa, L.F., 1981, Salt Lake Valley gravity map and data: Utah Geological and Mineral Survey, Open-File Report 39.

Arabasz, W.J., Smith, R.B., and Richins, W.D., eds., 1979, Earthquake studies in Utah, 1850 to 1978: Salt Lake City, University of Utah Special Publication, 552 p.

Arnow, Ted, and Mattick, R.E., 1968, Thickness of valley fill in the Jordan Valley east of the Great Salt Lake, Utah, in Geological Survey research 1968: U.S. Geological Survey Professional Paper 600-B, p. B79-B82.

Borcherdt, R.D., 1970, Effects of local geology on ground motion near San Francisco Bay: Seismological Society of America Bulletin, v. 60, p. 29-61.

______ed., 1975, Studies for seismic zonation of the San Francisco Bay region: U.S. Geological Survey Professional Paper 941-A, 102 p.

Borcherdt, R.D., and Gibbs, J.F., 1976, Effects of local geological conditions in the San Francisco Bay region on ground motions and the intensities of the 1906 earthquake: Seismological Society of America Bulletin, v. 66, p. 467-500.

Carver, D.L., Cunningham, D.R., and King, K.W., 1986, Calibration and acceptance testing of the DR-200 digital seismograph with S-6000 and the L-4C seismometers: U.S. Geological Survey Open-File Report 86-340, 28 p.

Cloud, W.K., and Hudson, D.E., 1961, A simplified instrument for recording strong motion earthquakes: Seismological Society of America Bulletin, v. 51, p. 159-274.

Evernden, J.F., and Thomson, J.M., 1985, Predicting seismic intensities, in Evaluating earthquake hazards in the Los Angeles region--An earth science perspective: U.S. Geological Survey Professional Paper 1360, p. 151-202.

Gutenberg, B., 1957, Effects of ground on earthquake motion: Seismological Society of America Bulletin, v. 47, p. 221-250.

Hays, W.W., Algermissen, S.T., Miller, R.D., and King, K.W., 1978, Preliminary ground response maps for the Salt Lake City area: International Conference on Microzonation, 2d, San Francisco, 1978 Proceedings, v. 2, p. 497-508.

Hays, W.W., and King, K.W., 1982, Zoning of the earthquake ground-shaking hazard along the Wasatch fault zone, Utah: International Earthquake Microzonation Conference, 3d, Seattle, 1982 Proceedings, p. 1307-1318.

Kanai, K., 1952, Relation between the nature of the surface layer and the amplitude of earthquake motion: Tokyo University Earthquake Research Institute Bulletin, v. 30, p. 31-37.

Knapp, R.W., 1985, Using half-integer source offset with split spread cdp seismic data: The Leading Edge, Society of Exploration Geophysics, v. 4, p. 66-69, 108.

Mayne, W.H., 1962, Common reflection point horizontal data stacking techniques: Geophysics, v. 27, p. 952-965.

McGregor, E.E., Van Horn, Richard, and Arnow, Ted, 1974, Map showing the thickness of loosely packed sediments and the depth to bedrock in the Sugar House quadrangle, Salt Lake County, Utah: U.S. Geological Survey Miscellaneous Investigations Map I-766-M, scale 1:24,000.

Medvedev, J.V., 1962, Engineering seismology: Moscow, Academia Nauk. [Translated into English by Israel Program for Scientific Translations, Jerusalem, 1965, 260 p.]

Miller, R.D., 1980, Surficial geologic map along part of the Wasatch Front, Salt Lake Valley, Utah: U.S. Geological Survey Miscellaneous Field Studies Map MF-1198, scale 1:100,000, 2 sheets and pamphlet.

Milne, J., 1908, Seismology (2d ed.): London, K. Paul, Trench, Trubner, and Col, 320 p.

Mower, R.W., and Van Horn, Richard, 1973, Map showing minimum depth to water in shallow aquifiers (1963-1972) in the Sugar House quadrangle, Salt Lake County, Utah: U.S. Geological Survey Miscellaneous Investigations Map I-766-I, scale 1:24,000.

Murphy, J.R., Weaver, N.L., and Davis, A.H., 1971, Amplification of seismic body waves by low-velocity surface layers: Seismological Society of America Bulletin, v. 61, p. 109-145.

Reid, H.F., 1910, The California earthquake of April 18, 1906; The mechanics of the earthquake: Carnegie Institute of Washington publ. 87, v. 2, 192 p.

Rogers, A.M., Covington, P.A., Park, R.B., Borcherdt, R.D., and Perkins, D.M., 1980, Nuclear event time histories and computed site transfer functions for locations in the Los Angeles region: U.S. Geological Survey Open-File Report 80-1173, 207 p.

Rogers, A.M., and Hays, W.W., 1978, Preliminary evaluation of site transfer functions developed from nuclear explosions and earthquakes: International Conference on Microzonation, 2d, San Francisco, 1978 Proceedings, v. 2, p. 753-764.

Rogers, A.M., Tinsley, J.C. and Borcherdt, R.D., 1985, Predicting relative ground response, <u>in</u> Ziony, J.I., ed., Evaluating earthquake hazards in the Los Angeles region: U.S. Geological Survey Professional Paper 1360, p. 221-247.

Rogers, A.M., Tinsley, J.C., Hays, W.W., and King, K.W., 1979, Evaluation of the relation between near-surface geological units and ground response in the vicinity of Long Beach, California: Seismological Society of America Bulletin, v. 61, p. 1603-1622.

Swan, F.H., II, Schwartz, D.P., and Cluff, L.S., 1980, Recurrence of moderate to large magnitude earthquakes produced by surface faulting on the Wasatch fault zone, Utah: Seismological Society of America Bulletin, v. 70, p. 1431-1462.

Van Horn, Richard, 1972, Surficial geologic map of the Sugar House quadrangle, Salt Lake County, Utah: U.S. Geological Survey Miscellaneous Investigations Map I-766-A, scale 1:24,000.

Widess, M.B., 1973, How thin is a thin bed: Geophysics, v. 38, p. 1176-1180.

IN SITU POISSON'S RATIO
MEASUREMENTS NEAR PROVO, UTAH

by

Richard, D. Miller, Don W. Steeples, and Ralph W. Knapp
Kansas Geological Survey
Lawrence, Kansas

and

Kenneth W. King
U.S. Geological Survey
Denver, Colorado

ABSTRACT

Intensity variations of several units on the MM scale at sites only a few kilometers apart have been well documented. Classification of sites according to response to earthquake energy would enable engineers to accurately determine minimum structural requirements for individual sites in high-to-moderate earthquake risk zones. It is possible to produce shallow P-wave and S-wave reflection data containing the necessary information to allow direct in situ determination of Poisson's ratio (which is directly related to site response). During two separate visits to Provo, Utah, and the surrounding area, high-resolution shallow P- and S-wave surveys were conducted. The P- and S-wave data from Provo airport are of excellent quality and yield average velocity values accurately enough to allow determination of Poisson's ratio as a function of depth in the upper 50 meters of the geologic section. Poisson's ratio at the Provo airport (a high response site) is calculated to be 0.44, while a low response site near a cherry orchard has a Poisson's ratio of 0.27.

INTRODUCTION

Intensity of ground shaking during an earthquake is determined in part by local near-surface geological conditions. Intensity differences of three to four units on the MM scale at sites no more than a few kilometers apart have been well established for nearly a century (Lawson et al., 1908). Because of these differences, prediction of individual site response is an important part of urban earthquake hazard mitigation. Borcherdt et al. (1975) have estimated such specific site responses in the San Francisco Bay area. They used intensity maps from the 1906 San Francisco earthquake combined with data from recording far-field ground motion in the San Francisco Bay area from explosions at the Nevada Test Site (NTS).

The use of NTS explosions in other urban areas is not feasible now because of the decreasing size of NTS explosions in the past few years and the distance of many of these areas from NTS, (e.g., Seattle, Los Angeles, Salt Lake City, Memphis, St. Louis, Evansville, Charleston, and Boston). While moderate-to-strong earthquakes in these areas in the future will provide an energy source to evaluate ground motions, it is these very earthquakes whose hazards we wish to mitigate.

Knowledge of site response would allow engineers the data necessary to better calculate minimum structural requirements for development of individual sites in high-to-moderate earthquake risk zones. It also would help to more accurately determine the present risk to structures already completed and occupied.

Shallow P- and S-wave reflection data contain the necessary information to allow direct in situ determination of some dynamic properties of materials within the upper hundred meters of the earth's surface. It has long been known that the ratio of acoustic impedance of juxtaposed layers theoretically relates to amplification. Medvedev (1965) empirically demonstrated the use of seismic shear impedance (the product of density and S-wave velocity) to predict relative ground response. The potential for amplification of shaking increases as the impedance contrast between layers increases, provided other parameters are constant.

It is possible to produce shallow P-wave and S-wave reflection profiles along the same surface line. This allows interpretation of more geological information than the use of P-waves or S-waves alone. With the determination of interval velocities, it is possible to determine variations in Poisson's ratio with depth. Equation (1) uses average P-wave and S-wave velocities from the surface to a reflecting interface to determine Poisson's ratio.

$$\sigma = \frac{1}{2}\,\frac{\alpha^2 - 2\beta^2}{\alpha^2 - \beta^2} \tag{1}$$

σ = Poisson's ratio, α = P-wave velocity, β = S-wave velocity

While it would be possible to produce similar results with an expensive drilling program that included cross-hole, downhole, or uphole P- and S-wave velocity measurements, logistical problems that accompany drilling are sometimes significant, particularly in urban areas. High-resolution seismic surveys can be safely performed with shallow reflection techniques in areas such as parks and school yards with essentially no environmental damage. For example, we performed one such survey across the baseball fields at Sylmar High School in the San Fernando Valley, of California while the students were practicing baseball and softball.

TECHNIQUES

Seismic reflection techniques have been used in petroleum prospecting for about a half century. Although examples are occasionally cited in the literature, shallow reflection techniques in engineering and groundwater applications have met with only limited success because of the difficulty encountered in identifying reflections from layers at shallow depths. The shallowest reflections documented in the literature are from 10 m by Steeples and Knapp (1982). The amplitudes of the reflected waves at commonly recorded frequencies, when present, are smaller than the amplitudes of unwanted waves, particularly ground roll composed of Rayleigh waves and Love waves. Further, the generation and recording of frequencies much above 100 Hz has not been routinely done on land.

Typical energy sources that have been tried include sledge hammer (Hunter at al., 1981, and Meidav, 1969), weight drop (Doornenbal and Helbig, 1983) and small explosive charges (Pakiser and Warrick, 1956). These energy sources normally produce seismic waves with unfiltered dominant frequencies less than 100 Hz. In order to provide better resolution (both precision and accuracy) of shallow reflective interfaces, high frequencies are needed. Resolution of "thin beds" is theoretically limited to about 1/8 wavelength (1/4 wavelength by conventional methods) of the recorded seismic energy (Widess, 1973), so improvement in resolution and imaging of shallower reflectors can be obtained directly by increasing the frequency of the energy recorded.

A worthy goal of shallow reflection surveys is to provide bed resolution in the approximate dimension of one-half meter. Typical velocities of near-surface soil and/or alluvial materials range from about 300 to about 1200 m/sec for P-waves and from 100 to about 300 m/sec for S-waves. Using classic quarter wavelength methods, the desired one-half meter resolution cannot be obtained without frequencies greater than 75 Hz for a P-wave velocity of 300 m/sec and 25 Hz for S-wave velocity of 100 m/sec. We have been able to routinely produce dominant P-wave frequencies greater than 200 Hz and S-wave frequencies greater than 75 Hz.

The source for a shallow high-resolution reflection survey must possess a high frequency signature; it must be field durable, and time-efficient enough for cost-effective seismic data acquisition. Most of our P-wave reflection research has involved the use of common hunting rifles modified for safe and quiet operation when fired vertically into the ground. Our most productive source has been a steel arrow forced hydraulically into the ground, rotated by hammer impact, and then removed hydraulically. The arrow is equipped with an arm protruding laterally from its base. This arm is impacted by a sledge hammer causing a rotational motion about the center of the arrow.

High-resolution compressional wave surveys have generally had the best success when severe low-cut filtering and high natural frequency geophones were used (Hunter et al., 1984; Steeples and Knapp, 1982; Miller and Steeples, 1986). As previously mentioned, the higher the dominant frequency of the seismic data, the greater the bed resolution. Our most commonly used low-cut filter suppresses energy down 3 dB at 220 Hz and down 24 dB/octave below 220 Hz. We have had success with single 100 Hz geophones spaced as closely as one-quarter meter. In certain environments higher low-cut filters (340 Hz or 480 Hz) have proven useful in improving near-surface bed resolution (Treadway et al., 1985).

Field parameters for obtaining good shallow shear wave reflections are extremely site dependent. Usually the lower frequency spectrum of S-waves in comparison to P-waves from the same site dictates the use of lower natural frequency geophones sensitive to ground motion perpendicular to the direction of wave propogation. Recently we have had the best results with 30 Hz horizontal geophones. The most frequently used low-cut filter has a -3 dB point at 110 Hz.

S-wave reflection surveys have an added potential for suppressing undesirable noise. Due to the nature of S-waves, the polarity of reflections recorded are dependent on the direction of initial particle displacement. By independently recording shots with initial source rotations clockwise and then counterclockwise and subtracting the recorded signal from the 2 shots, the signal-to-noise ratio is improved.

Geophone spacing is dictated by degree of lateral resolution needed and desired accuracy of the velocity function. In most instances when the target depth range is from 5 to 50 m, we space single geophones at 1.25 m intervals.

FIELD METHODS

We use an Input/Output, Inc. DHR 2400 seismic recording system to amplify, filter, and digitize the data in the field and to record the data on digital tape. Our amplifier gains can be adjusted from 42 to 120 dB, depending upon the distance from the shot point to the geophone for the individual channels. The upper limit of amplifier gains to avoid clipping of the signal is limited by digital word size rather than by the amplifier gains available. Our low-cut filters have 24 dB/octave rolloff to decrease the amplitude of ground roll. Data sample interval on each channel can vary from 1/4 to 4 msec with a total record length of 1000 samples per channel. Anti-alias filters are used to attenuate energy at frequencies above the Nyquist frequency (signal down 60 dB at that frequency).

Relatively severe low-cut filters have the beneficial effect of eliminating substantial amounts of cultural noise. Cultural noise in urban areas is relatively severe at frequencies below 50 Hz, but vehicular traffic and other vibratory sources don't produce much energy above 100-150 Hz. The noise that is produced at these high frequencies attenuates rapidly with distance from the source because of the low-pass nature of the earth's transfer function. Low-cut filtering also allows limited control over the dominant frequency of the recorded energy. Boosting the dominant frequency increases the possible bed resolution and, therefore, the accuracy of the survey. Care must be taken, however, when increasing the low-cut filter. Too severe filtering of lower frequencies decreases the signal-to-noise ratio and causes a ringiness in the data, generally resulting in a poorer quality section and a loss of bed resolution.

Provo Airport

Compressional wave data were recorded during the spring trip. The line for the P-wave data consisted of 65 shot locations occupied by two different sources. The line was set-up with a 1.25 m shot interval and single 100 Hz geophones spaced on 1.25 m intervals. A 30-06 hunting rifle with a specially designed airblast containment device was used. Recording was done with 220 Hz low-cut filters and the dominant frequency of the 30-06 seismic data was about 150 Hz. The second source was a 50-caliber single-shot sport rifle with its own airblast and particle containment apparatus. Recording was done with 110 Hz low-cut filters and the dominant frequency of the 50-caliber data was about 100 Hz.

The 50-caliber source was fired twice at each source location with the second projectile fired into the hole made by the first projectile. The repetitious firing of projectiles into the same hole allows the energy from later shots to dissipate more efficiently into more competent material. The two shots were recorded on tape separately and processed through CDP stack as independent data sets. Then the two stacked sections were cross-correlated and CDP stacked into a single 12-fold CDP seismic section.

The S-wave survey conducted in the spring of 1985 at the Provo Airport was the first real test of the arrow shear wave source in a 12-fold CDP production mode of operation. The source was a quad-winged arrow pointing vertically downward with each wing oriented either parallel or perpendicular to the survey line. After insertion into the ground, the arrow was forced (by sledge hammer) to rotate clockwise, then counterclockwise and each impact was recorded independently. The receivers were single 40 Hz horizontal geophones. The low-cut filter used had a -3 dB point at 55 Hz. Source and receivers were laid out in a split-spread orientation with a 5 m offset from source to closest receiver. Due to the lower bandpass recorded, the dominant frequency of the CDP stacked section was only about 30 Hz. Therefore, resolution was poor and surface waves overpowered the early portions of the seismograms.

As a result of the inappropriate choice of field recording parameters in the spring, a second shear wave survey was conducted at the Provo airport during the summer of 1985. After analysis of the spring survey data and slight modifications to the acquisition technique, new field parameters were chosen to improve the previous data quality. The new low-cut filter had a -3 dB point at 110 Hz. Due to the slower than expected S-wave velocity and the complex radiation pattern of S-waves, an end-on source/receiver orientation with an 11 m source-to-closest-receiver offset was chosen.

A new source was designed for the summer trip which was similar to the previous quad-winged arrow except the new arrow had only two wings separated by 180 degrees and by 0.25 m from the base. The new arrow design exploited some basic principles in an attempt to boost the frequency spectrum as well as reduce the generation of Love waves. The surface area of the second arrow head was reduced by about 70 percent. This was accomplished by cutting off the base half of the arrow and replacing the base half with a 0.15 m long, 2.5 cm diameter shaft. The smaller surface area of the double-winged arrow decreased the energy source volume and increased the dominant frequency. Also, the addition of the shaft allowed deeper penetration of the arrow into the soil layer resulting in a noticeable reduction in recorded Love waves.

It has been well documented that shear waves have a direction-dependent radiation pattern (for example, see Garland, 1971). On-site studies showed the radiation pattern of S-waves, generated by the smaller arrow, was strongly dependent on orientation of the arrow's wings. A lobe maximum traveled in the direction of the line when the arrow's wings were oriented 45 degrees to the line, so that orientation was used for the summer survey.

Springville Cherry Orchard

Compressional wave data at the cherry orchard were collected using field parameters similar to those used at the airport in Provo. On both runs the receiver (single 100 Hz geophones) and shot spacing was 1 m. The low-cut filter on the 30-06 survey attenuated signal by 3 dB at 220 Hz. This resulted in a dominant frequency on the 12-fold CDP stack of about 130 Hz. The 30-06 survey only required a single shot per shot point in a split-spread source/receiver array, with a source-to-closest-receiver spacing of 1.5 m. The 50-caliber rifle occupied about the first 50 of the 100 shot locations recorded using the 30-06 rifle. The low-cut filter for the 50-caliber survey attenuated signal by 3 dB at 110 Hz. Those field and recording parameters resulted in a dominant frequency on the stacked section of about 90 Hz. The 50-caliber data set at the cherry orchard had 2 shots per shot point with the second projectile traveling down the hole made by the first projectile. It was collected using a split-spread array with a source to closest receiver spacing of 4.5 m.

The shear-wave survey at the Springville cherry orchard was conducted using the same field parameters as the spring S-wave survey at the Provo airport. The cherry orchard survey included the use of single 30 Hz horizontal geophones, 55 Hz low-cut filters, and the quad-winged arrow.

DATA PROCESSING

The processing flow of the data was similar to ordinary oil company routines (Table 1). The seismic computer software used limits flexibility in engineering applications due to the nature of its originally intended application for large scale petroleum exploration surveys. However, techniques normally used to reduce 10 seconds of data can be scaled down to work on 0.1 sec of data. This is done by processing in units of decimeters and tenths of seconds instead of meters and seconds.

The 24-channel compressional wave field data was reduced to 12-fold stacked Common Depth Point (CDP) sections. If more than a single shot was fired at a location, a time shift was generally necessary to align the same CDP from different shots. This time mismatch was the result of source sensor irregularities and delays in the energy transfer of a second projectile fired into the hole made by a previous projectile. Determining the value of this time shift was accomplished by cross-correlating traces from the same CDP and shot location with successive projectiles.

Shear-wave data were processed quite similarly to the compressional wave data up to the point where the same CDP from two different shots with the same source location were mixed to form a single CDP trace. In order to compensate for possible time inconsistencies between shot 1 with straight polarity and shot 2 with reverse polarity, the same cross-correlation performed on compressional-wave data was used (after the signal from shot 2 was reversed in polarity). The resulting calculated time shift necessary to align reflecting events was then applied to the individual trace in the same fashion as with the 2-shot compressional-wave process. With the data time shifted, polarity matched, and stacked, a pseudo 24-fold S-wave reflection section resulted.

DISCUSSION

Provo Airport

The seismic line at the Provo, Utah, airport was occupied during two separate visits in 1985. The line was located in the flat grassy runway median with an apparently uniform soil layer underlain by lacustrine sediments. Geophone and source coupling with the ground on both the spring and summer trips were excellent, yielding high quality seismic data.

The P-wave seismic section from Provo airport, using the 50-caliber rifle, is shown in Figure 1. Note that excellent reflections were detected to 450 msec, a depth of roughly 300 m. Depth estimates are difficult to make for these data because the maximum source-to-receiver offset was only 20 m. This restricted the capability to do velocity analysis because of the short sampling of the normal-moveout curve. The data seemed to process equally well at velocities from as low as 450 m/sec to 2000 m/sec. This example illustrates the shallow reflection seismologist's dilemma: close source-to-receiver offsets are necessary to detect shallow reflections, but if deep reflections are present as a bonus on the data, their depth cannot be accurately calculated because of velocity uncertainties.

Two other facets of this P-wave section should be pointed out. First, there is a lack of reflections between 150 and 250 msec. The choice of offsets was such that this time window was nearly saturated with surface waves, obliterating any reflections that may be present.

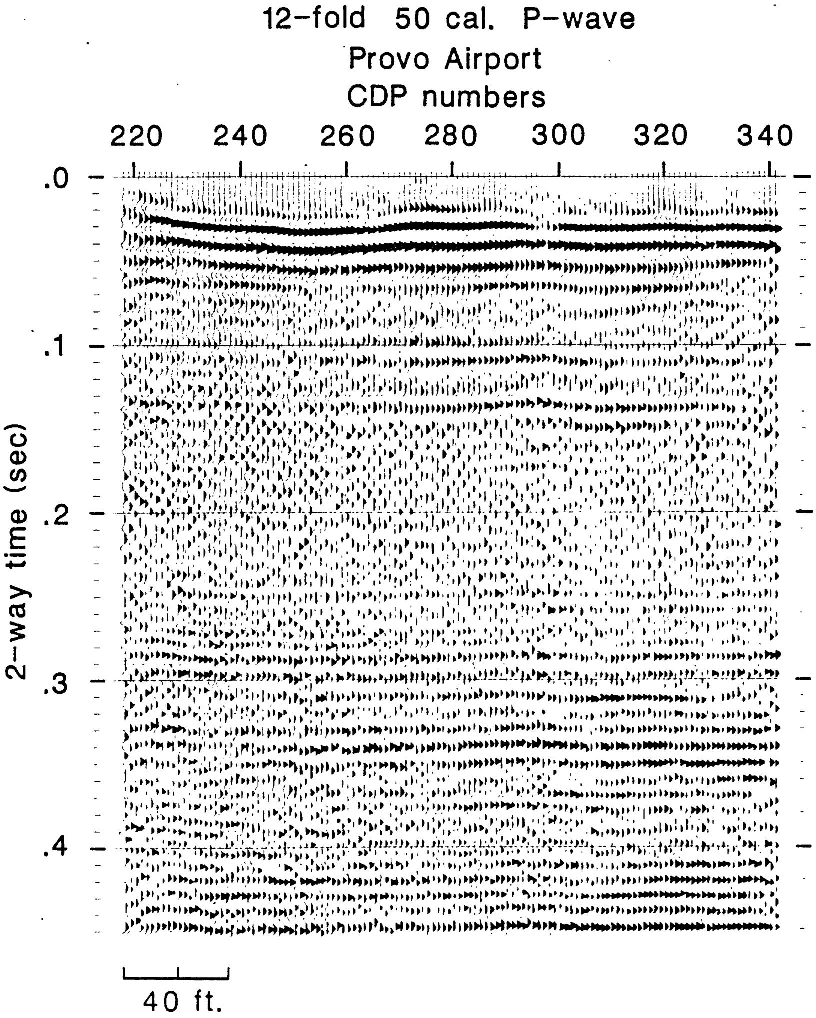

FIGURE 1. The 50-caliber rifle data from the Provo airport is excellent quality to 450 msec. The quiet zone between 170 msec and 240 msec resulted from the stacking of ground roll which dominated the 12-fold CDP gathers from 170 to 240 msec. The stacking process is intended to attenuate noise. Comparison of the P-wave data here and the S-wave data on Figure 2 is possible between 80 msec and 180 msec on the P-wave data, and 250 msec and 550 msec on the S-wave data. Reflections below 250 msec lack a good velocity function and, therefore, calculation of depth to reflecting events is not possible. This is a result of close geophone and source spacing which was necessary to record the shallow horizons.

During the CDP stacking process, the surface waves were attenuated but not to the extent of showing any reflections. In this case, absence of evidence is not necessarily evidence of absence of reflections. Second, the top two coherent wavelets on the section above 50 msec may be refractions that stacked in during processing. Overall, however, the P-wave data is excellent at this locality.

The S-wave seismic section from the second survey at Provo airport is shown in Figure 2. Note the existence of reasonably good reflections in the time window between 250 and 500 msec. The stacking velocity used was 170 m/sec for the S-wave data as compared to 550 m/sec for the P-waves. This suggests possible correlation of the S-wave reflection at 400-450 msec with the P-wave reflection at 140 msec. The S-wave reflection at 340-350 msec could correlate with the P-wave reflection at 110 msec. The S-wave reflection at 270-280 msec could correlate with the P-wave reflection at 90-100 msec.

While the above mentioned time correlations are reasonable with a Vp/Vs ratio of 3.1 which, using equation (1), yields a Poisson's ratio of 0.44 within the upper 50 m of sediment, the character of the reflections is different between the P-wave section and the S-wave section. This can be explained in part by noting that the frequency is almost identical between the two sections. Since the frequency is the same and the velocity differs by a factor of three, the resolution is better by a factor of three on the S-wave sections. In other words, what one sees on the seismic sections is resolution dependent to some degree. In any event, the combined data sets from the Provo airport represent our first successful effort to record shallow (less than 50 m) P-wave and S-wave reflections along the same line.

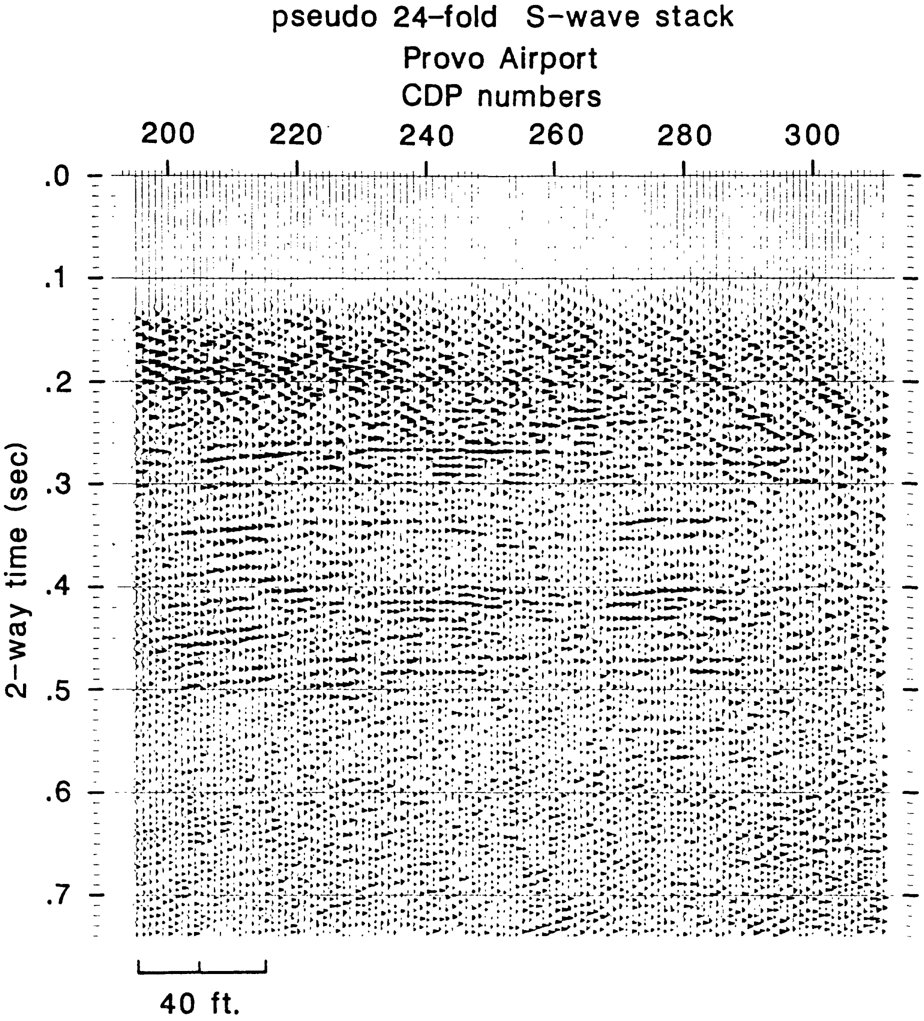

FIGURE 2. The rotational arrow proved a good source of S-wave energy. Information above 220 msec was lost due to the dominance of Love waves and a source-to-closest-receiver offset of 11.25 meters. There are several strong reflections that are coherent across the entire section. High frequency events near 400 msec between CDP 240 and CDP 220 may be indicative of a cut and fill stream deposit.

Springville Cherry Orchard

During the spring of 1985 trip to Provo, Utah, high-resolution P- and S-wave reflection surveys were conducted at a cherry orchard in Springville, Utah. Compressional wave surveys were done with both a 30-06 rifle and a 50-caliber rifle. The shear wave survey used the quad-winged arrow discussed in the previous section as the source. All three surveys occupied the same source and receiver locations with equipment unique to each particular technique.

The soil conditions hampered penetration of both source and receivers. Poor coupling to the ground from these soil conditions in part is responsible for the lower data quality in comparison with the Provo airport data. The soil layer consisted of very poorly sorted, unconsolidated sediments with grain sizes from silts to cobbles with scattered boulders.

In general, the data from the cherry orchard are not as good as those from the Provo airport. There are several notable features, however. Figures 3 and 4 represent the P-wave sections from the 50-caliber rifle and the 30-06 rifle, respectively, while Figure 5 is a shear-wave section. The 50-caliber rifle shell ejector broke during field work on this line, so Figure 3 is a shorter line than originally planned. The 30-06 data on Figure 4 are of low quality because of the bad near-surface seismic recording conditions discussed earlier.

The important point to notice about this line is the anticlinal nature of the most prominent reflector on Figures 3-5, inclusive, between CDP 219 and CDP 290. All three seismic sections show this feature, suggesting that it is geologically prominent in the subsurface. It is not known what causes this reflection, but it is

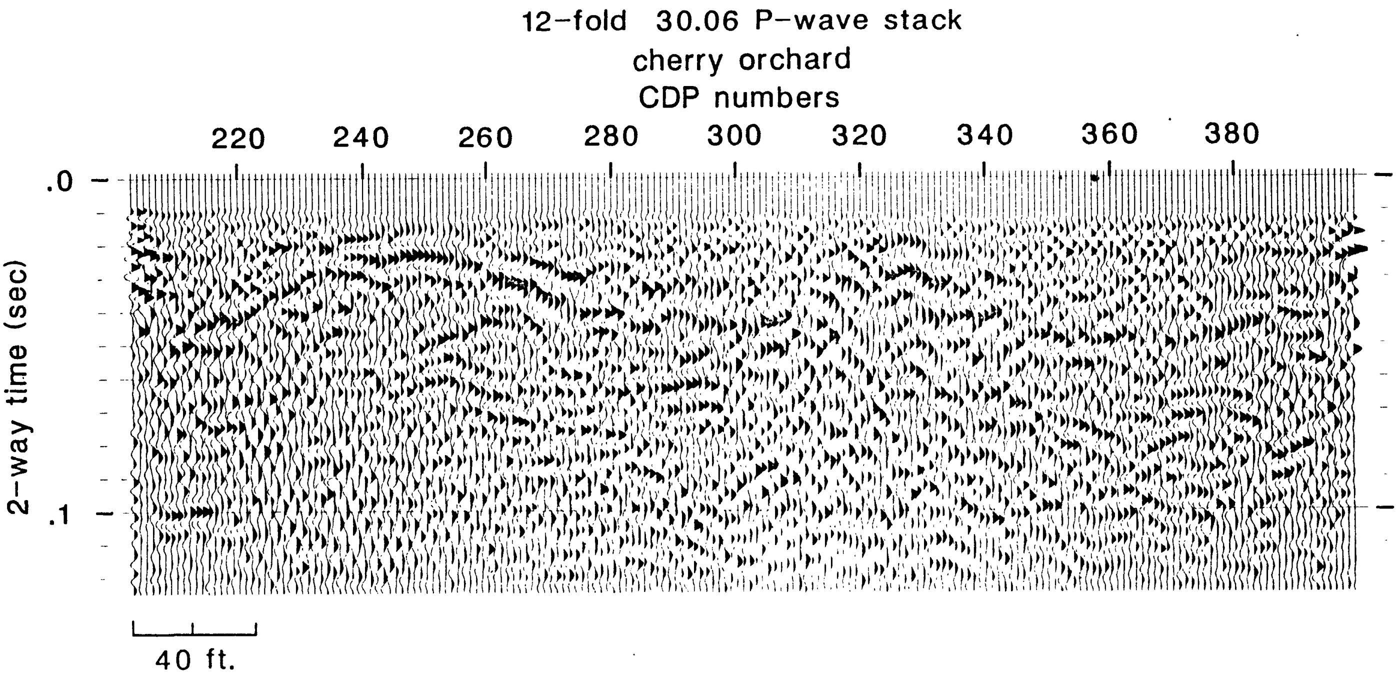

FIGURE 3. The 30-06 reflection line at the cherry orchard shows similar structure to the other cherry orchard lines (Figures 4 and 5). An anticlinal event can be followed from CDP 210 to CDP 275 between 45 msec and 20 msec. Hints of coherent events can be seen scattered over the entire right half of the section. Penetration was adequate to identify the dominant anticlinal event but lacked good energy penetration below about 40 msec.

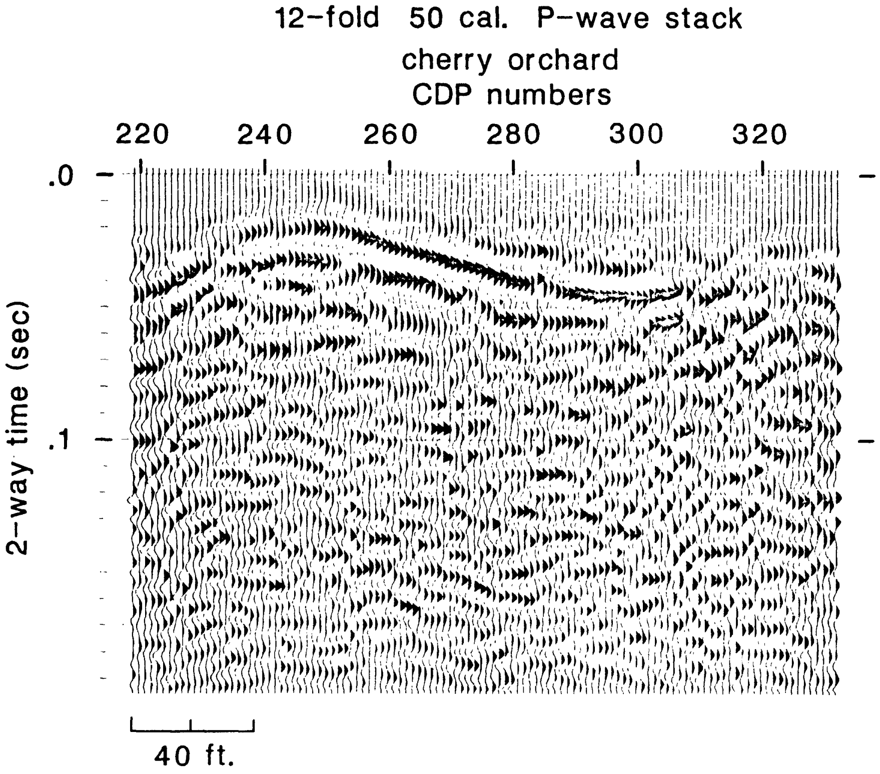

FIGURE 4. The 50-caliber line represents few processed field records, but coherent events can be picked out as deep as 140 msec. The same anticlinal event can be seen here as on Figure 3.

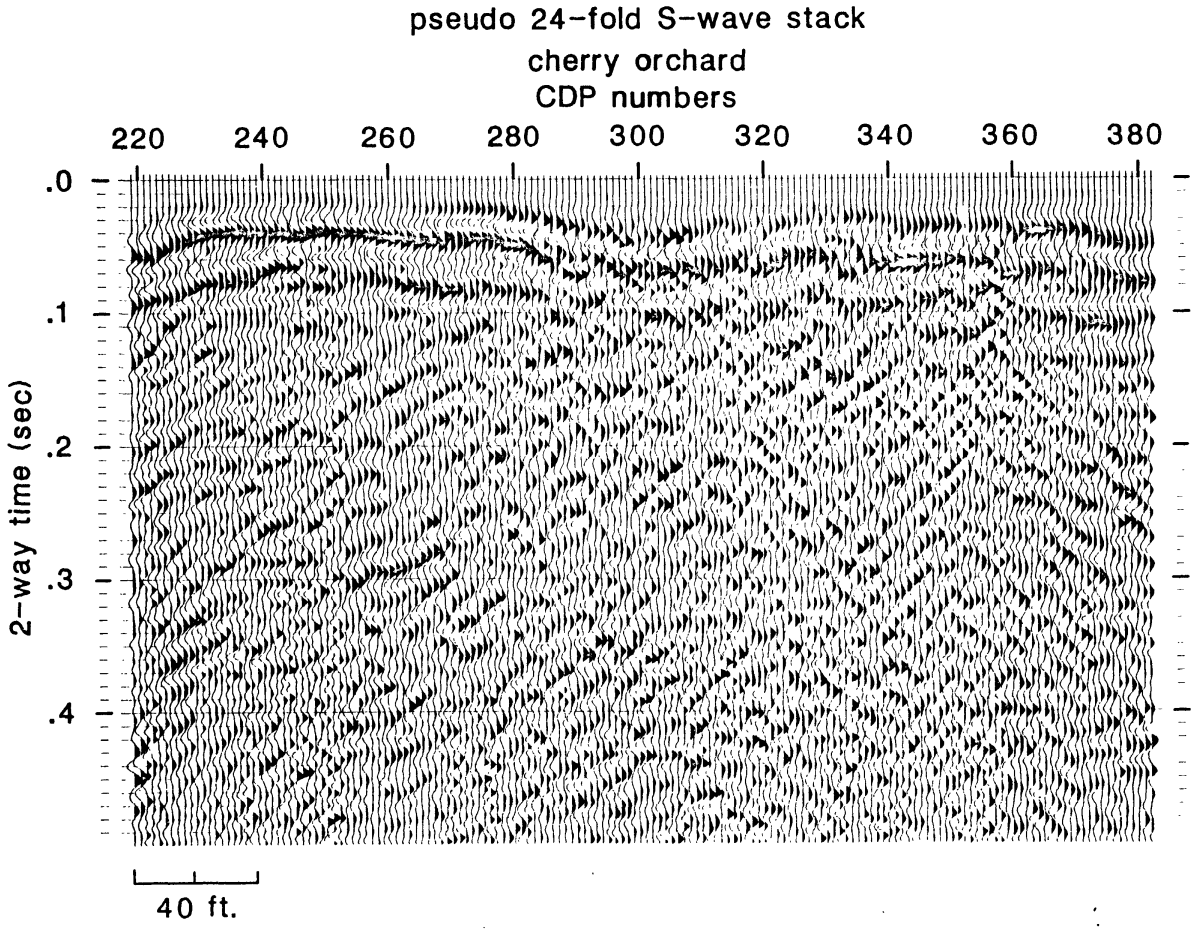

FIGURE 5. This S-wave data were collected using a quad-winged rotating arrow. The shallow reflecting event present here has a very similar shape to the events identified as anticlinal on Figures 3 and 4. Excessive ground roll (Love waves) drowned out the deeper reflecting events.

apparently in the depth range between 35 and 60 m. The USGS also ran a P-wave survey along this line independently using similar recording equipment and field parameters but with different personnel and different seismic processing software. The results (not shown here) are essentially identical.

The data from the shear wave survey were processed very similar to the Provo airport S-wave data. Two shots with opposite polarity were recorded separately at each shot location. The individual shots were time shifted, the second shot reversed, and stacked together. The resulting section possesses a dominant frequency around 40 Hz. The processed section lacked the good quality, continuous reflecting events observed on the summer S-wave survey from Provo airport.

The Vp/Vs ratio at this location is lower than at the Provo airport, with the ratio being about 1.8 in the near-surface sediments at the cherry orchard. Using equation (1), this yields a Poisson's ratio of 0.27.

While we do not have 50-caliber data beyond the middle of Figures 4 and 5 due to equipment malfunction, it is notable that the data quality from CDP 290 to CDP 340 is poor on the S-wave section and even worse on the 30-06 P-wave section. Beyond CDP 340 the data quality improves somewhat on both sections.

In brief, the cherry orchard data provide another example of the use of P-wave and S-wave reflection data to determine dynamic properties of the near-surface materials to a depth of about 50 m. The S-wave reflection technique has been improved since these data were shot, and the 50-caliber rifle would most certainly give better seismic sections for P-waves than did the 30-06. These two factors lead us to conclude that while the data from the cherry orchard discussed here are useful, considerable improvement can be expected in the future.

CONCLUSIONS

The shallow seismic P-wave reflection method is now a well developed technique. The seismic P-wave sections shown in this report are typical of the resolution that can be obtained with proper selection of recording parameters. The seismic sections at the cherry orchard demonstrate the repeatability of the technique. The results obtained with the 30-06 source and the 50-caliber source were essentially the same in the upper 60 msec. Furthermore, the USGS used its own crew and equipment to shoot the same line for comparison purposes. The prominent features of the two lines are identical, even though the data were processed by different people using different software. In particular, the anticlinal feature between CDP 210 and CDP 280 is obvious on all three P-wave sections as well as on the S-wave section.

The shallow S-wave reflection technique has room for improvement. At the Provo airport, the second survey provided excellent reflection data. The dominant frequency of the S-waves using the arrow source appears to be somewhere between 60 Hz and 100 Hz, a bit higher than expected. The recording of S-wave reflections shallower in time than 100 msec has not yet been attained by us. The problem involves getting rid of substantial amounts of Love-wave energy. Since Love waves are essentially multiply-reflected S-waves trapped in near-surface layers, they exhibit many of the same characteristics as the desired S-wave reflections. We have made progress toward solving that problem by moving the S-wave source below the surface and by increasing its frequency.

The actual calculation of Poisson's ratio is simple arithmetic once the P-wave and S-wave velocities are known. For example, at the Provo airport, P-wave velocity (determined from normal moveout equation) is approximately 550 m/sec and S-wave velocity is approximately 170 m/sec within the upper 100 m of lake sediments, yielding an average Poisson's ratio of 0.44. Whereas, at the cherry orchard, P-wave velocity is approximately 355 m/sec and the S-wave velocity is approximately 200 m/sec in the upper 30 m resulting in an average Poisson's ratio in the upper 100 m of 0.27. We were not able to correlate individual reflections between the P-wave and S-wave seismic sections well enough to allow direct calculation of Poisson's ratio, depth interval-by depth interval. Part of this difficulty stems from the fact that the S-wave reflections had about a factor of 3 greater resolution than did the P-wave reflections at the Provo airport and more than a factor of 2 greater resolution at the cherry orchard.

Finally, the ultimate goal of this project is to relate the engineering properties of near-surface materials to amplification of ground-shaking at specific sites. That phase of the project is just beginning and will be examined in late 1985 and early 1986.

BIBLIOGRAPHY

Barbier, M.G., Bondon, P.J., and Mellinger, R., 1975, Results of shallow seismic prospecting using the "MiniSOSIE" process, [Abs.]: Soc. Explor. Geophysicists annual meeting, Denver, CO.

Barry, K.M., Cavers, D.A., and Kneale, C.W., 1967, Special Report: Recommended standards for digital tape formats: Geophysics, v. 40, no. 2, p. 344-352.

Bondon, P.J., 1975, MiniSOSIE Denver field tests, unpublished report.

Borcherdt, R.D., Joyner, W.B., Warrick, R.E., and Givvs, J.F., 1975, Response of local geologic units to ground shaking, In USGS Prof. Paper 941-A, edited by R.D. Borcherdt, p. 52-68.

Cook, J., 1965, Seismic mapping of underground cavities using reflection amplitudes: Geophysics, v. 30, p. 527-538.

Cooley, J.W. and Tukey, J.W., 1965, An algorithm for the machine calculation of complex Fourier series, Mathematics of Computation, v. 19 p. 297-301.

Costain, J. and Robinson, E., 1972, Some seismic measurements on the Virginia coastal plain: Water Resources Research Center Bull. 56, Virginia Polytechnic Institute, Blackburg, 69 p.

Dobrin, M.B., 1976, Introduction to geophysical prospecting: McGraw-Hill Book Co., New York.

Doornenbal, J.C. and Helbig, K., 1983, High resolution reflection seismics on a tidal flat in the Dutch Delta-acquisition, processing and interpretation: First Break, May, p. 9-20.

Fry, J.C. and Leonard, A.B., 1954, Significant new exposures of Pleistocene deposits at Kirwin, Phillips County, Kansas: Kansas Geol. Survey Bull. 109, pt. 3.

Gardner, L.W., 1939, An areal plan of mapping subsurface structure by refraction shooting: Geophysics, v. 4, p. 247-259.

Gardner, G.H.F., Gardner, L.W., and Gregory, A.R., 1974, Formation velocity and density: The diagnostic basics for stratigraphic traps: Geophysics, v. 39, p. 770-780.

Green, C.H., 1938, Velocity determinations by means of reflection profiles: Geophysics, v. 3, p. 295-305.

Hagedoorn, J.G., 1954, A process of seismic reflection interpretation: Geophys. Prospect., v. 21, p. 85-127.

Hobson, G.D. and Grant, A.C., 1964. Tracing buried river valleys in the Kirkland Lake area of Ontario with a hammer seismograph: Canadian Mining Journal, p. 3-7, April.

Hobson, G., 1970, Seismic methods in mining and groundwater exploration: Geological Survey of Canada, Economic Geology Report 26, p. 148-170.

Hobson, G. and Jobin, C., 1975, A seismic investigation - Peyto Glacier, Banff National Park, and Woolsey Glacier, Mount Revelstoke National Park: Geoexploration, v. 13, p. 117-127.

Hunter, J.A., 1981, Mating the digital engineering seismograph with the small computer - some useful techniques, [Abs.]: Geophysics, v. 46, p. 451-452.

Hunter, J.A., Burns, R.A., and Good, R.L., 1981, Optimum field techniques for bedrock mapping with the multichannel engineering seismograph [Abs.]: Geophysics, v. 46, p. 451.

Hunter, J.A., Pullan, S.E., Burns, R.A., Gagne, R.M., and Good, R.L., 1984, Shallow seismic reflection mapping of the overburden-bedrock interface with the engineering seismograph: some simple techniques: Geophysics, v. 49, p. 1381-1385.

Jakosky, J.J., 1950, Exploration geophysics: Trija Publishing Co., Newport Beach, CA.

Knapp, R.W. and Steeples, D.W., 1981, Investigation of salt dissolution collapse using high-resolution MiniSOSIE reflection seismology [Abs.]: EOS Trans. Am. Geophys. Union 62, p. 954-955.

Lawson, A.C., 1908, The California earthquake of April 18, 1906: Report of the State Earthquake Investigation Commission, v. I, Carnegie Institute of Washington, Washington, D.C.

Mayne, W.H., 1962, Horizontal data stacking techniques: Supplement to Geophysics, v. 27, p. 927-938.

McNellis, J.M., 1973, Geology and ground-water resources of Rush County, Kansas: Kansas Geol. Survey Bull. 207.

Medvedev, S.V., 1965, Engineering seismology: National Technical Information Service, NTIS no. TT65-50011, 260 p.

Meidav, T., 1968, A multilayer seismic refraction nomogram: Geophysics, v. 33, p. 524-526.

Meidav, T., 1969, Hammer reflection seismics in engineering geophysics: Geophysics, v. 34, p. 383-395.

Merriam, D.F., 1954, Electrical resistivity studies in the Kansas river valley: State Geol. Survey of Kansas Bull. 109, pt. 7, Lawrence, KS.

Miller, R.D., and Steeples, D.W., 1986, Shallow structure from a seismic reflection profile across the Borah Peak, Idaho, fault scarp: Geophysical Research Letters, in press.
Mota, L., 1954, Determination of dips and depths of geological layers by the seismic refraction method: Geophysics, v. 19, p. 242-254.

Musgrave, A.W., 1967, Seismic refraction prospecting: Society of Exploration Geophysicists, Banta, Menasha, Wisconsin.

Muskat, M., 1933, The theory of refraction shooting: Physics, v. 4, p. 14-38.

Nuttli, O.W., 1973, The Mississippi valley earthquakes of 1811 and 1812: Intensities, ground motion, and magnitudes: Seism. Soc. Am. Bull. v. 63, 227-248.

O'Connor, H.G., 1960, Geology and groundwater resources of Douglas County, Kansas: Kansas Geol. Survey Bull. 148, 200 p.

O'Connor, H.G. and Fowler, L.W., 1963, Pleistocene geology in a part of the Kansas City area: Trans. Kansas Acad. Sci., 66, no. 4.

Pakiser, L. and Warrick, R., 1956, A preliminary evaluation of the shallow reflection seismograph: Geophysics, v. 21, p. 388-405.

Robinson, E.A. and Treitel, S., 1964, Principles of digital filtering: Geophysics, v. 29, p. 394-404.

Saske, J.L., 1959, Discussion on the blind zone problem in engineering Geophysics: Geophysics, v. 24, p. 359-416.

Schepers, R., 1975, A seismic reflection method for solving engineering problems: Journal of Geophysics, v. 41, p. 367-384.

Schneider, W.A. and Backus, M.M., 1968, Dynamic correlation analysis: Geophysics, v. 33, p. 105-126.

Sengbush, R.L. and Foster, M.R., 1968, Optimum multichannel velocity filters: Geophysics, v. 33, p. 11-35.

Steeples, D.W., 1979, A repeatable seismic energy source for shallow groundwater exploration [Abs.]: EOS Trans. Am. Geophy. Union, v. 62, p. 683.

Steeples, D.W. and Knapp, R.W., 1982, Reflections from 25 feet or less, (expanded abstract): Soc. Explor. Geophys. program, p. 469-471.

Treadway, J.A., Steeples, D.W., and Miller, R.D., 1985, Seismic reflections within the upper 100 feet near Borah Peak, Idaho, earthquake scarp: Soc. Explor. Geophys. 55th annual meeting, Washington, D.C., in Technical Program, Abstracts and Biographies, [expanded abstract] p. 161-163.

Warrick, R. and Winslow, J., 1960, Application of seismic methods to a groundwater problem in northeastern Ohio: Geophysics, v. 24, p. 505-519.

Widess, M.B., 1973, How thin is a thin bed?: Geophysics, v. 38, p. 1176.

EFFECTS OF SIX DAMAGING EARTHQUAKES IN SALT LAKE CITY, UTAH

by

Sherry D. Oaks
Department of Geography
University of Colorado
Boulder, Colorado

ABSTRACT

The geographic distribution of Modified Mercalli (MM) intensity is identified and analyzed for six damaging earthquakes in Salt Lake City, Utah. These events include the October 5, 1909; May 22, 1910; March 12, 1934; February 22, 1943; March 6, 1949; and September 5, 1962, earthquakes. Some of these earthquakes are large events ($\geq 6.0\ M_L$) with epicenters distant from Salt Lake City ($>$100 km) and some are moderately large earthquakes ($5.0.6.0 M_L$) with epicenters close to Salt Lake City ($<$ 15 km). Both types of earthquakes have caused structural damage in that urban area. Building type and damage are detailed for sites within Salt Lake City from each of the earthquakes.

Intensity is found to increase across the city from the Wasatch Fault zone on the east side of the city to the Jordon River Valley in the west sections of the city by 2 to 3 intensity units. There are also increases of 1 to 1.5 units from the northern section of the city (in the vicinity of the State Capitol Building) to the southern parts of the city near Twenty-First South Street. Based on work by Evernden and Thomson (1985), these values are estimated to be 1 to 1.5 intensity units greater if a higher water table (such as the one that exists in Salt Lake City today) is assumed. The distribution of intensity from the historic earthquakes investigated in this study is found to correlate with values from instrumental site response studies conducted in the region.

This study was supported through a doctoral student appointment at the Branch of Geologic Risk Assessment at the U.S. Geological Survey and by a doctoral dissertation assistance grant from the Geopraphy and Regional Science Program at the National Science Foundation.

Introduction

Six moderate-to-large earthquakes that caused damage in the Salt Lake City urban area were investigated in the study (Figure 3-1). Earthquakes with epicenters near the Wasatch Fault zone running to the east of the city or on Basin and Range faults in the Salt Lake valley to the north and west of the city were examined. Investigations to determine Modified Mercalli (MM) intensity (Wood and Neumann 1931) for these events show that a large earthquake ($\geq$ 6.0 M_L) near Salt Lake City or a moderately large earthquake (5.0-6.0 M_L) close to Salt Lake City can cause damage in that urban area even if the event is not as large as the postulated-7.5 M_L event that is commonly used for hazard and loss estimates in that urban area. Data from the investigations of these moderately large earthquakes illustrate the distribution of

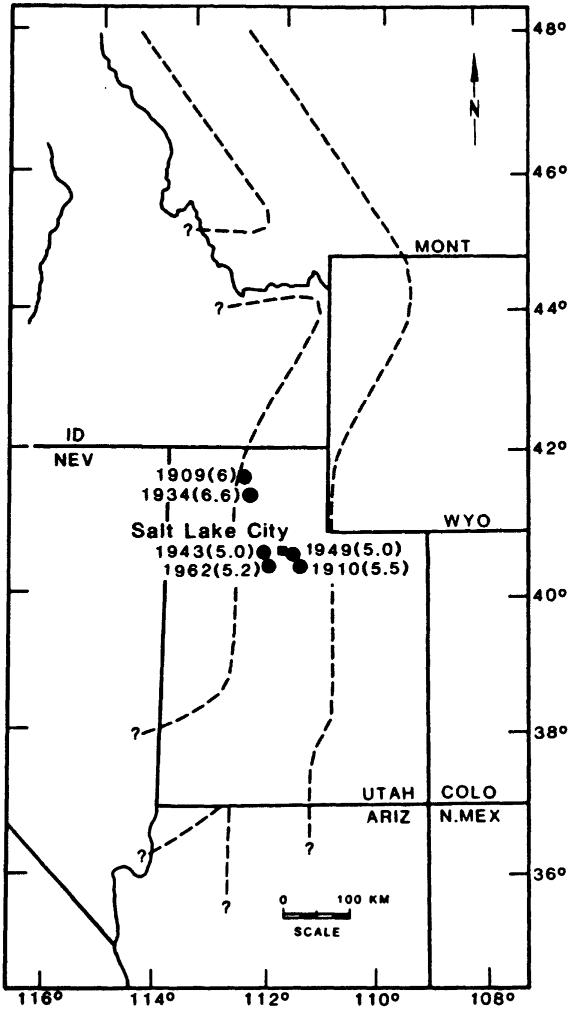

Figure 3-1. Epicenters of the six earthquakes investigated in this study. The dashed lines represent the Intermountain Seismic Belt.

intensities throughout the city. The observed intensities were derived from historical documentary evidence and were plotted throughout the city on U.S. Geological Survey 1:24,000 topographic maps (Plates 1-6, Appendix III). Figures 3-2 - 3-7 also illustrate these intensity distributions.

Instrumental site response studies (Hays et al. 1978; Hays and King 1982, 1984; King et al., in press) have greatly increased the knowledge of potential damage from ground shaking effects in the Salt Lake City urban area. The six earthquakes detailed in this paper also add to an understanding of the earthquake effects at specific sites throughout the Salt Lake City urban area by providing a large geogaphical sample of earthquake effects showing patterns of observed intensity throughout the city. These intensity patterns are compared to the recent site response work of King et al. (in press).

Intensity Determinations for the October 5, 1909, Earthquake

Figure 3-2 shows the MM intensity assigned to reports found in documentary sources for the October 5, 1909, I_O VIII (maximum intensity), Hansel Valley earthquake. This earthquake is

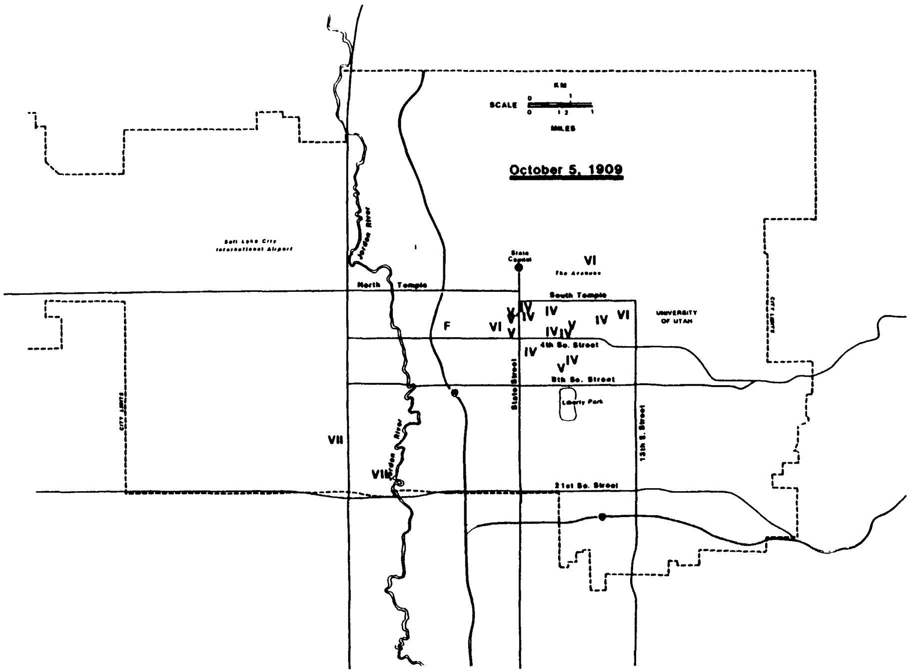

Figure 3-2. Distribution of intensity (MM) in Salt Lake City from the October 5, 1909 earthquake.

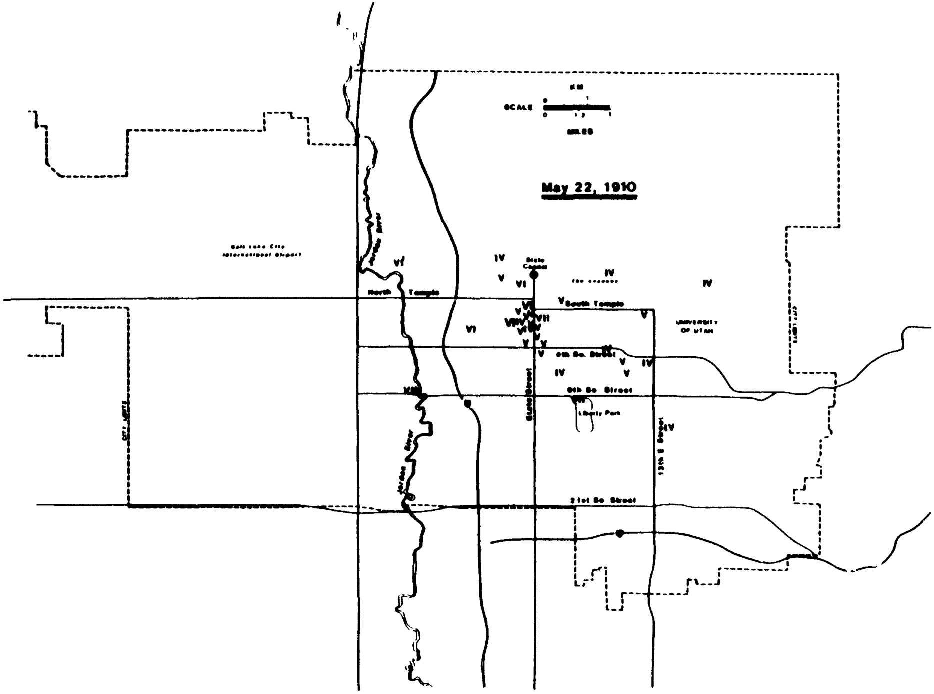

Figure 3-3. Distribution of intensity (MM) in Salt Lake City from the March 22, 1910 earthquake.

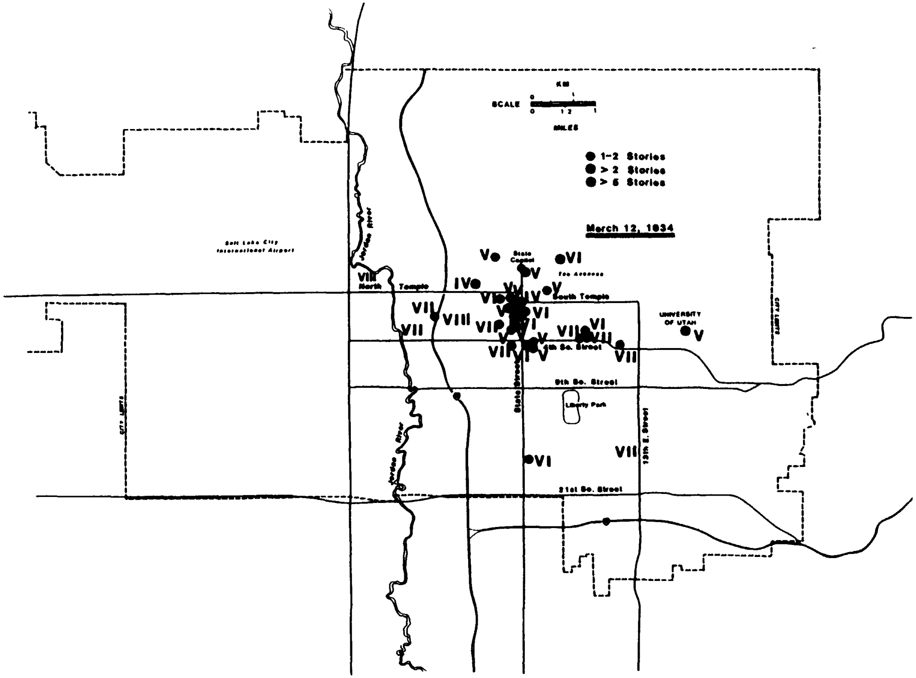

Figure 3-4. Distribution of intensity (MM) in Salt Lake City from the March 12, 1934 earthquake.

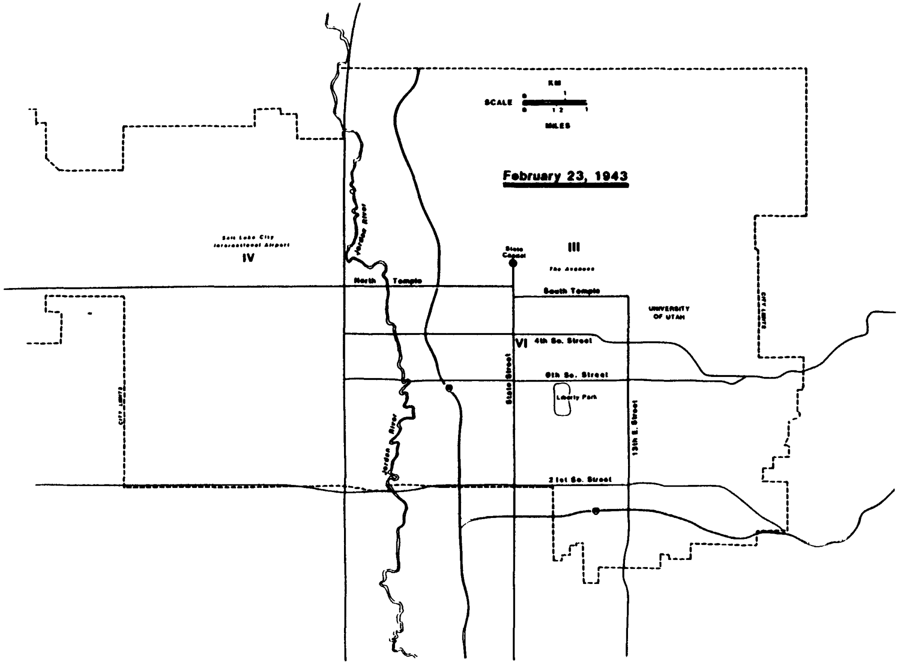

Figure 3-5. Distribution of intensity (MM) in Salt Lake City from the February 22, 1943 earthquake.

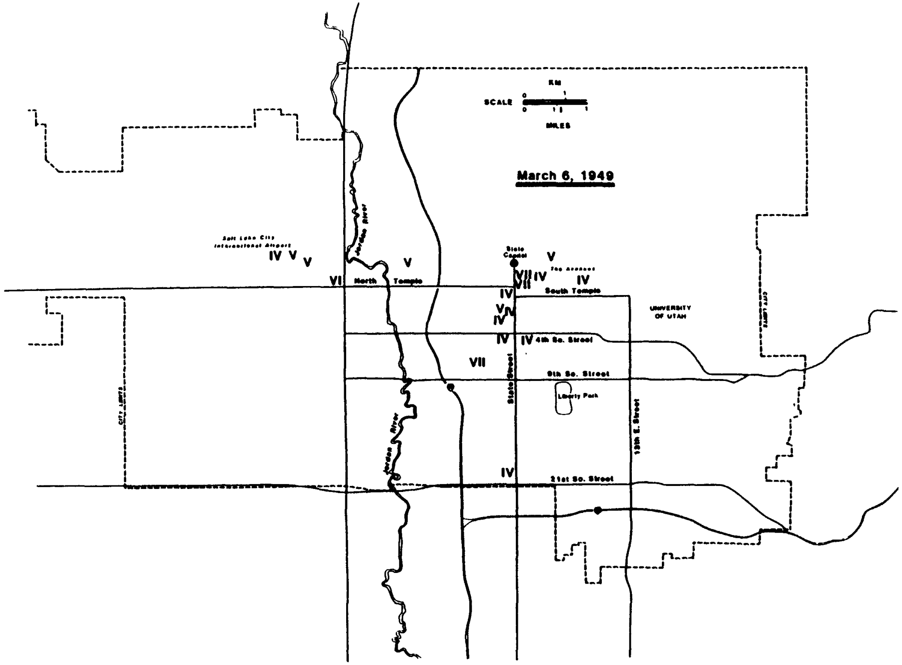

Figure 3-6. Distribution of intensity (MM) in Salt Lake City from the March 6, 1949 earthquake.

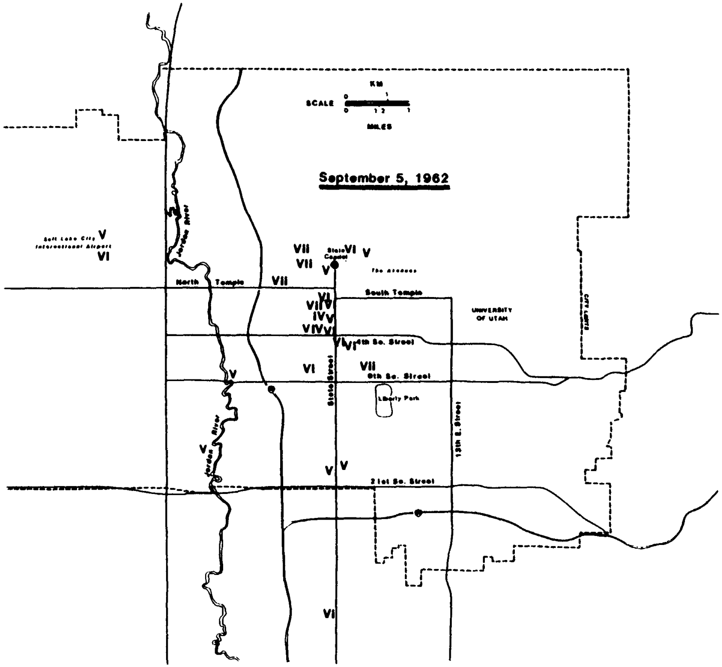

Figure 3-7. Distribution of intensity (MM) in Salt Lake City from the September 5, 1962 earthquake.

assigned epicentral intensities of VIII by Arabasz et al. (1979) and VII by Stover et al. (1986). The higher value is consistent with reports of surface faulting that are alleged to have occurred in the epicentral area based on an interview by R. B. Smith at the University of Utah (personal commun., 1986) and records of damage to buildings in the area (Salt Lake City, LDS Archives, Curlew Stake, Snowville Ward, Manuscript History). The earthquake was recorded at the University of Utah's seismograph station, but extensive searches in connection with this study, as well as others (Arabasz et al. 1979), have not been successful in locating the original records. A copy of the original instrumental record was located with weather records (Asheville, N.C., National Climatic Data Center, Salt Lake City station records) and a description of the recording was reproduced in a copy of the <u>Salt Lake Telegram</u> newspaper. Epicentral coordinates for the earthquake are estimated to be at 41.46° N and 112.40° W by Arabasz et al. (1979) and 41.8° N and 112.7° W by Stover et al. (1986). Since this study concentrates on the effects of the event within Salt Lake City, the building type at each of the sites was investigated in detail so accurate MM intensity could be assigned. A list of the site names and addresses, the type of building, a brief description of the earthquake effects at that site, and the MM intensity assignment are listed in Appendix II.

Reports of general effects in Salt Lake City included houses shifting on their foundations, cracked walls and windows, people on the street wavering in their steps and experiencing nausea, and people in higher story buildings reporting strong tremors (Salt Lake Tribune, Deseret News). At the U.S. Weather Bureau office on the top floor of the newly built, 11-story steel-framed Boston Building there was a "decided swaying motion" and clocks stopped (Deseret News; Asheville, N.C., National Climatic Data Center, Salt Lake City station records).

Damage within the city limits was observed at the Armory on Pierpont Street (Figure 3-8). There were also reports of broken windows in homes at higher elevations in north and east bench neighborhoods. Since the specific addresses for these homes could not be determined, the points are not included in Figure 3-2. Buildings twisted, boards cracked, and waves rolled over the bath house pier at the Saltair Resort, located on the south shore of the great Salt

Figure 3-8. Damage sustained at the Armory on Pierpont Street during the October 5, 1909 earthquake. (Photograph courtesy of the Utah State Historical Society.)

Lake. A seiche was reported as having "passed over" the Union Pacific Railroad's Lucin cut-off near the northern part of the lake.

Intensity Determinations for the May 22, 1910, Earthquake

Figure 3-3 shows the intensity distribution from the May 22, 1910 I_o VII earthquake. This event was recorded on the seismograph at the University of Utah, but like the 1909 earthquake, the original record has not been located despite extensive searches conducted during this study and by scientists at the University of Utah (Arabasz et al., 1979; Arabasz, personal commun., 1986; Smith, personal commun., 1986). The epicentral coordinates were determined as 40.44° N and 111.50° W by Arabasz et al. (1979) and as 40.7° N and 111.8° W by Stover et al. (1986). At the time of the earthquake, Professor Pack, Deseret Professor of Geology at the University of Utah, theorized that the epicenter was on the Wasatch Fault under the University of Utah (Deseret News). The important point is that the event's epicenter was close to, if not within, the boundaries of Salt Lake City. A list of site names and addresses, building type, reports of earthquake effects, and MM intensities are listed in Appendix II

This earthquake was reported to have been felt by everyone throughout the city (Salt Lake Tribune; Deseret News). In some areas, there was a "great exodus" of people from their homes and businesses. This was especially true in the section of Salt Lake City between Third South, Sixth South, Main and Third East, which was predominantly settled by blacks; along Plum Alley which was the oriental neighborhood between Main, State, First South, and Second South at that time; in the Greek neighborhood on the west side along Second South from Fourth West to Sixth West; and in the Fifth Ward along Third West from about Fifth South to Seventh South. These neighborhoods had a 3:1 ratio of brick and adobe houses to wood-frame residences (Salt Lake City, University of Utah, Special Collections; Sanborn Maps).

Damage in Salt Lake City consisted mainly of cracked and fallen plaster and broken mirrors and windows. Some chimneys toppled and the earthquake separated joints in gas mains on Ninth South between Eighth East and Second West, causing leaks and some loss of service (Deseret News; Salt Lake City, State of Utah Archives, Public Works records). Plaster fell at the Bitner Residence at 60 Center Street, a one-story frame, stone and brick residence; at the American Sunday School Chapel at Fifth North and Oakley; and at the Oregon Short Line Depot, a two- to six-story reinforced concrete, steel-framed structure (Deseret News; Salt Lake City, University of Utah, Special Collections, Sanborn Maps, Union Depot architectural plans). A brick chimney fell at the police station, a two-story stone building located at 120 East First South (Deseret News; Salt Lake Tribune).

Intensity Determinations for the March 12, 1934, Earthquake

Figure 3-4 shows the intensity distribution in Salt Lake City for the March 12, 1934, I_O IX, Hansel Valley earthquake. The University of Utah seismograph station was not operating at the time of the shock, although the shock was recorded on a number of other instruments in the country (United States Earthquakes, 1934). The main shock from this earthquake began at 8:06:45 a.m. and continued until 8:08 a.m. local time. A large aftershock occurred at 11:21 a.m. the same day and dozens of aftershocks occurred in the months that followed (Boulder, Colorado, World Data Center for Geophysics, manuscript of field study of 1934 Hansel Valley earthquake; Shenon, 1934). The earthquake was assigned a 6.6 M_L by Richter (1935) and is the largest to have occurred in northern Utah since settlement there by Mormons and others in the 1840's. Many believe this event to be the only earthquake to have caused surface faulting in the region, although the 1909 Hansel Valley earthquake may have produced surface faulting as mentioned. A list of site names and addresses, types of buildings, reports of earthquake effects, and MM intensity are listed in Appendix II.

Significant damage within Salt Lake City occurred east of downtown where chimneys of two adjacent homes at 817 and 823 East Second South were destroyed. The 817 East Second South home was a two-story brick house and the 823 East Second South residence was a one-and-one-half story brick structure (Deseret News; Salt Lake Tribune; Salt Lake Telegram; Salt Lake City, University of Utah, Special Collections, Sanborn Maps) (Figure 3-9). The LDS Thirty-Third Ward meeting house, at Eleventh East between Fourth South and Fifth South, sustained damage when part of an interior wall collapsed. This structure

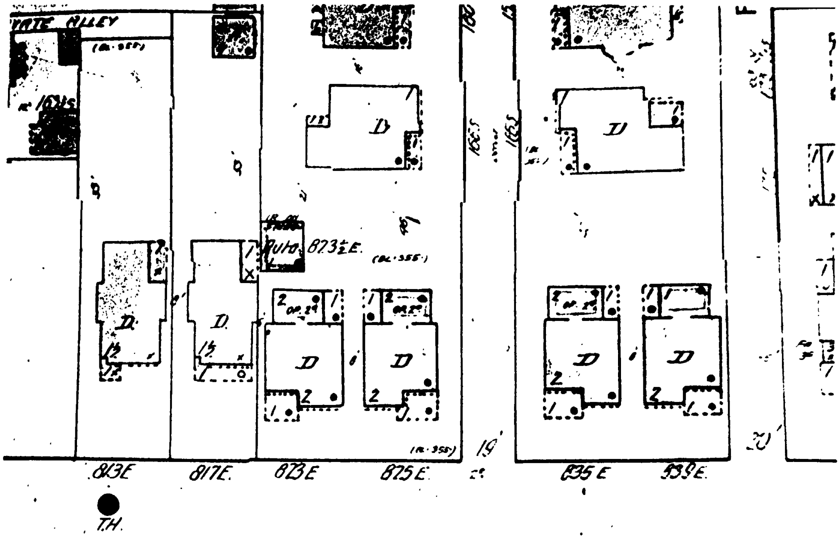

Figure 3-9. Sanborn map detail of construction type of two residences damaged during the March 12, 1934 Hansel Valley earthquake. (Reproduction of Sanborn Map, courtesy of the University of Utah.)

was a one-and-one-half story brick building (Salt Lake City, LDS Archives, Thirty-Third Ward Manuscript History; Architectural Records Ward meeting houses; University of Utah, Special Collections, Sanborn Map) (Figure 3-10).

North of downtown, nonstructural damage occurred at the Ensign School at 431 Ninth Avenue, a three-story steel, reinforced-concrete and stone building (Deseret News; Salt Lake City, University of Utah Special Collections, Sanborn Map). Just to the south of the main downtown commercial center, damage occurred at the City and County Building, an unreinforced-stone, 4- to 5-story structure at State Street between Fourth and Fifth South. Chimneys and capstones collapsed and bricks fell to the street (Deseret News; Salt Lake Tribune; Salt Lake Telegram; Salt Lake City, University of Utah, Special Collections, Sanborn Map). Kaliser (1971) reports that "some two-and-one-half tons of mechanical clock equipment fell from the main tower and crashed down through the building" and that the "center floor-well on the fifth floor was permanently closed soon after."

In the central business district, damage consisted mainly of cracked plaster, fallen plaster, and

Figure 3-10. Damage was sustained by the Thirty-Third Ward Meetinghouse (LDS) during the March 12, 1934 earthquake. (Photo courtesy of the Church of Jesus Christ of Latter-day Saints.)

broken windows. Considerable amounts of plaster fell at the Dooly Building, a six-story, unreinforced-brick structure and at the Newhouse Building, a twelve-story, steel-frame structure (Deseret News; Salt Lake Tribune; Salt Lake Telegram; Salt Lake City, University of Utah, Special Collections, Sanborn Map) (Figure 3-11).

On the west side of town, several vehicles were affected by the earthquake including one driven by Dillard Hamilton on the way to the airport (exact location on North Temple not specified). At 143 South Seventh West, a driver was injured when he was thrown forward in the auto by the earthquake (Deseret News).

South of downtown, the most serious effect from the earthquake was the collapse of a ditch on Public Works employee Charles Bitthell who died of the injuries (Deseret News; Salt Lake Tribune; Salt Lake Telegram).

There were several reports of long-period effects from this earthquake, including those at the City and County Building, the LDS Salt Lake Temple, and the Tribune and Ezra Thompson buildings. At the City and County Building at State Street between Fourth and Fifth South, the statue on the top of the

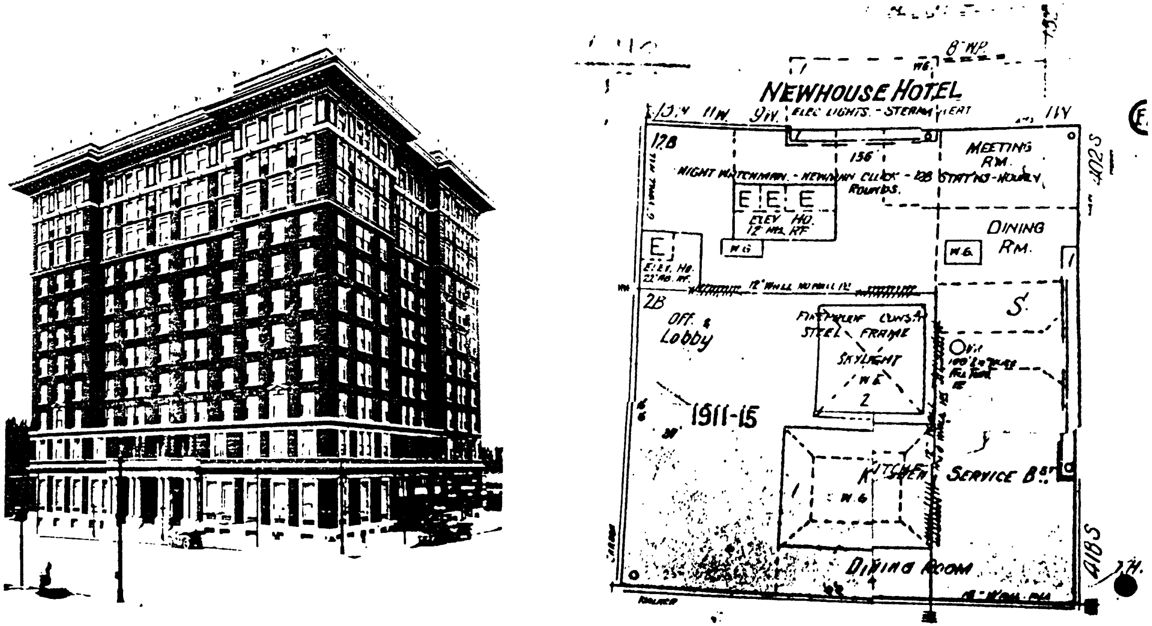

Figure 3-11. The Newhouse Hotel was damaged by the March 12, 1934 Hansel Valley earthquake. (Photograph courtesy of the Church of Jesus Christ of Latter-day Saints.) (Sanborn map courtesy of Marriott Library, Special Collections, University of Utah.)

building's tower (210-ft. elevation) was shaken nearly a foot out of line and was later removed (Salt Lake Tribune, Salt Lake Telegram, Deseret News) (Figure 3-12). At the LDS Salt Lake City Temple on Main Street between North and South Temple, the Angel Moroni statue, although anchored securely atop the main tower (234-ft height) was moved and twisted toward the southeast by the earthquake (Salt Lake Tribune, Deseret News, Salt Lake Telegram), (Figure 3-13). The most dramatic report of long-period effects involved the adjacent Ezra Thompson and Tribune buildings at 143 and 145 South Main which were observed to batter against each other (Deseret News, Salt Lake Tribune, Salt Lake Telegram). The Ezra Thompson Building is a ten-story, steel-frame and brick structure built in 1924. It is still standing as of this writing. The old Tribune Building was a six-story, unreinforced-brick building that has been demolished. As a result, the exact distance between the buildings is not known. Sanborn maps and historic photographs (Salt Lake City, University of Utah, Special Collections) show the proximity of the two buildings circa 1934 (Figure 3-14).

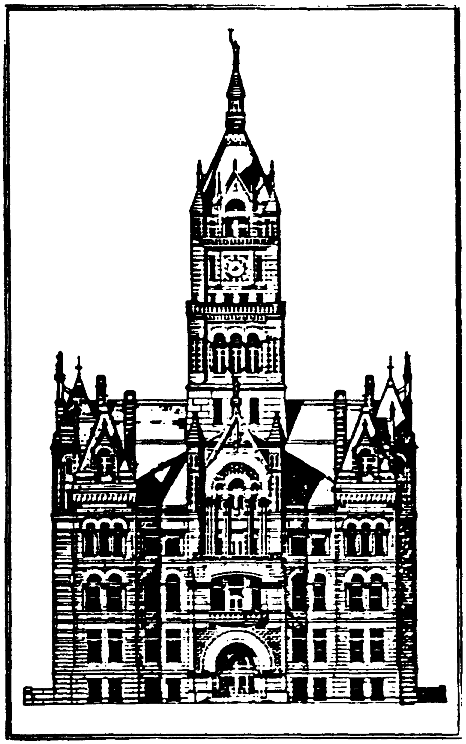

Figure 3-12. The Salt Lake City and County Building was affected by long-period effects of the March 12, 1934 earthquake. The statue atop the tower (210-ft. elevation) was shaken a foot out of line and later removed. (Drawing courtesy of Reaveley Engineers and Associates.)

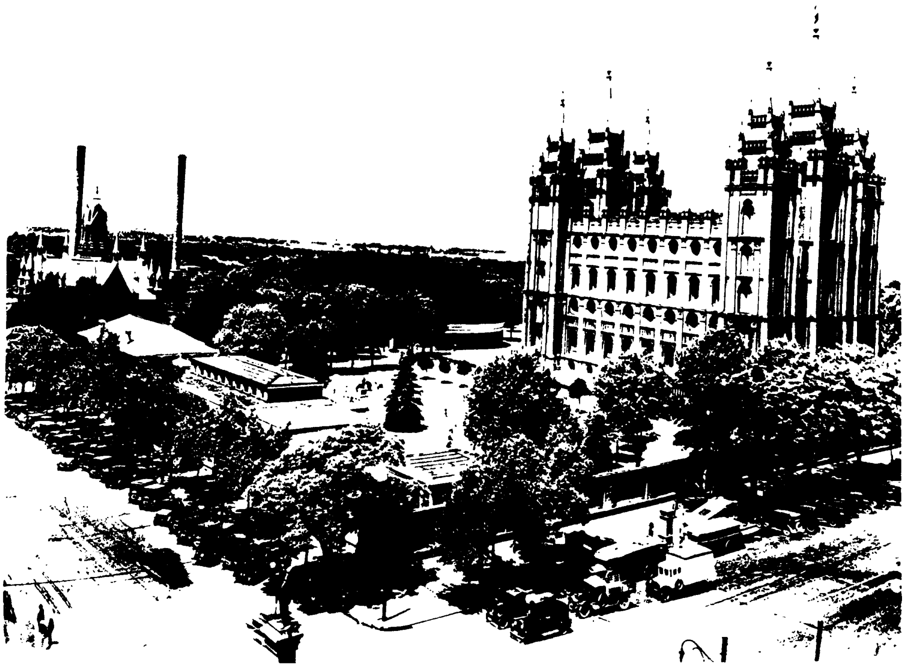

Figure 3-13. Long-period effects also affected the statue atop the tower (234-ft. elevation) of the Salt Lake City Mormon Temple during the March 12, 1934 earthquake. (Photo courtesy of the University of Utah, Marriott Library, manuscripts.)

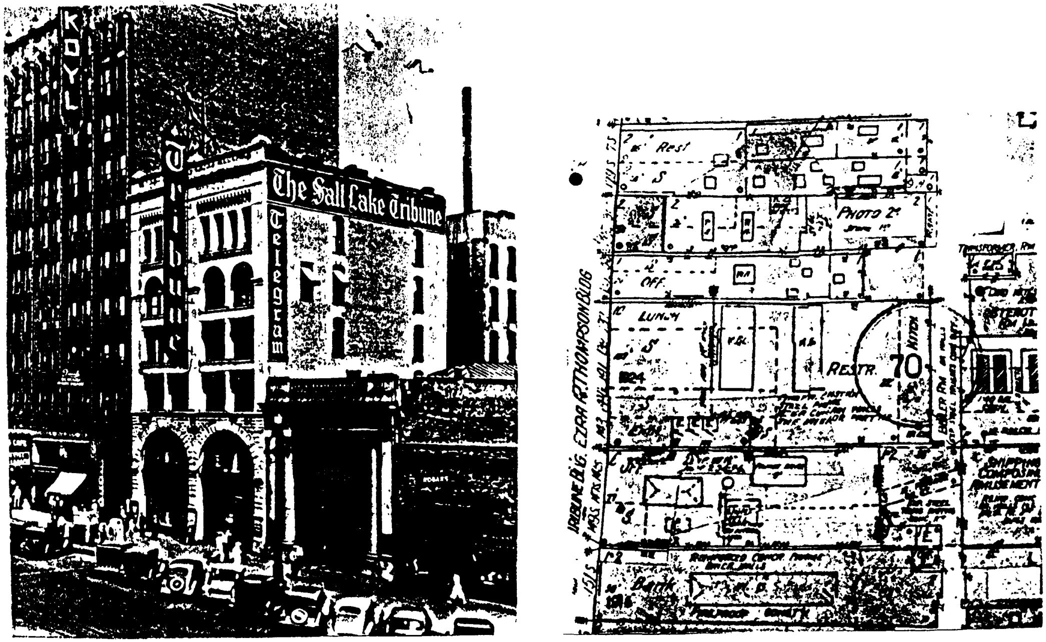

Figure 3-14. The Ezra Thompson and Tribune buildings battered against each other during the March 12, 1934 earthquake. (Photograph courtesy of the Utah State Historical Society; Sanborn map courtesy of Marriott Library, Special collections, University of Utah.)

Intensity Determinations for the February 22, 1943, Earthquake

Figure 3-5 shows the intensity distribution of the February 22, 1943, I_o VI earthquake. The event was recorded on the University of Utah seismograph (Boulder, Colorado, World Data Center for Geophysics Seismograph Records). According to Dr. Hyrum Schneider, a professor at the University of Utah at the time of the earthquake, the shock lasted for about 30 seconds (Salt Lake Tribune). The epicentral coordinates have been determined to be 40.7° N and 112.0° W by Stover et al. (1986) and 40.42° N and 112.40° N by Arabasz et al. (1979). At the time of the event, Dr. Hyrum Schneider estimated the origin to be on a fault at the north end of the Oquirrh Mountains, and characterized the event as most pronounced on the west side of the Salt Lake Valley, especially at the towns of Kearns and Magna. The event was also recorded on the Utah State University seismograph and Dr. J. Stewart Williams placed the location as uncertain, but approximately 150 miles from Logan (Deseret News; Salt Lake Tribune; United States Earthquakes 1943). A list of the site names and addresses, the types of buildings, descriptions of the earthquake effects, and MM intensity assignments are listed in Appendix II.

Few reports of earthquake effects from which intensity assignments can be made were found for this earthquake. United States Earthquakes (1943) noted that there were reports of cracked plaster in Salt Lake City; however, examination of the original cards from which the determinations were made failed to provide exact addresses (Boulder, Colorado, World Data Center for Geophysics, Earthquake Felt Reports). The only report of damage found by this study was the building engineer's report concerning the City and County Building. That report determined that the earthquake must have increased prior damage to the roof of the building and caused additional leakage (Deseret News, Salt Lake City, State of Utah Archives, Salt Lake County Engineer's Records).

Intensity Determinations for the March 6, 1949, Earthquake

Figure 3-6 shows the intensity distribution from the March 6, 1949, I_o VI earthquake. The event was recorded on the University of Utah seismograph, lasting approximately 2 minutes (Boulder, Colorado, World Data Center for Geophysics, Seismograph

Records). The epicentral coordinates have been determined to be 40.7° N and 111.8° W by Stover et al. (1986) and 40.44° N and 111.50° W by Arabasz et al. (1979). Professor C. Edward Jacob of the University of Utah at the time of the earthquake, termed the shock to be of "minor intensity" (*Salt Lake Tribune*). Most of the intensity reports located by this study were in the IV and V range; however, damage corresponding to higher intensities was observed in Salt Lake City. A 10-inch water main was broken at 233 Canyon Road and caused some local flooding and disruption of city water service for a few hours (*Deseret News*, Salt Lake City, State of Utah Archives, Salt Lake City Public Works records).

Other damage in the city included a destroyed chimney at 720 Kilby Court, a one-and-one-half-story brick dwelling in the southwest part of the city. Windows were broken at a cafe at 1726 West North Temple. *United States Earthquakes* (1949) reported damage to walls in some west-side homes, but exact addresses were not found in the original records (Boulder, Colorado, World Data Center for Geophysics, Earthquake Felt Reports). A list of site names, the types of buildings, the descriptions of earthquake effects, and the MM intensity assignments for Salt Lake City are listed in Appendix II.

Intensity Determinations for the September 5, 1962, Earthquake

Figure 3-7 shows the intensity distribution in Salt Lake City from the September 5, 1962, I_O VI Magna earthquake. The event was recorded on the University of Utah seismograph and a copy of the east-west and north-south components of that record is available (Boulder, Colorado, World Data Center for Geophysics, Seismograph Records). The earthquake occurred just days after the August 30, 1962, Cache Valley earthquake (I_O VII, 5.7) which caused over a million dollars damage in the northern Utah cities of Ogden and Logan. The damage from the September 5 earthquake was actually greater than the August 30th event in Salt Lake City (United States Earthquakes 1962). Sources examined by this study did not include reports of significant damage in Salt Lake City from the August 30 event, whereas the September 5 earthquake caused structural and nonstructural damage.

The epicentral coordinates of the September 5, 1962, earthquake are listed as 40.72° N and 112.09° W by Stover et al. (1986) and 40.42° N and 112.5° W by

Arabasz et al. (1979). The magnitude is listed as M_L=5.2 and M_b=5.1 by Stover et al. (1986) and as 5.2W. by Arabasz et al. (1979). This earthquake was investigated by Algermissen (Deseret News, Salt Lake Tribune). A list of the site names and addresses, the types of buildings, the descriptions of earthquake effects, and the MM intensity assignments for Salt Lake City are listed in Appendix II.

There was a great deal of concern over the September 5 earthquake, probably because of the extensive damage in northern Utah as a result of the Cache Valley earthquake that occurred a few days prior. Because of this increased concern, all schools in the Salt Lake City school district and surrounding suburban school districts were inspected after the September 5 event. Damage was found to consist mainly of plaster cracks, loose acoustical tile, and related architectural damage. Cyprus High School in the Granite School District just west of Salt Lake City required a parapet removal after the facade of the building was pulled away from the infrastructure by about 2 inches on the north and west sides of the building (Deseret News; Salt Lake Tribune). Appendix

II lists the damage to schools in the Salt Lake City school district.

There was widespread nonstructural damage in downtown buildings including plaster cracks, cracks in walls, fallen plaster, and broken windows. A few buildings sustained structural damage. At 430 East Seventh South, a wall and ceiling collapsed as blocks from an inner wall fell through the ceiling. An outside wall cracked from the foundation to the roof (Deseret News, Salt Lake Tribune). The house was a one-story brick-faced structure of hollow- or cinder-block construction (Salt Lake City, University of Utah, Special Collections, Sanborn Map). At 17 North Fifth West, the ceiling of a one-story brick dwelling fell in, and at 271 West Fifth North a portion of a plaster ceiling and an inner wall collapsed from a two-story brick and adobe apartment building (Salt Lake Tribune; Deseret News; Salt Lake City, University of Utah, Special Collections, Sanborn Map) (Figure 3-15). At 809 North Redwood Road a house was displaced from its foundation (Deseret News). At 1600 Wallace Road, in the southwest part of town, the LDS Bishops' Central Storehouse suffered damage to windows and plaster walls (Bishop Charles M. Knighton; Deseret

Figure 3-15. Damage sustained to houses during the September 5, 1962 earthquake. (Photographs courtesy of the Deseret News.)

News). The Twenty-Second Ward Chapel on the southeast corner of Second West and Fourth North Streets, a brick-faced concrete-block building, sustained enough damage that the local ward and the LDS Church Building Department recommended its removal and the building of a new ward house (Salt Lake City, LDS Archives, Church Building Records, Twenty-Second Ward, Manuscript History; Church Building Officials; personal communication) (Figure 3-16).

Analysis Intensity Data

Intensities were calculated for these earthquakes. The high and low values were derived from the equation

$$I_o - I = n \, \mathrm{Log}_{10}[(\Delta^2+h^2)1/2h]$$

for the six events where

n = empirical component to be determined,
Δ = epicentral distance (km),
h = depth of focus (km), and
I_o = the maximum intensity at the epicenter (Ergin, 1969).

Plates 7a and b, and 8a and b in Appendix III show the differences between the calculated and observed intensities assuming focal depths of 3 km

Figure 3-16. The Twenty-Second Ward chapel sustained damage during the September 5, 1962 earthquake. (Photograph courtesy of the Church of Jesus Christ of Latter-day Saints.)

and 10 km, respectively. Plates 9a and b in Appendix III show a similar plot for a focal depth of 7 km, the average depth determined by the University of Utah for Utah earthquakes (Arabasz et al. 1980). Plates 10a and b in Appendix III show the values for the estimated and observed intensity only for the points derived from the intensity data for the September 5, 1962 earthquake which was determined to have a depth of 7 km. Each pair of figures shows the values for structures greater than 8 stories and less than 8 stories.

Isoseismal contours are difficult to draw through these data points due to the wide variation in intensity at many proximate locations. Nevertheless, general statements concerning the distribution of intensities can be made from these data. The high and low values generally correlate with thickness of Quarternary deposits determined by Arnow (1981) and by Adhidjaja et al. (1981). Their maps indicate that the thickness of these deposits varies throughout the city ranging from 100 ft. in the north and northeast neighborhoods, to 250 ft. in the north-northwest and east neighborhoods, to 400 ft. in most of the downtown area and part of the east neighborhoods, to 650 ft. in the south and west neighborhoods. Depth of sediments derived from drill hole data from Anderson et al. (1986) and Case (1986) help define these areas and depth to bedrock work by Tinsley (in progress) in the Salt Lake City area may help define these areas more precisely. As Evernden and Thomson (1985) stated, predictions concerning intensity must include site geology and depth to water table for specific sites and specific periods (such as fluctuating water table depths due to seasonal changes or in the case of Salt Lake City, the recurrence intervals of the inundations by the Great Salt Lake). Generally, as the Quaternary sediments increase in depth, the intensity determinations from the six historic earthquakes investigated by this study increase by two to three intensity units from the east side of the city to the west and from the north to the south. This distribution is similar to the range in intensity across the city calculated by Algermissen and Steinbrugge (1984) using Rosenblueth's (1964) expression:

$$I = \frac{\log 14v}{\log 2}$$

where I is intensity, v is velocity of ground shaking in cm/sec, as applied to data from instrumental site response studies by Hays et al. (1978) and Hays and King (1982, 1984) for a hypothesized 7.5-M_S earthquake in Salt Lake City (Figure 3-17)

It is evident from the data presented here, as in studies by Borcherdt and Gibbs (1976), Hays and King (1982, 1984), Rogers et al. (1985), and King et al. (in press), that local site conditions have a significant influence on ground shaking. Hays and King (1982) state that the

> greatest potential hazard from earthquake ground shaking in the Wasatch Front area would occur at sites underlain by thick, fine-grained, water-saturated, nearshore and offshore deposits of silts and clays.

Hays and King (1984) observed that "site amplification of as much as a factor of 10 in the period band that coincides with the natural period of vibration of 2-7-story buildings can occur in Salt Lake City" (Figure 3-18).

In addition, findings of King et al. (in press) for the Wasatch Front region from site response recording sites on all types of surficial material (as defined by Miller 1980) including onshore, near-shore, and offshore deposits and on bedrock show

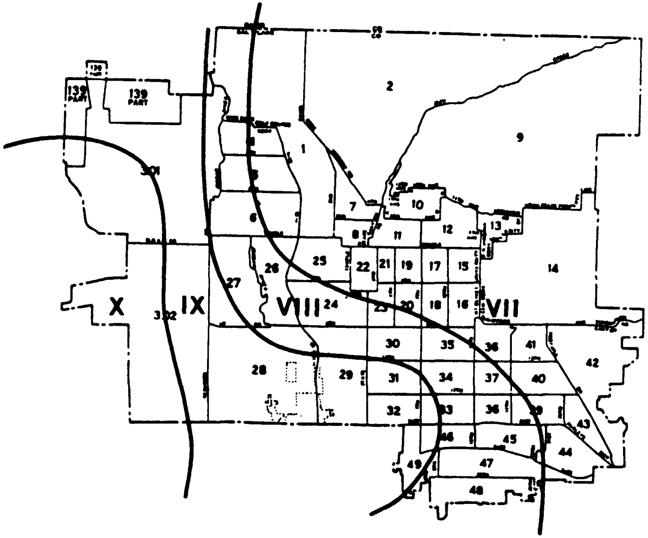

Figure 3-17. Hypothesized intensities for a 7.5 M_S earthquake in Salt Lake City. (From Algermissen and Steinbrugge 1984.)

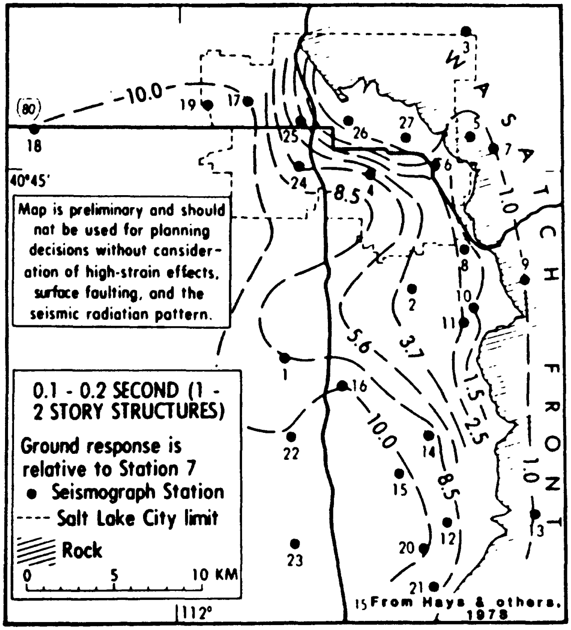

Figure 3-18. Map showing an estimated site response for a period band of 0.20-0.7 seconds (from Hays and King 1984).

variance in site response. Most of their work was based on records of nuclear test shots recorded on different site types. Their results on spectral ratios of rock versus alluvial sites agreed with the results of Rogers and Hays (1978) which were derived from earthquake-induced ground motion (see King et al., in press). Briefly, the findings (King et al., in press) showed that the "level of amplification factors ranges from approximately 1.5 to 3.0 for sites near the Wasatch Front underlain by thinner sections of alluvium" to factors of 7 to 12 in areas that are located near "the center of the valley and are underlain by more than 300 m of alluvium."

King et al. (in press) also concluded that recordings in the mid-valley locations (similar to the mid-valley Salt Lake City locations used by Hays and King [1982] that are now inundated by the Great Salt Lake) showed response numbers in the 0.2-0.7-second period-band to be higher than that on rock by a factor of 7 to 12. The Hays and King (1982, 1984) and King et al. (in press) studies show a systematic increase in site response as the distance westward from the Wasatch Front increases. This is in total agreement with the general pattern observed from the historical intensity data presented in this study.

There is also a correlation between the increase in intensity and the potential for liquefaction as mapped by Anderson et al. (1986) for the Salt Lake County region. Plate 11 in Appendix III shows the Anderson et al. (1986) low, moderate, and high potential liquefaction areas in relation to the highs and lows of the calculated intensity versus observed intensities derived in this study.

It is also relevant to consider the work of Evernden and Thomson (1985) which assumes the potential for increased intensity with decreasing ground water table depth levels. Recently, the inundation of the Great Salt Lake and the corresponding decrease in the water table depth in the Salt Lake City area may have increased the potential of earthquake-induced ground shaking. Evernden and Thomson calculated a relationship between ground shaking and depth of water table for the Los Angeles area and concluded that intensity could increase by one unit based on a rise in the water table depth from 30 to 0 ft and by one half an intensity unit for a rise of water table depth from 100 to 30 ft.

In addition to the potential effects of soil and geologic conditions on expected intensity, something must be said about the characteristics of the buildings themselves. The intensity maps for the six earthquakes investigated in this study sometimes show great variation in the intensity at several sites within a one-block area. This is probably due to the type of construction as well as site conditions. An excellent example of high intensity assignments due to construction is the City and County Building which, because of its site location and construction (Kaliser 1971), is especially vulnerable to ground shaking. In contrast, many of the LDS buildings and the newly constructed high-rise hotels and office buildings in Salt Lake City are engineered to withstand the shear forces of earthquake shaking (Reaveley; Jackson; Salt Lake City, LDS Church Building officials, personal commun. 1986). These structures generally exhibit less damage than older, unreinforced-masonry buildings. Type of construction is an important consideration today in the Salt Lake City urban area because of the high proportion of brick structures still in use (Algermissen and Steinbrugge 1984). Although retrofitting and modernization projects are underway in the city, many of the changes are architectural rather than structural. For instance, only some of the structures that sustained damage from the earthquakes investigated in this study have been demolished (such as the Newhouse Hotel) or retrofitted. Others simply have been given a modern facade over the original infrastructure (such as the old Deseret News Building, present-day location of Citibank). The importance of strictly enforced building codes in the Salt Lake City urban area is paramount to the reduction of losses from not only the hypothesized-7.5 M_L earthquake on the Wasatch front, but from much smaller earthquakes similar to those investigated in this study. It is also important to note that the occurrence of an hypothesized-7.5 earthquake on any of the Wasatch Fault segments identified by Machette et al. (1986), as well as a moderate-size earthquake on a Salt Lake Valley fault (such as the West Valley Fault), would cause damage in the Salt Lake City urban area (Keaton 1986). This point is illustrated by the investigations of the historic earthquakes in this study which included a far-field event (the M_L=6.6, March 12, 1934, Hansel Valley earthquake) and a near-field event (the M_L=5.2, September 5, 1962, Magna earthquake), both of which caused structural damage in Salt Lake City.

Another important consideration in relation to the historic earthquakes in Salt Lake City is the changing size of the urban area through time. Although some older structures have been torn down, there are still a large number of unreinforced-masonry buildings in the city (Algermissen and Steinbrugge 1984). It is also important to note the density of buildings. Figures 3-19, 3-20, and 3-21 illustrate the changing density of downtown Salt Lake City from 1909 until 1986.

Conclusions

The damage patterns in Salt Lake City due to six near- and far-field historic earthquakes investigated in this study have been used to determine the distribution of MM intensity throughout that urban area. Generally, the results indicate that the intensity increases across the city from the Wasatch fault zone (rock sites) to Jordan River valley locations (alluvial sites) by 2-3 intensity units and from the Avenues area east of the Utah State Capitol building south to approximately Seventeen South by 1-1½

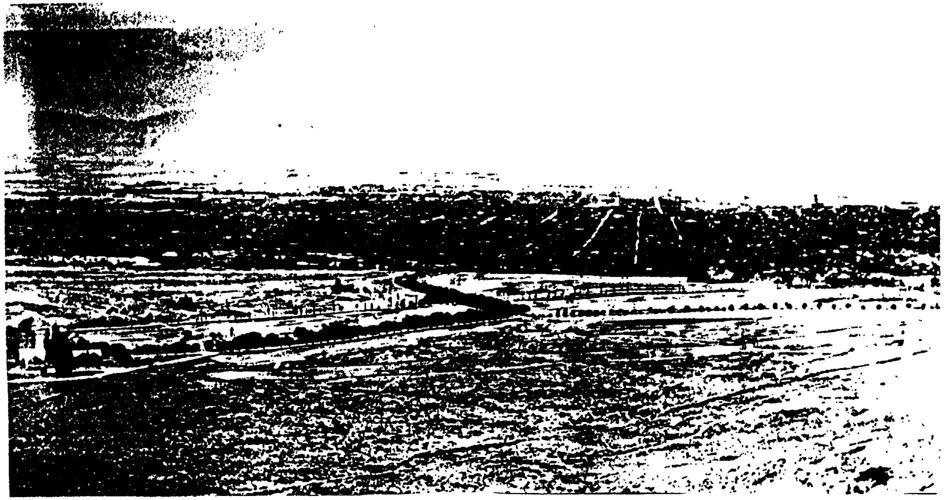

Figure 3-19. Looking west toward downtown Salt Lake City, circa 1909. (Photograph courtesy of the Church of Jesus Christ of Latter-day Saints.)

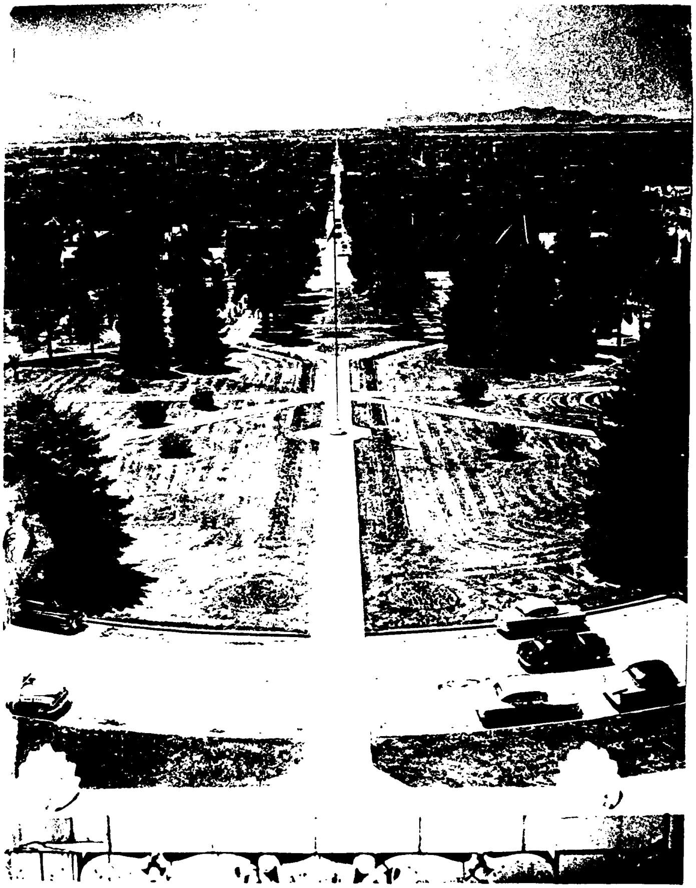

Figure 3-20. Looking west toward downtown Salt Lake City,circa 1950's. (Photograph courtesy of the Marriott Library, Manuscripts, University of Utah.)

Figure 3-21. Looking west toward downtown Salt Lake City in 1986.
(Photo by S. Oaks.)

intensity units. These increases may be estimated to be greater by 1-1½ intensity units if a higher water table (such as the one that exists in Salt Lake City today) is assumed. The distribution of increase in intensities derived from the historic earthquake reports is found to correlate with values from instrumental site-response studies presented by King et al. (in press) which show an increase in ground shaking from east to west and from north to south across the city.

REFERENCES

Adhidjaja, J. I., Cook, K. L., and Serpa, L. F. 1981. Salt Lake valley gravity map and data. Open File Report 39. Salt Lake City, Utah: Utah Geological and Mineral Survey.

Algermissen, S. T., and Steinbrugge, K. V. 1984. Seismic hazard and risk assessment--Some case studies. The Geneva Papers on Risk and Insurance 9:8-26.

Anderson, L. R., Keaton, J. R., Spitzley, J. E., and Allen, A. C. 1986. Liquefaction potential map for Salt Lake County, Utah. Logan and Salt Lake City, Utah: Utah State University Department of Civil and Environmental Engineering, and Dames and Moore.

Arabasz, W. J. 1979. Historical review of earthquake related studies and seismograph recording in Utah. In Earthquake studies in Utah 1850-1978, eds. W. J. Arabasz, R. B. Smith, and W. D. Richins. Salt Lake City, Utah: University of Utah Seismograph Stations, University of Utah.

________ 1984-1987. Personal communication. Utah Seismograph Stations, Department of Geology, Geophysics, University of Utah, Salt Lake City.

Arabasz, W. J., Smith, R. B., and Richins, W. D. (eds.). 1979. Earthquake studies in Utah 1850-1978. Salt Lake City, Utah: University of Utah Seismograph Stations, Department of Geology and Geophysics, University of Utah.

__________. 1980. Earthquake studies along the Wasatch fault, Utah--Network monitoring seismicity and seismic hazards. Seismological Society of America 20: 1479-1499.

Arnow, T. D. 1981. Contours of the base of the Quaternary deposits in the Jordan Valley, Utah. Groundwater Quality Management-background report. Salt Lake City, Utah: Salt Lake County Division of Water Quality and Water Pollution Control.

Asheville, North Carolina, National Climatic Data Center. Salt Lake City, Utah station records 1909, 1910, 1934, 1943, 1949, 1962.

Borcherdt, R. D., and Gibbs, J. F 1976. Effects of local geological conditions in the San Francisco Bay region on ground motions and the intensities of the 1906 earthquake. Bulletin of the Seismological Society of America 66:467-508.

Keaton, J. R. 1986. Potential earthquake-induced damage along the Wasatch Front. Workshop on Earthquake hazards along the Wasatch Front, Utah. Salt Lake City, Utah.

King, K. W., Williams, R. A., and Carver, D. A. In press. A relative ground response study in east Salt Lake City and areas of Springville-Spanish Fork, Utah.

Machette, M., Lund, B., and Arabasz, W. 1986. Tectonic framework and earthquate potential of the Wasatch Front Area. Presented at Workshop on Earthquake Hazards Along the Wasatch Front, Utah, Salt Lake City, Utah.

Miller, R. D. 1980. Surficial geologic map along part of the Wasatch Front, Salt Lake Valley, Utah. Map MF-1198, scale 1:100,000. Washington, D.C.: U.S. Geological Survey.

Reaveley, L. R. 1987. Personal communication. Structural engineer, Reaveley Engineering and Associations and Department of Engineering, University of Utah, Salt Lake City, Utah,

Richter, C. F. 1935. An instrumental earthquake magnitude scale. Bulletin of the Seismological Society of America 25:1-32.

Rogers, A. M., Tinsley, J. C., and Borcherdt, R. D. 1985. Predicting Relative Ground Response. In Evaluating Earthquake Hazards in the Los Angeles Region--an earth science perspective, ed. J. K. Ziony. U.S. Geological Survey Professional Paper 1560, pp. 221-248. Washington, D.C.: U.S. Government Printing Office.

Rogers, A. M., and Hays, W. W. 1978. Preliminary evaluation of site transfer functions developed from nuclear explosions and earthquales. In Proceedings of the Second International Conference on Microzonation, pp. 753-764. San Francisco, California: International Conference on Microzonations.

Rosenblueth, E. 1964. Probablistic design to resist earthquakes. American Society of Civil Engineers, Proceedings 90:189-219.

Salt Lake City, Utah, LDS Archives. Snowville Ward, Manuscript History; Thirty-third Ward, manuscript history; Twenty-second Ward, manuscript history, quarterly reports; Salt Lake City wards and stakes, Manuscript History, quarterly reports 1909, 1910, 1934, 1943, 1949, 1962; Church Building Department Records, architectural drawings and

Boulder, Colorado, World Data Center for Geophysics Seismograph Records 1943, 1949, 1962; Earthquake felt reports 1934, 1943, 1949, 1962; Manuscript of field study of 1934 Hansel Valley earthquake by Shenon.

Case, W. F. 1985. Significant drill holes of the Wasatch Front valleys including Cache Valley and Tooele Valley. Open-File Report 82. Salt Lake City, Utah: Utah Geological and Mineral Survey.

Ergin, K. 1969. Observed intensity-epicentral distance relations in earthquakes. Bulletin of the Seismological Society of America 59: 1227-1238.

Evernden, J. F. and Thomson, J. M. 1985. Predicting seismic intensities. In Evaluating earthquake hazards in the Los Angeles region--An earth science perspective, ed. J. K. Ziony. U. S. Geological Survey Professional paper 1560, pp. 151-202. Washington, D.C.: U.S. Government Printing Office.

Hays, W. W., Algermissen, S. T., Miller, R. D., and King, K. W. 1978. Preliminary ground response map for the Salt Lake City area. In Proceedings of the Second International Conference on Microzonation, pp. 497-508. San Francisco, California: International Conference on Microzonation.

Hays, W. W., and King, K. W. 1982. Zoning of the earthquake ground-shaking hazard along the Wasatch front zone, Utah. In Proceedings of the Third International Conference on Microzonation, pp. 1307-1318. Seattle, Washington: International Conference on Microzonation.

Hays, W. W., and King, K. W. 1984. The ground-shaking hazard along the Wasatch Fault zone, Utah. In Workshop on "Evaluation of regional and urban earthquake hazards and risk in Utah, ed. W. W. Hays and P. L. Gori. U.S. Geological Survey Open-File Report 84-763, pp. 133-147. Reston, Virginia: U.S. Geological Survey.

Jackson, R. H. 1985-1987. Personal communication, Church Building Department, Church of Jesus Christ of Latter-day Saints, Salt Lake City, Utah.

Kaliser, B. N. 1971. Engineering geology of the City and County Building, Salt Lake City, Utah. Special Studies 38. Salt Lake City, Utah: Utah Geological and Mineral Survey.

records, ward meeting house design drawings, miscellaneous building records, report to the committee on expenditures, September 1962; Relief Society, Minutes of General Board; Church Historian's Office, daily log; diaries of Salt Lake City ward bishops, 1934; Welfare Services, Disaster file; Moyle Oral History Collection, Young, Harvey, Lewes, Patterson, Pohlman, Proctor, Romney, Ryser, Simpson, and Spafford inter-
Salt Lake City (continued) views; Statements of the First Presidency, greetings December 18,1909, remarks about the Teton Dam disaster; Manuscript History of the church, December 27, 1832, February 27, 833, March 17, 1842; Teton Flood interviews of Brown, Barth, Hillam, Smith, Simpson, and Tanner; Minutes of meetings of the First Presidency, October-December 1909; Visiting teachers monthly report booklet 1930-1941; Salt Lake City Stake and Ward Relief Society Minutes, March-June, 1934; Melchizedek Priesthood minutes, March-June, 1934; High Priest Quorum Minute Book, March-June, 1934; Elders Minutes, March-June, 1934; General Minutes of the Weekly Ward Priesthood Meeting, March-June, 1934.

Salt Lake City, Utah, State of Utah Archives, Salt Lake City Engineer's Records, Salt Lake City Public Works Records.

Salt Lake City, Utah. University of Utah, Marriott Library Special Collections, Sanborn maps.

________. University of Utah, University Archives, Frederick J. Pack files.

Stover, C. W., Reagor, B. G., and Algermissen, S. T. 1986. Seismicity map of Utah. Map MF-1856, scale 1:1,000,000. Washington, D.C.: U.S. Geological Survey.

United States Earthquakes, 1934. Washington, D.C.: U.S. Government Printing Office.

United States Earthquakes, 1943. Washington, D.C.: U.S. Government Printing Office.

United States Earthquakes, 1949. Washington, D.C.: U.S. Government Printing Office.

United States Earthquakes, 1962. Washington, D.C.: U.S. Government Printing Office.

Wood, H. O., and Neumann, F. 1931. Modified Mercalli intensity scale of 1931. Bulletin of the Seismological Society of America 21(1):39-43.

APPENDICES

APPENDIX I

MODIFIED MERCALLI INTENSITY SCALE OF 1931

MODIFIED MERCALLI INTENSITY SCALE OF 1931

(From Wood and Neumann, 1931)

I

Not felt--or, except rarely under especially favorable circumstances.
Under certain conditions, at and outside the boundary of the area in which a great shock is felt:
I sometimes birds, animals, reported uneasy or disturbed;
R.F.[1] sometimes dizziness or nausea experienced;
sometimes trees, structures, liquids, bodies of water, may sway--doors may swing, very slowly.

II

Felt indoors by few, especially on upper floors, or by sensitive, or nervous persons.
Also, as in grade I, but often more noticeably:
I sometimes hanging objects may swing, especially when
to delicately suspended;
II sometimes trees, structures, liquids, bodies of water, may
R.F. sway, doors may swing, very slowly;
sometimes birds, animals, reported uneasy or disturbed;
sometimes dizziness or nausea experienced.

III

Felt indoors by several, motion usually rapid vibration.
Sometimes not recognized to be an earthquake at first.
Duration estimated in some cases.
III Vibration like that due to passing of light, or lightly
R.F. loaded trucks, or heavy trucks some distance away.
Hanging objects may swing slightly.
Movements may be appreciable on upper levels of tall structures.
Rocked standing motor cars slightly.

---

[1] Indicates corresponding degree of intensity in the Rossi-Forel scale, an intensity scale widely used in the United States before the publication of the Modified Mercalli Scale in 1931.

IV

Felt indoors by many, outdoors by few.
Awakened few, especially light sleepers.
Frightened no one, unless apprehensive from previous experience.
Vibration like that due to passing of heavy, or heavily loaded trucks.
IV Sensation like heavy body striking building, or falling of
to heavy objects inside.
V Rattling of dishes, windows, doors; glassware and
R.F. crockery clink and clash.
Creaking of walls, frame, especially in the upper range of this grade.
Hanging objects swung, in numerous instances.
Disturbed liquids in open vessels slightly.
Rocked standing motor cars noticeably.

V

Felt indoors by practically all, outdoors by many or most; outdoors direction estimated.
Awakened many, or most.
Frightened few--slight excitement, a few ran outdoors.
Buildings trembled throughout.
Broke dishes, glassware, to some extent.
V Cracked windows--in some cases, but not generally.
to Overturned vases, small or unstable objects, in many
VI instances with occasional fall.
R.F. Hanging objects, doors, swing generally or considerably.
Knocked pictures against walls, or swung them out of place.
Opened, or closed, doors, shutters, abruptly.
Pendulum clocks stopped, started, or ran fast, or slow.
Moved small objects, furnishings, the latter to slight extent.
Spilled liquids in small amounts from well-filled open containers.
Trees, bushes, shaken slightly.

VI

Felt by all, indoors and outdoors.
Frightened many, excitement general, some alarm, many ran outdoors.
Awakened all.
VI Persons made to move unsteadily.
to Trees, bushes, shaken slightly to moderately.
VII Liquid set in strong motion.
R.F. Small bells rang--church, chapel, school, etc.
Damage slight in poorly built buildings.
Fall of plaster in small amount.
Cracked plaster somewhat, especially fine cracks chimneys in some instances.
Broke dishes, glassware, in considerable quantity, also some windows.
Fall of knick-knacks, books, pictures.
Overturned furniture in many instances.
Moved furnishings of moderately heavy kind.

VII

Frightened all--general alarm, all ran outdoors.
Some, or many, found it difficult to stand.
Noticed by persons driving motor cars.
Trees and bushes shaken moderately to strongly.
Waves on ponds, lakes, and running water.
Water turbid from mud stirred up.
Incaving to some extent of sand or gravel stream banks.
Rang large church bells, etc.
Suspended objects made to quiver.
VIII-- Damage negligible in buildings of good design and
R.F. construction, slight to moderate in well-built ordinary
buildings, considerable in poorly built or badly designed
buildings, adobe houses, old walls (especially where laid up
without mortar), spires, etc.
Cracked chimneys to considerable extent, walls to some extent.
Fall of plaster in considerable to large amount, also some stucco.
Broke numerous windows, furniture to some extent.
Shook down loosened brickwork and tiles.
Broke weak chimneys at the roof-line (sometimes damaging roofs).
Fall of cornices from towers and high buildings.
Dislodged bricks and stones.
Overturned heavy furniture, with damage from breaking.
Damage considerable to concrete irrigation ditches.

VIII

Fright general--alarm approaches panic.
Disturbed persons driving motor cars.
Trees shaken strongly--branches, trunks, broken off, especially palm trees.
Ejected sand and mud in small amounts.
Changes: temporary, permanent; in flow of springs and wells; dry wells renewed flow; in temperature of spring and well waters.
VIII+ Damage slight in structures (brick) built especially to
to withstand earthquakes.
IX- Considerable in ordinary substantial buildings, partial
R.F. collapse: racked, tumbled down, wooden houses in some
cases; threw out panel walls in frame structures, broke off
decayed piling.
Fall of walls.
Cracked, broke, solid stone walls seriously.
Wet ground to some extent, also ground on steep slopes.
Twisting, fall, of chimneys, columns, monuments, also factory stacks, towers.
Moved conspicuously, overturned, very heavy furniture.

IX

Panic general.
Cracked ground conspicuously.
Damage considerable in (masonry) structures built
especially to withstand earthquakes:
IX+ threw out of plumb some wood-frame houses built
R.F. especially to withstand earthquakes;
great in substantial (masonry) buildings, some collapse in large part; or wholly shifted frame buildings off foundations, racked frames;
serious to reservoirs; underground pipes sometimes broken.

X

Cracked ground, especially when loose and wet, up to widths of several inches; fissures up to a yard in width ran parallel to canal and stream banks.
Landslides considerable from river banks and steep coasts.
Shifted sand and mud horizontally on beaches and flat land.
X Changed level of water in wells.
R.F. Threw water on banks of canals, lakes, rivers, etc.
Damage serious to dams, dikes, embankments.
Severe to well-built wooden structures and bridges, some destroyed.
Developed dangerous cracks in excellent brick walls.
Destroyed most masonry and frame structures, also their foundations.
Bent railroad rails slightly.
Tore apart, or crushed endwise, pipe lines buried in earth.
Open cracks and broad wavy folds in cement pavements and asphalt road surfaces.

XI

Disturbances in ground many and widespread, varying with ground material.
Broad fissures, earth slumps, and land slips in soft, wet ground.
Ejected water in large amount charged with sand and mud.
Caused sea-waves ("tidal" waves) of significant magnitude.
Damage severe to wood-frame structures, especially near shock centers.
Great to dams, dikes, embankments, often for long distances.
Few, if any (masonry), structures remained standing.
Destroyed large well-built bridges by the wrecking of supporting piers, or pillars.
Affected yielding wooden bridges less.
Bent railroad rails greatly, and thrust them endwise.
Put pipe lines buried in earth completely out of service.

XII

Damage total--practically all works of construction damaged greatly or destroyed.

- Disturbances in ground great and varied, numerous shearing cracks.
- Landslides, falls of rock of significant character, slumping of river banks, etc., numerous and extensive.
- Wrenched loose, tore off, large rock masses.
- Fault slips in firm rock, with notable horizontal and vertical offset displacements.
- Water channels, surface and underground, disturbed and modified greatly.
- Dammed lakes, produced waterfalls, deflected rivers, etc.
- Waves seen on ground surfaces (actually seen, probably, in some cases).
- Distorted lines of sight and level.

APPENDIX II

SITES, TYPES OF BUILDINGS, EARTHQUAKE EFFECTS AND MM INTENSITIES FOR EARTHQUAKES INVESTIGATED IN THIS STUDY

October 5, 1909, earthquake

Site name and address	Description of building[1]	Report of earthquake effects[2]	MM assignment
National Guard Armory 120-140 Pierpont Ave.	2-story brick; wooden post- and beam-construction.	Seams at the junction of walls and ceilings cracked open throughout the building; plaster shaken from ceiling (DN)[3].	VI
Hotel Kenyon SE corner of Main St. and Second South	4-story brick	People rushed from their rooms into the street (DN)[3].	V
Utah Light & Railway Co. 133 South West Temple	2- and 3-story brick	No disturbance in the power supply (SLT)[3].	F
Utah Light & Railway Co. East Side Car House	1- and 2-story brick	Similar sensations to those experienced during 1906 San Francisco earthquake (SLT)[3].	F
Tribune Building 145 South Main St.	6-story brick	Swaying of the building and felt it was going to fall; office of L.D. Martin hanging electric lights swung violently and furniture was moved (SLT)[3].	V

October 5, 1909, earthquake--Continued

Site name and address	Description of building[1]	Report of earthquake effects[2]	MM assignment
Thomas Bowen residence 667 East Third South	1½ and 2-story frame house.	Glass in front windows cracked (SLT)[3].	V
Independent Telephone Company Exchange Building 115 South State	3-story fireproof construction; cast iron columns.	Felt the building shake and "were with difficulty restrained from rushing from the structure" (SLT)[3].	IV
Apartment above the Wagener Brewing Company 142 East First South	2-story brick	Glass vases on table rocking (SLT)[3] (Ms. Frank Latler's apartment).	IV
Colonial Flats 458 East Third South	3-story brick	Bed shook and chairs rattled (SLT)[3]	IV
Ivor Redman residence 548 East Seventh South	1-story brick	Thought house was falling down, articles of furniture were moved and bric-a-brac fell from shelves (SLT)[3].	V
527 East Fifth South	2-story brick	Felt disturbances; 3 shocks; things were badly shaken up and articles of furniture moved (SLT)[3].	V

October 5, 1909, earthquake--Continued

Site name and address	Description of building[1]	Report of earthquake effects[2]	MM assignment
E.W. Taylor residence 962 East Second South	2-story brick	Two distinct shocks (SLT)[3]	F
Judge O.W. Powers residence Linger-Longer West St. (Virginia) and Douglas Ave. in Newhouse Park	---	Two shocks (SLT)[3]	F
654 East Sixth South	1½-story brick- and frame-composition	"Very perceptible movements" (SLT)[3]	IV
252 East Fifth South	1-story brick	"Very perceptible movements" (SLT)[3]	IV
Wm. R. Duvall residence 324 South Sixth East	2-story brick	Distinct shock (SLT)[3]	F
443 East First South	2½-story frame	Distinct shock (SLT)[3]	F

October 5, 1909, earthquake--Continued

Site name and address	Description of building[1]	Report of earthquake effects[2]	MM assignment
Boston Bldg. Main St. NE corner Exchange Place	11-story brick with stone facade, steel-frame construction.	Decided swinging motions; clock stopped (11th floor) (WBR)[3].	V
University of Utah	2-story brick	Recorded on seismograph station (WBR)[3]	F

[1] Descriptions of buildings were found in manuscript and photographic collections at the Church of Jesus Christ of Latter-Day Saints, the Utah State Historical Society, the Salt Lake City Public Library, and the University of Utah.

[2] Reports of earthquake effects were gathered from newspaper reports, manuscript records of the United States Weather Bureau, manuscript records of the Church of Jesus Christ of Latter-Day Saints, and manuscript records from the World Data Center for Geophysics and the U.S. Geological Survey which were used for U.S. Earthquakes.

[3] DN - Desert News; SLT - Salt Lake Tribune; T - Salt Lake Telegram; WBR - records of U.S. Weather Bureau; LDS - records of the Church of Jesus Christ of Latter-Day Saints; WDCG - World Data Center Geophysics; USGS - U.S. Geological Survey, Branch of Global Seismology, UU - University of Utah Archives, Manuscripts, and Special Collections.

May 22, 1910 earthquake

Site name and address	Description of building[1]	Report of earthquake effects[2]	MM assignment
Rocky Mountain Bell Bldg. 56 South State	5-story, reinforced-concrete and brick fireproof construction.	Chairs moved, switchboard may have moved (SLT)[3].	V
Independent Telephone Company office 115 South State	3-story, fireproof construction, cast iron columns.	General panic of people (DN)[3]	V
S.A. Bitner residence 59 Center Street	1-story, frame, stone, and brick.	House rocked back and forth and large amounts of plaster and adobe fell in sitting room (DN,SLT)[3].	VII
Touraine Hotel 42 East Third South	3-story brick	Light oscillated in Dewitt B. Louie's room (DN,SLT)[3].	III
State Prison Fourteenth East at Twelfth South	---	Distinctly felt (DN)[3]	F
University of Utah	1-story brick	Recorded at seismograph station (WBR)[3]	F

May 22, 1910 earthquake--Continued

Site name and address	Description of building[1]	Report of earthquake effects[2]	MM assignment
Ft. Douglas	1- and 2-story, frame and brick.	Distinctly felt (DN)[3]	F
Judge Mercy Hospital Tenth East between Sixth and Seventh South	3½-story brick with 4-story brick towers.	Buildings "rocked perceptibly for some time" no damage (DN)[3].	IV
Webster School 421 South Eighth East	3-story brick, outside wall on 1st-story stone.	Shaken, swayed to and fro (DN)[3]	IV
Deseret News Bindery Deseret News Annex 15-19 West South Temple	8-story steel-frame, fireproof construction.	Bookcases jarred down (6th floor); scrubwoman's bucket tipped over (4th floor) (DN)[3].	V
Boston Building Main St. NE corner Exchange Place	11-story brick with stone facade, steel-frame construction.	Swayed back and forth; clock stopped on top (11th floor); employees rushed out into street (1st floor), rumbling of building was "quite appreciable." (DN,SLT,WBR)[3].	V

May 22, 1910 earthquake--Continued

Site name and address	Description of building[1]	Report of earthquake effects[2]	MM assignment
Hotel Kenyon	4-story brick	guests not sure what happened, some awakened (SLT)[3].	IV
LDS Salt Lake Temple Main and South Temple	11-story stone construction, 3 subfoundations	trumpet of Angel Moroni jarred approximately a foot by the quake (SLT)[3]	V
Buena Vista Race Track SPLA&SL tracks west of McKinley (Redwood Rd.)	---	People panicked, ran for open; horses broke out of stables (DN)[3].	V
Julian Riley residence 614 South Fourth East	2-story brick	Doors rattled loudly, chandeliers vibrated in "an astonishing manner" (DN)[3].	IV
Hotel Knutsford State NE corner of Third South	6-story brick (some sections 7-story) stone facade; iron support posts.	Bottle of water knocked from dresser and broke on floor (S.B. Ricaby's room), recognized as earthquake shock by manager, H. M. Hawkins, waiters fled the building (DN,SLT)[3].	V

May 22, 1910 earthquake--Continued

Site name and address	Description of building[1]	Report of earthquake effects[2]	MM assignment
Cullen Hotel 33 West Second South	5-story brick	Water in tub dashed to and fro and splashed over top, building rocked, per manager, W. D. Ahern (DN,SLT)[3].	V
American Sunday School Chapel Fifth North and Oakley	---	Badly shaken, plaster jarred from interior onto floor; books in library thrown to floor (DN,SLT)[3].	VI
Near Tribune Bldg. at Second South near State	---	Buildings swayed to and fro, and oscillated (DN,SLT), windows creaked (SLT)[2].	IV
Tribune Building 145 South Main Street	6-story brick	Top swayed, morter broke loose from brick, clouds of dust from building, people fled building (SLT)[3].	VI
Oregon Short Line Depot (Union Depot) South Temple at Third West	2-story brick; rotunda 6-story brick; reinforced concrete frame.	Plaster on walls of ticket office badly cracked and a portion fell; no damage to rotunda (DN,SLT)[3].	VI

May 22, 1910 earthquake--Continued

Site name and address	Description of building[1]	Report of earthquake effects[2]	MM assignment
J.S. Morgan residence 339 West Third North	1-story brick	"Distinct shocks;" thought house across the street would collapse (DN)[3].	IV
Commercial Club (new) 34 East Exchange Place	6-story, stone and brick	Shock severe, feet by Captain Tibbetts and others (DN,SLT)[3].	F
Jerrold R. Letcher residence 575 South Tenth East	1½story, frame	House rocked violently (DN)[3]	V
A.B. Hirth residence 7 South Twelfth East	1½story, frame	House shaken violently; weights rattled in the casings (DN)[3].	V
Cummings Apartments 39 D Street	3-story, concrete block	Difficult to stand; glasses were thrown from table (Ms. L.K. Demus's apt.) (DN)[3].	V
City and County Bldg. State St. between Fourth and Fifth South	5-story unreinforced stone.	Big tower "swayed back and forth"; water slopped out of bucket (4th floor) not noticed (basement).	V
Police Station 120 East First South	2-story stone and 2-story brick	Brick chimney fell; people ran out of building (DN)[3]	VII

May 22, 1910 earthquake--Continued

Site name and address	Description of building[1]	Report of earthquake effects[2]	MM assignment
St. Mark's Hospital Second West between Seventh and Eighth North	3-story and 4-story brick	Patients alarmed and hysterical (DN)[3]	IV
Charles O. Farnsworth residence 47 East First South	3-story brick	Coffee thrown out of cup (DN)[3]	V
Lorenzo O. Camomile residence 1090 South Ninth East	1½-story brick	Sleeping children awakened (DN)[3]	IV
Cannon Farm in Jordan Bottoms SW of town	---	Bricks shaken loose from chimneys (DN)[3] Open flowing well "sprouted" 30 feet high during earthquake and for five minutes after (SLT)[3]	VII
Anthon H. Lund 127 North West Temple	2-story brick	Furniture moved (personal diary-UU)	V

May 22, 1910 earthquake--Continued

Site name and address	Description of building[1]	Report of earthquake effects[2]	MM assignment

---

[1] Descriptions of buildings were found in manuscript and photographic collections at the Church of Jesus Christ of Latter-Day Saints, the Utah State Historical Society, the Salt Lake City Public Library, and the University of Utah.

[2] Reports of earthquake effects were gathered from newspaper reports, manuscript records of the United States Weather Bureau, manuscript records of the Church of Jesus Christ of Latter-Day Saints, and manuscript records from the World Data Center for Geophysics and the U.S. Geological Survey which were used for U.S. Earthquakes.

[3] DN - Desert News; SLT - Salt Lake Tribune; T - Salt Lake Telegram; WBR - records of U.S. Weather Bureau; LDS - records of the Church of Jesus Christ of Latter-Day Saints; WDCG - World Data Center Geophysics; USGS - U.S. Geological Survey, Branch of Global Seismology; UU - University of Utah Archives, Manuscripts, and Special Collections

March 12, 1934 earthquake

Site name and address	Description of building[1]	Report of earthquake effects[2]	MM assignment
City and County Bldg. State St. between Fourth and Fifth South	5-story unreinforced stone.	Statue on top of building shaken a foot out of line; capstone on south chimney collapsed; chunks of mortar fell to pavement; cracks in ceiling (5th floor); plaster fell in several rooms; numerous cracks in interior and across entire archway on 3rd floor; woman fainted (3rd floor); many people ran out of building before evacuation ordered; caused elevator to stop (DN, SLT, T).	VII
LDS Salt Lake Temple Main and South Temple	11-story stone construction, 3 subfoundations.	Movement of Angel Moroni statue twisted to right (DN, SLT).	V
Ensign School 431 9th Avenue	3-story steel and concrete fireproof construction, reinforced concrete and stone.	Ceiling cracked in two rooms (DN)	V

March 12, 1934 earthquake--Continued

Site name and address	Description of building[1]	Report of earthquake effects[2]	MM assignment
South High School 1575 South State	3-story fireproof construction and reinforced concrete, brick walls, steel frame in auditorium.	Portable panels moved in auditorium; students badly frightened; lights shaken loose, slight cracking of wall near ramp on 3rd floor (DN, T).	V
West High School 241 North Second West	3-4-story fireproof reinforced concrete construction, brick curtain walls.	Blackboard moved away from wall and swung (DN).	IV
Washington School 163 West Fourth North	2-story brick	Small objects (bird cage) knocked over (DN).	V
Utah State Capitol Bldg. North end of State Street	4-story fireproof construction, reinforced concrete, granite faced.	CWA workers were "swung around on scaffold" (DN).	V
Hotel Utah Main at NE corner of South Temple	10-story fireproof steel frame construction, reinforced brick.	Floor rose and fell (DN)	IV

March 12, 1934 earthquake--Continued

Site name and address	Description of building[1]	Report of earthquake effects[2]	MM assignment
Dooly Bldg. 109-113 West Second South	6-story unreinforced brick.	Crack from top to bottom on north side; considerable plaster fell (DN).	VII
Chemistry Bldg. University of Utah campus	1-story frame	Clocks stopped (interview with Richard Jackson).	V
Geology Bldg. University of Utah campus	3-story brick	Two distinct shocks	F
Tribune Bldg. 145 South Main	6-story brick	Pounded against Ezra Thompson Bldg. (DN, T).	VI
Ezra Thompson Bldg. 143 South Main	10-story brick, steel frame construction.	Pounded against Tribune Bldg.; water shaken out of tank on top of building and showered roof (DN, T).	VI
Belvedere Apartments 29 South State	9-story fireproof, reinforced concrete and brick	Clocks stopped, plaster cracks, fallen plaster.	VI
Ms. G.T. Dooley residence 823 East Second South	1½-story brick	Bricks fell from chimney and fell through window (DN).	VII

March 12, 1934 earthquake--Continued

Site name and address	Description of building[1]	Report of earthquake effects[2]	MM assignment
Henrietta McMonegal 817 East Second South	2-story brick	Chimney dislodged and crashed through window (DN, T).	VII
Clift Building 10 West Third South	8-story fireproof construction, reinforced concrete frame, brick curtain walls.	No damage (DN, SLT, T).	F
Newhouse Hotel 11 West Fourth South	12-story steel frame	Plaster tumbled into the lobby and president's suite (DN, SLT, T).	VII
Salt Lake County Jail 437½ South Second East	2-story brick	General panic of prisoners (DN, T).	V
Salt Lake County heating plant adjacent to jail	1-story brick	Boiler room swayed (DN, T)	V
Lincoln House 68 East First South	3-story brick	Clock thrown from shelf and restarted (T).	V
Spencer-Stewart Apartments 740 East Third South	3-story brick with frame interior support walls.	Chandeliers fell, dishes were broken as they crashed from shelves (T).	V

March 12, 1934 earthquake--Continued

Site name and address	Description of building[1]	Report of earthquake effects[2]	MM assignment
ZCMI Drug Store 13-31 South Main	3-story brick with iron facade.	Clock stopped (T)	V
LDS Church Office Bldg. 47 East South Temple	5-story stone-faced reinforced by stone columns and steel frame.	Felt in elevator (DN)	IV
Dunfield Store 111 South Eighth West	2-story brick	All windows broken (ON)	VII
Schramm-Johnson Drug Store 203 South Main	4-story brick	Bottles fell in a heap (T)	V
Robinson Apartments 268 C Street	2-story brick	Pictures fell from walls, piano and and beds moved.	V
143 South Seventh West	---	Injury to man driving automobile	VIII
West Side Drainage Project	---	Stoves were overturned and started fires.	VII
Administration Bldg. Salt Lake City Airport 2150 West North Temple	2- and 3-story fireproof construction reinforced concrete, stone front.	Felt, (WBR)	F

March 12, 1934 earthquake--Continued

Site name and address	Description of building[1]	Report of earthquake effects[2]	MM assignment
LDS Thirty-third Ward Meeting House Eleventh East between Fourth and Fifth South	1-story brick with wood truss.	Plaster fell, wall damaged (LDS)	VII

---

[1] Descriptions of buildings were found in manuscript and photographic collections at the Church of Jesus Christ of Latter-Day Saints, the Utah State Historical Society, the Salt Lake City Public Library, and the University of Utah.

[2] Reports of earthquake effects were gathered from newspaper reports, manuscript records of the United States Weather Bureau, manuscript records of the Church of Jesus Christ of Latter-Day Saints, and manuscript records from the World Data Center for Geophysics and the U.S. Geological Survey which were used for U.S. Earthquakes.

[3] DN - Desert News; SLT - Salt Lake Tribune; T - Salt Lake Telegram; WBR - records of U.S. Weather Bureau; LDS - records of the Church of Jesus Christ of Latter-Day Saints; WDCG - World Data Center Geophysics; USGS - U.S. Geological Survey, Branch of Global Seismology; UU - University of Utah Archives, Manuscripts and Special Collections.

February 22, 1943 earthquake

Site name and address	Description of building[1]	Report of earthquake effects[2]	MM assignment
City and County Bldg. State St. between Fourth and Fifth South	5-story, unreinforced stone.	Roof pulled away from building (per city engineer) (SLT).	VI
Administration Bldg. Muncipal Airport 2450 West North Temple	2- and 3-story fireproof construction, reinforced concrete.	Shook for 30 seconds, no damage (WBR)	IV
Ninth Avenue and J. Street	---	A thud as though someone had fallen out of bed.	III
University of Utah	1-story concrete	Recorded on seismograph	F

---

[1] Descriptions of buildings were found in manuscript and photographic collections at the Church of Jesus Christ of Latter-Day Saints, the Utah State Historical Society, the Salt Lake City Public Library, and the University of Utah.

[2] Reports of earthquake effects were gathered from newspaper reports, manuscript records of the United States Weather Bureau, manuscript records of the Church of Jesus Christ of Latter-Day Saints, and manuscript records from the World Data Center for Geophysics and the U.S. Geological Survey which were used for *U.S. Earthquakes*.

[3] DN - Desert News; SLT - Salt Lake Tribune; T - Salt Lake Telegram; WBR - records of U.S. Weather Bureau; LDS - records of the Church of Jesus Christ of Latter-Day Saints; WDCG - World Data Center Geophysics; USGS - U.S. Geological Survey, Branch of Global Seismology; UU - University of Utah Archives, Manuscript and Special Collections.

March 6, 1949 earthquake

Site name and address	Description of building[1]	Report of earthquake effects[2]	MM assignment
Hotel Utah Main Street NE Corner South Temple	10-story fireproof steel frame construction, reinforced brick.	Guests felt the tremor; no panic resulted. Guests on upper floors reported earthquake as "very distinct" (SLT).	IV
Newhouse Hotel Main Street SW corner Fourth South	12-story; some fireproof construction, steel frame.	Guests felt the tremor; no panic resulted. Guests on upper floors reported earthquake as "very distinct" (SLT).	IV
Adele Parks residence 1275 Third Avenue	1½story frame	Felt a very sharp jar and heard the grandfather clock creak; a crystal dropped from chandelier (SLT).	IV
Salt Lake County Jail 437½ South Second East	4-story brick, concrete floors.	Iron gates and cell doors rattled (SLT).	IV
Frank Cabrera residence 720 Kilby Court (between Second and Third South from Seventh South)	1½story brick	Big chimney destroyed (SLT).	VII

March 6, 1949 earthquake--Continued

Site name and address	Description of building[1]	Report of earthquake effects[2]	MM assignment
Salt Lake Municipal Airport 2450 West North Temple	---	Ground jumped up and down; sounded like an explosion (SLT).	IV
University of Utah	1-story concrete	Recorded on seismograph	F
Utah Theatre 148 South Main	1-4-story reinforced concrete frame, some fireproof construction, steel roof trusses.	Patrons jumped to their feet and began to rush out; a few screamed.	V
Capital Theatre 46 West Second South	3-story reinforced concrete construction, brick exterior walls.	Felt the tremor; no one especially afraid.	IV
Pilot Cafe 1726 West North Temple	1-story	Shattered two windows	VI
Jane Butcher residence 707 Sagebrush Airbase Village	---	Knocked mirror from wall	V

March 6, 1949 earthquake--Continued

Site name and address	Description of building[1]	Report of earthquake effects[2]	MM assignment
Walter Scott 794 Project Road Airbase Village	---	Loud noise, broken dishes and mirrors	V
713 E Street	---	Broken dishes	V
Herschel P. McGuinness 329 North Tenth West	1-story stone	Afraid to go to bed	V
Lizzie O. White residence 222 Fourth Avenue	2-story brick	Desk lamp shook; stairs creaked	IV
Tribune-Telegram Offices Ezra Thompson Bldg. 143 South Main	10-story brick; fireproof construction, steel frame.	Persons throughout the building; feet; building swayed.	IV
Salt Lake General Hospital 2033 South State	4-story brick; some fireproof construction, exposed steel joists.	Felt on upper levels but not in basement.	F

March 6, 1949 earthquake--Continued

[1] Descriptions of buildings were found in manuscript and photographic collections at the Church of Jesus Christ of Latter-Day Saints, the Utah State Historical Society, the Salt Lake City Public Library, and the University of Utah.

[2] Reports of earthquake effects were gathered from newspaper reports, manuscript records of the United States Weather Bureau, manuscript records of the Church of Jesus Christ of Latter-Day Saints, and manuscript records from the World Data Center for Geophysics and the U.S. Geological Survey which were used for U.S. Earthquakes.

[3] DN - Desert News; SLT - Salt Lake Tribune; T - Salt Lake Telegram; WBR - records of U.S. Weather Bureau; LDS - records of the Church of Jesus Christ of Latter-Day Saints; WDCG - World Data Center Geophysics; USGS - U.S. Geological Survey, Branch of Global Seismology; UU - University of Utah Archives, Manuscripts and Special Collections.

September 5, 1962, earthquake

Site name and address	Description of building[1]	Report of earthquake effects[2]	MM assignment
Deseret Bldg. 75 South Main	4-story steel frame construction, 12-in. brick curtain walls.	Plaster cracks on the 4th floor; water from water tanks splashed up walls walls about 8 in. (DN).	VI
Newhouse Bldg. 10 Exchange Place	11-story steel frame construction, brick with stone facade.	Plaster cracks (DN)	VI
Continental Bank Bldg. 200 South Main	13-story reinforced concrete, brick and stone-faced building.	Felt stronger than other earthquake [Cache Valley, Aug. 30, 1962]. The building had a rolling motion (13th floor). "Terrifying experience" (11th floor) (DN).	V
Karl Wesemann residence 430 East Seventh South	1-story hollow cinder or concrete blocks; brick-faced.	Wall and ceiling collapsed; blocks from from inner wall fell through ceiling, outside wall cracked from foundation to roof (DN).	VII

September 5, 1962, earthquake--Continued

Site name and address	Description of building[1]	Report of earthquake effects[2]	MM assignment
LDS Twenty-second Ward Meeting House SE corner of Second West and Fourth North Streets	1-2-story hollow cinder or concrete block, brick-faced.	Damage was sufficient to cause building to be demolished (LDS).	VII
Walker Bank Bldg. 175 South Main	16-story steel frame, fireproof construction.	A slight swaying sensation (16th floor)	III
Salt Lake General Hospital 2033 South State	3-4-story, some fireproof, reinforced concrete, brick.	Glass partitions were shaking and the whole building was rattling; many of the people ran out.	V
LDS Hospital 318-325 Eighth Ave.	5-7-story reinforced concrete columns and beams, steel frame.	Operations were suspended; no damage but building received a good shaking.	V
Control Tower Salt Lake City Airport 4000 West Eighth North	8-story	"Things really rocked;" no damage	V

September 5, 1962, earthquake--Continued

Site name and address	Description of building[1]	Report of earthquake effects[2]	MM assignment
FAA Building Salt Lake City Airport 4000 West Eighth Ave.	---	Cracks, light fixtures weakened and fell	VI
Terminal (New) Salt Lake City Airport 4000 West Eighth North	---	Plaster shaken loose, cracks in walls	VI
Ms. Joseph (Edith) M. James residence 809 North Redwood road	---	Foundation of north side of house had pulled away both in back and in front.	VII
Paul Robinson residence 558 Dowington Ave.	1-story	"Quite sharp" in that area; the house and pictures on the wall swayed.	V
1325 South 1700 West	---	Felt like the whole earth shook; tile roof "sounded like teeth chattering."	IV

September 5, 1962, earthquake--Continued

Site name and address	Description of building[1]	Report of earthquake effects[2]	MM assignment
Utah State Office Building North end of State Street north of Utah State Capitol Building	6-story, reinforced concrete, on metal deck.	Plaster shaken loose, cracks in plaster on third floor, wall and doorline cracks, other hairline cracks.	VI
Tribune Offices Ezra Thompson Bldg. 143 South Main	10-story brick; fireproof construction steel frame.	Floor shook violently (DN)	V
Utah State Capitol Bldg. North end of State St.	4-story fireproof construction, reinforced concrete, granite faced.	Appeared to be bouncing during earthquake (DN, SLT).	V
Federal Bldg. 350 South Main	5-story stone	Wall and doorway cracks (DN, USGS)	VI
City and County Bldg. 421 South State	5-story unreinforced stone.	Cracks 2nd, 3rd, and 4th floors. Plaster shaken loose (DN).	VI
Police Station 244 East Fourth South	2-story metal sash and glass	Plaster shaken loose; cracks in walls (DN)	VI

September 5, 1962 earthquake--Continued

Site name and address	Description of building[1]	Report of earthquake effects[2]	MM assignment
LDS Bishop Central Store- 1655 Wallace Road	---	Severe damage to windows and plaster walls; 1/4-in. cracks along walls; 90 ft of wallboard pulled loose on 2nd floor; 70 ft damaged on 1st floor (DN).	VII
Deseret News Bldg. 31-33 Richards	8-story fireproof construction; steel frame.	16 windows broken; cracks in walls and and ceiling; entire wall pulled away from interior supports (DN).	VII
Ms. Valjean Chapman 808 Coatsville		Clock that had not run for years restarted.	V
Catholic Church Cathedral of the Madeleine 331 East South Temple	3-story, stone	Some plaster dust fell as it does during a wind storm.	V
181 West Eighth South	1-story	Windows, mirrors, a showcase, and bottles shattered during the tremor.	VI
Ms. George Miller residence 17 North Fifth West	1-story brick	Ceiling fell in, inside wall shattered (DN, USGS).	VII

<u>September 5, 1962 earthquake</u>--Continued

Site name and address	Description[1] of building	Report of earthquake effects[2]	MM assignment
Ms. Oral Martineau residence 271 West Fifth North	2-story brick, with attached 1-story adobe.	Portions of ceiling and an inner wall collapsed.	VII
ZCMI 15 South Main	3-story brick with cast iron facade.	Crystal display shken down, broken	V
University of Utah Campus		Recorded on seismograph	F
South High School 1575 S. State	---	Very little damage except for a few cracks around the exterior of the main entrance.	VI
West High School 241 N. 2nd West	---	Some plaster cracks in the technical building.	VI
Jordan Junior High School 1040 W. 6th South	---	Some cracks in the gym area	VI
Bonneville Elementary School 1145 South Nineteenth East	---	Crack in the exterior brick work on the SE corner.	VI
Dilworth Elementary School 1959 Twenty-First East	---	Plaster down and a crack in the main office	VI
Hamilton Elementary School 711 East Eighth South	---	Loose acoustical tile	V

September 5, 1962 earthquake--Continued

Site name and address	Description of building[1]	Report of earthquake effects[2]	MM assignment
McKinley Elementary School 1864 South State	---	Clock knocked from wall	V
Onequa Elementary School 513 North Tenth West	---	Cracks in pipe tunnel below building	V
Washington Elementary School 163 West Fourth North	---	Plaster cracks in four classrooms	VI
Webster Elementary School 429 Eighth East	---	One interior wall crack	VI
Grant Elementary School 627 South First West	---	Old interior wall cracks reopened	VI
Jackson Elementary School 750 West First North	---	Old interior wall cracks reopened	VI
Jefferson Elementary School 1071 South West Temple	---	Old interior wall cracks reopened	VI

September 5, 1962 earthquake--Continued

Site name and address	Description of building[1]	Report of earthquake effects[2]	MM assignment

---

[1] Descriptions of buildings were found in manuscript and photographic collections at the Church of Jesus Christ of Latter-Day Saints, the Utah State Historical Society, the Salt Lake City Public Library, and the University of Utah.

[2] Reports of earthquake effects were gathered from newspaper reports, manuscript records of the United States Weather Bureau, manuscript records of the Church of Jesus Christ of Latter-Day Saints, and manuscript records from the World Data Center for Geophysics and the U.S. Geological Survey which were used for U.S. Earthquakes.

[3] DN - Desert News; SLT - Salt Lake Tribune; T - Salt Lake Telegram; WBR - records of U.S. Weather Bureau; LDS - records of the Church of Jesus Christ of Latter-Day Saints; WDCG - World Data Center Geophysics; USGS - U.S. Geological Survey, Branch of Global Seismology; UU - University of Utah Archives, Manuscripts and Special Collections.

APPENDIX III

LIST OF PLATES

Plate 1--MM intensity distribution in Salt Lake City for the October 5, 1909 earthquake.

Plate 2--MM intensity distribution in Salt Lake City for the May 22, 1910 earthquake.

Plate 3--MM intensity distribution in Salt Lake City for the March 12, 1934 earthquake.

Plate 4--MM intensity distribution in Salt Lake City for the February 22, 1943 earthquake.

Plate 5--MM intensity distribution in Salt Lake City for the March 6, 1949 earthquake.

Plate 6--MM intensity distribution in Salt Lake City for the September 5, 1962 earthquake.

Plate 7a and 7b--High and low values for MM intensity for buildings < 8 stories (7a) and buildings ≥ 8 stories (7b) in Salt Lake City (based on observed and calculated intensities) for a focal depth of 3 km.

Plate 8a and 8b--High and low values for MM intensity for buildings < 8 stories (8a) and ≥ 8 stories (8b) in Salt Lake City (based on observed and calculated intensities) for a focal depth of 10 km.

Plate 9a and 9b--High and low values for MM intensity for buildings < 8 stories (9a) and ≥ 8 stories (9b) in Salt Lake City (based on observed and calculated intensities) for a focal depth of 7 km.

Plate 10a and 10b-- High and low values for MM intensity for buildings < 8 stories (10a) and ≥ 8 stories (10b) in Salt Lake City (based on observed and calculated intensities) for a focal depth of 7 km using data collected from the September 5, 1962 earthquake.

Plate 11--High and low values for MM intensity for Salt Lake City for buildings > 8 stories and ≥ 8 stories for a focal depth of 7 km. Also shown are areas of high, moderate, and low liquefaction potential as mapped by Anderson et al. 1986.

EARTHQUAKE HAZARDS TO DOMESTIC WATER DISTRIBUTION SYSTEMS IN SALT LAKE COUNTY, UTAH

by

Lynn M. Highland
U.S. Geological Survey
Denver, Colorado

ABSTRACT

In an estimated magnitude-7.5 earthquake occurring along the Wasatch Front, Utah, significant damage may occur to Salt Lake County's domestic water system. This system is composed of water treatment plants, aqueducts, distribution mains, and other facilities that are vulnerable to ground shaking, liquefaction, fault movement, and slope failures. Other recent investigations into earthquake recurrence, liquefaction potential and site characteristics provide important data for evaluating the potential earthquake hazards to water-distribution systems in the event of a large earthquake. Water system components may be vulnerable to one or more of these earthquake effects, depending on site conditions at the various locations. Presentation of case studies of water-system damage by both recent and historical large earthquakes in Utah and in other regions of the United States offers an additional method for evaluating this problem. A recent field investigation of landslide damage to the domestic water systems of four towns in central Utah has also contributed information about potential damage to water systems that may occur during future large earthquakes.

Purpose and Scope of This Study

The objective of this investigation is to identify and map the geologic hazards caused by an earthquake which could reasonably be expected to occur in the vicinity of Salt Lake County, Utah. These hazards will be evaluated as to how they may affect the potable water supply and distribution system of Salt Lake County. Specifically, the following components of water supply and distribution will be evaluated.

1. Water purification facilities
2. Major aqueducts
3. Pumping stations
4. Wells
5. Above ground water tanks
6. Underground water-storage reservoirs
7. Penstocks and flumes
8. Distribution mains

The information presented is intended for use as a general guideline for identification of high hazard areas to aid future water system planning and emergency preparedness.

This study is organized into the following sections:

1. A geographic and demographic profile of Salt Lake County including its domestic water use and water-distribution system.
2. Seismic setting of Salt Lake County and explanation of the rationale for the possible occurrence of a large earthquake.
3. Review of the types of geologic hazards related to earthquakes and how water system components, in general, are affected.

4. Discussion of four hazard maps for Salt Lake County, and a detailed analysis as to how each hazard may affect the water system components in Salt Lake County.
5. Conclusions and recommendations for futher study.

A GEOGRAPHIC AND DEMOGRAPHIC PROFILE OF SALT LAKE COUNTY AND ITS DOMESTIC WATER USE AND WATER-DISTRIBUTION SYSTEM

The study area for this analysis is confined to Salt Lake County. There are 12 incorporated cities in Salt Lake County, and municipal expansion is occurring on previously irrigated agricultural land. The total population of the State of Utah, based on the 1980 United States census is 1,468,596, of which 42 percent reside in Salt Lake County. The population of Salt Lake County has increased about 62 percent in the past 20 years and is expected to increase another 52 percent, to 900,000, by the year 2,000 (Metropolitan Water District, 1982). Figure 1 shows a map of Utah's planning districts and counties; a perspective may be gained by noting the fact that there is a relatively dense population residing in the small area of land comprising Salt Lake County. Planning is currently being implemented to facilitate the future water needs of the county, and many proposals calling for new facilities for water storage, treatment, and distribution are being evaluated for location and feasibility (Metropolitan Water District, 1982).

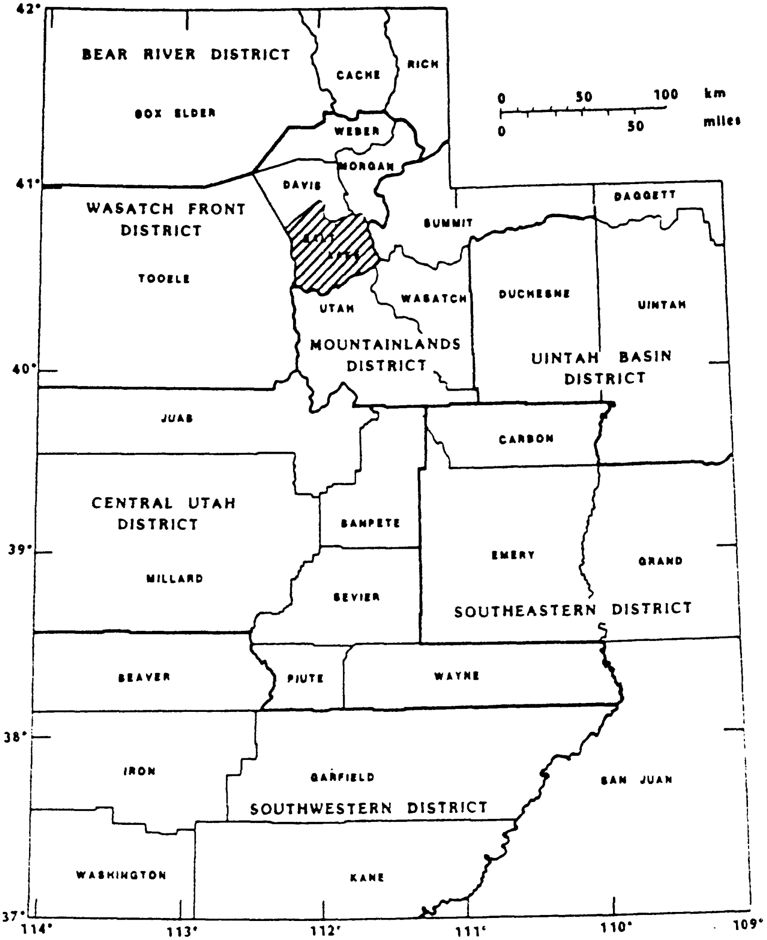

FIGURE 1. Utah planning districts. Salt Lake County is shown cross-hachured. (After Salt Lake County area-wide water study, 1982.)

It is helpful to visualize the area by providing a short description of its setting. Salt Lake County, Utah, covers an area of 765 mi^2 (1,231 km^2) of which 65 percent is alluviated valley. The remainder is composed of steep mountainous terrain. The Wasatch range rises to elevations of over 11,000 ft (3,400 m) east of Salt Lake Valley. These mountains rise very steeply and are eroded on their lower slopes in the shape of a series of triangular facets, characteristic of fault-block mountains. The Oquirrh Mountains, to the west of Salt Lake Valley, reach heights of 9,500 ft (2,900 m) and finally, the Traverse Mountains form the south end of the valley, at elevations of 6,500 ft (2,000 m). The valley floor consists of a series of ancient lake shoreline benches dropping in elevation from the mountains to the Jordan River, which flows north to the Great Salt Lake, through the entire length of the valley. The valley soils consist of clay, silt, sand and gravel to a depth of at least 2,000 ft (600 m). Figure 2 illustrates a map of the Jordan River drainage.

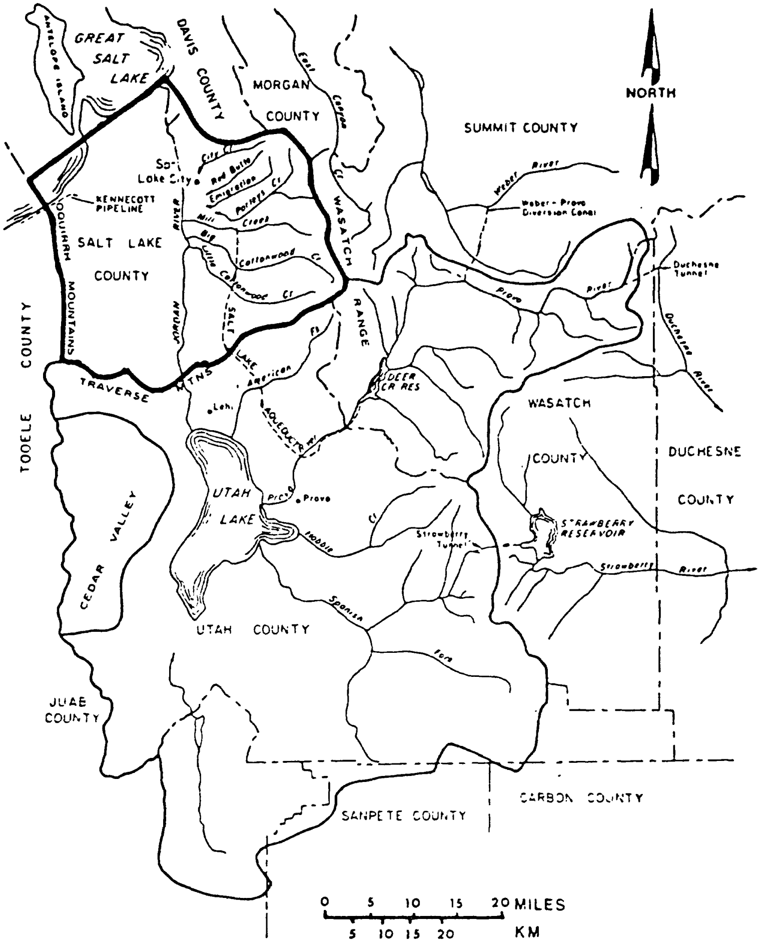

FIGURE 2. Water drainage and Jordan River system for study area. Salt Lake County is outlined. (After Salt Lake County area-wide water study, 1981.)

Because precipitation has an effect on water supply and on the severity of some geologic hazards in the area, it will be briefly mentioned. The major portion of the area's precipitation occurs during the winter months. Normal annual precipitation ranges from 12 to 16 in. (30 to 40 cm) on the valley floor, to 60 in. (152.4 cm) in the high mountain areas of the Wasatch range. Melting snow in the Wasatch range results in very high levels of runoff during the spring snowmelt period. The Oquirrh Mountains and the valley receive relatively little snow. A large percentage of the winter precipitation is absorbed into the soil and underlying bedrock resulting in recharge of the valley ground water. During recent years (since about 1982), snow accumulation has been higher than normal and has caused a marked increase in both ground water and lake levels throughout the Wasatch front areas, a change which may intensify geologic hazards in the area, especially those already intensified by earthquakes.

Water profile for Salt Lake County--sources and distribution

In Utah, as in most areas of the semi-arid, western United States, one of the major resources of concern is water--both sources and distribution systems. A disrupted water system is serious in any populated area, but for the Wasatch front area, where potable water flows from a very narrow range of geographic sources, distribution could be very seriously impeded in the event of a damaging earthquake.

It is useful to map and discuss the system of water distribution for Salt Lake County--where water originates and to where it flows. Seven major and 12 smaller streams with significant water flows originate in the Wasatch Range on the east side of the valley. These streams provide more than 97 percent of the surface water supply originating in the Salt Lake Valley drainage. Six streams originate in the Oquirrh Mountains on the west side of the valley, which supply less than 3 percent of the surface water. Water is diverted from the Weber River and from the North Fork of the Duchesne River into the Provo River where it is stored in Deer Creek Reservoir. From there it is transported to Salt Lake County via the Salt Lake aqueduct and Provo River canal. Utah Lake, just south of Salt Lake City, is also used as a primary reservoir. The outflow from Utah Lake is the Jordan River. The Jordan River flows north through Salt Lake County into the Great Salt Lake, which acts as a catchment area for the county. The high salinity, mineral, and waste content of the Great Salt Lake renders it unsuitable as a source for drinking water. It is pertinent here to mention a word about irrigation. The valley's farmland has been heavily irrigated since 1847 with diversions from mountain streams onto the land. In addition, Utah Lake water was brought into the valley by canals in the 1880's. Since Utah Lake water is not potable, many exchange agreements have been made to substitute Utah Lake water for irrigation use so the high-quality mountain stream water could be used for municipal and industrial purposes. Much of the valley's irrigation water is treated so that it can be used later for drinking water for parts of Salt Lake County.

Existing Water Sources

On the east side of the valley (Wasatch Front area), there are seven major canyon drainages which contribute to water supply. These include City Creek, Red Butte, Emigration, Parleys, Mill Creek, Big Cottonwood, and Little Cottonwood Canyons. The minor east side drainages consist of Neffs, Tolcats, Heughs, Ferguson, Deaf Smith, Bells, Middle Fork Dry Creek, South Fork Dry Creek, Rocky Mouth, Big Willow, Little Willow, Bear, and Corner Canyons. On the west side of the valley, the Oquirrh range side, the essential drainages include Rose, Butterfield, Bingham, Barneys, Harkers, and Coon Canyons.

The Wasatch Range, to the east, is generally much higher in elevation than the Oquirrh Mountains of the west, and is also on the windward side of major storms. As a result, the Wasatch watersheds receive more precipitation than the Oquirrh watersheds, and the majority of the surface flow into the valley originates from the Wasatch range. Less than 3 percent of the surface-water supply originating in the Salt Lake Valley drainage area is provided by Oquirrh Mountain streams, and most future planning for new water networks is concentrated on the extreme east side of the Salt Lake Valley (Salt Lake City Area-wide Water Study, 1982).

Imported Water

Water is imported from sources outside the Jordan River drainage area to Salt Lake County. Spring runoff and winter flows from the Weber River are diverted to the Provo River through the Weber-Provo diversion canal. Water from the North Fork of the Duchesne Rivers is stored in Deer Creek Reservoir on the Provo River and, at times, in Utah Lake. Approximately 7.6 percent of the total water supply for Salt Lake County comes from the Deer Creek Reservoir through the Salt Lake Aqueduct. The Salt Lake Aqueduct joins with the Metropolitan Treatment Plant at about 9th South. This aqueduct has a capacity of 150 ft3/s (50 m$^{3/s}$), which is significant in that fire-fighting needs require approximately 30 ft$^{3/s}$ ($_{10}$m$^{3/s}$). Water is then delivered to the Salt Lake County area through the Salt Lake Aqueduct, Provo reservoir canal, and the Jordan aqueduct. The outlet from Utah Lake is the Jordan River which flows north through Salt Lake County. Its basin includes the major drainage of the American Fork, Provo, and Spanish Fork Rivers. In Salt Lake County, the Jordan River is joined by tributary inflows along the Wasatch and Oquirrh Mountains, and terminates in the Great Salt Lake. In addition to this system, there are 13 underground water-storage reservoirs in Salt Lake County with a million gallon (75.6 million litres) capacity or more. Drinking water is closely tied in with irrigation water, and many complex interchanges occur in order to trade potable water for lower quality irrigation water that has not been treated. Water ownership and rights are also extremely complex and diverse in the Jordan River valley--by the time it is treated and used, drinking water may pass through several jurisdictions and ownership companies involved in supplying both drinking water and irrigation water (Terry Way, Salt Lake County Division of Flood Control and Water Quality, written commun., 1984).

Ground Water

Ground water occurs in subsurface materials throughout Salt Lake County, but only water in the Healy aquifer in the valley fill is a major source for wells. The ground water is recharged primarily from the precipitation and snowmelt on the mountain watersheds. The ground water east of the Jordan River is generally of high quality, while the ground water west of the Jordan River is of lower quality. Approximately 20 percent of the total amount of Salt Lake County's potable water supply is produced by ground water wells. The wells produce over 45 percent of the water diverted for municipal and industrial use.

SEISMIC HISTORY AND SETTING

> "It is useless to ask when this disaster will occur. Our occupation of the country has been too brief for us to learn how fast the Wasatch grows; and, indeed, it is only by such disasters that we can learn. By the time experience has taught us this, Salt Lake City will have been shaken down and its surviving citizens will have sorrowfully rebuilt it of wood: to use a homely figure, the horse will have escaped, and the barn door, all too late, will have been closed behind him." (As quoted from G. K. Gilbert, Salt Lake City Tribune, Sept. 16, 1883.)

Since G. K. Gilbert's time, much has been learned about the nature of earthquakes, and many well-documented examples of damage to structures have provided clues as to what can be done to lessen an earthquake's impact. As Gilbert pointed out, we have limited historical information for assessment of the rates of recurrence of earthquakes--indeed, the "when" of an earthquake is as crucial a question as "how big" in terms of citizen preparedness. Much of western Utah has experienced sizable earthquakes as evidenced by surface faulting and old landslide remains which were possibly earthquake induced. Utah's historical catalog of documented earthquakes, however, dates only from

1850, about the time the area was first settled (Arabasz and others, 1979). The rest of Utah's seismic pre-history is being studied by geologists through field investigation methods such as fault scarp dating and trenching of subsurface faults.

Utah occupies a large segment of the Intermountain Seismic Belt, a zone of pronounced seismic activity that encompasses more than 792 mi^2 (1,300 km^2) beginning from the junction of the States of Utah, Nevada, and Arizona to northwestern Montana (Arabasz and others, 1979). Outside of California and Nevada, Utah has one of the highest levels of potential earthquake hazard in the United States. The term hazard in this instance refers to the probability of occurrence, within a specified period of time and within a given area, of a potentially damaging phenomenon. Within this belt of seismic activity lies the 225 mi (370 km) long Wasatch Fault, along which mountain blocks have been uplifted to form a prominent, west-facing scarp known as the Wasatch front, extending from Malad City, Idaho, southward to Gunnison, Utah. Figure 3 shows a generalized map of young faults in Utah including the Wasatch Fault.

Geologic Investigations

During the last 10 years, the Wasatch Fault has been the subject of increased geologic study with respect to its prehistoric seismic behavior. In 1977, the first trenches were excavated across the fault for the specific purpose of quantifying large earthquake recurrence, based on physical evidence of past earthquakes. These investigations have yielded information on slip rate, recurrence intervals of past earthquakes, displacement per event for past earthquakes, fault geometry, and additional evidence that the Wasatch fault is segmented (Schwartz and others, 1984). These investigations have provided a basis for evaluating the past behavior of the fault (Schwartz and others, 1984). A normal fault as long as the Wasatch Fault will probably only rupture along part of its total length during a surface-faulting earthquake. There is evidence that there are at least ten major segments (possibly more) comprising the Wasatch fault and that each segment may have a different earthquake frequency, derived from available radiocarbon dates of displaced horizons (Machette, 198_, this volume). Schwartz and others (1984) has presented calculations of a range of 400 to 600 years (and a preferred value of 444 years) for the average recurrence interval for the magnitude range of 6-3/4-7.5 along the entire Wasatch Fault zone.

For the section of the fault zone in Salt Lake County, Schwartz and others also suggest that the average ground displacement during a large earthquake would likely be about 6 ft (2 m). There is no record of historic faulting having occurred on the Wasatch Fault, but it is known that average displacement for large earthquakes in the past 10,000 years has been from 4.8 to 7.8 feet (1.6 to 2.6 m).

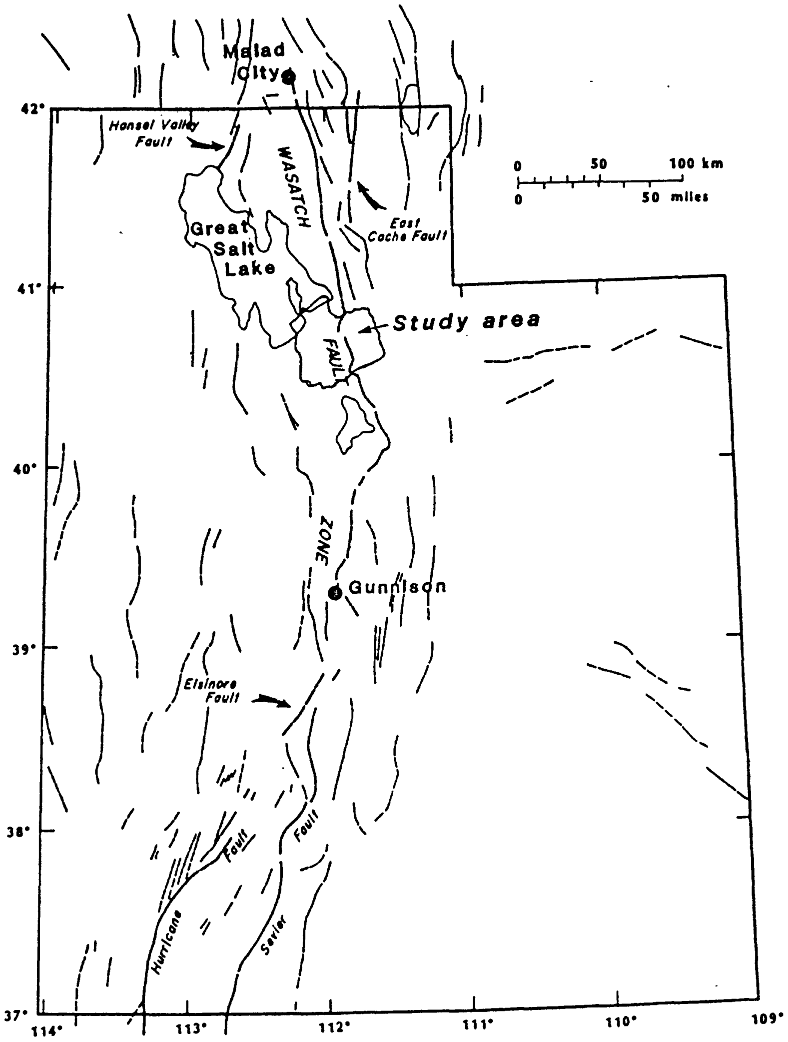

FIGURE 3. Fault map of Utah. Study area is outlined. (After Arabasz and others, 1979.)

Evaluating Earthquake Hazards

The number of people and monetary value of structures at risk from earthquake hazards is significant in Salt Lake County as 85 percent of Utah's population is concentrated along the seismically active Wasatch and East Cache Fault zones, as well as along adjacent smaller surface faults. The Wasatch Front, which includes Salt Lake County, has significant potential for strongest earthquake shaking in Utah. Expressed in terms of ground motion, there is a 90 percent probability that the acceleration in rock will not exceed .28 g (acceleration) in a 50-year period of time. Expected ground motion increases when time periods of interest greater than 50 years are considered. Figure 4 shows ground-motion values for the contiguous United States to which Utah can be compared.

FIGURE 4. Map of horizontal acceleration in rock from earthquakes (expressed as percent of gravity) with 10 percent probability of being exceeded in 50 yrs. (From Algermissen and others, 1982.)

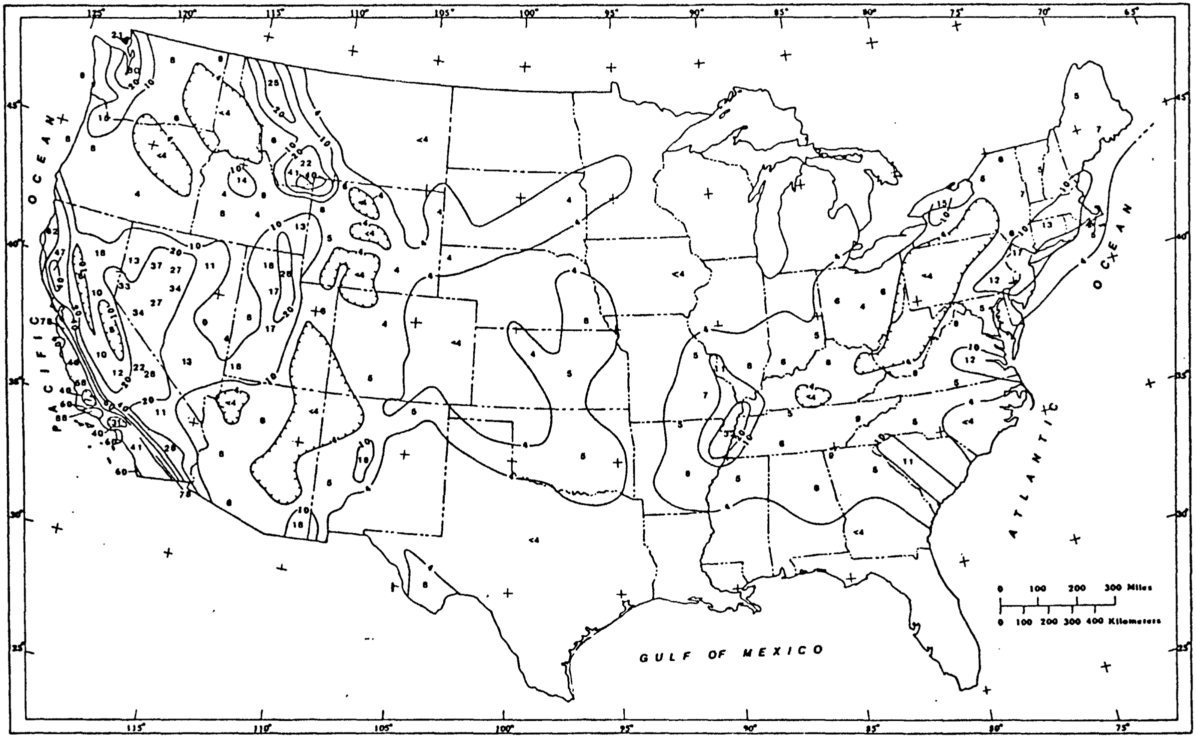

Damaging Historical Earthquakes in Utah

The most damaging earthquake in Utah's history was the 1962 event, near the town of Richmond, north of Logan. Although the epicenter was outside the immediate study area, it was felt at Intensity V and VI in Weber and Davis Counties (adjacent to Salt Lake County) and at V or less in Salt Lake and Utah Counties. The earthquake was relatively moderate in size (magnitude 5.7, maximum MM Intensity VII) but produced damage in three-fourths of the houses in Richmond, nine being unsafe to reoccupy. Mudslides and rockfalls closed several highways in the foothills east of the epicenter and damaged water flumes and irrigation canals, causing minor flooding.

Four Intensity VI earthquakes have occurred in Salt Lake City, the largest city in the Salt Lake County study area. The earthquakes occurred in 1910, 1943, 1949, and 1962, within the immediate Salt Lake City area. Table 1 shows dates and epicentral locations of the largest earthquakes (maximum MM intensity VI or greater) in the Utah region, including those in the study area. Figure 7 shows a plot of Utah's largest earthquakes dating from 1850-1978. Damage from these earthquakes occurred in the form of cracked walls, fallen plaster, toppled chimneys, and broken windows. Significantly for this study, the 1949 event ruptured a 10-in. (25.4 cm) water main, which resulted in the loss of water to a sizable portion of Salt Lake City (Arabasz and others, 1979).

TABLE 1 FOLLOWING PAGE

FIGURE 5 FOLLOWING PAGE

TABLE 1 --Largest earthquakes in the Utah region, 1850 through 1978

[Magnitudes in parenthesis were estimated from intensity value. All information from Arabasz and others, 1979, except where noted]

Local date Year Month Day	Latitude (°N)	Longitude (°W)	Intensity (I_0)	Magnitude (M_L)	Location
1884 Nov. 10	42.0	111.3	8	(6)	Bear Lake Valley
1887 Dec. 5	37.1	112.5	7	(5 1/2)	Kanab
1900 Aug. 1	40.0	112.1	7	(5 1/2)	Eureka
1901 Nov. 13	38.8	112.1	9	(6 1/2+)	Richfield
1902 Nov. 17	37.4	113.5	8	(6)	Pine Valley
1909 Oct. 5	41.8	112.7	8	(6)	Hansel Valley
1910 May 22	40.8	111.9	7	(5 1/2)	Salt Lake City
1914 May 13	41.2	112.0	7	(5 1/2)	Ogden
1921 Sep. 29	38.7	112.2	8	(6)	Elsinore
1921 Oct. 1	38.7	112.2	8	(6)	Elsinore
1934 Mar. 12	41.7	112.8	9	6.6	Hansel Valley
1943 Feb. 27	41.0	111.5	6	5.7	Salt Lake City[1]
1949 Mar. 6	40.8	111.9	6	5.7	Salt Lake City[1]
1959 Jul. 21	37.0	112.5	6	5.5+	Utah-Arizona Border (Kanab).
1962 Aug. 30	42.0	111.7	7	5.7	Cache Valley (Logan).
1966 Aug. 16	37.5	114.2	6	3.6	Nevada-Utah border
1975 Mar. 27	42.1	112.5	8	6.0	Idaho-Utah border (Pocatello Valley).

---

[1] From U.S. Geological Survey, 1976.

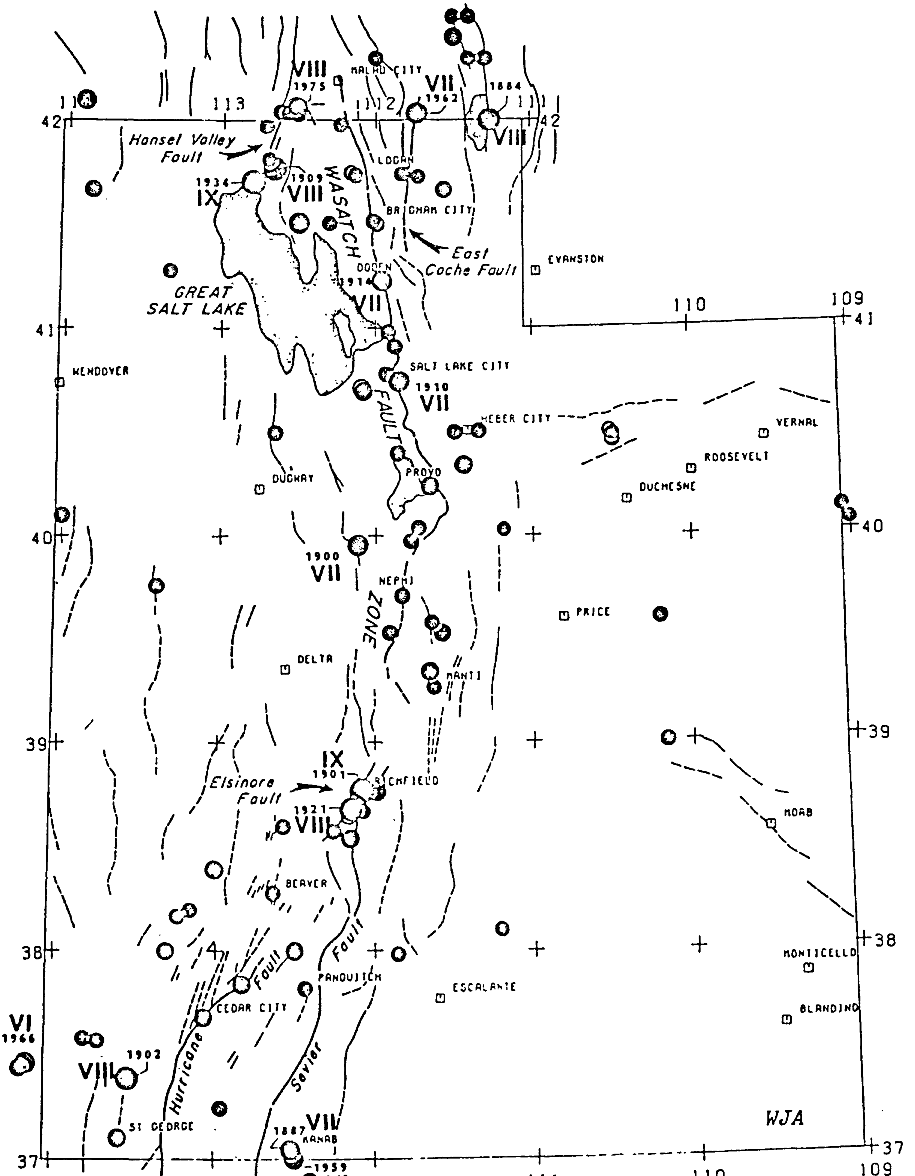

FIGURE 5. Largest earthquakes in Utah from 1850 to 1978. (After Arabasz and others, 1979.)

Characteristic Earthquake

The characteristic earthquake is defined here as an event that may reasonably be expected to occur in a given area, based on prior seismic events (size and recurrence) and on the geologic characteristics of the given area. A 1976 U.S. Geological Survey report entitled "Earthquake Losses in Salt Lake City," (Rogers and others) selected a magnitude-7.5 event as a very possible future occurrence along the Wasatch Front area. In that report, six magnitude 7.5 events were selected for simulation of resultant earthquake effects, 2 of which were hypothetically located in the Salt Lake City area. One epicenter was located in the northwestern part of Salt Lake City, near the mouth of Emigration Canyon. The other epicenter was situated near the town of Granger, immediately west of Salt Lake City. Briefly, the reason a 7.5-magnitude event was selected as a possible occurrence is because geological evidence exists indicating that an event this size shook the area in the recent past--perhaps as recently as 300 years ago. Newer evidence substantiates this estimate. Little Cottonwood Canyon contains fault scarps with a total offset of 188 ft (57 m) and individual scarps having offsets of 10 to 45 ft (3.3 to 15 m). A more significant indicator of large events is fault length. Some individual scarps are traceable for about 7 mi (11 km) (Rogers and others, 1976). In addition, according to information appearing in Schwartz and others (1984), linear frequency-magnitude distributions over a full range of earthquake magnitudes may not be appropriate for individual faults or fault segments, and moderate magnitude events smaller than the characteristic earthquake may be relatively less likely to occur than the larger event. Also, the magnitude of the characteristic earthquake may approximate the maximum earthquake (magnitude 7-7.5) for the Wasatch Fault zone. For this current study, a magnitude 7.5 earthquake occurring on the Wasatch Fault will also be considered the characteristic event.

GEOLOGIC HAZARDS RELATED TO EARTHQUAKES AND THEIR EFFECTS ON WATER SYSTEMS

Based on evidence from past damaging earthquakes and a recent field study, there are four major hazards resulting from earthquakes which may possibly damage water systems:

1. Fault movement
2. Ground shaking
3. Liquefaction of soils
4. Slope failures (landslides, rockfalls, slumps, etc.)

Each of these will be discussed briefly in general and then related to their effects on specific water system components and facilities.

Fault Movement

During fault movement caused by an earthquake, two planes of the Earth's surface slip differentially along a plane of weakness. As a result, energy is released and differentially displaces very long or relatively short sections of ground surface. The ground may move horizontally or vertically, motions called strike-slip and dip-slip movement, respectively. Also, one side of the two weakened planes may even thrust over the other in what is known as a thrust fault. During an earthquake, fault movement may occur on an already existing fault or may be newly manifested as surface rupture. Faults may also move below the surface of the ground, shaking the surrounding area but having no apparent visible surface rupture.

Fault movement damage to water facilities includes shearing of pipelines and wells, cracking interiors and (or) exteriors of buildings, such as concrete purification plants and, in extreme cases, toppling of buildings, such as pump facilities and tanks. Pipelines are very vulnerable to fault movement and, depending on the materials of which they are constructed, may shear both above and below the ground surface. During the 1971 San Fernando, Calif., earthquake, both above-ground and underground reinforced concrete-box channels which carried water were cracked and sheared as a result of surface fault displacement (Murphy, 1971). The Parkfield-Cholame, California earthquake of 1966 (magnitude 5.7) ruptured an irrigation pipeline which crossed the main fracture zone, nine hours before the actual event. The rupture occurred near an elbow on a 400-ft- (133-m-) long exposed segment of pipe that was parallel to and about 20 ft (6.6 m) east of the main fracture zone. A short segment of the pipe was buried (upon installation) where it crossed the fracture zone. Since the shifting could not be attributed solely to gravitational movement during foreshocks, as the first recorded foreshock occurred long after the pipeline break, This unusual occurrence was explained as pre-earthquake deformation of the ground surface near the main fracture zone (Brown and others, 1967). Pre-seismic damage has not been reported elsewhere, but the possibility of pre-earthquake deformation could possibly have implications for facilities, especially pipelines, in other areas.

Ground Shaking from Earthquakes

Ground shaking damages to water system facilities include breaking or shearing of pipes or pipe connections. Heavy shaking may cause cracking of unreinforced concrete or adobe buildings, rotation of wall casings and changes in well water levels in some cases. General loosening or breaking of connective apparatus, such as inlet-outlet piping may occur. In general, underground facilities such as pipelines are somewhat less vulnerable to damaging effects of ground shaking than are the same above ground facilities (Taylor and Ward, 1981).

Ground shaking generally causes the most widespread damage during an earthquake. As a result of the 1964 Alaskan earthquake, the Anchorage water treatment plant suffered pipeline damage due to severe shaking. At Kodiak, over 200 mi (320 km) from the epicenter, both water and sewer lines were cracked from earth vibrations. A situation worth noting was the absence of any sewer or water line damage in the town of Cordova, a city very close to the 1964 epicenter. Cordova is built almost entirely on indurated bedrock. Its airport however, located 13 mi (20.8 km) from the city and situated on thick alluvial deposits, suffered extensive water line and utility damage (Schuster and Krizek, 1978).

The 1971 San Fernando, Calif., earthquake caused widespread and severe damage to the area's water system. Most of the damage occurred in and around the most heavily shaken area which included Sylmar, San Fernando, and the Van Norman Reservoirs. The sole supply of water, before the earthquake, was from wells north of the city of San Fernando. The wells themselves were contaminated by seepage from ruptured sewer lines and septic tanks, and the underground delivery conduit from the well field was shattered. The distribution system was so fractured by ground cracking and violent shaking as to require a new water system for San Fernando. An extensive account of earthquake ground-shaking damage to dams, flood-control systems, treatment plants, wells, and water distribution facilities in the 1971 San Fernando earthquake is given in Murphy, (1971).

Soil Liquefaction

Liquefaction of soils is another common effect of earthquakes in low-lying coastal areas, or wherever soft soils and (or) sand and high water tables exist. The compaction of the water-saturated soil from earthquake vibrations causes the ground water to flow upward, and the usually coherent sandy or muddy soils become liquified into a kind of quicksand (Yanev, 1979). In addition, ground shaking causes adjustments in the packing of particles in the sand layer, and causes disrupted grain to grain contacts. These actions increase the pressure in the water, reduce the strength of the soil, and generate an upward flow of water through the ground. Structures located on such soils may suffer buckling, tilting, and possible cracking. Pipes and inlet-outlet connections may break or crack during differential compaction of liquefied soils.

Slope Failures

An important and potentially damaging effect of earthquakes on water systems is the threat of landslides, rockslides, and other associated slope movements such as debris slides, slumps, and ground cracking. Besides the obvious destructive effects of slope movements on structures such as buildings, dams, and telephone and powerline supports, landslides have caused well-documented damage to pipelines and aqueducts situated both below and above ground. Earthquakes may trigger landslides and other slope movements by shaking already weak and poorly consolidated slope materials such as clay, loose gravel or talus, or causing previously formed zones of weakness to shake loose and shear off with resultant movement down a slope. High water saturation of slope materials aggrevates and intensifies this type of movement.

It is difficult to predict the magnitude and (or) intensity level at which landslides and other slope movements occur, because many site-specific conditions determine the threshold of shaking that will induce slope movement. Slope angle, soil material, water pore pressure, and precipitation all have variable effects on the potential of an area to experience landslides, seismically induced, or not. Documented cases of moderate earthquakes in California of magnitudes in the range of 5.3 to 5.7 have generated landslides. The August 13, 1978, Santa Barbara, Calif. earthquake which caused extensive landslides was determined to have a maximum MM Intensity of only V-VI. Further aspects of landslide potential will be discussed in the hazard map section of this study.

Figure 6 shows five categories of slope movements identified by D. Varnes, which appear in Schuster and Krizek, (1978). A short description of each follows.

FIGURE 6 FOLLOWING PAGE

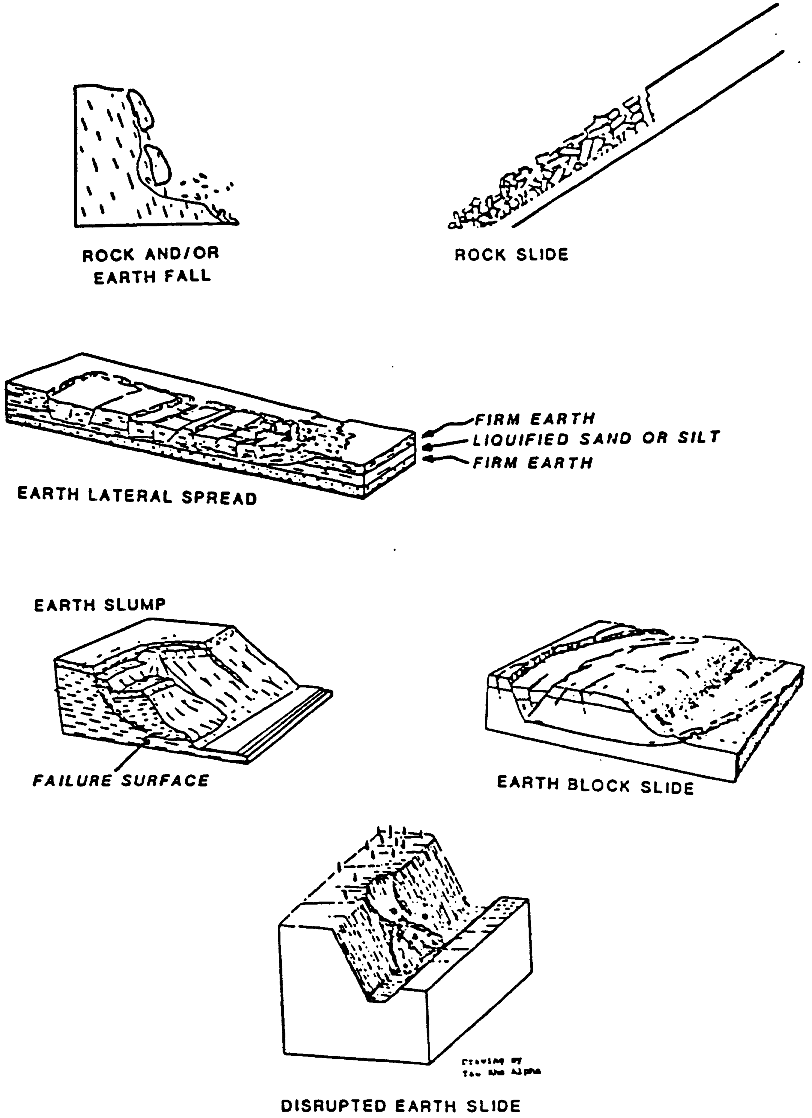

Figure 6. Five categories of slope failures. (After Schuster and Krizek,

Falls.-- Falls involve earth or rock that becomes detached from a cliff or slope. The material falls, bounces, or rolls through the air in a very rapid movement.

Slides.--This term refers to the movement of soil or rock along an identifiable surface called a rupture zone. The zone developes within layers of soil or bedrock or between soil and bedrock layers.

Flows.--Many types of slope movement cannot be classed as falls, topples, slides, or spreads. In unconsolidated materials, these generally take the form of fairly obvious flows, either fast or slow, wet or dry (Schuster and Krizek, 1978, p. 17).

Topples.--A block of rock that tilts or rotates forward on a pivot point is called a topple. A topple does not involve much movement nor does it necessarily trigger a rockfall or rock slide.

Lateral spreads.--A lateral spread is a nearly horizontal movement that occurs across a slope and on very gentle terrain. Such spreads are often initiated by earthquakes which liquify a layer beneath the material that moves. For example, if an earthquake liquifies a layer of sensitive clay just beneath rock, the rock above may break apart causing the pieces to separate very slowly.

Many cases of slope failure causing water system damage have been documented. The 1964 Alaska earthquake, (magnitude 8.5) caused extensive damage to the water distribution system in Anchorage. Ground fractures and landslides broke pipes in nearly 100 places--all types of pipe were affected. The underground systems, built primarily of concrete pipe, were broken by landslides and earth cracks. Whittier, a town near Anchorage, suffered extensive damage to its water distribution system due to ground fractures and large landslide-generated sea waves. Information in Harp and others (1980) has shown from results of reconnaissance investigations of effects resulting from the 1978 magnitude-5.5 Santa Barbara, Calif. earthquake that roadcuts experienced rockslides and rockfalls during the earthquake and are highly susceptible to slope failures. Tanks and purification plants which are often located near roadcuts may be vulnerable to heavy damage from rockfalls, or other failures, depending on the roadcut material.

A good example of the effects of a large landslide on a water system was provided by the June 19, 1975 landslide at the eastern end of 21st Street in Ogden, Utah (Rogers and others, 1976). The slide was not seismically induced, but was part of an older reactivated landslide formed from lake deposits consisting of silts, clays, and fine sands. This landslide ruptured a 42-in. (1.1 m) water main which had a 53 million-gallon (200,000-litre) capacity. Repair was costly and difficult since the slide continued moving. A second slide also occurred during repair work, aggrevating the situation further. Repair was completed two weeks after the date of the first landslide.

Though not seismically induced, the recent landslides which occurred in central Utah during May, 1984, dramatically illustrate the effect of slope failures on water systems. The slopes in the vicinity of central Utah contain soils composed of clays and unconsolidated materials (Davis, 1984). Because of steep slopes in the area, it has long been known that the area is very susceptible to slope failures. It is also a seismically active region, which makes the combination of conditions even more potentially damaging. Recent heavy rains and heavy snow runoff during May aggrevated the conditions and triggered a series of landslides, debris slides, and mudslides which plagued central Utah for weeks. The major damage to the cities and towns in the area came in the form of highway blockage by flow debris, and damage to drinking-water systems. A field survey of landslide damage was undertaken by the author because of the possible implication for Salt Lake County, which is also a region of moderate to high landslide potential.

The towns in central Utah which suffered water-system damage were Mt. Pleasant, Ephraim, Manti, Levan, and Fairview. Three of these cities, Ephraim, Manti, and Fairview had to install new drinking water systems after mudslides devastated their original systems. Ephraim, a town of about 2,810 people, was hardest hit by a series of slides in the surrounding canyons, which are the primary source of potable water. Two slides at the Great Basin Experiment Station at Major's Flat (Ephraim Canyon) interrupted the flow of water. The water from the city's springs was finally reconnected to the city's water tank after an 1800-ft-(550-m) long, 6-in.-(15-cm) diameter plastic water pipeline was successfully connected over the slide. The original pipe had been made of galvinized iron and was severed at a joint by the movement of the slide. The slide also ruptured the Birch and Maple Springs water lines which supplement the main line. The city of Ephraim originally diveréted the water from the severed main line into an old line in the same area which was ultimately severed by the slide. A state geologist suggested running the flexible pipe over the top of the slide, but this pipe was only a temporary measure until the original iron pipe could be repaired. The city was without water for 3 days, from May 3 to May 6 (Manti Messenger, May 17, 1984, p. 1).

In Manti (population 2,080,) a massive slope movement destroyed the lower shoulder of a section of Manti Canyon Road, severing a buried water pipeline which ran under the road. The slide exposed about 15 ft (63 m) of the line and caused it to buckle and to break open at a joint. The remaining pipeline was in imminent danger of dropping off into the canyon.
Two guy wires were attached to the exposed section of pipe and anchored above the road for support. Approximately 400 ft (133 m) of plastic pipe was installed to bypass the broken section of pipe. Fortunately, due to the occurrence of previous slides, Manti had devised a backup system for water delivery (Manti Messenger, May 10, 1984, p. 1).

In the same region of central Utah, Fairview, a small town of 916 people,. experienced 23 slides in its adjacent canyon to the east. Interestingly, the slides with the most bulk occurred on the north side of the canyon (the drier side) rather than the south side. Last year's slides also had the same ratio of north to south-oriented slides. Only 16-20 homes in Fairview were affected by a severed water main resulting from one of the slides. There was still drinking water left in a storage tank, but affected residents were told to boil their water because the tank water would become stale with no fresh water feeding into the tank. Fairview has devised a plan to provide a well as a backup system for future emergencies (The Pyramid, May 9, 1984, p. 1).

MAPS OF EARTHQUAKE HAZARD FOR SALT LAKE COUNTY

The following section presents five plates (pls. 1-5) illustrating proximity of water distribution facilities to four potential hazards. Plate 1 shows a base map of the study area which includes major towns and cities, and primary water sources and facilities. Plates 2-5 show four earthquake hazards which could potentially damage Salt Lake County's water system in the event of a magnitude 7.5 earthquake. The following hazards are mapped for Salt Lake County:

Plate 2--The Wasatch Fault

Plate 3--Regional patterns of expected intensity levels

Plate 4--Soil liquefaction potential

Plate 5--Landslide potential

Faulting, liquefaction, and landslide potential are mapped separately from intensity because they may occur at different levels of intensity. The intensity map will be used primarily to describe ground shaking. It should also be noted that these hazards may occur at higher or lower magnitudes than 7.5. The recurrence interval for a surface-faulting earthquake is approximately 444 years, based on information in Schwartz and others (1984). A recurrence interval for a magnitude 7.5 earthquake is less well defined. The U.S. Geological Survey report (Rogers and others, 1976) on loss studies for the Salt Lake City, Utah, area concludes that the time interval for which there is a 63 percent probability of an event exceeding or equaling magnitude 7.5 may be as short as 100 years. It is not currently known when the last time a 7.5 event occurred in the Salt Lake County area.

Plate 1. Salt Lake County Domestic Water Supply Base Map

This plate shows major reservoirs, aqueducts, purification plants, pumping stations, wells, underground reservoirs, and above-ground tanks. In addition, some waste-water treatment plants are shown. The information on this map is modified from material found in the Salt Lake County Area wide Water Study (1980), from information found in Taylor and Ward (1981), and from Rogers and others, (1976).

Plate 2. Map of the Wasatch Fault, Salt Lake County

This plate shows the Wasatch fault as it has been mapped, in Salt Lake County. The dots indicate at which points fault movement may be expected to damage a water system facility at that point. It should be noted that movement along the fault in any given surface-faulting earthquake will probably occur only along a segment of the fault. Which portion of the fault may fail in the next large earthquake cannot presently be determined. The surface location of the Wasatch Fault was taken from a geologic map series prepared by Davis (1984).

Plate 3 shows the estimated regional patterns of MM intensity that could possibly be generated by a magnitude 7.5 earthquake on the Wasatch Fault. The intensity information is derived from studies of the average relative ground response in the 0.1 to 0.2 second period range in the Salt Lake County area. The ground response is based on rates of ground motion from the effects of mining blasts and small earthquakes in the area (Hays and others, 1978). Site amplification studies are ongoing and the results may be modified at a future time.

Estimating seismic-intensity patterns which will result from a specific earthquake is complicated. The degree of ground shaking at a specified location based on a given magnitude value is dependent upon a number of conditions. Among the most influential are the distance from the source of the event and the nature of the earth materials through which earthquake vibrations pass. Further complicating the estimation is the fact that manmade structures are of diverse materials and design and, thus, behave differently in an earthquake. Intensity evaluations may be the best way in estimating damage patterns, since the MM Intensity Scale provides some uniformity as to building type and construction.

Plate 4. Map of Potential Liquefaction for Salt Lake County

This map shows areas of Salt Lake County which are classified as having high, moderate, or very low potential for soil liquefaction in the event of an earthquake along the Wasatch Fault. (Maps are from Anderson and others, this volume). Data for the map came from borings made to learn the depth of liquefiable soils. Critical accelerations are the basis for the divisions on the liquefaction potential map, which are in turn based on the use of exceedence probability curves applied uniformly throughout the county (J. Spitzley, Dept. of Civil Engineering, Utah State Univeristy, Logan, Utah, written commun., 1984).

Plate 5. Map of Landslide Potential for Salt Lake County, Utah

This map is contoured to show areas of high, moderate, and low potential for landsliding. Areas of historic landsliding are also shown on this map. The map is based on known areas of past landsliding, bedrock type, topography, and average annual rainfall. A methodology for regional assessment of earthquake-induced landslides has been developed by D. Keefer (1984). From that study, it has been concluded that areas judged highly susceptible to earthquake-induced landslides have slopes steeper than 35°, overlie water-saturated sand and silty alluvium, and (or) are on active and recently active landslides. At present, there are no such earthquake-induced landslide susceptibility maps in completed form for Salt Lake County. As landslide studies become more detailed and site specific, the mechanisms of earthquake-induced landslides become better known, landslide susceptibility maps will become better tools in estimating loss to water systems and other vulnerable facilities. Note, for a detailed slope stability map of the Sugar House Quadrangle (near Salt Lake City) see Van Horn (1972).

EARTHQUAKE VULNERABILITY OF DOMESTIC WATER SYSTEMS IN SALT LAKE COUNTY

The following section will provide an overview of water supply and distribution components utilized in Salt Lake County, and also discuss the extent to which these facilities are vulnerable to the four earthquake hazards previously discussed. Some of the following discussion includes information found in a water system vulnerability study for Salt Lake City prepared for the Utah Seismic Safety Commission by (Taylor and Ward, 1981).

Past earthquakes have shown that various components of water supply systems are vulnerable to damage at various intensity thresholds and goelogic effects. It is pertinent here to describe the effects that earthquake hazards might possibly have on the particular components that make up the Salt Lake County water system. The following components will be discussed and evaluated as to their vulnerability to a magnitude 7.5 earthquake located on the Wasatch Fault:

Building Code, 1976). All of these treatment plants are bifurcated so that part of the plant can be shut down to clean the purification tanks. All six plants have emergency power. Chlorine cylinders are typically chained down and chlorinators are bolted to the floors. According to sources used in the Utah Seismic Safety Commission Report (Taylor and Ward, 1981), none of the plants have bypass valving. The Metropolitan plant has a bypass line that would permit chlorination in an emergency if chlorine is available.

FIGURE 7 FOLLOWING PAGE

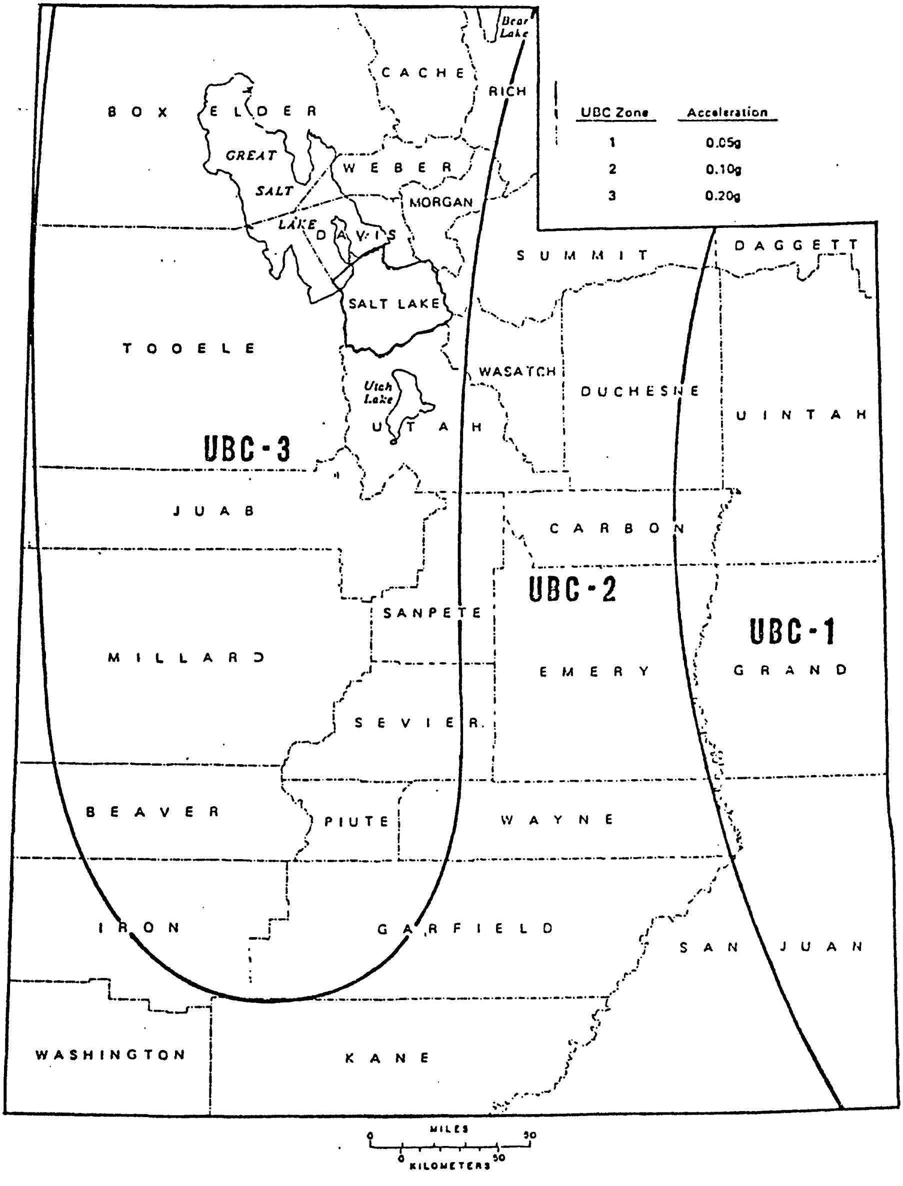

FIGURE 7. Uniform building code zones for Utah. Study area is outlined. (After Uniform Building Code, 1976.) The zones are differentiated as to the ground motion (% g) from earthquakes, which might be expected to occur.

At the Big Cottonwood Plant, a liquid fiberglass tank outdoors and at the eastern end of the plant is likely to fail at higher intensities due to two factors: a high height-diameter ratio for the tank and anchor bolts that are stronger than the fiberglass to which they are connected. Inside the Big Cottonwood treatment plant, chlorine tanks in use are chained down. However, reserve chlorine tanks are in cradles and could possibly slide if subjected to extreme lateral forces. Even though chlorine can be harmful in excessive amounts, damage from chlorine spills would not result in plant nonfunctionality. Another point of vulnerability to the Big Cottonwood plant for instance, is its total reliance upon electrical power for processes such as screening and treatment. The screening process at the City Creek plant may be manually operated. For these purification plants, power dependency and water outlet connections appear to be the chief points of earthquake vulnerability. Rupture of outlet connections may be expected to occur at Intensities IX or X. However, fault movement, liquefaction and (or) landsliding may be additional threats to that of ground shaking, since they may occur at lower intensities. Table 2 shows the vulnerability of the six water purification plants to four major earthquake effects. This information was taken from plates 2-5. The conclusions shown in table 2 are by no means substantiated by actual earthquake effects in the area, but are an educated estimate as to how earthquakes may affect the water purification plants in Salt Lake County.

TABLE 2 FOLLOWING PAGE

TABLE 2.--Expected earthquake effects on Salt Lake County's water-purification plants in the event of a magnitude-7.5 earthquake

Location of purification plant	Fault movement (pl. 2)	Ground shaking (pl. 3)	Liquefaction potential (pl. 4)	Landslide poten- (pl. 5)
Parley's----	No fault trace in the vicinity.	Probably light ground shaking--no site amplification data currently available.	Very low--	High.
City Creek--	Possible damage, less than 0.1 mi (0.16 km) from fault trace.	May experience heavy ground shaking--no site amplification data currently available.	--do------	Do.
Big Cottonwood.	Possible heavy damage, less than 100 ft (33 m) from fault trace.	Possible VII intensity according to site amplification.	--do------	Do.
Metropolitan	Possible damage; 0.2 mi (0.32 km) from fault trace.	Intensity VI according to site amplification studies.	--do------	Do.
Draper------	Plant is located on fault; possible heavy damage may be expected if fault moves here.	VII to VII according to site amplification studies.	--do------	Do.
Jordan------	None to very little damage; at some distance from fault trace.	Not enough site amplification studies.	--do------	Do.

Major Aqueducts

The aqueducts and major conduits comprising the Salt Lake County water systems are vulnerable at many points, principally because many are aligned with the Wasatch Fault trace and cross it at several points (see plate 2 for major fault cross points). Aqueducts are also vulnerable to ground shaking, liquefaction, and ground failures such as landsliding.

It is known that underground aqueduct systems perform better than those at the surface when both are subjected to heavy ground shaking (Dowding and Rozen, 1978), but less is known about the effects of liquefaction on such pipe. Landsliding and fault rupture may disrupt both underground and above ground conduits and (or) aqueducts.

There are several major aqueducts in the Salt Lake County region. The Salt Lake Aqueduct extends about 41.7 mi (67 km) from the Provo River to Salt Lake City and, as shown on plate 2, many segments lie on or very close to the Wasatch Fault. The sections of this aqueduct just east of Tolcats and Heughs Canyons are subject to high liquefaction potential (Plate 4). Approximately one-tenth of the aqueduct passes through an area of Intensity VIII-IX at its northernmost extension at the Jordan River. This area also has moderate to high liquefaction potential. Approximately 25 percent of Salt Lake County's and approximately 7 percent of Salt Lake City's water is delivered from Deer Creek Reservoir through this aqueduct. The Salt Lake Aqueduct (as well as the Jordan Aqueduct), is a 69-inch (175-cm) diameter conduit which is constructed in two layers. The inner pipe is steel and the outer layer, called shock coat, is a form of reinforcement constructed in concrete. This double-layered piping is laid in 30-foot (91-m) lengths which are, in turn, fastened with rubber joints called bell-spigot joints (rubber from one section fits inside the next section of pipe). These segments are specifically designed to withstand extensive ground movement. Original concrete piping still comprises some segments of the Salt Lake Aqueduct, but these older sections are being gradually replaced by the newer, bell-spigot, double-layered pipe (Scott Haslam, oral communication, 1984). The Salt Lake Aqueduct joins with the Metropolitan Water Treatment Plant at about 90th South (near the mouth of Little Cottonwood Canyon), and water is taken off at 78th South, 70th South, at the Tanner Reservoir, 45th South, and at the Park Reservoir. The Salt Lake Aqueduct is represented on Plate 1 as it runs from mountainous portions of the water system (from Deer Creek Reservoir) and continues north to the Jordan River, at times above the surface, at times below.

The Jordan Aqueduct, a part of the Bureau of Reclamation's Central Utah Water Project, supplies approximately 94,000 acre-feet (116,000,000 m^3) of water to Salt Lake County. This aqueduct runs from the mouth of Provo Canyon to the Jordan water-purification plant near Point-of-the-Mountain. From there, treated water flows north along the west side of the valley, terminating at 40th West and 21st South, to the west part of Salt Lake City (Rogers and others, 1976). As shown on plates 3 and 4, the Jordan Aqueduct is susceptible to both liquefaction effects and potential intensity IX-X ground shaking near Granger, about 4 mi (6.4 km) southwest of Salt Lake City. This affects the northern one-third of the aqueduct. However, this aqueduct is built to be resistant to heavy ground shaking due to its shock-coat and bell-spigot connective design. The various canals, also shown in Plate 1 in this same vicinity, are irrigation canals and do not convey drinking water.

It should be noted that many waste-water treatment plants and their inlet and outlet piping are located in these same areas of expected heavy ground shaking and (or) liquefaction effects. Damage to such facilities could affect drinking water systems by contamination of ground water and seepage of contaminants into the purified water distribution system. Waste-water treatment plants are also shown on Plate 1.

The Wasatch fault is not evident in the areas of the Jordan Aqueduct system, and intensity effects postulated from site amplification studies have not been mapped for the area of Provo Canyon. Landsliding may be a potential hazard in the steep portions of the Provo Reservoir Canal (see Plate 4).

The Big Cottonwood Conduit starts at the Big Cottonwood Treatment Plant and is intersected at the entrance to Big Cottonwood Canyon, at about 70th South, by the Little Cottonwood Conduit from the Metropolitan water district's Little Cottonwood Treatment Plant. The Big Cottonwood Conduit has parallel outlets with the Salt Lake Aqueduct for interchange of feeds. Both the Salt Lake Aqueduct and the Big Cottonwood Conduit cross the Wasatch Fault barely north of 70th South, and both cross an inferred fault barely south of 45th South. A major earthquake could lead to fault movement-related damage to the lines at one or both locations (Taylor and Ward, 1981). The Big Cottonwood Conduit is also subject to high liquefaction potential in the area around Tolcats and Heughs Canyons.

In assessing conduit and aqueduct vulnerability to earthquake damage, the relative ease and time with which repairs can be made is important. If damage occurs either to the aqueduct or to the smaller conduits, no in-line valves exist to isolate the damage sections. Instead, water must be turned off at the treatment plant or plants. Repair might consist of sandbagging or baffling to control surface flow, but little can be done until the line is emptied. If failure occurs to only one of the major supply lines, then the other one can be used to supply water to major portions of the Salt Lake County system. If failure should occur to both lines south of 70th South, then the Big Cottonwood conduit still could supply large portions of the water needed in the system. If, in contrast, failure occurred north of 70th South, then large portions of the system would need to rely upon reservoir supplies. Those portions of the system where reserve supplies would be depleted rapidly would soon lack supplies.

Pumping Stations

Pumping facilites vary widely in size and structural details. Most are small, reinforced concrete-box structures are only slightly vulnerable to seismic damage, and equipment anchorage or bracing also reduces seismic vulnerability. Power failure can also lead to nonfunctioning or temporary failure of pumping stations expecially if no emergency generators are available. An example of the effects of power-outage (which may occur during an earthquake occurred on July 5, 1976. At this time, there was a general 4-hour power outage and the bench area above 35th South, the bench area in the southernmost portion of the system, and the northernmost bench area went dry (Taylor and Ward, 1981).

Power is also needed for deep pump wells, for boosting of artesian sources, and for treatment-plant operation. In spite of the predominant use of gravity flow in the Salt Lake County system, it is still heavily dependent upon power sources. Since power outages very often accompany earthquakes, back-up power systems could significantly reduce the impact on pumping stations and (or) treatment plants.

An example of a pumping station which might suffer damage is the 3rd East pumping station. This station is an unreinforced concrete structure which is particularly vulnerable to earthquakes and could receive slight damage at shaking levels as low as MM Intensity VI. Loss of the 3rd East pumping station would entail loss of at least artesian supplies of about 15 million gallons per day, which is not as critical as the loss of other higher capacity facilities

Wells

Deep pump wells and artesian wells supply almost 50,000 gallons (189,000 litres) of water per minute, or 70 million gallons (264.6 million litres) per day (MGD). Artesian wells can supply a maximum flow of 15 MGD for about 4 hours maximum. Even though flows from wells meet fire-flow requirements, wells are localized and cannot supply all parts of Salt Lake County. Plate 1 shows locations of deep wells.

Damage to wells themselves is usually caused by contamination due to seepage from damaged sewer lines or septic tanks. As discussed previously, wells damaged in the 1971 San Fernando earthquake suffered concrete casing failure as well as damage to pump stands and other connective apparatus of pumps. A number of wells in the Murray area (shown on Plate 1) supply water to Salt Lake City and would be relatively unaffected by fault movement. However, liquefaction and ground shaking would still be threats in the event of a magnitude 7.5 earthquake. The delivery pipe for these wells is a thin-walled, three-sixteenth-inch (.34 cm) in diameter, that is in poor condition, because of numerous breaks and electrolysis damage which occurred in the past. Such pipe could be seriously damaged by a strong earthquake. The source of water in this area is also vulnerable due to the likelihood of contamination by broken sewer lines. Table 3 summarizes earthquake damage to deep pump wells in Salt Lake County. The data is based on the maps presented on Plates 2-5. The wells are numbered on the plates to coincide with numbers in tabular material.

TABLE 3 FOLLOWING PAGE

TABLE 3.--Deep pump wells in Salt Lake County--exposure to earthquake hazard

Well No. (pl. 1)	Fault movement (proximity to fault)	Liquefaction potential	Intensity (MM)	Landslide potential
1	Within 0.2 mi (0.32 km)	Low	VII	Low
2	Within 0.1 mi (0.15 km)	--do---	VII	High
3	----do--------------------	--do---	VII	Low
4	Within 0.2 mi (0.32 km)	Low	VIII	High
5	----do--------------------	Moderate	VII	Do.
6	----do--------------------	Low	VII	Do.
7	More than 0.5 mi (0.75 km)	--do---	VII	Do.
8	----do--------------------	--do---	VII	Do.
9	Within 0.1 mi (0.15 km)	High	VII	Low
10	More than 0.5 mi (0.75)	--do---	VIII	Do.
12	----do--------------------	--do---	VIII	Do.
13	----do--------------------	--do---	VIII	Do.
14	----do--------------------	--do---	VIII	Do.
15	----do--------------------	--do---	VIII	Do.
16	----do--------------------	--do---	VIII	Do.
17	----do--------------------	Low	VIII	Do.
18	----do--------------------	--do---	VIII	Do.
19	----do--------------------	Moderate	IX	Do.
20	----do--------------------	--do----	IX	Do.
21	----do--------------------	Low	X	Do.

Above ground Water Tanks

Above ground water storage tanks in Salt Lake County have a combined capacity of approximately 20 million gallons (71.8 million litres). They are constructed of steel plates, which are riveted together to form cylinders. Many of the storage tanks are located on the bench areas and can supply water to almost all surrounding areas. They do not, however, supply enough water for fire-flow needs.

Tanks which suffered damage in the 1971 San Fernando earthquake were located on poor soil and were extensively damaged at intensities VII-VIII. The predominent mode of failure was displacement leading to buckling in the base of the tank. Inlet and outlet lines to tanks apparently suffered damage almost universally in higher intensity regions. Also, poorly designed tank roofs failed at lower intensities. Proper anchorage can lessen the damage to storage tanks as will ball-and-socket joints used in inlet and outlet lines (Taylor and Ward, 1981).

Locations of water tanks in Salt Lake County are shown on Plate 1. Table 4 summarizes the exposure of above ground water tanks in Salt Lake County to the 4 earthquake hazards shown on Plates 2-5. Each tank is numbered to coincide with tabular material. Most of the 22 tanks are in areas of low potential liquefaction (see Plate 4). Three tanks located near Magna, a city located in western Salt Lake County, however, may be subjected to high liquefaction effects and intense ground shaking during a strong earthquake. It has been shown from information provided from past earthquakes in other areas of the world that at Intensity X, anchored tanks as well as buried reservoirs may be severely damaged (Taylor and Ward, 1981). Other tanks, located on or near bench areas close to Salt Lake City, are near areas of potential fault movement. Also, landslide potential in steep areas is a consideration where tanks are concerned because they can be knocked over or displaced by mass earth movements. Because tanks, for the most part, provide water for very narrow bands of population along the bench areas near Salt Lake City, damage to these facilities would not severely impact Salt Lake County's water supply. Implications, however, lie in the use of similar types of tanks for oil refinery operations which, in addition to potential tank damage and leakage, may suffere damage to piping inlet and outlet connections, and pose a fire hazard.

TABLE 4 FOLLOWING PAGE

TABLE 4.--Above-ground tanks in Salt Lake County--exposure to earthquake hazard

Tank No. (pl. 1)	Fault movement (proximity to fault)	Liquefaction potential	Intensity	Landslide potential
1	More than 1 mi (1.6 km)	Low	VII	High
2	Within 0.1 mi (0.32 .16 km)	--do---	VII	Do.
3	----do-------------------	--do---	VII	Do.
4	0.75 mi (~~0.9~~ 1.2 km)	--do---	VII	Do.
5	1.5 mi (2.4 km)	--do---	VII	Do.
6	----do-------------------	--do---	VII	Do.
7	1.7 mi (2.7 km)	--do---	VII	Do.
8	1.75 mi (2.8 km)	--do---	VII	Do.
9	0.05 mi (0.08 km)	--do---	VII	Do.
10	0.3 mi (0.~~7~~5 km)	--do---	VII	Low
11	Directly on fault	--do---	X	High
12	2 mi (3.2 km)	--do---	VII	Do.
13	5 mi (8.0 km)	--do---	VII or less	Low
14	+8 mi (+12.2 km)	--do---	X	Do.
15	----do-------------------	--do---	X	Do.
16	----do-------------------	--do---	X	Do.
17	----do-------------------	--do---	IX to X	Do.
18	----do-------------------	--do---	IX to X	Do.
19	----do-------------------	--do---	IX to X	Do.
20	----do-------------------	--do---	IX to X	Do.
21	----do-------------------	--do---	IX to X	Do.
22	----do-------------------	--do---	IX to X	Do.

Underground Water-Storage Reservoirs

As shown in Plate 1, many of Salt Lake County's underground-storage reservoirs are on or within 1/4 mi (0.40 km) of the Wastach Fault. An additional five reservoirs are within 1 m (0.61 km) of the fault and could be damaged by fault movement. All of the reservoirs are constructed of reinforced concrete or are lined with concrete. One reservoir, near Murray, is located in a potential Intensity VIII region, a site which also lies in an area of high liquefaction potential. Little data is available for liquefaction effects on underground reservoirs, but a study by Eguchi and others (1982) shows that when liquefaction occurs in the vicinity of an underground reservoir, primary damage consists of tank-wall buckling and damage to external connections. During the 1971 San Fernando earthquake, six of eight buried reservoirs in regions of Intensity X suffered damage. Four reservoirs suffered roof damage, which was generally followed by cracking or bending of sidewalls. Two other reservoirs sustained horizontal cracking in walls. As with other types of storage facilities, leakage can occur at breaks in the inlet and outlet pipes.

Buried reservoirs are able to supply all parts of the Salt Lake County water system except for areas dependent on tanks, which as mentioned, supply thin strips of population located along eastern bench areas. The reservoirs would be able to supply fire-flow over a two-day period in the event of a large earthquake, if they remain operable. According to Rowland Jensen of the Salt Lake City Department of Public Utilities, rupture of outlet connections or sidewall cracking at reservoirs could lead, in some cases, to secondary flood damage, since the natural drainage zones of some reservoirs contain residences, commercial development, and streets (Rowland Jensen, oral commun., 1984). Table 5 summarizes possible damage to individual reservoirs in Salt Lake County. The reservoirs are numbered to coincide with tabular data. Information on this hazard is taken from Plates 2-5.

TABLE 5 FOLLOWING PAGE

TABLE 5.--Underground water-storage reservoirs in Salt Lake County--exposure to earthquake hazard

Reservoir No.	Fault movement (proximity to fault)	Liquefaction potential	Intensity (MM)	Landslide potential
1	On small surface fault system-	Low-------	VII	High
2	More than 1 mi (1.6 km)-------	--do------	VII	Do.
3	Within 0.5 mi (0.32 km)-------	--do------	VII	Moderate
4	----do------------------------	--do------	VII	High
5	More than 1 mi (1.6 km)	--do------	VII	Do.
6	----do------------------------	--do------	VII	Do.
7	----do------------------------	--do------	VII	Do.
8	----do------------------------	--do------	VII	Do.
9	----do------------------------	--do------	VII	Do.
10	----do------------------------	--do------	VII	Do.
11	Within 0.5 mi (0.32 km)	High	VII	Moderate
12	More than 1 mi (1.6 km)	Low	VIII	Low
13	----do------------------------	High	X	Do.

Penstocks and Flumes

Penstocks and flumes, often designed to generate power, could lead to flood damage in the event they were damaged by an earthquake. In the 1971 San Fernando earthquake, a power penstock in an Intensity X region had its supporting piers displaced both horizontally and vertically up to 2 feet (0.6 m). Anchor bolts failed, the pipe elongatged at two expansion joints, and rivets were sheared. The location of a nearby generating plant penstock and flume at the mouth of Big Cottonwood Canyon may present a potential source of damage to the Big Cottonwood Water Treatment Plant located near it. The penstock and flume, owned by Utah Power and Light, and constructed in 1895, are approximately 430 feet (132 m) above the plant. Water flows through the flume and the penstock at about 10 to 32 MGD, or, on the average, between about 7,000 and 22,000 gallons/min (26,460 and 83,160 litres/min). Were a rupture of the penstock and (or) flume to occur, considerable water could be released before a shutoff could be implemented. That water would flow into the Big Cottonwood Treatment Plant. Since the flume is wooden and the penstock is steel, failure of the flume is likely to occur first. Water released in this case is not likely to damage the plant itself. Also, the Big Cottonwood Plant has a backup system in case the inflow penstock is damaged--untreated water can still be admitted through a concrete ditch from the Big Cottonwood Creek. However, this ditch is very near the Wasatch Fault and fault movement could potentially damage all three intake components of the plant--penstock, flume, and concrete ditch. Penstocks and flumes of this construction are not common in Salt Lake County, but the one at Big Cottonwood Canyon is a major facility.

Feeder and Major Distribution Pipes

In order to simplify a water-system network, pipelines can be classified as follows: (1) supply mains which transport water from the source of supply (catchment reservoirs) to the centralized point of distribution (distribution reservoirs), (2) as feeder mains, which begin at distribution reservoirs, and carry water to centralized points of distribution and (3) as distribution mains which supply the individual consumer. Feeder mains can be further divided into primary and secondary mains which supply individual consumers. It is not within the scope of this paper to discuss possible earthquake damage to every main in a system but, it is necessary to discuss possible damage to the supply and larger feeder mains.

Ductile iron pipe is believed to be very resistent to heavy shaking from earthquakes (Taylor and Ward, 1981). Although ductile iron pipe is now being laid in Salt Lake County, except in corrosive areas in the west valley, only about five percent of the system now contains such pipe. Older pipes in the system are of a variety of other types, some of which are very vulnerable to earthquake damage. At least 50 percent of the pipe in the Salt Lake County distribution system is made of cast iron and another 10 percent is asbestos-concrete (Taylor and Ward, 1981).

Vulnerability Models for Distribution Pipe

Figures 8, 9, and 10 show vulnerability models for four types of distribution pipe: asbestos cement, cast iron, welded steel with caulked joints, and welded steel with gas-welded joints. The graphs shown in these figures are differentiated by kind of earthquake effect: fault breakage, shaking, and nontectonic ground failure such as landsliding. Each of these effects is gauged by average number of breaks per 1,000 feet (333 m). The data for these comparisons resulted from studies of 25 worldwide earthquakes (Eguchi and others, 1982). Interestingly, welded steel-welded joint pipes experience less breakage during fault rupture and nontectonic ground failure when compared to the other three types of pipe; however, this same welded steel-welded joint pipe does not perform well during high levels of ground shaking, as indicated by Figure 12.

The 1976 U.S. Geological Survey (Rogers and others) loss report indicated that 75 percent of the total of Salt Lake County could expect to experience Intensity IX effects from a magnitude 7.5 earthquake aldong the Wasatch Fault--Figure 13 indicates the average number of breaks per 1,000 feet (333 m) for each type of pipeline. From this figure, it can be roughly estimated that at Intensity IX levels of shaking Salt Lake County will sustain pipeline damage as follows:

FIGURES 8, 9, 10 FOLLOWING PAGES

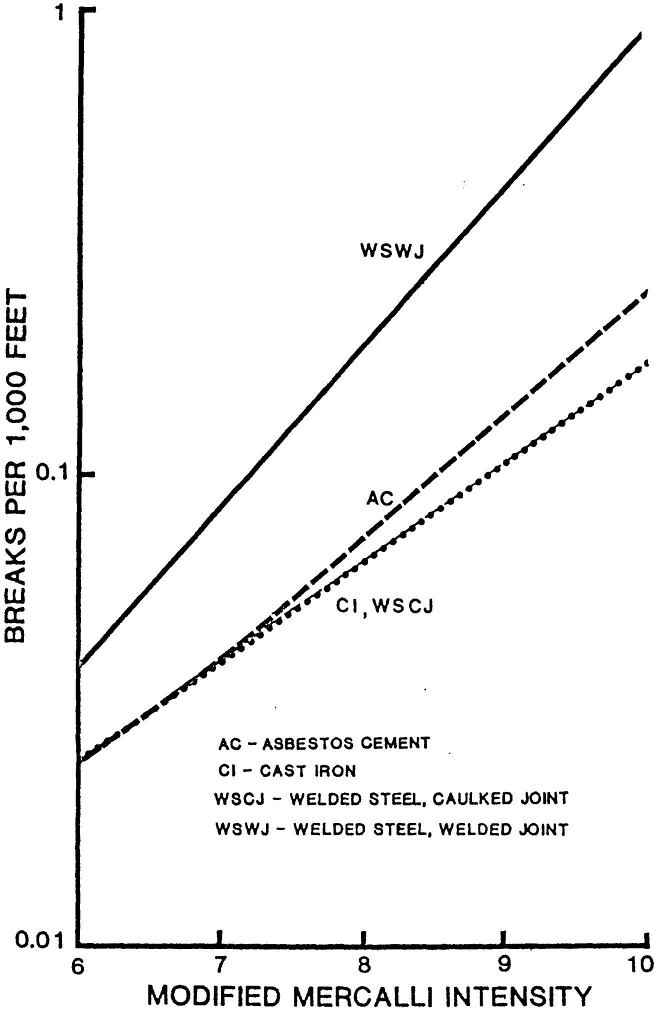

FIGURE 8. Earthquake vulnerability of different types of pipe at different levels of ground shaking. (After Eguchi and others, 1982.)

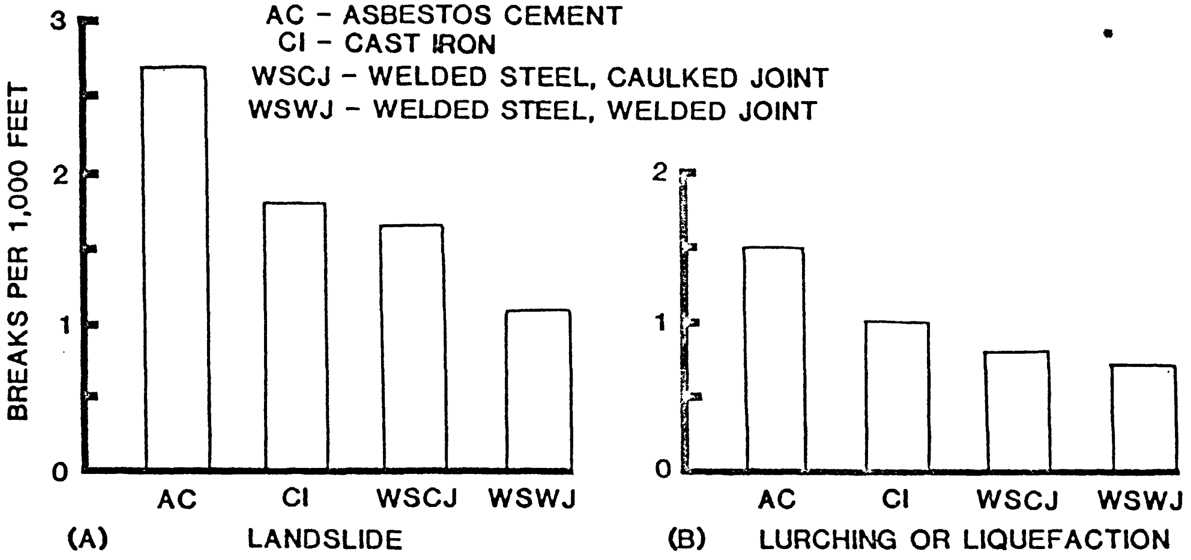

FIGURE 9. Vulnerability relationships of different types of pipe to ground failure and liquefaction. (After Eguchi and others, 1982.)

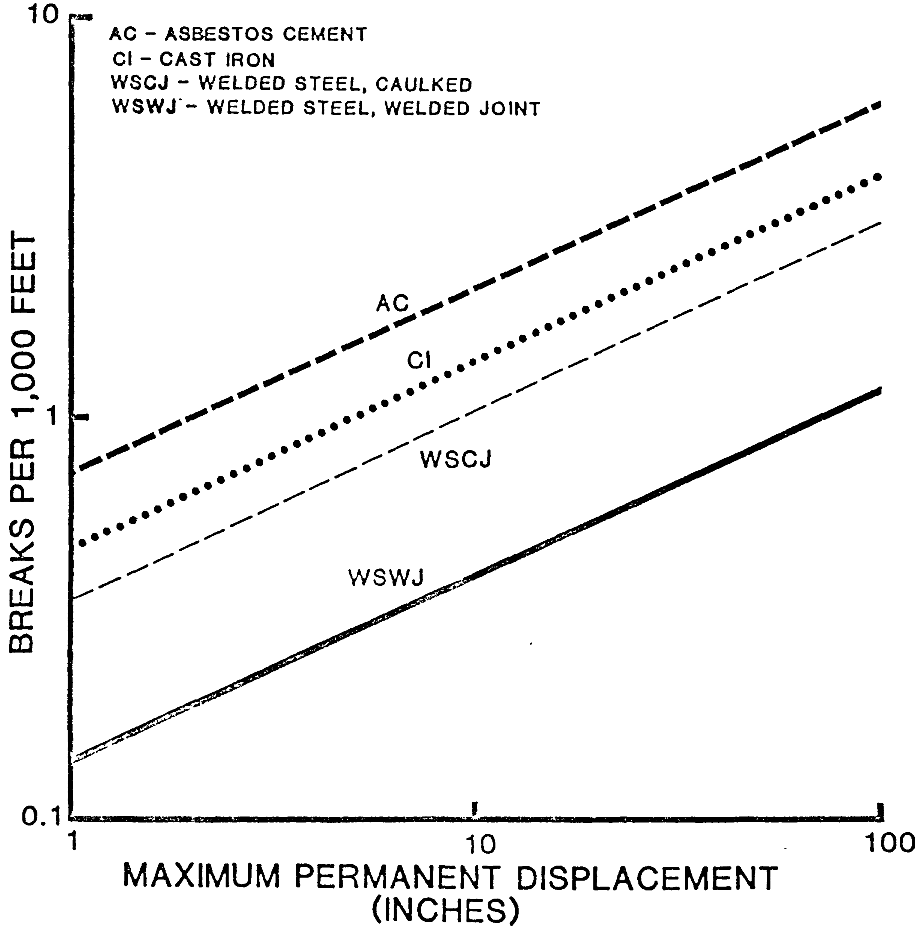

FIGURE 10. Vulnerability relationships for underground water pipe during ground fault displacement.

Asbestos cement lines will likely suffer 0.1 breaks per 1,000 feet (333 m) on average, or equivalently, an average one break per 5,000 feet (1.5 km).

Cast iron lines and welded steel (caulked joints) lines may experience 0.8 breaks per 1,000 feet (333 m) or approximately one break per 10,000 ft or 2.9 miles (3.2 km).

Welded steel (welded joint) lines average approximately 0.4 breaks per 1,000 feet (333 m), or one break per 2,000 feet (666 m).

Again, the previously stated conclusions assume no fault rupture or ground failure and would only be applicable to areas experiencing ground shaking of Intensity IX levels. If fault movement and ground failure were added, a higher frequency of pipe breakages would probably occur.

A study appearing in the Journal of the American Society of Civil Engineers (Dowding and Rozen, 1978), has drawn several conclusions about seismic effects on pipeline structures based on occurrences during two Japanese earthquakes and three California earthquakes:

1. At short periods, surface displacements of pipelines are larger than subsurface displacements.
2. The ratio of surface to underground displacements depends on the type of ground. It is greater for alluvium than for weathered rock and may reach a value of at least 10.
3. Severe tunnel and pipeline damage appears to be inevitable when the tunnel is crossed by a fault which slips during the earthquake.

4. In tunnels and pipelines away from fault rupture, severe damage may be caused by shaking the lining and portals, particularly where the construction is of marginal quality. Substantial reinforced concrete linings are seldom damaged.
5. While it seems reasonable that the competence of the surrounding rock would reduce the likelihood of damage due to shaking, inadequate comparative evidence is available to substantiate this point.
6. Intensity of shaking below ground is less severe than on the surface.

In addition to these general conclusions, more specific observations for the behavior of specific pipelines were discussed, based on the 1971 San Fernando earthquake experience:

1. Modern electrically butt-welded pipelines survived; old acetylene (pre-1940) bell-spigot welds and riveted or cast lines failed.
2. On active fault rupture crossings, subsurface structures generally failed. Butt-welded lines were not tested across faults.
3. In areas of mass movement, that is, landslide or liquefaction, buried structures failed except for butt-welded pipelines.

Similar experience has also been collected on the behavior of undergound box culverts. Major damage in those instances was attributed directly to fault displacements, with ground acceleration a contributing factor at but one location.

A second study which examined earthquake effects on tunnels and pipelines (Dowding and Rozen, 1978) examined effects of nine earthquakes of magnitudes ranging from 6.4 to 8.4. The tunnels studied were from 10 to 20 feet (3 to 6.1 m) in diameter--larger than those now currently in use in Salt Lake County. Nevertheless, insights applicable to for Salt Lake County may be gained. It was found that pipes and tunnels failed due to three basic earthquake effects--ground shaking, fault movement, and ground failure (landsliding, liquefaction, etc.). Several conclusions about pipeline and tunnel failure were drawn:

1. Collapse of tunnels from shaking occurs only under extreme conditions. It was found that there was no damage in both lined and unlined tunnels at surface accelerations up to 0.1 g. In addition, very few cases of minor damage due to shaking were observed at surface accelerations up to 0.25 g.
2. Tunnels are much safer than above ground structures for given intensity of shaking. While only minor damage to tunnels was observed at Mercalli Intensity VIII-IX levels, the damage in above ground structures at the same intensities is considerable.
3. Tunnels in poor soil or rock, which suffer from stability problems during excavation, are more susceptible to damage during earthquakes.
4. Tunnels deep in rock are safer than shallow tunnels.
5. Total collapse of a tunnel was found associated only with movement of an intersecting fault.

A Word About Fire

Experience has shown that a potentially major consequence of water pipeline breakage resulting from earthquakes is the unchecked spread of fire. In the case of the 1906 San Francisco earthquake, damage to three major supply conduits and to city distribution mains resulted in the loss of all potable water supply to the city of San Francisco. This loss of water also left the city defenseless against the 50 fires which erupted during and after the earthquake and, as a result, fires raged for three days, leaving only two percent of the shaken city unburned. Later, it was found that there were over 300 water line breaks in the San Francisco area. However, there were in excess of 23,200 service connections broken, largely due to the collapse of burning buildings rather than to soil failure due to the earthquake itself (Schussler, 1906).

The 1971 San Fernando earthquake, which is considered only a moderate event, was directly responsible for the outbreak of 116 fires. In this case, however, all fires were contained due to the presence of normal and near normal fire department staff levels and the generally distributed nature of these fires. However, water distribution systems were impaired throughout most of the northern portion of San Fernando, necessitating a lareg number of mobile tank trucks for provision of fire-fighting and drinking water (Murphy, 1971).

In Salt Lake County, water needed to fight fires must flow at a minimum of about 30 ft$^{3/s}$ ($_{10\text{m}}{}^{3/s}$). Most facilities such as deep well pumps, major aqueducts, and underground reservoir outlets are capable of providing the flow rate necessary to fight fire. Tanks, however, do not.

CONCLUSIONS

In summation, intensity may be the best way to generalize the expected damage patterns to systems with known construction and when information on past patterns of damage to these same types of components is known and can be compared. It is not definitively known what maximum intensity a postulated magnitude 7.5 earthquake will produce, or what the regional pattern will be, but it is fairly safe to hypothesize that a magnitude 7.5 earthquake located near Salt Lake City, on the Wasatch Fault will probably generate maximum intensities in the IX to X range (as shown on Plate 3). High intensities are expected in areas overlain by lake deposits which composes the surface soils of the Salt Lake Valley, an idea that seems to be substantiated by site aamplification studies previously discussed.

At Intensities VI and VII, poorly sited tanks and pipes in poor condition may break. The wooden flume at Big Cottonwood Treatment Plant may rupture so that the creek must serve as a means of flow on the inlet side of this facility. The generating station at Big Cottonwood Canyon may suffer enough damage to require the dependence upon other sources of power. There is also a chance that the 3rd East pumping station will be damaged.

As observed in past earthquakes at intensity VIII, pipe breakage becomes widespread. Some unanchored mechanical systems may cease to function. Some inlet or outlet connections may break. Some wells that are near sewage lines or cesspools may become contaminated. There may be some damage to the deteriorated and (or) unreinforced aqueduct or conduit lines such as the Salt Lake aqueduct and the Big Cottonwood conduit. If intensities higher than VII are not experienced and no system failures such as widespread power outage occur, it should be possible to make repairs quickly and to supply water. It was noted in Eguchi and others (1982) that in many earthquakes, facilities in intensity-VIII areas or higher experienced power outages. It is known that liquefaction can occur at this intensity level and possibly even at lower levels. Settling and (or) buckling of tanks as well as inlet-outlet breakages could occur especially in areas of differencial compaction due to liquefaction.

At Intensity IX, minor fault offsets may damage structures in the zone of deformation, such as tanks and buried reservoirs and possibly the Salt Lake aqueduct or Cottonwood conduits. Considerable damage would occur to pipes, and also to outlet connections. Treatment plants affected at such intensities may be rendered nonfunctional (except for bypass use if chlorine reserves exist) because of power outage or other breakdown of mechanical systems, such as air compressors, or outlet ruptures. Tanks are expected to buckle. Damage will likely occur to deteriorated sections of the aqueducts and conduits.

At Intensity X, pipe damage may be beyond immediate repair, especially in areas where pipes are smaller or already in poor condition. Major fault offsets may damage the Salt Lake Aqueduct and/or Cottonwood Conduits. Cracking will occur in reservoir walls, and reservoirs with poorly designed roof systems may suffer roof damage (Taylor and Ward, 1981).

Salt Lake County will probably experience slope failures only in areas of steep slopes such as the bench areas (on the east side of the valley) which do not slope gently, but rather abruptly and steeply. If Salt Lake County continues to experience wetter than normal years, the situation will definitely be aggravated and landslides may occur even at lower levels of shaking. While landslides cannot usually be prevented, the towns in central Utah, faced with the inevitability of landslides have devised back-up water systems, some which were tested successfully during the recent May 1984, landslides.

Less is known about what actually will happen if liquefaction occurs in the Salt Lake Valley--there is no past history of liquefaction in the valley. Conditions will usually rule out landslides and liquefaction occurring at the same site because of differing site conditions which facilitate these phenomenon. For example, soils that are prone to liquefaction are not usually located on a slope; rather, they accumulate in valleys. In this sense, there is little concurrent hazard from liquefaction and landslide.The information presented in tables previously in this study shows no water system facility built on a high liquefaction potential site which also has a high landslide potential.

Fault movement and displacement are constrained to an immediate area within the vicinity of the Wasatch Fault--but during large displacements, the effects may be geographically more widespread. Fault movement may only affect segments of the water system network and facilities which are closest to it.

Based on information provided by the four hazard maps (Plates 2-5), the six purification plants located in Salt Lake County are vulnerable mainly to potential landsliding. Four of these plants are very close to the Wasatch Fault and could suffer structural damage in the event of a large earthquake.

Liquefaction potential is low at the treatment plant sites. The Draper Plant may experience heavy ground shaking and this same plant seems to be the most vulnerable to the earthquake effects discussed.

The Salt Lake Aqueduct and Big Cottonwood Conduit may be the most vulnerable of the major aqueducts to at least three earthquake-relate effects: landsliding, liquefaction, fault movement and possibly heavy shaking. The Jordan Aqueduct could be primarily affected by liquefaction effects and possibly heavy shaking.

Six of the deep pump wells in Salt Lake County are located in areas of high landslide potential. Seven are within .2 miles (.32 km) of the Wasatch Fault. Seven of these wells are in areas of high liquefaction potential and 11 wells may experience shaking at intensity levels of VIII-X. Tanks located in the eastern part of the Salt Lake Valley are vulnerable to effects from landslides and fault movement. Wells located in the western part of the valley are more prone to effects from liquefaction and heavy ground shaking.

Eleven above ground tanks in Salt Lake County could be damaged by landslides due to an earthquake. These are located in the eastern part of Salt Lake Valley. Nine tanks located in the western part of the valley are in areas of low landslide potential but are located in areas that could be heavily shaken. Liquefaction potential is low in all areas where above ground tanks are located. Tank number 11 is located on the Wasatch Fault, and others are located within .1 miles (.16 km) of the Wasatch Fault.

Eight underground reservoirs are located in areas of high potential landsliding. One is located in an area of high potential liquefaction and Intensity X ground shaking effects. The liquefaction potential is low for the soil on which 85 percent of the reservoirs are located. Landsliding and heavy ground shaking may be the predominant hazards to underground water storage reservoirs.

Planning Considerations

Most of Salt Lake County's population lives in the eastern side of Salt Lake County--an area which has the highest probability of experiencing the most intense hazards from a magnitude 7.5 earthquake. Most plans for water system expansion involve the building of additional reservoirs in the western slope areas of the Wasatch Mountains, with pipelines and conduits delivering the water to the valley. Very little development is planned for water sources in the Oquirrh Mountains, since runoff and snow accumulation render them a much less reliable source of water (Salt Lake County Area Wide Water Study, 1981).

Hazard maps and subsequent analysis and interpretation of them can serve as useful planning tools. For example, when planning a new treatment facility, these maps can indicate where a back-up system might be needed, and serve as a guide for a uniform standard of construction. Indeed, much is known about reinforcing structures against earthquakes. If there is a reasonable choice in locating a facility, hazard maps should make the selection of the safer site easier. Hazard maps also indicate areas of multiple hazards, which might increase the perceived risk of building a structure at that site. Proper reinforcement can then be planned. Finally, emergency procedures can be planned for areas of likely damage.

Suggested Mitigation--An Example

The following discussion outlines some key procedures implemented by Mountain Fuel Supply (Salt Lake City) in order to lessen the impact of a damaging earthquake on its gas pipeline system. Gas pipelins distribution systems are not dissimilar to water distribution systems in that they are often composed of the same materials, have valve systems for shutoff, run underground for the most part, and have component above-ground structures for control and maintenance.

Mountain Fuel Supply has an active cast iron pipe retirement program. Cast iron pipe is acknowledged to be the most brittle of the various materials used in piping systems and the most brittle of the various materials used in gas piping systems. The company also maintains a corrosion control department where nine members have the responsibility of monitoring pipelines for corrosion and, either electrically protecting the facility or, if corrosion induced leakage is suspected, recommending replacement.

A decision was made in the early 1970's to utilize polyethylene pipe in Mountain Fuel's distribution system. Thirty-seven per-cent of its system is composed of polyethylene, a type of plastic which is very ductile and is one of the best materials available to withstand deflections resulting from ground movement. Additionally, when this pipeline is installed it is "roped" from one side of the trench to the other, to help the pipeline withstand Mountain Fuel also maintains a very extensive valve system (over 550 valves in the Salt Lake area alone), which when used in an emergency can isolate areas containing approximately 5,000 people. The location of these valves are found in emergency valve books which are available to key personnel within the company. Also, continuously updated maps are maintained which show all locations of subsurface piping, along with areas of known faulting.

Current design calls for above-ground pressure reduction equipment to be housed in steel buildings, rather than the previously used design of brick and stucco. These buildings, in addition to providing superior shear strength are economical to use.

Lastly, Mountain Fuel provides public information about reducing earthquake hazards from damaged gas lines in the home, through presentations to community groups--it also maintains a written emergency plan dealing with response to all types of emergencies. Its employees are also kept aware of their emergency responsibilities (written communication, Peter W. McDonough, P.E., Salt Lake North Division engineer, Mountain Fuel Supply Company, Salt Lake City, Utah).

Many of these mitigation plans used by Mountain Fuel Supply can be applied to water distribution systems, although slight alterations would have to be implemented, allowing for differences in the two systems.

Recommendations for Further Study

This study is a general overview and an attempt to present current work on the nature and effects associated with the occurrence of a large earthquake with implications to water supply systems of Salt Lake City. Salt Lake County is unique because it is subject to a number of hazards, about which considerable knowledge information has been accumulated. However, gaps exist in the application of geologic, geophysical, and related hazard studies to mitigation.

A more detailed study of hazards to the water system is required beyond the overview presented here. The complex network of facilities and an even more complex organization of water jurisdiction and ownership must be sorted out. A large scale map of all pipelines and other facilities would be helpful. A study of the feasibility of a uniform policy of reinforced construction of facilities is appropriate as well as implementation of a policy of retrofitting unsafe structures to be earthquake resistant. Irrigation water is still intricately tied up with the domestic water supply and distribution; a fact which could possibly be an asset for emergency procedures and back-up systems. Waste water treatment plants are also intimately associated with the water system--these facilities should be studied in greater depth.

Intensity studies are currently being re-evaluated as new evidence about earthquake effects arises from actual events. The MM Intensity Scale has not been radically changed since its inception (Wood and Neumann, 1931) and refinement is necessary. As mentioned, site amplification studies are being further refined and improved--however, there is a need for more such studies in other areas of Utah and wherever a high earthquake hazard potential exists.

Liquefaction effects may occur sporadically since certain preconditions such as soil type and high water table must exist. Many places in the world do not experience liquefaction effects during an earthquake, and if they do, the effects are not always in the vicinity of structures. Maps such as those prepared by Utah State University (potential liquefaction) are extremely helpful when accompanied by other hazard information. Further mapping of this hazard is necessary.

REFERENCES

Algermissen, KS.T., and Steinbrugge, K.V., 1984. Seismic hazard and risk assessment: some case studies, Proceedings, First Meeting of the International Working Group on Natural Disasters and Insurance, UNDRO, Geneva, Switzerland, 26 p.

Algermissen, S.T., Perkins, D.M., Thenhaus, P.C., Hanson, S. T., and Bender, B.L., 1982, Probabilistic estimates of maximum acceleration and velocity in rock in the contiguous United States, U.S. Geological Survey Open-File Report 82-1033, 99 p.

Anderson, L., 1984. Liquefaction for Salt Lake City County, Utah, Utah State University, Logan Utah, this volume.

Arabasz, W. J., Smith, R. B., and Richins, W. D., 1979. Earthquake studies in Utah, 1850-1978. University of Utah Seismograph Station, Department of Geology and Geophysics, University of Utah, Salt Lake City, Utah, Special Publication, 552 p.

Brown, R. D., Jr., Vedder, J. G., Wallace, R. E., Roth, E. F., Yerkes, R. F., Castle, R. O., Waanamen, A. O., Page, R. W., and Eaton, G. P.,1967, Surface geologic effects, water- resources aspects and preliminary seismic data: The Parkfield-Cholame, Calif. earthquakes of June-August, 1966, U S., Geological Survey Professional Paper 579, 66 p.

Davis, F. D., 1983, Geologic map of the central Wasatch Front, Utah, Utah Geological and Mineral Survey Map 55-a.

Dowding, C. H., and Rozen, A., 1978, Damage to rock tunnels from earthquake shaking, Journal of the Geotechnical Engineering Division, American Society of Civil Engineers, 104, no. GT2, pp. 62-78.

Eguchi, R. T., Philipson, L. L., and Wiggins, J. H., 1982. An approach for evaluating the earthquake performance of water supply systems in International Earthquake Microzonation Conference Proceedings, June 28, 1982, Seattle, Washington, pp. 1625 - 1652.

Hays, W. W., Algermissen, S. T., Miller, R. D., and King, K. W., 1978, Preliminary ground response maps of the Salt Lake City, Utah area, Proceedings, Second International Conference on Micorozonation, San Francisco, Calif.

Keefer, D. K., 1984, Landslides caused by earthquakes, Geological Society of America Bull., vol. 95, April, 1984, pp. 406-421.

Machette, M. N., 198_, Quaternary geology along the Wasatch Front--evidence foradditional segmentation and for large changes in slip rate on the Wasatch fault zone, in Hays, W. W., and Paula Gori, eds., Evaluation of Urban and regional earthquake hazards and risks in Utah, U. G. Geological Survey Professional Paper, pp __ - __.

McDonough, P., 1984, A Utah utility addresses seismic hazards. Proc. of the Ninth World Conference on Earthquake Engineering, San Francisco, California, Vol. 7, pp. 593-600.

Metropolitan Water District of Salt Lake City, Salt Lake County Water Conservancy Distict, 1982. Salt Lake County Area-Wide Water Study.

Murphy, Leonard, ed., 1971, The San Fernando, California, earthquake of February 9, 1971, U. S. Geological Survey Professional Paper 733, vol. 2.

Rogers, A. M., Algermissen, S. T., Hays, W. W., and Perkins, D. M., 1976, A study of earthquake losses in the Salt Lake City, Utah area, U. S. Geological Survey open-file report 76-89, 357 p.

Schussler, H., 1906, The water supply of San Francisco, California, before, during and after the earthquake of April 18, 1906 and the subsequent conflagration, Spring Valley Water Co., California, 103 p.

Schuster, R. L., and Krizek, R. J., eds., 1978, Landslides: analysis and control, Special Report 176, National Academy of Sciences, Transportation Research Board, 210. Constitution Ave., N.W., Washington, D.C.

Schwartz, D. P., Swan, III, F. H., and Cluff, L S., 1984, Fault behavior and earthquake recurrence along the Wasatch zone, in Workshop on Evaluation of Regional and Urban Earthquake Hazards and Risk in Utah, August 13-16, 1984, Salt Lake City, Utah, U. S. Geol. Survey open-file report 84-763, 950 p.

Taylor, C., and Ward, Delbert, 1981, Seismic risk assessment of public culinary water supply systems in Utah, and recommendations for risk reduction, Seismic Safety Advisory Council Publication, State of Utah, Salt Lake City, Utah, 91 p.

Uniform Building Code, 1976, International Conference of Building Officials, 5360 S. Workman Mill Road, Whittier, California 90601, 950 p.

Van Horn, Richard, 1972, Slope map of the Sugar House quadrangle, Salt Lake County, Utah: U.S. Geol. Survey Misc. Geol. inv., Map I-766-C.

Wiggins, J. H., Slosson, J. E., and Krohn, J. P., 1978, Natural hazards--earthquake, landslide, expansive soil loss models, J. H. Wiggins, Co. Technical Report, Redondo Beach, Calif.

Wood, H. O., and Neuman, F., 1931, Modified Mercalli Intensity Scale of 1931, Bull. Seis. Soc. Amer., 21, pp. 277-283.

Yanev, P., 1974, Peace of mind in earthquake country, Chronicle Books, San Francisco, California, 304 p.

NEWSPAPERS

The Pyramid, May 9, 1984, Mt. Pleasant, Utah.

The Manti Messenger, Thursday, May 17, 1984, Manti, Utah.

Salt Lake Daily Tribune, September 16, 1883, Salt Lake City, Utah.

PERSONAL COMMUNICATIONS

Terry G. Way, oral commmunication, Water Quality Engineer, Division of, Flood Control and Water Quality, Salt Lake County, Augu98412,

Rowland Jensen, oral communication, Salt Lake City Dept. of Public Utilities, September 5, 1984.

Scott Haslam, oral communication, Water Resources Division, Salt Lake County, September 13, 1984.

John Spitzley, Utah State University, Logan, Utah, written communication, September 21, 1984.

MAKING THE IMPLEMENTATION PROCESS OF THE NATIONAL EARTHQUAKE HAZARDS REDUCTION PROGRAM WORK IN UTAH

by

Walter W. Hays
U.S. Geological Survey
Reston, Virginia 22092

ABSTRACT

Implementation of loss-reduction measures designed to mitigate the earthquake hazards of ground shaking, surface fault rupture, earthquake-induced ground failure, regional tectonic deformation, seiches, and (where applicable) tsunami runup in earthquake-prone parts of the Nation is a complex long-term process. Experience has shown that five interrelated elements are required to foster the process of implementation in a community:

- A comprehensive body of geologic, seismological, and engineering data and accumulated knowledge that is available for use by a wide variety of user groups to mitigate specific earthquake hazards.

- People who are trained, concerned, and committed to performing explicit actions to mitigate earthquake hazards.

- Programs that are focused, integrated, and coordinated in terms of specific short- and long-term goals to conduct research and mitigation activities.

- Experience with at least one damaging earthquake that provides a realistic basis for assessing the risk to the community, or for defining an

earthquake scenario that is considered to be representative of what could happen in the community.

- o The availability of practical, proven techniques or measures for reducing potential losses from earthquake hazards that can be applied in a cost effective manner in the community by a wide range of individuals, groups, institutions, and agencies.

Although all of these elements are required to accomplish the process of implementation, worldwide experience has shown that the greatest progress in implementation in a community is made after a damaging earthquake occurs. Consequently, the challenge faced by every earthquake-prone part of the Nation is to implement loss-reduction measures before the damaging earthquake.

Utah has all of the elements in place now to accomplish an effective program of implementation during the next 10 years. Such a program will prevent the next damaging earthquake from being a disaster.

INTRODUCTION

Objectives and Scope

This paper describes the generic elements of the process to foster implementation of earthquake loss-reduction measures. Implementation, a dynamic process, has been tested since 1977 in the National Earthquake Hazards Reduction Program (NEHRP). The focus of the paper is the Wasatch front area, Utah, where a concentrated effort in the NEHRP began in 1983 to accelerate the research being conducted mainly in the universities and in the private sector and to identify the sequence of interrelated actions and activities that cause basic data and knowledge of earthquake hazards gained from research to be transformed into public policies and loss-reduction measures. When fully implemented in a community in an earthquake-prone region, these policies and measures will lead to greatly reduced losses from the earthquake hazards of ground shaking, surface-fault rupture, earthquake-induced ground failure, regional tectonic deformation, seiches, and (where applicable) tsunami runup. Damaging earthquakes will not be disasters.

Information and experience gained by USGS, FEMA, National Science Foundation, and National Bureau of Standards since 1977 in the NEHRP have shown that the implementation process is as complex as any reasearch study and that many issues (i.e., questions for which expert opinion is divided between "yes" "no") must be dealt with efficiently over a long time frame. In Utah and every other earthquake-prone region of the Nation, three principal issues impact the implementation process. They are:

o Will implementation of loss-reduction measures happen without the occurrence of a major earthquake (Figure 1)?

FIGURE 1 FOLLOWS TEXT

- How much more will loss-reduction measures cost?

- Should the required money come from reprogramming of existing programs, or from new sources? That is, who pays and who wins or loses in the funding battles.

CRITICAL ELEMENTS OF THE IMPLEMENTATION PROCESS

Experience in the NEHRP has shown that implementation of loss-reduction measures tends to happen when 5 critical interrelated elements are present (Figure 2). Each element is described below.

FIGURE 2 FOLLOWS TEXT

Element 1: Existence of Technical Data Bases--Effective implementation requires explicit knowledge of the cause and effect relations of the earthquake hazards of ground shaking, surface fault rupture, earthquake induced ground failure, regional tectonic deformation, seiches, and (when applicable) tsunami runup in the urban area (Figure 3). The quantity and

---

FIGURE 3 FOLLOWS TEXT

---

quality of the geologic, seismological, and engineering data are the two most important factors that facilitate assessments of the earthquake hazards and risk as well as feeding the process of devising and implementating loss-reduction measures.

The critical issues of implementation that are directly related to the technical data bases of an urban area in Utah are:

- Can the existing data be utilized to foster implementation of loss-reduction measures, or must the data be translated, extrapolated or augmented by theory, experiments, and new data gathering programs?
- Does Utah have enough data for implementation of loss-reduction measures, at least in a preliminary way?
- Are the data at the right scale to achieve the desired applications?
- Is it possible to extrapolate beyond the limits of the data bases to address specific requirements of users in a reasonable, yet conservative manner?

In general, technical data are required on three scales:

- global (map scale of about 1:7,500,000 or larger) to give the "big picture" of the inter- and intra-plate tectonic forces.

- regional (map scale of about 1:250,000 or larger) to define the physical parameters and their range of values that provide a framework of understanding of the spatial and temporal characteristics of earthquake hazards in a region.

- local (map scale of about 1:24,000 or smaller) to determine the physical parameters and their range of values that control the local earthquake-resistant design requirements. (Note: site-specific design requirements are not covered by the regional- or local scale-data; they are based on site-specific data.)

All of the available data must be integrated and analyzed. Uncertainty must be quantified, as appropriate, to obtain explicit answers to six questions:

- Where have earthquakes occurred in the past? Where are earthquakes occurring now?

- How big in terms of epicentral intensity and/or magnitude were the past earthquakes? Has the maximum-magnitude earthquake occurred?

- What physical effects (hazards) have past earthquakes caused? What was their spatial and temporal distribution? What was their level of severity?

- What were the causative mechanisms for each earthquake? Each hazard?

- How often (on the average) do earthquakes of a given magnitude (or epicentral intensity) occur? How often (on the average) does ground shaking of a certain level occur?

- What are the viable options for mitigating the earthquake hazards expected to occur in the region in a 50 year exposure time (i.e., the useful life of an ordinary building)?

Limitations of the Technical Data - Typical limitations of the technical data bases (in the context of the Wasatch Front) include the following:

- The Wasatch fault zone consists of listric-type faults buried beneath the surface. The surface and subsurface trances of the faults can not be mapped in all cases except by geophysical methods, which have some ambiguity.

- Knowledge of Late Quaternary (125,000 years before the present) and Holocene (10,000 years before the present) faulting is limited because of the lack of suitable stratigraphic exposures or inadequate resources to establish a paleoseismicity investigative program.

- Knowledge of shear-wave velocities, thicknesses, water content, and dynamic strain-dependent properties of the soil-rock columns in an urban area is meager.

- Data needed for site-specific design are not generally available. Typically these data are very limited, or they are unabailable because of proprietary interests.

- The catalog of historical seismicity in the region is short, unreliable, and incomplete for large magnitude earthquakes.

- Seismicity networks are nonexistant or archaic, or they have detection thresholds that limit analyses and applications of the data.

- Isoseismal maps of historic earthquakes are either inaccurate, inconsistent, or too general or too conservative.

- No strong ground motion records of past earthquakes exist in the region, or if they exist, the data sample has significant gaps (for example, no near-field data from large- to great-magnitude earthquakes, no soil-rock instrument pairs, no attenuation arrays, etc.).

Element 2: Trained, Concerned, and Committed People--Utah needs trained people to analyze the technical data bases, to extrapolate beyond the limits of the data, and to translate the basic data into maps and other products that can be applied in the community as practical and reasonable loss-reduction measures (Figure 4). The critical issues of implementaion that are directly related to Utahans are:

FIGURE 4 FOLLOWS TEXT

- Is appropriate training available to transfer the available knowledge to Utah professionals in a way that will impact practice?

- Can Utahans who have never experienced a damaging earthquake in their lifetime be motivated to have increased concern about earthquakes and their effects?

- Can Utahans who have been uncommitted in the past with respect to implementation of loss-reduction measures be transformed into leaders who are committed to providing leadership for changing the "status quo" of implementation in their community?

The people who are making the implementation process happen in Utah communities must deal with a wide range of geologic, seismological, and engineering data and produce credible, practical loss-reduction measures. To succeed, they must know that fundamental differences exist in the perspectives of scientists/engineers and decisionmakers (see Table 1), and they must have experience in minimizing these differences.

TABLE 1 FOLLOWS TEXT

Types of Products Needed for Implementation - The people who foster the process of implementation in Utah must be able to utilize the following types of technical products:

- Maps showing the actual and inferred surface and subsurface locations, types, and spatial extent of faults and other geologic structures in the region known or suspected to have seismogenic potential.

  Objective: To establish the location, physical characteristics, and earthquake potential of each individual seismogenic source in the region.

- Logs and maps of trenches across specific fault zones, emphasizing detailed studies of the Late Quaternary and Holocene stratigraphy and the age of faulting and paleoliquefaction episodes.

  Objective: To establish slip rates and average recurrence intervals of major earthquakes on specific faults; to define the paleoseismicity of the fault zone.

- Maps showing the subsurface configuration of faults and structures having seismogenic potential.

Objective: To define the plastic-brittle zone of the crust and to quantify the fault rupture model.

- Maps showing the geometry and physical properties of the soil-rock columns in the region, including shear wave velocities, thicknesses, and water content.

Objective: To define the regional seismic-wave-propagation model, local soil response, and soil failure models.

- Maps of topography.

Objective: To assist in the definition of the slope stability, a key parameter for evaluating the potential for landslides.

- A reliable and complete catalog of preinstrumental-and instrumentally-located earthquakes containing the epicenter, hypocenter, and size of the earthquake as well as a description of the ground-shaking and ground-failure effects.

Objective: To define where?, how big?, how often?, and what happened? in past earthquakes.

- Maps of the historical and current seismicity.

Objective: To define where earthquakes have occurred and to delineate seismogenic source and seismotectonic models precisely.

- Isoseismal maps of past major earthquakes.

  Objective: To define the damage distribution in past major earthquakes and to derive an appropriate seismic-wave-attenuation relation for the region.

- Seismotectonic maps showing the relationship between earthquakes and geologic structure.

  Objective: To define seismogenic sources and a regional seismotectonic model.

- Maps showing the distribution of stress in the crust and its correlation with geologic structures and the contemporary strain field.

  Objective: To define the ultimate causative mechanism for earthquakes.

- Strong motion records from earthquakes having magnitudes ranging from 5 to 8 or greater and epicentral distances ranging from the epicenter to 600 km. The records should include both free-field and building locations.

  Objective: To define the peak amplitudes, spectral composition, and duration of shaking for a wide range of earthquake magnitudes, epicentral distances, and soil-rock columns.

- Data on seismic-wave attenuation.

Objective: To define frequency-dependent seismic-wave attenuation relations.

- Data on soil (or ground) response.

Objective: To define the frequency- and strain-dependent characteristics of ground response. To determine linear and nonlinear behavior under different ground-shaking loads. To identify the potential for soil-structure interaction.

- Data on building response.

Objective: To define how various types of buildings respond to a broad range of earthquake loads. To determine the damage thresholds and damage states under large amplitude and long-duration earthquake loads. To identify the potential for soil-structure interaction.

- Data on respons of lifelines.

Objectives: To define how lifelines respond to a broad range of earthquake loads.

- Data on damage distribution.

Objective: To develop fragility curves for a range of damage states and a broad range of earthquake loads that can be used in loss estimation scenarios.

- Lessons from past earthquakes.

  Objectives: To take advantage of the fundamental knowledge gained from the "laboratory" provided by a damaging earthquake to determine how people as well as buildings and lifelines of various types perform in an earthquake.

Element 3: Focused, Coordinated, and Integrated Programs-- The data, information, and people provide the resource base for programs in Utah. The programs include research studies; the assessment of earthquake hazards, potential vulnerability, and risk for parts or all of an urban area; a seismic safety organization; mitigation and preparedness actions; and the implementation of new and improved loss-reduction measures. The success of each program depends on: how well it is focused, the degree of integration, and the extent of the coordination between the various disciplines and agencies. The critical issues of implementation that are directly associated with programs in Utah are:

- Do the expected benefits of the program justify the cost and the anguish associated with reallocation of resources from existing programs?

- Are the technological, societal, and political considerations appropriately balanced?

- Does the program have a definite ending point; if not, should it? Can the end point be negotiated before the program begins?

Element 4: A Damaging Earthquake, The "Laboratory"--A damaging earthquake provides the best opportunity to acquire unique geologic, seismological, engineering, and social science information and to foster implementation of specific loss-reduction measures in a community. The critical issues of implementation in Utah that are directly related to the occurrence of a damaging earthquake are:

- Does the earthquake provide experience and relevant information for stimulating increased earthquake preparedness in Utah communities?
- Can "lessons" that are useful for Utah be extracted from the earthquake experience in another part of the Nation or world?
- Is Utah prepared to conduct post earthquake investigations to increase its knowledge base?

Postearthquake Investigations - Five types of investigations are typically conducted after a damaging earthquake. They provide a rapid way of infusing new data and knowledge (Hays, 1986) into the process of implementation:

- Geologic studies--field investigations to determine the nature, degree, and spatial distribution of surface faulting, regional tectonic deformation, landslides, liquefaction, and wave inundation from seiches and tsunami runup.

- Seismological studies--measurement programs using arrays of portable seismographs to locate earthquakes comprising the aftershock sequence, to define the spatial extent of the fault rupture zone and its temporal changes, and to determine the focal mechanisms of the earthquake.

- Engineering Seismology Studies--measurement programs using arrays of portable strong motion accelerographs and broad band seismographs to measure the characteristics of strong ground motion at various epicentral locations underlain by various soil-rock columns. Both the main shock and the aftershock sequence are utilized.

- Engineering Studies--Investigations on a building-by-building scale to determine the nature, degree, and spatial distribution of damage to a wide range of structures, including: low-, medium-, and high-rise buildings, lifelines, and critical facilities.

- Societal Studies--Investigations to determine how the populace reacts before, during, and after an earthquake and to devise ways the new technical information can be transformed into public policy and new or improved loss-reduction measures.

Worldwide experience has shown that comprehensive studies conducted after an earthquake provide a basis for:

- Improving understanding of the causative physical mechanisms of ground shaking, surface faulting, regional tectonic deformation, landslides, liquefaction, seiches, and tsunamis.

- Correlating the occurrence of earthquakes with concepts of plate tectonics and with regional tectonic elements to define seismogenic sources (and, in coastal areas, tsunamigenic sources).

- Identifying regional tectonic elements and their seismogenic potential on the basis of the rate of activity of specific faults and the correlation of regional seismicity and geologic structure.

- Improving the knowledge of the amplitude, spectral composition, temporal, and spatial distribution of ground shaking and its causative relation with damage in buildings and triggering of other physical effects such as ground failures.

- Extending the state-of-knowledge on seismic zoning, and seeking to push the limits of seismic microzonation to bounds set by the local and site-specific engineering scales.

- Improving the state-of-practice on land use, engineering design, and construction.

- Improving the seismic-design provisions of building codes.

- Improving the state-of-practice in lifeline engineering.

- Motivating legislation to incorporate, implement, and enforce new knowledge that will lead to loss reduction.

- Motivating new and revitalized programs of research, mitigation, preparedness, response, and recovery.

- Calling for change in public policy concerning earthquake hazards.

Investigations of Important Earthquakes - A number of important earthquakes have been investigated in the past two decades that can benefit Utah. These investigations have contributed important new knowledge toward the long-term goal in the United States of reducing potential losses from earthquake hazards. The following brief accounts of past investigations of important earthquakes are provided to illustrate ways the Utahans benefit from the past and to highlight the inescapable conclusion--the greatest progress in implementation of loss-reduction measures takes place after dmaging earthquakes. The investigations include the following:

1. 1964 Prince William Sound, Alaska, earthquake--This great (M_w=9.2) earthquake occurred in one of the most active tectonic areas of the world where the Pacific tectonic plate is being subducted under the North American tectonic plate at a rate of about 2 inches per year. It caused widespread regional tectonic deformation over an area of at least 77,000 square miles--a phenomenon that is now recognized as a characteristic feature of great earthquakes (Hansen and others, 1966). Structural damage and collapse occurred in buildings located at distances of more than 60 miles from the epicenter. Damaging tsunami waves were generated by the earthquake and affected local and very distant locations.

Sensitive clay formations failed, causing extensive ground failures in 30 blocks of downtown Anchorage. No strong motion accelerograms were recorded in the earthquake. A new scientific field, earthquake prediction, was initiated after this earthquake, and researchers began to seek explicit answers to three questions: where? how big? and when? will future earthquakes occur. The answer to "where?" is the most elusive.

2. <u>1971 San Fernando, California, earthquake</u>--The moderate (Ms=6.4) San Fernando earthquake served as a greater catalyst for knowledge gathering, applications, and changes in public policy than any other earthquake, before or after 1971. The earthquake occurred on a thrust fault in the Transverse Ranges structural province. The fault had not been recognized previously as tectonically active and potentially dangerous, so the earthquake was a "surprise." The earthquake produced the largest horizontal ground shaking ever recorded (at that time) at a site underlain by rock near the epicenter--1.24 g at Pacoima dam (U.S. Department of the Interior and U.S. Department of Commerce, 1971). Severe damage and partial collapse were experienced in the epicentral region in buildings designed to meet the intent of seismic design provisions of a modern building code. More than 200 accelerograms were added to the existing, but inadequate, strong ground motion data sample that consisted mainly of a few records from each prior earthquake. These new records provided a basis for comprehensive damage studies, deterministic and probabilistic hazards assessments, and the reevaluation of seismic design criteria for critical facilities (hospitals, dams, nuclear power plants) and lifelines (highways, bridges, gas, water, and electric utilities, sewers, airports, harbors). Lifeline engineering began as an institutionalized activity as

a result of the nature and extent of damage sustained by lifelines in the San Fernando earthquake.

The Pacoima dam accelerogram stimulated debate over the effects of soil and rock and the local topography on the amplitude and frequency composition of ground shaking. An extensive array of portable broadband seismographs was deployed to record the aftershock sequence. These data provided information on site amplification, the effects of topography on ground motion, and the estimated spectral composition of the main shock ground motion at sites that sustained damage but did not record it. The concept of a seismic safety element as a part of a community's general plan was introduced after the San Fernando earthquake, and legislation was passed in California to implement it. The value of a seismic safety organization was increased by the San Fernando earthquake, and resulted eventually in the California Seismic Safety Commission, the Utah Earthquake Advisory Council, the South Carolina Seismic Safety Consortium, the Kentucky Task Force on Earthquake Hazards and Safety, the Central United States Earthquake Consortium, and the New York Earthquake Advisory Council.

3. The 1972 Managua, Nicaragua, earthquake--This moderate (Ms=6.2) earthquake occurred on a shallow well-known stike-slip fault system beneath the city, which was the source of another earthquake in 1931 (Earthquake Engineering Research Institute, 1973) It caused severe damage to buildings that were designed to meet the intent of earthquake resistant design provisions of a modern building code. A network of portable broadband instruments was deployed to augment the single strong motion record of the main shock

obtained at the Esso refinery (peak horizontal acceleration of 0.39 g and peak vertical acceleration of 0.33 g). These data provided insight into the characteristics of ground shaking at sites that did not record the main shock and site response under low-strain conditions. Managua was relocated in the 1970's to avoid the system of active faults identified in detail by the postearthquake investigations.

4. The 1976 Guatamala earthquake--This large (Ms=7.5) earthquake was generated by left-lateral slip on the Motagua fault, a well-known stike slip fault zone marking the active boundary between the North American and Caribbean plates (Espinosa, 1976). The fault ruptured over a distance of about 180 miles, the most extensive surface rupture in the Northern Hemisphere since the 1906 San Francisco, California, earthquake, which was generated by right-lateral slip on the San Andreas fault. The westward-propagating fault rupture caused extensive damage to buildings, roads, and the railroad system. Structural damage from the ground shaking was extensive, affecting hospitals and buildings in Guatemala City designed in accordance with the seismic provision of a modern building code and causing the collapse of nonengineered adobe structures in a number of communities located 10 to 60 miles from the epicenter. Hundreds of landslides were triggered by the ground shaking generated by the main shock and the thousands of aftershocks that followed during the next several months. Although no accelerograms of the main shock were recorded, the Modified Mercalli intensity data obtained from detailed surveys of the damage distribution provided a basis for constructing a seismic zoning map of Guatemala for use in redevelopment of the city. Earthquake prediction research was stimulated by this earthquake. The

National Earthquake Hazards Reduction Program of the United States was initiated in 1977, partly as a result of the magnitude of the disaster caused by the 1976 Guatemala earthquake and partly because 1976 was one of the worst years on record for damaging earthquakes.

5. The 1976 Tangshan, China, earthquake--This large (Ms=7.8) earthquake that occurred under Tangshan was a surprise. Tangshan was located in a seismic zon of the Chinese building code that did not call for earthquake-resistant design. The buildings of the city, consisting mainly of unreinforced brick, were unable to resist the strong ground shaking and the forces generated by the dynamic fault rupture. Eighty five percent of the city's buildings collapsed or were damaged severely, and several hundred thousand people were killed. The need for earthquake prediction research was made clearer by this earthquake. The magnitude of the disaster stimulated legislation such as the 1977 Earthquake Hazards Reduction Act.

6. The 1978 Argentina earthquake--This large (Ms=7.4) earthquake produced avery important new result--that significant liquefaction can occur at distances of more than 120 miles from the epicenter of an earthquake. This result means that the potential for liquefaction at a site must be considered for levels of ground shaking as low as VI on the Modified Mercalli Intensity scale when saturated, young, fire-grained sand deposits underlie the construction site.

7. The 1979 Imperial Valley, California, earthquake--This large (Ms=7.5) earthquake, which had its epicenter in Mexico on the well-known Imperial

fault, occurred in the midst of a dense array of seismic instruments that included short-period vertical seismographs and strong motion accelerometers (Johnson and others, 1982). It provided a unique opportunity to study in detail the changes in seismicity attending and preceding a moderately strong earthquake and the characteristics of damage produced by ground shaking. The earthquake generated the most detailed and integrated set of strong ground motion data ever recorded from a damaging earthquake. These data were unique because they included (1) the first set of accelerograms ever obtained close to a fault rupture zone activated in an earthquake, showing the effects of directivity, (2) the first data set of accelerograms from an extensive array located in a severely damaged building (the Imperial County Services Building), (3) the first data set from an array of closely spaced instruments, and (4) an array on a highway overpass bridge located less than 1/2 mile from the fault rupture zone. The strong motion data also included the largest vertical ground acceleration (1.66 g) ever recorded in the United States. Because another earthquake of about the same magnitude had occurred in the Imperial Valley in 1940, comparative studies of the distribution of damage and the correlation of intensity data with strong ground motion parameters were possible. For the first time, adequate data were available to extend seismic wave attenuation laws to the very near field for strike-slip faults (Seed and Idriss, 1982).

8. The 1980 El Asnam, Algeria, earthquake--This large (Ms=7.3) earthquake, the largest historic earthquake of north Africa, occurred as a consequence of the collision of the Eurasian and African tectonic plates. The Oued Fodda fault, a well-known 26-mile-long active thrust fault, ruptured the

surface from the southwest to the northeast over a distance of 21 miles. About 85 percent of the buildings in El Asnam (now called Ech Cheliff), located 6 miles east of the epicenter, collapsed or suffered severe damage (Earthquake Engineering Research Institute and the National Research Council, 1983; United Nations Educational Scientific and Cultural Organization (UNESCO, 1985). Although no records of the main shock were obtained, seismologists and engineers conducting postearthquake investigations concluded that the level of vertical ground acceleration exceeded the horizontal acceleration and may have approached 1 g. Construction was frozen in the damaged portion of the Ech Cheliff region for more than 4 years to permit the completion of a comprehensive seismic microzontion study of northern Algeria and the incorporation of the results in land use, building codes, and construction practices. Thirty trenches were excavated to determine the recurrence interval of large earthquakes and to augment an incomplete record of seismicity. Ninety strong motion instruments were deployed in Algeria. The Algerian building code was modified extensively to reflect the new knowledge gained in the seismic microzontion study. Although damaging earthquakes also had occurred in the vicinity of El Asnam in 1922, 1934, and 1954, public policy and applications in terms of seismic zoning and construction practices had lagged behind knowledge. Except for activity in 1976 to revise the building code, specific mitigation activities did not make much progress until after the 1980 event. The earthquake stimulated the creation of the Algerian Institute of Earthquake Engineering and Applied Seismology in 1985.

9. The 1983 Coalinga, California, earthquake--This moderate (Ms=6.7) earthquake occurred in an area of moderate seismicity along the eastern front of the Coast Ranges (Earthquake Engineering Research Institute, 1984). It occurred on faults in the Anticline Ridge which, although, they had been identified previously as potentially seismogenic, were not considered to be the likely location of the next moderate earthquake in California. The ground shaking at Pleasant Valley, 5 miles from the eipcenter, was 0.54 g horizontal and 0.37 g vertical. The earthquake devastated the central business district of Coalinga, which consisted mainly of unreinforced one- and two-story brick masonry buildings constructed in the early part of the 20th century. In contrast, newer reinforced brick, block masonry, or reinforced concrete buildings perfored very well, sustaining only nonstructural damage. The earthquake demonstrated that an industrial facility (for example, oil company facilities) can withstand high ground motion if its structures are well designed and constructed and if its equipment is anchored.

10. The 1983 Borah Peak, Idaho, earthquake--This large (Ms=7.3) earthquake provided conclusive validation of the importance of studying Holocene (10,000 years before present) and Late Pleistocene (125,000 years before present) fault scarps to assess the potential for future large earthquakes (Stein and others, 1985). In the Borah Peak earthquake, a 21-mile-long normal fault surface rupture was formed. It repeated with great precision the Holocene fault scarp that had been excavated and examined in detail 10 years earlier, proving once again that Holocene fault scarps provide an unsurpassed tool for identifying likely sites in the Great Basin for future earthquakes. In contrast, microseismicity provided no clue of the

1983 earthquake; no earthquakes having a magnitude greater than or equal to 3.5 have occurred in the epicentral region of the Borah Peak earthquake during the past 20 years. About 30 giant sandblows formed or were revitalized in the epicentral region which was assigned a rating of VII on the Modified Mercalli Intensity scale. The fault slip, length, and width of the 1983 earthquake provide a technical basis for assessing the maximum seismic moment and magnitude of future seismic events, especially in the heavily populated urban corridor along the Wasatch Front, Utah, which has not experienced a large earthquake since the area was settled in 1845, but which is considered to have the potential for a magnitude 7.5 earthquake (Hays and Gori, 1985).

11. The 3 March 1985 Chile earthquake--This large (Ms=7.8) earthquake occurred in the subduction zone west of Chile where the Nazca tectonic plate is being subducted under the South American tectonic plate (Earthquake Engineering Research Institute, 1985). The Nazca plate dips to the east under Chile at approximately 20°. Damaging earthquakes have occurred in the subduction zone near Chile about once every 10 years. The largest known earthquake in history (Mw=9.5) occurred there in 1960. The 1985 earthquake had special seismological significance because an extensive network of strong ground motion accelerographs were operating at the time of the earthquake, and about 30 records of the ground shaking were obtained. The levels of peak horizontal and vertical ground acceleration reached 0.67 g and 0.85 g, respectively. This data sample, one of the most comprehensive from a subduction zone earthquake, showed that the ground shaking was strong, rich in high and low frequencies, and had a long duration. Although damage from the earthquake was extensive and

losses may ultimately exceed $2 billion, modern reinforced concretc buildings performed very well. As expected, adobe buildings generally were destroyed, and small wooden homes typically were undamaged. A reinforced concrete hospital in San Antonio sustained considerable structural damage from the ground shaking. Many buildings experienced foundation failure or minor settlement due to ground failures. Water systems were affected severely due to ruptures of the aqueducts. The death (176) and injury (2,500) tolls, relative to the damage, were surprisingly low for a large earthquake. Information from this subduction zone earthquake is considered to be relevant for Puerto Rico, the Puget Sound, Washington, area, and southern Alaska, three areas of the United States thought to have the potential for large to great subduction zone earthquakes.

12. The 19 September 1985, Mexico earthquake--This great earthquake, initially rated as Ms = 7.8 but later upgraded to Ms=8.1, occurred as a consequence of subduction of the Cocos tectonic plate beneath the North American plate. The existence of a possible seismic gap in this portion of the Cocos plate and a general forecast of a large earthquake having an average recurrence interval of about 35 years had been made in 1981 (McNally, 1981). The specific time of the earthquake had not been predicted, however. This earthquake was noteworthy because about 400 tall buildings located in Mexico City, about 240 miles from the epicenter, collapsed partially or totally, causing an estimated 5,000 to 10,000 deaths, numerous injuries, and possible economic losses of $5 to 10 billion. The extraordinarily high degree of damage at this large epicentral distance was partly due to soil-structure interaction

(Rosenblueth, 1986). The long-period (2 second) ground motion was amplified by the 150-foot-thick, water-saturated sediments of a former lake bed forming the foundation under part of Mexico City. The lake bed zone was recognized by Zeevaert (1964) as having a characteristic site period of about 2 seconds, roughly the natural period of vibration of a 20-story building. Past distant earthquakes (for example, 1957 and 1962, Mexico earthquakes) also had caused damage to Mexico City that clearly was attributed to site amplification. In the 1985 earthquake, six buildings collapsed at the Mexico General Hospital, and about 400 doctors, nurses, and patients were trapped in the ruins of the Juarez Hospital located just eight blocks from the Presidential Palace. Government buildings, as a group, sustained considerable damage. long-distance telecommunications with the rest of the world were eliminated for several days after the earthquake due to the destruction of the main microwave transmitter and the lack of a redundant system. Because of prior planning by United States and Mexican scientists and engineers, a number of strong motion accelerographs were in place at the time of the earthquakes. According to early reports (Jim Brune, November, 1985, personal commun.), the earthquake was a low stress drop event and had epicentral accelerations of about 18 percent g. These strong motion data, together with that data acquired in the March 3, 1985, Chile earthquake, provided a valuable sample of strong ground motion data for subduction zone earthquakes. A building code having a factor for soil conditions had been adopted and implemented in Mexico City since 1976.

Collectively, postearthquake investigations have produced evidence for the following set of general conclusions:

- Earthquakes tend to recur where they have occurred in the past. Faults have average recurrence intervals for a given magnitude earthquake that can be quantified by intergration of paleoseismicity studies and historical seismicity data.

- The theory of plate tectonics provides an explanation of many of the world's intraplate earthquakes. The explanation for interplate earthquake is less clear.

- A long fault (greater than 20 miles) is required to generate a large or a great earthquake (magnitudes of 7 or greater).

- Understanding the fault-activity during the Holocene (10,000 years before present), and Late Quaternary (125,000 years before present) is critically important in defining the earthquake potential of a region.

- The parameters of the fault (rupture mechanics, length, width, slip rate, type) and changes in the thickness and physical properties of the soil-rock column underlying the building site control the main features of the peak amplitudes, frequency composition, and duration of the ground shaking induced on a building.

- Earthquake-resistant buildings always tend to have a lateral-force-resisting system that is: 1) continuous (forced: are transferred from their point of application to their point of resistance), 2) ductile (construction materials are stable when strained beyond their yield limits), and 3) complete (no missing links, inadequate joints, or brittle elements are present).

- Earthquake-resistant buildings tend to be: 1) regular in plan and elevation, 2) designed to have the same relative degree of strength and stiffness throughout the load-resisting elements, 3) tied together to respond as a unit to the ground-motion load, 4) separated from adjacent buildings, and 5) designed to avoid reentrant corners and zones of high stress concentrations.

- The primary causes of damage to buildings are almost always a result of one or more of the following factors: 1) use of inadequate lateral force-resisting systems (for example, unreinforced masonry, adobe, brittle concrete columns), 2) omissions in engineering analysis (for example, neglect of torsion effects, overturning effects, and static equilibrium of all force), 3) lack of adequate connections and detailing, 4) poor quality of construction, 5) underestimation of the amplitude, frequency composition, and duration of ground shaking that the building or facility will experience in its lifetime, and 6) underestimation of the geotechnical properties of the foundation materials with respect to their potential for failure when subjected to the ground shaking.

- Significant changes in public policy are triggered primarily by the occurrence of a disaster.

Scenario Earthquake - When a long time has elapsed in the region since the last historic damaging earthquake (e.g., such as in the Mississippi Valley) or no historic earthquake has occurred (e.g., such as along the Wasatch front, Utah), a scenario earthquake can be used to foster the implementation process by heightening awareness and concern. In Utah the main issues associated with scenario earthquakes are:

- Is the scenario earthquake sufficiently credible in terms of present knowledge that it will be used to guide the development of a community's response plans?

- Is the scenario earthquake realistic in terms of the actual geologic setting of the community and the social and political conditions in the community and, if so, will it be used as the basis for specific mitigation activities?

Element 5: Loss Reduction Measures--A wide range of practical loss-reduction measures are now available for implementation in Utah communities. The overriding issue of implementation that is directly related to each loss-reduction measure being considered by the community is:

- How much more does the loss-reduction measure cost in comparison with the cost of maintaining the "status quo?"

Loss-Reduction Measures - Loss-reduction measures applicable for Utah can be grouped in seven categories:

- Hazard maps - Maps showing the relative severity and spatial variation of a specific hazard (for example, the ground-shaking hazard) that can be used in applications ranging from design guidelines to seismic microzoning to regulations.

- Design criteria - Criteria for siting a wide range of structures (including those covered by building codes as well as by other regulations), such as: public buildings, schools, private buildings, critical public facilities, dams, hospitals, and nuclear power plants.

- Guidelines and regulations - Guidance for regional and urban planning to improve land-use in the context of earthquake hazards.

- Seismic microzonation - A procedure that utilizes the existing technical data as a basis for the division of a region into zones expected to experience the same relative severity of a specific earthquake hazard in a given exposure time (such as the level of ground shaking expected in a 50 year period). Seismic microzoning provides the prospective user of an area with the design criteria that will permit selection of the most suitable part of the area for the proposed use.

- Inspection and review - Procedures to regulate design and construction, practices.

- Education and training - Short- and long-term activities designed to close specific gaps in knowledge. Training prepares people to do a wider variety of tasks than they could do without training.

- Response planning - Planning that improves the capability of the community, region, and State to respond effectively to a damaging earthquake.

SUMMARY OF ACCOMPLISHMENTS IN UTAH AND RECOMMENDATIONS TO ACCELERATE PROGRESS

All of the critical elements required to foster the implementation process in Utah exist. The expectation is that implementation of earthquake-hazards loss-reduction measures will take place (Figure 4). Although the technical data bases have some limitations, they are adequate for many applications (listed above) that require regional- and local-scale data. The resources for acquiring site-specific data also exist.

FIGURE 4 FOLLOWS TEXT

Utah has trained, concerned, and committed professionals who are working full time on the problem of earthquake hazards reduction. They constitute a valuable resource. Ongoing research programs have well-defined short- and long-term goals and are producing high-quality scientific results. Programs have a high degree of integration and coordination at Federal and State levels.

In the eyes of many scientists, Utah now has a damaging earthquake to use as a model--the 1983 Borah Peak, Idaho earthquake. Coupled with loss scenarios completed in 1976, many Utahans have adequate experience with earthquakes to know what needs to be done and how to do it. The next step is to call for change where it is needed. All of the categories of loss-reduction measures listed above have been judged to be relevant for communities in Utah. They need to be implemented.

RECOMMENDATIONS

For the Wasatch front area, the basic question is "Will significant implementation of effective loss-reduction measures happen in Utah without a major earthquake on the Wasatch fault zone?" To ensure that the answer is "yes", Utahans are encouraged to take the appropriate actions now, in advance of the inevitable damaging earthquake on the Wasatch front.

Short-and long-term recommendations (1-10 years) include:

- Compile and publish a portfolio of maps depicting specific hazards. The portfolio should contain maps that are adequate for use in planning, design, and construction. The portfolio of maps should be disseminated widely to all potential users in Utah along with guidelines for their use during the next 5-10 years, a period expected to be characterized by rapid urban development.

- Perform a careful evaluation of the maps that depict the perceived risk zones in Utah. These maps are contained in the various building codes (e.g., uniform Building Code, 1985; Applied Technology Council, 1978). Such an evaluation should also include consideration of soil amplification effects, identifying those areas in communities along the Wasatch front that have the potential for damaging soil-structure interaction effects similar to those that occurred in the 1985 Mexico and the 1967 Caracas, Venezuella, earthquakes.

- By 1990, the date for which changes in the 1991 edition of the Uniform Building Code can be made, conduct an extensive evaluation of the risk zones and the soil-structure interaction factors in Utah.

- Adopt and enforce realistic inspection and review procedures to ensure compliance with the requirements of the 1991 edition of the Uniform Building Code.

- Revise existing guidelines and regulations to promote regional and urban land-use planning, and, as appropriate, incorporate new knowledge of earthquake hazards (as depicted in the portfolio of hazard maps).

- Initiate state-of-the-art training programs to transfer the technology required by a wide variety of user groups who want to apply the hazards maps in design, construction, and land-use planning.

- Develop plans for conducting comprehensive post-earthquake investigations following damaging earthquakes in Utah or in other areas having analogous: a) seismotectonic settings, b) design and construction practices, and c) inventory of structural types exposed to the groundshaking hazard expected along the Wasatch front in a 50-year period of time.

Implementation of these actions during the next decade will be a major step toward achieving the goal of a high level of earthquake preparedness in Utah, and will prevent the next damaging earthquake in Utah from being a disaster.

REFERENCES

Algermissen, S. T., 1978, Postearthquake field investigations: Acquisition and transfer of scientific and engineering data, in Hays, W. W. (Editor), Communicating Earthquake Hazards Reduction in Formation, Proceedings of Conference V, May 1978, U.S. Geological Survey Open-File Report 78-933, p. 198-204.

Applied Technology Council, 1978, Tenative Provisions for the Development of Seismic Regulations for Buildings, Atc 3-06, Palo Alto, California, 950 p.

Earthquake Engineering Research Institute, 1985, Preliminary Evaluation of Research Opportunities in Connection with the March 3, 1985, Earthquake in Chile, 35 p. (in press).

_____ 1984, Coalinga, California Earthquake of May 2, 1983, Report number 84-03, 300 p.

Earthquake Engineering Research Institute and National Research Council, 1983, El Asnam, Algeria Earthquake of October 10, 1980.

_____ 1979, Learning from Earthquakes, Report to the National Science Foundation, 79 p.

_____ 1973, Managua, Nicaragua Earthquake of December 23, 1972, Conference Proceedings, 2 Vols. 975 p.

Espinosa, A. F. (Editor), 1976, The Guatemalan Earthquake of February 4, 1976, A Preliminary Report., U.S. Geological Survey Professional Paper 1002, 90 p.

Hansen, W. R., Eckell, E. B., Schaem, W. E., Lyle, R. E., George, Warren, and Chance, Genie (Editors), 1966, The Alaska Earthquake March 27, 1964: Field Investigations and Reconstruction Effort, U.S. Geological Survey Professional Paper 541, 111 p. (Note: Nine 9 Professional Papers on the Alaskan earthquake were prepared by the U.S. Geological Survey).

Hays, W. W., 1986, The Importance of Postearthquake Investigations, Earthquake Spectra, v. 2, p. 653-668.

Hays, W. W., 1985, An Introduction to Technical Issues in the Evaluation of Seismic Hazards for Earthquake-Resistant Design, U.S. Geological Survey Open-File Report 85-371 (ICSSC TR-6), 102 p.

Hays, W. W. (Editor), 1981, Facing Geological and Hydrological Hazards:Earth Sciences Considerations, U.S. Geological Survey, Professional Paper 1240-B, 109 p.

Hays, W. W., and Gori, P. L., (Editors) 1985, Evaluation of Regional and Urban Earthquake Hazards and Risk in Utah, Proceedings of Conference XXVI, U.S. Geological Survey Open-File Report 84-763, 694 p.

Johnson, Carl E., Rojahn, Christopher, and Sharp, Robert V. (Editors), 1982, The Imperial Valley Earthquake of October 15, 1979, U.S. Geological Survey Professional Paper 1254, 451 p.

Marshall, Richard D., 1985 Guidelines for ICSSC Post-Earthquake Response Activities, National Bureau of Standards Report 85-3123, (ICSSC TR-5), 71 p.

McNally, Karen C., 1981, Plate subduction and prediction of earthquakes along the Middle American Trench, in Simpson, D. W., and Richards, P. G. (eds), Earthquake prediction, an international review, American Geophysical Union, Maurice Ewing Series, 4, pp. 63-72.

Rosenblueth, Emilo.,1986, The Mexico Earthquake--A First hand Report, Civil Engineering, American Society of Civil Engineers, New York, January, pp. 3840.

Seed, H. B., and Idriss, I. M., 1982, Ground Motions and Soil Liquefaction, Earthquake Engineering Research Institute Monograph, El Cerrito, California, 134 p.

Stein, Ross S., Bucknam, Robert C., and Breckenridge, Roy M. (Editors), 1985, On the Borah Peak, Idaho Earthquake, Proceedings of Conference XXVIII, U.S. Geological Survey Open-File Report 85-290, 686 p.

Uniform Building Code, 1985, International Conference of Building Officials, Whittier, California (updated every 3 years), 704 p.

United Nations Educational Scientific and Cultural Organization (UNESCO), 1985, Assistance for the realization of a seismic microzoning study in the Chlef region of Algeria, UNDP/ALG/83/004, 23 p. (in French).

U.S. Department of the Interior and U.S. Department of Commerce, 1971, The San Fernando, California Earthquake of February 9, 1971, U.S. Geological Survey Professional Paper 733, 254 p.

Zeevaert, L., 1964, Strong Ground Motions Recorded During Earthquakes of May the 11th and 19th, 1962 in Mexico City, *in* Bulletin of the Seismological Society of America, December 1973, Vol 63, part 2, pp. 209-232.

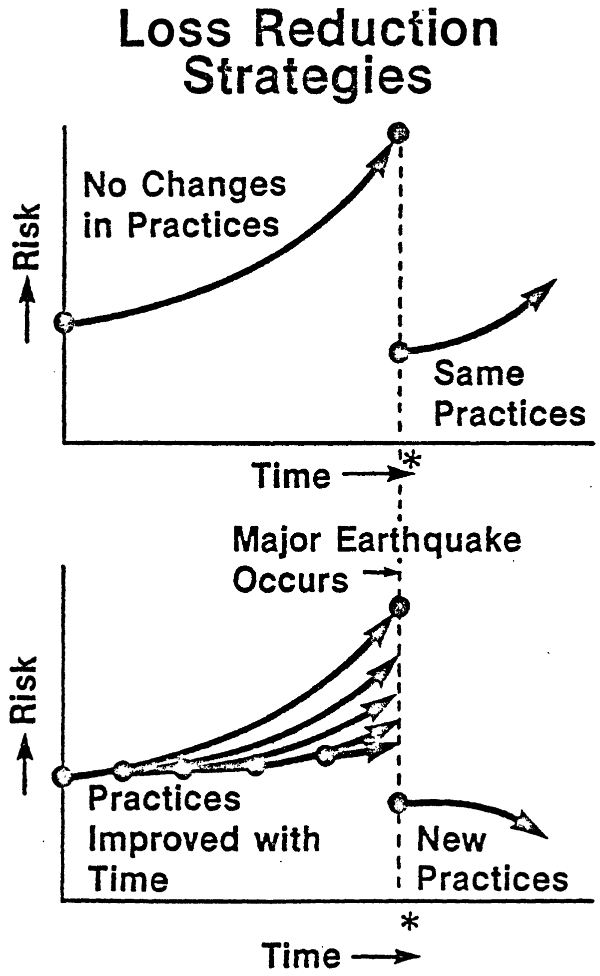

Figure 1.--Schematic illustration of the critical issue in the implementation process for every earthquake-prone region of the Nation--"Will significant implementation of loss-reduction measures take place without a major earthquake?"

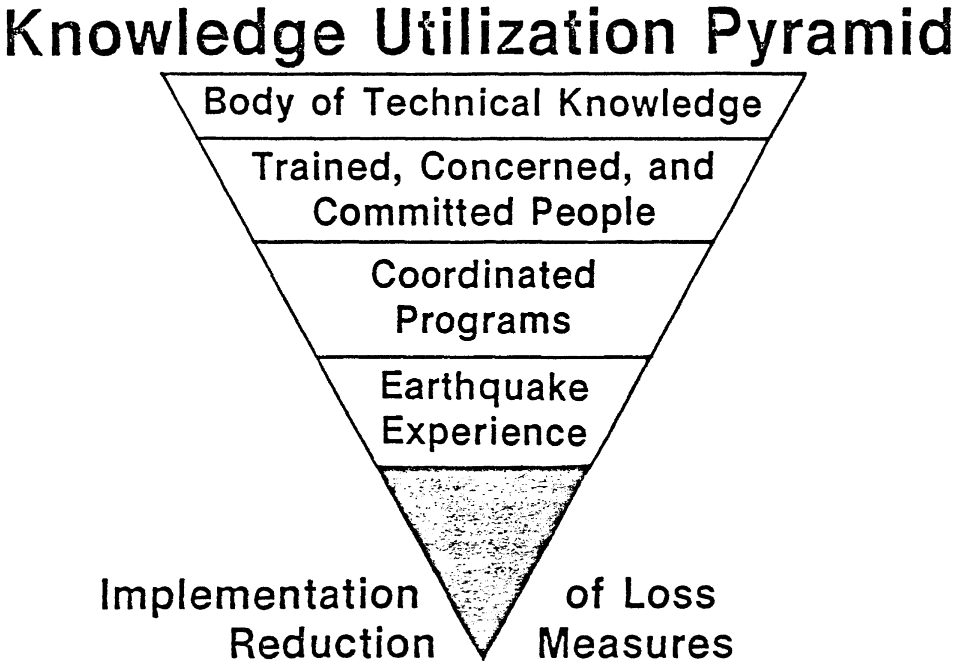

Figure 2.--Schematic illustration of the five critical elements of the earthquake-hazards-reduction implementation process. The flow is from top to bottom. The most important element seems to be the occurrence of a damaging earthquake.

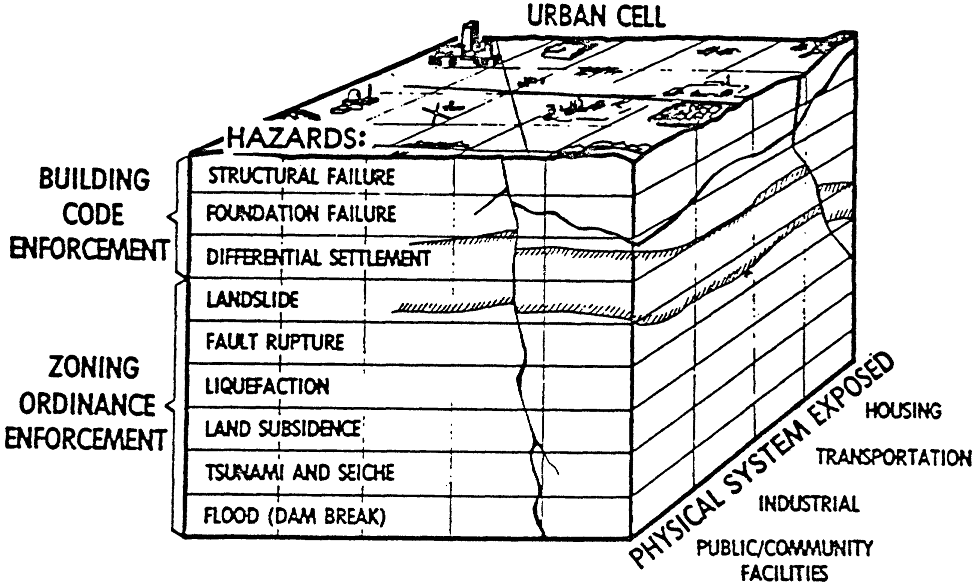

Figure 3.--Schematic illustration of an urban community facing potential losses from the earthquake hazards of ground shaking, surface fault rupture, earthquake-induced ground failure, regional tectonic deformation, seiches, and (in coastal area) tsunami runup. The community must develop the capability to implement a wide range of loss-reduction measures to minimize the potential impacts of each hazard. Decisionmakers in the community must decide which loss-reduction measures are best for their community and foster their implementation.

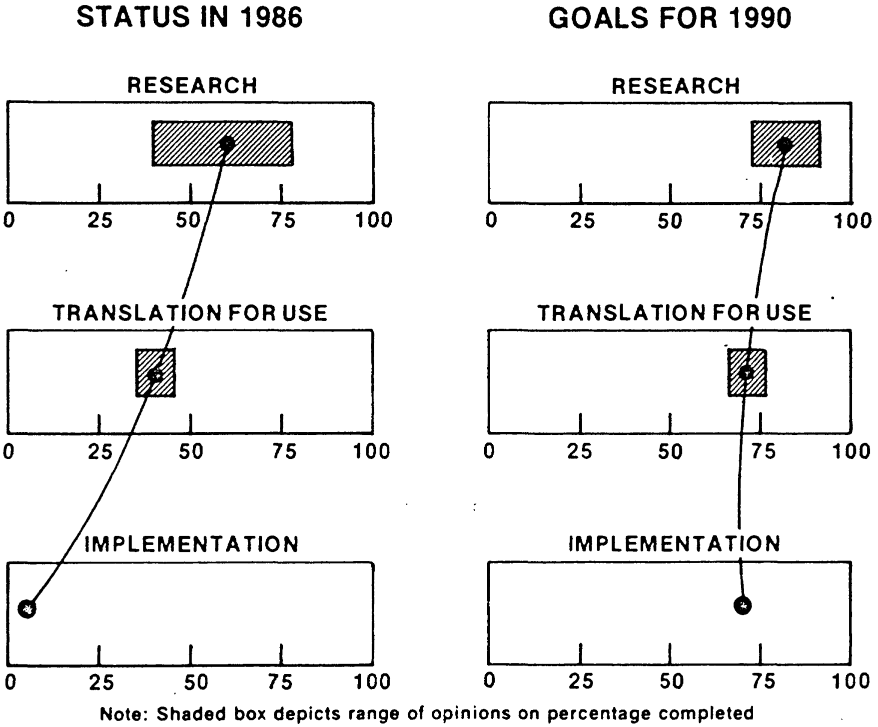

Figure 4.--Status and goals of research, translation of research results for user groups, and legislation in Utah.

Table I

Differences in the perspectives of scientists/engineers and decisionmakers (from Szanton, 1981).

Attributes	Perspectives	
	Scientists/Engineers	Decisionmaker
1. Ultimate objective	Respect of Peers	Approval of electorate
2. Time horizon	long	Short
3. Focus	Internal logic of the problem	External logic of the problem
4. Mode of thought	Inductive, generic	Deductive, particular
5. Most valued outcome	Original insight	Reliable solution
6. Mode of expression	Abstruse, qualified	Simple, absolute
7. Preferred form of conclusion	Multiple possibilities with uncertainties emphasized	One-best-solution with uncertainties submerged

Reducing Earthquake Risk in Utah:

Past trends and future opportunities

Genevieve Atwood and Don R. Mabey

Utah Geological and Mineral Survey

Salt Lake City, Utah

ABSTRACT

Earthquakes are the geologic hazard with the greatest potential for destruction of life and property in Utah, but because Utah has not experienced a highly destructive earthquake in historic time the public and official perception of the earthquake risk differs from areas with a history of destructive earthquakes. Utah's political and social structure produces factors that both enhance and impede programs to reduce earthquake risk. In the one hundred years since G. K. Gilbert informed the public of the earthquake hazard along the Wasatch Front some progress toward reducing earthquake risk has been made, mostly in the last two decades. A resistance to extensive land-use planning and to state and federal controls inhibits statewide seismic safety efforts. The LDS Church's emphasis on preparing for disasters provides support for preparations to respond to earthquakes and for some measures to reduce risk. The primary responsibility for many actions to reduce earthquake risk in Utah rests with county and city governments but there is need for strong leadership at the state level. If elected and appointed state and local officials, engineers, architects, and the public are to take actions to reduce earthquake risk in Utah, the geologic community must provide them with translated geologic data upon which to base actions.

INTRODUCTION

In Utah, earthquakes are the geologic hazard with the greatest potential for catastrophic destruction of life and property, although other geologic hazards such as flooding and landslides in the past have caused much more damage in Utah than earthquakes. Geologists and many residents of Utah have been concerned about earthquakes along the Wasatch Front for over a century, but only in the last three decades has significant progress been made to reduce earthquake risk.

Utah has taken the initial steps toward reducing earthquake risk and the stage is set for increased success. This paper reviews the history of efforts to reduce earthquake risks in Utah, analyzes some of the positive and negative forces that tend to enhance or thwart these efforts, and looks to the future to analyze how risks can be reduced successfully in the next decade. Earthquake "hazard", as used here, refers to the phenomena accompanying an earthquake and includes surface rupture, ground-shaking, liquefaction, rockfalls, tectonic tilt, slope failure, avalances, and other physical phenomena. Earthquake "risk" as used here, refers to the threat posed by the hazard as a potential danger to lives and property. Over the last few decades, the understanding of the earthquake hazard in Utah has vastly improved at a rapidly increasing rate. Meanwhile, the earthquake risk also has increased, hopefully at a decreasing rate in response to conscientious efforts to avoid certain types of earthquake hazards and to engineer for them.

Prior to 1950 several committed citizens warned of the Wasatch Front earthquake hazard but such individuals, mostly geologists, rarely could elicit the support of their colleagues, let alone the public. During the 1950s, 1960s and into the mid-1970s, the scientific understanding of the hazards developed, the public became more conscious of the risks, and individuals concerned about earthquakes were able to make some progress educating their professional colleagues. This rather sporadic progress was counterbalanced by greatly increased exposure to earthquake risks as homeowners, entrepreneurs, and governmental entities, encouraged by a political environment that was often hostile to certain types of planning, designed and constructed buildings and critical facilities particularly vulnerable to earthquakes. The Utah Seismic Safety Advisory Council (USSAC) working from 1977 through 1981 focused attention on the hazards and legitimized risk reduction efforts. Although few local or state policies changed as a direct result of their work, some progress was made and a foundation established for action. Now in the 1980s, earthquake hazards awareness and mitigation advances through the efforts of many advocates, and successes appear to outdistance setbacks.

In addition to chronicling the history of success of actions to reduce earthquake risks in Utah, this paper looks at the forces that contribute to or oppose these actions. One of the purposes of this report is to provide those in Utah as well as others who are interested in earthquake risk reduction an understanding of the Utah story, its successes and its failures, and the implementation issues that are special to Utah. Clearly, the state is affected by national trends and, most importantly, by the state-of-the-science which has national leadership on earthquake hazards from the U. S. Geological Survey (USGS).

Utah is not unique, and can and should apply lessons learned in other parts of the country. However, some important problems in reducing earthquake risks are special to Utah or at least are not shared with most states. Implementation of risk reduction strategies in Utah must be made in the context of these special factors: 1) responsibilities of each level of government, 2) the Church of Jesus Christ of Latter Day Saints (LDS, Mormon) as an organization and policymaker, and 3) the nature and extent of our knowledge of earthquake hazards. In Utah, local governments have the authority and responsibility, although not the mandate, to plan for use of land and the responsibility to implement building codes and other construction practices. No state land-use-planning authority, nor a coordinating statewide policy, nor statewide building code mandates construction practices. Therefore, the regulation of building and construction professionals by the state is weak and the success of earthquake risk reduction primarily depends on implementation at the local level. The federal government is looked to for some types of standardization, for research, and, of course, for money to support projects of mutual concern. The role of the LDS Church is unique to Utah and parts of adjacent states. The church is very powerful and its members are widely distributed across the state. The organization either overtly or subconsciously exerts an influence on all state policies including earthquake risk reduction. Finally, Utah's heavily populated areas have not experienced a highly destructive earthquake so the understanding of the hazard is based on geological and geophysical data and information translated from other areas rather than from firsthand experience. State and local policymakers' perception of the risk and the problems of implementation of risk reduction efforts in Utah differ from other areas that have a history of destructive earthquakes.

The final section of this paper turns from past and present events and looks to the future...with optimism. Several actions (such as adoption of building codes, delineation of fault-rupture areas, definition of liquefaction susceptibility zones, review of dams for safety, development of innundation models) have been taken to reduce earthquake risk and there is reason to hope that others will be taken. Research on earthquakes is producing information that will help reduce earthquake risk. The need for effective translation and dissemination of hazard information is clear, and its application can be furthered by a reasonable outlay of creative effort, talent, and additional research.

METHODOLOGY

This paper is the product of interviews and discussions with several individuals who have had or presently have a role in implementing earthquake risk reduction in Utah. These individuals are: Delbert Ward (Director, Utah Seismic Safety Advisory Council, 1977-1981), Scott M. Matheson (Governor, State of Utah, 1977-1985), Robert Huefner (University of Utah, Department of Political Science), Albert Haines (Salt Lake City Administrator, 1980-1986), Christopher Nelson (Director, Utah State Division of Facilities Construction and Management), Lawrence Reaveley (structural engineer), Harry D. Goode (consulting geologist), Ellis Armstrong (Commissioner, Bureau of Reclamation, 1969-1973), Lorayne Tempest (Director, Utah Division of Comprehensive Emergency Management), Bruce Kaliser (State Hazards Geologist, Utah Geological and Mineral Survey), Robert Smith (Chairman of the Department of Geology and Geophysics, University of Utah), and Walter Hays (Deputy Chief for Research Application, Office of Earthquakes, Volcanoes, and Engineering, U.S. Geological Survey). Bruce Kaliser and Robert Smith served as members of the Utah Seismic Safety Advisory Council (1977-1981) and Walter Hays served ex officio as a liaison member from USGS. These interviews have been supplemented by a review of literature and by the experience of the authors. This paper is not a complete history of earthquake risk reduction in Utah.

HISTORY OF EARTHQUAKE RISK REDUCTION IN UTAH

Earthquake potential -

The first important warning of the threat earthquakes pose to communities along the Wasatch Front (specifically Salt Lake City) was issued by G. K. Gilbert in a letter to the Salt Lake Daily Tribune published in 1883 (Figure 1.). Gilbert correctly identified the geologic evidence of the earthquake hazard but seemed convinced that this evidence would not move the citizens of Salt Lake City to take action to reduce the risk. That action, he prophesied, would be taken only when the city had been largely destroyed by an earthquake. Indeed, at that time it was not clear to Gilbert what reasonable

DAILY TRIBUNE.

The Salt Lake Daily Tribune.

VOL. XXV. SALT LAKE CITY SUNDAY MORNING, SEPTEMBER 16, 1883—SIX PAGES. NO. 131

WEEKLY TRIBUNE

EARTHQUAKES.

A Prophetic Discourse by G. K. Gilbert, United States Geologist.

The Matter Brought Home to the People of Salt Lake.

There are many geologists who are very wise, but even they do not understand the forces which produce mountains. And yet it must be admitted, not only that mountains have been made, but that some mountains are still rising. The mysterious forces appear to act in different ways in different places, and it is possible that their nature is not universally the same. Suffice it to say that in the Great Basin the movements they cause are vertical. It is as though something beneath each mountain was slowly, steadily, and irresistibly rising, carrying the mountain with it.

In yielding to this all-compelling upward thrust, the earth's crust sometimes bends and stretches, but more often it breaks; and when it breaks, the fracture occurs in a peculiar place. It does not run along the medial axis of the mountain, but along one margin. On one side of the fracture the crust is lifted and tilted; on the other side it either sinks or remains undisturbed. The uplifted part of the crust is the mountain, and the storms carve out its canyons; the unlifted part remains a lowland or valley, and receives the debris washed out from the canyons.

A mountain is not thrown up all at once by a great convulsive effort, but rises little by little. The subterranean upthrust is continuous and slow, and would produce a continuous upward movement of the mountain if the mountain's weight were the only resisting factor. But there is also a great friction to overcome, the friction along the surface of fracture, between the rising and stationary parts of the crust; and friction gives to slow motion an interrupted or rhythmic character.

The disagreeable jarring of a railway car started while the brake is set is due to the interruption of motion by friction, the wheels alternately sliding and stopping. The musical vibration of a violin strings is due to the alternate cohesion and sliding of the bow upon it, and fails when the friction of the bow is insufficient. Attach a rope to a heavy box and drag it slowly, by means of a windlass, across a floor. As the crank is turned the tension of the rope gradually increases until it suffices to overcome the starting friction, as it is called. Once started, the box moves easily, because sliding friction is less than starting friction. The rope shortens or sags until its tension is only sufficient for the sliding friction, and it would continue in that state but that the box, having acquired momentum, is carried a little too far. This slacks the rope still more, and the box stops, to be started only when the tension again equals the starting friction. In this way the box receives an uneven, jerky motion.

Something of this sort happens with the mountain. The upthrust produces a local strain in the crust, involving a certain amount of compression and distortion, and this strain increases until it is sufficient to overcome the starting friction along the fractured surface. Suddenly, and almost instantaneously, there is an amount of motion sufficient to relieve the strain, and this is followed by a long period of quiet, during which the strain is gradually reimposed. The motion at the instant of yielding is so swift and so abruptly terminated as to constitute a shock, and this shock vibrates through the crust with diminishing force in all directions. Movable objects are displaced, and the soil, which is moveable as compared with solid rock, is cracked. In consequence of earth-cracks subterranean waters find new channels, leading to the stoppage of some springs and the starting of others. In fine, all the phenomena of an earthquake are produced.

This is not a universal theory of earthquakes—some of them are doubtless to be accounted for in a different way; but it affords a sufficient, and I do not doubt that it affords the true, explanation of the earthquakes of the Great Basin. In this region a majority of the mountain ranges have been upraised by the aid of a fracture at one side or the other, and in numerous instances there is evidence that the last increase of height was somewhat recent.

Let us look a moment at this evidence. The material eroded from a mountain by the elements is washed out through the canyons and deposited in the adjacent valleys. The coarser part of it lodges at the mountain base, and is built into a sloping mass called the foot-slope, or colloquially the "bench." When an earthquake occurs a part of the foot-slope goes up with the mountain, and another part goes down (relatively) with the valley. It is thus divided, and a little cliff marks the line of division. A man ascending the foot-slope encounters here an abrupt hill, and finds the original grade resumed beyond. This little cliff is, in geologic parlance, a "fault-scarp;" and the earth fracture which has permitted the mountain to be uplifted is a "fault." In the course of time the same slow process of erosion and deposition which originally formed the foot-slope restores its shape and obliterates the fault-scarp. When a mountain ceases to grow its fault-scarp soon disappears; and conversely, when we find a fault scarp at the base of a mountain we are assured that the uplifting force has not ceased to act. Fault scarps have now been found at the bases of so many ranges of the Great Basin that it is safe to say that the subterranean forces are generally active in this region, and this is especially true of all the large mountain masses. The Wasatch is a conspicuous example, and residents of this city need not go far for ocular demonstration. A fault scarp, thirty or forty feet high, divides the powder houses north of the Hot Spring, so that some of them stand above and some below it, and considerable grading was necessary to lead the road to the upper magazines. With one exception, all the lime kilns between the powder houses and the Warm Springs are built in the face of the fault scarp, the lime rock being conveniently delivered to the kilns from the upper level, and the lime as conveniently drawn out at the lower level. At the mouth of Little Cottonwood Canyon a smelter has been built on the edge of the upper bench for the convenience of dumping its slag over the fault scarp. At the mouth of Spanish Fork Canyon the D. & R. G. railroad encounters the scarp, and the engineers have started an embankment a long way back to climb it. Similar features may be seen, with rare intervals, all along the mountain base from Nephi to Willard.

The fault scarps of the Wasatch follow the western base. Those of the Sierra Nevada follow the eastern base, and it happens that one of them has been formed since the settlement of the country. It occurred in 1872, and produced one of the most notable earthquakes ever recorded in the United States. The height of the scarp varies from five to twenty feet, and its length is forty miles. Various tracts of land were sunken a number of feet below their previous positions, and one tract, several thousand acres in extent, was not only lowered, but carried bodily about sixteen feet northward. The ground was cracked in various directions, and several springs permanently disappeared. All houses of adobe or stone in the immediate vicinity were thrown down, and about thirty persons lost their lives. In the little town of Lone Pine, numbering some three hundred inhabitants, twenty-one were killed by falling walls.

There was only one violent shock, and the damage was all done in a few seconds, but for two months there were occasional tremors. Theoretically, the main strain of the earth's crust was relieved at once, but a complete equilibrium was brought about more slowly.

The surviving inhabitants of Lone Pine observed that the only houses which remained standing were of wood, and in rebuilding they employed that material exclusively. Such a course was natural, but I conceive that their precaution was unnecessary. They may indeed feel feeble shocks propagated from earthquakes centering elsewhere, but in their own locality the accumulated earthquake force is for the present spent, and many generations will probably pass before it again manifests itself. The old maxim "Lightning never strikes the same spot twice," is unsound in theory and false in fact; but something similar might truly be said about earthquakes. The spot which is the focus of an earthquake (of the type here discussed) is thereby exempted for a long time. And conversely, any locality on the fault line of a large mountain range, which has been exempt from earthquake for a long time is by so much nearer to the date of recurrence—and just here is the application of what I have written. Continuous as are the fault scarps at the base of the Wasatch, there is one place where they are conspicuously absent, and that place is close to this city. From the Warm Springs to Emigration Canyon fault scarps have not been found, and the rational explanation of their absence is that a very long time has elapsed since their last renewal. In this period the earth strain has been slowly increasing, and some day it will overcome the friction, lift the mountains a few feet and re-enact on a more fearful scale the catastrophe of Owens Valley.

It is useless to ask when this disaster will occur. Our occupation of the country has been too brief for us to learn how fast the Wasatch grows; and, indeed, it is only by such disasters that we can learn. By the time experience has taught us this, Salt Lake City will have been shaken down and its surviving citizens will have sorrowfully rebuilt it of wood: to use a homely figure, the horse will have escaped, and the barn-door, all too late, will have been closed behind him.

When the earthquake comes, the severest shock is likely to occur along the line of the great fault at the foot of the mountain. This line follows the upper edge of the upper bench from Big Cottonwood canyon to the rifle targets back of Fort Douglas, cutting across each creek just where it issues from between walls of bed rock, and passing only a short distance back of the Fort. At a point not far north of the targets the fault divides; one branch continuing northward, across the spur, toward Farmington, the other turning westward, running just back of that hopeless artesian boring, and following the upper edge of the gravel bench to the vicinity of the Warm Springs. Should the earthquake follow the former of these branches, the city will not fare so badly as the Fort; should it follow the latter, or follow both, city and fort will alike suffer severely.

What are the citizens going to do about it? Probably, nothing. They are not likely to abandon brick and stone and adobe, and build all new houses of wood. If they did, they would put themselves at the mercy of fire, and fire, in the long run, unquestionably destroys more property than earthquakes. It is the loss of life that renders earthquakes so terrible. Possibly some combination of building materials will afford security against both dangers.

G. K. GILBERT.

Figure 1. G. K. Gilbert's letter to the Salt Lake Daily Tribune published in 1883.

actions could be taken that would provide protection from earthquakes because construction of frame houses and structures that were earthquake resistant could create an even greater fire hazard.

First seismograph -

For many years, it seemed that Gilbert would be proven correct. Although a few individuals expressed their concern and argued for recognition of the hazard, their efforts were largely ineffective. James E. Talmage, Professor of Geology and President of the University of Utah, worked for several years to obtain support to install a seismograph on the university campus. He capitalized on the San Francisco earthquake of 1906 and finally succeeded in 1907 when a seismograph was installed in the basement of the university museum (Arabasz, 1979).

Past events and crusaders for change -

Early this century, most individuals and organizations did not perceive a significant earthquake risk, even organizations that would logically have provided such leadership. The first office of Superintendent of Public Works established in 1852 to advise communities on technical and financial aspects of irrigation and other engineering works did not consider earthquakes as a potential threat although it recognized the flooding of Great Salt Lake and the feasibility of reducing the flooding hazard by diverting water from the lake into the west desert (Armstrong, 1986, personal communication).

The first earthquake reported in Utah was felt in Nephi and Provo on December 1, 1853, six years after the first Mormon settlements were established. Early damaging earthquakes that occurred in northeastern Utah

(1884, Bear Lake Valley), central Utah (1901, Richfield), and southwestern Utah (1902, Pine Valley) had little effect on public policy. Frederick Pack, Chairman of the University of Utah Geology Department, documented the effects of the 1921 Elsinore earthquake in southcentral Utah, but his work did not result in public recognition of earthquake hazards. However, the 1934 Hansel Valley earthquake which is the only documented surface faulting event in Utah in historic time heightened awareness by directly causing one death, liquefying lake sediments, and toppling one sculpted figure from the Salt Lake City and County Building. F. F. Hintze, Professor of Geology at the University of Utah, unsuccessfully argued for a seismological society that could share knowledge about earthquakes and the risk to structures and relate it to the city's building standards (Arabasz, 1979). However, only a few hazardous parapets were removed including three additional figures from the City and County Building. Suggestions for earthquake risk reduction through better construction seemed to have no effect; however, the 1934 earthquake appears partly responsible for establishing the beginnings of Utah's seismograph network. In 1935, the U.S. Coast and Geodetic Survey supported installation of two seismograph stations, one at the University of Utah Seismograph Laboratory Building and the other at the Oldham Seismograph Station at the Utah State Agricultural College in Logan.

Studies of active faults -

Work by G. K. Gilbert, W. M. Davis, and others provided geologic evidence of the earthquake hazards represented by the active faults in western Utah, and earthquakes provided proof. Major earthquakes in western and central Nevada in 1915 and 1932 as well as the Hansel Valley earthquake confirmed earthquake hazards related to Basin and Range structures. During the 1940s through 1960s, Utah's geologists began to document active fault traces and to study earthquakes. Ray Marsell and Armand Eardley of the University of Utah and J. Stewart Williams and Clyde Hardy of Utah State University worked on these studies and advocated reduction of earthquake risk.

Building codes -

As more and better data on Utah earthquakes became available, more earthquake research was undertaken and the available information base expanded. At the same time, the state's building wealth exposed to earthquake hazards also increased. After World War II, construction activities boomed in Utah. A backlog of construction needs had accumulated since the building boom of the 1920s and the post-war years saw tremendous growth of some of the most earthquake-vulnerable types of frame and masonary construction with virtually no provisions to withstand lateral forces (Reaveley, 1986, personal communication). Through the 1950s and into the 1960s, unreinforced masonry buildings added to an ever increasing inventory of structures at risk. Arguments made for reducing earthquake risk at a local level were ineffective until the Uniform Building Code (UBC) provided a model that included seismic safety provisions. Salt Lake City first adopted construction standards that considered lateral earthquake forces for certain types of buildings when the UBC was adopted in 1958. This code contained seismic provisions in its appendix. In 1961 when the provisions became part of the main body of the code, the first privately financed buildings in Utah were designed for seismic forces. Even so, many professionals resisted the incorporation of these standards and were reluctant to use them. Additional upgrades of seismic provisions of UBC were adopted in 1964 and in 1967 when the Wasatch seismic zone classification was changed from zone 2 to zone 3.

Champions for earthquake resistant design -

The individuals who brought about these changes are not well remembered except for Ray Marsell who made significant impacts for earthquake hazard reduction in Salt Lake City's waterworks and the construction of certain state water facilities. His studies and documentation of the Wasatch fault and his great enthusiasm as a teacher influenced literally hundreds of policymakers, geology students, and professional geologists and engineers. He accomplished earthquake risk reduction simply by working directly with engineers, pointing out obvious risks, suggesting corrective measures, and seeing that they followed through. Meanwhile, significant scientific advances were made that later influenced seismic risk and its documentation. With the better understanding of soil mechanics and its application to foundations, it became possible to build much larger facilities. For example, when the Bureau of Reclamation built 235 foot high Deer Creek dam in the 1940s, it was one of the highest dams in the nation and incorporated the latest in soils science research and even a consideration of earthquake risk (Armstrong, 1986, personal communication).

Instrument arrays -

Geophysical instrumentation and detection of seismic events in Utah rapidly advanced during the 1950s to meet military demands to document Soviet underground nuclear tests and to monitor tests from the Nevada Test Site. Kenneth Cook, University of Utah geophysicist, built the University of Utah Seismograph Stations by responding to these needs. By 1967, when the first Governor's Conference on Geologic Hazards discussed earthquakes, the seismograph network, although skeletal, was well established, the Wasatch fault zone was partly mapped, geologists at Utah State University had inventoried Utah's historic seismic events, civil engineers at the University of Utah had made some strain measurements across segments of the fault, and the Utah Geological and Mineralogical Survey (UGMS) under William Hewitt had begun inspections of excavations in order to document fault traces. As the understanding of the earthquake hazards continued to increase, so did the risk. Widespread construction of unreinforced masonry buildings and critical buildings such as schools, hospitals, watertanks, etc., without geologic site evaluations, created increased vulnerability that outpaced implementation of measures to reduce the hazard. During the 1970s and early 1980s, perhaps one-third to one-half of all commercial buildings did not comply with UBC requirements (Reaveley, 1986, personal communication).

The 1970s -

The decade of the 1970s saw the transformation from individual scientists and engineers working within their specialities to influence risk reduction to a networking of these individuals and groups to effect earthquake risk reduction in political as well as technical arenas. Work at the University of Utah appears to have set the stage. (For a collection of papers summarizing this work through 1976, see "Earthquake studies in Utah 1850 to 1978, edited by W. J. Arabasz, R. B. Smith, and W. D. Richins.) By mid-1970, a permanent network of seismograph stations monitored the Wasatch Front and much of the Intermountain seismic belt, and research by geologists and geophysicists had provided considerable knowledge of the potential for a major earthquake. About a dozen professionals including structural engineers, building officials, architects, and planners tried to raise the consciousness of their colleagues. In retrospect, progress and interest appears almost haphazard. The Committee on Geologic Hazards for Utah which was established in 1967 later became the Governor's Committee on Geologic Hazards and provided a limited forum for sharing information, ideas, and dilemmas. The Utah Geological and Mineral Survey worked with local governments, and its members gave talks to interested citizens and continued to inspect excavations. It also funded the Woodward-Clyde (Cluff and others, 1970) low-sun-angle aerial photo analysis of the surface traces of the Wasatch fault, which provided a major increase in knowledge that also could be easily applied by planners and understood by interested citizens. After several attempts, encouraged by the national concern for the environment and shocked by unscrupulous land development activity, the 1973 legislature passed Utah's Land Sales Disclosure Act. This act required identification of environmental concerns including geologic hazards before developing large parcels of land in unincorporated areas. Another act, S.B. 27 - Utah Land Use Act, passed in 1974 by the legislature provided for a state role in coordinating land-use concerns, but later that year the act was submitted to a public referendum. It was soundly defeated resulting in a major setback to state leadership in hazards disclosure, facilities siting, and coordination of local government activities.

Meanwhile, at the county level, at least one county, Davis County, appeared concerned with geologic hazards, while others such as Salt Lake County did not incorporate hazards into their decisions even though social pressures against foothill development were increasing. Planning ordinances were defeated on the basis of protecting individuals' liberties and freedom for the pursuit of happiness. Widespread commercial and residential development and government construction of critical facilities continued, and only the exception considered seismic risk unless pressured by national concerns. For example, a positive exception where seismic risks were evaluated was some of the waste water systems funded by the U. S. Environmental Protection Agency (Kaliser, 1986, personal communication). The State funded the construction of numerous facilities, only a few of which incorporated seismic design such as the 1976-77 portion of the University of Utah Medical Center.

While these uncoordinated activities to foster implementation went on, some organizations began to support reduction of earthquake risk: e.g., members of the League of Women Voters, the Parent Teachers Association, and the League of Cities and Towns pushed their organizations to take a stand. The Utah legislature showed some interest and C. DeMont Judd, a state representative from Ogden, urged an interim legislative committee to study the earthquake problem along the Wasatch Front. His efforts were unsuccessful due to opposition from state and local agencies responsible for constructing water impoundments (Judd, 1986, personal communication).

Building officials organization -

A key group that banded together in 1972 and continued as an effective agent of change was the Building Officials Association, an affiliate of the International Congress of Building Officials (Reaveley, 1986, personal communication). In general, they are not engineers or architects. They are responsible for issuing permits and checking plans for local governments. Under the leadership of staff of the Salt Lake City and County building departments, this group reinforced its own membership with training, technical assistance, and moral support when members were faced with political and other pressures to allow poor building design or construction. This group served as an example to other professional groups that later took up the banner of earthquake risk reduction, such as the Structural Engineers Association formed in 1977-78 to improve the quality of structural engineering work in Utah. They, too, have improved the quality of their profession and influenced actions by the State Board of Registration to discipline members of their profession for flagrantly poor construction designs (Ward, 1986, personal communication). Their active membership presently numbers approximately 85.

1975-76 legislation -

The years 1975-76 saw significant political advances. Senator Frank Moss held U. S. Senate public hearings in April 1975 at the Utah State Capitol on the nation's vulnerability to earthquakes (U.S. Senate, 1975). Various scientists and policymakers testified. That year, House Joint Resolution 29 (Atwood, sponsor) which recommended a seismic safety council failed but was transformed in the 1976 legislative session into a legislative study which recommended the following actions to the 1977 legislature (Sharp, 1976, p. 2-3):

1. It is recommended that the Legislature adopt an act organizing a seismic safety advisory council to develop seismic safety programs and educate state and local agencies and the public at large concerning the possibilities for earthquake hazard reduction programs. Authorization for this advisory council would end in four years.
2. It is recommended that the Legislature support the amendment of the Utah Geological and Mineral Survey enabling statute to include the directive to delineate special seismic risk areas, to provide seismic risk information to the appropriate state and local agencies and, at the request of other state or local agencies, to review the siting of critical facilities. It is also recommended that the Legislature support the request of the Survey for a workload increase to accomplish the mapping and review functions described in the amendment.
3. It is recommended that the Legislature direct the State Building Board to instigate a strong motion instrumentation pilot program in order to help insure earthquake resistant design in future buildings.

4. It is recommended that the Legislature amend Section 73-5-5, U.C.A. 1953 (Dam Safety Statute), to remove the exemption of dams constructed by the U.S. Bureau of Reclamation from review by the State Engineer's Office.

> These recommendations are by no means considered to be the final solution to the problems of earthquake hazard reduction. However, they provide a very real and direct attack on the problem. The Legislature should doggedly pursue the study of earthquake hazard reduction until it is satisfied that all that can reasonably be done has been done. What is finally accomplished to reduce the hazard will depend on the will of the people and what is perceived to be a justifiable cost for the benefits received.

Three of the four recommendations passed (1, 2, and 4). The following three factors helped bring about this success...an expanded information base, an earthquake event in 1975, and political commitments.

According to the legislative summary, "In the summer of 1976, the USGS sent a team of experts to the State of Utah to estimate the probability of an earthquake and the resulting damage.... Upon determining that a major earthquake was likely to strike the Salt Lake area within the next 100 years and postulating where surface ruptures were apt to occur, those conducting the study developed a total damage profile through careful consideration of seismicity, geological history, population density, and distribution and physical status of structural and lifeline installations throughout the region" (Sharp, 1976, p. 22-23). Concerning the probability of a major earthquake, the USGS Open File Report 76-89 actually had stated "the time interval for which there is a 63 percent probability of an event exceeding or equaling magnitude 7.5 may be as short as 100 years" (USGS, 1976, p. 37). This report which outlined damages that would likely be sustained along the Wasatch Front also awakened political support from politicians representing Utah's urban areas.

On March 28, 1975, the magnitude 6.0 Pocatello Valley earthquake near the Utah-Idaho border caused considerable damage, mostly in Idaho, and helped focus support for earthquake legislation. The earthquake was felt throughout the Salt Lake Valley and the northern portion of the state and damaged several buildings in Salt Lake County. Considerable political attention focused on damage to the Oquirrh School located in a politically vociferous neighborhood of downtown Salt Lake City.

Additional support for legislation was gained through political loyalty and commitments. According to R. S. Olson (written communication, 1984, p. 9-10), "The Utah Legislature passed the Utah Seismic Safety Advisory Council (USSAC) bill but only after several amendments and considerable difficulty. Insiders agree that passage was primarily due to three factors: (1) Many legislators liked Genevieve Atwood [sponsor of the bill], respected her professional credentials, and accorded her high credibility on the earthquake issue. Moreover, they wanted to 'give her a program, something she could point to'. (2) Atwood repeated her commitment to the bill's sunset clause, ending the USSAC after a four-year run. One especially key actor said that the sunset clause swung the Senate and kept the House coalition more or less intact. (3) The fiscal picture was reasonably bright that year, and there were sufficient funds to support a number of these modest government programs".

Utah Seismic Safety Advisory Council -

Thus began the first successful, multidisciplinary attempt to reduce earthquake risk. The Utah Seismic Safety Advisory Council (USSAC), with Delbert Ward as Executive Director, brought together a group of eleven diverse members whose mandate was to devise and to recommend within four years a consistent and comphrensive public policy framework for earthquake risk reduction in Utah. In retrospect, USSAC products are highly praised but disappointment is widely expressed that no agency or group followed through on the recommendations. The 22 reports received limited distribution, and by the time the reports were issued the political climate had changed and the legislature did not act to integrate the function of reduction of earthquake risk into the Governor's planning office. As a result, very few of the recommendations were implemented and none of the suggested legislation became law. The 1981 legislature consisted of many new members, several of whom had campaigned on a Proposition 13 platform to reduce government. According to R. S. Olson (1984, written communication):

> The Republican party is the traditional home of the anti-regulation, anti-government elements in U.S. society, and it would be difficult to conceive of a more uncongenial set of bills than the USSAC proposals: The first four were classically regulatory, and the fifth was a bill to add a new, permanent government office, offering the prospect of even more regulatory legislation in the future. In one of our interviews, an opposing legislator expressed the opinion that "Representative Nielsen and Senator Swan were brave as hell even to bring the USSAC package to the 1981 session."

Even so, there is general agreement that the USSAC made a quantum difference in earthquake risk reduction by: (1) linking several of the isolated scientists and earthquake-safety activists into a network, (2) focusing attention on earthquake hazards, (3) writing a series of reports that documented the status quo of earthquake preparedness and provided a framework for action, (4) bringing together local leaders with national experts, (5) providing visibility for all individuals and agencies who wanted to contribute to earthquake risk reduction, (6) providing an umbrella of political legitimacy to engineering, political, scientific, and other professional groups who lobbied their membership for increased acceptance of state-of-the-art techniques, and (7) providing a collegiality and supportive network that lasted beyond the lifetime of the organization. Governor Matheson had been and continued to be verbally very supportive of hazards preparedness and mitigation. In 1975, the Second Governor's Conference on Geologic Hazards stressed several hazards including earthquakes. In 1980, the Governor transformed the unwieldly Council of Defense into the Division of Comprehensive Emergency Management (CEM) with the hope it would be less focused on bomb shelters and more concerned with natural hazards (Matheson, 1986, personal communication). Shortly thereafter, CEM began its statewide hazard preparedness plans with funding assistance from Federal Emergency Management Agency (FEMA) and their public information programs included personal preparedness for earthquakes. A few local communities responded to concerns expressed by members of the USSAC and contracted for hazard maps, others passed ordinances containing provisions for identification of geologic hazards. The UGMS responded to their requests for geologic investigations of critical facilities.

In 1983, the second well-organized surge of effort to reduce earthquake vulnerability along the Wasatch Front began as part of the USGS Regional and Urban Earthquake Hazards Assessments element of the National Earthquake Hazards Reduction Program. This program targeted the Wasatch Front as its highest priority and the USGS invited the UGMS to participate in developing and carrying out the program's five components: information systems, hazard evaluation and synthesis, ground motion modeling, loss estimation models, and implementation. One of the important accomplishments of the program has been installation of a network of strong motion seismographs along the Wasatch Front located to record the ground motion in several geologic environments during a shaking event. None of the USGS scientists involved in the Wasatch Front earthquake program are headquartered in Utah; therefore, much of the local leadership role fell to the UGMS. The 1983 Borah Peak earthquake in neighboring Idaho and in a geologic setting similar to the Wasatch Front has provided much scientific information applicable to the Wasatch Front and in conjunction with the 1985 Mexico City earthquake, has increased public awareness of the nature and extent of earthquake hazards.

FACTORS THAT TEND TO ENHANCE OR IMPEDE EARTHQUAKE RISK REDUCTION

Events outside of Utah have enhanced decisionmakers' awareness of the need to reduce risks from earthquakes in Utah. For example, the 1906 San Francisco earthquake resulted in the installation of Talmadge's instruments in 1907 (Arbasz, 1979). The Cold War in the 1950s and 1960s greatly advanced the understanding of Utah's seismicity when the military provided funding for instruments in Utah to monitor nuclear tests at the Nevada Test Site and other locations around the world. Professor Kenneth Cook and others capitalized on this to establish the skeletal network of seismograph stations. The first station locations were selected primarily to gather information about nuclear tests rather than about the seismicity of the state, but under the direction of Professor Robert Smith, the number of seismograph stations was expanded and located strategically to better understand earthquakes. The Borah Peak earthquake which occurred in central Idaho on October 28, 1983 is proving to be of great importance to understanding Utah's earthquake hazards because its geologic setting is similar in important ways to Utah's Wasatch Front. As such, it can be used as the model earthquake along the Wasatch fault for emergency response planning. Even so, although it reinforced USGS efforts and provided valuable information to the scientific community, it has had little noticeable impact on state or local policy. As several people have said, "not enough people were killed to get the politicians' or the public's attention".

Perhaps the most telling factor acting against adoption of earthquake risk reduction measures is that Utah has not experienced a highly destructive earthquake in a heavily populated area. Earthquakes have been felt in Utah since shortly after the first permanent settlements were established in 1847 and destructive earthquakes have caused extensive damage in several small communities. The main population centers along the Wasatch Front, however, have not sustained substantial damage. Destructive earthquakes in California, Alaska, Nevada, Montana, and Idaho have convinced most of Utah's leaders and many of the citizens that an earthquake along the Wasatch Front would cause great loss of life and destruction of property, but the earthquake problem seems removed from most people's everyday perceptions. Even those who endorse the science have not had their lives personally affected by an earthquake the way that many Californians have. Most state politicians easily can convince themselves that it will not be a problem during their term in office or even in their lifetime. Their constituents are not clamoring for safety measures. Considerable personal evidence supports the idea that "it won't happen to us". Many individuals still concur with Gilbert that it will take an extensive damaging earthquake to change present practices of architects and structural engineers and to incorporate a respect for geologic hazards into site evaluation. This conclusion is in spite of the favorable geography, topography, and geology of Utah's urbanized areas that allow for planning without denying growth.

In discussing those forces which seemed to have brought about reduction of earthquake risk and those forces which seemed to thwart these efforts, by far the most frequently cited negative force is inadequate information about earthquake hazard and risk in Utah. In spite of the considerable progress in understanding the physical phenomena of earthquakes and many engineering solutions, major questions remain unanswered. Scientists understand the Wasatch fault system much better than a decade ago, and successful implementation of earthquake risk reduction measures by other communities, particularly in California, serve as an example to Utah's communities. Some decisionmakers believe that a critical mass of information has already been developed and that cries of "too little information" are uncalled for. But, the majority of policymakers in Utah believe that, although an important body of knowledge has been developed and that a destructive event will happen during their lifetimes, not enough has been learned for them to apply it. Implicit in this concern for more information is the additional concern that even if the earthquake hazard were better understood, the application of that knowledge to effectively reduce the risk to life and property would require much further work. How much information has to be in hand to make decisions that will be cost effective? Apparently, not enough exists today and perhaps the information in hand has not been fully translated so it can be easily used by non-technical people. Scenarios of probable events and consequences have not been sufficiently developed to convince preparedness, response, and recovery planners of the reality of response exercises. Even when scientists such as S. T. Algermissen and Walter W. Hays (USGS) have estimated bedrock ground motion and generated maps that could be used as the basis for building codes, design professionals in Utah express suspicions that the engineers who translate this information into national building codes do not understand what the science means.

In Utah, as elsewhere, decisionmakers want a solid information base and are discomfitted when the information they thought they understood changes with the advancement of scientific understanding. When codes change too often, credibility can be lost. The information base has changed considerably in the last twenty years. Recent advancement in our understanding of the earthquake hazards along the Wasatch Front now emphasizes ground-shaking hazards versus surface-rupture hazards that were emphasized ten years ago. The recurrence interval of breaks along segments of the Wasatch fault is now estimated to be significantly longer than many had assumed ten years ago. New concerns are being raised about hydrologic effects of earthquakes including eastward tilting of the valleys and the resulting eastward transgressions of Great Salt Lake and Utah Lake. The lack of strong-motion data continues as a major weakness in Utah's information base and must be extrapolated from elsewhere. Thus, there is a tendency to wait for better information. Decisionmakers would like to have estimates of the probability of a major earthquake occurring within the next 50 or 100 years and most investigators do not believe that the existing information is adequate to justify this kind of forecast. Decisionmakers need to know what actions are most effective in reducing risk. This information is particularly important when decisionmakers consider proposals to invest large sums of money in retrofitting historic buildings to improve seismic safety or when they consider additional expenditures to fund seismic safety features that were not included in the original construction design. Unfortunately, decisionmakers often receive conflicting advice when faced with these dilemmas.

Translating scientific information for use by non-scientists has inherent difficulties. Many users of hazards information in Utah are state and local officials who are unfamiliar with geologic processes and, even when they recognize a hazard exists, are confused about what information is available or where it is available. When provided with this information most do not know how to use it because technical reports are rarely presented to the public in lay terms. Taking people into the field and showing them evidence of a hazard is usually more effective in developing an understanding of a hazard than simply providing a technical report. Another difficulty seems to be that many of the users of hazard information are engineers with a propensity to enjoy the challenge of solving problems rather than seeking to avoid them. They question the credibility of hazard statements especially if given in alarmist tones. If the hazards and risks cannot be quantified, many engineers question their reality, reasoning that if a problem cannot be clearly defined, standards cannot be drawn. If apparently differing opinions are expressed by scientists, some decisionmakers convince themselves that not enough reliable information exists to influence decisions. And...if they have two experts who disagree, they are off the hook. Today's information base makes the definition of the hazard appear too complex, the assumptions too numerous, and the conclusions too speculative to be the basis for political decisions. Lay people may conclude that geologists and seismologists may not really know what they are talking about.

Such skepticism is human nature and not unique to Utah. Many officials and the public do not want to recognize what they assume will be an expensive problem. Recommendations for special construction standards and many other earthquake risk reduction measures require additional funding. Property owners often assume that the recognition of a geologic hazard on their property will decrease its value and that a geologic site investigation will disclose only negative information. Most building owners believe that retrofitting structures to achieve seismic safety and delays in construction of new facilities to allow for detailed site characterization and seismic design are prohibitively expensive. For instance, Utah's water projects are considered vital to the state's economic future and their proponents have viewed geology and geologists as disrupting projects by causing costly delays, and by adding costs to redesign.

Most homeowners and developers have not had experience with earthquake risk reduction and do not understand the economics of earthquake preparedness and response. They see no way to distribute the costs of earthquake risk reduction before the earthquake happens. They wonder who will pay and question who should pay, before or after an earthquake. They often assume that the federal government will come to the rescue and this assumption alleviates much of their concern. The price of earthquake insurance has discouraged its acquisition by most property owners. To most business people, the incentives to encourage private enterprise to take seismic safety seriously are either lacking or are counter-productive. The prevailing economic incentives to build as much as possible for as little as possible put pressure on planning and zoning boards and on elected officials at both the local and state levels and on local building inspectors to ignore problems related to natural hazards. Building code provisions are expressly defined as minimum standards, but they commonly are perceived as the maximum. If design professionals are doing less than the minimum they may be sued, and if they overdesign they may not be retained.

This creates financial disincentives for innovation or for additional protection.

Private businesses in Utah rarely have enough resources to build what they really want to have constructed and they tend to invest in what is required immediately and not much more. State government funding can be even less rational because the Utah legislature generally funds repairs to buildings and corrects even major deficiencies, however, it almost never provides sufficient funds to meet the needs for new construction projects (Matheson, 1986, personal communication). Thus, original designs are kept as inexpensive as possible in order to provide funds for as many projects as possible. This has often compromised safety. The Utah legislative appropriations act spells out, line item by line item, expenditures of the Division of Facilities Construction and Management (DFCM). Reduction of exposure to geologic hazards has never been a priority expressed to the division by the legislature (Nelson, 1986, personal communication). Rarely do the state and other owners specifically request earthquake design (but at least they are no longer rejecting such suggestions on the basis that they cost too much). More often, earthquake safety is used by DFCM with other arguments as an excuse to retrofit or tear down a building in need of major repair for other reasons.

Limited and unpredictable funding also hurts state programs for earthquake risk reduction. At the federal level, relatively reliable funding has been one of the reasons the National Earthquake Hazards Reduction Program has succeeded as a research and mitigation program. At the state level, the progress in earthquake risk reduction is remarkable given the virtual absence of state-funded earthquake programs and the lack of understanding about geologic processes by governmental officials and the public.

On the positive side, several economic factors help reduce earthquake risk in Utah. Early recognition of earthquake hazards and the incorporation of seismic design in new construction appears to add between 2 and 5 percent to the cost of most buildings and incorporates protection against several other natural hazards such as wind and foundation problems (Ward, 1986, personal communication). Early recognition of problems saves delays and costs later on. The potential liability of some public officials for not incorporating geologic hazard information in the decisionmaking process has encouraged some to seek such information. Similarly, increasing premiums for liability insurance is leading to the development of minimum standards of practice for architects, engineers and geologists. In this environment, earthquake risk reduction may follow the pattern of the energy conservation program which succeeded in getting life cycle energy costing built into the construction of public facilities. The economy of the state can support earthquake risk reduction in construction practices, and the concern for quality of life and the goals of attracting tourism and clean industry argue for planning and zoning that considers the impact on the natural environment.

Utah's topography, geography, geology, population density and demography are such to make sensible land-use planning effective. Past political experience indicates that this is most likely to occur in Utah at a local, not a state, government level. Local governments in Utah exhibited a sense of genuine governmental responsibility to their citizens during the flooding/landslide/mudflow events of 1983 and 1984. Cities and counties in

Utah have not had a "good earthquake but we have had a great flood, from the emergency response point of view" (Haines, 1986, personal communication). The flooding events tested the communities' capability and willingness to respond. The neighborhood organizations worked extraordinarily well using the LDS Church's organizational structure to quickly communicate information to workers and volunteers. Another positive social factor is that the LDS Church espouces the ethics of preparedness, organization, and responsibility for self and family during economic and natural hazard emergencies. The church has had considerable experience in helping others recover after major disasters and has taken considerable interest in earthquakes perhaps because their church headquarters is in known earthquake country or perhaps because a few well respected members have been influential in pointing out the hazard. For whatever reasons, the LDS Church constructs its buildings with seismic safety considerations and trains its members to respond to emergencies.

During the spring and early summer of 1983 and again in 1984, communities along the Wasatch Front and along the plateaus to the south and east experienced widespread flooding, numerous landslides, and mudflows. Local officials became familiar with the destructive power of these natural hazards and gained first hand experience on how to avoid the hazard or engineer to lessen the risk. Organizations such as the Association of Counties advised their members that the doctrine of "governmental immunity" reduces liability of public officials if they have tried to abate the risk; however, if they have done nothing, they are liable (Hester, 1984, personal communication). The increased migration of Californians and others to Utah from areas where geologic hazards are taken into account has heightened awareness. These newcomers are negatively impressed when local promoters downplay the hazard.

Countering these positive forces are several strong statewide sentiments against organized, government-sponsored activities such as land use planning, and some sentiment that natural disasters are "acts of God" and hence, attempts at risk reduction are futile. An extreme example of the sentiment against statewide regulations was the support for state legislation in 1981 to exempt schools from conforming to building codes. This bill, vetoed by Governor Matheson, would have exempted the schools from safety and health factors in the interest of economy and local control. It was dubbed the "burn the children bill" (Matheson, 1986, personal communication). The legislative debate reflected a perception that all regulations lead to inflexible rules prescribing exactly how to cope rather than encouraging reasonable and flexible case-by-case analysis (Nelson, 1986, personal communication). With an almost religious fervor, many people consider development and risk-taking commendable whereas intellectualism and scientific pronouncements evoke wariness. In fact, "religious" statements are made to discourage preparedness in spite of LDS Church activities to the contrary. In the Utah House of Representatives, arguments were made against the establishment of the Utah Seismic Safety Advisory Council because earthquakes were "sent by God" (Atwood, 1977, personal observation). Richard S. Olson wrote a summary of the origins, activities, and demise of USSAC as an unpublished contribution to the August 14-16, 1984 USGS et al workshop on "Evaluation of Regional and Urban Earthquake Hazards and Risk in Utah" as part of his research on the influence of partisan politics in the establishing of policies for seismic safety in Utah. In that paper, he details the difficulties the seismic safety bills have had in the Utah legislature from 1972 to 1982, including highly conservative sentiments against regulation and governmental encroachment into private decisionmaking.

State government's reluctance to require land use planning almost certainly harks back to the 1974 defeat by a popular vote of 242,068 against to 157,438 for the Utah Land Use Act. This is the only law passed by the Utah legislature that has been so unpopular that it was revoked by popular referendum. More recently, as communities have grown, the perceived need for reasonable and coordinated planning has increased (Haines, 1986, personal communication). Planning is justified as a way for Utah to maintain its quality of life and environment. As urbanization concentrates population, it increases the vulnerability of the public and its lifelines to earthquakes. A lack of leadership at the state level is perceived for both long term mitigation and response (Huefner, Haines, 1986, personal communication). Interjurisdictional problems (i.e., turf) abound both vertically among federal, state and local entities, and horizontally among state agencies. The Division of Comprehensive Emergency Management (CEM) and Federal Emergency Management Agency (FEMA) are saddled with a reputation that they put response first and preparation second. This perception however may change. FEMA, after years of nominally coordinating the earthquake programs of all federal agencies, now invests an increased, albeit a small, amount in mitigation and hazards awareness. The effectiveness of some state and many local agencies may be compromised by members of their policy boards who are developers or building contractors with conflicting interests (Haines, 1986, personal communication). The effectiveness of UGMS in advising on geologic hazards has been limited by a perception of being alarmist and having a tendency to righteously criticize rather than assist other state agencies' efforts (Nelson, 1986, personal communication). In short, the bureaucracies within federal, state, and local governments create their own political hazards to be reckoned with.

Countering the adage that old ways are comfortable ways, several professional societies in Utah reinforce the best intentions of their members and persevere in their goal to upgrade their own professionalism and that of state government. When state government has been ineffective in providing leadership in hazard mitigation or coordinating land-use practices, these professional societies have encouraged local governments to do so. In 1980, a small group of structural engineers and architects halted the Crossroads/Beneficial Life tower in downtown Salt Lake City in mid-construction because of questionable structural design (Reaveley, 1986, personal communication). The time it took to revise the plans resulted in millions of dollars in lost time and increased costs. Salt Lake City's Building Department now exercises more careful plan review.

Key individuals and organizations in Utah are primarily responsible for the successes in hazard reduction. Several of these individuals were members of the USSAC, Structural Engineers Association, or University of Utah staff. All see a need, enjoy the fight, like the professional and national recognition, and express a personal commitment to leave their profession "better" than when they entered it. They stress that they feel good that they are not "selling junk" and are translating complicated science into workable policy. Key organizations such as the USSAC, Association of Building Officers, Structural Engineers Association, the Utah Chapter of the American Planners Association, UGMS, and several academic departments at Utah's universities have provided technical and moral support to their membership and staff and to others associated in the political process. The University of Utah, the USGS, the UGMS, and the LDS Church have been particularly influential in bringing about change. Although the LDS Church has not made proclamations, it has set policies in more subtle ways by requiring seismic design on its buildings, stressing personal preparedness and community response, and demonstrating a willingness to coordinate with state and local governments in time of disaster. The USGS and the University of Utah have helped to develop the information base, coordinated scientific and engineering studies, and provided professional esprit de corps that has added much of the excitement and challenge. Scientists at Utah State University, Brigham Young University, and individuals in private enterprise also have made significant contributions to advances in research. As the understanding of the Wasatch fault system has increased, so has the visibility of their programs. And finally, time itself influenced the rate at which earthquake risk has been reduced. Over the years, the reduction efforts add up. Continued articulation of the problem, bolstered by more and better information, has gained recognition of the hazard, increment by increment.

IMPLEMENTATION EFFORTS IN CURRENT EARTHQUAKE PROGRAM

The ultimate success of the Wasatch Front Earthquake Hazards Program in reducing the earthquake risk will depend on the effectiveness of the implementation component. The goal of this component is the effective use of scientific information to reduce loss of life and damage to property caused by major geologic and hydrologic hazards. Achieving this requires communication of translated scientific information to responsible officials and interested parties seeking to reduce losses from the hazards. This is a major challenge to the program because many of the products of scientific research are not directly useable by responsible officials and the public. To accomplish the goals of this component, it is essential to involve the user of the information early in the program. A series of workshops has been conducted to work with user groups to define the kinds and format of information that would be most useful to them. The implementation component of the USGS-UGMS program is closely related to the preparedness and response programs of FEMA and CEM, and the four agencies are working together to develop this component.

Action by county and city government is essential if earthquake risk reduction measures are to be implemented along the Wasatch Front, but none of the local governments had geologists or seismologists on their staffs before 1985. As part of the National Earthquake Hazards Reduction Program, funds have been provided for five Wasatch Front counties to employ three geologists. The three geologists are located in the counties' planning departments: one for Salt Lake County, one shared between Weber and Davis Counties, and one located in Utah County who also advises Juab County. During the three years of USGS/UGMS support, they will compile published and unpublished reports that contain information about the geologic hazards in their counties, compile this information at 1:24,000 scale, and respond to requests for assistance from city and county agencies for site investigations, project reviews, and technical advice. The technical work of these three geologists is coordinated and supervised by the UGMS. The UGMS also provides advice and assistance directly to local governments on matters relating to earthquakes and other geologic hazards. Two pilot programs have been funded by the USGS to assist Wasatch Front communities in developing techniques to implement earthquake risk reduction. The major cities of Utah are all working on significant implementation efforts. The Utah Museum of Natural History, with support from the National Earthquake Hazards Reduction Program through the UGMS, has developed an instruction kit on earthquake and other geologic hazards for use in schools. Through talks and workshops, a major effort is being made to inform the public of the earthquake hazard. The UGMS and CEM are working within government to convince state agencies that the state should set an example in risk reduction actions. This includes state construction activities and state preparedness.

A major effort is being made by the UGMS to make information on earthquake hazards available to users in forms that will be most useful to them. This information system is largely computer based and is designed to transfer as much information as possible in digital form and facilitate frequent upgrading of the information. A bibliography of approximately 900 publications related to earthquake hazards has been prepared by the UGMS (Jarva, 1986). Other information on earthquake hazards is being integrated into a statewide geologic hazards information data base.

FUTURE OF EARTHQUAKE RISK REDUCTION IN UTAH

Clearly, progress has been and is being made in Utah. Not only is the earthquake threat better understood, the factors that inhibit and promote earthquake risk reduction are also better understood. However, as we look to the future, many needs remain.

Some needs are just wishes...almost fantasies, such as: 1) that the Utah legislature would play a greater role in promoting seismic safety, 2) that bureaucratic turf problems would go away, 3) that all developers would consider geologic hazards in their developments, 4) that many more exceptional people with diverse backgrounds would champion seismic safety, and 5) that Utah could be exposed to an earthquake event that could shake us to our senses and provide needed data without inflicting much damage. Being more realistic, although optimistic, there appear to be a number of areas which need continued emphasis. Many individuals express the need for re-establishing the Utah Seismic Safety Advisory Council or a similar organization to provide well-coordinated leadership, a central reporting point, and accountability at the state level. There is a need for statewide leadership in construction practices. Certainly, all state-funded buildings should be required to meet UBC seismic provisions. The USSAC recommended that all publicly occupied buildings meet UBC seismic provisions (USSAC, 1981). The 1983 Governor's Conference on Geologic Hazards recommended legislation that would require that a buyer of property in Utah be informed of known geologic hazards that could affect that property (UGMS, 1983). Many geologists would like to see local governments require a geologic report before tracts of land are developed or before state funds are used to construct a public facility. FEMA and CEM could place greater emphasis on prevention, mitigation, and avoidance of hazards. UGMS could fill the need for a state repository and distribution point for earthquake information. If universities and other research groups would identify new information and techniques that are developed to the stage they can be applied, the UGMS, county geologists, and others could translate, disseminate, and encourage their use. Peer review by geologists and structural engineers can increase professionalism of the local consulting community and achieve higher quality reports, especially review of siting and design plans for public schools. Most agencies and professional organizations have not defined response roles after a major earthquake in such a way that their geologists and engineers know their responsibilities for participating in rescue and public safety operations or for collecting important geologic information on short-lived phenomena.

The need to translate the technical information so that engineers, planners, and policymakers can use it cannot be stressed too much. As one person said "if we're so smart, why aren't we using it?" (Nelson, 1986, personal communication). The users of the information, especially planners and regulatory agencies, need to understand certain aspects of earthquake risk. Policymakers need information on economic repercussions to recognize the payback for their investment. Loss estimates for specific geographic areas that detail potential loss of life, property losses, damage to essential services, and indirect economic losses effectively capture public attention. The results of such studies do not need to be translated in order to impact decisionmakers.

Most often voiced by information users and generators alike is the need for clearer, more definitive information about earthquake events and the true risk in the state. What are the characteristics of an event that could be expected along the Wasatch Front? For a given site, what would be the repercussions? What will be the effects on ground water, on Great Salt Lake and Utah Lake? Where will landslides occur? Which are the most seismically active segments of the Wasatch fault? What is the geometry of the faults? Are some active faults blind, i.e., hidden at the surface? What are the levels of peak accelerations related to normal faulting, given certain focal depths and the geometry of the fault? What event is most likely to occur and what are the limits of what could occur; is magnitude 7.5 really the upper limit? What will ground response be for a really big earthquake and what is peak response for other earthquakes? How often do these events recur?

To answer these questions requires continuing basic data collection as well as special studies. Just as the weather service keeps sending out balloons and collecting various types of data, so the network of seismographs needs to continue to monitor the Intermountain seismic belt. Other specific studies to address some of the questions listed above include systematic high quality reflection profiling of the fault to better define the geometry of faults; drill holes through the Wasatch fault to precisely locate the fault at depth and collect information about the physical characteristics of the rocks close to the fault at depth; trenching to try to determine event magnitude and recurrence intervals of large earthquakes on different fault segments; frequent remapping of the geodetic network in Utah to better document the state of stress; development of models to predict ground-motion parameters such as acceleration, velocity, displacement, and spectral response at locations for postulated hypothetical earthquakes; and strong-motion devices to capture site specific information about ground response that can be used in building design and for construction standards.

Efforts to answer these questions will require money, talent, and time. The past three-year USGS effort has shown that concentration of resources can result in a major increase in the amount and quality of available information. Only time will tell if a critical mass has been achieved. If it is not quite achieved yet, then it seems close. Although real progress has been made in the sciences, only incremental successes have been made in implementation. The scientific and engineering advances and the achievements of implementation of the first half of this century appear in hindsight to be almost random. Those of the 1970s are mixed with significant defeats and backward slides. Now in the 1980s, it looks as if we will not slip backward as often. Local government entities are clearly aware and concerned about earthquake hazards and risk. At the state level, policymakers want to preserve Utah's quality of life and reputation as a grand place to live and that may mean a shift toward policies that stress wise development. The time seems right to get information into the hands of those who can and want to use it. However, detailed maps delineating earthquake hazards are probably years away, although generalized maps for most of the metropolitan areas will be available in 2 years. And, of course, there will be skepticism, inertia, and other obstacles inherent to bureaucracies. Even so, there is ample evidence that Utah is moving to implement earthquake risk reduction measures and hopefully, we will prove that G. K. Gilbert was wrong in 1883 when he wrote:

> Our occupation of the country has been too brief for us to learn how fast the Wasatch grows: and, indeed, it is only by such disasters that we can learn. By the time experience has taught us this, Salt Lake City will have been shaken down and its surviving citizens will have sorrowfully rebuilt it of wood: to use a homely figure, the horse will have escaped, and the barndoor, all too late, will have been closed behind him.

References Cited

Arabasz, W. J., 1979, Historic review of earthquake-related studies and seismographic recording in Utah, in Arabasz, W. J., Smith, R. B., and Richins, W. D., eds., Earthquake studies in Utah 1850 to 1978: University of Utah Seismograph Stations special publicantion, p. 33-56.

Arabasz, W. J., Smith, R. B., and Richins, W. D., editors, 1979, Earthquake studies in Utah 1850 to 1978: University of Utah Seismograph Stations special publication, 552 p.

Cluff, L. S., Brogan, G. E., and Glass, C. E., 1970, Wasatch Fault, Earthquake Fault Investigation and Evaluation; Consultants report by Woodward-Clyde Associates for Utah Geological and Mineral Survey, 3 volumes.

Gilbert, G. K., 1883, Earthquakes: The Salt Lake Daily Tribune, September 16, 1883.

Jarva, J. L., 1986, Bibliography of Utah Earthquake Hazards, computer and hardcopy publication of Utah Geological and Mineral Survey, in press.

Olson, R. S., 1984, Seismic safety and party differences: the case of Utah, unpublished manuscript prepared for USGS/UGMS/CEM/FMEA workshop on evaluation of regional and urban earthquake hazards and risk in Utah, August 14-16, 1984, paper number 21, 18 p.

Sharp, V. J., 1976, Earthquake hazard reduction in Utah, a report to the 42nd Legislature: Utah Office of Legislative Research report no. 14, 58 p.

Utah Geological and Mineral Survey, 1983, Governor's Conference on Geologic Hazards, UGMS Circular 74, 99 p.

Utah Seismic Safety Advisory Council, 1981, A brief summary of earthquake safety in Utah and abbreviated recommendations for risk reduction, USASC report 22, 13 p.

U. S. Senate, 1975, Earthquake research and knowledge, a hearing before the Committee on Aeronautical and Space Sciences, April 26, 1975, U. S. Government Printing Office, 261 p.

U. S. Geological Survey, 1976, A study of earthquake losses in the Salt Lake City, Utah area, USGS Open-File Report 76-89, 357 p.

EMERGENCY MANAGEMENT IN UTAH FOR EARTHQUAKES

BY JAMES L. TINGEY AND RALPH F. FINDLAY
UTAH DIVISION OF COMPREHENSIVE EMERGENCY MANAGEMENT
SALT LAKE CITY, UTAH 84018-0100

ABSTRACT

Since 1982, the Federal Emergency Management Agency has sponsored programs in Utah under the National Earthquake Hazard Reduction Program (NEHRP) through the Utah Division of Comprehensive Emergency Management (CEM) for earthquake preparedness along the Wasatch Front. The major emphasis of these programs has been in three areas 1) Preparedness and response planning, including the development of mutual aid agreements 2) Mitigation strategies involving the education of builders, architects and planners and 3) Public awareness and education.

While most of the particular needs of the State as they relate to earthquake hazard mitigation have been established in the past by the comprehensive work of the Utah Seismic Safety Advisory Council (1977-1981), CEM's major challenge has been to provide management leadership for the implementation of preparedness and other mitigation strategies within the cities, counties and state agencies of Utah.

Eighty percent of the population is concentrated along the Wasatch Fault Zone. With a projected increase in population of 16 percent through 1990 and 62 percent through the year 2010, a great deal of emphasis will be placed on public awareness programs.

Initial efforts of CEM's programs were on the development, coordination and integration of the State/Four County Earthquake Response Plan which provides central coordinating direction and organization during the response

phase of an earthquake. This document ties together city, county and state government emergency plans so that response procedures can be monitored at each level.

During 1985, mock earthquake or "Table Top" exercises were held in each county and at the State Emergency Operations Center to test the plan and familiarize coordinating officials with the plan. A table top exercise requires the participants to respond to messages requesting resources, information or describing damage. As a result of the exercises, especially at the State level, several areas for improvement were identified, including radio networks, communication backlog, emergency operation center organization, and interagency communication.

Mutual aid agreements, which formally tie together the emergency response capabilities of Weber, Davis, Salt Lake, and Utah counties under the coordination of CEM, were executed in 1985. Other mutual aid agreements, cooperative agreements, and memorandums of understanding were negotiated with public and private entities including the University of Utah Seismograph Stations, private volunteer agencies, military entities, and others.

Because of an increased amount of public interest in earthquake information from a scientific and safety standpoint as expressed by the distribution of approximately 750,000 brochures and many public presentations, CEM's direction for 1986 is the development of public education and awareness material. The work program includes the production of a locally focused earthquake education/ preparedness and safety film for public broadcast and possible reuse as an "in-class" tool. This film is to be supplemented by a public education and awareness packet.

A very important objective for activities in 1985 was the establishment of specific requirements for hazard maps. The major goal of the 1985 Workshop on Earthquake Hazards in the Wasatch Front Region was to provide urban planners with a sounding board for their specific map needs.

As a result, a scale requirement of at least 1:24,000 was arrived at as the best for overall use at the state, county and city levels. Specific overlay topics were also determined, these included fault zones, isoseismal zones, liquefaction zones, lifeline routes, and critical facilities. Thirty-eight 7 1/2 minute USGS quadrangle maps and two 15 minute quadrangles covering critical planning areas, were identified as needing hazard overlays.

The 1986 USGS National Mapping Division digital mapping project for Salt Lake County will provide an excellent way to produce and transmit this data at the desired scale, or possibly larger, in order to benefit detailed planning at local levels.

The continued support of FEMA through the NEHRP is essential at this time as momentum builds toward efforts to implement the more difficult hazard reduction activities.

INTRODUCTION

One of FEMA's roles under the National Earthquake Hazards Reduction Program (NEHRP) is to develop the capability within state and local governments to be prepared for, respond to, recover from, and mitigate the effects of earthquakes. As in other programs, their objectives are to save lives, and to reduce injuries, property losses and outages.

FEMA's efforts in Utah have been directed toward the implementation component of the Regional and Urban Earthquake Hazards program element. The development of the Regional and Urban Earthquake Hazards program evolved from the discussions held at Pacific Grove, California in 1982. Five interrelated components were adapted and eight regional and urban areas were chosen for further emphasis. The Wasatch Front Region, Utah was ranked as priority number one; and it was recognized that the

Wasatch Front Region was the only region in which all five components are being pursued. Utah has concentrated on three elements under FEMA's current program guideline standards (FEMA, 1986 CCA): 1) Preparedness and response planning, including the development of mutual aid agreements 2) Mitigation strategies involving the education of builders, architects and urban planners and 3) Public awareness and education.

The Utah Division of Comprehensive Emergency Management's (CEM) role in locally implementing NEHRP through the Utah Earthquake Preparedness Program is controlled by three fundamental elements: 1) NEHRP guidelines outlined by the governing bodies of the Federal Emergency Management Agency, USGS, National Bureau of Standards, and the National Science Foundation 2) Funding and directional authority of FEMA National and FEMA, Region VIII, and 3) The needs of the State of Utah which are reinforced by the current public willingness to pursue programs outlined by NEHRP and Utah's Earthquake Preparedness Program.

CEM and the earthquake program are the central links between the national and regional offices of FEMA, which have established the basic guidelines for state and local implementation of NEHRP, and the user oriented preparedness and response office of state and local governments and private-volunteer agencies.

PROGRESS BY THE FEDERAL EMERGENCY MANAGEMENT AGENCY AND UTAH DIVISION OF COMPREHENSIVE EMERGENCY MANAGEMENT

In 1977, the Utah State Legislature established the Utah Seismic Safety Advisory Council (USSAC). In addition to the fourteen technical reports and the compilation of important data; in 1981, the USSAC published "A Brief Summary of Earthquake Safety in Utah and Abbreviated Recommendations for Risk Reduction" (USSAC-22, 1981). This summary listed 18 general recommendations for comprehensive earthquake hazard mitigation and response. Many of these concerns and the expanded recommendations contained in the twenty-two publications issued during the four years of the USSAC are being addressed in Utah's Earthquake Preparedness Program.

Since 1982, FEMA has sponsored earthquake hazards reduction, preparedness, and mitigation programs with funding support as follows:

FY 1982	$24,000
FY 1983	$25,000
FY 1984	$30,000
FY 1985	$33,000
FY 1986	$75,000

The efforts of the Earthquake Preparedness Program have been focused on the Wasatch Front Region/Wasatch Fault Zone where most of Utah's population is concentrated. This area expects a 16 percent increase in population over the next five years and a 62 percent increase over the next 25 years (Utah State Office of Planning and Budget, 1986). There are good reasons why this region (10 counties) has been recognized as one of the high risk urban areas within the United States to receive primary attention from the NEHRP.

In 1983, CEM published the "Utah Earthquake Program - Five Year Plan and Preparedness Elements". The program objectives are to achieve a coherent, comprehensive program for reducing the earthquake hazard to populations, lifeline systems, and vital life support systems and to save lives and conserve resources during and following an earthquake.

Included in the program under the main objectives are elements to obtain incremental and overall success. These include hazard analysis (the development of maps and identification of risks), emergency response plans, public awareness and education, mutual aid agreements, involvement of the public and private sector, and legislative implementation.

The funding support to the Division of Comprehensive Emergency Management has provided for the salary of a geologist with experience in geologic hazards and planning. The first efforts (FY 82-84) were directed toward the development of the State/Four County Earthquake Response Plan. This plan establishes the response procedures and guidance, in one comprehensive volume, to be used jointly by the State and counties in response to a damaging earthquake (Fig. 1). The four counties involved in this plan are Weber, Davis, Salt Lake, and Utah, with provisions for all Wasatch Front counties (Fig. 2) to. The plan is aimed toward immediate and flexible employment of all available assets, response forces, and outside aid to meet the demands throughout the region where the needs are greatest. It provides for central coordinating support and local on-scene controls. Communications emphasis is on radio networks to control rescue and response operations. Immediate response from military resources are provided through the U.S. Sixth Army. Coordinating procedures are established for the non-governmental organizations such as, American Red Cross, Civil Air Patrol, Rocky Mountain Rescue Dogs, churches, and general contractors. Coordination of lifeline restoration is addressed in order to focus available resources on priority needs.

During 1985, Utah's Earthquake Preparedness Program concentrated on three important elements, two were follow-up items from the development of the Four County Response Plan and consisted of coordinating and integrating the plan with the participating counties and holding earthquake exercises.

The exercises were held separately at each county emergency operation center and were "Table Top" in nature. They were organized to bring together county and city emergency management personnel and exercise the plan by responding to preconceived messages about the extent of damage, deaths, injuries, and public information distribution within the county. A combined

P = Primary

S = Support

	Warning	Emergency Communications	Emergency Public Infomation	Evacuation	Rescue and Recovery	Public Safety & Security	Medical, Health & Sanitation	Mass Care & Feeding	Debris Clearance	Damage Assessment	Damage Survey	Temporary Housing & Shelter	Emergency Manpower	Public Education Services	Fire Fighting	Public Utilities/Trans.	Hazardous Materials Accidents	Military Support	Voluntary Organizations	Federal Disaster Assistance Programs	Claims and Disbursements	Audits	Long-range Disaster Recovery Planning	Legal Services	Insurance Assistance
Division of CEM	P	P	S	P	S	S	S	S	S	S	S	S	S	S	S	S	S	S	P	P	S	S	S	S	S
Office of the Governor			P																	S					
State Fire Marshal					P		S								P					S					
Department of Public Safety	S	S		S	S	P	S					S			S		P			S					
Department of Social Services				S				P		S	S						S		S	S					
Department of Health				S			P	S		S	S						S			S					
Department of Community & Economic Dev.										S		P								S					
Department of Employment Security							S						P							S					
State Office of Education				S				S		S	S	S		P	S	S				S					
Department of Natural Resources		S							S	S	S				P		S			S					
Department of Business Regulation				S						S	S					P				S					
Department of Administrative Services										P	P					S				S	P				
State Auditor																				S		P			
State Planning Coordinator																				S			P		
Utah National Guard		S		S	S	S	S	S	S	S	S	S			S	S	S	P		S					
Utah Civil Air Patrol		S								S	S									S					
State Board of Regents				S				S		S		S		S						S					
Department of Agriculture										S	S						S			S					
Department of Transportation		S		S		S			P	S	S						S			S					
Office of Attorney General																				S				P	
Department of Insurance																				S					P
Utah Geological & Mineral Survey	S									S	S									S					

Figure 1 -- Utah State Emergency Response Functions

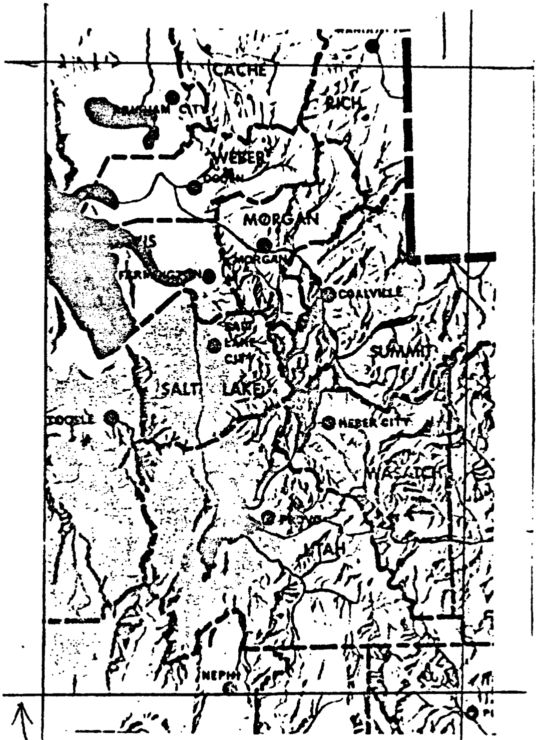

FIGURE 2.-- Wasatch Front and adjacent counties

county and state exercise was conducted at the State Emergency Operation Center for all State agencies and non-governmental organizations.

In addition to familiarizing city, county, and state agencies with the plan, the exercises brought out other important considerations and pitfalls that may be encountered during the response phase of an earthquake. Among these were communication backlogs, radio network coordination, Emergency Operations Center organization and the ability of EOC personnel to coordinate with the agencies they are representing and with other agencies within the EOC.

The third element completed in 1985 was the development and execution of mutual aid agreements between counties, state agencies, and private entities involved in emergency response.

This particular task involved the cooperation of autonomous groups which usually do not have much interaction. Because many of the mutual aid agreements are contractual in form, numerous iterations and negotiations with county governments and legal entities were necessary before an acceptable document could be drafted and adopted. Agreements already in existence were collected and reviewed.

Mutual aid agreements typically consist of six parts:

1. Statement of the need for a mutual aid or cooperative agreement.
2. Statement of authority for entering into an agreement.
3. Brief description of the parties to the agreement.
4. Statement of how and when the agreement is to be activated and coordinated.
5. Outline of responsibilities of the parties.
6. Statement of financial and legal liability for resources used.

It is also helpful to include a statement on how the agreement should be updated, amended, or terminated as the need arises.

Agreements entered into by CEM in 1985 ranged from informal "memorandums of understanding" to structured contractual types which detail responsibility and liability. Not only do these documents provide a legal basis for mutual aid, they also help establish procedural steps in acquiring aid and build a framework for the development of more comprehensive plans and working relationships between agencies involved in response and recovery.

Organizations which entered into mutual aid, cooperative agreements, or memorandums of understanding involving emergency response are Weber, Davis, Salt Lake, and Utah counties; University of Utah Seismograph Stations; military entities, and private volunteer organizations.

The development and negotiation of mutual aid agreements continues into 1986 with the Army Corps of Engineers, Veterans Administration, and others.

PUBLIC EDUCATION TO REDUCE EARTHQUAKE HAZARDS

Experts have agreed that in the wake of the Mexican earthquake it was evident that tragic losses could have been averted or reduced if sufficient attention had been given to public awareness and education prior to the event. During 1985 an increased amount of interest in the subject of earthquakes along the Wasatch Fault led to the distribution of a large number of brochures discussing earthquake awareness and safety. The reason for this increased interest can probably be attributed to the flooding disasters of 1983 and 1984, the subsequent Governor's Conference on Ceologic Hazards, the 1984-85 Earthquake Workshop held in Salt Lake City, Utah and increased media attention.

On a monthly basis during 1985, CEM distributed by unsolicited request approximately 6000 pamphlets and brochures on emergency preparedness. More than three quarters of these pamphlets were concerned with earthquake preparedness. When combined with literature distributed to county and city emergency offices and those given out during lectures and workshops the total number of earthquake related brochures distributed during the 1985 fiscal year was approximately 735,000. The distribution by CEM of USGS, FEMA, and CEM produced literature in 1985 is listed in Table 1.

A sampling of academic and governmental offices which regularly receive requests for public presentations revealed the following:

AGENCY	Approximate number of Requests for Public Presentations on Earthquake Related Subjects in 1985
Utah Division of CEM	60
Utah Geological & Mineral Survey	36
University of Utah Seismograph Stations	30
[1]Utah Museum of Natural History	40

[1] In the time period from November 85 through February 86, over 65 requests were received.

This kind of interest, much of it unsolicited, has generated the 1986 project goals which will focus on the FEMA/USGS Public Education-Awareness component of NEHRP.

Our intention is to develop and produce a television series or video program to reach the public in their homes through Public Broadcasting System (PBS) stations. Another a possible use could be in schools and at public presenta- tions. Increased funding in the FY 1986 budget is to initiate these programs. It is recognized that for local preparedness and education to be

TABLE 1 - Literature Distribution

Publication	Unsolicited	Solicited	Approximate Number Distributed
[1]FEMA-In Time Of Emergency	25,000	25,000	50,000
[1]Earthquake Checklist	25,000	25,000	50,000
[1]FEMA-Safety Tips For Earthquakes	25,000	25,000	50,000
[1]FEMA-Family Home Earthquake Drill	25,000	25,000	50,000
FEMA-Coping With Children's Reactions To Earthquakes and other Disasters	25,000	25,000	50,000
[1]CEM-Debris & Erosion Control	25,000	25,000	50,000
[1]CEM-Utah Flood Awareness	25,000	25,000	50,000
[1]CEM-Utah Flood Checklist	25,000	25,000	50,000
[2] CEM-Are You Prepared For The Next Earthquake/Flood	6,000	450,000	456,000

---

[1] Given out as a "Disaster Information Packet" during the 1985 Flood Awareness Campaign.

[2] Distributed by Utah Power and Light Company during routine billings in 1985.

effective, production of the television programs are necessary although costly. However, efforts will be made to achieve home-oriented education through the support of corporations involved in public services. It is hoped that such public education programs will go well beyond the usual public service brief messages. The initial concept is to produce a program at least 30 minutes to one hour in length which will educate the public about the geology, seismic history, and seismic risk of the Wasatch Front and concentrate on providing for specific locales, the hazards information and preparedness guidance which will enable individuals and families to be prepared. The programs should tell what can be done before the quake to reduce vulnerabilities and what to do at the time of and immediately after the event to reduce loss of lives and injuries.

Associated with this effort is the publication of a concise information packet on the earthquake hazard in Utah. The literature now available, published by FEMA, is excellent for general preparedness purposes but does not focus or address the problem from a state or local community aspect and is general in approach.

In order to be meaningful, these packets should contain maps showing earthquake hazard, similar to those provided by the National Flood Insurance Program. The requirement is large-scale maps for each geographic locality, showing the hazards which may exist in each locality related to a worst case earthquake. In lay terms, the hazards should be shown and explained, followed by specific guidance for residents, schools, businesses, hospitals, health-care institutions, high-rise dwellings, dense housing complexes, etc.

REQUIREMENTS FOR GEOLOGIC HAZARDS MAPS

The main goal of Utah's 1985 Workshop on Earthquake Hazards in the Wasatch Front Region was to create a means whereby technical information could be transferred to and applied by local users. The most beneficial result of the Workshop was the establishment of basic requirements for mapping of earthquake hazards. The topics were treated and the participants were selected in order to convey to the users what is now available and to evoke from users what is yet required. Considerable effort was directed toward reaching a consensus among the users and technologists regarding such elements as: scale most useful, depictions most useful and the integration of needed information on maps to satisfy unique requirements.

Topics presented by the following scientists, engineers, and planners included:

1) Zoning and Mapping of the Earthquake Ground-Shaking Hazard Along the Wasatch Fault Zone - Walter W. Hays, Deputy for Research Applications, U.S. Geological Survey, Reston, Virginia
2) Zoning and Mapping of Earthquake Liquefaction Hazards Potential Along the Wasatch Fault Zone - Jeffrey R. Keaton, Dames and Moore Engineering, Loren R. Anderson, Utah State University and T. Leslie Youd, Brigham Young University.
3) Mapping of Earthquake Faulting Along the Wasatch Fault Zone - David P. Schwartz, U.S. Geological Survey, Menlo Park, California.
4) Application of Technical Information on Earthquake Ground-Shaking, Liquefaction and Fault/Tectonic Reformation to Mitigation and Hazard Reduction by Users - William Kockelman, U.S. Geological Survey, Menlo Park, California, Robert D. Brown, U.S. Geological Survey, Menlo Park, California and George Mader, William Spangle and Associates, Portola Valley, California.
5) Applications of Technical Information on Earthquake hazards to Land Use Planning, Community Safety and Risk Reduction - Kenneth C.

Topping, Development Services, County of San Bernadino, California, and George Mader.

6) Applications of Earthquake and Soil Stability Technology to the Mapping of Hazards and Ways to Depict Risks - Russell H. Campbell, Research Applications, U.S. Geolgical Survey, Reston, Virginia.

The target users were drawn from Utah's state, county and community levels. They were the emergency response planners and mitigation planners from the Utah Division of Comprehensive Emergency Management; county emergency response planners, county engineers and county land use planners from the ten counties along the Wasatch Front; and city planners and engineers from the communities along the Wasatch Front.

Scale

The basic scale of 1:24,000 is required for use at state, county, and city levels. This scale will provide a detail and resolution of hazard useful to land use planners, community developers, lifeline operators, hazards mitigators, emergency responders, and emergency preparedness planners, at regional, county, community, and general neighborhood levels. It was recognized that mapping of the Wasatch Fault Zone at this large scale would be costly and time consuming. However, consideration for smaller scales were outweighted by the user oriented needs for a consistent scale of this size. Thirty-eight 1:24,000 scale USGS quadrangles and two 15 minute quadrangles have been identified for the principal coverage from Logan to Santaquin, Utah (Table 2).

TABLE 2 - Wasatch Front/Wasatch Fault Zone
7 1/2" and 15" Map Coverage

Trenton
Cutler Dam
Tremonton
Logan
Willard
Huntsville
Clearfield
Bountiful Peak
Fort Douglas
Sugar House
Jordan Narrows
Orem
Springville
Nephi (1:48,000)
Richmond
Newton
Honeyville
Bear River
Plain City
Roy
Kaysville
Saltair
Magna
Midvale
Lehi
Bridal Veil Falls
Spanish Fork
Riverside
Smithfield
Wellsville
Brigham City
North Ogden
Ogden
Farmington
Salt Lake City North
Salt Lake City South
Draper
Timpanogos Cave
Provo
Santaquin (1:48,000)

Depictions

The consensus was that single hazard maps are required to focus on specific user needs. However, some areas should be covered by several hazards. Topographic maps, which show man-made features and one hazard, such as potential fault rupture, will be most useful.

An example of what is needed is the USGS series of the Sugar House, Utah, Quadrangle by Van Horn and others. Two presentations in this series are very useful in earthquake hazards reduction applications:

Map I-766-B, showing faults

and

Map I-766-O, showing Inferred Relative Stability of the Land Surface During Earthquakes

To further provide the required information to users, a map in the same series is needed showing: isosiesmal zones of inferred damage for the maximum credible earthquake (Richter Magnitude 7.5) in Modified Mercalli Scale Intensities (Intensity values of VII and higher).

The results of a recent survey which sampled the planning and engineering requirements for counties and cities along the Wasatch Front, indicate that over 80% have requirements for the use of some type of geologic seismic or other hazard information in their planning and engineering process and nearly all counties and cities feel the need for more accurate and detailed geologic information especially as it relates to possible hazards which can be used on a site specific basis. Suggestions ranged from the specific location of active or potentially active fault traces to potential avalanche hazard areas.

Digitized Applications

Application of some form of computer manipulated Geographic Information System is required to accelerate the creation and updating of the maps with their relevant information. By use of an Automated Geographic Reference System, such as the one in Utah's Office of Planning and Budget, the manipulation and use of mapping information can suit the users' unique needs. The minicomputer used is a Prime 550. For example, a user can edit, integrate, display, modify, and print geographic information. As the data base is established, by the use of specific software, such as ARC-INFO, the user can quickly synthesize single topic overlays to create customized maps.

The application of digitized processes to the mapping function makes the establishment of a consistent base map scale even more important. Users of the Geographic Information System in Utah, as well as the USGS National Mapping Division, Denver, Colorado, have stated that their base map data is at a scale of 1:24,000.

Digitized data which should be mapped for synthetic hazards analyses and customized mapping should include:

Geophysical data base at a scale of 1:24,000.

Location of faults and zones of tectonic deformation.

Location of inferred soils instabilities.

Location of isoseismal damage zones.

Cultural features, such as roads, railroads, streets, etc.

Locations of critical facilities, such as hospitals, EOC's, fire stations, airports, etc.

Locations of lifelines, such as natural gas lines, electric power lines, water lines, telephone networks, sanitary sewer systems, etc.

In addition to the earthquake preparedness program, CEM is involved in local multi-hazard mitigation planning, state natural hazard planning and coordination, county integrated emergency management system planning, Great Salt Lake expansion planning, and energy resources transport systems vulnerability studies. This extended role permits access to many resources and increases our ability to inform and educate the public and private sector on the Wasatch Front earthquake hazard.

REFERENCES

Federal Emergency Management Agency FY86 Comprehensive Cooperative Agreement Program Guidelines for Earthquake Preparedness.

Utah State Office of Planning and Budget, 1986; Revised Population Estimates and State Population Projections 1986.

VanHorn, Richard, 1972, Map Showing Relative Ages of Faults in the Sugar House Quadrangle, Salt Lake County, Utah: U.S. Geological Survey Folio Map I-766-B.

---------------- and Van Driel, J. Nicholas, 1977, Computer Composite Map Showing Relative Stability of the Land Surface During Earthquakes, Sugar House Quadrangle, Salt Lake County, Utah: U.S. Geological Survey Folio Map I-766-0.

UTAH GEOLOGICAL AND MINERAL SURVEY EXCAVATION INSPECTION PROGRAM

A TOOL FOR EARTHQUAKE HAZARD RECOGNITION IN UTAH

By Harold E. Gill
Utah Geological and Mineral Survey
Salt Lake City, Utah

ABSTRACT

A source of geologic information commonly overlooked in urban areas is data available from construction excavations. For nearly two decades the Utah Geological and Mineral Survey (UGMS) has maintained a construction excavation inspection program to identify evidence of past earthquake activity. The program has dealt primarily with large excavations in Salt Lake County, and has been most successful in collecting information on past ground displacement and liquefaction in developed areas not otherwise available to standard trenching methods.

Results of the UGMS excavation inspection program have shown the zone of deformation along the Wasatch Fault to be highly variable and in some locations up to several hundred meters wide. Therefore, a standard set-back distance for the entire fault (as used in California) is not appropriate for the Wasatch Fault. The excavation inspection program has identified a possible zone of deformed and liquefied material extending in an east-west direction across the south-central part of Salt Lake County. Evidence has been found for five large prehistoric lateral spread landslides in Davis County, and a major lateral spread (1 km by 0.5 km) in downtown Salt Lake City. In 1984, a cooperative program with the U. S. Geological Survey (USGS) allowed for expansion of the

UGMS excavation inspection program to other counties along the Wasatch Front. All available geologic hazard data will ultimately be placed in a statewide computer geographic reference system for users in need of hazard information.

INTRODUCTION

A major component of the Urban and Regional Hazards element of the National Earthquake Hazards Reduction Program (NEHRP), is the creation and implementation of hazard-reduction measures in urban areas along the Wasatch Front. Earth-science information (geologic, seismologic, hydrologic, and soils) is vital to the formulation of seismic safety studies, plans, and programs intended to reduce seismic hazards. Much of the information presently available is not of the detail and scale needed for planning purposes. The Utah Geological and Mineral Survey (UGMS) excavation inspection program is intended to collect and distribute site-specific information on past seismic events, geology, soils, and ground water to engineers, planners, and those charged with protecting public health and safety from the effects of an earthquake.

As early as 1963, the Utah Geological and Mineralogical Survey (as it was called at that time) was involved in excavation inspections. Osmond and others (1965) identified faulting and deformation in the Hall of Justice building excavation in downtown Salt Lake City. For almost two decades, Bruce N. Kaliser, chief of the UGMS Urban and Engineering Geology Section, maintained a program of inspecting foundation excavations throughout Salt Lake City as part of the UGMS seismic hazards reduction program. In 1978, Robert Klauk, geologist with the Urban and Engineering Geology Section, in an attempt to increase the number of inspections, contacted both the Salt Lake City and Salt Lake County Building Departments to request monthly lists of recent building permits. The lists allowed the UGMS to monitor major construction projects in the Salt Lake Valley. He also initiated a systematic monthly reconnaissance of excavations along the Wasatch Fault zone in Salt Lake County. In 1980, a standard form for documenting geologic and soils data from excavation inspections, and a set of large scale maps for plotting excavation locations in Salt Lake County, were developed by the author. As part of a cooperative program with the USGS, the UGMS excavation inspection program was expanded in 1984 to include all counties along the Wasatch Fault, however, the majority of the inspections are done in Weber, Davis, Salt Lake, and Utah Counties, where the bulk of construction activity occurs. The time and personnel allotted to the program were increased, and a computer geographic reference system is presently being developed that will incorporate data from both the excavation inspections and other site evaluations performed by UGMS and USGS personnel.

The UGMS excavation inspection program documents soil, ground-water, and geologic conditions at each site. When a significant feature (deformed bedding, evidence of liquefaction, a fault, etc.) is encountered, a complete photo log and schematic diagram is made, and if time permits, the feature is logged in detail. The UGMS program has been successful in collecting data on ground displacement (faulting, lateral spreading), and liquefaction.

APPLICATION OF EXCAVATION INSPECTION PROGRAM TO HAZARD-REDUCTION MEASURES

The potential for large earthquakes along the Wasatch Fault presents planners, engineers, and others with major concerns regarding earthquake hazard reduction. The following examples illustrate the type of data collected by the UGMS and how that information may be applied to earthquake hazard reduction.

Surface Rupture and Zone of Deformation

Extensive development continues along the foothills of the Wasatch Range in the vicinity of the Wasatch Fault. Recently, local governments have become increasingly concerned about the geologic hazards that exist near the fault. Some cities and counties have written ordinances requiring geologic reports delineating hazards such as active faults and unstable slopes prior to development. The reports are required primarily in hillside areas, but some municipalities include suspected hazardous areas in the valleys. The UGMS has received many of those reports for review. In a number of cases, the geotechnical consultant has recommended a set-back distance from faults. The recommendation usually states that structures should not be built within 15 m of a mapped fault trace. It has been the experience of the UGMS that these recommendations generally are not based on geologic exploration at the site, but are taken from ordinances developed in California. It also appears the recommendation is made without a good understanding of the type of faulting and surface deformation associated with the Wasatch Fault zone.

In California, the restriction adopted by most municipalities requires that no structure for human occupancy shall be placed across or within 15 m of the trace of an active fault. The area within 15 m of an active fault is assumed to be underlain by branches of that fault. The criteria is based chiefly, if not exclusively, on data collected from strike-slip faults which exhibit mostly lateral movement and commonly do not have a wide zone of deformation. However, the Wasatch Fault is a normal fault and thus is characterized by vertical movement. The zone of deformation associated with normal faulting can be very wide consisting of grabens, back-tilted blocks, and antithetic faults. Results of the UGMS excavation inspection program in Salt Lake and Utah Counties have shown that the zone of deformation along the Wasatch Fault is commonly much greater than the 15 m recommended in many reports, as the following examples demonstrate.

Site F1: An excavation on the University of Utah campus for expansion of Rice Stadium (fig. 1, site F1) revealed faulted pre-Lake Bonneville alluvial-fan deposits. A detailed log and soil descriptions are presented in figure 2. Four faults, with a minimum displacement of 1 m, were observed within 305 m north-northwest of a branch of the East Bench Fault as mapped by Van Horn (1969). The faults which trend parallel to the East Bench Fault are believed to be antithetic faults within the zone of deformation associated with the larger structure. Overlying Lake Bonneville sediments were removed during construction, therefore, it is not known if they were displaced. However, the East Bench Fault has been active in Pleistocene and possibly Holocene time (Scott and Shroba, 1985), and the possibility of surface fault rupture affecting any structure in this zone needs to be considered.

Site F2: A 1984 geologic hazards study prepared for the City of Provo, mapped the main trace of the Wasatch Fault approximately 153 meters west of where it had been mapped by previous investigators (Cluff and others, 1973). The study also delineated a restricted zone extending 15 m on either side of the trace (based arbitrarily on California restrictions for a major fault and associated zone of deformation). This fault would trend through the site of a 1978

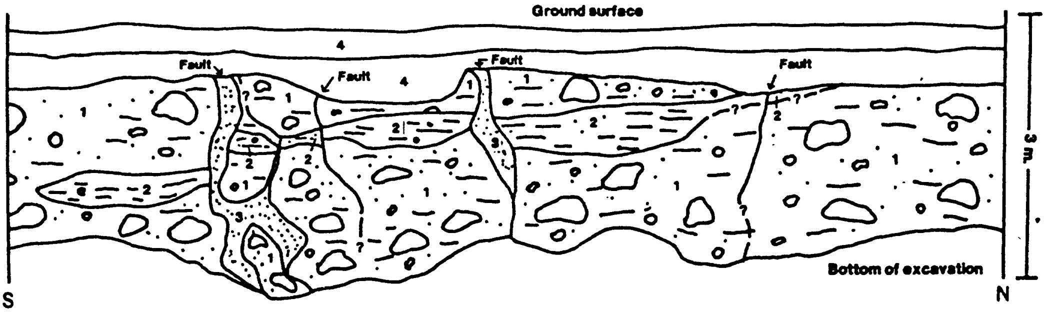

Figure 2. Log of University of Utah Rice Stadium excavation, Salt Lake City, Utah (figure 1 site F1). Faults displace pre-Lake Bonneville alluvial-fan deposits (unit 1). Overlying Lake Bonneville sediments were removed during construction and it is not known if they were displaced.

Unit 1	Silty gravel with sand (GM); light tan, medium dense, none to low plasticity, moist; 20% sand, 20% fines, 30% cobbles, pre-Lake Bonneville alluvium.
Unit 2	Gravelly lean clay with sand (CL); red, firm, medium plastic, moist; 20% gravel, 20% sand, caliche filaments observed.
Unit 3	Poorly graded sand (SP); yellow-white, loose, nonplastic, dry to moist; fine sand, apparently wind deposited, filled open cracks along the faults.
Unit 4	Fill material, variable clay to gravel, brown, red, green, asphalt layers evident.

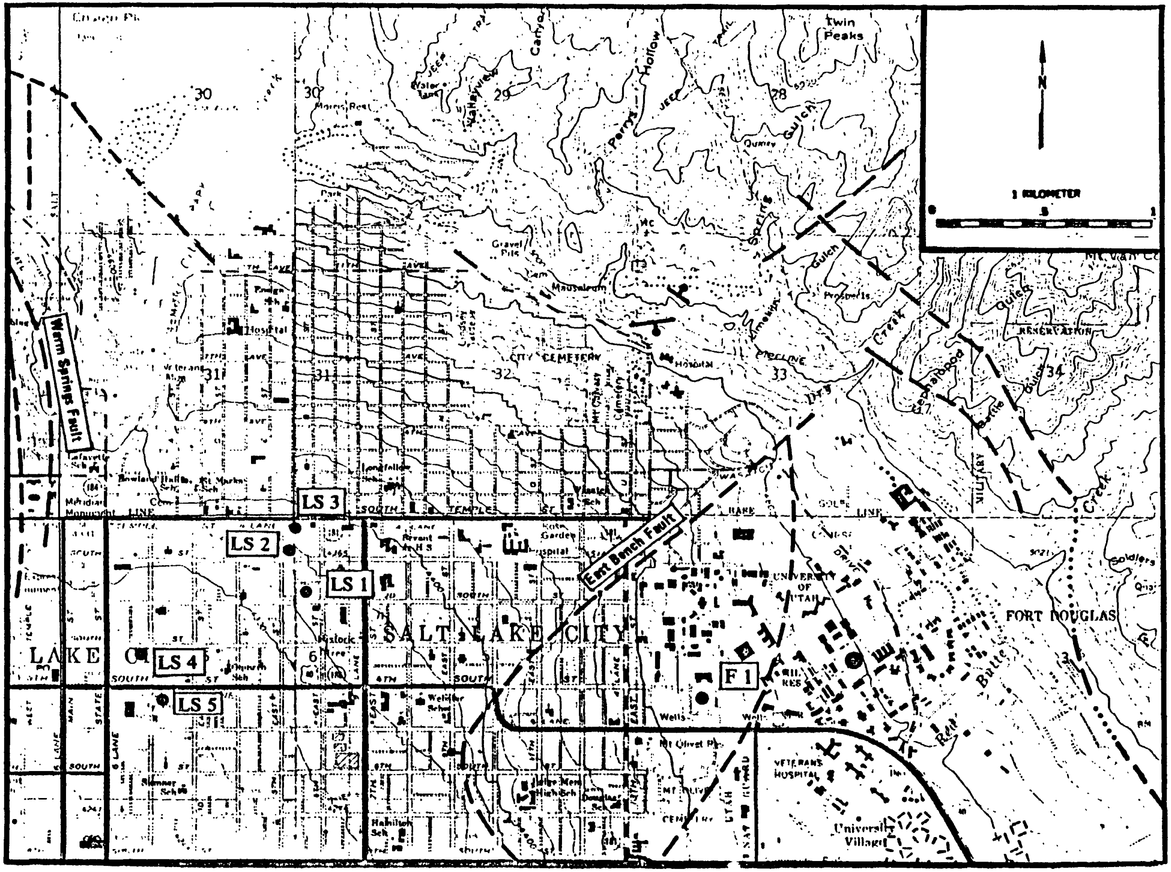

Figure 1. Location map for selected excavation inspections. Sites F1 and LS1 through LS4 are excavation inspections done by UGMS after 1979; Hall of Justice excavation (LS5) from UGMS Special Studies No. 11 (Osmond and others, 1965). Mapped faults (solid where it forms scarp; dashed where approximately located or inferred; dotted where concealed; bar and ball on downthrown side) from Scott and Shroba, 1985; Van Horn, 1981, and 1969. Base map from Salt Lake City North and Fort Douglas, Utah, U.S. Geological Survey 7.5 minute topographic quadrangles.

excavation inspection performed by the UGMS along the Provo-Orem bench in Utah County (fig. 3, site F2). However, no evidence of a major fault, as mapped during the 1984 study, was observed in that excavation (Klauk, 1985). Although more than 35 fractures, dipping between 60 and 80 degrees, mostly to the west, were observed along a 46 m segment of the excavation, no offset greater than 0.6 m was observed. This minor faulting is interpreted to be the result of antithetic faulting paralleling the main trace of the Wasatch Fault, as mapped in 1973, 92 m east of the excavation. Indications are, that the western limit of the disturbed zone extends to the west beyond the 1978 excavation. Therefore, the zone of deformation extends at least 214 m west of and parallel to the main fault trace (Klauk, 1985). Thus the 1984 "fault trace" was mislocated 153 m to the west of the true Wasatch Fault, and the 30-m wide "zone of deformation" falls significantly short of the actual width of the disturbed zone. Any critical facility built near the 1984 trace, but outside the 30-m wide restricted zone, would nevertheless lie in the disturbed zone, where a hazard from surface rupture exists. The 1984 hazard study illustrates not only the need for site-specific geologic investigations for critical facilities, but also the utility of previously collected excavation information.

As illustrated by the preceding examples, the width of the zone of deformation along the Wasatch Fault is variable and can be up to several hundred meters wide. Therefore, a standard set-back distance for the entire fault is not useful as a hazard mitigation policy. Appropriate set-back distances, particularly for critical facilities, should be defined on a site-specific basis.

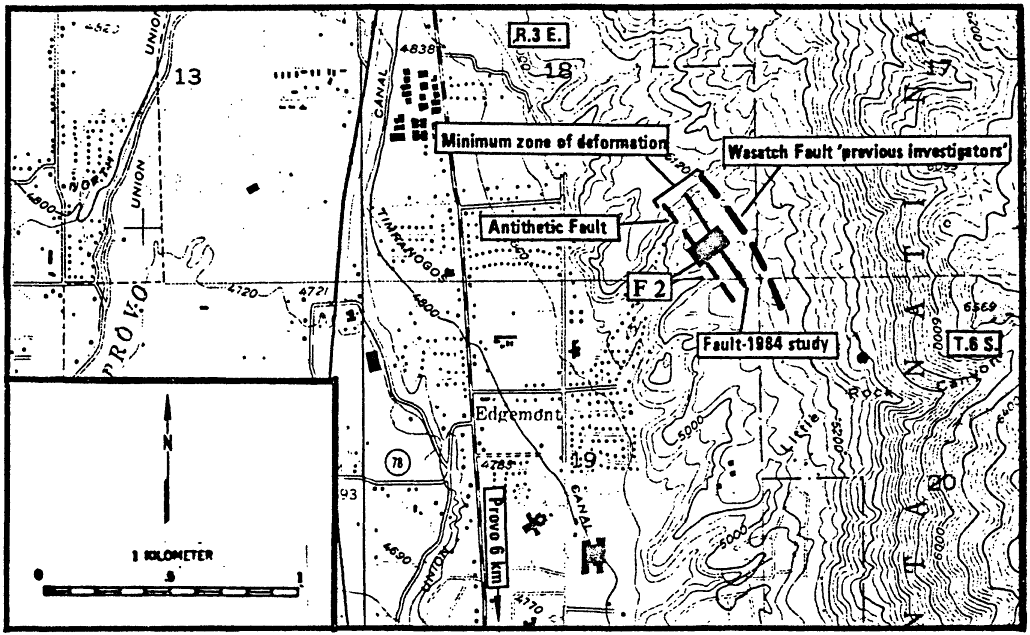

Figure 3. Location map for 1978 excavation F2. In a 1984 Provo City hazard study the main trace of the Wasatch Fault was mapped approximately 153 m west of the main fault trace as mapped by previous investigators, and a 15 m wide restricted zone (based abritrarily on California restrictions for a zone of deformation associated with a major fault) was defined on either side of the fault. A major fault trace was not encountered at this location during a 1978 excavation inspection at F2. During this inspection it was also determined that a minimum width for the zone of deformation associated with the Wasatch Fault (as previously mapped) was 214 meters. After Klauk, R. H., 1985. Base map from Orem, Utah, U.S. Geological Survey 7.5 minute topographic quadrangle.

Liquefaction Potential

Ground failure associated with liquefaction has resulted in major damage to facilities in many parts of the world. Shallow deposits of saturated, fine to medium sand exist along the Wasatch Front and are susceptible to liquefaction. Evidence of past earthquake activity in northern Utah clearly indicates that ground shaking has been sufficient to induce liquefaction in susceptible soils. Evidence of liquefaction was observed following the 1934 Hansel Valley earthquake in Box Elder County, Utah and again following the Cache Valley earthquake of 1962 (Anderson, 1984). As part of the U.S. Geological Survey's Earthquake Hazard Reduction program "Liquefaction Potential Maps" have been prepared for Davis, Salt Lake, and Utah Counties by Loren Anderson and Jeffrey Keaton (this volume).

Liquefaction may occur more than once at the same location (L. Youd, oral commun. 1985). As soil liquefies, it becomes dense from the bottom up. After an earthquake, the upper layers of a soil horizon may be less dense than those below and again be susceptible to liquefaction. Therefore, it is important for planners, engineers, and others to know where liquefaction has occurred in the past, and where similar conditions exist today. The excavation inspection program has identified a possible zone of deformed and liquefied material extending in an east-west direction across the south-central part of Salt Lake County. Deformation has been observed in two locations thus far, however, development in the area is rapid and the UGMS is watching carefully for additional exposures.

Site L1: An excavation inspection at 5300 South and 600 West, Salt Lake City, Utah (south central Salt Lake County, approximately 3 km southeast of the Taylorsville fault, Keaton, Curry, and Olig, this volume), (fig. 4, site L1), revealed extensive deformation of Lake Bonneville sediments. Site stratigraphy includes homogeneous, lean clay and silt deposits interbedded with lenses of poorly graded sand and silty sand. The sand lenses are highly distorted, including recumbent folding and minor fracturing. The deformation is likely due to liquefaction and associated lateral spreading of the subaqueous lake sediments, but this is not certain.

Site L2: Approximately 3 km east of site L1, an excavation at 5600 South and 735 East, Salt Lake City, Utah (fig. 4, site L2), exposed deformation in bedded Lake Bonneville sediments. Two episodes of deformation appear to have occurred at this site. The south end of the excavation contains highly deformed horizons of fine-grained sand and silt interbedded with undeformed clay beds. These minor disturbances may have occurred during deposition while the sediments were saturated. A second and larger event is indicated by a set of fractures into which fine-grained sand has been injected. Figure 5 presents a photograph and detailed log of the sand injection and deformed bedding. The liquefaction and resulting injection of saturated sand could have occured whenthe lake was only slightly higher than its present level, and may have been caused by earthquake induced ground shaking. A large recumbent fold (axial plane approximately 6 to 7 m in length) found at the north end of the excavation (fig. 6), is also believed to be associated with the latest event.

It is expected that future excavation inspections will identify additional locations where liquefaction has occurred along the Wasatch Front. This

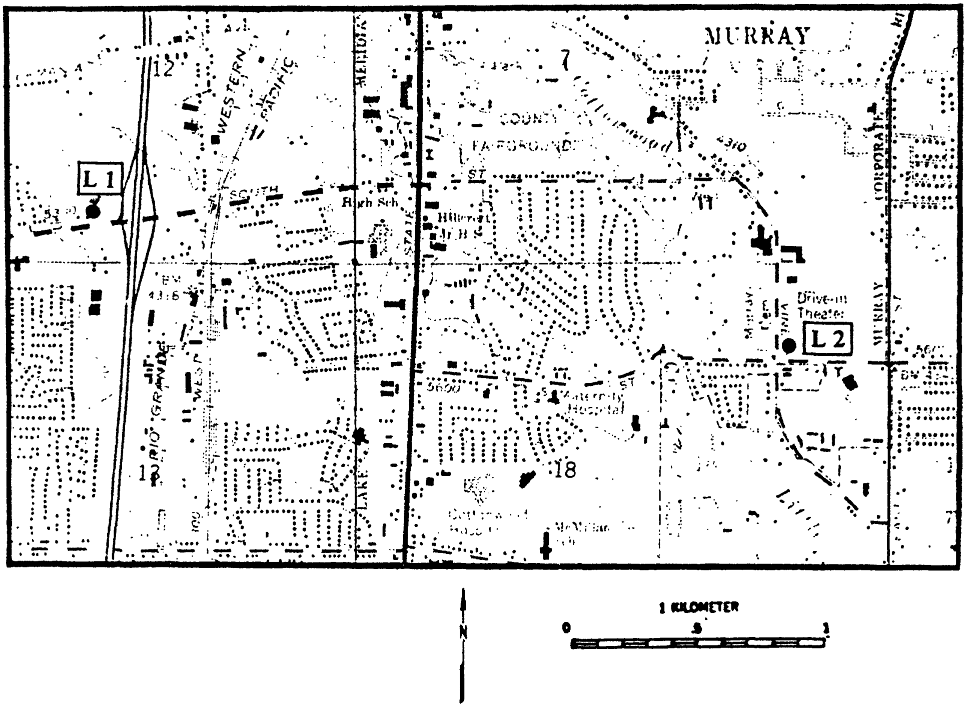

Figure 4. Location map for selected excavation inspections in south central Salt Lake County, Utah. Base map from Salt Lake City South and Sugar House, Utah, U.S. Geological Survey 7.5 minute topographic quadrangles.

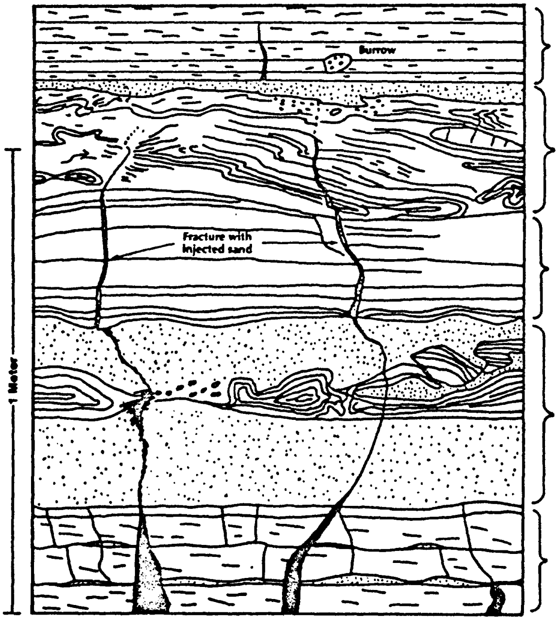

Unit 1 Lean to fat clay (CL/CH); light brown, medium to high plasticity; interbedded lean and fat clay, no deformation, fractured, liquefied sand in fracture.

Unit 2 Interbedded poorly graded sand (SP) and silt (ML); light tan, nonplastic; highly deformed lenses of silt and sand, evidence for liquefaction.

Unit 3 Lean to fat clay (CL/CH); brown, medium to high plasticity; interbedded lean and fat clay, no deformation, fractured, liquefied sand in fracture, very fine sand lenses offset by fractures.

Unit 4 Interbedded poorly graded sand (SP) and silt (ML); light tan, nonplastic; highly deformed lenses of silt and sand, evidence that this horizon has liquefied and has been injected upward along fractures.

Unit 5 Fat clay (CH) with interbedded lenses of lean clay (CL); brown, highly plastic, minor lenses of lean clay offset by numerous fractures.

Figure 5. Photograph and detailed log of the sand injection and deformed bedding in an excavation at 5600 South and 735 East, Salt Lake City, Utah (figure 4, site L2). Lake Bonneville sediments appear to have undergone two episodes of deformation at this site. Highly deformed horizons of fine-grained sand and silt, interbedded with undeformed clay beds, indicate minor disturbances may have occurred during deposition while the sediments were in a subaqueous state. A second and larger event is indicated by a set of fractures into which fine-grained sand has been injected. This post-depositional event, with subsequent liquefaction, may have been due to earthquake induced ground shaking.

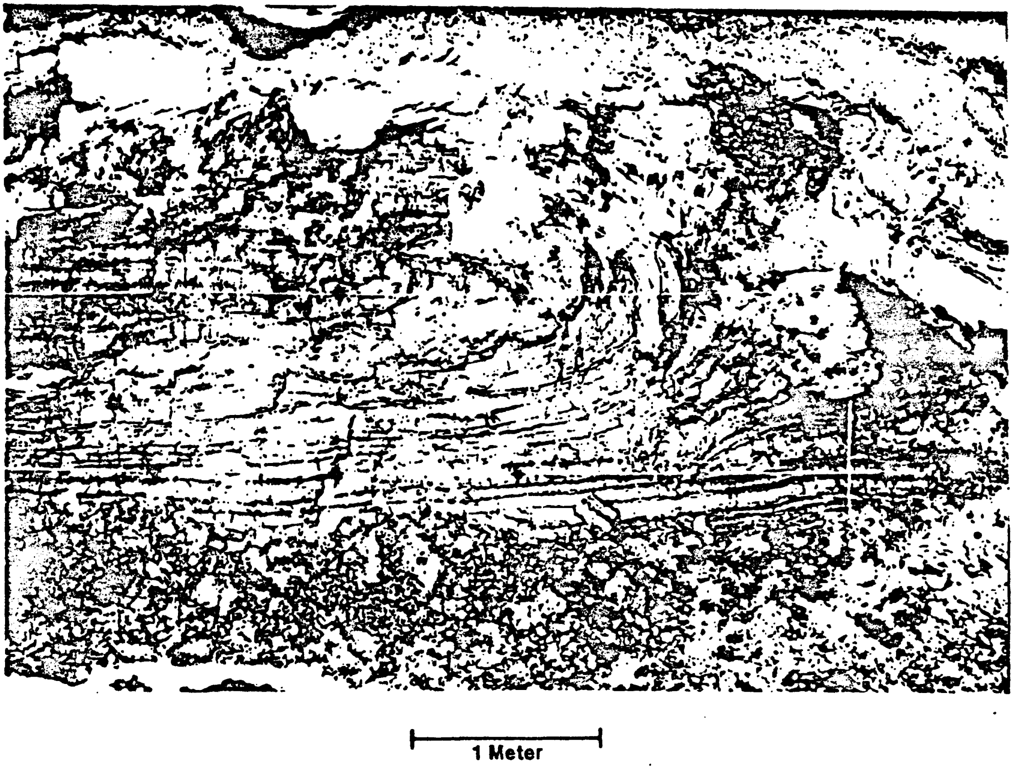

Figure 6. Photograph of large recumbent fold in excavation at 5600 South and 735 East, Murray, Utah (figure 4, site L2). Lake Bonneville sediments have undergone extensive deformation. The recumbent fold (axial plane approximately 6 to 7 m in length) may have been caused by earthquake induced shaking.

information, in combination with shallow ground-water maps (being prepared by the UGMS and USGS) and the liquefaction potential maps by Anderson and Keaton (this volume), will contribute greatly to the data base needed for informed decisions regarding hazard reduction in liquefaction-susceptible areas.

Slope Stability and Lateral Spread

Results of research by Anderson and Keaton (this volume) on liquefaction potential along the Wasatch Front has led them to conclude that lateral spread landsliding is the type of ground failure most likely to accompany soil liquefaction. Slopes with gradients ranging from about 0.5 to 5.0 percent, of which there are many along the Wasatch Front, are susceptible to failure by lateral spreading (Anderson, 1984). Commonly, a coherent upper block is broken into strips or blocks and extended or stretched by underlying plastic flow or liquefaction of a lower layer. Lateral spread landslides are of considerable concern because a small amount of movement can do a great deal of damage. Although all types of structures are susceptible to damage, buried utilities are particularly vulnerable. Evidence has been found in Davis County for five large lateral spread landslides, all of which were prehistoric (pre-1847, Anderson, 1984). A review of the Hall of Justice excavation study (fig. 1, site LS5), 300 East 400 South, Salt Lake City, Utah, (Osmond and others, 1965)and several other excavations in the vicinity, was performed by Scott and Shroba (1985). They concluded that deformation seen in Lake Bonneville sediments at those locations was probably caused by a pre-historic lateral spread and not related to tectonic activity. The UGMS has inspected four other excavations in the area that support this conclusion (fig. 1, sites LS1 through LS4, all within an area approximately 1 km long and 0.5 km wide in downtown

Salt Lake City). In the event of a contemporary slide of similar volume, several square blocks of downtown Salt Lake City could be involved.

Documenting lateral spread failures in the valleys along the Wasatch Front provides data directly applicable to hazard reduction. The information will also enable geologists and others to recognize where similar conditions exist today and flag those areas for special study prior to development.

COMPUTERIZED GEOGRAPHIC REFERENCE SYSTEM

A computer data file is maintained for each excavation identified for inspection until it has been completed. A second data file is being developed to store geologic data and soil information from the excavation inspection program and from other studies performed by the UGMS along the Wasatch Front. Planners, engineers, geologists, and others will be able to access this information for a specific site or for an entire quadrangle or county. For example, it will be possible to locate all excavations in a county or quadrangle in which possible lateral spread landslides or faults were observed to ascertain where damage to buried utilities or other facilities may occur during an earthquake. The data will also be digitized so that selected information can be plotted on maps. All available geologic hazard data, including the most recent UGMS, USGS, and geotechnical consultant reports, will ultimately be placed in a statewide computer geographic reference system, maintained by the UGMS and the Utah Planning and Budget Office, for users in need of hazard information.

SUMMARY

The effective application of scientific information by responsible officials is a prerequisite to successful hazard mitigation. The UGMS Excavation Inspection Program is an ongoing, inexpensive way to accumulate that scientific information and make it available to users at a level of detail and scale applicable to site-specific determinations. The program focuses on those areas of greatest need, primarily the collection of data along the Wasatch Front where construction is the heaviest and the earthquake hazard the highest. Construction is continuing in areas of known geologic hazards and it is imperative that as more information is collected it be made available to those who require it for earthquake hazard reduction. Therefore, it is to the advantage of engineering, architectural, construction, and geotechnical firms to notify the UGMS of upcoming foundation and exploratory excavations.

ACKNOWLEDGMENTS

I gratefully acknowledge the many helpful comments and suggestions of those who reviewed this paper in draft form: Robert C. Rasely, United States Department of Agriculture, Soil Conservation Service; Robert Klauk, William R. Lund, Don Mabey, and William Case, from the Utah Geological and Mineral Survey.

SELECTED REFERENCES

Anderson, L. R., 1984, Liquefaction potential and slope stability Wasatch Front area: in Hays, W. W. and Gori, P. L., ed., 1984, A workshop on "Evaluation of regional and urban earthquake hazards and risk in Utah": U.S. Geological Survey Proceedings of Conference XXVI, Open-File Report 84-763, p. 126-132.

Baker, A. A., 1964, Geologic map and sections of the Orem quadrangle, Utah: U.S. Geological Survey Quadrangle Map GQ-241, scale 1:24,000.

Cluff, L. S., Brogan, G. E., and Glass, C. E., 1973, Wasatch fault southern portion, earthquake fault investigation and evaluation: Woodward-Lungren and Associates, Oakland, California, 79 p.

Everitt, B. L., 1980, Geology of some foundation excavations in northeastern Salt Lake City: Utah Geological and Mineral Survey Report of Investigation No. 149, 24 p.

Gordon, W. J., 1977, Report of soils and engineering geology study, proposed Victory Road water reservoir near 600 North Victory Road, Salt Lake City, Utah, for the Department of Water Supply and Water Works Salt Lake City Corporation: Dames & Moore, Salt Lake City, Utah, Job No. 02090-034-06, 50 p.

Hunt, C. B., Varnes, H. D., and Thomas, H. E., 1953, Lake Bonneville - geology of northern Utah Valley, Utah: U.S. Geological Survey Professional Paper 257-A, 99 p.

Kaliser, B. N., 1968, Engineering geology of the Victory Road reservoir site Salt Lake City, Utah: Utah Geological and Mineral Survey Report of Investigation No. 38, 17 p.

Keefer, D. K., 1984, Landslides caused by earthquakes: Geological Society of America Bulletin, v. 95, p. 406-421.

Klauk, R. H., 1985, Zone of deformation determination along a portion of the Wasatch Fault in Provo, Utah: Utah Geological and Mineral Survey unpublished report, 5 p.

-----1986, Engineering geology for land-use planning for Research Park, University of Utah, Salt Lake City, Utah: Utah Geological and Mineral Survey Report of Investigation No. 204, 30 p.

Murphy, Peter, and Gwynn, J. W., 1979, Geothermal investigations of the Warm Springs fault geothermal system Salt Lake County, Utah: Utah Geological and Mineral Survey Report of Investigation No. 140, 29 p.

Osmond, J. C., Hewitt, W. P., and Van Horn, Richard, 1965, Engineering implications and geology, Hall of Justice excavation Salt Lake City, Utah: Utah Geological and Mineralogical Survey Special Studies No. 11, 35 p.

Scott, W. E., and Shroba, R. R., 1985, Surficial geologic map of an area along the Wasatch fault zone in the Salt Lake Valley, Utah: U.S. Geological Survey Open-File Report 85-448, 18 p.

Van Horn, Richard, 1969, Preliminary geologic map of the southern half of the Fort Douglas Quadrangle, Salt Lake County, Utah: U.S. Geological Survey Open-File No. 69-308, scale 1:24,000.

-----1972a, Surficial geologic map of the Sugar House Quadrangle, Salt Lake County, Utah: U.S. Geological Survey Map I-766-A, scale 1:24,000.

-----1972b, Map showing relative ages of faults in the Sugar House Quadrangle, Salt Lake County, Utah: U.S. Geological Survey Map I-766-B, scale 1:24,000.

-----1979, Surficial geologic map of the Salt Lake City South Quadrangle, Salt Lake County, Utah: U.S. Geological Survey Map I-1173, scale 1:24,000.

-----1981, Geologic map of pre-Quaternary rocks of the Salt Lake City North Quadrangle, Davis and Salt Lake Counties, Utah: U.S. Geological Survey Map I-1330, scale 1:24,000.

Youd, T. L., 1985, Landslides caused by earthquakes: discussion and reply: Geological Society of America Bulletin, v. 96, p 1091-1094.

Ziony, J. I., editor, 1985, Evaluating earthquake hazards in the Los Angeles region - an earth-science perspective: U.S. Geological Survey Professional Paper 1360, 505 p.

ROCK FALL HAZARD SUSCEPTIBILITY DUE TO EARTHQUAKES CENTRAL WASATCH FRONT, UTAH

William F. Case
Utah Geological & Mineral Survey
Salt Lake City, Utah

ABSTRACT

Urban encroachment into rock fall susceptible areas is increasing as the demand for "view lots" increases. This study identifies rock fall susceptible areas in the Central Wasatch Front. Rock falls are the most common type of landslide initiated by an earthquake; a magnitude 7.0-7.5 earthquake anywhere in the Wasatch Fault Zone could trigger tens of thousands of rock falls in the entire Wasatch Front area. Rock falls consist of the free-fall, saltation, rolling, sliding, or toppling of blocks that have been separated along the discontinuities in a rock mass due to tensile forces. The study area consists Wasatch Mountain spur faces which project into the Salt Lake Valley from Kaysville to Draper and Oquirrh Mountain spur faces which project into the Tooele Valley from Lake Point to Tooele and into the Salt Lake Valley from Lark to Magna. The following parameters were mapped at a scale of 1:24,000 for each spur face; extent of face, lithology, bedrock outcrop area, bedrock dip, maximum slope, discontinuities, unconsolidated deposits, and presence of rock fall clast deposits. A spur face was considered susceptible if there was a source of rock fall clasts from bedrock outcrops or unconsolidated sedimentary deposits on the face. Out of 124 spurs investigated 71 (57%) were determined to be susceptible to rock falls. Runout zones were estimated for some spur areas from the presence of rock fall deposits; the maximum rock fall clast runout distance in the study area is approximately 250m. Sixty-four percent of the clastic and carbonate bedrock spurs and twenty-four percent of the igneous and volcanic bedrock spurs are susceptible to rock falls. Bedrock spurs composed of combinations of lithologies are more susceptible to rock fall than single lithology spurs. Boulder lacustrine beaches, glacial moraines, and talus deposits provide rock fall clasts on some spurs. The most common rock fall clasts in existing rock fall deposits are Paleozoic carbonates, Precambrian quartzites, Tertiary conglomerates, and Tertiary granitic intrusives. Maximum slope angles for susceptible spurs have a bimodal distribution; 24-26 degrees for unconsolidated deposits and 30-41 degrees for bedrock spurs.

INTRODUCTION:

Rock falls are a significant hazard associated with earthquakes along the Wasatch Front but to date they have received little attention. According to Keefer (1984) rock fall is one of the most common landslides to be caused by an earthquake, and the most damaging to property and life.

During the night of 17 August, 1959, in the Hebgen Lake area of Montana, 28 lives were lost due to a rock fall and rock avalanche which were caused by an earthquake (Nolan, 1964). The 1976 Guatemalan earthquake generated over 10,000 rock falls which caused extensive property damage and the loss of hundreds of lives (Harp, Wilson, & Wieczorek, 1981). Between 1887 and 1982 there were at least nine Utah earthquakes which caused rock falls and rock slides (Table 1). Widespread areas of the Wasatch Front might experience property damage and loss of life due rock falls induced by a major earthquake.

As population growth in Wasatch Front communities moves toward "view lots" on steep slopes and higher elevations, previously benign geologic hazards including rock falls induced by earthquakes become a risk to life and property. Areas of rock fall and other geologic hazards need to be identified to facilitate mitigation, and when possible the identification should be made before the encroachment of urbanization. This report describes a study of the rock fall hazard of part of the Wasatch Front region with particular emphasis on the rock falls that might be triggered by earthquakes.

The landslide is one of the most common geologic hazards on steep slopes. Landslides can occur on isolated slopes because of local conditions of static loading such as construction near the crest, addition of moisture from lawns or closed drainages, or slope steepening due to removal of the toe of the slope. Widespread landsliding can also be initiated by dynamic loading of slopes due to an earthquake. An earthquake of a magnitude 7.0-7.5 could produce over 10,000 rock falls over an area of 5,000 square kilometers (Keefer, 1984). According to Keefer (1984) the rock fall is one of the most common landslides to be caused by an earthquake, and therefore the most damaging to property and life. Property and life loss along a widespread area of the Wasatch front could result from rock falls because of nearby earthquakes.

TABLE 1: Utah earthquakes that have produced rock slope failures

Date DD/MM/YY	Magnitude,M, Intensity,MMI	Location	Remarks, Reference
30/09/77	M=5,MMI=VI	Mountain Home	Rock slab failure along Farnsworth Canal Rock fall in Rock Creek Canyon (Coffman & Stover, 1979)
11/10/77	M=4.8,MMI=VI	Duchesne	Small rock falls near mouth of diversion tunnel in Peterson Gulch (Coffman & Stover,1979)
04/10/67	MMI=VII	Marysvale	Rock slides noted (Coffman, von Hake, & Stover, 1982)
30/08/62	M=5.7,MMI=VII	Logan	Rock fall in Logan Canyon (Coffman, von Hake, & Stover, 1982)
12/03/34	MMI=VIII	Kosmo	Rock slides reported (Coffman, von Hake, & Stover,1982)
01/10/21	MMI=VIII	Elsinore	Large rock falls produced on both sides of Sevier Valley (Williams & Tapper, 1953)
17/11/02	Rossi-Forel Intensity= VIII-IX	Pine Valley Washington Co.	Dust produced by rock falls over an area 25 miles across (Williams & Tapper, 1953)
13/11/01	MMI=VIII	Marysvale	Rock slides noted (Williams & Tapper, 1953)
05/12/87	MMI=VII	Kanab	Vast dust clouds produced by rock falls (Williams & Tapper, 1953)

AREA STUDIED:

Figure 1 is an index map showing the study area which consists of mountain spurs along the west flank of the Wasatch Range from the Draper area to the Layton vicinity and the Oquirrh Mountain spurs from the northern tip southward to Tooele on the west and near Lark on the east. For the purpose of this study the concept of a mountain spur follows the Bates and Jackson (1980) definition, that is, a "..subordinate ridge...that projects sharply from the crest... of a... mountain..". Others, inluding Gilbert (1928) have referred to the salients such as City Creek salient, of the Wasatch Range as spurs. Gilbert (1928) refers to the subordinate ridges as mountain "ribs". The area investigated consists of the faces of these mountain spurs, some of which are triangular facets, others are rounded topographic features (figure 2). Only the spurs projecting into Tooele and Salt Lake Valleys were studied because of their proximity to community development. Spurs from Magna to Lark, along the eastern front of the Oquirrh Mountains, were not investigated because they are developed in alluvial fan deposits and are too small to be studied at the map scale of this report, 1:100,000. Side canyons of the ranges present obvious rock fall hazards because of steep slopes and widespread outcrop areas but are not being rapidly settled.

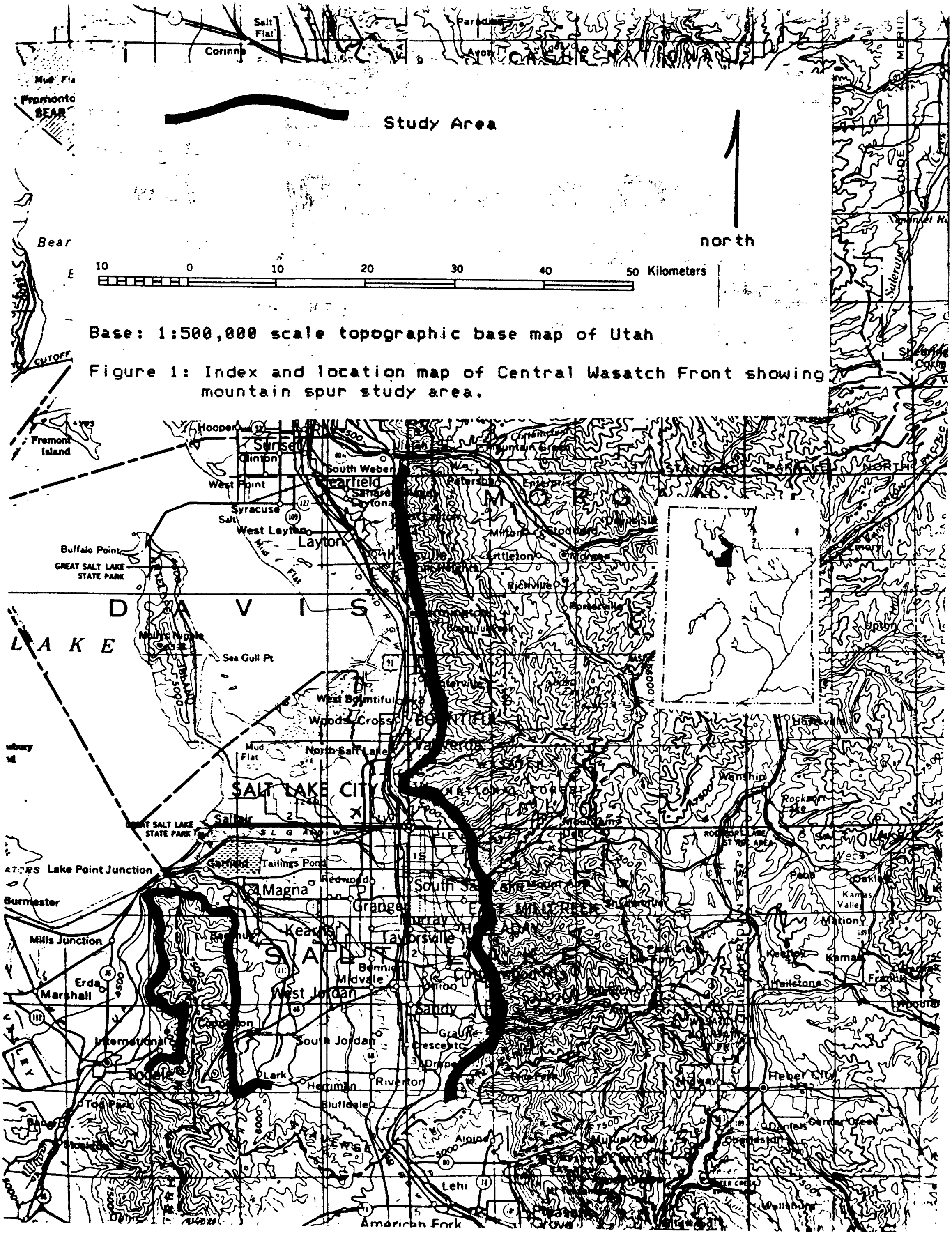

Base: 1:500,000 scale topographic base map of Utah

Figure 1: Index and location map of Central Wasatch Front showing mountain spur study area.

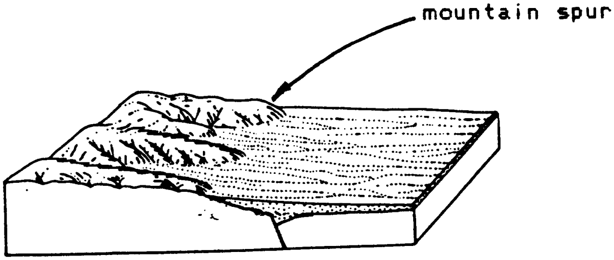

old fault activity

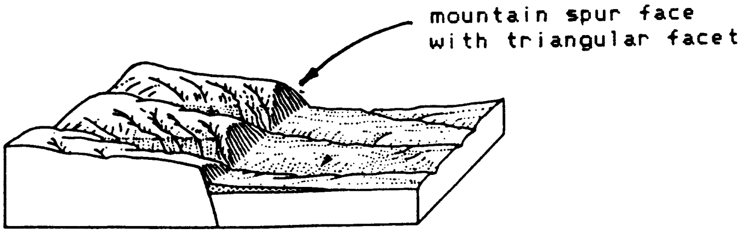

recent fault activity

Figure 2: Mountain spur appearance with young and old fault after Johnson (1939) and Anderson (1977).

WASATCH FAULT ZONE SEISMICITY & EARTHQUAKE CHARACTERISTICS:

The Wasatch fault zone trends from the Gunnison, Utah vicinity northward toward Collinston, Utah in an area approximately 370 km long by 30 km wide. The zone is located at the juncture of the Basin and Range physiographic province on the west and the Middle Rocky Mountains physiographic province on the east. The Wasatch fault zone is within the Intermountain Seismic Belt, an area of high seismicity which may be due to interaction of various subplates of the North American contintental plate. The fault zone is composed of at least six fault segments (Schwartz and Coppersmith, 1984), each of which has unique seismological and geological characteristics. Faults within the zone are basin and range type normal faults which generally parallel mountain fronts. The dip, or slope of the fault can range from 70 degrees from the horizontal at the surface to 10-40 degrees at focal depths of basin and range earthquakes (10-15 km). The epicenter of an earthquake, and possible zone of maximum ground motion, may be several kilometers valleyward from the surface expression of faults. Schwartz and Coppersmith (1984) have proposed the concept of a "characteristic earthquake" of the Wasatch fault zone, that is, the earthquake that is most likely to occur. Fault exposures in trenches across Wasatch fault segments show that vertical displacements due to past earthquakes are fairly consistantly within a range of 1.6 to 2.6 m which would seem to indicate that the most common earthquakes to have occurred within the last 8000 years are of magnitude 7-7.5 (Schwartz and Coppersmith, 1984). The recurrence interval for the most common or "characteristic" earthquake to occur somewhere within the entire Wasatch fault zone is 400-666 years (Schwartz and Coppersmith, 1984).

Altough no historic earthquakes of magnitude 7-7.5 have occurred in the Wasatch fault zone, earthquakes of this magnitude have occurred in similar geologic situations in the Intermountain Seismic Belt and indicate possible extent and type of damage to be expected. Doser (1985) has postulated that the 1983 Borah Peak, Idaho earthquake (magnitude 7.3) represents a typical earthquake to be expected along the Wasatch fault and that the 1959 Hebgen Lake, Montana earthquake (magnitude 7.5) would be the maximum event expected in the Intermountain Seismic Belt.

Surface rupture as a result of the Borah Peak event extended at least for 34km in the north-central portion of the Lost River fault and maximum surface displacement was 2.7 m (Doser, 1985). The surface break occurred on an scarp that had one or two events on the order of 12,000 to 14,000 years before present, no events of magnitude greater than 3.5 had occurred during the last two decades of instrumental monitoring (Stein and Bucknam, 1985). The epicenter of the 1983 Borah Peak main event was 14 km southwest (valleyward) of the surface break and all events (main and all eight aftershocks greater than magnitude 4.0) were concentrated in a 500 square kilometer area valleyward of the Lost River fault (Doser, 1985).

The Hebgen Lake event produced approximately 23 km of surface rupture along the Red Canyon fault (Witkind, 1964). The main event and all 21 aftershocks greater than magnitude 4.0 were within an area of approximately 2200 square kilometers on both sides of the fault (Doser, 1985).

The typical (Borah Peak type) earthquake event to occur in the Wasatch fault zone would have the following characteristics: 1) magnitude would be approximately 7.0-7.5, 2) surface expression would be around 2 m maximum vertical displacement and approximately 20 km maximum horizontal surface rupture, possibly along a presently exposed scarp 3) the epicenter (and maximum ground shaking) may be up to 15 km valleyward of the surface expression of the fault, 4) aftershocks of magnitude greater than 4.0 would be concentrated within an area of approximately 500 square kilometers of the epicenter, 5) focal depth would be near 15 km, and 6) the fault would dip approximately 45 degrees at the surface.

INVESTIGATIVE PROCEDURES:

Spur faces were first outlined on 1:24,000 scale topographic maps before field work. All spurs were investigated in the field directly and/or remotely to determine: 1) extent of spur face, 2) rock outcrop area, 3) dip of outcrop, either absolutely or a remote visual estimate of whether the dip is into or out of slope and the relationship of dip angle to slope angle, 4) if outcrops are partially buried and thus unlikely to produce rock fall clasts, 5) extent of discontinuities (faults, joints, shear zones, rock cleavage) either by actual measurements or estimated, 6) orientation of discontinuities on spurs which were investigated directly, 7) presence of rock fall clasts and runout zone, maximum clast diameter, average large-size clast diameter, and relative clast abundance, 8) sedimentary deposits which could provide rock fall clasts during an earthquake, 9) talus areas, 10) predominant rock type, 11) possible risk to cultural entities, and 12) whether clast deposits were produced by means other than rock fall or were influenced by cultural construction.

A spreadsheet (Table 2) was constructed with the following categories: 1) map quadrangle and spur number (arbitrary numbering system), also an indication of a the presence of a rock fall deposit and if the deposit was man-made or represents a wave-cut cliff deposit, 2) slope of spur face in degrees, 3) lithology of spur using a modified classification from Davis (1984), 4) presence of outcrop (no, yes, or yes but partially buried and therefore would not provide rock fall clasts), 5) bedding (yes, no); dip into or out of slope and dip angle, 6) faulting (yes, no), and 7) if the spur face presents a rock fall hazard, according to the judgement of the investigator, that is, if there are clasts available for falling, or if rock fall clasts are evident on the spur face or at the base of the spur. All spur faces that were investigated including those that have high rock fall susceptibility are illustrated on Plates 1a through 1d.

ROCK FALL INTRODUCTION:

For the purpose of this report rock topple and rock fall mass movement types will be considered collectively as rock fall (figure 3). Whalley (1984) limits a rock fall to a volume of rock mass well below 1,000,000 cubic meters and a failure surface less than 50 m from the ground surface. All the rock falls noted in the study area were well below 1,000,000 cubic meters and most were simply isolated rock fall clasts. A few of the talus deposits are probably on the order of hundreds of cubic meters. Piteau and Peckover (1978) define a rock mass as a "...heterogeneous and discontinuous medium composed essentially of partitioned solid blocks that are separated by discontinuities." Rock falls are produced when clasts (blocks) composed of semi-consolidated to consolidated rock move downslope by pure movement of, or movement combinations of: free-fall, saltation (travelling in the air after collision), rolling, sliding, or toppling. The minimum slope for a rock fall is the angle of repose of its clasts; at this slope scree is deposited as talus (Whalley, 1984).

Plate 1a. Mountain Spurs from Centerville Canyon to Hobbs Canyon, Wasatch Range, Utah.

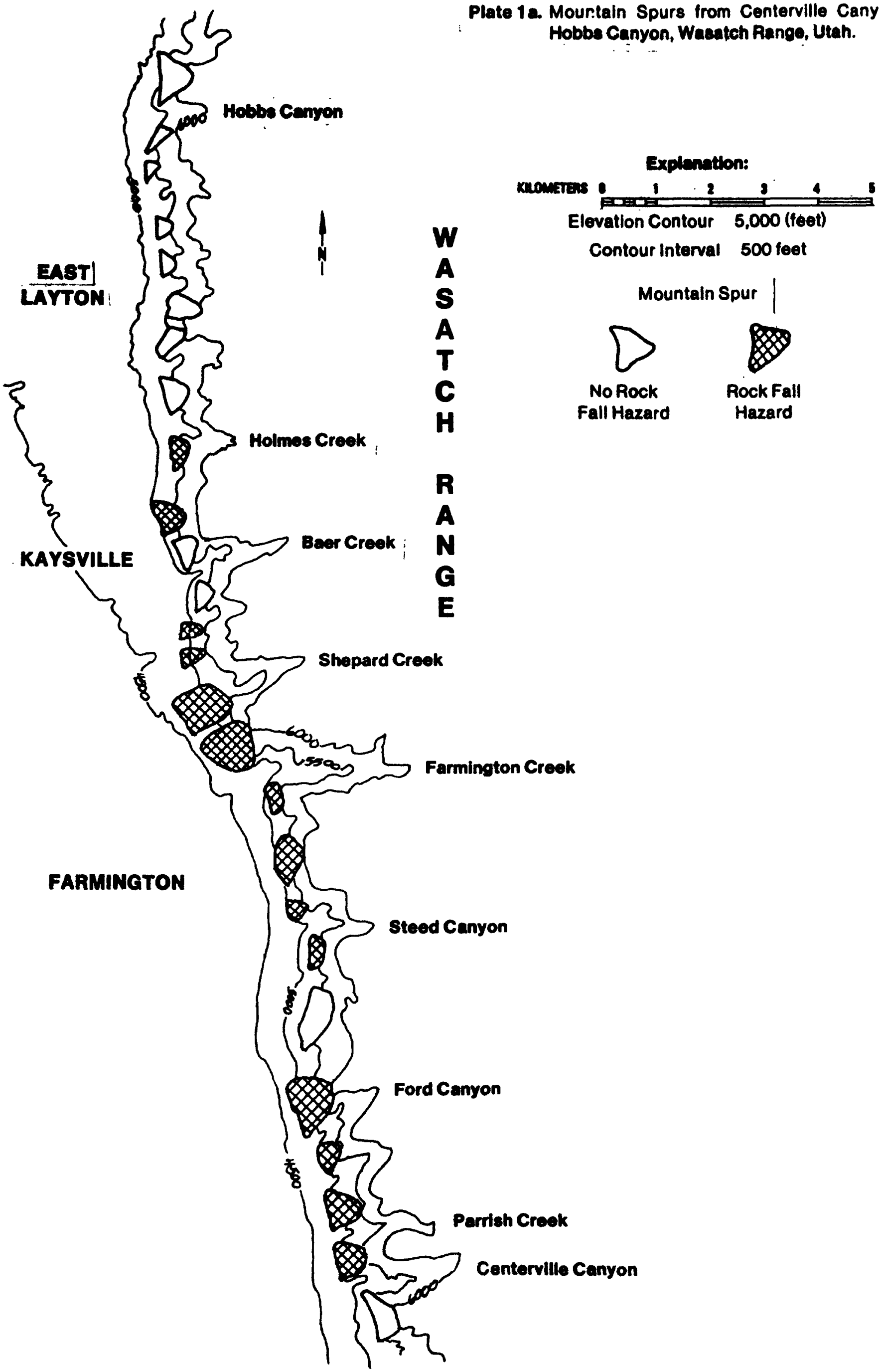

Plate 1b. Mountain Spurs from Millcreek to Centerville Canyon, Wasatch Range, Utah.

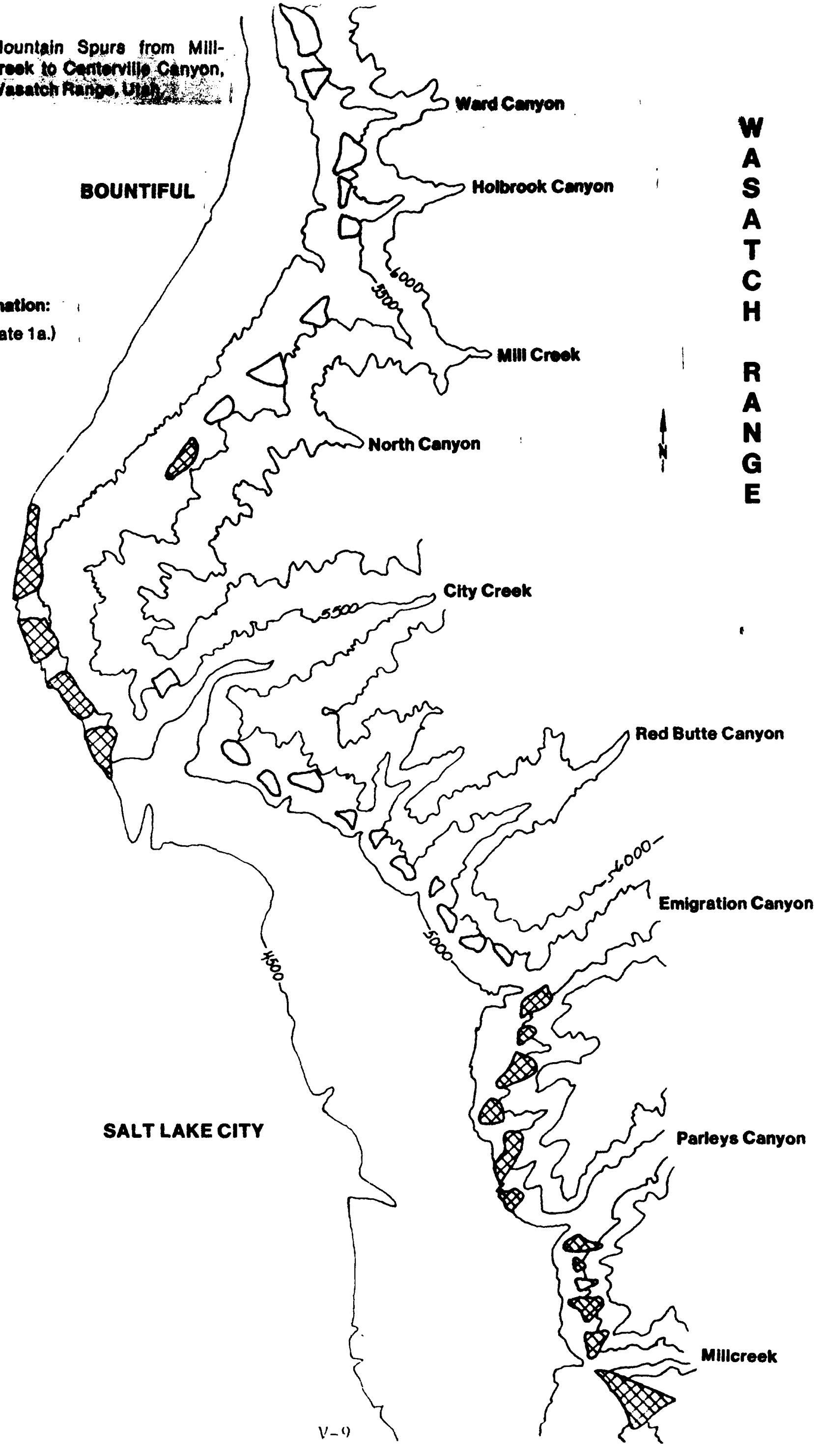

Explanation:
(see Plate 1a.)

Plate 1c. Mountain Spurs from Draper to Millcreek, Wasatch Range, Utah.

Explanation:
(see Plate 1a.)

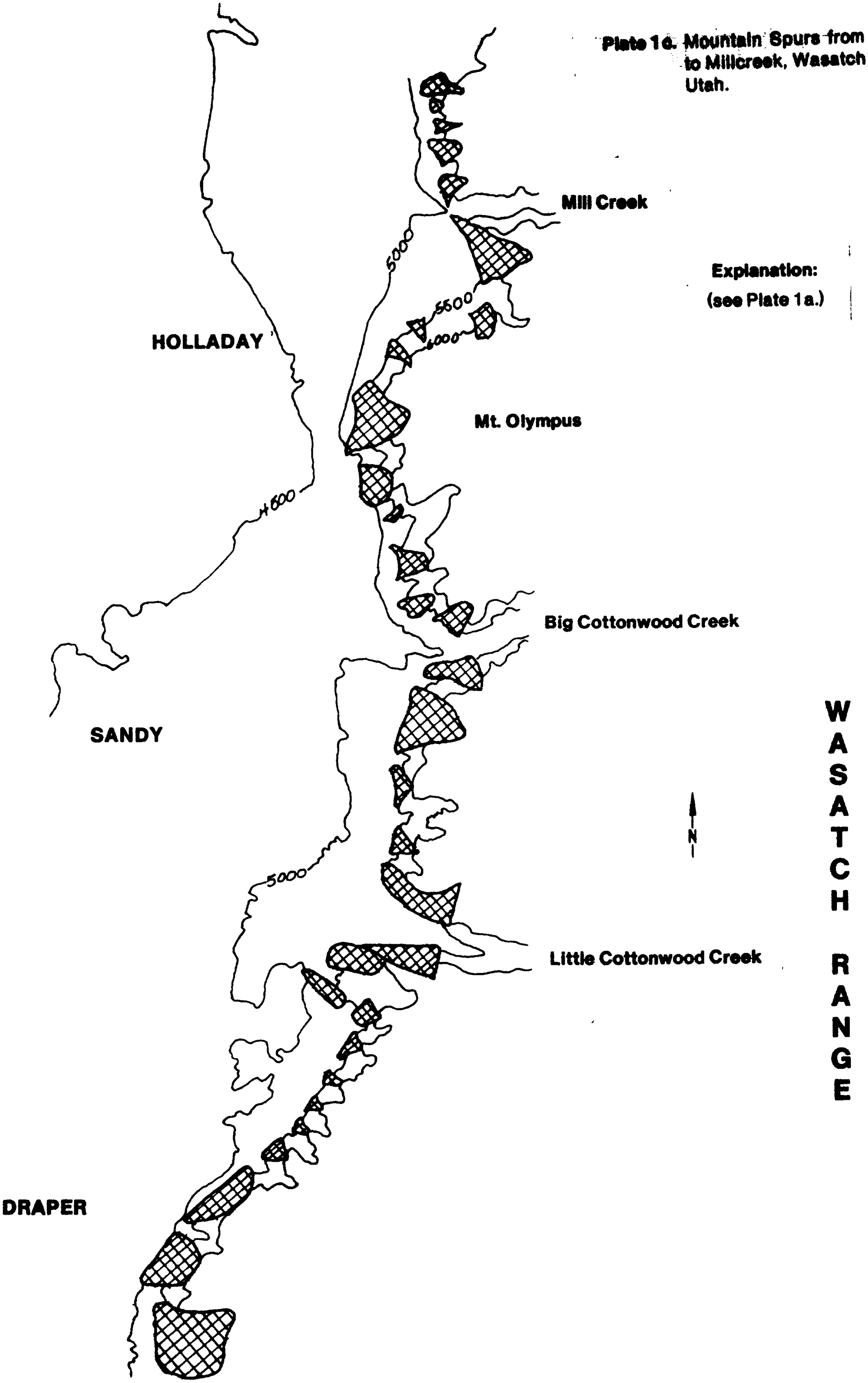

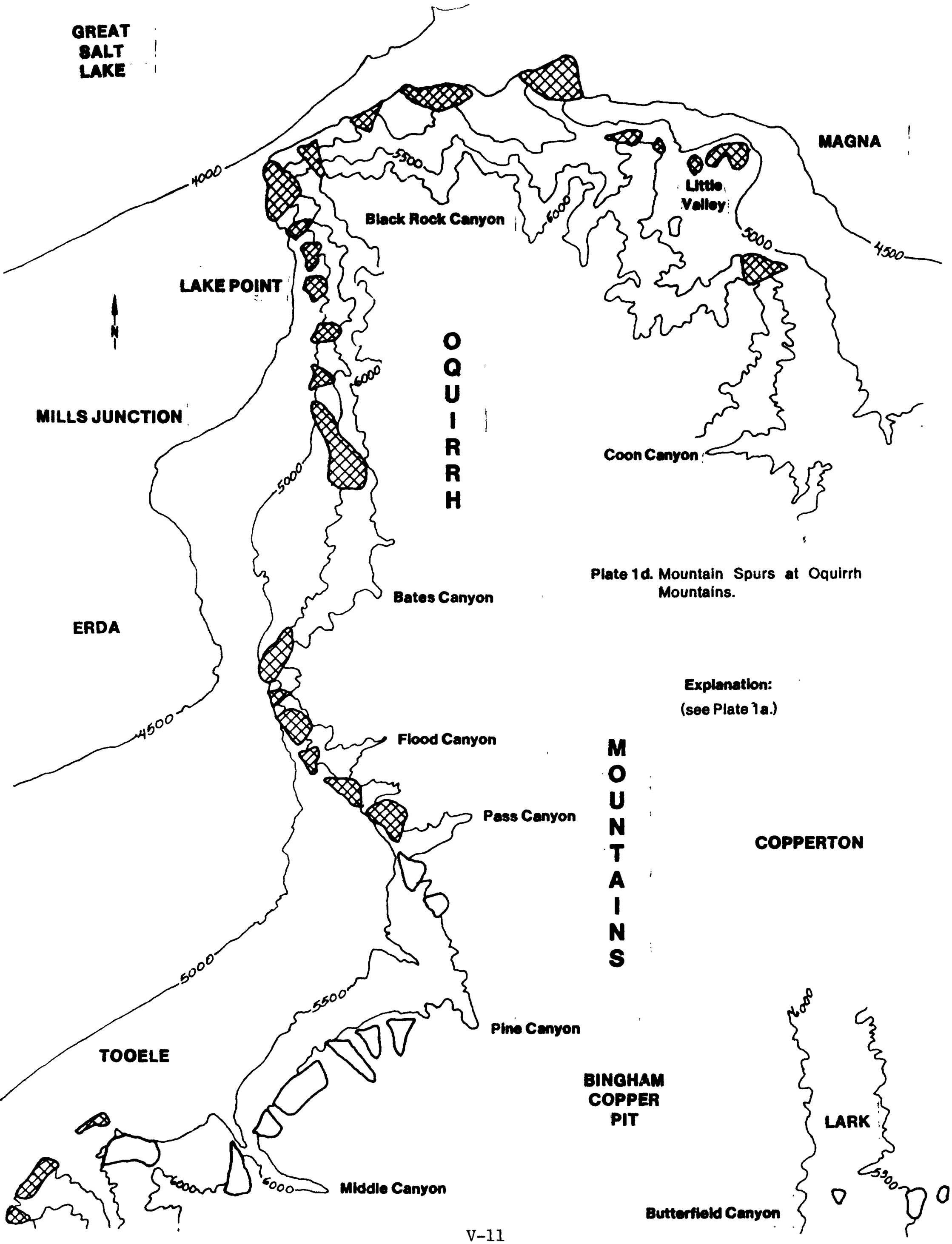

Plate 1d. Mountain Spurs at Oquirrh Mountains.

Explanation:
(see Plate 1a.)

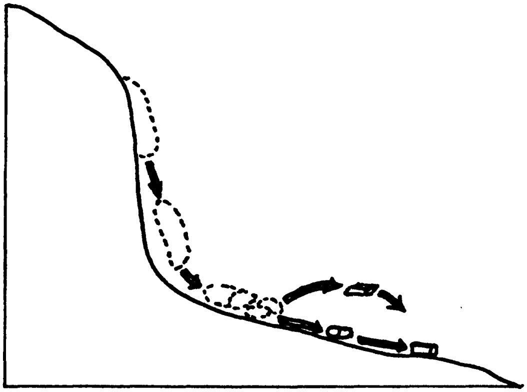

Rock Fall: dislodged rock mass which travels mostly in the air by free-fall, saltation, rolling, and sliding.

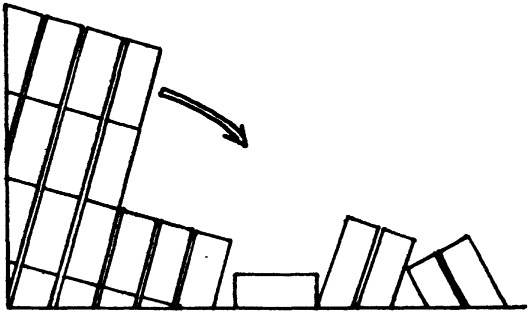

Rock Topple: Rock Fall due to top loading and shear about a pivot point below the center of gravity of a rock mass.

Figure 3: Rock fall and rock topple movements, after Varnes (1978)

Table 2: Central Wasatch Front Spur Rock Fall Susceptibility Spreadsheet

Explanation:

QUAD.= 7 1/2' Topographic Quadrangle

SPUR= mountain spur, arbitrarily numbered; *=rock fall deposit of unknown origin; *w=wave-cut cliff deposit(?); *m=man-made

SPUR SLOPE=degrees, steepest slope on spur

LITHOLOGY CLASSIFICATION= 1. metamorphics; 2. carbonates; 3. coarse-grained clastics; 4. fine-grained clastics
(after Davis, 1984) 5. intrusives; 6. extrusives; 7. lake gravels
8. Prefixes: Q=Quaternary, T=Tertiary; Qa=alluvium, Qt=talus, Qm=moraine, Qf=fan, Qls=landslide, QTf=fan, Tg=gravels

OUTCROP PRESENT?= YES/NO; YES(B)=buried, few clasts available

BEDDING= dip degrees; IN, OUT of slope; @ HI-A= at high angle; @ SLOPE=at slope angle

FAULT PRESENT?= YES/NO

ROCK FALL SUSCEPTIBILITY= YES/NO; (ALL)=all lithologies provide clasts; (7)=lithology class which provides clasts; (@)=quarry site

QUAD.: BINGHAM CANYON

SPUR #	SPUR SLOPE	LITHOLOGY CLASSIFICATION	OUTCROP PRESENT?	BEDDING	FAULT PRESENT?	ROCK FALL SUSCEPTIBILITY
1	29.1	3	NO	——	YES	NO
2	26.6	3	NO	——	YES	NO
3	24	3,8(QTf)	NO	——	YES	NO
4	28.6	3	NO	——	YES	NO
5	24.4	3	NO	——	YES	NO
6	26.6	3,8(QTf)	NO	——	NO	NO
7	36.5	3,8(QTf)	NO	——	NO	NO
8	27.2	3,8(QTf)	YES	OUT 22	NO	YES
9	35.5	3,8(QTf)	YES	OUT 55	NO	YES
10*	30.5	3,7	YES	IN @ HI-A	NO	YES
11	32	3,7,8(Qt)	YES	OUT 30-57	NO	YES
12	28.7	3,7,8(Qt)	YES	OUT 35	NO	YES
13	24.8	3,7,8(Qt)	YES	OUT 35	NO	YES

QUAD.: BOUNTIFUL PEAK

SPUR #	SPUR SLOPE	LITHOLOGY CLASSIFICATION	OUTCROP PRESENT?	BEDDING	FAULT PRESENT?	ROCK FALL SUSCEPTIBILITY
1	20	1	NO	——	NO	NO
2	26.6	1,7,8(Qls)	YES	IN	NO	YES(1,7)
3	30.3	1,7,8(Qls)	YES(B)	IN	NO	YES(1,7)
4	21.8	1,7	YES(B)	OUT 5	NO	NO
5	34.6	1,7	YES(B)	OUT 5-20	YES	NO
6	24.9	1,7	YES(B)	IN 20-35	NO	YES(7)
7	19.2	1,7	YES(B)	OUT 20-30	NO	YES(7)
8	26.6	1,7	YES(B)	OUT 10-35	NO	YES(7)
9	24.9	1,7	YES(B)	OUT 5-45	NO	YES(7)
10	26.9	1,7,8(Qls)	NO	——	NO	NO
11	20.9	1,7	YES(B)	IN 35-45	NO	YES(7)
12	25.5	1,7	YES	OUT 25	NO	YES(7)
13	24.9	1,7	YES	OUT>SLOPE	NO	YES(7)
14	18.4	1,7,8(Qls)	YES(B)	OUT 25-40	NO	YES(7)

QUAD. : DRAPER

SPUR #	SPUR SLOPE	LITHOLOGY CLASSIFICATION	OUTCROP PRESENT?	BEDDING	FAULT PRESENT?	ROCK FALL SUSCEPTIBILITY
1*	38.7	5,8(Qa)	YES	———	NO	YES(5,8)
2*w	34.4	5,7	YES	OUT H-55	NO	YES(7)
3*	39.8	4,5	YES	IN 15-70	NO	YES
4*	45	4,5,8(Qt,Qa)	YES	OUT 35-70	YES	YES(5,8)
5	38.7	4	YES	———	YES	YES
6	42.3	4,5	YES	IN 60	YES	YES
7	42	5	NO	———	YES	NO
8	45	5,8(Qa)	NO	———	YES	NO
9	18.4	5,8(Qm)	NO	———	NO	YES(8)
10	25.8	7,8(Qm)	NO	———	YES	YES(8)
11	24.8	8(Qm)	NO	———	YES	YES(8)
12	36.9	3,4,8(Qm,Qt)	YES	IN 10-60	YES	YES
13*	38.7	1,3,4,5,8(Qm,Qt)	YES	OUT 25-55	YES	YES(ALL)
14	36	1,8(Qm)	NO	———	NO	YES(8)
15	33.7	3,4,8(Qm,Qa)	YES	OUT 60	NO	YES
16	37.9	4,5,8(Qa)	YES	OUT 40-80	YES	YES
17*	45	3,4,5,8(Qm,Qt,Qa)	YES	OUT 25	NO	YES
18*	36.3	3,4,8(Qt)	YES	IN 60	YES	YES

QUAD.: FARNSWORTH PEAK

SPUR #	SPUR SLOPE	LITHOLOGY CLASSIFICATION	OUTCROP PRESENT?	BEDDING	FAULT PRESENT?	ROCK FALL SUSCEPTIBILITY
1*w	33	2,3,7,8(Qt)	YES	OUT 25-35	YES	YES(ALL)
2*w	35.8	2,3,7,8(Qt)	YES	OUT 15-60	YES	YES(ALL)
3	24.4	2,3,7	YES	OUT 25-55	YES	YES(ALL)
4	27.6	2,3,7	YES	OUT 22-42	NO	YES(ALL)
5	36.9	2,3,7,8(Qt)	YES	OUT 20-30	NO	YES(ALL)
6	48.9	2,3,7	YES	OUT 30-65	YES	YES(ALL)
7	43.6	2,3,7,8(Qt)	YES	OUT 45-70	YES	YES
8	41.6	2,7	YES	OUT 70-75	YES	YES
9	39.8	2,7	YES	IN 70-80	YES	YES
10	31.5	2,3,7	YES	IN 57-62	YES	YES(ALL)
11*	33.1	2,7	YES	IN 27-58	YES	YES
12*	42	2,7	YES	IN 35	YES	YES
13*	26.6	2,7	YES	OUT 35-60	YES	YES
14	46.2	2,7,8(Qt)	YES	IN 22	NO	YES(ALL)
15	27.9	2,7,8(Qt)	YES	OUT 10-41	YES	YES
16*	35.5	2,7,8(Qt)	YES	IN 12-35	YES	YES

QUAD.: FORT DOUGLAS

SPUR #	SPUR SLOPE	LITHOLOGY CLASSIFICATION	OUTCROP PRESENT?	BEDDING	FAULT PRESENT?	ROCK FALL SUSCEPTIBILITY
1	18.4	2	YES(B)	OUT 33	YES	NO
2	28.6	2	YES(B)	IN 40	YES	NO
3	32.3	3	YES(B)	OUT 47	YES	NO
4	31	3,4	YES(B)	OUT 82	YES	NO
5*	26.6	2,4	YES(B)	OUT@ SLOPE	YES	YES
6	28.3	2,4	YES(B)	OUT@ SLOPE	YES	NO
7	33.7	2,3,7	YES(B)	IN 50	YES	NO
8	19	3	NO	———	NO	NO
9	27.8	3,7	NO	———	NO	NO
10	31	3,8(Qf)	YES(B)	IN 14	YES	NO
11	33.7	8(Tg)	NO	———	NO	NO
12	25.8	8(Tg)	NO	———	NO	NO
13	24.4	8(Tg)	NO	———	NO	NO

QUAD.: KAYSVILLE

SPUR #	SPUR SLOPE	LITHOLOGY CLASSIFICATION	OUTCROP PRESENT?	BEDDING	FAULT PRESENT?	ROCK FALL SUSCEPTIBILITY
1	25.4	1,7	YES(B)	IN	NO	YES(7)
2	29.1	1,7	YES(B)	IN	NO	YES(7)
3*	32.7	1,7	YES	IN	NO	YES
4*	26.6	1,7	YES	IN	NO	YES(7)
5	39.8	1,7	YES(B)	OUT 45	YES	NO
6	38.7	1	YES(B)	OUT 10-20	YES	NO
7	34.7	1,7	YES(B)	IN	NO	YES
8	32	1	YES(B)	IN 20	NO	YES
9	28.1	1,7	YES(B)	IN 15-35	NO	NO
10	37.6	1,8(Qls)	YES(B)	IN 30	YES	NO
11	35.5	1	YES(B)	IN 70	YES	NO
12	38.7	1	NO	———	NO	NO
13	21.8	1,7	YES(B)	IN 70-80	NO	NO
14	31.2	1,7	NO	———	YES	NO
15	28.6	1,7,8(Qls)	YES(B)	IN 40	NO	NO
16	33.7	1,7	YES(B)	OUT 20	YES	NO

QUAD.: LARK

SPUR #	SPUR SLOPE	LITHOLOGY CLASSIFICATION	OUTCROP PRESENT?	BEDDING	FAULT PRESENT?	ROCK FALL SUSCEPTIBILITY
1	21.8	6	NO	———	NO	NO
2	18.4	6	YES(B)	———	NO	NO
3	35.5	6	YES(B)	———	NO	NO

QUAD.: SALT LAKE CITY NORTH

SPUR #	SPUR SLOPE	LITHOLOGY CLASSIFICATION	OUTCROP PRESENT?	BEDDING	FAULT PRESENT?	ROCK FALL SUSCEPTIBILITY
1	29.1	2,3	YES(B)	OUT 25-32	YES	NO
2*m	35.5	2,3,8(Tg)	YES	OUT 62	YES	YES(@,8)
3*m	33.7	2,3,8(Tg)	YES	OUT 25-55	YES	YES(@,8)
4*m	28.2	2,3,8(Tg)	YES	IN 23-30	YES	YES(@,8)
5*m	37.6	2,3,8(Tg)	YES	IN 26	YES	YES(@,8)
6*	35.5	8(Tg)	YES	IN 33	NO	YES(8)

QUAD.: SUGAR HOUSE

SPUR #	SPUR SLOPE	LITHOLOGY CLASSIFICATION	OUTCROP PRESENT?	BEDDING	FAULT PRESENT?	ROCK FALL SUSCEPTIBILITY
1	39.8	3	YES	-----	NO	YES
2*m	33.7	3,4	YES	IN 70	YES	YES(@)
3*	34.6	3,4,7	YES	IN 35	YES	YES
4*	35.5	3,4,7	YES	IN	YES	YES(3,4)
5*w	43.3	3,7,8(Qt)	YES	OUT 40	YES	YES
6*	29.7	2,3,4,7,8(QTf)	YES	OUT 50-80	YES	YES(7)
7	37.6	4,8(QTf)	YES	-----	YES	NO
8	21.8	2,3,4,8(QTf)	YES	OUT 65	YES	YES(ALL)
9	39.8	2,3	YES	IN 35-60	YES	YES
10	33.7	2,3,4	YES	OUT 35-40	YES	YES
11	39.8	2,4	YES	-----	YES	YES
12*	39.8	2	YES	IN	NO	YES(@)
13*	39.8	2	YES	OUT 55	YES	YES
14*w	37.6	4,8(Qt)	YES	OUT 55	NO	YES
15*	24	2,7	YES	IN 45-70	YES	YES
16	31.6	3,4,8(Qt)	YES	IN 70	YES	YES
17*	33.7	2,4,7	YES	IN 50-80	NO	YES(7)
18	45	2,4	YES	IN@ HI-A	NO	NO
19	41	3,8(Qt)	YES	IN	YES	YES
20	38.7	2,3	YES	IN@ HI-A	YES	YES

QUAD.: TOOELE

SPUR #	SPUR SLOPE	LITHOLOGY CLASSIFICATION	OUTCROP PRESENT?	BEDDING	FAULT PRESENT?	ROCK FALL SUSCEPTIBILITY
1	32	2,5,8(Qt)	YES	-----	YES	YES
2	26.6	2,5,8(Qt)	YES	OUT 30-40	YES	YES
3	41.6	2,5,8(Qt)	YES	OUT 55-65	YES	YES
4	32	2,5	YES(B)	OUT 30-50	YES	NO
5	24	2,3,4,7	NO	-----	YES	NO

Rock fall clasts are produced by the development of discontinuities such as joints, faults, rock cleavage, bedding separations, or shear zones in a rock mass due to tectonic activity, unloading of overburden by erosion, weathering, or shrinkage due to cooling of volcanic flows. The shear strength of a rock mass is controlled by the extent of discontinuities (Piteau & Peckover, 1978). Discontinuities weaken rock particularly if they are closely spaced and open. Given a constant slope, rocks with open fractures were more susceptible to failure during the Mammoth Lake earthquakes in 1980 (Harp, Tanaka, Sarmiento, and Keefer, 1984). Open discontinuity surfaces are exposed to weathering, plant and animal activities, and infilling of materials which are often weaker than the rock mass. Once the discontinuities are developed and the rock is exposed, a rock fall can occur because of: 1) slope failure due to weaker rock such as shale at the base of a cliff, presence of ground water along bedding or a discontinuity, or removal of supporting material at the base of a cliff by erosion or construction, 2) static loading at the top of a cliff, 3) cleft pressure, such as freeze-thaw, hydration of minerals, and salt crystallization (Whalley, 1984) within discontinuities, and 4) dynamic loading due to an earthquake or blasting.

Practically any lithology can produce rock falls, although the most damaging rock falls are produced by rock types which tend to sustain discontinuities because of internal strength and induration and by rock types which tend to weather rapidly along fractures and exposed surfaces. Lithologies such as sandstones, quartzites, limestones, and gneisses are well-indurated, while volcanic and intrusive rocks tend to weather along exposed surfaces. Some igneous rocks such as basalts have columnar jointing, which provides large rock fall clasts, and tend to exhibit spheroidal weathering which reduces movement friction. The surface of failure in rock tends to follow discontinuity surfaces and does not trend through the rock mass itself unless the rock is very soft (Piteau & Peckover, 1978). Lithologies that produced rock falls in the Mammoth Lakes region of California include well-indurated Paleozoic marbles, quartzites, hornfels, slates, and Mesozoic granitic intrusives, and weakly cemented, weathered, rhyolites, rhyolitic tuffs, and basalts, some of which exhibit columnar jointing (Harp, Tanaka, Sarmiento, & Keefer, 1984). Harp, Wilson, and Wieczorek (1976) report that 90% of the rock falls caused by the 1976 Guatamalan earthquake were in poorly-cemented, non-welded, pumice, 10% occurred in Tertiary volcanic rocks, and less than 1% occurred in Cretaceous limestone and Paleozoic metamorphic rocks. The 1959 Hebgen Lake, Montana earthquake (main shocks and aftershocks) caused many rock falls in volcanic rock (altered rhyolites and jointed tuffs) and Paleozoic limestones (Hadley, 1964). Fractured volcanic rocks and jointed Paleozoic sedimentary rocks produced rock falls during the Borah Peak earthquake. Sedimentary deposits such as glacial moraines (figure 4), alluvial fans (figure 5), landslides, boulder beach deposits (figure 6), and man-made deposits (figure 7) can provide large rock fall clasts which can travel great distances, particularly because of spheroidal or diskoidal shapes common in the deposits. Talus and existing landslide deposits tend to be metastable and do not become reactivated during an earthquake (Hadley, 1964), (Keefer, 1984), (Harp, Wilson, Weiczorek, 1976).

The runout zone of a rock fall deposit is the area between the base of the mountain spur face and the maximum extent of rock fall clasts (figure 8). In a study of 40 major earthquakes the maximum reported distance a rock fall clast moved was approximately 800 m (Keefer, 1984). Harp, Tanaka, Sarmiento, and Keefer (1984) reported a diskoidal rock fall clast from a glacial moraine, approximately 8 m in diameter by 1.5 m thick, crashed through cottonwood trees at the base of a slope and rolled 50m beyond. Prediction of runout distance for any particular rock fall clast is dependent on factors such as: 1) driving forces; acceleration of ground surface which dislodges clast and initiates clast movement and clast momentum at the base of slope, 2) frictional components such as; slope distance, slope angle, and slope and runout zone roughness, and 3) clast parameters such as; clast shape, type of movement, and clast strength. The most practical way to estimate runout zone is to map existing rock fall clast runout assuming that the base of the slope is not culturally disturbed and the mechanism of emplacement is rock fall.

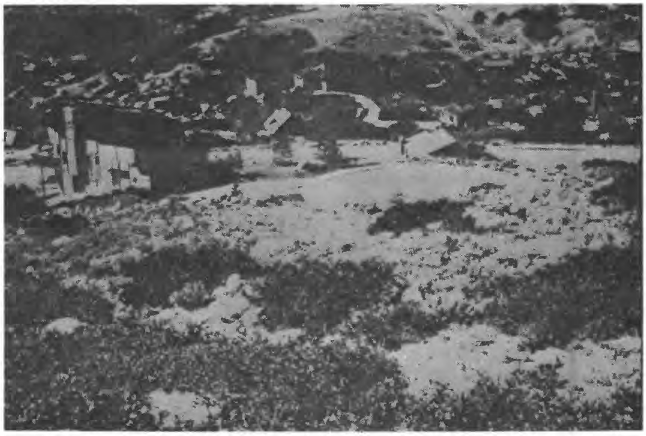

Figure 4: Glacial moraine surface in a subdivision below the Bells Canyon reservoir, Salt Lake City. View is toward the west. Rock clasts which dot the surface of the moraine are Precambrian quartzites and Tertiary quartz monzonites. The maximum rock clast diameter is approximately 2m.

Figure 5: Alluvial fan at mouth of Big Willow Creek, Salt Lake City. Tertiary quartz monzonite rock clasts may dislodge and move during an earthquake. The average large size of clasts is approximately 0.75m and the maximum size is almost 3m. The fan is above the highest level of Lake Bonneville and probably has not been disturbed by lake processes, however, cultural construction may have altered the density of rock clasts near the bottom of the slope. Note the triangular facetted spur face in the middle distance. View is to the southwest.

Figure 6: Lake Bonneville bench near Centerville. Many large rock clasts are perched precariously on a steep slope above development. All clasts are Precambrian metamorphic rocks such as gneisses, amphibolites, and quartzites. The Maximum size is appproximately 1.5m and the average large size is about 0.5m. The elevation ranges from 5200 feet at the slope crest to 4800 feet at the base of the slope. View is to the northeast.

Figure 7: Retaining wall in subdivision in Olympus Cove area, Salt Lake City. Rock clasts in and around the wall are approximately 1m in diameter. There is no infilled mortar between the rock clasts which will be ready to move during an earthquake.

Figure 8: Rock fall runout due to Borah Peak earthquake at Challis, Idaho. Homes and property were damaged but no loss of life was caused due to rock fall. The largest rock clast is approximately 2m. Weakly cemented and open-jointed volcanic rocks make up the greater than 30m high cliff which provided the clasts. View is to the east. Photo by Harold E. Gill, Nov. 1983.

CHARACTERISTICS OF SPURS WITH ROCK FALL SUSCEPTIBILITY:

If an outcrop existed anywhere on a spur face, regardless of its size, the entire spur face was regarded as being susceptible to rock falls unless the outcrop was partially buried to the point that it could provide no rock fall clasts. Column 4 of Table 2 lists spurs with outcrops and spurs with partially buried outcrops. Most of the partially buried outcrops were in rounded topographic terrain around Kaysville, Bountiful, and northeastern Salt Lake City, which may indicate an older surface or more easily eroded bedrock. Most of the lacustrine boulder beach deposits which may provide 1/2 m to 2 1/2 m diameter rock fall clasts during an earthquake are located between Bountiful and Kaysville. Some of the clasts appear to be ready to move at the slightest disturbance although the slopes are rather low for long runout distances (figure 6). Glacial moraines, located at the mouth of Little Cottonwood Canyon, have spheroidal, rounded, quartzite and quartz monzonite clasts up to 2 m in diameter which are perched precariously on the slopes (figure 4). All spurs with talus deposits are considered susceptible, not because the talus may provide clasts but because the clasts represent previous rock falls from outcrops above (figure 9).

ROCK FALL DEPOSITS:

No rock fall deposit was identifiable as being definitely triggered by an earthquake. Other possible agents of rock fall deposits include man, slope failure at the base of a cliff, erosion of sediment around clasts, exfoliation of bedrock, or wave-cut cliff erosion. Wave-cut cliff erosion consists of erosion of outcrops near a shoreline and deposition of clasts below and on the shoreline beach. The Bonneville level of Lake Bonneville (Currey, Atwood, & Mabey, 1983) is near the 5200 foot contour, and the Provo level is near the 4800 foot contour on the map quadrangles. Rock deposits from outcrops near these elevations are deposited in a relatively wide area laterally and downslope from the outcrop, and are on promotories which appear to have experienced wave action. Rock deposits that may be wave-cut cliff deposits are marked *w in Table 2. Man-made rock deposits that are associated with quarry activity are marked *m in Table 2. The maximum runout of a rock fall in the Central Wasatch Front area is approximately 250 m.

Figure 9 : North side of the mouth of Little Cottonwood Canyon, Salt Lake City, showing vegetated and open talus slopes with larger rock fall clasts. Rock outcrop on left skyline is Precambrian quartzite which has been intruded by a Tertiary quartz monzonite shown on the right skyline. View is to the northeast.

Figure 10 View looking north of mountain spur on north side of mouth of Big Cottonwood Canyon, Salt Lake City. Prominent feature in the middle distance is the Big Cottonwood delta which was deposited while the valley was occupied by Pleistocene Lake Bonneville. The mountain spur above the lake bench is composed of Precambrian quartzite which outcrops at bench level near the right edge of the photograph and in the middle foreground behind the Big Cottonwood water treatment plant. The Holladay Gun Club is located on the lake bench.

GEOLOGY OF THE CENTRAL WASATCH FRONT:

The following description of the geology of the mountain spur areas is adapted from Davis (1983). Middle and Upper Precambrian rocks consist of metamorphic rocks, mainly gneisses, granulites, quartzites, slates, argillites, schists, and amphibolites which crop out at Wasatch Range spur areas from Bountiful to the northern edge of the study area and near the mouth of Little Cottonwood Canyon and on spur faces between Draper and Holladay. The Paleozoic rocks consist of limestones, dolomites, sandstones, quartzites, siltstones, and shale from the Cambrian and Late Paleozoic periods. Paleozoic rocks crop out in mountain spurs along the Wasatch Range from Holladay to northern Salt Lake City and along the western front of the Oquirrh Range. Conglomerates, sandstones, siltstones, mudstones, shales, and limestones make up the Mesozoic rocks which crop out in Wasatch Range mountain spurs near northeastern Salt Lake City. Tertiary rocks include a quartz monzonite intrusive in mountain spurs east of Draper; volcanic flows near Lark at the eastern front of the Oquirrh Range, and coarse clastics of the Salt Lake Salient near northern Salt Lake City. The Quaternary/Tertiary Harkers Alluvium consists of coarse clastics deposited in pre-Lake Bonneville fans along the eastern Oquirrh Mountain front from Lark northward almost to Magna and northeast/east of Tooele City in western Oquirrh Mountain front spurs. There are also small, isolated Quaternary/Tertiary, pre-Lake Bonneville, alluvial fans along the Wasatch Range front. The most common Pleistocene deposts near the mountain spurs are coarse clastics of the highest beach of Lake Bonneville. The lake deposits occur along all mountain fronts in the study area (figure 10).

Pleistocene glacial moraines are located at mountain spurs near Little Cottonwood Creek. Coarse clastics of talus, alluvium, landslide, and fan deposits associated with mountain spurs are Pleistocene/Holocene age. These deposits occur in isolated spur areas along all mountain fronts.

LANDSLIDE SUSCEPTIBILITY:

Various investigators have estimated landslide susceptibility by using a combination of factors such as slope, lithology, and existing landslide deposits (Brabb, Pampeyan, & Bonilla, 1978), all of the above factors plus bedding and slope relationships (Vecchia, 1978). Carrara and Merenda (1976) have expanded the determinant factors of landsliding to include uniformity of slope (simple or complex), aspect of slope, and uniformity of lithology (one lithologic type versus various lithologies in the landslide source area). DeGraff and Romesburg (1980) developed a matrix of lithology, slope angle, and slope aspect to determine thresholds of landslide susceptibility for land management purposes. Pack (1985) used four factors in a multivariate debris slide model of Davis County, Utah; type of terrain, distance to nearest landslide, slope-shape (convex/concave) across the slope face, and slope angle. Wright, Campell, and Nilsen (1974) prepared isopleth maps which show landslide distribution in contour form based on percentage of area covered by landslides. Krohn and Slosson (1976) estimated landslide potential of the United States by combining topographical relief, annual rainfall, and landslide activity of geologic formations. Wieczorek, Wilson, and Harp (1985) developed an index of susceptibility based on the estimated shear strength of lithologies and critical earthquake ground acceleration to initiate sliding of rock mass.

This report considers rock fall susceptibility as a function of slope angle, production of rock fall clasts, and the likelihood of rock fall. A spur is susceptible to rock fall if a) there are rock clasts available for falling , b) if there are rock fall clasts on the spur face, or c) if there are rock fall clasts at the base of the spur face, in a runout zone. The susceptibility of rock fall hazard in this report is a go/no-go situation, a mountain spur face is or is not susceptible to rock fall hazards due to any mechanism.

EARTHQUAKE INITIATION OF ROCK FALLS:

Rock fall initiation is difficult to predict quantitatively because of a variety of factors of driving forces such as tensile stress and ground acceleration required to trigger movement, and resisting forces such as burial depth of rock clasts, shear strength of infilling materials in discontinuities, rock clast inertia, and discontinuity orientation, spacing, and tightness. Wilson (1984) using a procedure after Newmark (1965) consulted strong motion accelerographs of Californian earthquakes to determine the critical acceleration needed to produce ground displacements of 5 cm for rock slides and 2 cm for rock falls. Wilson (1984) assumes a 2 cm ground displacement necessary to initiate a rock fall. Rock falls have a lower critical acceleration threshold because the tensile strength mobilized by rock falls is lower than shear strength mobilized by rock slides (Wilson, 1984). There are no strong motion accelerographs of a Wasatch fault zone earthquake which can be used in the Newmark analysis. Keefer (1984) estimates that a magnitude 4.0 earthquake is probably the smallest needed to induce rock falls, although he remarks that landslides can be caused by nonseismic events and slopes of marginal stability may fail because of weaker shaking. Harp, Wilson, and Wieczorek (1976) indicate that a MMI intensity of VI is the threshold of ground shaking to trigger landslides in susceptible terrain and that many landslides were triggered by topographic amplification of seismic waves along canyon wall crests and ridges during the Guatamalan earthquake of 1976. From a study of 40 major earthquakes Keefer (1984) reports that rock falls can be triggered from a maximum distance of 200-300 km from the epicenter, or 150-200 km from the fault rupture due to an earthquake of magnitude 7.0-7.5, the magnitude range of the characteristic earthquake of the Wasatch fault zone. Given these distances, a characteristic earthquake occurring anywhere in the Wasatch fault zone could cause rock falls from susceptible slopes almost along the entire zone. The aftershocks, assuming the Borah Peak earthquake model, of magnitude greater than or equal to 4.0 could initiate rock falls within a 500 square kilometer area of the epicenter. In other words, assuming a mid-valley epicenter, the aftershocks could cause rock falls in the Oquirrh Mountains as well as the Wasatch Range.

RESULTS:

Lithology:

Table 3 and column 3 of Table 2 are listings of the lithologies, combinations of lithologies, and sedimentary deposits that compose each spur face investigated. The numerical nomenclature is from a classification of Central Wasatch front lithologies by Davis (1984). The numbers represent the following rock types: 1) Precambrian metamorphic rocks except clastics, 2) carbonate rocks of Paleozoic and Mesozoic age, 3) coarse-grained clastic rocks which are of Precambrian through Tertiary (Paleocene & Eocene) age, 4) Precambrian to Mesozoic fine-grained clastic rocks, 5) Tertiary igneous intrusive rocks, 6) Tertiary volcanic flows, 7) Pleistocene Lake Bonneville sand and gravel deposits, and 8) other coarse-grained clastic deposits of Tertiary (Oligocene through Pliocene) and Quaternary age. Classification #8 consists of Tertiary gravel (Tg), Quaternary/Tertiary fans (QTf), Quaternary talus (Qt), Quaternary glacial moraines (Qm), Quaternary alluvium (Qa), and Quaternary landslides (Qls).

Mountain spurs with combinations of rock types have a higher rock fall susceptiblity than spurs with only one rock type. Of the mountain spurs composed of one rock type, a higher percentage of spurs with clastic bedrock are more susceptible to rock fall than spurs with crystalline bedrock. Table 4 lists the percentages of rock types and combinations of rock types in spurs that have high rock fall susceptibility. Carbonate rocks, boulder beache' deposits, and talus make up the majority of the spur slopes with high rock fall susceptibility.

Table 3: Lithology of mountain spur faces, Central Wasatch front, Utah. (Lithology classification after Davis (1984))

Lithology Classification	Total Number of Spurs	Number of Spurs with high Rock Fall Susceptibility, (%)
Lithologies: (note: some catagories include sedimentary deposits)		
1(metamorphics)	30 spurs	4 spurs (13%)
2(carbonates)	13 spurs	11 spurs (85%)
3(coarse clastics)	20 spurs	9 spurs (45%)
4(fine clastics)	3 spurs	2 spurs (67%)
5(intrusives)	13 spurs	7 spurs (54%)
6(extrusives)	3 spurs	
Sedimentary Deposits:		
7(lake gravels)	51 spurs	39 spurs (77%)
8(other deposits)	56 spurs	39 spurs (70%)
Tg(gravel)	8 spurs	5 spurs (63%)
QTf(fan)	7 spurs	4 spurs (57%)
Qls(landslide)	6 spurs	
Qt(talus)	22 spurs	22 spurs(100%)
Qm(moraine)	8 spurs	6 spurs (75%)
Qa(alluvium)	4 spurs	2 spurs (50%)
Qf(fan)	1 spur	

Lithology Combinations: (note: catagories may include sedimentary deposits)

1,4(metamorphics & fine clastics)	1 spur	1 spur(100%)
2,3(carbonates & coarse clastics)	16 spurs	10 spurs (63%)
2,5(carbonates & intrusives)	4 spurs	3 spurs (75%)
2,3,4(carbonates, coarse & fine clastics)	2 spurs	2 spurs(100%)
3,4(coarse & fine clastics)	7 spurs	6 spurs (86%)
3,5(coarse clastics & intrusives)	1 spur	1 spur (100%)
4,5(fine clastics & intrusives)	3 spurs	3 spurs(100%)

Table 4: Percentages of rock types and combinations of rock types of bedrock in spurs with rock fall susceptibility.

Spurs with single bedrock type	Percentage of spurs with rock fall susceptibility
Clastic rock types (classification numbers 2, 3, & 4)	64%
Crystalline rock types (classification numbers 1, 5, & 6)	24%
Spurs with combinations of bedrock types	
Combinations of clastic rock types	73%
Combinations of clastic & crystalline rocks	77%

Thirty-two spurs which have rock fall deposits (other than talus) at their bases are marked with an asterik on Table 2. The most common rock types in the deposits are Paleozoic carbonates, Precambrian quartzites, Tertiary conglomerates, and Tertiary granitic intrusives. Other rock types that occur in rock fall deposits are Quaternary conglomerate, Triassic shale, Paleozoic sandstones, Precambrian hornfels and slates, and Precambrian crystalline metamorphic rocks.

Slope Angle:

The 1980 Mammoth Lakes, California earthquakes triggered rock falls from bedrock slopes and glacial moraines which were at slope angles at least 35 degrees but generally more than 50 degrees (Harp, Tanaka, Sarmiento & Keefer, 1984). Rock falls of pumice originated on slopes steeper than 50 degrees and debris slides orginated on slopes generally between 20 and 50 degrees as a result of the 1976 Guatamala earthquake (Harp, Wilson, & Wieczorek, 1981). Keefer (1984) reports that rock falls recorded in data from 40 major earthquakes originated on slopes steeper than 40 degrees, and rock slides on slopes steeper than 35 degrees. Wieczorek, Wilson, and Harp (1985) assume that all slopes steeper than 70% (35 degrees) are highly susceptible to rock fall.

Slope angles in this report were calculated from measurements of the steepest area of spur faces and sedimentary deposit slopes as outlined on 1:24,000 scale topographic maps. Slope angles are listed in column 2 of Table 2. Slopes of the thirty-six spur faces that have rock fall deposits (not including talus deposits) range from 24 to 49 degrees. Six of the spurs that have rock fall deposits have culturally controlled slopes due to quarry operations. Peak spur slope angles for spurs with no rock fall susceptibility range from 24-38 degrees. Spurs with rock fall susceptibility have a bimodal distribution of peak slope angles, 24 to 26 degrees for sedimentary deposits and 30 to 41 degrees for bedrock spurs.

The slope angle of spurs seems to be controlled by sedimentary processes, faulting, bedrock structure, and cultural manipulations. Six spurs, all of which have rock fall deposits, have slopes controlled by quarry operations near Big Cottonwood Creek and north Salt Lake City. Gravel pits are common along the Wasatch front but generally do not constitute a hazard because the grain size of the sand and gravel deposits averages only a few centimeters. Many spurs are influenced by subdivision development near Wasatch front communities (figure 11). Development near or on spurs includes cutting the toe of slopes, steepening slopes, clipping slope crests, changing vegetation, altering drainage, and redistributing rock fall clasts.

Bedrock type does not seem to directly control spur face slope angle except in a general sense; crystalline metamorphic bedrock spurs have an average slope of 25 degrees between Bountiful and Farmington and 32 degrees from Farmington to the north edge of the study area, carbonate bedrock spurs have an average slope of 34 degrees, and coarse-grained clastic bedrock spurs have an average slope of 30 degrees. Bedrock structure does affect some slope angles; spur slopes at the northern end of the Oquirrh Mountains generally are dip slopes which range up to 90 degrees.

Sedimentary processes which affect slope angles include: lacustrine beach erosion and deposition, glacial deposition, alluvial deposition, landslide deposition, and talus deposition. Lake Bonneville beach processes formed slopes at the base of most spurs along mountain fronts in the study area, but only locally do beaches contribute rock fall clasts. Slopes of spurs with rock fall susceptibility near Farmington and Centerville Canyon are developed on Quaternary Lake Bonneville beaches near the elevations of 5200 feet (1585 m) and 4800 feet (1463 m). Glacial moraines make up the primary slopes of spurs near the mouth of Little Cottonwood Creek. Alluvial deposits provide rock fall clasts and to some extent influence slope angle of spurs near Draper and the mouth of Little Cottonwood Creek. Talus slopes make up variable proportions of most spur faces but are extensive in areas south of Tooele, northwest and northern Oquirrh Mountains, near Holladay, and along southern edge of the mouth of Parleys Canyon. Landslide deposits in the study area do not increase the rock fall susceptibility of a spur because a) they are limited in areal extent and number, b) the deposits occur in soils and fine-grained material, and c) the slope of a landslide deposit is relatively low (27 degrees for a landslide south of Farmington).

Figure 11 Subdivision near the mouth of Emigration Canyon, Salt Lake City, looking east. Homes are situated at the base of Mesozoic sandstone slopes which may fail because of natural or human causes, there are children on the outcrop behind the white house.

The major control of spur face slope angle is related to normal faulting. Spurs along the western slopes of the Wasatch Range ahd the Oquirrh Mountains have been influenced by basin and range type normal faulting. Figure 2 is a block diagram of triangular facets formed when a mountain spur is truncated by a steeply dipping normal fault. Anderson (1977) suggests that the fault surface that forms the spur face can dip from 45 to 60 degrees originally but weathers to 20 to 40 degrees after the earthquake. Spur face slopes along the western fronts of the Oquirrh mountains and Wasatch Range in the study area range from 18 to 46 degrees. From Tooele to Erda (Table 2, Bingham Canyon quadrangle, spurs #1-13) slope angles are generally lower than from Erda to the northwest corner of the Oquirrh Mountains (Table 2, Farnsworth Peak quadrangle, spurs #16-10). Along the western front of the Wasatch Range spur slope angles are generally higher from Draper to Emigration Canyon (Table 2, Draper and Sugarhouse quadrangles) than from Emigration Canyon to Farmington (Table 2, Fort Douglas, Salt Lake City North, & Bountiful Peak quadrangles). North of Farmington spur slope angles tend to increase (Table 2, Kaysville quadrangle). Bedrock does not seem to control this pattern since similar slopes exist within the western front of the Oquirrh Mountains consisting of carbonate and coarse-grained clastic strata, and both the Bountiful Peak and Kaysville quadrangles are underlain by crystalline metamorphic rocks. The best developed triangular facets tend to be on the steeper spurs. Anderson (1977) also noted that spur slopes retreat from the fault as time after the faulting increases. Spurs with steep slopes tend to have boundary faults and form linear north-south and northeast fronts, whereas the embayment of the front at Bountiful as well as northwest trending fronts near northeastern Salt Lake City and northeast of Tooele tend to have more gentle slopes and are not as faulted. Perhaps these slopes have retreated farther from faults and are older than other fronts.

CONCLUSIONS:

Widespread damage could occur in the Central Wasatch Front area if an earthquake of magnitude 7.0-7.5 should occur. Some of that damage would be due to thousands of rock falls that would be the result of ground shaking during the event and aftershocks greater than magnitude 4. The Borah Peak and Hebgen Lake earthquakes are examples of such earthquakes that can be reasonably expected in the future somewhere along the Wasatch Front.

As the population of Wasatch Front communities increases, more urban pressure is exerted toward scenic lots available along the mountain fronts (figure 12). In addition to reducing slope stability of spurs, urban construction may encroach into rock fall runout zones. The rock fall susceptible spurs identified in this report should be studied in site-specific detail before building is permitted.

Figure 12: Subdivision at mouth of Big Cottonwood Canyon, Salt Lake City, looking south. Homes are located within runout zone of rock clasts from outcrops at the crest of the slope. Rock clasts consist of Precambrian quartzite and Tertiary quartz monzonite.

CITED REFERENCES:

Anderson, Thomas C, 1977, Compound faceted spurs and recurrent movement in the Wasatch Fault Zone, north central Utah; Brigham Young University Geology Studies, v.24, pt.2, p.83-101

Bates, Robert L and Jackson, Julia A, 1980, editors, Glossary of Geology, second edition; American Geological Institute, Falls Church, Virginia, 751p.

Brabb, Earl E, Pampeyan, Earl H, & Bonilla, Manuel G, 1978, Landslide susceptibility in San Mateo County, California; United States Geological Survey Miscellaneous Field Studies Map MF-360.

Bryant, Bruce, 1984, Reconnaissance geologic map of the Precambrian Farmington Canyon Complex and surrounding rocks in the Wasatch Mountains between Ogden and Bountiful, Utah; United States Geological Survey Miscellaneous Investigations Series Map I-1447

Carrara, A & Merenda, L, 1976, Landslide inventory in northern Calabria, southern Italy; Geological Society of America Bulletin, v.87, n.8,p.1153-62.

Coffman, Jerry L & Stover, Carl W, 1979, United States earthquakes, 1977; National Oceanographic and Atmospheric Adiministration/United States Geological Survey Publication, 81p.

Coffman, Jerry L, von Hake, Carl A, & Stover, Carl W, 1982, Earthquake history of the United States; National Oceanographic and Atmospheric Adiministration/United States Geological Survey Publication 41-1, 258p.

Crittenden, Max D, Jr, 1965a, Geology of the Draper Quadrangle, Utah; United States Geological Survey Geologic Quadrangle Map GQ-377

Crittenden, Max D, Jr, 1965b, Geology of the Sugar House Quadrangle, Utah; United States Geological Survey Geologic Quadrangle Map GQ-380

Currey, Donald R, Atwood, Genevieve, & Mabey, Don R, 1983, Major levels of Great Salt Lake and Lake Bonneville; Utah Geological and Mineral Survey Map 73.

Davis, Fitzhugh D., 1983, Geologic map of the central Wasatch front, Utah; Utah Geological and Mineral Survey Map 54-A.

Davis, Fitzhugh D., 1984, Mineral resources of the central Wasatch front, Utah; Utah Geological and Mineral Survey Map 54-D.

DeGraff, Jerome V & Romesburg, H Charles, 1980, Regional landslide-susceptibility assessment for wildland management: a matrix approach; in Coates, Donald R & Vitek, John D, editors, Thresholds in Geomorphology, George Allen & Unwin, p.401-414

Doser, Diane I, 1985, The 1983 Borah Peak, Idaho and 1959 Hebgen Lake, Montana earthquakes: models for normal fault earthquakes in the Intermountain Seismic Belt; in Stein, Ross S & Bucknam, Robert C, editors, Proceedings of Workshop XXVIII on the Borah Peak, Idaho, Earthquake, Volume A, United States Geological Survey Open-file Report 85-290, p.368-384

Gilbert, Grove Karl, 1928, Studies of Basin-Range Structure; United States Geological Survey Professional Paper 153, 92p.

Hadley, Jarvis B, 1964, Landslides and related phenomena accompanying the Hebgen Lake earthquake of August 17, 1959; United States Geological Survey Professional Paper 435-k, p.107-138

Harp, Edwin, Wilson, Raymond C, & Wieczorek, Gerald F, 1981 Landslides from the February 4, 1976, Guatamala Earthquake; United States Geological Survey Professional Paper 1204-A, 35p.

Harp, Edwin L, Tanaka, Kohei, Sarmiento, John, & Keefer, David K, 1984, Landslides from the May 25-27, 1980, Mammoth Lakes, California, earthquake sequence; United States Geological Survey Miscellaneous Investigation Series Map, I-1612, 1:62,500

Johnson, Douglas, 1939, Fault scarps and fault line scarps; Journal of Geomorphology v.2, p.174-177

Keefer, David K, 1984, Landslides caused by earthquakes; Geological Society of America Bulletin, v. 95, p. 406-421

Krohn, James P & Slosson, James E, 1976, Landslide potential in the United States; California Geology, October 1976, p.224-231

Moore, William J & Sorensen, Martin L, 1979, Geologic map of the Tooele 1 degree by 2 degree Quadrangle, Utah; United States Geological Survey Miscellaneous Investigation Series Map, I-1132

Newmark, N M, 1965, Effects of earthquakes on dams and embankments; Geotechnique, v. XV, p. 139-160

Nolan, Thomas B, 1964, The Hebgen Lake, Montana earthquake of August 17, 1959; United States Geological Survey Professional Paper 435, p.v-vi.

Pack, Robert T, 1985, Multivariate analysis of relative landslide susceptibility in Davis County, Utah; PhD, Utah State University, Logan, 231p.

Piteau, Douglas R & Peckover, F Lionel, 1978, Engineering of rock slopes; in R L Schuster & R J Krizek, editors, Landslides: Analysis & Control, Transportation Research Board, Commission on Socio-technical Systems, National Research Council, National Academy of Sciences, Washington D C, Chapter 9, p. 192-228

Schwartz, David P & Coppersmith, Kevin J, 1984, Fault behavior and characteristic earthquakes: examples from the Wasatch and San Andreas Fault Zones; Journal of Geophysical Research, v.89, no.B7, p.5681-98.

Stein, Ross S & Bucknam, Robert C, 1985, editors, Proceedings of Workshop XXVIII on the Borah Peak, Idaho, Earthquake, Volume A, United States Geological Survey Open-file Report 85-290, 686p.

Swensen, A Jaren, 1975, Geologic map of the Bingham District; in Bray, R Eldon and Wilson, John C, editors, Guide Book to the Bingham Mining District, sponsored by the Society of Economic Geologists, Bingham Canyon, Utah, October 23, 1975, 156p.

Tooker, Edwin W, 1980, Preliminary geologic map of the Tooele Quadrangle (7 1/2) minute Tooele County, Utah; United States Geological Survey Open-file Report 80-623.

Tooker, Edwin W & Roberts, Ralph J, 1961, Preliminary geologic map and sections of the north end of the Oquirrh Range (Mills Junction, Garfield, and Magna 7 1/2 minute Quadrangles) Tooele and Salt Lake Counties, Utah; United States Geological Survey Mineral Investigations Field Studies Map MF-240

Tooker, Edwin W & Roberts, Ralph J, 1971a, Geologic map of the Garfield Quadrangle Salt Lake and Tooele Counties, Utah; United States Geological Survey Geologic Quadrangle Map GQ-922

Tooker, Edwin W & Roberts, Ralph J, 1971b, Geologic map of the Magna Quadrangle Salt Lake County, Utah; United States Geological Survey Geologic Quadrangle Map GQ-923

Tooker, Edwin W & Roberts, Ralph J, 1971c, Geologic map of the Mills Junction Quadrangle Tooele County, Utah; United States Geological Survey Geologic Quadrangle Map GQ-924

Van Horn, Richard, 1969, Preliminary geologic map of the southern half of the Fort Douglas Quadrangle, Salt Lake County, Utah; United States Geological Survey Open-File Report 69-0308.

Van Horn, Richard, 1981, Geologic map of pre-Quaternary rocks of the Salt Lake City North Quadrangle, Davis & Salt Lake Counties, Utah; United States Geological Survey Map Miscellaneous Investigations I-1330

Varnes, David J, 1978, Slope movements and types and processes; Landslides: Analysis and Control, Special Report 176, Transportation Research Board National Academy of Sciences, Washington D C, 100p.

Vecchia, Orlando, 1978, A simple terrain index for the stability of hillsides or scarps; in Geddes, James D, editor, Large ground movements and structures, Proceedings of the Conference held at the University of Wales Institute of Science and Technology, Cardiff, July, 1977, sponsored by Department of Civil Engineering and Building Technology, University of Wales Institute of Science and Technology, and Institution of Structural Engineers, Pentech Press, p.449-461

Whalley, W B, 1984, Rockfalls; in D. Brunsden & D B Prior, editors, Slope Instability, John Wiley & Sons, p.217-256

Wieczorek, Gerald F, Wilson, Raymond C, & Harp, Edwin L, 1985, Map showing slope stability during earthquakes in San Mateo County, California; United States Geological Survey Miscellaneous Investigations Series Map I-1257-E.

Williams, J Stewart and Tapper, Mary L, 1953, Earthquake history of Utah, 1850-1949; Seismological Society of America Bulletin, v.43, n.3, p.191-218

Wilson, Raymond C, 1984, Quantitative prediction of earthquake-induced landslides; United States Geological Survey Open-file Report 84-760, p.398-413

Witkind, Irving J, 1964, Reactivated faults north of Hebgen Lake; United States Geological Survey Professional Paper 435-G, p.37-50.

Wright, Robert, Campbell, Russell H, & Nilsen, Tor H, 1974, Preparation and use of isopleth maps of landslide deposits; Geology, October, p. 483-485

LEGAL ISSUES RELATED TO HAZARD MITIGATION POLICIES

by

James E. Slosson
Slosson and Associates
Van Nuys, California 91401

ABSTRACT

Within the past decade, professionals involved in design, construction, and maintenance of structures/facilities have become the target of litigation when failures and losses have occurred. Slowly, but consistently, court decisions nationwide have moved toward holding the professionals responsible where negligence, errors, or omissions have been involved. Prior to this change in court philosophy, professionals only had to conform to "standard of practice" in a geographic area. "Same" or "similar" concept is now part of the legal vocabulary in California, Utah, and many other states. "Standard practice" in a given geographic area may be judged substandard relative to professional standards utilized elsewhere. A professional who uses a lower standard acceptable to a local jurisdiction, may be held responsible for a failure or losses resulting from the use of those lower standards, when higher standards, such as those established in California, are known and available to the professional. In addition, planners, planning commissions, elected and appointed officials involved may become targets in future litigation and share court-imposed penalties.

Professionals involved in design, construction, and maintenance of structures, facilities, and graded areas have become the target of litigation within the past decade when failures and losses have occurred. Court decisions nation-wide have moved slowly, but consistently, in the direction of holding the professionals responsible where negligence, errors, or omissions have been involved. Recent out-of-court (or pre-trial) settlements and superior court decisions in California have carried that another step and have developed a recognizable trend toward holding the professional responsible when there is an indication of negligence and/or work that falls below that which a responsible, prudent professional would perform.[1] Prior to this change in philosophy by the courts, the professional had only to reach the level of work or quality commonly attained or agreed upon by members of a prescribed discipline or profession in the geographic area in which those professionals practice; that locally - applicable level of work had been called "standard practice". In some geographic areas, it has been noted that persons of a given profession may have, by group action or agreement, set an agreed upon "standards-of-practice" -- in some instances stating that, for a variety of reasons or rationale, "they" need not meet as high a standard as achieved elsewhere.[2] Some local governments, such as the City of San Diego, have agreed with local professional organizations that because it seldom rains in San Diego, the standards need not be as rigid as in areas such as Los Angeles.[3] In the past, some professionals have set their personal standards of care to the lowest allowed by local government.[4]

Responsible professionals should be aware that the "same or similar" concept is now a part of the legal vocabulary in California, Utah, and many other states.[5] Some California judges during the past decade have suggested that it may be possible for "standard practice" in a given geographic area to be judged substandard relative to professional standards utilized elsewhere. A professional who uses a lower standard adopted by a lax governmental jurisdiction for a project within that jurisdiction, but who knows or should have known of higher standards utilized elsewhere, can be held responsible for a failure or losses resulting from the use of those lower standards. In a recent case in San Diego, California,[6] the consulting firm was found responsible for losses related to what the court determined to be substandard practice, even though the local government had accepted the work and the professional standards utilized.

The practicing professional architect, engineer, geologist, and planner should be aware of their responsibilities and to what "responsible, prudent practice" equates. They should be aware that many states have adopted the concept of "same or similar" for area of practice and/or method of practice. Thus, a professional architect working in Salt Lake City, Utah may be held responsible for knowing and utilizing the prudent practices normally used for earthquake resistant design used in California considering that:

- Earthquakes are anticipated in both areas.
- Many of the highrise structures and critical facilities are sited on water saturated alluvial fans, deltas, and/or lake deposits which possess a potential for prolonged shaking and liquefaction and/or landslide activity.
- For example, the state of Utah has all of the geologic and seismicity indicators suggestive of a high potential earthquake activity, but recent history has been somewhat lacking in strong motion shaking. One can easily argue that this may indicate a seismic gap, increasing the potential for a future large earthquake which is likely to occur within the next century.
- Similar construction materials are used.
- The professional societies dealing with architecture and seismic design critera are nationwide in membership;
- The universities teach similar subjects.
- Conferences dealing with earthquakes and design are held in both cities.
- Geologic mapping and seismic zonation has been accomplished in both geologic areas and with similar techniques.

- Active faults have been identified as well as other miscellaneous factors.
- The relative ease in locating the techniques and procedures of the "similar" jurisdiction. The case can easily be made for use of the "same" or "similar" concept.

Many professionals and/or firms practice in both Salt Lake City and Los Angeles, thus, it would be almost impossible for them to argue that it would be prudent to drop to a lower standard of practice just because "Salt Lake City was less stringent at the time of design and construction than Los Angeles".

It will be interesting to monitor the decisions of the courts in states such as Utah during the next decade as they determine whether professionals and/or their firms will be permitted to ignore the higher standards (related to site analysis and design criteria) which must be met in California (which has been held to be a "similar" locality) in order to use the lower requirements acceptable in Utah. In cases involving severe damage to structures and loss of life, will the professional be able to argue that he or she knowingly dropped professional standards to address only the lower standards of care accepted in Utah with full knowledge that failure or loss of life might occur? Granted cost is a factor and the client may not be willing to pay for more than the bare minimum required by local government (that may lack professional expertise and political support)[7] Should the professional be willing to work at a substandard and subprofessional level? The courts will certainly answer this question and dilemma when a building collapses and kills scores of people and a substantial cause of the damage can be shown to be substandard design or construction -- this will not be deemed to be an act of God, but rather will constitute legal negligence. An act of God had been defined in Utah as a natural act of such magnitude that it cannot be reasonably protected against.[8] Certainly an earthquake of 6.5 on the Richter Scale is predictable. There is further no question that we have the expertise to minimize the damage caused by an earthquake of this magnitude.

It is the opinion of the author that the courts will hold the professionals responsible for the high standards that have been established in jurisdictions such as the City of Los Angeles or the State of California. Furthermore, the engineering geologist will most likely be held responsible to meet or exceed the standard of care outlined in the guidelines for reports developed more than a decade ago (1971) by the Association of Engineering Geologist. These guidelines were adopted by the California Division of Mines and Geology in 1973 (CDMG Notes #37) and the California Board of Registration for Geologists and Geophysicists in 1979.

In addition, it is the opinion of the author that eventually the courts will recognize that the planners and planning commissions usually make the land-use and planning decisions that set the stage for the planning of and construction events that follow. Thus, the planners and planning commissions as well as other involved elected and appointed officials may become targets in future litigation and share the burden of court-imposed penalties.[9] If a planning commission approves a housing development to be designed and constructed below or downstream from a known, older, unsafe dam located near a known active fault (such as the Wasatch Fault) and a predictable 6½ to 7 magnitude earthquake occurs causing failure of the dam, flooding of the subdivision, and loss of life -- who then is responsible?

ACKNOWLEDGEMENT

This paper was reviewed by Michael F. Richman, Esq., Salt Lake City, Utah and his comments and counsel were very useful in the preparation of this paper.

REFERENCED NOTES

[1]

- (e.g.) King/Hanamure v Baldwin Co., Orange County, California, Superior Court, 1986; fill settlement
- Simon, et al v Chilcote, Inc., San Diego County Superior Court, 1985; fill settlement plus movement on ancient landslide
- Country Hills Inc., et al v Converse-Davis and Associates, Orange County, California, Superior Court, 1978; landslide failures
- Kearney, et al v MCS Development, et al, San Diego County Superior Court, 1984; fill settlement and slope failure
- Valley Circle Estates el al v VTN Consolidated, Inc., Los Angeles County Superior Court, 1983; grading and compaction
- Tech-Bilt v Woodward-Clyde and Associates, San Diego County Superior Court, 1982; fill causes damage to structures
- James W. and Katherine T. Harvey, et al v Christiana Companies, Inc., a Delaware Corp. et al, San Diego County Superior Court, 1984
- Kearney, et al v MCS Development, et al, 1983

[2]

- San Diego Union, September 19, 1982
- Country Hills Inc., et al v Converse-Davis and Associates, Orange County, California, Superior Court, 1978; landslide failures

[3]

- Slosson and Havens, "Government Appears to be Failing in Enforcement", 1985, at Natural Hazards Conference, University of Colorado
- Slosson, J.E., "Encouraging Government Mitigation: The Forensic Geologist/Expert Witness Perspective", 1985, at American Bar Association International Symposium, Miami, Florida

[4]

- Baldwin v Carleton Santee Corp., San Diego Superior Court, 1981
- Country Hills, Inc., et al v Converse-Davis and Associates, Orange County Superior Court, 1978
- Country Hills East Community Association et al v Lusk, Orange County Superior Court, 1986

[5] Swan v. Lamb (Ut) 584 P.2d 814 (Los Angeles doctor can testify in Utah as to California standards)

[6]

- Baldwin v Carleton Santee Corp, San Deigo County Superior Court, 1982
- Tech-Bilt v Woodward-Clyde and Associates, San Diego County Superior Court, 1982

[7] Kockelman, W. J, "Some Techniques for Reducing Landslide Hazards", Bulletin of the Association of Engineering Geologists, U.S. Geological Survey, Menlo Park, California, 1986

[8] Dougherty v. Cal-Pacific Utilities Co. 546 P.2d 880

[9] Meehan, Richard L., "The Battered Exclusion: Who Pays How Much for California Landslides?" (in press)

*U.S.GOVERNMENT PRINTING OFFICE:1987-201-933:60054

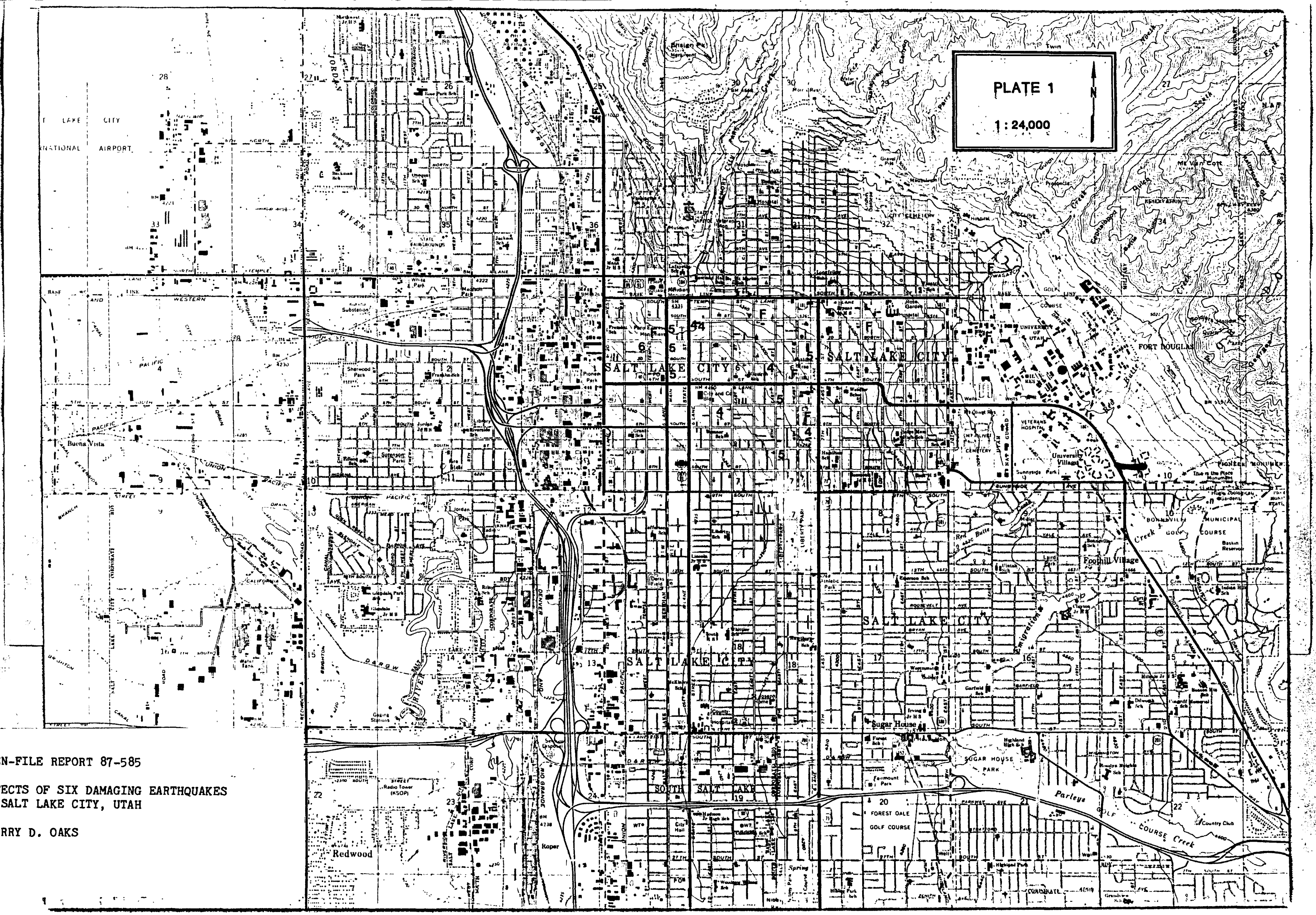

PLATE 1

1 : 24,000

OPEN-FILE REPORT 87-585

EFFECTS OF SIX DAMAGING EARTHQUAKES IN SALT LAKE CITY, UTAH

SHERRY D. OAKS

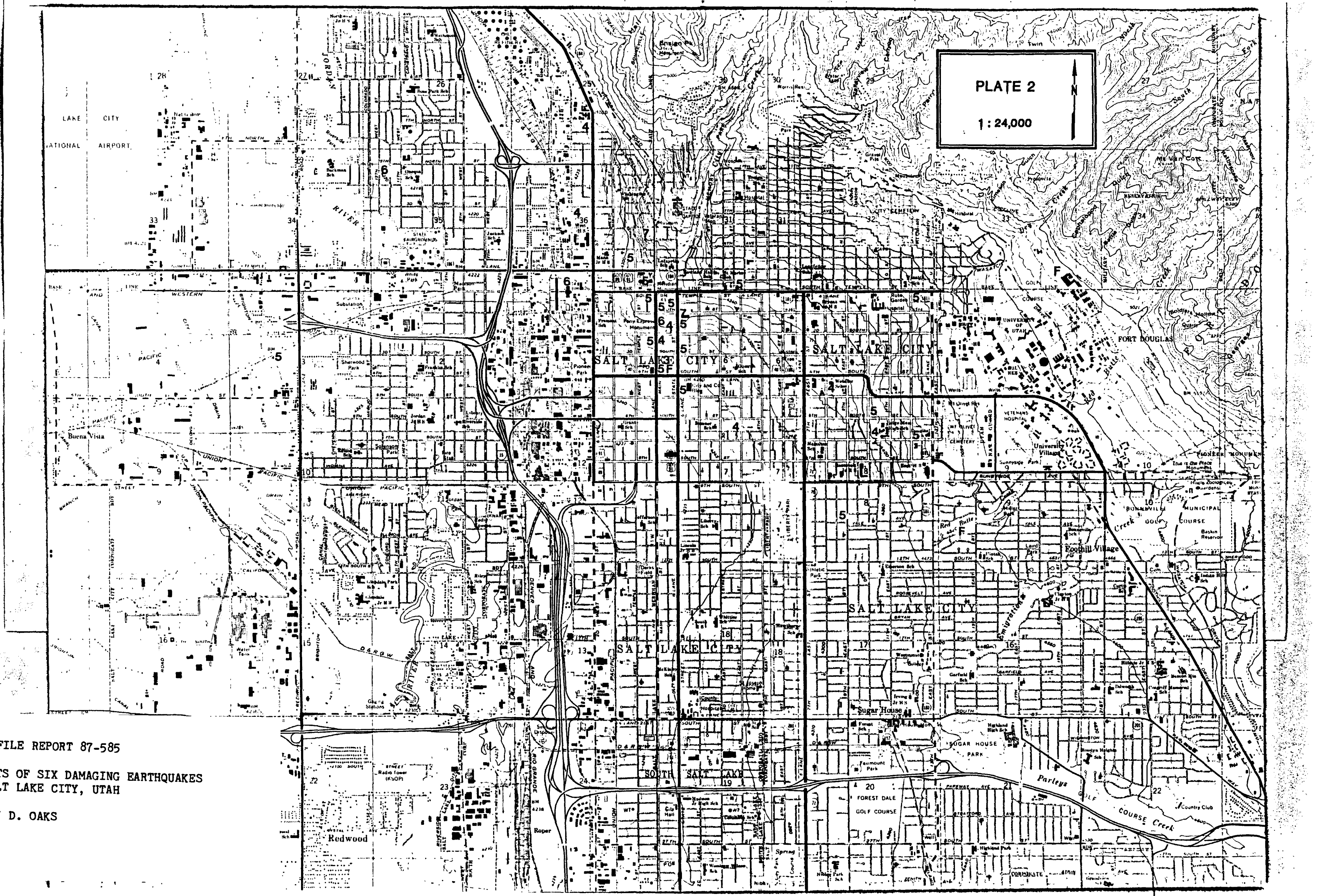

OPEN-FILE REPORT 87-585

EFFECTS OF SIX DAMAGING EARTHQUAKES
IN SALT LAKE CITY, UTAH

SHERRY D. OAKS

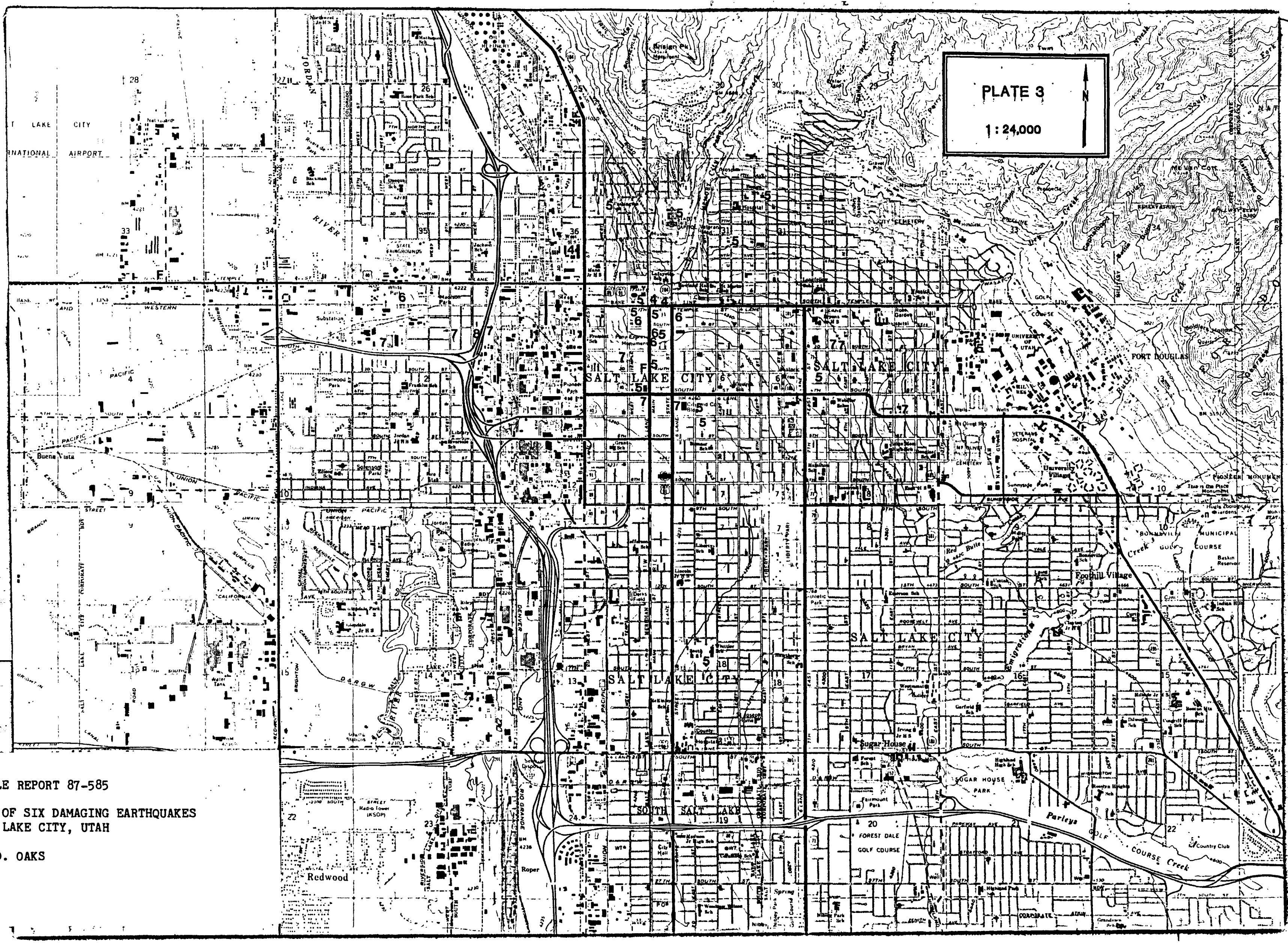

PLATE 3

1:24,000

OPEN-FILE REPORT 87-585

EFFECTS OF SIX DAMAGING EARTHQUAKES
IN SALT LAKE CITY, UTAH

SHERRY D. OAKS

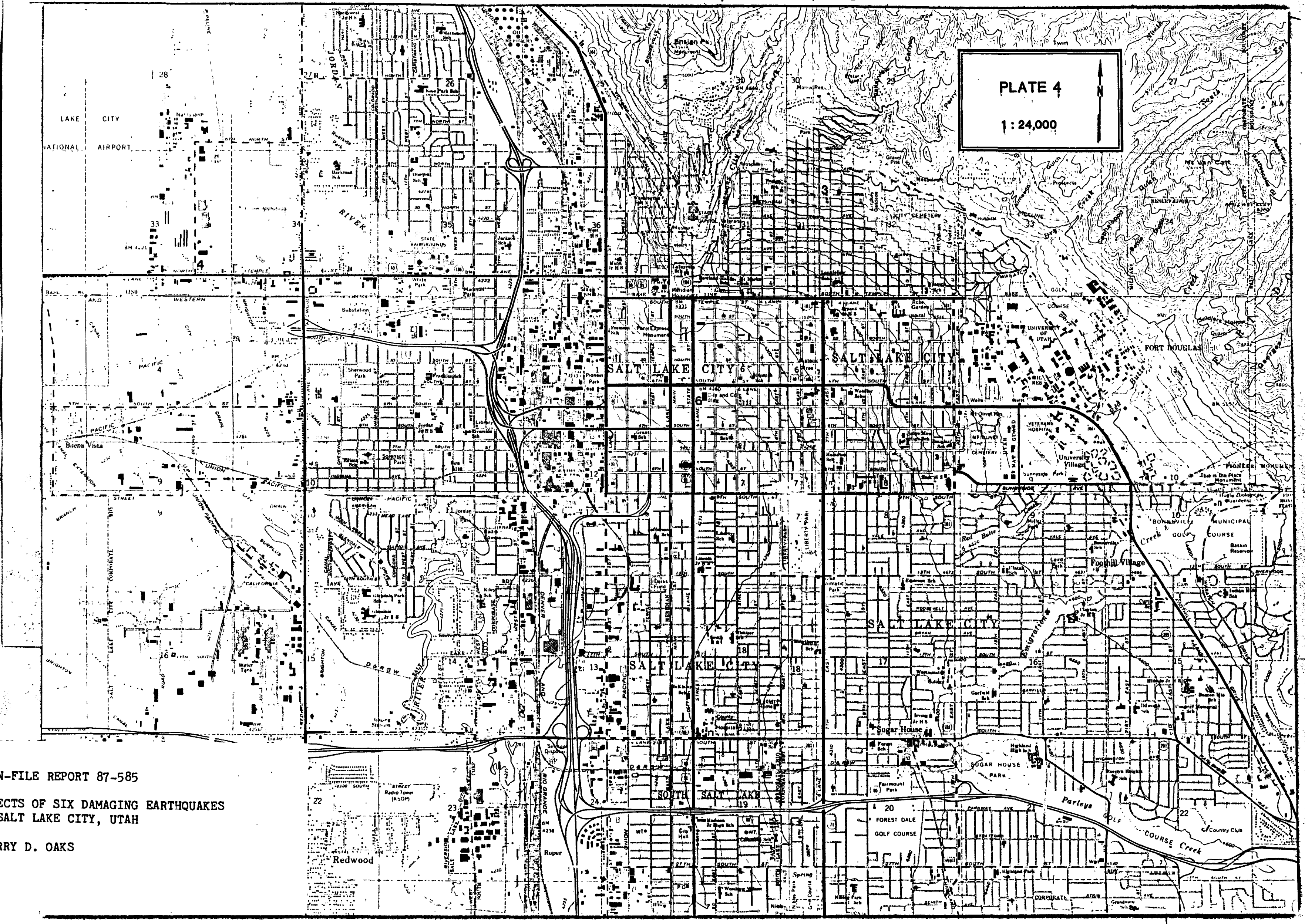

OPEN-FILE REPORT 87-585

EFFECTS OF SIX DAMAGING EARTHQUAKES
IN SALT LAKE CITY, UTAH

SHERRY D. OAKS

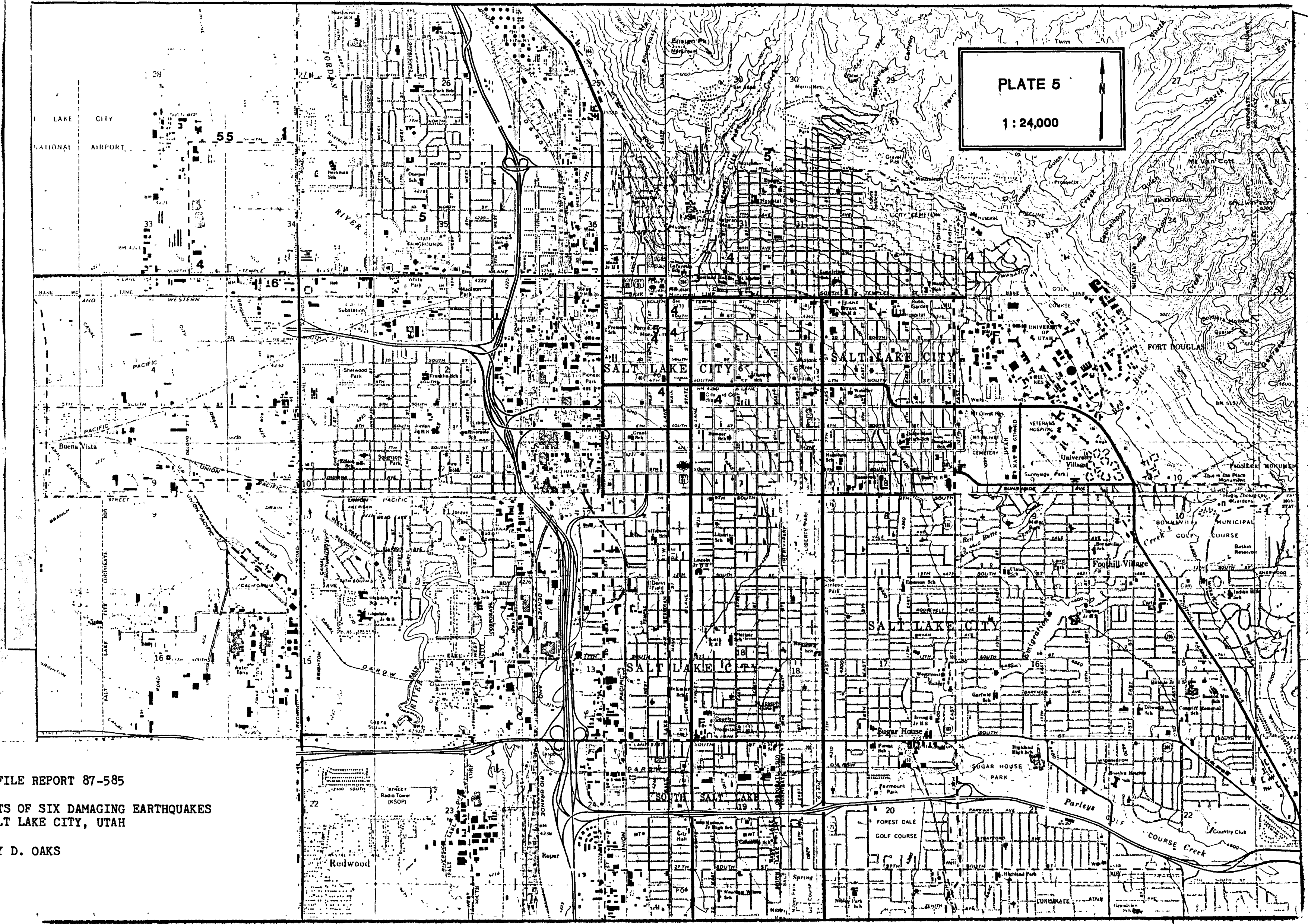

OPEN-FILE REPORT 87-585

EFFECTS OF SIX DAMAGING EARTHQUAKES
IN SALT LAKE CITY, UTAH

SHERRY D. OAKS

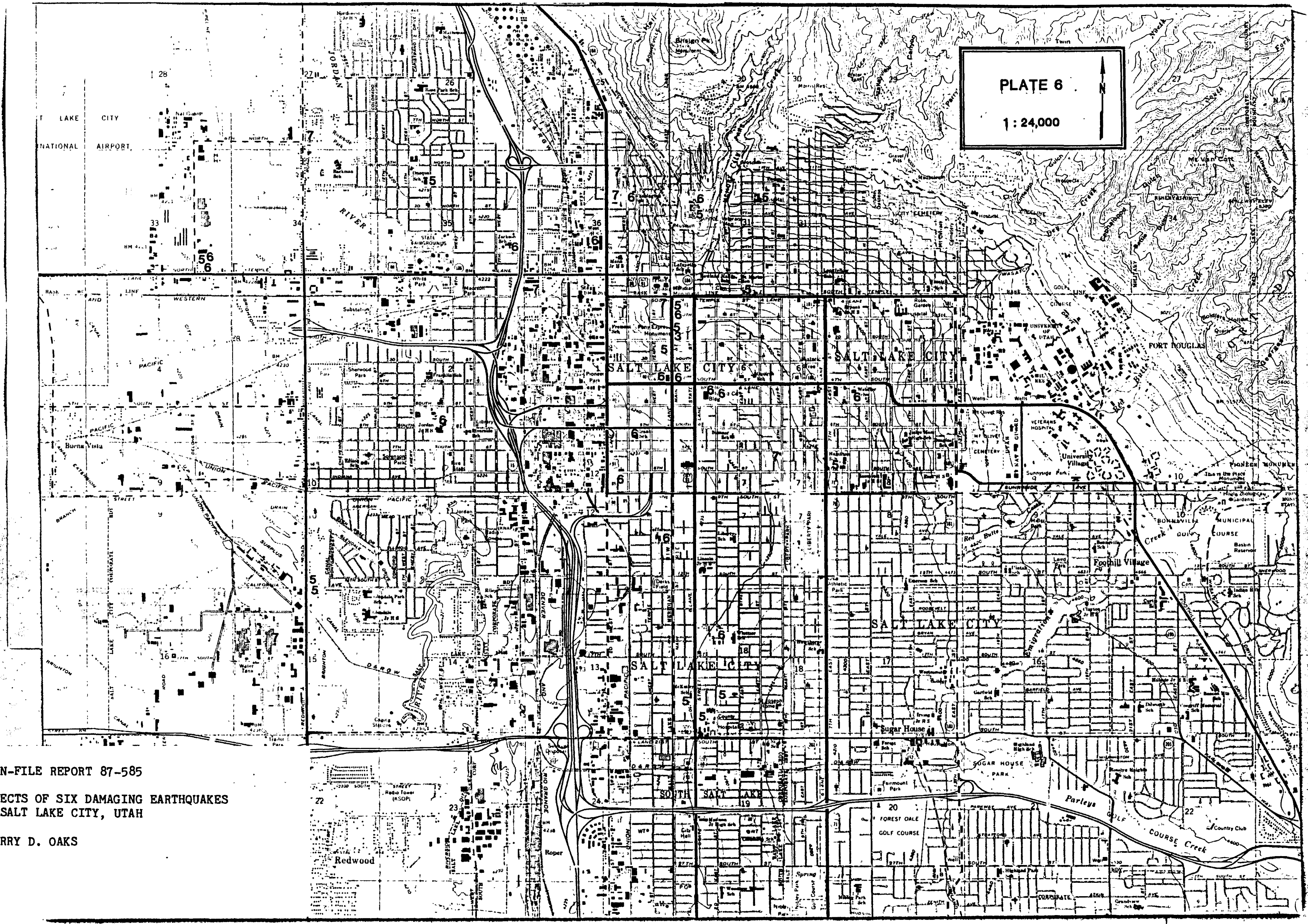

OPEN-FILE REPORT 87-585

EFFECTS OF SIX DAMAGING EARTHQUAKES
IN SALT LAKE CITY, UTAH

SHERRY D. OAKS

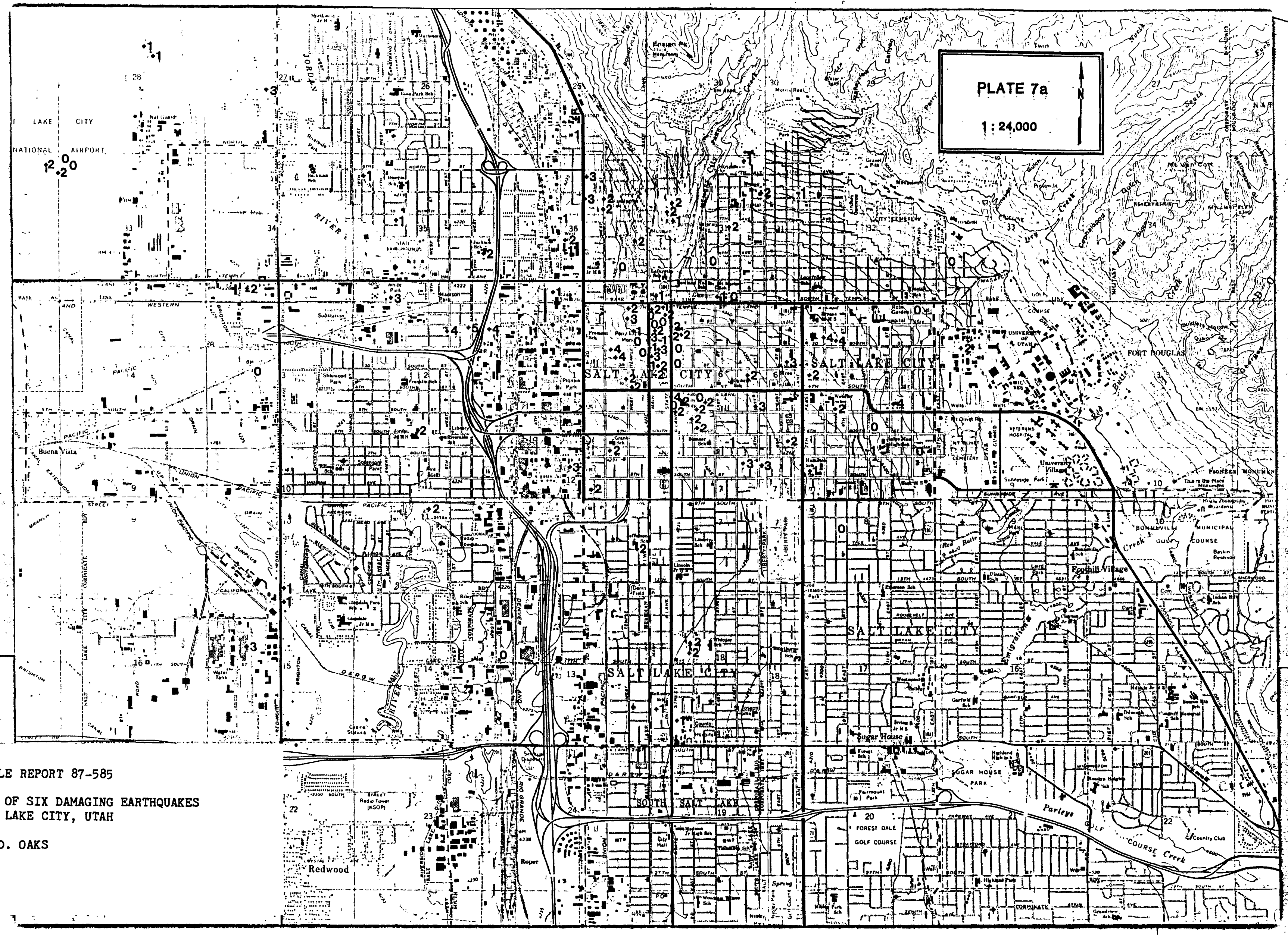

OPEN-FILE REPORT 87-585

EFFECTS OF SIX DAMAGING EARTHQUAKES
IN SALT LAKE CITY, UTAH

SHERRY D. OAKS

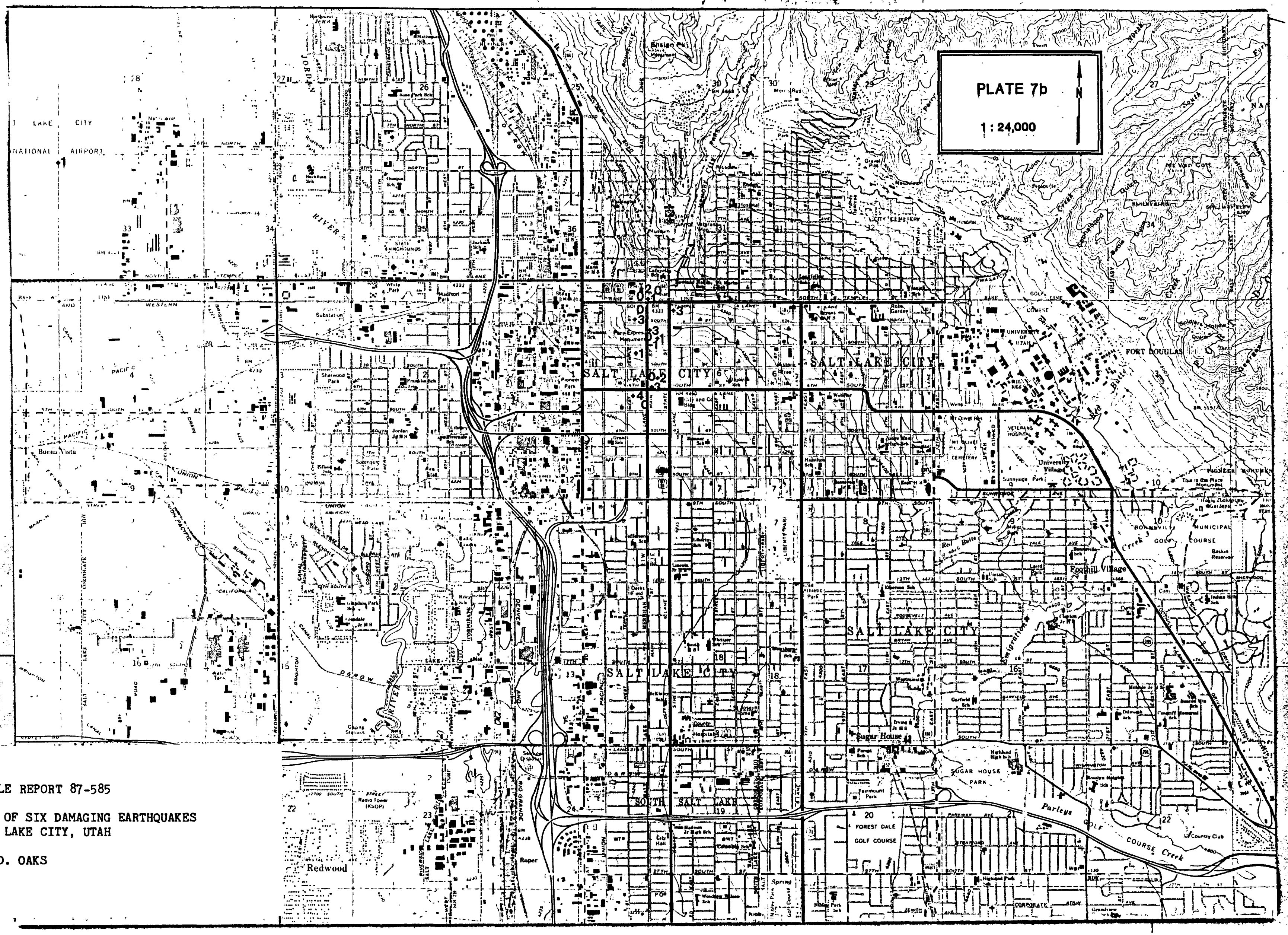

OPEN-FILE REPORT 87-585

EFFECTS OF SIX DAMAGING EARTHQUAKES
IN SALT LAKE CITY, UTAH

SHERRY D. OAKS

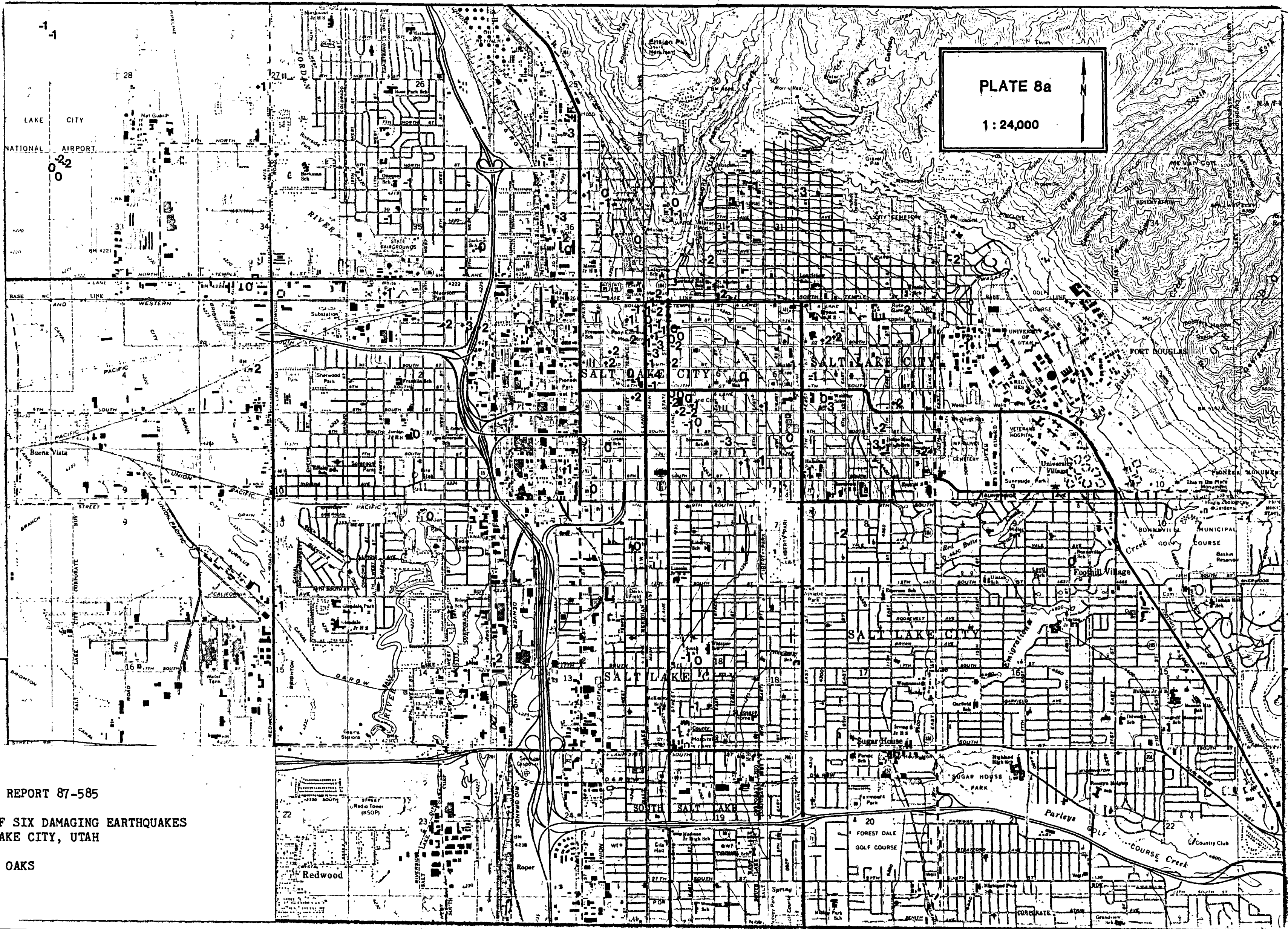

OPEN-FILE REPORT 87-585

EFFECTS OF SIX DAMAGING EARTHQUAKES
IN SALT LAKE CITY, UTAH

SHERRY D. OAKS

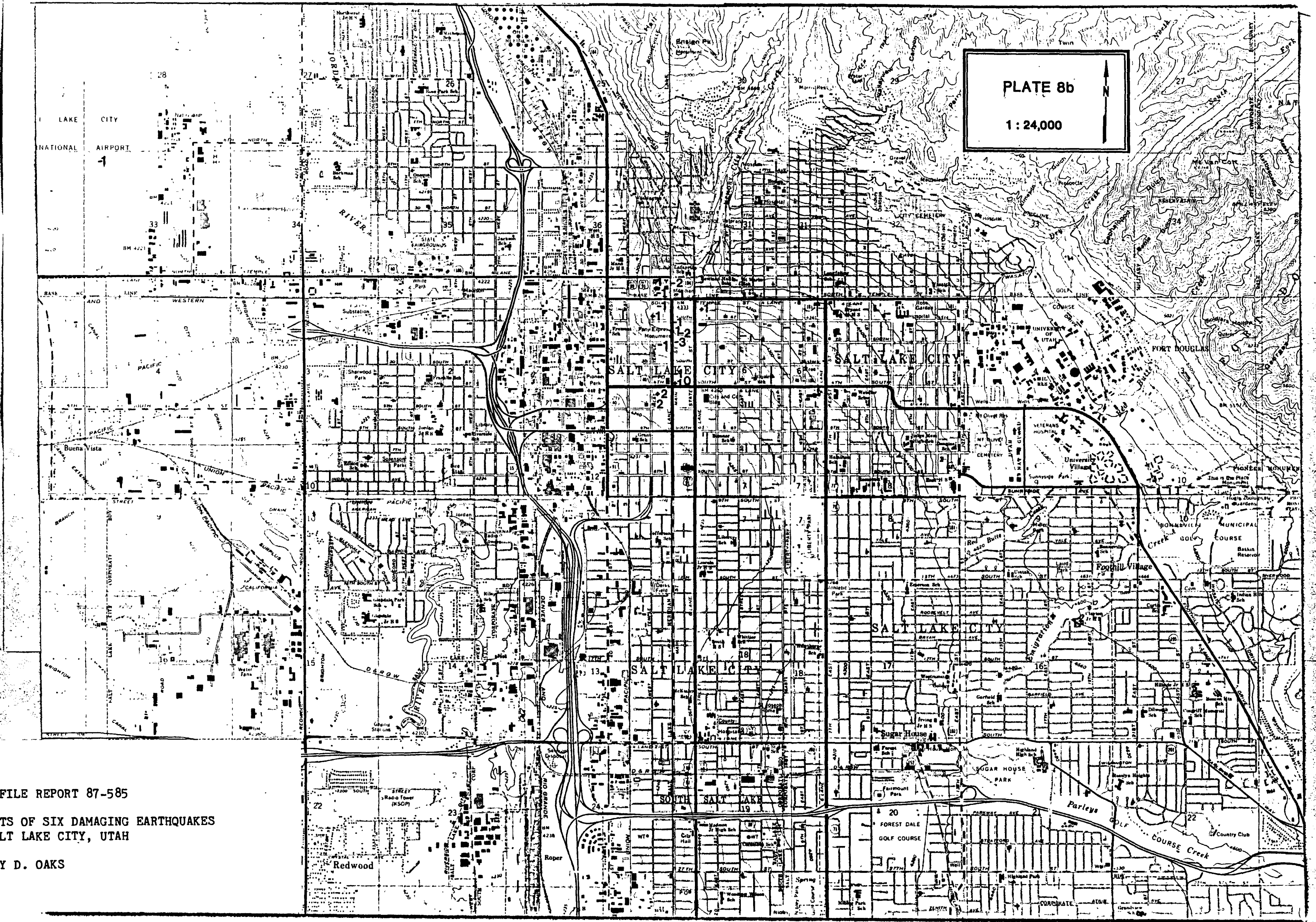

OPEN-FILE REPORT 87-585

EFFECTS OF SIX DAMAGING EARTHQUAKES
IN SALT LAKE CITY, UTAH

SHERRY D. OAKS

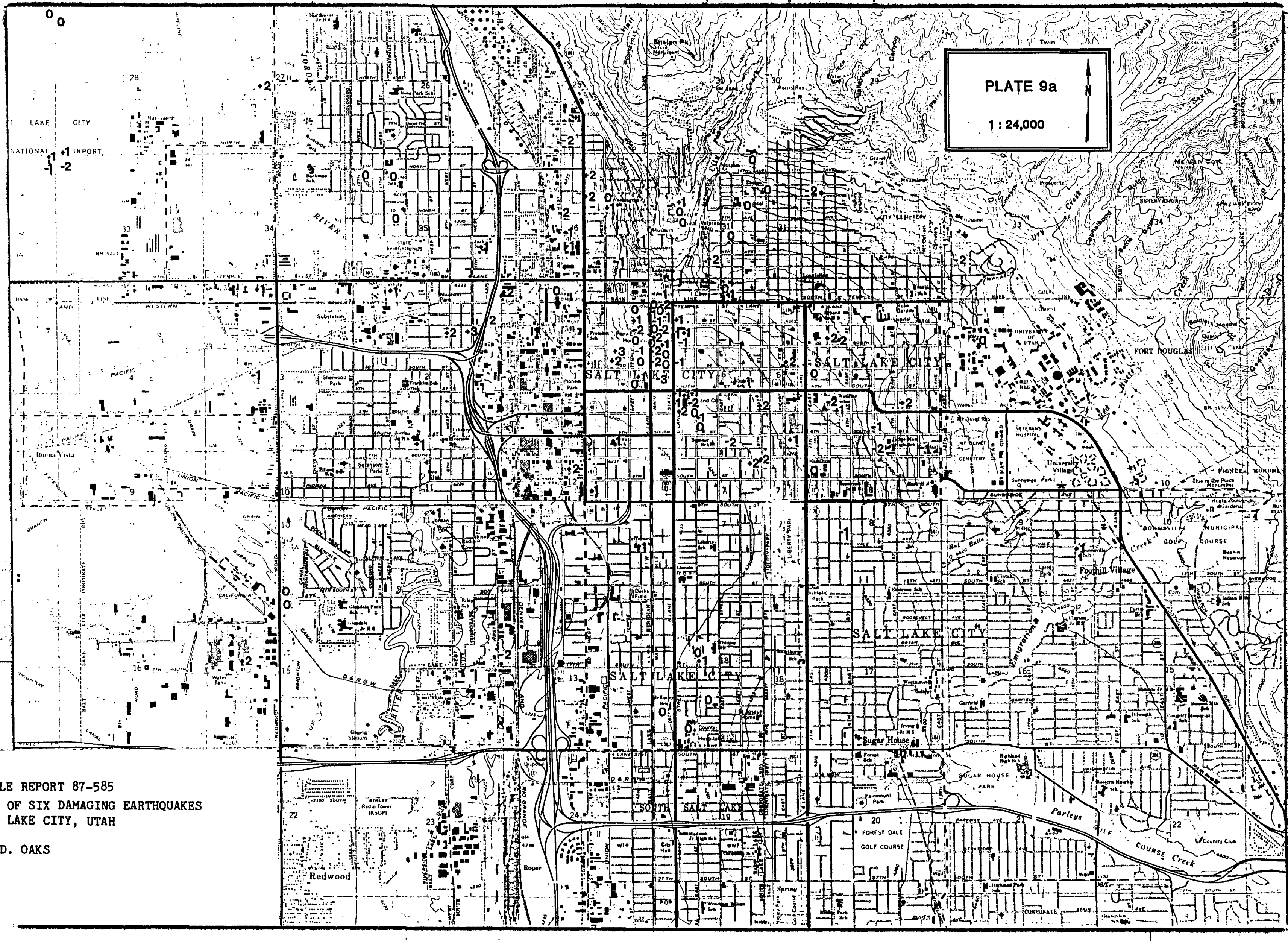

OPEN-FILE REPORT 87-585
EFFECTS OF SIX DAMAGING EARTHQUAKES
IN SALT LAKE CITY, UTAH

SHERRY D. OAKS

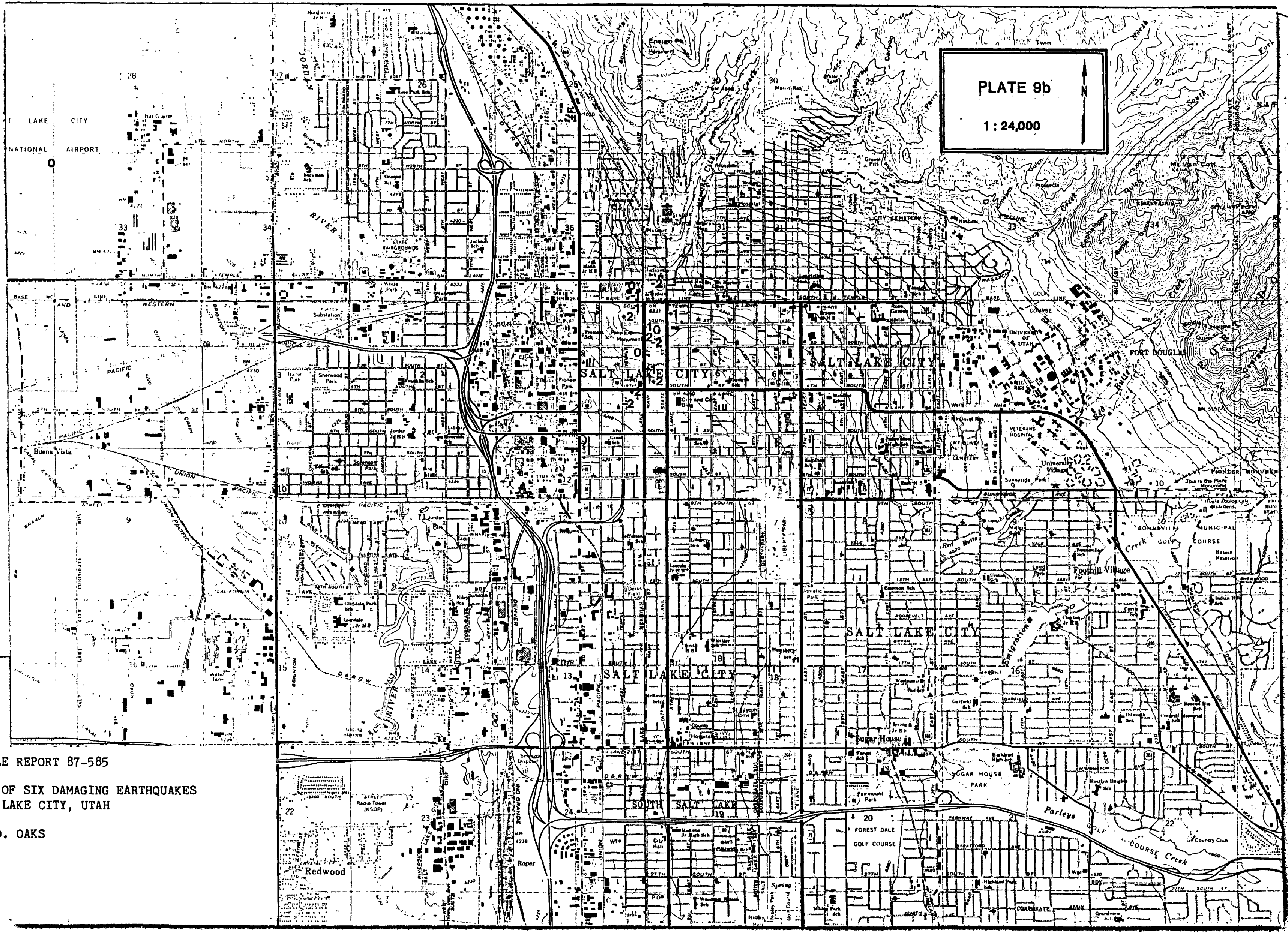

OPEN-FILE REPORT 87-585

EFFECTS OF SIX DAMAGING EARTHQUAKES
IN SALT LAKE CITY, UTAH

SHERRY D. OAKS

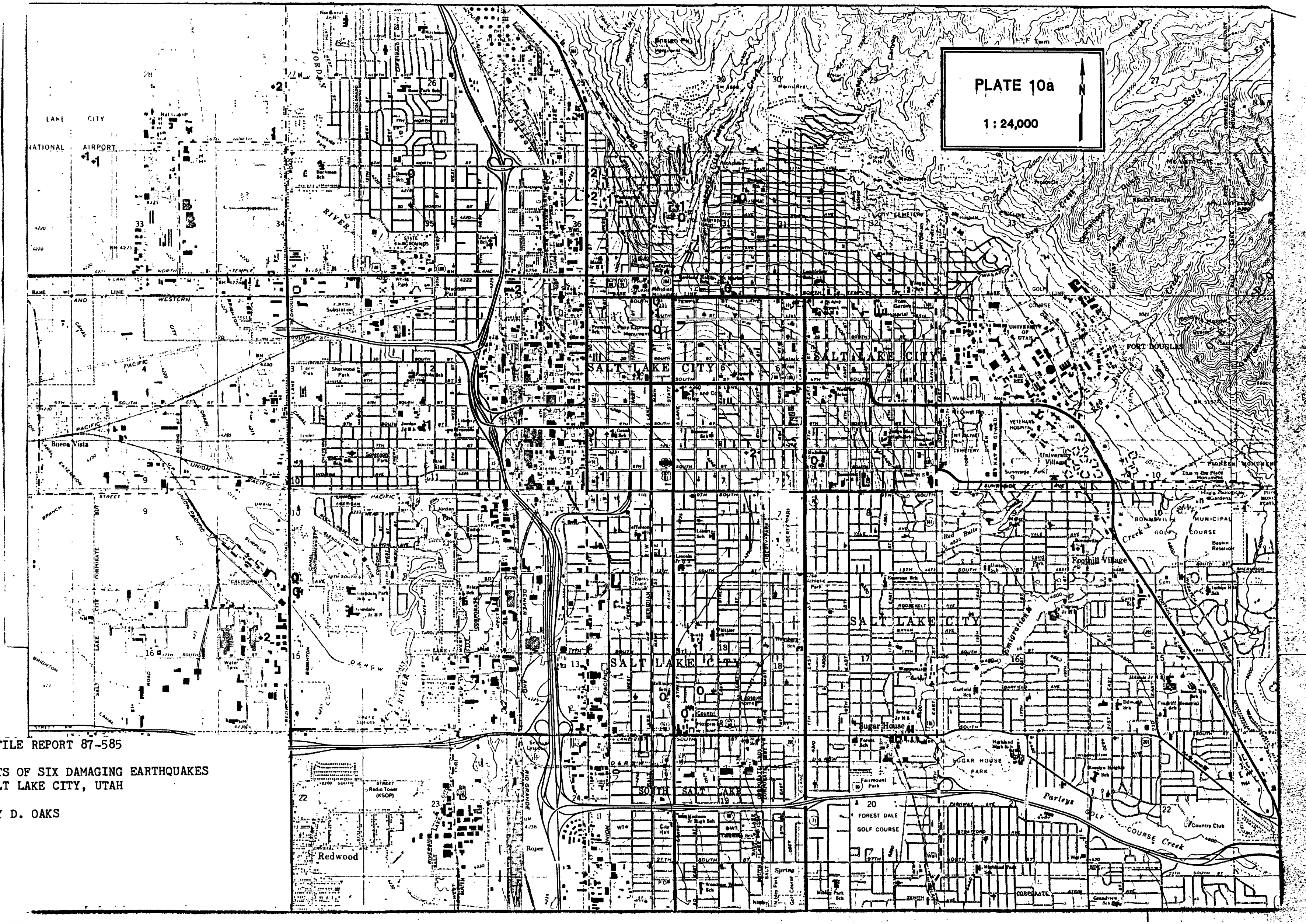

OPEN-FILE REPORT 87-585

EFFECTS OF SIX DAMAGING EARTHQUAKES
IN SALT LAKE CITY, UTAH

SHERRY D. OAKS

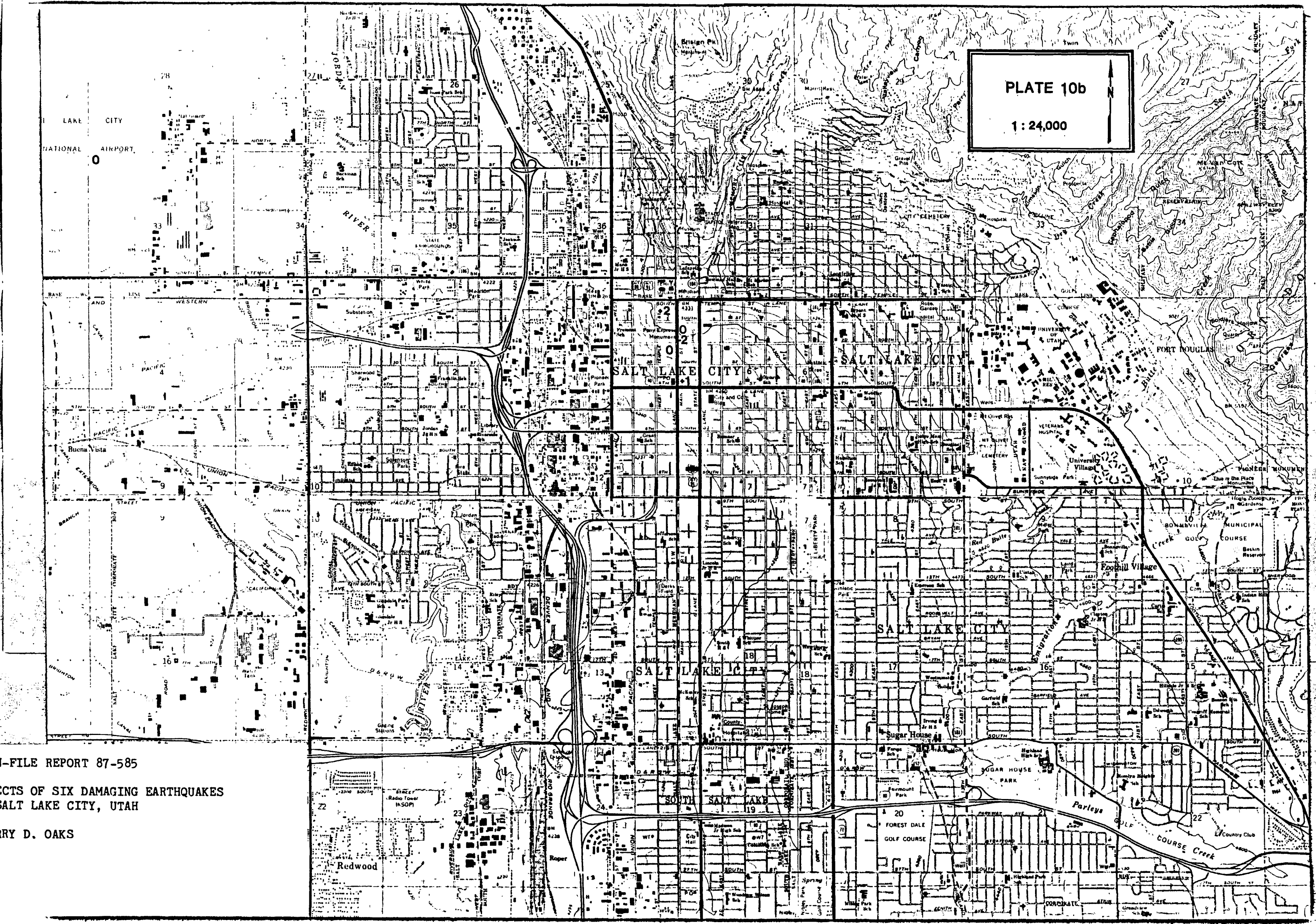

OPEN-FILE REPORT 87-585

EFFECTS OF SIX DAMAGING EARTHQUAKES
IN SALT LAKE CITY, UTAH

SHERRY D. OAKS

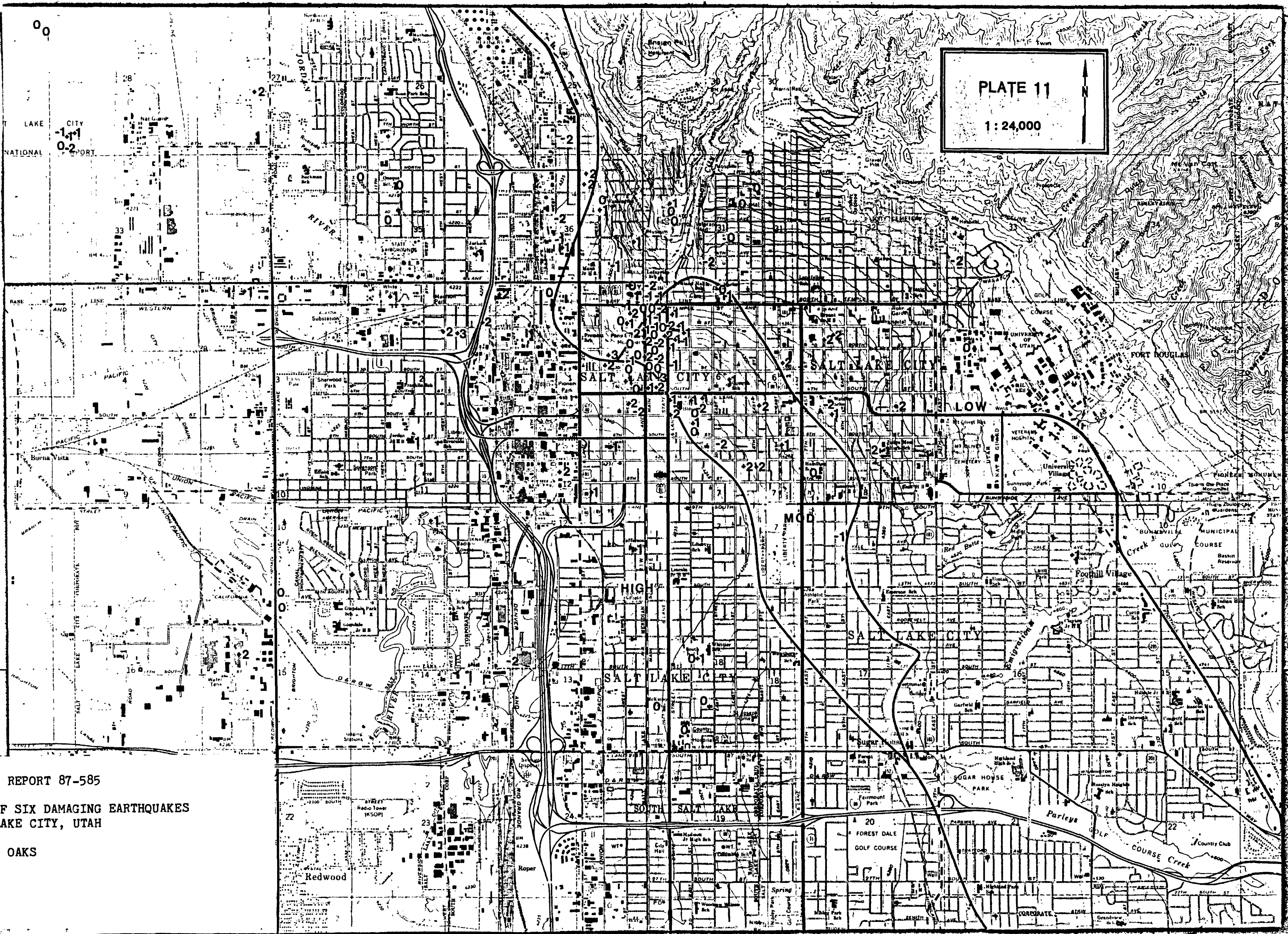

OPEN-FILE REPORT 87-585

EFFECTS OF SIX DAMAGING EARTHQUAKES
IN SALT LAKE CITY, UTAH

SHERRY D. OAKS